This is a digital copy of a book that was preserved for generations on library shelves before it was carefully scanned by Google as part of a project to make the world's books discoverable online.

It has survived long enough for the copyright to expire and the book to enter the public domain. A public domain book is one that was never subject to copyright or whose legal copyright term has expired. Whether a book is in the public domain may vary country to country. Public domain books are our gateways to the past, representing a wealth of history, culture and knowledge that's often difficult to discover.

Marks, notations and other marginalia present in the original volume will appear in this file - a reminder of this book's long journey from the publisher to a library and finally to you.

Usage guidelines

Google is proud to partner with libraries to digitize public domain materials and make them widely accessible. Public domain books belong to the public and we are merely their custodians. Nevertheless, this work is expensive, so in order to keep providing this resource, we have taken steps to prevent abuse by commercial parties, including placing technical restrictions on automated querying.

We also ask that you:

+ *Make non-commercial use of the files* We designed Google Book Search for use by individuals, and we request that you use these files for personal, non-commercial purposes.

+ *Refrain from automated querying* Do not send automated queries of any sort to Google's system: If you are conducting research on machine translation, optical character recognition or other areas where access to a large amount of text is helpful, please contact us. We encourage the use of public domain materials for these purposes and may be able to help.

+ *Maintain attribution* The Google "watermark" you see on each file is essential for informing people about this project and helping them find additional materials through Google Book Search. Please do not remove it.

+ *Keep it legal* Whatever your use, remember that you are responsible for ensuring that what you are doing is legal. Do not assume that just because we believe a book is in the public domain for users in the United States, that the work is also in the public domain for users in other countries. Whether a book is still in copyright varies from country to country, and we can't offer guidance on whether any specific use of any specific book is allowed. Please do not assume that a book's appearance in Google Book Search means it can be used in any manner anywhere in the world. Copyright infringement liability can be quite severe.

About Google Book Search

Google's mission is to organize the world's information and to make it universally accessible and useful. Google Book Search helps readers discover the world's books while helping authors and publishers reach new audiences. You can search through the full text of this book on the web at `http://books.google.com/`

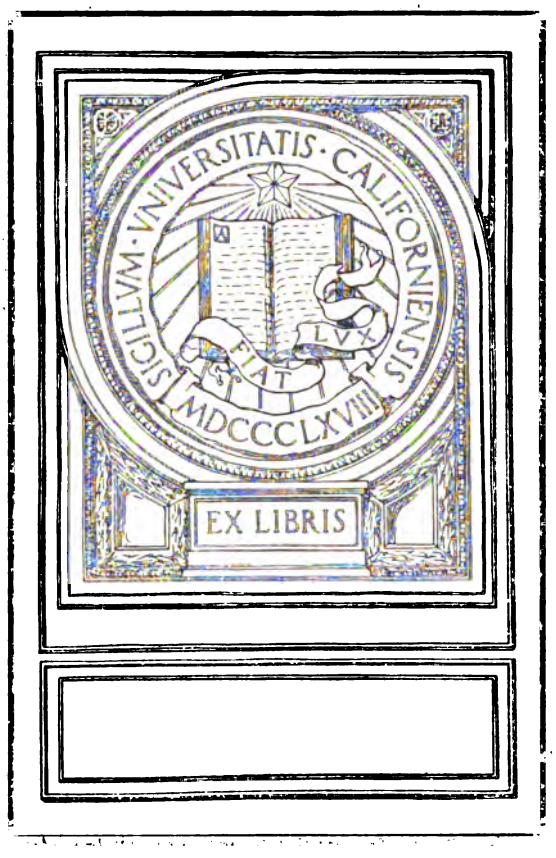

Digitized by Google

Digitized by Google

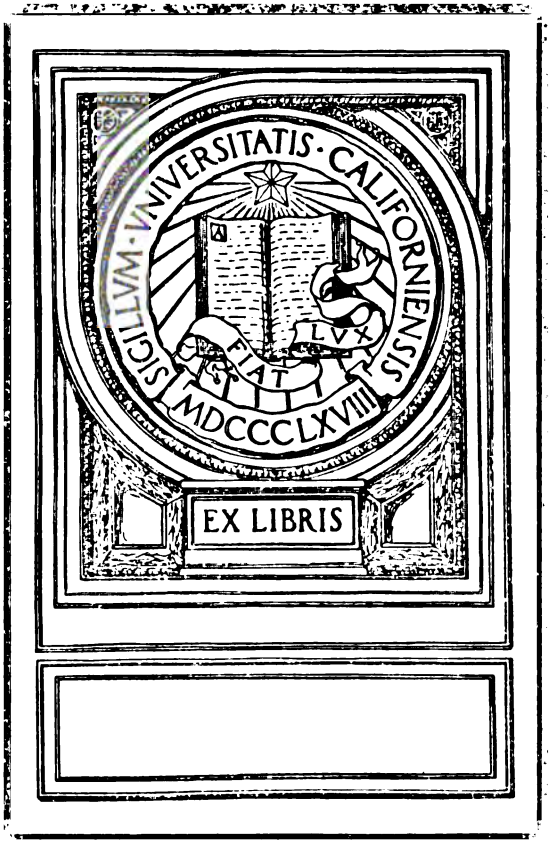

Digitized by Google

Digitized by Google

Digitized by Google

Digitized by Google

Digitized by Google

FEB 28 1923

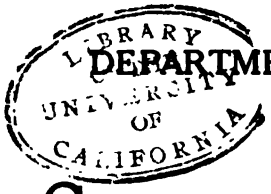

DEPARTMENT OF COMMERCE

SCIENTIFIC PAPERS

OF THE U.S.

BUREAU OF STANDARDS

S. W. STRATTON, DIRECTOR

(Prior to Volume 15 this series was called the "Bulletin of the Bureau of Standards")

VOLUME 17

1922

WASHINGTON
GOVERNMENT PRINTING OFFICE
1922

Digitized by Google

T1
W34
v.17

Digitized by Google

CONTENTS OF VOLUME 17.

		Page.
405.	A Simple Portable Instrument for the Absolute Measurement of Reflection and Transmission Factors ... *A. H. Taylor*	1
406.	Present Status of the Constants and Verification of the Laws of Thermal Radiation of a Uniformly Heated Inclosure ... *W. W. Coblentz*	7
407.	Recent Modifications in the Construction of Platinum Resistance Thermometers ... *T. S. Sligh, jr.*	49
408.	Effect of the Rate of Cooling on the Magnetic and Other Properties of an Annealed Eutectoid Carbon Steel ... *C. Nusbaum and W. L. Cheney*	65
409.	A New Method for the Measurement of Photographic Filter Factors ... *Raymond Davis*	79
410.	Thermal Expansion of Copper and Some of its Important Industrial Alloys ... *Peter Hidnert*	91
411.	Wave-Length Measurements in Arc Spectra Photographed in the Yellow, Red, and Infra-Red ... *F. M. Walters, jr.*	161
412.	Spectrophotoelectrical Sensitivity of Proustite ... *W. W. Coblentz*	179
413.	A Portable Vacuum Thermopile ... *W. W. Coblentz*	187
414.	Interference Measurements in the Spectra of Argon, Krypton, and Xenon ... *W. F. Meggers*	193
415.	Use of the Ulbricht Sphere in Measuring Reflection and Transmission Factors ... *Enoch Karrer*	203
416.	Preparation of Galactose ... *E. P. Clark*	227
417.	The Spectral Distribution of Energy Required to Evoke the Gray Sensation ... *Irwin G. Priest*	231
418.	Spectroradiometric Investigation of the Transmission of Various Substances, II ... *W. W. Coblentz*	267
419.	The Production of Liquid Air on a Laboratory Scale ... *J. W. Cook*	277
420.	Specific Volume of Liquid Ammonia ... *C. S. Cragoe and D. R. Harper, 3d*	287
421.	Wave Lengths Longer than 5500 A in the Arc Spectra of Yttrium, Lanthanum, and Cerium and the Preparation of Pure Rare Earth Elements ... *C. C. Kiess, B. S. Hopkins, and H. C. Kremers*	317
422.	Studies in Color Sensitive Photographic Plates and Methods of Sensitizing by Bathing ... *Francis M. Walters, jr., and Raymond Davis*	353
423.	Operation of the Modulator Tube in Radio Telephone Sets ... *E. S. Purington*	377
424.	Mathematical Theory of Induced Voltage in the High-Tension Magneto ... *Francis B. Silsbee*	407
425.	Characteristic Soft X Rays from Arcs in Gases and Vapors ... *F. L. Mohler and Paul D. Foote*	471
426.	Thermal Expansion of Nickel, Monel Metal, Stellite, Stainless Steel, and Aluminum ... *Wilmer H. Souder and Peter Hidnert*	497
427.	Some Effects of the Distributed Capacity Between Inductance Coils and the Ground ... *Gregory Breit*	521
428.	The Radio Direction Finder and its Application to Navigation ... *Frederick A. Kolster and Francis W. Dunmore*	529

Digitized by Google

Page.

429. NOTE ON THE PREPARATION OF MANNOSE.....*E. P. Clark* 567
430. HIGH-FREQUENCY RESISTANCE OF INDUCTANCE COILS.....*Gregory Breit* 569
431. THE FIELD RADIATED FROM TWO HORIZONTAL COILS.....*Gregory Breit* 589
432. AN IMPROVED METHOD FOR PREPARING RAFFINOSE.....*E. P. Clark* 607
433. THERMAL EXPANSION OF A FEW STEELS..*Wilmer Souder and Peter Hidnert* 611
434. ELECTROMOTIVE FORCE OF CELLS AT LOW TEMPERATURES.....
.....*G. W. Vinal and F. W. Altrup* 627
435. METALLOGRAPHIC ETCHING REAGENTS: II, FOR COPPER ALLOYS, NICKEL, AND THE ALPHA ALLOYS OF NICKEL.....
.....*Henry S. Rawdon and Marjorie G. Lorentz* 635
436. INTERFERENCE METHODS FOR STANDARDIZING AND TESTING PRECISION GAGE BLOCKS.....*C. G. Peters and H. S. Boyd* 677
437. THE SOLUBILITY OF DEXTROSE IN WATER.....
.....*Richard F. Jackson and Clara Gillis Silsbee* 715
438. TESTS OF STELLAR RADIOMETERS AND MEASUREMENTS OF THE ENERGY DISTRIBUTION IN THE SPECTRA OF 16 STARS.....*W. W. Coblentz* 725

Digitized by Google

FEB 1921

DEPARTMENT OF COMMERCE

SCIENTIFIC PAPERS

OF THE

BUREAU OF STANDARDS

S. W. STRATTON, DIRECTOR

No. 405

A SIMPLE PORTABLE INSTRUMENT FOR THE ABSOLUTE MEASUREMENT OF REFLECTION AND TRANSMISSION FACTORS

BY

A. H. TAYLOR, Associate Physicist
Bureau of Standards

NOVEMBER 30, 1920

PRICE, 5 CENTS

Sold only by the Superintendent of Documents, Government Printing Office
Washington, D. C.

WASHINGTON
GOVERNMENT PRINTING OFFICE
1920

Digitized by Google

UNIV. OF
CALIFORNIA

Digitized by Google

T1
U34
V.11

A SIMPLE PORTABLE INSTRUMENT FOR THE ABSOLUTE MEASUREMENT OF REFLECTION AND TRANSMISSION FACTORS

By A. H. Taylor

Early this year the author presented at the convention of the Optical Society of America a paper giving a brief review of the methods which had previously been used in measuring reflection factors, and describing a new type of absolute reflectometer. The complete description of that instrument, with the derivation of the theory, is now available in a scientific paper of this Bureau.[1]

The instrument described at that time was very thoroughly tested and was found to give correct results. However, certain precautions are necessary in its use and the mathematical equations are somewhat complex. These factors might tend to limit its use in the hands of inexperienced observers, though not necessarily so, as a calibration curve can be calculated and drawn for use in routine measurements.

One of the extremely interesting and important developments in that work was the high reflection factor obtained for magnesium carbonate. Measurements by four absolute methods gave an average factor of 99 per cent for a particular block of magnesium carbonate, whereas the previously accepted value was 88 per cent.

It has lately occurred to the author that a very simple reflectometer, based on one of the absolute methods employed in verifying the factor found for magnesium carbonate, could be constructed. It is the purpose of this paper to describe the new instrument, which is entirely different in principle from the one previously described.

THEORY OF REFLECTOMETER

If light is projected onto the inner wall of a small hollow sphere, painted with a diffusely reflecting white paint, it can be shown that the illumination of the surface by *reflected light only* will be equal in intensity at all points.

[1] B. S. Scientific Paper No. 391. Also Journal of the Opt. Soc. of America, 4, January, 1920.

499613

Digitized by Google

Let a small hollow sphere be arranged as shown in Fig. 1. A small segment of the surface is cut away, leaving a hole over which the surface to be tested is placed. At another point on the sphere about 90° from this one there is a small hole through which the opposite wall of the sphere is viewed by means of a portable photometer. The spot viewed is screened from the test surface by means of a small opaque screen.

Let F = total light flux (lumens) entering the sphere.

m = reflection factor of sphere surface.

m' = reflection factor of test surface.

E' = illumination of observation point when the direct light is projected onto the test surface.

E = illumination of observation point when direct light is projected onto the sphere surface at a point unscreened from the observation point.

When the light is projected onto the test surface, it must be reflected from it and from the sphere wall once each before any of it can reach the observation point, since this spot is screened from the test surface. Hence the flux which is effective in illuminating the spot observed is $m'mF$. In other words, the flux F, incident on the test surface, produces the same illumination of the observation spot as a point source of light placed at the center of the sphere and radiating $m'mF$ lumens. When the incident beam is projected onto the sphere surface at a point unscreened from the spot observed, it is readily seen, by the same method of reasoning, that its effect on the observation spot is the same as that of a point source radiating mF lumens. Hence in each case the illumination of the spot is directly proportional to these flux values, and the ratio of the illumination in the two cases is the reflection factor of the test surface. Therefore

$$\frac{E'}{E} = \frac{m'mF}{mF} = m'$$

It is to be noted here that no assumption has been made in regard to the way in which the light flux is reflected from the test surface. Hence the reflection factor of the test surface will be correctly evaluated no matter how the flux reflected from the test surface is distributed over the sphere wall. Also, the reflection factor measured is the factor for light of the color delivered by the lamp and is unaffected by selective reflection by the sphere walls.

Digitized by Google

Digitized by Google

FIG. 2.—*Method of using instrument to measure the reflection factor of a wall*

Digitized by Google

DETAILS OF CONSTRUCTION

The details of the instrument constructed are shown in Fig. 1. The hollow sphere used was a spun copper ball, 5 inches in diameter, such as is used with steam float valves. The lighting tube, which is set at an angle to the sphere surface, can be rotated about an axis normal to the surface of the sphere. This allows the direct light to be thrown on the test surface or the sphere wall as may be desired, the angle of incidence being

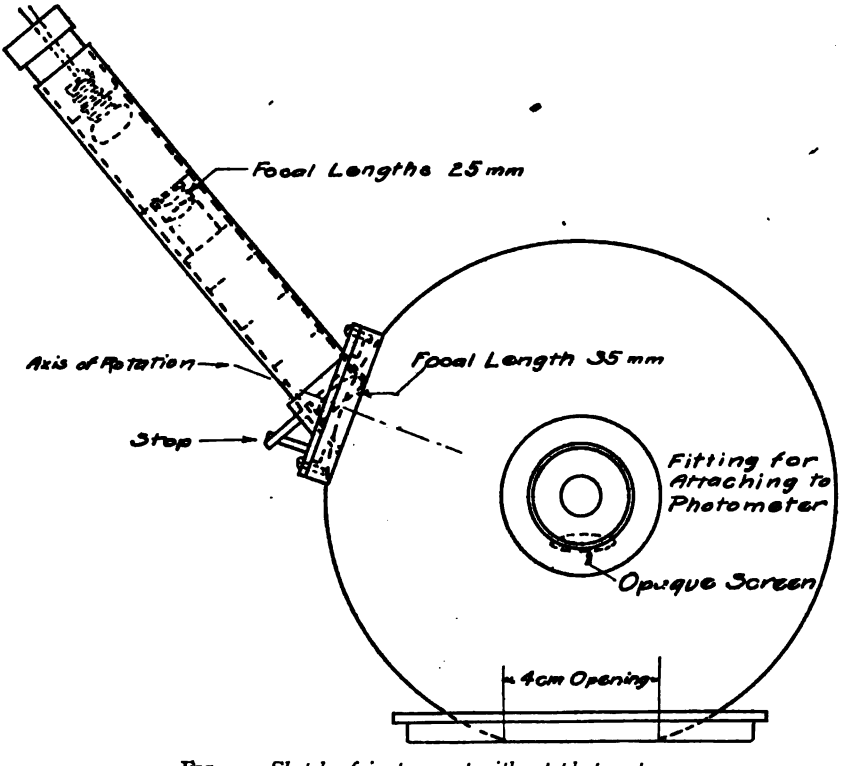

FIG. 1.—*Sketch of instrument without photometer*

about 40° from the normal. By means of a good lens system a narrow beam of light, without scattered light, is obtained. This results in a fairly uniform sharply defined spot of light about 2.0 cm in diameter, so that the opening over which the test surface is placed need not be very large. A 2.8-volt opal-back flashlight lamp is used in the tube.

The particular instrument used in these tests was designed and built to be used with a Macbeth illuminometer. A lens of 61 mm focal length inserted in the elbow tube of the illuminometer

Digitized by Google

restricts the spot observed to a diameter of about 4 mm, and hence a very small screen can be used to screen this spot from the test surface.

EXPERIMENTAL WORK

In order to verify the results obtained with the reflectometer previously described, a graded series of test objects was made up. Neutral gray objects were obtained by mixing black drawing ink and lampblack with a white cement (Keene's Fine). They were surfaced with coarse sandpaper, resulting in fairly good diffusers. These surfaces were tested for reflection factors by observation of surface brightness at intervals of 10°, using the apparatus shown in Fig. 3. The amount of flux reflected was calculated from these

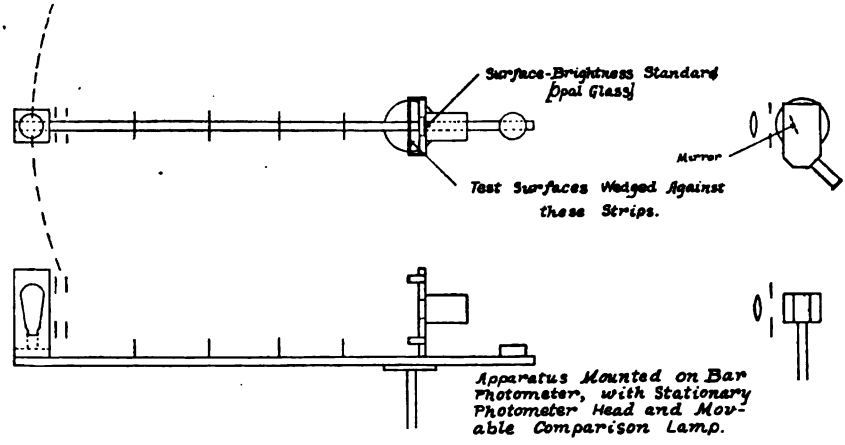

FIG. 3.—*Apparatus used in determining reflection factors by measurements of surface brightness at 10° intervals*

observations, and since the incident flux was known, the ratio of the reflected to the incident flux gave the reflection factors. These test objects were restandardized and used in verifying the results given by the new reflectometer. To these were added a block of magnesium carbonate previously tested, a polished sheet of milk glass, and a white cardboard painted with the same paint as that used in an 88-inch integrating sphere. The reflection factor of this paint had been previously determined by measuring the total illumination of the sphere wall when a lamp of known candlepower was burned in the sphere.

The tests of the cement surfaces with the first type of reflectometer (described in Scientific Paper No. 391), when used in the way recommended, showed that its results were in almost perfect agreement with those obtained by the point-by-point method.

Digitized by Google

The results of the measurements with the new type reflectometer described above are shown in Table 1.

TABLE 1.—Reflection Factors by Two Methods of Measurement

Test object	Reflection factor		Test object	Reflection factor	
	Point-by-point method	New type reflectometer		Point-by-point method	New type reflectometer
	Per cent	Per cent		Per cent	Per cent
Cement Standard No. 1	18.5	19.2	Cement Standard No. 6	82.3	81.3
Cement Standard No. 2	38.4	39.3	Cement Standard No. 7	86.6	86.4
Cement Standard No. 3	43.2	43.2	Polished milk glass	76.2	76.4
Cement Standard No. 4	60.4	60.5	Sphere paint	[a] 94.0	93.9
Cement Standard No. 5	67.8	68.1	Magnesium carbonate	[b] 99.0	98.5

[a] Value obtained by measurement of total illumination in 88-inch sphere when a lamp of known candlepower was burned in the sphere.

[b] Average of all previous measurements by four absolute methods, including the point-by-point method.

Such differences as exist in the above table may very easily be experimental errors. For all practical purposes the two methods may be considered to be in perfect agreement.

In using the instrument, no accurate voltage adjustment of the lamps in the photometer and the reflectometer is necessary, as both operate from the same battery. If only approximate factors are desired, the voltages can be adjusted so that the photometer reads 10 when the light is directed onto the sphere wall, and then the reading when the light is directed onto the test surface is one-tenth of the percentage reflection factor. This eliminates the necessity for any computations.

USE OF INSTRUMENT FOR MEASUREMENT OF TRANSMISSION FACTORS

By the addition of an exterior light source, giving a concentrated beam of the proper intensity, the same instrument may be used to measure transmission factors of clear or diffusing media. In the laboratory such a light source is easily obtained by proper screening of a lamp with reflector. For precision work the method of procedure would be as follows:

1. Turn the reflectometer lighting tube to project its beam onto the sphere wall at a point unscreened from the photometer observation point, then read the photometer.

2. Place over the opening in the sphere the substance to be tested for transmission, and again read the photometer. Then extinguish the lamp in the lighting tube.

3. Project the beam from the exterior lighting source through the large opening in the sphere and make a photometer reading.

Digitized by Google

4. Leaving the exterior lighting source unchanged, place over the opening the substance to be tested, and again read the photometer.

Let the photometer reading (in brightness or illumination units) in the four cases be respectively a, b, c, and d. Then the transmission-factor of the substance is $\frac{ad}{bc}$.

In using the instrument in this way the exterior light source should produce a beam which is somewhat smaller in diameter than the hole where it enters the sphere in order that when the substance to be tested is in place the light diffused by the substance at the edges of the beam will not escape around the edges of the hole.

This method of measuring transmission factors is similar in principle to that employed by Luckiesh and Mellor,[2] but the apparatus and test procedure are different. Transmission factors for diffused illumination might be determined by illuminating the test substance by means of a diffusing hemisphere, as in the method used by Luckiesh and Mellor.

CONCLUSION

Only one adaptation of the principle of this instrument has been shown, but there is no reason why it could not be adapted for use with almost any good type of portable photometer.

There is a considerable advantage in using an absolute instrument of this type rather than an instrument giving relative values, since no standard surface is required, and it is not necessary for lamps or sphere surface to remain constant from day to day.

The use of a low-voltage flashlight lamp in the lighting tube makes the instrument easily portable and convenient. A further improvement as regards portability would be to eliminate the battery-meter set and substitute therefor a large three-cell flashlight battery and miniature resistances.

The use of the instrument for measuring both reflection and transmission factors doubles its usefulness. No other instrument having this dual value has been proposed.

This instrument gives further proof of the very high reflection factor of magnesium carbonate, and establishes the value of 99 per cent for a particular block beyond much doubt.

WASHINGTON, October 22, 1920.

[2] Measurement of Transmission Factors, by M. Luckiesh and L. L. Mellor, Jour. Franklin Inst., 186, p. 529, October, 1918; also Jour. Optical Soc. of America, 2 and 3, January–March, 1919.

Digitized by Google

LIBRARY OF THE UNIVERSITY OF CALIFORNIA

DEPARTMENT OF COMMERCE

SCIENTIFIC PAPERS

OF THE

BUREAU OF STANDARDS

S. W. STRATTON, DIRECTOR

No. 406

PRESENT STATUS OF THE CONSTANTS AND VERIFICATION OF THE LAWS OF THERMAL RADIATION OF A UNIFORMLY HEATED INCLOSURE

BY

W. W. COBLENTZ, Physicist

Bureau of Standards

DECEMBER 20, 1920

PRICE, 10 CENTS

Sold only by the Superintendent of Documents, Government Printing Office, Washington, D. C.

WASHINGTON
GOVERNMENT PRINTING OFFICE
1921

Digitized by Google

Digitized by Google

DEPARTMENT OF COMMERCE

SCIENTIFIC PAPERS

OF THE

BUREAU OF STANDARDS

S. W. STRATTON, DIRECTOR

No. 406

PRESENT STATUS OF THE CONSTANTS AND VERIFICATION OF THE LAWS OF THERMAL RADIATION OF A UNIFORMLY HEATED INCLOSURE

BY

W. W. COBLENTZ, Physicist

Bureau of Standards

DECEMBER 20, 1920

PRICE, 10 CENTS

Sold only by the Superintendent of Documents, Government Printing Office, Washington, D. C.

WASHINGTON
GOVERNMENT PRINTING OFFICE
1921

Digitized by Google

Digitized by Google

PRESENT STATUS OF THE CONSTANTS AND VERIFICATION OF THE LAWS OF THERMAL RADIATION OF A UNIFORMLY HEATED INCLOSURE

By W. W. Coblentz

CONTENTS

	Page
I. Introduction	8
1. The Reichsanstalt investigations	9
2. The Bureau of Standards investigations	9
3. Object of the present paper	11
II. Discussion of black-body radiation, radiators, and shutters	11
1. Radiators	12
2. Water-cooled shutters and diaphragms	13
3. Statement of the laws of radiation	14
III. Discussion of various determinations of the coefficient of total radiation	15
1. Bolometric methods of electric compensation	15
(*a*) Observations of Kurlbaum	15
(*b*) Observations of Valentiner	16
(*c*) Observations of Gerlach	18
(*d*) Observations of Coblentz	20
(*e*) Observations of Kahanowicz	24
(*f*) Observations of Foote	25
(*g*) Observations of Puccianti	25
2. Thermometric methods with "black" receivers	27
(*a*) Observations of Féry	27
(*b*) Observations of Féry and Drecq	27
(*c*) Observations of Bauer and Moulin	28
(*d*) Observations of Puccianti	29
(*e*) Observations of Keene	30
3. Indirect and substitution methods	31
(*a*) Observations of Shakespear	31
(*b*) Observations of Todd	31
(*c*) Observations of Westphal	32
(*d*) Deductions of Lewis and Adams	33
IV. Discussion of various determinations of the constant of spectral radiation	34
(*a*) Observations of Paschen	35
(*b*) Observations of Lummer and Pringsheim	37
(*c*) Observations of Warburg and Collaborators	38
(*d*) Observations of Coblentz	39
V. Verification of the laws of thermal radiation of a uniformly heated inclosure	43
1. The formula and the coefficient of total radiation	44
2. The formula and the constant of spectral radiation	44
3. Confirmatory evidence	44
VI. Bibliography	46

Digitized by Google

I. INTRODUCTION

This seems to be an appropriate time for a retrospect of past accomplishments and for a starting point once more in the determination of the constants of thermal radiation, which investigations everywhere have suffered much from interruption during the past six years.

The various determinations of the numerical values of the constants of radiation have been hampered by the lack of exact knowledge of numerous contributory constants which enter into their evaluation.

Among these factors are the temperature scale, the absorptive coefficients and refractive indices of the prisms used, the correction for atmospheric absorption, and the correction for reflection from the radiometer receivers.

When the writer began studying this subject, about 14 years ago, it appeared desirable to determine more exactly the numerical values of the contributory constants, first of all, and then take up the determination of the constants of thermal radiation. At this day it is quite evident that such a procedure would have been the most efficient in obtaining the desired results. While such a program could not be fully carried out, some progress was made by determining the diffuse reflection of various substances,[1]—for example, plantinum black—the absorption constants of quartz,[2] and the correction for atmospheric absorption.[3,4] Somewhat similar experiments have been made by Warburg [5] on the absorptivity of quartz and by Gerlach [6] on atmospheric absorption.

Instead of a unified program of research, we find that, while one set of experimenters was engaged in establishing the temperature scale, another experimenter was determining the optical constants of the prism material; and a third group, using both the temperature scale and the optical constants, was attempting to determine the radiation constants. In turn, the first set of experimenters had to apply the results of those working on the radiation constants in order to verify and extrapolate the temperature scale beyond that attainable with the gas thermometer. In the meantime, the second experimenter improved his measurements of the optical constants (refractive indices) of the prism material (fluorite and quartz), while a fourth entered the field and added refinements by determining the temperature coefficients of these refractive indices. This in turn necessitated the recalculation of the prism calibration

[1] References are given in bibliography on pages 46–48.

Digitized by Google

and the numerical values of the spectral radiation constants. Added to these difficulties is the constant change in personnel, as is apparent from perusal of the title-pages of the published papers. The foregoing is an impersonal statement of the difficulties under which experimenters have been laboring. Fortunately, the spectral radiation observations are in terms of the scale of the spectrometer circle, and if the necessity arises, as described on a subsequent page, one can revise the corresponding wave lengths and recalculate the constants.

As a result of these various difficulties there is scarcely a determination of the constant σ of total radiation, and of the constant C of spectral radiation, which does not require corrections, some of which are obvious and could have been made by the experimenter.

It seems appropriate to point out specifically some of the difficulties experienced by the two national laboratories.

1. THE REICHSANSTALT INVESTIGATIONS

The determinations of the radiation constants, made at the German Reichsanstalt during the past two decades, involved measurements extending to about 1600° C, or even higher, and hence they have suffered from both the lack of knowledge of the temperature scale and of the refractive indices of the prisms used. In the later work the determination of the temperature scale was rightfully combined with the measurements of the radiation constants, instead of having the former measurements made in a separate laboratory.

The published papers do not state whether an attempt was made to harmonize the various determinations of the refractive indices of fluorite. The most recent work was done with quartz prisms, and the determination of the refractive indices of quartz was undertaken,[7] but as yet no data have been published.

2. THE BUREAU OF STANDARDS INVESTIGATIONS

The determinations of the radiation constants, especially the more recent ones, made at the Bureau of Standards, have suffered but little from a lack of knowledge of the temperature scale, owing to the fact that the radiators were not operated at a temperature much above 1200° C, and usually near the melting point of copper—1083° C. The chief difficulty has been the lack of exact knowledge of the refractive indices of fluorite; or, as it appears from the present inquiry into the matter, the lack of

Digitized by Google

exact knowledge of the refractive index of the yellow sodium line, and especially the yellow helium line which was used as a reference point in calculating the infra-red calibration of the prism.

The size of the apparatus used in determining indices of refraction is an important element in the accuracy attained. Langley [8] used a spectrometer having an image-forming mirror of over 4.5 meters focal length, in an inclosure which could be kept at a constant temperature. Paschen's [9,10,11,12] apparatus had an image-forming mirror of only 1/10 to 1/12 that of Langley's, and hence could not compete with it in accuracy. Hence, from the beginning, more weight should have been given to Langley's measurements. On applying Micheli's [13] temperature coefficients of refraction, Paschen's various determinations are found in good agreement with those published by Langley [8] whose reference point is the solar absorption line (the "A line") $\lambda = 0.7604\mu$; refractive index $n = 1.431020$ for fluorite at 20° C. From this point into the infra-red, the various determinations of the infra-red refractive indices of fluorite are in excellent agreement.

However, the fiducial line in this Bureau's spectroradiometry is the yellow helium line. From the present study of the data it appears that prior to 1913 the refractive indices of fluorite, for the visible spectrum, and in particular that of the yellow helium line $\lambda = 0.58758\mu$, were not known with sufficient accuracy to meet the present-day demands for refinements in the radiation constants. As a result, erroneous wave lengths were assigned to the infra-red (minimum deviation) settings of the spectrometer circle. This error is only 3″ (true value, 6″) in the Wadsworth system of spectrometer settings, and hence scarcely observable experimentally. However, it enters as a constant error of 0.3 to 0.4 per cent in the calculations of the calibration curve. Errors of such small magnitude were considered insignificant eight years ago, when there was a disagreement of 1 to 2 per cent, or even more, in the various determinations of the constant of spectral radiation.

As will be shown on a subsequent page, using Paschen's [12] recent measurements of the refractive index of fluorite for the yellow helium line (which measurements were made with a new and very accurately graduated spectrometer), all the apparent errors seem to be eliminated from this Bureau's determination of the constant of spectral radiation, which is now in good agreement

Digitized by Google

with the value that is to be expected from the Bureau's determination of the constant of total radiation [15] and from theoretical considerations.[4]

3. OBJECT OF THE PRESENT PAPER

In previous papers [15, 4] corrections were applied to the determinations of the radiation constants made by various experimenters. The object of the present paper is to make an up-to-date examination into the various instruments and methods employed in these various determinations and to give an estimate of the accuracy of the results therewith obtained.

At first glance, the various determinations of these constants appear to cover a wide range of numerical values. This is especially true of the values of the coefficient of total radiation, in which all sorts of ill-considered methods have been used. Moreover, no corrections were made for atmospheric absorption of the thermal radiation in its passage from the radiator to the receiver. As will be shown presently, most of these older determinations are in remarkably close agreement with the newer ones after making obvious corrections for atmospheric absorption and for reflection of the incident radiation from the receiver.

This paper does not include a discussion of the attempts which have been made to determine the constant, C, by means of an optical pyrometer, which at least in its ordinary form can not be considered an instrument of high precision. There are many difficulties to be overcome before one can conclude that the data so obtained are trustworthy. One of the uncertainties is the effective wave length of the red glass used in the eyepiece of the pyrometer. Other difficulties are encountered when using a spectral pyrometer. Also the temperature scale is in doubt. Hence recent experimenters have not attempted to determine C, but have reversed the process and, working on the assumption that C is a certain value, say, $C = 14350$, have determined the melting point of palladium. This seems to be the preferable procedure.

II. DISCUSSION OF BLACK-BODY RADIATION, RADIATORS, AND SHUTTERS

In order to arrive at an intelligent understanding of what has been accomplished in the determination of the constants of radiation, and in order to indicate the way to future progress in this subject, it is important to consider very briefly some of the

Digitized by Google

conceptions, as well as some of the most recent instruments and methods used in the production and measurement of the radiation from a uniformly heated inclosure, or so-called black body.

Every substance has a characteristic emission spectrum. On the other hand, the emission spectrum of a uniformly heated cavity is independent of the composition of the material forming the walls of the inclosure. It is a function only of the temperature.

The emission of thermal radiation from and the absorption of thermal radiant energy of all wave lengths entering into the cavity is complete. In a material substance this can occur only on the short-wave length side of the region of anomalous dispersion where the absorptivity is high, but where the reflecting power is practically nil; for example, in quartz[29] selenite and aluminum oxide, in the region of 7μ to 10μ ($\mu = 0.001$ mm).

Modern conceptions of black-body radiation are the result of slow development from such simple experiments as those of Draper[19] who found that the interior of a rifle barrel became luminous at a certain temperature; of Christiansen[21] who observed that the scratches and conical-shaped holes in an incandescent metal surface were brighter than the smooth surface and of St. John[22] who found that the selective emission, commonly observed in the rare oxides, disappeared when these substances were heated in a uniformly heated porcelain tube.

1. RADIATORS

The modern uniformly heated cavity or so-called black body is the result of such observations and facts as just enumerated. It is the invention of Wien and Lummer[23] and, for attaining fairly high temperatures, such as are used in many of the investigations mentioned in a subsequent part of this paper, consists of a diaphragmed porcelain tube wound with platinum ribbon, which is electrically heated.

In the modification used by the writer[30] the radiator consisted of two concentric tubes suitably wound with platinum ribbon in order to obtain a uniform temperature throughout a great length of the interior of the radiator, as shown by Waidner and Burgess.[31] The use of platinum ribbon instead of thick platinum wire eliminates local nonuniformity of temperature in the porcelain tube.

In radiators of this type the porcelain tubes sag on heating to 1200° C. To overcome this difficulty, in the determination of the radiation constants, to be described presently, the writer[30] placed a wedge-shaped fragment of porcelain, with a sharp edge,

Digitized by Google

about 2 mm long, about 25 to 30 mm to the rear of the radiating diaphragm. This support causes no local cooling, and it preserves the life of the radiator. Further improvements were made in the completeness of the emission of the radiation by painting the inside walls and the front side of the radiating diaphragm with a mixture of chromium oxide and cobalt oxide. Since these oxides become electrically conducting at 1200°, the front thermocouple was completely inclosed in a porcelain insulating tube. The short piece of porcelain which lies across the radiating wall of the black body was covered with cobalt oxide. Since the cobalt oxide did not adhere well to the porcelain tube, the latter was first covered with a thin layer of iron oxide, obtained by wetting the porcelain tube with writing ink which was burned into the tube. The cobalt oxide paint was then applied and also burned upon the tube by means of a blast lamp. After replacing the thermocouple, inclosed in this short tube, in the radiator, the whole interior was again painted with a mixture of cobalt and chromium oxides.

The cobalt oxide has a high temperature coefficient of absorption so that it appears black on slight heating. Its emission spectrum [29] is continuous, so that there is less difficulty in producing a perfect radiator than when the radiating inclosure is of white porcelain. However, porcelains which have a low melting point are less selective in their emission than the "Marquardt porcelain," from which are made the black bodies ordinarily used.

2. WATER-COOLED SHUTTERS AND DIAPHRAGMS

In discussing the relative merits of the various determinations of the radiation constants, and in particular the coefficient of total radiation, the writer will have occasion to refer frequently to the use, or misuse, of shields for preventing the receiver from being heated by the radiator, and of shutters for exposing the receiver to radiation. It is, therefore, important to consider briefly the functions of this apparatus.

The determination of the coefficient of total radiation usually consists in noting the heat interchange when the receiver is exposed to two radiators which are at widely different temperatures, say 0 and 100° C; that is, ice and boiling water. The radiator at the lower temperature may be, and usually is, used as a shutter. If the temperature of the shutter is lower than that of the receiver, the latter radiates to the shutter. Hence, it is important to have the receiver face a large (say, water-cooled) diaphragm, maintained at a constant temperature, back of which is placed the

Digitized by Google

shutter and the radiator. In this manner the surrounding conditions, facing the receiver, are not changed when the shutter is moved in order to expose the receiver to radiation.

There is no doubt that some of the unusual results obtained in the determination of the radiation constants are attributable to the operation of the shutter under such conditions that the receiver did not face uniform conditions when the shutter was opened in making the measurements.

Experience shows that the arrangement of the shutter should be similar to that used [3] (loc. cit., p. 516, Fig. 5) in the determination of the coefficient of total radiation. In this arrangement the water-cooled shield employed consisted of a tank 35 cm in diameter and 1.5 cm in thickness, which faced the radiator, and a second tank, 20 cm in diameter and 3 cm in thickness, which faced the radiometer. The water-cooled shutter, consisting of a thin metal box 3.5 by 3.5 by 0.8 cm, was operated in vertical ways between these two shields. A mercurial thermometer was used to measure the temperature of the water flowing through this shutter. The side of the shutter facing the radiometer was smoked in a sperm candle, and, in connection with the conical-shaped opening (painted black and smoked) in the water-cooled diaphragm which faced the radiator, it formed a miniature black body the temperature of which remained constant throughout a series of measurements.

3. STATEMENT OF THE LAWS OF RADIATION

The law of total radiation, generally called the Stefan-Boltzmann law,[17] states that the total emission of thermal radiation, R, of all wave lengths passing from a uniformly heated inclosure, at temperature T_1 to another body at a temperature T_0 is proportional to the difference of their absolute temperatures, to the fourth power, or

$$R = \sigma(T_1^4 - T_0^4)$$

In this formula σ is the coefficient or constant of total radiation under discussion. The numerical value of this coefficient is of the order $\sigma = 5.7 \times 10^{-5}$ erg per cm^2 per sec. per deg.^{4} In this paper only the first three significant figures will be mentioned; for instance, $\sigma = 5.32$.

The law of spectral radiation, which specifies the distribution of thermal emission intensities in the spectrum of the radiation

Digitized by Google

emitted by a uniformly heated inclosure, or so-called black body, is best represented by Planck's [18] formula

$$E_\lambda = C_1 \lambda^{-5} (e^{c/\lambda T} - 1)^{-1}.$$

In this formula the constant C determines to a great extent the shape of the isothermal spectral-energy curve. Suffice it to say that these laws are based on well-grounded theoretical foundations, and after almost two decades of discussion they remain unchanged.

III. DISCUSSION OF VARIOUS DETERMINATIONS OF THE COEFFICIENT OF TOTAL RADIATION

It has been shown by Stefan,[16] Schneebeli,[25] Wilson,[26] Lummer and Pringsheim,[24] Valentiner,[27] and others [3,15] that the total radiation emitted from a uniformly heated cavity is proportional to the fourth power of the absolute temperature. The measurements extend over a temperature range of perhaps 1500° C. They verify the fourth power law within the accuracy of the temperature scale and the general errors of observation, which are small owing to the fact that the measurements are relative.

The evaluation of the coefficient of thermal radiation in absolute measure is an extremely difficult task which has been attempted by numerous experimenters, whose data will now be considered.

The early determinations of the coefficient of emission of a substance (for example, blackened plates or balls of glass or copper) by Lehnebach,[34] Christiansen,[35] and others are of great historical interest, but they can not be considered in connection with present-day determinations of the coefficient or constant, σ, of total radiation of a uniformly heated inclosure.

1. BOLOMETRIC METHODS OF ELECTRIC COMPENSATION

(*a*) *Observations of Kurlbaum.*[36]—The first determination of the constant of total radiation in absolute value, by a method which is free from the gross experimental errors that are inherent in the work, was made by Kurlbaum.

The principle of the method is as follows: Three branches of a Wheatstone bridge (bolometer) consist of thick manganin wires which are not affected by a change in current through the bridge. The fourth branch consists of thin bolometer platinum, the resistance of which is affected by a change in current in the bridge. Starting with the bridge balanced, the bolometer branch of thin

Digitized by Google

platinum, at a distance of 18 to 20 cm, is exposed to the radiation from a black body at 100° C, and the change in resistance (or galvanometer deflection) is noted. With the bolometer branch shielded from radiation, the bridge current is varied until the change in resistance in the bolometer branch is equal to that attained when exposed to radiation. In other words, the bridge current is increased by a sufficient amount to produce the same galvanometer deflection as was caused by radiation falling on the bolometer strip. From a knowledge of the change in the bridge current, the bolometer resistance, etc., Kurlbaum was able to compute the energy input. He used two very different surface bolometers and found very concordant values. He found a value of $\sigma = 5.32$. In a subsequent communication [37] he made a correction of 2.5 per cent for loss by reflection from the platinum black surfaces of the bolometer. This gives a value of $\sigma = 5.45$. The writer [1] has determined the reflecting power of platinum black and has found that, using the blackest obtainable deposits, the reflecting power is almost 2 per cent for wave lengths at 8 to 9μ. An examination of six surface bolometers (12 branches or 24 surfaces of about 3 by 4 cm area), purchased abroad, showed that all of them had microscopically small bright patches of bare platinum, and that none of them were as black as the samples upon which the reflectivity measurements were made.[1] These bright areas would increase the loss by reflection. From this it appears that Kurlbaum's correction to his work is none too large.

(*b*) *Observations of Valentiner.*[37]—This method of measuring the coefficient of total radiation by means of a large surface bolometer was continued by Valentiner, who found quite different values, depending upon the blackness (kind) of radiators employed, which were heated as high as 1450° C. For the two blackest radiators (the steam-heated radiatior "W. S. K." and the electrically heated unblackened porcelain tube radiator "G. S. K.") he found a value of $\sigma = 5.36$.

In a subsequent paper,[38] he made a correction of about 4 per cent for various causes (for example, 1 per cent for lack of blackness of the radiator, 2.5 per cent for reflection from the bolometer, etc.) giving a value of $\sigma = 5.58$. No correction was made for atmospheric absorption.

The numerical values of the various determinations made by Valentiner, upon any one radiator, have a range of about 3 per cent, which was usually higher than allowable in order to ascertain the effect of atmospheric absorption in a space of 30 to 50 cm. How-

Digitized by Google

ever, when using a larger porcelain tube radiator,[27] "G. S. K.," the distances were rather longer than usual, being, respectively, 89 to 125 cm, and the effect of absorption seems unmistakable. The value of the radiation constant is about 2 per cent smaller for the greater distance, i. e., an increase of 35 cm in optical path introduced an absorption of about 2 per cent. It is difficult to say how great a correction should be applied to Valentiner's values in order to eliminate atmospheric absorption. The observations were made in the winter, when the humidity was, no doubt, much lower than for the test made by the writer,[15] in which an absorption of over 5 per cent was found in an air path of 124 cm, the temperatures of the radiator being of the same order as used by Valentiner. A conservative estimate of the correction to Valentiner's data, for absorption by atmospheric water vapor and carbon dioxide is 2 to 3 per cent. This increases Valentiner's value to $\sigma = 5.68$ with a possibility of the value being as high as $\sigma = 5.75$, which is in remarkably close agreement with the various determinations made by other methods. That a correction of not less than 1 per cent is to be applied to these data is indicated in Gerlach's [44] recent work on atmospheric absorption of black body radiation.

The surface bolometers used by Kurlbaum and by Valentiner consisted of two grids of thin platinum foil, placed one back of the other, with the surfaces overlapping. In this manner a continuous surface is formed, but part of the rear bolometer strips are shielded from the radiation incident on the front strips. The operation of the receiver is, therefore, unsymmetrical. Gerlach [40] has discussed the effect of this overlapping and has shown that in some cases it might lower the value of the observed radiation constant by a very considerable amount. The writer [39] has found that, using one bolometer strip back of the other, 50 per cent of the energy, incident upon the first receiver, is reradiated to the rear one. In the reverse process of heating the strip electrically, this effect would enter symmetrically and a low value of σ would result.

It was found by Kurlbaum and by Valentiner that the rate of temperature rise was different for heating the bolometer by absorption of radiation and by electrical heating. The low values of the radiation constant obtained by Valentiner are explained,[40] in part, as the result of reading the galvanometer deflection before temperature equilibrium was fully attained. Callendar [41] has described surface bolometers which would overcome some of the defects of conduction, etc. However, using radiators at 600 to

Digitized by Google

1000° C, there is no need of using such large receivers with the unavoidable defects just noted.

(*c*) *Observations of Gerlach.*[42, 48, 106]—The following method is not exactly bolometric in principle, but it may be considered here, since its virtues have been under discussion in connection with the results obtained by the bolometric methods just mentioned. Gerlach determined the constant of total radiation, σ, by a modification of Ångström's electric compensation pyrheliometer. In the original pyrheliometer of Ångström,[43] there are two thin, narrow sheets of manganin to each of which is attached one junction of a thermoelement which is joined through a galvanometer. One of these manganin strips is exposed to solar radiation. Through the other manganin strip is passed an electric current of such strength that it is heated to the same temperature as is the strip which is exposed to solar radiation. The equality of temperature is indicated when there is no current flowing through the galvanometer.

In the instrument as used by Gerlach there is but one strip of manganin which is 0.01 mm in thickness, and 2 to 4 mm wide (length 2.7 to 3 cm). At the back of this manganin strip and close to it was a thermopile of 45 elements (joined through a galvanometer) which is heated by radiation from the manganin strip, thus differing from Ångström's device in which a single thermojunction was heated by conduction from the manganin strip. The idea of using many junctions was to integrate over the whole strip, thus eliminating any irregular heating caused by inequalities in the thickness of the manganin strip, which was blackened electrolytically with platinum black. This manganin strip was heated electrically to the same temperature as that attained by the strip when exposed to the radiation from a black body. From a knowledge of the resistance of the strip and the electric current it was possible to determine the energy input, and hence the value of the radiation constant.

Gerlach experienced some difficulty in determining when he had exact compensation when heating the receiver electrically and radiometrically. Covering the sides of the receiver with knife-edged slits had no effect upon the radiation constant; but shielding the ends of the manganin strip from radiation caused the value of σ to increase from $\sigma = 5.83$ for the unshielded ends to a constant value of $\sigma = 6.14$ when the shields covered 1.5 mm, or more, of the ends of the strips. This is owing, perhaps, to heat conduction from the

Digitized by Google

ends and to the fact that in heating the strip electrically no correction was made for the excess electrical energy used in the ends of the receiver, which were not exposed to radiation. In practice he exposed the whole length of the receiver to radiation, claiming that the heat conducted from the ends is the same when the metal strip is heated radiometrically and electrically.[44]

The weak point in the device appears to be the uncertainty of (1) the effective length of the receiver, which is exposed to radiation, and (2) the length which is contained between the potential terminals and which is used in the evaluation of the energy in absolute measure. In the instrument used by the writer, [8, 15] this uncertainty was eliminated by placing the potential terminals upon the receiver, and at some distance from the heavy electrodes; thus providing uniform heating over a greater length of the receiver than is actually used in evaluating the constant. This seems to be the logical way to use such a receiver.

The mean value obtained by Gerlach is $\sigma = 5.803$. He made no correction for losses by reflection (2 per cent). This was done by Paschen,[45] who gives the value $\sigma = 5.9$.

Gerlach's value is based upon the determinations made with four receivers, the individual values of which depend somewhat upon the receiver, as was observed by the writer.[8] No attempt was made to remove the atmospheric water vapor from the space between the radiator and the receiver. There is a systematic decrease of 1 to 2 per cent in the radiation constant for an increase of 32 to 42 cm in the distance of the receiver from the radiator.

The work of Gerlach aroused considerable discussion among experimenters previously engaged on this same problem. This brought forth a very considerable amount of laborious experimental work by Gerlach [46] in defense of his method, in which he showed that his apparatus gave the same values as when operated by the bolometric method employed by Kurlbaum.[36]

In subsequent investigations, Gerlach determined the effect of atmospheric absorption[6] and of blackening the receiver[47] upon the radiation constant. He operated the radiator at higher temperatures (to 450° C), but the radiometric apparatus remained the same as in the earlier work. With this outfit his[48] new value of the coefficient of radiation, uncorrected for reflection of radiation from the receiver and for atmospheric absorption, is decidedly lower than that previously observed under similar conditions, being of the order $\sigma = 5.6$ to 5.7, as observed by the writer. Applying a correction of about 1.7 per cent for reflection[1] and, depending

Digitized by Google

upon the temperature of the radiator, a correction of 0.2 to 1.2 per cent for absorption of CO_2, the mean value of 52 independent sets of measurements is $\sigma = 5.85$. In a recent discussion of the constant of total radiation, Gerlach[106] places his value at $\sigma = 5.80$ when corrected for reflection.

Gerlach has done an enormous amount of experimental work and his determination is one of several which should be a convincing demonstration that the extreme values of $\sigma = 5.3$ to 6.5 are subject to correction, in so far as the corrections can be determined.

(*d*) *Observations of Coblentz.*[3,15,4]—This research was undertaken after making a study of the instruments and methods used in the earlier determinations, and an effort was made to embody the good features and eliminate the defective ones. It is, therefore, proper to discuss the work in considerable detail.

In designing the apparatus, an attempt was made to embody black-body conditions in the radiator (including the shutter and the receiver, as described under Section II). The lack of blackness of the radiator has been discussed by Wien and Lummer,[22] who gave a method for computing the correction for the opening in the radiator, on the assumption that the inclosure is spherical and diffusely reflecting. The amount of energy that can escape by diffuse reflection through the opening is determined practically by the size of the opening as compared with the total area of the interior of the radiator. In the porcelain tube radiator used in the present work the interior is uniformly heated over a length of 8 to 10 cm. However, for the purpose of the present computation, a length of only 2.5 cm which is defined by the first diaphragm, is considered. The area of the inclosure is 37.6 cm^2 and that of the opening is 3.1 $cm.^2$ On the basis that the reflecting power of the interior of the painted radiator is 7 per cent (loc. cit.,[3] p. 523, Table 3), the loss of energy by diffuse reflection through the inner diaphragm is 0.63 per cent. Using an unpainted Marquardt porcelain radiator, the coefficient of radiation is decreased by about 1 per cent (loc. cit.,[15] p. 571), showing that the question of lack of blackness of the radiator is important.

For a receiver[50] it was decided to use a modified Ångström pyrheliometer,[43] embodying novel features which had not yet been tried by others. In order to reduce the heat capacity of the manganin receiver and provide better insulation, the thermopile of bismuth and silver, having a continuous receiving surface, was placed a short distance back of the receiver. The apparatus used by Gerlach embodied this same idea.

Digitized by Google

The crucial and novel part of the apparatus was a receiver with potential terminals attached thereto, at a sufficient distance from the ends to avoid the uncertainty of the effective length of the receiver which is exposed to radiation and the length utilized in making the potential measurements. These potential wires, which were from 0.003 to 0.025 mm in diameter, defined the effective length of the central part of the receiver (which was utilized in the radiation measurements) more accurately than seems to be possible by measuring the distance between two heavy electrodes to which the receiver is soldered and to which the potential terminals are attached. By exposing the whole length of the receiver to radiation, conduction losses from the ends of the receiver do not enter the problem.

By means of an extra terminal the effect of the presence of the potential terminals was determined[3] and found negligible, viz, 0.3 per cent. The method of finding the difference of potential between two potential terminals seems more certain than to find the difference of potential between two heavy electrodes as used by Gerlach.[43] For, when the soldering is well done, a narrow band of solder protrudes from under the heavy electrode and fills up the sharp edge where the receiver joins the electrode. Hence the effective length of the receiver is less than that measured from the sharp edge of the electrode, and an erroneous value is assigned to the area of the receiver.

The operation of this type of radiometer would have involved the use of a hemispherical mirror placed in front of the receiver.[3,1,49] This may introduce errors when the strip is heated by electrical means. Hence, after conferring with specialists in geometrical optics who were in agreement with the writer's opinion that a reflecting inclosure is likely to introduce errors, the receiver was used without the hemispherical mirror, which was employed in a separate experiment to determine the diffuse reflection[1] from lampblack and platinum black, and finally, in determining the loss by reflection from some of the receivers actually used in making these observations. Hence, the loss of radiation incident upon the receivers was probably accounted for as accurately as it would have been by employing a "blackening" device in front of the mirror.

In order to test the question of the accuracy of the corrections used for eliminating the loss by reflection, a series of observations was made on receiver No. 10. In this test the slits in front of the receiver and all other conditions remained unchanged (not so in

Digitized by Google

No. 6). The only variation was in smoking the platinum-black receiver with a sperm candle after making the first set of observations. The reflecting power of platinum black was taken to be 1.7 per cent [4] and that of lampblack 1.2 per cent. The respective determinations are $\sigma = 5.822$ and $\sigma = 5.814$. They differ only by about 0.1 per cent, which is very satisfactory and shows that the reflection factors were (relatively, at least) well determined.

Subsequent tests showed that in this outfit the effect of atmospheric absorption was less than 0.1 per cent.[4] This conclusion is substantiated by recent measurements made by Gerlach.[6]

The thermopile was connected with a magnetically (unusually well) shielded ironclad Thomson galvanometer of special design,[49, 51] which served merely to indicate the relative rise in temperature of the receiver when exposed to radiation and when heated electrically.

The method of observation consisted in exposing the receiver to radiation and noting the galvanometer deflection; then in heating the strip by passing an electric current through it to give, within 1 per cent, the same deflection. The measurements of the power put into the strip were made with the same potentiometer used in measuring the temperature of the radiator. No difficulty was experienced in determining temperature equilibrium on heating the receiver by radiation and by electrical means.

The exact amount of energy necessary to cause the same deflection as that produced by absorbing radiant energy is obtained by multiplying the observed energy input by the ratio of the galvanometer deflections. This gives the "constant" of each receiver. In order to reduce all the measurements to a common basis, and at the same time obtain a value of the coefficient, or the so-called Stefan-Boltzmann constant, of total radiation, the custom of previous experimenters was followed in reducing the data.

The radiator was operated at a temperature of 800 to 1000° C, within which range the temperature scale is quite well determined.

The data obtained with receivers Nos. 8 and 9 are not included in the final value, because, at the time the measurements were made, they were known to be defective (as was quite fully explained in the original paper), and hence the reliability of the results would be open to question. For example, receivers Nos. 8 and 9, which were of platinum, were heated to redness to clean and brighten their surfaces before covering them with platinum black. As a result, the solder at the ends alloyed with the platinum, in one case leaving a large hole between the potential ter-

Digitized by Google

minal and the electrode. These receivers should never have been used for precision measurements.

To the data (304 pairs of measurements) obtained with 10 receivers a correction of 1.2 per cent for losses by reflection was applied to measurements made with receivers covered with lampblack (soot), and a correction of 1.7 per cent to measurements made with receivers covered with platinum black. The reflection from a receiver covered with platinum black, then smoked, is 1.2 per cent. As just mentioned these corrections were determined by direct measurements upon some of the receivers used in this investigation and by comparison of the surfaces of the other receivers with samples of lampblack whose reflection losses had been determined in a previous investigation.[1] The value of the coefficient of total radiation, after applying the corrections just mentioned, is

$$\sigma = (5.722 \pm 0.012) \times 10^{-12} \text{ watt cm}^{-2} \text{ deg.}^{-4}$$

If we took the average of the measurements made with all of the receivers, including the two defective ones, the value of the radiation constant would be increased by only about 0.3 per cent, or $\sigma = 5.74$. This is owing to the fact that these two defective receivers represent only 44 out of a total of 348 pairs of measurements.

No correction was made for absorption by atmospheric carbon dioxide, because in actual test,[4] the effect of the presence of CO_2, to the extent of 0.1 per cent, could not be detected. However, assuming that the effect is as large as indicated by Gerlach's[6] measurements, this correction might perhaps amount to 0.1 per cent to 0.2 per cent, thus increasing the value to $\sigma = 5.73$.

The method of operation is unsymmetrical in that when the receiver is exposed to radiation the heating is produced in the lampblack surface, while in passing an electrical current through the strip the heat is generated within the receiver. However, from the data obtained with receivers differing ten times in thickness, and covered with different kinds and thicknesses of absorbing material, it appears that the manner of heating the receiver has but little effect upon the final results.

For any one receiver, operated under different conditions, the precision attained is usually much better than 1 per cent. For the different receivers the maximum range in the value of σ is of the order of 1.5 to 2 per cent. This seems to be independent of

Digitized by Google

the length and width of the receiver and of the kind of slits used. The accuracy attained with this method of evaluating energy in absolute measure, as estimated by the departure of individual determinations from the mean value, appears to be of the order of 1 per cent.

Recently, Gerlach[106] has discussed these data, and, since his paper contains some inaccurate interpretations of this work, it is relevant to add a few comments in reply. A careful and unbiased examination of the original papers [8, 15] will show (1) that receiver No. 1, as well as Nos. 8 and 9, gave values which were greater than $\sigma = 5.8$; (2) that Nos. 8 and 9 were excluded from the beginning,[15] because they were defective—not subsequently,[107] because they gave values greater than $\sigma = 5.8$, as Gerlach's remarks (loc. cit., [106] p. 81) would leave one to infer; and (3) that the "Good series" mentioned by Gerlach refers to experimental conditions for series CX (just as in series CVI we read "Galv. unsteady") and has nothing to do with defects in the receiver itself which cause a constant error in the work. An examination of Gerlach's [42] original paper (see Table 8, loc. cit.[42]) shows that he also omitted from his final values data obtained with the defective receivers, which happened also to give abnormally high values. In fact, his first value is based upon only about one-half (4) of the total number of receivers constructed, while the writer's value is based upon 10 out of 13 receivers.

(*e*) *Observations of Kahanowicz.*[54]—The apparatus used by Kahanowicz, is essentially a modification of the Ångström pyrheliometer.[43] The receiver was placed at the center of a spherical mirror with an opening in one side to admit radiation. In this manner the correction for reflection was eliminated. The shutter was close to the receiver. If its temperature was different from that of the water-cooled diaphragm which was before the radiator, errors in the radiation measurements would occur. As mentioned eleswhere in this paper, the shutter should be placed between the water-cooled diaphragm and the radiator to avoid a change in surroundings facing the receiver when the shutter is raised for making the radiation measurements.

The temperature range was from 260 to 530° C. The distance from the radiator to the receiver was 35 to 55 cm. A series of 28 measurements gave an average value of $\sigma = 5.61$. Of this number 11 gave a value of $\sigma = 5.7$. Out of a series of four measurements made in December, 1916, with the distance $d = 56$ cm, three gave a value of $\sigma = 5.7$.

Digitized by Google

No corrections were made for atmospheric absorption, which for the temperatures used is not negligible. In a previous paper (loc. cit.,[3] p. 576) it was shown that on removing the moisture (vapor pressure of 10 to 12 mm) from a column of air 52 cm in length, the radiation constant was increased from $\sigma = 5.41$ to 5.55, or about 2.6 per cent. Other measurements mentioned in the paper just cited indicate an absorption of 2 to 3 per cent of the radiations emitted by a black body at 1000° C for the average humidity of Washington. The vapor pressures at Naples are considerably higher than at Washington. From these,[4] as well as Gerlach's, [44, 106] data it would appear that the corrections for atmospheric absorption must be at least 1 per cent. For the low temperatures at which the radiator was operated, a conservative estmate of the correction to the radiation data obtained by Kahanowicz is 1.5 to 2 per cent, or a value of $\sigma = 5.69$ to 5.73. In other words the Naples value of the coefficient of total radiation is comparable with other recent determinations which indicate a value of $\sigma = 5.7$.

(*f*) *Observations of Foote.*[108]—It is of interest to record Foote's deductions of the probable value of the coefficient of total radiation as obtained in the course of an investigation of the Marvin pyrheliometer.

The receiver of this pyrheliometer consists of a silver disk about 45 mm in diameter and 3 mm in thickness, inside of which is a spirally wound insulated nickel wire in the form of a 3-lead resistance thermometer This coil serves both as a thermometer and as a heater for calibrating the device by means of electrical energy.

Foote calibrated the instrument by the usual electric method and then radiometrically by exposure to the radiation of a black body. On the assumption that the coefficient of total radiation is $\sigma = 5.7$, he found the two methods of calibration in agreement within the limit of the errors of observation.

(*g*) *Observations of Puccianti.*[53]—The method of operation is just the opposite of that usually employed, and, in view of the small radiant energy exchanges involved, in comparison with the transfer of energy by heat conduction and by convection, this may perhaps be the weak point in his method.

Puccianti constructed a bolometer in the form of a black body, which is kept at room temperature. This black body really is the radiator. The other black body (which is really the receiver,

Digitized by Google

consisting of a blackened glass bulb) instead of being at a higher temperature, as usually is the case, is at the temperature of carbon dioxide snow or of liquid air. He measured the electric power which had to be supplied to the first black body to keep the temperature constant in order to compensate for the energy lost by radiation to the second black body. He very ingeniously constructed two black-body bolometer branches exactly alike, the one to be exposed to the cold receiver and the other to be protected from it. Each of these bolometer branches consisted of a vessel of 0.1 mm sheet copper having the form of a cone and a frustum of a cone united at the bases. The internal surface was smoked. The external surface was polished, and upon it were wound two thin insulated wires. One of these wires, of iron, formed the bolometric branch, and the other wire, of manganin, was used as a heating resistance. The other two branches of the bolometer bridge were formed of resistance coils and the whole was connected with a galvanometer and storage battery as in any ordinary bolometer. The two sensitive black-body branches of the bolometer were in an evacuated vessel, which was kept in a tank of water.

Puccianti measured the (electrical) energy necessary for compensation to prevent the bridge from being unbalanced when one branch was exposed to the receiver. He obtained a value of $\sigma = 5.96$.

The method is an ingenious variation from the usual procedure. The apparatus should have been constructed so that both bolometer branches could have been used as radiators. From the illustrations it appears that radiation from one branch could fall upon the other, which would introduce errors. Another uncertainty is the temperature and the manner of operation of the shutter. Tests might have been made to determine whether the bolometer remained balanced when a heating current was applied to both branches, without allowing one branch to radiate to the receiver. Furthermore, to repeat the herein oft-mentioned device, a heating coil should have been inserted temporarily within the radiator to determine the energy input as compared with the energy input required in the outer heating coils in order to maintain a balance. The device, as used, is unsymmetrical in that the heating coil is not in the proper place to operate the most efficiently. From this it appears that the constant is less than that indicated by these measurements.

Digitized by Google

2. THERMOMETRIC METHODS WITH "BLACK" RECEIVERS

(*a*) *Observations of Féry.*[55]—In order to eliminate the question of reflection from the surface, Féry,[55] made a series of determinations of the radiation constant, σ, by means of a thermojunction which is formed into a long conical-shaped metal receiver, which is blackened on the inside. On the outside of the cone, and insulated from it, was wound a heating coil of known resistance for calibrating the receiver. This was done by noting the temperature rise (galvanometer deflections) with the electrical energy input. The receiver was then exposed to an electric furnace, which was heated to various temperatures from 500 to 1200° C. and the corresponding galvanometer deflections were observed. He obtained a value of $\sigma = 6.30$.

(*b*) *Observations by Féry and Drecq.*[46]—The work was undertaken anew by Féry and Drecq,[46] the receiver being a cone of brass having an opening of 30° placed within a large sphere of brass, which was surmounted by a glass tube with a capillary 1 mm in diameter. The large brass sphere was filled with alcohol, the whole forming a thermometer in which 1 mm rise in height of the column in the capillary indicated a rise in temperature of 0°.005. Surrounding the outside of the brass case was a coil of wire through which an electric current was passed and the energy input noted to cause the same temperature as that produced by exposing the opening of the cone to the radiator. They found a mean value of $\sigma = 6.51$. This is the highest value yet reported. The relative values obtained with the instrument show a fair constancy over the whole temperature range which extended to the melting point of gold. However, the same is true of Valentiner's values obtained by the bolomteric method. This indicates that there is some constant factor, which is not eliminated and which causes the numerical value of σ to be high or low. Various suggestions have been made as to the cause of their excessively large values. It appears that part of the difficulty lies in the unsymmetrical way in which the instrument is operated. It is calibrated by a heating coil which is in contact with the alcohol (or air, in the first case) and can warm the latter by conduction and by absorption of radiant energy. On the other hand, the incoming radiation must be transformed by absorption in the cone, and the effect produced reaches the alcohol principally by conduction. As a result of this type of calibration, the apparent value of the radiation constant is

Digitized by Google

higher than the true value. The weak point is in not having the heating coil within the receiver, which should be constructed so that but little, if any, of the entering radiation, or the energy radiated from the heating coil, can escape through the opening in the receiver. This might easily have been done by forming the receiver into a double-coned receiver, such as was used by Puccianti. However, even with all these precautions, this type of receiver does not appear satisfactory.

A further determination of this constant was made by Féry and Drecq,[57] in which the radiations from an electric furnace fell upon a strip of platinum (area 36 by 55 and 0.03 mm in thickness), blackened electrolytically with platinum black. The radiation measurements were made by sighting upon the front and the rear surfaces of the platinum strip by means of a Féry pyrometer, the angle of incidence being 48°. Their new value of the radiation constant is $\sigma = 6.2$. The measurements upon the posterior surface lead to the value $\sigma = 5.57$, which is said to correspond with the measurements on the anterior surface made with plane receivers. If we correct the latter value by 2 per cent for reflection we obtain the value $\sigma = 5.68$, which is of the same magnitude as observed by the writer. This new determination of σ by Féry and Drecq appears to have been made defective by their reduction of the original observations; for example, they claim that the coefficient of absorption of the receiver was only 0.82 to 0.84, which seems impossible from numerous and diverse experiments on the diffuse reflecting power of platinum black made by others. Attention was called to this fact by Bauer,[58] who places their value of σ between 5.1 and 5.8, and, by making a correction of 2 per cent for reflection, deduced a value of $\sigma = 5.68$. In all three methods the data are meager as to elimination of the various errors which may occur. For example, an error may arise in determining the power put into the platinum strip. Another important source of error lies in the manner of operation of the water-cooled shutter, which should be placed between the water-cooled diaphragm and the radiator.

(*c*) *Observations of Bauer and Moulin.*[59]—In order to obviate the difficulties encountered by Féry and Drecq [57] in calibrating their conical-shaped receivers, Bauer and Moulin calibrated their receiver (which was a Féry pyrometer) by sighting it upon a strip of platinum which was heated to different temperatures by

Digitized by Google

an electric current. In order to determine the amount of radiant energy falling upon the receiver it was necessary to eliminate the losses from the strip by conduction and convection. For this purpose the platinum strip was heated in air and in a vacuum, the power consumed being determined for a definite length of platinum, defined by potential terminals as used in the present paper. Having calibrated the pyrometer by noting the galvanometer deflections for the various amounts of energy put into the platinum strip, they sighted the pyrometer upon a black body heated to various temperatures and noted the galvanometer deflections. Their first announced value was $\sigma = 6.0$. However, as in numerous other cases herein cited, they introduced errors in the final reduction of their data. They had observed the radiation emitted from the platinum strip at an angle of 13° from the normal and applied a correction [60] of about 12 per cent, which reduced their value to $\sigma = 5.3$. This correction is recognized to be much too large,[58] so that their value of the radiation constant lies between $\sigma = 5.3$ and 6.0, which indicates the close grouping of all the determinations about the value $\sigma = 5.7$. They made no correction for atmospheric absorption which would increase their value from $\sigma = 5.3$ to $\sigma = 5.6$ or 5.7. In a previous communication on the solar constant Bauer and Moulin (loc. cit.,[60] p. 1658), using an Ångström pyrheliometer, found the value $\sigma = 5.7$.

(*d*) *Observations of Puccianti.*[61]—In a continuation of his investigations Puccianti gives a determination in absolute measure of the radiation of a black body in which the temperature change is measured by means of a toluene thermometer, the bulb of which is formed into a hollow cone that is allowed to radiate to a black-body receiver, which is at the temperature of liquid air. The measurement is made by compensating the heat lost by the thermometer by the application of an electric current.

The apparatus not being differential in construction, the temperature of the water bath had to be kept rigorously constant in order to have the meniscus of the thermometer move slowly and regularly. The response of the apparatus was, of course, slow and sluggish, which is a common property of this type of receiver (radiator), so that it required from four to eight minutes to obtain a measurement.

The same criticisms apply to this instrument that have been mentioned in the cruder form of thermometer used by Féry and Drecq.[56] The energy for compensation is supplied by a heating

Digitized by Google

coil which is in contact with the liquid (a good scheme in so far as it applies to heating the liquid) and on the side of the wall of the receiver opposite to that upon which the incoming radiations impinge. The arrangement is therefore unsymmetrical. The heat of compensation should have been supplied by a coil inserted within the receiver, provision being made that little or none could escape by reflection and by direct radiation through the opening. In this manner the condition of heat interchanges would have been the most closely fulfilled. In the instrument as used the opportunity for escape of energy seems greater, so that in compensation there is a tendency to produce a value which is higher than the true value for radiation unaccompanied by conduction. By placing the heating coil within the receiver and using a high temperature radiator, Puccianti's device should be applied in the manner recently used by Keene.[62]

Puccianti considered the precision of this method as high as that of the bolometric apparatus, but the sensitivity of the thermometric apparatus was very much inferior to the bolometer. Nevertheless, he seems to prefer the thermometric method in spite of its small sensitivity. He obtained a value of $6.00 < \sigma < 6.3$, and his intermediate value is $\sigma = 6.15$.

(*e*) *Observations of Keene.*[62]—In the determination of the constant σ by Keene, the radiator consisted of an electric furnace which could be heated to 1000° C. The receiver consisted of a hollow, spherical, double-walled thermometer bulb provided with a small aperture in its side to admit the radiation to be measured. The space between the walls is filled with aniline, which served as thermometric substance, its expansion being observed in a capillary tube in the ususal way, 1 mm division = 0.0005° C.

In order to eliminate the effect of the variation of room temperature, two such thermometers were used differentially, radiation being admitted into one of them, the differential effect giving a measure of the energy supply. The interior of the bulb receiving the radiation was provided with an electric heating coil for the purpose of calibration. The paper contains the derivation of an exact expression for the energy interchange between two radiating coaxial circular openings. For he found that the approximate formula, which is ordinarily used when the distance between the opening is large, was not accurate enough for his work. His value of the radiation constant is $\sigma = 5.89$.

Digitized by Google

3. INDIRECT AND SUBSTITUTION METHODS

(*a*) *Observations of Shakespear.*[63]—The value of the constant σ is obtained by a method which is based upon the principle that a heated body in air, in surroundings at a lower temperature, loses heat (*a*) by conduction, (*b*) by convection, and (*c*) by radiation. If the rate of heat loss by a body be observed in two cases, the only difference being that the emissivity of the radiating surfaces varies, other conditions remaining the same, it is quite correct to assume that the losses (*a*) and (*b*) will be the same and that the difference between the observed rate of loss of energy in the two cases is due only to the difference in the losses by radiation. If, now, these two different surfaces, at the temperature of boiling water, be exposed in turn to a radiomicrometer at the room temperature, we obtain the ratio of the rates of the energy radiated by the two surfaces.

In the experiments a plate of metal with a silvered surface was heated electrically to 100° C, and close to it was another plate, blackened with soot, which was cooled with water. Between the plates was air at atmospheric pressure. Shakespear measured the energy input in order to maintain the plate at 100° when (1) the surface of the plate was highly polished and (2) when it was blackened. He measured also the ratio of the emissivities of the plate under these two conditions, using a radiomicrometer for the purpose. From this he obtained a value, σ' in absolute units. He then compared the emissivity of the lampblack surface at 100° with that of a black body at the same temperature by means of a radiomicrometer. From this latter comparison combined with the value of σ' he found a value of $\sigma = 5.67$.

From this description it may be noticed that the essential parts of the method differ from that of Westphal [65] in that the radiator was a flat metal plate which was used in air instead of a vacuum, and that the black body, with which the emissivity of the plate had to be measured, was separate from it; while in Westphal's instrument the black body was self-contained within the metal (in the form of a cylinder), of which the emissivity of the surface had to be measured.

(*b*) *Observations of Todd.*[64]—In his experiments on the thermal conductivity of gases Todd used a thin layer of air inclosed between two horizontal, parallel, good-conducting plates, which were maintained at different temperatures The colder plate, of course, receives heat by radiation and by conduction through the air from

Digitized by Google

the hotter plate, which is above it. Communication from the surrounding air is shut off by an insulating ring, and the two plates being close together in comparison with their linear dimensions the convection currents are eliminated. He determined the energy lost by radiation by varying the distance x between the two plates and noting the corresponding variation in the quantity Q of heat passing from the upper to the lower plate. These values of x and Q, when plotted, form a rectangular hyperbola and the horizontal asymptote gives the value R of the radiation. The energy input was determined by a calorimetric method. In order to determine the constant σ, he had simply to find the ratio of emissivities of the blackened plate to that of a black body at the same temperature, for which purpose a radiomicrometer was employed. The value of this ratio and the constants obtained in the main part of his experiment enabled him to compute the radiation constant which he found to be $\sigma = 5.48$.

This, like the preceding method, is likely to give a low value of the coefficient of total radiation owing to uncertainty of the exact temperature of the radiating surface of lampblack. A thin layer of soot is fairly efficient in its emission and absorption. But a thick layer of soot is quite nonconducting of heat, as was found by the writer [1] in the measurements of diffuse reflection.

(*c*) *Observations of Westphal.*[65, 66]—An important determination of the coefficient of total radiation was made by Westphal. The experiment consisted in comparing the emissivity of a cylindrical block of copper, when it was highly polished and when it was blackened; with the emissivity of a black body at the same temperature. The novelty involved in the method is in having the black body contained within the cylinder. The copper cylinder was heated electrically, and, to reduce the energy losses by gaseous heat conduction, this copper cylinder was suspended in a glass flask, from which the air could be exhausted to 1 mm pressure. The outer surface of the cylinder was either highly polished to give it a low emissivity or painted with lampblack to give it a high emissivity. The end surfaces remained unchanged. The heat losses by conduction and convection were therefore the same throughout the experiment, and the difference in energy input, when the surface of the cylinder had a high emissivity and when it had a low emissivity, was a measure of the energy lost by radiation.

Using the surface of the cylindrical body when highly polished, Westphal proceeded to find the curve of energy input of the body

Digitized by Google

as a function of the temperature between the temperatures 350 and 425° absolute. Then the surface of the body was brought to a high emissivity by applying in succession different blackening materials, and the energy input was measured at different temperatures.

The emissivities of the surface and of the interior of the copper cylinder were compared by means of a thermopile. The numerous details need not be discussed. Suffice it to say, that the work appears to have been thoroughly done, and from the nature of the method it seems free from gross systematic errors. His mean value is $\sigma = 5.54$.

He modified the apparatus, extending the observation over a wider range of temperature with a view to increasing the accuracy, and obtained the value $\sigma = 5.57$. Although nothing further seems to have been published subsequently, Westphal obtained further measurements, which yielded the value $\sigma = 5.67$.[66]

This is in excellent agreement with Shakespear's results,[63] showing that the coefficient of radiation as determined by reliable methods is the order $\sigma = 5.7$.

As already noted in discussing Todd's data, it is uncertain whether in all cases the surface of a layer of lampblack soot has the temperature of the metal plate upon which it is deposited. Gerlach [47] performed experiments which led him to question whether Westphal's results were not slightly low owing to the use of lampblack.

This and the preceding measurements of the coefficient of total radiation are excellent variations from the direct method. They are likely to give slightly low values, just as the thermometric methods, just described, give high values. Hence, these two methods serve the purpose of establishing upper and lower limits of the radiation constants.

(*d*) *Deductions of Lewis and Adams.*[67]—In concluding the survey of what the writer considers the most reliable experimental determinations of the coefficient of total radiation, it is of interest to include in this paper a theoretical computation by Lewis and Adams based upon data on the elementary electric charge, e, the gas constant, R, and the Faraday equivalent, F. Their calculations lead to a value of $\sigma = 5.7$.

The foregoing data are assembled in Table 1, which gives also the corrected values after making conservative corrections for atmospheric absorption, which important factor was in many cases neglected by experimenters.

Digitized by Google

It is interesting to find that these data, which were obtained by widely different methods and which appear so discordant on first perusal of the original papers, are in excellent agreement. The various values range about the number, $\sigma = 5.7$. In fact, two-thirds of the total number (12) of determinations are close to $\sigma = 5.7$. The mean value of all the data which are free from obvious errors is $\sigma = 5.72$ to 5.73. If we neglected Todd's low value, determined from gas conduction experiments, and Puccianti's high value, which is, no doubt, too high, the mean value remains unchanged. As we shall see presently, experimental data on ionization potential, X-rays, and photoelectric work show that the value of the coefficient of total radiation is of the order $\sigma = 5.7 \times 10^{-5}$ erg cm^{-2} sec.$^{-1}$ deg.$^{-4}$

TABLE 1.—Observed Value and the Most Probable Value of the Constant of Total Radiation after Correcting for Reflection, Atmospheric Absorption, etc.

Observer	Date	$\sigma \times 10^5$	Probable value of $\sigma \times 10^5$	Method
Kurlbaum	1898	5.45	?	Bolometer.
Féry	1909	6.3	?	Thermometer.
Bauer and Moulin	1909	5.30	5.7	Thermopile.
	1910	5.7	5.7	Pyrheliometer.
Todd	1909	5.48	5.48	Gas-conduction experiments.
Valentiner	1910	5.58	5.68to5.75	Bolometer.
Féry and Drecq	1911	6.51	?	Thermometer.
Do	1912	6.2	5.68	Calibrated pyrometer.
Do	1912	5.57	.....	
Shakespear	1912	5.67	5.67	Ratio of emissivities, metal; black body.
Gerlach	1916	5.85	.....	Modified Ångström pyrheliometer.
	1920	5.80	5.80	
Puccianti	1912	5.96	5.96	Bolometer.
	.....	6.15	?	Thermometer.
Westphal	1916	5.67	5.67	Ratio of emissivities, metal; black body.
Keene	1913	5.89	5.89	Thermometer.
Coblentz	1915	5.72	5.72	Modified Ångström pyrheliometer.
Kahanowicz	1917	5.61	5.69to5.73	Modified Ångström pyrheliometer.
Foote	1918	5.70	5.70	Marvin pyrheliometer.

Mean value $\sigma = 5.72$ to 5.73×10^{-5} erg cm^{-2} sec.$^{-1}$ deg.$^{-4}$

IV. DISCUSSION OF VARIOUS DETERMINATIONS OF THE CONSTANT OF SPECTRAL RADIATION

Planck's[18] equation $E_\lambda = c_1 \lambda^{-5} (e^{c_2/\lambda T} - 1)^{-1}$ is, no doubt, the closest representation yet formulated of the observed energy distribution in the spectrum of a black body. The constant C (often written in the more cumbersome form C_2) determines to a great extent the slope of the isothermal spectral energy curve. In the

Digitized by Google

spectral region, free from atmospheric absorption, to 6μ, the observed and the computed curves obtained by the writer,[76] are in agreement to within the errors of observation, viz, 0.5 to 1 per cent.

Rubens and Kurlbaum [77] have made isochromatic observations using the residual rays of fluorite in the spectral region of 24μ and 52μ. Their data are also in exact agreement with those computed by the Planck equation. From these data it appears that the Planck equation may be considered as representing, within the errors of observation, the energy distribution of a black body in the spectrum extending from 0.5μ to 50μ.

The Planck formula is based on theoretical considerations, and after almost two decades of discussion it remains unchanged. Recently, Nernst and Wulf [78] have arbitrarily modified the coefficient in the above equation, changing C_1 to $C_1(1+\alpha)$, where α is a variable. The whole procedure is based upon the assumption that the numerical value of the constant is $C = 14\,300$, as observed from isochromatic observations. Hence, in view of the fact that the (older) values of C, obtained from isothermals, are somewhat higher, they must be reduced by a factor $(1-\alpha)$, depending upon the temperature of the radiator. They point out explicitly that the whole procedure depends upon the truth or falsity of the value of $C = 14\,300$; or, rather, as will be seen presently, upon the truth or falsity of the older values of $C = 14\,400$ (about) obtained from isothermal measurements. Their deductions lead to a value of $\sigma = 6.04$, which from a consideration of the whole subject, on a subsequent page, appears to be much higher than the true value. Until we have more reliable experimental data, using isothermals, it does not appear necessary to consider a modification of the Planck equation.

In spite of all that has been published on the partition of energy in the spectrum of a black body, there are but few data at hand which are more than qualitative in value.

To the writer it seems that all these early data should be considered from the standpoint of historical interest, since it seems impossible to give them much weight in connection with the results obtainable at the present day.

(*a*) *Observations of Paschen.* [69, 70]—The pioneering work in spectral radiation measurements and constants was inaugerated by Paschen,[69] who observed an extensive series of spectral energy curves at temperatures ranging from 100 to 450° C, using six different kinds of bolometers covered with different kinds of ab-

Digitized by Google

sorbing material—for example, lampblack and platinum black or copper oxide—also having the bolometers in the focus of a hemispherical mirror. The radiators were heated by means of boiling water, aniline, sulphur, etc. The mean value of all his observations, which are in close agreement, was $A = \lambda_m T = 2891$ and $C = 14352$. He continued the work at temperatures ranging from 400 to 1050° C using a large porcelain radiator. He used also metal cups of copper or platinum blackened with oxides of copper or iron, and heated within this porcelain radiator, making in all about a dozen different arrangements of the radiators The bolometer was covered with platinum black and was situated in the focus of a hemispherical mirror to "blacken" it. The mean of the new series was $A = 2907$, with a probable error of ± 16.

In a further investigation Paschen [70] undertook the work anew, after redetermining the reflecting power of silver and the refractive indices of fluorite. He used a porcelain tube radiator, also three other radiators, which he blackened, as in the preceding research. He took the wise precaution to project an image of the radiating wall of the black body upon the spectrometer slit in order to avoid possible radiations from the side walls and diaphragms falling upon the prism and bolometer. Complete corrections for the selective reflection of the silver mirrors, and also for the loss by reflection from the prism, were made He then found that his observations fitted neither the Wien nor the Planck equation, the values on the long wave-length side of the energy curves falling between the two theoretical curves He found that if (for reasons he himself could not explain, loc. cit., p. 295) he multiplied his observations by factors varying from 1.02 at 2.91μ to 1.195 at 8.25μ, etc., the observed energy curve would fit the Planck equation and fulfilled better the condition of congruence. Upon this basis he obtained a value of $A = 2921$ for his newest data. He then applied factors to some of his previous data, thus making them agree better with the Planck equation, and the value of A was increased from 2891 to 2915, or about 0.87 per cent From this it appears that, if he had not multiplied his observations by these arbitrary factors, his latest results would have been about 0.87 per cent lower or $A = 2894$, which is practically the same as the value previously obtained.

The writer [30, 76] has obtained an estimate of the correction to Paschen's values, and the conclusion arrived at (loc. cit.,[76] p. 468) is that Paschen's recent determination is of the order $A = 2894$. This is close to the earlier determination, $A = 2891$, which is prob-

Digitized by Google

ably more reliable as regards the temperature scale. In other words, Paschen's original data fall within the range of the recent and more accurately determined values, being of the order $C = 14\,360$.

(*b*) *Observations of Lummer and Pringsheim.*[71,73,83]—Their spectral radiation measurements were made on porcelain tube radiators, described in the first part of this paper. The radiator was placed directly in front of the spectrometer slit. This reduces the length of air path, and hence the absorption; but there is uncertainty in keeping the alignment, especially since in the early designs no attempt was made to prevent the tube from sagging.

As is true of all the older measurements on radiators, operated, above 1200° C, the temperature scale is defective (too high)-giving values of C, which are too high.

The values of the constants published by Lummer and Pringsheim [71] require a treatment similar to that just given to Paschen's data. They used the earlier indices of refraction of fluorite, published by Paschen [10] in 1894, which are in error in wave length by 0.02μ for the region of 1 to 2.5μ. Fortunately, most of their values of λ_m are greater than 2.5μ, and no correction is required.

In their first investigation a series of four spectral energy curves, observed at temperatures of 837 to 1416° Abs, gave a value of $A = 2879°$.

For a second series of measurements, they inclosed the spectrometer in order to dry the air. A series of five spectral energy curves observed between the temperatures of 814 and 1426° Abs gave a value of $A = 2876$. These two values are in close agreement with Paschen's determinations made at that time. They found that their data did not fit the Wien equation, and this, no doubt, gave impetus to the formulation of the Planck equation. Suffice it to say that their data, obtained up to this time, if reduced on the basis of the Planck factor $\alpha = 4.9651$, leads to a value of $C = 14\,290$.

In a subsequent investigation [73] the radiator was heated to a much higher temperature, to 1646° Abs. A series of eight isothermal spectral energy curves gave a value of $A = 2940$ and $C = 14\,590$. In view of the fact that a correction of about 0.02μ must be made for the calibration at 1 to 2.5μ, this would reduce the value of C by 2 per cent or $C = 14\,310$. Although the apparatus was inclosed in order to remove the CO_2 and water vapor, the energy curves are appreciably affected by atmospheric absorption.

Digitized by Google

As in previous work, their temperature scale, above 1000° C, was obtained by extrapolation. Just how much the thermocouple calibration may be in error is not recorded. In a subsequent paper [83] they revised the temperature scale used in the previous test [24] of the Stefan-Boltzmann, fourth-power law. The revised temperatures are 10 to 12° lower, and, at the highest temperatures, they are 20 to 25° lower than previously used. Whether any temperature correction of this magnitude must be made to the spectral radiation data is not stated; though the researches on the gas thermometer by Holborn and Day [84] were then in progress. Suffice it to say that although their later value of $A = 2940$ is the one frequently quoted in books, none of the subsequent investigators have found a value of A, which is within 15 per cent as high as is this one.

From the foregoing consideration of the data obtained by Lummer and Pringsheim it appears conservative to place their value at $C = 14\ 300$.

(*c*) *Observations of Warburg and Collaborators.*[86 to 95]—During the past 20 years the determination of the constants of radiation and their application to the temperature scale has been relentlessly pursued by the Phys. Tech. Reichsanstalt,[83] at Berlin.

During the past 10 years these investigations have been pursued by Warburg and his collaborators. They used fluorite and quartz prisms and vacuum radiators. The sodium line was used as a zero setting of the spectrometer. The radiometer was a vacuum bolometer, which was operated by a null method. In this manner the galvanometer acted merely as an indicator. The temperature fixed points were the melting point of gold and some higher temperature, for example, melting point of palladium.

In their first communication,[86, 87] they reported a value of $C = 14\ 570$ on the basis that the melting point of palladium is 1549° C. On the other hand, if the higher temperature was determined radiometrically, by extrapolation from the gold point, using the Stefan-Boltzmann law, then the value of C was found to be smaller. Hence, they rightly questioned the gas-thermometer scale and proceeded to make their investigations by using the radiation laws to establish their scale of temperatures, thus avoiding the scale as transferred from the gas thermometer by means of thermocouples. They retained only one temperature fixed point, viz, gold at 1064° (later 1063°). The higher temperatures (1400°) were determined radiometrically. For this purpose they observed the position, λ_m, of the maximum emission E_m, of the isothermal spectral energy curve.

Digitized by Google

Using Paschen's refractive indices of fluorite and Carvallo's [90] indices of quartz, in their next communication,[88] they report values which varied from $C = 14\ 200$ to $14\ 600$.

Using improved methods for adjusting the sodium lines on the bolometer and making further provision so that radiation emanating from only the central diaphragm of the radiator was incident upon the bolometer, in the next report [89] the fluorite prism gave values ranging from $C = 14\ 300$ to $14\ 600$ and it was discarded. A quartz prism gave a value of $C = 14\ 360$.

In a very complete investigation [90, 91] they repeated the previous work. Using a quartz prism, the values obtained are $C = 13\ 270 \pm 40$ and $A = 2894 \pm 8$, for the temperature interval of 1337 and 2238° Abs.

The next step was to cut a prism out of a block of quartz, of which the absorptivity had been determined previously. With this and other improvements, including different radiators, a value of $C = 14\ 250$ was obtained [93, 94] from the temperature scale based on the Stefan-Boltzmann law of total radiation and a value of $C = 14\ 300$ or $14\ 400$ was obtained by using the Wien displacement law to establish the temperature. The uncertainty in the value of $C = 14\ 300$ or $14\ 400$ is owing to the uncertainty in their calibration curve (refractive indices) of the quartz prism.

The present status is the adoption [95] of the value of $C = 14\ 300$ and the melting point of palladium = 1557° C. Subsequent investigations [96, 97] appear to be made on this basis. There is an uncertainty of perhaps 1° in the temperature scale at the melting point of palladium,[98] and, in view of the great variations in the various determinations of C, it was perhaps a wise decision for Warburg to adopt the rounded number $C = 14\ 300$ micron degrees, for the spectral radiation constant; though, as we shall see presently, theory and other experimental data would place the value somewhat higher.

(*d*) *Observations of Coblentz.*[30, 76, 4]—In this investigation the spectrum was produced by means of a mirror spectrometer and a perfectly clear fluorite prism. In the first work an air bolometer, and later a vacuum bolometer was used for measuring the partition of energy in the spectrum. The radiator was a porcelain tube, wound with platinum ribbon, through which electric current was passed. It was operated at temperatures ranging from 450 to 1500° C. Various incidental questions, such as the adjustments of the optical parts of the apparatus, the temperature uniformity

Digitized by Google

and control of radiator, the water-cooled shutters, the temperature scale, the method of reduction of the observations to the normal spectrum, the proper formulas for computing the numerical constants, etc., were investigated.

The first paper [10] contains also data on various subsidiary problems, such as (1) the variation of the reflecting power of silver with angle of incidence and with wave length, (2) the variation of reflecting power of fluorite with angle of incidence and with wave length (refractive index), and (3) data for reducing the observations from prismatic to normal spectrum.

From the very beginning of this investigation on black-body radiation it was found that the Wien equation did not fit the spectral energy curves. The assumption was, therefore, tentatively made that the observed curves fit the Planck equation; and, at the completion of the investigation, this was found to be true for about 75 per cent of all the observed curves. This conclusion was based upon the uniformity of the values of λ_m, which resulted from computation (by the method of equal ordinates $E_{\lambda_1}=E_{\lambda_2}$) of the values of λ_1 and λ_2 which were taken far apart, and also close together on the observed isothermal spectral energy curve.

The observations were made in the winter, when the humidity was low, and the investigation extended over four winter seasons. An attempt was made to obtain a great many isothermal spectral energy curves, so as to avoid the personal bias which can enter the working over of a few curves. It now seems that this was probably a mistake; for no attempt could be made to correct the observations for small changes in temperature of the radiator and small variations in sensitivity of the vacuum bolometer.

In the meantime, owing to impairment of eyesight, the reduction of the data had to be intrusted to others who were not familiar with the work. The first calculation of the data gave a value of about $C=14\ 350$. But doubts arose concerning the calibration curve of the prism. A new calibration curve was worked out, using Paschen's[11] refractive indices (uncorrected for temperature) and the data recalculated and published as being $C=14\ 456$.

Data were obtained also with a fluorite prism which was full of cleavage planes. This produced much scattered radiation, which distorted the energy curves at 4μ to 5μ. These data were, therefore, not used in the final calculations. (This explains the queries by Nernst and Wulf.[78])

Digitized by Google

In the meantime Paschen [12] published further data on the dispersion of fluorite, which indicated that the calibration curve, and hence the value of $C = 14\,456$, was wrong.

In the earlier work the temperature scale was also in doubt. The last series (1912) was not observed at temperatures much above 1200° C and hence is quite free from doubts about the temperature scale.

The second paper[76] on this subject, therefore, dealt with a recalculation of these data, using a revised calibration curve. The mean value of the spectral radiation constant, based on 93 spectral energy curves (series of 1912) is $C = 14\,353$. If the corrections to the temperature scale (mentioned in the previous paper) are applied, the value is $C = 14\,362$. A further correction ($= +7$) is necessary, because in the second term of the equation used for calculating the data the value $C = 14\,300$ instead of $C = 14\,350$ was employed. Hence, the final corrected value, as published in the second paper, was $C = 14\,369$ and $A = 2894$ micron degrees.

In order to obtain a check on the methods of calculation of the constant a least square reduction of the first isothermal curve of the series of 1912 was undertaken by Roeser.[81] He obtained a value of $C = 14\,342$, which is in agreement with the value computed by the method of equal ordinates, viz, $C = 14\,339$.

Recently a further examination [4] was made of the accuracy of the factors used in converting the previously observed [80] prismatic spectral-energy data into the normal energy distribution. The graphical methods previously employed were checked, and similar factors were obtained by computation, using the first differential of the dispersion formula, which best represents the observed refractive indices of fluorite.[101] These refractive indices were obtained from consideration of all the available data, which in the region of 1 to 2μ are represented by the curve published by Langley and Abbot.[8] The best dispersion formula is that of Paschen.[101] However, owing to incompleteness of the formula, the graphical method was found to be just as accurate as was the method of computation.

The conclusion [4] arrived at was that the spectral radiation constant, $C = 14\,353$ micron degrees, determined some years ago,[76] remains unchanged. However, at that writing [4] there was some doubt as to whether some of the corrections then applied should have been made, giving a value of $C = 14\,369$; that is, the mean value might be $C = 14\,366$.

Digitized by Google

Rather curiously and unfortunately, in all these inquiries into the small errors that eight years ago were considered negligible the one concerning the zero setting has remained unconsidered until now. The calculation of the calibration curve was based on the sodium lines, $\lambda = 0.5893\mu$ for a reference point. Subsequently the writer adopted the then novel procedure of using the yellow helium line, $\lambda = 0.58758\mu$, instead of the sodium lines for adjusting the zero setting of the bolometer. For this purpose the refractive index $n = 1.43\ 390$ was adopted. Subsequently Paschen [12] published the value of $n = 1.433\ 907$ (17.°5 C) for the refractive index of the helium line, and $n = 1.433\ 866$ for the sodium lines. He observed a difference of 12″ in the minimum deviation settings of the sodium and the helium lines.

On the basis of the new value of the refractive index of fluorite for the yellow helium line, $n = 1.433\ 877$ (at 20° C), there is a difference of 6″ between the newly computed (zero) minimum deviation setting of the spectrometer circle and the setting used in this investigation on the basis of $n = 1.43\ 390$. As a result, the average values of λ_m, in terms of the spectrometer circle, must be reduced by 6″. Since the wave lengths, λ_m, occur between 2μ and 3μ (and the majority at about 2.2μ) the 6″ are equivalent to 0.003μ to 0.004μ in this part of the spectrum. This amounts to a reduction of the previously published value of the constant $C = 14\ 369$ by 0.3 to 0.4 per cent, giving a value of $C = 14\ 311$ to $14\ 326$.

As already stated, the second paper [76] was the result primarily of a revision of the calibration curve of the fluorite prism used; and it is unfortunate that at that time the above application of the temperature coefficient of the refractive index of the helium line was overlooked.

The various determinations of the constant of spectral radiation, C, are assembled in Table 2. The sixth column gives the probable value, as determined from consideration of the data in the text. The mean value is $C = 14\ 320$ micron degrees. The latest and most reliable determinations of the national laboratories are close to this value. Unfortunately, perhaps, this average is so close to the theoretical value arrived at from consideration of photo-electrical and similarly related phenomena that experimenters may consider their task finished, instead of just begun.

Digitized by Google

TABLE 2.—Observed Value and the Probable Value of the Constant C of Spectral Radiation

Observer	Date	$\lambda_m T - A$ observed	$\lambda_m T - A$ corrected	$C = \alpha\lambda_m T$, and from isochromatics	C, probable value in micron deg	Remarks
Paschen	1899	2891	2891	.....	14 360	Fluorite prism.
	.....	2907	2907	.....	.....	Temperature scale is questioned.
	1900	2921	2894	.....	.....	
Lummer and Pringsheim.	1900	2879	2879	14 290	.....	Fluorite prism. The wave length calibration of the prism is questioned; also temperature scale.
	.....	2876	2876	.....	.....	
	.....	2940	2882	14 310	14 300	
Warburg and collaborators.	1911	.....	.....	14 200–14 600	.....	Fluorite prism.
	1912	.....	.....	14 300–14 400	.....	Do.
	1912	.....	.....	14 360	.....	Quartz prism.
	1913	2894	.....	14 370	.....	Do.
	1915	.....	.....	14 250	.....	Temperature from Stefan-Boltzmann law.
	1915	.....	.....	14 300–14 400	14 300	Refractive indices (calibration of quartz prism) questioned.
Coblentz	1913	2911	.....	14 456	.....	Fluorite prism.
	1916	2894	.....	14 369	.....	Revised calibration (refractive indices) of prism; 1912 data are recalculated.
	1920	.....	.....	14 311–14 326	14 318	Correction for zero setting of bolometer.
Average value	.....	.....	.....	.....	14 320	

V. VERIFICATION OF THE LAWS OF RADIATION

In the foregoing pages an inquiry was made into the instruments and methods used in, and the numerical values of, various determinations of the constants of radiation.

The various methods are classified, and a brief description is given of each research. An attempt is made to indicate the good and the defective features in each research. This represents not only the writer's opinions, but also those of other experimenters.

It is shown that the great variation in the various determinations of the numerical values of the constants, especially the constant of total radiation, is owing mainly to the fact that, in the original papers, no corrections were made for atmosphere absorption of radiation in its passage from the radiator to the receiver.

In this paper conservative corrections for atmospheric absorption are applied to the various determinations, to which such corrections had not been made. As a result, instead of wide variations in the various determinations, which are free from other obvious defects, there is a remarkably close agreement among the

Digitized by Google

various numerical values. While it can not be said that the true numerical values are exactly as here recorded, obviously the time is past when the value of the constants of radiation are swayed by a single, and perhaps novel, method of research. The best that an experimenter should expect is that his own little contribution to the subject may have sufficient merit to go into the melting pot with the other determinations.

1. THE FORMULA AND THE COEFFICIENT OF TOTAL RADIATION

In the foregoing review the data are assembled and the evidence weighed pro and con. It is shown from various experiments that, beyond all reasonable doubt, the total radiation emitted from a uniformly heated inclosure is proportional to the fourth power of the absolute temperature—the so-called Stefan-Boltzmann law. Furthermore, the tabulated data show that the numerical values of the majority of the various determinations of the coefficient σ, which enters into the mathematical formula of total radiation, range about the value, $\sigma = 5.7 \times 10^{-5}$ erg cm^{-2} sec.$^{-1}$ deg.$^{-4}$ The average of 12 of the most reliable determinations is $\sigma = 5.72$ to 5.73×10^{-5} erg cm^{-2} sec.$^{-1}$ deg.$^{-4}$

2. THE FORMULA AND THE CONSTANT OF SPECTRAL RADIATION

Experimental evidence is cited showing that throughout the spectrum from 0.5μ to 50μ Planck's formula fits the observed spectral-energy distribution more closely than any other equation yet proposed. This formula is based upon theoretical principles, and after two decades of discussion it remains unchanged.

The constant C, which determines the shape of the spectral energy curve, has been the subject of numerous investigations. The numerical value of C has fluctuated greatly in the various determinations. In the foregoing pages it is shown that this is owing to experimental difficulties, such as, for example, lack of precise knowledge of the temperature scale and of the refractive indices of the prisms used. The tabulated data show that the various determinations of the constant of spectral radiation are of the order of $C = 14\,300$ to $14\,350$ with a mean value of $C = 14\,320$ micron degrees.

3. CONFIRMATORY EVIDENCE

One of the most interesting phases of the inquiry into the laws and constants of radiation is the confirmatory data which one obtains from a consideration of the interrelated phenomena of

Digitized by Google

atomic structure, of X rays, of ionization and resonance potential, and of photo-electrical action. From these data, as well as from the foregoing data on the two constants of radiation, one can compute the value of Planck's element of action, h. This gives seven independent methods of determining the universal constant, h. Or, from any one of four of these methods one can calculate [103, 104, 105], the radiation constants, and it seems truly remarkable how close is the agreement with the observed values.

For example, the writer's[4] value of the coefficient of total radiation, discussed on a preceding page, is $\sigma = (5.72 \pm 0.012) \times 10^{-5}$ erg cm^{-2} sec.$^{-1}$ deg.$^{-4}$ This indicates[105] a value of $C = 14\,320$ micron degrees and a value of $h = 6.55 \times 10^{-27}$ erg sec. The value of h, determined by Blake and Duane, [102] by X rays, is $h = 6.555 \times 10^{-27}$ erg sec., or an indicated value of $C = 14\,330$ micron degrees, which is close to experimental determinations of this constant. (See Table 2.)

Again, starting with Warburg's value of $C = 14\,300$, the corresponding value of the coefficient of total radiation is $\sigma = 5.74$, which is the higher estimated limit of the average of 12 different determinations of this constant, see Table 1. Hennig,[103] on the basis of Sommerfeld's theory, the measurement of spectral lines and the value of the electron, obtains $C = 14\,320$ and $\sigma = 5.717$.

In summing up the evidence, it is of interest to include Birge's[104] comprehensive and exact calculations of the constant h. In these calculations he, of course, assumes the truth of; (1) Lewis and Adams's[67] theory of ultimate rational units; (2) of the relation between C, σ, and h, as given by Planck's radiation formula; (3) of the quantum relation as applied to X-ray data;[102] (4) of Einstein's photo-electric equation; (5) of Bohr's theory of atomic structure; and (6) of the quantum relation as applied to ionization and resonance potentials.

In this manner he obtains seven separate calculations of Planck's constant of action, h, the mean value of which, as shown in Table 3, is $h = 6.5543 \times 10^{-27}$ erg sec.

This is close to the average of the value of h, which results from consideration of the two radiation constants.

From this calculation and intercomparison by Birge[104] of the data on C, σ, and h, as determined by thermal radiometric, photo-electric, X rays, and ionization potential measurements, it appears that the value of h, computed from radiometric data, compares very favorably with that obtained by more direct measurement. In other words, it appears to prove the validity of laws of

Digitized by Google

radiation and to establish the level of the numerical values of the constants entering therein.

TABLE 3.—Birge's [104] Calculation of Planck's Universal Constant h by Various Methods

Value of h	Method	Remarks
6.551±0.009	σ=5.72	Total radiation.
6.557±0.013	C=14 330	Spectral radiation.
6.542±0.011	Rydberg constant	Bohr's theory of atomic structure.
6.578±0.026	Photo-electric equations	Einstein's equations.
6.555±0.009	X rays	Quantum relation.
6.560±0.014	Ultimate rational units	Theory of Lewis and Adams.
6.579±0.021	Ionization potential	

Mean value h=6.5543±0.0025.

The outstanding disagreement between all the observed and computed data appears to be of the order of 1 to 3 parts in 1000, whatever the method of experimentation. This is a very close agreement, considering the variety of the data and the difficulties involved in making the experiments, which seems to indicate something more than a fortuitous relation between properties of matter.

In conclusion it may be added that, to a close approximation, we have the following constants:

$$A = \lambda_m T = 2885 \text{ micron degrees.}$$
$$C = 14\,320 \text{ micron degrees.}$$
$$\sigma = 5.72 \times 10^{-5} \text{ erg cm}^{-2} \text{ sec.}^{-1} \text{ deg.}^{-4}$$
$$h = 6.554 \times 10^{-27} \text{ erg sec.}$$

VI. BIBLIOGRAPHY

[1] Coblentz, B. S. Bul., **9**, p. 283; 1913 (diffuse reflection).

[2] Coblentz, B. S. Bul., **11**, p. 471; 1914 (optical constants of quartz).

[3] Coblentz and Emerson, B. S. Bul. **12**, p. 503; 1916 (radiation in absolute value; atmospheric absorption).

[4] Coblentz, B. S. Bul., **15**, p. 529; 1920 (constants of radiation; atmospheric absorption).

[5] Warburg and Müller, Ann. der Phys. (4) **48**, p. 410; 1915 (constants of spectral radiation; absorption of quartz).

[6] Gerlach, Ann. der Phys. (4) **50**, p. 233; 1916 (atmospheric absorption).

[7] Warbürg and Muller, Zs. für Instr., **35**, p. 103; 1915.

[8] Annals Astrophys. Obs. Smithsonian Institution **1**, p. 222, Plate XXVI B; 1902.

[9] Paschen, Ann. der Phys., (3) **53**, p. 334; 1894 (refractive indices).

[10] Paschen, Ann. der Phys., (3) **56**, p. 762; 1896.

[11] Paschen, Ann. der Phys., (4) **4**, p. 302; 1901.

[12] Paschen, Ann. der Phys., (4) **41**, p. p. 670; 1913.

Digitized by Google

[13] Micheli, Ann. der Phys., (4) **7**, p. 772; 1902 (temperature coefficients of refraction).
[14] Liebreich, Verh. Phys. Gesell., **18**, p. 1; 1911 (temperature coefficients of refraction).
[15] Coblentz, B. S. Bul., **12**, p. 553; 1916 (constant of total radiation).
[16] Stefan, Sitzungsber, d. K. Gesellsch., d. Wissensch. zu Wien (2) **79**, p. 391; 1879.
[17] Boltzmann, Ann. d. Phys., (3) **22**, pp. 31 and 291; 1884.
[18] Planck, Vorlesungen über Wärmestrahlung.
[19] Draper, Amer. Jour. Sci. (2) **4**, 1847, and Collected Papers.
[20] Kirchhoff, Pogg. Ann. d. Phys., **109**, p. 275; 1860.
[21] Christiansen, Ann. d. Phys. (3) **21**, p. 364; 1884.
[22] St. John, Ann. d. Phys. (3) **56**, p. 433; 1895.
[23] Wien and Lummer, Ann. d. Phys. (3) **56**, p. 451; 1895.
[24] Lummer and Pringsheim, Ann. der Phys. (3) **63**, p. 395; 1897; (4) **3**, p. 159, 1900.
[25] Schneebeli, Ann. d. Phys. (3) **22**, p. 430; 1884.
[26] Wilson, Astrophys. Jour., **10**, p. 80; 1899.
[27] Valentiner, Ann. der Phys. (4) **31**, p. 272; 1910.
[28] Lummer and Pringsheim, Verh. d. Deutsch. Phys. Gesell., **1**, pp. 33 and 215;1899.
[29] Coblentz, Carnegie Inst. of Washington, Publ. No. 65, pp. 77 and 80, 1906, and Pub. No. 97, p. 18, 1908.
[30] Coblentz, B. S. Bul., **10**, p. 1; 1913 (constant of spectral radiation).
[31] Waidner and Burgess, B. S. Bul., **3**, p. 163; 1907.
[32] Coblentz, B. S. Bul., **7**, p. 169; 1908 (emission spectra).
[33] Coblentz, B. S. Bul., **9**, p. 106; 1912 (selective emission).
[34] Lehnebach, Pogg. Ann. d. Phys., **151**, p. 96, 1873.
[35] Christiansen, Ann. d. Phys. (3) **19**, p. 267; 1883.
[36] Kurlbaum, Ann. d. Phys. (3) **65**, p. 746; 1898.
[37] Kurlbaum, Verh. d. D. Phys. Gesell., **14**, p. 576; 1912.
[38] Valentiner, Ann. der Phys. (4) **39**, p. 489, 1912; **41**, p. 1059, 1913.
[39] Coblentz, B. S. Bul., **14**, p. 532; 1918 (instruments and methods of radiometry).
[40] Gerlach, Ann. der Phys. (4) **41**, p. 99; 1913.
[41] Callendar, Proc. Roy. Soc., London, **28**, p. 1; 1910.
[42] Gerlach, Ann. der Phys. (4) **38**, p. 1; 1912 (constant of total radiation).
[43] Ångström, Phys. Rev., **1**, p. 365; 1893. Ann. der. Phys. (3), **67**, p. 633; 1899 (pyrheliometer).
[44] Gerlach, Phys. Zs., 17, p. 150; 1916.
[45] Paschen, Ann. der Phys., (4) **38**, p. 30; 1912.
[46] Gerlach, Ann. der Phys. (4) **40**, p. 701, 1913; **41**, p. 99, 1913; **42**, pp. 1163, 1167, 1913.
[47] Gerlach, Ann. der Phys. (4), **50**, p. 245, 1916.
[48] Gerlach, Ann. der Phys., (4) **50**, p. 259, 1916 (constant of total radiation).
[49] Coblentz, B. S. Bul., **9**, p. 40; 1911 (bolometers, hemispherical mirrors).
[50] Coblentz, B. S. Bul., **11**, p. 157, 1914 (thermopiles).
[51] Coblentz, B. S. Bul., **13**, p. 423, 1916 (ironclad galvanometers)
[52] Christiansen, Wied. Ann. der Phys., **19**, p. 267, 1883 (formulas).
[53] Puccianti, Nuovo Cimento (6) **4**, p. 31; 1912.
[54] Kahanowicz, Nuovo Cimento (6) **13**, p. 142, 1917.
[55] Féry, Compt. Rendus, **148**, p. 915, 1909.
[56] Féry and Drecq, Jour. de Phys. (5), **1**, p. 551, 1911
[57] Féry and Drecq, Compt. Rend., **155**, p. 1239, 1912.
[58] Bauer, Soc. Franç. de Phys., Procès Verbaux, No. 41, 1913.
[59] Bauer and Moulin, Compt. Rend., **149**, p. 988, 1909; Bull., Séances Soc. Fr. de Phys., p. 58, 1910.
[60] Bauer and Moulin, Compt. Rend., **150**, p. 167, 1910.

Digitized by Google

[61] Puccianti, Nuovo Cimento (6), **4**, p. 322, 1912.
[62] Keene, Proc. Roy. Soc., **88** A, p. 49, 1913; London Electrician, **70**, p. 541, 1912.
[63] Shakespear, Proc. Roy. Soc. London, **86** A, p. 180, 1012.
[64] Todd, Proc. Roy. Soc., **83** A, p. 19, 1909.
[65] Westphal, Verh. d. Deutsch. Phys. Gesell., **14**, p. 987, 1912.
[66] Westphal, Verh. d. Deutsch. Phys. Gesell., **15**, p. 897, 1913.
[67] Lewis and Adams, Phys. Rev. (2), **8**, p. 92, 1914.
[68] Millikan, Phys. Rev., **7**, p. 379, 1916.
[69] Paschen, Sitzber, Akad. Wiss., Berlin, **21**, pp. 403 and 959, 1899.
[70] Paschen, Ann. der Phys. (4), **4**, p. 277, 1901.
[71] Lummer and Pringsheim, Verh. Phys. Gesell., **1**, p. 23, 1899.
[72] Lummer and Jahnke, Ann. der Phys. (4), **3**, p. 383, 1900.
[73] Lummer and Pringsheim, Verh. Phys. Gesell., **1**, p. 215, 1899.
[74] Holborn and Valentiner, Ann. der Phys. (4), **22**, p. 1, 1906.
[75] Valentiner, Ann. der Phys. (4), **29**, p. 489, 1912.
[76] Coblentz, B. S. Bul., **13**, p. 459, 1916.
[77] Rubens and Kurlbaum, Ann. der Phys. (4), 4, p. 649, 1901.
[78] Nernst and Wulf, Verh. Phys. Gesell., **21**, p. 294, 1919.
[79] Warburg, Hupka, and Müller, Zs. Instrk., **32**, p. 134, 1912.
[80] Dellinger, B. S. Bul., **13**, p. 535, 1916.
[81] Roeser, B. S. Bul., **14**, p. 237, 1917 (least square calculation of *C*).
[82] Lummer and Pringsheim, Verh. Phys. Ges., **2**, p. 163, 1900.
[83] Lummer and Pringsheim, Ann. der Phys. (4), **3**, p. 159, 1900.
[84] Holborn and Day, Ann. der Phys. (3), **68**, p. 817, 1899; Ann. der Phys. (4), **2**, p. 505, 1900.
[85] Hoffmann and Meissner, Zs. für Instrk., **33**, p. 157, 1913.
[86] Warburg and Leithauser, Sitzber., **44**, p. 225, 1910.
[87] Warburg and Leithauser, Zs. für Instrk., **30**, p. 118, 1910.
[88] Warburg and Leithauser, Zs. für Instrk., **31**, p. 124, 1911.
[89] Warburg, Hupka, and Müller, Zs. für Instrk., **32**, p. 134, 1912.
[90] Warburg, Leithauser, Hupka, and Müller, Sitzer Akad. Wiss. Berlin, **1**, p. 35, 1913.
[91] Warburg, Leithauser, Hupka, and Müller, Ann. der Phys. (4), **40**, p. 609, 1913.
[92] Warburg, Hupka, and Müller, Zs. Instrk., **34**, p. 115, 1914.
[93] Warburg and Müller, Zs. Instrk., **35**, p. 98, 1915.
[94] Warburg and Müller, Ann. der Phys. (4), **48**, p. 410, 1915.
[95] Warburg, Verh. Phys. Ges., **18**, p. 1; January, 1916.
[96] Hoffmann and Meissner, Ann. der Phys. (4), **60**, p. 201, 1919.
[97] Holst and Oosterhuis, Proc. K. Akad., Amsterdam, **19**, p. 549, 1917.
[98] Hyde and Forsythe, Phys. Rev., **15**, p. 540, 1920.
[99] Carvallo, Compt. Rend., **126**, p. 728, 1898.
[100] Paschen, Ann. der Phys. (4), **26**, p. 120, 1908.
[101] Paschen, Ann. der Phys. (4), **4**, p. 299, 1901, Fl. II.
[102] Blake and Duane, Phys. Rev. (2), **10**, p. 624, 1917.
[103] Hennig, Verh. Deutsch. Phys. Gesell., **20**, p. 81, 1918.
[104] Birge, Phys. Rev. (2), **14**, p. 361, 1919.
[105] Coblentz, B. S. Bul., **15**, p. 617, 1920.
[106] Gerlach, Zs. für Physik, **2**, p. 76, 1920.
[107] Coblentz, Phys. Rev. (2), **14**, p. 174, 1919.
[108] Foote, B. S. Bul., **14**, p. 605, 1918.

WASHINGTON, August 22, 1920.

Digitized by Google

APR 7 1921

LIBRARY OF THE UNIVERSITY OF CALIFORNIA

DEPARTMENT OF COMMERCE

SCIENTIFIC PAPERS

OF THE

BUREAU OF STANDARDS

S. W. STRATTON, DIRECTOR

No. 407

RECENT MODIFICATIONS IN THE CONSTRUCTION OF PLATINUM RESISTANCE THERMOMETERS

BY

T. S. SLIGH, Jr., Associate Physicist
Bureau of Standards

JANUARY 5, 1921

PRICE, 5 CENTS

Sold only by the Superintendent of Documents, Government Printing Office
Washington, D. C.

WASHINGTON
GOVERNMENT PRINTING OFFICE
1921

Digitized by Google

Digitized by Google

RECENT MODIFICATIONS IN THE CONSTRUCTION OF PLATINUM RESISTANCE THERMOMETERS

By T. S. Sligh, Jr.

ABSTRACT

After a brief résumé of some phases of platinum resistance thermometry a description is given of some recent modifications in the construction of resistance thermometers as regards the heads, leads, terminals, and sealing of the strain-free type. The elimination of the drying head and the use of an all-metal case with the calorimetric type of resistance thermometer are also discussed. The necessity for relieving strains in the winding of the latter type is shown, and means of accomplishing this are pointed out.

Some practical notes regarding the construction of resistance thermometers and a description of the construction of a convenient and effective form of laboratory heating coil are given.

CONTENTS

	Page
1. Introduction	49
2. Historical	50
3. Resistance-temperature relations	51
4. Strain-free thermometers	53
5. Calorimetric thermometers	55
(a) Drying head	56
(b) All-metal case	56
(c) Lag	57
6. Materials and methods for thermometer construction	57
(a) Thermometer wire	57
(b) Leads	58
(c) Mica	59
(d) Arc-fusing	60
7. Sheath heating coil	61
8. Summary	62

1. INTRODUCTION

During the past six or eight years in the process of testing commercial thermometers and constructing thermometers for use at this Bureau a number of modifications in the construction of resistance thermometers have been made. Some of these are desirable on account of the accuracy to be gained, others for the simplification of construction, increased mechanical strength, etc.

Digitized by Google

It now seems well to describe these modifications representing the present practice of this Bureau, indicating the reasons for such changes as have been made from former practice. However, extended experimental evidence is beyond the scope of this paper and will not be dealt with here as such.

2. HISTORICAL

Since the failure of the original proposal of Siemens [1] of a platinum resistance thermometer having the coil wound on a clay cylinder and protected by an iron tube, nearly all successful forms of resistance thermometers have been constructed with the coil wound on mica, as proposed by Callendar,[2] with a protecting tube of glass, porcelain, or quartz. Heraeus introduced a thermometer in which the winding is sealed into quartz, but this form, although used with some success for industrial work, is not fitted for exact work on account of its unstable resistance, naturally resulting from the stress to which the winding must be subjected. Jaeger and von Steinwehr [3] have described a thermometer consisting of a silk insulated wire protected by a metal capillary tube, but this thermometer exhibited thermal after effects similar to those shown by the mercury-in-glass thermometer. Numerous forms of thermometers have been made in which glass and other materials were used to support and insulate the winding, notably by E. H. Griffiths.[4] None of these forms, with the exception of the Callendar mica cross, have come into general use. Dickinson and Mueller [5] described a calorimetric platinum resistance thermometer in which the wire was wound on a strip of mica which was inclosed in a flat closely fitting metal sheath between thin plates of mica.

Three methods of compensating for or eliminating the effects of the resistance of the thermometer leads and terminal contacts which have been in general use are the Siemens three-lead method, the Callendar compensating-loop method, and the potential-terminal method. Measurements with the last-named method may be made by the use of a potentiometer and current-measuring shunt, a Thompson bridge, by the Kohlrausch differential galvanometer method, or by the use of a Wheatstone bridge [6] and reversing commutator, as is the practice at this Bureau. Measure-

[1] Proc. Roy. Soc., 19, p. 351; 1871.
[2] Phil. Mag., 32, p. 104; 1891.
[3] Zs. für Instrk., 26, p. 237; 1906.
[4] Phil. Trans., A, 182, pp. 43–72; 1891.
[5] B. S. Bulletin, 9, p. 483; 1913. B. S. Sci. Papers, No. 200.
[6] E. F. Mueller, B. S. Bull., 13, p. 547; 1917.

Digitized by Google

ments of the resistance of a potential-terminal thermometer by any of these methods are independent of the lead and terminal-contact resistances, while the indications of the three-lead and compensating-loop thermometers are not wholly independent of these resistances.

3. RESISTANCE TEMPERATURE RELATIONS

As the result of the large amount of experimental work which has been done with the platinum resistance thermometer since the appearance of Callendar's original work [7] it is known that in the interval $-40°$ to $1100°$ C the relation between the resistance, R, and the temperature, t, of a platinum resistance thermometer can be very accurately represented by a parabolic equation of the form

$$R = R_o\,(1 + \alpha t + \beta t^2).$$

For purposes of computation this may be put in the more convenient form proposed by Callendar, which involves the use of two formulas, one of which introduces the very convenient concept of platinum temperatures (pt) which are related to resistances by the equation

$$pt = 100\,\frac{R_t - R_o}{F\,I},$$

where R_t is the resistance of the thermometer at $t°$ C, R_o is the resistance at o° C, and FI, the fundamental interval, is $R_{100} - R_o$. Thus the platinum temperature is a linear function of the resistance of the thermometer.

The fundamental coefficient, c, of the thermometer wire is defined by the relation

$$c = \frac{R_{100} - R_o}{100 R_o}$$

and serves, as explained below, as a criterion of the purity of the platinum.

The reduction of platinum temperatures to °C use is made of the difference formula $t - pt = \delta(1 - t/100)t/100$ where δ is a constant of the thermometer wire and is determined by a measurement of resistance at some temperature in addition to o° C or 100°. Where the construction of the thermometer permits the boiling point of sulphur (SBP = 444.6° C) is used for the deter-

[7] Phil. Trans., A, 178, p. 161; 1887.

Digitized by Google

mination of δ. The Callendar formulas are reducible to the form $Rt = R_0(1 + \alpha t + Bt^2)$ by means of the relations,

$$\alpha = c\left(1 + \frac{\delta}{100}\right) \text{ and } B = \frac{c\,\delta}{(100)^2},$$

where the symbols have the meanings stated previously.

The scale of temperature defined by a thermometer of pure platinum calibrated at the ice point, the steam point, and the sulphur boiling point has been adopted as the standard scale in the interval $-40°$ C to $450°$ C. Even at temperatures up to $1100°$ C this scale is found to agree with the thermodynamic scale of temperature to the accuracy with which that scale can be realized by the use of the gas thermometer.

Pure platinum has a fundamental coefficient, $c = 0.0039+$, and a delta value, $\delta = 1.5-$. The impurities usually associated with platinum tend to lower the value of c and to increase the value of the SBP δ. Further, thermometers of impure platinum when calibrated in the usual manner have been found to define a temperature scale which differs somewhat from the standard scale.[8]

The several national laboratories which use the platinum resistance thermometer to define the standard scale in the interval $-40°$ C to $450°$ C are in agreement in specifying that the purity of the platinum employed for thermometer construction is determined by the mean temperature coefficient of resistance in the interval 0 to $100°$ C, which coefficient should not be less than 0.00388, and by the value of the constant, δ, in the Callendar difference formula, which value[9] should not be greater than 1.52. These specifications should be understood to refer to wire which is pure, perfectly annealed, and free from strain. Some experimental work now nearing completion at this Bureau indicates that strain may affect the constants of thermometer wire, the effect being a lowering of the fundamental coefficient and also a lowering of the value of δ. Furthermore, there is some[illegible]ence that a thermometer wound of pure platinum wire in [illegible]ined condition does not define exactly the same scale as do[illegible] thermometer wound of the same wire free from strain, t[illegible] the difference is negligible in the range 0 to $100°$ C for the[illegible]eters which by comparison with a strain-free standard at 30[illegible]ow a δ not less than 1.47. These recent findings have a be[illegible] upon some modifications in the construction of calorimetric[illegible]tance thermometers, which will be discussed later in this p[illegible]

[8] Waidner and Burgess, B. S. Bull. 6, p. 150, 1909.

[9] Waidner, Mueller, and Foote, Bull. Am. Inst. Min. and Met. Eng., pp. 2051–2063; [illegible], 1919.

Digitized by Google

4. STRAIN-FREE THERMOMETERS

During the progress of some earlier work at this Bureau the accuracy attainable at high temperatures was limited by the fact that the constants of the thermometers used were changed by exposure to such temperatures. These changes were attributed to possible contamination of the thermometer wire by the hot mica and to the straining of the wire due to changes in volume of the mica supports; accordingly a mounting was devised (*E*, Figs. 1 and 2), which supported the winding in such a manner as to give a minimum of contact with the mica form and to preclude the setting up of strains in the winding due to swelling of the mica.

For this strain-free mounting two rows of holes spaced 0.6 mm from center to center are drilled or punched about 0.5 mm from the edges of a strip or core of mica (*a*, Fig. 2) 8 mm wide and 0.1 mm thick. A similar row of holes is punched in each of two mica strips or fins (*b*, Fig. 2) 2 mm wide by 0.1 mm thick. This core, with the fins lined up with the holes in its edges, is clamped between the two halves of a split mandrel (*C*, Fig. 1) 7 mm in diameter, and the winding is passed around the mandrel and through the holes. When the winding is completed the mandrel is carefully removed and the fins displaced through 90° so as to space the winding.

A simpler strain-free mounting which is probably as effective as the above was proposed by H. C. Dickinson of this Bureau in 1916 and has since been used by one of the manufacturers of resistance thermometers in this country. This construction makes use of the mica cross as in the Callendar mounting but substitutes deep narrow slots for the V-shaped notches for the winding. The winding is put on over a quartered mandrel whose diameter is slightly greater than the root diameter of the slots.

A modification of this mounting which would seem to line the coil up better consists in cutting the slots in one arm of the cross with a root diameter equal to the diameter of the mandrel and the slots in the other arm a few tenths of a millimeter deeper. Thus when the winding is put on and the mandrel removed the wire is supported on the bottoms of the shallower slots and on the edges of the deeper ones.

After the winding is put on the mounting, the short platinum leads (the branch terminals) are passed through small holes in the upper end of the mica core and are arc-welded to the ends of the gold internal leads, which are anchored through holes in two short

Digitized by Google

strips of mica. These lead anchorages are secured to the core by two small platinum clamps (*c*, Fig. 2). The gold leads are insulated from each other for about 10 cm above the thermometer "bulb" by mica washers (*e*, Fig. 2) spaced 5 mm apart and only a trifle smaller in diameter than the tube into which the thermometer is to be placed. These washers serve to reduce the convection currents in the thermometer tube which would tend to lower the temperature of the thermometer when used in a hot bath. The mica washers are punched from 0.1 mm mica, and four small holes are punched for the leads. Two of these holes, opposites, are spaced about half as far from the center of the washer as are the other two holes. The washers are put on the leads staggered, that is, a given lead will be passed through one of the inner holes in one washer and through an outer hole in the next, etc., thus putting a slight bend in the lead at each washer which serves to keep the washers spaced. (This method of punching and mounting the washers was devised by H. K. Griffin of this Bureau.) Glass capillary tubes (*p*, Fig. 1) serve to insulate the remainder of the internal leads.

The thermometer with its leads is now slipped into a closely fitting glass, porcelain, or quartz tube, and the leads are brought out of the tube around a small glass evacuating tube (*f*, Fig. 1) which is then cemented in place with De Khotinsky cement. The thermometer is thoroughly dried by evacuating and washing out the tube with air which has been passed through a drying tube, and the evacuating tube is sealed off with dry air in the thermometer tube, or with hydrogen if the thermometer is to be used at very low temperatures.

A winding of this type of 0.1 mm wire will dissipate the heat generated by a current of 1.5 milliamperes in the winding with a temperature rise of about 0.001° C.

The head, the construction of which is shown in Fig. 1, is slipped onto the tube from the bottom, and is cemented or secured to the tube by a wrapping of shellacked silk thread (*g*, Fig. 1). This latter method permits of easy removal of the head. The internal leads are now arc-fused to short gold wires which have been silver-soldered to the copper studs in the thermometer head. The flexible leads (*J*, Fig. 1), which are soft-soldered to the terminal studs, consist of four strands insulated and covered with a braid, each strand consisting of three No. 28 enameled copper wires double-silk covered, twisted together, and again double-silk covered. This lead was designed to eliminate the variable lead

Digitized by Google

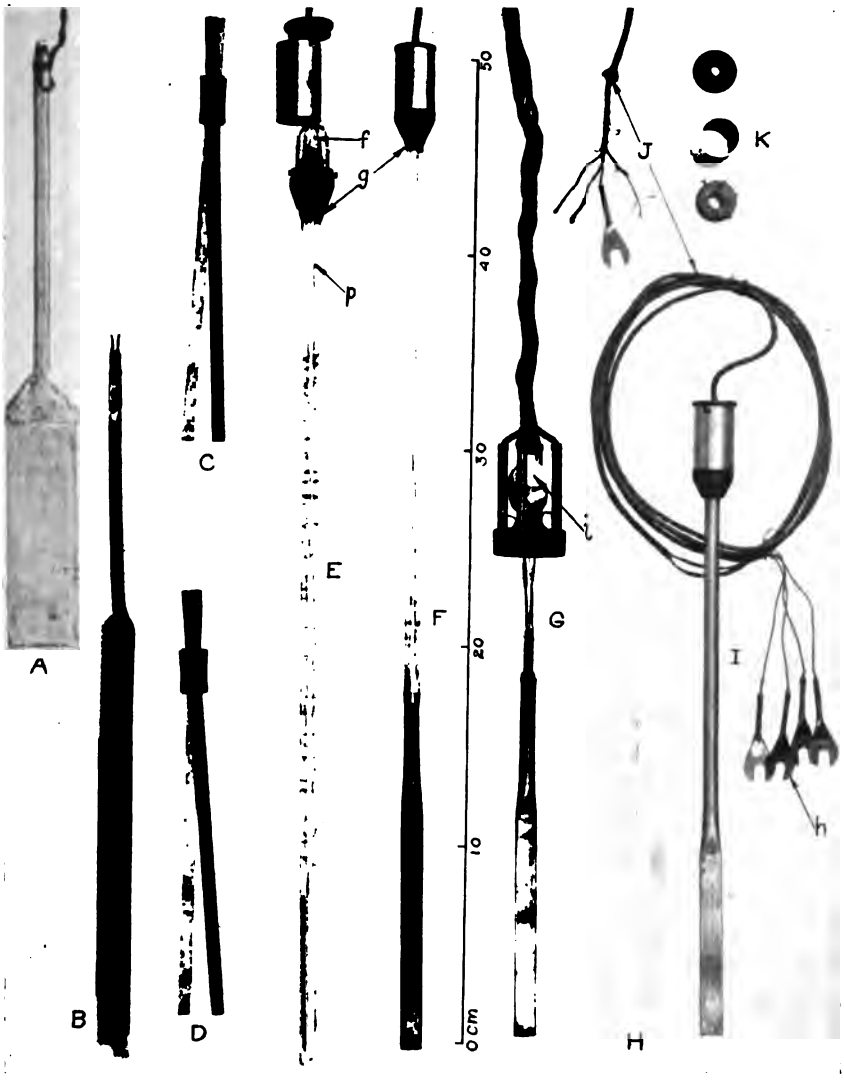

FIG. 1.—*Sheath type heating coils, core mandrels, and various types of resistance thermometers*

A, Sheath heating coil. Capacity, 600 watts, with a loading of 10 watts/cm² of surface
B, Sheath heating coil sectioned. Note that copper leads are flattened and wound for a few turns on the core before joining the resistance winding. Leads are insulated by mica. Cap is of bakelite cemented to the lead duct
C, Smooth mandrel on which strain-free coils are wound
D, Threaded mandrel for notching calorimetric cores
E, Standard strain-free thermometer B. S. No. C_{22}. Only about 10 cm of mica washers are needed instead of the 25 cm shown here
F, Calorimetric thermometer B. S. No. Pt_7 for use at temperatures up to 500° C. Method of sealing tube and attaching leads in head as shown at *f*
G, Commercial form of calorimetric resistance thermometer
H, Calorimetric winding showing gold leads and side-plates
I, Calorimetric resistance thermometer B. S. No. Pt_{11} with German-silver case and without drying head. Method of sealing tube and attaching leads in head as shown at *f*
J, Flexible lead for resistance thermometers
K, New style thermometer head of the size shown at *F* and *I*. Head at *E* is of a slightly larger size

Digitized by Google

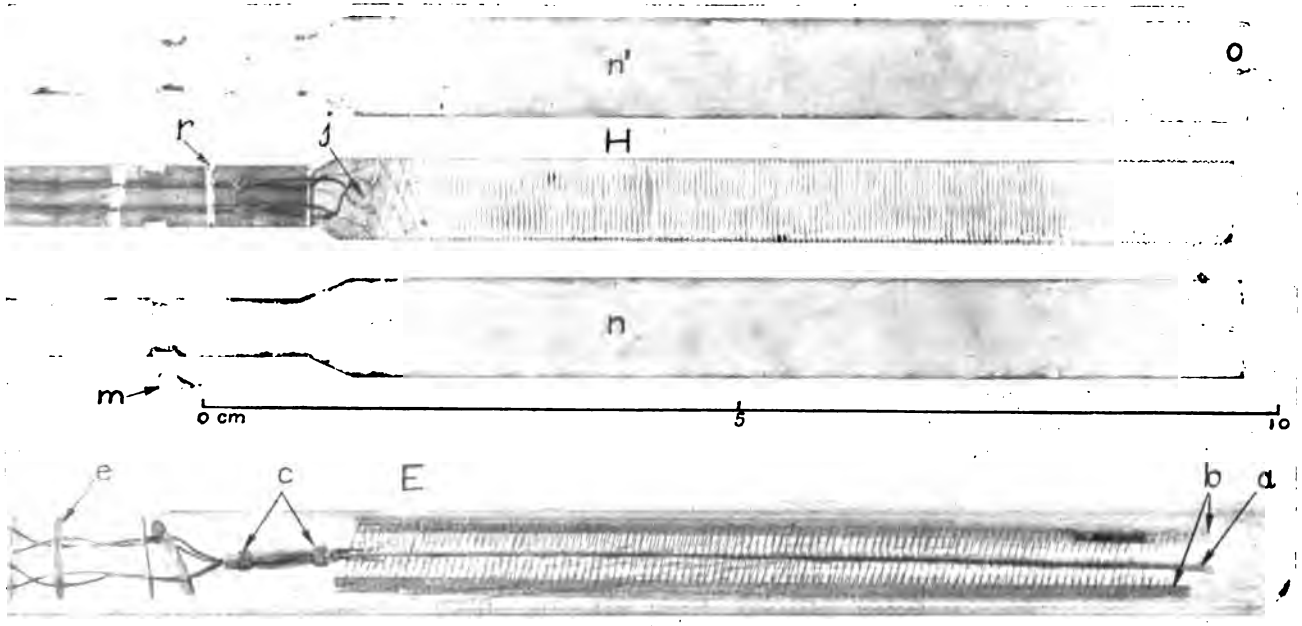

FIG. 2.—*Details of strain-free and calorimetric thermometer coils*

E, Strain-free coil. Enlargement of coil of *E*, Fig. 1. Spacing 14 turns per centimeter. Note floating fins *b* and washers *e*
H, Calorimetric winding. Enlargement of *H*, Fig. 1. Spacing 20 turns per centimeter. Note method of supporting flattened leads on mica strips and the accidental displacement of the winding about the middle of the coil which indicates the looseness of the windings. Temporary binding at *r* is to be removed when the side-plates *n* and *n'* are attached by means of the clamps, one of which is shown at *m*, and the tie wire at *o*

Digitized by Google

resistance so often experienced with lamp-cord flexibles due to the slip resistance of one or more strands which have become broken or were not originally properly soldered to the terminals.

The light copper terminals (*h*, Fig. 1) are cut from 0,2 mm sheet copper, and owing to their small heat capacity and good thermal conductivity, tend to minimize troublesome thermal electromotive forces at the commutator or bridge terminals. A thin gold plating will prevent oxidation and insure good electrical contact at the binding posts.

5. CALORIMETRIC THERMOMETERS

This type of thermometer was developed at this Bureau by Dickinson and Mueller.[10] A detailed description of the original construction is given in the reference cited.

Since the construction of the commercial form (*G*, Fig. 1) of these thermometers precludes their use at temperatures above about 150° C, it has been the practice at this Bureau to calibrate them by observations in ice and in steam and to determine their delta by comparison at 30° C with a strain-free thermometer which had been calibrated at ice, steam, and at the SBP.

These thermometers showed values of δ of about 1.47 both when calibrated against the strain-free thermometers and against the verre-dur mercury-in-glass standards of the Bureau. Later some thermometers of the calorimetric type (*F*, Fig. 1) were constructed with platinum sheaths sealed to long glass stems and were calibrated at ice, steam, and at the SPB. These thermometers were then compared with the strain-free thermometers at lower temperatures and the results previously mentioned; that is, the lowering of the δ value by mechanical strain, were arrived at. This led to the construction of coils very loosely wound on thick (0.5 mm) mica cores, thoroughly annealed before and after winding by passing an electric current through the wires. These coils were placed in sheaths which were lightly flattened down on the windings and fused at the bottoms. The thermometers were then annealed by flashing the coils on a voltage of 120–150 volts, care being taken not to overheat the mica. (The temperature of the wire calculated from voltmeter and ammeter readings was about 1000° C.) These thermometers were then finished as described for the strain-free type.

Thermometers so constructed, with special care taken both to avoid the introduction of strains in construction and to anneal the thermometer thoroughly after incasing, compare very favor-

[10] B. S. Bull. 9, pp. 483 and 1013; B. S. Sci. Papers, No. 200.

Digitized by Google

ably with the strain-free type, showing a value of δ which approaches 1.49. Further, the temperature scale defined by these thermometers is, within the limits of accuracy of the comparison of platinum resistance thermometers, identical with that defined by the strain-free type thermometers.

(*a*) DRYING HEAD.—The glass drying head (*i*, Fig. 1) used on the original calorimetric type of thermometers has been eliminated in this latter design because it has now been found easy to secure tubing for the sheaths which is free from flaws, and the technique of construction has been developed to a point where the joints can be made permanently tight and the thermometer and case thoroughly dried before sealing.

(*b*) ALL-METAL CASE.—With the elimination of the drying head it seemed worth while to go a step further toward a robust construction by eliminating the glass stem between the sheath and the thermometer head. German silver was selected for the sheath (*I*, Fig. 1) on account of its low thermal conductivity, its freedom from excessive oxidation, and its availability in the desired form. It is evident that any metal of low thermal conductivity, if not subject to corrosion, could be used. As a matter of fact there are several such metals which are superior to German silver in some respects, but they are not at present available in the form of thin-walled tubing. For use in chemical reagents the sheath could well be made of platinum or some of its alloys, the latter having in general the advantages of greater stiffness and lower thermal conductivity.

The case is made of tubing 30 cm long by 0.75 cm diameter by 0.02 cm thick, flattened over a brass strip or form 0.1 cm thick for a length of about 15 cm. The coil, head, and external leads are as described above.

The internal leads consist of four No. 30 copper wires with silk and enameled insulation; these are stripped of insulation for about 4 cm of their length and rolled to a width of 1 mm. To these flattened ends short lengths (5 mm) of gold wire are silver soldered, and this wire is arc soldered to the ends of the winding. The flattened portions of the leads are laid between thin strips of mica and fastened by clamps (*M*, Fig. 2) to the mica core and the mica side plates, and the coil is slipped into the sheath from the bottom; the insulated ends of the leads are cabled and led out of the end of the tube through a collar of bakelite and around a glass evacuating tube as in the strain-free construction (*f*, Fig. 1). The sheath is now flattened down lightly on the coil and on the mica-

Digitized by Google

covered portion of the leads and the end of the sheath silver soldered. This soldering may be accomplished without injury to the mica if the core terminates about 8 mm above the bottom of the sheath, and the sheath is clamped lightly in a vise at this point to conduct the heat from the winding.

The winding is again flashed as described above. The evacuating tube is then plugged temporarily with cement, and the thermometer immersed in a tube of water from the surface of which the atmospheric pressure is removed by a suction pump. Any leaks can then be located by means of the air bubbles which will form. If the thermometer is tight the evacuation tube is sealed off, and the thermometer tube is fitted to the head, secured with a small set screw, and the internal and external leads soldered to the terminal studs.

It has been found that no effect of stem conduction can be detected when the thermometer bulb is immersed in the ice bath to a point a little above the flattened portion. This immersion is about that required for the glass-stem type. The same immersion appears sufficient in the steam bath.

(*c*) LAG.—The use of thicker core plates and lighter sheath pressures together with the all-metal case entails some sacrifice as regards rapidity of action; that is, the lag of the thermometer is increased, and the current-carrying capacity for a given temperature rise is slightly reduced. However, the sacrifice is slight, as the lag of the thermometers tested including the lag of the galvanometer (period 5 seconds) has been found to be between 2.5 and 3.5 seconds in the ice bath. By lag is meant the number of seconds required for the temperature difference between the thermometer and the bath to be reduced to $1/e$ of its initial value. The lag could be reduced somewhat by reducing the amount of metal in the case, or by making the stem of a low-conductivity metal and the sheath of a high-conductivity metal, such as copper or silver. However, since lags of the magnitude encountered introduce no complications in the use of these thermometers for the service for which they are designed, the slight possible gain due to the changes mentioned has not appeared to be worth the additional complication of construction.

6. MATERIALS AND METHODS FOR THERMOMETER CONSTRUCTION

(*a*) THERMOMETER WIRE.—Thermometer wire should be of the highest purity platinum, 0.1 mm diameter serving for most purposes. Smaller wire is more difficult to handle, is more easily

Digitized by Google

contaminated, and, while it would seem at first glance that a more compact thermometer could be constructed by its use, the sensitivity of such a thermometer is necessarily reduced on account of the reduced area for the dissipation of heat because the permissible heating by the measuring current is limited. Wire of 0.1 mm diameter, calorimetric construction, will dissipate about 0.000003 watt/cm of length (a current of 5 milliamperes in the winding), with a temperature rise of 0.001° C.

Heavier wire, 0.2 to 0.4 mm in diameter, is preferable for work at higher temperatures because the larger wire is more nearly self-supporting, is less easily contaminated, and because it has been found that low-resistance thermometers ($R_0 = 2.5$ ohms) are entirely suitable for work at such temperatures. The wire should be thoroughly annealed before winding by heating to 1000 to 1200° C by the passage of an electric current, should be wound with as little tension as practicable, and should be as thoroughly annealed after winding as the construction of the thermometer will permit.

With the strain-free coil there is little danger of dehydrating the mica by electrically heating the winding to a temperature of about 1000° C with the coil in the open. With the calorimetric construction the wire can be heated to this temperature only momentarily by "flashing" on a high voltage. The annealing is to be secured by a series of flashes, allowing the mica to cool after each flash. This flashing is especially valuable after the sheath has been flattened down on the winding because it tends to ease up any local strains which may have been set up by such flattening.

It has been found convenient to adjust the resistance of the winding so as to give a fundamental interval of approximately either 10 or 1 ohms, which permits rapid and accurate calculations of temperature by the use of the slide rule only.

(*b*) LEADS.—The internal leads are of gold wire 0.3 mm in diameter for use up to temperatures of 1000° C. Gold is selected because of its freedom from oxidation, its low thermal emf against the copper studs in the head, and because it may be readily arc-fused to platinum. Internal leads are made of platinum only for use above 1000° C. Copper leads may be used only below 200° C.

Thermal conduction along the leads should be shunted to the case in the calorimetric construction by having at least 4 cm of the internal leads rolled thin and mounted between thin strips of mica in the flattened portions of the sheath.

Digitized by Google

With the potential terminal construction for use with a Wheatstone bridge and commutator it is desirable that the two current leads have nearly equal resistances in order that it may be necessary to shift only one or two bridge dials when changing from the "normal" to the "reverse" setting. It is further desirable that the changes in resistance of these leads with changes in temperature be nearly equal. These results may be attained by cutting all four of the branch terminal platinum leads, two current and two potential leads, to the same length and making the remainder of the leads as nearly alike as practicable. When finished there are four possible combinations of leads, of which the best combination may be selected by measurements in the ice bath. In nearly every case it will be possible to so select the combination as to give normal and reverse settings which differ by not more than 0.01 ohm. By an adjustment similar to the adjustment of the value of R_0 these settings have been made alike to within 0.001 ohm. It should be noted that this adjustment of leads is merely for convenience and in no way improves the accuracy of measurement. For instance, a constant resistance of 10 ohms in one lead would have no effect upon the accuracy of the resistance measurements except as it slightly reduces the galvanometer sensitivity.

(*c*) MICA.—Clear ruby mica free from iron oxide, which shows up as a brownish stain, should be used for the construction of resistance thermometers. The mica used in the construction of strain-free thermometers should be as thin as can be conveniently worked (0.1 mm or less) in order that the heat capacity and consequently the lag of the thermometer may be reduced. The same is true of the calorimetric thermometer except as regards the central core, which should be about 0.5 mm thick in order that the wire may not be unduly strained by bending around the thin edges.

Mica may be cut nicely with foot shears such as are used for cutting light sheet metal. If such are not available or if only a narrow strip is to be trimmed off the mica may be clamped between steel straightedges and cut with a safety-razor blade. Small holes may be made with a punch and die (a jeweler's staking tool is convenient for this work), or by drilling with a jeweler's pivot drill or a small drill made of piano wire or a needle. Drilling may be done by hand, in which case a neater hole is secured by drilling from first one side and then the other, or by a high-speed power drill, in which case it is best to back the mica up by a smooth surface such as hard rubber or brass. Notches for the calorimetric winding may be cut by clamping the mica between the two halves

Digitized by Google

of a split hardened-steel screw (*D*, Fig. 1) of 14 to 20 threads per centimeter and cutting out the V-shaped notches with a hacksaw blade the teeth of which have been ground down to a V-shape to fit the threads and slightly rounded on the edge. A smoother cut is secured if the first cut is taken backwards rather than in the usual way. After the notches have been cut loose bits of mica, etc., may be cleaned off by "sawing" a bundle of loose cotton threads across the edge of the mica while it is still clamped in the form. When the core is removed from the form its edges should be beveled slightly on a medium-grit carborundum stone.

Holes for the strain-free winding may be spaced by clamping the mica between one-half of the threaded form and a strip of hard rubber and drilling at the base of the notches. A flexible drill made of 0.2 mm piano wire is serviceable for this work. Where a row of holes is to be drilled near an edge it is often better to leave about a millimeter extra width on the strip to be trimmed off later between straightedges.

The clamps used for holding the various parts of the mica together in the assembled thermometer are made of platinum wire rolled to strip and annealed. Copper clamps may be used for work at temperatures below about 200° C.

The side plates (*n*, *n'*, Fig. 2) on the calorimetric coil are held in place at the bottom of the winding by a small platinum wire passed through a hole in the plates and the core. (*o*, Fig. 2.)

(*d*) ARC-FUSING.—There are two general methods of arc-fusing which are suitable for resistance thermometer work. The two-carbon method, in which an arc is drawn out between two carbons and brought up to the work, is suitable for heavy work such as closing the ends of platinum or silver sheaths or for work with base metals where a flux is necessary. The two-carbon method does not localize the heat so well as the single-carbon method, in which the work to be fused is made the positive pole of a dc arc of which a single carbon is the negative pole. The currents and voltages required vary with the size of the work to be fused. Thirty volts and 1 ampere are usually sufficient to join two 0.1 mm platinum wires. Somewhat larger voltages and currents are required to join the 0.3 mm gold wire to the winding. No flux is required in the fusing of gold, silver, and platinum.

A convenient method of securing the variable voltages and currents required for this work consists in tapping off through a rheostat from the sliding contact of a 50-ohm rheostat which is connected across the 110-volt dc mains.

Digitized by Google

7. SHEATH HEATING COIL

It does not seem out of place in this paper to describe a very effective type of heating coil (*A* and *B*, Fig. 1) which has been developed at this Bureau for use in baths of stirred liquid. The winding consists of a constantan ribbon rolled from wire of sizes No. 20 to No. 36, according to requirements, and wound bifilarly on a notched mica strip. The spacing of the notches from center to center is usually made about twice the width of the ribbon.

The notches may be punched, or cut on a form similar, except as regards size and notching, to that used for the calorimetric thermometers, or cut with a small circular saw driven at high speed. In this last case the mica strip should be backed up with a strip of hardwood, or the edge of the saw should be rotating in a slot cut in the edge of a metal strip which serves as a support for the mica. Leads are of copper silver-soldered to the ends of the winding, anchored to the core by being passed through slits and brought out through the lead duct, and insulated by silk or mica strips as seems best.

The winding with sideplates of thin mica is slipped into a case made by flattening a thin-walled copper tube. The sheath is squeezed down *tightly* on the coil in a vise and the end soldered. The lead duct consists of a smaller tube, round or flattened as is convenient, which has previously been hard-soldered to the sheath.

Hard or silver solder is used in the place of soft solders in the construction of thermometers and heating coils wherever possible because it gives a more permanent union of the parts.

The form of heating coil described has small lag and heat capacity together with large dissipating capacity, which makes it especially adapted for use with thermoregulated baths. Tests of heat dissipation made in stirred water baths indicate a dissipation of 0.07 watt/cm^2 of sheath surface for each degree difference in temperature of winding and bath. Thus with a loading of 10 watts/cm^2 the temperature of the winding runs about 140° C above the temperature of the bath. A loading of 30 watts/cm^2, probably the safe maximum value, requires a difference of temperature of 430° C. Without stirring of the bath the transfer coefficient drops to about 0.05 watt/cm^2 for each degree centigrade difference of temperature between winding and bath.

No tests on the rate of transfer in oil baths have as yet been made, but it is known that the coefficient is very much smaller than in water; 0.03 would probably be a safe value.

Digitized by Google

These coils are usually wound for a loading of about 10 watts/cm^2 and are tested for leak in a manner similar to that applied to the calorimetric thermometers. It is essential that the coils be sealed against the bath liquid (water), and if used at low temperatures the lead duct should be sealed with De Khotinsky cement or by some other method to prevent the condensation of atmospheric moisture on the winding and consequent almost inevitable short-circuit.

In conclusion acknowledgement is made of the assistance rendered by E. F. Mueller of this Bureau in the preparation of this paper. The construction of resistance thermometers therein described is due to the combined efforts of the members of this Bureau who have worked along these lines during the past few years.

8. SUMMARY

The potential terminal type of thermometer is preferred in view of its more complete elimination of lead resistance.

Thermometer leads are now made of four strands, each made up of three No. 28 enameled copper wires. This construction affords sufficient flexibility and avoids the difficulties caused by the breakage of strands and the consequent variable lead resistance which is so often encountered with the fine-strand flexibles.

Thermometer bridge terminals are made of thin sheet copper, which may be gold or silver plated.

A thermometer head of simpler construction and neater appearance than the metal-cased head previously used on the strain-free type of thermometer is now used on both the strain-free and the calorimetric thermometers.

The only essential modification in the construction of the strain-free type of thermometer is the change from unsealed to sealed thermometer tubes. This sealing eliminates the possibility of the condensation of moisture in the thermometer when it is being used at low temperatures.

The calorimetric construction has been modified in several particulars, notably, (1) the glass drying head has been found to be unnecessary if the thermometer case is tight and the initial drying has been complete; (2) a case made from German-silver tubing flattened into a sheath at one end has been substituted for the glass stem and the metal sheath previously used. This case, if constructed of German-silver tubing 0.75 cm in diameter and 0.02 cm thick, requires an immersion to a point only about 5 cm

Digitized by Google

above the top of the winding in order that stem and lead conduction effects may be eliminated.

It is essential for the most accurate work that the winding of the calorimetric thermometer be free from strain. This freedom from strain may be attained by thoroughly annealing the wire before winding by winding, with very light tension, on a mica core which is not less than 0.5 mm thick, so that the wire may not be unduly strained by bending around a sharp edge, and by flash-annealing the winding both before and after placing it in the case. Flash-annealing consists in connecting the winding for a few seconds across a voltage sufficiently high to heat the winding to a temperature of about 1000° C before the mica has time to heat above 600° C.

A heating coil constructed along the lines of the calorimetric type of thermometer, with the substitution of a ribbon of resistance material for the platinum winding, has been found very effective and convenient for general laboratory use. Due to its small heat capacity and its large heat-transfer coefficient (0.07 watt/cm² per degree difference in temperature between the winding and the water bath), it is especially suited for use in temperature-controlled baths and for energy-measurement work.

WASHINGTON, September 18, 1920.

Digitized by Google

Digitized by Google

APR 7 1921

LIBRARY OF THE UNIVERSITY OF CALIFORNIA

DEPARTMENT OF COMMERCE

SCIENTIFIC PAPERS

OF THE

BUREAU OF STANDARDS

S. W. STRATTON, DIRECTOR

No. 408

EFFECT OF THE RATE OF COOLING ON THE MAGNETIC AND OTHER PROPERTIES OF AN ANNEALED EUTECTOID CARBON STEEL

BY

C. NUSBAUM, Associate Physicist
W. L. CHENEY, Assistant Physicist
Bureau of Standards

JANUARY 22, 1921

PRICE, 5 CENTS

Sold only by the Superintendent of Documents, Government Printing Office
Washington, D. C.

WASHINGTON
GOVERNMENT PRINTING OFFICE
1921

Digitized by Google

Digitized by Google

EFFECT OF THE RATE OF COOLING ON THE MAGNETIC AND OTHER PROPERTIES OF AN ANNEALED EUTECTOID CARBON STEEL

By C. Nusbaum and W. L. Cheney

ABSTRACT

This paper discusses the results of a study of the effect of the rate of cooling upon the magnetic and other properties of an annealed eutectoid steel. In carrying out the experiment, six specimens of this steel were selected, heated to 800° C, and allowed to cool at various rates—one in air, another in lime, and the remainder in the furnace at slower and slower rates. The following properties were then measured: Normal induction for ordinary and large magnetizing forces, residual induction, coercive force, resistivity, and Shore scleroscope hardness. In order to study the metallographic structure of the steel, micrographs of each specimen were made at a magnification of 500 diameters.

A study of the experimental results show that as the cooling rate is diminished there is a pronounced increase in the value of the maximum induction for a given small magnetizing force, a decided increase in the maximum permeability, but a decrease in the coercive force. The values of the coercive force agree very well with the scleroscope hardness number.

In plotting the reluctivity line as calculated from the magnetization curve, it is found that the reluctivity line consists of two straight lines with the bend occurring at a definite point. As the structure of the steel changes from an essentially sorbitic one to "divorced" pearlite, there is a gradual shifting of this bend toward the origin and a greater difference between the values of the "real" and "apparent" values of the saturation intensity of magnetization as calculated from the slopes of the reluctivity line.

CONTENTS

	Page
I. Introductory	66
II. Experimental method	66
1. Material	66
2. Heat treatment	67
3. Magnetic measurements	67
4. Resistivity	67
5. Hardness	67
III. Observations and results	68
1. Rates of cooling	68
2. Magnetic properties	69
3. Microscopical analysis	72
IV. Discussion	74
V. Summary	76

Digitized by Google

I. INTRODUCTORY

In a previous paper [1] the effect of the quenchings and subsequent tempering on the magnetic properties of a eutectoid carbon steel were presented and the metallurgical significance of these effects were discussed. Particular use was made of the magnetic reluctivity relationship. The investigation has since been extended to slower rates of cooling, some of which are within the annealing range. This investigation is discussed in the present paper.

That the physical properties and the crystalline structure of steel are greatly affected by various rates of cooling from or through the critical range is universally recognized by metallurgists. The influence of the rate of cooling on the magnetic properties is also generally recognized, yet there does not appear to be a full appreciation of its importance. In much of the published magnetic data mention is made that the steel was in the "annealed condition," but generally no information is given as to the initial temperature, the length of time the material had been kept at such temperature, or the rate of cooling. Perhaps the data of Yensen [2] on electrolytic iron and silicon steel are the most complete in this respect. The present paper is an attempt to emphasize the importance of these factors by presenting data on the magnetic and other physical properties and also on the microstructure resulting from various cooling rates.

II. EXPERIMENTAL METHOD

1. MATERIAL

The specimens were of the following chemical composition:

	Per cent
C	0.85
Mn	.23
Si	.23
Cr	.05
P	.016
S	.014
Fe (by difference)	98.61

The specimens were in the form of cylindrical rods 1 cm in diameter and 25 cm long, and had been previously heated to 800° C and furnace annealed.

[1] Nusbaum, Cheney, and Scott, B. S. Sci. Papers, No. 404; 1920.
[2] T. D. Yensen, Univ. of Illinois Engineering Experiment Station, Bull. No. 72; 1914.

Digitized by Google

2. HEAT TREATMENT [3]

Each specimen was heated to a temperature of 800° C in a small Hoskins resistance furnace and kept at this temperature for a definite interval of time. The temperatures were measured by a platinum platinum-rhodium thermocouple. Oxidation of the specimens at the high temperatures was reduced by the presence of a gas flame within the furnace. Since, at the slow cooling rates, decarburization of the outer portions of the specimen becomes appreciable, all of the specimens were turned down to a diameter of 8 mm so that the specimens throughout their entire cross section would be uniform in properties and composition. One end of each specimen was kept for microscopic examination.

3. MAGNETIC MEASUREMENTS

The magnetic measurements at ordinary magnetizing forces were made with a Burrows [4] permeameter. At high field values the measurements were made by a modified form of the "isthmus" method.[5] For the latter measurements it was necessary to reduce the diameter of the specimens to 6 mm.

4. RESISTIVITY

The resistance measurements were made by a comparison method: The "fall of potential," both across the terminals of a standard shunt connected in series with the current-carrying specimen, and across knife-edge potential terminals in contact with the specimen and 20 cm apart, was measured by a high-resistance Wolff potentiometer. A series of alternate measurements were taken. In order to minimize the effects on the specimen of temperature changes caused by the heating effects of the current, observations were not taken until an equilibrium temperature had been reached.

5. HARDNESS

One end of each specimen was polished for the determination of the scleroscope hardness, and the determinations were made by a self-recording Shore scleroscope. The size and form of the specimens did not permit of Brinell hardness tests.

---

[3] The heat treatment was carried out by Messrs. H. Scott and T. G. Digges, of the heat-treating laboratory of the Bureau of Standards. Mr. Scott also gave the writers valuable assistance in selecting the most suitable cooling rates for these experiments.

[4] C. W. Burrows, B. S. Sci. Papers, No. 117; 1909.

[5] W. L. Cheney, B. S. Sci. Papers, No. 361; 1920.

Digitized by Google

III. OBSERVATIONS AND RESULTS

1. RATES OF COOLING

Such rates of cooling were chosen as to cause a gradual variation from an essentially sorbitic structure to one in which the matrix is essentially divorced pearlite. Specimen *16* was allowed to cool in air, and specimen *17* in lime, while specimens *18*, *19*, *20*, and *21* were furnace cooled at various rates and under different conditions. In Fig. 1 are plotted the time-temperature curves for the furnace-cooled specimens. In the case of specimen *18* the current was cut off after the temperature had been held at 800° C for 12 minutes, and the specimen was then allowed to cool with the furnace. Specimen *19* was held for a time interval of 13 minutes at a temperature of 800° C, and then slowly cooled by reducing the current, which was cut off when the temperature

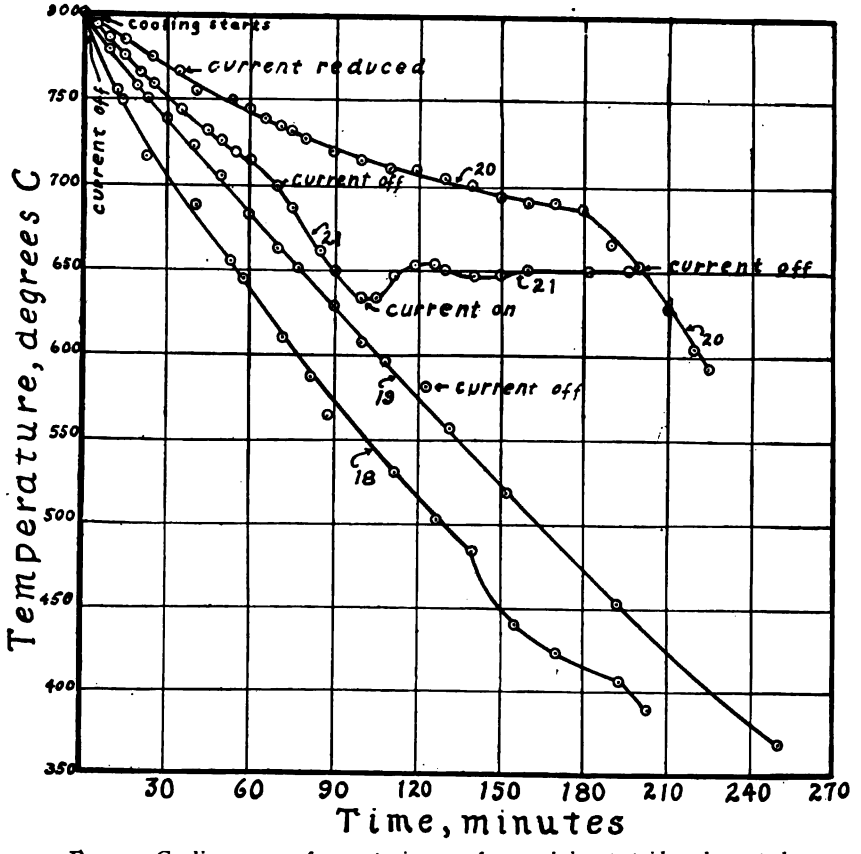

FIG. 1.—*Cooling curves for 4 specimens of annealed eutectoid carbon steel*

Digitized by Google

had fallen to 580° C; the specimen was then allowed to cool with the furnace. Specimen *20* was held for a period of 20 minutes at the initial temperature and allowed to cool in a definite manner by suitable reductions of the current. Specimen *21* was cooled to 650° C in a definite manner and then held at this temperature for a period of 75 minutes in order to determine the effect upon the physical properties and structure of maintaining the material below its critical temperature during a given time interval. The times of cooling for the various specimens from 800° C to 650° C are recorded in Table 1.

TABLE 1.—Effect of Rate of Cooling on Magnetic and Other Properties of Eutectoid Carbon Steel

Specimen number	Time held at 800° C	Method of cooling	Time cooling from 800°–650° C	Maximum permeability	Magnetic induction			Residual induction H_m 150	Coercive force H_m 150	Saturation intensity of magnetization (calculated)	Scleroscope hardness	Specific resistance
					H=15	H=150	H=1000					
	Minutes		Minutes		Gausses	Gausses	Gausses	Gausses	Gausses	C. g. s. units		Microhms
16	.....	Air cooled	.....	385	5150	16 100	20 050	10 050	13.4	1564 1520	43.3	0.2025
17	.....	Lime cooled	.....	437	6150	16 300	20 000	10 540	12.4	1550 1500	42.3	.2006
18	12	Furnace cooled	56	630	9300	16 100	20 030	12 300	10.18	1580 1490	33.0	.1941
19	13	Furnace cooled	78	630	9300	16 100	20 030	12 300	10.0	1600 1430	30.4	.1950
20	20	Furnace cooled	200	698	10 000	16 300	20 000	12 360	9.2	1610 1430	29.9	.1931
21	13	Furnace cooled	90	633	9300	16 100	20 080	11 970	9.2	1540 1400	33.6	.1963

2. MAGNETIC PROPERTIES

Fig. 2 gives the normal induction curves for low and medium values of the magnetizing force, and Fig. 4 gives the curves for high values. It is interesting to observe the increase in the magnitude of the induction for a given value of the magnetizing force, as the rate of cooling is varied from air cooling to slow furnace cooling. The change in the values of the induction is most marked in the magnetizing force intervals, 10 to 20 gausses, and between the rates for the lime-cooled and normal furnace-cooled specimens. The curves for specimens *18*, *19*, and *21* practically agree throughout the entire range of the magnetizing force, and for higher values the three corresponding curves are plotted as one curve.

Digitized by Google

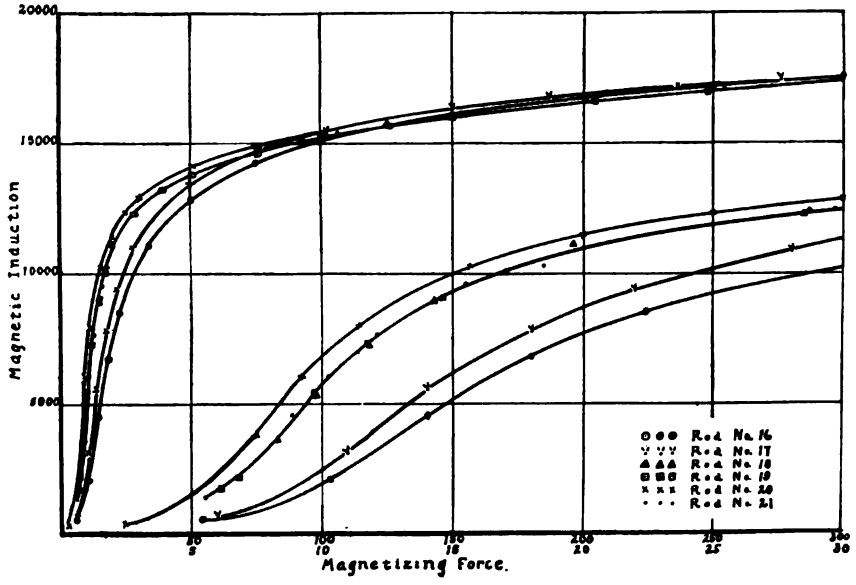

FIG. 2.—*Curves showing effect of rate of cooling annealed eutectoid carbon steel upon magnetic induction for small and intermediate magnetizing forces*

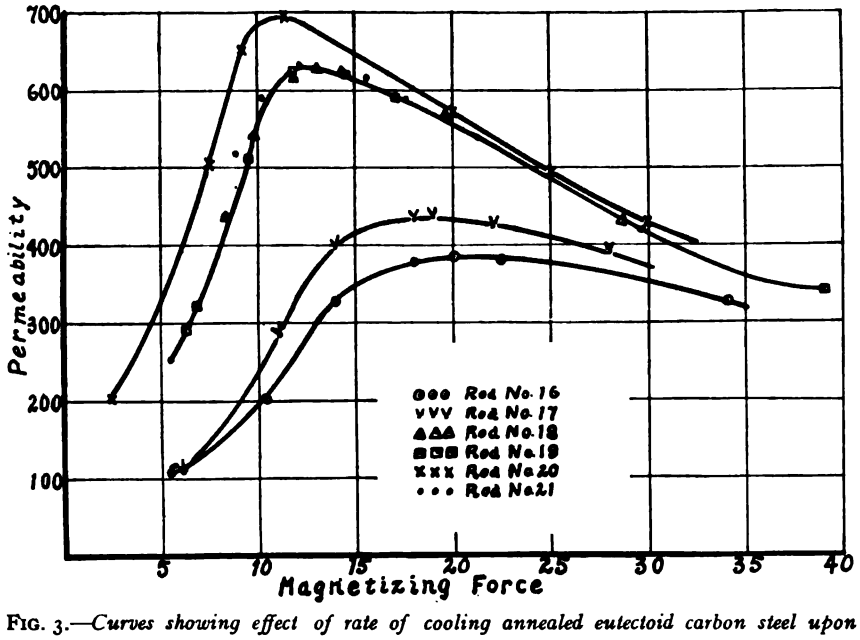

FIG. 3.—*Curves showing effect of rate of cooling annealed eutectoid carbon steel upon permeability*

Digitized by Google

The relationship between the magnetizing force and the corresponding induction can, perhaps, best be noted by plotting the permeability against the magnetizing force as the independent variable, as shown in Fig. 3. Each curve passes through a maximum of increasing magnitude as the rate of cooling of the corresponding specimen decreases. A continual shifting of this maxi-

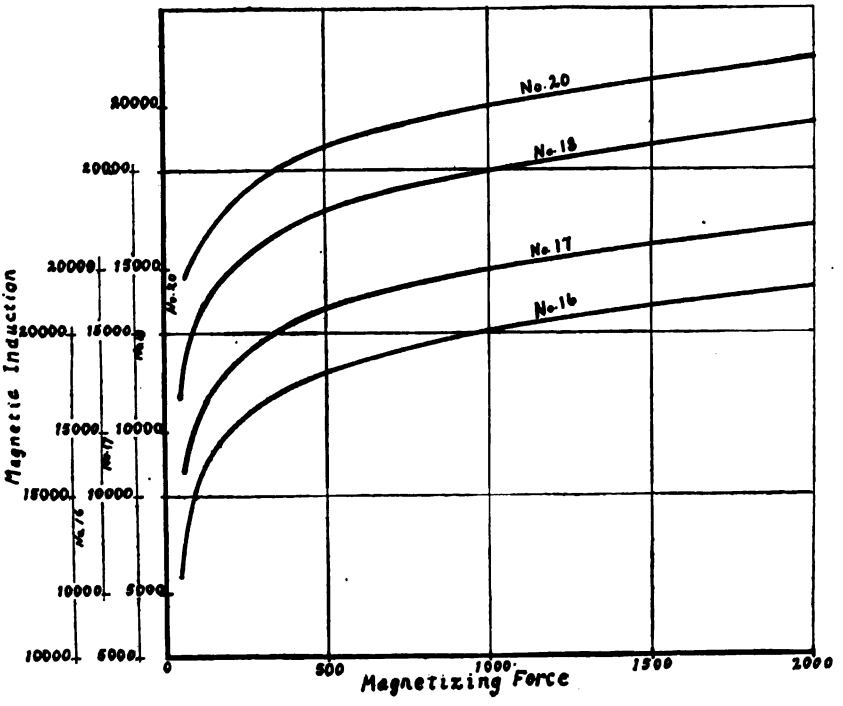

FIG. 4.—*Curves showing effect of rate of cooling annealed eutectoid carbon steel upon magnetic induction for large magnetizing forces*

mum toward the origin is also to be noted. The values of the maximum permeability are given in Table 1.

In Fig. 5 are plotted for the respective specimens the reciprocals of the susceptibility, $\frac{I}{K}$, against the magnetizing force, H, as the independent variable. All of the curves have a quite pronounced bend in the straight-line portions of the curve. As has been shown in a previous paper,[6] this bend is due to the presence of a magnetically harder constituent, the cementite in the form of conglomerate, stratified, or "divorced" masses. The reciprocal of the slope of the lower straight-line portion of the curve is pro-

[6] Nusbaum, Cheney, and Scott, B. S. Sci. Papers, No. 404; 1920.

Digitized by Google

portional to the "apparent" maximum intensity of magnetization, while the reciprocal of the slope of the upper part of the straight-line portion of the curve is proportional to the "real" maximum intensity of magnetization of the material for the particular arrangement of the constituents. Both the apparent and real saturation values are given in Table 1. Attention is called to the

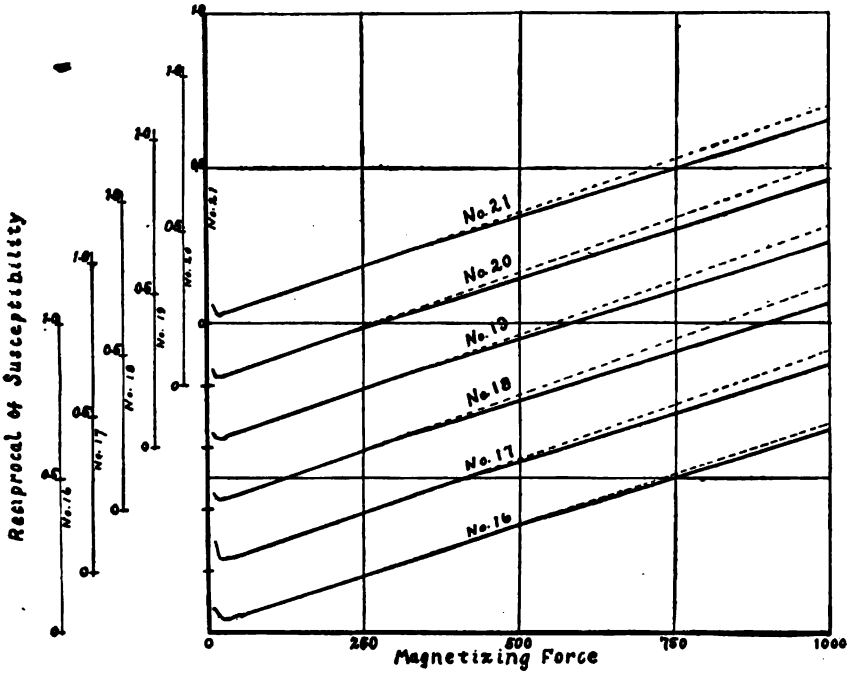

FIG. 5.—*Curves showing effect of rate of cooling annealed eutectoid carbon steel upon reciprocal of susceptibility*

gradual shift of the bend in the curves toward lower values of the magnetizing force with decreasing values of the rate of cooling.

3. MICROSCOPICAL ANALYSIS

The micrographs of Figs. 6 to 11, inclusive, all at a magnification of 500 diameters, represent the average structural condition shown by etching for 10 seconds in 5 per cent alcoholic picric acid. The difference between the furnace-cooled, the air-cooled, and the lime-cooled specimens is very marked. The air-cooled material (specimen *16*, Fig. 6) consists largely of sorbite with intervening patches of coarse pearlite. In these patches "free" ferrite is seen

[1] This analysis was made by H. S. Rawdon, chief of the metallographic laboratory of the Bureau of Standards, to whom the writers are greatly indebted for his painstaking work.

Digitized by Google

FIG. 6.—*Micrograph of specimen 16, cooled in air from 800° C*

FIG. 7.—*Micrograph of specimen 17, cooled in lime from 800° C*

Digitized by Google

to exist, often in masses of considerable size. The effect of the slow cooling in lime (specimen *17*, Fig. 7) was to allow most of the grains, sorbitic when air cooled, to form as lamellar pearlite. The patches of coarse pearlite with the conspicuous free ferrite still persist after cooling in lime.

The four specimens (Nos. *18*, *19*, *20*, and *21*, Figs. 8, 9, 10, and 11), cooled slowly in the furnace, are very similar in structure. Patches of lamellar pearlite were found in the structure of each, the amount decreasing somewhat as the rate of cooling of the specimen was decreased. The matrix of the material in each case (specimens *18*, *19*, *20*, and *21*) consists largely of divorced pearlite; that is, cementite particles in a matrix of ferrite. The size of the cementite particles increases somewhat as the rate of cooling of the specimen is decreased.

IV. DISCUSSION

The magnetization curves for specimens *18* to *21*, inclusive, are quite characteristic of magnetic materials in the annealed condition. This is indicated by the comparatively high values of the maximum permeability. The results obtained are similar to those of Yensen[8] on electrolytic iron melted in vacuo. In his experiments much slower rates of cooling were used. However, the effect of magnetizing forces of *15* gausses in the eutectoid steel is more pronounced than for corresponding rates of cooling in pure iron. This effect is evidently due to the influence of the cementite in the resulting sorbitic and pearlitic structures acting both as a magnetically harder medium and as a retarding agent for the transformation from gamma to alpha iron. The first of these is more likely the predominant factor.

The experiments of Howe[9] show a quite definite relationship between the logarithm of the time of cooling from 800 to 650° C and the resulting structure of a eutectoid carbon steel. While the results here presented show no mathematical relationship between the cooling rates and the magnetic constants, there is, however, a marked correspondence. The maximum induction increases or decreases directly, and the coercive force, inversely, with the time of cooling from 800 to 650° C. The residual induction does not show as marked a relationship. Since both the magnetic constants and the metallographic structure are in-

[8] T. D. Yensen, Univ. of Illinois Engineering Experiment Station Bull. No. 72; 1914.
[9] Howe and Levy, Jour. Iron and Steel Inst., 94, pp. 210–232; 1916.

Digitized by Google

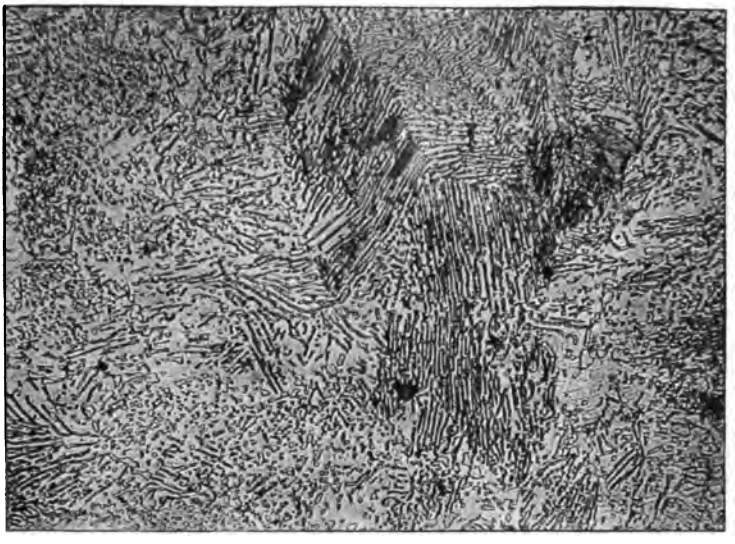

FIG. 8.—*Micrograph of specimen 18, cooled in furnace from 800° C*

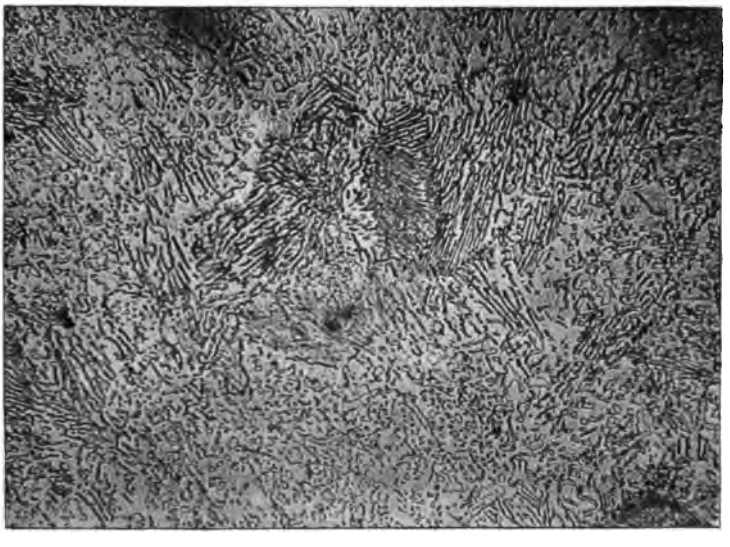

FIG. 9.—*Micrograph of specimen 19, cooled slowly in furnace from 800° C*

Digitized by Google

fluenced by the rate of cooling, these constants should be useful in the application of magnetic tests for determining the quality and structure of steel.

As already stated, the break in the reluctivity line increasingly shifts toward the origin with slower cooling rates. In the air-cooled specimen, where the structure consists largely of sorbite with intervening patches of coarse pearlite, the break occurs at the highest value of the magnetizing force. As the material is allowed to cool at various rates so as to form a gradation in structure from sorbite to divorced pearlite, the break is shifted toward lower values of the magnetizing force. There is also a greater difference between the real and apparent maximum intensity of magnetization. In specimens *18*, *19*, and *21*, where patches of lamellar pearlite exist, the shifting of the break toward the origin is still more pronounced, all of the breaks occurring at approximately the same magnitude of the field values. There is also the largest difference between the real and apparent values of the maximum intensity of magnetization. The break in the reluctivity line occurs at the lowest field value in specimen *20*, where the pearlite is most completely divorced. For a more complete degree of "divorcing" (the "spheroidal" state) the break would probably occur at still lower values of the magnetizing force. This shifting is very likely due not only to changes in the magnetic properties of the ferrite matrix, one of the magnetic constituents, but also to the change in the flux distribution produced by the change in the arrangement of the cementite relative to the ferrite.

The scleroscope hardness and the resistivity as related to the cooling rates are interesting and significant. There is also a quite definite relationship between the coercive force and the scleroscope hardness, except for specimen *21*, which was maintained at 650° C for a definite time. It should be remembered, however, that the scleroscope measures essentially a property of the material quite near the surface, while the coercive force is a property of the material as a whole.

V. SUMMARY

In this paper are presented data showing the influence of various rates of cooling on the magnetic and other physical properties and the resulting metallographic structure of a eutectoid carbon steel. The results may be briefly summarized as follows:

Digitized by Google

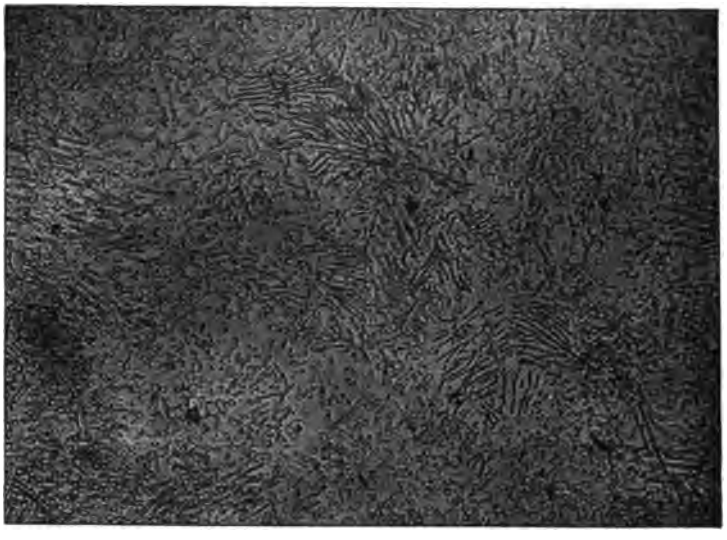

FIG. 10.—*Micrograph of specimen 20, cooled slowly in furnace from 800° C*

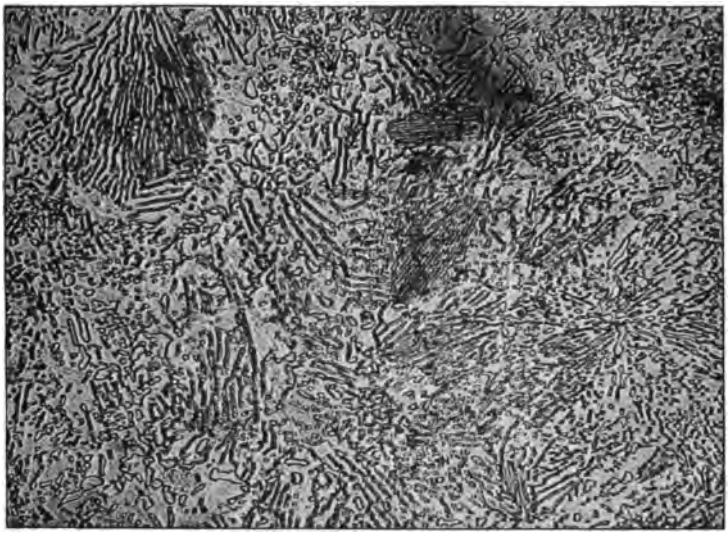

FIG. 11.—*Micrograph of specimen 21, cooled slowly in furnace from 800° C and held at 650° C for definite period of time*

Digitized by Google

1. With decrease in the cooling rate there is a marked increase in the value of the maximum induction for a given value of the magnetizing force, an increase in the magnitude of the maximum permeability, and a decrease in the magnitude of the coercive force.

2. As the structure is changed from an essentially sorbitic one, through lamellar pearlite to divorced pearlite, there is a gradual shifting of the break in the reluctivity line toward the origin. Also the difference between the magnitudes of the real and apparent values of the maximum intensity of magnetization is greatest when the structure is that of lamellar pearlite.

3. There is a marked agreement between the values of the coercive force and the scleroscope hardness, as influenced by the various cooling rates, except when the specimen is held at a temperature of 650° C for a definite time.

WASHINGTON, October 20, 1920.

Digitized by Google

MAY ⌣ 1921

LIBRARY OF THE UNIVERSITY OF CALIFORNIA

DEPARTMENT OF COMMERCE

SCIENTIFIC PAPERS

OF THE

BUREAU OF STANDARDS

S. W. STRATTON, DIRECTOR

No. 409

A NEW METHOD FOR THE MEASUREMENT OF PHOTOGRAPHIC FILTER FACTORS

BY

RAYMOND DAVIS, Photographic Technologist

Bureau of Standards

FEBRUARY 5, 1921

PRICE, 5 CENTS

Sold only by the Superintendent of Documents, Government Printing Office
Washington, D. C.

WASHINGTON
GOVERNMENT PRINTING OFFICE
1921

Digitized by Google

Digitized by Google

A NEW METHOD FOR THE MEASUREMENT OF PHOTOGRAPHIC FILTER FACTORS

By Raymond Davis

ABSTRACT

A new method is described whereby the filter factors for orthochromatic and panchromatic plates with various filters may be determined with apparatus using a source of light which is corrected in its spectral energy distribution to closely approximate that of average noon sunlight.

The apparatus is essentially a single light source photometer in which two beams one from either side of the lamp, are reflected so that they fall side by side on the photographic plate which is used in conjunction with the filter. In the path of one of these beams the filter is inserted, consequently weakening the light in that beam. The lamp, being movable between two of the reflectors, is shifted toward the filter, thus increasing the intensity of the beam on the filter side and diminishing it on the other. Successive exposures are thus made at different lamp positions, so chosen that some fall on one side of the photographic match and some on the other. After development the differences in density between each pair of exposures is measured, and the position of a photographic match obtained therefrom by plotting these differences against the scale of the instrument. Knowing the length of the path of the two beams of light the law of inverse squares is applied to calculate the filter factor.

CONTENTS

	Page
I. Introductory	80
II. Apparatus and method of procedure	80
1. Description of instrument	80
2. Experimental procedure	81
3. Measurement of the plates	83
III. Necessary precautions	84
1. Adjustment to out-of-doors conditions	84
2. Exposure time	84
3. Reliable shutter	85
4. Absorbent backing for the plates	85
5. Avoiding uneven densities	86
IV. Precision attainable	86
V. Possible applications of this photometer	88
VI. Summary	89

24634°—21

Digitized by Google

I. INTRODUCTORY

Orthochromatic and panchromatic plates are almost always used with photographic filters (colored screens of glass or gelatin) to control the color and intensity of the light falling on the photographic plates. Since the use of a filter decreases the intensity of certain colors on the plate the photographic exposure through a filter will be greater than that required for the same plate used without a filter.

A filter factor is the ratio of the exposure required with a given filter to the exposure without the filter; hence, to obtain the proper time of exposure when using the filter, the proper time of exposure without the filter should be multiplied by the filter factor.

Heretofore, so far as the author knows, filter factors have been determined by either of two methods. First, the method of trial and error; and second, the measurement, in some form of sensitometer, of plate speeds without and with the given filter. In the course of a study of the plates and films made in the United States it was desired to measure, among other things, the filter factors of all orthochromatic and panchromatic emulsions for a number of different filters. A method was thereupon devised with which it has been possible to measure filter factors with an accuracy equal to or better than that attained in careful speed measurements, and yet with much less effort.

II. APPARATUS AND METHOD OF PROCEDURE

1. DESCRIPTION OF APPARATUS

The apparatus, Fig. 1, is as follows: Light from the two sides of a standard metal filament lamp L is reflected by similar reflectors M_1, M_2, M_3, M_4, and by similar prisms, P_1 and P_2, so that the two beams fall side by side on the photographic plate E, the filter factors of which are to be determined. In front of the plate E is a simple shutter. The source of light L is movable along the line joining M_1 and M_3. At F, between M_3 and M_4, supports to hold the filters are inserted.

The lamp initially at the position a will give two beams of equal intensity at the photographic plate if the distances traversed by them are the same and if identical optical conditions of reflection and absorption obtain for the various media through which they pass. If a filter be inserted in one path, the intensity of that beam is decreased, so in order to make the beams of the same intensity

Digitized by Google

it is necessary to shift the lamp toward the filter, position *b*, thus shortening that path and increasing the other. In the case without a filter equal illumination is obtained with equal paths; the ratio by which the filter decreases the intensity of the light is equal to the square of the length of the path without the filter, divided by the square of the length of the path which contains the filter. This ratio is the filter factor sought.

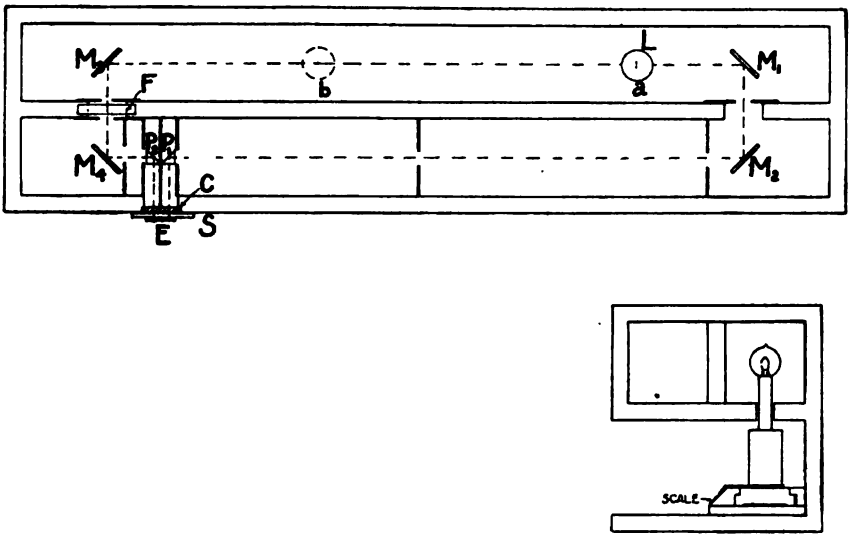

FIG. 1.—*Plan and sectional view of filter-factor apparatus*

2. EXPERIMENTAL PROCEDURE

In practice the point of balance is determined by making a series of exposures on the plate with the lamp at such distances that some are distributed on one side of the point of balance and some on the other. The plate is developed and fixed, and the density differences corresponding to the given positions of the lamp are measured on a polarization photometer. These differences are then plotted (as shown in Fig. 2) against the position of the lamp—positive or negative according to whether the setting made the lamp distance too large or too small—and the setting for a balance located where the smooth curve crosses the position axis.

In the plot given the scale zero is taken as the point of balance without a filter. With the K_1 filter, the curve is found to cross the instrument scale at 27 cm. Hence, 27.0 is the distance in centimeters of the new point of balance with the K_1 filter from the point of balance of the instrument without the filter.

Digitized by Google

Knowing the length of the paths of light to the point of balance without a filter and the distance of the new point of balance with the filter from the position of equilibrium without the filter, the law of inverse squares can be applied to calculate the filter factor. For example:

Length of path of each beam of light when both beams give equal exposure without the filter = 100 cm;

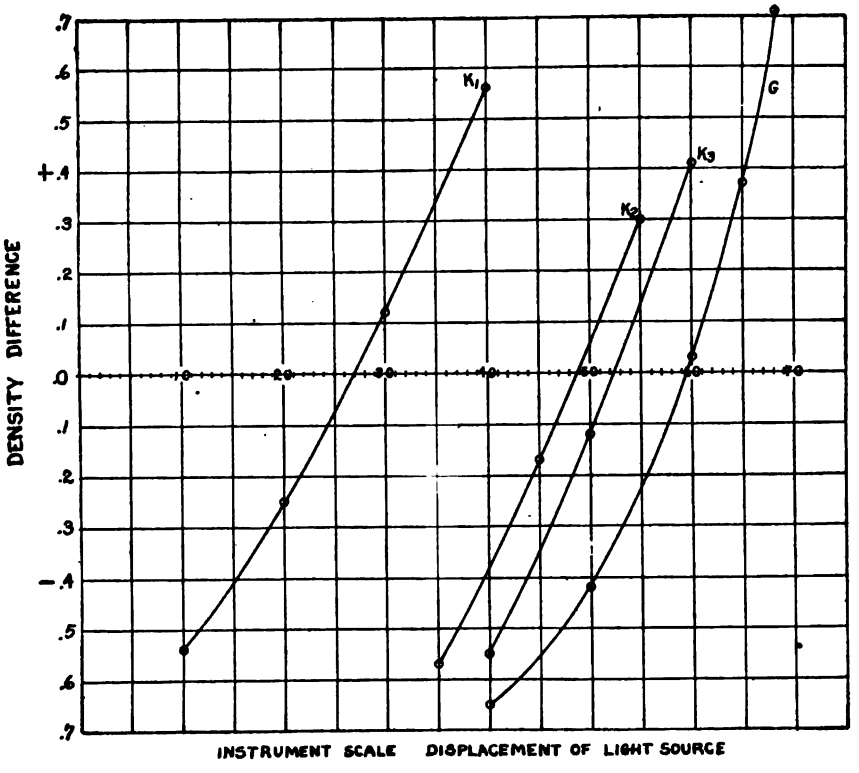

FIG. 2.—*Typical curves of density differences, showing the method of plotting*

Point of balance with the K_1 filter (that is, distance by which one of the beams was lengthened and the other shortened) = 27.0 cm;

Hence, Length of path on one side = 100 + 27.0 = 127.0 cm;

Length of path on other side = 100 − 27.0 = 73.0 cm;

Applying the law of inverse squares:

$$\text{Filter factor sought} = \frac{127^2}{73^2} = 3.03.$$

The apparatus as constructed has each path about 1 m long when the lamp is in the zero position, and the lamp has a move-

Digitized by Google

FIG. 3.—*Photometer for measuring test plates*

Digitized by Google

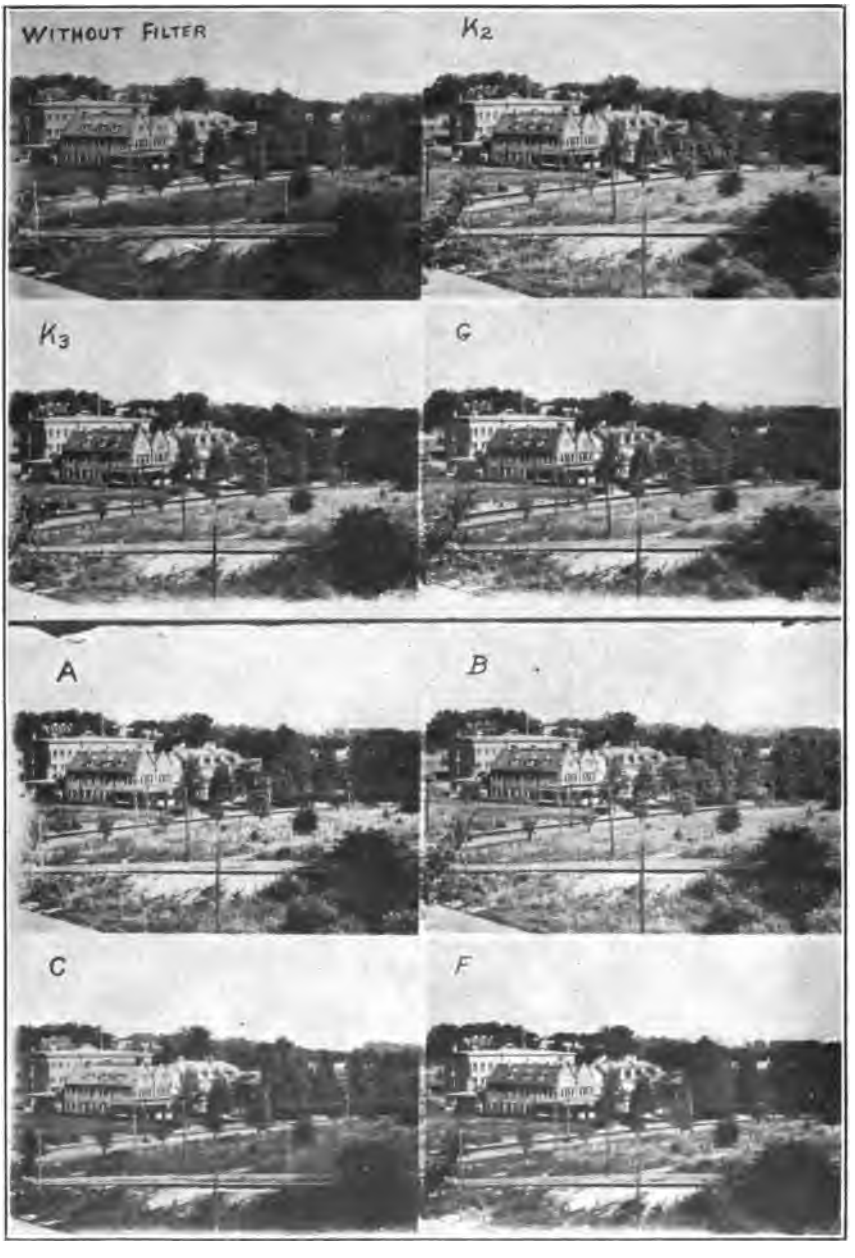

FIG. 4.—*Photographs taken with and without filters*

The exposure times with filters were adjusted according to the measured factors

Digitized by Google

ment of about 69 cm, so that the range of factors which can be measured is from 1 to 30. The filters used must be larger than one-half inch square. The strips of the photographic plate tested are 1⅛ by 5 inches, permitting two filter factors to be measured conveniently on each.

In measuring filter factors, four or five settings (one exposure at each setting) are made with each filter as described in Section II, 2. Since nine exposures can be made on each test plate, a single plate serves to test two filters.

The trouble and loss of time required to make preliminary tests were avoided by preparing tables, such as Table 1, which give the range of settings of the lamp suitable to the color sensitivity of the various types and brands of plates and filters. For example, filter K_1 with a panchromatic plate was tested for the scale positions 10, 20, 30, and 40. This procedure is practicable because the variation in color sensitivity with emulsions of the same brand is as a rule not nearly so large as the differences in the same type of emulsions of different manufacture.

TABLE 1.—Range of Settings for Class C Plates

PANCHROMATIC PLATES

Filter	Factor range	Use scale settings
K_1	1.5 to 5.5	10—20—30—40
K_2	2.8 to 12.3	25—35—45—55
K_3	5.5 to 23	40—50—60—65
G	5.5 to 30	40—50—60—65—68.2
A	9.3 to 30	50—60—65—68.2
B	5.5 to 23	40—50—60—65
C	5.5 to 23	40—50—60—65
F	9.3 to 30	50—55—60—65—68.2

ORTHOCHROMATIC PLATES

K_1	1.5 to 5.5	10—20—30—40
K_2	2.8 to 12.3	25—35—45—55
K_3	5.5 to 23	40—50—60—65
G	5.5 to 30	40—50—60—65—68.2

3. MEASURING THE TEST PLATES

The photometric apparatus used to measure the density differences was constructed primarily for measuring the density of the test plates exposed in the sensitometer. In this the photometer P, Fig. 3, is a Martens polarization instrument. The illumination in box B is diffuse, the light entering the photometer being reflected

Digitized by Google

from a ground opal glass plate, surrounded on four sides with ground glass, outside of which are placed electric lamps symmetrically arranged to give uniform illumination. The test strip is placed in the sliding holder *S*, which by means of stops brings the center of the two squares under the respective apertures of the photometer. The angular readings of the polarization instrument are reduced to densities by means of a table computed for the purpose.

III. NECESSARY PRECAUTIONS

1. ADJUSTMENT TO OUT-OF-DOORS CONDITIONS

In order to have filter factors which can be used out of doors, it is necessary to modify the distribution of spectral energy of the metal-filament lamp. This is accomplished by placing in both beams a suitable screen (at *C*, Fig. 1). It is also necessary to run the lamp at a constant and specified current so as to keep its spectral distribution constant. This combination of lamp and filter gives a close approximation in spectral energy distribution to that of average noon sunlight at Washington and is identical with that used as the standard light source of the Bureau of Standards sensitometer. That the apparatus furnishes satisfactory results in this respect is shown by the illustrations in Fig. 4, in which the calculated exposures used ran as high as 24 times that without the filter. As can be seen, the exposures, which were proportional to the filter factors as measured, were made on two plates, the two being developed together for the same length of time and printed simultaneously on one sheet of paper. The filters used (Wratten) and their factors for the plate used (Wratten M) were as follows:

Filter	None	K_2	K_3	*G*	*A*	*B*	*C*	*F*
Factor	1	4	4.5	5.5	18	14	12	24

2. THE EXPOSURE TIME

The exposure time is of considerable importance and should be such that the operation is confined to the straight-line portion of the characteristic (*H* and *D*) curve for the plate tested. With a few exceptions, this straight-line portion is sufficiently long so that difficulties arising from this cause are not to be expected. Table 2 shows the effect of using exposures longer than the straight-line part. For this series of tests a thinly coated plate having a

Digitized by Google

scale of only 15 was selected and from it two test pieces cut and exposed as indicated—one plate with the light source on one side of the position of photographic match (scale 35) and the other with it on the opposite side (scale 45).

Thus, compared with a plate in the filterless arm, the plate for position 45 had an excess density (density difference +0.15, for exposure ½); while the other plate for position 35 had a less density (−0.03). Each of these pairs of densities was used as in Fig. 2 for determining the position of match, and therefrom the corresponding filter factor in column 4 calculated. Nine exposures varying in time from one-half to four seconds were thus made on each plate. They show that a three-fourth-second exposure has carried the effect on the undimmed part beyond the straight-line portion of the characteristic curve.

TABLE 2.—Effect of Overexposure on the Calculated Filter Factor

Position of lamp on scale		Approximate exposure	Filter factor (calc.)
35	45		
		Seconds	
−0.03	+0.15	½	3.00
− .03	+ .15	½	3.00
− .03	+ .14	½	3.05
− .04	+ .15	½	3.08
− .05	+ .13	¾	3.20
− .09	+ .10	1	3.40
− .12	+ .08	2	3.70
− .10	+ .05	3	3.76
− .12	+ .02	4	4.25

3. RELIABLE SHUTTER

For measurements of this kind the shutter should be mechanically operated and so arranged that the timing can be adjusted to suit the sensitiveness of the material to be tested. It should also, of course, be of such construction that the exposure time is repeated with moderate precision for all the exposures of a given set, else false density differences may result.

4. ABSORBENT BACKING FOR THE PLATES

It is necessary to back all plates used for sensitometric tests with some light-absorbing medium to prevent halation. This backing to be effective must be in optical contact with and of about

Digitized by Google

the same refractive index as the glass plate. In all of our sensitometric work black shellac has been used for this purpose. When properly made and applied, it is very effective, but is more difficult to remove than the burnt-sugar backing usually recommended. The chief advantage of the shellac mixture is that it dries very quickly and does not come off or injure the developing and fixing solutions. It may be removed by scraping with the edge of a rectangular block of wood. The plates should be exposed and developed soon after the backing has become dry because it is much easier to remove it then than if applied several hours before developing.

5. AVOIDING UNEVEN DENSITIES

The condition of the surface of the test plate when placed on the racks to dry is also important. Besides being sponged off with wet absorbent cotton to remove sediment accumulated from the solutions and wash water, all drops of water must be removed from the surface of the film, otherwise the densities will be uneven, due to the unequal rate of drying of the different parts.

IV. PRECISION ATTAINABLE

High precision can not be obtained with any apparatus where the results depend on the density of the silver deposit on commercial photographic plates and films. This is clearly shown by the results of a series of tests recorded in Table 3. For this, six 5 by 7 plates were selected and numbered 1 to 6, inclusive. Plates 1, 2, and 3 were of the same manufacture—the second, seventh, and last plate in a package—the rest of different manufacture. Each plate was cut into five standard-size test pieces, four of which were selected for test. Each strip furnished two determinations for the filter factor—four exposures being used in each case to locate the position of photometric balance. Thus the vertical columns in the table give the variation in the factor over the same plate, and its mean value; the first three columns show how it varies with different plates of the same manufacture; the first five, how the factor for the same filter (K_2) varies with the plates of different manufacture; while column 6 is added merely to show the variation over a single plate for a *G* filter.

Digitized by Google

TABLE 3.—Showing Filter Factor Variations

Plate	No. 1	No. 2	No. 3	No. 4	No. 5	No. 6
Filters	K_3	K_3	K_3	K_3	K_3	G
Filter factors	13.75	13.20	13.60	5.18	4.80	27.0
	13.92	13.41	13.68	5.41	4.85	27.0
	14.00	13.35	13.82	5.37	4.82	26.6
	14.18	13.95	14.00	5.12	4.76	26.6
	13.92	13.82	14.10	5.41	4.85	26.6
	13.68	14.10	13.65	5.41	4.82	27.0
	14.10	13.41	14.80	5.45	(a)	26.4
	14.42	13.60	14.60	5.37	(a)	27.4
Average	13.99	13.60	14.03	5.34	4.82	26.8
Max. dev., per cent	3.1	3.7	5.5	4.1	1.2	2.2

[a] Defective plates.

The maximum variation from the mean for any single plate, 1.2 per cent to 5.5 per cent, may seem large, but it is after all very satisfactory when compared with the variation in the sensitiveness of the commercial materials.

The following experiments demonstrate the corresponding density variation of different parts of single plates. Two 5 by 7 inch plates of different makes were placed behind a grid consisting of five opaque black bars separated by their own width—each bar half as wide as the standard test plate. Each plate was first given a timed exposure to the regular source (compensated to sunlight distribution) placed at 3 m distance. The plate was then shifted across the grid so that the parts just exposed were covered by the bars and the parts unexposed uncovered. With a color filter introduced in the light path, in one case a K_3 and the other a G filter, a second exposure was then made. For the K_3 filter the second exposure was adjusted by the filter factor to give equal density, while for the G filter a somewhat lower density was purposely sought. The two plates were developed together to a moderate contrast, and after fixing, washing, and drying were cut into standard size test strips, each test strip having a pair of exposures running the full length, one the result of the exposure with the color filter and one without. The difference in density, measured at intervals of one-half inch along the length of the strip—given in Tables 4 and 5—shows the resulting variations in density differences.

Digitized by Google

TABLE 4.—Variation in Density Over a Single Plate—K_2 Filter

Strip No. 1	Strip No. 2	Strip No. 3	Strip No. 4	Strip No. 5
−0.01	−0.02	+0.01	−0.02	−0.01
+ .01	− .01	− .01	− .01	− .01
+ .01	+ .01	− .01	+ .01	− .01
+ .03	.00	.00	+ .01	+ .01
.00	+ .01	− .01	− .01	+ .03
0.00	−0.01	−0.01	0.00	+0.04
+.01	.00	− .02	− .01	+. 03
.00	− .01	+ .01	− .01	+. 02
−.03	− .01	+ .02	− .03	+. 01

TABLE 5.—Variation in Density Over Another Plate—G Filter

Strip No. 1	Strip No. 2	Strip No. 3	Strip No. 4	Strip No. 5
−0.17	−0.13	−0.15	−0.15	−0.16
− .12	− .15	− .17	− .15	− .12
− .16	− .15	− .15	− .14	− .11
− .13	− .12	− .14	− .15	− .16
− .11	− .14	− .14	− .13	− .08
−0.09	−0.14	−0.12	−0.14	−0.08
− .09	− .12	− .10	− .09	− .09
− .09	− .12	− .11	− .13	− .09
− .07	− .12	− .09	− .09	− .11

Table 4 shows, for one type of plate and filter, a range of density differences from +0.04 to −0.03, that is of 0.07; while Table 5 shows, for another plate and filter, a range from −0.07 to −0.17, that is 0.10. It should be added that the density differences recorded in Table 4 were proved to be real by setting the photometer for zero difference and observing that the match was thereby destroyed. Furthermore, it was observed that if the photometer were set for a match at a fixed place on the test plate, the match was destroyed when the test plate was moved to another position. It is therefore obvious that the method of testing is distinctly more reliable than the emulsion is uniform.

V. OTHER POSSIBLE APPLICATIONS OF THE PHOTOGRAPHIC PHOTOMETER

By replacing the filter under test with sectored wheels the intermittency effect in photographic exposures, with light sources of different intensity and different intermittency, can readily be investigated.

Digitized by Google

The apparatus could be modified so as to measure the relative energy in different parts of the spectrum of two light sources provided suitable monochromatic filters were at hand. This method would be specially valuable where comparisons in the blue end of the spectrum are of importance, such as perhaps in the effect of humidity, etc., in the study of the variation of flame standards as compared with electric standards. Such information would be of special value in the application of flame standards for sensitometry.

VI. SUMMARY

A new method is described whereby the filter factors for orthochromatic and panchromatic plates with various filters may be determined with apparatus using a single source of light. The energy distribution of the lamp is corrected to closely approximate that of average noon sunlight, so that the values obtained are applicable in actual practice.

The test procedure is described, and an example given to illustrate the method of calculating the factor.

Some of the most important precautions necessary for accurate work are enumerated.

Experimental evidence is given to show that the accuracy of the instrument is distinctly greater than the emulsions are uniform.

Suggestions as to the possible applicability of the apparatus to other problems are made.

WASHINGTON, July 31, 1920.

Digitized by Google

Digitized by Google

JUL 5 1921

LIBRARY OF THE UNIVERSITY OF CALIFORNIA

DEPARTMENT OF COMMERCE

SCIENTIFIC PAPERS

OF THE

BUREAU OF STANDARDS

S. W. STRATTON, DIRECTOR

No. 410

THERMAL EXPANSION OF COPPER AND SOME OF ITS IMPORTANT INDUSTRIAL ALLOYS

BY

PETER HIDNERT, Assistant Physicist

Bureau of Standards

MARCH 21, 1921

PRICE, 25 CENTS

Sold only by the Superintendent of Documents, Government Printing Office
Washington, D. C.

WASHINGTON
GOVERNMENT PRINTING OFFICE
1921

Digitized by Google

Digitized by Google

THERMAL EXPANSION OF COPPER AND SOME OF ITS IMPORTANT INDUSTRIAL ALLOYS

By Peter Hidnert

ABSTRACT

Data on the thermal expansion of 128 samples of copper and its important alloys of various compositions, heat treatments, mechanical treatments, etc., are presented. The specimens contained from 56 to 100 per cent copper and were prepared in a number of ways—cast, cast and cold-rolled, extruded, extruded and cold worked, hot-rolled and cold worked. Most of the samples were examined from room temperature to about 300° C. (Several specimens were cooled to −50° C and then heated to +300° C.)

Practically all available information on the thermal expansion of copper and its alloys is briefly reviewed.

A description of the apparatus and the preparation of the samples, etc., are given.

Definite mathematical relations were found to exist between the coefficients of expansion and the copper content of most of the alloys investigated (Series II, III, V, VI). In general, the coefficient of expansion increases with a decrease in the copper content. The addition of lead or tin has a decided effect on the coefficient; the former element generally decreases and the latter increases the coefficient.

Cast and Cold-Rolled Copper-Zinc Alloys (Series II and III).—In the case of alloys containing 62 per cent copper, it was found that the coefficients did not materially differ in cast or cold-rolled specimens, and for alloys containing 90 per cent copper a similar agreement existed. For alloys with a copper content from about 62 to 90 per cent the cold-rolled alloys have greater coefficients than the castings, and for alloys containing more than 90 per cent copper the reverse is true. The coefficients of the inside sections of the castings are generally slightly less than those of the outside sections. A relation exists between the density and thermal expansion of the cold-rolled copper-zinc alloys (Series II).

Cast and Cold-Rolled Copper-Tin Alloys (Series V and VI).—The coefficients of the cold-rolled tin alloys are less than those of the castings. Cold-rolling and drawing, therefore, cause a diminution in the values of the coefficients.

Hot Rolled and Extruded Specimens (Series I, IV, and VII).—Owing to the large number of varying elements in the hot-rolled and extruded samples, it was impossible to determine the exact effect of each constituent element. In general, however, the coefficients are greater than the extrapolated values obtained from the quadratic equations of the copper-zinc alloys (Series II and III).

The differences between the various series of samples are discussed in the section "Comparison of Results" and presented graphically in Figs. 39 to 43.

The appendix gives average coefficients of expansion of all the samples investigated.

Digitized by Google

CONTENTS

	Page
I. Introduction	92
II. Previous determinations	93
III. Materials investigated	98
IV. Apparatus and evaluation of constants	101
V. Experimental and derived results	107
1. Series I. Copper: Electrolytic, nickeliferous, arsenical	107
2. Series II. Cold-rolled copper-zinc alloys	109
3. Series III. Sections of copper-zinc castings	116
4. Series IV. Extruded and hot-rolled copper-zinc alloys	125
5. Series V. Cold-rolled copper-tin alloys	132
6. Series VI. Sections of copper-tin castings	133
7. Series VII. Aluminum bronze	136
8. Relation of density to thermal expansion	138
VI. Comparison of results	140
VII. Summary and conclusions	149
VIII. Appendix	151

I. INTRODUCTION

A general demand for reliable information on the thermal expansion of copper and its alloys, caused the Bureau, with the cooperation of the American Brass Co., to undertake a comprehensive investigation on this subject. An attempt has been made to determine how the coefficients of expansion vary with temperature, chemical composition, heat treatment, mechanical treatment, etc. In structural work and in the design and construction of various apparatus, such as steam and pressure gages, thermostats, automatic valves, etc., many questions relating to expansion arise. The following article should answer many questions of expansivity in so far as these refer to apparatus constructed of these alloys.

Most of the samples were examined from room temperature to about 300° C. (Several specimens were cooled to −50° C and then heated to +300° C.) None of the determinations were made on alloys that had been annealed after cold working. The alloys investigated contain various percentages of copper (from 56 to 100 per cent), zinc (0 to 40 per cent), and tin (0 to 10 per cent). The percentages of other elements contained are relatively small. The samples are divided into seven series, according to chemical composition and treatment.

The samples and photomicrographs were prepared by the technical department of the American Brass Co., which also furnished the chemical composition. The author wishes to express his appreciation for valuable suggestions, comments, and data on

Digitized by Google

the micrographs and the preparation of the samples, given by W. H. Bassett and F. G. Smith of this company.

II. PREVIOUS DETERMINATIONS

Some of the work by previous observers on the thermal expansion of copper and copper alloys will be briefly reviewed here.

Matthiessen [1] divided the physical properties of alloys into two classes, namely, (1) Those which do not indicate their chemical nature, and (2) those which do indicate their chemical nature. He investigated the property of thermal expansion, in order to determine to which of these classes this property belongs, as well as to find the law which regulates the expansion of alloys.

His method by which the expansion of small quantities of metals and alloys could be determined was to weigh the body in water at different temperatures. The sample was slightly gilded to prevent the action of water on it. Before each weighing the water was boiled in order to expel absorbed air.

He found that copper does not behave, in one respect, like glass. The glass rods which he examined "do not return directly to their original length after being heated to 100° and cooled rapidly; copper, however, does so; for no differences in the coefficients were observed after heating the rod to 100°, determining its expansion, allowing it to stand over night, and redetermining the coefficients."

The following formulas applicable between 0° and 100° C are given for the linear and the cubical thermal expansion of copper:

$$L_t = L_0 (1 + 10^{-4} \times 0.1481t + 10^{-6} \times 0.0185t^2)$$

and $$V_t = V_0 (1 + 10^{-4} \times .4463t + 10^{-6} \times .0555t^2)$$

The corresponding formulas for a copper-zinc alloy containing 71 per cent copper are

$$L_t = L_0 (1 + 10^{-} \times 0.1720t + 10^{-6} \times 0.0186t^2)$$

and $$V_t = V_0 (1 + 10^{-4} \times .5161t + 10^{-6} \times .0558t^2).$$

These equations represent the mean of two determinations on the same sample. The results were as follows (if $V_0 = 1$):

First heating, $V_{100} = 1.005723$.

Second heating, $V_{100} = 1.005716$.

Matthiessen states that "a difference in the crystalline form will in all probability cause a slight difference in the coefficients of expansion. It is well known that alloys crystallize much more

[1] Matthiessen, Phil. Trans., 156, pp. 231, 861; 1866.

Digitized by Google

Turner and Levy [6] investigated the annealing of copper with special reference to dilatation. They state "It is common knowledge that hard copper becomes perfectly annealed by heating to 500° C; that the heating need not be for any lengthened period, and the rate of cooling afterward is unimportant."

An extensometer was employed, which was made in the metallurgical department of the University of Birmingham. Two expansion curves of hard-drawn and of annealed copper from 18° to about 600° C are shown, but no definite quantitative data are given. Turner and Levy observed "that both the heating and cooling curves are quite regular, there being no break such as would be caused by the slightest abrupt change of volume at a critical temperature. There was nothing observed which would serve to indicate at exactly what temperature hard copper passes into the soft variety."

These observers also examined five hard-drawn copper alloys, four of which, "namely, 70:30 brass, 66:34 brass, gun metal, and phosphor bronze gave perfectly regular and uniform curves as the temperature rose, and no indication was afforded as to the point at which the hard metal became annealed." They did not obtain a satisfactory curve for the fifth sample, 60:40 brass.

"The conclusion to be drawn from these experiments would appear to be that the alterations which take place when hard copper is by annealing converted into the soft variety are unaccompanied by any change in linear dimensions. It is known that the separation of a constituent as of graphite from cast iron or pearlite from steel, is accompanied by marked dilatometric changes. Le Chatelier [7] has shown that a dimorphic transformation, such as that which ferrous sulphide undergoes between 100 and 150 °, is accompanied by a marked change of volume. Allotropic changes in an element are also usually accompanied by marked alterations of volume, as in the case of pure iron at about 880° C. It is evident therefore, that such changes in the properties of copper and of copper alloys as are caused by mechanical work or annealing, respectively, are of a different order to those which are due to allotropic or dimorphic transformations, or to the separation or rearrangement of constituents. The results here recorded lead us to believe that mechanical work produces only internal rearrangement

[6] Turner and Levy, Proc. Roy. Soc., London, 80 (series A), p. 1; 1908.

[7] Metallographist, 1903, p. 23; Bull. de la Société d' Encouragement pour l'Industrie Nationale; September, 1902.

Digitized by Google

Hot-rolled S340 Cold-worked

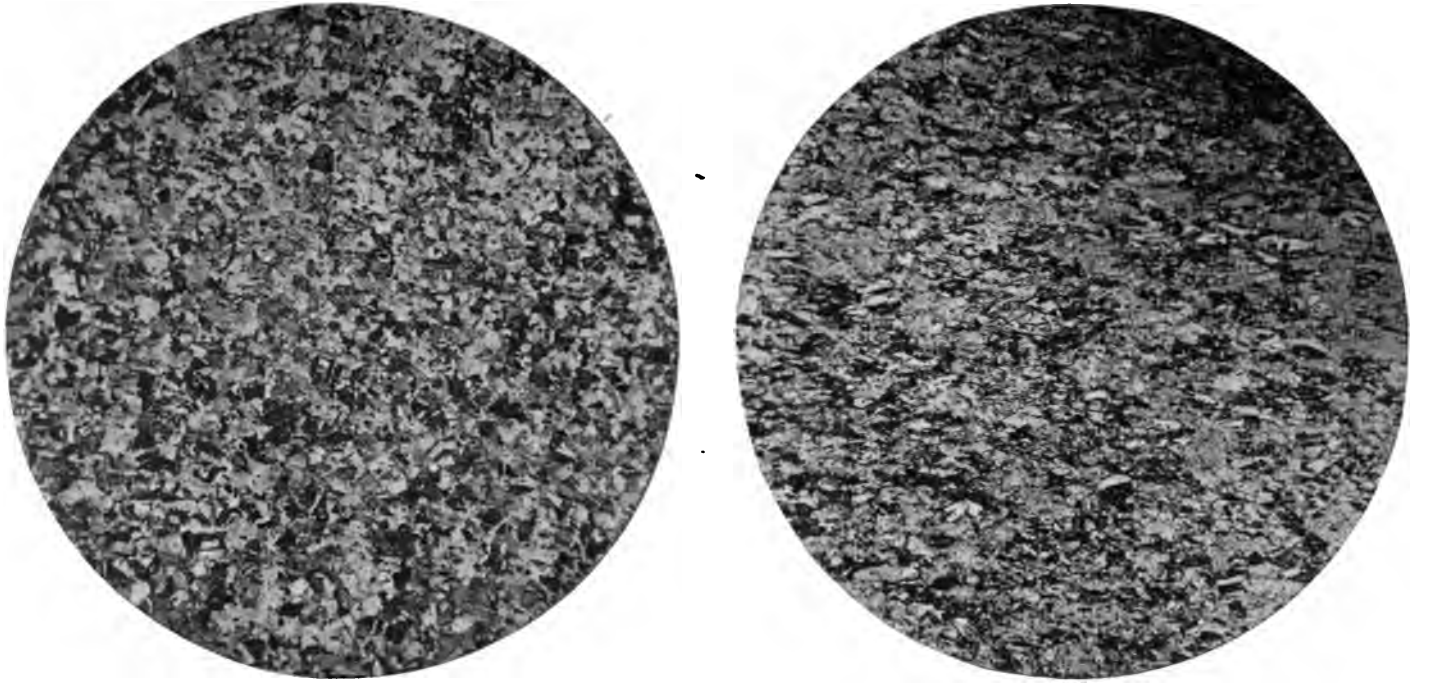

H Series I HD

FIG. 1.—*Electrolytic copper.* ×75

Copper 99.968

Digitized by Google

Digitized by Google

of the metallic grains or molecules, but does not lead to any chemical or physical changes such as are correctly regarded as allotropic. We have met with no evidence to support the view that allotropic change results from mechanical work."

Price and Davidson [8] reported Bureau of Standards observations [9] on the thermal expansion of 17 samples of rolled brass cut longitudinally and of 12 samples cut transversely to the direction of rolling. The specimens varied from 0.256 to 0.034 inch in thickness. The various thicknesses were obtained by cold-rolling. The chemical composition of these specimens was as follows:

	Per cent
Copper	64.71
Zinc	35.27
Iron	.02
Lead	None

Observations on the expansion of the 29 samples were made from room temperature to about 300° C.

Several curves are shown, but no attempt was made to determine the coefficients of expansion, their relation to the percentage reduction in thickness due to rolling, nor the differences between the coefficients of corresponding longitudinal and transverse samples. It is hoped to compute and discuss the coefficients of expansion of these brasses in a future publication.

Merica and Schad [10] investigated the thermal expansion of alpha and of beta brass between 0 and 600° C in relation to the mechanical properties of heterogeneous brasses of the Muntz metal type.

The expansion curves for alpha brass are regular, but those of beta show a transformation point at about 450°, due to a change of beta into beta prime. Alpha brass usually showed a slight permanent elongation after heating to 600° C and cooling, but in the case of beta brass a shrinkage always took place. The quadratic equations given with the curves do not, however, best fit the observations in each case.

The average coefficients of expansion of a number of brasses over different termperature intervals are given in the table on next page.

[8] Price and Davidson, Transactions of the American Institute of Metals, 10, p. 133; 1916.

[9] Observations made by L. W. Schad and Peter Hidnert of the Bureau of Standards.

[10] Merica and Schad, Journal of the American Institute of Metals, 11 (No. 3), p. 396, 1917; and B. S. Scientific Papers, No. 321; 1918.

Digitized by Google

TABLE 4.—Coefficients of Expansion of Alpha and Beta Brasses

Specimen	Phase	Chemical analysis					Average coefficients $\times 10^6$ from—					
		Copper	Zinc	Tin	Lead	Iron	20 to 100° C	100 to 200° C	200 to 300° C	300 to 400° C	400 to 450° C	500 to 600° C
		P. ct.	P. ct.	P. ct.	P. ct.	P. ct.						
215A	Alpha	65.6	32.9	1.3	0.2	0.1	19.2	20.0	22.0	22.5	23.5	24.5
216C	Beta	54.5	43.9	1.3	.1	.2	21.6	21.8	22.8	29.6	35.0	30.5
250A	Alpha	53.5	45.6	.9	Tr.	Tr.	20.1					
252A	Beta	54.7	44.5	.7	.1	.1	22.8	19.4	23.5	27.5	39.2	26.9
256A	Alpha	65.3	34.5	.23	.2	Tr.	18.7	20.0	22.0	22.5	23.0	23.7
259A	Alpha	64.6	35.4	.06	.04	< .04	22.8	22.2	21.9	22.2	23.4	23.6
261F	Beta	55.5	44.5	.07	.05	< .04	20.0	21.0	23.6	28.0	35.0	27.0

III. MATERIALS INVESTIGATED

The samples investigated are grouped into seven series as given in Table 5.

TABLE 5.—Classification of Materials

Series	Copper content range	Number of samples
	Per cent	
I. Copper: Electrolytic, nickeliferous, arsenical	99.38–99.97	4
II. Cold-rolled copper-zinc alloys	62.1 –97.0	18
III. Sections of copper-zinc castings	62.1 –97.0	72
IV. Extruded and hot-rolled copper-zinc alloys	56.4 –61.4	12
V. Cold-rolled copper-tin alloys	89.7 –95.4	4
VI. Sections of copper-tin castings	89.7 –95.4	16
VII. Aluminum bronze	92.2	2

Other details (commercial names, heat treatments, etc.) relating to these specimens will be given later. However, the following typical photomicrographs are shown and briefly explained in this section, for they are considered as partial definitions of the materials investigated.

SERIES I: COPPER (Fig. 1).—The micrograph of S340H shows the normal crystalline character of very pure copper due to self-annealing during hot-rolling. It also shows the distribution of cuprous oxide in lengthwise streaks. The micrograph of S340HD shows principally the elongation of the grains due to cold working; i. e., the structure of typical hard-drawn copper.

SERIES II AND III: COLD-ROLLED AND CAST COPPER-ZINC ALLOYS (Figs. 2 to 9).—(*a*) *Alpha Brass.*—S320 shows the structure of cast alpha brass. The grains are practically pure alpha, which agrees with the well-known equilibrium diagrams. The color shading

Digitized by Google

Cast S320 Cold-rolled

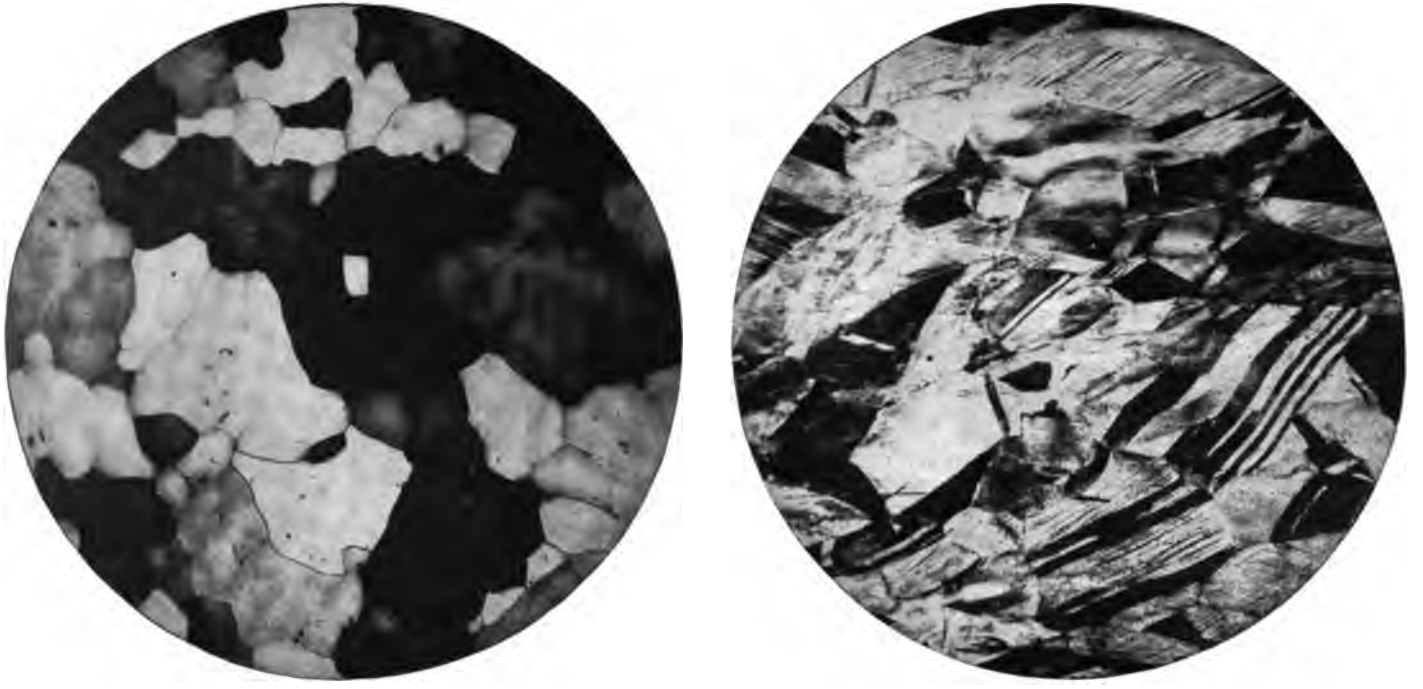

Series III Series II

FIG. 2.—*Alpha brass.* ×75

Copper 70.28, zinc 29.66, lead 0.03, iron 0.03 (cartridge brass)

Digitized by Google

Cast S328 Cold-rolled

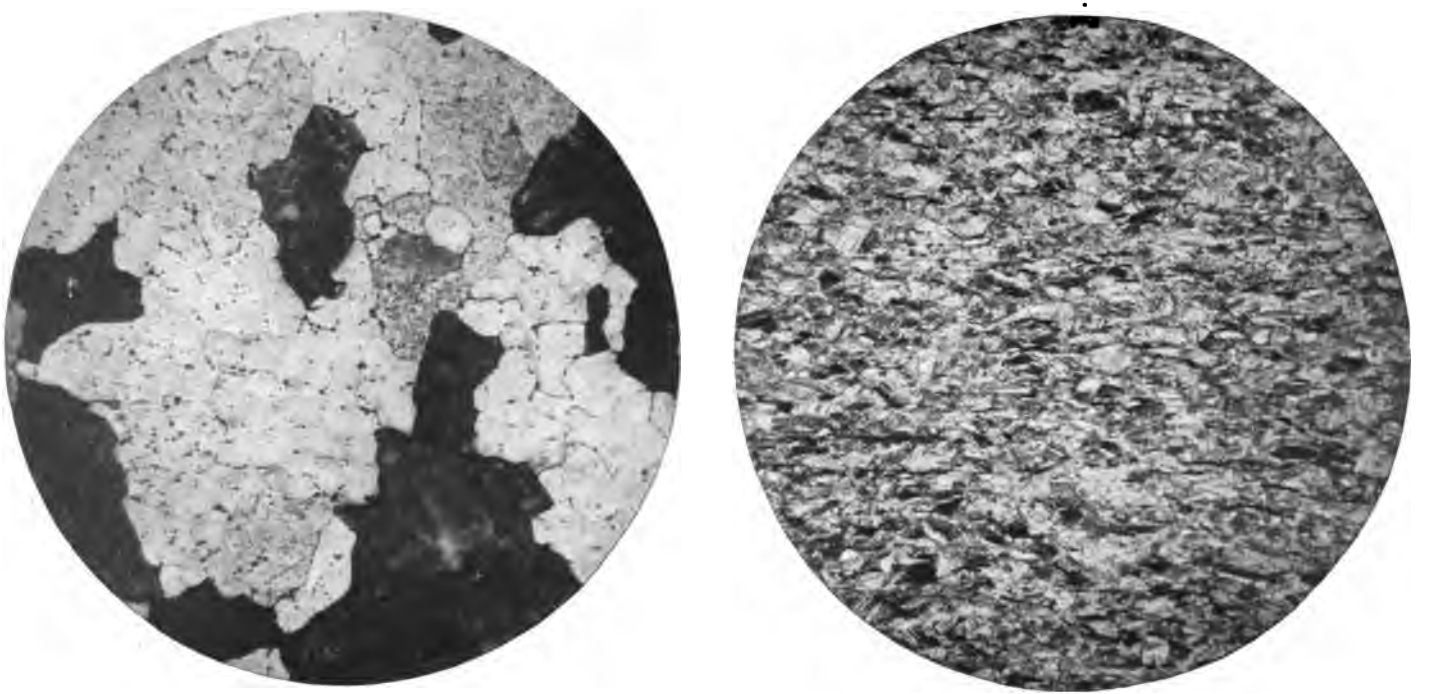

Series III Series II

FIG. 3.—*Alpha brass containing lead.* ×75

Copper 78.28, zinc 20.01, lead 1.68, iron 0.03 (leaded low brass)

Digitized by Google

Cast S333 Cold-rolled

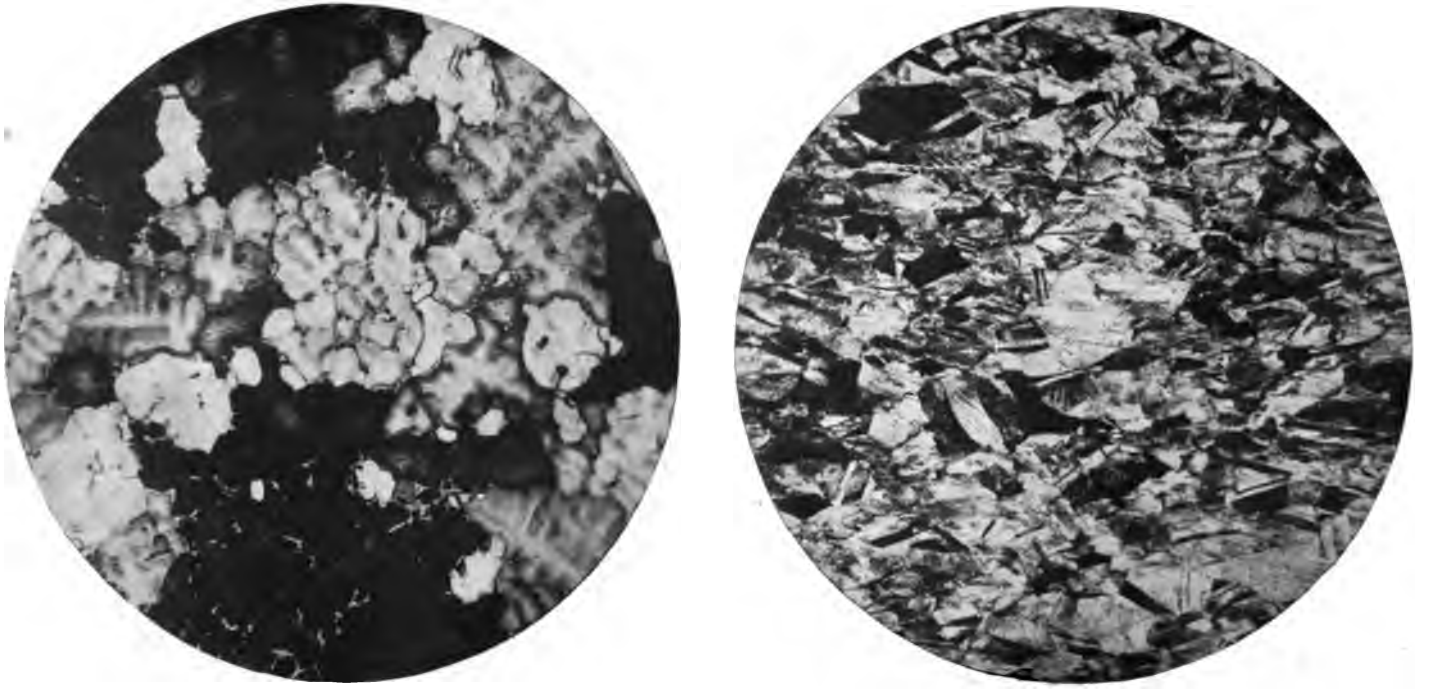

Series III Series II

FIG. 4.—*Alpha brass containing tin.* ×75

Copper 70.64, zinc 28.21, tin 1.10, lead 0.04, iron 0.01 (Admiralty condenser tubes)

Digitized by Google

Cast S321 Cold-rolled

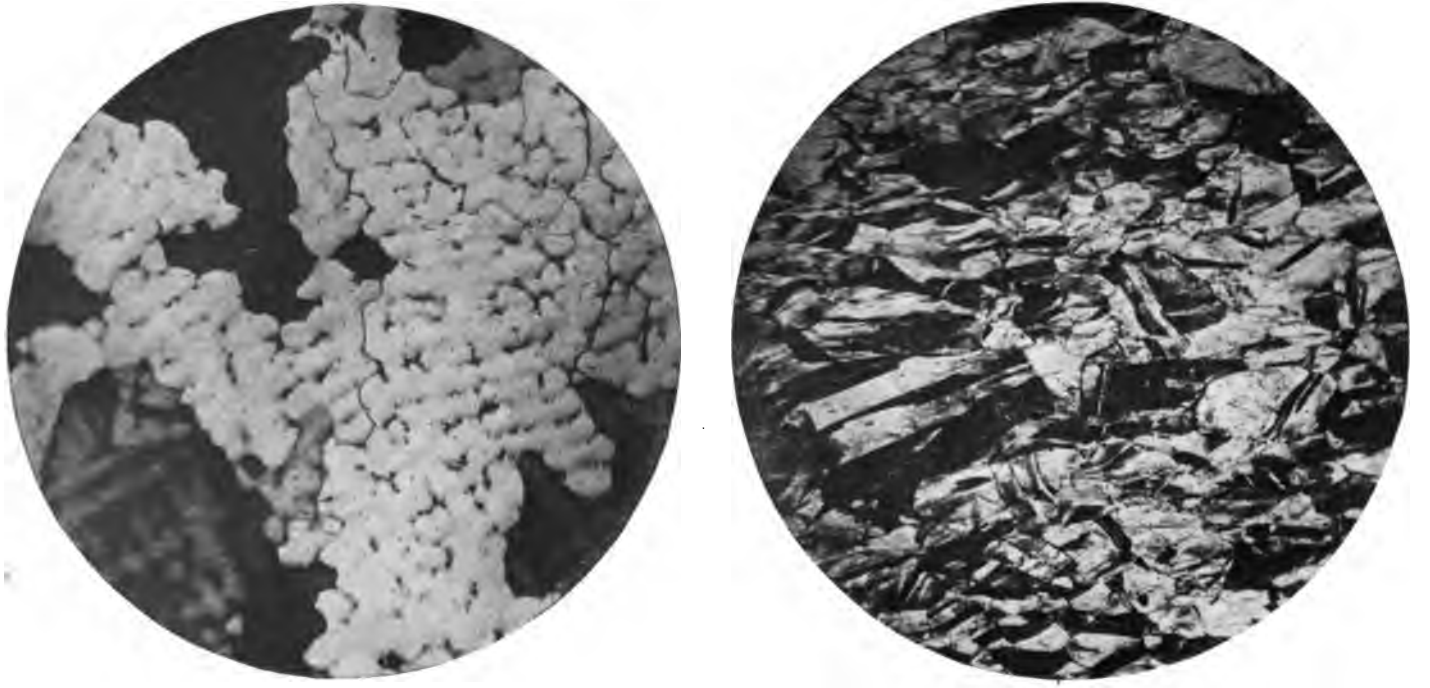

Series III Series II

FIG. 5.—*Alpha beta brass.* ×75

Copper 66.50, zinc 33.43, lead 0.04, iron 0.03 (cartridge brass)

Digitized by Google

Cast S322 Cold-rolled

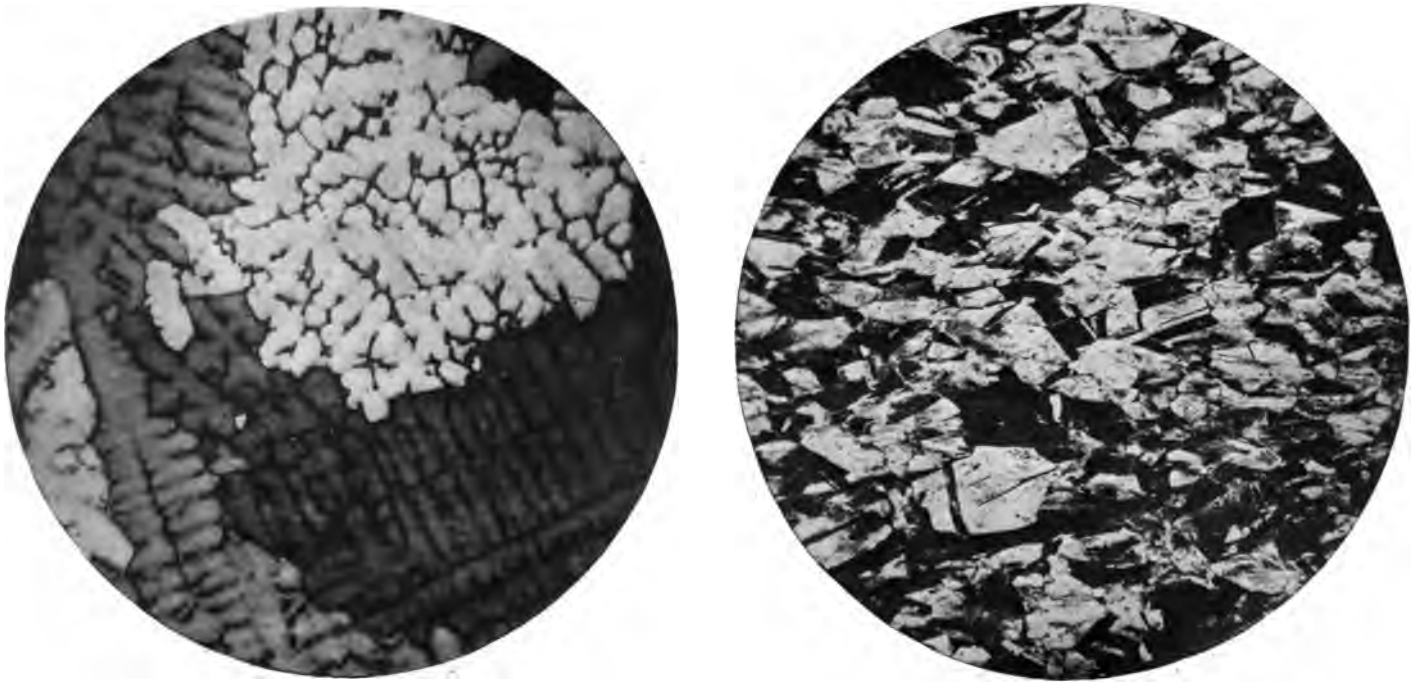

Series III Series II

FIG. 6.—*Alpha beta brass.* ×75

Copper 64.81, zinc 34.92, lead 0.24, iron 0.03 (commercial brass)

Digitized by Google

Cast S323 Cold-rolled

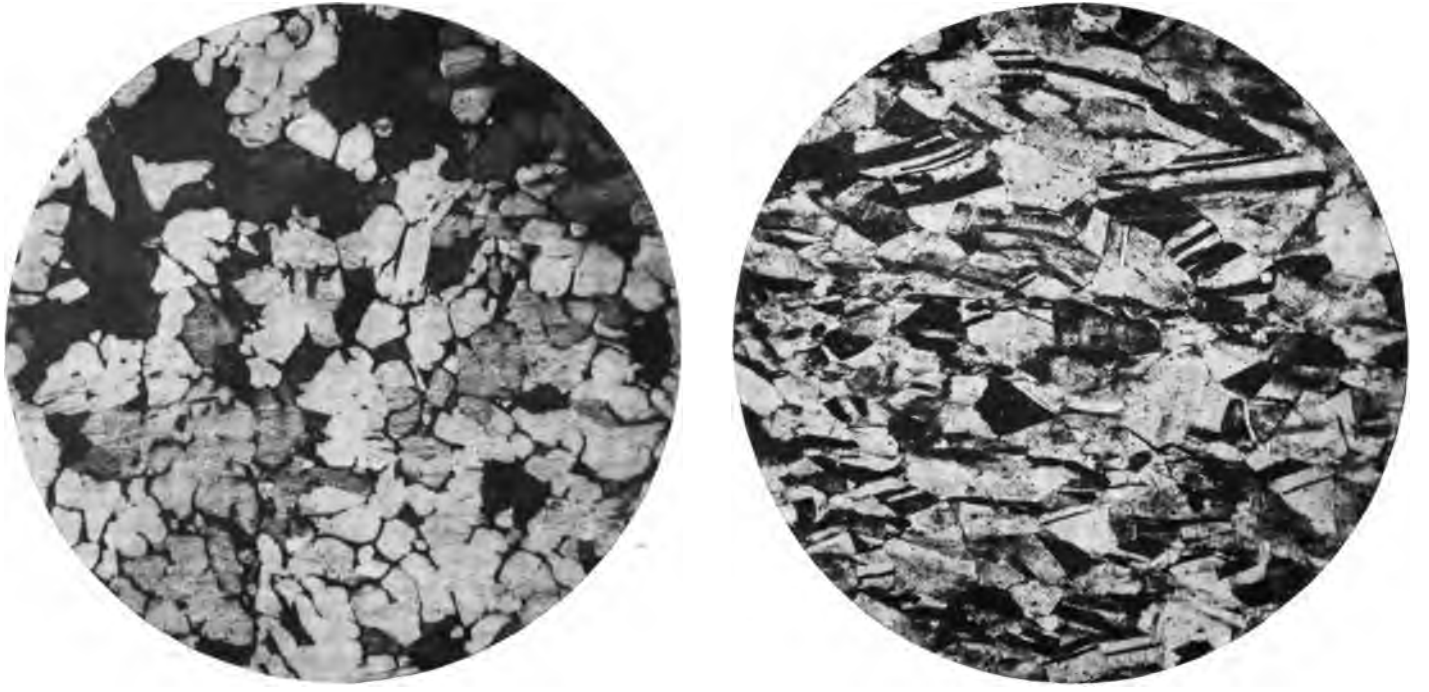

Series III Series II

FIG. 7.—*Alpha beta brass.* ×75

Copper 63.63, zinc 36.17, lead 0.17, iron 0.03 (commercial brass wire)

Digitized by Google

Cast S324 Cold-rolled

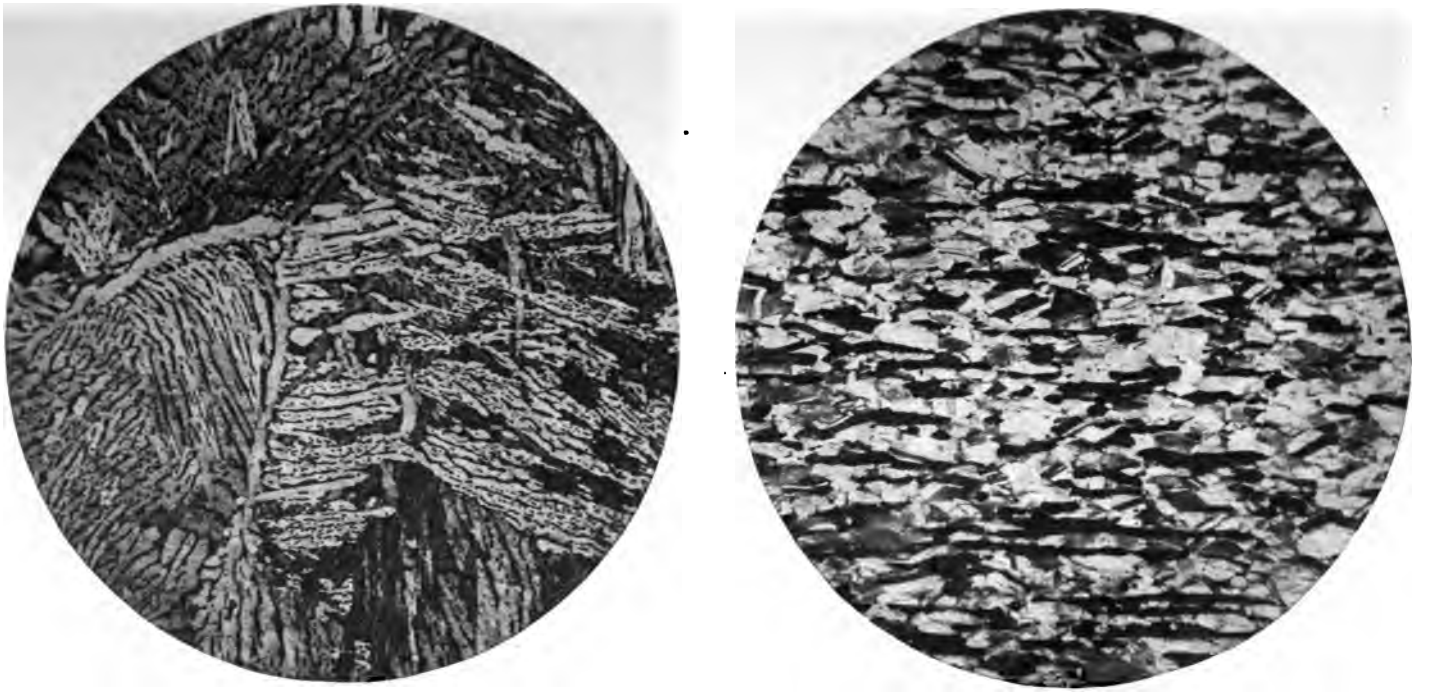

Series III Series II

FIG. 8.—*Alpha beta brass.* ×75

Copper 62.10. zinc 37.71, lead 0.17, iron 0.02 (hot-rolled brass tube)

Digitized by Google

Cast S330 Cold-rolled

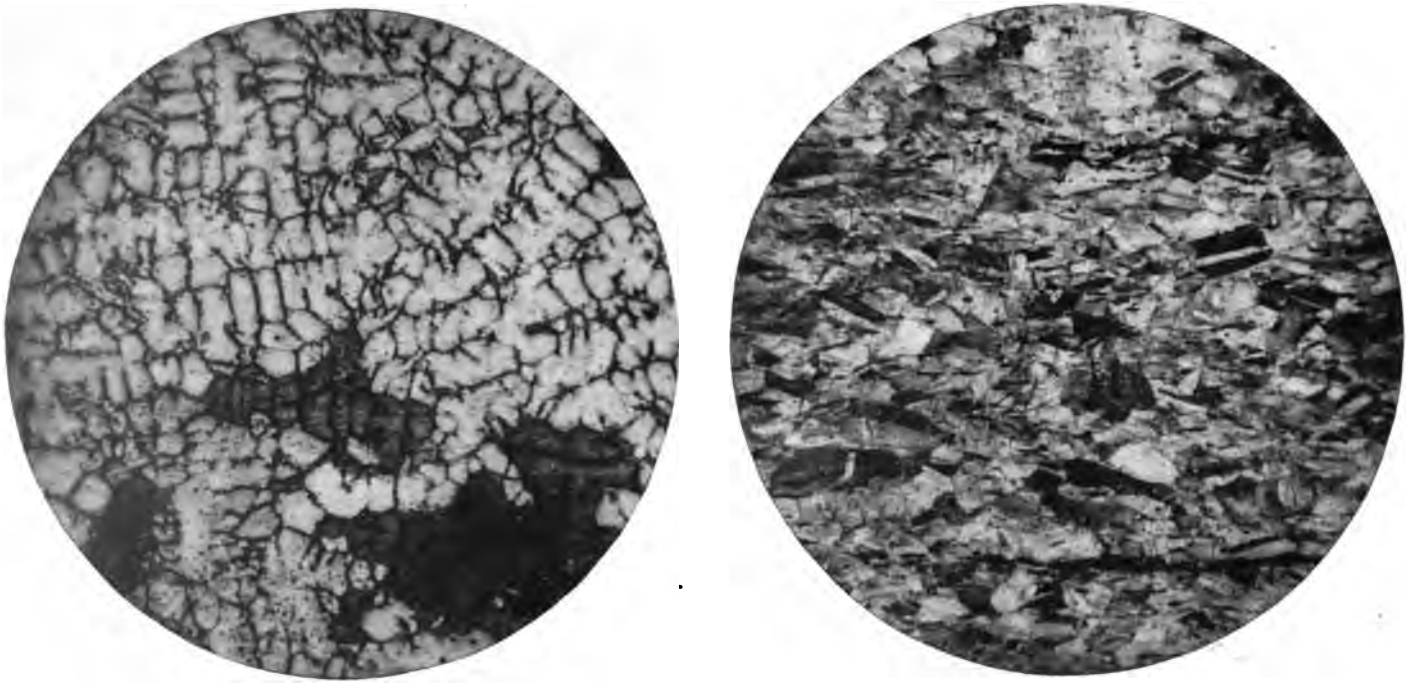

Series III Series II

FIG. 9.—*Alpha and beta brass containing lead.* ×75

Copper 62.33, zinc 35.04, lead 2.57, iron 0.06 (free turning rod)

Digitized by Google

of dendritic form indicates lack of homogeneity within the grains. The micrograph of the cold-rolled sample shows twinned alpha crystals which are the result of annealing and cold working. The elongated appearance is due to cold-drawing as the last operation.

(*b*) *Alpha Brass Containing Lead.*—S328 shows a structure similar to the casting of S320, the principal difference being that part of the lead can be seen as small dark dots mostly along borders of the grain. The corresponding micrograph of the cold-rolled sample shows the elongated twinned alpha crystals with streaks of lead scattered among them.

(*c*) *Alpha Brass Containing Tin.*—S333 shows a structure of alpha grains similar to S320. Small islands of a tin-rich alloy can be seen segregated from the alpha. The micrograph of the cold-rolled alloy shows elongated twinned alpha crystals. Annealing and cold working caused the tin to diffuse and become absorbed in the alpha grains.

(*d*) *Alpha Beta Brass.*—The structure of cast brass in which there is a varying amount of beta depending on the zinc content is shown in the micrographs of S321 to S324, inclusive. In micrograph S321 the alpha dendrites (referred to in the micrograph of the casting of S320) are bordered with islands of beta, in S322 the beta nearly envelops the alpha dendrites, in S323 there are no dendrites on account of the larger proportion of beta, and in S324 there is a new grain formation in which the grains are relatively large and consist of mixed alpha and beta surrounded by a network of alpha.

The changes in the structure due to annealing and cold working may be seen from a comparison of the micrographs of the cast and cold-rolled alloys (S321 to S324, inclusive). In the cold-rolled alloys S321 and S322 the beta, which could be seen in the castings, has diffused and none but alpha crystals can be seen. Only a small amount of beta, appearing as dark streaks, can be seen in the cold-rolled alloys of S323 and S324.

(*e*) *Alpha and Beta Brass Containing Lead.*—The structure of a cast alpha and beta brass containing lead is shown in micrograph S330. The proportion of zinc is great enough so that in the cold-rolled alloy S330 (like S323) the beta is not all diffused by the cold-rolling and annealing. A small proportion of the lead can be seen as dots in the alpha crystals. (This alloy will be compared with S343 later.)

Digitized by Google

SERIES IV: EXTRUDED AND HOT-ROLLED COPPER-ZINC ALLOYS. (Figs. 10 to 15).—(*a*) *Alpha-Beta Brass.*—The micrographs of S341 and S342 show typical structural differences between hot-rolled and extruded alloys having nearly the same composition. Both alloys have the alpha and beta Muntz structure, but the distribution of the phases is entirely different, due to the different methods of hot-working.

(*b*) *Extruded Alpha and Beta Brass Containing Lead.*—The micrograph of S343E shows elongated grain of alpha and beta. Some of the undissolved lead probably accompanies the beta.

The micrograph of S343ED shows a greater proportion of beta than casting S330 (a leaded brass of practically the same composition) of Series III, principally on account of the lesser amount of cold working and annealing the former received. The fact that the extruded alloy carries a slightly greater amount of zinc and lead has a slight bearing on the amount of beta phase. From a comparison of the micrographs of S343 and S330, the structural differences in the two leaded brasses, due to extrusion and cold-rolling, may be observed.

(*c*) *Alpha and Beta Brass Containing Tin.*—The structural differences between the hot-rolled (S344) and extruded (S345) brasses (having nearly the same composition) are shown in Figs. 13 and 14. These alloys are of the same type as S341 and S342 and have the same structural character. The small tin content has no apparent effect on the structure.

(*d*) *Alpha and Beta Bronze Containing Tin and Iron.*—The structure of a typical manganese bronze is shown in the micrographs of S346, both extruded and drawn. It is an alloy of the same general type as S342 and S345, but on account of the greater proportion of zinc the beta crystals predominate. It consists principally of beta grains through which are scattered needles and globules of alpha.

SERIES V AND VI: COLD-ROLLED AND CAST COPPER-TIN ALLOYS (Fig. 16).—The micrograph of the cast alpha tin bronze (S408) shows dendrites of alpha surrounded by beta. Within the beta there are small areas of delta or alpha and delta complex.

The corresponding micrograph of the cold-rolled sample shows elongated alpha crystals. The tin-rich parts (beta) of the castings have been completely diffused by annealing and cold working, which produced a homogeneous alloy.

SERIES VII: ALUMINUM BRONZE (Fig. 17).—The micrograph of the alpha aluminum bronze (S347H) shows the crystalline

Digitized by Google

Hot-rolled S341 Cold-worked

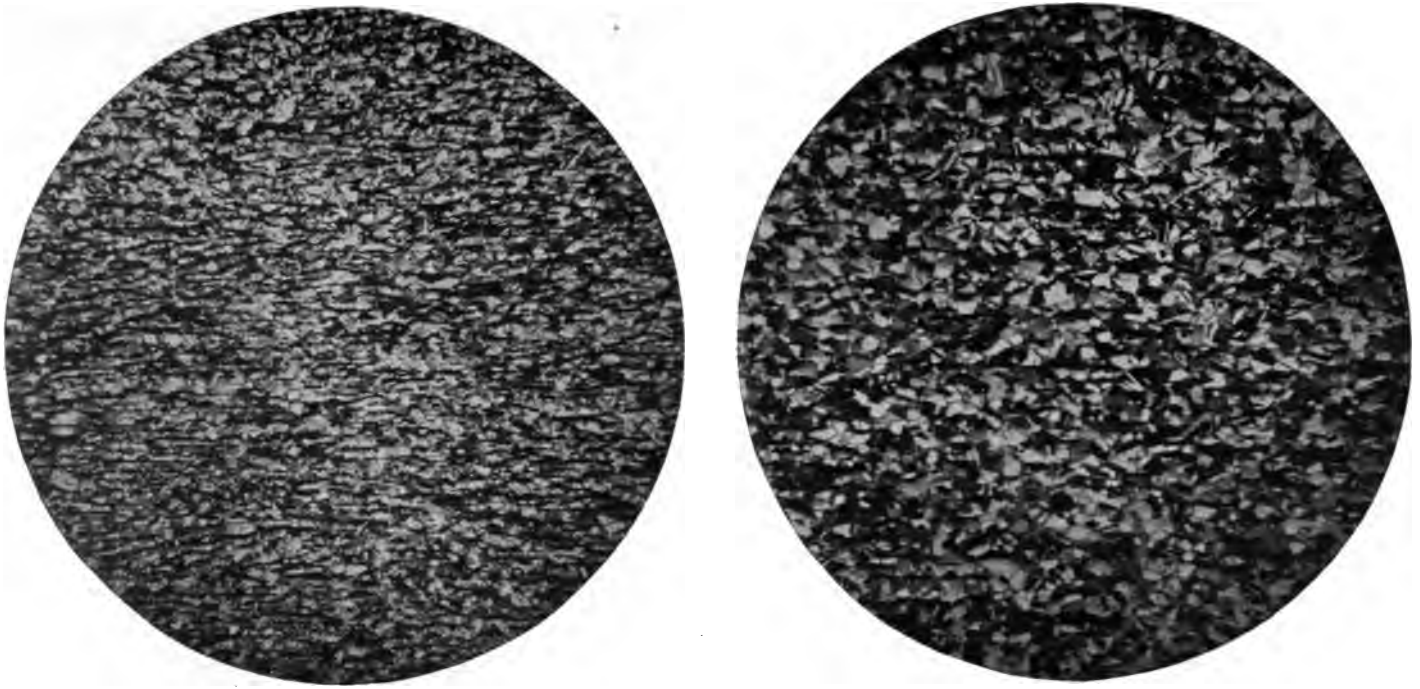

H Series IV HD

FIG. 10.—*Alpha beta brass.* ×75

Copper 61.07, zinc 38.66, lead 0.24, iron 0.03 (Muntz metal)

Digitized by Google

Extruded S342 Cold-worked

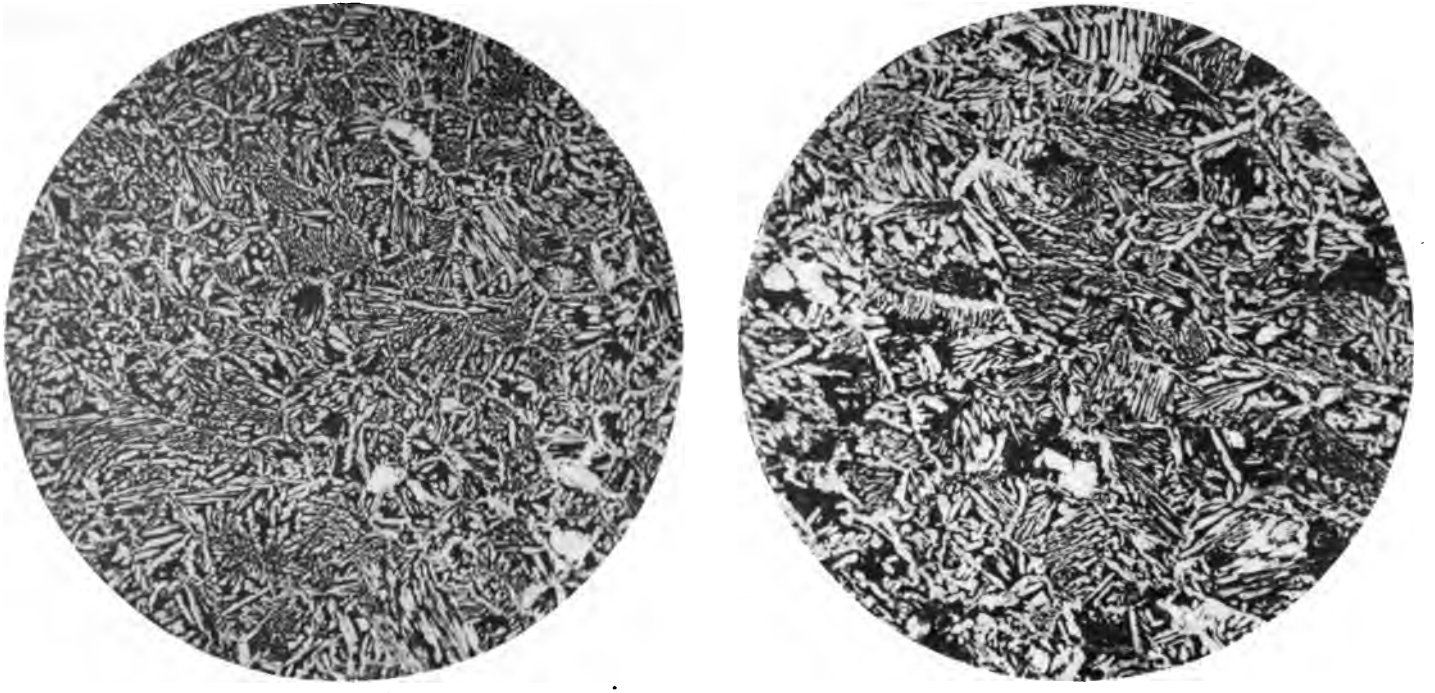

E Series IV ED

FIG. 11.—*Alpha beta brass.* ×75

Copper 59.12, zinc 40.49, lead 0.35, iron 0.04 (Muntz metal)

Digitized by Google

Extruded S343 Cold-worked

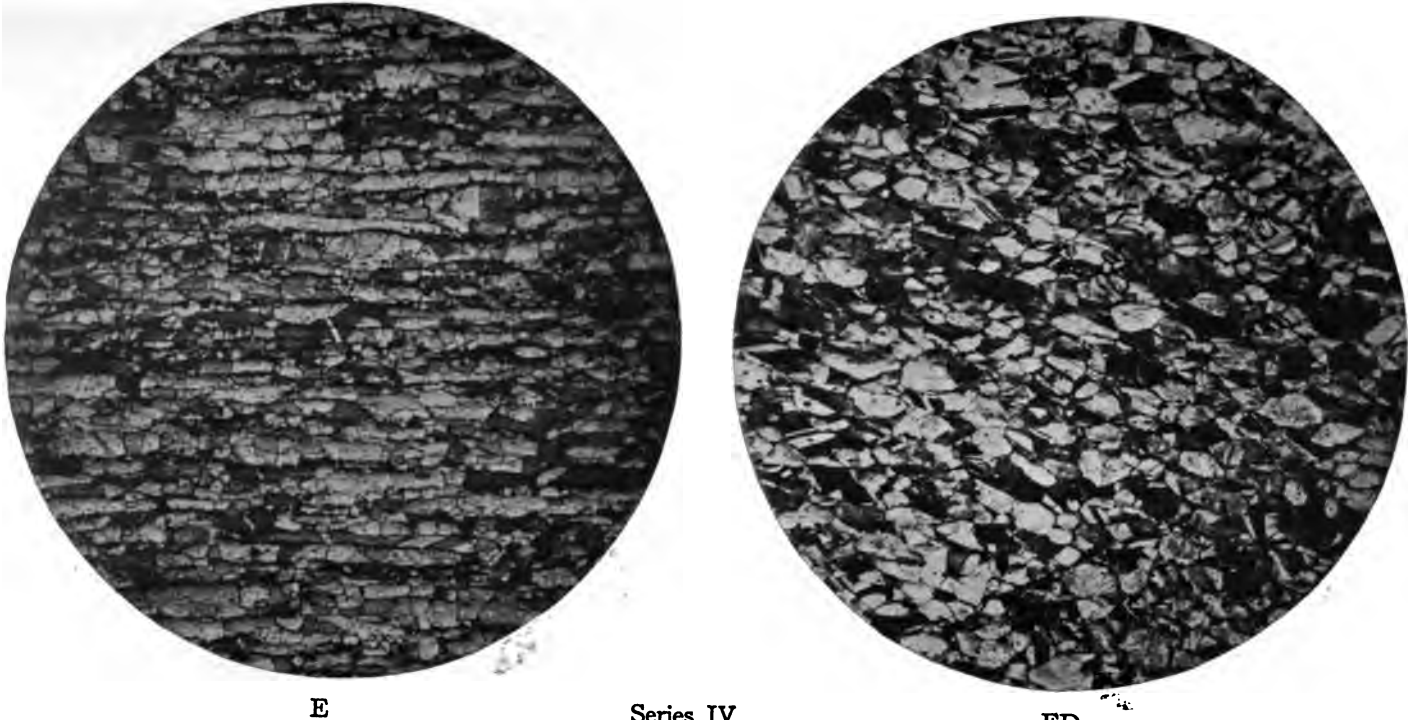

E Series IV ED

FIG. 12.—*Alpha and beta brass containing lead.* ×75

Copper 61.44, zinc 35.68, lead 2.85, iron 0.03 (free turning rod)

Digitized by Google

Hot-rolled S344 Cold-worked

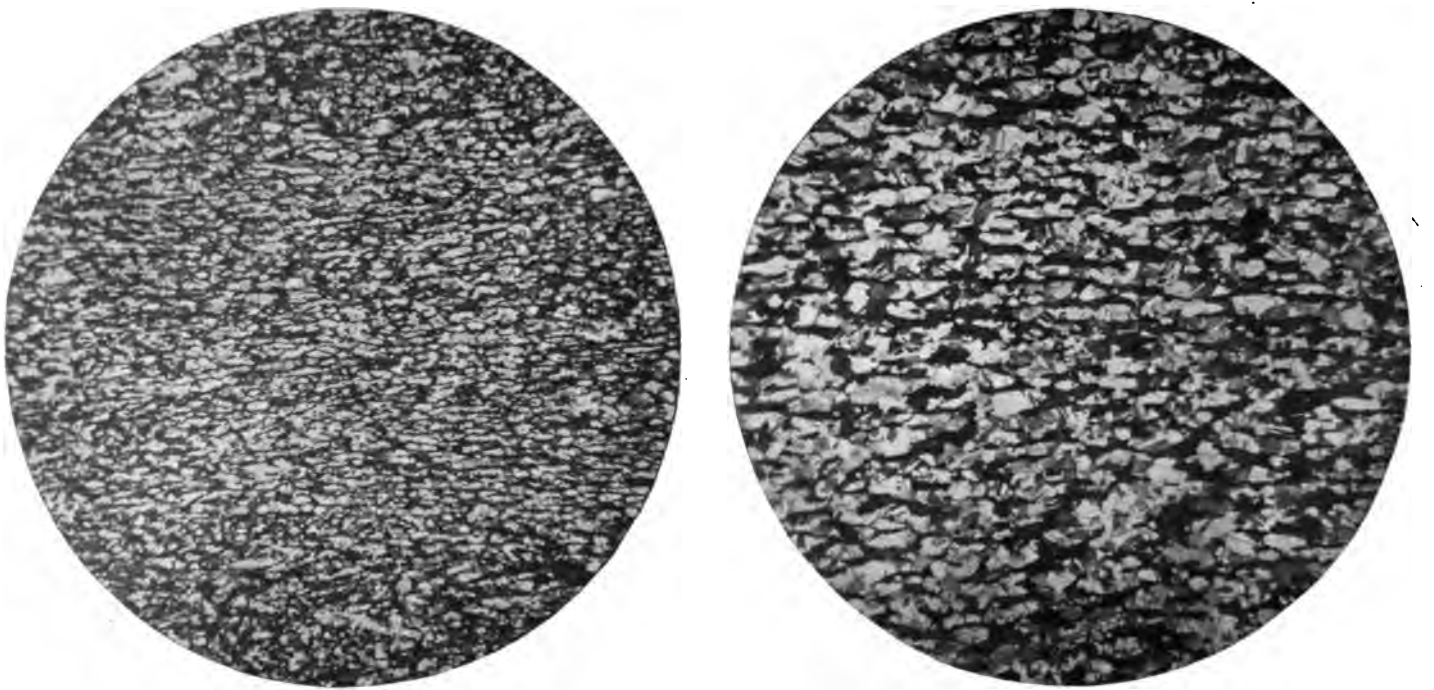

H Series IV HD

FIG. 13.—*Alpha and beta brass containing tin.* ×75

Copper, 60.21 zinc 38.86, tin 0.71, lead 0.20, iron 0.02 (naval brass)

Digitized by Google

Extruded S345 Cold-worked

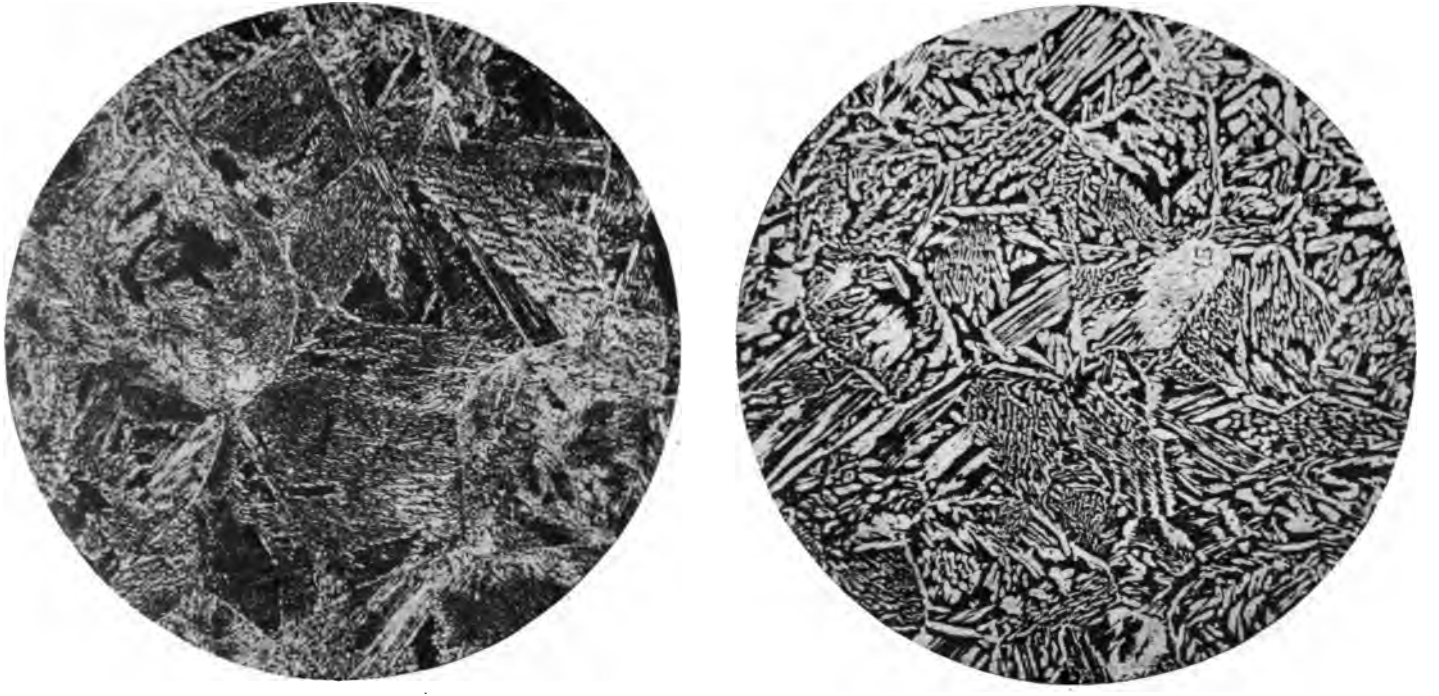

E Series IV ED

FIG. 14.—*Alpha and beta brass containing tin.* ×75

Copper 58.96, zinc 40.16, tin 0.84, lead 0.06, iron 0.01 (naval brass)

Digitized by Google

Extruded S346 Cold-worked

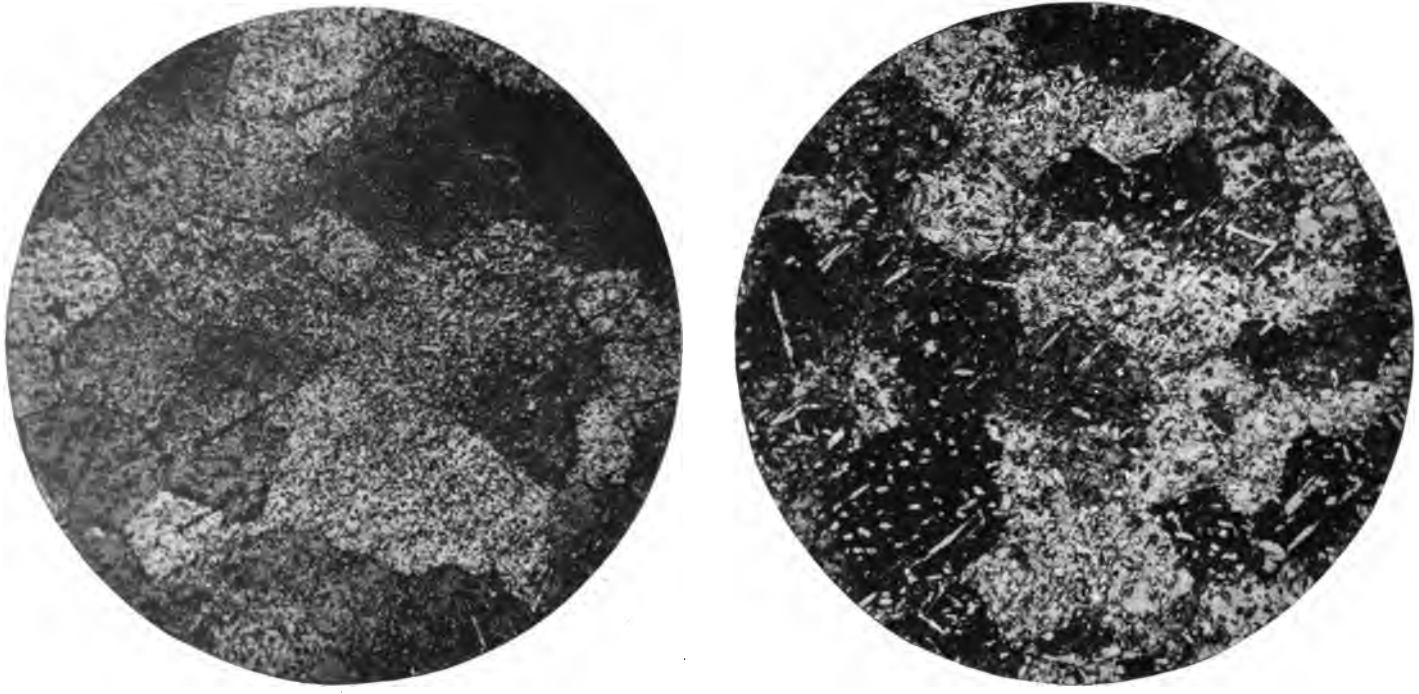

E Series IV ED

FIG. 15.—*Alpha and beta bronze containing tin and iron.* ×75

Copper 56.39, zinc 40.95, tin 1.52, iron 0.96, lead 0.09, manganese 0.09 (manganese bronze)

Digitized by Google

Cast

S408

Cold-rolled

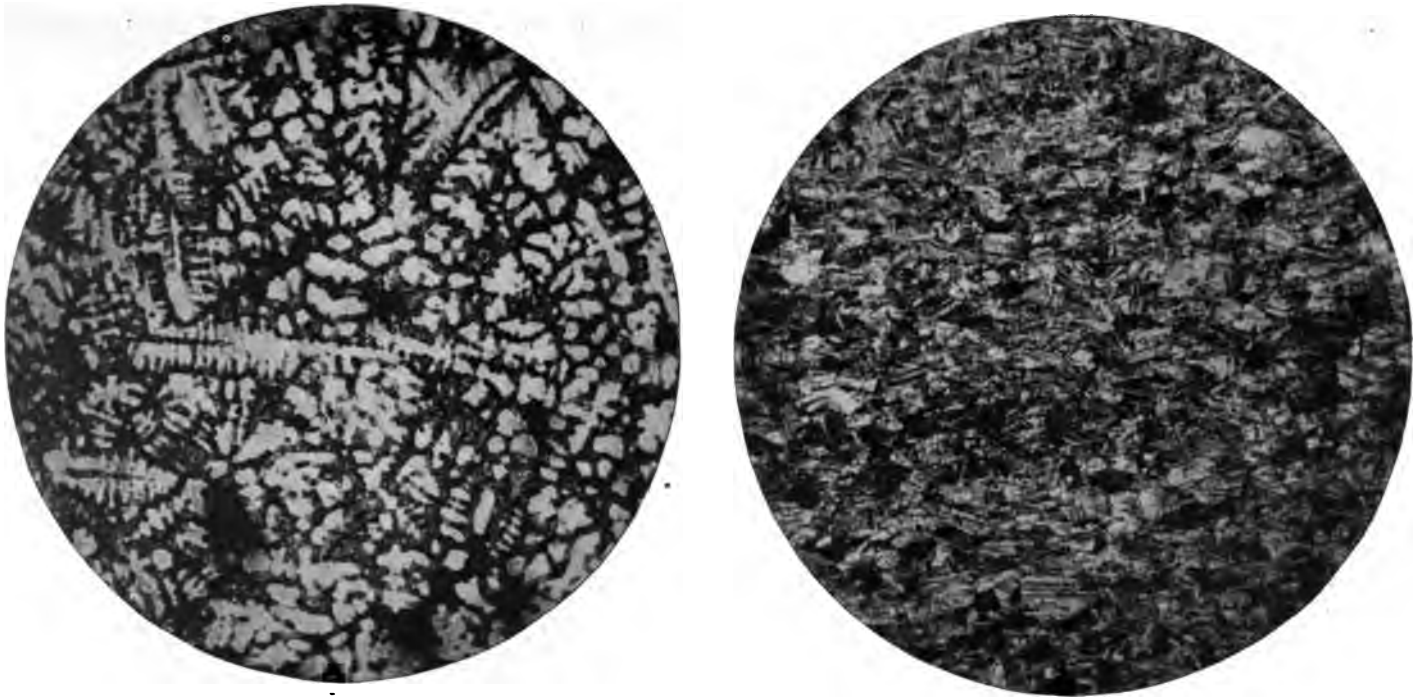

Series VI

Series V

FIG. 16.—*Alpha bronze.* ×75

Copper 89.69, tin 10.14 (gun metal)

Digitized by Google

Hot-rolled S347 Cold-worked

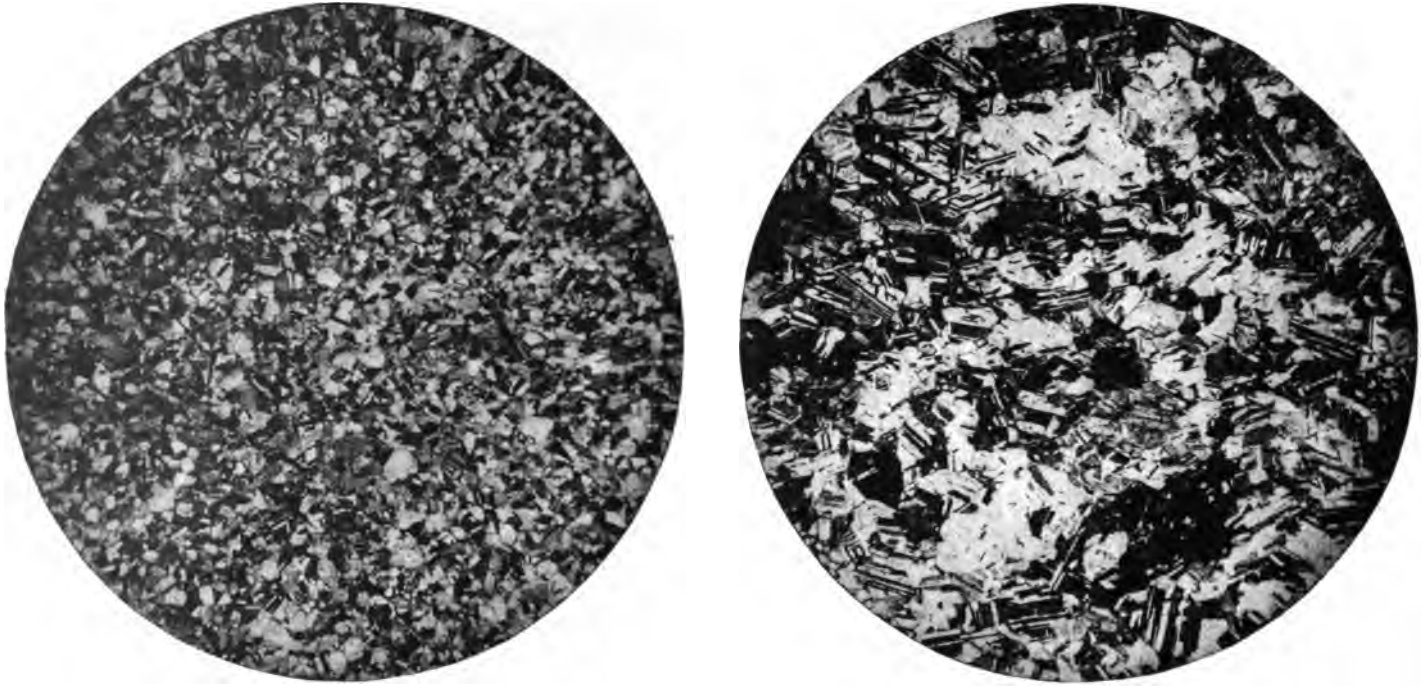

Series VII

FIG. 17.—*Alpha aluminum bronze.* ×75

Copper 92.17, aluminum 7.34, zinc 0.40, silicon 0.09, nickel, trace (aluminum bronze)

Digitized by Google

character due to self-annealing during hot-rolling. In this respect it is similar to copper.

The micrograph of S347HD shows similar but larger alpha crystals. This alloy was drawn only slightly and the consequent elongation of the grains can not be seen.

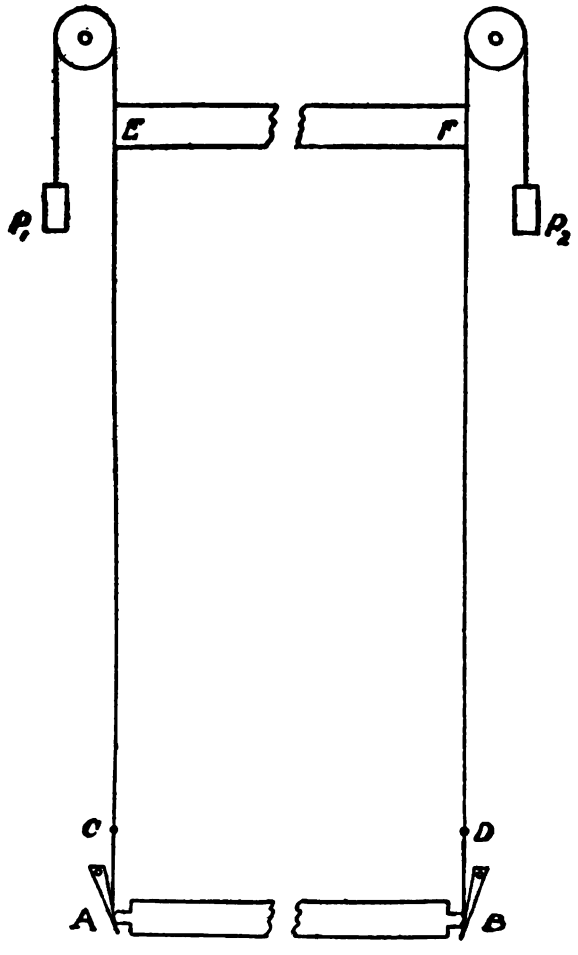

FIG. 18.—*Diagrammatic representation of specimen and contact wires*

IV. APPARATUS AND EVALUATION OF CONSTANTS

The apparatus employed was essentially the same as that used for the determination of the thermal expansion of molybdenum.[11]

Each specimen was supported horizontally in a return flow bath. The method of arrangement [12] is shown diagramatically in

[11] B. S. Scientific Papers, No. 332; 1919.
[12] A. W. Gray, J. Wash. Acad. Sci., 2, p. 248; 1912.

Digitized by Google

Fig. 18. *AB* represents the specimen, and *C* and *D* are points on the 1 mil tungsten wires *ACE* and *BDF*, which points represent the foci of two horizontal micrometer microscopes. These wires are in contact with the ends of the specimen *AB*, and are stretched upward to a rigid bar *EF* (shown in part). Each wire passes over a pulley, and supports a small weight, *P*, at its upper end. *AC*

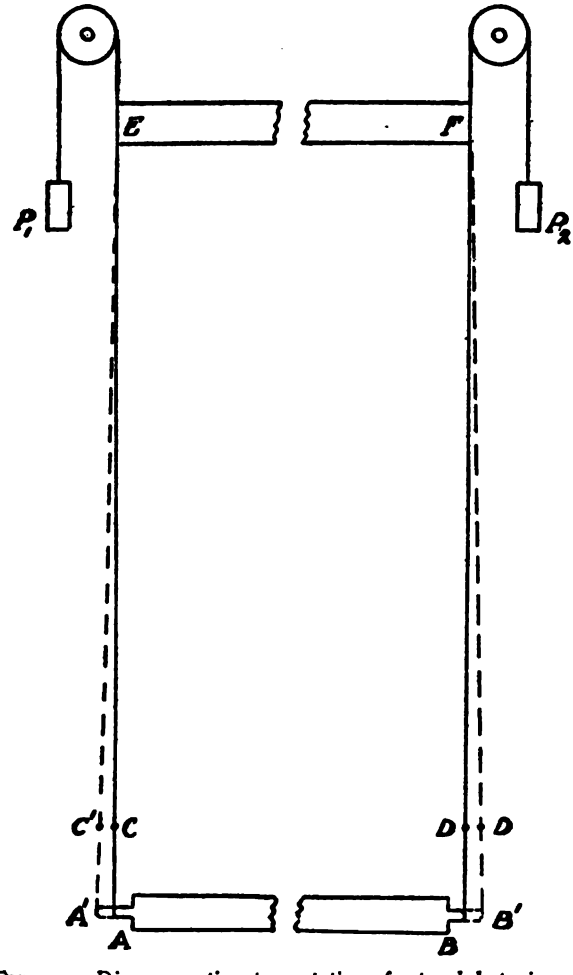

FIG. 19.—*Diagrammatic representation of expanded specimen*

is $\frac{1}{10}$ the distance of *AE*, and, similarly, *BD* is $\frac{1}{10}$ the distance of *BF*. *EF* is a hollow invar bar which is kept at room temperature.

The length changes of *AB* were measured indirectly. The distance, *CD*, was compared with a standard bar kept at the same temperature as *EF*. If the temperature of the specimen is increased, it expands as shown in Fig. 19. *A'B'* represents the

Digitized by Google

length of the specimen at some increased temperature, and $(AA'+BB')$ represents the true expansion. The microscopes first measured the distance CD and then $C'D'$. The difference between $C'D'$ and CD, which is equal to $(CC'+DD')$, gives the apparent expansion, from which the true expansion $(AA'+BB')$ may be determined. Since AC is $\frac{1}{10}$ of AE, and triangle $C'CE$

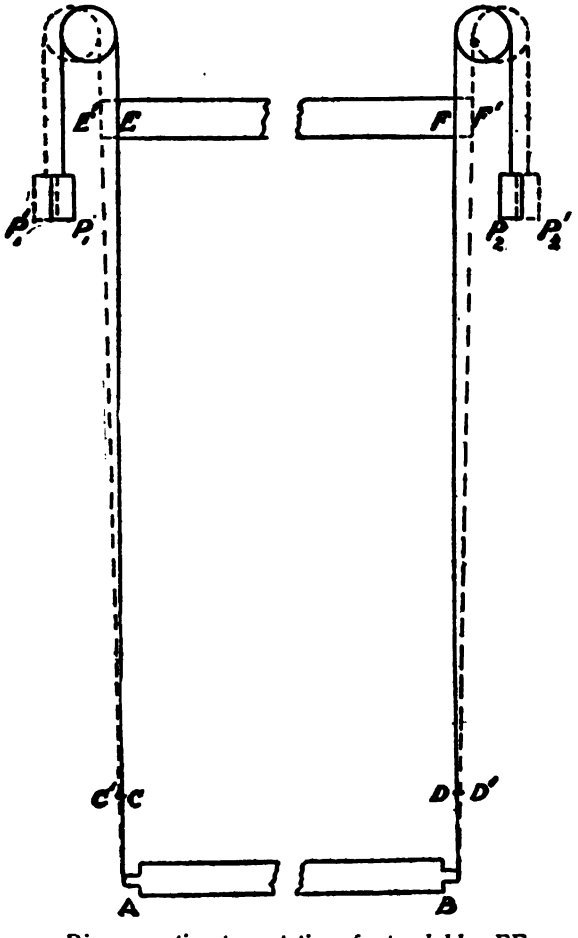

FIG. 20.—*Diagrammatic representation of expanded bar EF*

is similar to triangle $A'AE$, then $\frac{CC'}{AA'}=\frac{1}{10}$ or $AA'=\frac{10}{9}\ CC'$. Similarly, $BB'=\frac{10}{9}\ DD'$. The true expansion is therefore equal to $\frac{10}{9}$ of the observed or apparent expansion.

If the temperature of EF varies from the assumed constant temperature, it is necessary to apply a correction to the observed length of CD. If the temperature of the upper hollow bar, EF,

Digitized by Google

increases its temperature above the standard temperature and expands an amount equal to $EE'+FF'$, then the wires will incline as shown in Fig. 20. The microscopes will sight the points C' and D' instead of the points C and D. It is necessary, therefore, to subtract the distance, $CC'+DD'$, from the observed distance, $C'D'$, in order to obtain the distance, CD. Since AC is $\frac{1}{10}$ of AE, and triangle ACC' is similar to triangle AEE', then $\frac{CC'}{EE'}=\frac{1}{10}$ or CC' is $\frac{1}{10}$ EE'. In like manner DD' is $\frac{1}{10}$ FF'. $CC'+DD'$, the correction to be applied (added when the temperature is below the

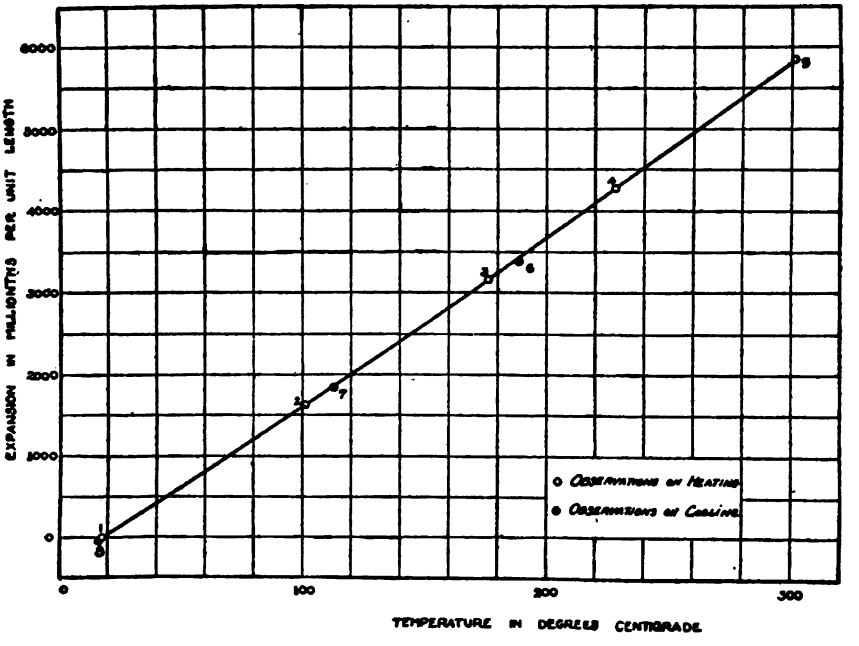

FIG. 21.—*Linear expansion as a function of temperature*

standard temperature and subtracted when above the standard temperature), is equal to $\frac{1}{10}$ $(EE'+FF')$. The correction to be applied to the length, CD, is $\frac{1}{10}$ of the change of EF. This correction is usually very small.

The return flow bath was filled with oil or pentane, the liquid used depending on the temperature desired. Between room temperature and 300° C, "Renown" engine oil was used, while for low temperatures pentane was employed. An electric resistance coil surrounded by, and in contact with, the liquid was used for heating. Cooling below room temperature was effected by the expansion of compressed air within a coil of copper tubing immersed in the

Digitized by Google

bath containing pentane. The liquid surrounding the specimen was kept in circulation by means of a propeller. The temperature variation over the entire specimen was probably not greater than 0.1° C during an observation.

The length changes were determined with a movable comparator consisting of two micrometer microscopes rigidly clamped on an invar bar at a distance from each other equal to the length of the specimen (30 cm). The microscopes were so arranged that they could first be sighted on a standard length bar kept at nearly constant temperature and then on the 1 mil wires which were in contact with the ends of the specimen.

The temperatures were determined by means of a copper-constantan thermoelement and a potentiometer calibrated respectively by the heat and electrical divisions of this Bureau.

In order to indicate how the observations were used in deriving empirical equations of expansion, the observations on a single specimen (S341) are given in the following table. The accompanying curve (Fig. 21) shows the results graphically.

TABLE 6.—Expansion Observations on a Sample

Observation number	Temperature	Δl	Observation number	Temperature	Δl
	°C	$\times 10^{-6}$		°C	$\times 10^{-6}$
1	17.5	0	5	301.2	5864
2	101.3	1621	6	188.5	3380
3	175.8	3159	7	112.6	1838
4	228.1	4289	8	15.9	−47

[a] Δl represents the change per unit length from the length at the initial temperature 17.5° C.

If it is assumed that the specimen expands in accordance with a second degree equation of the form

$$\Delta l = (t-17.5)a + (t-17.5)^2 b,$$

where t represents any temperature between 17.5 and 301.2° C, then from the values of Δl, obtained from the observations on heating, it is possible to derive the following empirical equation by the method of least squares:

$$\Delta l = 19.02(t-17.5)10^{-6} + 0.00590(t-17.5)^2 10^{-6}.$$

Table 7 gives a comparison of the observed values with those computed from this empirical formula.

Digitized by Google

TABLE 7.—Results on Heating

Temperature, degrees centigrade	Observed Δl	Computed Δl	Residuals
	$\times 10^{-6}$	$\times 10^{-6}$	$\times 10^{-6}$
101.3	1621	1635	−14
175.8	3159	3159	0
228.1	4283	4267	+16
301.2	5864	5871	− 7

The probable error is

$$0.6745\sqrt{\frac{501\times 10^{-12}}{4-2}} = \pm 11\times 10^{-6}.$$

The deviations of the observed values taken on cooling, from this empirical equation representing the heating curve, are given in the following table, where Δl represents the change per unit length from the length at the initial temperature 17.5° C.

TABLE 8.—Results on Cooling

Temperature, degrees centigrade	Observed Δl	Computed Δl	Deviations
	$\times 10^{-6}$	$\times 10^{-6}$	$\times 10^{-6}$
301.2	5864	5871	− 7
188.5	3380	3425	−45
112.6	1838	1862	−24
15.9	−47	−30	−17

From inspection of the preceding table, it is evident that the observations on cooling lie below the heating curve and that the specimen at the end of the test was about 0.002 per cent shorter than at the beginning.

The first derivative of the empirical equation of expansion

$$\Delta l = 19.02(t-17.5)10^{-6} + 0.00590(t-17.5)^2 10^{-6}$$

gives

$$\frac{d}{dt}[\Delta l] = 19.02\times 10^{-6} + 0.01180(t-17.5)10^{-6}$$

and represents the tangent to the expansion curve. This tangent also represents the rate of expansion or instantaneous coefficient, a_t, at any temperature, t, within the proper limits.

From inspection of the preceding linear equation and the following table which gives the instantaneous coefficients computed for every 50° from 50 to 250° C, it is evident that the rate of expansion increases with temperature.

Digitized by Google

TABLE 9.—Relation between Coefficient of Expansion and Temperature

Temperature, degrees centigrade	Instantaneous coefficients	Temperature, degrees centigrade	Instantaneous coefficients
	$\times 10^{-6}$		$\times 10^{-6}$
50	19.40	200	21.17
100	19.99	250	21.76
150	20.58		

The equation

$$\Delta l = 19.02(t-17.5)10^{-6} + 0.00590(t-17.5)^2 10^{-6}$$

may be transformed into the following:

$$L_t = L_o(1 + 18.81\ t \times 10^{-6} + 0.00590t^2 \times 10^{-6}),$$

where L_t is the length of the specimen at any temperature, t, between 17.5 and 301.2° C and L_o the length at 0° C.

V. EXPERIMENTAL AND DERIVED RESULTS

1. SERIES I.—COPPER: ELECTROLYTIC, NICKELIFEROUS, ARSENICAL

In this series there are four samples of copper. The method of working of these samples before the thermal expansion tests is given in the following table. The specimen marked "*H*" was hot-rolled and those marked "*HD*" were drawn, annealed, and finished hard after being hot-rolled.

TABLE 10.—Treatment Before Expansion Tests

Laboratory number	Method of working
S340H	Hot-rolled in one heat from wire bar to ¾-inch diameter.
S340HD	Hot-rolled in one heat from wire bar to ¾-inch diameter, drawn to 0.300 inch, annealed, and finished hard at ¼ inch.
S339HD	Hot-rolled to ¾-inch diameter, cold-drawn to 0.300 inch, annealed, and finished hard at ¼ inch.
S338HD	Same method as S339HD.

Table 11 gives the composition, the temperature range of the thermal expansion test, the values of a and b of the general quadratic equation

$$L_t = L_o(1 + at + bt^2),$$

where L_t is the length at any temperature within the specified range, the probable error of L_t, and the instantaneous coefficients at every 50° from 50 to 250° C.

Digitized by Google

TABLE 11.—Summary of Values of Series I

Laboratory number	Commercial name	Composition			Temperature range	Coefficients	
		Copper	Nickel	Arsenic		$a \times 10^6$	$b \times 10^6$
		Per cent	Per cent	Per cent	°C		
S340H	Electrolytic copper	99.968			+16–300	16.23	0.00483
S340HD					−49–305	16.32	.00413
S339HD	Nickeliferous copper	99.601	0.346		+19–300	16.65	.00336
S338HD	Arsenical copper	99.378		0.5361	21–300	16.69	.00322

Laboratory number	Probable error of L_t	Instantaneous coefficients $\times 10^6$				
		At 50° C	At 100° C	At 150° C	At 200° C	At 250° C
	$\times 10^{-6}$					
S340H	3	16.71	17.20	17.68	18.16	18.64
S340HD	9	16.73	17.15	17.56	17.97	18.38
S339HD	1	16.99	17.82	17.66	17.99	18.33
S338HD	2	17.01	17.33	17.66	17.98	18.30

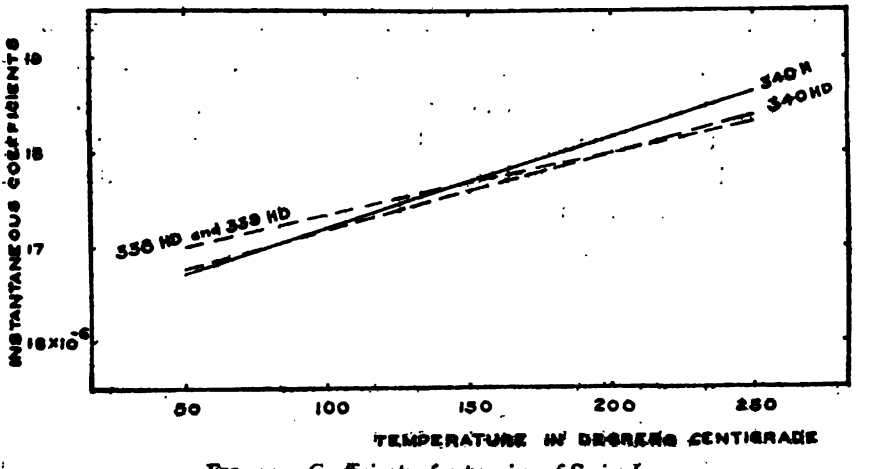

FIG. 22.—*Coefficients of expansion of Series I*

The curves in Fig. 22 show graphically the relation between the instantaneous coefficients and the temperature from 50 to 250° C.

ELECTROLYTIC COPPER.—These samples were prepared from high-grade electrolytic copper wire bar.

The instantaneous coefficients of the drawn sample of electrolytic copper are less (nearly over the whole temperature range) than those of the hot-rolled specimen. The maximum difference in the coefficients is 0.26×10^{-6} and occurs at 250° C.

Digitized by Google

In general, annealing and drawing of the hot-rolled bar caused a slight lowering of the values of the coefficients.

NICKELIFEROUS AND ARSENICAL COPPER.—The instantaneous coefficients of the cold-drawn nickeliferous and arsenical copper samples are practically equal, and somewhat larger than those of the drawn electrolytic copper rod (to 200° C). The substitution of small amounts of nickel or arsenic tends to raise the instantaneous coefficients.

The cooling curves of S340HD, S339HD, and S338HD lie below the heating curves, and the cooling curve of S340H lies above. The maximum variation between the heating and cooling curves is ±50 millionths per unit length. After cooling to room temperature, the variation in length from the original length was found to be as follows. The minus (−) sign indicates a decrease in length.

TABLE 12.—Changes in Length After Test

Laboratory number	Hot-rolled	Hot-rolled and drawn
	Per cent	Per cent
S340	0.000	−0.002
S339		[a] −.001
S338		[a] −.005

[a] The maximum deviation between the heating and cooling curves did not exceed this value.

2. SERIES II.—COLD-ROLLED COPPER-ZINC ALLOYS

Series II includes 16 samples of copper-zinc alloys, cold-rolled from 2-inch chill castings to twenty-one thirty-second inch, cold-drawn to 0.300-inch, annealed, and finished hard at one-fourth-inch, and 2 samples (S332 and S333) similarly rolled from chill castings of 1⅝-inch diameter.

This series may be subdivided into four groups of alloys: (*a*) Alpha brass, S313 to S320, inclusive; (*b*) alpha beta brass, S321 to S324, inclusive; (*c*) leaded brass (alpha or alpha beta), S327 to S330, inclusive; (*d*) alpha brass containing tin, S332 and S333.

The following table gives the composition, the temperature range of the thermal expansion test, the values of a and b of the general quadratic equation

$$L_t = L_0 (1 + at + bt^2),$$

where L_t is the length at any temperature within the specified range, the probable error of L_t, and the instantaneous coefficients at every 50° from 50 to 250° C.

Digitized by Google

TABLE 13.—Summary of Values of Series II

Metallurgical subdivision	Laboratory number	Commercial name	Composition				Temperature range	Coefficients		Probable error of L_t	Instantaneous coefficients $\times 10^6$				
			Copper	Zinc	Lead	Iron		$a \times 10^6$	$b \times 10^6$		At 50° C	At 100° C	At 150° C	At 200° C	At 250° C
			Per ct.	Per ct.	Per ct.	Per ct.	° C			$\times 10^{-4}$					
Alpha brass	S313	Primer gilding	97.00	2.97	0.01	0.02	−49–301	16.48	0.00363	6	16.84	17.21	17.57	17.93	18.30
	S314	Gilding	94.87	5.11	.01	.01	+28–305	16.81	.00389	5	17.20	17.59	17.98	18.37	18.76
	S315	Commercial bronze	90.26	9.70	.01	.03	26–302	17.01	.00379	2	17.39	17.77	18.15	18.53	18.90
	S316	Rich low brass	85.21	14.76	.01	.02	−50–300	17.03	.00512	5	17.54	18.05	18.57	19.08	19.59
	S317	Low brass	80.02	19.89	.05	.03	+28–302	17.22	.00590	7	17.81	18.40	18.99	19.58	20.17
	S318	Brazing brass	75.31	24.64	.02	.03	28–300	17.58	.00624	1	18.20	18.83	19.45	20.08	20.70
	S319	Spring brass	72.02	27.95	.01	.02	25–306	17.73	.00652	5	18.38	19.03	19.69	20.34	20.99
	S320	Cartridge brass	70.28	29.66	.03	.03	19–301	17.75	.00653	3	18.40	19.06	19.71	20.36	21.02
	S321	.....do	66.50	33.43	.04	.03	−50–301	18.26	.00561	5	18.82	19.38	19.94	20.50	21.06
Alpha beta brass	S322	Commercial brass	64.81	34.92	.24	.03	+20–299	18.15	.00645	5	18.80	19.44	20.08	20.73	21.38
	S323	Commercial brass wire	63.63	36.17	.17	.03	21–299	18.11	.00725	7	18.84	19.56	20.28	21.01	21.74
	S324	Hot-rolled brass tube	62.10	37.71	.17	.02	23–308	18.05	.00855	7	18.90	19.76	20.62	21.47	22.32
Leaded brass (alpha or alpha beta)	S327	Leaded bronze	88.30	10.00	1.68	.02	21–301	17.06	.00389	3	17.45	17.84	18.23	18.62	19.00
	S328	Leaded low brass	78.28	20.01	1.68	.03	22–301	17.48	.00524	4	18.00	18.53	19.06	19.58	20.10
	S329	Leaded screw wire	68.65	29.67	1.65	.03	20–304	17.91	.00652	4	18.56	19.21	19.87	20.52	21.17
	S330	Free turning rod	62.33	35.04	2.57	.06	21–302	18.26	.00656	3	18.92	19.57	20.23	20.88	21.54
Alpha brass, containing tin.	[a]S332	Fourdrinier wire	81.70	17.94	.04	.01	19–301	17.31	.00580	1	17.89	18.47	19.05	19.63	20.21
	[b]S333	Admiralty condenser tubes	70.64	28.21	.04	.01	20–301	17.94	.00693	6	18.68	19.33	20.02	20.71	21.40

[a] Tin=0.31 per cent.

[b] Tin=1.16 per cent.

Digitized by Google

The observations on three of the above alloys were plotted, and the curves obtained are shown in Fig. 23.

From inspection of the previous table, it is seen that, in general, the coefficients increase with a decrease in the copper content of these copper-zinc alloys. If the values of the instantaneous coeffi-

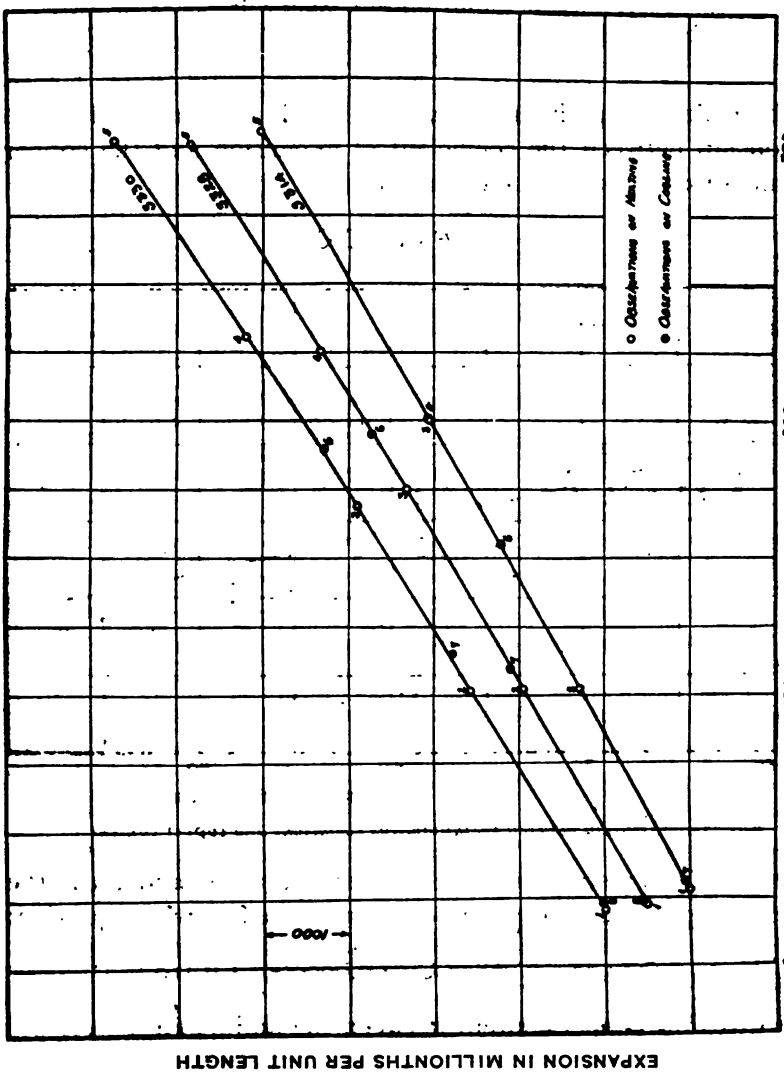

FIG. 23.—*Linear expansion of three cold-rolled copper-zinc alloys*

cients at 50° C are plotted against the copper content, the curve shown in Fig. 24 is obtained. It is obvious that it is possible to derive a mathematical relation between the instantaneous coefficient at 50° C and the copper (or zinc) content of these alloys, if it is assumed that the other elements present are impurities which

Digitized by Google

may be neglected. Since the leaded brasses (S327 to S330, inclusive) and the brasses containing tin (S332 and S333) contain lead and tin, respectively, which were added intentionally, it was decided to ignore these alloys in deriving the relation between copper content and expansivity. The instantaneous coefficients computed from the quadratic equation of expansion

$$L_t = L_0 (1 + at + bt^2)$$

may be called "experimental" values. If it is assumed that the relationship between the coefficient of expansion and the copper content is expressed by the equation

$$a_{50} = A + B\,\mathrm{Cu} + C\,\mathrm{Cu}^2$$

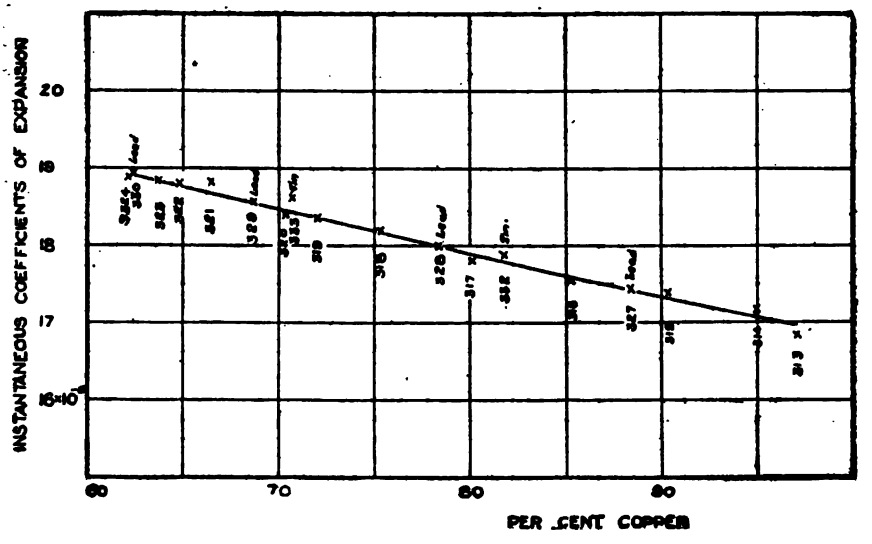

FIG. 24.—*Relation between instantaneous coefficient and copper content*

where a_{50} is the instantaneous coefficient at 50° C and Cu is the per cent copper, then it is possible to derive the following equation:

$$a_{50} = (22.923 - 0.06833\,\mathrm{Cu} + 0.0000695\,\mathrm{Cu}^2)\,10^{-6},$$

where Cu is the copper content between the limits 62.1 and 97 per cent.

The following is a comparison of the experimental values of the instantaneous coefficients of expansion at 50° C with those computed from this formula. The residuals show that the equation holds.

Digitized by Google

TABLE 14.—Comparison of Experimental and Computed Coefficients at 50° C

[The probable error of a_{50} is $\pm 0.06 \times 10^{-6}$.]

Laboratory number	Copper	Coefficients		Residuals
		Experimental a_{50}	Computed a_{50}	
	Per cent	$\times 10^{-6}$	$\times 10^{-6}$	$\times 10^{-6}$
S313	97.00	16.84	16.95	−0.11
S314	96.87	17.20	17.07	+ .13
S315	90.26	17.39	17.32	.07
S316	85.21	17.54	17.61	− .07
S317	80.02	17.81	17.90	− .09
S318	75.31	18.20	18.17	+ .03
S319	72.02	18.38	18.36	.02
S320	70.28	18.40	18.46	− .06
S321	66.50	18.62	18.49	+ .13
S322	64.81	18.80	18.79	.01
S323	68.63	18.84	18.86	− .02
S324	62.10	18.90	18.95	− .05

In a similar manner the instantaneous coefficients, a_{100}, a_{150}, a_{200}, and a_{250}, at 100, 150, 200, and 250° C, respectively, were computed and the equations derived are

$$a_{100} = (24.673 - 0.08794\ Cu + 0.0001252\ Cu^2 \pm 0.05)10^{-6}$$
$$a_{150} = (25.790 - .09119\ Cu + .0000775\ Cu^2 \pm .08)10^{-6}$$
$$a_{200} = (23.406 - .00386\ Cu - .0005421\ Cu^2 \pm .13)10^{-6}$$
$$a_{250} = (28.681 - .11451\ Cu + .0000874\ Cu^2 \pm .16)10^{-6}.$$

The last term in the parenthesis of each equation represents the probable error.

Fig. 25 represents graphically the instantaneous coefficients at every 50° from 50 to 250° C.

A change in temperature causes a greater change in the value of the instantaneous coefficient of a copper-zinc alloy of low copper content than in that of an alloy of higher copper content, as is apparent from Fig. 25 and the following comparison:

TABLE 15

Laboratory number	Composition				Coefficients $\times 10^6$		Change $(a_{100} - a_{50})$
	Copper	Zinc	Lead	Iron	a_{50}	a_{100}	
	Per cent	Per cent	Per cent	Per cent			$\times 10^{-6}$
S313	97.00	2.97	0.01	0.02	16.84	17.21	0.37
S320	70.28	29.66	.03	.03	18.40	19.06	.66

Digitized by Google

The change in the rate of expansion or instantaneous coefficient of S320 from 50 to 100° C is nearly twice as large as that for S313. This change increases with a decrease in the copper content (and a corresponding increase in the per cent zinc) of the alloy.

The average residuals of the alpha beta brasses (S321 to S324, inclusive) above 100° C, exceed the corresponding probable errors, which indicates that this group of alloys is not in as close agreement with the empirical equations as the group of alpha brasses (S313 to S320, inclusive).

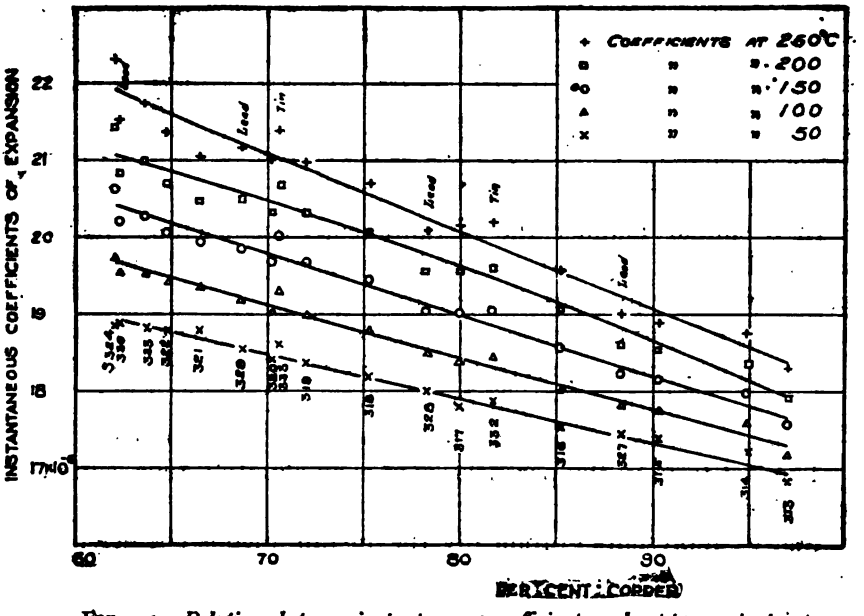

FIG. 25.—*Relations between instantaneous coefficients and copper content*

The two copper alloys (S332 and S333) containing tin, which was added intentionally, have coefficients which are greater than the theoretical values of alloys of corresponding copper content (but without tin), as may be seen from Fig. 25 and the following comparison:

Digitized by Google

TABLE 16.—Comparison of Experimental and Theoretical Coefficients

A. S332 (COPPER 81.70, TIN 0.31)

	Instantaneous coefficients $\times 10^6$				
	At 50° C	At 100° C	At 150° C	At 200° C	At 250° C
Experimental	17.89	18.47	19.05	19.63	20.21
Theoretical [a]	17.80	18.32	18.86	19.47	19.91
Deviations	.09	.15	.19	.16	.30

B. S333 (COPPER 70.64, TIN 1.10)

Experimental	18.63	19.33	20.02	20.71	21.40
Theoretical [a]	18.44	19.09	19.74	20.43	21.08
Deviations	.19	.24	.28	.28	.32

[a] These values refer to a cold-rolled copper-zinc alloy of corresponding copper content (but without tin).

The deviations are greater than the probable errors, and are attributable to the large amounts of tin. It should be noted that for the alloy containing 1.10 per cent tin (S333), the observed values deviate from the theoretical curves of instantaneous coefficients more than those of the alloy containing less tin (S332).

The four leaded brasses containing from 1.65 to 2.57 per cent lead, which was intentionally added, have instantaneous coefficients that are less than the theoretical values of alloys of corresponding copper content (but without appreciable amounts of lead). The average deviations at 150, 200, and 250° C are -0.10×10^{-6}, -0.17×10^{-6}, and -0.20×10^{-6}, respectively, which exceed the probable errors and are due to the added lead.

From the equations of instantaneous coefficients it is possible to predict the coefficients of a cold-rolled copper-zinc alloy, the copper content of which varies from 62.1 to 97 per cent. There is a remarkable uniformity between the coefficients of expansion and the copper content of these alloys. This uniformity might be better if copper and zinc were the only two elements to vary.

In general, it was found that the cooling curves from the maximum temperature (about 300° C) to room temperature did not coincide exactly with the heating curves. At any given temperature the variation did not exceed ± 70 millionths per unit length. In each case the maximum variation occurred at room temperature; that is, the cooling curve deviated more from the heating curve as the temperature decreased from about 300° C (the maximum temperature) to room temperature. The following table shows the deviations at room temperature or the changes

Digitized by Google

in length after test. The plus (+) sign indicates an increase in length, and the minus (−) sign a decrease in length.

TABLE 17.—Change in Length Due to Heat Treatment Received During Test

Laboratory number	Change in length after test	Laboratory number	Change in length after test
	Per cent		Per cent
S313	−0.005	S322	−0.004
S314	− .001	S323	− .002
S315	− .001	S324	+ .006
S316	+ .001	S327	− .004
S317	+ .004	S328	+ .002
S318	+ .007	S329	.000
S319	+ .005	S330	− .002
S320	+ .002	S332	+ .005
S321	− .001	S333	+ .006

As a general rule, materials fail to return to their original dimensions after heating unless they are well annealed before test. This means that the cooling curve does not coincide with the

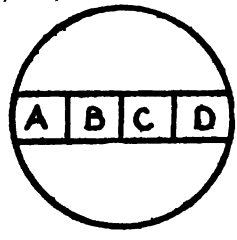

FIG. 26.—*Cross section of copper-zinc casting*

heating curve, and may lie above or below the heating curve, or may intersect it, depending on the material.

Since the specimens of Series II were in the hard condition (not annealed), it is not surprising to find that these samples did not return to their original lengths and that the cooling curves did not coincide with the heating curves. It should be remembered, however, that the deviations between the heating and cooling curves are very small.

3. SERIES III: SECTIONS OF COPPER-ZINC CASTINGS

Series III includes 72 samples cut from 18 castings of copper-zinc alloys, the compositions of which correspond to those of Series II. From each casting, four specimens were cut as shown in the diagram (Fig. 26).

Digitized by Google

A and *D* represent outside sections, and *B* and *C* inside sections. All the samples except S332 and S333 (cut from 1⅝-inch castings) were cut from 2-inch castings. It should be noted that the samples of Series II were obtained from castings similar to those of Series III, which castings were treated as described in the first paragraph of Series II (p. 109). S313A, S313B, S313C, and S313D of Series III have the same chemical composition as S313 of Series II, and in like manner for the other specimens of this series.

The following table gives the composition, the temperature range of the thermal expansion test, the values of a and b of the general quadratic equation

$$L_t = L_0 (1 + at + bt^2),$$

the probable error of L_t, and the instantaneous coefficients at every 50° from 50 to 250° C.

Digitized by Google

TABLE 18.—Summary of Values of Series III

Metallurgical subdivision	Laboratory number	Commercial name	Composition				Temperature range	Coefficients		Probable error of L_t	Instantaneous coefficients $\times 10^6$				
			Copper	Zinc	Lead	Iron		$a \times 10^6$	$b \times 10^8$		At 50° C	At 100° C	At 150° C	At 200° C	At 250° C
			Per cent	Per cent	Per cent	Per cent	°C			$\times 10^{-4}$					
	S313 A	Primer gilding	97.00	2.97	0.01	0.02	+29 to +299	16.82	0.00368	2	17.19	17.56	17.92	18.29	18.66
	S313 B						18– 300	16.66	.00384	4	17.04	17.43	17.81	18.20	18.58
	S313 C						27– 300	16.71	.00373	3	17.08	17.46	17.83	18.20	18.58
	S313 D						28– 300	16.75	.00345	2	17.10	17.44	17.78	18.13	18.48
	S313 Ac						*19– 303*	*16.68*	*.00383*	*2*	*17.06*	*17.45*	*17.83*	*18.21*	*18.60*
	S314 A	Gilding	94.87	5.11	.01	.01	28– 307	16.89	.00340	3	17.23	17.57	17.91	18.25	18.59
	S314 B						29– 302	16.87	.00340	2	17.21	17.55	17.89	18.23	18.57
	S314 C						19– 303	16.89	.00367	1	17.26	17.62	17.99	18.36	18.72
	S314 D						27– 301	16.84	.00382	1	17.22	17.60	17.99	18.37	18.75
	S315 A	Commercial bronze	90.26	9.70	.01	.03	24– 304	17.01	.00416	2	17.43	17.84	18.26	18.67	19.09
	S315 B						17– 300	16.84	.00437	2	17.28	17.71	18.15	18.59	19.02
	S315 C						24– 305	16.90	.00413	2	17.31	17.73	18.14	18.55	18.96
	S315 D						26– 304	16.81	.00462	4	17.27	17.73	18.20	18.66	19.12
	S316 A	Rich low brass	85.21	14.76	.01	.02	16– 302	17.11	.00478	2	17.59	18.07	18.54	19.02	19.50
	S316 B						25– 300	17.04	.00483	3	17.52	18.01	18.49	18.97	19.46
	S316 C						26– 301	17.27	.00423	2	17.69	18.12	18.54	18.96	19.38
	S316 D						27– 302	16.90	.00551	4	17.45	18.00	18.55	19.10	19.66
Alpha brass	S316 Bc						*17– 305*	*17.24*	*.00426*	*3*	*17.67*	*18.09*	*18.53*	*18.94*	*19.37*
	S317 A	Low brass	80.02	19.89	.05	.03	17– 301	16.98	.00586	6	17.57	18.15	18.74	19.32	19.91
	S317 B						25– 301	17.38	.00505	5	17.88	18.39	18.90	19.40	19.90
	S317 C						25– 306	17.17	.00569	8	17.74	18.31	18.88	19.45	20.02
	S317 D						29– 303	17.09	.00568	5	17.66	18.23	18.79	19.36	19.93
	S318 A	Brazing brass	75.31	24.64	.02	.03	19– 301	17.52	.00648	6	18.17	18.82	19.46	20.11	20.76
	S318 B						23– 300	17.25	.00639	7	17.89	18.53	19.17	19.81	20.44
	S318 C						23– 307	17.11	.00662	5	17.77	18.43	19.10	19.76	20.42
	S318 D						27– 305	17.32	.00619	6	17.94	18.56	19.18	19.80	20.42

Digitized by Google

Alpha beta brass..	S319...	A	Spring brass.....	72.02	27.95	.01	.02	23- 304	17.39	.00703	6	18.09	18.80	19.50	20.20	20.90
		Be						27- 308	*17.50*	*.00689*	*7*	*18.19*	*18.88*	*19.59*	*20.08*	*20.70*
		C						25- 300	17.47	.00685	8	18.16	18.85	19.53	20.22	20.91
		D						18- 304	17.50	.00649	6	18.13	18.80	19.45	20.10	20.74
	S320...	A	Cartridge brass	70.28	29.66	.03	.03	21- 303	17.87	.00692	9	18.46	19.05	19.65	20.24	20.83
		B						25- 304	17.74	.00633	5	18.37	19.00	19.64	20.27	20.90
		C						18- 301	17.58	.00621	8	18.20	18.82	19.44	20.06	20.68
		De						20- 303	*17.74*	*.00717*	*8*	*18.36*	*18.97*	*19.59*	*20.21*	*20.83*
	S321...	A	....do.....	66.50	33.43	.04	.03	25- 304	17.98	.00676	7	18.66	19.33	20.01	20.68	21.36
		B						22- 304	18.06	.00626	5	18.69	19.31	19.94	20.56	21.19
		C						20- 301	18.12	.00614	1	18.73	19.35	19.96	20.58	21.19
		D						17- 302	18.08	.00653	8	18.73	19.39	20.04	20.69	21.34
	S322...	A	Commercial brass	64.81	34.92	.24	.03	19- 302	18.28	.00647	5	18.93	19.57	20.22	20.87	21.52
		B						20- 302	17.99	.00691	7	18.68	19.37	20.06	20.75	21.44
		C						20- 301	18.12	.00658	6	18.78	19.44	20.09	20.75	21.41
		D						23- 302	17.95	.00705	8	18.66	19.36	20.06	20.77	21.48
	S323...	A	Commercial brass wire	63.63	36.17	.17	.03	21- 307	18.32	.00624	8	18.94	19.57	20.19	20.82	21.44
		B						20- 303	18.33	.00611	8	18.93	19.54	20.15	20.76	21.38
		C						17- 304	18.24	.00648	7	18.89	19.54	20.18	20.83	21.48
		D						27- 301	18.22	.00671	5	18.89	19.56	20.23	20.90	21.58
	S324...	A	Hot-rolled brass tube	62.10	37.71	.17	.02	23- 304	18.46	.00634	4	19.09	19.73	20.36	21.00	21.63
		B						20- 302	18.29	.00671	4	18.96	19.63	20.30	20.97	21.64
		C						17- 302	18.58	.00638	5	19.22	19.86	20.49	21.13	21.77
		D						19- 303	18.02	.00776	7	18.80	19.57	20.35	21.12	21.90

* Results on second heating.

Digitized by Google

TABLE 18—Continued

Metallurgical subdivision	Laboratory number		Commercial name	Composition				Temperature range	Coefficients		Probable error of L_t	Instantaneous coefficients $\times 10^6$				
				Copper	Zinc	Lead	Iron		$a \times 10^6$	$b \times 10^6$		At 50° C	At 100° C	At 150° C	At 200° C	At 250° C
								°C			$\times 10^{-6}$					
Leaded brass (alpha or alpha beta).	S327...	A	Leaded bronze ..	88.30	10.00	1.68	.02	24- 303	17.22	.00344	4	17.56	17.91	18.25	18.60	18.94
		B						19- 305	17.25	.00369	4	17.62	17.99	18.36	18.73	19.10
		C						24- 303	17.13	.00396	2	17.53	17.92	18.32	18.71	19.11
		D						25- 310	16.98	.00441	3	17.42	17.86	18.30	18.74	19.18
	S328...	A	Leaded low brass	78.28	20.01	1.68	.03	19- 301	17.60	.00451	3	18.05	18.50	18.95	19.40	19.86
		B						25- 303	17.37	.00470	6	17.84	18.31	18.78	19.25	19.72
		C						26- 302	17.38	.00501	3	17.88	18.38	18.88	19.38	19.88
		D						25- 303	17.30	.00507	3	17.81	18.31	18.82	19.33	19.84
		C[a]						*17- 306*	*17.48*	*.00458*	*4*	*17.94*	*18.40*	*18.86*	*19.31*	*19.77*
	S329...	A	Leaded screw wire	68.65	29.67	1.65	.03	27- 302	17.78	.00597	6	18.38	18.97	19.57	20.17	20.76
		B						25- 301	17.94	.00604	5	18.54	19.15	19.75	20.36	20.96
		C						26- 302	17.81	.00630	4	18.44	19.07	19.70	20.33	20.96
		D						30- 302	18.14	.00547	7	18.69	19.28	19.78	20.33	20.88
	S330...	A	Free - turning red	62.33	35.04	2.57	.06	21- 305	18.02	.00739	7	18.76	19.50	20.24	20.98	21.72
		B						26- 304	17.88	.00768	4	18.65	19.42	20.18	20.95	21.72
		C						28- 302	18.30	.00681	6	18.98	19.66	20.34	21.02	21.70
		D						24- 302	18.26	.00661	3	18.92	19.58	20.24	20.90	21.56
		D[a]						*16- 306*	*18.96*	*.00656*	*6*	*18.92*	*19.57*	*20.23*	*20.88*	*21.54*
Alpha brass containing tin.	S332[b]...	A	Fourdrinier wire	81.70	17.94	.04	.01	20- 299	17.16	.00558	5	17.72	18.28	18.83	19.39	19.95
		B						24- 303	17.27	.00518	4	17.79	18.31	18.82	19.34	19.86
		C						25- 303	17.08	.00565	4	17.64	18.21	18.78	19.34	19.90
		D						27- 305	16.86	.00672	6	17.53	18.20	18.88	19.55	20.22
	S333[c]...	A	Admiralty condenser tubes	70.64	28.21	.04	.01	27- 303	17.69	.00658	3	18.35	19.01	19.66	20.32	20.98
		B						27- 301	17.61	.00691	8	18.30	18.99	19.68	20.37	21.06
		C						26- 302	17.66	.00704	6	18.36	19.07	19.77	20.48	21.18
		D						24- 308	17.53	.00704	7	18.23	18.94	19.64	20.35	21.05

[a] Results on second heating. [b] Tin=0.31 per cent. [c] Tin=1.10 per cent.

Digitized by Google

The observations on four of the above samples were plotted, and the curves obtained are shown in Fig. 27.

Similar to Series II, the coefficients of this series, in general, increase with a decrease in the copper content of the casting.

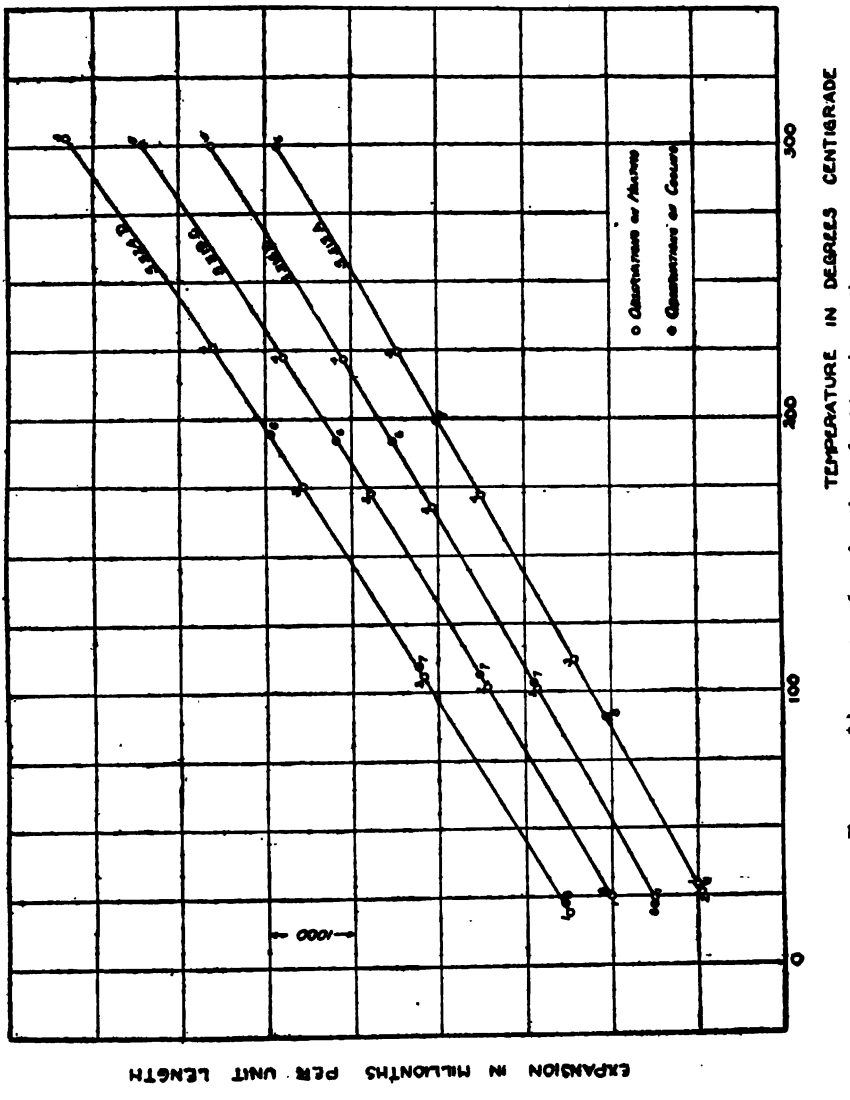

FIG. 27.—*Linear expansion of sections of copper-zinc castings*

The following mathematical relations between the instantaneous coefficients and the copper content of the castings were derived. In deducing these equations, the sections of the four leaded castings, S327 to S330, and those of the two castings containing tin, S332 and S333, were neglected, for these samples contained

Digitized by Google

large amounts of lead and tin, respectively, which were added intentionally.

OUTSIDE SECTIONS

$$a_{50} = (29.391 - 0.23978\ Cu + 0.0011741\ Cu^2 \pm 0.07)\ 10^{-6}$$
$$a_{100} = (29.023 - .20604\ Cu + .0009006\ Cu^2 \pm .06)\ 10^{-6}$$
$$a_{150} = (28.646 - .17212\ Cu + .0006263\ Cu^2 \pm .05)\ 10^{-6}$$
$$a_{200} = (29.250 - .16345\ Cu + .0005105\ Cu^2 \pm .06)\ 10^{-6}$$
$$a_{250} = (28.543 - .12104\ Cu + .0001830\ Cu^2 \pm .08)\ 10^{-6}$$

INSIDE SECTIONS

$$a_{50} = (29.533 - 0.24272\ Cu + 0.0011871\ Cu^2 \pm 0.07)\ 10^{-6}$$
$$a_{100} = (29.371 - .21524\ Cu + .0009569\ Cu^2 \pm .06)\ 10^{-6}$$
$$a_{150} = (29.207 - .18780\ Cu + .0007269\ Cu^2 \pm .04)\ 10^{-6}$$
$$a_{200} = (29.704 - .17729\ Cu + .0006029\ Cu^2 \pm .05)\ 10^{-6}$$
$$a_{250} = (29.237 - .14192\ Cu + .0003222\ Cu^2 \pm .06)\ 10^{-6}$$

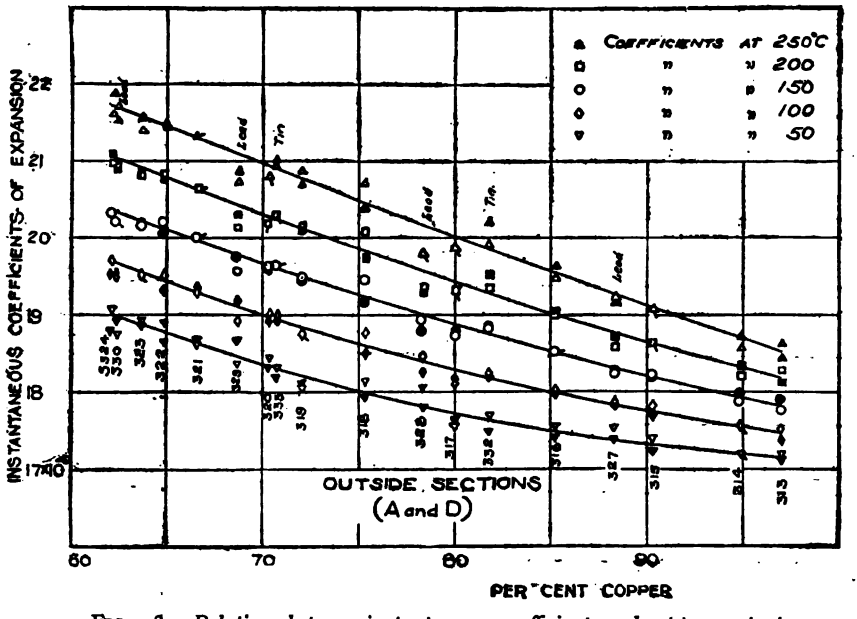

FIG. 28.—*Relations between instantaneous coefficients and copper content.*

The light symbols represent the observed values of sections *A* and the dark symbols those of sections *D*. Where the values of two sections (*A* and *D*) are equal or nearly so, a tagged symbol was employed as shown

These equations apply for copper-zinc castings, the copper content of which varies from 62.1 to 97 per cent. In each case the last term of the parenthesis represents the probable error in the value of the coefficient as determined from the corresponding equation.

Digitized by Google

Fig. 28 represents graphically the instantaneous coefficients of the outside sections at every 50° from 50 to 250° C, and Fig. 29 the coefficients of the inside sections.

In general, the residuals of this series are not as large as those of Series II.

From an examination of Figs. 28 and 29 it is seen, as was the case for the cold-rolled alloys of Series II, that the instantaneous coefficient of a copper-zinc casting of high copper content is not affected by a temperature change as much as that of a casting of low copper content.

In Series II the average residuals of the cold-rolled alpha beta brasses (S321 to S324, inclusive) exceed the probable errors.

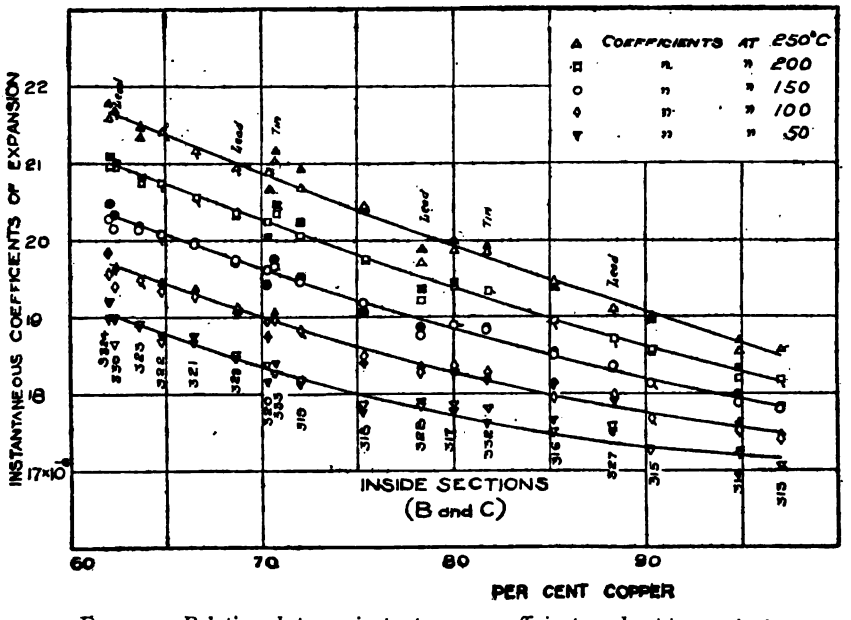

FIG. 29.—*Relations between instantaneous coefficients and copper content*

The light symbols represent the observed values of sections *B*, and the dark symbols those of sections *C*. Where the values of two sections (*B* and *C*) are equal or nearly so, a tagged symbol was employed as shown

The residuals of the alpha beta castings of Series III, however, are generally less than the probable errors, which shows that this group of castings is in close agreement with the derived quadratic equations.

The instantaneous coefficients of the two castings (S332 and S333) which contain tin were found to be usually greater (deviations somewhat more than the probable errors) than the theoretical values of alloys of corresponding copper content (but without tin).

Digitized by Google

Most of the instantaneous coefficients of the leaded castings, S327 to S330, are less than the theoretical values. The average deviations are as follows:

TABLE 19.—Deviations of Leaded Castings

Temperature, degrees centigrade	Average deviations $\times 10^6$	
	Outside sections	Inside sections
50	0.14	0.13
100	.10	.08
150	.10	.07
200	.16	.07
250	.23	.13

As was the case in Series II, these deviations exceed the probable errors and are attributable to added lead.

The coefficients of the specimens which were reheated agree fairly well with those of the first heating, the maximum variation being $\pm 0.15 \times 10^{-6}$. In most cases the coefficients were lower on the second heating. It may be possible to apply the equations (given on p. 122) to calculate the instantaneous coefficients of copper-zinc castings on second heatings without introducing large errors.

TABLE 20.—Change in Length after Test

Laboratory number	Outside sections		Inside sections		Laboratory number	Outside sections		Inside sections	
	A	D	B	C		A	D	B	C
	Per cent	Per cent	Per cent	Per cent		Per cent	Per cent	Per cent	Per cent
S313	0.000	−0.001	0.000	[a] 0.000	S322	[a]−0.002	[a]−0.002	[a] 0.000	−0.001
S314	−.001	[a]+ .001	−.001	[a].000	S323	− .003	[a]− .003	− .002	− .002
S315	[a].000	.000	.000	[a].000	S324	− .001	− .001	− .004	[a]− .002
S316	.000	.002	+.006	[a].000	S327	− .003	[a].000	.000	− .002
S317	−.003	.000	[a].004	.000	S328	.000	[a].000	[a]− .001	[a].000
S318	.000	.000	.000	−.001	S329	[a]− .003	[a].000	[a].000	[a]− .002
S319	[a].000	[a].000	[a]−.003	.000	S330	.000	− .002	− .002	− .001
S320	[a]+.002	.001	.000	+.002	S332	[a]+ .002	.000	[a].000	+ .002
S321	[a].000	− .001	−.002	−.002	S333	[a].000	+ .001	.000	[a].004

[a] The maximum deviation between the heating and cooling curves did not exceed this value.

The cooling curves of this series, as in Series II, did not coincide exactly with the heating curves. Unlike Series II, however, the maximum variation did not always occur at room temperature. At any given temperature from room temperature to 300° C the variation did not exceed ±70 millionths per unit length (except

Digitized by Google

S320C, which showed a variation of +130 millionths at 206° C). The preceding table gives the differences between the lengths after cooling to room temperature and the original lengths of the specimens of this series.

The heating and cooling curves of the four samples which were reheated coincided. These specimens, therefore, returned to the same lengths they had before the second heating. The first heating evidently had an annealing effect.

4. SERIES IV: EXTRUDED AND HOT-ROLLED COPPER-ZINC ALLOYS

In this series there are eight specimens of extruded copper-zinc alloys, the copper content of which varies from 56.4 to 61.4 per cent, and four samples of hot-rolled alloys.

EXTRUDED.—Three specimens were extruded at 0.265 inch, and three having corresponding compositions were extruded at 0.265 inch, drawn to 0.256 inch, annealed, and finished hard at one-fourth inch. The remaining two specimens (S343E and S343ED) containing 61.4 per cent copper were extruded at nine-sixteenths inch. One of these was then drawn to 0.300 inch, annealed, and finished hard at one-fourth inch. The specimens marked "E" were extruded, and those marked "ED" were drawn, annealed, and finished hard after being extruded.

HOT-ROLLED.—The method of working these samples before the thermal expansion tests is given in the following table:

TABLE 21.—Treatment Before Expansion Tests

Laboratory number	Method of working
S341H.....	Hot-rolled from 2½ inches square in one heat to ¾-inch diameter.
S341HD.....	Hot-rolled from 2½ inches square in one heat to ¾-inch diameter, drawn to 0.256 inch, annealed, and finished hard at ¼ inch.
S344H.....	Hot-rolled from 2½ inches square to ½-inch diameter.
S344HD.....	Hot-rolled from 2½ inches square to ½-inch diameter, cold-drawn to 0.256 inch, annealed, and finished hard at ¼ inch.

The specimens marked "H" were hot-rolled, and those marked "HD" were drawn, annealed, and finished hard after being hot-rolled.

Table 22 gives the composition, the temperature range of the thermal expansion test, the values of a and b of the general quadratic equation

$$L_t = L_o\,(1 + at + bt^2),$$

the probable error of L_t, and the instantaneous coefficients at every 50° from 50 to 250° C.

Digitized by Google

TABLE 22.—Summary of Values of Series IV

Previous treatment and metallurgical type	Laboratory No.	Commercial name	Composition						Temperature range
			Copper	Zinc	Lead	Iron	Tin	Manganese	
			P. ct.	P. ct.	P. ct.	P. ct.	P. ct.	P. ct.	°C
Extruded: Alpha beta brass containing lead.	S343E	Free turning rod.	61.44	35.68	2.85	0.03	.....	.....	+20–+318
	S343ED								18– 301
Extruded: Alpha beta brass.	S342E	Muntz metal.	59.12	40.49	.35	.04	.....	.....	12– 305
	S342ED								−49– 301
Extruded: Alpha beta brass containing tin.	S345E	Naval brass.	58.96	40.16	.06	.01	0.84	.....	+15– 302
	S345ED								18– 308
Extruded: Alpha beta bronze containing tin and iron.	S346E	Manganese bronze.	56.39	40.95	.09	.96	1.52	0.09	18– 299
	S346ED								17– 300
Hot-rolled: Alpha beta brass.	S341H	Muntz metal.	61.07	38.66	.24	.03	.....	.....	17– 301
	S341HD								−50– 301
Hot-rolled: Alpha beta brass containing tin.	S344H	Naval brass.	60.21	38.86	.20	.02	.71	.....	+26– [a]288
	S344HD								18– 301

Previous treatment and metallurgical type	Laboratory No.	Commercial name	Coefficients		Probable error of L_t	Instantaneous coefficients $\times 10^6$				
			$a \times 10^6$	$b \times 10^6$		At 50° C	At 100° C	At 150° C	At 200° C	At 250° C
					$\times 10^{-6}$					
Extruded: Alpha beta brass containing lead.	S343E	Free turning rod.	18.66	0.00777	14	19.44	20.21	20.99	21.77	22.54
	S343ED		18.17	.00692	5	18.86	19.55	20.25	20.94	21.63
Extruded: Alpha beta brass.	S342E	Muntz metal.	18.42	.00867	9	19.29	20.15	21.02	21.89	22.76
	S342ED		18.79	.00737	5	19.53	20.26	21.00	21.74	22.48
Extruded: Alpha beta brass containing tin.	S345E	Naval brass.	18.94	.00813	6	19.75	20.57	21.38	22.19	23.00
	S345ED		18.68	.00827	8	19.51	20.33	21.16	21.99	22.82
Extruded: Alpha beta bronze containing tin and iron.	S346E	Manganese bronze.	19.21	.01077	12	20.29	21.36	22.44	23.52	24.60
	S346ED		18.93	.00816	15	19.75	20.56	21.38	22.19	23.01
Hot-rolled: Alpha beta brass.	S341H	Muntz metal.	18.81	.00590	11	19.40	19.99	20.58	21.17	21.76
	S341HD		18.56	.00689	5	19.25	19.94	20.63	21.32	22.00
Hot-rolled: Alpha beta brass containing tin.	S344H	Naval brass.	19.98	.00569	3	20.57	21.16	21.75	22.34	22.92
	S344HD		18.86	.00681	5	19.54	20.22	20.90	21.58	22.26

[a] Before test, specimen was heated to 200° C and cooled to room temperature, after which the test was carried to 524° C in an electric furnace. Coefficients, however, apply only within the range given in the table.

Curves showing the relation between the instantaneous coefficients and the temperature from 50 to 250° C are given in Fig. 30.

Digitized by Google

The large number of varying elements makes it impossible to definitely determine the effect of each on the value of the coefficient of expansion. In general, a decrease in the copper content causes an increase in the coefficient.

ALPHA BETA BRASS.—*S342E and S342ED.*—The drawn specimen has greater coefficients below 140 (approximately), and smaller coefficients above 140° C than the extruded sample. At about 140° C the coefficients of these specimens are equal, and therefore the temperature-coefficient curves intersect at that temperature. At 50 and 250° C the differences are 0.24 and 0.28×10^{-6}, respectively. Annealing and drawing seem to have

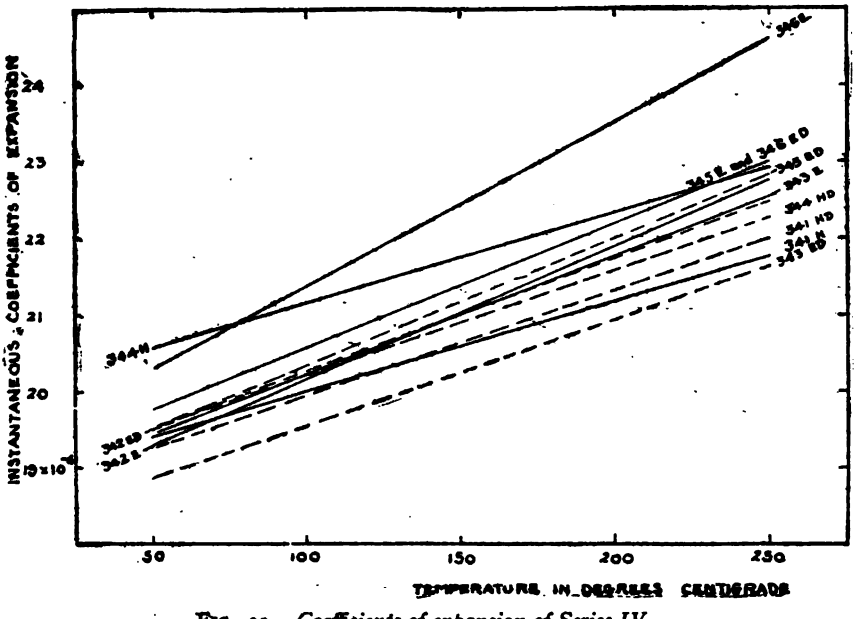

FIG. 30.—*Coefficients of expansion of Series IV*

much less effect on the coefficients of this extruded alloy than on the alloy with 61.4 per cent copper. The latter alloy has 2.5 per cent more lead than the former. The curve of S343E (copper 61.4 per cent) lies between these two curves. The maximum variation of the former from either of the other two curves occurs at 250° C and is 0.22×10^{-6}.

S341H and S341HD.—At about 140° C the rates of expansion of the hot-rolled and the drawn samples are the same. Below this temperature the instantaneous coefficients of the drawn sample are less than those of the hot-rolled, and above this temperature the latter is less than the former. The maximum difference in the coefficients is 0.24×10^{-6}.

Digitized by Google

ALPHA BETA BRASS CONTAINING LEAD.—*S343E and S343ED.*—The drawn sample has lower instantaneous coefficients of expansion than the extruded. At 50° C the difference in the coefficients is 0.58×10^{-6}. This difference increases with increase of temperature, and is equal to 0.91×10^{-6} at 250° C. Annealing and drawing of this alloy, therefore, caused a marked diminution in the instantaneous coefficients.

ALPHA BETA BRASS CONTAINING TIN.—*S345E and S345ED.*—These specimens differ in composition from the preceding ones of this series in the following respects:

(*a*) They contain considerably less lead.

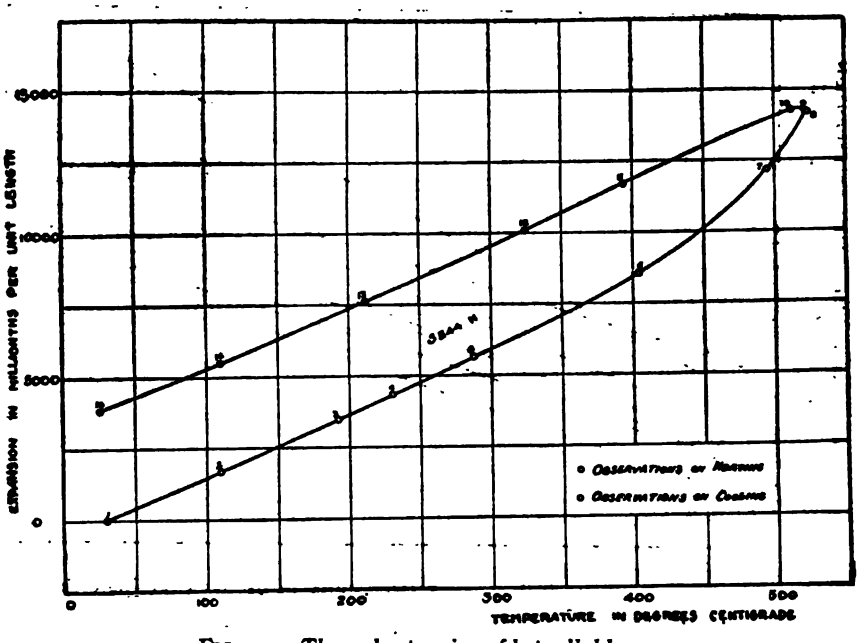

FIG. 31.—*Thermal expansion of hot-rolled brass*

(*b*) They contain an appreciable amount of tin.

The coefficients of the drawn sample are less than those of the extruded. At 250° C the difference in the coefficients is 0.18×10^{-6}. This difference increases very slowly with decrease in temperature and is equal to 0.24×10^{-6} at 50° C. For this alloy, annealing and drawing also caused a diminution in the instantaneous coefficients, but considerably less effect than was produced in the alloy with 61.4 per cent copper.

S344H and S344HD.—These two samples also contain tin.

The instantaneous coefficients of the drawn sample are less than those of the hot-rolled. At 50° C the difference in the coefficients

Digitized by Google

is 1.03×10^{-6}. This difference decreases with temperature and is 0.66×10^{-6} at 250° C. Annealing and drawing of the hot-rolled specimen containing 0.71 per cent tin caused the greatest change in the values of the instantaneous coefficients of hot-rolled samples of Series I and IV, probably due to the amount of tin contained in the alloy.

The hot-rolled specimen (S344H) was heated to 524° C in an electric air furnace. The observations were plotted, and the curves shown in Fig. 31 were obtained. It was impossible to derive a second degree equation applicable over the entire temperature range. Average coefficients of expansion are given in the following table:

TABLE 23.—Coefficients of Expansion

Temperature interval	Average coefficient
°C	$\times 10^{-6}$
30-100	20.7
100-200	21.7
200-300	23.0
300-400	24.9
400-500	40.8

The coefficients increase with temperature. Above 400° C the coefficient increased very rapidly. The rate of expansion between 400 and 500° C was equal to about two times the rate between room temperature and 100° C. The sudden increase in the coefficient indicates that a polymorphic change occurred in the alloy. It should be noted that the average coefficients from 100 to 200° and 200 to 300° C are practically equal to the instantaneous coefficients at 150 and 250° C, respectively.

The observations on cooling lie considerably above the heating curve. The average coefficients of contraction are as follows:

TABLE 24.—Coefficients of Contraction

Temperature interval	Average coefficient
°C	$\times 10^{-6}$
500-400	21.6
400-300	23.0
300-200	22.0
200-100	20.8
100- 30	19.0

Digitized by Google

On cooling to room temperature, this specimen was found to be 0.39 per cent longer than before the test.

After the test, another micrograph was made of this sample (Fig. 32). This record shows how completely the structure has been changed from that of the hot-rolled rod before the test. (See micrograph Fig. 13.) The change indicates that the grains have become equiaxed, in other words, the metal has been thoroughly annealed. The rate of expansion increased abruptly at about 400° C, due to the beginning of this change in structure.

ALPHA-BETA BRONZE CONTAINING TIN AND IRON.—*S346E and S346ED.*—These samples contain 0.09 per cent manganese (not present in the other samples of this series) and comparatively large percentages of iron and tin.

The instantaneous coefficients of the drawn sample are considerably less than those of the extruded. At 50° C the difference in the coefficients is 0.54×10^{-6}. The difference increases very rapidly with increase in temperature, as shown in Fig. 30 and by the large differential rate of expansion $da_t = a - a' + 2t\,(b - b')$, where a and b are the coefficients in the expansion equation of the extruded specimen and a' and b' the coefficients of the drawn sample. The differential rate of expansion for these specimens is

$$da_t = [0.28 + 2t\,(0.00261)]\,10^{-6}$$
$$= (0.28 + 0.00522t)\,10^{-6}.$$

At 250° C the difference in the coefficients is 1.59×10^{-6}. Annealing and drawing of this alloy produced the greatest changes in the coefficients of the alloys of this series. It is interesting to note that this treatment on the extruded alloy, S346E, produced a sample the coefficients of which are practically equal to those of S345E (curves of S346ED and S345E coincide), which specimen contains less copper, lead, iron, and tin (and no manganese).

The cooling curves of S343E, S343ED, and S341H lie below the heating curves, and those of S342E, S345E, S345ED, S346E, and S344H lie above the heating curves. The cooling curves of the other specimens in the series intersect the heating curves. The maximum variation between the cooling and heating curves occurred at room temperature, except for the following two specimens:

Digitized by Google

S344H

FIG. 32.—*Alpha beta brass containing tin, after heating to 524° C.* ×75

Copper 60.21, zinc 38.86, tin 0.71, lead 0.20, iron 0.02 (naval brass)

Digitized by Google

Digitized by Google

TABLE 25

Laboratory number	Maximum deviation per unit length	Temperature
		°C
S343ED	−0.00005	100
S342E	+ .00004	180

After cooling to room temperature, the variation in length from the original length was found to be as follows:

TABLE 26.—Changes in Length After Test

Laboratory number	Extruded	Extruded and drawn
	Per cent	Per cent
S343	−0.014	−0.004
S342	+ .002	+ .003
S345	.011	.006
S346	.026	.002

Laboratory number	Hot-rolled	Hot-rolled and drawn
	Per cent	Per cent
S341	−0.002	+0.004
S344	a+ .39	− .001

a Specimen heated to 524° C.

For the drawn specimens the deviations of the cooling curves from the heating curves are less than the corresponding deviations for the extruded samples. Annealing and drawing of the extruded alloys evidently tend to make the cooling curves approach the heating curves.

The differences in the changes in length at room temperature (see preceding table) between the extruded and drawn samples are comparable to the corresponding differences in the coefficients of the extruded and drawn samples. For S342 and S345 the differences in both cases are small, but for S343 and S346 the reverse is true. In the latter (S346), the difference in the changes of length between the extruded and drawn samples is 0.026 − 0.002 = 0.024 per cent, which is the greatest difference in this series. The greatest difference in the coefficients of expansion between the extruded and drawn samples was observed in this alloy.

Digitized by Google

5. SERIES V: COLD-ROLLED COPPER-TIN ALLOYS

Series V includes four samples of copper tin alloys (alpha bronzes), cold-rolled from 1⅝-inch chilled castings to twenty-one thirty-seconds inch round, cold-drawn to 0.300 inch, annealed, and finished hard at one-fourth inch.

The following table gives the composition, the temperature range of the thermal expansion test, the values of a and b of the general quadratic equation

$$L_t = L_0 (1 + at + bt^2),$$

the probable error of L_t, and the instantaneous coefficients at every 50° from 50 to 250° C.

TABLE 27.—Summary of Values of Series V

Laboratory number	Commercial name	Composition			Temperature range	Coefficients		Probable error of L_t	Instantaneous coefficients $\times 10^6$				
		Copper	Tin	Phosphorus		$a \times 10^6$	$b \times 10^6$		At 50° C	At 100° C	At 150° C	At 200° C	At 250° C
		P. ct.	P. ct.	P. ct.	°C			$\times 10^{-6}$					
S409....	Phosphor bronze.	95.40	4.25	0.37	+20–302	16.61	0.00859	11	17.17	17.53	17.89	18.25	18.60
S406....	Chain bronze	94.86	4.88	.12	20–301	16.63	.00867	13	17.00	17.36	17.73	18.10	18.46
S407....	Gun metal..	92.04	7.67	.11	19–298	16.82	.00425	12	17.24	17.67	18.10	18.52	18.94
S408....	...do	89.69	10.14	.00	20–301	17.13	.00870	4	17.50	17.87	18.24	18.61	18.98

For this series it was also found possible to derive quadratic equations showing the relation between the instantaneous coefficient at a given temperature and the copper (or tin) content of these alloys, if the comparatively small amount of phosphorus is considered negligible. The instantaneous coefficients of cold-rolled copper-tin alloys (89.7 to 95.4 per cent copper) at every 50° from 50 to 250° C may be calculated from the following equations, derived by the method of least squares:

$$a_{50} = (35.492 - 0.32422\ \mathrm{Cu} + 0.0013737\ \mathrm{Cu}^2 \pm 0.11)\ 10^{-6}$$
$$a_{100} = (26.056 - .10752\ \mathrm{Cu} + .0001793\ \mathrm{Cu}^2 \pm .10)\ 10^{-6}$$
$$a_{150} = (26.840 - .11263\ \mathrm{Cu} + .0001877\ \mathrm{Cu}^2 \pm .10)\ 10^{-6}$$
$$a_{200} = (38.042 - .34214\ \mathrm{Cu} + .0014036\ \mathrm{Cu}^2 \pm .11)\ 10^{-6}$$
$$a_{250} = (28.601 - .12544\ \mathrm{Cu} + .0002091\ \mathrm{Cu}^2 \pm .12)\ 10^{-6}.$$

Fig. 33 represents graphically the instantaneous coefficients at every 50° from 50 to 250° C.

As was the case in Series II and III, the instantaneous coefficients of these alloys increase with a decrease in the copper content.

Digitized by Google

From Fig. 33 it is seen that the curves are nearly parallel. A given increase in temperature, therefore, will cause approximately the same change in the instantaneous coefficients of alloys of this series within the range 89.7 to 95.4 per cent copper. For example, the change in the computed values of the instantaneous coefficients at 100 and 150° C of the alloy containing 89.69 per cent copper is 0.39×10^{-6}, and the corresponding change for the alloy containing 95.40 per cent copper is 0.37×10^{-6}. These changes are approximately the same.

The cooling curves of the specimens of this series lie below the heating curves. The maximum variation between these curves occurred at room temperature, except for S408 (at 100° C, deviation was −0.011 per cent). After cooling the specimens were found to be about 0.008 per cent shorter than before the tests.

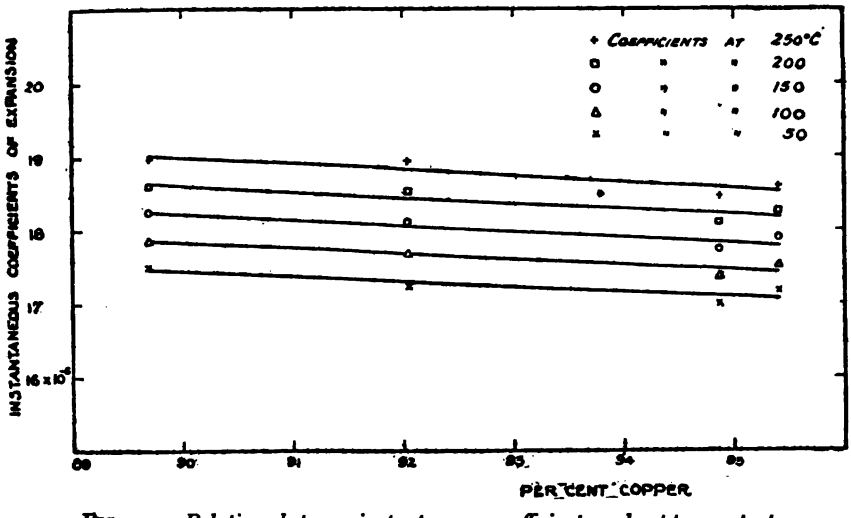

FIG. 33.—*Relations between instantaneous coefficients and copper content*

6. SERIES VI: SECTIONS OF COPPER-TIN CASTINGS

Series VI includes 16 samples cut from 4 castings (1⅝ inches) of copper-tin alloys (alpha bronzes), the compositions of which correspond to those of Series V. From each casting, four specimens (A, B, C, D) were cut similar to the sections of Series III. (See p. 116.) The samples of Series V were obtained from castings like those of Series VI, which castings were cold-rolled to twenty-one thirty-seconds inch round, cold-drawn to 0.300 inch, annealed, and finished hard at one-fourth inch. S409A, S409B, S409C, and S409D of Series VI have the same chemical composition as S409 of Series V, and in like manner for the other samples of this series.

Digitized by Google

The composition, the temperature range of the thermal expansion test, the values of a and b of the general quadratic equation

$$L_t = L_o (1 + at + bt^2),$$

the probable error of L_t, and the instantaneous coefficients at every 50° from 50 to 250° C are given in the following table:

TABLE 28.—Summary of Values of Series VI

Laboratory number		Commercial name	Composition			Temperature range	Coefficients		Probable error of L_o	Instantaneous coefficients $\times 10^6$				
			Copper	Tin	Phosphorus		$a \times 10^6$	$b \times 10^9$		At 50° C	At 100° C	At 150° C	At 200° C	At 250° C
			P. ct.	P. ct.	P. ct.	°C			$\times 10^{-6}$					
S409	A.	Phosphor bronze	95.40	4.25	0.37	+25–+302	16.89	0.00416	2	17.31	17.72	18.14	18.55	18.97
	B.					21– 302	17.12	.00348	1	17.47	17.82	18.16	18.51	18.86
	C[a]					20– 305	16.77	.00423	1	17.19	17.62	18.04	18.46	18.88
	D.					26– 299	16.83	.00452	2	17.28	17.73	18.19	18.64	19.09
S406	A.	Chain bronze	94.86	4.88	.12	25– 302	16.92	.00356	2	17.28	17.63	17.99	18.34	18.70
	B.					27– 303	16.77	.00415	2	17.18	17.60	18.02	18.43	18.84
	C.					25– 303	16.91	.00409	1	17.32	17.73	18.14	18.55	18.96
	D.					24– 302	16.78	.00384	4	17.16	17.55	17.93	18.32	18.70
S407	A.	Gun metal	92.04	7.67	.11	28– 303	17.12	.00347	2	17.47	17.81	18.16	18.51	18.86
	B.					28– 305	17.02	.00381	4	17.40	17.78	18.16	18.54	18.92
	C.					25– 305	17.16	.00315	3	17.48	17.79	18.10	18.42	18.74
	D.					23– 299	17.15	.00336	1	17.49	17.82	18.16	18.49	18.83
S408	A.	Gun metal	89.69	10.14	.00	25– 305	16.99	.00520	2	17.51	18.03	18.55	19.07	19.59
	B.					26– 303	16.98	.00440	2	17.42	17.86	18.30	18.74	19.18
	C.					22– 302	17.33	.00366	3	17.70	18.06	18.43	18.79	19.16
	D.					28– 299	17.17	.00479	2	17.65	18.13	18.61	19.09	19.56

[a] Results on second heating.

The derived equations giving the relation between the instantaneous coefficient at every 50° from 50 to 250° C and the copper content of these castings are as follows:

OUTSIDE SECTIONS

$$a_{50} = (+37.776 - 0.37966\ \mathrm{Cu} + 0.0017247\ \mathrm{Cu}^2 \pm 0.05)10^{-6}$$
$$a_{100} = (+41.783 - .44669\ \mathrm{Cu} + .0020292\ \mathrm{Cu}^2 \pm .06)10^{-6}$$
$$a_{150} = (-52.360 + 1.60752\ \mathrm{Cu} - .0091195\ \mathrm{Cu}^2 \pm .13)10^{-6}$$
$$a_{200} = (+50.397 - .59178\ \mathrm{Cu} + .0026883\ \mathrm{Cu}^2 \pm .14)10^{-6}$$
$$a_{250} = (-92.532 + 2.51757\ \mathrm{Cu} - .0141623\ \mathrm{Cu}^2 \pm .23)10^{-6}$$

INSIDE SECTIONS

$$a_{50} = (+33.580 - 0.30147\ \mathrm{Cu} + 0.0013695\ \mathrm{Cu}^2 \pm 0.10)10^{-6}$$
$$a_{100} = (-16.009 + .77588\ \mathrm{Cu} - .0044331\ \mathrm{Cu}^2 \pm .08)10^{-6}$$
$$a_{150} = (-15.622 + .77588\ \mathrm{Cu} - .0044331\ \mathrm{Cu}^2 \pm .07)10^{-6}$$
$$a_{200} = (-15.835 + .78703\ \mathrm{Cu} - .0044838\ \mathrm{Cu}^2 \pm .08)10^{-6}$$
$$a_{250} = (-114.191 + 2.91918\ \mathrm{Cu} - .0159864\ \mathrm{Cu}^2 \pm .13)10^{-6}$$

Digitized by Google

Again, it should be remembered that, as in previous series, these equations are not to be applied beyond the proper limits. For this series of copper-tin castings the limits are from 89.7 to 95.4 per cent copper.

The instantaneous coefficients of the outside sections at every 50° from 50 to 250° C, and the coefficients of the inside sections are shown graphically in Figs. 34 and 35, respectively.

The experimental values of the instantaneous coefficients at 250 and 200° C of the outside sections deviate appreciably from the computed values, especially for the casting containing about 92 per cent copper. The deviations of the experimental coefficients

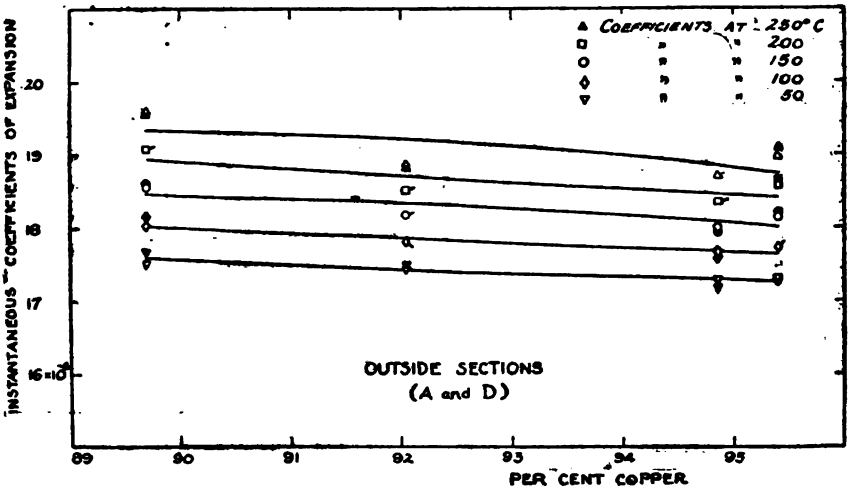

FIG. 34.—*Relations between instantaneous coefficients and copper content*

The light symbols represent the observed values of sections *A*, and the dark symbols those of sections *D*. Where the values of two sections (*A* and *D*) are equal or nearly so, a tagged symbol was employed as shown

of the inside sections are generally smaller than those of the outside sections.

The experimental values of the coefficients of sections *A* agree with the corresponding values of sections *D* much better than do the coefficients of sections *B* with *C*.

The coefficients of the outside sections at 50 and 100° C are nearly the same as the corresponding values of the inside sections at these temperatures. However, at higher temperatures there are appreciable differences. The values of the coefficients of the inside and outside sections containing about 94 or 95 per cent copper are approximately the same, but for specimens with less copper the

Digitized by Google

differences increase with a decrease in the copper content of the castings.

Most of the cooling curves of the specimens of Series VI lie below the heating curves. The cooling curves of S409A, S409C, S406C, S408A, and S408D lie above the heating curves. The maximum variation between these curves did not exceed ±60 millionths per unit length except for S407A (at 190° C deviation was −180 millionths per unit length). After cooling to room temperature, the average variation in length from the original lengths was ±0.002 per cent.

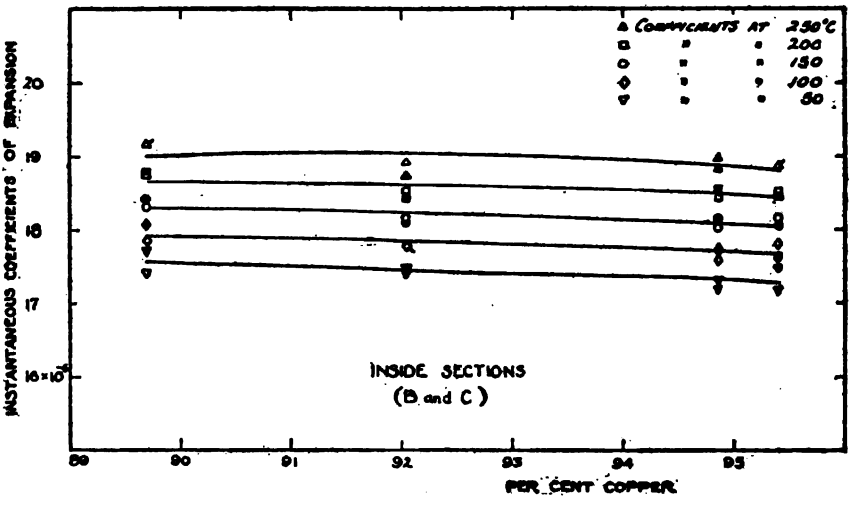

FIG. 35.—*Relations between instantaneous coefficients and copper content*

The light symbols represent the observed values of sections *B*, and the dark symbols those of sections *C*. Where the values of two sections (*B* and *C*) are equal, or nearly so, a tagged symbol was employed as shown

7. SERIES VII: ALUMINUM BRONZE

This series contains two aluminum bronzes, S347H and S347HD, having the following composition: Copper, 92.17 per cent; aluminum, 7.34 per cent; zinc, 0.40 per cent; silicon, 0.09 per cent; and a trace of nickel. The first specimen was hot-rolled from 3 inches round to one-half inch diameter, and the second sample was hot-rolled from 3 inches round to one-half inch diameter, cold-drawn to 0.256 inch, annealed, and finished hard at one-fourth inch.

The expansion equations derived for these bronzes are

$$\text{S347H} \quad L_t = L_0 [1 + (15.57t + 0.00805t^2 \pm 7)\ 10^{-6}].$$
$$\text{S347HD} \quad L_t = L_0 [1 + (15.79t + .00645t^2 \pm 12)\ 10^{-6}].$$

Digitized by Google

These equations are applicable between 21 and 319°, and from 19 to 301° C, respectively.

The instantaneous coefficients at every 50° from 50 to 250° C are given in Table 29.

TABLE 29

Laboratory number	Instantaneous coefficients $\times 10^6$				
	At 50° C	At 100° C	At 150° C	At 200° C	At 250° C
S347H	16.37	17.18	17.99	18.79	19.60
S347HD	16.44	17.08	17.72	18.37	19.02

These alloys are the only ones investigated that contain aluminum and silicon.

Below 75° (approximately) the instantaneous coefficients of the drawn sample are slightly larger than those of the hot-rolled, but for higher temperatures the coefficients are less, the difference in the coefficients increasing with temperature. At 250° C this difference is 0.58×10^{-6}. Annealing and drawing of the hot-rolled aluminum-copper alloy caused a greater diminution in the coefficients than was observed in the case of the hot-rolled electrolytic copper.

The maximum variation between the heating and cooling curves did not exceed ±70 millionths per unit length. After cooling to room temperature, the variations in lengths from the original lengths of S347H and S347HD were found to be −0.002 and +0.002 per cent, respectively.

The cold-drawn aluminum-copper specimen was reheated from 20 to 302° C. The equation

$$L_t = L_0 [1 + (16.17t + 0.00523t^2 \pm 10)\ 10^{-6}]$$

was found to fit the observations on the second heating. The last term of the parentheses represents the probable error of L_t at any temperature within the range. The following comparison gives the instantaneous coefficients on the first and second heatings:

TABLE 30

	Instantaneous coefficients $\times 10^6$				
	At 50° C	At 100° C	At 150° C	At 200° C	At 250° C
First heating	16.44	17.08	17.72	18.37	19.02
Second heating	16.69	17.32	17.74	18.26	18.78

Digitized by Google

At about 150° C the coefficients are equal. Below this temperature the coefficients on the second heating are greater than those of the first, but at higher temperatures the reverse is true. The maximum difference in the coefficients is 0.25×10^{-6}.

8. RELATION OF DENSITY TO THERMAL EXPANSION

In order to find a possible relation between thermal expansion and density, it was decided to examine the densities of a number of samples of Series II and III.

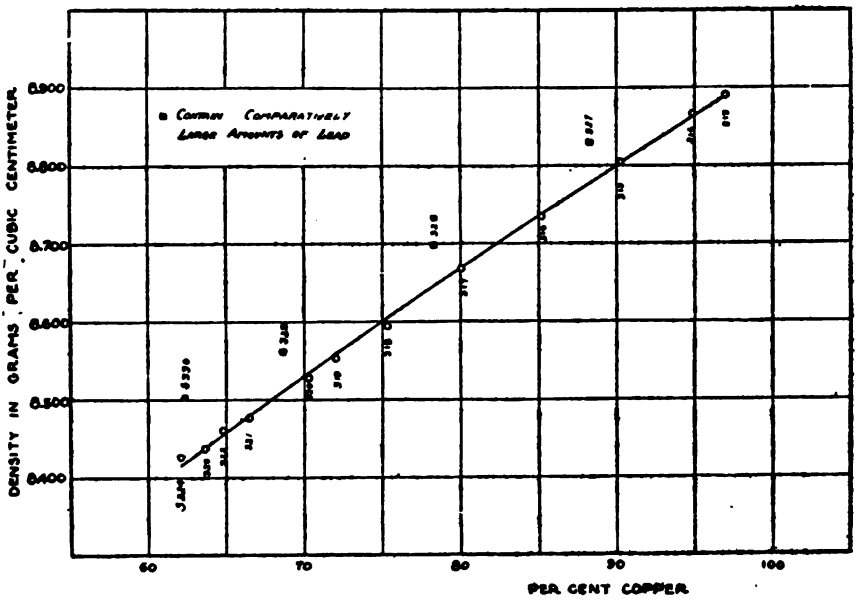

FIG. 36.—*Relation between density and copper content of cold-rolled copper-zinc alloys*

The densities of 16 samples of 2-inch cold-rolled copper-zinc alloys of Series II were determined [13] after the thermal expansion tests, and are plotted in Fig. 36. The empirical equation

$$D_{15} = 7.3605 + 0.019147\ \mathrm{Cu} - 0.00003509\ \mathrm{Cu}^2$$

gives the density of a cold-rolled copper-zinc alloy containing from 62.1 to 97 per cent copper, and the remainder zinc with comparatively small percentages of lead and iron. In deriving this equation, where D_{15} is the density in grams per cubic centimeter at 15° C and Cu is the percentage of copper contained in the alloy the four specimens (S327, S328, S329, and S330), containing appreciable amounts of lead, were ignored. The observed densi-

[13] By E. L. Peffer of this Bureau.

Digitized by Google

ties of these four alloys are considerably greater than those computed from the formula, on account of the comparatively large density of the lead constituent. The following table shows a comparison between the observed and computed densities:

TABLE 31.—Densities of Cold-Rolled Copper-Zinc Alloys

Laboratory number	Composition				Density		Residuals
	Copper	Zinc	Lead	Iron	Observed	Computed	
	Per cent	Per cent	Per cent	Per cent			
S313	97.00	2.97	0.01	0.02	8.890	8.888	0.002
S314	94.87	5.11	.01	.01	8.866	8.861	.005
S315	90.26	9.70	.01	.03	8.804	8.803	.001
S316	85.21	14.76	.01	.02	8.734	8.737	−.003
S317	80.02	19.89	.05	.03	8.667	8.668	−.001
S318	75.31	24.64	.02	.03	8.594	8.604	−.010
S319	72.02	27.95	.01	.02	8.553	8.558	−.005
S320	70.28	29.66	.03	.03	8.528	8.533	−.005
S321	66.50	33.43	.04	.03	8.476	8.479	−.003
S322	64.81	34.92	.24	.03	8.460	8.454	+.006
S323	63.63	36.17	.17	.03	8.437	8.437	.000
S324	62.10	37.71	.17	.02	8.426	8.414	.012
S327	88.30	10.00	1.68	.02	8.830	(8.778)	(.052)
S328	78.28	20.01	1.68	.03	8.698	(8.644)	(.054)
S329	68.65	29.67	1.65	.03	8.562	(8.510)	(.052)
S330	62.33	35.04	2.57	.06	8.503	(8.418)	(.085)

The probable error above is ±0.004.

From the relations existing between expansion and copper content and between density and copper content, it is possible to predict the expansion of a cold-rolled copper-zinc alloy from a density determination. By substituting the observed density in the previous equation the copper content may be found. The instantaneous coefficient of expansion—for example, at 100° C—may be determined by substituting this value of the copper content in the equation (p. 113)

$$a_{100} = (24.673 - 0.08794\ \mathrm{Cu} + 0.0001252\ \mathrm{Cu}^2 \pm 0.05)10^{-6}.$$

The densities (in grams per milliliter at 18° C) of the sections of four castings of Series III were also determined. The results were found to be as follows:

Digitized by Google

TABLE 32.—Densities of Sections of Some Copper-Zinc Castings

Laboratory number	Copper	Density			
		Outside sections		Inside sections	
		A	D	B	C
	Per cent				
S317	80.02	8.626	8.612	8.612	8.480
S318	75.31	8.571	8.569	8.479	8.486
S321	66.50	8.442	8.443	8.434	8.415
S323	63.63	8.410	8.413	8.392	8.419

On cutting through the surfaces of S317C, S321C, and S323B, inclosed pores and cavities were found to exist. This accounts for the comparatively low values of the densities of these sections.

In general the density increases with an increase in the copper content of the casting, but no definite relation could be found for this series of castings. The densities of the cold-rolled alloys (Series II) of corresponding composition are greater than the densities of these castings. In this case cold-rolling evidently closed the pores and cavities in the casting and produced a more compact alloy.

VI. COMPARISON OF RESULTS

A discussion of each particular series of samples has already been given at the close of each series. In this section, however, it is proposed to compare the various series and indicate the more obvious relations or differences.

The curves of instantaneous coefficients of Series II and III were plotted on the same scale and are shown in Fig. 37. Since the curves for the inside sections are slightly below those for the outside sections, they were omitted in order to avoid confusion. An examination of this figure yields important facts, showing the differences produced in copper-zinc castings (Series III) if cold-rolled, cold-drawn, annealed, and finished hard (Series II).

In the case of alloys containing 62 per cent copper, it was found that the coefficients did not materially differ in cast and cold-rolled specimens, and for alloys containing 90 per cent copper a similar agreement existed. For alloys with a copper content from about 62 to 90 per cent, the cold-rolled alloys give greater coefficients than the castings, and for alloys containing more than 90 per cent copper the reverse is true. In the former case, the maximum

Digitized by Google

deviations occur at about 75 per cent copper (except at 250° C), and in the latter case at 97 per cent copper; that is, the coefficients of expansion of castings containing 75 or 97 per cent copper, if cold-rolled, cold-drawn, annealed, and finished hard, change more than the coefficients of castings containing other percentages of copper between 62 and 97 per cent. The maximum deviations between the coefficients of Series II and those of Series III (over the range 62 to 97 per cent copper) occur in alloys with a copper content of 97 per cent (except at 250° C). The differences between the computed coefficients of a casting (Series III, outside

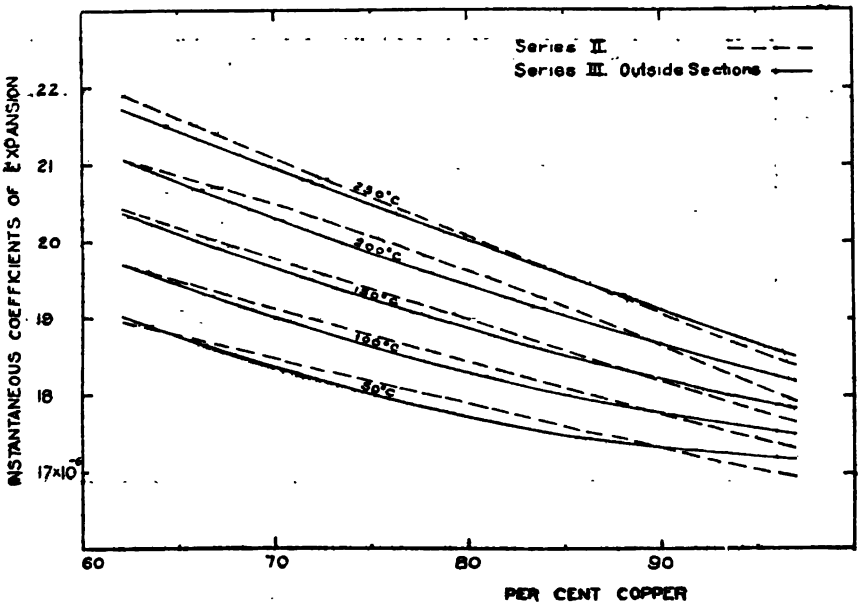

FIG. 37.—*Comparison of instantaneous coefficients of Series II and III*

sections) containing 97 per cent copper, and of a cold-rolled copper-zinc alloy (Series II) of the same composition, are shown in the following comparison:

TABLE 33

	Instantaneous coefficients $\times 10^6$			
	At 50° C	At 100° C	At 150° C	At 200° C
Series III (outside sections)	17.18	17.51	17.84	18.20
Series II	16.95	17.32	17.67	17.93
Deviations (Series III—Series II)	.23	.19	.17	.27

Digitized by Google

The corresponding deviations between the two series for alloys containing 75 per cent copper are given in Table 34.

TABLE 34

	Instantaneous coefficients $\times 10^6$			
	50° C	100° C	150° C	200° C
Series III (outside sections)	18.01	18.64	19.26	19.86
Series II	18.19	18.78	19.39	20.07
Deviations (Series III—Series II)	−.18	−.14	−.13	−.21

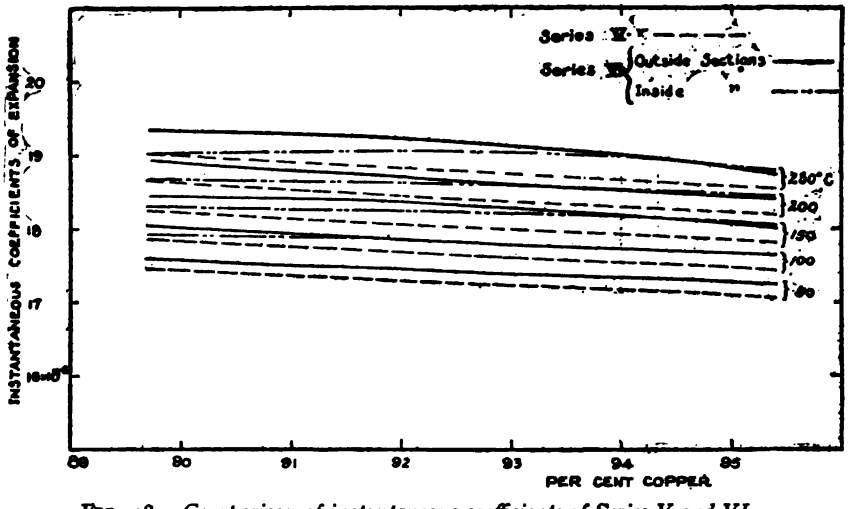

FIG. 38.—*Comparison of instantaneous coefficients of Series V and VI*

Fig. 38 shows the curves of instantaneous coefficients of Series V and VI. The curve for the instantaneous coefficients of the inside sections at 50° was omitted to avoid confusion, for it is very close to the corresponding curve for the outside sections.

Some of the essential differences produced in copper-tin castings (Series VI), if cold-rolled, cold-drawn, annealed, and finished hard (Series V), are as follows:

1. The coefficients of the cold-rolled tin alloys are less than those of the castings; that is, cold rolling and drawing cause a diminution in the values of the instantaneous coefficients. In general, the difference between the instantaneous coefficients of the outside sections and the cold-rolled specimens increases as the temperature increases.

Digitized by Google

2. The instantaneous coefficients of the inside sections and the cold-rolled alloys, both containing 90 per cent copper, are approximately equal. For specimens containing from 90 to 95 per cent copper, the difference between these coefficients generally increases with increase of copper content.

The following five figures (Figs. 39 to 43, inclusive) give a general graphical résumé of the instantaneous coefficients of the seven series of alloys investigated.

The curves derived from the observations of Series II, III, V, and VI are shown, except several which are omitted to avoid confusion. The curves of the inside sections of Series III are not shown, for they nearly coincide with the corresponding curves of the outside sections. The curve of Series V at 150° and the curve of the inside sections of Series VI at 50° were also omitted, for they are close to those of Series II and Series VI (outside sections), respectively.

There do not seem to be great differences between the curves of Series II and V and Series III and V, respectively. The maximum deviation (0.12×10^{-6}) between the curves of instantaneous coefficients of Series II and V occurs at 200° C (95.4 per cent copper), and the greatest difference (0.12×10^{-6}) between the curves of Series III (outside sections) and Series V, at 250° C (about 95 per cent copper).

For the curves of Series II and Series VI (outside sections) the maximum variation (0.36×10^{-6}) occurs at 250° C (about 93 per cent copper). The differences between Series III and VI are considerably less.

At 50° the instantaneous coefficients of S347H and S347HD, which contain about 7 per cent aluminum, are considerably below the values of Series II, III, V, and VI. With increasing temperature, to about 200° C, the values of the instantaneous coefficients approach those of the alloys of these series containing the same amount of copper. At 250° the instantaneous coefficient of S347H is greater than any copper alloy of these series containing about 92 per cent copper. The aluminum evidently has a great effect on the rate of expansion.

At 50° C the values of the instantaneous coefficients of S340H and S340HD (99.97 per cent copper) lie slightly below the extrapolated curve of Series II. As the temperature increases, these values gradually approach this curve, and then with further increase in temperature there is a tendency to depart more and more above this curve. The values of the coefficients of the

Digitized by Google

FIG. 39.—*Résumé of coefficients of expansion of Series I to VII at 50° C*

NOTE.—The light symbols indicate specimens that were hot rolled or extruded, and the heavy symbols indicate samples that received additional treatment (drawn, annealed, and finished hard)

Digitized by Google

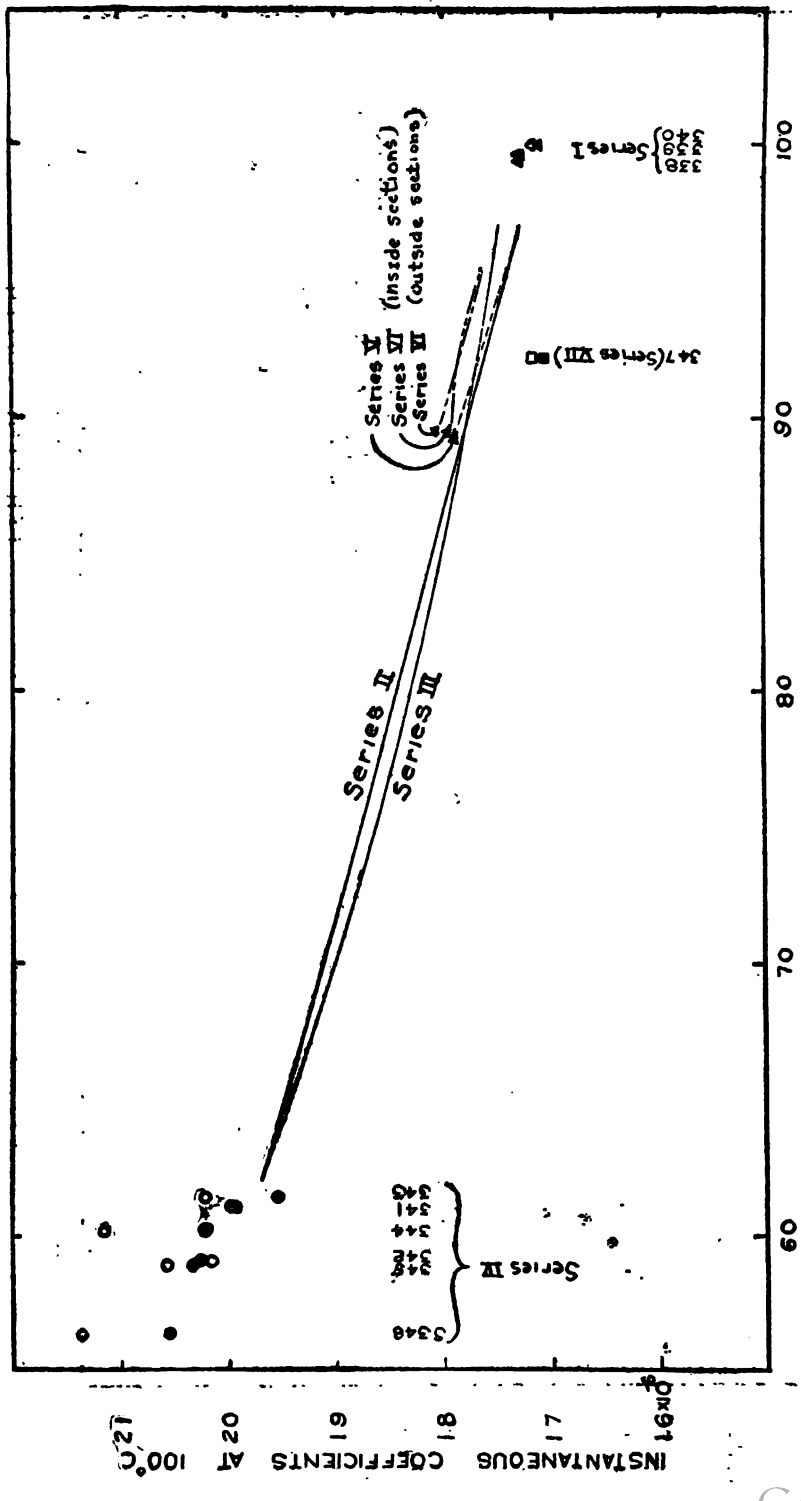

FIG. 40.—*Résumé of coefficients of expansion of Series I to VII at 100°C. (See note, Fig. 39)*

Digitized by Google

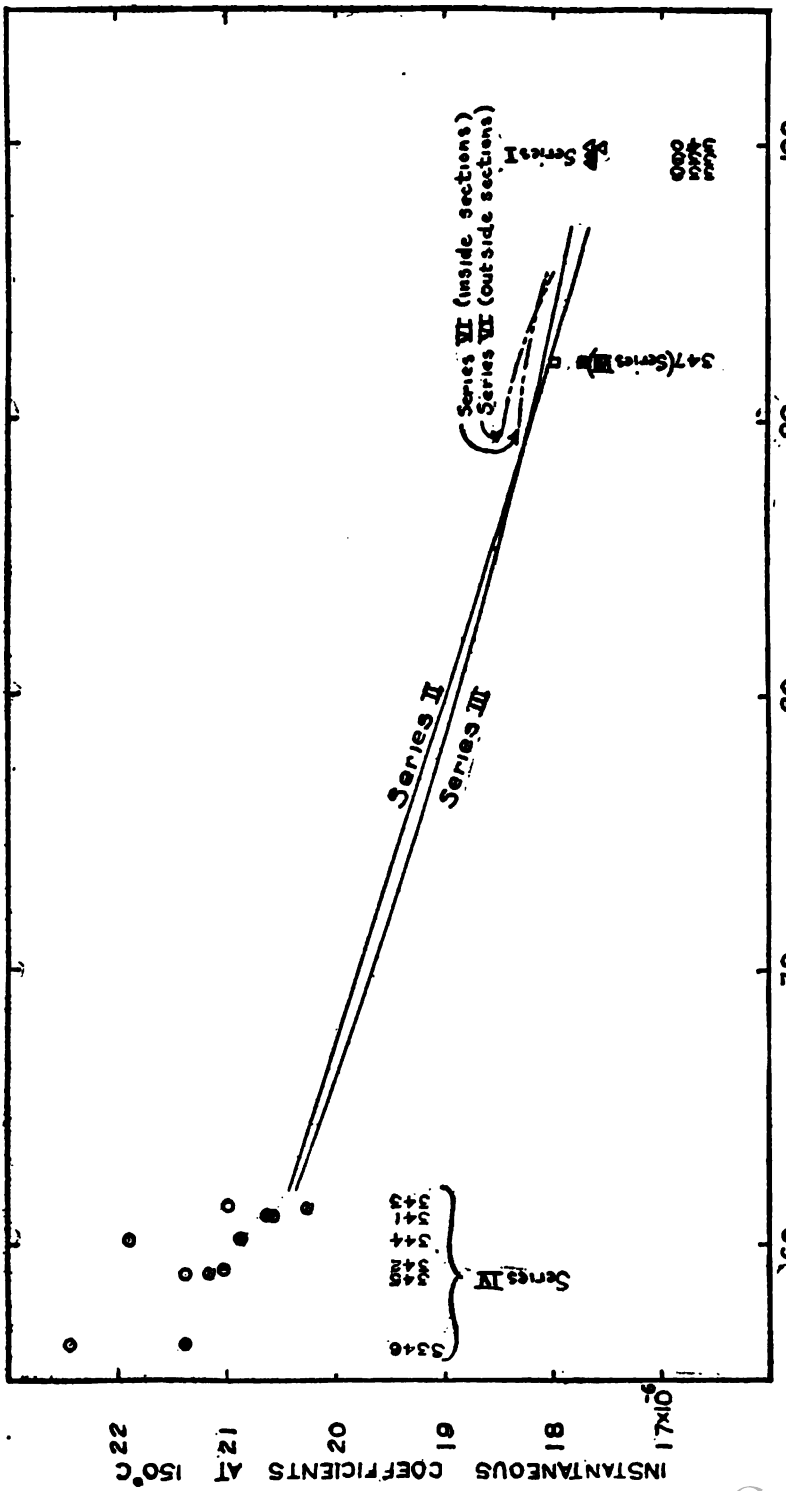

FIG. 41.—*Résumé of coefficients of expansion of Series I to VII (V omitted) at 150° C. (See note, Fig. 39)*

Digitized by Google

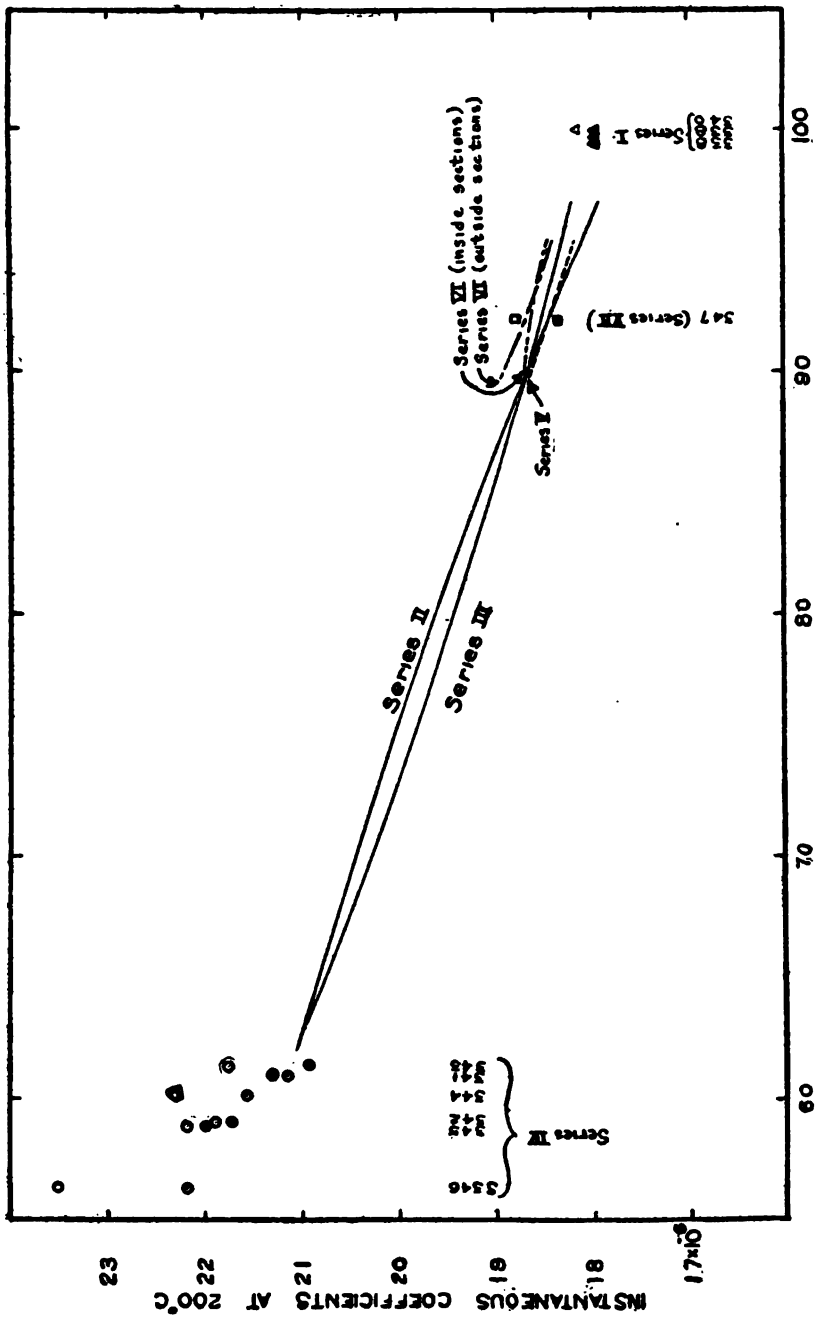

FIG. 42.—*Résumé of coefficients of expansion of Series I to VII at 200° C. (See note, Fig. 39)*

Digitized by Google

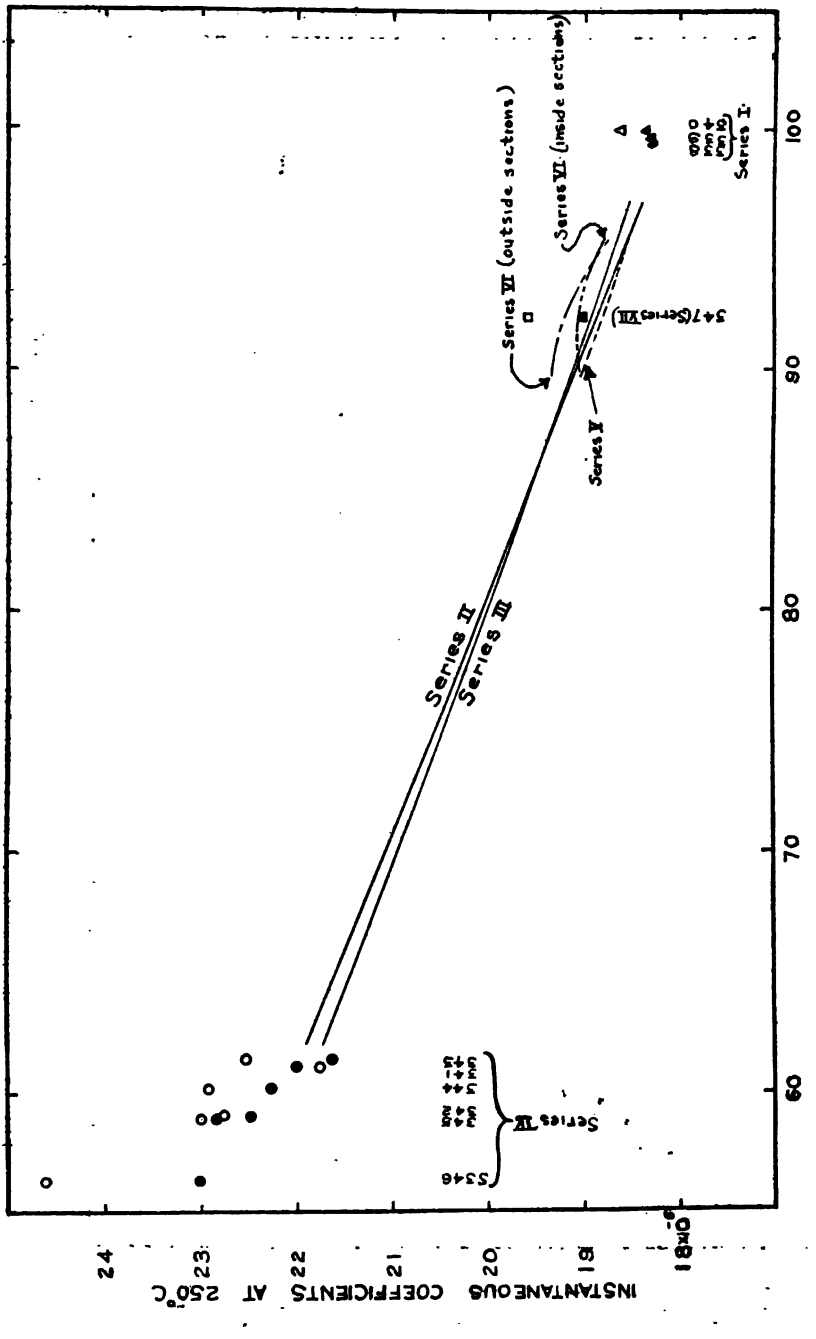

FIG. 43.—*Résumé of coefficients of expansion of Series I to VII at 250° C. (See note, Fig. 39)*

Digitized by Google

nickeliferous and arsenical copper lie near the extrapolated curves of Series III and above those of Series II.

The instantaneous coefficients of the hot-rolled and extruded alloys containing from 56.4 to 61.4 per cent copper, are scattered more or less, on account of the comparatively large number of varying factors. In general, these values lie above the extrapolated curves of Series II and III.

VII. SUMMARY AND CONCLUSIONS

In the present investigation data on the thermal expansion of 128 samples of copper and its important industrial alloys of various compositions, heat treatments, mechanical treatments, etc., are presented. The alloys contained from 56 to 100 per cent copper and were prepared in a number of ways—cast, cast and cold-rolled, extruded, extruded and cold worked, hot-rolled, and hot-rolled and cold worked. Most of the samples were examined from room temperature to about 300° C. (Several specimens were cooled to −50° C and then heated to +300° C.)

Practically all available information on the thermal expansion of copper and its alloys is briefly reviewed.

A description of the apparatus and the preparation of the samples, etc., are given.

Definite mathematical relations were found to exist between the instantaneous coefficients of expansion and the copper content of most of the alloys investigated. (See Series II, III, V, VI.) In general, the coefficient of expansion increases with a decrease in the copper content. The addition of lead or tin has a decided effect on the coefficient; the former element generally decreases, and the latter increases, the coefficient.

SERIES II AND III (COPPER-ZINC ALLOYS).—In the case of alloys containing 62 per cent copper, it was found that the coefficients did not materially differ in cast or cold-rolled specimens, and for alloys containing 90 per cent copper a similar agreement existed. For alloys with a copper content from about 62 to 90 per cent, the cold-rolled alloys have greater coefficients than the castings, and for alloys containing more than 90 per cent copper the reverse is true. The coefficients of the inside sections of the castings are generally slightly less than those of the outside sections. A relation exists between the density and thermal expansion of the cold-rolled copper-zinc alloys of Series II.

SERIES V AND VI (COPPER-TIN ALLOYS).—The coefficients of the cold-rolled tin alloys are less than those of the castings. Cold-

Digitized by Google

TABLE 36.—Average Coefficients of Expansion of Cold-Rolled Copper-Zinc Alloys [a] (Series II)

Laboratory number	Commercial name	Composition				Average coefficients of expansion per degree centigrade				Average coefficients of expansion per degree Fahrenheit. Room temperature (77° F) to 212° F
		Copper	Zinc	Lead	Iron	Room temperature (25° C) to 100° C	100 to 200° C	200 to 300° C	Room temperature (25° C) to 300° C	
		Per cent	Per cent	Per cent	Per cent					
S313	Primer gilding	97.00	2.97	0.01	0.02	0.0000169	0.0000176	0.0000183	0.0000177	0.0000094
S314	Gilding	94.87	5.11	.01	.01	.0000173	.0000180	.0000188	.0000181	.0000096
S315	Commercial bronze	90.26	9.70	.01	.03	.0000175	.0000181	.0000189	.0000182	.0000097
S316	Rich low brass	85.21	14.76	.01	.02	.0000177	.0000186	.0000196	.0000187	.0000096
S317	Low brass	80.02	19.89	.05	.03	.0000180	.0000190	.0000202	.0000191	.0000100
S318	Brazing brass	75.31	24.64	.02	.03	.0000184	.0000195	.0000207	.0000196	.0000102
S319	Spring brass	72.02	27.95	.01	.02	.0000185	.0000197	.0000210	.0000198	.0000103
S320	Cartridge brass	70.28	29.66	.03	.03	.0000186	.0000197	.0000210	.0000199	.0000103
S321	do	66.50	33.43	.04	.03	.0000190	.0000199	.0000211	.0000201	.0000105
S322	Commercial brass	64.81	34.92	.24	.03	.0000190	.0000201	.0000214	.0000202	.0000105
S323	Commercial brass wire	63.63	36.17	.17	.03	.0000190	.0000203	.0000217	.0000205	.0000106
S324	Hot-rolled brass tube	62.10	37.71	.17	.02	.0000191	.0000206	.0000223	.0000208	.0000106
S327	Leaded bronze	88.30	10.00	1.68	.02	.0000175	.0000182	.0000190	.0000183	.0000097
S328	Leaded low brass	78.28	20.01	1.68	.03	.0000181	.0000191	.0000201	.0000192	.0000101
S329	Leaded screw wire	68.65	29.67	1.65	.03	.0000187	.0000199	.0000212	.0000200	.0000104
S330	Free turning rod	62.33	35.04	2.57	.06	.0000191	.0000202	.0000215	.0000204	.0000106
S332 [b]	Fourdrinier wire	81.70	17.94	.04	.01	.0000180	.0000190	.0000202	.0000192	.0000100
S333 [c]	Admiralty condenser tubes	70.64	28.21	.04	.01	.0000188	.0000200	.0000214	.0000202	.0000104

[a] The previous treatments of these alloys are given on p. 109.

[b] Tin=0.31 per cent.

[c] Tin=1.10 per cent.

Digitized by Google

TABLE 37.—Average Coefficients of Expansion of Sections of Copper-Zinc Castings [a] (Series III)

Laboratory number	Commercial name	Composition				Average coefficients of expansion per degree centigrade				Average coefficients of expansion per degree Fahrenheit. Room temperature (77° F) to 212° F
		Copper	Zinc	Lead	Iron	Room temperature (25° C) to 100° C	100 to 200° C	200 to 300° C	Room temperature (25° C) to 300° C	
S313 A	Primer gilding	Per cent 97.00	Per cent 2.97	Per cent 0.01	Per cent 0.02	0.0000173	0.0000179	0.0000187	0.0000180	0.0000096
S313 B						.0000171	.0000178	.0000186	.0000179	.0000095
S313 C						.0000172	.0000178	.0000186	.0000179	.0000095
S313 D						.0000172	.0000178	.0000185	.0000179	.0000095
S313 A [b]						.0000172	.0000178	.0000186	.0000179	.0000095
S314 A	Gilding	94.87	5.11	.01	.01	.0000173	.0000179	.0000186	.0000180	.0000096
S314 B						.0000173	.0000179	.0000186	.0000180	.0000096
S314 C						.0000173	.0000180	.0000187	.0000181	.0000096
S314 D						.0000173	.0000180	.0000188	.0000181	.0000096
S315 A	Commercial bronze	90.26	9.70	.01	.03	.0000175	.0000183	.0000191	.0000184	.0000097
S315 B						.0000174	.0000182	.0000190	.0000183	.0000097
S315 C						.0000174	.0000181	.0000190	.0000182	.0000097
S315 D						.0000174	.0000182	.0000191	.0000183	.0000097
S316 A	Rich low brass	85.21	14.76	.01	.02	.0000177	.0000185	.0000195	.0000187	.0000098
S316 B						.0000176	.0000185	.0000195	.0000186	.0000098
S316 C						.0000178	.0000185	.0000194	.0000186	.0000099
S316 D						.0000176	.0000186	.0000197	.0000187	.0000098
S316 B [b]						.0000178	.0000185	.0000194	.0000186	.0000099
S317 A	Low brass	80.02	19.89	.05	.03	.0000177	.0000187	.0000199	.0000189	.0000098
S317 B						.0000180	.0000189	.0000199	.0000190	.0000100
S317 C						.0000179	.0000189	.0000200	.0000190	.0000099
S317 D						.0000178	.0000188	.0000199	.0000189	.0000099
S318 A	Brazing brass	75.31	24.64	.02	.03	.0000183	.0000195	.0000208	.0000196	.0000102
S318 B						.0000180	.0000192	.0000204	.0000193	.0000100
S318 C						.0000179	.0000191	.0000204	.0000193	.0000100
S318 D						.0000181	.0000192	.0000204	.0000193	.0000101

[a] The previous treatments of these castings given on p. 116.

[b] Results on second heating.

Digitized by Google

TABLE 37—Continued

Laboratory number	Commercial name	Composition				Average coefficients of expansion per degree centigrade				Average coefficients of expansion per degree Fahrenheit. Room temperature (77° F) to 212° F
		Copper	Zinc	Lead	Iron	Room temperature (25° C) to 100° C	100 to 200° C	200 to 300° C	Room temperature (25° C) to 300° C	
S319 A	Spring brass	72.02	27.95	.01	.02	.0000183	.0000195	.0000209	.0000197	.0000101
S319 B[a]						.0000183	.0000194	.0000207	.0000196	.0000102
S319 C						.0000183	.0000195	.0000209	.0000197	.0000102
S319 D						.0000183	.0000194	.0000207	.0000196	.0000102
S320 A	Cartridge brass	70.28	29.66	.03	.03	.0000186	.0000196	.0000208	.0000198	.0000103
S320 B						.0000185	.0000196	.0000209	.0000198	.0000103
S320 C						.0000184	.0000194	.0000207	.0000196	.0000102
S320 D[a]						.0000185	.0000196	.0000208	.0000197	.0000103
S321 A	do	66.50	33.43	.04	.03	.0000188	.0000200	.0000214	.0000202	.0000105
S321 B						.0000188	.0000199	.0000212	.0000201	.0000105
S321 C						.0000189	.0000200	.0000212	.0000201	.0000105
S321 D						.0000189	.0000200	.0000213	.0000202	.0000105
S322 A	Commercial brass	64.81	34.92	.24	.03	.0000191	.0000202	.0000215	.0000204	.0000106
S322 B						.0000189	.0000201	.0000214	.0000202	.0000105
S322 C						.0000189	.0000201	.0000214	.0000203	.0000105
S322 D						.0000188	.0000201	.0000215	.0000202	.0000105
S323 A	Commercial brass wire	63.63	36.17	.17	.03	.0000191	.0000202	.0000214	.0000203	.0000106
S323 B						.0000191	.0000202	.0000214	.0000203	.0000106
S323 C						.0000190	.0000202	.0000215	.0000203	.0000106
S323 D						.0000191	.0000202	.0000216	.0000204	.0000106
S32 A	Hot-rolled brass tube	62.10	37.71	.17	.02	.0000193	.0000204	.0000216	.0000205	.0000107
S32 B						.0000191	.0000203	.0000216	.0000205	.0000106
S32 C						.0000194	.0000205	.0000218	.0000207	.0000108
S32 D						.0000190	.0000203	.0000219	.0000205	.0000106
S327 A	Leaded bronze	88.30	10.00	1.68	.02	.0000176	.0000183	.0000189	.0000183	.0000098
S327 B						.0000177	.0000184	.0000191	.0000184	.0000098
S327 C						.0000176	.0000183	.0000191	.0000184	.0000098
S327 D						.0000175	.0000183	.0000192	.0000184	.0000097

Digitized by Google

S328	A	Leaded low brass	78.28	20.01	1.66	.03	.0000182	.0000190	.0000199	.0000191	.0000101
	B						.0000180	.0000188	.0000197	.0000189	.0000100
	C						.0000180	.0000189	.0000199	.0000190	.0000100
	D						.0000179	.0000188	.0000198	.0000189	.0000100
	E						.0000181	.0000189	.0000198	.0000190	.0000100
S329	A	Leaded screw wire	68.65	29.67	1.65	.03	.0000185	.0000195	.0000208	.0000197	.0000103
	B						.0000187	.0000198	.0000210	.0000199	.0000104
	C						.0000186	.0000197	.0000210	.0000199	.0000103
	D						.0000188	.0000198	.0000209	.0000199	.0000105
S330	A	Free turning rod	62.33	35.04	2.57	.06	.0000189	.0000202	.0000217	.0000204	.0000105
	B						.0000188	.0000202	.0000217	.0000204	.0000105
	C						.0000192	.0000203	.0000217	.0000205	.0000106
	D						.0000191	.0000202	.0000216	.0000204	.0000106
	E						.0000191	.0000202	.0000215	.0000204	.0000106
S332	A	Fourdrinier wire	81.70	17.94	.04	.01	.0000179	.0000188	.0000200	.0000190	.0000099
	B						.0000179	.0000188	.0000199	.0000190	.0000100
	C						.0000178	.0000188	.0000199	.0000189	.0000099
	D						.0000177	.0000189	.0000202	.0000190	.0000098
S333[c]	A	Admiralty condenser tubes	70.64	28.21	.04	.01	.0000185	.0000197	.0000210	.0000198	.0000103
	B						.0000185	.0000197	.0000211	.0000199	.0000103
	C						.0000185	.0000198	.0000212	.0000199	.0000103
	D						.0000184	.0000196	.0000210	.0000198	.0000102

[a] Results on second heating.

[b] Tin=0.31 per cent.

[c] Tin=1.10 per cent.

Digitized by Google

TABLE 38.—Average Coefficients of Expansion of Extruded and Hot-Rolled Copper-Zinc Alloys [a] (Series IV)

Laboratory number	Commercial name	Composition						Average coefficients of expansion per degree centigrade				Average coefficients of expansion per degree Fahrenheit. Room temperature (77° F) to 212° F
		Copper	Zinc	Lead	Iron	Tin	Manganese	Room temperature (25° C) to 100° C	100 to 200° C	200 to 300° C	Room temperature (25° C) to 300° C	
S343E	Free turning rod	Per cent 61.44	Per cent 35.68	Per cent 2.85	Per cent 0.03	Per cent	Per cent	0.0000196	0.0000210	0.0000225	0.0000212	0.0000109
S343ED								.0000190	.0000202	.0000216	.0000204	.0000106
S342E	Muntz metal	59.12	40.49	.35	.04	.....	.....	.0000195	.0000210	.0000228	.0000212	.0000108
S342ED								.0000197	.0000210	.0000225	.0000212	.0000110
S345E	Naval brass	58.96	40.16	.06	.01	0.84	.....	.0000200	.0000214	.0000230	.0000216	.0000111
S345ED								.0000197	.0000212	.0000228	.0000214	.0000110
S346E	Manganese bronze	56.39	40.95	.09	.96	1.52	0.09	.0000206	.0000224	.0000246	.0000227	.0000114
S346ED								.0000200	.0000214	.0000230	.0000216	.0000111
S341H	Muntz metal	61.07	38.66	.24	.03	.....	.....	.0000195	.0000206	.0000218	.0000207	.0000109
S341HD								.0000194	.0000206	.0000220	.0000208	.0000108
S344H	Naval brass	60.21	38.86	.20	.02	.71	.....	.0000207	.0000217	.0000229	.0000219	.0000115
S344HD								.0000197	.0000209	.0000223	.0000211	.0000110

[a] The previous treatments of these alloys are given on p. 125.

Digitized by Google

TABLE 39.—Average Coefficients of Expansion of Cold-Rolled Copper-Tin Alloys [a] (Series V)

Laboratory number	Commercial name	Composition			Average coefficients of expansion per degree centigrade				Average coefficients of expansion per degree Fahrenheit. Room temperature (77° F) to 212° F
		Copper	Tin	Phosphorus	Room temperature (25° C) to 100° C	100 to 200° C	200 to 300° C	Room temperature (25° C) to 300° C	
		Per cent	Per cent	Per cent					
S409	Phosphor bronze	95.40	4.25	0.37	0.0000173	0.0000179	0.0000186	0.0000190	0.0000096
S406	Chain bronze	94.85	4.88	.12	.0000171	.0000177	.0000185	.0000178	.0000095
S407	Gun metal	92.04	7.67	.11	.0000174	.0000181	.0000189	.0000182	.0000096
S408	Gun metal	89.69	10.14	.00	.0000176	.0000182	.0000190	.0000183	.0000098

[a] The previous treatments of these alloys are given on p. 132.

Digitized by Google

TABLE 40.—Average Coefficients of Expansion of Sections of Copper-Tin Castings [a] (Series VI)

Laboratory number	Commercial name	Composition			Average coefficients of expansion per degree centigrade				Average coefficients of expansion per degree Fahrenheit.
		Copper	Tin	Phosphorus	Room temperature (25° C) to 100° C	100 to 200° C	200 to 300° C	Room temperature (25° C) to 300° C	Room temperature (77° F) to 212° F
		Per cent	Per cent	Per cent					
S409 A	Phosphor bronze	95.40	4.25	0.37	0.0000174	0.0000181	0.0000190	0.0000182	0.0000097
S409 B					.0000176	.0000182	.0000189	.0000183	.0000098
S409 C [b]					.0000173	.0000180	.0000189	.0000181	.0000096
S409 D					.0000174	.0000182	.0000191	.0000183	.0000097
S406 A	Chain bronze	94.86	4.88	.12	.0000174	.0000180	.0000187	.0000181	.0000096
S406 B					.0000173	.0000180	.0000188	.0000181	.0000096
S406 C					.0000174	.0000181	.0000190	.0000182	.0000097
S406 D					.0000173	.0000179	.0000187	.0000180	.0000096
S407 A	Gun metal	92.04	7.67	.11	.0000176	.0000182	.0000189	.0000182	.0000098
S407 B					.0000175	.0000182	.0000189	.0000183	.0000097
S407 C					.0000176	.0000181	.0000187	.0000182	.0000098
S407 D					.0000176	.0000182	.0000188	.0000182	.0000098
S408 A	do	89.69	10.14	.00	.0000176	.0000186	.0000196	.0000187	.0000098
S408 B					.0000175	.0000183	.0000192	.0000184	.0000097
S408 C					.0000178	.0000184	.0000192	.0000185	.0000099
S408 D					.0000178	.0000186	.0000196	.0000187	.0000099

[a] The previous treatments of these castings are given on p. 133.

[b] Results on second heating.

Digitized by Google

TABLE 41.—Average Coefficients of Expansion of Aluminum Bronzes [a] (Series VII)

Laboratory number	Commercial name	Composition					Average coefficients of expansion per degree centigrade				Average coefficients of expansion per degree Fahrenheit. Room temperature (77° F) to 212° F
		Copper	Aluminum	Zinc	Silicon	Nickel	Room temperature (25° C) to 100° C	100 to 200° C	200 to 300° C	Room temperature to 300° C	
		Per cent	Per cent	Per cent	Per cent	Per cent					
S347H	Aluminum bronze	92.17	7.34	0.40	0.09	Trace	0.0000166	0.0000180	0.0000196	0.0000182	0.0000092
S347HD							.0000166	.0000177	.0000190	.0000179	.0000092
S347HD [b]							.0000168	.0000177	.0000188	.0000179	.0000093

[a] The previous treatments of these bronzes are given on p. 136.

[b] Results on second heating.

Digitized by Google

Digitized by Google

JUL 5 1921

DEPARTMENT OF COMMERCE

LIBRARY OF THE UNIVERSITY OF CALIFORNIA

SCIENTIFIC PAPERS

OF THE

BUREAU OF STANDARDS

S. W. STRATTON, DIRECTOR

No. 411

WAVE-LENGTH MEASUREMENTS IN ARC SPECTRA PHOTOGRAPHED IN THE YELLOW, RED, AND INFRA-RED

BY

F. M. WALTERS, Jr., Associate Physicist
Bureau of Standards

APRIL 9, 1921

PRICE, 5 CENTS
Sold only by the Superintendent of Documents, Government Printing Office
Washington, D. C.

WASHINGTON
GOVERNMENT PRINTING OFFICE
1921

Digitized by Google

Digitized by Google

WAVE-LENGTH MEASUREMENTS IN ARC SPECTRA PHOTOGRAPHED IN THE YELLOW, RED, AND INFRA-RED

By F. M. Walters, Jr.

ABSTRACT

For several years the Bureau of Standards has been conducting grating measurements in red and infra-red arc spectra by the aid of specially sensitized photographic plates to improve the data in this region and to find some element which would furnish lines suitable for wave-length standards in this region. To the 25 elements already measured the following are here added: Silver, aluminum, gold, bismuth, cadmium, mercury, lead, antimony, tin, and zinc.

The wave-length measurements are in the international system and are given to 0.01 A.

The elements were brought to luminosity by inserting a sample in copper or graphite electrodes between which the arc was maintained. The grating used had 299 lines per millimeter and a 640-cm radius. The spectra were photographed in the first order on plates sensitized with pinacyanol or dicyanin. The comparison spectrum was iron in the first, second, or third order, and in the reductions the wave lengths established by interference methods were used.

Impurity and spurious lines must be looked for very carefully. It is necessary to describe exactly the source of light and specify the observing conditions. The accuracy possible in wave-length measurements from the direct photography of normal spectra exceeds that in measurements from phosphor photography and bolometer measurements.

CONTENTS

	Page
I. Introduction	161
II. Apparatus and method	162
III. Results	164
1. Silver	165
2. Aluminum	166
3. Gold	167
4. Bismuth	168
5. Cadmium	168
6. Mercury	169
7. Lead	170
8. Antimony	171
9. Tin	174
10. Zinc	175
IV. Discussion	177
V. Summary	177

I. INTRODUCTION

Several years ago the Bureau of Standards began a program of grating measurements of the red and infra-red arc spectra of the chemical elements. The purpose was to find some element which

Digitized by Google

would furnish lines suitable for wave-length standards in this region, and also to improve the data on arc spectra with the aid of specially sensitized photographic plates. Wave-length measurements in spectra obtained by photography have already been published for 25 elements, namely, lithium, sodium, potassium, rubidium, caesium, copper, beryllium, calcium, strontium, barium, and magnesium;[1] iron, cobalt, and nickel;[2] helium;[3] neon;[4] krypton and xenon;[5] titanium, vanadium, chromium, manganese, molybdenum, tungsten, and uranium.[6] The greater the number of elements which have been measured the easier it is to eliminate the impurity lines in the observed spectrum of the next. Only in this way can the true spectra which are characteristic of each element be ultimately determined.

This paper is a continuation of the program and presents wave-length measurements in international Angstrom units in the spectra of silver, aluminum, gold, bismuth, cadmium, mercury, lead, antimony, tin, and zinc from wave lengths 5500 A to about 10 000 A.

II. APPARATUS AND METHOD

The Anderson grating employed in this work—radius of curvature, 640 cm, and 299 lines to the millimeter—is mounted in parallel light[7] and has a dispersion in the first order of about 10 A per millimeter.

Plates 8 inches long were used so that a wave-length interval of 2000 A was recorded in one exposure to the first order spectrum. The photographs were made on Seed's 23 and Seed's 30 plates sensitized to the long waves by staining in dye baths containing water, alcohol, and ammonia. The dye used, the time of exposure, the current in the arc, and slit width for the various regions are given in the following table:

Region	Dye	Time	Current	Slit width
		Minutes	Amperes	mm
5500–7500 A	Pinacyanol	20– 60	6.5	0.025
6400–8400 A	Dicyanin	45–100	7.5	.035
7300–9300 A	do	75–300	8.5	.045
8300–10 300 A	do	300	8-12	·055

[1] B. S. Bull., 14, p. 371; 1917.
[2] B. S. Bull., 14, p. 637; 1918.
[3] B. S. Bull., 14, p. 157; 1917.
[4] B. S. Bull., 14, p. 771; 1918.
[5] B. S. Sci. Papers, 15, p. 251; 1919.
[6] B. S. Sci. Papers, 16, p. 51; 1920.
[7] B. S. Bull., 14, p. 371; 1917.

Digitized by Google

The overlapping second and third orders were screened out by a cell of potassium bichromate or a piece of Jena red glass.

On account of the relatively low melting points of most of the metals used in this work it was impossible to employ electrodes of the metals themselves, so they were brought to luminosity by inserting a sample in a hole bored in one of two copper or graphite terminals between which the arc was maintained. Copper rods about 7 mm and graphite rods 12 mm in diameter were used with the positive electrode below, and the arc was fed with direct current from a power line of 240 volts. The average length of the arc was about 6 mm, and light from the central portion was focused on the slit of the spectrograph by means of a lens so placed as to give a threefold magnification. The use of copper electrodes for spectrographic analysis offers certain advantages over the older practice of using electrodes of carbon or graphite, in that very pure copper can readily be obtained and its spectrum in the region of longer waves is comparatively simple, so that there is less chance of being confused with lines due to the electrodes and impurities. Spectroscopic analysis of the graphite employed in this work showed that the alkali metals, alkaline earths, and iron, titanium, and vanadium were present as impurities. Graphite electrodes were frequently used, especially in cases where it appeared that copper lines were nearly coincident with lines due to other elements and might thus interfere with the accurate measurement of the latter.

In either case, whether copper or graphite electrodes were used, the intensity of the spectrum of copper or of carbon and its impurities was somewhat reduced by keeping the positive electrode loaded with the metal under investigation, so that the arc stream was always charged with the vapor of the element. When this condition existed for the elements dealt with in this work, the arc made a loud hissing sound and also exhibited colors in core and aureole which are more or less characteristic for each of the metals. If the arc burned much more quietly and showed that only the undesirable spectrum of copper or of graphite was being produced, the circuit was broken, a new supply of metal was placed in the crater, and the arc was again struck. The relatively low boiling points of the metals under discussion and the rapidity with which most of them oxidize made it necessary to feed the arc at short intervals of time, so that in some cases 100 or more grams of metal were consumed in making a five-hour exposure.

Digitized by Google

For the comparison spectrum electrodes of Norwegian or electrolytic iron were used under the conditions recommended by the International Wave Length Committee.[8]

The plates were measured on a large Gaertner engine, first with the scale reading increasing with the wave length, and then reversed, so as to eliminate personal error in setting on lines of different intensity and width. The iron in the first, second, or third order served as the reference spectrum, and in the reductions the wave lengths determined by interference methods[9] were used.

Lines due to impurities were eliminated from the spectra by reference to Kayser's Handbuch, to the work already done at the Bureau of Standards on the spectra of other elements, and by intercomparison among the wave lengths of the elements observed in this paper. Faint lines common to two or more elements were removed even when they could not be ascribed to any known element. Among these the most persistent were 5727.96 A, 6739.11 A, and 8184.86 A. It is possible that these three are new lines of copper. Ghosts of both the Rowland and also the Lyman[10] type were looked for and eliminated from the tables. The wave lengths were examined also for second order lines which might have passed through the screens used.

III. RESULTS

The first column of each of the following tables gives the wave lengths measured in international Angstrom units. The second column gives notes on the intensity and character of the lines. The strongest lines are given an intensity of 10 and the faintest measurable lines an intensity of 1. This estimate was applied to the work as a whole rather than to the spectrum of any particular element, so that a value of 10, for example, varied somewhat with the region under observation. To illustrate, with the methods employed 6438 A of cadmium gives a much greater photographic effect than 8273 A of silver, but an intensity of 10 is assigned to each of these lines in the tables. The character of a line is indicated by letters having the following meanings:

b = broad.
h = hazy.
H = very hazy.
L = shaded to the red.
v = shaded to violet.

[8] Astrophys. J., 39, p. 93; 1914. [9] B. S. Bull., 13, p. 245; 1915. [10] Am. Astron. Soc. Publ., p. 101; 1919.

Digitized by Google

It is difficult to express definite wave lengths for lines which are unsymmetrical in structure; i. e., shaded to red or to violet. An effort was always made to set on the "center of gravity" of the image, but in the case of unsymmetrical lines this setting becomes a function of the photographic exposure. For lines shaded to the red a strongly exposed spectrogram will thus give longer wave lengths than those obtained from weaker spectrograms. The uncertainty in expressing the wave lenghts of unsymmetrical lines may be several hundredths of an Angstrom on this account. The third column indicates the probable error of the measurements of each wave length, the significance of the letters being as follows:

A = probable error 0.01 A.
B = probable error of 0.01 A to 0.02 A.
C = probable error of 0.02 A to 0.03 A.
D = probable error > 0.03 A.
E = only one determination.

The wave-length measurements of other observers are included in the tables for the purpose of comparison. Whenever these wave lengths are expressed in international Angstrom units it is so indicated by I. A. in the table headings. The remaining values are based on Rowland's system of wave-length standards and may be changed to the international system by subtracting the following quantities:

0.22 A from 5500 to 6050 A.
.21 A from 6050 to 6500 A.
.22 A from 6500 to 6570 A.
.23 A from 6570 to 6750 A.
.24 A from 6750 to 6850 A.
.25 A from 6850 to 7000 A.
.26 A from 7000 to 7200 A.
.27 A from 7200 to 7400 A.
.28 A from 7400 to 7700 A.
.29 A from 7700 to 8000 A.
.30 A from 8000 to 8200 A.
.31 A from 8200 to 8300 A.
about .35 A from 8300 to 8800 A.

1. SILVER

Metallic silver and silver nitrate were burned in copper. Nineteen plates were measured; three of them were 5-hour exposures in the region 8400–10 400 A, but no wave lengths greater than 8273.58 A were found.

Digitized by Google

TABLE 1.—Silver

Walters			Kaspar [a]		Kayser and Runge [b]		Lehmann [c]	
λ I. A.	Notes	Probable error	λ I. A.	Notes	λ	Notes	λ	Notes
5523.74	3	B						
5529.91	2	A						
5545.67	3, L	B	5545.635		5545.86	4		
5667.34	4, h	B	5667.494		5667.72	4		
							7386.1	4
							7653.2	4
			Randall [d]		Lewis [e]			
			λ	Notes	λ	Notes		
7687.79	10	B	7688.2	200	7688.4		7684.0	1
8273.58	10	C	8274.1	250	8274.08		8275.4	1

[a] Kaspar, Zs. für wissenschaftliche Photographie, **10**, p. 53; 1912.
[b] Kayser and Runge, Wied. Ann., **46**, p. 225; 1892.
[c] Lehmann, Ann. d. Phys., **39**, p. 53; 1912 (phosphor photography).
[d] Randall, Astrophys. J., **43**, p. 1; 1911 (bolometer measurements).
[e] Lewis, Astrophys. J., **2**, p. 1; 1895 (bolometer measurements).

Eder (Wien, Ber., **124**; 1915) gives the wave length of the deep red line as 7687.89 and recommends its use in place of the red doublet of potassium for the calibration of small spectroscopes.

2. ALUMINUM

The commercial metal was burned in copper or graphite. Some observations were made with the positive electrode aluminum, but with this arrangement a current of more than 5 amperes could not be used without melting the aluminum.

TABLE 2.—Aluminum

Walters			Paschen [a]		Eder and Valenta [b]		Grünter [c]		Eder [d]		Lehmann [e]	
λ I. A.	Notes	Probable error	λ	Notes	λ	Notes	λ I. A.	Notes	λ I. A.	Notes	λ	Notes
5557.02	3	D	5557.283	7	5557.57	3	5557.08	1, u				
5557.96	3	D	5558.167	5	5558.37	2	5557.95	1, u				
5635.15	2	D										
5651.69	2, h	B										
6176.36	2, h	D										
6696.12	7	A	6696.269	6			6696.064	3	6696.08	5		
											6696.8	2
6698.78	5	A	6698.936	4			6698.734	3	6698.77	4		
7362.5	2, H, L	D										

[a] Paschen, Ann. d. Phys. (4), **29**, p. 625; 1909.
[b] Eder and Valenta, Atlas Typischer Spectren, Wien; 1911.
[c] Grünter, Zs. f. wiss. Phot., **13**, p. 11; 1913–14.
[d] Eder, Wien, Ber.; 1915.
[e] Lehmann, Ann. d. Phys., **39**, p. 53; 1912.

Digitized by Google

TABLE 2—Continued

Walters			Paschen		Meissner [a]		Grünter		Eder		Lehmann	
λ I. A.	Notes	Probable error	λ	Notes	λ I. A.	Notes	λ I. A.	Notes	λ I. A.	Notes	λ	Notes
					7466	3, u	.....	.....	.....	.....	.....	.....
7837.1	6, H, L	D	.....	.....	7836.85	5	.....	.....	.....	.....	.....	.....
											7833.5	2
8774.48	6, L	C	8775.1	50	8774.56	4	.....	.....	.....	.....	8770.1	2

[a] Meissner, Ann. d. Phys., 50, p. 713; 1916.

3. GOLD

Gold chloride or metallic gold was burned in copper or graphite. Thirteen plates were measured. Silver was the principal impurity. The lines 6122 and 6162 A observed by Quincke are in close agreement with strong calcium lines.

TABLE 3.—Gold

Walters			Quincke [a]		Eder and Valenta [b]		Kayser and Runge [c]	
λ I. A.	Notes	Probable error	λ I. A.	Notes	λ	Notes	λ	Notes
5629.27	1, H	D	.....	.....	.....	.....	.....	.....
5651.07	1	D	.....	.....	.....	.....	.....	.....
5655.79	3	C	5655.764	1	5656.00	4	5656.00	4
5660.46	1	D	.....	.....	.....	.....	.....	.....
5837.40	5	A	5837.396	4	5837.64	10	5837.64	6
5841.44	2	B	.....	.....	.....	.....	.....	.....
5859.34	1, h	D	.....	.....	.....	.....	.....	.....
5862.92	2	A	5862.943	1, u	5863.17	4	5863.17	6
5956.98	3	B	5956.984	1, u	5957.24	5	5957.24	4
5962.72	2	A	.....	.....	.....	.....	.....	.....
5968.96	1, H	D	.....	.....	.....	.....	.....	.....
			6101.654	2	.....	.....	.....	.....
			6122.28	1, u	.....	.....	.....	.....
			6162.228	3	.....	.....	.....	.....
6278.20	6	A	6278.179	4	6278.37	8	6278.37	4
6377.41	1, h	D	.....	.....	.....	.....	.....	.....
			6634.22	1, u	.....	.....	.....	.....
			6692.811	1, u	.....	.....	.....	.....
6781.97	2, h	B	.....	.....	.....	.....	.....	.....
7023.28	1, h	B	.....	.....	.....	.....	.....	.....
7156.82	1	A	.....	.....	.....	.....	.....	.....
					Eder [d]		Lehmann [e]	
					λ I. A.	Notes	λ	Notes
7510.69	5	C	.....	.....	7510.74	5	7509.8	1

[a] Quincke Zeits. f. wiss., Phot., 14, p. 257; 1914.
[b] Eder and Valenta, Atlas Typischer Spectren, Wien; 1911.
[c] Kayser and Runge, Wied. Ann., 46, p. 225; 1892.
[d] Eder, Wien, Ber.; 1915.
[e] Lehmann, Ann. d. Phys., 89, p. 53; 1912.

Digitized by Google

4. BISMUTH

Chemically pure metallic bismuth was burned in copper or graphite. Fourteen plates were measured. The principal impurities detected spectroscopically were silver and lead. The lines 8501.8 and 8627.9 A are very diffuse and are more than five Angstroms wide on the spectrograms.

TABLE 4.—Bismuth

Walters			Eder and Valenta[a]		Kayser and Runge[b]		Lehmann[c]		Randall[d]	
λ I. A.	Notes	Probable error	λ	Notes	λ	Notes	λ	Notes	λ	Notes
5552.35	10, B	C	5552.43	5	5552.43	8, r	.....	.....	.....	.....
5599.41	3	A	.....	.....	.....	.....	.....	.....	.....	.....
[e]5718.81	2	E	.....	.....	.....	.....	.....	.....	.....	.....
5742.55	6	B	5742.77	1	42.74	4, r	.....	.....	.....	.....
6134.82	6	B	6135.08	4	.....	.....	.....	.....	.....	.....
6184.99	2, H	D	.....	.....	.....	.....	.....	.....	.....	.....
6364.75	1, h	C	.....	.....	.....	.....	.....	.....	.....	.....
6475.73	3	C	.....	.....	.....	.....	.....	.....	.....	.....
6476.24	3	B	.....	.....	.....	.....	.....	.....	.....	.....
6991.12	4, H	C	.....	.....	.....	.....	.....	.....	.....	.....
7036.15	2	B	.....	.....	.....	.....	.....	.....	.....	.....
7335.01	1	D	.....	.....	.....	.....	.....	.....	.....	.....
7441.25	1, h	D	.....	.....	.....	.....	.....	.....	.....	.....
7502.33	2	C	.....	.....	.....	.....	.....	.....	.....	.....
7838.70	3	B	.....	.....	.....	.....	.....	.....	7841.1	7
7840.33	2	D	.....	.....	.....	.....	.....	.....	.....	.....
8210.83	1, h	D	.....	.....	.....	.....	8205.5	4	.....	.....
							8343.2	4	.....	.....
8501.8	1, H, b	D	.....	.....	.....	.....	8508.3	4, u	.....	.....
8544.54	2	A	.....	.....	.....	.....	.....	.....	.....	.....
8579.74	1	B	.....	.....	.....	.....	.....	.....	.....	.....
8627.9	1, H, b	D	.....	.....	.....	.....	8621.4	4	8628.5	10
8754.88	2	C	.....	.....	.....	.....	.....	.....	.....	.....
8761.54	3	D	.....	.....	.....	.....	8763.3	3	8761.8	10
8907.81	2	D	.....	.....	.....	.....	.....	.....	8910.0	10
9058.62	1	D	.....	.....	.....	.....	9054.4	3	9059.5	15
9342.60	1, h	D	.....	.....	.....	.....	9343.1	3	9344.1	40
9657.20	2	C	.....	.....	.....	.....	9646.9	1	9657.9	300

[a] Eder and Valenta, Atlas Typischer Spectren.
[b] Kayser and Runge, Wied. Ann., **52**, p. 93; 1894.
[c] Lehmann, Ann. d. Phys., **39**, p. 53; 1912 (phosphor photography).
[d] Randall, Astrophys. J., **34**, p. 1; 1911 (bolometer measurements).
[e] Given as spark line by W. Schwetz, Dissert., Bonn; 1908.

5. CADMIUM

Metallic cadmium was burned in copper or graphite electrodes. Fourteen plates were measured. Lead was found as an impurity. The lines measured by Paschen, 5599 to 6330 A, were observed in cadmium arc in vacuo, and this may account for the absence of

Digitized by Google

some of them in the present observations. It should be stated, however, that the first three lines were observed as a hazy group on spectrograms of the arc operated at atmospheric pressure, but the lines were too broad and poorly resolved to permit satisfactory measurements of wave lengths. The lines 6099, 6111, and 6116 A constitute a similar group, and it is seen that they are very hazy, unsymmetrical, and of greater effective wave length when the arc is surrounded by atmospheric pressure instead of vacuum.

TABLE 5.—Cadmium

Walters			Paschen [a]		Eder and Valenta [b]		Lehmann [c]	
λ I. A.	Notes	Probable error	λ	Notes	λ	Notes	λ	Notes
			5598. 989	6				
			5604. 903	4				
			5607. 068	2				
			5637. 44	5				
			5784. 15	4				
6099.90	3, H, L	D	6099. 393	8				
6112.05	2, H, L	D	6111. 729	6				
6116.10	1, H, L	D	6116. 395	4				
			6128. 87	2				
6165.28	3, H, v	D						
6325.05	7, h	D	6325. 404	15	6325. 40			
6329.91	5	B	6330. 18	8				
[d]6438.4696	10							
6777.66	2, H	D						
7346.01	1, H	A	7346. 5	15			7346. 2	8
7382.32	2, H	C	7385. 3	10				
7396.67	1, H	B	7399. 2	5				
8200.07	1, H	D						
							8870. 8	
							9174. 8	4
							9280. 7	4
10 395.22	1, h	E	10 395. 17	200				

[a] Paschen, Ann. d. Phys., 29, p. 625.
[b] Eder and Valenta, Atlas Typischer Spectren, Wien; 1911.
[c] Lehmann, Ann. d. Phys., 39, p. 53; 1912.
[d] International value.

6. MERCURY

A vacuum arc in glass taking 3 amperes was used as the source. Exposures of 30 hours were made for the region beyond 8000 A. The arc in air was tried but rejected on account of the broadness of the lines.

Wiedmann measured 15 lines of intensity 2 or less in prismatic spectra in the region 6878 to 8198 A which were too weak to photograph with a grating.

Digitized by Google

TABLE 6.—Mercury

Walters			Styles [a]		Wiedmann [b]		Eder and Valenta [c]		Kayser and Runge [d]	
λ I. A.	Notes	Probable error	λ I. A.	Notes	λ	Notes	λ	Notes	λ	Notes
5676.01	3	D	5675.811	1	.....	.....	5676.01	2	.....	.....
e5769.5984	.....	.....	.....	.....	.....	.....	.....	.....	.....	.....
			5789.521	2	.....	.....	.....	.....	.....	.....
e5790.6543	.....	.....	.....	.....	.....	.....	.....	.....	.....	.....
5803.65	3	C	.....	.....	.....	.....	5804.28	4	5804.28	2, r
									5819.05	1, u
5859.38	3	A	5859.49	1, u	5860.28	1	5859.90	2	.....	.....
					5868.28	1	.....	.....	.....	.....
5872.03	1	E	.....	.....	5872.37	2	5872.78	2	5871.301	3, u
6072.64	2	A	6072.66	1	6072.839	5	6072.93	2	.....	.....
6123.48	3	A	6123.48	1	6123.672	6	6123.65	2	.....	.....
6234.36	4	A	6234.31	2	6234.536	8	.....	.....	.....	.....

Lehmann [f]	
λ	Notes
6521.1	3
6553.3	3, u
.....	.....
6917.03	3
7085.7	4, u
.....	.....
.....	.....
.....	.....
.....	.....

6716.34	4	B	6716.315	1	6716.680	5	.....	.....	.....	.....
6907.46	8	D	6907.47	4	6907.776	10	6908.13	4	6917.03	3
7081.94	4	D	7081.96	1	7082.273	4	7082.43	3	7085.7	4, u
7091.87	2	D	.....	.....	7092.456	3	7092.32	2	.....	.....
7370.06	2	E	.....	.....	7371.00	3	.....	.....	.....	.....
7728.85	2	C	.....	.....	7729.456	u	.....	.....	.....	.....
8195.60	1	D	.....	.....	8198	2	.....	.....	.....	.....

[a] Styles, Astrophys. J., **30**, p. 48; 1909.
[b] Wiedmann, Ann. d. Phys., **38**, p. 1091; 1912.
[c] Eder and Valenta, Atlas Typischer Spectren, Wien; 1911.
[d] Kayser and Runge, Wied. Ann., **43**, p. 384; 1891.
[e] Interferometer Measurements, Fabry and Perot, Comptes Rendus, **170**, p. 492; 1900.
[f] Lehmann, Ann. d. Phys., **39**, p. 53; 1912.

7. LEAD

The arc spectrum was obtained from ordinary metallic lead burning in copper electrodes or in graphite electrodes.

Eder states that the two red lines which he gives are reproduced in the Atlas Typischer Spectren, Chart XXI, No. 13. Although this reproduction shows 7229 with considerable intensity, no lines of longer wave length appear and the wave length 7700.18 A, if real, is probably not due to lead.

The line 5895.70 A was measured in the fourth order. With low dispersion its presence is indicated by the increased intensity of the D_1 line of sodium which usually occurs as an impurity.

Digitized by Google

TABLE 7.—Lead

Walters			Eder and Valenta [a]		Kayser and Runge [b]		Lehmann [c]	
λ I. A.	Notes	Probable error	λ	Notes	λ	Notes	λ	Notes
[d]5608.85	4	B	5609.14	1				
5692.26	4	B	5692.36	2				
5895.70	6, h, L	B	5896.18	2+Na				
6002.24	8, h, L	D	6002.20	8, r	6002.08	2, r		
6011.98	5, h, L	C	6012.36	3, r				
6059.71	4, h, L	B						
6110.70	3, h, L	B	6111.32	2, r				
6169.40	2, h	C	6169.66	2, u				
6235.44	4	B	6235.73					
[d]6660.17	3, h	B						
			6791.54	1, u				
			6878.67	1, u				
7099.78	2	C						
			Eder [e]					
			λ I. A.	Notes				
7229.11	10	C	7228.93	6			7228.6	1
7330.12	2	D						
			7700.18	5				
8272.85	3, h	C					8267.2	3N

[a] Eder and Valenta, Wien, Ber., **119**, IIa, p. 519; 1910.
[b] Kayser and Runge, Wied. Ann., **52**, p. 93; 1894.
[c] Lehmann, Ann. d. Phys., **89**, p. 53; 1912.
[d] Given by Klein as spark lines, Zeits. f. wiss. Phot., **12**, p. 16; 1913.
[e] Eder, Wien, Ber., 1915.

8. ANTIMONY

Two samples of antimony were used. One was Kahlbaum pure metal and the other was less pure, containing lead, tin, calcium, sodium, potassium, cadmium, and iron. Twenty plates were measured. Five lines were observed which are given by Kretzer as occurring in the spark but not in the arc spectrum. The lines given by Kretzer beyond 7000 A are probably second order lines, since he used a potassium bichromate screen and a commercial panchromatic plate not particularly sensitive in this region. 7145.840, 7279.591, 7367.408, and 7480.194 A correspond to the lead lines 3572.95, 3639.72, 3683.62, and 3740.20 A, which are the strongest in this region. 7276.081 and 7445.895 A correspond to the strongest antimony lines, 3638.00 and 3822.94 A. Two lines 5700 and 5782 A observed by Schippers and by Kretzer are probably due to the presence of copper as an impurity. The sign + in the column of notes referring to my wave lengths indicates that these lines were very much stronger near the positive electrode than in any other part of the arc.

Digitized by Google

TABLE 8.—Antimony

Walters			Eder and Valenta [a]		Schippers [b]		Kretzer [c]	
λ I. A.	Notes	Probable error	λ	Notes	λ I. A.	Notes	λ	Notes
5531. 89	1, h	D						
5556. 21	3	B	5556. 37	2	5556. 084	2		
5568. 09	3	B			5567. 963	1		
5599. 93	3	B	5600. 05	2	5599. 762	1		
5602. 30	3	B	5602. 39	2	5602. 113	2		
5631. 97	5	C						
5639. 74	2, h	A						
5660. 78	2, h	A			5660. 778	1		
5691. 26	2	A			5691. 071	2	5691. 367	4
					5700. 29	0	5700. 439	3
5707. 47	2	A	5707. 52	.2	5707. 494	2	5707. 700	5
5730. 46	4	B	5730. 56		5730. 314	2	7730. 517	6
					5774. 557	3	5774. 769	3
					5782. 150	3	5782. 299	4
5806. 30	1, h	D						
					5813. 97	0	5814. 040	2
5844. 66	1, H	D						
5910. 64	1, h, v, +	D						
5912. 33	2	C			5912. 160	2	5912. 357	5
5948. 37	1	D						
[d]6005. 00	4, h, +	B						
[d]6079. 55	3, H, +	C						
					6081. 14	0	6081. 432	3
6097. 60	2	B			6097. 633	3	6097. 839	5
					6112. 70	0	6112. 961	1
6129. 98	3, H, +	B						
6178. 85	1	D						
6179. 80	1	B						
					6204. 51	0	6204. 682	3
6214. 00	2	B						
6221. 45	3	A						
					6332. 220	3	6332. 395	5
					6345. 955	2	6346. 098	4
					6388. 324	2	6388. 522	2
					6392. 175	3	6392. 391	3
					6405. 406	2	6405. 611	3
6415. 93	1, H	B						
6454. 95	2	B						
6490. 25	2	B						
							6495. 173	
6503. 03	1, H	C						
					6505. 404	1	6505. 657	3
6517. 10	2	B						
					6558. 150	3	6558. 353	5
					6564. 052	3	6564. 269	5
6611. 48	3	B			6611. 411	3	6611. 146	3
6634. 63	2, H	B						
6640. 55	1, H	B						
					6648. 134	2	6648. 344	4

[a] Eder and Valenta, Atlas Typsicher Spectren, Wien; 1911.
[b] Schippers, Zeits. f. Wiss. Phot., 11, p. 235; 1912–13.
[c] Kretzer, Zeits. f. Wiss. Phot., 8, p. 56; 1910.
[d] Given by Kretzer as spark lines.

Digitized by Google

TABLE 8—Continued

Walters			Eder and Valenta		Schippers		Kretzer	
λ I. A.	Notes	Probable error	λ	Notes	λ I. A.	Notes	λ	Notes
6738. 99	2	D						
[a]6778. 38	2, H, +	B						
6806. 35	2, H, +	C						
6811. 42	1	B						
6995. 91	2, h, +	C						
7006. 19	1, h	C						
7032. 88	1	C						
7122. 28	1	A						
7136. 29	1	D						
							7145. 840	5
							7181. 089	4
7222. 50	2, h	D						
							7276. 081	8
							7279. 591	8
							7343. 407	3
7362. 30	1, h	D						
							7367. 404	8
7405. 50	2, h	C						
7442. 0	1, H	D						
							7445. 985	7
							7480. 194	6
7592. 82	1, h	D						
7648. 28	3	B						
7755. 85	2	B						
7764. 9	2, H	D						
7816. 9	2, H	D						
7834. 6	1, H	D						
7837. 25	2	C						
7844. 44	4	A						
7867. 17	2	D						
7906. 73	2	C						
7924. 65	6	B						
7933. 38	1	D						
7969. 47	2, h	D						
8062. 1	2, H	D						
8241. 74	1	D						
8257. 56	2, H	D						
8289. 0	2, H	D						
8314. 21	1	D						
8411. 65	2	C						
8572. 59	2	C						
8619 60	2	C						
8682. 88	1	D						
8700. 20	1	D						
8719. 79	1	C						
8735. 0	1, H	D						
8789. 2	1, H	D						
8860. 3	1, H	E						
8903. 1	1, H	E						
9019. 5	1, H	E						
9132. 30	1	D						

[a] Given by Kretzer as spark lines.

Digitized by Google

9. TIN

Metallic tin was used in copper or graphite electrodes for the production of the arc spectrum. Sodium and potassium were observed as impurities, and by the same token the line at 7800.282 A observed by Arnolds may be due to rubidium.

TABLE 9.—Tin

Walters			Arnolds [a]		Kayser and Runge [b]		Eder and Valenta [c]	
λ I. A.	Notes	Probable error	λ I. A.	Notes	λ	Notes	λ	Notes
5631.70	8	A	5631.696		5631.91	5	5631.89	5
5753.61	3	B						
5761.77	2	A						
5801.79	1	A						
5925.48	4	B						
5934.72	2,H	D						
5970.30	5	A						
6011.08	2,h	D						
6037.70	5	B						
6054.90	5	D						
6060.75	2	C						
6068.94	8,h	C	6069.08	2,u				
6073.52	4,h	C	6073.55	1,u				
6149.67	6	B	6149.620	3	6149.81	2,v		
6154.60	5	B						
6171.49	4	B						
6203.62	3	B						
6275.78	2	B						
6310.83	4	C						
6254.36	2	B						
6444.83	2,H	D						
6453.58	3	A						
6462.36	2,+,Ca ?	D						
6844.20	2	B						
6909.29	1,H	D						
6924.72	1,H	E						
7685.29	1	A						
7754.94	2	A						
			7800.282	1				
7808.25	1	E						
8100.42	2	D						
8114.06	7	C						
8121.42	2,H	C						
8249.6	1,H	D						
8338.0	1,H	D						
8345.38	1,h	D						
8349.35	3	D						
8357.03	4	C						
8391.27	2	D						
8422.77	3,h	D						
8457.6	2,H	D						

[a] Arnolds, Zeits. f. Wiss. Phot., 13, p. 313; 1913–14.
[b] Kayser and Runge, Wied. Ann., 52, p. 93; 1894.
[c] Eder and Valenta, Wien, Ber., 119, IIa, p. 519; 1910.

Digitized by Google

TABLE 9—Continued

Walters			Randall [a]		Kayser and Runge		Eder and Valenta	
λ I. A.	Notes	Probable error	λ	Notes	λ	Notes	λ	Notes
8552.60	7	B	8554.7	12				
8649.2	1,H	D						
8681.4	1,H	D						
8708.9	1,H	D						
8886.61	1	D						
8908.11	1,h	E						
9018.9	1,h	D						
9023.1	1,h	D	9023.2	8				
9146.3	1,H	D						

[a] Randall, Astrophys. J., **34**, p. 1; 1911 (bolometer measurements to 13022 A).

10. ZINC

Chemically pure zinc was burned in copper electrodes and also with a 10 mm zinc rod as the positive electrode and copper as the negative electrode. Lead, cadmium, sodium, and potassium were found as impurities. Of the "new" lines given by Eder from 7026 to 8256 A, 18 correspond to the stronger vanadium lines in this region; 7664.84 and 7698.93 A, since they both appear, look suspiciously like potassium, and 7625 A may be due to nickel. This accounts for all except 7932.95 and 7937.93 A which are in all probability also due to some impurity. Eder admits that "these red and infra-red lines of zinc appear to be but slightly characteristic and are scarcely suited for spectral analytical indications of the metal."

TABLE 10.—Zinc

Walters			Eder and Valenta[a]		Wiedmann [b]		Paschen[c]		Lehmann [d]	
λ I. A.	Notes	Probable error	λ	Notes	λ	Notes	λ	Notes	λ	Notes
					5654.48	1				
5772.64	4, L	D			5772.33	5	5772.218	10		
5775.94	2, L	D			5775.75	4	5775.645	8		
5777.81	1, L	D			5777.36	3	5777.240	6		
5894.38	2	B			5894.65	6	5894.53	10		
							5937.93	3		
					6022	1				
					6102.38	2				
6183.97	5, h, v	D								
6214.62	1	D			6214.86	5	6214.89	7		
6237.82	3, h	C			6238.20	6	6238.21	8		

[a] Eder and Valenta, Wien, Ber., **118**, IIa, p. 1077; 1909.
[b] Weidmann, Ann. d. Phys., **35**, p. 660; 1911.
[c] Paschen, Ann. d. Phys., **29**, p. 625; 1909.
[d] Lehmann, Ann. d. Phys., **39**, p. 53; 1912.

Digitized by Google

TABLE 10—Continued

Walters			Eder and Valenta		Wiedmann		Paschen		Lehmann	
λ I. A.	Notes	Probable error	λ	Notes	λ	Notes	λ	Notes	λ	Notes
6239.14....	2	C	.....	.....	6239.46	3	6239.43	6	.....	.....
[a]6362.345..	10	.....	6362.58	8	6362.58	10	6362.58	20	.....	.....
							6471.19	4	.....	.....
6478.84....	2, h	D	.....	.....	6479.50	5	6479.37	8	.....	.....
							6914.15	2	.....	.....
6928.69....	8, L	D	6929.0	4	5928.54	8	6928.582	8	.....	.....
6938.77....	6, L	D	6939.2	3	6938.68	6	6938.733	6	6937.2	2
6943.55....	3, L	D	6943.9	2	6943.46	4	6943.474	4	.....	.....
			Eder [b]							
			λ I. A.	Notes						
			7026.07	4	.....	.....	.....	.....	.....	.....
									7234.9	3
			7264.22	4	.....	.....	.....	.....	.....	.....
			7338.88	4	.....	.....	.....	.....	.....	.....
			7356.45	4	.....	.....	.....	.....	.....	.....
			7358.54	4	.....	.....	.....	.....	.....	.....
			7361.33	3	.....	.....	.....	.....	.....	.....
			7363.11	3	.....	.....	.....	.....	.....	.....
7468.44....	1	D	.....	.....	.....	.....	.....	.....	.....	.....
7478.71....	2	C	.....	.....	7479.03	6	.....	.....	.....	.....
			7578.75	3	.....	.....	.....	.....	.....	.....
			7624.77	3	.....	.....	.....	.....	.....	.....
									7675.1	4
			7664.84	4	.....	.....	.....	.....	.....	.....
			7698.93	4	.....	.....	.....	.....	.....	.....
7799.04....	4, h, v	D	.....	.....	7799.62	6	.....	.....	.....	.....
			7932.95	2	.....	.....	.....	.....	.....	.....
			7937.93	2	.....	.....	.....	.....	.....	.....
									8005.2	3, u
									8112.1	4, u
			8116.74	4	.....	.....	.....	.....	.....	.....
			8144.57	2	.....	.....	.....	.....	.....	.....
			8161.01	3	.....	.....	.....	.....	.....	.....
			8186.65	2	.....	.....	.....	.....	.....	.....
			8187.38	1	.....	.....	.....	.....	.....	.....
			8198.85	2	.....	.....	.....	.....	.....	.....
			8202.91	2	.....	.....	.....	.....	.....	.....
			8241.50	1	.....	.....	.....	.....	.....	.....
			8253.46	1	.....	.....	.....	.....	.....	.....
			8255.76	1	.....	.....	.....	.....	.....	.....

[a] Interferometer measurement, vibrator in vacuo, Fabry and Perot, Comptes Rendus, 180, p. 242; 1900.
[b] Eder, Wien. Ber., 124, IIa, p. 120; 1915.

Digitized by Google

IV. DISCUSSION

A comparison of the wave lengths measured for the same element by different observers shows several important facts. In the first place impurity and spurious lines must be looked for very carefully. The determination, in a given spectral region, of the wave lengths of related or contaminating elements makes increasingly more certain the lines belonging to each particular element, and only when the spectra of all the elements are intercompared on the same basis can the true standard spectrum of each element be arrived at. Spurious lines due to false spectra given by gratings or to unrecognized overlapping spectral orders are responsible for some of the divergences in spectroscopic data. Careful examination of the optical performance of gratings should remove the first, and improvements in ray filters and photographic plates are necessary to reduce errors of the second kind. It is important to describe the source of light and specify the observing conditions since the spectrum of each element in general is different under various operating conditions (arc or spark, either in air, vacuum, or under pressure, etc.) and appreciably different spectra are obtained even from the same source if light from different parts of it is examined (pole effect, electrode lines, etc.). The accuracy possible in wave-length measurements from the direct photography of normal spectra exceeds that of phosphor photography and bolometer observations, but at the present time the photographic method is limited to waves shorter than about 10 000 A. The development of a photographic plate sensitive further into the infra-red is much to be desired.

V. SUMMARY

The arc spectra of 10 metals, silver, aluminum, gold, bismuth, cadmium, mercury, lead, antimony, tin, and zinc, were photographed in the red and infra-red on plates bathed with pinacyanol and dicyanin. These elements have relatively few strong lines in this region when compared with the spectra of iron, cobalt, and nickel observed under the same conditions.

In conclusion, acknowledgment is made to Prof. O. M. Stewart and to Dr. W. F. Meggers for their interest and encouragement in this work.

WASHINGTON, December 9, 1920.

Digitized by Google

Digitized by Google

DEPARTMENT OF COMMERCE

SCIENTIFIC PAPERS

OF THE

BUREAU OF STANDARDS

S. W. STRATTON, DIRECTOR

No. 412

SPECTROPHOTOELECTRICAL SENSITIVITY OF PROUSTITE

BY

W. W. COBLENTZ, Physicist
Bureau of Standards

APRIL 9, 1921

PRICE, 5 CENTS
Sold only by the Superintendent of Documents, Government Printing Office
Washington, D. C.

WASHINGTON
GOVERNMENT PRINTING OFFICE
1921

Digitized by Google

Digitized by Google

SPECTROPHOTOELECTRICAL SENSITIVITY OF PROUSTITE

By W. W. Coblentz

ABSTRACT

The present investigation is a continuation of previous work on the spectrophotoelectrical sensitivity of various substances.

At 20° C the spectrophotoelectrical sensitivity curve of proustite has a slight maximum at about 0.61μ and a marked sensitivity with a wide maximum (at about 0.3μ) in the ultra-violet.

At −170° C the intrinsic spectrophotoelectrical sensitivity is greatly increased; but the maximum reaction is confined mainly in a sharp maximum at 0.578μ. No photoelectrical sensitivity was observed for radiation stimuli of wave lengths extending from 0.7μ to 2μ.

CONTENTS

	Page.
I. Introductory statement	179
II. Apparatus and procedure	180
III. Experimental data	182
1. Voltage effect	182
2. Response-time curves	182
3. Spectrophotoelectrical sensitivity of proustite	183
4. Effect of temperature	184
IV. Summary	185

I. INTRODUCTORY STATEMENT

The present investigation is a continuation of previous work on the spectrophotoelectrical sensitivity of various substances.[1] As a result of these earlier investigations it has been possible to formulate a few general characteristics of photoelectrical conduction in solids.[2] It was shown that, in general, the photoelectric response of a substance at room temperatures, when exposed to equal-energy stimuli, is fairly uniform over a wide region of the visible spectrum, terminating in a band or bands of higher sensitivity in the extreme red or near infra-red.

Cuprous oxide[3] was cited as the only example then known in which the maximum sensitivity is in the ultra-violet, and in which the characteristic band in the red differs from that of the other substances investigated in being almost absent at 20° C. However, like other substances exhibiting photoelectrical sensitivity,

[1] Molybdenite, B. S. Sci. Papers, 15, p. 121; 1919. Silver sulphide, B. S. Sci. Papers, 15, p. 231; 1919.
[2] B. S. Sci. Papers, 16, p. 635; 1920.
[3] Pfund, Phys. Rev., 7, p. 289; 1916.

Digitized by Google

at low temperatures the reaction of cuprous oxide relative to the rest of the spectrum is confined almost entirely to this band in the red.

In the present paper it will be shown that the spectrophotoelectrical characteristics of proustite, Ag_3AsS_3, are similar to those of cuprous oxide. Furthermore, they exhibit similar characteristics in their spectral transmission of thermal radiation. Both are opaque to ultra-violet radiation and begin to transmit freely in the red end of the spectrum, thus imparting to them a bright red or vermilion color.

The one characteristic that all these photoelectrically sensitive substances have in common is a great opacity in the ultra-violet and violet end of the spectrum, followed by a rapid increase in transparency in the red and near infra-red spectrum. This is the long wave-length side of a region of optical resonance with a possible anomalous dispersion. The transmission data at hand on cuprous oxide, proustite, selenium, molybdenite, silver sulphide, etc., show a gradual shifting (or widening) of the absorption band from the ultra-violet into the infra-red. Similarly there is a regular sequence in the decrease in the general spectrophotoelectrical reaction in the short wave lengths and an increase in intensity of the band of high photoelectrical reaction in the red as we go from the spectrically more transparent substances, for example, cuprous oxide and proustite, to the more opaque substances, such as silver sulphide. From this it would appear that the explanation of the photoelectric reaction is to be sought for in an optical resonance phenomenon rather than a change in crystal structure, though the latter of course may contribute to the phenomenon by a change in pleochroism.

Proustite, Ag_3AsS_3, is a double sulphide of silver and arsenic. Case[4] recorded that it is sensitive photoelectrically. One of the reasons for making the examination of this mineral was to obtain a comparison of its spectrophotoelectrical sensitivity with that of silver sulphide.[5] It is interesting to note that their spectrophotoelectric reactions are entirely different.

II. APPARATUS AND PROCEDURE

The arrangement of the apparatus and the methods of operation were practically the same as used in the investigation of molybdenite.[6] Instead of a fluorite prism, a quartz prism was employed.

[4] Case, Phys. Rev., (2) 9, p. 305; 1917.
[5] B. S. Sci. Papers, 15, p. 231; 1919.
[6] B. S. Sci. Papers, 15, p. 120, Fig. 2; 1919.

Digitized by Google

The dispersion of quartz is about twice that of fluorite. The source of radiation was a 500-watt, gas-filled tungsten lamp, mounted in front of the spectrometer slit. Repeated calibrations of the lamp showed that any aging it may have undergone had not affected the equal-energy values used.

The measurements in the ultra-violet were made with a quartz-lens spectropyrheliometer,[7] the source of radiation being a Cooper-Hewitt 600-watt quartz-mercury lamp. The emission lines of mercury were reduced to equal-energy stimuli by suitably diaphragming the quartz lens which was used to focus an image of the burner upon the spectrometer slit. In this manner high intensities were obtained which permitted an extension of the photoelectrical measurements into the ultra-violet. (See Fig. 1.) High intensities were required in view of the fact that the material examined is not very sensitive and has peculiar electrical properties which prevent the application of a high potential.

The proustite, Ag_3AsS_3, used in this investigation came from Chañarcillo, Chile. Two samples were examined. They were of large size, semitransparent, and of a light vermilion color, indicating a high absorptivity for wave lengths less than 0.55μ ($\mu = 0.001$ mm).

SAMPLE NO. 1 was a well-formed, homogeneous crystal 16 by 4 by 3 mm. The terminals were of No. 36 copper wire wound tightly in grooves cut close to the ends of the crystal. The wire and the ends of the crystal were then covered with Woods alloy, which adhered well to the crystal when not applied too hot. The electrodes were attached in this manner with the view of obtaining symmetrical conduction through the crystal. The exposed part of the crystal between the electrodes was 8 mm.

SAMPLE NO. 2 was not so homogeneous in structure, having the appearance of a mass of semitransparent crystals forming a rod 18 by 6 by 4 mm. The electrodes were applied to sample No. 2 in the same manner as to sample No. 1, just described. The exposed part of the crystal between the electrodes was 10 mm.

The electrodes of both crystals were covered with cardboard to prevent exposure to radiation. For making the observations at low temperatures the samples were mounted in the evacuated glass container described in previous papers. When making the measurements at 22° C the sample was mounted at the exit slit of the spectrometer. The intensity of the radiation stimulus was

[7] B. S. Sci. Papers, 16, p. 233; 1920.

Digitized by Google

therefore three to four times larger than usually employed, and it was possible to investigate the visible spectrum more accurately.

The photoelectrical changes in conductivity were determined by connecting the crystal of proustite in series with a high resistance (10 000 to 30 000 ohms), a potential of 1.4 to 4 volts, and a d'Arsonval galvanometer.

Proustite is classed as a good conductor and hence a special arrangement of batteries and shunts [8] would be required in order to apply high voltages.

III. EXPERIMENTAL DATA

Considerable difficulty was experienced in making observations on these crystals, owing to the unsteadiness of the zero reading. This is probably attributable to the large mass of material under examination. At least that was the explanation arrived at in an examination [9] of stibnite where thin samples were also obtainable.

In the preliminary examination of different parts of the crystal it was found that, unlike molybdenite, these two samples of proustite were fairly uniform in sensitivity.

No "positive-negative" effect, such as was found in a certain sample of molybdenite,[10] could be observed in proustite.

1. VOLTAGE EFFECT

The increase in conductivity with increase in the applied voltage, which has been described by previous experimenters, was especially marked in proustite. Moreover, on applying a constant voltage the conductivity increased greatly with time. This was overcome to some extent by applying a high potential for a while, then reducing it to 1.4 volts (a single dry battery). Even then it was necessary to wait an hour or more before making observations.

2. RESPONSE-TIME CURVES

For proustite, the curve illustrating the progress of the photoelectric reaction with time was found quite similar to that of other substances (for example, molybdenite) described in previous papers. When the reaction was small, the maximum deflection was observed in 5 to 10 seconds and the time for recovery was not greatly prolonged. On the other hand, when observing in the region of the maximum photoelectric action (at 0.578μ) at low temperatures the time to attain a maximum reaction was prolonged

[8] B. S. Bull., 14, p. 591; 1918.
[9] B. S. Sci. Papers, 16, p. 596; 1920.
[10] B. S. Sci. Papers, 16, p. 596; 1920.

Digitized by Google

to 45 seconds or longer, and the time necessary for recovery was two to three times the time of exposure.

3. SPECTROPHOTOELECTRICAL SENSITIVITY OF PROUSTITE

The spectrophotoelectric reaction of proustite at 22° C. is illustrated in Fig. 1, the samples being exposed at the exit slit of the spectrometer, as already explained. In this illustration the observations on sample No. 1 are indicated by the continuous curves and those on sample No. 2 by the dotted curves.

The two curves to the right, marked *B*, depict the results of a careful examination of the small maximum in the region of 0.61μ It will be shown presently that, with decrease in temperature, this maximum very rapidly overtakes and exceeds the reaction in the rest of the spectrum and shifts to shorter wave lengths as observed in previous work on other substances.

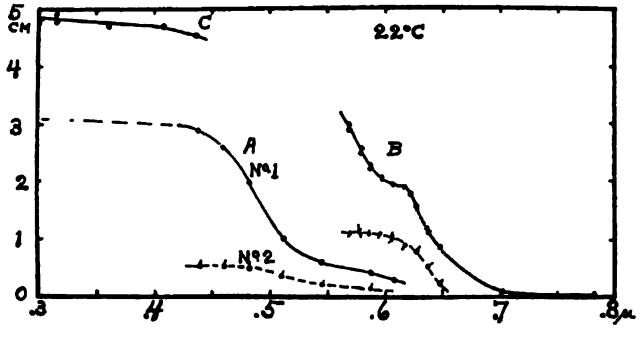

FIG. 1.—*Spectrophotoelectrical sensitivity of proustite. (Ordinates are galvanometer deflections)*

In the two curves marked *A*, which are to the left in the illustration, the observations are extended into the violet. For this purpose the tungsten lamp had to be operated on a lower current in the region of 0.6μ. The radiation intensities are $B = 7A$. For sample No. 1 curve *A* is extended by a dashed line to illustrate what is to be expected in the ultra-violet.

The observations on sample No. 1 in the ultra-violet are illustrated in curve *C*, Fig. 1. They were obtained by using a quartz-mercury vapor lamp and a quartz spectropyrheliometer, as already described.

The results of this examination show that, at 22° C, the spectrophotoelectrical sensitivity curve of proustite consists of a wide band, with a maximum in the ultraviolet, and a small, ill-defined maximum in the orange-yellow of the spectrum. In this respect

Digitized by Google

the spectrophotoelectric response curve is similar to that of cuprous oxide.

No photoelectric reaction could be observed for radiations extending to 2μ.

4. EFFECT OF TEMPERATURE

In order to make this test the sample was mounted in an evacuated glass container which was immersed in liquid air as already described.[11]

The effect of temperature upon the spectrophotoelectric reaction of proustite is illustrated in Figs. 2 and 3. The former gives the photoelectric reaction of samples No. 1 and No. 2 (curves *1* and *2*, Fig. 2) at $-125°$ C and $-126°$ C, respectively. They are interesting in showing that, although the intrinsic sensitivity of sample

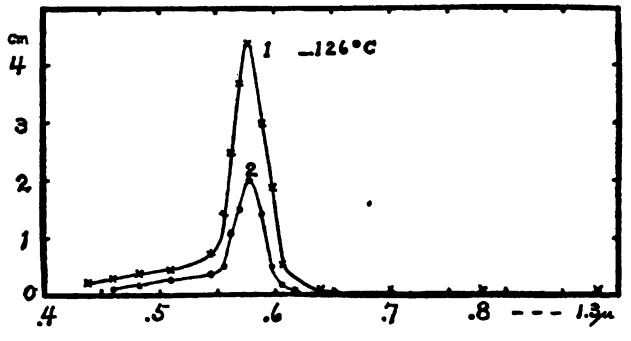

FIG. 2.—*Effect of temperature upon the spectrophotoelectrical sensitivity of proustite*

No. 2 is much less than that of No. 1, their spectrophotoelectric reactions are similar, both showing a marked development of the band at 0.578μ.

In Fig. 3 is depicted the rapid growth of the band at 0.578μ. From $+22°$ C to $-49°$ C this band is imperceptible. At $-93°$ C the wide maximum in the violet is still observable, while the one at 0.578μ has become sharp and well defined. From $-101°$ C to $-125°$ C the band at 0.578μ greatly exceeds the violet band. From these curves it appears that the band at 0.578μ does not suddenly envelop the ultra-violet band at a definite temperature, but that between $-50°$ C and $-90°$ C there is a gradual interchange in the relative intensities of the two maxima.

While observing these three curves the applied potential (1.4 volts) remained constant. Consequently, as the temperature de-

[11] B. S. Sci. Papers, 15, p. 120, Fig. 2; 1919.

Digitized by Google

creased the resistance increased, and, although the intrinsic spectrophotoelectrical sensitivity was greatly increased, the galvanometer deflections remained of the same order of magnitude. Hence, for the purpose of clearly depicting the isothermal spectrophotoelectric reactions in this illustration (Fig. 3), the ordinates of the $-49°$ C curve are two times that of the 22° C curve; also the ordinates of the $-93°$ C curve and of the $-101°$ C curve are five times that of the 22° C curve.

Furthermore, in order to avoid confusion in Fig. 3, the zero of the ordinates of the isothermal spectrophotoelectric reaction curves observed at $-125°$ C and at $-167°$ C is raised. In these

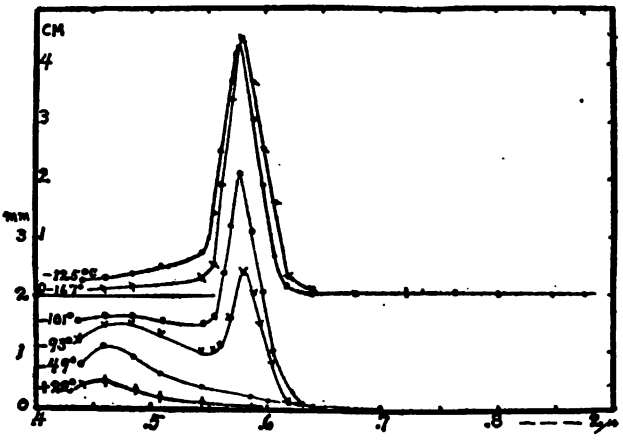

FIG. 3.—*Spectrophotoelectrical sensitivity curves of proustite at various temperatures*

two curves the galvanometer deflections were much larger than those observed at the higher temperatures. However, owing to the long time required for the reaction to attain equilibrium, as already explained, the observations at 0.578μ were subject to some uncertainty. The conclusion to be drawn for these curves is that the sharp maximum at 0.578μ remains fairly constant in position with decrease in temperature

IV. SUMMARY

In the foregoing pages experimental data are given on the spectrophotoelectrical sensitivity of the mineral proustite, which is a double sulphide of silver and arsenic. The results obtained show that the photoelectric reaction is entirely different from that of silver sulphide.

Digitized by Google

The samples were exposed to thermal radiation stimuli extending from 0.3μ to 2μ. The greatest photoelectrical activity occurs in the region of the spectrum (0.5μ to 0.7μ) where there is a rapid decrease in spectral absorption. No photoelectric reaction was observed for wave lengths greater than 0.7μ.

It was found that at 22° C the photoelectric reaction of proustite consists of a wide maximum in the ultra-violet, with a weak, ill-defined maximum in the region of 0.61μ.

On lowering the temperature to −167° C the intrinsic sensitivity is greatly increased throughout the spectrum. The ill-defined maximum at 0.61μ increases greatly in intensity and shifts to 0.578μ.

At low temperatures the greatest spectrophotoelectric reaction is localized in the band at 0.578μ.

All the data are in agreement with the previously formulated general characteristics of spectrophotoelectrical sensitivity in solids.

WASHINGTON, January 7, 1921.

Digitized by Google

Digitized by Google

Digitized by Google

OCT 3 1921

LIBRARY OF THE UNIVERSITY OF CALIFORNIA

DEPARTMENT OF COMMERCE

SCIENTIFIC PAPERS

OF THE

BUREAU OF STANDARDS

S. W. STRATTON, DIRECTOR

No. 413

A PORTABLE VACUUM THERMOPILE

BY

W. W. COBLENTZ, Physicist
Bureau of Standards

JULY 15, 1921

PRICE, 5 CENTS
Sold only by the Superintendent of Documents, Government Printing Office
Washington, D. C.

WASHINGTON
GOVERNMENT PRINTING OFFICE
1921

Digitized by Google

Digitized by Google

A PORTABLE VACUUM THERMOPILE

By W. W. Coblentz

ABSTRACT

A description is given of a portable vacuum thermopile of glass, in which the calcium evacuator is permanently attached to the container. The paper gives general directions for operating the device, as well as data on the thermopile, which is of bismuth silver.

Observations extending over a period of about seven years are given on the behavior of vacuum thermopiles in which the vacuum is maintained by means of calcium, which has the property of combining with gases when it is heated.

CONTENTS

		Page
1.	Introductory statement	187
2.	Description of the thermopile	189
3.	Description of the vacuum thermopile container	189
4.	Concerning radiation sensitivity tests of vacuum radiometers	191

1. INTRODUCTORY STATEMENT

The object of this paper is to describe a vacuum thermopile mounting which is rendered portable by attaching a calcium evacuator permanently to the radiometer container.

By this simple means one can maintain a vacuum without being obliged to keep the radiometer attached to a pump.

One of the chief complaints of workers in thermal radiometry is the uncertainty of the measurements caused by unsteadiness of atmospheric conditions. Radiometers are necessarily of small heat capacity and as a consequence are greatly affected by air currents. The loss of heat by convection is very large. The sensitivity of a modern thermopile—that is, its rise in temperature when exposed to radiation—is doubled and that of a thermocouple of fine (0.01 mm) wire is quadrupled by placing it in an evacuated receptacle.[1]

The container for a vacuum bolometer or thermopile differs from that of an evacuated, glass bulb, incandescent lamp in that it can not be thoroughly heated to expel the adsorbed water vapor and occluded gases. The radiometer container is usually provided

[1] B. S. Bull., 11, pp. 132 and 613; 1914.

Digitized by Google

with a fluorite or rock salt window which can not be heated without risk of breakage, and hence is attached with a cement that may give off vapors. Furthermore the radiometer receiver is covered with lampblack, etc., containing absorbed gases which slowly escape into an evacuated container.

As a result of these difficulties attempts to seal off the vacuum radiometer permanently from the evacuating device have not been successful.[2] Consequently it is necessary to provide a vacuum pump or other means for removing the hydrocarbon vapors coming from the stopcock grease and the gases disengaged from the walls or leaking through the joints of the vacuum chamber.

In a previous paper [3] a simple radiometric attachment was described for maintaining a vacuum by means of metallic calcium, which has the property of chemically combining with all atmospheric gases except argon. It is a simplification of the method used by Soddy,[4] in that the calcium is contained in a quartz tube which is heated to a low red by either a Bunsen burner, an alcohol lamp, or electrically. The calcium, being covered with a thin coating of oxide, does not combine with the quartz container unless it is heated to a bright red color.

Portable vacuum thermopiles in which the vacuum is maintained by means of calcium have been in use by the writer for nearly seven years. One of the vacuum thermocouple containers (No. 7) used in stellar radiometry[5] was provided with a new quartz tube and calcium on March 22, 1919. On January 19, 1921, there was found only a slight decrease in vacuum (total pressure perhaps 0.5 mm). This was easily remedied by warming the quartz tube containing the calcium. Container No. 6 used in stellar radiometry was heated December 10, 1917, for the first time after August, 1914, and then again the second time on January 19, 1921—twice in seven years. This vacuum container, which began to leak soon after it was finished, was easily repaired by applying a coat of shellac. However, as mentioned in the previous paper, sufficient air had entered to impart to the Geissler tube discharge the characteristic blue color of argon. In the most recent attempt to remove this residual gas (pressure less than 1 mm after standing three years) prolonged heating of the calcium evacuator had no effect in diminishing the argon.

---

[2] Buchwald, Ann. der Phys. (4), **33**, p. 928; 1910.

[3] B. S. Bull., 11, p. 185; 1914.

[4] Soddy, Proc. Roy. Soc., 78, p. 429; 1907. Baly's Spectroscopy, new ed., p. 433. Magnesium is also reported to be good for "vacuum cleanup."

[5] B. S. Bull., 11, p. 624, Fig. 3; 1914.

Digitized by Google

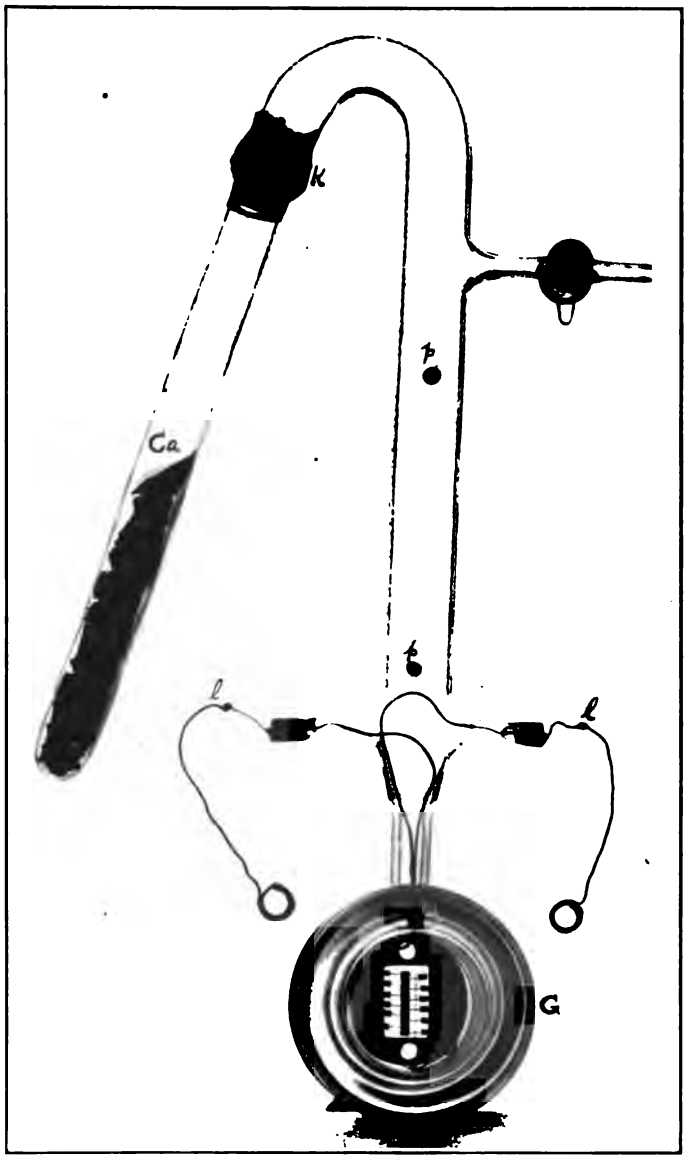

FIG. 1.—*Vacuum thermopile*

Digitized by Google

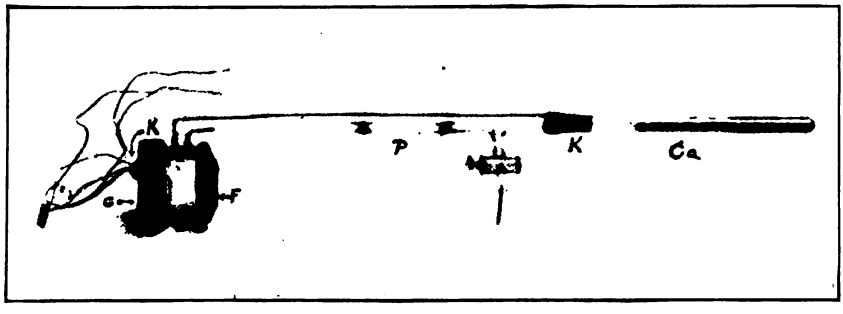

FIG. 2.—*Vacuum thermocouple mounting for stellar radiometry*

Digitized by Google

The linear vacuum thermopile, to be described presently, has been in use for about four years. The first container in which it was mounted always leaked seriously. Nevertheless, after closing the stopcock (in 1917) and sealing it with Chatterton wax, the vacuum was maintained by occasionally heating the calcium.

2. DESCRIPTION OF THE THERMOPILE

The thermopile is constructed of bismuth wire, 0.08 mm in diameter (0.1 mm would be less fragile and hence adapted for general use), and silver wire, 0.031 mm in diameter. The individual receivers are of tin, 1.7 by 1.1 by 0.018 mm. The total length of the receiver of the completed instrument of 12 elements is 12.5 mm, and the resistance is 6.7 ohms. The bismuth wire is cut to the proper length (4 mm) and pressed flat between glass plates to increase thermal conduction where it is in contact with the receivers and thus facilitate the attainment of thermal equilibrium.[6] The base upon which the thermoelements are mounted may be of ivory or of red fiber (shown in Fig. 1) which has been boiled in paraffin to shrink it and to expel the air.

The rate of rise of emf of the thermopile, when exposed to radiation, is so rapid that a galvanometer swing of 2 seconds is not retarded. In fact, when using a galvanometer having a single swing of 2 seconds, the response of the thermopile is too rapid for making observations comfortably. For example, 90 per cent—that is 18 cm—of a total deflection of 20 cm is obtained in about 1 second.

3. DESCRIPTION OF THE VACUUM THERMOPILE CONTAINER

Radiometer containers which can be evacuated have been described in previous papers.[7]

The thermopile in its new vacuum mounting (20 cm in height) is shown in Fig. 1, which is a rear view. This mounting is in the form of a cup made out of one piece of glass, which is covered with a thick glass window, *G*. Fig. 2 is a side view of a similar vacuum thermopile container used in stellar radiometry. In these illustrations similar parts are referred to by similar letters. The quartz tube (standard size quartz test tube), containing the calcium, *Ca*, is attached to the glass tube by means of Khotinsky cement, *K*. Pyrex glass tubing may be used instead of quartz and joined directly to the glass, thus dispensing with the cement, but it is likely to collapse on accidental overheating.

[6] B. S. Bull., 11, pp. 132 and 613; 1914.
[7] B. S. Bull., 9, p. 39, 1911; 13, p. 444, 1916.

Digitized by Google

The electrodes, *p*, *p*, of platinum wire 0.3 to 0.4 mm in thickness, are used for testing the evacuation. For this purpose either an induction coil or a 2000 to 10 000 volt transformer is used.

The glass window, *G*, covering the rear of the container, is 7 mm thick. Experience shows that a thick plate of glass is necessary in order to prevent warping by atmospheric pressure and consequent leaking through the ground joint. The latter is closed with a combination of beeswax and tallow (stopcock grease) and the edge is covered with Chatterton wax.

The fluorite window, *F*, Fig. 2, covering the front of the container, is about 3 mm in thickness, which is sufficient to prevent warping when placed over the slot (8 by 16 mm, Fig. 1) in the fine-ground face of the glass receptacle. It is joined to the glass by means of stopcock grease and the outer edge is covered with Chatterton wax.

The lead wires to the thermopile, *l*, Fig. 1, are of copper, sealed to the glass with a platinum wire. This refinement is not necessary, though it is desirable to reduce the number of places where leakage may occur.

The glass receptacle is mounted in a brass box which slides in vertical ways as illustrated in previous papers.[8]

In concluding this description of the thermopile container it is relevant to add a few remarks concerning the operation of the calcium evacuator. The calcium is cut into small fragments with a chisel or by other means and placed in the quartz tube, which is then attached to the thermopile container. The device is then evacuated with an oil pump. While the pumping is in progress the calcium is heated with a Bunsen flame in order to cause it to combine with the water vapor, the residual air, and the acetylene gas which is generated from the water vapor and the calcium carbide which is formed in previous use. Keeping the calcium hot, fresh air is allowed to enter and the pumping is continued. This operation should be repeated several times to sweep the water vapor from the walls of the container, after which the stopcock is permanently closed.

With reference to the efficiency of the device, it may be stated that, after the gases have been absorbed by the calcium, the vacuum is so high that the discharge from an induction coil passes through the 5 cm air space between the electrodes, *p*, *p*, Fig. 1, in preference to passing through the evacuated tube.

[8] B. S. Bull., 11, p. 156, 1914; 13, p. 446, 1916 ("Mounting for vacuum thermopiles").

Digitized by Google

As mentioned elsewhere, an electric heater may be used, but it requires close attention to avoid overheating of the quartz tube. It is not absolutely necessary to use a pump to start the evacuation. However, explosions may result from the increase in pressure of the water vapor, acetylene, etc., when the calcium is first heated in a closed tube at atmospheric pressure. Hence provision must be made for increase in gas pressure during the initial heating of the calcium in a closed tube containing air at atmospheric pressure. For it is to be remembered that the chemical action begins at about 300° C and is most effective at a low, red heat.

The first samples of the vacuum chamber with attached calcium evacuator, described in the foregoing pages, were prepared about seven years ago and taken 3200 miles to an observatory without mishap. This experience showed that equipped with several vacuum radiometers of this type one can go to the remotest station without taking a pump.

A further improvement will come from the discovery of a cement for securing the windows which will not give off vapors, and thus increase the efficiency of the device.

4. CONCERNING RADIATION SENSITIVITY TESTS OF VACUUM RADIOMETERS

It is beyond the scope of this paper to describe fully the methods of calibration of radiometers and the various methods which may be employed to test the variation in their radiation sensitivity.

In this connection it is to be remembered that the sensitivity of the auxiliary Thomson galvanometer varies with the diurnal change in terrestrial magnetism, etc. The current sensitivity may therefore be tested by a simple device described in previous papers.[9]

The radiation sensitivity of a vacuum bolometer and to a less extent of a thermopile (because of its greater heat capacity) is a function of the kind and the pressure of the residual gas. The sensitivity of a bolometer is 2.5 as great in hydrogen as in air at the same gas pressure. It has been found by Reinkober[10] and also by the writer that the radiation sensitivity of the Ruben's thermopile (of wire 0.15 mm in diameter) in a vacuum is only about 1.5 times that in air. The radiation sensitivity of

[9] B. S. Bull., **10**, p. 19, 1913; **11**, p. 171, 1914, "Specification of the radiation sensitivity of a thermopile."

[10] Reinkober, Ann. der Phys. (4), **34**, p. 343; 1911. Lebedew (Ann. der Phys. (4), **9**, p. 209; 1902) found that above 5 mm (also below 0.01 mm) a variation in gas pressure has but little effect upon the sensitivity.

Digitized by Google

the present thermopile is doubled in a vacuum. In this instrument the sensitivity varies but little during the course of a day's work. In making transmissivity (and reflectivity) measurements it is sufficient to have the radiation sensitivity remain constant while making the two sets of measurements, namely, (1) the intensity of the radiation transmitted through the substance, and (2) the intensity of the direct radiation.

If it is desired, the variation in radiation sensitivity of the vacuum thermopile (and of vacuum radiometers in general) may be determined by means of a standard incandescent lamp,[11] or other suitable means.

In conclusion, it is relevent to empasize the fact that the increase (say, 50 to 100 per cent) in radiation sensitivity by placing the ordinary laboratory radiometer (thermopile) in a vacuum is relatively small, and that the chief gain lies in elimination of unsteadiness of the galvanometer reading by elimination of convection currents. This is easily accomplished by keeping the air pressure less than 0.1 mm.

WASHINGTON, March 4, 1921.

[11] McCauley, Astrophys. J., 37, p. 164; 1913.

Digitized by Google

3 1921

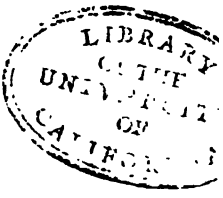

DEPARTMENT OF COMMERCE

SCIENTIFIC PAPERS

OF THE

BUREAU OF STANDARDS

S. W. STRATTON, DIRECTOR

No. 414

INTERFERENCE MEASUREMENTS IN THE SPECTRA OF ARGON, KRYPTON, AND XENON

BY

W. F. MEGGERS, Associate Physicist
Bureau of Standards

AUGUST 1, 1921

PRICE, 5 CENTS

Sold only by the Superintendent of Documents, Government Printing Office, Washington, D. C.

WASHINGTON
GOVERNMENT PRINTING OFFICE
1921

Digitized by Google

Digitized by Google

INTERFERENCE MEASUREMENTS IN THE SPECTRA OF ARGON, KRYPTON, AND XENON

By W. F. Meggers

ABSTRACT

The spectra of the inert gases, especially of the heavier ones, contain strong lines which represent wave lengths possessing a high degree of homogeneity and reproducibility and these lines are therefore suitable for use as standards of wave length. This paper gives the values of 50 wave lengths in the spectrum of argon (3948 to 8521 A), 18 of krypton (4273 to 7601 A), and 12 of xenon (4500 to 4923 A), all of which have been compared with the wave length of the red radiation from cadmium (6438.4696 A) which is the international primary standard. These wave-length comparisons were made by means of etalon interferometers and most of the values are probably correct to one part in several millions. The elegance and precision of the interferometer methods for wave-length comparisons are demonstrated by the close agreement between values obtained by different observers, and also by the constant frequency differences of many of the lines belonging to combination series. There are only a few cases where independent observers differ by 0.004 A or more. From the wave-length measurements in argon and krypton, frequency differences are obtained which are constant within the probable error of the measurements. This further confirms the exactness of the Combination Principle of Ritz. If these frequency differences are regarded as true constants, they testify to the accuracy in relative value of the wave-lengths involved.

CONTENTS

	Page
I. Introduction	193
II. Apparatus and method	195
III. Results	198
IV. Summary	202

I. INTRODUCTION

Interferometer comparisons of wave lengths with the object of establishing satisfactory secondary standards were undertaken by this Bureau some years ago and have resulted in the following publications in this Bulletin:

1. "Wave lengths of neon,"[1] in which the wave length of the neon line 5852 A is compared with the cadmium standard and values for nine other neon lines are obtained relative to 5852 A.

2. Interference measurements of "Wave lengths in the iron spectrum,"[2] giving the values for 125 iron lines (2851 to 3701 A)

[1] B. S. Bull., 6, p. 673, 1911; 8, p. 539, 1912.

[2] B. S. Bull., 12, p. 179; 1915.

Digitized by Google

as suitable standards derived from the international primary standard.

3. "Interference measurements of wave lengths in the iron spectrum,"[3] where 402 wave-length values (3761 to 6750 A) are given, most of which are tertiary standards interpolated between the accepted international secondary standards by the Buisson and Fabry interferometer method.

4. "Wave lengths of the stronger lines in the helium spectrum,"[4] presenting 21 values (2945 to 7281 A).

5. "Measurements of wave lengths in the spectrum of neon."[5] The wave lengths of 55 lines lying in the region 3369 to 8495 A are given in this paper.

Further work of this kind has recently been resumed in the spectroscopic laboratory of this Bureau and values obtained for the stronger lines in the spectra of argon, krypton, and xenon are presented in this paper.

The importance of accurate measurements of wave lengths in the spectra of the inert gases can scarcely be overestimated. It was shown by Buisson and Fabry[6] that spectrum tubes of these gases, especially the heavier ones, give lines which possess a high degree of homogeneity. In fact, they are the narrowest spectral regions of emission which are known at the present time. The wave lengths are therefore susceptible of very precise measurement, and this precision together with reproducibility and convenience in operating the source are considerations which recommend the use of these lines as standards of wave length, or even as fundamental units of length. For several years the wave lengths of helium and neon lines have been in continuous use at this Bureau for the accurate length measurements of precision end standards and gage blocks, and for a study of the doubtful permanency of such material standards.[7]

In addition to their practical value as units of length or standards of wave length, emission lines in the spectra of the inert gases, because of the precision with which they can be measured, are of great theoretical interest in unravelling the laws of spectral series, calculation of fundamental spectroscopic constants, etc.

In the case of each of the gases—neon, argon, krypton, and xenon—frequency differences which were suspected of being constant had long been observed but it remained for the interfer-

[3] B. S. Bull., 13, p. 245; 1916.
[4] B. S. Bull., 14, p. 159; 1917.
[5] B. S. Bull., 14, p. 765; 1918.
[6] J. de Phys. (5), 2, p. 442; 1912.
[7] Peters and Boyd, Am. Machinist, Sept. 30 and Oct. 7, 1920.

Digitized by Google

ometer comparisons, first made in the case of neon, to prove that these frequency differences are really constant to the limit of accuracy obtainable in wave-length measurements at the present time. This was a complete confirmation of the Combination Principle of Ritz and gives some conception of the extreme nicety with which the atom is constructed. It will be shown below that frequency differences in the spectra of argon and krypton are also constant to the same degree as in neon. It should also be mentioned that these constant differences in the spectra of the inert gases which have attracted attention for many years have only recently disclosed their physical significance and hence assumed considerable theoretical value. The constant differences in neon, for example, have very recently been arranged into spectral series by Meissner [8] and more completely by Paschen.[9] Thus the spectrum of neon which had puzzled spectroscopists for a long time has suddenly become one of the most completely and accurately defined sets of series, comprising over 800 lines between the wave-length limits 2561 and 9314 A. More extensive wave-length measurements are required before the spectra of argon, krypton, and xenon can be discussed in a similarly complete and final manner. Whereas in the case of neon, the greatest number of related convergence limits was found to be 10, the maximum number of related subordinate series limits in argon, according to Nissen, [10] is 18. In the helium spectrum a series system of doublets is known. It may therefore be expected that in the remaining rare gases, krypton and xenon, the number of related subordinate series limits will be found equal to the number of electrons in the atom; that is, 36 to 54, respectively.

II. APPARATUS AND METHOD

The apparatus consisted of spectrum tubes, Fabry and Perot etalon-type interferometers, spectrographs, and a measuring engine. The general method of making wave-length comparisons with such equipment was originated by Fabry and Perot.[11] It is the approved method by which the international secondary standards have been obtained and has been described so often [12] that it is unnecessary to repeat its description here.

[8] Ann. d. Phys., 58, p. 333; 1919.
[9] Ann. d. Phys., 60, p. 405; 1919.
[10] Phys. Zs., 21, p. 25; 1920.
[11] Ann. d. Chim., 25, p. 110; 1902.
[12] Lord Rayleigh, Phil. Mag. (6), 11, p. 685; 1906. Eversheim, Ann. d. Phys., 30, p. 815; 1909. Fabry and Buisson, Astroph. J., 28, p. 169; 1908. Pfund, Astrophys. J., 28, p. 197; 1908.

Digitized by Google

Tubes containing either cadmium vapor or one of the inert gases (neon, argon, krypton, xenon) were made luminous by a high potential alternating current of 10 to 30 milliamperes. All the tubes were made with internal electrodes of aluminum. Light was taken from the central portion (5 mm.) of tube capillaries except in the case of cadmium, which was used "end on." The neon, argon, and cadmium tubes were made at this Bureau but tubes of krypton and xenon were imported, it being impossible to obtain in America sufficient quantities of these gases in a pure state. One quartz tube each of krypton and xenon was filled a number of years ago by the late Sir William Ramsey, and several small glass tubes containing krypton and xenon were recently obtained from Geissler Nachfolger.

All the rare gases, especially the heavier ones, cause sputtering of the electrodes on the walls of the tubes. It appears that this electrode deposition imprisons some of the gas so that ultimately the tubes become vacuous and resist the passage of any current. This phenomenon has been described by Collie,[18] who states that heating the tube recovered part of the gas in the case of krypton, but had little effect on xenon. Collie tried xenon tubes with cathodes of platinum, aluminum, or copper and found that "with copper, although a very large amount of the cathode is volatilized, the disappearance of the xenon proceeds more slowly." It may be that some other metal which has even less effect than copper could be found.

The electrode deposit occurs very rapidly when the gas pressure in the tube is very low. Such was the case with the Geissler tubes which, though filled with pure gas, were at such low pressure that the cathode dark space reached the walls of the tube and cathode ray bombardment caused the well-known green fluorescence in the glass. These tubes deposited the electrode material on the walls with such speed that a 15 to 30 minute run put bright mirrors on the bulbs, the tubes thereafter becoming vacuous and worthless.

It is also observed that with increasing deposit and consequent decreasing gas pressure the tubes have a tendency to emit the so-called second spectrum instead of the first. At a certain stage near the end of the life of the tube a flickering color change takes place in the capillary and examination with a direct-vision spectroscope shows that the first and second spectra are emitted

[18] Proc. Roy. Soc., 97, p. 349; 1920.

Digitized by Google

either together or alternately. These facts are mentioned as more or less objectionable features in the use of rare gas tubes as sources of standard wave lengths. Tubes filled in our laboratory with helium, neon, and argon to pressures corresponding to several millimeters of mercury have been operated for several hundred hours without becoming vacuous and it seems probable that tubes of krypton and xenon would be relatively permanent if filled in the same way. It is worth while to experiment further to discover the specifications as to gas pressure, electrode material, current strength and potential, etc., which will increase the life and usefulness of spectrum tubes of the heavier inert gases.

A spectrograph with rock-salt prism and quartz lenses, designed especially for work in the ultra-violet spectrum, was used to record the interference rings for lines between 3300 and 7600 A on plates stained with pinacyanol. The spectrum of argon was further investigated from 6000 to 8500 A by means of interferometers used with a concave grating mounted in parallel light. Plates stained with dicyanin were used for these longer waves. The exposures with the prism spectrograph ranged from 30 to 60 minutes each for the rare gas spectra and 1 or 2 minutes for the cadmium spectrum. Work with the concave grating involved exposures of from 2 to 10 hours for the gases. As a rule, the cadmium was exposed before and after each of the others. A neon exposure was added to each plate because of the convenience in using the neon wave lengths for determining the order of interference or size of etalon.[14]

A series of etalons made of invar was used to separate the interferometer plates by distances of 2, 3.75, 10, 15, 20, 25, and 40 mm. Most of the wave lengths given in the tables are the mean values of 6 to 10 or more comparisons with the primary standard and the majority of these values are derived from the use of 25 or 40 mm etalons. The relative values obtained from the small etalons (2 and 3.75 mm) were used with those derived from the larger ones (25 and 40 mm) to find the corrections which were applied to the final wave lengths to eliminate differences in apparent penetration of the interferometer films as described elsewhere.[15] The interferometer plates used with the prism spectrograph were of fused quartz, plated with nickel, and for the work with the grating glass plates coated with thin copper films were used. These interference etalons were mounted in the chamber for temperature

[14] B. S. Bull., 12, p. 203; 1915. [15] B. S. Bull., 12, p. 199; 1915.

Digitized by Google

control used in the work of this Bureau on the index of refraction of air and described previously.[16]

The long exposures mentioned above required careful temperature control of the interferometer so as to guard against changes either in the dimensions of the interferometer or in the refractive index of the air between the plates. For about half of the exposures the interferometer was maintained at 15° C and for the remainder it was held closer to room temperature (20 to 22° C). The small corrections necessary for deviations of air pressure and temperature from normal conditions were made from tables prepared for this purpose.[17]

III. RESULTS

Wave lengths of the stronger lines in the spectra of argon, krypton, and xenon are given in Tables 1, 3, and 5, respectively, in which the values for 50 argon lines, 18 krypton, and 12 xenon are presented. Most of the values are thought to be correct within one or two thousandths of an angstrom. Values obtained by other observers, using the same method and based on the international primary standard, are added for purposes of comparison. All the wave lengths are therefore expressed in international angstrom units and represent the lengths of waves in air at a temperature of 15° C and pressure of 760 mm mercury.

TABLE 1.—Wave Lengths in the Argon Spectrum

Intensity	Bureau of Standards	Meissner [a]	Intensity	Bureau of Standards	Meissner [a]
	λ			λ	
4	3948.980		3	6871.290	
6	4044.419		2	6937.666	
9	4158.591		10	6965.429	432
4	4164.180		2	7030.250	
4	4181.884		10	7067.217	218
4	4190.714		5	7147.043	
4	4191.027		2	7206.986	
6	4198.316		2	7272.938	
9	4200.676		2	7353.316	
3	4251.184		2	7372.119	
7	4259.362		9	7383.979	978
5	4266.286		8	7503.867	868
6	4272.169		7	7514.651	648
6	4300.101		10	7635.106	107
6	4333.561		2	7723.758	760
4	4345.168		4	7724.210	210
5	4510.733		8	7928.175	177
3	4522.325		7	8006.156	158
3	4596.096		9	8014.784	788
3	4628.445		8	8103.693	691
4	4702.317		9	8115.307	310
4	6032.127		5	8264.522	525
4	6416.307		4	8408.210	216
4	6677.282		6	8424.646	650
4	6752.831		3	8521.442	

[a] Ann. d. Phys. (4), 51, p. 95; 1916.

[16] B. S. Bull., 14, p. 712; 1918.

[17] B. S. Bull., 14, pp. 728 and 729; 1918.

Digitized by Google

Tables 2 and 4 show some of the frequency differences (differences in waves per centimeter in vacuum) which exist among wave lengths of argon and krypton. The constancy of these frequency differences is of interest in view of the high degree of precision which the wave-length measurements are believed to possess. Measurements on the refractive index of air [18] which were made at this Bureau were used in computing the frequencies in vacuum from the wave lengths in air.

Regularities in the spectrum of argon were first detected by Rydberg,[19] who listed 23 groups of lines having frequency differences which were repeated from group to group. Additional groups of the same type were pointed out by Paulson.[20] Then Meissner [21] determined some of the longer wave lengths by direct comparison with the cadmium standard and found that the frequency differences among the quadruplets were constant within the limits of probable error in the wave-length measurements. Twenty-eight of the argon lines in Table 1 belong to quadruplets of this type. Table 2 gives the quadruplets in which two or more of the lines in Table 1 are present.

Wave lengths given to two decimal places are taken from the measurements of Kayser [22] and are converted to the international scale. The line 8667.97 was obtained from diffraction-grating spectra made by this Bureau not yet published. The three decimal-place values are found in Table 1, except those contained in parenthesis, which are predicted from the others by means of frequency differences in parenthesis and assuming that each of the 12 groups of lines is really a complete quadruplet. It is evident that the frequency differences between lines measured by the interferometer are constant within one part in three or four millions which is the same order of accuracy as the wave-length measurements. This may be regarded as another verification of the exactness of the Combination Principle of Ritz. On the other hand, if these frequency differences are really constant, it follows from Table 2 that the measurements determining the relative values of wave lengths involved in these combinations can not be in error by more than one or two thousandths

[18] B. S. Bull., 14, p. 712; 1918.
[19] Astroph. J., 6, p. 338; 1897.
[20] Physik. Z., 15, p. 831; 1914.
[21] Physik. Z., 17, p. 549; 1916.
[22] Astroph. J., 4, p. 1; 1896.

Digitized by Google

of an angstrom. The following frequency relations may be considered to hold throughout each group of four lines:

$\nu_2 = \nu_1 + 606.837$

$\nu_3 = \nu_2 + 803.075 = \nu_1 + 1409.912$

$\nu_4 = \nu_3 + 846.162 = \nu_2 + 1649.237 = \nu_1 + 2256.074$

TABLE 2.—Frequency Differences in the Argon Spectrum

No.	λ in air	λ in vacuum	Frequency in vacuum $\nu_1, \nu_2, \nu_3, \nu_4$	$\nu_3-\nu_1$ $\nu_3-\nu_2$ $\nu_4-\nu_2$ $\nu_4-\nu_3$	$\nu_3-\nu_1$ $\nu_3-\nu_1$ $\nu_4-\nu_1$
1	(9354. 224)	9356. 788	10 687. 428		(1649. 237)
2	8667. 97	8670. 34	11 533. 57	803. 09	
3	8103. 693	8105. 918	12 336. 665	606. 844	
4	7723. 758	7725. 880	12 943. 509	1409. 94	
1	(9224. 502)	9227. 031	10 837. 722	(846. 162)	
2	(8556. 439)	8558. 797	11 683. 884	(803. 075)	
3	8006. 156	8008. 355	12 486. 959	606. 837	
4	7695. 106	7697. 205	13 093. 796		
1	8521. 448	8523. 781	11 731. 882	846. 168	846. 168
2	7948. 175	7950. 358	12 578. 050	(803. 075)	
3	(7471. 159)	7473. 213	13 381. 125		2256. 071
4	7147. 042	7149. 009	13 987. 953	1409. 903	
1	8408. 210	8410. 518	11 889. 876	(846. 162)	
2	(7849. 528)	7851. 735	12 736. 038		1649. 237
3	7383. 979	7385. 010	13 539. 113	606. 835	2256. 072
4	7067. 217	7069. 162	14 145. 948		
1	8264. 522	8266. 791	12 096. 593	846. 158	846. 158
2	7724. 210	7726. 333	12 942. 751	803. 075	1649. 233
3	7272. 935	7274. 936	13 745. 826	606. 840	2256. 073
4	6965. 429	6967. 347	14 352. 666	1409. 915	
1	4702. 317	4703. 629	21 260. 182	846. 161	846. 161
2	4522. 325	4523. 588	22 106. 843	(803. 075)	
3	(4364. 748)	4365. 970	22 909. 418		2256. 17
4	4251. 17	4252. 36	23 516. 35	1410. 01	
1	4628. 44	4629. 73	21 599. 59		
2	(4453. 955)	4455. 201	22 445. 676	(803. 075)	1649. 22
3	4300. 101	4301. 306	23 248. 751	606. 831	2256. 05
4	4190. 714	4191. 891	23 855. 582		
1	4596. 03	4597. 31	21 751. 85	846. 20	846. 20
2	4423. 92	4425. 16	22 598. 05	802. 70	1648. 90
3	4272. 169	4273. 367	23 400. 751	606. 837	2255. 74
4	4164. 180	4165. 350	24 007. 588	1409. 54	
1	(4610. 454)	4611. 741	21 683. 782	(846. 162)	
2	(4437. 297)	4438. 537	22 529. 944	(803. 075)	
3	4266. 286	4267. 483	23 433. 019	606. 833	
4	4158. 591	4159. 759	24 039. 852		
1	4510. 733	4511. 994	22 168. 151	(846. 162)	
2	(4344. 850)	4346. 066	23 009. 313		1649. 238
3	4198. 316	4199. 495	23 812. 389	(606. 837)	
4	(4093. 982)	4095. 134	24 419. 226		
1	4335. 33	4336. 54	23 059. 85	846. 10	846. 10
2	4181. 884	4183. 058	23 905. 954	803. 10	1649. 20
3	4045. 96	4047. 10	24 709. 05	606. 81	2256. 01
4	3948. 980	3950. 094	25 315. 858	1409. 904	
1	4333. 561	4334. 775	23 069. 247	(846. 162)	
2	(4180. 247)	4181. 422	23 915. 309		1649. 226
3	4044. 419	4045. 557	24 718. 473	606. 88	2256. 10
4	3947. 50	3948. 61	25 325. 35		

Digitized by Google

TABLE 3.—Wave Lengths in the Krypton Spectrum

Intensity	Bureau of Standards	Buisson and Fabry[a]	Intensity	Bureau of Standards	Buisson and Fabry[a]
	λ			λ	
8	4273.9696		7	4502.354	
3	4282.967		3	4807.065	
8	4318.552		4	5562.224	
10	4319.580		10	5570.2872	2908
10[b]	4355.478		10	5870.9137	9172
6	4362.6422		3	6456.290	
8	4376.122		8	7587.414	
4	4399.969		10	7601.544	
9	4453.9174				
9	4463.690				

[a] Comptes Rendus, 156, p. 945; 1913. [b] Second spectrum.

TABLE 4.—Frequency Differences in the Krypton Spectrum

No.	λ in air	λ in vacuum	Frequency in vacuum ν_1, ν_2	$\nu_2-\nu_1$
1	8776.73	8779.14	11 390.64	945.06
2	8104.33	8106.55	12 335.70	
1	8298.07	8300.35	12 047.68	945.00
2	7694.53	7696.64	12 992.68	
1	8190.02	8192.27	12 206.62	944.98
2	7601.544	7603.633	13 151.608	
1	5879.85	5881.48	17 002.52	944.91
2	5570.2872	5571.8396	17 947.426	
1	5870.9137	5872.5370	17 028.415	945.026
2	5562.224	5563.765	17 973.441	
1	4502.354	4503.613	22 204.396	945.030
2	4318.552	4319.765	23 149.426	
1	4463.690	4464.938	22 396.725	945.030
2	4282.967	4284.168	23 341.755	
1	4453.9174	4455.168	22 445.866	945.027
2	4273.9696	4275.168	23 390.893	

Pairs of lines in the spectrum of krypton having the same frequency difference were first discovered by Paulson.[23] Similar pairs among the longer wave lengths were found by Merrill.[24] Some of these are reproduced in Table 4 in which the last four pairs are completely represented by the wave lengths in Table 3. The constancy of these frequency differences is really remarkable since no value differs from the mean (945.028) by more than one part in about 10 millions of the wave number.

Pairs of lines suspected of having constant frequency differences have had attention called to them by Paulson,[25] but all of these associate rather faint lines with the stronger ones of Table 5 and these data are therefore not complete enough to

[23] Ann. d. Phys., 45, p. 428; 1914. [25] Astroph. J., 40, p. 298; 1914.
[24] B. S. Scientific Papers, 15, p. 251; 1919.

Digitized by Google

test the constancy of frequency differences in this spectrum. It is hoped to extend the wave-length measurements to fainter lines as soon as more spectrum tubes of xenon gas can be obtained.

TABLE 5.—Wave Lengths in the Xenon Spectrum

Intensity	Bureau of Standards	Intensity	Bureau of Standards	Intensity	Bureau of Standards
	λ		λ		λ
8.....	4500.978	9.....	4524.275	7.....	4807.019
6.....	4524.680	10.....	4671.225	4.....	4829.705
4.....	4582.746	6.....	4697.020	10 *.....	4844.883
10 *.....	4603.028	8.....	4734.154	5.....	4923.246

* Second spectrum.

IV. SUMMARY

The spectra of the inert gases contain strong lines which represent wave lengths possessing a high degree of homogeneity and reproducibility and are therefore suitable for use as standards of wave length. This paper gives the values of 50 wave lengths in the spectrum of argon, 18 of krypton, and 12 of xenon, all of which have been compared with the international primary standard by means of interferometers. The wave lengths are considered to be correct to 0.001 A in most cases. The elegance and refinement of the interferometer methods for wave-length comparisons are evidenced by the close agreement between values obtained by different observers, and also by the constant frequency differences of many of the lines belonging to combination series. There are only a few cases where independent observers differ by 0.004 A or more. From wave-length measurements in argon and krypton frequency differences are obtained which are constant within the probable error of the measurements. This further confirms the exactness of the Combination Principle of Ritz. If these frequency differences are considered as true constants, they certify to the accuracy in relative value of the wave lengths involved. More work of this kind on the part of different observers is very much to be desired so that an extended system of accurate secondary standards will ultimately be produced.

WASHINGTON, May 9, 1921.

Digitized by Google

LIBRARY OF THE UNIVERSITY OF CALIFORNIA

DEPARTMENT OF COMMERCE

SCIENTIFIC PAPERS

OF THE

BUREAU OF STANDARDS

S. W. STRATTON, DIRECTOR

No. 415

USE OF THE ULBRICHT SPHERE IN MEASURING REFLECTION AND TRANSMISSION FACTORS

BY

ENOCH KARRER, Physicist

Bureau of Standards

AUGUST 10, 1920

PRICE, 5 CENTS

Sold only by the Superintendent of Documents, Government Printing Office
Washington, D. C.

WASHINGTON
GOVERNMENT PRINTING OFFICE
1921

Digitized by Google

Digitized by Google

DEPARTMENT OF COMMERCE

SCIENTIFIC PAPERS

OF THE

BUREAU OF STANDARDS

S. W. STRATTON, DIRECTOR

No. 415

USE OF THE ULBRICHT SPHERE IN MEASURING REFLECTION AND TRANSMISSION FACTORS

BY

ENOCH KARRER, Physicist

Bureau of Standards

AUGUST 10, 1921

PRICE, 5 CENTS

Sold only by the Superintendent of Documents, Government Printing Office
Washington, D. C.

WASHINGTON
GOVERNMENT PRINTING OFFICE
1921

Digitized by Google

Digitized by Google

USE OF THE ULBRICHT SPHERE IN MEASURING REFLECTION AND TRANSMISSION FACTORS

By Enoch Karrer

ABSTRACT

A brief historical survey is given of the methods and instruments used in measuring the reflection factor of surfaces. The theory of the infinite luminous plane is discussed at some length in connection with the Nutting absolute reflectometer, which is based on this theory. Recent suggestions of the use of the Ulbricht sphere are noted and several new ways of using it are described. A reflectometer based on one of the latter ways is described in detail. This consists in a combination of the sphere with the Martens polarization photometer. The surface whose reflection factor is sought is laid over an aperture in the sphere. The brightness of it is compared with the brightness of the sphere wall. By screening the test surface from the first reflected light this comparison gives directly the unknown reflection factor. The theory of this use of the sphere is given in full. The reflection factor of a block of magnesium carbonate is shown to be 98.7 per cent by means of this instrument.

A transmissometer based on the same theory is also described. It is also pointed out that the spectral reflection and transmission factors may be obtained in this way as a step toward standardization of methods.

A simpler and less expensive reflectometer is also described, that will enable one to obtain the reflection factor of surfaces to within 10 to 15 per cent.

CONTENTS

		Page
1.	Introduction	203
2.	Historical	204
3.	Use of the sphere	205
4.	Theory and use of infinite planes	210
5.	Theory of the sphere	214
6.	Description of the present reflectometer	216
7.	General comments on methods of measuring reflection and transmission factors, and on standards	219
8.	A simpler instrument for commercial use	220
9.	A transmissometer	222
10.	Use of reflectometer and transmissometer with monochromatic light	225

1. INTRODUCTION

The purpose of this article is to present a general survey of the theory of the methods of measurement of the reflection factor of substances, and to describe in detail some new pieces of apparatus for the measurement of this quantity and for the measurement of the transmission factor.[1]

[1] The reflection and the transmission factors for light are formally defined by the Illuminating Engineering Society (report of committee on nomenclature and standards, 1918). The terms are here used in accordance with these definitions, with the understanding, however, that they are determined under conditions of diffused light. Other symbols used in this article conform also to the Illuminating Engineering Society nomenclature.

Digitized by Google

The apparatus described in greatest detail is a reflectometer consisting of a photometric sphere and the Martens polarization photometer. The novelty in this suggestion lies not in the use of this particular photometer in the study of the transmission and reflection by bodies nor in the use of the sphere in this connection, but in the use of the sphere in a way that is in accord with the simple theory of the sphere, and that, in conjunction with a photometer, such as the Martens, allows an absolute determination of either the transmission or reflection factor in one observation.

2. HISTORICAL

The measurement of reflection factors for surfaces that reflect more or less diffusely has received considerable attention. Thaler [3] made a thorough test of the behavior of a few substances in this respect. Although he was not interested in the total diffuse reflection factors, his data [3] for a surface smoked with magnesium oxide determine values between 0.89 and 0.90.

Sumpner [4] made use of the increased brightness of the walls resulting when a lamp was introduced within an inclosure, to study reflection and transmission by substances. Rosa and Taylor [5] used the same phenomenon with the sphere to obtain the reflection factor of their sphere paint. The method depends upon the comparison of illumination at a particular point from a given source when the direct flux only is considered and when this flux is altered by inclosing the source. Since the inclosure affects the flux in all directions from the source, the direct flux, with which comparison is made, must be the average direct flux from the source.

Gardner [6] gives data, obtained in The Electrical Testing Laboratories by the use of the sphere in a manner suggested by Little, on the reflection factors of colored surfaces. This method is relative, consisting of the measurement of the brightness of the sphere walls when illuminated by the test or standard surface placed successively inside the sphere. The test or standard surface only is illuminated directly by a source that is most conveniently placed outside the sphere.

[3] Ann. d. Phys., 816, p. 996; 1903. Good for reference to earlier work pertaining to Lambert's law. See also in this connection Mascart, "Traite d'optique," 3, p. 213.

[3] Ann. d. Phys., 816, p. 1006, Table 1. (There appears to be a typographical error here in the record of angles.)

[4] "The diffusion of light," Phil. Mag., 35, p. 81; 1893.

[5] "The integrating photometric sphere, its construction and use," Trans. Illum. Eng. Soc., 2, p. 453; 1906.

[6] "The light-reflecting values of white and colored paints," J. Franklin Inst., 181, p. 99; 1916.

Digitized by Google

Nutting[7] has made some interesting and important considerations on an instrument for determining the reflecting power of opaque bodies. This instrument was a very portable reflectometer, depending on no standards, and had the unique property of requiring no light source as a necessary adjunct. Any general illumination at the place where measurements were made might suffice. Because this reflectometer bears some semblance to that described in this article, some parts of the underlying theory are given below. The sources of error that exist in the Nutting reflectometer will not be dwelt on here. They have been pointed out by others.[8]

3. USE OF THE SPHERE

Luckiesh[9] has more recently called attention to the unsatisfactory state of the measurement of reflection factors, pointing out the desirability of arriving at some standard methods, and suggesting the use of the sphere in the following manner: Around a translucent sphere are distributed several light sources, and the whole is surrounded by a white-walled box. The surface, the reflection factor of which is sought, fills a small aperture in the sphere. The brightness of the test surface is measured by matching the brightness of it with that of the field in an auxiliary photometer. The proposed method is good, but it involves the use of all the photometric accessories required in the ordinary use of the sphere, and requires, further, a standard reflecting surface. The means employed of illuminating the sphere walls would have to be altered somewhat in order that full advantage may be taken of the theory of the sphere. In any case, however, the use of the principle of the sphere has decided advantages over the laborious method of measuring the reflection factor for various directions, and then by integration, graphically or otherwise, deriving the total reflection factor.

Much credit is due Taylor[10] for pointing out several ways by which the sphere may be used to determine the absolute reflection factor. The most obvious ways (including those of Mr. Taylor and others) of using the sphere to measure the reflection factor may be enumerated as follows:

1. By comparison of the illumination due to reflected flux alone with that due to both direct and reflected flux. If E_1

[7] Trans. Illum. Eng. Soc., 7, p. 412; 1912.

[8] "Measurement of diffuse reflection factors," J. Am. Op. Soc., 4, p. 9, 1920; B. S. Sci. Papers, Nos. 391 and 405; and Gen. Elec. Rev., 23, p. 72, 1920.

[9] "Measurement of the reflection factor," Electrical World, 69, p. 958; 1917.

[10] "Measurement of diffuse reflection factors," J. Am. Op. Soc., 4, p. 9; 1920. Also B. S. Sci. Papers, Nos. 391 and 405.

Digitized by Google

is the illumination due to the average direct flux and E_2 that due to the reflected flux, then

$$\frac{E_2}{E_1+E_2}=\rho$$

This is the method used by Sumpner and Rosa and Taylor, as described above, to obtain the absorption factor (α) directly and derive therefrom the reflection factor. In this case

$$\frac{E_1}{E_1+E_2}=\alpha=1-\rho$$

Sumpner, however, used an inclosure in the form of a hollow cylinder rather than in the form of a hollow sphere. Sumpner also used this method to obtain the transmission factor of substances. It is applicable only to materials that can be made into the form of a sphere, or that may be applied to the inner sphere walls.

2. By illuminating sphere walls as a whole indirectly by first illuminating a small portion of them. Brightness of the walls is measured when complete and when a known portion of the sphere is removed. This is the basis of a proposed reflectometer by Taylor [11] to obtain the reflection factor of painted sphere walls. The reflection factor ρ of the sphere wall is given by the equation

$$\rho^2\left[q\ (p+q-1)+\frac{b}{b_0}\ p\ (1-q)\right]+\rho\ (1-q)\left[q+(p+q-1)\ \left(1-\frac{b}{b_0}\right)\right]+(1-q)^2\left(1-\frac{b}{b_0}\right)=0$$

where q is the percentage of the sphere surface cut off by the hole; p, the percentage of area added to the sphere wall when the hole is covered by a plane surface; b and b_0 are brightnesses of the sphere wall due to reflected light when the test surface has a reflection factor of ρ and 0, respectively. A particular application of this method was made by Benford [12] for the determination of the reflection factor of magnesium carbonate as follows: The brightness (b_1 and b_2) of the sphere wall was measured after the removal in succession of two known fractional parts ($1-p_1$) and ($1-p_2$) of the sphere. The reflection factor is given by

$$\rho=\frac{b_1-b_2}{b_1\,p_1-b_2\,p_2}$$

[11] J. Am. Op. Soc., 4, p. 16; 1920.

[12] Gen. Elec. Rev., 23, p. 72; 1920.

Digitized by Google

This method, as the previous one, is applicable only when the test substance can be made into a sphere or can be applied to the inner sphere walls. It has one very desirable feature, in that not only is the illumination diffuse but the reflected flux which is measured is also, and the whole of it is directly contributory to the results. The degree to which the flux is diffused depends upon the test substance itself, for the latter constitutes the whole of the sphere wall. It must be applied with caution when the test substances are any other than highly diffusing.

3. By method (2), modified so that the specimen need not be the whole of the sphere wall but merely a small known portion of it. In this case the reflection factor ρ_x of the test surface is given by

$$\rho_x = \frac{1 - \frac{b_0}{b_x}}{\frac{q}{1-q} \cdot \frac{b_0}{b_x} + \frac{\rho p}{\rho p + (1-q)(1-\rho)}}$$

where p, q, ρ, and b_0 have the same meaning as in the method (2), and b_x is the brightness of sphere wall when the test surface is in place. The equation given under method (2) is derived from the present one when $\rho_x = \rho$. This method retains the desirable diffuseness in both incident and reflected light and obviates the restrictions of method (2) above, but the sensitivity of it depends upon the value of the reflection factor measured.

4. By use of part sphere, test (or standard) surface constituting a known portion of the sphere wall is illuminated directly. The standard is a specimen having the reflection factor of the sphere wall. The brightness of the sphere wall is measured first when illuminated by the specimen, then when illuminated by the standard. The reflection factor (ρ_x) of the test surface is given by [18]

$$\rho_x = \frac{\rho \frac{b_x}{b}}{1 - \frac{\rho^2 p \left(1 - \frac{b_x}{b}\right)}{1 - q + \rho(p + q - 1)}}$$

b_x and b are the values of the brightness of the sphere wall when the aperture is covered by the test surface and by the standard surface respectively. This method was one adopted by Taylor

[18] J. Am. Op. Soc., 4, p. 16; 1920.

Digitized by Google

in preference to the preceding one because it is more accurate and more sensitive.

5. By use of the complete sphere, the specimen being placed inside and illuminated directly (preferably by a narrow beam of light projected through a window). The standard is a specimen of known reflection factor. Two measurements of brightness of the sphere wall are necessary, first, when illuminated by the specimen, second, when illuminated by the standard. This method was suggested and used by Little,[14] whose standard was a magnesium-carbonate surface. The ratio of these gives the reflection factor of the sample in terms of the standard. This method may be improved by eliminating the standard surface. This may be accomplished by screening the test surface from the observation window, then comparing the brightness of the sphere wall, first, when illuminated by the sample, and second, when illuminated by illuminating a small portion of the wall. In the latter case no screen is interposed.

6. By use of the complete sphere, the specimen being placed inside and illuminated by the sphere wall. The brightness of the sample and of the sphere wall are compared by one observation. The sphere wall may be illuminated by illuminating a small portion of it. The reflection factors are in terms of that of the sphere wall. If the test surface only is screened from the illuminated portion the method is an absolute one.

7. By directly illuminating the specimen (constituting a negligible portion of the sphere wall). The walls are illuminated by the specimen. The brightness of the sphere wall at a point screened from the test surface is measured, first, as resulting from the illumination of the test surface, and second, as resulting from an equal illumination of a portion of the sphere walls unscreened from the observed spot. The ratio of these is the reflection factor of the surface. This is the method embodied in the reflectometer more recently designed by Taylor.[15] No standard is required.

8. By illuminating the specimen (constituting a negligible portion of the sphere) by means of the sphere walls, which in turn are illuminated by a narrow beam admitted through a small window. The specimen is screened from the illuminated spot.

[14] "The light-reflecting values of white and colored paints," J. Franklin Inst., 181, p 99; 1916.

[15] "A simple portable reflectometer," A. H. Taylor, Trans. Illum. Eng. Soc., paper read at 14th annual convention, Illum. Eng. Soc.; 1920. Also B. S. Sci. Papers, No. 405.

Digitized by Google

No standard is required. This method was used by Sharp and Little.[16] These authors showed that the reflection factor of a mirror as well as that of other surfaces may be correctly measured by this method. It may also be pointed out that all movements of the photometer in making the measurements required—namely, of the brightness of, first, the specimen and, second, the sphere wall—may be avoided by employing a mirror of known reflection factor. In some experimental work with this method the author used a glass prism, by the rotation of which either the specimen or the comparison spot could be brought into view.

9. By method (8) just described, simplified by the use of a Martens polarization photometer. One measurement, comparing the brightness of the specimen with that of the sphere wall, will then suffice. This is the method to which special attention is called in this article. It is the method embodied in the reflectometer described in detail below. It is suggestive of the best combination (for certain photometric work) in which the sphere is used in a manner that takes advantage of its properties and at the same time affords simplicity of parts, compactness, and directness.

10. Still other methods may be designed. For example, by using the specimen as a known portion of sphere wall. Another known portion removed. Two measurements of brightness of sphere wall are required, first, when sphere is complete, and, second, when the known portion is removed. This has the advantage that both the incident and the reflected light are diffused. The degree to which the light is diffused depends in this case and in method (3) above, not upon the specimen as in methods (1) and (2) above, but upon the sphere wall.

11. By modification of the foregoing methods, using two spheres simultaneously, so that only one measurement is necessary.

12. By use of a new method of obtaining the reflection factor of a substance that may be applied to the walls of the sphere or that may be made into a sphere, as suggested by the equation given below under the theory of the sphere. The relation between the brightness, b_s, of the sphere wall resulting when a portion, p,

[16] C. H. Sharp and W. F. Little, "Measurement of reflection factors," Trans. Illum. Eng. Soc., paper read at 14th annual convention, Illum. Eng. Soc.; 1920. See also paper by A. H. Taylor, presented at the same time, and discussion by Karrer.

Digitized by Google

of it is made luminous and the brightness, b, of the luminous portion is given by

$$b_s = p\, b \cdot \frac{\rho}{1-\rho}.$$

The reflection factor $\rho = \frac{r}{p+r}$, where $r = \frac{b_s}{b}$. The quantities p, b, and b_s may be measured. In particular, if p were changed until $b_s = b$, then $\rho = \frac{1}{1+p}$. It seems that this method is simpler than method (2), where portions of the sphere are removed, and simpler than method (1), where it is required to know the mean spherical candles of the source.

One simple way suggests itself whereby no beam of light need be projected into the sphere, namely, a plate of diffusing glass is illuminated on one side so that the brightness of the reverse side is b. The plate with the latter side toward the sphere is then placed against the sphere aperture of known dimensions. Finally the brightness of the sphere walls produced by this luminous plate is measured. This arrangement would readily allow of a variable aperture into the sphere.

Furthermore, the method of illuminating either the specimen or the sphere wall in some instances may be different from that stated above; for example, in method (8) above, the sphere wall might be illuminated by transmitted light as indicated by Luckiesh.[17]

4. THEORY AND USE OF INFINITE PLANES

The Nutting instrument is based upon the principle of the infinite luminous plane. The illumination [18] on a plane exposed to the flux from an infinite parallel plane source of uniform brightness b (lamberts) is $\pi\, b$, provided every element of the infinite plane radiates according to the cosine law. If a small reflecting surface be exposed to this illumination, it will reflect per unit area at the rate of $\pi \rho b$ lumens, where ρ is the reflection factor of the surface. Its brightness, therefore, is ρb. Hence the ratio of the brightness of the small plane to that of the infinite plane is the reflection factor sought. The surface under test should be small enough not to change the brightness of the luminous plane. Such simple conditions are not realized, however, in

[17] "Measurement of diffuse reflection factors," Jour. Am. Op. Soc., 4, p. 9, 1920; B. S. Sci. Papers, Nos. 391 and 405; and Gen. Elec. Rev., 23, p. 72, 1920.

[18] B. S. Bull., 6, p. 553; 1910

Digitized by Google

practice. In case of the Nutting reflectometer, two planes of the same size constitute the radiating and the receiving planes. In such a case, if we assume them infinite, their resulting brightness is readily calculable.

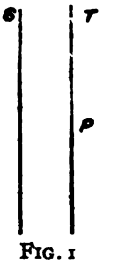

FIG. 1

The brightness of the planes is increased by the multiple reflection of light between them. Let S (Fig. 1) be the infinite plane of brightness b, illuminating the infinite plane T, and let the reflection factors of these planes be ρ_2 and ρ_1, respectively. As a result of the direct illumination from S, T will be of uniform brightness $\rho_1 b$, and will reradiate onto S at the rate $\pi\rho_1 b$. As a result of this S will have its brightness increased by an amount of $\rho_1\rho_2 b$. The plane S will in turn increase its illumination on T by an amount, $\pi\rho_1\rho_2 b$. The total illumination E_T of surface T will be

$$E_T = \pi b + \pi\rho_1\rho_2 b + \pi\rho_1^2\rho_2^2 b + \cdots\cdots \text{etc.}$$

The brightness of T is, therefore,

$$b_T = \rho_1 b\ (1 + \rho_1\rho_2 + \rho_1^2\rho_2^2 + \cdots\cdots + \rho_1^{n-1}\rho_2^{n-1} + \cdots\cdots) = \frac{\rho_1 b}{1 - \rho_1\rho_2}.$$

For the surface S we obtain the brightness

$$b_S = b\ (1 + \rho_1\rho_2 + \rho_1^2\rho_2^2 + \cdots\cdots + \rho_1^{n-1}\rho_2^{n-1} + \cdots\cdots) = \frac{b}{1 - \rho_1\rho_2}.$$

$$\frac{b_T}{b_S} = \rho_1.$$

In order to approach the condition of infinite planes, and at the same time retain limits consistent with a portable instrument, Nutting bounded the planes with a mirror.

The effect of the mirror is virtually to extend by multiple reflection the planes indefinitely. If the mirror were nonabsorbing, the finite planes bounded by it would give effects similar to infinite planes. The theory of them then would be also as simple as that of infinite planes. The mirror, however, will reflect only a certain proportion ρ_m of the flux falling upon it, and as a consequence, instead of an infinite plane with uniform brightness, we have an infinite plane composed of concentric zones of varying brightness. It becomes more difficult to calculate the illumination due to such a luminous plane at any point in space. This will be seen by considering, for sake of simplicity, the illumination at a point P which lies on the line perpendicular to the plane at the common

Digitized by Google

center of all the zones. Let S, Fig. 2, be a luminous disk of diameter $2a$ and of uniform brightness b, surrounded by an annular area of uniform brightness $\rho_m b$. For the present the annular area may be regarded as the reflection of the disk in a surrounding circular mirror which reflects an amount ρ_m. The width of the annular area is therefore $2a$; its brightness $\rho_m b$. The illumination due to the disk S at the point P is

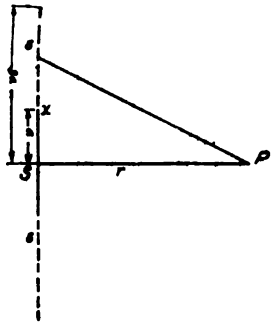

FIG. 2

$$E_d = \pi b \int_0^a \frac{2r^2 x dx}{(r^2+x^2)^2} = \frac{\pi b a^2}{r^2+a^2},$$

where r is the distance of the point P from the disk.[19]

Similarly the illumination at P due to the annular portion ss of the disk of brightness b_1 is

$$E_1 = \pi b_1 \int_a^{3a} \frac{2r^2 x dx}{(r^2+x^2)^2} = \frac{8\pi b_1 a^2 r^2}{(r^2+9a^2)(r^2+a^2)}.$$

So that the total illumination at P is the sum of these

$$E_t = \frac{\pi b a^2}{(r^2+a^2)}\left(1 + \frac{8\rho_m r^2}{r^2+9a^2}\right),$$

where $\rho_m = \frac{b_1}{b}$.

If the disks were of uniform brightness, that is, $\rho_m = 1.00$,

$$E_t = 2\pi b r^2 \int_0^{3a} \frac{x dx}{(r^2+x^2)^2} = \frac{9\pi b a^2}{(r^2+9a^2)}.$$

In the actual case there is an infinite number of concentric zones which contribute to the illumination at P and the resultant effect at P may be represented by a summation of such integrals as that given above for the annular zone ss due to the first order of reflection. The effect of the nth order of reflection may be written after noting that the position and boundary of the nth image are determined by its radii, which are $a(2n-1)$ and $a(2n+1)$.

[19] B. S. Bull. 6, p. 551; 1910.

Digitized by Google

The illumination at P due to the nth reflection is then

$$E_n = \pi b \rho_m^n \int_{a(2n-1)}^{a(2n+1)} \frac{2r^2 x dx}{(r^2+x^2)^2} = \frac{8\pi b a^2 r^2 n \rho_m^n}{[r^2+(2n-1)^2a^2]\,[r^2+(2n+1)^2a^2]}.$$

The illumination due to all zones is

$$E_a = \sum_{n=1}^{n=\infty} \pi b \rho_m^n \int_{a(2n-1)}^{a(2n+1)} \frac{2r^2 x dx}{(r^2+x^2)^2} = \sum_{n=1}^{n=\infty} \frac{8\pi b a^2 r^2 n \rho_m^n}{[r^2+(2n-1)^2a^2]\,[r^2+(2n+1)^2a^2]}.$$

And the total illumination becomes

$$E_t = E_d + E_a = \pi b a^2 \left\{ \frac{1}{r^2+a^2} + 8r^2 \sum_{n=1}^{n=\infty} \frac{n\rho_m^n}{[r^2+(2n-1)^2a^2]\,[r^2+(2n+1)^2a^2]} \right\}.$$

A few terms of this expression may be written out for the sake of the discussion.

$$E_t = \pi b a^2 \left[\frac{1}{a^2+r^2} + 8r^2 \left\{ \frac{\rho_m}{(r^2+9a^2)\,(r^2+a^2)} + \frac{2\rho_m^2}{(r^2+25a^2)\,(r^2+9a^2)} + \right\} \right.$$
$$+ 8r^2 \left\{ \frac{n\rho_m^n}{[r^2+(2n-1)^2a^2]\,[r^2+(2n+1)^2a^2]} \right.$$
$$\left. \left. + \frac{(n+1)\rho_m^{n+1}}{[r^2+(2n+3)^2a^2]\,[r^2+(2n+1)^2a^2]} + \cdots\cdots \text{etc.} \right\} \right].$$

This series is, in general, very rapidly converging. The ratio of the $(n+1)$th to the nth term being

$\rho_m \frac{n+1}{n} \left\{ 1 - \frac{(8+16n)a^2}{r^2+(2n+3)^2a^2} \right\}$, which approaches the value ρ_m for large values of n, but is always less than ρ_m if a is large compared with r (say, $a = 3r$ or more). The value of this ratio for the first and second terms is ρ_m if $a = 2r$. The effect of the illumination due to the nth reflection compared with that of the disk alone is:

$$e = \frac{8r^2 n \rho_m^n\,(a^2+r^2)}{[r^2+(2n+1)^2a^2]\,[r^2+(2n-1)^2a^2]}.$$

If a/r is assumed to be 5, and ρ_m to be 100, then the effect of the first and second images is about 5 per cent of that of the disk, and the effect of the first 10 images is slightly less than 6 per cent of that of the disk. It is evident that as the reflection factor of the mirror approaches unity the disk as extended by its images becomes more like an infinite plane.

Digitized by Google

From the equation for E_t it is also seen that as r becomes very small the illumination at P approaches that given by an infinite plane of uniform brightness, $E_t = \pi b$.

The foregoing considerations show that the theoretically simple conditions are not at all attained in the use of infinite planes as in the Nutting instrument. An improvement could be effected by making the test surface only a small portion of one of the planes. This would also be the case if one were to consider the instrument from the point of view of a finite inclosure rather than from the viewpoint of infinite planes.

A very good approach to two infinite planes can be had by two concentric spherical surfaces. Either of the surfaces may be made luminous with uniformity of brightness. The test surfaces may be made a part or the whole of the nonluminous sphere. A sphere uniformly bright illuminates all points on any given concentric spherical surface equally, and more nearly like an infinite plane as the points approach the surface of the luminous sphere.[20] Of course, the last condition would be impossible to realize in a practical instrument. Yet this interposes no hindrance to the practical use of two concentric spherical surfaces as described. For when the surfaces are separated any finite distance the relative distribution of the illumination from the one on to the other remains unaltered. The magnitude only of the illumination changes, becoming less than that which is given by an infinite plane in the ratio of the square of the radius of the sphere to the square of the distance from the center of the sphere to the concentric spherical surface. (The latter statement applies when the inner sphere is the luminous one.) Just what other difficulties would arise in the actual execution of this arrangement can not be foretold.

It is of interest to note that the flux between two infinite parallel planes depends upon the reflection factors of them in a manner quite different from that in which the flux in a sphere depends upon the reflection factor of the sphere wall.

5. THEORY OF THE SPHERE

For an inclosure we find the most satisfactory case to consider is that of the hollow sphere, for although the flux in any inclosure is everywhere the same [21] if the walls of the inclosure are uniformly bright, it is only in case of the sphere where this latter condition of uniformity of brightness is easily obtainable.

[20] B. S. Bull., 6, p. 558; 1910.

[21] B. S. Bull., 6, p. 562; 1910.

Digitized by Google

In the sphere, whose walls reflect according to Lambert's law, every element of surface illuminates every other element to the same degree,[23] no matter how the wall of the sphere or any portion of it is directly illuminated. This property of the spherical inclosure was first discovered by Sumpner.[25] It was rediscovered by Ulbricht,[24] who first demonstrated its great practical importance to photometry. So that, if the surface of the sphere has a uniform reflection factor and if a small portion of it is made luminous, the whole sphere will be uniformly bright, except for this spot which may be of negligible proportions. The brightness may be calculated as follows:

Let the illuminated spot of area A have an average brightness of b. It radiates πbA lumens. Owing to multiple reflections this flux will accumulate to a value F such that the rate of loss αF equals the rate of input πbA, where α is the absorption factor.

$$\alpha F = \pi bA$$

$$F = \frac{\pi bA}{\alpha} = \frac{\pi bA}{1-\rho}.$$

This was first derived by Mascart.[26] This reasoning may be employed for any inclosure whose walls obey Lambert's cosine law of emission. When the walls are not uniformly bright, b refers to the average brightness.

The illumination on every other element of the surface of the sphere will be

$$E = \frac{bA}{4\pi r^2} \cdot \frac{1}{1-\rho}.$$

Hence the brightness of every element of the surface of the sphere (except A) is

$$\frac{\rho bA}{4\pi r^2} \cdot \frac{1}{1-\rho} = b_s$$

The ratio of the area of the luminous spot to the area of the sphere is

$$\frac{A}{4\pi r^2} = p.$$

So that

$$b_s = \frac{pb\rho}{1-\rho}.$$

[23] Liebenthal, Praktische Photometrie, p. 301

[25] "The diffusion of light," Phil. Mag., **35**, p. 81; 1893.

[24] Electrotechn. Zs. **21**, p. 595, 1900; **26**, p. 512, 1905

[26] Palaz, Traité de Photométrie Industrielle, translation by the Pattersons, p. 297.

Digitized by Google

If now for a small portion of the sphere surface there is substituted another nonluminous surface whose reflection factor is ρ_x, the brightness b_x of the latter will be

$$b_x = \frac{\rho_x b\rho}{1-\rho} = \frac{\rho_x b_s}{\rho},$$

and

$$\frac{b_x}{b} = \frac{\rho_x}{\rho}.$$

The reflection factor of any specimen is given in terms of that of the sphere wall. To make it possible to obtain the reflection factor of the specimen absolutely, certain conditions must be imposed upon the manner in which the specimen is illuminated. If all of the flux illuminating the specimen is reduced by a factor ρ, the brightness of the specimen will also be reduced in the same proportion.

Then b_x becomes $b'_x = \rho\, b_x = \rho_x\, b_s$.

and $\frac{b'_x}{b_s} = \rho_x$.

This result is achieved by interposing a screen between the illuminated spot and the test surface. The screen is just sufficiently large to enable it to intercept all of the flux reflected from the former in the direction of the latter. The illuminated spot must be small in order that no appreciable illumination due to the second and higher order of reflections would come to the test surface if the screen were not present. The new surface also is assumed to be so small that its presence does not alter the brightness of the sphere walls.

All of these theoretical conditions can be attained to a satisfactory degree in practice. This is the idea underlying several uses of the sphere in reflectometry listed above and in particular the reflectometer [26] depicted in Fig. 3.

6. DESCRIPTION OF THE PRESENT REFLECTOMETER

The reflectometer sketched in Fig. 3 is essentially a sphere, having, firstly, an aperture which may be closed by any surface whose reflecting factor is sought, secondly, a means for comparing directly the brightness of the test surface with that of the

[26] This reflectometer was shown before the Illuminating Engineering Society at Cleveland, Oct. 5, 1920. A general description of it will appear in Trans. Illum. Eng. Soc., as discussion of the papers: "Measurement of reflection factor," C. H. Sharp and W. F. Little; and "A simple portable reflectometer of the absolute type," A. H. Taylor

Digitized by Google

sphere surface, such as a Martens[27] photometer, and thirdly, a lamp for illuminating a small portion of the sphere.

The most satisfactory photometer for comparing the brightness of two surfaces not far removed from each other is the Martens

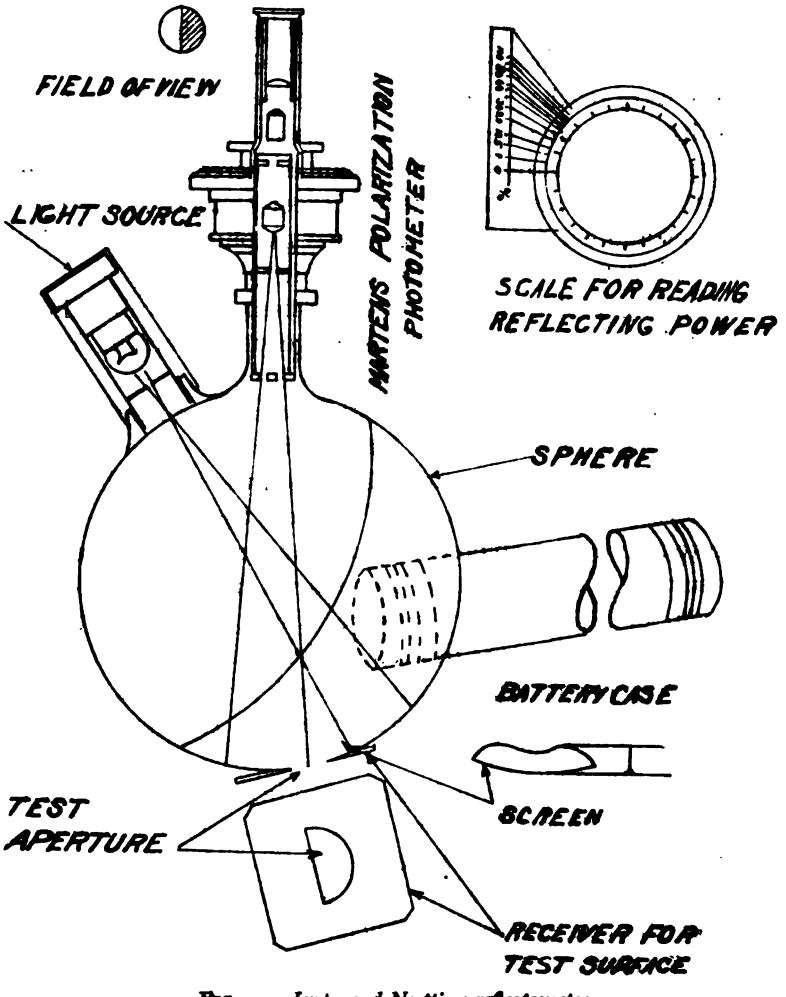

FIG. 3.—*Improved Nutting reflectometer*

Scale ½ natural size

polarization photometer. It is very compact, accurate, and has an extremely good photometric field.[28] Its optical parts are, in order of position in the optical path, Fig. 3, two apertures, lens, Wollaston prism, biprism, Nicol prism, and eyepiece containing

[27] Phys. Za., 1, pp. 299-303; 1900

[28] In spite of the fact that this instrument is not patented it is unfortunately not readily procurable.

Digitized by Google

lens and aperture. A scale reading directly the absolute reflection factor is attached to the circular scale already a part of the Martens photometer. The lamp is a small Mazda flashlight lamp operated at 3.8 volts by a small 3-cell flashlight battery. It is not difficult to get sufficient flux into the sphere and at the same time illuminate a rather small spot, say, 3 cm in diameter, when proper lenses are chosen. For the first instrument constructed no lenses were used. For ease and accuracy of setting, however, the resulting illumination was insufficient.

The spot illuminated by the beam is screened from the test aperture. This screen is made no larger than is necessary. Its dimensions and shape were determined graphically. The size and shape and location of it are shown in Fig. 3.

The battery is placed in an ordinary flash-lamp tube whose end is soldered to the sphere. Thus a very convenient handle is afforded at the same time.

The sphere is a copper-covered steel float, procurable at plumbers' supply houses. Its diameter is 6 inches. The copper coat was actually found to be undesirable when the sphere is enameled, and was removed. The screen between the test aperture and illuminated spot was riveted in place and enameled like the rest of the surface. A coat of white enamel facilitates greatly the attainment of a satisfactory surface, where a matt-white surface of high reflection factor is desired. The enameled surface is easy to paint and requires a much thinner coat of paint than otherwise. The paint used was that described by A. H. Taylor [29] of this Bureau.

A few results are recorded here to indicate the behavior of an instrument constructed along these lines. These results were obtained with the first instrument, constructed rather hastily and imperfectly. No lenses were used with the lamp; no adequate holder for the battery was attached; and no provision was made for readily turning the Martens photometer through 180° to eliminate any asymmetric errors. Settings were made in each of the four quadrants.

Magnesium carbonate block No. 1 (A. H. T.)—0.980;
Magnesium carbonate block No. 2 (A. H. T.)—0.972;
Magnesium carbonate block No. 1 (E. K.)—0.980.

The first two blocks of magnesium carbonate were loaned by Mr. Taylor, who has determined the reflection factor of them by

[29] B. S. Sci. Papers, in preparation, "The integrating sphere," Ross and Taylor

Digitized by Google

various methods, arriving at 0.99 for No. 1 and 0.982 for No. 2. There seems to be a consistent difference. Other tests were made on a series of surfaces which had been studied by Mr. Taylor using the point by point method. Differences in the factor were usually obtained (although not always), which indicated that the above reflectometer was reading slightly low. The value obtained here for the magnesium carbonate agrees with those found first by Mr. Taylor [30] and later by Mr. Benford [31] and others.[32]

The sample needs to be neither opaque nor diffusing. It may be a clear piece of glass or mirror. This condition follows on the assumption that the hole in the sphere over which the specimen is placed is so small that its area is negligible in comparison with that of the whole sphere. In the one described above the area of the hole is about 3 cm², or less than one-half per cent of that of the sphere. In the case of a mirror, however, precautions must be taken not to have the second reflecting surface too far removed from the opening. The angle subtended by the image of the test aperture must always be sufficiently large to fill the field of view of the photometer.

7. GENERAL COMMENTS ON METHODS OF MEASURING REFLECTION AND TRANSMISSION FACTORS, AND ON STANDARDS

Many aspects of the problem of measuring the diffuse reflection factor call for consideration, some of which may or may not turn out to be of any moment. For instance, in case of the reflection factor the surface may be diffusely illuminated, but in general can be observed from one direction only. Or it may be illuminated from one direction only, and the diffusely reflected flux measured. In either case the question of direction enters, concerning which nothing much can be said until more work is done; the use of the sphere is, however, a step toward uniformity and standardization. In case of the transmission factor the illumination on the specimen may be entirely diffuse and the whole of the transmitted flux measured. This can be accomplished by the use of two spheres, comparing the brightness of the walls of them, so that the question of direction may be easily eliminated in case of the transmission factor.

[30] A. H. Taylor, "Measurement of diffuse reflection factors and a new absolute reflectometer," J. Am. Op. Soc., 4, p. 9; 1920.

[31] F. A. Benford, "An absolute method for determining coefficients of diffuse reflection," Gen. Elec. Rev., 23, p. 72; 1920.

[32] C. H. Sharp and W. F. Little, "Measurement of reflection factors," Trans. Illum. Eng. Soc., paper read at 14th annual convention, Illum. Eng. Soc., 1920. (See also paper by A. H. Taylor, presented at the same time, and discussion by Karrer.)

Digitized by Google

Four of the methods enumerated above for determining the reflection factor—namely, (2), (3), (9), and (12)—afford diffusion in both the incident and the measured flux. The first and last of these place very serious limitations upon the nature and the form of the surface to be tested. The other two are insensitive for certain values of the reflection factor, their sensitivity depending upon this factor in a rather complicated manner. Method (1) virtually allows diffuseness in both incident flux and measured flux, but the extent to which this condition actually prevails depends upon the relative importance of the secondary flux, E_2, and therefore upon the reflection factor itself.

At all events, so far as a working standard is concerned, the procuring of a magnesium carbonate block at any market is to be discouraged so far as preliminary observations go. Magnesium carbonate blocks purchased at different times may have reflection factors varying by at least several per cent. It would be an admirable thing for some scientific supply house to have in stock magnesium blocks of guaranteed texture and purity. Yet those who have the facilities of a photometric sphere need not rely on even such standards.

8. A SIMPLER INSTRUMENT FOR COMMERCIAL USE

The Nutting reflectometer requires neither lamp nor battery, a great advantage in a portable instrument. This advantage could possibly be obtained with other reflectometers by sacrificing accuracy for serviceability. It might, for example, be possible to accomplish this by the use of a translucent sphere or one in part transparent. In the reflectometer shown in Fig. 3 a mirror mounted so as to have sufficient freedom of rotation was substituted for the lamp to obviate the necessity of maintaining a light source. Unless, however, an intense external light source is available, the brightness is too low. With sunshine it works admirably. For practical uses, however, even simpler instruments might be used, for example, the one shown in Fig. 4. In this an opal glass sphere has a rather large opening covered with a flat disk. The disk has a circular aperture against which the test surface is placed surrounded by an annular area divided into sectors, having different known reflection factors. The test surface and sectors are equally illuminated by the sphere wall, and are viewed through an aperture, W. The brightness of the test surface is taken to be that of the sector whose brightness most nearly matches it. The use of

Digitized by Google

a simple disk with graduated reflection factors was suggested many years ago. It is not satisfactory where any great amount of specular reflection exists. In the present instrument such is not the case. Furthermore, a definite direction determined by angle A, Fig. 4, for observing is given. This direction might be chosen

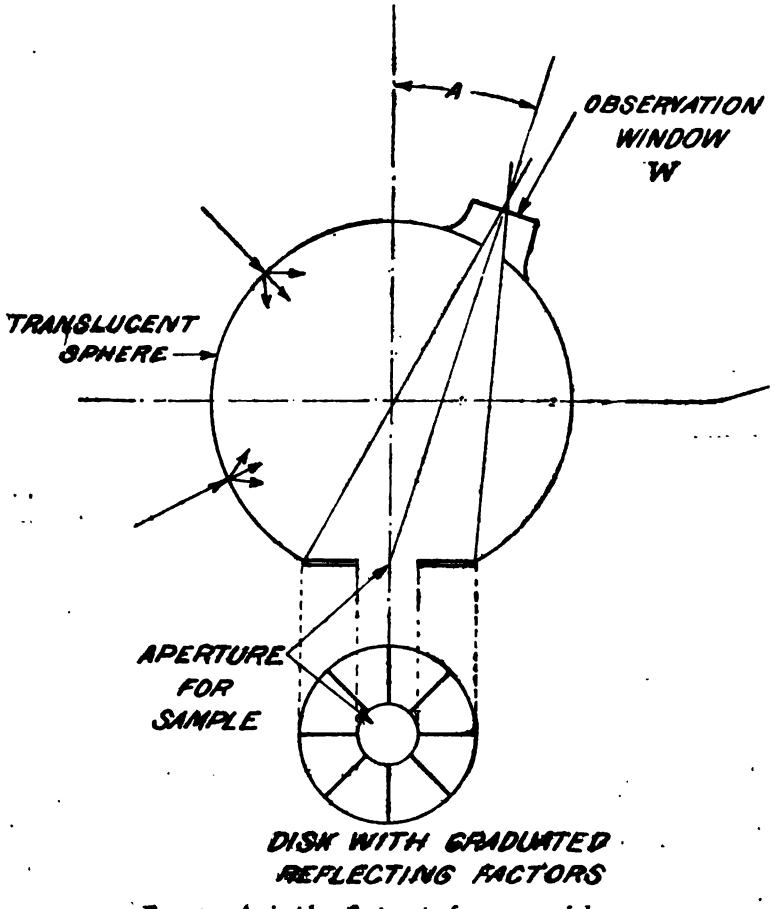

FIG. 4.—*A simple reflectometer for commercial use*

most favorably for many common materials met with in practice. Several workers [22] seem to find that at some angle of emergence for normal illumination many surfaces have a reflection factor nearly equal to that of a perfectly diffusing surface of the same diffuse reflection factor.

[22] A. H. Taylor finds this angle to be about 50° for many surfaces. Prof. W. J. Drisko informs me that he has found the angle to be about 46° for many surfaces.

Digitized by Google

9. A TRANSMISSOMETER

The diffuse transmission factor is sometimes more important than the reflection factor, as in the case of photographic negatives and in diffusing glassware for illumination purposes. It is therefore desirable to have at hand a means of readily measuring this quantity with a fair degree of accuracy. While there are several ways in which the properties of the Ulbricht sphere may be utilized for this purpose, let it suffice to point out in detail here only one such way, which is merely an extension of that involved in the reflectometer described above. Another similar sphere with an aperture equal to that in the reflectometer sphere, as is

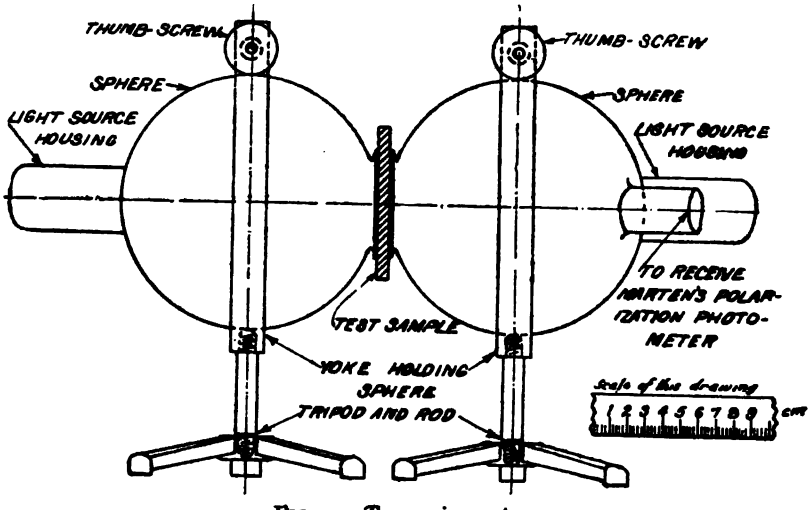

FIG. 5.—*Transmissometer*

shown in Fig. 5, is added. The second sphere is illuminated by the same lamp or by one similar to and in series with the one illuminating the first sphere. For a stationary piece of apparatus where no restrictions are placed on size, the same lamp could illuminate both spheres. The flux into the second sphere is controlled by means of a diaphragm with a variable aperture such as an iris, slit, or wedge. (See Fig. 6.) No exacting specifications are necessary. The aperture of the second sphere is screened from the direct flux, as in the reflectometer sphere. In this case, as in the reflectometer, we assume that the area of the aperture is so small that it will not affect the brightness of the sphere walls. This can probably always be sufficiently well attained. It is also assumed that the illuminated area is small.

Digitized by Google

The use of this apparatus as a transmissometer is as follows: The transmission sample is placed over the aperture of the reflectometer as usual, and its reflection factor ρ measured. The auxiliary sphere is then brought up so that the reverse side of the specimen covers its aperture. The brightness b_x of the sample now is due to two factors, (1) the flux reflected from its front surface (which is illuminated by the walls of the first sphere), and (2) the flux transmitted by the specimen in consequence of the illumination by the walls of the second sphere. Let the walls of these spheres have a brightness of b and b_1, respectively, and let the transmission factor of the sample be τ. Then $b_x = \rho b + \tau b_1$.

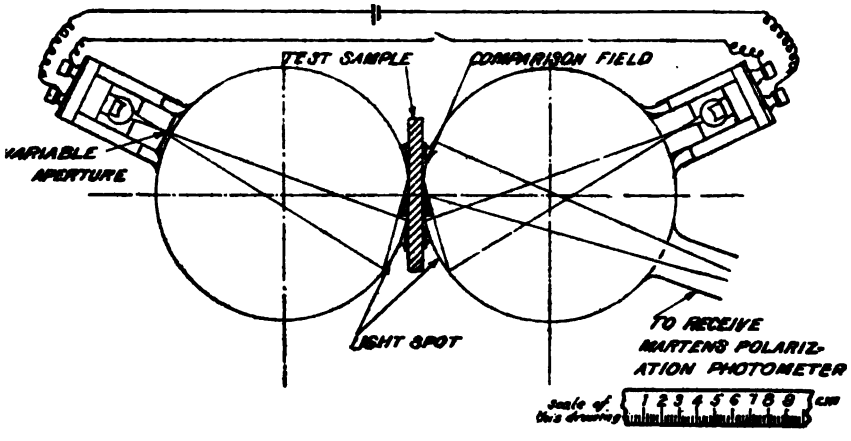

FIG. 6.—*Transmissometer, showing position of light sources, test sample, photometer, and screens*

The quantity b_1 may be measured in terms of b once for all, and may have any value, but for the sake of simplicity, we shall make $b_1 = b$.

Then $b_x = b(\rho + \tau)$.

$$\frac{b_x}{b} = \rho + \tau.$$

In this equation ρ has been determined; b_x is measured in terms of the brightness of the walls of the reflectometer sphere; τ is the factor desired; and $\frac{b_x}{b}$ is measured and read off directly by means of the reflectometer. We see, therefore, that it is just as simple so far as manipulation is concerned to obtain the value of the combined reflection and transmission factors as it is to obtain the reflection factor alone. The difference of these two quantities gives the transmission factor. In this way one piece of laboratory

Digitized by Google

apparatus enables us to obtain both the reflection factor and the transmission factor in an absolute manner, involving no calibration of a standard of transmission or reflection, no light standards, no measurement of distances, no manipulation of the specimen, and no electrical measuring instruments. One placing of the sample against the reflectometer is all.

Although the arrangement described appears to have certain advantages for laboratory purposes where duplication of costly photometric or spectrophotometric apparatus is not desired, or where it is desirable that such apparatus when once set up shall not be disturbed, it may be of interest to describe a few other arrangements that may be had. A simple method would be to insert the sample between the end of the photometer and sphere in such a way that one of the apertures only of the photometer is covered by it. The other aperture is illuminated by the sphere

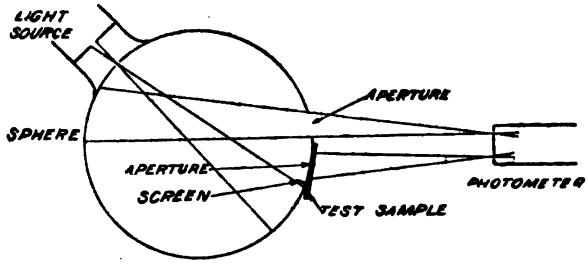

FIG. 7

wall, which in turn is illuminated by projecting a narrow beam into the sphere. Precautions must be taken to screen the test sample properly, as has been noted in the description of the reflectometer. Narrow limits are set to the size and shape of the sample that is to be tested.

A modification of this is shown in Fig. 7, where the photometer is removed from the sphere to a distance that allows greater freedom in the size and shape of the sample. In this case a comparison is made of the brightness b of the sphere wall with the brightness τb of the sample. The Martens polarization photometer measures τ directly.

In all these arrangements nothing novel can be claimed except in the use of the sphere rather than of an irregular inclosure or of superficial standards. The sphere affords two important essentials: (1) The kind of diffuse illumination desired in such measurements, and (2) the conditions for absolute determination. Neither of these can be so closely approximated by any other means.

Digitized by Google

The combination of the sphere with the Martens photometer has been suggested and used by Goldberg [84] in measuring the density of photographic plates. His suggestions differ from those given in this article regarding the general use of the sphere in measuring the transmission and reflection factors of substances in that in accordance with the latter the sphere is to be used not only to secure good diffuseness of the light but to obtain these factors in an absolute manner.

10. USE OF REFLECTOMETER AND TRANSMISSOMETER WITH MONOCHROMATIC LIGHT

Although the instruments discussed above were primarily intended for mixed light, obviously they may also be used in determining the diffuse reflection and transmission factors of substances for spectral light. For this purpose the Koenig-Martens spectrophotometer is admirably adapted. In this connection, too, the use of the sphere, in ways described above, would make for definiteness and standardization, and afford absolute methods.

Most of this work was carried out with the cooperation of the searchlight investigation section of the Engineers, U. S. Army, who also made the executing of it possible by providing for it. Acknowledgment is also made to U. M. Smith for the illustrations of the text.

WASHINGTON, January 31, 1921.

[84] Photographische korrespondenz; May–June, 1910. Densograph, ein registrierapparat zur messung der schwaerzung photographischer platten.

Digitized by Google

Digitized by Google

LIBRARY OF THE UNIVERSITY OF CALIFORNIA

DEPARTMENT OF COMMERCE

SCIENTIFIC PAPERS
OF THE
BUREAU OF STANDARDS

S. W. STRATTON, DIRECTOR

No. 416

PREPARATION OF GALACTOSE

BY

E. P. CLARK, Associate Technologist
Bureau of Standards

AUGUST 15, 1921

PRICE, 5 CENTS
Sold only by the Superintendent of Documents, Government Printing Office
Washington, D. C.

WASHINGTON
GOVERNMENT PRINTING OFFICE
1921

Digitized by Google

Digitized by Google

PREPARATION OF GALACTOSE

By E. P. Clark

ABSTRACT

Owing to the large demand made by bacteriologists for specifications and data on galactose and its derivatives, a convenient method is described for preparing galactose from lactose so that this work may be undertaken.

One kg of lactose is hydrolyzed by boiling two hours with 2.5 liters of water and 50 g of sulphuric acid. The solution is neutralized with barium carbonate, filtered and concentrated. The galactose is crystallized from the resulting syrup by the addition of a mixture of 1 part of ethyl and 2 parts of methyl alcohol. The yield of crude sugar is about 27 per cent.

During the past few years there has arisen a demand for accurate data on the physical properties of the less common sugars. Coincident with this demand is also the constantly increasing use of these materials and the necessity for more economical methods of preparation. As the result of these conditions, this Bureau has had numerous requests for information on the economical production of galactose, as well as for an accurate value of its specific rotation. In order to bring this about, as well as to supply the demand for a standard sample of this material, an investigation of the subject was undertaken.

A number of methods for preparing galactose [1] have been reported, but partly because the details of procedure are not given with sufficient exactness, and partly because, in many cases, unnecessarily drastic measures have been recommended which add to the cost and reduce the yield, these methods are not satisfactory. Recently, an unpublished method, originated in the Bureau of Chemistry, has been used quite successfully by many workers. However, it is not generally known. The method which we have worked out in order to meet the demands made upon the Bureau of Standards has the advantages over the above-mentioned methods of giving more uniform results and higher yield at a lower cost, and is reported here that it may be useful to those requiring a supply of this sugar.

[1] Lippmann, Die Chemie der Zuckerarten, III. Auflage, pages 698–700.: 1904.

Digitized by Google

One thousand five hundred g of lactose are dissolved in 3750 cc of hot water containing 75 g of concentrated sulphuric acid. The solution is brought to a boil and then simmered for two hours. A thin paste of barium carbonate is then added to the hot solution until it reacts neutral to congo paper. The precipitate of barium sulphate is allowed to settle overnight, after which as much as possible of the supernatant liquid is drawn off. This liquid is filtered through a thin layer of active carbon placed on a moistened filter paper in a Büchner funnel. When all has passed through, the precipitate is placed on the filter, drained as dry as possible, and finally washed by drawing a little water through it. The filter, prepared with a small amount of carbon, as outlined, clarifies the solution and at the same time prevents the sulphate from passing through and gives a relatively rapid filtration.

The filtrate is concentrated under diminished pressure until it has a weight of 1650 g. If a refractometer is available, the concentrated syrup should show a refractive index n_D^{20} between 1.5120 and 1.5125. The very thick syrup is warmed to between 60 and 70° and 250 cc of ethyl alcohol are dissolved in it by vigorous shaking. The solution is then poured into a beaker or jar and the remaining syrup is washed from the flask with 500 cc of methyl alcohol. This is best done by adding the methyl alcohol to the flask portion wise and warming and shaking in a water bath. The whole solution is thoroughly mixed and seeded with some pure galactose crystals and allowed to crystallize.

The crystallization is generally complete in about four days, after which the crystals are filtered off, washed with a little methyl alcohol, then with 85 per cent ethyl alcohol, and finally with 95 per cent alcohol. They are then dried. The yield of the crude sugar is about 27 per cent of the lactose taken.

In order to purify the crude galactose, it is dissolved in water, making about a 25 per cent solution. To this is added a few cc of glacial acetic acid. It is then concentrated under diminished pressure to about 75 per cent total solids, warmed to 60 or 70°, transferred to a beaker, and 95 per cent alcohol added to saturation. Almost immediately the contents of the flask become solid. After standing overnight, the crystals are filtered from the mother liquor, washed, and dried. The yield is generally 82 to 83 per cent of the crude sugar taken.

Digitized by Google

A thoroughly dried sample of this recrystallized product had the following properties:

Ash	0.034 per cent.
$[\alpha]_D^{20}$	$=80°.4$ (10.617 g per 100.00 cc).
$[\alpha]_{\lambda=5462\text{ A}}^{20}$	$=95.°8$.

The values are only given, however, to identify the product. Work upon the thorough purification and the accurate determination of its specific rotation is in progress.

WASHINGTON, April 6, 1921.

Digitized by Google

Digitized by Google

DEC 22 1921

DEPARTMENT OF COMMERCE

SCIENTIFIC PAPERS

OF THE

BUREAU OF STANDARDS

S. W. STRATTON, DIRECTOR

No. 417

THE SPECTRAL DISTRIBUTION OF ENERGY REQUIRED TO EVOKE THE GRAY SENSATION

BY

IRWIN G. PRIEST, Physicist
Bureau of Standards

AUGUST 25, 1921

PRICE, 10 CENTS
Sold only by the Superintendent of Documents, Government Printing Office
Washington, D. C.

WASHINGTON
GOVERNMENT PRINTING OFFICE
1921

Digitized by Google

Digitized by Google

THE SPECTRAL DISTRIBUTION OF ENERGY REQUIRED TO EVOKE THE GRAY SENSATION[1]

By Irwin G. Priest[2]

ABSTRACT

The chief significance of this paper lies in the development and testing of an experimental method for determining an objective physical standard of "white light." The standard to be determined is the Planckian ("black-body") distribution of energy required to evoke the hueless sensation of brilliance, commonly called "white" or "gray," under certain standard conditions stated in detail in the paper.

The method of producing and adjusting the spectral distribution of the stimulus is this: Light from a lamp of known spectral distribution is modified by rotatory dispersion in a system of quartz plates and nicol prisms in such a way that by rotating one of the nicols the light emerging from it can be made to assume the spectral distribution of a Planckian radiator at any desired temperature between 4000 and 7000° K. Such a system is, in effect, a selective light filter of adjustable spectral transmission.

Two methods of observation are described:

(1) The method of adjustment by trial, in which the observer himself adjusts the stimulus until he calls the sensation "white."

(2) The method of answers, in which the operator conducting the experiment adjusts the stimulus to correspond to certain fixed temperatures of the hypothetical Planckian radiator and records the observer's reactions as "blue," "white," or "yellow," as the case may be. The latter method proved to be the more satisfactory.

Experimental results are given from four observers. The average results of these observers indicate that "white light" may be represented: (1) Theoretically, by the light from a Planckian radiator at a temperature of about 5200° absolute; (2) practically, to a fair approximation, by average noon sunlight at Washington. It is, however, emphasized that the final establishment of such a standard should be based on a more extensive statistical investigation.

An appendix to the paper sets forth the desirability of an extensive statistical determination and correlation of the characteristics of vision.

[1] The substance of this paper was first presented at a joint meeting of the American Physical Society and the Optical Society of America in Chicago, Dec. 29, 1920.

[2] The author acknowledges the cooperation of Prof. C. A. Skinner, Dr. M. Katherine Frehafer, and Mr. H. J. McNicholas as observers in this investigation, and their advice as well as that of Dr. P. V. Wells in revising the manuscript of this paper. Special credit is due to Mr. J. Clacey, optician, Bureau of Standards, for the construction of a standard quartz plate.

Digitized by Google

CONTENTS

	Page
I. Introduction	232
1. General considerations	232
2. Purpose and scope of this investigation	236
II. Experimental methods	238
1. Apparatus	238
2. Method of adjusting the stimulus	238
(A) Theory of method	238
(B) Experimental verification of method	241
3. Methods of observation	246
(A) Method of adjustment by trial	246
(B) Method of answers	246
III. Experimental results	247
1. Effect of previous selective fatigue	247
2. Results by the method of adjustment by trial	248
3. Results by the method of answers	249
IV. Summary and conclusions	255
1. Principal conclusions	255
2. Incidental conclusions	256
3. Suggestions as to future work	259
Appendix: The desirability of an extensive statistical determination and correlation of the characteristics of vision	260
Bibliography	264

I. INTRODUCTION

1. GENERAL CONSIDERATIONS

The Planckian spectral distribution of energy serving to specify the normal stimulus for the hueless visual sensation commonly known as "white" or "gray" should naturally take rank among the most significant cardinal data of the pure science of physiologic optics. Moreover, a quantitative knowledge of the normal stimulus of gray is obviously of fundamental importance to the practical technologic problems of rational color specification; it must be, in fact, the basis of the solution of the problem of defining "white" light. Nevertheless, it does not appear that any serious attempt has been made heretofore to determine this stimulus experimentally.

The concept of a "black-body" energy distribution as a definition for the stimulus of "white" was definitely proposed by H. E. Ives in 1910. He also showed that the energy distribution of "average daylight" could be represented by a "black body" at about 5000° K, and inferred, without any rigorous demonstration or attempt at experimental proof, that this definition of "average daylight" might be considered interchangeable with the definition of "white light."[1]

[1] H. E. Ives, Trans. I. E. S., 5, pp. 198 and 202; 1910.

Digitized by Google

The desirability of making such an experimental determination was pointed out several years ago by Troland. He stated the case very clearly, as follows:[4]

> There has been considerable discussion, in connection with colorimetric procedure, concerning the definition of "white light." It seems to me obvious that "white light" or "white" radiation can be defined logically only with reference to the properties or reactions of the normal human visual apparatus. White radiation is radiation which produces the sensation of white, or the achromatic visual quality, whether it be white or some shade of gray. The existence of complementary pairs of colors makes it evident that there must be an infinite number of different combinations of wave lengths which will produce this sensation, and consequently it becomes desirable to add the further criterion that "white" radiation must have the distribution characteristic of a black body. The tendency to identify white light in this sense with solar radiation, or with black body radiation corresponding as nearly as possible with solar radiation, is based upon the hypothesis that sunlight actually produces the sensation of white. If Hering's assertion, already referred to, is correct, this hypothesis can not be retained. [Hering claims daylight is yellowish.]

About this same time the present author was making a few preliminary determinations.[5] Subsequent experience has shown that the tentative results of these first experiments have no quantitative value. They are without significance because of the following circumstances:

(1) The stimuli did not actually conform sufficiently closely to the Planckian formula.

(2) The field viewed was not large enough to permit of good color discrimination.

(3) Sufficient care was not taken as to standard conditions of observation, particularly in avoiding the effect of previous fatigue.[6]

(4) The method of observation (adjustment by trial) was not good.[7]

The elementary concepts upon which the present investigation is based are these:

(1) The energy radiated by a so-called complete or ideal radiator ("black body") may be expressed as a function of temperature and wave length by the Planckian[8] formula:

$$E = \frac{c_1}{\lambda^5\left(e^{\frac{c_2}{\lambda T}} - 1\right)}$$

where $\lambda \equiv$ wave length;

$T \equiv$ absolute temperature of source;

$e \equiv$ base of natural logarithms;

c_1 and c_2 are constants;

$E \equiv$ energy per unit wave length.

---

[4] Troland, Trans. I. E. S., 13, p. 26; 1918.

[5] Priest, Trans. I. E. S., 13, pp. 75–77; 1918.

[6] Compare Sec. III, 1, below.

[7] Compare Sec. III, 2, below.

[8] Max Planck, Verh. d. Deutsch. Phys. Ges., 2, pp. 202–204; 1900.

Digitized by Google

(7) However, as will be shown below, it is possible by suitable artifices to obtain radiant energy having the same spectral distribution (in the visible spectrum) as would be given by a hypothetical Planckian radiator at any temperature between about 4000 and 7000° K, and the transition temperature in question has been found to fall within this range.

2. PURPOSE AND SCOPE OF THIS INVESTIGATION

The purpose of the present investigation has been to determine, in a preliminary way, for a few individuals, the Planckian spectral energy distribution which evokes the gray sensation under the following conditions:

(1) The uniformly illuminated circular field viewed by the observer subtends about 3.5° at his eye.

(2) This field is surrounded by a completely dark field (except for the small amount of diffuse light in the apparatus in some of the observations). There is no comparison field.

(3) The absolute intensity is chosen to give a medium comfortable brilliance, such as to give no conspicuous afterimages in the dark; and it was determined that considerable positive and negative departures from this intensity had no effect on the results. In the second method of observation[13] the brilliance was maintained approximately constant for all spectral distributions.

(4) The observations are conducted in a dark room and the observer's eyes are further protected by an eye shade following the contour of the face. The observer is kept in the dark about 10 to 15 minutes before observations begin in order to eliminate the effect of previous fatigue.[14]

(5) The observer selects by one method or another[15] the spectral distribution which for him evokes the gray or hueless sensation. He is asked to distinguish between "cold bluish white," "white," and "warm yellowish white."

It will be observed that, while these conditions are to a certain extent arbitrary, they are probably the most rational ones to impose in a preliminary investigation of limited extent, and they at any rate *approximate closely the conditions of observation in colorimetry with instruments of usual design and methods of use.* The size of field should be at least that used here, for color discrimination is very difficult and uncertain with small fields. That a comparison field can not be used is obvious from the nature

[13] See Sec. II, 3, B, below.
[14] See Sec. III, 1, below.
[15] See Sec. II, 3, A and B, below for two methods used.

Digitized by Google

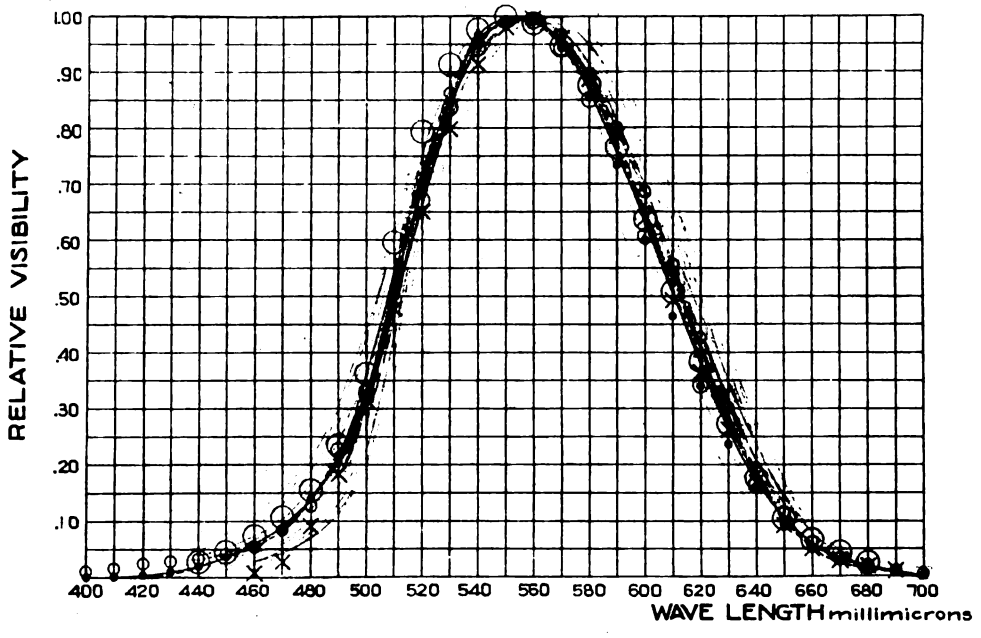

Gray background of curves: 125 individuals by Coblentz & Emerson: B.S. Sci Pap. 303, Fig. 13; 1917.
● ● ● Hyde, Forsythe & Cady: Astrop J. 45 p. 67, Table IV; 1918. (Average of 10–29 individuals)
O O O Coblentz & Emerson: B.S. Sci Pap. 303, Table 5, 1917. (Average of 125 individuals)
Nutting Trans. I.E.S. 9, p. 637, last line; 1914. (Average of 21 individuals)
Ives. Phil. Mag. (6) 24 p. 853, Table II; 1912. (Average of 18 individuals)
I.E.S. committee mean. (From Nutting: Jour. Op. Soc. Am. 4 p. 56; 1920)
Tentatively adopted by Priest, 'Leucoscope', Fig. 8, Jour. Op. Soc. Am. Nov. 1920. (nearly coincident with I.E.S.)
× × × Recommended by Ives as standard for physical photometry: J. Frank Ins. 188, p. 220, Table I; 1919.

FIG. 2.—*Synopsis of visibility data*

Digitized by Google

Digitized by Google

of the question to be answered. That fatigue must be guarded against is a reasonable precaution, the necessity of which will also be shown in the experimental part of this paper.[16]

Under these conditions we have determined the Planckian energy distribution which evokes the gray sensation for four different observers and have expressed the findings in terms of the absolute temperature of the Planckian hypothetical complete radiator. Sufficient observations have been made to determine these temperatures with considerable accuracy for these particular observers.

It has been shown that the transition from yellow to blue under these conditions is a real and obvious phenomenon, and that positive, unambiguous results may be obtained in determining the temperature of the source corresponding to this transition.

The purposes of this paper are:

(1) To describe the experimental method followed and show its utility for such investigations;

(2) To present the limited data already found for four individuals.

In regard to these observers, the following information may be given:

Visibility.—The visibility of radiant energy has been determined for two of the observers (H. J. M. and I. G. P.) by Coblentz and Emerson and is on record.[17] H. J. M. was classed by Coblentz and Emerson as "normal," I. G. P., as "subnormal red." The latter's departure from normal is comparatively small.[18]

Color perception.—The color perception of all the observers is approximately normal as judged by Holmgren's test and their ability to arrange colored samples in spectral order. As judged by Nagel's cards there is reason to *suspect* that two of the observers should be classed as "anomalous trichromats" (C. A. S. and H. J. M.), but this evidence is not conclusive. They exhibit a *slight* tendency to confuse green and gray in this test. All can read Stilling's charts.

[16] Compare Sec. III, 1.
[17] B. S. Sci. Papers, No. 303, pp. 184–185; 1917.
[18] Cf. J. Op. Soc. Am., 4, p. 471, Fig. 8; 1920.

Digitized by Google

II. EXPERIMENTAL METHODS

1. APPARATUS

The essential parts of the apparatus used in this investigation to control spectral distribution are shown in Fig. 4. The actual apparatus used was part of the Arons chromoscope[19] with an auxiliary quartz plate and nicol, as shown in Fig. 5, the auxiliary parts being placed between nicol P'' and the source. The auxiliary nicol and the nicol P'', with the auxiliary 0.500 mm plate between them, play, respectively, the parts of nicols 1 and 2 in Fig. 4. Likewise, nicols P and A with a 0.500 mm quartz plate between them play the parts of nicols 2 and 3. The angle ϕ_1 (nicol P'' and auxiliary nicol)[20] is set permanently at 170°. The angle ϕ_2 (nicols P and A) is variable.

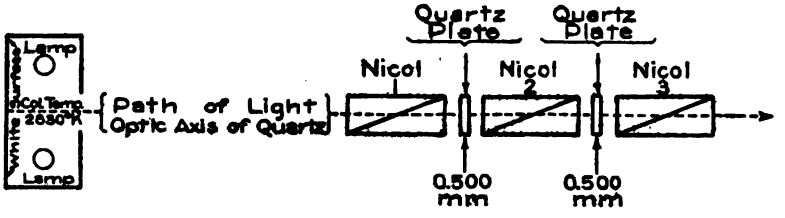

FIG. 4.—*Essential parts of apparatus used to adjust the spectral distribution of the stimulus*

Nicols 1 and 2 are fixed. The spectral distribution of energy emerging from nicol 3 in the direction of the dotted arrow may be adjusted by rotation of nicol 3 relative to nicol 2 (angle, ϕ_2).

In the use of the instrument for our present purpose, the Lummer-Brodhun cube (L,B) and the quartz plates Q_I to Q_{IV} (Fig. 5) are removed.

2. METHOD OF ADJUSTING THE STIMULUS[21]

(A) THEORY OF METHOD

The essence of the method of producing and adjusting the spectral distribution of the stimulus is this:

The spectral distribution of a source is modified by rotatory dispersion by allowing the energy to pass through the system of nicols and quartz plates shown in Fig. 4, which system is equivalent to a blue filter of adjustable spectral transmission, the adjustment being made by rotation of the nicol 3, as will be further explained below.

Illumination is obtained from two 300-watt, gas-filled tungsten lamps in a magnesia-lined box disposed as shown in Fig. 4. These lamps are operated at a constant current previously determined

[19] Ann. d. Phys. (4), **39**, pp. 545–568; 1912.
[20] Compare definition of ϕ_1 in Section II, 2, A.
[21] Cf. Priest, Radiant energy at high temperatures, J. Op. Soc. Am.; March, 1921.

Digitized by Google

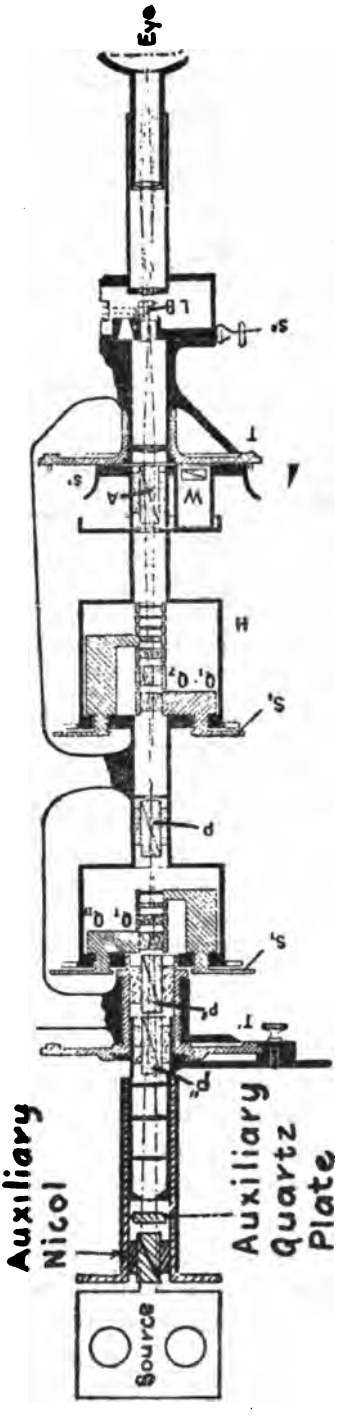

FIG. 5.—*Part of Arons chromoscope*
(From Ann. der Phy. (4), **89**, p. 541) with auxiliary nicol and quartz plate.

L, B= Lummer-Brodhun cube, *removed in present use of the instrument.*
A= Nicol prism.
Q_1—Q_2= Quartz plates, *all removed except one 0.300 mm. thick.*
P= Nicol prism in fixed position.
Q_1—Q_2= Quartz plates, *all removed in present use of instrument.*
P′ and P″= Nicol prisms.

Digitized by Google

such that the light *finally emerging from the ocular of the chromoscope with all quartz plates removed* is color matched with the light from the standard lamp, B. S. 1717 at 118 volts, known to have the spectral distribution of a complete radiator at 2830° K (Fig. 6).[22] This initial calibration by color match was accomplished by means of the Lummer-Brodhun cube in the chromoscope (LB, Fig. 5), the light from the standard lamp being reflected into the outer part of the Lummer-Brodhun field by means of a suitably positioned magnesium carbonate block.

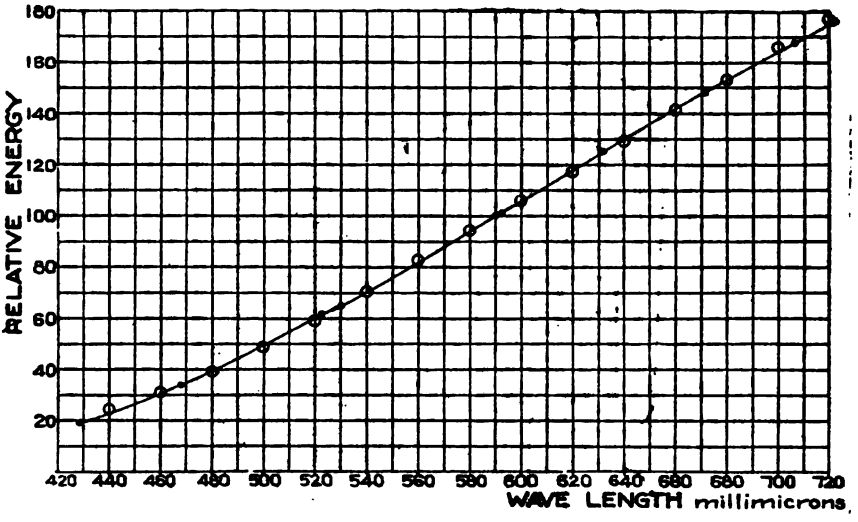

FIG. 6.—*Comparison of spectral distributions of energy for the Planckian radiator (hypothetical) and the standard lamp used in this investigation*

Solid curve: Planckian radiator at 2830° K. (The solid black dots show the points actually computed.) Open circles: B. S. lamp 1717 at 118.0 volts as determined radiometrically by W. W. Coblentz, Bureau of Standards.

Nicol P′ is set permanently relative to nicol P, so as to give a suitable brightness range. Rotation of nicol P″, together with the auxiliary quartz plate and auxiliary nicol as a unit, serves to keep the brilliance approximately constant for all values of ϕ_2 in the second method described below.[23]

The theory of the adjustment of spectral distribution is as follows:

$\phi_1 \equiv$ angle through which nicol 1 (Fig. 4) is rotated relative to nicol 2 in a direction contrary to the natural rotation of the quartz plate between 1 and 2 and measured from the extinction position with the quartz removed.

[22] From radiometric determinations by W. W. Coblentz, Bureau of Standards.
[23] Sec. II, 3, B.

Digitized by Google

$\phi_2 \equiv$ angle through which nicol 3 (Fig. 4) is rotated, relative to nicol 2 in the same direction as the natural rotation of the quartz plate between 2 and 3, and measured from the extinction position with the quartz removed.

These three nicols and two quartz plates constitute, in effect, a selective light filter, the spectral transmission of which may be continuously adjusted by changing ϕ_1 or ϕ_2. The relative transmission is given by:

$$\sin^2 (\phi_1 - 0.5\alpha_\lambda) \sin^2 (\phi_2 - 0.5\alpha_\lambda)$$

where $\alpha_\lambda \equiv$ rotation of the plane of polarization by 1.000 mm of quartz for light of wave length λ.

If the current in the lamps (Figs. 4 and 5) is adjusted so that the energy transmitted by the nicols (Fig. 5) with the quartz removed has the visible spectral distribution of a complete radiator at 2830° K, and the plates are then inserted and ϕ_1 set at 170°, the resultant spectral energy distributions are determined by ϕ_2. Distributions corresponding to certain values of ϕ_2 are shown in Fig. 7, in which are also shown the spectral energy distributions of a hypothetical complete radiator at various temperatures as computed by the Planckian formula. It will be noticed at once that the spectral energy distributions obtained by this artifice conform closely to those given by the Planckian formula. That is, radiant energy having the spectral distribution (visible spectrum) of a complete radiator at any desired temperature between about 4000 and 7000° K can be obtained by giving ϕ_2 a suitable value. In Fig. 8 such values of ϕ_2 are plotted as a function of temperature. Given any value of ϕ_2, we can obtain the corresponding temperature by reference to this graph.

(B) EXPERIMENTAL VERIFICATION OF METHOD

For the particular apparatus used the approximate validity of the relation shown in Fig. 8 has been checked experimentally by using the apparatus to determine color temperatures which could be checked fairly well by independent methods. More specifically stated, the checking procedure has been this: By means of the Lummer-Brodhun cube, L B (Fig. 5), light of known color temperature has been brought into juxtaposition in a photometric field with the light yielded by this apparatus (Figs. 4 and 5). ϕ_2 has then been set to give a match of color quality, a brilliance match being simultaneously made by other adjustments.

Digitized by Google

FIG. 7.—*Illustrating the production of radiant energy having the spectral distribution of a complete radiator by means of the apparatus in Figs. 4 and 5*

The curves represent the Planckian formula. The numbers attached to these curves indicate temperatures in degrees K. The various circles represent distributions obtained by the arrangement shown in Fig. 4. Each different style and size of circle refers to a particular value of ϕ_4, and the numbers attached to the circles indicate values of ϕ_4 in circular degrees. ϕ_1 constant = 170°. In all cases, energy = 100.0 at wave length 590 (arbitrary convention).

Digitized by Google

The color temperature corresponding to this value of ϕ_2 has then been read from the graph in Fig. 8 and compared with the independently known color temperature. Three separate cases of such checking are to be considered, as follows:

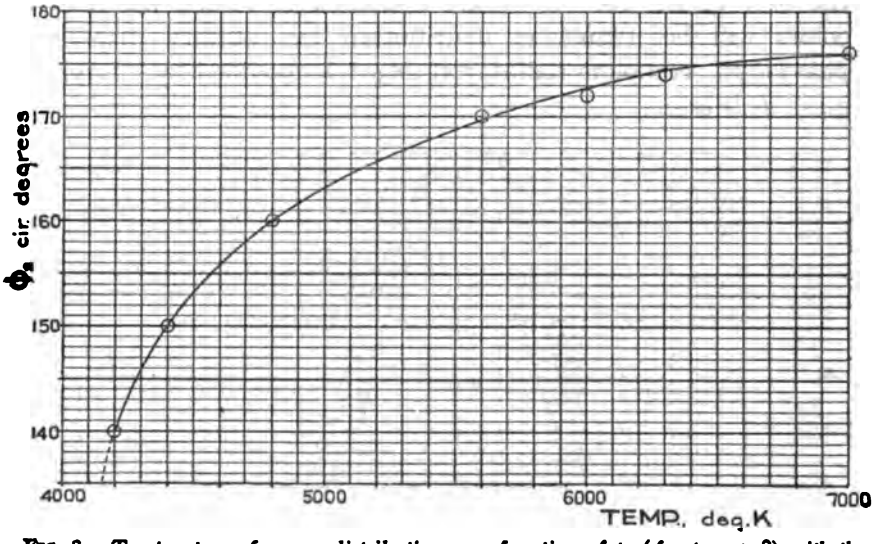

FIG. 8.—*Temperature of energy distribution as a function of ϕ_2 (for ϕ_1=170°) with the arrangement shown in Fig. 4*

Plotted from inspection of Fig. 7.

(*a*) DIFFUSE LIGHT FROM UNIFORM OVERCAST SKY.—

Date	Hour	Color temperature, degrees Kelvin
1920		By apparatus in Figs. 4 and 5
December 1....	9:10 a. m.....	6360
December 14...	8:45 a. m.....	6240
February.....	9:00 a. m. to 5:00 p. m....	Under approximately similar conditions by leucoscope [a] 6300 to 6500

[a] Priest, Leucoscope, J. Op. Soc. Am., 4, p. 483: November, 1920.

(*b*) LIGHT HAVING THE SPECTRAL DISTRIBUTION OF A COMPLETE RADIATOR AT 2830° K (B. S. LAMP 1717, AT 118.0 VOLTS) MODIFIED BY TRANSMISSION THROUGH "DAYLITE" GLASS, B. S. 15 648 A.—The resultant spectral distribution of light ("luminosity curve") is shown by the dotted curve in Fig. 9. The solid curves in the same figure show the distributions of light for a Planckian radiator at several temperatures. It will be noticed that the distribution of light transmitted by the glass departs from the Planckian form in the following respects:

The curve is narrower; that is, relative to a complete radiator, the light has an excess of greenish yellow.

Digitized by Google

There is a hump in the blue-green.

From the above it follows naturally that there is no value of ϕ_2 for which the light from the apparatus (Fig. 5) will evoke a color *perfectly* matched with the color evoked by the light through the blue glass. At the closest approach to match the relative colors will be: Planckian distribution by rotatory dispersion, *pale purple;* complete radiator at 2830° K modified by "Daylite" glass, *pale green.*

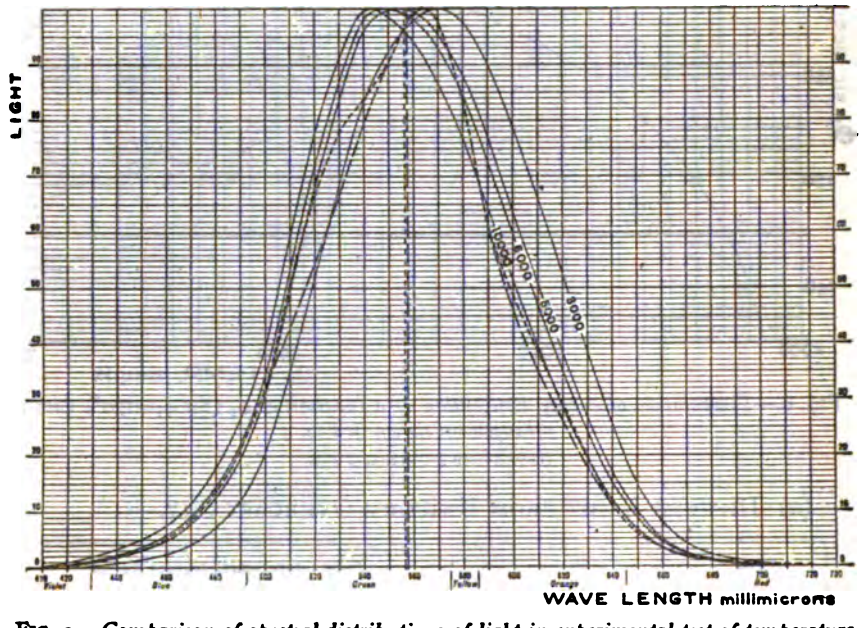

FIG. 9.—*Comparison of spectral distributions of light in experimental test of temperature scale*

Solid curves: Planckian radiator at temperatures indicated in degrees K by numbers attached to curves.
Dotted curve: Planckian radiator at 2830° K modified by "Daylite" glass, B. S. 15648A.
Dashed curve: Smoothed from dotted curve by removing humps.

This conclusion has been verified by direct observation in attempting to determine the color temperature by observation of the angle ϕ_2.

However, we have determined the value of ϕ_2 required to give the closest approach to color match; that is, the green-purple contrast mentioned just above. We then reason as follows:

We would obtain this same value of ϕ_2 for a distribution represented by the dashed curve in Fig. 9, while the approximation to color match in this case would be closer.

We would obtain this same value of ϕ_2 for a Planckian distribution having the same wave length of center of gravity as the dashed curve, and the color match would be perfect.

Digitized by Google

In line with this argument the following data are presented:

Color temperature from observed ϕ_2	6500° K
λ_0 Planckian radiator at this temperature (from Fig. 3)	557.4mμ
λ_0 dotted curve, Fig. 9	556.6mμ
λ_0 dashed curve, Fig. 9	557.6mμ
Temperature corresponding to this λ_0 (from Fig. 3)	6400° K

(*c*) LIGHT HAVING THE SPECTRAL DISTRIBUTION OF A COMPLETE RADIATOR AT 2360° K (NELA RESEARCH LABORATORY VACUUM TUNGSTEN STANDARD LAMP) MODIFIED BY TRANSMISSION THROUGH "DAYLITE" GLASS, B. S. 15 648 A.—The resultant spectral distribution of light is shown by the dotted curve in Fig. 10.

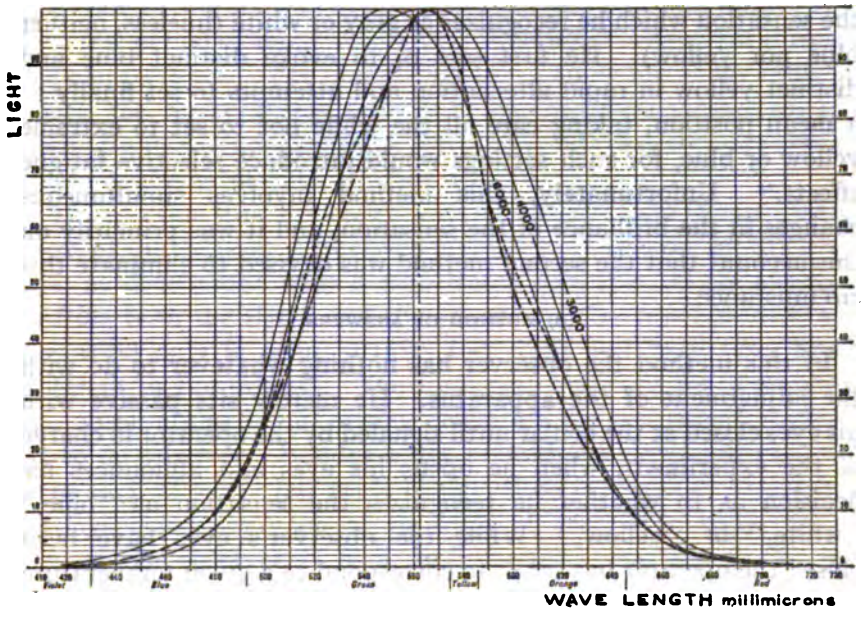

FIG. 10.—*Comparison of spectral distributions of light in experimental test of temperature scale*

Solid curves: Planckian radiator at temperatures indicated in degrees K by numbers attached to curves.
Dotted curve: Planckian radiator at 2360° K modified by "Daylite" glass, B. S. 15648A.
Dashed curve: Smoothed from dotted curve by removing humps.

The same remarks and line of argument presented under (*b*) just above apply here *with the exception that in this case the green-purple contrast is less; that is, a closer approximation to color match can be obtained by adjustment of* ϕ_2.

Similarly, the following data analogous to those given under (*b*) are presented in this case:

Color temperature from observed ϕ_2	4650° K
λ_0 Planckian radiator at this temperature (from Fig. 3)	562.25mμ
λ_0 dotted curve, Fig. 10	562.35mμ
λ_0 dashed curve, Fig. 10	562.2 mμ
Temperature corresponding to this λ_0 (from Fig. 3)	4675° K

Digitized by Google

While the data given under (*a*), (*b*), and (*c*) just above do not afford a rigorous check on the temperature scale, they do clearly indicate that no large errors exist. It seems safe to assume that temperatures near 5000° K determined from ϕ_2 by means of Fig. 8 will certainly not be in error by as much as 100° and will probably be correct to within 50° or perhaps 25°.

3. METHODS OF OBSERVATION

(A) METHOD OF ADJUSTMENT BY TRIAL

In this method the observer adjusts the angle ϕ_2 (nicol 3, Fig. 4; nicol A, Fig. 5) by trial until he finds the setting which gives the sensation which he recognizes as gray or white (hueless, neither blue nor yellow). He first sets ϕ_2 to evoke distinct blue and distinct yellow in rapid alternation and attempts to set finally at a mean position, taking care all the while not to set to extreme yellow or blue, for such settings would introduce selective fatigue effects.[24] Unfortunately, this method involves simultaneous changes in the brilliance of the sensation, and it was primarily on this account that the second method was devised to eliminate this circumstance.

(B) METHOD OF ANSWERS

In this method the observer has nothing whatever to do with the adjustment of the apparatus. He merely sits passive with his eyes closed at the ocular until signaled by the operator in charge of the experiment, when he opens his eyes and announces his decision as to whether he recognizes the sensation as "blue," "white," or "yellow." While the observer's eyes have been closed the operator has set ϕ_2 to correspond to a given temperature of the hypothetical source (calibration curve, Fig. 8) and has also rotated the nicol P'' (Fig. 5), together with the auxiliary plate and nicol, to a position previously determined to make the brilliance for this value of ϕ_2 approximately the same as given by other values of ϕ_2 with other corresponding rotations of P''. That is, for each value of ϕ_2, P'' is rotated so as to produce approximately the same brilliance for observations at all temperatures. Having made these settings and noted that the current in the lamps has its correct standard value, the operator says: "Look" or "Ready, look." The observer opens his eyes and answers, "Blue," "White," or "Yellow," depending upon the sensation evoked, and immediately closes his eyes again. The operator

[24] Compare Sec. III, 2.

Digitized by Google

records the answer in a suitable form. The same procedure is then repeated.

As standard temperatures for tests by this method the following have been chosen after preliminary trials showed them to cover the proper range: [25]

For three observers—H. J. M., M. K. F., and I. G. P. { 6200° K, 5700, 5300, 5000, 4700, 4450, 4200 } For one observer—C. A. S.

At one sitting 20 trials are made at each temperature, interrupted by a rest period of about 10 minutes, in the dark, when half through the complete set. The observer has no knowledge of the order in which the temperatures are set; [26] the observers themselves say there are no circumstances to prejudice their decisions (except in the first sitting for I. G. P., Dec. 13).

The reaction time between the signal "Look" and the announcement of the decision varies from about 1 to 4 seconds, on the average, as determined with a stop watch operated by an assistant hearing both the signal and the answer. (This reaction time was measured only in some sittings but could not have been much different in the others.) The total time required for completing the observations in one sitting, including the rest period, is about 45 to 60 minutes. Besides a few preliminary trials not reported here each observer has made observations throughout 5 complete sittings, consisting each of 20 trials at each of 6 temperatures (except one observer, C. A. S., in first sitting; see record, Fig. 12).

III. EXPERIMENTAL RESULTS

1. EFFECT OF PREVIOUS SELECTIVE FATIGUE

Preliminary trials by the first method showed that the results were affected to a noticeable degree by the previous stimulus acting on the observer's eye. For example, the author when recording his own observations in a lighted room and, consequently, looking at the record sheet between observations, found his results

[25] In future work it will be desirable to choose, in addition to these, several more temperatures at smaller intervals on each side of the transition temperature.

[26] The order of setting the temperatures appears to influence the apparent precision with which the stimulus of gray is determined, but not the final value found. If the order of setting is from extreme to median temperatures the observer (I. G. P.) answers white for a greater range of temperature than if the reverse order is followed. In the case of observers C. A. S., H. J. M., and M. K. F., the usual order has been from median to extreme temperatures. In the case of I. G. P. several orders have been followed. This question of the order of setting deserves further study.

Digitized by Google

to vary with the illumination on the sheet, as shown in Table 1. The column headed "Temperature" gives the temperature for the Planckian stimulus evoking the gray sensation under the several conditions specified.

The effect of severely fatiguing the eye selectively with the long wave lengths (yellow, orange, and red) was found as follows: At the end of a long series of observations in the dark the observer (I. G. P.) looked through an orange glass at a bright sky for several minutes and then immediately began observations again. The following temperatures for the stimulus for gray were found:

		°K
Mean of 49 observations within 30 minutes just before the fatigue		5580
Extremes of above observations		6350 and 4750
Observations immediately before fatigue		5900
Observations immediately after fatigue	less than	4000
Observations 5 minutes after fatigue	about	5400
Observations 8 minutes after fatigue	about	6000
Observations 10 minutes after fatigue	about	5800

It will be noticed that while the immediate effect of this selective fatigue was pronounced the recovery was rapid and complete within 10 minutes. Considering the extreme nature of the fatiguing stimulus in this case and the rapidity of recovery from it, we have concluded that under ordinary circumstances a 10 to 15 minute rest in the dark before beginning observations is sufficient to bring the eye to what may be considered a standard non-fatigued state. This preliminary period of rest has accordingly been observed in all of the experiments under the second method.[37]

2. RESULTS BY THE METHOD OF ADJUSTMENT BY TRIAL.

This method has been followed only by the author himself. The only other observer (H. J. M.) who attempted it did not obtain reasonable or consistent results and complained that the unavoidable changes of brilliance prejudiced and vitiated his readings to such an extent that it was deemed wise to abandon the attempt.

The author made 209 such settings distributed about equally over 4 days. The results are summarized graphically in Fig. 11 in the following way:

A count has been made of the number of individual observations falling within each of the following temperature intervals: 4675–4925, 4925–5175, 5175–5425, 5425–5675, 5675–5925, 5925–6175, 6175–6425, 6425–6675° K. These numbers (frequency of choice)

[37] Sec. III, 3.

Digitized by Google

are plotted as ordinates against the wave length of the center of gravity of the spectral distribution of light [28] for the mean temperature of the interval. Temperatures corresponding to λ_c are given in the upper margin of the figure. Inspection of Fig. 11 shows that the mode (maximum ordinate) of this distribution of choices falls at about 5400° K. The arithmetical mean of the 209 temperatures is 5480° K.

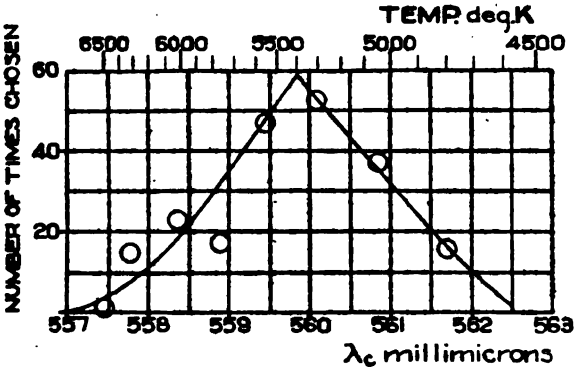

FIG. 11.—*Distribution of 209 choices of black body stimuli found to evoke the gray sensation by method of adjustment by trial*

Obs. I. G. P. Dates: Dec. 1–4, inc., 1920.

TABLE 1.—Showing Effect of Previous Stimulus on Determinations of the Stimulus of Gray

Date	Hour	Illumination on record sheet	Temperature, degrees Kelvin (means of 10 observations)	Comments
1920				
Nov. 30.....	10.27 a. m.	Daylight.....	5810	Note that these determinations were made about midday and that consequently the room illumination was "bluer" than in the next determination below
	10.33 a. m.	.....do.....	5750	
	11.12 a. m.	.....do.....	5880	
	4.10 p. m.	.....do.....	5220	Note late hour in afternoon, giving room illumination relatively weak in blue light
	5.10 p. m.	Gas-filled tungsten	4590	Note effect of fatigue by comparatively yellow light
Dec. 1.....	9.00 a. m.	Daylight.....	5870	
	10.20 a. m.	.....do.....	5410	
	11.25 a. m.	Gas-filled tungsten	4430	Note effect of fatigue by comparatively yellow light. Note particularly hours
	11.35 a. m.	Daylight.....	5460	
	11.45 a. m.	Record by assistant. Observer's eyes in dark	5050	Note that the observer's eyes were protected from room illumination in these two determinations
	11.55 a. m.		5810	

3. RESULTS BY THE METHOD OF ANSWERS

Aside from a few unsystematic preliminary trials, the complete transcript of the record of all determinations so far made by the

[28] Compare Figs. 1 and 3.

Digitized by Google

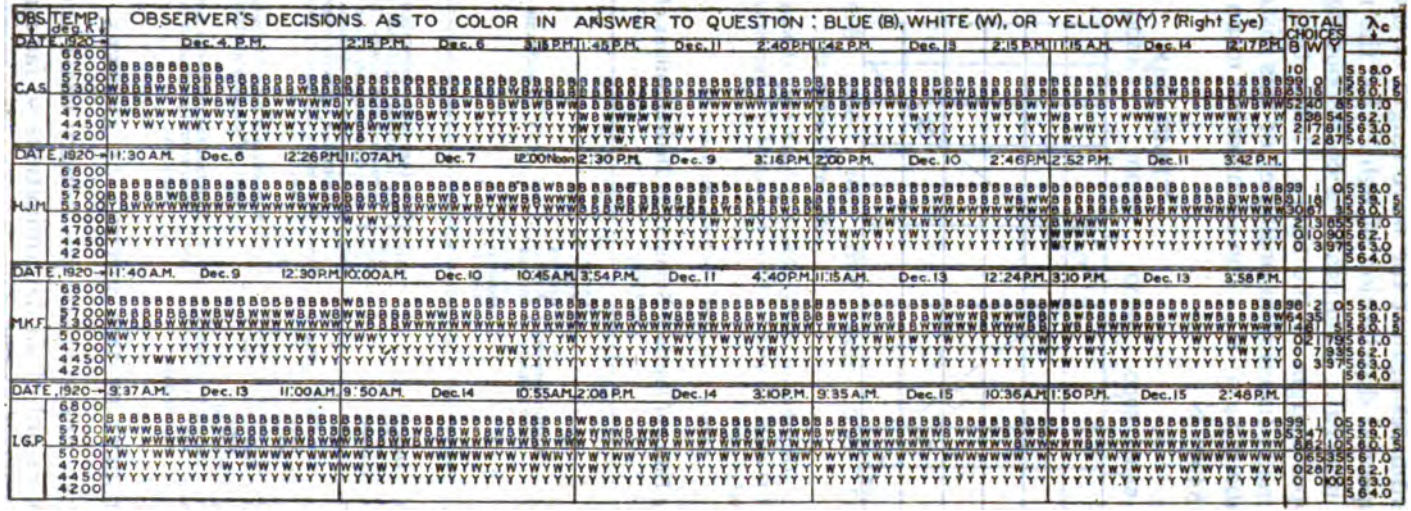

FIG. 12.—*Complete transcript of original data by the method of answers*

The letters *B*, *W*, *Y* indicate, respectively, blue, white, yellow, the observers' answers in response to the stimulus indicated by temperature of the hypothetical Planckian radiator. (Col. 2.) These same data are shown graphically in Figs. 13*a* and 13*b*.

Digitized by Google

method of answers is shown in Fig. 12, which, in connection with the description of the method given above, should be self-explanatory

While simple inspection of the tabular presentation of the data in Fig. 12 will serve to indicate roughly the temperature a Planckian radiator would have in order that the radiant energy would evoke the gray sensation, a graphic presentation is much more instructive and indicates the temperature much more definitely. Such a graphic presentation is shown in Figs. 13*a* and 13*b*. The scale of equal parts on the abscissa (bottom of each figure) is in terms of λ_c, while corresponding temperatures of the source are shown on a scale at the top of each figure.[29] The ordinates show the *probability* of the observer's recognizing the stimulus as "blue," "white," or "yellow," as the case may be.[30]. It is evident that the stimulus of gray is located (in terms of λ_c or temperature) by the intersection of the blue and yellow curves.

Within the experimental uncertainty, the λ_c coordinate of this intersection appears to be the same as the λ_c coordinate of the maximum of the white curve, as would be theoretically expected, while it can be determined more definitely. The probability of recognizing this stimulus as blue is equal to the probability of recognizing it as yellow; while the probability of recognizing it as either is rather low, since the probability of recognizing it as gray is a maximum.

Values of temperature and of λ_c corresponding to the intersection of the blue and yellow curves are shown in Table 2 under the caption "Average stimulus for gray." The stimuli, which, according to these curves (Figs. 13*a* and 13*b*), will always be recognized as blue or yellow are also specified in Table 2. The spectral distributions of energy in the several limiting cases found in this investigation are shown in Fig. 14, which is self-explanatory.

[29] Compare Fig. 3.

[30] Explicitly, these ordinates show the value of the ratio:

$$\frac{\text{Number of times the given color was named}}{\text{Total number of decisions at the given temperature}}$$

Digitized by Google

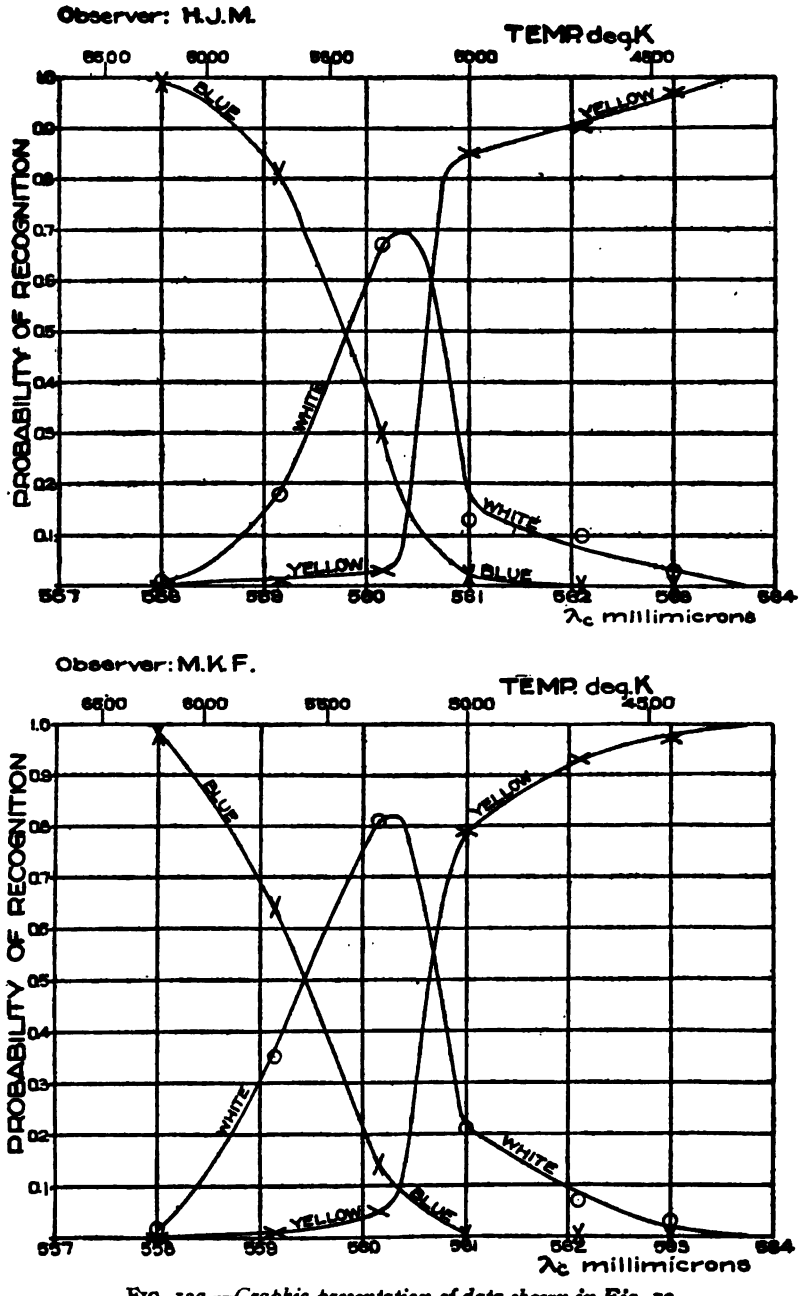

FIG. 13a.—*Graphic presentation of data shown in Fig. 12*

Digitized by Google

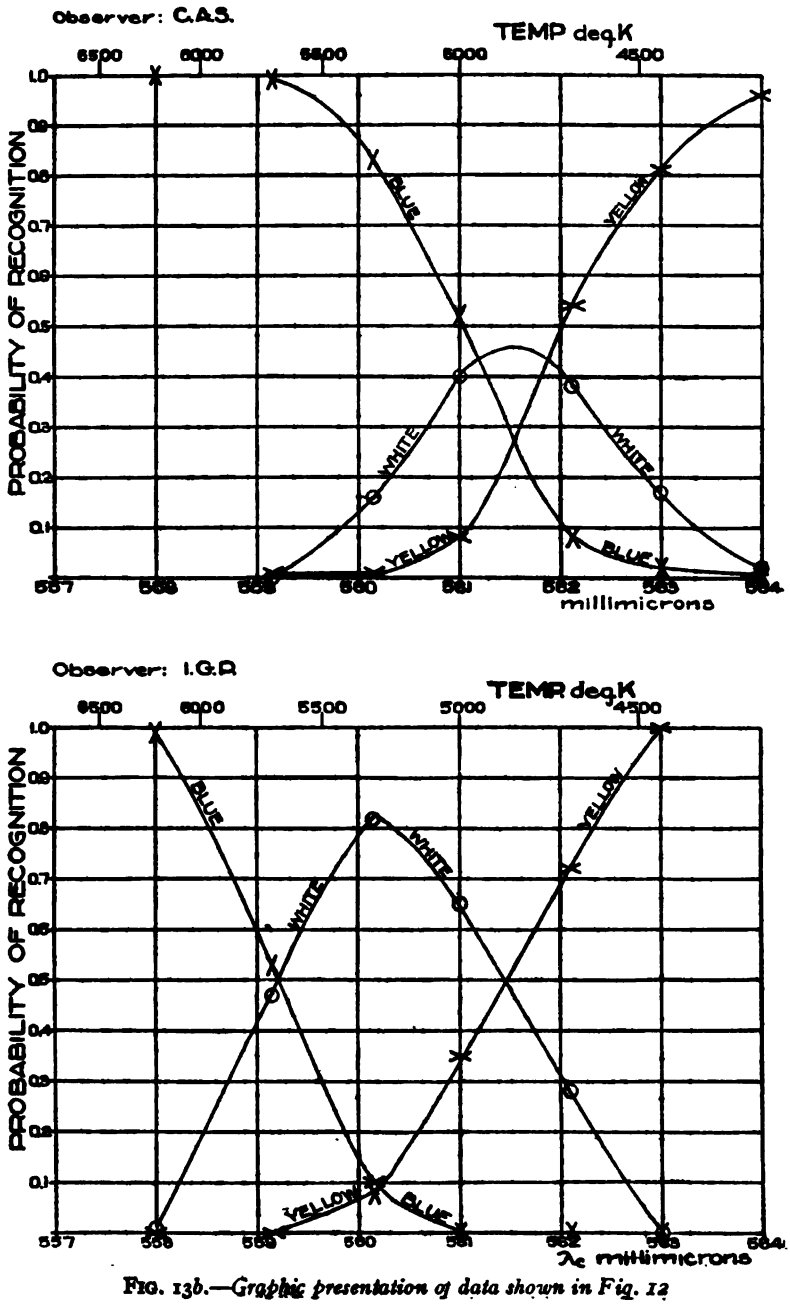

FIG. 13b.—*Graphic presentation of data shown in Fig. 12*

Digitized by Google

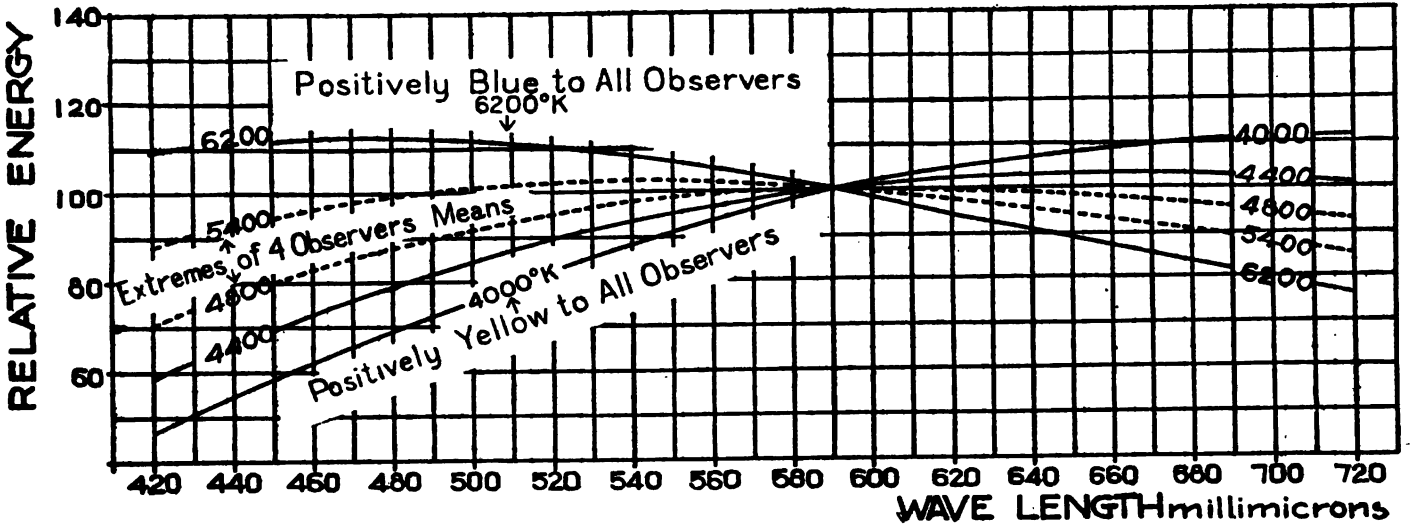

FIG. 14.—*Spectral distributions of radiant energy evoking the sensations gray, yellow, and blue*

Dotted curves, 5400 and 4800° K, delineate the extreme range of four observers' final averages in determining the stimulus for gray. The solid curve, 6200° K, shows the spectral distribution always recognized as blue by all four observers. The solid curve, 4000° K, shows the spectral distribution always recognized as yellow by all four observers. The solid curve, 4400° K, shows the spectral distribution always recognized as yellow by the three observers of ages less than 35 years.

Digitized by Google

TABLE 2.—Results of Determination of Stimulus of Gray by Method of Answers

Observer	Age	Sex	Average stimulus for gray		Stimulus ALWAYS evoking yellow		Stimulus ALWAYS evoking blue	
			Temperature	λ_c	Temperature	λ_c	Temperature	λ_c
			°K	mμ	°K	mμ	°K	mμ
C. A. S.[a]	50	Male	4850	561.5	4000	565	5750	559
H. J. M.	28	do	5200	560.4	4200	564	6200	558
M. K. F.	34	Female	5200	560.4	4200	564	6200	558
I. G. P.	35	Male	5300	560.2	4450	563	6200	558
Mean of all			5140	560.6	4200	564	6090	558.2
Mean of last three			5230	560.33	4280	563.7	6200	558

[a] The cornea of this observer's eye is injured, and this fact may invalidate his data to some extent.

IV. SUMMARY AND CONCLUSIONS

1. PRINCIPAL CONCLUSIONS

On account of the limited amount of data obtained no generalization as to the average stimulus of gray can be drawn from this investigation. However, the principal conclusions may be summarized as follows:

(1) A practical method suitable for determining the Planckian stimulus of gray has been developed and thoroughly tested experimentally. The yellow-blue transition has been found to be a much more definite phenomenon than was anticipated, and definite, unambiguous results can be obtained in determining the hypothetical source temperature marking this transition.[81] The method of observation settled upon (method of answers) is easy of application and entirely satisfactory.

(2) This yellow-blue transition temperature has been determined for four individuals, as follows:

Observer	Age	Temperature
		°K
C. A. S.	50	4850
H. J. M.	28	5200
M. K. F.	34	5200
I. G. P.	35	5300 (second method)
		5400 (first method)

(3) The most probable average value for the yellow-blue transition temperature, based on these four individuals, is about 5200° K. That is to say, *based on these limited data,* the best representative temperature for a Planckian radiator, in order that

[81] Compare Fig. 13 and Table 2.

Digitized by Google

its radiant energy shall evoke the gray sensation in the average individual, is 5200° K.

(4) There is an *indication* that the yellow-blue transition temperature depends upon the observer's age, but no conclusion on this point can be positively affirmed.

(5) With regard to change in the wave length of the center of gravity of the spectral distribution of light, the transition from yellow to blue is remarkably abrupt and well defined.[32] The wave length of the center of gravity for gray is determined for each observer with an uncertainty less than 1 millimicron. A change of about 6 millimicrons in the wave length of center of gravity changes the sensation from *undoubted* yellow to *undoubted* blue; that is, this change covers completely the observer's range of doubt as to whether the sensation should be called blue or yellow and within which it may be called white. The range of the four observers' determinations of the wave length of the center of gravity for white is about 1.3 millimicrons. The range for three of the observers of nearly the same age is only 0.2 millimicron.[33]

(6) The effect of previous selective fatigue on the determination of the yellow-blue transition temperature is very noticeable but disappears in a few minutes.[34]

2. INCIDENTAL CONCLUSIONS

A number of standards for "average daylight," "average sunlight," and "white light" (objective) have been proposed more or less definitely heretofore. Some of these are compared with our present results in the following table:

Authority	Designation of standard	Temperature	λ_c
		°K	mμ
This paper	Stimulus of gray	5200	560.4
Priest's representation of Abbot's data (Phys. Rev., 11, p. 502; 1918. Fig. 1, open circles)	Average noon sunlight at Washington	5300 (*Not strictly Planckian distribution*)	560.0
H. E. Ives's (Trans. I. E. S., pp. 198, 202; April, 1910)	"Average daylight." "White"	5000	561.0
H. P. Gage ("Daylite" glass, Sibley Jour. of Eng., 30, No. 8; May, 1916)	"Average daylight." "Sun outside the earth's atmosphere"	6500-7000 (*Not strictly Planckian distribution*)	557.5 to 556.7

[32] Compare Fig. 13 and Table 2.

[33] It should be noted that the wave length of center of gravity (λ_c) considered here is, in every case, that computed from our tentative standard of average visibility (dotted curve, Fig. 2) and is not referred to the observer's own individual visibility. In further work it will be desirable to compute also λ_c from each observer's individual visibility and attempt to correlate each observer's stimulus for gray with his visibility.

[34] Compare Sec. III, 1.

Digitized by Google

Accepting our stimulus of gray given above as a tentative standard, we may conclude that under our standard conditions [35] various stimuli will evoke sensations as follows:

Stimulus	Sensation
Abbot-Priest	
Average noon sun	Very nearly gray
Winter sun or sun in morning or afternoon	Pale greenish yellow. By simultaneous contrast standard gray appears pale purple. (Confirmed by experiment)
Noon summer sun	Pale blue
Ives's "Average daylight," 5000° K.	Very pale yellow or perhaps gray
Gage's "Average daylight," 7000° K.	Blue. (Confirmed by experiment with "Daylite" glass, B. S. 15 648 A)

The spectral distributions of these stimuli and of some common artificial sources are shown in Fig. 15.

The average noon sunlight derived from Abbot's data is accordingly found to be a close approximation to the stimulus for gray. However, it is to be noted that this average sunlight does not conform strictly to a Planckian ("black-body") spectral distribution, and on this account, as well as on account of the small difference in λ_c, the color match may not be perfect.

The spectral distribution of sunlight at the earth's surface in the winter or in the morning or evening departs notably from a Planckian distribution in such a way that the colors by simultaneous contrast are:

Sun, pale greenish yellow.

Complete radiator, pale purple.

While, relative to the tentative gray found in this investigation, Ives's "average daylight" would be slightly yellow, it is quite possible that a more extensive statistical investigation would show it to be a good representative gray.

Gage's "average daylight" (6500–7000° K) is definitely and unambiguously blue. This conclusion has been confirmed by direct experiment by the method of answers applied to this stimulus.[36] It was called blue 10 times out of 10, the observer (H. J. M.) being under the impression that the trials were being made with the variable rotatory dispersion stimulus, and that the stimulus was being changed.

[35] Compare I, 2, above

[36] Source at 2850° K modified by "Daylite" glass (B. S. 15 648 A.)

Digitized by Google

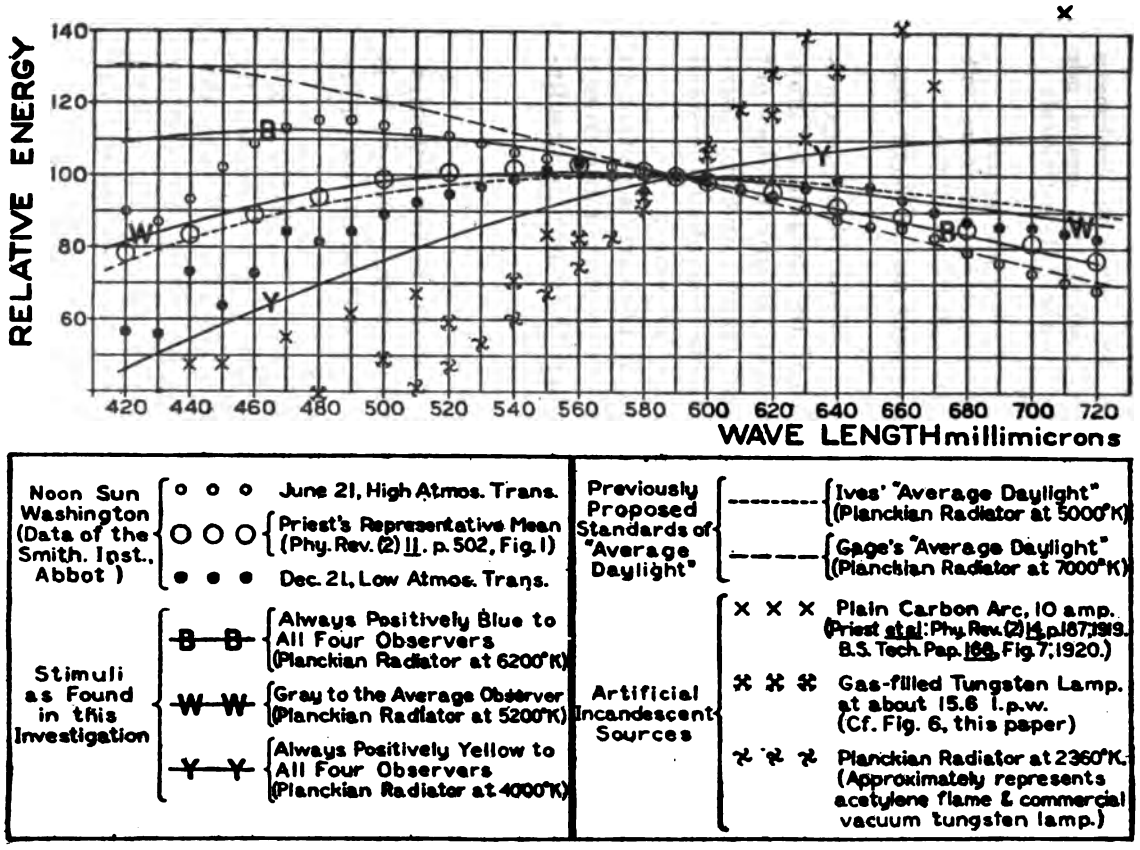

FIG. 15.—*Comparison of results with previous data on sunlight and "average daylight"*

Digitized by Google

3. SUGGESTIONS AS TO FUTURE WORK

It would seem desirable that an extensive statistical determination of the Planckian stimulus of gray be made by means of the method of answers described in this paper.

The following suggestions relative to details in the method of answers should be considered in planning future work:

(1) Standard temperatures at which decisions are made should be taken at smaller intervals in the neighborhood of the transition temperature.

(2) It might be desirable to substitute the operation of a shutter controlled by the operator for the opening and closing of the observer's eyes.

(3) The effect of changing the following factors should be studied:

(*a*) The intensity of the stimulus;

(*b*) The size of the field;

(*c*) The order of taking the different temperatures;

(*d*) The exposure time, to be investigated by means of a timed shutter controlled by the operator, presenting the stimulus for a definite period, *at the end of which* the observer is to announce his decision;

(*e*) The effect of fatigue. In particular, it is proposed to compare the results obtained immediately after a night's sleep and *before the eye has been subjected to any stimulus* with those obtained at the end of a working day, and also with those obtained after prolonged exposure to various specified stimuli of moderate intensity.

Some extension of the present work will probably be undertaken at the Bureau of Standards during the coming year, and it is also to be hoped that other investigators will undertake such determinations independently.

WASHINGTON, February 10, 1921.

Digitized by Google

APPENDIX

THE DESIRABILITY OF AN EXTENSIVE STATISTICAL DETERMINATION AND CORRELATION OF THE CHARACTERISTICS OF VISION

That part of visual optics dealing with the relations of stimulus and sensation (the visual psychophysical relations) long ago reached the stage where it would have been profitable to classify and set in order the problems awaiting solution to the end that they might be attacked in an orderly and effective manner. We are indebted to Nutting and to Richtmyer for several interesting and stimulating papers which point the way in this direction, but aside from these the author is not aware of any systematic attempt to survey this field. The outline below is the result of several years' thinking on this subject incident to the problems confronting one who has to deal daily with colorimetry and color specifications from a practical point of view. It represents a digest of purely scientific data urgently needed for practical (and often utilitarian) purposes. Careful consideration reveals the fact that these are the same data needed in order to advance "pure" science in the matter of elucidating the phenomena of color perception. The purpose of this appendix is to direct attention to this comparatively neglected field of research in the hope that it may act as a stimulus to more intensive cultivation. Occasion is also taken to point out, in this connection, the general utility of the "method of answers" used in the preceding paper.

This outline is to be regarded merely as the tentative result of an attempt to set in order, in a preliminary way, the subject matter dealt with. It will, of course, require revision and amplification and is of no permanent didactic value. It may serve as a temporary basis for discussion.

I

The cardinal features of the visual response to stimulation by radiant energy which are susceptible to quantitative study may be classified as follows (at least in part):

1. *To Be Determined as Functions of Frequency (or Wave Length) and Intensity of Stimulus and Size of Field Viewed.*
   - (A) The visibility of radiant energy. [1] [37]
   - (B) Contrast sensibility—the least change in intensity of stimulus perceptible as a change in brilliance. [2]
   - (C) Hue sensibility—the least change in frequency (or wave length) perceptible as a change in hue. [3] (Hue sensibility must also be determined as a function of purity. [4] (Cf. Watson, Proc. Roy. Soc., London, B, 84, pp. 118–121; 1911.)
   - (D) Saturation sensibility—the least change in purity perceptible as a change in saturation. [4]
   - (E) The three "primary sensations." [5]
   - (F) The time rates of adaptation—growth and decay of sensation with duration of stimulus—"persistence of vision." [6]
   - (G) The names for colors evoked by homogeneous stimuli. [7]

[37] A classified bibliography follows this Appendix. Reference to the bibliography is made in the Appendix by citing the bibliography group number in black-face type.

Digitized by Google

2. *To Be Determined as Functions of Intensity of Stimulus and the Size of the Field Viewed.*
   (A) The frequencies (or wave lengths) of the stimuli of complementary hues. [8]
   (B) The relative intensities of the homogeneous stimuli of complementary hues required to be mixed to evoke the gray sensation. [9]
   (C) The frequencies of the three homogeneous stimuli best suited to evoke the gray sensation by their joint action. [10]
   (D) The relative intensities of the three homogeneous stimuli required to be mixed to evoke the gray sensation.
   (E) The Planckian spectral distribution of energy required to evoke the gray sensation. [11]
3. *To Be Determined as Functions of Frequency (or Wave Length) of Stimulus and Size of Field Viewed.*
   (A) The least stimulus of perceptible brilliance (so-called "achromatic threshold").
   (B) The least stimulus competent to evoke a color of characteristic hue (so-called "chromatic threshold"). [12]

II

An extensive thoroughgoing statistical determination of these characteristics is desirable for the following reasons: (1) In order to provide reliable and comparable data for the study of vision as a pure science. (2) In order to provide a reliable scientific basis for practical colorimetry and color specification. (3) In order to provide a reliable scientific basis for the practical diagnosis of color-blindness.

III

In order to fully serve the purpose noted under II (3) above, it will further be necessary that the above data from each observer be correlated with his reactions to certain tests previously recommended and more or less generally used in the routine diagnosis of color-blindness. In the author's opinion, the more important of these tests are: [13]

1. Holmgren Yarns; [14]
2. Stilling Charts; [15]
3. Nagel Charts; [16]
4. Anomaloskop Reading (Rayleigh Equation); [17]
5. Leucoscope Reading; [18]
6. Edridge-Green "Colour Perception Spectrometer." [19] (The following improvements to the Edridge-Green instrument might perhaps be made for the sake of simple standard conditions: (1) Substitution of a grating for the dispersion prism in order to have a normal spectrum. (2) Use of standard artificial average noon sunlight for illumination by means of the arrangement proposed by Priest, Phys. Rev., (2), 11, p. 502, Fig. 1; 1918.
7. Practical Tests for the Recognition or Confusion of Signal Lights under Actual Working Conditions.

Certain "lantern" tests [20] have been proposed to simulate approximately such conditions. I would, however, propose in place of these a test, the essential features of which may be outlined as follows:

A test range would be provided, at opposite ends of which would be an *actual standard* railway signal lantern and the subject being tested. The length of this range should be the distance at which the engineer must recognize the signal in order to properly control his train.

The subject being stationed and his attention directed to the lantern, the signals shown *and the time of showing* would be automatically recorded on a chronograph record.

Digitized by Google

The subject would indicate his reaction by suitably prescribed motion of a lever (which might imitate the engineer's throttle lever), and the time of this reaction would be recorded on the same chronograph record.

Determinations should be made at several intensities, and a number of determinations should, of course, be made for each individual.

It will be observed that a notable merit of this proposed test lies in the fact that it records not only the subject's decision as to the signal, but also *the time it took him to make the decision*, which is a *vital* factor in this case.

IV

It is obvious that in order to yield the maximum information all of these characteristics should be determined for the same subjects.

It is also obvious that they should be correlated with reference to the following variables as to the subjects: (1) race, (2) sex, (3) age.

The magnitude of such an investigation, comprehending several hundred individual observers, is so discouraging that we are obliged to consider how it may be abridged with least loss. That is, of the whole outline above, what is most important to be done first?

The first question that arises is which of the above characteristics is it most important to determine on the same large group of individuals in order (1) to build up a consistent theory of color vision, (2) to elucidate the phenomena of "color-blindness" and its practical diagnosis, and (3) to provide the most needed data for practical colorimetry? These, in the author's opinion, are the ones listed under I, 1, A to E and I, 2, A to E, together with the practical tests for "color-blindness" under III.

In regard to the determination of the several characteristics as a function of the intensity of the stimulus, it appears that this should not be undertaken for the whole group, but rather in a very limited way as a subordinate auxiliary investigation. For the general investigation a standard intensity giving a comfortable brilliance high enough to avoid the Purkinje effect and low enough to avoid conspicuous or persistent afterimages should be chosen.

Likewise, the effect of field size should be studied in a similar limited subordinate investigation. The standard field size for the large group should be about 3 to 3.5°.

Similar remarks apply to other affecting conditions and circumstances, such as adaptation, previous fatigue, and simultaneous contrast, all of which may be studied in a limited way on small groups and suitable standard conditions chosen to apply to the large group.

In regard to determinations as a function of frequency (or wave length), such determinations should cover the whole group.

Visibility (I, 1, A above), the "three sensations" (I, 1, E above), and "hue sensibility" (I, 1, C above) should be determined at from 20 to 30 points in the spectrum.

"Contrast sensibility" or "photometric sensibility" (I, 1, B above) determinations might be limited to 3 (perhaps 5) homogeneous lights and "white" light (I, 2, E above).

The number of frequencies at which determinations of purity sensibility should be made will probably require a preliminary study.

Spectral colors should be named (I, 1, G above) at probably 20 different frequencies.

In order to avoid, for the present, complications (which may be studied in detail later), all subjects should be in an approximately normal state of general health and not addicted to drugs.

V

Even with the limitations just imposed, the magnitude of the investigation is such that no practicable plan for carrying it out can be suggested at once. Our present purpose is merely to outline the work definitely and stress its importance. The needs of "pure" science and the needs of "applied" science, particularly in colorimetry

Digitized by Google

and the diagnosis of "color-blindness," urgently require the results of such an investigation.

One point especially to be emphasized is the desirability of obtaining data on these several characteristics *from the same individuals* in order that—

(1) They may be correlated, merely as a matter of scientific interest.

(2) The results of the more or less empiric routine tests for color-blindness may be correlated with the more simple fundamental scientific data.

Of all these characteristics by far the most work of present value has heretofore been done on visibility, and comparatively reliable and satisfactory data on it are now extant. Nevertheless, there is at present some advocacy of a still more extensive statistical determination of this characteristic. In the author's opinion, it would be an exceedingly ill-advised and unfortunate expenditure of effort to undertake such an investigation *without simultaneously determining the other characteristics, outlined above, for the same group of subjects.* On the other hand, the getting together of a group of observers for such an investigation would afford the desired opportunity to carry out the other determinations, and the whole investigation would yield results of the utmost value.

VI [38]

In this section it is proposed to make a generalized suggestion relative to the experimental method of determining the psychophysical functions previously enumerated. The author is of the opinion that the "method of answers" described in the preceding paper, modified slightly to suit each particular case, would be advantageously applicable to most, and indeed probably all, of these determinations.

The advantages of this method over the more usual method of "adjustment by trial" are:

(1) PHYSIOLOGICAL.—A standard state of the visual apparatus may be more definitely prescribed and maintained, in that the effect of fatigue necessarily inherent in the method of adjustment by trial is eliminated.

(2) PSYCHOLOGICAL.—The decisions of the observer are bound to be less prejudiced by the incidental circumstances and conditions of the experiment.

(3) AS TO TREATMENT AND INTERPRETATION OF THE EXPERIMENTAL DATA.—The data obtained are conveniently amenable to treatment by statistical methods and can be graphically presented in a very cogent manner. (For example, Figs. 13*a* and 13*b* in the preceding paper.)

What is meant can best be made clear by an example, for which we take first the determination of the least stimulus competent to evoke the hueless sensation of brilliance. The observer's eye is brought to whatever state of adaptation may be desired and his attention fixed to a suitable fixation point, as is usual in such experiments. The operator controls the stimulus which is predetermined (but unknown to the observer) as to angular size, intensity, spectral composition, and time of duration. The observer answers "Yes" or "No," meaning thereby that the sensation is or is not evoked. The experiment proceeds in a manner quite similar to that described in the preceding paper. The probability of answering "Yes" and the probability of answering "No" are then plotted against the intensity of the stimulus (size, spectral composition, and duration being constant), or against any one of the variables, the others being constant. Equality of the probabilities of "Yes" and "No" evidently determines in a most rational manner the "just preceptible stimulus," while the slope of the curve indicates clearly the abruptness of the change from visible to nonvisible as the intensity of the stimulus changes.

As another example we may take the determination of least perceptible contrast (photometric sensibility). The operator sets the photometric field as to relative inten-

[38] In connection with the preparation of this section the author wishes to acknowledge the value of suggestions made by Dr. P. V. Wells, who, after reading the preceding paper, advised emphasizing the more general applicability of the "method of answers."

Digitized by Google

sity of stimuli in the two halves, the field being obscured by a shutter during this operation. He uncovers the field and asks the observer's decision. The observer answers: "right," "left," or "matched," meaning thereby, respectively, "the right half is brighter," "the left half is brighter," or "the field is matched." The "right," "left," and "matched" probability curves are then plotted against the ratio of intensities of stimuli in a manner quite analogous to the "blue," "yellow," and "white" curves in the preceding paper. Obviously, such curves will show contrast sensibility in a most definite and readily intelligible manner.

The same procedure will probably be found a valuable means of heterochromatic photometry, including the determination of the visibility of radiant energy.

Similar examples might be given for hue sensibility, saturation sensibility, etc., but it would involve a quite needless repetition of words; the reader can readily infer the slight modifications of method that would be made to suit each particular kind of determination.

It may or may not prove of interest later; but it is perhaps worth pointing out that by applying this same method we should be able to determine two other chromatic transition temperatures for the Planckian radiator, namely, red-yellow and blue-violet, analogous to the yellow-blue transition determined in the preceding paper.

BIBLIOGRAPHY OF REFERENCES CITED IN APPENDIX

The bibliographies given in the notes below are not complete, but are sufficiently comprehensive to give a good survey of the several subjects.

For general summarized information, see:

Nutting, The reactions of the retina to light, Am. J. of Physiol. Op., 1, pp. 142–170; 1920. Report of Standards Committee on Visual Sensitometry, J. Op. Soc. of Am., 4, pp. 55–79; 1920.

NOTES.

1. Koenig (and Ritter), Wied. Ann., 45, pp. 604–607; 1892. Beiträge zur psychologie und physiologie der sinnesorgane (Helmholtz festschrift), pp. 309–388; Leipzig, 1891. Koenig's Ges. Abh. Physiol. Op., pp. 144–213; Leipzig, 1903.
   Ives, Phil. Mag. (6), 24, pp. 853–863; 1912.
   Nutting, Trans. I. E. S., 9, pp. 633–642; 1914.
   Coblentz and Emerson, B. S. Sci. Papers, No. 303; 1917.
   Reeves, Com. No. 55, Eastman Kodak Res. Lab., Trans. I. E. S., 13, pp. 101–109; 1918.
   Hyde, Forsythe, and Cady, Astrophys. J., 48, pp. 65–88; 1918.
   Nutting, J. Op. Soc. Am., 4, pp. 55–60; 1920.
   Watson, Proc. Roy. Soc. London, A, 88, pp. 404–428; 1913.
   Watson, Proc. Roy. Soc. London, A, 89, pp. 36–38; 1913.
   Allen, Phil. Mag. (6), 21, pp. 604–607; 1911.
   Allen, Phil. Mag. (6), 38, pp. 81–89; 1919.
2. Koenig and Brodhun, Koenig's Ges. Abh. Physiol. Op., pp. 116–143; Leipzig, 1903.
   Nutting, B. S. Bulletin, 5, p. 285; 1908–1909.
   Blanchard, Phys. Rev. (2), 11, pp. 81–99; 1918.
   Nutting, J. Op. Soc. Am., 4, p. 66; 1920.
3. Mandelstamm, Archiv für Ophth., 13, Abt. 2, pp. 399–406; 1867.
   Dobrowolsky, Graefe's Archiv, 18, Abt. 1, pp. 66–74; 1872.
   Peirce, Am. J. of Sci., 126, pp. 299–302; 1883.
   Koenig and Diterici, Wied. Ann., 22, pp. 579–589; 1884.
   Graefe's Archiv, 30, Abt. 2, pp. 171–184; 1884.
   Koenig's Ges. Abh. Physiol. Op., pp. 23–33.
   Uhthoff, Graefe's Archiv, 34, Abt. 4, pp. 1–15; 1888.
   Exner, Wien. Sitzb., 111, 2A, pp. 875–877; 1902.
   Steindler, Wien. Sitzb., 115, 2A, pp. 39–62; 1906.
   Jones, J. Op. Soc. Am., 1, pp. 63–67; 1917.
   Nutting, J. Op. Soc. Am., 4, pp. 60–64; 1920.
   Rayleigh, Proc. Roy. Soc. London, A, 84, pp. 464–468; 1910.
4. Purity $\equiv \frac{l_\Lambda}{l_\Lambda + l_w}$,
   where
   $l_\Lambda \equiv$ homogeneous light,
   $l_w \equiv$ "white light,"
   as these stimuli are mixed in so-called monochromatic analysis.
   Compare: Nutting, J. Op. Soc. Am., 4, p. 60; 1920.
   Priest, J. Op. Soc. Am., 4, p. 400; 1920.
   Op. Soc. Am., Com. on Standards and Nomenclature, Subcom. on Colorimetry, Report 1919 (preliminary draft), copy in Bureau of Standards Library, pp. 38–40 and Table V.

Digitized by Google

5. Nutting, Outlines of applied optics, p. 130, Fig. 38; Philadelphia, 1912.
Exner, Wien. Sitzb., 111, 2A, pp. 857–875; 1902.
Koenig and Diterici, Zeit. für Psy. und Physiol. der Sinnesor., 4, pp. 241–347; 1892.
Koenig's Ges. Abh. Physiol. Op., pp. 214–321; Leipzig, 1903.
Abney, Researches in color vision, Chapter XV; London, 1913.
Allen, Phil. Mag. (6), 38, pp. 55–81; 1919.
Allen, Am. Jour. Physiol. Op., 1, pp. 94–134; 1920.
6. Nutting, J. Op. Soc. Am., 4, pp. 70–76; 1920.
Allen, Phys. Rev. (2), 11, pp. 257–280; 1900.
7. Helmholtz, Physiol. optics (third edition), 2, pp. 63–64.
Rood, Modern chromatics, p. 26; New York, 1879.
Crookes, Trans. Roy. Soc. London, A, 214, p. 4; 1914.
Bezold, Farbenlehre, pp. 24–30; Braunschweig, 1874.
8. Helmholtz, v. Kries, v. Frey, Koenig, Angier, Trendelenburg, and Diterici as quoted in Helmholtz; Physiol. optics (third edition), 2, p. 107.
Grünberg, Sitzb. Ak. Wien, 2A, 113, pp. 627–636; 1904.
9. Parsons, An introduction to the study of color vision, pp. 35–36; Cambridge University Press, 1915.
10. Rood, Modern chromatics, pp. 120–122; New York, 1879.
Watson, Text book of physics (fourth edition), p. 562; London, 1905.
Helmholtz, Physiol. optics (third edition), 2, pp. 138–140; 1911.
11. Troland, Trans. I. E. S., 13, p. 26; 1918.
12. Parsons, Introduction to the study of color vision, pp. 19, 60, 72, and 80; Cambridge University Press, 1915.
Abney, Proc. Roy. Soc. London, A, 83, pp. 290–297; 1910.
Abney and Watson, Trans. Roy. Soc. London, A, 216, pp. 91–128; 1916.
Ives, Astrophys. J., 44, pp. 124–127; 1916.
Russell, Astrophys. J., 45, pp. 60–64; 1917.
Reeves, Com. No. 51, Eastman Kodak Research Laboratory.
Reeves, J. de Phys. (5), 7, pp. 68–74; 1917.
Blanchard, Phys. Rev. (2), 11, pp. 81–99; 1918.
Reeves, Astrophys. J., 47, pp. 141–145; 1918.
13. Compare Black, Trans. I. E. S., 9, pp. 436–437; 1914.
Jennings, Am. J. Physiol. Op., 1, pp. 77–93; 1920.
14. Holmgren, Color-blindness and its relations to railroads and the marine. (Original in Swedish) Upsala, 1877.
Abridged translation, Smithsonian Inst. Report; 1877.
Sep. Pub. by Smithsonian Inst.; 1878.
Jeffries, Color-blindness; Boston, 1879.
Rep. Com. on Color Vision (Rayleigh, chairman), Proc. Roy. Soc. London, 51, p. 298, and pp. 375–391, 1892.
15. Stilling, Pseudo-isochromatische tafeln zur prüfung des farbensinnes (fourteenth edition); Leipzig, 1913.
Koellner, Die stoerungen des farbensinnes, p. 79; Berlin, 1912.
16. Nagel, Tafeln zur untersuchung des farbenunterscheidungs-vermögens, published by J. F. Bergmann; Wiesbaden, 1911.
Koellner, Die stoerungen des farbensinnes, pp. 67–69.
17. Nagel, Zwei Apparate, etc., Zeit. für Augenh., 17, p. 201; 1907.
Koellner, Die stoerungen des farbensinnes, pp. 69–77.
Rep. Com. on Standards and Methods of Examining the Color Vision (Williams, Black, and Jennings); Section on Ophthal., Am. Med. Assoc.; Chicago, 1914.
18. Koenig, Centralblatt für prak. Augenh., 8, pp. 375–377; 1884.
Brodhun, Ann. der Phys. und Chem., 34, pp. 897–918; 1888.
Priest, J. Op. Soc. Am., 4, pp. 448–495; 1920.
(See last citation for complete bibliography.)
19. Edridge-Green, Proc. Roy. Soc. London, B, 82, pp. 458–467; 1910.
Edridge-Green, Colour-blindness (second edition), p. 111; London, 1909.
Rayleigh, Proc. Roy. Soc. London, A, 84, pp. 464–468; 1910.
20. For example, Edridge-Green, Williams, Thomson.
Compare Rep. Com. on Standards and Methods of Examining the Color Vision (Williams, Black, and Jennings), Section on Ophthal., Am. Med. Assoc.; Chicago, 1914.
Thomson, A lantern for detection of color-blindness, Ry. Surg. J.; November, 1907.
Edridge-Green, Colour-blindness (second edition); London, 1909.
Collins, Color-blindness, Pub. Health Bull. No. 92, U. S. Pub. Health Service; 1918.

Digitized by Google

Digitized by Google

LIBRARY OF THE UNIVERSITY OF CALIFORNIA

DEPARTMENT OF COMMERCE

SCIENTIFIC PAPERS

OF THE

BUREAU OF STANDARDS

S. W. STRATTON, DIRECTOR

No. 418

SPECTRORADIOMETRIC INVESTIGATION OF THE TRANSMISSION OF VARIOUS SUBSTANCES, II

BY

W. W. COBLENTZ, Physicist
Bureau of Standards

AUGUST 29, 1921

PRICE, 5 CENTS
Sold only by the Superintendent of Documents, Government Printing Office
Washington, D. C.

WASHINGTON
GOVERNMENT PRINTING OFFICE
1921

Digitized by Google

Digitized by Google

SPECTRORADIOMETRIC INVESTIGATION OF THE TRANSMISSION OF VARIOUS SUBSTANCES, II

By W. W. Coblentz

ABSTRACT

This paper gives transmission data in the spectrum extending from 0.6μ to 3μ, using a mirror spectrometer, a quartz prism, and a vacuum thermopile. The substances examined are a group of mineral, animal, and vegetable oils (containing fatty acids), nitrocellulose, bakelite, and selenite. It is shown that the absorption spectra of the oils are so nearly identical that they can not be used for detecting the adulteration of one oil with another. The paper concludes with an examination of the accuracy of the author's previous work using a rock-salt prism. It is found that, using the recently determined refractive indices of rock salt, the corrections to the observations of 1903 to 1905 are of the order of 0.01 to 0.02μ and hence negligible.

CONTENTS

	Page
I. Introductory statement	267
II. Experimental apparatus and procedure	268
III. Transmission data	268
Appendix.—Concerning the accuracy of previous observations using a rock-salt prism	276

I. INTRODUCTORY STATEMENT

In previous papers data were published on the infra-red transmission of various substances particularly for wave lengths[1] extending from 2 to 15μ. One of the important conclusions arrived at is that the great groups of chemical compounds—for example, alcohols, fatty acids, etc.—have characteristic absorption spectra. Hence one could hardly expect to detect spectroradiometrically the adulteration of a vegetable oil with a similar oil containing fatty acids; for example, cottonseed oil in olive oil. This conclusion was verified in a subsequent examination of pure olive oil, linseed oil,[2] etc., in which the most conspicuous and characteristic absorption bands at 3 to 9μ occur so nearly at the same wave lengths that difficulties and uncertainties would arise in attempting to identify the substance producing them.

The object of the present paper is to record transmission data on the near infra-red spectrum, extending from 0.7 to 3μ, thus supplementing previous work, and incidentally showing that this

[1] Pub. No. 35, Carnegie Institution of Wash.; 1905. Also B. S. Bull., 2, p. 457; 1905.
[2] B. S. Bull., 7, p. 648; 1911.

Digitized by Google

region of the spectrum is likewise unsuited for spectroradiometrically detecting adulteration of animal and vegetable oils of similar composition. Furthermore, from a consideration of the present and of the previously published data, it appears that, as a rule, superposed upon the bands of selective absorption there is a general or nonselective absorption (perhaps it is merely a widening of the spectral activity of the band of selective absorption) which increases rapidly with wave length. Consequently, in order to extend the observations beyond 2μ, it is necessary to use thicknesses of material of the order of 0.1 to 0.01 mm to prevent complete opacity, whereas thicknesses of 1 to 10 cm are required in order to observe the absorption bands in the spectral region from 0.5 to 1.5μ. This appears to be true whether or not the substance—for example, dyestuffs—exhibits absorption in the visible spectrum.

II. EXPERIMENTAL APPARATUS AND PROCEDURE

The spectroradiometer used in the present investigation consisted of a mirror spectrometer described in previous work,[3] a quartz prism [4] which gives a relatively large dispersion in the region of 0.7 to 3μ, and a vacuum thermopile.[5] The source of radiation was a 500-watt, gas-filled tungsten lamp.

The absorption cell, 1 cm in thickness, was provided with thin, highly polished quartz windows. For examining thin layers of material cells 0.3 mm or less in thickness were employed. They were made of plates of microscope cover glass between which was placed a U-shaped wire or tin foil, then glued.

The experimental procedure was to note the galvanometer deflection with and without the cell before the spectrometer slit. No correction was made for loss of energy by reflection and absorption in the glass and quartz windows, which loss is quite uniform to 2.4μ. In some cases the transmission is higher than the theoretical value (92 per cent), from which it appears that there may have been internal reflection in the cell. However, since the main part of the problem was the accurate mapping of the location of the absorption bands, this is of no great importance.

III. TRANSMISSION DATA

The first observations to be described under this caption are on a series of animal and vegetable oils. These observations are illustrated in a series of spectral transmission curves, which are given

[3] B. S. Bull., 10, p. 1; 1913. [4] B. S. Sci. Papers, 16, p. 701; 1920. [5] B. S. Sci. Papers, No. 413; 1921.

Digitized by Google

at random, without special reference to the origin of the material (whether animal or vegetable) in order to show the great similarity of curves, and hence their unsuitability for detecting adulteration. All these oils, when in a 1 cm layer, exhibit three deep, wide bands in the region of 1.18, 1.39, and 1.75μ, respectively. Practically the only distinguishing characteristic is the absorption band at 0.65μ which occurs in vegetable oils containing chlorophyl. In the infra-red the writer found only slight indications of selective absorption,[6] in the region of 0.73μ, in an alcoholic solution of chlorophyl. Owing to the great opacity of alcohol at 1.2 to 1.4μ it remains to be determined whether the observed increase in absorption of chlorophyl at 1.4μ is correct.

Olive Oil.—The transmission curve of a 1 cm layer of pure olive oil is given in curve *A*, Fig. 1. Similar data were previously obtained[7] for the spectral region of 3 to 10μ, the thickness of the layer being only 0.007 mm. As already mentioned, the absorption band at 0.65μ is caused by chlorophyl.

Cottonseed Oil.—The sample examined was a standard commercial product (colorless and free from chlorophyl) known as Wesson oil. The transmission of a 1 cm layer is given in curve *B*, Fig. 1. From the close similarity of the transmission curve of cottonseed oil and that of olive oil it is evident that the spectroradiometric test can not be used to detect the adulteration of olive oil with cottonseed oil.

Peanut Oil.—The sample examined was a commercial product. The spectral transmission of a 1 cm layer is given in curve *C*, Fig. 1.

Tung Oil.—The sample examined was obtained from the chemistry division. It was made from nuts gathered especially for the purpose of procuring the pure product free from adulterants found in the commercial material, which is a liquid. The present sample was a white solid which liquefied on warming, after which it would remain liquid for several days.

The transmission of a 1 cm layer of this material, in the liquid state, is given in curve *A*, Fig. 2. Tung oil is adulterated with soya-bean oil, with cottonseed oil, and sometimes with fish oil. The transmission curves are so nearly identical that they can not be distinguished with certainty.

[6] Phy. Rev., 19, p. 27; 1904. In the transmission curves of a 10 cm layer of vegetable oils, published by Dr. K. S. Gibson. (The Cotton Oil Press, September, 1920), the absorption band of chlorophyl at 0.66μ is very conspicuous. His curves of vegetable oils which are free from chlorophyl do not show the characteristic band at 0.65 to 0.67μ.

[7] B. S. Bull., 7, p. 648; 1911.

Digitized by Google

Catfish Oil.—The transmission of a 1 cm layer of catfish oil is given in curve *B*, Fig. 2.

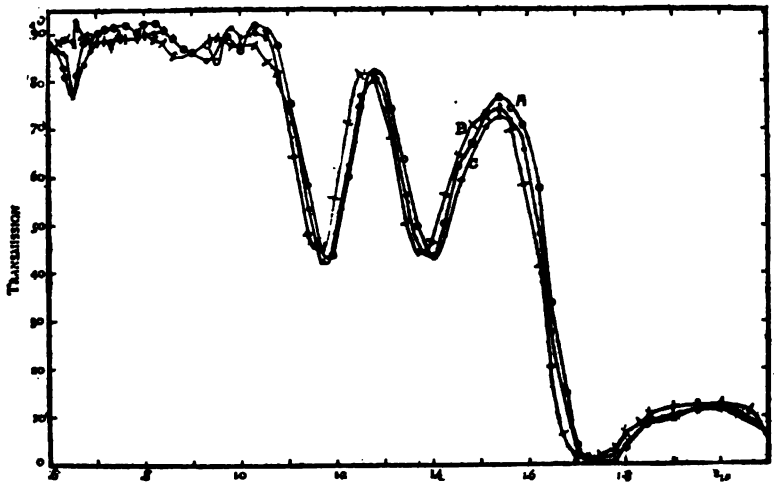

FIG. 1.—*A, olive oil; B, cotton seed oil; C, peanut oil*

Soya-Bean Oil.—The special transmission of a 1 cm layer of commercial soya-bean oil is given in curve *C*, Fig. 2. Soya-bean oil is used to adulterate linseed oil.

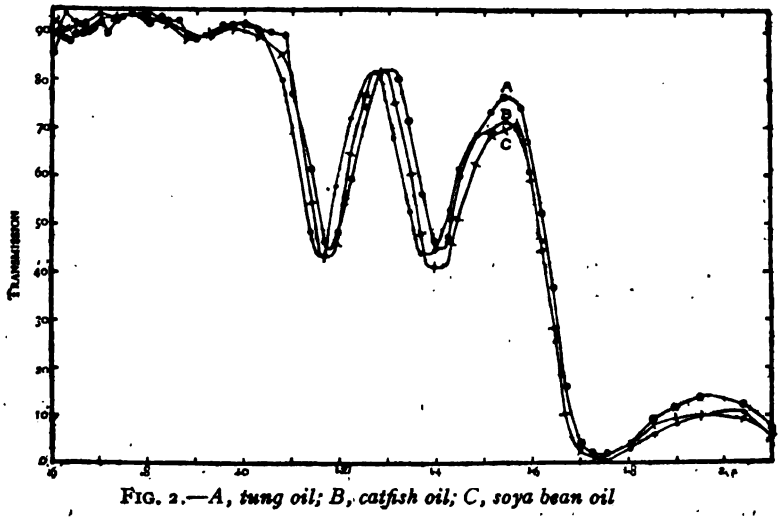

FIG. 2.—*A, tung oil; B, catfish oil; C, soya bean oil*

Lard Oil.—The spectral transmission of a 1 cm layer of clear lard oil is given in curve *A*, Fig. 3. It is conspicuous for the sharpness of its absorption bands at 0.7, 0.9, 1.18, and 1.41 μ.

Digitized by Google

Fatty Acids of Linseed Oil.—This material was prepared in the chemistry division of this Bureau. It was brownish in color,

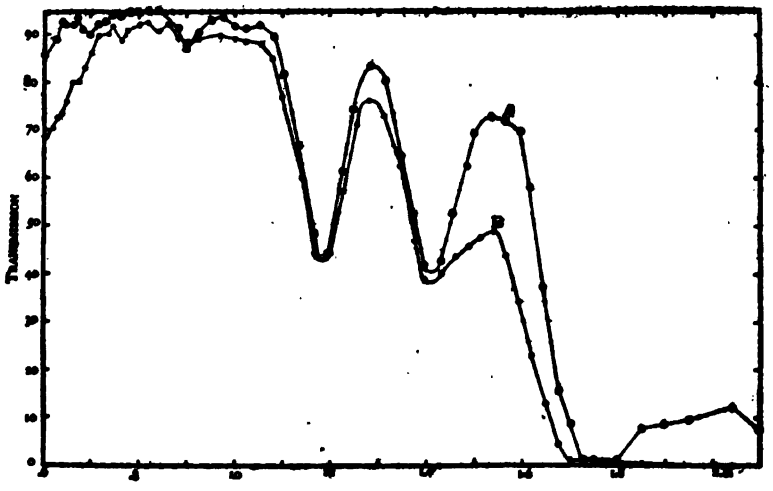

FIG. 3.—*Lard oil, A; fatty acids of linseed oil, B*

thus causing high absorption in the violet end of the visible spectrum. The spectral transmission of a 1 cm layer is given in curve *B*, Fig. 3.

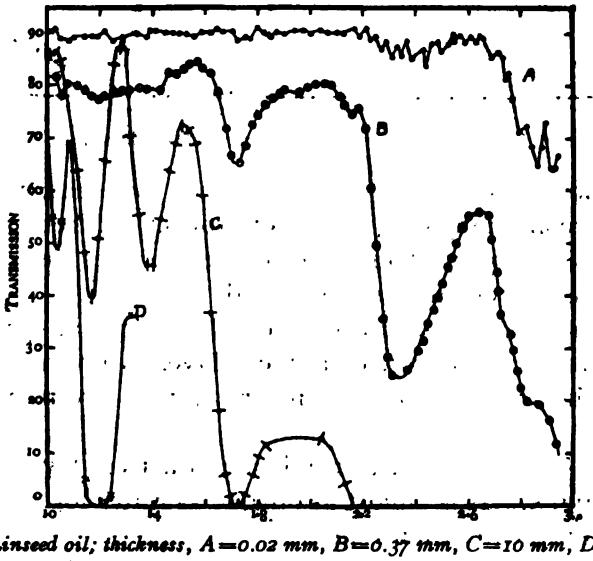

FIG. 4.—*Linseed oil; thickness, A=0.02 mm, B=0.37 mm, C=10 mm, D=100 mm*

Linseed Oil.—The spectral transmissions of various thicknesses of pure linseed oil are given in Fig. 4. Curve *A* gives the transmission through a thickness of 0.02 mm; curve *B*=0.37 mm; curve *C*=10 mm.

Digitized by Google

Curve *D* gives the transmission of a 10 cm layer of cottonseed oil. It is taken from a paper by Gibson[9] to illustrate the effect of thickness upon the intensity of the absorption bands mentioned in the first part of the paper. Curve *C* (1 cm layer) is drawn to a larger scale in curve *A*, Fig. 5.

These curves are interesting in illustrating a rapid increase in absorption in the spectrum beyond 1.5μ with increase in thickness of the material. The wide unsymmetrical band at 2.3μ appears to be a complex group of small bands. The sharp band at 1.72μ is to be noticed, since it is harmonic with the bands at 3.43μ, 6.86μ,

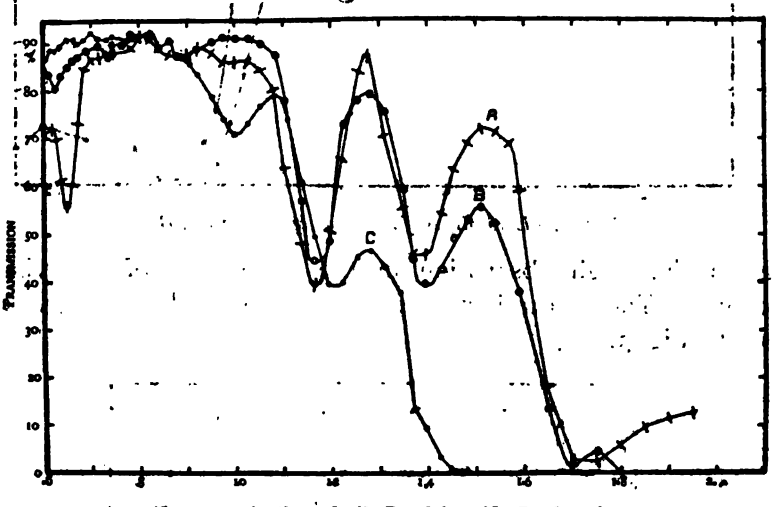

FIG. 5.—*A, linseed oil; B, oleic acid; C, glycerine*

etc., previously observed.[9] These bands are characteristic of substances containing CH_2 groups of atoms.[10] Whether the small band at 0.86μ observed in some of these curves belongs to this harmonic series remains undetermined.

Oleic Acid.—This substance is found in lard oil, olive oil, etc. The spectral transmission of a 1 cm layer is given in curve *B*, Fig. 5. The transmission of thinner layers is given in previous papers.[11]

Glycerin.—The spectral transmission of a 1 cm layer is given in curve *C*, Fig. 5. It is almost as opaque as water for radiations of wave lengths greater than 1.4μ.

[9] Gibson, "The Cotton Oil Press," September, 1910.
[9] B. S. Bulletin, 7, p. 649; 1911.
[10] Pub. No. 35, Carnegie Institution of Wash.; 1905.
[11] Pub. No. 35, Carnegie Institution of Wash., p. 71; 1905. Also B. S. Bul., 7, p. 648; 1911.

Digitized by Google

Nitrocellulose.—The samples examined were obtained under the trade names, Celluloid, Pyralin, and Viscoloid.[13] They were thin, uncolored, and quite free from scratches and other imperfections. The thickness was closely the same for all samples, being 0.23 mm for celluloid and viscoloid, and 0.26 mm for pyralin.

The observed data are illustrated in Fig. 6, in which *A* represents the observations on celluloid from 0.55 to 3 μ and A_1 represents the same observations drawn to a larger scale in order to show the numerous fine absorption lines which occur in the region

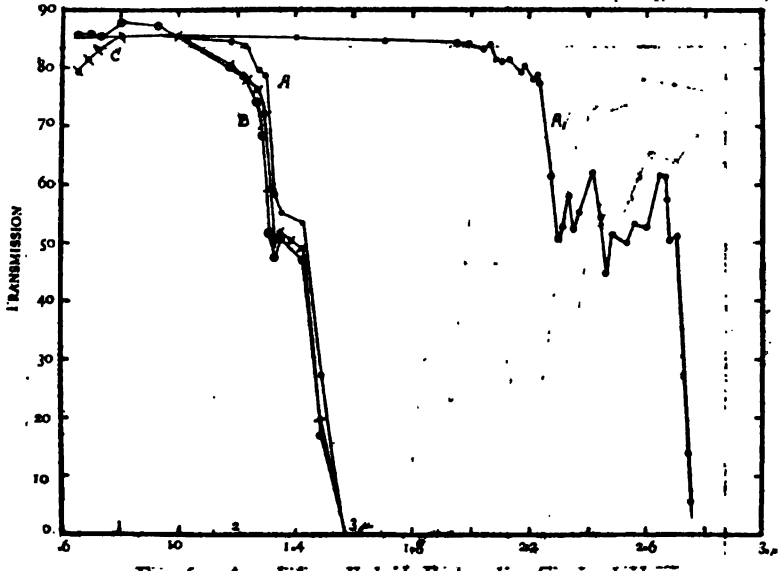

FIG. 6.—*A and A_1, celluloid; B, pyralin; C, viscoloid*

of 2.3 to 2.6 μ. Curve *B* gives the transmission of pyralin and curve *C* that of viscoloid.

The data show that the transmission of all three kinds of the colorless material is high, being 80 to 85 per cent in the visible and in the infra-red to 3μ. Beyond this point they are very opaque to infra-red rays.

Similar data on celluloid [15] and on collodium [16] were published by the writer some years ago when it was shown that these products of nitrocellulose have numerous absorption bands in the spectral region extending from 3 to 15μ, which was the extent of the spectrum examined.

[13] Celluloid from The Celluloid Co., New York City; pyralin from E. I. du Pont de Nemours & Co., Arlington, N. J.; and viscoloid from The Viscoloid Co., Leominster, Mass.

[15] Pub. No. 97, p. 42, Carnegie Institution of Wash.; 1908.

[16] Pub. No. 65, p. 60, Carnegie Institution of Wash.; 1906.

Digitized by Google

In the ultra-violet these samples show considerable absorption at 0.365μ and are opaque to radiations of wave lengths less than 0.3μ.

Judging from the behavior of other substances, the opacity of samples of celluloid, etc., which become discolored, is increased in the violet and ultra-violet, but not in the infra-red.

Selenite.—The spectral transmissions of various thicknesses of selenite, $CaSO_4+2H_2O$ are given in Fig. 7. For curve *A*, the thickness $t=0.11$ mm.; for curve B, $t=2.80$ mm; and for curve *C*, $t=9.32$ mm. The data were obtained in order to supplement

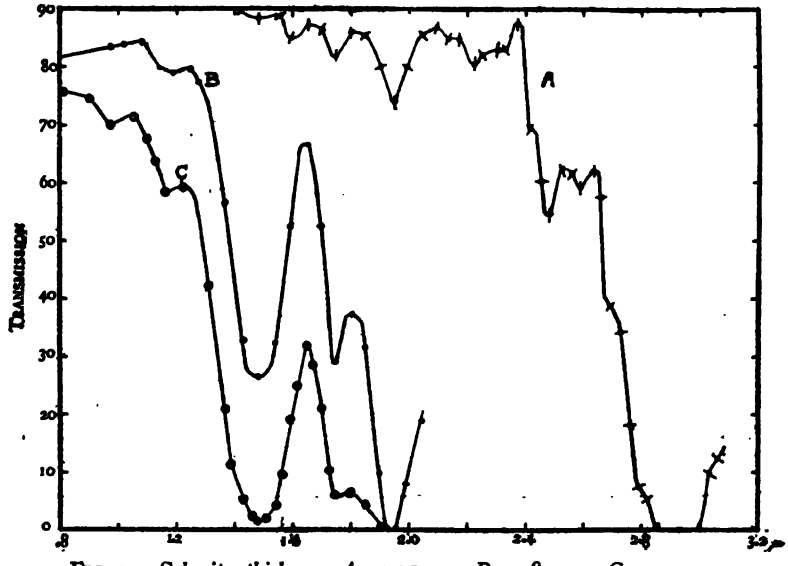

FIG. 7.—*Selenite; thickness, A=0.11 mm, B=2.80 mm, C=9.32 mm*

previous investigations of substances containing water of crystallization.[15] In the present work the previously observed asymmetrical absorption band at 2.5 to 3μ is resolved into several distinct absorption bands. Considered in connection with the previous observations it appears that all these absorption bands are caused by water.

Paraffin Oil.—The material examined was a colorless liquid petrolatum (liquid paraffin) of American origin and great purity, used for medicinal purposes.

The second sample was a petroleum distillate (paraffin base) having a light brown color and a boiling point of 272 to 274°C at 2 mm pressure.

[15] B. S. Bull., 7, p. 619; 1911.

Digitized by Google

The spectral transmissions of these two samples were found to be identical. The observations for 1 cm layer are illustrated in curve *C* of Fig. 8.

There are two sharp absorption bands, with maxima at 1.2 and 1.42μ, respectively, which are so close to similar absorption bands in olive oil, etc. (Figs. 1 to 3), that it would be difficult to distinguish adulteration by spectroradiometric tests.

Benzol.—The spectral transmission of a 1 cm layer of benzol, C_6H_6, is given in curve *A*, Fig. 8. The data are of interest in connection with a previous examination [16] of a thinner layer of

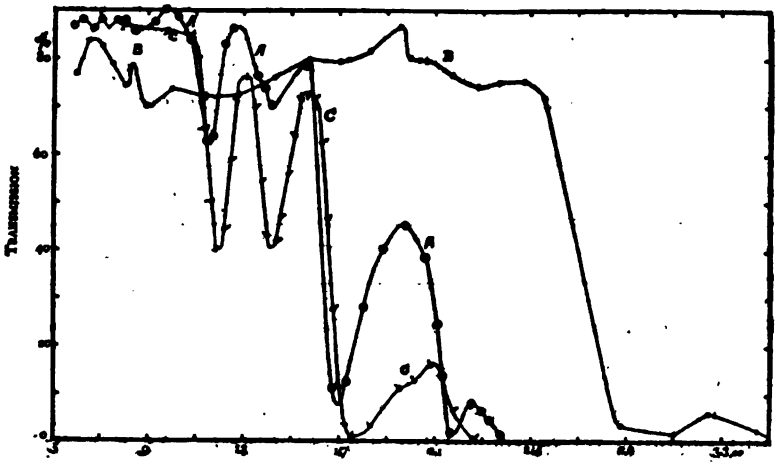

FIG. 8.—*A, benzol; B, bakelite; C, mineral oil, paraffin base*

this material which permitted an exploration of the bands at 2.18 and 2.49μ, using a quartz prism. The 1 cm layer is opaque to radiations of wave lengths greater than 2.5μ. It is useful in locating absorption bands at 1.14 and 1.41μ (complex) which are barely perceptible in a thin layer of this material.

Bakelite.—This is a condensation product of formaldehyde and phenol. It was obtained as a varnish dissolved in acetone. A layer 0.04 mm in thickness was mounted upon a thin piece of glass and baked to remove the solvent. It has a high absorptivity in the ultra-violet but, as shown in curve *B*, Fig. 8, shows no marked absorption bands (to 3μ) in the infra-red, when used in a thin layer as just described.

[16] Pub. No. 35, pp. 35–76, Carnegie Institution of Wash.; 1905.

Digitized by Google

APPENDIX.—CONCERNING THE ACCURACY OF PREVIOUS OBSERVATIONS USING A ROCK-SALT PRISM

In 1903 to 1905 the writer determined the infra-red transmission of various substances using a rock-salt prism. At that time the dispersion of rock salt was not accurately known. In the region of 3μ there was considerable disagreement in the refractive indices as determined by various observers, and the writer used a smooth curve drawn through the various determinations.[17] In the meantime a new determination[18] was made of the refractive indices of rock salt, and recently a study was made of all the data available.[19] It was therefore deemed desirable to recalculate the calibration curve of rock salt and compare it with the one used in the investigations of 1903 and 1905. The difference in the calibration curve then used and the correct curve is

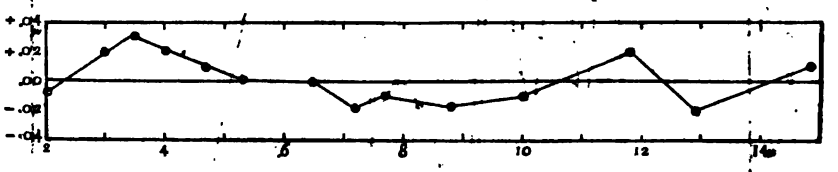

FIG. 9.—*Wave length corrections to maxima of absorption bands published in 1905*

illustrated in Fig. 9 from which it may be observed that in the region of 3 to 4μ the published maxima of absorption bands should perhaps be increased by 0.01 to 0.02μ. At 7 to 10μ the published maxima should be decreased by 0.01μ. These corrections are so small that they appear to be negligible in comparison with the errors of observation resulting from changes in temperature of the prism and the small dispersion used.

That these data are free from large systematic errors is indicated by comparison with similar observations using a fluorite prism which has almost three times the dispersion of rock salt in the spectral region from 3 to 8μ. For example, the maxima of characteristic absorption bands at 3.43 and 6.86μ, first observed with the rock-salt prism, in substances containing CH_3 and CH_2 groups, are in good agreement with similar maxima subsequently observed with a fluorite prism.

WASHINGTON, April 1, 1921.

[17] Pub. No. 35, Carnegie Institution of Wash.; 1905 (Investigation of Infra-red Spectra, p. 138).
[18] Paschen, Ann. der Phys., 4, pp. 120 and 1029; 1908.
[19] B. S. Sci. Papers, 16, p. 701; 1920.

Digitized by Google

DEC 22 1921

DEPARTMENT OF COMMERCE

SCIENTIFIC PAPERS

OF THE

BUREAU OF STANDARDS

S. W. STRATTON, DIRECTOR

No. 419

THE PRODUCTION OF LIQUID AIR ON A LABORATORY SCALE

BY

J. W. COOK, Assistant Physicist

Bureau of Standards

SEPTEMBER 6, 1921

PRICE, 5 CENTS

Sold only by the Superintendent of Documents, Government Printing Office
Washington, D. C.

WASHINGTON
GOVERNMENT PRINTING OFFICE
1921

Digitized by Google

Digitized by Google

Digitized by Google

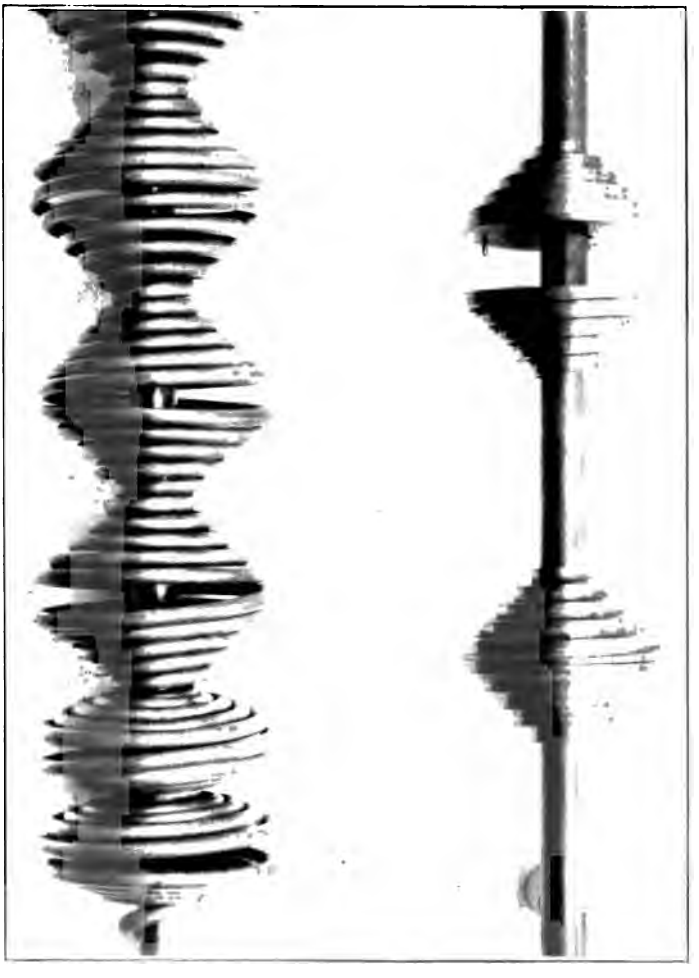

FIG. 2.—*Regenerator coil (at left) in course of construction and forms (at right) used in winding the coil.*

Digitized by Google

THE PRODUCTION OF LIQUID AIR ON A LABORATORY SCALE

By J. W. Cook

ABSTRACT

The essentials of a plant producing liquid air by the Hampson process are the compressor, purifying train, and liquefier. The compressor, usually of four stages, delivers air at room temperature and approximately 3000 pounds per square inch. The compressed air purifying train consists of, first, a trap for receiving oil and water, and second, suitable containers charged with chemical reagents, such as sodium hydroxide, calcium chloride, or lime, for removing carbon dioxide and water vapor. The air thus compressed and purified is delivered to the liquefier, in which, after passing through a coil of copper tubing, the air is allowed to expand freely to approximately atmospheric pressure. Where this drop in pressure takes place there is a corresponding drop in the temperature of the air. The expanded air before leaving the liquefier is caused to circulate around the copper coil which contains the compressed air, thus cooling the coil and in turn the compressed air, so that on continuous operation a cycle of progressive cooling is maintained until the temperature ultimately reaches the liquefying point. The liquefier is so constructed that the air which is condensed to liquid is delivered into a receiving vessel. The gaseous air exhausted from the liquefier is returned to the intake of the compressor for succeeding cycles because it has been purified and when used repeatedly will be less exhausting on the purifying reagents.

CONTENTS

	Page
I. Introduction	277
II. Construction of liquefiers	279
III. Purification of air	282
IV. Description of Bureau plant	284
V. Summary	286

I. INTRODUCTION

The following is a brief account of the liquefaction of air on a laboratory scale by the Hampson process and a description of the apparatus now used at the Bureau of Standards. It is not the purpose of this paper to enter into the theory of the Hampson liquefier, which has been treated elsewhere, nor to furnish a working drawing whereby the apparatus may be duplicated, because details and methods of mechanical construction are rarely duplicated exactly by different constructors. It is the purpose to show the general methods of construction which will serve as a guide for others working along similar lines.

Digitized by Google

It is well to call attention to the fact that the total cold available is determined by the initial temperature and pressure of the air at the point where it enters the regenerator and the exhaust pressure, which in practice is one atmosphere. It is independent of the internal construction or arrangement of the liquefier, of the material used in its construction, of the distribution of temperature in the regenerator coil, and of all other circumstances whatever, provided that the kinetic energies of the feed and the exhaust are negligible. This cold is used in the following three ways: (*a*) To offset the heat that leaks into the liquefier from outside, either through the insulation or along the metallic component parts of the liquefier; (*b*) to cool the whole quantity of gas from its initial temperature to the slightly lower exhaust tenperature; (*c*) to cool a fraction of the air from this exhaust temperature to the normal boiling point and then condense it into liquid.[1]

From these facts it is evident that to obtain the maximum amount of liquid air with a given expenditure of power a Hampson liquefier must be so constructed that the factors (*a*) and (*b*) are kept as small as possible. This results in a compromise, however, for by increasing the size of the regenerator indefinitely, which would make (*b*) negligible by exhausting at practically the initial temperature, the size of the liquefier, over all, is necessarily increased, thereby increasing (*a*) the heat leak. It is therefore apparent that, to be efficient, a liquefier should be as small, over all, as will exhaust air at a temperature just slightly below the initial temperature, which may be about room temperature or may be considerably lower if a precooler is used. The size of the regenerator coil required would be determined chiefly by the capacity of the compressor furnishing the air and by the temperature of the air entering the regenerator. Obviously, if a precooler us used, the size of the regenerator may be decreased.

In the foregoing discussion it has been assumed that the liquefier has been in operation long enough for complete thermal equilibrium to have been reached. Under these conditions the actual heat capacity would not be a factor. If a liquefier is to be run only intermittently for the production of small amounts of liquid at a time, the heat capacity of the liquefier will be an appreciable factor, influencing the length of time required to cool down the liquefier when starting, and effectiveness of heat interchange can be advantageously sacrificed in order to reduce the heat capacity.

[1] Buckingham, B. S. Bull. 6, p. 125; 1909 (Sci. Paper No. 123).

Digitized by Google

II. CONSTRUCTION OF LIQUEFIERS

In the liquefiers constructed at the Bureau the regenerator coil is a copper tube (*aa'*, Fig. 1) wound, starting at the top of the liquefier, in a spiral from outside to center for the first layer, then from center to the outside for the next layer, and so on down the liquefier, without multiplicity of tubes and without retracing in the reverse direction from bottom to top.[2] Thus, all the incoming air must pass through the entire length of the regenerator. Fig. 2 is a photograph of a section of a regenerator in the course of construction. The spiral is wound on the brass forms shown in Fig. 2; the core is then slipped out of one of the forms to permit removing the two halves of this form from the coil. The form is then replaced on the core from the other end and the winding continued, the process being repeated until the entire length of a tube, usually about 25 feet, has been wound. The several coils are then pressed down into a series of nearly flat spirals, and as many sections as are required for the regenerator are joined with silver solder. It is more convenient to make the joints at the outermost turn of the spiral. The complete regenerator coil is then mounted permanently on a German-silver tube just strong enough to serve as a core and support the apparatus.

In winding the copper tubing it sometimes has a tendency to collapse or flatten. To prevent this it is convenient to fill a length of the tube with water and, with a hydraulic pump, maintain during the winding a constant hydrostatic pressure on the tube equal to the pressure at which the liquefier will be operated with air, usually 3000 pounds per square inch. If this process does not suffice, the tube may be filled with water, then frozen in a bath of brine and ice, and wound while the water in the tube is frozen.[3] Annealed copper tubing will not burst on having water frozen once within it, and if winding is done before the ice has had time to melt a very true coil of small diameter may be made. Either of the above methods has the advantage that emptying and cleaning the tube are accomplished without difficulty, which is not the case if lead, rosin, etc., are used in a tube of this length. It is advisable to test the copper tubing before winding under sufficient hydraulic pressure to assure a reasonable factor of safety, and to test the completed regenerator at a lower pressure, but still somewhat higher than the normal working pressure.

[2] A regenerator of this type has been described and illustrated by H. Kammerlingh Onnes; Communications from the Phys. Lab. at the Univ. of Leiden, No. 87, 1903. Plate II, also No. 109*b*, 1909.

[3] This method w as devised by Dr. H. F. Stimson, of the Bureau of Standards.

Digitized by Google

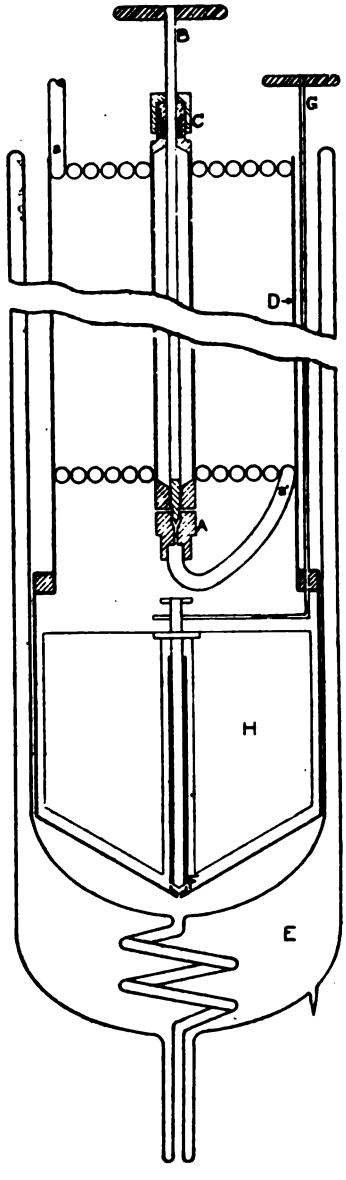

FIG. 1.—*Cross section, partly diagrammatic, of Hampson liquefier*

a, a' regenerator coil; *A*, expansion valve; *B*, valve stem; *C*, stuffing box; *D*, sheet metal casing; *E*, silvered glass Dewar cylinder; *F*, float valve; *G*, lifter for float valve; *H*, float

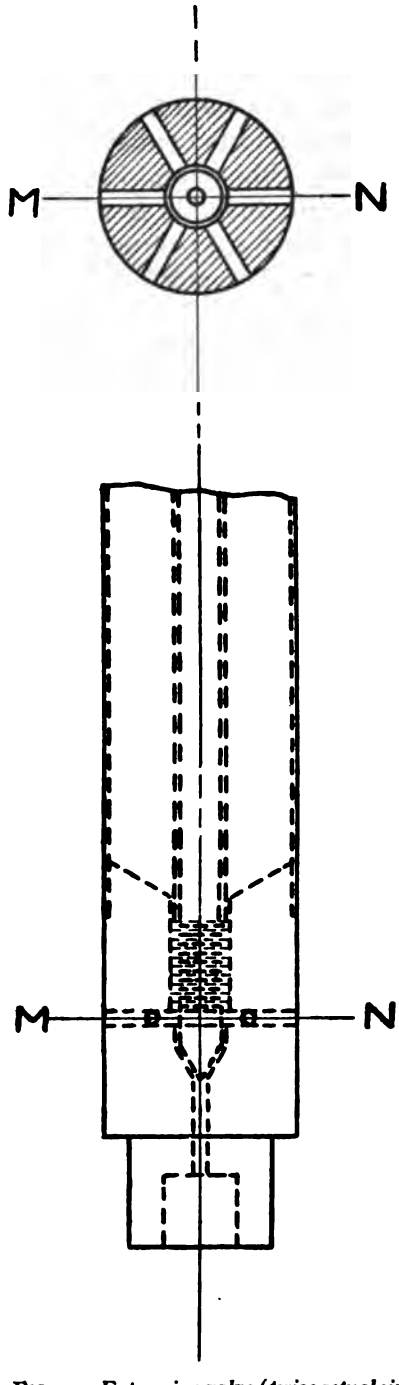

FIG. 3.—*Expansion valve (twice actual size)*

Digitized by Google

At the lower end of the core is soldered the expansion valve (*A*, Fig. 1), and at the lower end of this is silver soldered the end of the regenerator coil. Fig. 3 is a drawing of this expansion valve in detail, it being a needle valve of simple construction. A brass body and phosphor-bronze or gun-metal needle work well. The expansion valve is operated from above the top by means of the valve stem (*B*), which is a German-silver tube extending up the core and through a stuffing box (*C*), which holds the back pressure only. Any other type of valve that can be operated conveniently may be used, however, and even a fixed orifice, in the form of a few feet of copper capillary tube, has served in place of an expansion valve with fair success. It should be noted that the liquefier which was equipped with the capillary tube in place of an expansion valve did not permit of adjustment to accommodate variations in the speed of the compressor and also gave considerably more trouble by freezing and clogging, which will be discussed later.

A sheet-metal cylinder (*D*, Fig. 1) of thin German silver is made to fit tightly around the regenerator, open freely at the top to exhaust the gaseous air, and open through a small hole at the bottom to allow the liquid air to run out.

It is desirable to mount the complete liquefier in a suitable Dewar vessel (*E*) having an outlet at the bottom. However, very satisfactory results have been obtained by using 3 to 4 inches of "fine regranulated cork" instead of a Dewar vessel. Fine regranulated cork is made commercially by grinding trimmings from cork board.

To work efficiently, the liquefier should discharge air in the liquid state from the bottom of the sheet-metal cylinder mentioned above, and all of the cold vapor should be forced up over the regenerator coil and out at the top. To accomplish this either a fixed, an adjustable, or an automatic outlet valve must be arranged at the bottom. A fixed opening naturally works with least efficiency, because some cold vapor escapes with the liquid and is a direct loss. An adjustable opening requires attention while running. An automatic float valve (*F*) can be made to give high efficiency and very satisfactory service, but care must be taken in its design. It has been found that the violent turbulence of the air around the expansion valve and in the vicinity of the float (*H*) may lift the float against gravity, hold the valve open, and prevent its operation. It is therefore necessary to install baffles to screen the float. No entirely satisfactory arrangement

Digitized by Google

of baffles has been found, although several layers of fine copper gauze around the expansion valve serve fairly well. It is also necessary to remove moisture which will collect at the float valve when the liquefier is not in use and which would freeze if not removed when the apparatus was put into operation. If some mechanical means (*G*) is provided whereby the float valve can be lifted and held open while dry air is circulated through the liquefier just before starting a run, all moisture can thus be removed and the float mechanism will be free to open and close automatically. No ferrous metal should be incorporated in this part of the liquefier, as rusting would subsequently cause trouble.

When the liquid-air plant is in operation, the air after compression is cooled with running water to approximately 20° C. Since the Joule-Thomson effect is greater at lower temperatures, it is very desirable to further cool the air before it reaches the liquefier, which is done by immersing a line of copper tubing in a tank containing ice and salt. Should a refrigerating plant producing a still lower temperature be available—using, for example, ammonia or carbon dioxide—a precooler should be included in the liquefier above the regenerator coil.

III. PURIFICATION OF AIR

It is also necessary that some means be provided for purifying the air by removing the water vapor and carbon dioxide. Most of the water vapor is condensed during compression, and a trap is located to catch this water, which can be drawn off at intervals, together with the oil used for lubrication in the compressor. The air is subsequently passed through a container, where it bubbles through a solution of sodium hydroxide, which removes carbon dioxide, and then passes over calcium chloride, which removes water vapor. This method is very effective, delivering air which is purer than is actually needed for normal conditions of liquefaction by the Hampson process.[4] Calcium hydroxide in water (milk of lime) may be used to remove carbon dioxide, and calcium oxide (quicklime) may be used to remove water vapor, if preferred. If only one purifier is available, it can be used with dry sodium hydroxide in the lump or stick form, as this reacts with both carbon dioxide and water vapor.

[4] The compressed-air plant at the Bureau of Standards is also used for refrigerating low-temperature apparatus, such as expansimeters and calorimeters, where a steady flow of air, without clogging, can be maintained for several hours at a time. This work demands that a higher degree of purity be attained than would be required for liquefaction alone.

Digitized by Google

These purifiers are one of the chief sources of danger in a plant of this kind, as they contain comparatively large volumes of air under high pressure. They should, therefore, be designed with a considerable factor of safety and should be tested under hydraulic pressure considerably in excess of the working pressure. Each stage of the compressor is equipped with a spring safety valve, the one on the last stage also serving as the safety valve which protects the liquefier and purifiers as well as the compressor. It is suggested that a check valve, resembling the outlet valve of the last stage of the compressor, be placed in the air line between the first purifier and the high-pressure safety valve on the compressor to prevent a possible back flow of air in case of accident to this safety valve or to the compressor outlet valve and the gasket under the high-pressure cylinder head. If they should give way while pressure is on, any solution in the purifier would be atomized into the laboratory through the rupture unless such a check valve is provided.

A purifier for removing carbon dioxide may be placed in the intake line to the compressor, but as the volume of the air in the intake line is much greater than that in the high-pressure line more surface of the reagent must be exposed. When a purifier of proper size is placed in the intake line, it is effective for removing carbon dioxide, but very unsuitable for removing water vapor, because much water can be removed during compression, as mentioned above. Should any purifier be placed in the intake line, care must be taken to thoroughly filter the air before allowing it to enter the compressor, otherwise particles of the reagent used will be carried by the current of air into the valves of the compressor, eventually causing trouble. It is desirable, if feasible, to deliver to the intake of the compressor the exhaust air from the liquefier, because this air, having passed through the purifiers, has had most of the water and carbon dioxide removed.

When starting a Hampson liquid-air plant after pressure has been built up but before any liquid has been produced, there will be a very definite rate of flow of air through the apparatus. If the liquid-air outlet valve is closed before any liquid has been produced and the high-pressure gauge is watched closely, it will be observed that there is a definite time at which the pressure drops, indicating that the air flow has slightly increased. This corresponds with the first production of liquid. The mass rate of flow of partially liquefied air is probably greater than that of

Digitized by Google

gaseous air under the same conditions, owing to the greater density of liquid air. This greater density, however, is accompanied by lower velocity of flow, which favors the deposition of ice or solid carbon dioxide at the point in the expansion valve or its vicinity at which liquefaction occurs, resulting in partial or complete clogging. To remove the obstruction, it is necessary to temporarily change the point where liquefaction is taking place to a point farther on in the air current, thereby increasing the velocity at the point where clogging occurred and sweeping the obstruction from its point of lodgment. This can be accomplished by momentarily opening the expansion valve a little and then reclosing it to its proper position. If the expansion valve is frozen in place and can not be moved, the same effect may be obtained by allowing some of the expanded air to escape directly out of the bottom of the apparatus (through the liquid-air outlet valve), thereby raising the temperature of the air in the expansion valve slightly. This causes a temporary vaporization and a consequent increase in velocity which will clear the valve of the accumulation of snow.

The difficulty just described does not ordinarily occur when the purifying train is in proper working order, because slight impurities will pass through the liquefier without causing obstruction and will be collected with the liquid air. Pure liquid air is clear and transparent, but when a very noticeable white precipitate is observed it may be taken as an indication that the reagents are exhausted and need to be replaced.

IV. DESCRIPTION OF BUREAU PLANT

The following brief specifications give a general idea of the size and output of the Bureau of Standards liquid-air plant. The four-stage compressor, driven by a 35-horsepower direct coupled steam engine, has a rated capacity of 75 cubic feet of free air per minute. The container for the sodium hydroxide solution used for removing the carbon dioxide is 8 feet long and 4½ inches in inside diameter and is placed in a vertical position, the air entering at the bottom and bubbling up through the solution. This container is nearly filled with pieces of broken marble, which cause better contact of the air with the solution and also prevent the carrying over of spray. About 1 gallon of a 25 per cent solution is used, which half fills the container. The flanged ends are bolted on, compressing a red fiber ring, which seals air-tight. Three

Digitized by Google

calcium chloride purifiers, each 3 feet long and 2 inches in inside diameter, are used in series for removing water vapor. They are placed in a vertical position, and the air enters each successively from the bottom. A drain is located at the bottom of each tube for drawing off the calcium chloride solution which is formed during use. About 5 pounds of lump anhydrous calcium chloride are used to fill the three purifiers, and when replenishment is necessary only the first purifier in the series is removed and refilled. This refilled purifier is then replaced as the third one in the series, thus economizing on the reagent. All the purifiers are of seamless steel tubing. Connections to the purifiers are made by means of ball-and-socket unions of the type used on high-pressure gas cylinders.

The compressed air after being purified at ordinary temperature is cooled to about 0° C by a circulation of calcium chloride brine (cooled by an ammonia plant) and then to from −20 to −35° C by a CO_2 cycle.

The regenerator coil consists of about 200 feet of copper tubing of $\frac{3}{16}$ inch outside diameter and 0.035-inch wall, mounted on a ½-inch core. This coil when mounted is about 18 inches long and 3 inches in outside diameter and is completely jacketed by a glass Dewar vessel. An automatic float delivery valve is installed with mechanical adjustment for holding it open when desired. When working at full capacity, the plant produces 3 gallons of liquid air per hour. The general operation of the plant indicates that the above proportions are approximately correct.

Fig. 4 shows the construction of a very serviceable needle valve, which will be convenient in a laboratory where high-pressure air lines are desired for various purposes or where there is more than one liquefier available. This type of valve has been used at the Bureau of Standards for many years, but the origin of its design is not known. The body is usually of brass and the needle of steel, but where there is a possibility of the presence of moisture phosphor bronze is recommended in place of steel. The high-pressure lines are connected to the valve by means of unions, one of which is represented. A thin gasket of pressboard is placed between the flat faces (*a*) and (*b*) and compressed air-tight by the nut (*c*). The copper line is joined with silver solder at (*d*).

Acknowledgments.—Many of the features described are similar to those of other commercial liquid air plants. The development of the liquid-air plant at the Bureau of Standards is due largely

Digitized by Google

to F. S. Durston and the late T. B. Ford, who were formerly in charge. Acknowledgment is also due to Dr. C. W. Kanolt, at present in charge of the cryogenic laboratory, for a careful criticism of the manuscript.

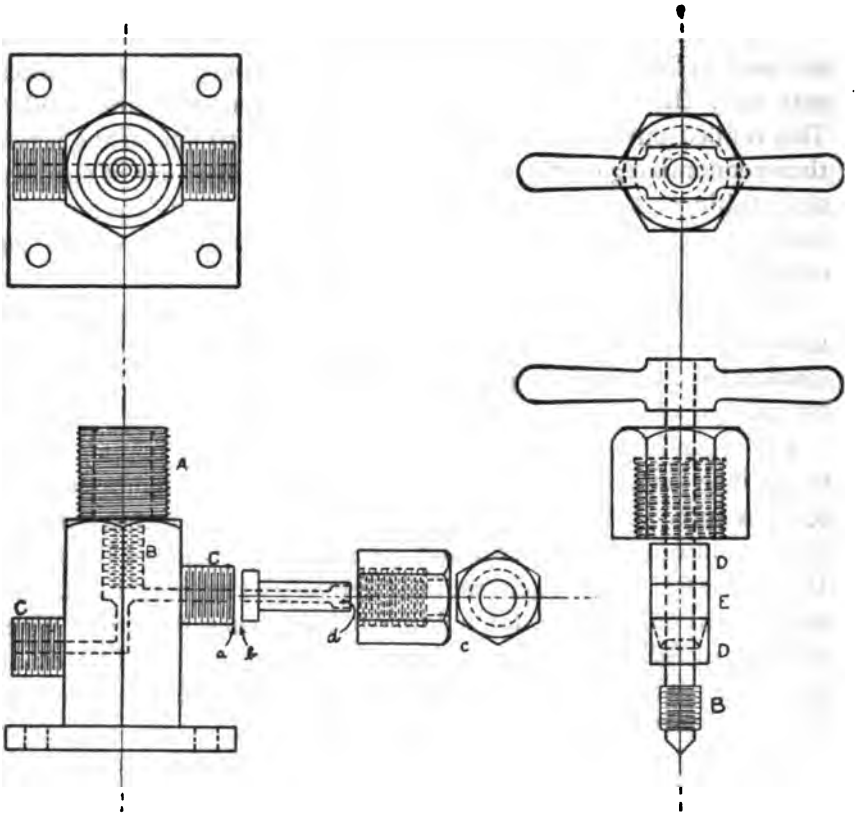

FIG. 4.—*Needle valve for gases under high pressure*

A, 1" x 14 thread; *B*, 7/16" x 20 thread; *C*, 3/8" x 20 thread; *D*, brass packing rings; *E*, leather packing; *b*, *c*, union connection

V. SUMMARY

The design and construction of laboratory apparatus for liquefying air by the Hampson process are described. Brief descriptions of necessary or useful accessories, such as purifiers for the air, precoolers, and a high-pressure needle valve, are included.

WASHINGTON, May 11, 1920.

Digitized by Google

JAN 24 1922

DEPARTMENT OF COMMERCE

SCIENTIFIC PAPERS

OF THE

BUREAU OF STANDARDS

S. W. STRATTON, DIRECTOR

No. 420

SPECIFIC VOLUME OF LIQUID AMMONIA

BY

C. S. CRAGOE, Associate Physicist
D. R. HARPER 3d, Physicist
Bureau of Standards

OCTOBER 15, 1921

PRICE, 5 CENTS

Sold only by the Superintendent of Documents, Government Printing Office
Washington, D. C.

WASHINGTON
GOVERNMENT PRINTING OFFICE
1921

Digitized by Google

Digitized by Google

SPECIFIC VOLUME OF LIQUID AMMONIA

By C. S. Cragoe and D. R. Harper 3d

ABSTRACT

The specific volume—that is, the numerical reciprocal of density—of pure liquid ammonia under the pressure corresponding to saturation conditions was determined throughout the temperature interval −78 to +100° C, with an accuracy of about 1 part in 10 000. A comprehensive review of previous work is included. Tables of specific volume and density in both metric and English units are appended.

CONTENTS

	Page
I. Introduction	287
II. Previous measurements	288
III. Description of method and design of picnometers	292
IV. General description of apparatus	295
1. Picnometers	295
2. Balance and weighing chamber	297
3. Thermoregulated bath	297
4. Thermometers	298
V. Calibration of picnometers	298
VI. Purification of samples and description of picnometer fillings	301
VII. Results of measurements	304
VIII. Form of empirical equation to represent specific volume of liquid ammonia as a function of temperature	307
IX. Discussion of results	309
X. Summary	311
Appendix:—Tables of specific volume and density of liquid ammonia under saturation pressure in metric and English units	313

I. INTRODUCTION

The extensive use of ammonia in the refrigerating industries lends commercial importance as well as scientific interest to the accurate measurement of its physical properties. Among the properties which are necessary to the preparation of engineering tables for this industry is the specific volume, namely the volume occupied by unit mass, or the numerical reciprocal of density.

Direct measurements of this property of the vapor under saturation conditions were undertaken at this Bureau some time ago. The method employed in these measurements (which will be published later) required an accurate knowledge of the specific volume

Digitized by Google

of the saturated liquid; that is, under the pressure corresponding to saturation conditions. It was to meet this requirement that the measurements here presented were made. They serve also as a convenient means of the several samples of ammonia purified by somewhat different methods and used in the determinations of the various thermodynamic properties of ammonia.[1]

II. PREVIOUS MEASUREMENTS

The earliest measurements were made with apparatus that did not lend itself to precision work, and also under very unfavorable conditions, so that no great significance is to be attached to the results. They have historic interest, in common with pioneer measurements of any kind, and are accordingly summarized in Table 1, but do not merit individual detailed discussion. For comparison, the authors' results are included in the last column.

TABLE 1.—Early Measurements of the Specific Volume of Liquid Ammonia, in Cubic Centimeters per Gram

Temperature in degrees centigrade	Faraday[a] (1823)	Andreef[b] (1859)	Jolly[c] (1861)	Lange[d]	Lange and Herz[e] (1897)	Urban[f] (1897)	Bureau of Standards (1920)
−20					1.47		1.4545
−10		1.540					1.5328
−5		1.555					1.5496
0		1.571	1.604				1.5669
+5		1.588					1.5851
+10	1.52	1.605					1.6008
+15		1.625					1.6198
+15.5	1.568						1.6312
+20		1.642		1.626			1.6386
(?)						1.69	

[a] Phil. Trans. Roy. Soc., London, 113, p. 197; 1823. Phil. Trans. Roy. Soc., London, 135, p. 169; 1845. Collected works, edition of 1859, pp. 95 and 114.

[b] Ann. d. Chemie und Pharmacie (Liebig's), 110, p. 1; 1859.

[c] Ann. d. Chemie und Pharmacie (Liebig's), 117, p. 281; 1861. Phil. Mag. (4), 21, p. 364; 1861.

[d] Taschenbuch der soda industrie (inaccessible, and figures taken from Lange, see footnote e).

[e] Zeitschrift für angewandte chemie, p. 224; 1897.

[f] Chemikerzeitung, 21, p. 790; 1897.

The first measurement worthy of detailed consideration is that made by Lange[2] in 1898. The method was to fill a bomb almost full of ammonia at a temperature somewhat below that desired for a determination, connect the bomb to a manometer, and immerse it in a bath the temperature of which could be raised at a suitable rate. Complete fullness of the system was indicated by the

[1] Latent heat of vaporization, B. S. Bull., 14, p. 439; 1917 (Scientific Paper No. 315). Specific heat, B. S. Bull., 14, p. 397; 1917 (Scientific Paper No. 313). Vapor pressure, B. S. Bull., 16, p. 7; 1920 (Scientific Paper No. 369).

[2] Chemische Industrie, 21, p. 191; 1898. Za. f. d. gesamte kälte-industrie, 5, p. 39; 1898.

Digitized by Google

manometer changing its rate of rise from that corresponding to increase of vapor pressure to that corresponding to the expansion of the liquid. The temperature was then noted, the outlet valve of the bomb closed so as to entrap a definite volume of ammonia, and the temperature at once lowered to prevent bursting. Necessary weighings and volumetric calibrations supplied the data for the density. An effort was made to exclude errors due to air. For temperatures below that of the weighing room, a modification of the above method was made by introducing a series of overflow or spill bombs. The principles were not altered, only a considerable increase made in the number of necessary weighings. The series of determinations, made with a bomb of about 1.17 liters capacity, is given in Table 2.

TABLE 2.—Measurements by Lange

Temperature in degrees centigrade	Specific volume	Temperature in degrees centigrade	Specific volume
	cm³/g		cm³/g
−49	1.4403	+36.7	1.7221
−35	1.4747	+40.8	1.7425
−32.5	1.4832	+44.7	1.7630
−31.2	1.4881	+48.6	1.7838
−25	1.5036	+52.5	1.8051
−16.2	1.5306	+56.4	1.8275
−10.2	1.5413	+60.2	1.8505
− 6	1.5605	+63.6	1.8727
0	1.5770	+71.6	1.9301
+ 6	1.5985	+75.8	1.9623
+ 7.9	1.6090	+78.8	1.9869
+14.7	1.6284	+81.8	2.0139
+19.4	1.6469	+84.7	2.0412
+23.9	1.6647	+90.2	2.0960
+28.4	1.6838	+97.8	2.1853
+32.6	1.7021		

Lange computed a smoothed table of results from the above data. These are given in Table 5, and the percentage deviations from the results of the present work are plotted as a smooth curve in Fig. 1. The report of the work is comprehensive and offers fair information for analysis, but it has not seemed possible to locate a probable error of 1 per cent throughout the range.

The measurements by Dieterici and Drewes[3] were made in calibrated glass containers. The method employed is discussed briefly in the following section. An accuracy of 0.1 per cent is claimed for the results, but the report is entirely lacking in those details which would permit an independent estimate of final accuracy, or even the precision attainable in the apparatus used. The individual observations show an average deviation from the mean

[3] Za. f. d. gesamte kälte-industrie, 11, p. 21; 1904.

Digitized by Google

curve of about 1 part in 1000. The observations extended from 0 to +105° C and are given in Table 3. Dieterici gives a table of interpolated values between 0 and 100° C which are shown in Table 5.

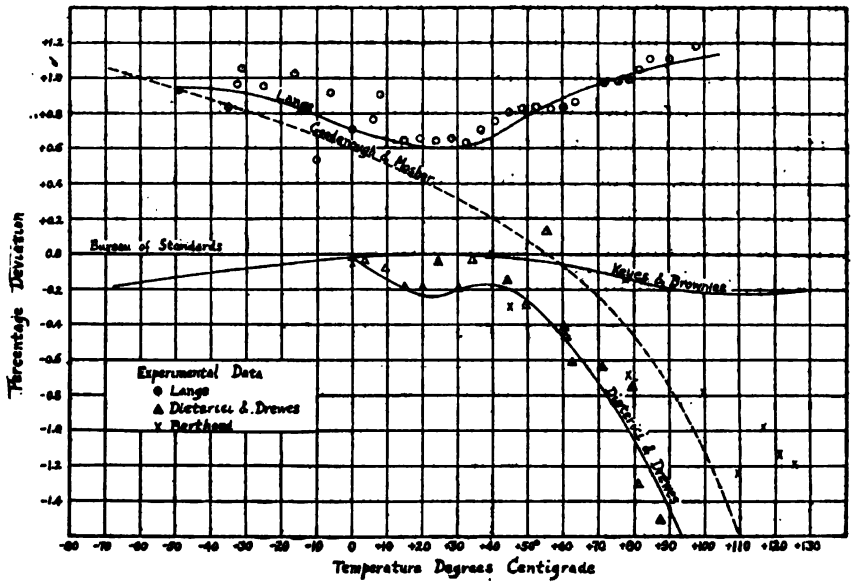

FIG. 1.—*Comparison of laboratory measurements, since 1898, of the specific volume of anhydrous liquid ammonia under saturation pressure*

(The dotted curve is from the tabulation by Goodenough and Mosher and does not represent an independent laboratory measurement.) The scale adopted was selected so that a deviation of 1 part in 10 000 can be distinguished

TABLE 3.—Measurements by Dieterici and Drewes

By Dieterci		By Drewes	
Temperature in degrees centigrade	Specific volume	Temperature in degrees centigrade	Specific volume
	cm³/g		cm³/g
0	1.5656	55.4	1.8090
3.0	1.5769	60.4	1.8289
9.5	1.5977	60.9	1.8309
15.0	1.6161	62.8	1.8403
20.1	1.6358	71.1	1.8957
24.65	1.6565	79.8	1.9619
30.3	1.6778	81.2	1.9618
34.3	1.6983	87.2	2.0119
39.3	1.7221	92.6	2.0524
44.4	1.7448	98.1	2.1211
49.6	1.7695	102.1	2.1878
		105.6	2.2425

Fitzgerald[4] in his work with ammonia solutions made several determinations of the specific volume of liquid ammonia at −33.5°.

[4] J. Phys. Chem., 16, p. 654; 1912.

Digitized by Google

He obtained as the mean of seven determinations 1.4652 cm ^{3}/g, which agrees with the authors' measurements to about 1 part in 1000.

In the research laboratory of the Massachusetts Institute of Technology, Keyes and Brownlee[5] made a series of absolute measurements of specific volume at the normal boiling point, 0°, and +35° C, in a special picnometer, and a series of relative measurements at higher temperatures in a calibrated steel piston chamber. The specific volume at +35° C was chosen as the reference point, and the increase in volume at higher temperatures was measured at pressures slightly greater than the saturation pressure. The individual determinations, made at about −33.5, 0, 35, 68, 110, 120, and 125° C, are not recorded. Values are tabulated at 20° intervals from −50 to +120° C, which are shown in Table 5. The agreement with the results of the present work is remarkably good, as shown in Fig. 1.

Berthoud[6] recently published his results on the specific volume of the saturated liquid and vapor of ammonia at high temperatures obtained in an attempt to determine the critical volume. Two calibrated glass tubes of different volumes were immersed in the vapors of various liquids boiling under a constant pressure, and the volumes of the liquid and vapor were observed in each tube. The temperatures in each experiment were obtained from the vapor-pressure curve of the particular liquid employed. No details are given which would permit an estimate of the precision attained. The results obtained are reproduced in Table 4. Berthoud plotted the observed liquid and vapor densities against temperature and estimated the critical density from the "slightly curved" rectilinear diameter. He gives no reason for the apparently arbitrary choice of the critical temperature.

TABLE 4.—Measurements by Berthoud

Temperature in degrees centigrade	Specific volume	Temperature in degrees centigrade	Specific volume
	cm ^{3}/g		cm ^{3}/g
0.00	1.5652	121.30	2.6103
45.00	1.7556	123.20	2.6667
78.70	1.9531	125.45	2.7902
98.75	2.1532	129.60	3.0809
109.25	2.3047	(132.30)	(4.2337)
119.40	2.4655		

[5] Thermodynamic properties of ammonia, John Wiley & Sons; 1916. J. Am. Soc. Refrigeration Engineers, 1, pp. 34; 1914.

[6] Helvitica chemica acta, 1, p. 84; 1918.

Digitized by Google

TABLE 5.—Specific Volume of Ammonia under Saturation Pressure

[Smoothed values based on experimental measurements]

Temperature in degrees centigrade	Specific volume				
	Lange [a] (1898)	Dieterici [b] (1904)	Goodenough and Mosher [c] (1913)	Keys and Brownlee [d] (1916)	Bureau of Standards (1920)
	cm³/g	cm³/g	cm³/g	cm³/g	cm³/g
−50	1.4380	.....	1.4377	1.4227	1.4245
−40	1.4631	.....	1.4621	.....	1.4493
−30	1.4892	.....	1.4876	1.4745	1.4757
−20	1.5167	.....	1.5151	.....	1.5037
−10	1.5458	.....	1.5439	1.5332	1.5338
0	1.5770	1.5636	1.5751	1.5657	1.5660
+10	1.6111	1.5985	1.6008	.....	1.6008
+20	1.6483	1.6342	1.6456	1.6367	1.6385
+30	1.6898	1.6765	1.6856	.....	1.6800
+40	1.7373	1.7227	1.7298	1.7256	1.7257
+50	1.7908	1.7719	1.7786	.....	1.7766
+60	1.8505	1.8250	1.8329	1.8331	1.8341
+70	1.9183	1.8875	1.8970	.....	1.9000
+80	1.9964	1.9595	1.9700	1.9747	1.9774
+90	2.0947	2.0390	2.0550	.....	2.0708
+100	2.2114	2.1525	2.1660	2.1836	2.1885
+120	.....	.....	2.4050	2.5891	2.5948

[a] Chemische Industrie, 21, p. 191; 1898.
[b] Za. f.d. gesamte kälte-industrie, 11, p. 81; 1904.
[c] These values are taken from Goodenough and Mosher's tables, Properties of saturated and superheated ammonia, University of Illinois Experiment Station Bulletin, 68; 1913.
[d] Thermodynamic Properties of Ammonia, John Wiley & Sons, 1916; J. Am. Soc. Refrigeration Engineers, 1, p. 34; 1914.

III. DESCRIPTION OF METHOD AND DESIGN OF PICNOMETERS

The method employed in the measurement of the specific volume of the liquid under saturation pressure was similar to that used by Dieterici.[7] It consists essentially in observing, at various temperatures, the volumes of the liquid and vapor phases in equilibrium in a closed vessel.

Assuming that the two phases, liquid and vapor, are present and in equilibrium—that is, saturated—and that the walls of the vessel in the vapor space are dry, then at any given temperature the total mass of ammonia, M, in any closed vessel is given by the equation:

$$M = \frac{v}{u} + \frac{V - v}{u'}, \qquad (1)$$

where u and u' represent the specific volume of the liquid and vapor, respectively, V the total volume of the vessel, and v the volume of the liquid. In any experiment under saturation conditions the walls of the vapor space are very likely to be wet with a

[7] Za. f. d. gesamte kälte-industrie, 11, p. 81: 1904.

Digitized by Google

thin film of liquid unless special precautions are taken to avoid this. However, if the volume of the vapor space is small, the mass of this film of liquid will be small in comparison with the total mass.

The method employed by Dieterici was to fill two vessels of different total volumes with equal masses of ammonia. Both vessels were immersed simultaneously in a thermoregulated bath, and observations were taken of the volume of liquid in each vessel. He then computed the ratio of the specific volumes at the various observed temperatures by the expression:

$$R=\frac{u'}{u}=\frac{(V_2-v_2)-(V_1-v_1)}{v_1-v_2},$$

where the subscripts refer to vessels 1 and 2. With these values of R the specific volume of the liquid was obtained from the measurements with the smaller vessel by means of the relation

$$u=\frac{v}{M}+\frac{V-v}{MR},$$

and finally u' from $Ru=u'$.

In the present investigation the procedure was simplified somewhat by designing vessels, here called picnometers, of widely different total volumes and filled with unequal masses of ammonia. From equation (1) the specific volume of the liquid and vapor may be expressed, respectively, as:

$$u=\frac{v}{M-\frac{V-v}{u'}},$$

$$u'=\frac{V-v}{M-\frac{v}{u}},$$

in which M, V, and v are the measurable quantities. It will be noted that both specific volumes u and u' occur in each equation, but by suitable design of picnometers the terms $\frac{V-v}{u'}$ or $\frac{v}{u}$ may be made small in comparison with M such that they enter only as small correction terms. This may be accomplished with comparative ease in the determination of the specific volume of the liquid by designing picnometers of sufficient volume so that M,

Digitized by Google

V, and v are easily measurable to the precision desired (about 1 part in 10 000 in the present case) and so that the mass of the vapor, $\frac{V-v}{u'}$, is not over 0.1 per cent of the total mass. Then by the use of approximate values of u' (within 10 per cent), u can be determined with the desired precision.

For determinations of the specific volume of the vapor, it is difficult and inconvenient to make the mass of the liquid, $\frac{v}{u}$, small in comparison with the total mass, especially at low temperatures, and it appeared desirable to determine first the specific volumes of the liquid with fair precision in order to make this correction with a satisfactory degree of certainty.

In a series of measurements of the specific volume of the liquid, the volume of the liquid in the picnometer was observed by reading at various temperatures the position of the meniscus upon a previously calibrated scale. The temperature of the thermoregulated bath was maintained constant to 0.01 or 0.02° C for an interval of about one-half hour and readings of the ammonia meniscus taken at 5-minute intervals. The effect of drainage or evaporation of the liquid was found to be small, equilibrium being reached usually within 10 minutes. The total volume of the picnometer was obtained from its calibration at the highest scale division visible and adding to this the estimated volume of the tip formed in sealing off. Both of these volumes were, of course, corrected for temperature and pressure changes. The total mass of ammonia in the picnometer was a constant during any series of measurements and was usually determined afterwards by weighing the picnometer filled with ammonia, then breaking the tip, and reweighing filled with dry air.

Considerable care was exercised in the determination of the mass. A short deep scratch was made at the tip of the picnometer with a diamond or special glass-cutting tool. The picnometer was then cleaned with chromic acid, water, and acetone, successively. After being permitted to hang in the weighing chamber for nearly an hour, in order to come to temperature equilibrium, it was weighed independently by two observers. In all of the weighings a counterpoise of equal external volume was employed and weighings were made by substitution. The picnometer was then cooled with a mixture of solid carbon dioxide and gasoline, or with commercial liquid ammonia until the pressure inside was less than atmospheric and by applying a heated

Digitized by Google

glass rod the tip was broken carefully, so as to lose no glass by splintering. The picnometer was then evacuated several times, filled with dry air and weighed, as before, by two observers.

In the earlier determinations an attempt was made to obtain a check on the total mass of ammonia by absorbing it in an evacuated flask of concentrated sulphuric acid of known weight. For this operation a small steel tube was inclosed in rubber tubing connecting the picnometer and acid flask. Just enough length of rubber tubing was used to furnish the necessary flexibility for breaking the tip of the picnometer with the steel tube. Considerable difficulty was experienced in getting good, clean breaks. A small mercury manometer was sealed into the neck of the acid flask which served to indicate any leakage of air into the flask during the operation. From the observed increase in pressure, which was usually small, a correction was applied for the weight of this air leakage. The results obtained by this method were consistently lower by about 1 or 2 mg—that is, about 1 part in 2000 of the total mass—than those obtained by the method of direct weighing, which discrepency was probably due to the action of the ammonia on the rubber tubing. No weight was given in the final results to the mass determinations by this method because of the great uncertainty as to the action of the ammonia on the rubber.

In the later determinations the total mass of ammonia was measured before filling the picnometer, as well as after each series of measurements. For this purpose a small auxiliary tube was used which consisted of a graduated glass tube soldered to a steel needle valve by a method described in another communication from this laboratory.[8] This auxiliary tube was evacuated and weighed, then filled with approximately the desired amount of ammonia and weighed again. The total mass determined in this manner agreed in each case, within better than 1 part in 10 000 with that determined later by the direct weighing of the picnometer filled and empty. A different balance and a different set of weights were used for the two determinations.

IV. GENERAL DESCRIPTION OF APPARATUS

1. PICNOMETERS

The picnometers used in these measurements were made from soda glass and annealed thoroughly. Capillary tubing of about 2 mm internal diameter and 3 mm wall thickness was selected with

[8] McKelvy and Taylor, J. Am. Chem. Soc., 42, p. 1364; 1920.

Digitized by Google

special attention to uniformity of bore. Scales were etched upon those capillary tubes by ruling divisions at intervals of 1.5 mm with a dividing engine.

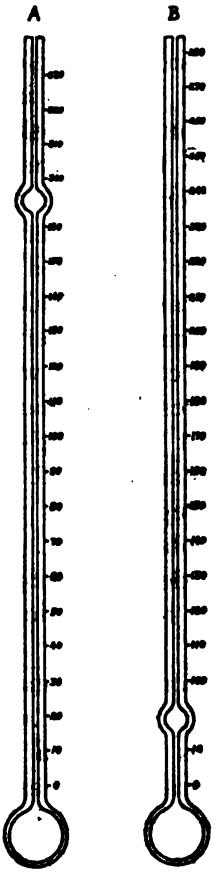

FIG. 2.—*Sketch of picnometers, showing position of arbitrary scaling (Tables 6 and 7)*

Picnometer A used for lower part of temperature range, with one check reading at high temperature; B for higher part of range with one check at a low temperature

Two types of picnometers were used (Fig. 2). Type A was used in the measurements considerably below room temperature, usually from 0 to −50° C. The small upper bulb served as an expansion reservoir for the ammonia when at room temperature. The volume of this upper bulb was so adjusted as to give a measurement at about +40° C and thus afford a means of comparison with measurements in the other types.

Digitized by Google

Similarly in type B, the short capillary between the two bulbs permitted one measurement at a low temperature for the purpose of comparison. This design proved to be very convenient in filling with approximately the desired amount of ammonia, which was accomplished by immersing the bulb in liquid ammonia exposed to the air and condensing just enough liquid to bring the meniscus into this short capillary. The upper capillary was of sufficient length to permit measurements over a range of about 50° C.

2. BALANCE AND WEIGHING CHAMBER

The balance used in the calibrations of the picnometers and in the determinations of the mass of ammonia was made by A. Collot, Paris. It was equipped with air dashpots to make the swings practically aperiodic. The picnometers were suspended in a closed chamber directly beneath the balance by means of small rods connected to the scale pans. Weighings could be made to about 0.1 mg. The weights used in all the weighings were calibrated by the weights and measures division of this Bureau and corrections given to 0.01 mg.

3. THERMOREGULATED BATH

The thermoregulated bath used in all of the measurements consisted of a cylindrical Dewar vacuum flask of about 6 liters capacity. The temperature regulating mechanism was assembled as a unit in a long cylindrical brass tube about one-fourth the diameter of the flask, so as to leave more than three-fourths of the useful area available for introduction of the picnometers. This regulating unit included a motor-driven direct-connected screw propeller stirrer, an electric heating coil, a carbon dioxide expansion cooling coil, and a thermostat coil filled with toluene. A fixed contact in the thermostat head served to maintain the temperature constant to about 0.01°. The details of the construction of a similar unit have been previously described.[9] The liquid used in the bath for the temperature interval −50 to +50° C was a mixture of about 65 per cent carbon tetrachloride and 35 per cent gasoline, a mixture selected with reference to fluidity and transparency at temperatures down to −50° C, combined with maximum safety from fire hazard when at room temperature or warmer. The volatile hydrocarbons which meet the greatest number of requirements

[9] Osborne, B. S. Bull., 14, p. 145; 1917 (Scientific Paper No. 301).

Digitized by Google

of a low-temperature bath are not safe alone in proximity to electric motors and heating circuits which may possibly fail and spark but the admixture of a large carbon tetrachloride content makes the fluid entirely safe in this respect and does not destroy transparency to a serious degree, provided reasonable precautions are taken to exclude atmospheric moisture from getting dissolved in it and freezing out when cooled. The flash point was about +50° C. For temperatures in the interval +50 to +100° C a high boiling point kerosene was used. As a protection from possible failure of the picnometers under pressure and also failure of the Dewer flask itself, the bath was inclosed in a metal case which was provided with celluloid windows about 3 mm in thickness.

4. THERMOMETERS

In the earlier measurements mercurial thermometers graduated in tenth-degrees were used over the temperature interval −30 to +50° C. These thermometers were calibrated against platinum resistance thermometers. Below −30° C Baudin toluene thermometers were used in the first series, but were found to be unreliable to better than 0.1°, due to drainage. In the later measurements resistance thermometers were employed in this region and also at higher temperatures, together with mercurial thermometers. The Wheatstone bridge used in connection with the resistance thermometers was of the 4-dial type and has been described previously.[10]

V. CALIBRATION OF PICNOMETERS

The volume per scale division of the capillaries in each picnometer was determined by the usual method of observing the lengths of a mercury thread of known mass. Threads of different lengths were used. A check on this value of the volume per scale division was obtained from the calibration at various divisions on the scale.

Distilled water and mercury, which had been purified by the anode process and by distillation, were used in the volumetric calibrations. Volumes were determined by observing the level of the meniscus at a given temperature, usually 20° C, weighing in air, and using the factor given in the Landolt and Börnstein tables of physical and chemical constants, which contain the

[10] B. S. Bull., 13, p. 547; 1916 (Scientific Paper No. 288).

Digitized by Google

buoyancy and specific volume corrections.[11] Special precautions were taken in the calibrations with water to dry the walls of the capillary above. The portion of the picnometer filled with liquid was immersed in ice and the upper space evacuated to a pressure of about 1 mm.

Readings were taken upon the lower surface of the concave water meniscus and upon the upper surface of the convex mercury meniscus which, of course, introduced a systematic difference between the two calibrations. As an illustration of this, the initial calibration of picnometer A is given in Table 6.

TABLE 6.—Initial Calibration of Picnometer A

Calibration with—	Volume in cubic centimeters to scale division—		
	10	160	320
Mercury	4.8143	5.3058	5.8702
Do	4.8145	5.3057	5.8702
Water	4.8154	5.3066	5.8714
Do	4.8158	5.3070	5.8715
Mean water	4.8156	5.3069	5.87145
Mean mercury	4.8144	5.3055	5.8702
Difference	0.0012	0.0013	0.00125

Assuming that the shapes of the water and mercury menisci are concave and convex hemispheres, respectively, in capillaries of the particular size used (about 2 mm in diameter), the difference in the volume determined by reading to any graduated mark is equal to the difference between the volume of a sphere and its circumscribed cylinder whose length and diameter are the diameter of the capillary. Numerically the difference is

$$2r\,(\pi r^2) - \frac{4}{3}\pi r^3 = \frac{2}{3}\pi r^3,$$

where r is the radius of the capillary. The diameter of the capillary in the preceding illustration was found from the calibration to be 1.66 mm, which gives for the calculated difference in volume 0.0012

[11] Although the Landolt-Börnstein tables are labeled cubic centimeters, the factor given actually reduces volumes to milliliters rather than to cubic centimeters, but the difference in the two units is insignificant for the results of work described in this paper. The volume of 1 kg of water at 4° C, defined as 1 liter, is 1000.027 cm³, namely, differs from a cube of 10 cm edge by about 27 parts in 1 000 000. The final results of this paper are carried to the point where 1 or 2 parts in 10 000 have significance; one more decimal place is retained in the intermediate stages—that is, volume measurements are recorded to 1 part in 50 000 (20 parts in 1 000 000)—but the last figure is in doubt by considerably more than a single unit, and the distinction between milliliters and cubic centimeters for its expression may well be neglected.

Digitized by Google

cm³. The results from several calibrations indicate that the above method of calculating the difference in volume between the two menisci is fairly reliable for capillaries of the particular dimensions used.

Since liquid ammonia wets the walls of the tube and has a meniscus similar to that of water, the desired volumes are obviously those determined by the calibrations with water. The calibrations with mercury, however, are probably the more accurate. The final volumes adopted were obtained from the mean of several mercury calibrations plus the calculated correction for the shape of the meniscus. These agreed well in most cases with the mean of the water calibrations.

The pressure coefficient of expansion of each picnometer was determined by applying air pressure from a cylinder of compressed air with the picnometer almost completely filled with water. Readings were taken at intervals of 5 or 10 atmospheres up to 50 atmospheres. The value for the compressibility of water obtained from the Landolt and Börnstein tables was taken as 45×10^{-6} per atmosphere. The expansion with pressure was small and appeared to be uniform over the above range of pressure.

The temperature coefficients of expansion of picnometers A and B between -20 and $+40°$ C were measured by observing the apparent change in volume of a known weight of mercury. The difference between the observed volume change and the expansion of the mercury (taken from Landolt and Börnstein physical tables) furnished an approximate value for the expansion coefficient of the glass. The results obtained by this method were inconsistent, the values for the temperature coefficient of cubical expansion varying from 0.000025 to 0.000028 per degree centigrade. The coefficient of linear expansion of a sample taken from picnometer B was determined by C. G. Peters of this Bureau, using a Fabry and Perot interferometer. He obtained the value 9.8×10^{-6}. The temperature coefficient of cubical expansion used throughout the measurements here presented was based upon the above determination and taken as 2.9×10^{-5} per degree centigrade.

The final results of the picnometer calibrations are given in Table 7. The capillaries selected were found to be so uniform that application of the caliber corrections would not have changed any result by more than 1 part in 10 000. Interpolation was effected by the use of the factors—volume per scale division. The initial calibration of A was used in the calculations of the first

Digitized by Google

series of specific volume measurements (Table 8). In the process of filling A the second time a small crack developed in the capillary at about the 140 scale division, probably caused by cooling too rapidly with liquid air. This crack was healed and the picnometer recalibrated after the second series of measurements. The lower bulb of A was accidentally broken in cleaning preparatory to filling the third time and a new one blown. The third calibration was made after the measurements of series 5. The pressure coefficient of expansion of A with its new lower bulb was not determined, since measurements were taken only at low pressures.

TABLE 7.—Final Results of Picnometer Calibrations

Date	Volume in cubic centimeters to scale division—				Volume per scale division in cubic centimeters	Increase in volume per unit volume	
	10	130	160	300		Per atmosphere	Per degree centigrade
PICNOMETER A_1							
February, 1915	4.8156	.....	5.3067	5.8201	0.00327	0.000009	0.000029
March, 1916	4.8158	5.2089	5.3068	5.8143	.00327	.....	.....
February, 1917	6.1768	6.5699	6.6618	7.1743	.00327	.....	.....
PICNOMETER A_2							
	10	50	150	300			
May, 1920	4.3993	4.7065	5.4007	6.3313	.00694	.000009	.000029
PICNOMETER A_3							
	100	150	200	300			
July, 1918	5.6205	5.8424	6.0642	6.3664	.00444	.000010	.000029
PICNOMETER B							
	5	100	200	300			
December, 1915	5.0112	5.6205	6.0642	6.5079	.00444	.000010	.000029
May, 1920	5.0113	5.6201	6.0644	.....	.00444	.....	.....

VI. PURIFICATION OF SAMPLES AND DESCRIPTION OF PICNOMETER FILLINGS

The ammonia used in these measurements was prepared by McKelvy and Taylor of the chemical division of this Bureau, by four methods described more in detail in an independent paper.[12]

[12] To be published later.

Digitized by Google

Only a brief description of the processes of purification will therefore be given here.

METHOD 1.—A commercial sample in which no traces of pyridine or ammonium acetate could be detected chemically and which showed a very small residue on evaporation was used as the starting material. This material was converted into ammonium sulphate by passing the gas into sulphuric acid after it had been passed through a tube containing lime heated to a red heat. The ammonium-sulphate solution obtained was heated with sodium hydroxide and the ammonia gas thus liberated. The gas was dried by passing it through an all-glass train of potassium hydroxide, ignited lime, and barium oxide, and was then condensed in a glass bulb cooled with a mixture of carbon dioxide and petroleum ether. The ammonia was then fractionally distilled several times, frozen with liquid air repeatedly, and then frozen by its own evaporation, the vapor being pumped off through a vacuum pump. The final products obtained by the above procedure are designated in Table 8 as samples F, G, and H.

METHOD 2.—A sample of ammonia the same as the one used in method 1 was used as the starting material. This was transferred by distillation into a small steel container which would hold about a kilogram. The first portion was discarded and the middle portion was distilled into a similar vessel containing metallic sodium in the form of a fine wire to remove any traces of water. Following this dehydration the liquid was distilled into a high-pressure fractional-distillation apparatus and fractionally distilled 8 times, rejecting the first and last fractions (a little less than 0.1 the total volume of the liquid) in each distillation. The product thus obtained was distilled into a vacuum-fractional distillation apparatus of glass and fractionally distilled about 10 times, the first and last portions being rejected in each case. The ammonia was then frozen in liquid air and the residual vapor and gas were pumped off. The ammonia was then allowed to warm up until it was entirely liquid and some of the vapor was escaping through a mercury seal. It was again frozen in liquid air and the vapor pumped off as before. This process was repeated several times. Finally the ammonia was frozen into small flocculent crystals by its own evaporation, the resulting vapor being pumped off and discarded. This final product, designated sample L in Table 8, was used for filling the picnometers.

METHOD 3.—This method was the same as method 2, except that a sample of synthetic ammonia made by the Haber process

Digitized by Google

was used as a starting material, instead of the sample previously described. This synthetic sample proved to be extremely pure except for a comparatively large amount of water, which was easily removed by means of the metallic sodium. The samples designated I and P in Table 8 were prepared by this method.

METHOD 4.—The procedure employed in this method was similar to that followed in method 2, using the same source of ammonia, the dehydration with metallic sodium, and the high-pressure fractional distillations. No vacuum fractional distillations were made. The sample designated A in Table 8 was prepared by this method.

The tests for purity on the final samples of ammonia obtained from the above methods gave the following results: Water, less than 0.003 per cent, by weight, which was the limit of sensitivity of the chemical test applied; noncondensing gases, from approximately 1 part in 10 000 to 1 part in 1 000 000, by volume.

The picnometers were cleaned with a mixture of concentrated nitric and sulphuric acids, aqueous potassium hydroxide solution, and washed with distilled water. The upper ends of the picnometers were always constricted so as to facilitate satisfactory seals. They were then sealed directly into the glass line of the vacuum-distillation apparatus and evacuated to a pressure less than 0.001 mm of mercury. After a sufficient quantity of the purified ammonia had been distilled into one of the picnometers, the supply reservoir was cut off by closing an intervening stopcock and the ammonia frozen by means of liquid air. The vapor phase was pumped off with the aid of a high-vacuum pump, and the picnometer was sealed by fusing the constricted capillary. The method of filling with approximately the desired amount varied somewhat. In most instances commercial liquid ammonia in an open Dewar flask was used as a cooling agent to condense the desired amount into the picnometers directly, or into a small graduated tube of known volume for transfer by distillation into the picnometers. A mixture of carbon dioxide and petroleum ether was sometimes used for cooling. In the last fillings, for the measurements at the higher temperatures, it was necessary to exercise particular care to fill within a few milligrams of the desired mass. For this purpose a small glass tube, soldered to a steel needle valve, was filled with a slight excess of ammonia and then small amounts were blown off through the valve. This method proved very convenient in adjusting to the required amount and also furnished an excellent check upon the mass

Digitized by Google

determinations, since the auxiliary tube lent itself most readily to direct weighings.

VII. RESULTS OF MEASUREMENTS

The results of all the measurements of the specific volume are collected in Table 8. They have been divided into separate series, since each series consists of measurements with a particular sample, picnometer, and filling. The various factors which enter into the results have also been included.

TABLE 8.—Measurements of Specific Volume of Liquid Ammonia

SERIES 1

Date	Sample	Picnometer	Reading of meniscus	Volume of liquid, v	Total mass NH_3, M	Volume of vapor, $(V-v)$	Mass of vapor, $\frac{(V-v)}{u'}$	Temperature of experiment	Specific volume of liquid, u	Deviations from equation
			Scale division	cm³	g	cm³	g	°C	cm³/g	Parts in 100 000
Nov. 20, 1915.....	F	A_1	300.6	5.8272	3.3400	0.093	0.0013	+44.01	1.74535	−4
	F	A_1	316.2	5.8538	3.3400	.056	.0008	+46.02	1.75605	+10
Nov. 26, 1915.....	F	A_1	4.5	4.7890	3.3400	1.119	.0005	a−46.02	1.43405	−10
	F	A_1	49.5	4.9192	3.3400	.998	.0010	a−30.66	1.47326	−42
	F	A_1	89.5	5.0706	3.3400	.840	.0017	−14.80	1.51892	−11
	F	A_1	134.7	5.2209	3.3400	.692	.0029	− .53	1.56422	− 1
Nov. 27, 1915.....	F	A_1	300.9	5.8282	3.3400	.092	.0013	+44.07	1.74555	−10
	F	A_1	317.2	5.8577	3.3400	.053	.0007	+46.22	1.75695	+16
	F	A_1	89.4	5.0703	3.3400	.840	.0017	−14.83	1.51888	−11
	F	A_1	134.6	5.2206	3.3400	.764	.0023	− .50	1.56413	− 1
	F	A_1	161.5	5.3097	3.3400	.605	.0027	+ 7.28	1.59102	− 3
Nov. 29, 1915.....	F	A_1	4.8	4.7898	3.3400	1.117	.0005	a−45.87	1.43429	−18
	F	A_1	49.2	4.9172	3.3400	.992	.0010	a−30.89	1.47265	−40
	F	A_1	89.4	5.0703	3.3400	.840	.0017	−14.80	1.51883	−19
	F	A_1	134.7	5.2209	3.3400	.692	.0023	− .56	1.56422	− 5
	F	A_1	161.4	5.3094	3.3400	.605	.0027	+ 7.25	1.59093	− 3
	F	A_1	4.7	4.7895	3.3400	1.118	.0005	a−45.92	1.43439	−18
	F	A_1	43.3	4.9175	3.3400	.992	.0010	a−30.88	1.47275	−36

SERIES 2

Mar. 2, 1916.....	G	A_1	14.0	4.8184	3.3834	1.050	0.0004	−49.96	1.42430	−22
	G	A_1	26.0	4.8582	3.3834	1.020	.0005	−45.12	1.43611	−23
	G	A_1	38.7	4.9008	3.3834	.964	.0006	−40.14	1.44874	−16
	G	A_1	66.3	4.9921	3.3834	.857	.0009	−29.87	1.47586	−11
	G	A_1	108.7	5.1329	3.3834	.738	.0014	−15.22	1.51771	− 8
Mar. 3, 1916.....	G	A_1	303.6	5.8307	3.3834	.051	.0007	+39.55	1.72369	+ 9
	G	A_1	132.3	5.2119	3.3834	.660	.0017	− 7.57	1.54120	−12
	G	A_1	159.2	5.2949	3.3834	.579	.0026	− .05	1.56589	+ 4
Mar. 6, 1916.....	G	A_1	14.5	4.8200	3.3834	1.050	.0004	−49.68	1.42478	−34
	G	A_1	26.5	4.8600	3.3834	1.020	.0005	−44.88	1.43664	−28
	G	A_1	40.1	4.9051	3.3834	.964	.0006	−39.59	1.45011	−24
	G	A_1	66.2	4.9917	3.3834	.857	.0009	−29.91	1.47574	−12
	G	A_1	109.4	5.1352	3.3834	.736	.0014	−14.94	1.51839	−19
	G	A_1	132.2	5.2116	3.3834	.660	.0017	− 7.63	1.54112	− 5
	G	A_1	159.6	5.2962	3.3834	.578	.0020	+ .05	1.56627	− 6
Mar. 7, 1916.....	G	A_1	302.6	5.8274	3.3834	.054	.0006	+39.27	1.72366	+26

a Temperatures measured with toluene thermometers, uncertainty about 0.1° C.

Digitized by Google

TABLE 8.—Measurements of Specific Volume of Liquid Ammonia—Continued

SERIES 3

Date	Sample	Piezometer	Reading of meniscus	Volume of liquid, v	Total mass NH_3 M	Volume of vapor, $(V-v)$	Mass of vapor, $\frac{(V-v)}{u'}$	Temperature of experiment	Specific volume of liquid, u	Deviations from equation
			Scale division	cm^3	g	cm^3	g	°C	cm^3/g	Parts in 100 000
Mar. 3, 1916.....	G	B	100.5	5.6184	3.6476	0.975	0.0025	− 7.57	1.54135	− 2
	G	B	120.2	5.7071	3.6476	.886	.0031	− .05	1.56595	+ 8
	G	B	148.3	5.8336	3.6476	.762	.0037	+10.00	1.60093	+ 7
	G	B	178.7	5.9701	3.6476	.627	.0043	+20.01	1.63861	− 4
	G	B	212.0	6.1200	3.6476	.479	.0044	+29.98	1.67984	− 6
	G	B	247.4	6.2796	3.6476	.320	.0041	+39.56	1.72351	− 5
	G	B	269.9	6.3805	3.6476	.222	.0032	+45.09	1.75077	− 6
	G	B	291.0	6.4747	3.6476	.127	.0020	+49.90	1.77608	− 2
Mar. 6, 1916.....	G	B	100.4	5.6180	3.6476	.975	.0025	− 7.63	1.54124	+ 3
	G	B	120.4	5.7079	3.6476	.886	.0031	+ .05	1.56617	0
Mar. 7, 1916.....	G	B	246.5	6.2750	3.6476	.825	.0040	+39.27	1.72230	+ 5
	G	B	270.1	6.3812	3.6476	.222	.0032	+45.13	1.75096	− 7
	G	B	290.5	6.4725	3.6476	.131	.0021	+49.80	1.77547	+20
	G	B	148.4	5.8341	3.6475	.761	.0037	+10.00	1.60106	+15
	G	B	179.4	5.9730	3.6476	.624	.0042	+20.23	1.63940	− 9
	G	B	212.6	6.1222	3.6476	.477	.0044	+30.16	1.68043	−16

SERIES 4

Apr. 4, 1916.....	A	B	6.4	5.0077	3.4951	1.508	0.0009	−46.43	1.43386	− 8
Apr. 6, 1916.....	A	B	100.7	5.6228	3.4951	.882	.0047	+12.82	1.61093	−15
	A	B	122.0	5.7186	3.4951	.798	.0053	+20.03	1.63866	− 6
	A	B	154.3	5.8637	3.4951	.665	.0059	+30.10	1.68059	+ 4
	A	B	189.0	6.0198	3.4951	.501	.0060	+39.94	1.72531	− 5
	A	B	208.4	6.1070	3.4951	.416	.0058	+44.99	1.75021	− 9
	A	B	228.4	6.1959	3.4951	.327	.0052	+49.84	1.77566	− 4
Apr. 8, 1916.....	A	B	9.9	5.0296	3.4951	1.483	.0007	−44.62	1.43761	− 4
	A	B	100.8	5.6232	3.4951	.882	.0047	+12.87	1.61104	−19
	A	B	122.4	5.7204	3.4951	.796	.0053	+20.18	1.63917	−10
	A	B	153.3	5.8592	3.4951	.660	.0059	+29.87	1.67924	−14
Apr. 12, 1916.....	A	B	190.0	6.0242	3.4951	.497	.0060	+40.21	1.72658	− 7
	A	B	209.6	6.1128	3.4951	.410	.0058	+45.28	1.75176	− 5
	A	B	229.8	6.2032	3.4951	.320	.0051	+50.17	1.77742	− 4

SERIES 5

Feb. 12, 1917.....	H	A_1	68.6	6.3586	4.3189	0.962	0.0010	−30.99	1.47262	−26
	H	A_1	160.0	6.6563	4.3189	.668	.0018	− 7.42	1.45184	− 1

SERIES 6

Mar. 4, 1917.....	H	B	104.5	5.6392	3.5234	1.022	0.0051	+10.55	1.60282	0
Apr. 4, 1917.....	H	B	135.2	5.7775	3.5234	.886	.0062	+21.00	1.64264	+ 2
	H	B	219.2	6.1850	3.5284	.514	.0071	+44.92	1.75842	+22

SERIES 7

May 29, 1917.....	I	B	6.5	5.0085	3.4908	1.548	0.0008	−45.58	1.43510	−13
June 11, 1917.....	I	B	120.0	5.7102	3.4908	.848	.0057	+19.98	1.63869	+ 8

SERIES 8

Aug. 11, 1917.....	I	B	1.1	4.9901	3.2432	1.541	0.0040	− 7.84	1.54054	0
	I	B	9.4	5.0272	3.2432	1.503	.0045	− 4.18	1.55223	0
	I	B	186.6	5.8549	3.2432	.886	.0122	+44.97	1.75020	− 4
	I	B	125.3	5.7390	3.2432	.802	.0127	+49.94	1.77650	+13

Digitized by Google

TABLE 8.—Measurements of Specific Volume of Liquid Ammonia—Continued

SERIES 9

Date	Sample	Piezometer	Reading of meniscus	Volume of liquid, v	Total mass NH_3, M	Volume of vapor, $(V-v)$	Mass of vapor, $\frac{(V-v)}{u'}$	Temperature of experiment	Specific volume of liquid, u	Deviations from equation
			Scale division	cm^3	g	cm^3	g	°C	cm^3/g	Parts in 100 000
July 9, 1918.....	L	A_3	141.6	5.7928	4.0708	1.737	0.0006	−50.49	1.42323	− 3
	L	A_3	151.6	5.8382	4.0708	1.693	.0008	−45.91	1.43445	− 2
	L	A_3	165.9	5.9009	4.0708	1.631	.0010	−39.70	1.45002	−10
	L	A_3	188.8	6.0037	4.0708	1.529	.0016	−30.04	1.47540	−11
	L	A_3	301.5	6.3678	4.0708	1.171	.0040	0.00	1.56580	−12
SERIES 10										
May 11, 1920.....	P	B	6.5	5.0227	2.8665	1.352	0.0198	+ 47.64	1.76439	+19
May 12, 1920.....	P	B	100.2	5.6333	2.8665	.748	.0255	+ 80.58	1.98286	+29
	P	B	167.0	5.9328	2.8665	.452	.0201	+ 91.24	2.08432	+26
	P	B	206.5	6.1097	2.8665	.276	.0139	+ 96.27	2.14181	+40
	P	B	240.4	6.2617	2.8665	.125	.0069	+100.05	2.18971	+24
SERIES 11										
May 11, 1920.....	P	A_3	301.6	6.3515	3.4625	0.105	0.0022	+60.22	1.83553	+ 6
	P	A_3	311.2	6.4186	3.4625	.039	.0009	+63.22	1.85423	− 3
	P	A_3	152.6	5.4159	3.4625	1.029	.0036	− .03	1.56579	− 8
May 13, 1920.....	P	A_3	82.6	4.7111	3.4625	1.716	.0081	−78.59	1.36065	+ 3

In the temperature interval −50 to +50° C the values for the specific volume of the saturated vapor which enter into the correction for the mass of the vapor were based upon preliminary measurements made at this Bureau, the final results of which will be published in a separate paper. In the interval +50 to +100° C, the vapor specific volumes were obtained by extrapolation of the mean diameter of the temperature-density dome (often called the Cailletet and Mathias rectilinear diameter), Fig. 3. This diameter was found to be represented accurately by a second degree equation.

The scale of temperature used in these measurements is the scale defined by the resistance thermometer of pure platinum, calibrated in ice, steam, and sulphur vapor (444.6° C taken as the normal boiling point of sulphur). Using the Callender equation

$$t=\frac{R_t-R_0}{R_{100}-R_0}\,100+\delta\left(\frac{t}{100}-1\right)\frac{t}{100}$$

as an interpolation equation, the temperature scale so defined represents the centigrade thermodynamic scale in the interval −50 to 450° C to the accuracy with which that scale is at present known, and has been adopted as the standard working scale of

Digitized by Google

this Bureau in that interval. By direct comparison of several platinum resistance thermometers with a constant-volume hydrogen thermometer at temperatures below $-50°$ C, Henning[18] found the corrections necessary to reduce to the gas scale the temperatures determined with the above equation. From Henning's results a correction of $+0.08°$ has been applied to the measurement at $-78.59°$ C

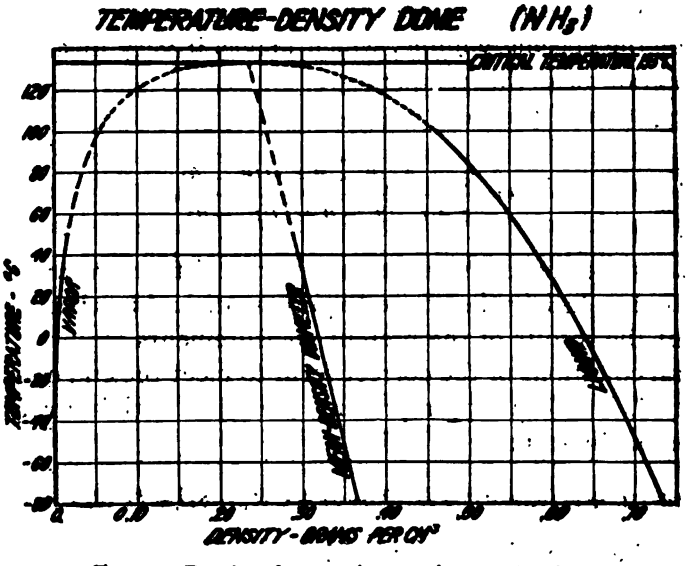

FIG. 3.—*Density of ammonia at various temperatures*

The arithmetical average of the liquid density and vapor density at given temperature locates the abscissa of the mean density diameter for that temperature

Solid lines are located from experimental measurements, dash lines by extrapolation of the diameter. The dotted top of the dome is shaped in accordance with the requirement of meeting the critical temperature line as a tangent at the point of its intersection with the mean diameter. As drawn, it agrees with measurements by Berthoud

VIII. FORM OF EMPIRICAL EQUATION TO REPRESENT SPECIFIC VOLUME OF LIQUID AMMONIA AS A FUNCTION OF TEMPERATURE

A form of empirical equation was sought which would represent the experimental results closely and which would also satisfy the terminal conditions at the critical temperature. To be consistent with our present knowledge of the behavior of substances at the critical temperature, θ_c, the equation should give a finite value for the specific volume, u. and for the derivative $\frac{du}{d\theta}$ should give a value of $+\infty$.

[18] Ann. d. Phys., (4), p. 653; 1913.

Digitized by Google

The Avenarius [14] equation,

$$u = A + B \log (\theta_c - \theta),$$

has frequently been used to express the volume of the liquid as a function of temperature. Using the constants $A = 3.68$, $B = 1$, and $\theta_c = 130$, this equation was found to represent the experimental results in the range -50 to 50° C remarkably well. However, at the critical temperature this equation gives an infinite value for the specific volume, which makes it very unsuitable for extrapolation near this temperature.

An equation of the form [15]

$$u = \frac{u_c + A\sqrt{\theta_c - \theta} + B(\theta_c - \theta)}{1 + C\sqrt{\theta_c - \theta} + D(\theta_c - \theta)},$$

where u_c is the specific volume at the critical temperature, θ_c, has been found to satisfy the above requirements and has been used to represent the results of the present measurements.

Several equations of the correct form to meet the end conditions were tried, but did not represent the data satisfactorily. An equation of the form

$$u = u_c + A(\theta_c - \theta)^{\frac{1}{2}} + B(\theta_c - \theta) + C(\theta_c - \theta)^{\frac{3}{2}} + D(\theta_c - \theta)^2$$

proved to be surprisingly unsuitable.

---

[14] Klewsche universitätsnachrichten, 6, p. 249; 1884 (reference taken from Goodenough and Mosher).

[15] This equation is entirely empirical in that it is based on purely empirical relations. The selection of the particular form was not, however, pure guesswork, a rational development leading to its trial. The Cailletet and Mathias relation for the mean diameter of the temperature-density dome is that of a linear equation between mean density and temperature. Preliminary data obtained for the specific volumes of both the vapor and liquid phases showed that the mean diameter is not strictly linear, but is more exactly expressed by the empirical relation (where ρ = densities; where θ = temperatures):

$$\frac{\rho + \rho'}{2} = \rho_c + A\sqrt{\theta_c - \theta} + B(\theta_c - \theta). \qquad (1)$$

A well-known relation for expressing approximately the vapor pressure of ammonia as a function of temperature is:

$$\log p = A' + \frac{B'}{\theta}. \qquad (2)$$

Osborne and Van Dusen (footnote 1) found the relation between latent heat of vaporisation and temperature to be expressed very closely by the empirical equation:

$$L = A''\sqrt{\theta_c - \theta} + B''(\theta_c - \theta). \qquad (3)$$

Assuming the gas law to hold for saturated vapor ($p = R\rho\theta$), and using the Clapyron equation to eliminate latent heat, the acceptance of the validity of the empirical relations (2) and (3) transforms (1) into the form given in the text of the paper. The justification of the form rests not on the above derivation but solely on the test of applying it to the data obtained in the measurements described in this paper. This test is discussed in the text of the succeeding sections.

Digitized by Google

IX. DISCUSSION OF RESULTS

The results of the measurements may be expressed by means of the following empirical equation:

$$v = \frac{4.2830 + 0.813055\sqrt{133-\theta} - 0.0082861\,(133-\theta)}{1 + 0.424805\sqrt{133-\theta} + 0.015938\,(133-\theta)},$$

where the positive values of the square roots are to be used. The units for θ are degrees centigrade, and for v, cubic centimeters per gram. The value for the critical temperature is based upon the experimental determination by Cardoso and Giltay.[16] The critical volume was obtained from the extrapolation of the mean diameter of the temperature-density dome (Fig. 3).

The deviations, in parts in 100 000, of the individual measurements from values computed by the above equation are shown in Table 7. It may be noted that nearly all of the measurements were made in the temperature interval -50 to $+50°$ C. The last two series were made in order to establish the trend of the curve outside of this range. In each of these series one measurement was made in the range previously investigated to permit of comparison with the earlier series.

Since the empirical equation expresses closely the experimental results from -78 to $+100°$ C and also fits the critical volume as determined by the generally accepted method, it is believed that the interpolated values between $+100$ and $+133°$ C are a fair approximation to the volumes of the liquid in this region. Values computed from this equation for every degree between the freezing point and the critical temperature, in both metric and English units, are given in the appendix.

An estimate of the accuracy of the measurements may be obtained by assigning average and maximum errors to each element which enters into the final result. Table 9 contains a tabulation of the magnitude of these errors which were estimated from the experience gained in making the measurements. They apply more particularly to the temperature range, -50 to $+50°$ C.

[16] Arch. Sci. Phys. Nat., Genève, 24, p. 20; 1922.

Digitized by Google

TABLE 9.—Estimation of Errors

[All errors are parts in 100 000 produced in the final result u]

Source of error	Nature of error	Average error	Maximum error
Calibration of picnometer	Systematic	4	15
Reading of meniscus	Accidental	6	15
Total mass of ammonia	do	7	25
Volume of vapor	do	1	5
Specific volume of vapor	Systematic	3	10
Measurement of temperature	Accidental	4	10
Total estimated	Systematic and accidental.	7	30
Observed deviations from empirical equation	do	11	42

The fair agreement between the observed and estimated average error indicates that the precision attained in the measurements was about that to be expected from the precision of the various factors. The observed maximum error is less than the estimated, which means that all of the possible errors of the same sign were never present in any single measurement.

In the above discussion no mention has been made of the possible systematic error introduced in any given series by the sample itself. From the above analysis the observed errors may easily be attributed to errors of observation. This leads to the important conclusion that the seven different samples of ammonia made by four different methods of purification yield results for the specific volume of the saturated liquid which are in agreement within the precision of the measurement.

The measurements described in this paper were made with very pure samples of ammonia. The question immediately arises in the practical application of the results as to how much the results would be affected by the impurities commonly found in commercial samples. Tests [17] made at this Bureau upon eight standard American brands of commercial ammonia, which are believed to represent fairly well the material now used in the refrigeration industries, indicate that most commercial brands of ammonia contain less than 0.1 per cent of impurities. The nature of the impurities and the quantity of each present were not widely different in all eight brands, and it seemed that for the purpose in view any one might properly be taken as a fair representative of commercial ammonia and that no need existed for comparing each sample with chemically pure ammonia. A sample designated as

[17] McKelvy and Taylor, J. Am. Soc. Refrigeration Engineers, 8, No. 5, p. 45; 1917.

Digitized by Google

B in a previous analysis [16] was used for three determinations of density at +25° C in a glass picnometer of about 125 cm³ capacity. A separate filling was made for each determination. The mean of the three measurements agreed with the results on the highly purified ammonia within 1 part in 3000. It seems reasonably certain that the density tables appended to this paper, representing values for pure ammonia, can be applied with an error well within 1 part in 1000 to usual commercial ammonias of 99.9 per cent purity. In carrying the accuracy of this work on pure ammonia much beyond the needs of engineering practice due regard was had for the general desirability of accurate values of physical constants for pure substances and for the fact that extreme accuracy of measurement on the liquid phase was essential to securing a high enough accuracy of measurement on the vapor phase, by the methods used, to meet the needs of industrial refrigeration engineering, 1 or 2 per cent in some parts of the temperature range.

Credit is due to G. F. O'Conner, who assisted in making many of the measurements.

X. SUMMARY

The results of previous measurements of the specific volume of saturated liquid ammonia are discussed briefly and compared with the authors' results.

Four glass picnometers of about 5 cm³ capacity were calibrated with water and mercury to an accuracy of a few parts in 100 000. The temperature coefficient of expansion of the glass was obtained from a determination with an interferometer of the coefficient of linear expansion. The expansion of the picnometers with pressure was determined experimentally, using a liquid of known compressibility.

Seven samples of ammonia, purified by four somewhat different methods, were used in these picnometers, and volume measurements made throughout the temperature interval −78 to +100° C. Special tests showed less than 1 part in 10 000, by volume, of noncondensing gases present and less than 0.01 per cent, by weight, of other impurities.

The picnometers, after being partially filled with liquid ammonia, were immersed in a thermoregulated bath, the temperature of which could be maintained constant to about 0.°01 C. Readings at various temperatures were then taken of the position of the ammonia meniscus in the calibrated capillary of the picnometer.

[16] See footnote 17.

Digitized by Google

Readings were taken at five-minute intervals for a period of about one-half hour in order to insure equilibrium.

The total mass of ammonia in each picnometer during any series of measurements was always determined afterwards by weighing the picnometer filled with ammonia, then breaking the tip and reweighing filled with dry air. In the later series the total mass was also determined before filling the picnometers, using a small auxiliary bulb soldered to a steel valve. The mass so determined agreed with the subsequent determination to better than 1 part in 10 000.

The picnometers were so designed as to make the mass of the vapor phase small in comparison with the total mass of ammonia. The values for the specific volume of the saturated vapor which enter as a correction term were obtained from preliminary measurements made at this Bureau. In the interval +50 to +100° C these values were obtained by extrapolating the mean diameter of the temperature-density dome.

An empirical equation was found which represents closely the results in the temperature range covered experimentally and also conforms to what is known about the behavior of liquids at the critical temperature. The average deviation of all the measurements from this equation is 1 part in 10 000 and the maximum deviation is 4 parts in 10 000.

As a final result the specific volume of saturated liquid ammonia is expressed by the equation:

$$u = \frac{4.2830 + 0.813055\sqrt{133-\theta} - 0.0082861\ (133-\theta)}{1 + 0.424805\sqrt{133-\theta} + 0.015938\ (133-\theta)},$$

where u is expressed in cubic centimeters per gram and θ in degrees centigrade.

WASHINGTON, October 8, 1920.

Digitized by Google

APPENDIX.—TABLES OF SPECIFIC VOLUME AND DENSITY OF LIQUID AMMONIA UNDER SATURATION PRESSURE IN METRIC AND ENGLISH UNITS

Specific Volume of Liquid Ammonia under Saturation Pressure, in Cubic Centimeters per Gram

°C	0°	1°	2°	3°	4°	5°	6°	7°	8°	9°
−70	1.3788	1.3766	1.3745	1.3724	1.3702	1.3681	1.3660	1.3639	1.3618	1.3597
−60	1.4010	1.3988	1.3965	1.3942	1.3920	1.3898	1.3876	1.3854	1.3832	1.3810
−50	1.4245	1.4221	1.4197	1.4173	1.4150	1.4126	1.4103	1.4079	1.4056	1.4033
−40	1.4493	1.4468	1.4442	1.4417	1.4392	1.4367	1.4342	1.4318	1.4293	1.4269
−30	1.4757	1.4730	1.4703	1.4676	1.4649	1.4623	1.4597	1.4571	1.4545	1.4519
−20	1.5037	1.5008	1.4980	1.4951	1.4923	1.4895	1.4867	1.4839	1.4811	1.4784
−10	1.5338	1.5307	1.5276	1.5245	1.5215	1.5185	1.5155	1.5125	1.5096	1.5066
− 0	1.5660	1.5627	1.5594	1.5561	1.5528	1.5496	1.5464	1.5432	1.5400	1.5369
+ 0	1.5660	1.5694	1.5727	1.5761	1.5795	1.5831	1.5866	1.5901	1.5936	1.5972
10	1.6008	1.6045	1.6081	1.6118	1.6156	1.6193	1.6231	1.6270	1.6308	1.6347
20	1.6386	1.6426	1.6466	1.6506	1.6547	1.6588	1.6630	1.6672	1.6714	1.6757
30	1.6800	1.6844	1.6888	1.6932	1.6977	1.7023	1.7069	1.7115	1.7162	1.7209
40	1.7257	1.7305	1.7354	1.7404	1.7454	1.7504	1.7555	1.7607	1.7659	1.7713
50	1.7766	1.7820	1.7875	1.7931	1.7987	1.8044	1.8102	1.8160	1.8220	1.8280
60	1.8341	1.8403	1.8465	1.8529	1.8593	1.8658	1.8725	1.8792	1.8860	1.8930
70	1.8980	1.9072	1.9145	1.9219	1.9294	1.9370	1.9448	1.9528	1.9608	1.9690
80	1.9774	1.9859	1.9946	2.0034	2.0124	2.0217	2.0311	2.0407	2.0505	2.0605
90	2.0708	2.0813	2.0920	2.1030	2.1143	2.1259	2.1377	2.1498	2.1623	2.1752
100	2.1885	.....	.....	.....	.....	2.261	.....	.....	.....	.....
110	2.348	.....	.....	.....	.....	2.455	.....	.....	.....	.....
120	2.80	.....	.....	.....	.....	2.80	.....	.....	.....	.....
130	3.18	.....	.....	[a] 4.283	.....	.....	.....	.....	.....	.....

Density of Liquid Ammonia under Saturation Pressure, in Grams per Cubic Centimeter

°C	0°	1°	2°	3°	4°	5°	6°	7°	8°	9°
− 70	0.7253	0.7264	0.7275	0.7287	0.7298	0.7309	0.7321	0.7332	0.7343	0.7354
− 60	.7138	.7149	.7161	.7172	.7184	.7195	.7207	.7218	.7230	.7241
− 50	.7020	.7032	.7044	.7056	.7067	.7079	.7091	.7103	.7114	.7126
− 40	.6900	.6912	.6924	.6936	.6948	.6960	.6972	.6984	.6996	.7008
− 30	.6777	.6789	.6801	.6814	.6826	.6839	.6851	.6863	.6875	.6889
− 20	.6650	.6663	.6676	.6688	.6701	.6714	.6726	.6739	.6752	.6764
− 10	.6520	.6533	.6546	.6559	.6572	.6585	.6598	.6611	.6624	.6637
− 0	.6386	.6399	.6413	.6426	.6440	.6453	.6467	.6480	.6493	.6507
+ 0	.6386	.6372	.6358	.6345	.6331	.6317	.6303	.6289	.6275	.6261
10	.6247	.6233	.6218	.6204	.6190	.6175	.6161	.6146	.6132	.6117
20	.6103	.6088	.6073	.6058	.6043	.6028	.6013	.5998	.5983	.5968
30	.5952	.5937	.5921	.5906	.5890	.5875	.5859	.5843	.5827	.5811
40	.5795	.5779	.5762	.5746	.5729	.5713	.5696	.5680	.5663	.5646
50	.5629	.5612	.5594	.5577	.5560	.5542	.5524	.5507	.5489	.5471
60	.5452	.5434	.5416	.5397	.5378	.5359	.5341	.5321	.5302	.5283
70	.5263	.5243	.5223	.5203	.5183	.5163	.5142	.5121	.5100	.5079
80	.5057	.5036	.5014	.4991	.4969	.4946	.4924	.4900	.4877	.4853
90	.4829	.4805	.4780	.4755	.4730	.4704	.4678	.4652	.4625	.4597
100	.4569	.4541	.4512	.4483	.4453	.4422	.4391	.4360	.4327	.4294
110	.426	.....	.....	.....	.....	.407	.....	.....	.....	.....
120	.385	.....	.....	.....	.....	.357	.....	.....	.....	.....
130	.315	.....	.....	[a] .2335	.....	.....	.....	.....	.....	.....

[a] Critical.

Digitized by Google

Specific Volume of Liquid Ammonia under Saturation Pressure, in Cubic Feet per Pound

[1 ft.³/lb.=62.429cm³/g]

°F	0°	1°	2°	3°	4°	5°	6°	7°	8°	9°
−180	0.02197	0.02195	0.02193	0.02191	0.02190	0.02188	0.02186	0.02184	0.02182	0.02180
− 90	.02216	.02214	.02213	.02211	.02209	.02207	.02205	.02203	.02201	.02199
− 80	.02236	.02234	.02232	.02230	.02228	.02226	.02224	.02222	.02220	.02218
− 70	.02256	.02254	.02252	.02250	.02248	.02246	.02244	.02242	.02240	.02238
− 60	.02278	.02275	.02273	.02271	.02269	.02267	.02265	.02263	.02261	.02259
− 50	.02299	.02297	.02295	.02293	.02291	.02288	.02286	.02284	.02282	.02280
− 40	.02322	.02319	.02317	.02315	.02313	.02310	.02308	.02306	.02304	.02301
− 30	.02345	.02342	.02340	.02338	.02335	.02333	.02331	.02328	.02326	.02324
− 20	.02369	.02366	.02364	.02361	.02359	.02357	.02354	.02352	.02349	.02347
− 10	.02393	.02391	.02388	.02386	.02383	.02381	.02378	.02376	.02374	.02371
− 0	.02419	.02417	.02414	.02411	.02409	.02406	.02404	.02401	.02399	.02396
+ 0	.02419	.02422	.02424	.02427	.02430	.02432	.02435	.02438	.02440	.02443
10	.02446	.02449	.02451	.02454	.02457	.02460	.02462	.02465	.02468	.02471
20	.02474	.02476	.02479	.02482	.02485	.02488	.02491	.02494	.02497	.02500
30	.02503	.02505	.02508	.02511	.02514	.02518	.02521	.02524	.02527	.02530
40	.02533	.02536	.02539	.02542	.02545	.02548	.02551	.02555	.02558	.02561
50	.02564	.02568	.02571	.02574	.02577	.02581	.02584	.02587	.02590	.02594
60	.02597	.02601	.02604	.02608	.02611	.02614	.02618	.02621	.02625	.02628
70	.02632	.02635	.02639	.02643	.02646	.02650	.02653	.02657	.02661	.02664
80	.02668	.02672	.02675	.02679	.02684	.02687	.02691	.02695	.02699	.02703
90	.02707	.02711	.02715	.02719	.02723	.02727	.02731	.02735	.02739	.02743
100	.02747	.02752	.02756	.02760	.02764	.02769	.02773	.02777	.02782	.02786
110	.02790	.02795	.02799	.02804	.02808	.02813	.02817	.02822	.02827	.02832
120	.02836	.02841	.02846	.02851	.02855	.02860	.02865	.02870	.02875	.02882
130	.02885	.02890	.02895	.02901	.02906	.02911	.02916	.02922	.02927	.02930
140	.02938	.02943	.02949	.02954	.02960	.02966	.02971	.02977	.02983	.02989
150	.02995	.03001	.03007	.03013	.03019	.03025	.03031	.03037	.03045	.03050
160	.03056	.03063	.03069	.03076	.03082	.03089	.03096	.03103	.03110	.03117
170	.03124	.03131	.03138	.03145	.03153	.03160	.03167	.03175	.03183	.03190
180	.03198	.03206	.03214	.03222	.03230	.03238	.03247	.03255	.03264	.03272
190	.03281	.03290	.03299	.03309	.03317	.03326	.03336	.03346	.03355	.03365
200	.03375	.03385	.03395	.03405	.03415	.03426	.03437	.03448	.03459	.03470
210	.03482	.03494	.03506	.03518	.03530	.03543	.03556	.03569	.03582	.03595
220	.0361	.....	.....	.....	.....	.0368	.....	.....	.....	.....
230	.0376	.....	.....	.....	.....	.0385	.....	.....	.....	.....
240	.0395	.....	.....	.....	.....	.0407	.....	.....	.....	.....
250	.0422	.....	.....	.....	.....	.0440	.....	.....	.....	.....
260	.0463	.....	.....	.....	.....	.0499	.....	.....	.....	.....
270	.0577	a.0686	.....	.....	.....	.....	.....	.....	.....	.....

a At 271.4° (critical).

Digitized by Google

Density of Liquid Ammonia under Saturation Pressure, In Pounds per Cubic Foot

[1 lb./ft.³ = 0.0160183 g/cm³]

°F	0°	1°	2°	3°	4°	5°	6°	7°	8°	9°
−100	45.52	45.55	45.59	45.63	45.67	45.71	45.75	45.79	45.83	45.87
− 90	45.12	45.16	45.20	45.24	45.28	45.32	45.36	45.40	45.44	45.48
− 80	44.72	44.76	44.80	44.84	44.88	44.92	44.96	45.00	45.04	45.08
− 70	44.32	44.36	44.40	44.44	44.48	44.52	44.56	44.60	44.64	44.68
− 60	43.91	43.95	43.99	44.03	44.07	44.11	44.15	44.19	44.24	44.28
− 50	43.49	43.54	43.58	43.62	43.66	43.70	43.74	43.78	43.83	43.87
− 40	43.08	43.12	43.16	43.20	43.24	43.28	43.33	43.37	43.41	43.45
− 30	42.65	42.69	42.74	42.78	42.82	42.86	42.91	42.95	42.99	43.03
− 20	42.22	42.26	42.31	42.35	42.39	42.44	42.48	42.52	42.57	42.61
− 10	41.78	41.83	41.87	41.91	41.96	42.00	42.05	42.09	42.13	42.18
− 0	41.34	41.38	41.43	41.47	41.52	41.56	41.61	41.65	41.70	41.74
+ 0	41.34	41.29	41.25	41.20	41.16	41.11	41.07	41.02	40.98	40.93
10	40.89	40.84	40.79	40.75	40.70	40.66	40.61	40.56	40.52	40.47
20	40.43	40.38	40.34	40.29	40.24	40.20	40.15	40.10	40.05	40.01
30	39.96	39.91	39.87	39.82	39.77	39.72	39.68	39.63	39.58	39.53
40	39.49	39.44	39.39	39.34	39.29	39.24	39.19	39.15	39.10	39.05
50	39.00	38.95	38.90	38.85	38.80	38.75	38.70	38.65	38.60	38.55
60	38.50	38.45	38.40	38.35	38.30	38.25	38.20	38.15	38.10	38.05
70	38.00	37.95	37.90	37.84	37.79	37.74	37.67	37.64	37.59	37.53
80	37.48	37.43	37.37	37.33	37.27	37.21	37.16	37.11	37.05	37.00
90	36.95	36.90	36.85	36.80	36.74	36.67	36.62	36.56	36.51	36.45
100	36.40	36.34	36.29	36.23	36.18	36.12	36.07	36.01	35.95	35.89
110	35.84	35.78	35.72	35.67	35.51	35.55	35.49	35.43	35.37	35.32
120	35.26	35.20	35.14	35.08	35.02	34.96	34.90	34.84	34.78	34.72
130	34.66	34.60	34.54	34.48	34.41	34.35	34.29	34.23	34.17	34.10
140	34.04	33.98	33.91	33.85	33.78	33.72	33.65	33.59	33.52	33.46
150	33.39	33.33	33.26	33.20	33.13	33.06	32.99	32.93	32.86	32.79
160	32.72	32.65	32.58	32.52	32.45	32.37	32.30	32.23	32.16	32.09
170	32.01	31.94	31.87	31.80	31.72	31.65	31.57	31.50	31.42	31.35
180	31.27	31.19	31.11	31.04	30.96	30.88	30.80	30.72	30.64	30.56
190	30.48	30.40	30.32	30.23	30.15	30.06	29.98	29.89	29.81	29.72
200	29.63	29.54	29.45	29.37	29.28	29.19	29.10	29.01	28.91	28.82
210	28.72	28.62	28.53	28.43	28.33	28.23	28.13	28.02	27.92	27.82
220	27.7					27.2				
230	26.6					26.0				
240	25.3					24.6				
250	23.7					22.7				
260	21.6					20.1				
270	17.3	a14.6								

a At 271.4° (critical).

Digitized by Google

Digitized by Google

DEPARTMENT OF COMMERCE

SCIENTIFIC PAPERS

OF THE

BUREAU OF STANDARDS

S. W. STRATTON, DIRECTOR

No. 421

WAVE LENGTHS LONGER THAN 5500 Å IN THE ARC SPECTRA OF YTTRIUM, LANTHANUM, AND CERIUM AND THE PREPARATION OF PURE RARE EARTH ELEMENTS

BY

C. C. KIESS, Associate Physicist
Bureau of Standards

B. S. HOPKINS
H. C. KREMERS
University of Illinois

OCTOBER 14, 1921

PRICE, 5 CENTS

Sold only by the Superintendent of Documents, Government Printing Office, Washington, D. C.

WASHINGTON
GOVERNMENT PRINTING OFFICE
1921

Digitized by Google

Digitized by Google

WAVE LENGTHS LONGER THAN 5500 A IN THE ARC SPECTRA OF YTTRIUM, LANTHANUM, AND CERIUM AND THE PREPARATION OF PURE RARE EARTH ELEMENTS

CONTENTS

PART I.—WAVE LENGTHS LONGER THAN 5500 A IN THE ARC SPECTRA OF YTTRIUM, LANTHANUM, AND CERIUM

Page

I. Introduction 318
II. Apparatus and methods 319
III. Results 321
1. Yttrium 321
2. Lanthanum 323
3. Cerium 326
IV. Summary 335

PART II.—THE PREPARATION OF PURE RARE EARTH ELEMENTS

I. Introduction 337
II. The cerium group 338
1. Cerium 338
2. Samarium 339
3. Lanthanum 341
4. Neodymium 342
5. Gadolinium 342
III. The yttrium group 344
1. Yttrium 344
2. Dysprosium 348
3. Erbium 350

Digitized by Google

PART I.—WAVE LENGTHS LONGER THAN 5500 A IN THE ARC SPECTRA OF YTTRIUM, LANTHANUM, AND CERIUM

By C. C. Kiess

ABSTRACT

This paper contains the results derived from a study of the yellow, red, and infra-red regions of the arc spectra of yttrium lanthanum, and cerium. Spectrograms were photographed with the dyes pinacyanol, kryptocyanin, and dicyanin. The rare earth compounds studied were derived from two sources: From the University of Illinois were obtained the oxalates of yttrium and lanthanum and the oxide of cerium, prepared under the direction of Prof. B. S. Hopkins; from Eimer and Amend were obtained the chlorides of yttrium and lanthanum and the nitrate of cerium, the last being a Kahlbaum preparation. In addition to spectrograms of the above-named materials secured with the concave grating spectrograph of the Bureau of Standards there were available for measurement two spectrograms made by Dr. Eder, of Vienna, with his grating spectrograph. These spectrograms were of yttrium and cerium salts prepared by C. Auer von Welsbach. The tables submitted herewith contain about 175 lines in the spectrum of yttrium, 410 in the spectrum of lanthanum, and about 1700 in that of cerium. Many of the wave lengths are those of heads of bands which are prominent in the spectra of yttrium and lanthanum. Part II of this paper, prepared by Prof. B. S. Hopkins and Dr. H. C. Kremers at the University of Illinois, describes the methods used in purifying the samples of yttrium, lanthanum, and cerium, which were used in this work.

I. INTRODUCTION

The rare earths present many interesting problems not only to the chemist, but to the spectroscopist as well. Indeed, the chemist, in separating and purifying his various preparations of the compounds of the rare earth metals, avails himself to a great extent of spectroscopic methods. And in one instance, at least, the spectroscopist has indicated the presence of a new and unsuspected element which had escaped detection by the chemist.[1]

In addition to its work of measuring standard wave lengths in the spectra of the chemical elements, the spectroscopy laboratory at the Bureau of Standards makes frequent spectroscopic analyses of various metals, salts, alloys, etc., to ascertain their composition and purity. The opportunity which arose when a number of samples of rare earth compounds (prepared at the University of Illinois by Prof. Hopkins and his coworkers) were submitted for

[1] Kaiser, Akad. der Wiss. Sitz. Wien., 126, IIa, p. 473; 1917.

Digitized by Google

analysis was taken advantage of to study the yellow, red, and infra-red regions of their arc spectra. This work was done in continuation of a program which was begun several years ago and is now well on the way toward completion. This program has as one of its objects the mapping of the red and infra-red spectra of the chemical elements as far out into the region of longer wave lengths as modern photographic methods will permit. To date results for about 35 elements have been published,[2] and work on the remainder is in various stages of progress. This paper presents the data derived from a study of the arc spectra of yttrium, lanthanum, and cerium. Wave lengths in the spectra of other rare earth elements have been measured and will be published as soon as the work of compiling the tables is completed.

II. APPARATUS AND METHODS

Most of the spectograms upon which the present study is based were secured with the concave grating spectograph of the Bureau of Standards. This instrument has been described in a previous publication.[3] Four gratings, all ruled at the Johns Hopkins University and of 640 cm radius, were used in the spectrograph. The third order of a grating ruled with 10 000 lines to the inch, was used in photographing the regions of the spectra between 5500 A and 5900 A. The dispersion was 2.3 A per millimeter. The first orders of two 20 000 lines-per-inch gratings (dispersion 3.6 A per millimeter) were used to photograph the spectral regions between 5500 A and 8000 A. For the region from 8000 A to 10 000 A the first order of the 7500 lines-per-inch grating, regularly in use in this laboratory, was employed. A few spectrograms in shorter wave-length regions were also made in the third and fourth orders of the last-named grating.

The materials whose spectra were studied were derived from two sources. From Eimer and Amend were obtained the chlorides of yttrium and lanthanum and the nitrate of cerium, the last named being a Kahlbaum preparation. As mentioned above, several preparations of rare earths were received for analysis from the chemistry department of the University of Illinois. Among these were the oxalates of yttrium and lanthanum and the oxide of cerium. A statement of the methods of extracting these compounds from their ores and purifying

[2] B. S. Bull., 14, pp. 371, 637, 765, 1918; B. S. Scientific Papers, 15, p. 251, 1919; 16, p. 51, 1920. Also Popular Astronomy, 29, p. 18; 1921.

[3] B. S. Bull., 14, p. 373; 1918.

Digitized by Google

them has been prepared by Profs. Hopkins and Kremers and constitutes the second part of this paper.

The salts were vaporized either on graphite or copper electrodes, the latter, however, being used for the greater portion of the work. Although the spectrum of copper has some strong lines in the regions studied, yet it is believed that few lines, if any, in the spectra examined have been omitted because of coincidence with copper lines. We have found the use of copper preferable to the use of graphite because of the steadiness with which the copper arc burns, especially when a bead from the upper electrode is fused with the metal in the lower. The advantage of this feature in the case of long exposures can be appreciated. Current strengths of 6 to 10 amperes were used under 240 volts pressure, depending on the spectral region being photographed.

The spectrograms were made on Seed 23 and Seed 30 plates measuring 2½ by 8 inches. They were sensitized to the yellow, red, and infra-red regions of the spectrum with pinacyanol, kryptocyanin,[4] and dicyanin, respectively. Dyes produced in this country and abroad were used with equal success. The exposure times ranged from 2½ minutes for the yellow regions to 5 hours for the infra-red. The arc spectrum of iron served as comparison spectrum, and its wave lengths determined by interference methods[5] were used in the reductions. The iron spectrum was photographed both at the beginning and at the end of long exposures in order to eliminate any possible temperature shift. Inasmuch as the grating is mounted in a small room whose temperature changes are gradual through long periods of time, corresponding to seasonal changes, no trouble from this source was experienced. A potassium bichromate cell or a screen of red glass, Jena 4512, was used in front of the slit of the spectrograph to remove overlapping higher orders of spectra.

In addition to the spectrograms made here, as described above, the Bureau of Standards has received from Prof. J. M. Eder, of Vienna, a number of spectrograms of the rare earth preparations of C. Auer von Welsbach. Among them, two—one of erbium nitrate containing yttrium, the other of cerium chloride—extend into a portion of the same spectral regions investigated here. These spectrograms were secured by Eder with a Rowland concave grating of 4.6 m radius and containing 13 000 lines per inch. The

[4] J. Op. Soc. of Am., 4, p. 91, 1920; J. Am. Chem. Soc., 42, p. 2661, 1920.
[5] B. S. Bull., 13, p. 245, 1916.

Digitized by Google

dispersion was 3.7 A per millimeter. The results derived from these plates are included with those given in the tables of this paper.

All the plates were measured on a large engine of which the smallest scale division is 0.001 mm. The spectrograms were measured directly in the sense increasing wave lengths with increasing scale readings, and then in the reversed position. In both directions of measurement from two to six settings with the micrometer wire were made on each line according to its sharpness.

III. RESULTS

In the following tables are brought together the results derived from the measurement of the plates. The tabulated wave lengths are, in the case of yttrium and lanthanum, the averages of from 2 to 12 determinations, and in the case of cerium, from 2 to 7. The majority of the tabulated wave lengths, however, are the means of 4 observations. Lines observed only once were recorded on plates exposed longer than the average to a particular spectral region.

The second and third columns of the tables give symbols describing the intensity, character, and accuracy of the lines. The intensities range from 1 or <1 for the faintest lines measured to 10 for the strongest. An asterisk (*) in the second column denotes that the line was not observed in the spectra of the preparations submitted by the University of Illinois. Lines so marked may be due to impurities, but it is very probable, since most of them are faint, that they failed to appear on the spectrograms because the exposures were not sufficiently long. The letters and symbols in the explanatory columns have the following significance:

b=broad.
coin=coincident.
d=double.
g=ghost.
h=hazy.
l=shaded to red.
n=band head.
p=part of band structure.
R=reversed.
v=shaded to violet.
A=probable error of 0.000 A to 0.010 A.
B=probable error of 0.010 A to 0.020 A.
C=probable error of 0.020 A to 0.030 A.
D=probable error >0.030 A.
E=only one determination.

Lines with probable errors A and B were measured three times or more.

1. YTTRIUM

About 175 lines in the arc spectrum of yttrium were measured between the limits 5503 A and 7882 A. Of these, approximately

Digitized by Google

one-fifth are the heads of bands which form a prominent feature of the orange and red regions of the yttrium spectrum. Prolonged exposures, up to five hours in length, failed to show any lines in the spectrum beyond that at 7881.87 A.

The yttrium oxalate received from the University of Illinois was very pure, the only impurities present, if any, being indicated by several faint lines which occur also in the spectra of lanthanum or erbium. These lines are marked in the second column of Table 1. The yttrium chloride received from Eimer and Amend contained a considerable amount of calcium, but was uncontaminated by other rare earths.

An extensive study of the spectrum of yttrium has been made by Eder.[6] Using yttrium sulphate prepared by C. Auer von Welsbach he has measured the arc spectrum from 2231 A to 7881 A. An earlier work by Eder[7] gives practically the same list of lines in the orange and red regions.

In general, the agreement between his two sets of results and those presented here is very good. Slight discrepancies, not accounted for, are the appearance in each list of wave lengths of faint lines not to be found in the other.

TABLE .1—Arc Spectrum of Yttrium

λ I. A.	Notes	Probable error	λ I. A.	Notes	Probable error	λ I. A.	Notes	Probable error
5503. 474	4	A	5675. 303	4	A	5841. 898	1 l	B
5509. 936	3	A	5675. 642	1	A	5858. 824	1 n?	A
5513. 658	2	A	5686. 683	1 b	B	5871. 764	1	B
5521. 654	4	B	5693. 639	2	A	5876. 134	1 b, p?	B
5526. 729	1	B	5706. 758	4 R	A	5879. 958	1	A
5527. 589	5 R	B	5713. 845	2 h, n?	B	5893. 140	1 h, p?	B
5541. 647	1	B	5714. 918	2 b	B	5893. 929	1 h, p?	B
5544. 599	3	A	5720. 609	2	A	5902. 940	2	A
5546. 084	2	A	5728. 454	1	A	5939. 082	2 n	B
5550. 996	1	A	5726. 912	1 Er?	A	5945. 711	2	B
5556. 484	4 R	A	5728. 911	3	A	5949. 999	2	B
5567. 759	3	A	5730. 147	1 n	A	5956. 429	2 n	B
5577. 429	4 R	A	5740. 213	1	A	5972. 158	7 n	B
5581. 085	2	B	5743. 874	4	A	5987. 706	5 n	B
5581. 894	5 R	A	5746. 953	1 n	B	6003. 636	6 n	B
5590. 958	1	A	5765. 668	3	A	6009. 196	3 p?	B
5594. 126	1	A	5773. 937	2	A	6019. 920	5 n	B
5606. 345	3	A	5781. 696	1	B	6036. 647	4 n	B
5610. 352	1	A	5787. 740	2 g, coin	B	6053. 844	4 n	B
5619. 945	1	B	5797. 130	1	A	6072. 817	2 n	C
5623. 907	1	B	5800. 009	1 n?	B	6089. 373	2 n	C
5630. 144	6 R	A	5809. 289	1 p?	B	6096. 823	2 n	C
5632. 245	2	A	5812. 671	1	B	6107. 834	2 n	C
5632. 911	1	A	5818. 548	1	A	6114. 729	2 n	C
5641. 812	<1	B	5819. 258	1 b, p?	B	6127. 387	1 n	B
5644. 704	4 R	A	5820. 023	1 h	B	6132. 156	7 n	B
5648. 490	4 R	A	5821. 879	2 Er?	A	6135. 056	2 p?	B
5660. 909	1	B	5823. 774	1 l, p? La?	A	6138. 417	2	B
5662. 949	7 R	A	5832. 255	2	A	6148. 454	6 n	B
5669. 229	1	A	5838. 060	1 l	A	6165. 142	6 n	B

[6] Kaiser, Akad. der Wiss. Sitz. Wien., 125, IIa, p. 383; 1916.
[7] Kaiser, Akad. der Wiss. Sitz. Wien., 124, IIa, p. 118; 1915.

Digitized by Google

TABLE 1.—Arc Spectrum of Yttrium—Continued

λ I. A.	Notes	Probable error	λ I. A.	Notes	Probable error	λ I. A.	Notes	Probable error
6182. 250	4 n	B	6664. 378	3	B	7191. 628	2	B
6191. 719	4	A	6687. 975	4	A	7195. 942	1	B
6199. 859	2 n	A	6691. 848	2	B	7229. 119	1	E
6217. 981	2 n	B	6694. 749	2	B	7264. 186	2	C
6222. 572	2	A	6699. 259	2 La?	B	7330. 641	1 d?	C
6236. 719	2 n	B	6700. 707	3	A	7346. 444	2	A
6251. 039	2 n?*	E	6713. 195	2	A	7398. 871	1 b	C
6275. 013	2 n, Er?	B	6735. 991	2	A	7442. 258	1	D
6295. 489	2 n?*	C	6798. 694	4	A	7450. 286	2	B
6316. 308	2 n?*	C	6795. 402	2	A	7452. 978	1 b	E
6368. 120	1 n?*	C	6808. 152	2 b	C	7466. 365	1	E
6402. 016	2	B	6815. 147	2	B	7535. 696	1 b	C
6435. 029	6	A	6832. 474	1	B	7563. 061	2	E
6437. 173	2	A	6845. 226	3	B	7617. 744	1	D
6501. 263	2 n?	B	6858. 216	2	A	7622. 939	1	B
6503. 024	1 p?	C	6887. 214	3	A	7719. 893	2	E
6504. 579	1 p?	C	6895. 968	2	B	7734. 014	2	C
6518. 364	2 l, n?	B	6908. 266	2	B	7788. 390	1	C
6535. 873	2 l, n?	B	6933. 533	2	A	7796. 286	1	C
6588. 571	4	A	6950. 310	2	A			
						7802. 485	1	C
6553. 876	2 l, n?	B	6951. 662	1	A	7812. 132	1	C
6557. 360	3	A	6958. 005	1 La?	B	7855. 546	1	C
6572. 621	1 l, n?	B	6979. 860	2	A	7881. 868	2	A
6576. 859	2 Er?	A	7008. 946	2	B			
6584. 878	2	A	7009. 952	2	B			
6599. 588	1	C	7035. 188	2	B			
6618. 740	3	B	7052. 972	2	B			
6622. 511	2	B	7054. 323	1	B			
6636. 478	2 La?	B	7087. 71	1 h	D			
6650. 599	2	A	7127. 928	2	B			

2. LANTHANUM

In the regions studied, the spectrum of lanthanum is characterized by numerous lines of intensity 3 or greater. Superposed on the line spectrum is a banded spectrum which remains prominent out into the infra-red regions. In all, about 400 lines, including band heads, are tabulated below between the limits 5501 A and 9079 A. Both samples of lanthanum analyzed were very pure. Lines suspected as not being true lanthanum lines are appropriately marked. Among these, the two at 6262.30 A and 6645.19 A agree very closely with the strongest lines in the red region of the spectrum of europium.

Eder and Valenta [8] have measured on the Rowland scale the arc spectrum of lanthanum between the limits 5455 A in the green and 7066 A in the red. Shortly afterwards they also published measurements of heads of bands observed in the lanthanum arc.[9] A later work by Eder [10] using various compounds of lanthanum prepared by C. Auer von Welsbach resulted in the

[8] Kaiser, Akad. der Wiss. Sitz., Wien., 119, IIa, p. 39; 1910.
[9] Kaiser, Akad. der Wiss. Sitz., Wien., 119, IIa, p. 547; 1910.
[10] Kaiser, Akad. der Wiss. Sitz., Wien., 123, IIa, p. 2304; 1914.

Digitized by Google

determination of about 120 wave lengths in international units in the red from 6468 A to 8051 A. The stronger lines of his list are in close agreement with the wave lengths given below; but among his faint lines are many not to be found in the accompanying table. In like manner, Table 2 contains faint lines not to be found in Eder's list.

TABLE 2.—Arc Spectrum of Lanthanum

λ I. A.	Notes	Probable error	λ I. A.	Notes	Probable error	λ I. A.	Notes	Probable error
5501.349	6 R	B	5823.829	4 R	A	6035.120	1 b, p?	E
5502.229	2	C	5827.550	3	A	6038.597	4 R	A
5502.656	2	C	5828.494	3	B	6041.587	2	A
5503.858	3	B	5829.729	4 R	B	6044.849	2 b, p?	B
5506.067	2*	B	5832.842	1	B	6046.050	1 b, p?	C
5515.315	2	B	5834.330	1	B	6061.430	1 b, p?*	C
5517.386	3	B	5835.931	1	B	6067.154	2	B
5529.895	1	B	5839.785	2	A	6068.703	4 R	A
5532.071	1	B	5845.021	4 R	A	6072.062	2	A
5541.284	4 R	B	5848.357	4 R	A	6074.007	1	A
5544.924	2	B	5848.949	2	A	6075.239	1	A
5565.396	3	B	5852.265	3	A	6084.931	3	A
5565.736	2	B	5855.582	4 R	A	6085.462	2	B
5566.938	2	B	5863.681	5 R	B	6087.950	1 p?	B
5568.482	4	B	5866.428	3 n	B	6092.271	2	B
5570.385	1	C	5869.554	3 n, p?	B	6100.364	3	A
5588.346	4 R	A	5869.965	2	A	6107.266	2	A
5600.065	5 n	C	5872.935	1 p?	E	6108.499	5 R	A
5602.559	5 n, p?	C	5873.986	2	A	6111.730	4 R	A
5626.148	4 n	C	5874.731	4	A	6120.399	1	A
5628.678	4 n, p?	C	5877.630	3	B	6121.274	1	B
5631.215	3	A	5877.984	3	B	6123.806	1	A
5632.055	3	B	5880.615	5 R	B	6126.084	4 R	A
5639.298	2	A	5892.664	1 p?	B	6127.051	3	A
5648.260	4	A	5893.592	3 n	B	6129.554	5 R	A
5652.518	2 n	C	5894.826	4 R	B	6134.403	5 R	A
5654.891	2 n, p?	C	5896.690	3 n, p?	B	6136.526	1	A
5657.743	4	A	5900.721	2 p?	A	6143.994	4	A
5671.560	3	A	5901.958	2	A	6145.339	3	A
5696.193	3 Gd?	A	5904.298	2	A	6146.552	2	B
5703.292	3	B	5917.622	4	A	6165.040	2	B
5712.412	3	A	5720.852	3 n	B	6165.716	5 R	A
5714.016	3	B	5723.969	2 p	A	6172.730	2	A
5714.547	2	B	5927.660	2 p	B	6174.192	1	B
5720.031	2	B	5928.495	2	B	6188.107	2	A
5727.298	2	A	5930.598	6 R	B	6203.540	2	A
5734.951	3	A	5935.263	3	B	6218.220	2	A
5740.647	6 R	A	5936.216	2	B	6219.522	1*	B
5742.946	3	A	5940.858	2	B	6233.522	2	A
5744.415	5 R	A	5948.286	2 n	B	6234.843	3	A
5761.840	5 R	A	5951.378	2 p	B	6236.230	2	A
5769.070	7 R	B	5960.583	2	B	6236.775	2	A
5769.368	7 R	B	5962.582	1	B	6238.586	3	A
5769.993	5 R	A	5965.331	1	A	6249.921	7 R	A
5789.234	6 R	A	5971.096	1 p?	E	6262.297	5 R Eu?	A
5791.331	7 R	A	5973.513	2	A	6266.030	4 R	A
5797.594	7 R	B	5975.785	3 l, n?	E	6273.780	1	B
5802.083	1 b, p?	B	5978.895	2 l, p?	B	6287.748	2	A
5805.767	5 R	A	5982.337	3	A	6288.584	2	A
5806.620	1 p?	B	5992.378	3	A	6293.571	4 R	A
5808.291	5 R	B	6007.367	4	A	6296.095	5 R	A
5810.372	1	A	6017.222	2	A	6305.463	2	A
5813.385	2	A	6025.108	1 p?	B	6307.265	1	A
5820.533	1*	B	6031.494	1 b, p?	B	6308.269	2	B
5821.998	6 R	A	6034.548	1 p?	B	6308.991	1 b*	B

Digitized by Google

TABLE 2.—Arc Spectrum of Lanthanum—Continued

λ I. A.	Notes	Probable error	λ I. A.	Notes	Probable error	λ I. A.	Notes	Probable error
6310.224	2 b	B	6699.842	1	A	7257.187	2 b, n?	B
6310.939	3	A	6709.496	4	A	7270.075	2	A
6315.817	1	A	6714.091	2	A	7282.323	4	A
6318.290	2	A	6716.011	1	B	7289.296	2 n? *	B
6320.389	5 R	A	6718.664	1	B	7308.321	1 n? *	C
6325.919	5 R	A	6732.794	1	A	7320.901	1	B
6330.476	1*	A	6748.125	2	A	7322.001	1 n? *	C
6333.218	1 n?*	B	6753.039	3	A	7334.146	4	A
6333.833	2*	B	6774.268	4	A	7345.314	3	A
6337.915	2*	B	6776.785	1*	B	7354.840	1 n? *	B
6339.249	2*	B	6778.243	1*	B	7379.711	2	C
6356.438	2	B	6783.500	1 v*	B	7380.081	5 n	B
6358.130	3 Cu?	B	6796.707	1	B	7382.668	2 p	B
6360.242	3	A	6808.850	2	A	7403.576	7 n	B
6374.144	1	A	6813.655	1	A	7411.391	4 p	B
6375.110	2*	B	6816.290	1 b, d?*	B	7434.357	7 n	B
6380.558	1*	B	6821.530	2 v, h	B	7442.896	4 p, air?	B
6390.453	5 R	A	6823.785	3	A	7463.075	2	B
6394.242	6 R	A	6834.055	2	A	7465.276	5 n	B
6399.064	3	A	6837.912	2	A	7474.803	2 p?	C
6410.982	4	A	6859.044	1	B	7483.454	3	B
6417.223	1	A	6898.414	1 h*	B	7496.564	5 n	B
6443.086	1	B	6899.545	1 h*	B	7498.756	2 p?	B
6446.618	2	B	6902.117	1	B	7506.766	2 l, n?	B
6448.151	2	A	6903.073	1	B	7528.249	3 n	B
6450.331	2	A	6917.244	2	A	7539.203	2 p?	B
6454.508	3	A	6918.273	2	A	7560.161	3 n	B
6455.980	5 R	B	6925.235	3	A	7592.348	2 n	B
6468.438	2 b	B	6934.981	3	A	7612.959	1 p?	B
6485.544	3 h	C	6952.500	2 b	B	7624.922	2 n	B
6492.903	1 l, n?	B	6954.514	2	A	7657.867	1 n? *	B
6498.187	2	A	6956.176	1*	B	7664.331	2	B
6506.273	1 b, n?	A	6958.092	3	A	7666.731	1 n?	B
6519.332	1	A	6961.084	1	E	7691.079	1 n? *	B
6520.772	2 b, n?	A	6968.716	2	A	7698.830	1	B
6523.904	1	A	6976.837	1	A	7701.922	1 b, n? *	B
6526.976	4	A	6978.039	1	B	7716.687	1 b, p? *	B
6529.756	1	A	6994.473	2 n?	B	7724.360	1 n? *	C
6543.154	4	A	6996.867	2 b, p? Gd?	B	7737.780	1 n? *	C
6549.194	1	A	7011.196	2 n	B	7789.29	1 b, h	D
6554.136	1	A				7809.733	1 n	C
6555.054	1	B	7023.625	3 n?	B	7826.388	1	C
6555.950	1	E	7024.454	1	E	7841.856	2 b, n?	C
6565.415	3 b, h, Cu?	B	7032.009	2	B	7877.226	5 n	A
			7040.815	2 l, n?	B	7908.757	2 p?	B
6570.937	1	A	7045.933	4	A			
						7910.556	6 n	A
6578.518	4	A	7054.831	2 n*	B	7912.308	1 p? *	C
6582.207	1	A	7066.194	4	A	7945.013	5 n	B
6593.458	3	A	7068.323	3	A	7947.915	1 p?	C
6599.484	1 b	E	7070.799	2 n	A	7964.834	1	B
6600.166	2	A	7076.368	1*	B			
6605.090	1	A	7085.417	2 n*	B	7979.746	3 n	A
6607.676	1	E	7101.052	2 n	B	7983.304	1 p?	B
6608.253	3	A	7116.442	3 n*	C	8001.964	1 p?	B
6616.588	4	A	7131.680	2 n*	B	8014.830	2 n	A
6628.387	1	B	7147.480	2 n*	B	8019.541	1 p?	B
6631.218	1	A	7149.704	1 p?*	E	8050.250	2 n	A
6636.521	1 Yt?	A	7158.059	2	B	8051.360	1	B
6642.779	2	A	7161.192	3	A	8055.783	1 p? *	C
6644.389	3	A	7162.398	2 n*	B	8086.074	2	A
6645.188	2 Eu?	A	7179.029	2 n*	B	8122.213	1 n	A
6650.799	4	A	7193.674	2 b, n?	B	8129.808	1	E
6661.405	4	A	7211.015	2 n?*	B	8158.997	2	B
6671.402	2	A	7219.884	2	A	8196.017	1	C
6682.880	3	A	7225.235	2 v, n?	B	8203.391	1	C
6689.243	1 Yt?	A	7242.873	2 b, n?	B	8216.383	1 air?	E

Digitized by Google

TABLE 2.—Arc Spectrum of Lanthanum—Continued

λ I. A.	Notes	Probable error	λ I. A.	Notes	Probable error	λ I. A.	Notes	Probable error
8238.054	1 h * air?	C	8519.15	<1	E	8709.16	<1 Cn?	E
8247.475	2	B	8526.66	2 n	B	8714.70	<1 n?	E
8316.031	1 *	B	8543.48	2	B	8720.40	1	C
8324.694	3	A	8545.428	3	A	8748.420	2	B
8346.547	3	A	8557.24	<1	E	8753.64	<1 n?	E
8379.728	2*	B	8568.54	2 n	B	8798.13	<1 n?	E
8453.86	1 n? *	D	8590.98	1	C	8818.95	1	E
8467.53	2 n?	C	8595.74	<1 b	E	8825.84	2	B
8476.483	2	A	8600.86	2 n	B	8839.67	1	E
8480.78	<1	E	8624.29	1	E			
						8957.70	1	B
8484.38	<1	E	8634.53	<1	E	8963.48	<1	E
8490.01	1 h, n?	C	8638.48	1 n?	C	9078.99	<1	E
8507.35	1	C	8672.13	2	B			
8513.55	1	C	8674.383	3	A			
8514.63	1	C	8676.50	1 n	E			

3. CERIUM

Table 3 contains about 1700 lines in the arc spectrum of ceriun between the limits 5500 A and 9025 A. Most of the lines are faint; that is, of intensity 2 or less. A band spectrum is indicated by the presence of a few band heads, but this feature does not display the prominence in cerium that it does in yttrium and lanthanum.

Using cerium ammonium nitrate and cerium chloride prepared by C. Auer von Welsbach, Eder and Valenta [11] measured the arc spectrum of cerium from 4800 A to 7253 A on the Rowland scale. A later work by Eder [12] yielded wave lengths between 6466 A and 8025 A, expressed in the international units. In the regions common to their work and that done at the Bureau of Standards there is very good agreement between the two sets of results.

TABLE 3.—Arc Spectrum of Cerium

λ I. A.	Notes	Probable error	λ I. A.	Notes	Probable error	λ I. A.	Notes	Probable error
5500.91	1	B	5510.70	2	B	5520.20	1	B
5501.43	1	C	5511.19	1	E	5520.81	1	B
5501.79	1	E	5511.61	2	E	5521.05	<1	E
5502.80	1	B	5512.08	6	B	5521.88	2	B
5503.55	1	C	5513.14	2	B	5522.50	3	B
5504.19	1	C	5514.23	1	B	5523.01	1	B
5504.56	1	C	5515.23	1	C	5523.65	1	B
5505.11	1	C	5515.37	1	C	5524.42	2	C
5505.52	1	E	5516.07	2	B	5524.73	1	C
5506.04	2	B	5516.32	1	B	5525.58	1	E
5506.48	2	B	5517.40	2	B	5526.09	1	B
5508.04	1	B	5517.86	1	B	5526.78	2	B
5508.69	<1	C	5518.52	3	B	5527.15	2	B
5509.02	1	C	5519.02	1	B	5527.56	1	B
5509.44	1	C	5519.78	1	E	5527.93	1	C

[11] Kaiser, Akad. der Wiss. Sitz., Wien., 119, IIa, p. 531; 1910.
[12] Kaiser, Akad. der Wiss. Sitz., Wien., 123, IIa, p. 2308; 1914.

Digitized by Google

TABLE 3.—Arc Spectrum of Cerium—Continued

λ I. A.	Notes	Probable error	λ I. A.	Notes	Probable error	λ I. A.	Notes	Probable error
5528.75	1	B	5568.79	1	E	5617.46	1	B
5529.13	1	E	5569.30	2	B	5618.18	1	B
5529.48	1	E	5570.48	1	B	5618.64	1	B
5529.90	<1	E	5570.94	2	B	5618.87	<1	E
5530.46	1	B	5571.61	1	B	5619.36	1	C
5531.18	1	B	5572.23	3	B	5619.69	1	C
5531.53	<1	E	5573.12	1	B	5620.38	2	A
5532.04	2	C	5574.36	<1	E	5620.77	<1	E
5532.92	1	C	5575.08	1	B	5621.76	<1	E
5533.21	1	B	5576.04	1	B	5622.23	1	B
5533.49	<1	E	5577.05	1	B	5622.65	2	B
5534.64	<1	E	5577.28	2	A	5623.00	2	B
5535.25	3	B	5578.29	3	A	5623.76	1	B
5535.84	1	E	5578.92	2	A	5624.84	1	B
5536.41	1	E	5579.24	1	B	5625.23	2	B
5537.26	2	B	5579.50	1	B	5626.01	1	A
5537.52	3	B	5580.60	<1	E	5626.73	1	A
5538.09	1	B	5582.58	2	B	5627.24	1	B
5538.51	1	C	5582.70	4	A	5627.63	1	A
5539.24	1	C	5583.87	1 d?	B	5628.17	2 d	A
5539.61	1	C	5584.72	2 d	B	5629.01	1	B
5540.57	2	B	5585.48	1	B	5629.71	1	B
5541.25	1	E	5586.72	2	A	5630.39	2	A
5541.59	<1	E	5587.24	<1	E	5630.98	1	A
5542.13	1	B	5588.12	1	B	5631.31	1	B
5542.77	2	B	5588.33	3	A	5632.07	1 d	B
5543.70	1	B	5589.25	1	A	5632.49	3	B
5544.12	1	C	5590.13	2	B	5633.09	4	A
5544.65	2	B	5590.52	2	B	5633.48	1	B
5545.24	<1	C	5592.16	1	A	5634.48	2	A
5545.50	1	C	5592.58	<1	E	5635.28	1	A
5546.16	1	B	5592.93	<1	E	5636.44	1	A
5546.52	1	B	5593.72	2	B	5636.91	1	E
5546.86	1	B	5594.17	1	B	5637.37	3	A
5547.48	1	A	5594.74	2	A	5638.18	4	A
5548.81	4	A	5594.97	3	A	5638.66	2 v, d?	A
5549.29	<1	D	5595.89	4	A	5640.14	2	A
5550.03	2	B	5596.54	1 d	B	5640.78	2	A
5550.64	1	B	5597.13	1	A	5641.43	1	B
5551.40	1	B	5597.96	3	A	5641.71	1	B
5551.63	<1	E	5598.96	3 d	A	5642.80	1	B
5552.30	1	B	5600.18	1	B	5643.88	1	B
5553.33	<1	E	5601.29	5	A	5644.29	1	B
5554.36	1	B	5602.09	<1	E	5644.72	2 h, d	B
5556.26	5	B	5602.79	1	A	5645.45	1	B
5556.95	3	A	5603.63	1	B	5645.96	1	B
5557.58	<1	E	5604.15	1	B	5646.60	3	B
5558.31	1	B	5604.39	2	A	5647.09	2	B
5558.65	2	B	5605.03	1	A	5647.74	1	B
5559.22	4	A	5606.13	1	A	5649.29	1	A
5560.06	2	A	5606.47	2	A	5649.95	<1	E
5560.96	1	B	5607.63	1	A	5650.59	3	A
5561.46	2	A	5608.48	1	B	5651.28	1	B
5562.21	2	B	5608.99	1	B	5652.20	1	B
5563.02	3	B	5609.44	2	B	5652.98	2	A
5563.74	<1	E	5610.27	4	B	5653.51	1	B
5564.26	3	B	5610.93	3	A	5654.21	<1	E
5564.99	5	A	5611.68	1	B	5655.17	6	A
5565.28	1*	A	5612.65	1	B	5656.21	2	A
5565.97	4	B	5613.71	3	A	5656.89	1 l, m?	E
5566.49	2	A	5614.22	1	B	5658.25	1	A
5567.06	<1	E	5614.75	4	A	5659.81	2	A
5567.52	1	B	5615.98	2	A	5660.48	1	B
5567.82	3	B	5616.53	1	A	5661.19	1	B
5568.23	<1	E	5617.12	1	A	5662.11	<1	E

Digitized by Google

TABLE 3.—Arc Spectrum of Cerium—Continued

λ I. A.	Notes	Probable error	λ I. A.	Notes	Probable error	λ I. A.	Notes	Probable error
5662.72	1	A	5718.42	2 b, d?	B	5768.05	1	A
5663.24	3	B	5719.09	5	A	5768.94	5	A
5663.48	2*	B	5719.55	2	A	5769.95	2	A
5664.00	5*	A	5720.78	1 l, d?	C	5770.45	3	A
5664.68	2	B	5721.97	3	A	5771.55	1	B
5665.38	1	A	5722.62	1	A	5771.97	2	A
5667.14	1	B	5723.25	1	B	5772.23	3	A
5667.67	1	B	5724.47	1	B	5773.04	5	A
5668.00	1	C	5724.96	1	B	5773.58	3	A
5668.94	4	A	5725.85	4	A	5774.37	2	A
5669.97	6	A	5726.15	2	A	5775.03	2	A
5670.75	1	B	5727.27	2	A	5775.80	2	A
5671.42	2	A	5728.06	1	B	5776.23	2	C
5671.92	3	B	5728.63	1	B	5776.73	1	B
5673.73	1	A	5729.38	2	A	5777.26	1	B
5675.10	2	A	5730.46	1	A	5778.35	3 b, g coin?	B
5676.38	1	B	5730.81	1	B	5779.23	2	B
5676.89	3	A	5731.28	1	B	5780.22	2	B
5677.24	1	A	5731.91	1	B	5780.75	1	B
5677.76	5	A	5733.85	2 b, d	B	5781.32	<1	B
5678.33	1	A	5735.77	2 b, d	B	5782.43	2	B
5678.98	2	B	5736.58	1	B	5782.80	1	B
5680.27	2	B	5737.08	1	B	5783.99	3	A
5681.77	1	B	5737.49	1	B	5784.86	3	A
5682.22	1	A	5737.75	1	A	5785.76	1	B
5682.77	2	B	5738.32	2	A	5786.85	2	B
5683.12	2	A	5739.17	1 d	B	5787.21	2	A
5683.77	3	A	5739.63	2	A	5788.14	5	A
5684.38	1	A	5740.20	1 b	A	5788.58	1	A
5684.94	2	A	5741.13	1	A	5789.95	3 d, g coin?	B
5685.86	4	A	5741.92	1	B	5791.32	2	A
5687.82	1	A	5742.45	1 d	B	5791.67	2	A
5688.12	1	B	5743.52	5	A	5792.38	1	A
5688.48	2	B	5744.35	1*	B	5792.96	1	B
5689.90	2 b	B	5744.68	2	A	5794.32	1	A
5690.35	1 b, d?	B	5746.05	1	B	5794.79	2	A
5691.48	2	A	5746.48	2	A	5795.27	1	B
5692.12	2	A	5746.92	1	A	5796.05	3 d	A
5692.98	5	A	5747.36	1	A	5796.45	1	A
5694.05	1	B	5748.29	1	A	5797.40	2	A
5694.93	1 b, d?	A	5748.94	2	A	5798.09	2 d	B
5695.88	4	A	5749.36	1	B	5799.38	1	B
5697.02	5	A	5750.64	1	A	5799.80	3	A
5699.24	3	A	5751.20	1	B	5800.33	1	A
5699.92	<1	E	5752.12	1	B	5801.16	1	A
5700.45	<1	E	5752.51	2	A	5801.61	1	B
5700.86	<1	E	5753.03	1	A	5802.89	1	B
5701.51	1	B	5754.05	1	A	5803.23	1	A
5702.34	3	A	5754.71	1	A	5804.42	4	A
5703.25	3	A	5755.42	1	E	5804.96	1	A
5704.53	1 d	A	5756.00	1	B	5806.15	2	A
5705.21	1 b	B	5756.59	1 d	B	5806.53	1 d	B
5706.87	1	A	5757.48	1	B	5807.07	1	B
5707.44	2	A	5758.24	3	B	5807.50	1	A
5708.49	1	A	5758.79	1	A	5808.43	<1	E
5709.06	2	A	5759.71	<1	E	5809.35	1 d	A
5709.64	1	B	5760.16	1	A	5809.72	1	A
5710.07	1	A	5760.59	2	A	5810.73	3	A
5710.83	1	B	5760.97	2	A	5811.83	1	A
5711.45	3	A	5762.57	1	B	5812.93	6	A
5712.29	2	A	5763.00	2	B	5814.07	<1	B
5713.86	1	B	5763.36	1	B	5815.47	2	A
5714.33	1	A	5764.72	3 d	B	5815.91	1	B
5715.28	3	A	5765.34	3	A	5816.41	1	A
5716.49	3	A	5766.43	2 b, d?	B	5817.06	1	B

Digitized by Google

TABLE 3.—Arc Spectrum of Cerium—Continued

λ I. A.	Notes	Probable error	λ I. A.	Notes	Probable error	λ I. A.	Notes	Probable error
5817.78	2	A	5872.94	2 d	B	5922.95	3	B
5818.80	1	B	5873.91	2	A	5923.55	1	B
5820.38	3 b, d?	B	5874.90	<1	E	5924.05	3	A
5820.80	1	A	5875.85	1	C	5924.90	2	A
5822.99	3	A	5876.44	1	B	5926.28	4	A
5823.46	2	A	5877.12	<1	E	5927.31	1	B
5824.60	1	A	5877.69	1	C	5927.76	1	B
5825.22	1 b, d?	C	5878.07	2	B	5928.32	4	B
5826.56	1	A	5878.94	3	B	5928.74	2	A
5826.88	1*	A	5879.92	1	C	5929.46	3	B
5827.25	2	A	5880.43	1	C	5929.84	3	B
5828.00	<1	B	5880.97	1	C	5931.71	1	BC
5828.40	1 Cu?	B	5881.69	2	B	5932.17	2	B
5828.82	1	B	5882.69	2	B	5932.64	1	C
5829.33	1	B	5884.89	1 d	B	5933.05	1	C
5830.03	3 d	B	5885.82	1	B	5933.58	2	B
5830.67	1	B	5886.26	1	B	5934.43	5	B
5831.37	2 Cu?	B	5886.69	1	B	5935.44	1	BC
5831.92	5	A	5887.55	2	B	5936.76	1	C
5832.29	1	B	5888.00	1	B	5937.69	4	B
5832.88	1 d	B	5888.50	2	A	5938.38	2 d	B
5834.25	2	A	5888.99	1	B	5939.80	1	B
5835.84	5	A	5889.60	3	B	5940.84	5	B
5837.66	1	B	5891.29	1	C	5941.51	3	B
5838.13	4	A	5892.48	2	B	5941.87	2	B
5838.88	1	A	5893.24	3	B	5942.66	3	B
5839.36	3	A	5893.90	1	C	5943.57	2 l, n?	B
5840.01	<1*	B	5894.32	1	B	5944.88	3	B
5841.59	<1	B	5894.93	2	A	5945.40	1	C
5842.11	1	B	5895.85	3 d, Na coin?	B	5946.23	1	C
5843.10	2	A				5947.03	1 d	B
5843.73	3	A	5896.34	3 b, l	B	5947.64	3	B
5844.36	2 b	B	5897.72	1	C	5948.19	2	B
5845.37	1	B	5898.10	2	A	5948.78	1 d	B
5845.98	3	B	5898.89	1	B	5950.23	1	B
			5899.23	1	B			
5846.73	1	A				5950.60	3	B
5847.61	1 v	B	5899.70	2	A	5951.21	2	B
5848.32	2	A	5900.66	2	B	5952.25	1	B
5848.86	2	A	5901.33	3	A	5952.88	2	B
5849.56	1 l	B	5902.65	2	B	5956.04	1	C
			5903.03	1	B			
5851.08	3*	E						
5853.07	3 b	A	5903.54	<1	E	5956.77	2	B
5853.34	3*	A	5904.74	1	C	5959.07	1	B
5853.68	3	A	5905.27	1 d	C	5959.73	3	B
5854.85	1	B	5906.00	2	B	5960.17	1	B
			5906.85	1 b, d	B	5960.81	2 d	B
5855.19	1	A						
5856.64	1	B	5907.49	2	B	5962.61	1	E
5857.12	3	A	5908.34	<1	E	5963.35	2	B
5857.60	1	B	5909.20	1	B	5964.07	1	C
5858.19	2	B	5910.00	5 R	B	5964.67	2	B
			5910.68	1	C	5966.26	4 d	B
5858.56	2	B						
5859.37	3	A	5911.28	<1	E	5967.36	1	C
5862.50	5	A	5912.25	1	C	5967.72	1	C
5863.86	1	A	5912.88	3 d	B	5968.08	2	B
5864.53	1	A	5913.75	1	B	5968.60	1	B
			5914.84	3	B	5969.20	1	C
5865.16	1	A						
5865.75	1	C	5915.57	1	B	5969.80	1	B
5867.89	1	B	5916.29	1	C	5970.25	1	C
5868.49	1	B	5916.68	1	C	5970.75	1	B
5869.32	1 d	B	5917.43	1	B	5972.08	3	B
			5919.06	1	B	5972.80	2	B
5869.97	1	B						
5870.34	<1	B	5919.43	1	B	5973.50	1 v	B
5870.85	1	B	5919.93	1*	C	5974.62	1 b	B
5871.61	4	A	5920.40	3	B	5975.25	2	B
5872.30	1	B	5921.32	1 b	B	5975.90	5	A
			5922.11	2	A	5978.43	1	A

Digitized by Google

TABLE 3.—Arc Spectrum of Cerium—Continued

λ I. A.	Notes	Probable error	λ I. A.	Notes	Probable error	λ I. A.	Notes	Probable error
5979.39	2 l, nl?	A	6018.41	1	C	6069.46	4	A
5979.74	1	B	6018.83	2	A	6070.17	1	B
5980.56	1	B	6020.59	1	B	6072.00	3	B
5981.18	2	B	6021.24	1	B	6072.32	1	B
5981.83	2	B	6021.64	2	B	6073.07	1	B
5982.35	<1	E	6022.36	1	C	6073.90	1 b	C
5982.91	1	C	6023.14	1	C	6074.26	1	C
5983.57	1	B	6024.19	5	A	6075.16	1	C
5984.25	1	B	6025.28	2 d	B	6075.58	2	B
5985.40	1 v	B	6026.05	2 d	B	6075.91	2	B
5986.24	2	B	6027.16	2	A	6076.63	3	B
5986.66	1	B	6027.78	1	B	6077.16	2	B
5987.38	2	B	6028.28	1	B	6077.55	2	B
5988.29	1	C	6029.07	2 d	B	6078.44	1	C
5988.79	2	B	6029.72	1	B	6079.37	2	B
5989.37	3	B	6030.35	1	C	6080.37	2	A
5990.22	1 l, nl?	B	6030.67	2 Cu?	B	6081.27	2	B
5990.85	2	B	6031.25	2	A	6082.08	2	B
5991.62	2	B	6032.10	1	B	6082.80	1	C
5992.06	<1	E	6032.53	1	B	6083.39	1	C
5992.64	3	B	6033.57	3	A	6083.93	1	C
5993.31	1 Cu?	C	6034.20	4	B	6084.90	1 d	C
5993.83	1	C	6034.59	2 d	B	6085.40	1	C
5994.29	1	C	6035.48	3	A	6086.62	2	B
5994.74	1	C	6035.85	1	B	6087.38	1	B
5995.35	4	B	6036.62	2	B	6087.62	1	B
5996.20	1	C	6037.07	1	B	6088.21	1	B
5997.00	3	B	6038.40	1	B	6088.88	3	B
5997.38	1	C	6039.05	1	C	6089.40	1	B
5997.77	1	C	6039.80	1	B	6089.65	2	C
5998.11	1	C	6040.59	2	B	6090.97	2	B
5998.46	1	C	6041.37	1	C	6091.74	1	C
5999.31	1	C	6041.92	1	C	6092.34	2	B
6000.17	2	B	6043.39	5	A	6093.19	3	B
6000.86	1	C	6044.14	1 l	B	6093.56	1	B
6001.83	4	B	6045.44	3	B	6093.83	1	C
6002.27	1	C	6045.88	2	B	6094.29	1	B
6002.68	1	C	6046.72	1 d	B	6096.96	1	B
6003.09	1	C	6047.39	4	A	6097.60	2	B
6003.66	2	B	6050.07	2 v	B	6098.34	5	A
6004.03	1	E	6051.30	1	B	6099.40	1	C
6004.50	1	C	6051.78	3	B	6099.77	2	B
6005.33	1	E	6052.60	2	A	6100.11	2	B
6005.85	4	A	6053.29	1	E	6100.79	1	B
6006.21	2	B	6053.94	1	B	6101.24	1	C
6006.80	4	A	6054.63	1	B	6101.56	1	C
6007.38	2	A	6055.30	1	B	6102.74	2	B
6008.47	1	B	6056.08	1	C	6103.42	2	B
6009.03	1	E	6056.45	1	B	6104.02	2	B
6009.63	1	B	6057.42	4 d	B	6104.84	1	B
6010.09	1	B	6057.99	3	B	6107.04	1	C
6010.44	2	B	6058.60	1	C	6107.79	1	B
6011.04	1	E	6059.32	2 d	B	6108.74	4	B
6011.55	1	B	6060.70	3	B	6109.72	1	B
6011.96	1	B	6061.67	1	B	6111.92	2	B
6012.31	1	B	6062.40	1	C	6112.90	1	C
6013.40	5	A	6062.75	1	C	6113.33	1	C
6014.06	2	B	6063.43	1	C	6114.27	1	C
6014.65	1	E	6064.05	1	E	6114.69	1	B
6015.44	1	B	6064.48	2	A	6115.15	1	B
6015.99	1	B	6066.23	1	B	6115.44	1	C
6016.56	2	A	6066.72	2	B	6116.47	1	C
6017.02	1	B	6067.02	2	B	6117.71	1	B
6017.28	1	A	6068.17	1	B	6118.56	2	B
6017.86	1	B	6068.65	2	B	6118.87	2	B

Digitized by Google

TABLE 3.—Arc Spectrum of Cerium—Continued

λ I. A.	Notes	Probable error	λ I. A.	Notes	Probable error	λ I. A.	Notes	Probable error
6119.79	2	B	6190.07	1	C	6271.18	1	B
6120.63	1	C	6192.27	1	B	6272.05	4	A
6123.66	4	A	6192.92	<1	E	6273.71	2 b	B
6124.31	1	B	6194.21	1	C	6274.35	1	B
6124.98	1	B	6194.75	1	B	6275.32	1	B
6125.43	1	C	6195.27	2	B	6276.45	3	B
6126.09	2 v, d?	B	6195.55	2	A	6276.86	1	C
6128.54	1	C	6196.29	2	A	6277.10	1	B
6129.00	1	B	6198.04	2	A	6279.10	1	B
6130.15	2	B	6200.65	1*	B	6281.58	1 l	B
6131.13	1	C	6201.83	2 b	B	6282.85	1	A
6132.06	3 d	B	6204.83	1 b, d?	B	6283.57	1	A
6132.76	1 d	B	6206.74	1	B	6283.99	1	A
6133.24	1	C	6208.32	1	B	6285.75	2	B
6133.61	2	B	6208.99	3	A	6286.34	2	B
6134.58	1	B	6209.58	2	B	6287.14	1	B
6135.51	2	A	6211.05	2	A	6287.64	1	C
6136.59	1	B	6211.67	<1	E	6290.49	1	B
6137.23	2	B	6212.51	2	A	6291.42	1	B
6138.33	1	B	6214.11	1	B	6294.36	1 d	B
6139.09	3	B	6216.07	2	A	6295.58	3	A
6139.82	1	C	6216.83	2	A	6296.15	1	B
6140.63	1	C	6220.72	1 d	B	6296.99	1	B
6141.34	1	B	6221.33	1	B	6299.51	3	A
6141.88	1 l, d?	B	6222.28	1	B	6300.23	3	A
6142.92	2	B	6223.23	2	B	6302.15	1	A
6143.39	4	B	6223.65	3 d	B	6302.77	1	B
6146.42	3	B	6225.50	1 d	B	6304.01	1	B
6146.95	1 d	B	6226.88	1	B	6305.26	1	B
6147.85	2	A	6227.32	1 l	C	6306.63	2	A
6149.58	2	B	6228.24	2	B	6307.55	1	B
6150.20	1	B	6229.00	4 d	B	6308.08	1	C
6151.20	1 v, d?	B	6230.26	1	B	6308.64	1	C
6151.73	2	A	6231.43	1 d	B	6309.29	1	B
6153.24	1	B	6232.46	3	A	6310.03	3	A
6153.92	1 d	B	6233.79	1 Cu?	C	6310.53	1	A
6155.05	1 b, d?	C	6237.45	3	A	6312.58	1	A
6155.49	2	B	6238.71	2	A	6316.44	1	B
6156.75	2	B	6241.47	1	B	6318.00	2	A
6157.63	1	C	6241.91	2	B	6318.57	2	A
6158.14	1	C	6242.92	2	A	6320.82	1	B
6158.93	2	A	6243.93	1	B	6321.25	2	A
6159.82	3	A	6244.87	1 b, f	B	6321.61	1	A
6161.36	1	B	6247.80	1	C	6322.37	1	B
6162.14	2	A	6249.64	1	C	6322.87	1	B
6162.73	1	B	6250.32	1	B	6323.87	1	B
6163.20	2	A	6250.91	1	B	6327.46	1	A
6164.43	1	B	6251.66	1	B	6328.16	1	B
6164.70	2	B	6253.27	1	B	6328.89	1 b, v	B
6165.54	2 d?	B	6253.62	2	B	6329.43	2	A
6166.56	1	B	6254.72	1	B	6330.05	1	B
6167.88	2	B	6255.74	1	B	6330.92	1	B
6172.91	2 d, air?	A	6256.36	2	A	6331.27	1	B
6174.00	1	E	6257.98	2	A	6332.00	2	A
6174.51	1	C	6258.60	1	C	6334.12	1	B
6175.28	2	A	6259.11	1 Dy?	B	6334.83	1	B
6177.96	2	A	6259.35	1	B	6335.39	3	A
6178.39	2	A	6259.78	1	C	6336.29	1	A
6180.08	1	A	6260.36	1 d	B	6337.22	2	A
6182.23	1	A	6261.06	1	B	6338.28	1	B
6184.04	2 d	A	6262.05	1 b, d?	B	6338.73	1	B
6186.16	3	A	6264.26	2	A	6339.89	1	A
6186.91	2	A	6266.23	1	A	6340.69	3	A
6187.91	2	A	6269.80	1	A	6341.85	1	B
6188.46	1	A	6270.28	2	A	6343.96	3	A

Digitized by Google

TABLE 3.—Arc Spectrum of Cerium—Continued

λ I. A.	Notes	Probable error	λ I. A.	Notes	Probable error	λ I. A.	Notes	Probable error
6344.87	1 l	B	6448.46	<1	E	6682.29	1	B
6345.82	1	B	6449.77	1	E	6684.49	2	A
6346.72	1 str?	A	6450.95	<1	E	6687.48	2 v	B
6347.35	1	A	6451.38	<1	E	6687.99	1	B
6348.28	1	A	6451.98	1	B	6690.34	1	B
6348.80	1	A	6453.86	1	B	6691.67	1 b, d?	C
6349.40	1	A	6454.92	1	A	6692.06	<1	E
6351.27	1	B	6456.84	1	B	6692.96	1	B
6351.59	1	B	6458.06	3	B	6693.60	1	B
6352.18	1	B	6458.54	<1	E	6694.46	2 b, Cu?	C
6353.52	1	A	6458.96	<1	E	6696.45	1 b	E
6360.23	2	A	6460.59	<1	E	6698.58	1	C
6366.60	1	B	6461.86	2	B	6699.20	1	C
6367.79	1	B	6462.77	1	B	6699.88	1	C
6369.19	2	A	6466.86	2	B	6700.09	<1	E
6370.60	1	B	6467.40	3	A	6701.69	2	A
6371.10	3	A	6468.46	1	C	6705.65	3	A
6372.48	1	A	6468.97	2	A	6709.40	1	B
6372.99	1	A	6470.96	1	A	6709.92	1	B
6374.82	1	B	6471.73	1	B	6710.75	1	B
6379.23	1	A	6472.54	1	B	6712.12	1	E
6379.75	1	A	6473.08	1	A	6712.98	1	B
6380.11	1	A	6473.67	4	B	6713.47	2	B
6383.13	1	B	6477.89	1	B	6715.71	1	B
6383.50	1	B	6478.53	1	B	6717.85	1	C
6386.16	2	A	6479.33	1	B	6718.52	2	C
6386.86	3	A	6480.75	1 v	B	6720.82	1	C
6390.32	1	A	6481.98	1 str?	A	6723.65	1	C
6390.66	1	B	6482.53	<1	E	6724.04	1	C
6393.02	2	B	6482.84	1 b	C	6724.45	1	C
6394.09	<1	E	6485.97	1	A	6725.52	1 b	E
6395.12	1	B	6487.56	1	A	6727.47	1	B
6396.26	1	A	6488.01	1	A	6729.09	2	B
6399.90	1	B	6488.68	1	B	6730.46	1	C
6400.66	1?	E	6490.97	2	A	6731.14	<1	E
6403.68	1	E	6494.59	1	E	6731.98	<1	E
6411.68	1	E	6494.93	2	C	6732.79	1	E
6412.85	1	E	6496.90	1	C	6733.45	1 b	E
6415.41	<1?	E	6497.92	1	C	6733.63	1 b	E
6416.39	1	B	6499.56	1	C	6739.34	<1	E
6418.06	<1	E	6500.42	1	B	6740.48	1	C
6419.06	<1	E	6501.82	1	C	6741.19	1	C
6422.91	1	B	6503.26	2	A	6742.32	1	C
6423.34	1	B	6504.06	1	A	6744.55	<1	E
6424.47	1	B	6506.22	1 b, v	E	6746.52	1	B
6425.30	2	B	6507.18	2	A	6747.00	1	B
6425.87	1	B	6507.74	<1	E	6747.57	1	B
6426.53	1	B	6509.01	2	A	6748.42	1	B
6429.04	1	A	6511.44	<1	E	6748.99	1	C
6430.07	2	A	6513.61	3	A	6749.61	2	B
6431.51	1 b, v	C	6517.28	2	A	6800.16	1	C
6431.92	1	B	6519.12	1	A	6801.57	1	C
6433.41	2	A	6521.51	1	C	6802.20	1	C
6434.38	2	A	6522.05	1	B	6803.32	1 b	C
6435.48	<1	E	6522.55	1	B	6804.06	1	C
6436.40	2	A	6525.33	1	B	6805.37	2	B
6438.16	1	B	6526.15	1	B	6806.33	2	B
6439.95	1	B	6527.03	1	B	6806.87	2	B
6440.45	1	B	6527.85	1	B	6808.31	1 b	E
6441.02	1	B	6528.76	1	B	6809.72	1	B
6442.08	1	B	6529.42	1	B	6811.13	1	C
6445.22	1	B	6530.17	1	B	6812.06	2	C
6446.16	2	B	6530.70	1 l	A	6813.20	1	C
6447.10	<1	E	6530.98	<1	E	6814.38	1	C
6448.00	<1	E	6531.80	1	B	6815.53	1	B

Digitized by Google

TABLE 3.—Arc Spectrum of Cerium—Continued

λ I. A.	Notes	Probable error	λ I. A.	Notes	Probable error	λ I. A.	Notes	Probable error
6616.30	1 b, df	C	6713.42	1 b, v	B	6836.53	2	B
6617.81	1	C	6715.41	1	B	6837.05	1	B
6618.84	<1	E	6720.32	2	B	6853.06	1	C
6632.98	2	B	6721.53	1	C	6865.68	<1	E
6633.72	1	C	6722.36	1	C	6867.15	<1 b	E
6634.39	1	B	6725.46	1 v	B	6867.98	1	B
6635.03	1	B	6726.52	1	B	6868.94	1	B
6635.50	1	B	6728.25	<1	E	6869.56	1	C
6637.50	1 l	C	6728.69	2	A	6871.07	<1	E
6638.88	3	A	6729.55	2	A	6871.75	<1	E
6643.32	1	B	6730.06	<1 l	B	6872.12	<1	E
6639.78	2	C	6733.21	1	B	6873.41	1	B
6635.06	2	B	6735.56	1	B	6873.86	1	B
6635.92	1	B	6736.79	<1	E	6875.43	1	C
6637.32	1	B	6743.48	<1	E	6876.97	1	C
6641.13	1	B	6744.03	<1	E	6878.26	1	B
6643.15	1	B	6744.70	1	B	6880.18	1	C
6645.01	1	B	6746.89	1	B	6882.49	<1	E
6646.77	1	C	6749.44	1	B	6883.41	<1	E
6647.38	2	B	6750.20	1	B	6885.56	1 b	E
6649.32	<1 b, l	E	6755.08	1	B	6886.38	1	B
6650.87	2	B	6757.12	1	C	6887.71	1	C
6651.40	1	B	6761.17	<1	E	6892.29	1	C
6652.75	3	A	6764.40	1	C	6893.64	2	C
6653.00	1	A	6766.92	<1	E	6894.55	2	C
6658.56	1	C	6767.65	1	C	6898.48	2	B
6658.29	2	C	6769.29	1	C	6899.07	2	B
6654.81	2	C	6769.72	1	C	6901.50	<1	E
6655.47	1	C	6770.15	1	C	6902.10	1	C
6656.98	<1	E	6771.12	<1	E	6903.11	1	C
6656.96	1 b	E	6773.33	<1	E	6903.51	1	C
6657.71	1	B	6774.25	2	B	6904.56	1 l	C
6658.55	1	B	6775.57	1 Cul	B	6907.83	1	C
6659.13	<1	E	6778.23	1	B	6909.31	1	C
6660.00	1	B	6780.15	1	B	6910.51	<1	E
6661.41	2	A	6780.72	1	C	6911.25	1 K?	C
6662.55	1	A	6785.06	<1	E	6912.24	1	C
6663.72	<1	E	6789.90	1	C	6914.18	<1	E
6665.65	2 b, l	A	6791.36	1	C	6914.77	1	C
6665.94	1	A	6792.61	1	C	6916.27	1	C
6666.57	1	B	6798.81	1	C	6919.27	1	C
6670.63	1	B	6794.68	1	C	6921.14	1	C
6665.53	2	B	6795.46	1	C	6922.77	3	C
6668.71	<1	E	6800.75	1	C	6927.32	1	C
6677.32	1	B	6805.20	1	C	6928.02	1	C
6668.84	2	A	6806.10	1	B	6931.31	1	C
6668.55	1	A	6807.33	2	B	6932.12	1	C
6668.83	<1	E	6808.89	1	B	6933.32	1	C
6665.30	<1	E	6811.72	1	B	6933.64	1	C
6685.70	<1	E	6812.99	<1	E	6934.02	1	C
6685.59	2	B	6815.29	1	C	6939.40	2	C
6687.34	1	B	6818.20	1	C	6941.97	1 b	C
6688.74	<1	E	6826.43	1	C	6943.04	<1	E
6688.25	<1	E	6828.37	1	C	6943.50	1	C
6689.71	1	B	6829.75	2	C	6944.37	1 b	C
6689.96	<1 b	E	6838.37	<1	E	6946.76	1 b, v	C
6691.93	<1 b	E	6834.21	1	B	6948.29	<1 h	C
6692.59	1	B	6839.98	1	B	6948.72	1 h	C
6694.35	1	B	6844.43	1 b	B	6949.57	1 h	C
6696.16	1 b, l	A	6846.78	2	B	6953.18	1	C
6699.67	3	A	6847.27	2	B	6953.54	1	C
6704.38	3 d	A	6848.76	<1	E	6954.70	1	C
6705.03	2	A	6849.21	1	B	6955.28	1	C
6708.07	1	B	6850.77	1	B	6956.28	1	C
6710.16	1	B	6856.61	2	B	6957.21	1	C

Digitized by Google

TABLE 3.—Arc Spectrum of Cerium—Continued

λ I. A.	Notes	Probable error	λ I. A.	Notes	Probable error	λ I. A.	Notes	Probable error
6957.75	1	B	7132.08	1	C	7397.76	2	A
6959.11	1	C	7136.05	<1	E	7401.21	1 b, n?	B
6959.68	1	C	7141.40	2	B	7414.86	<1	E
6960.69	2	B	7141.71	1	B	7417.93	1 v	B
6963.08	1	E	7150.20	2	B	7424.84	1 b, n?	C
6963.54	1	E	7151.66	2	B	7433.04	1	C
6966.32	1	B	7155.20	1	B	7438.55	<1	E
6968.70	1	E	7156.96	2	B	7440.45	<1	E
6969.16	<1 b	E	7162.40	<1	E	7444.46	1	C
6970.40	1	C	7163.77	<1	E	7462.29	<1	E
6972.33	1	B	7166.04	<1	E	7472.39	<1	E
6973.48	2	B	7166.71	<1 d	E	7486.53	<1	E
6981.24	1 b, l	B	7167.48	<1	E	7500.68	1	E
6981.99	<1 b	E	7167.88	<1	E	7505.46	<1	E
6983.77	1	B	7170.12	<1	E	7508.12	<1	E
6985.98	2	A	7174.95	1	B	7509.43	1 b	E
6991.48	1	B	7177.43	1	B	7509.75	1	E
6992.50	<1	E	7182.26	1	B	7511.36	<1	E
6993.10	<1	E	7186.18	<1	E	7527.58	1 b, d?	E
6999.85	2	B	7189.40	1 l, n?	B	7528.85	<1	E
7001.56	<1	E	7191.70	1	B	7539.53	<1	E
7003.18	<1	E	7196.78	<1	E	7540.64	<1 n?	E
7004.85	<1	E	7201.51	1	B	7541.24	<1	E
7006.52	<1	E	7201.86	2	B	7561.25	1 n?	E
7009.16	<1	E	7203.58	1	B	7556.63	<1 b	E
7009.86	<1	E	7205.23	1	B	7562.47	1	B
7010.59	1	C	7208.09	1	B	7562.92	1 l, n?	B
7013.33	1	C	7210.66	1	C	7563.52	1	C
7014.36	<1	E	7213.95	1	C	7616.06	1	C
7014.71	1	B	7217.34	2	B	7646.07	1	C
7017.18	1	B	7231.20	1	B	7663.37	<1	E
7017.72	<1	E	7232.44	<1	E	7670.89	2	C
7018.73	1	B	7232.95	1	B	7671.19	<1	E
7024.70	<1	E	7233.96	1	B	7678.11	1	C
7026.72	1	B	7235.70	2 n	B	7682.47	2	C
7029.90	1	B	7238.37	2	B	7689.13	2	A
7030.96	2	B	7241.69	2 n	B	7702.85	1	C
7040.75	1	C	7252.72	2	B	7734.70	<1	E
7049.60	1	C	7257.58	<1 p?	E	7782.32	2	C
7052.93	<1	E	7259.38	<1 p?	E	7748.35	1	B
7054.41	1	C	7262.63	1 p?	B	7797.73	2	C
7057.85	1	C	7275.57	1 p?	E	7835.81	2	B
7058.56	1	C	7277.92	1 n	B	7842.57	2	B
7059.91	1	C	7279.93	1 p?	B	7844.92	2	B
7061.69	3	B	7287.10	1 p?	E	7850.00	1	A
7064.41	1	B	7288.03	1 p?	E	7851.25	2	B
7065.68	1	B	7296.15	<1	E	7857.50	1	A
7066.41	1	C	7301.40	1	B	7859.05	2	B
7068.18	1	B	7310.24	<1	E	7860.54	2	B
7071.56	<1	E	7310.86	<1	E	7864.49	1	B
7075.13	<1	E	7311.75	<1	E	7866.05	1	B
7075.71	<1	E	7313.40	1	C	7874.10	1	B
7086.31	3	B	7329.90	2	A	7879.67	2 n	C
7087.04	<1	E	7334.69	1	B	7899.03	2 n?	B
7105.01	1	C	7337.65	<1	E	7904.84	1 n?	B
7110.25	<1	E	7343.41	1	B	7913.43	1	B
7113.10	1	C	7345.57	<1	E	7924.04	2 b*	C
7114.65	1	C	7361.81	<1 b	E	7927.53	2 n?	C
7115.07	1	E	7362.38	1	B	7953.57	1*	E
7118.72	<1	E	7363.11	1	B	7964.50	1*	E
7120.07	<1	E	7372.49	<1	E	7972.34	2 b*	E
7120.82	<1	E	7379.64	<1	E	7975.49	2 b*	C
7121.30	1 d?	E	7383.71	1	B	8002.66	2	C
7122.05	<1	E	7390.42	1	C	8018.94	1 b*	B
7123.45	<1	E	7393.42	1	B	8025.57	2	A

Digitized by Google

TABLE 3.—Arc Spectrum of Cerium—Continued.

λ I. A.	Notes	Probable error	λ I. A.	Notes	Probable error	λ I. A.	Notes	Probable error
8066.97	1 nl*	C	8332.30	1 b	B	8516.24	1	B
8109.09	1	B	8336.89	1	B	8523.32	1	B
8114.53	1	D	8349.19	1	C	8526.88	1 l, n?	D
8116.70	1 b*	C	8352.39	2	C	8535.26	1	B
8120.32	2	A	8355.32	2	B	8539.04	1	B
8165.35	1	B	8358.05	1	B	8543.30	1	E
8171.32	1	B	8363.82	2	B	8545.40	<1	E
8175.35	1	C	8368.55	1	B	8548.13	1	C
8179.81	1 b	C	8371.90	2	B	8560.60	2	C
8195.28	1	B	8376.35	1	C	8564.56	1	B
8199.09	1	B	8381.02	1	B	8567.36	1	C
8215.50	1	A	8383.14	1	C	8575.56	1	B
8220.65	1	A	8386.22	<1	E	8583.87	2 h,l,Cu?	B
8223.69	2 b, df?	B	8387.71	<1	E	8612.62	2	B
8226.94	1	B	8396.20	2	D	8613.58	1	E
8234.12	3 b	B	8403.67	1	D	8633.25	<1	C
8237.73	1	B	8405.02	1	D	8636.40	1	B
8239.37	1	B	8408.65	1 h, Cu?	D	8647.59	2	B
8241.53	1	B	8417.96	2	C	8672.45	1	C
8245.10	2	B	8426.16	<1	E	8677.46	1	D
8246.79	1	C	8427.24	1	C	8702.32	1	C
8250.53	1	C	8441.05	1	B	8704.25	1	B
8251.21	1	B	8442.39	<1	E	8716.64	1	C
8252.52	1	B	8446.88	1	E	8756.26	1	C
8258.35	1 b	B	8455.97	<1	E	8772.08	3	B
8261.03	2	B	8459.98	1 b, d	B	8782.30	1	E
8276.36	1	B	8467.38	2 b	C	8810.77	1	E
8278.02	1	B	8475.78	1	B	8891.14	1	C
8296.06	1 nl?	B	8483.34	1 b	B	8910.98	1	C
8299.84	<1	E	8488.21	1	B	8927.42	1	D
8300.58	2	B	8491.67	<1	E	8970.41	<1	E
8310.22	2	B	8495.64	3	B	8992.36	<1	E
8312.30	1	B	8503.57	1 b	B	8998.85	<1	E
8322.85	1 b	C	8511.16	1	C	9024.68	1	B
8327.58	1	C	8513.70	1 b	C			

IV. SUMMARY

The yellow, red, and infra-red regions of the arc spectra of yttrium, lanthanum, and cerium have been photographed with various concave gratings in the spectrograph of the Bureau of Standards. Plates specially sensitized with the dyes pinacyanol, kryptocyanin, and dicyanin were used for making the spectrograms. Two sets of materials were burned in copper or graphite arcs to furnish the luminous sources studied. These consisted of the chlorides of yttrium and lanthanum and the nitrate of cerium obtained from Eimer and Amend; and the oxalates of yttrium and lanthanum and the oxide of cerium obtained from the chemical laboratory of the University of Illinois, where they were prepared under the direction of Prof. B. S. Hopkins. The tables contain a total of about 2300 wave lengths, many of which are heads of bands. In yttrium about 175 lines were measured from 5003 A to 7882 A where the spectrum seems to end abruptly. In lan-

Digitized by Google

thanum about 400 lines were measured between 5501 A and 9079 A; and in cerium 1700 lines were measured between 5500 A and 9025 A.

To F. J. Stimson and Mr. Myers credit is due for assistance in the securing and reduction of many of the spectrograms, to Prof. B. S. Hopkins, of the University of Illinois, for the generous samples of materials used in the work, and to Prof. J. S. Ames, of Johns Hopkins University, for the loan of the several gratings with which some of the work was done.

Digitized by Google

PART II.—THE PREPARATION OF PURE RARE EARTH ELEMENTS

By B. S. Hopkins and H. C. Kremers

ABSTRACT

At the University of Illinois compounds of Ce, Sa, La, Nd, and Gd were extracted from sodium rare-earth sulphate, donated by the Welsbach Co.; and compounds of yttrium, dysprosium, and erbium were extracted from gadolinite obtained from Norway and Texas, and from an oxalate prepared from xenotime.

Cerium was removed from the Welsbach residues by boiling the neutral solution with potassium bromate to precipitate basic ceric nitrate. After removal of Ce, Sa was concentrated at the soluble end of a magnesium double nitrate series of fractional crystallizations, and La at the insoluble end of the series, the middle fractions of the series being used in the preparation of Nd. Gd was obtained from the fractions at the soluble end of the series, Sa being nearly all removed by adding bismuth magnesium nitrate.

The yttrium-group material was first freed from the cerium-group elements. It was then converted to bromate and subjected to a long series of fractional crystallizations. From the various bromate fractions, Y, Dy, and Er were prepared, respectively. Y probably contained not more than 0.005 per cent Ho and was reasonably free from other earths. The best samples of Dy contained some Tb and Ho; and the best Er fractions contained considerable Y and probable small amounts of other rare earths.

I. INTRODUCTION

The work upon the rare earths which has been in progress for several years at the University of Illinois has been concerned with both the cerium-group and yttrium-group elements. Of the cerium-group elements, compounds of samarium, lanthanum, neodymium, cerium, and gadolinium have been furnished to the Bureau of Standards for the accurate measurement of spectrum lines. These materials were practically all derived from the same source, which was a shipment of 182 kg of sodium cerium-group sulphates obtained through the courtesy of the Welsbach Co., of Gloucester, N. J., and its chief chemist, Dr. H. S. Miner. The early steps in the purification of compounds of these elements are identical, and consequently the process is described under the first elements, cerium and samarium, and the description for the other elements is taken up where each is separated from the general process.

The materials from the yttrium group include compounds of yttrium, erbium, dysprosium, and gadolinium. The sources of

Digitized by Google

o kg of gadolinite which came from Norway
th oxalates which had been prepared from
sed from Drossbach & Co., Freiburg, Saxony.
gadolinite were obtained from the deposit at
, Tex. The first steps in the purification of these
are identical, since the elements of this group resemble
other closely in properties. When, however, the material
s treated for some time by the method of fractional crystallization, separations began to appear, and each element was in turn separated from the general process. Accordingly, in this description the treatment of the ore and the first steps in the separation are explained under yttrium, while the discussion of the other elements is taken up at the point where each was removed from the general process.

II. THE CERIUM GROUP

1. CERIUM [13]

The rare earth residues obtained from the Welsbach Co. were chiefly the sodium double sulphates of lanthanum, praseodymium, neodymium, samarium, gadolinium, and cerium, with small amounts of europium and the yttrium-group elements. These double sulphates were boiled for a few hours with a 50 per cent sodium hydroxide solution until they were completely disintegrated. The mass was diluted and the resulting hydroxides filtered and washed with boiling water until free from sulphates. The hydroxides were dissolved in nitric acid, and the rare earths precipitated from hot solution by oxalic acid. After a thorough washing on a Büchner funnel with hot water, the oxalates were drained as dry as possible and dissolved in pure nitric acid. The resulting nearly neutral solution was heated to boiling and potassium bromate added in 10 g portions as proposed by James and Pratt.[14] When the liberated acid became strong enough to set free the fumes of bromine, lumps of marble were added to keep the solution neutral. Then the solution was boiled until the cerium present was thrown down as the deep yellow, insoluble basic ceric nitrate. This operation was continued until all but about 1 per cent of the cerium had been removed. This point is determined roughly by the intensity of the color of the precipitate formed in the hydrogen peroxide test for cerium and also

[13] This work was carried out in conjunction with Dr. Edward Wichers.
[14] J. Am. Chem. Soc., 33, p. 1326; 1911.

Digitized by Google

by the fact that the last portions of cerium are thrown down very slowly by this treatment.

In this manner almost chemically pure cerium was separated. About 1 per cent was left in the solution because if an attempt had been made to precipitate the last of the cerium in the same manner it would have been contaminated by other rare earths.

The basic ceric nitrate was filtered off and washed thoroughly with a 5 per cent solution of ammonium nitrate, which prevented the precipitate from becoming colloidal. The cerium material was then dissolved in nitric acid with the aid of a little alcohol and again precipitated as the basic ceric nitrate in the same manner as before. After another thorough washing the material was once more converted to the nitrate. A 20 cm layer of this solution showed no absorption lines, when viewed with a spectroscope.

The final purification consisted in precipitation of the oxalate in the presence of free nitric acid, followed by a thorough washing of the precipitate. This process was repeated twice more and finally the oxalate was converted to the oxide by ignition in platinum.

2. SAMARIUM [15]

The solution from which most of the cerium material had been removed, as just described, was boiled still further to remove the last traces of cerium, an excess of marble being present to keep the solution neutral. In this manner all the remaining cerium and a small amount of the other rare earths were thrown down. The boiling was continued until a small filtered portion of the solution failed to respond to the hydrogen peroxide test for cerium. When this point was reached, the residue, which consisted of a mixture of marble and ceric basic nitrates intermingled with some of the other rare earths, was filtered off. Then the remaining rare earths were precipitated from a boiling solution by hot oxalic acid solution. The precipitated rare earth oxalates were washed thoroughly first by decantation and then on a large Büchner funnel. The oxalates were dried in an air bath and ignited in an electric furnace and the resultant oxides dissolved in nitric acid. A quantity of nitric acid equal to that used in the solution of the rare earth oxides was neutralized by adding magnesium oxide. The two nitrate solutions were then filtered, mixed, and evaporated until crystals of the magnesium rare earth nitrate began to

[15] The samarium material was prepared by Dr. A. W. Owens, formerly of the Bureau of Standards while he was a student at the University of Illinois.

Digitized by Google

form on the surface. To prevent the formation of a crust on the surface as the solution cooled, a layer of water was added carefully and the dish left undisturbed for 24 hours. At the end of this time the solution was thoroughly drained off from the crystals and both crystals and mother liquor put through the process of fractional crystallization. Whenever the solution at the insoluble end no longer showed in the spectrum the absorption lines of neodymium, this dish was set out of the series and reserved for work on lanthanum and praseodymium. When the soluble end began to crystallize poorly, this portion was diluted, filtered, and the rare earths separated from other soluble salts by precipitation with oxalic acid. The fractionation was continued as long as samarium continued to appear at the soluble end.

When it became evident that the samarium had all been removed from the series, the oxalates from the soluble end were ignited and again converted into the magnesium rare earth nitrate by the method already described. The second fractionation was carried out in the same manner as before with the object of more completely separating samarium and neodymium. When the absorption bands of neodymium disappeared from any fraction at the soluble end it was set out of the series and the samarium precipitated by oxalic acid. When the samarium lines disappeared from any fraction at the insoluble end it was set out for the preparation of pure neodymium material.

The samarium oxalate, prepared as stated, contained appreciable amounts of gadolinium, some europium, and most of the yttrium group earths contained in the original monazite residues. To free the samarium from the yttrium-group elements the method of fractional crystallization of the magnesium double nitrate in 30 per cent nitric acid was used. After 180 fractionations in this manner it was found that practically all the yttrium earths had been removed. Double magnesium bismuth nitrate was then added at the soluble end of the series, as first proposed by Urbain and Lacomb.[16] The fractionation was now continued in the same manner as formerly, with the samarium coming out at the insoluble end, with the bismuth salt next, and the europium and gadolinium following in order at the soluble end. As the fractionation continued the concentration of the nitric acid solvent increased to 50 per cent or more, which probably aided the complete isolation of samarium. After 35 fractionations in this manner, the material at the insoluble end was thought to be pure

[16] C. R., 187, p. 793; 1903.

Digitized by Google

samarium, since no absorption lines other than samarium had been visible for some time. Accordingly atomic weight determinations, using the oxide to chloride ratio, were run on 6 fractions, as follows:

Fraction No.	Atomic weight
9	155.35
10	154.32
11	152.64
12	153.06
13	152.60
14	153.81

The lack of uniformity in the results and the high values were interpreted as indicating considerable variations in the composition of the fractions. Accordingly the fractionation was continued through 150 additional crystallizations, and then the atomic weights of fractions 32 to 43 determined by the same ratio. The values obtained in this second series were somewhat lower than in the first, but again there was a discouraging lack of checks upon duplicate analyses. Several considerations pointed to the fact that the oxide-chloride ratio was at fault. When the same material was used in determining the atomic weight by the chloride-silver ratio splendid results were obtained, showing that the material was uniform in composition and free from other salts. Eighteen successful determinations made on material taken from 14 different fractions gave extreme values varying between 150.49 and 150.40, with a mean of 150.43, which agrees with the accepted value 150.4.

The material sent to the Bureau of Standards was taken from these purest fractions, the final purification being accomplished by alternate precipitations as hydroxide and oxalate.

3. LANTHANUM [17]

Those fractions of the magnesium double nitrate crystallization which were set out at the insoluble end of the series, as explained in the preceding discussion, contained lanthanum with small amounts of praseodymium. These lanthanum-rich fractions were then removed and converted into the double ammonium nitrates and given a long series of recrystallizations. Lanthanum can best be separated from small amounts of praseodymium by means of the double ammonium nitrates. Since praseodymium, with possible small amounts of neodymium, would be the only other rare earths present here, a simple absorption spectrum analysis of the

[17] The preliminary part of the fractionation of the double magnesium nitrates was carried out by Dr. E. Wichers and the fractionation of the double ammonium nitrates was carried out by Dr. E. W. Engle.

Digitized by Google

solution would indicate the purity of the lanthanum. The purest lanthanum thus obtained showed no absorbtion bands when observed through a 10 cm layer of the concentrated solution. The final purification of the lanthanum material was accomplished by precipitation from hot solution with oxalic acid in the presence of free nitric acid; the precipitate was thoroughly washed, dried, ignited, and redissolved in nitric acid. This process was repeated twice more, the final treatment stopping with the oxalate, which was the material supplied for spectrum work.

4. NEODYMIUM [18]

The fractionation of the neodymium-rich portion of the double magnesium nitrate series from which the lanthanum had been obtained as described above was continued for some time. Since neodymium is more abundant than any other earth of this group, after the separation of cerium, the problem of obtaining relatively large quantities of neodymium of high purity is not difficult. The concentration of neodymium in the fractionation of the double magnesium nitrates is more rapid than that of any other earth whose isolation is effected by fractional crystallization methods. Thus if the fractionation of a series of high-grade neodymium material of several kilograms in weight is continued for a considerable length of time—e. g., some hundreds of fractionations—the middle fractions will consist of very pure material. All of the lanthanum and smaller amounts of praseodymium together with a high per cent of neodymium concentrate toward the least soluble end. The more soluble end will consist of a high per cent of neodymium of course, with the remainder composed mostly of samarium plus very small traces of gadolinium and europium. As fractionation continued in the above series the end fractions were removed from time to time. When it became apparent that no further concentration of the middle fractions took place the fractionation was discontinued. The oxide was prepared by the same method as that described under cerium and lanthanum.

5. GADOLINIUM

In the separation of the yttrium and cerium groups with either potassium or sodium sulphate, the terbium group of earths will be divided between the two groups. From this condition it follows that either or both the cerium or yttrium group may be taken as the source of gadolinium material. The gadolinium oxide

[18] The fractionation of the neodymium-rich material was carried out by Dr. E. W. Engle.

Digitized by Google

supplied to the Bureau of Standards was obtained from the cerium group. The raw material originally came from the Welsbach Co. as previously described.

In the fractionation of the double magnesium nitrates of the cerium group the increasing solubility of the earths is as follows: Lanthanum, praseodymium, neodymium, samarium, europium, gadolinium, and terbium. The more soluble end of this series which very frequently does not crystallize well will contain mostly samarium, europium, gadolinium, and terbium. The soluble end of a large double magnesium nitrate series was mixed with bismuth nitrate and subjected to a long series of recrystallizations by other workers in this laboratory. The purpose in mind was the removal of the samarium at the insoluble end and the concentration of the gadolinium at the soluble end of the series. This separation was made completely by taking advantage of the fact that bismuth-magnesium nitrate is isomorphous with the magnesium rare earth nitrates and intermediate in solubility between samarium on the one hand and gadolinium on the other. The fractions obtained at the soluble end showed a high concentration of gadolinium. This material formed the basis for the work on gadolinium by Jordan and Hopkins.[19] These authors removed the bismuth and magnesium from this material in the regular way and subjected the oxide to a few precipitations with oxalic acid. The atomic weight of this oxide as determined by the permanganate method of Gibbs was 157.20. This value seemed to indicate very pure gadolinium. This material did, however, show some samarium absorption lines and the color of the oxide indicated some terbium. Since the atomic weight of samarium is 150.4 and terbium 159.2, these two values would neutralize each other. Bettendorf[20] discovered that if gadolinium oxide containing small amounts of terbium oxide was gently heated in hydrogen a pure white oxide resulted, and when again heated in air the oxide turned brown. The present authors found this to be the case with respect to the material at hand. This was then high-grade gadolinium with small amounts of samarium and terbium and perhaps traces of europium.

The usual methods of purification for the preparation of the oxide were used; that is, the complete removal of traces of bismuth with hydrogen sulphide and several alternate precipitations with freshly prepared ammonia and recrystallized oxalic acid.

[19] J. Am. Chem. Soc., 39, p. 2614; 1917.
[20] Ann. Chem. Liebig., 268, p. 167; 1891.

Digitized by Google

III. THE YTTRIUM GROUP

1. YTTRIUM [21]

The gadolinite was pulverized in a ball mill, treated with an excess of HCl to which a little HNO_3 was added occasionally. After complete decomposition the silica was dehydrated and filtered off, then the rare-earth material was precipitated from a slightly acid solution with oxalic acid, both solutions being hot. The rare earth oxalate prepared in this way was mixed with the purchased oxalate derived from xenotime. The dry oxalates were converted to anhydrous sulphates by mixing with enough concentrated sulphuric acid to form a thick paste and then heating till fumes were no longer given off. The sulphates were dissolved in ice water and solid sodium sulphate sifted in, the solution being stirred continuously. The addition of sodium sulphate was continued until a 3-inch layer of the solution did not show the absorption lines of neodymium, when it was assumed that the relatively small per cent of the cerium group elements present was nearly all precipitated. The solid cerium-group sodium sulphates were filtered off and set aside, the solution containing the more soluble yttrium-group sodium sulphates was first treated with ammonium hydroxide and the precipitated hydroxides were washed very thoroughly to remove the sodium salts. The hydroxides were dissolved in hydrochloric acid and precipitated from hot solution by oxalic acid.

The first method of fractionation used was the method of fractional crystallization of the bromates as proposed by James.[22] The bromates were prepared by adding to a solution of the rare-earth sulphates a hot solution of barium bromate. The bromate solution was added slowly, the solutions being thoroughly agitated by a mechanical stirring device. The rare earth bromate solution was filtered off and subjected to fractional crystallization, the progress of the separation being observed by a direct vision spectroscope. After a few hundred series of fractionations had been carried out, it was found that certain portions of the series showed the color and absorption lines characteristic of various members of the group. As the fractional crystallization of the main series continued, certain portions, showing sufficient concentration of the individual earths, were set out of the main series forming a number of smaller subseries, whose treatment was

[21] The preliminary purification of yttrium material was done by Dr. J. E. Egan and other workers.
[22] J. Am. Chem. Soc., 30, p. 182; 1908.

Digitized by Google

continued for the purpose of further purification of the elements present.

The richest yttrium material selected from the fractional crystallization of the bromates was precipitated by oxalic acid, ignited to the oxide and the dry oxide, mixed with the calculated amount of chromic acid in an 8-liter round-bottom Jena flask. After thorough mixing, a small amount of water was added, when a violent reaction took place. Water was then added until the flask was about half full, then a 10 per cent solution of potassium chromate was added with shaking, until a faint cloudiness indicated that a permanent precipitate had begun to form. The material was then heated to boiling on a sand bath, a lively current of steam was passed into the solution to prevent the precipitate from collecting on the bottom and 10 per cent solution of potassium chromate was added drop by drop from a separatory funnel. The amount of chromate added was determined by the size of the precipitate desired. After adding the precipitant, boiling was continued for from one to two hours, the steam and burners being so regulated that the volume of solution remained constant. Finally, the material was cooled, the precipitate filtered out, dissolved in hydrochloric acid, a few cubic centimeters of alcohol added to reduce the chromate, and the rare earth precipitated with oxalic acid.

The chromate method of fractional precipitation was found to be efficient for removing from the yttrium material all of the rare earths present except erbium and holmium. From this treatment nearly 400 g. were obtained, with an average atomic weight of 90.3, as determined by the oxide to sulphate ratio. The absorption spectra of this material showed considerable holmium and erbium but none of the other rare earths.

Purification by fractional precipitation with dilute ammonia was carried out on two series of salts. One was obtained from the best fractions of the chromate fractionation (called the H series) and the other included 246 g of yttrium oxalate prepared in a similar manner, but showing no holmium lines (called the E series). In both series the rare earth chlorides were dissolved in water and diluted largely. Then 2 or 3 liters of ammonia of approximately 0.01 N strength were added. Under these conditions no precipitate appeared when the solutions were first mixed but on standing several hours a cloudiness appeared and after 24 hours a slight precipitate collected in the bottom of the flask.

Digitized by Google

After the precipitate was filtered out and purified the filtrate was evaporated to its original volume and the process repeated. The H series was fractionated 42 times in this way and the E series 37 times, the average fraction weighing about 3.1 g. The fractions of the H series below number 30 showed a constant atomic weight of 89.9, with holmium lines still prominent, but very little erbium. The E series shows an atomic weight of 88.7 in the fractions below number 25, the lower value being attributed to the absence of holmium, which the ammonia precipitation does not remove efficiently. The low atomic weights found are probably due to the fact that the values were obtained by a method which gives lower results than the oxide to sulphate ratio.

The purest fractions from both the E and H series of ammonia precipitations were further purified by fractional precipitation with sodium nitrite following in general the method of Holden and James.[28] This method consists in adding a strong solution of sodium nitrite to a dilute solution of rare earth material which has been carefully neutralized, and then boiling for a time, usually about one hour. It was found that the purification took place somewhat more rapidly if the rare earth solutions were sufficiently dilute so no precipitate formed when the ammonia was added. On boiling, the precipitate appeared. After standing some hours, the precipitate was filtered out, dissolved in nitric acid and purified, while the mother liquor was again fractionated. The best material from the H ammonia series was fractionated as the N series, which was split into 8 fractions, the last 4 of which showed an entire absence of color, while the first 4 fractions showed a decreasing pink color, indicating that erbium was concentrated in the first precipitates. Fractions N_3, N_4, N_5, and N_6 showed a constant atomic weight of 88.8 by the Gibbs method, while fractions N_7 and N_8 gave a value of 87.6. In spite of the fact that N_3 and N_4 showed a very faint pink tint, it was concluded that fractions N_3, N_4, N_5, and N_6 were presumably more nearly uniform than the last 4 fractions.

The fall in atomic weight shown at N_7 was thought to be due to the presence of some more basic material such as scandium or sodium. No trace of scandium was revealed by test with a saturated K_2SO_4 solution. The presence of sodium in these last fractions was considered probable because in the method of fractionation the mother liquor becomes heavily loaded with sodium salts. Accordingly N_7 and N_8 were very thoroughly purified by

[28] J. Am. Chem. Soc., 36, p. 1419; 1914.

Digitized by Google

alternate precipitations with ammonia and oxalic acid, together with two precipitations with ammonium sebacate. In spite of these steps the atomic weight of fractions N_7 and N_8 remained unchanged, and no explanation has yet been made for this peculiar fact. To prevent the possible use of material of lower atomic weight, fractions N_7 and N_8 were set aside and fractions N_3, N_4, N_5, and N_6 were combined, giving 106.2 g of material of average atomic weight of 88.87. This material was fractionated again by the nitrite method as series O, six fractions being obtained. The first 2 fractions showed the concentration of the erbium in the faint pink color and atomic weights 89.18 and 89.42, respectively. Fractions O_3, O_4, O_5, and O_6 were white, with atomic weights from 88.69 to 88.42.

A quantity of yttria corresponding to 37 g of the oxide was collected from the best fractions of the E ammonia series. This was split into five fractions by the sodium nitrite method forming series R. All of the fractions were pure white and showed a constant atomic weight, the values obtained varying between 88.58 and 88.40, which is only slightly more than the probable experimental error of the Gibbs method. Both these fractions and the O fractions showed very faint holmium lines when viewed through an accurate spectroscope looking through a 5 cm layer of concentrated solution. By comparison of this line with a standard holmium solution it was estimated that the amount of holmium present could not exceed 0.005 per cent.

The work of preparing the pure yttria was performed by Egan and Balke,[24] and by Hopkins and Balke.[25] Additional details are to be found in these papers.

Of the fractions prepared as described, O_4, O_5, O_6, R_3, R_4, and R_5 were used for the determination of atomic weight as described by Hopkins and Balke. Portions of the same material were used by Kremers and Hopkins[26] for the determination of the atomic weight by the chloride to silver ratio. The value obtained by the latter method, 89.33, has been accepted by the International Committee.[27] The material supplied the Bureau of Standards was taken from the mixed O_{4-6} fractions.

[24] J. Am. Chem. Soc., 35, p. 365; 1913.
[25] J. Am. Chem. Soc., 38, p. 2332; 1916.
[26] J. Am. Chem. Soc., 41, p. 718; 1919.
[27] J. Am. Chem. Soc., 41, p. 1881; 1919.

Digitized by Google

2. DYSPROSIUM

The dysprosium material came entirely from the gadolinite and xenotime oxalate previously mentioned. From the main series of bromate fractions there were set out subseries C and D, as described by Engle and Balke.[38] These were further fractionated as the bromates for the concentration of dysprosium. After a long series of fractionation, series D indicated a high concentration of dysprosium collecting toward the middle fractions. Small amounts of neodymium and praseodymium had continually collected toward the less soluble end and were removed from time to time. Likewise the fraction showing stronger holmium bands had been removed from the more soluble end from time to time. Series C, which was composed mostly of dysprosium and holmium, with very small amounts of terbium and other earths, after a long series of fractionation indicated a concentration of high-grade dysprosium in the less soluble end.

The dysprosium-rich material from series D was then converted into a nitrate series. Bismuth nitrate was also added to the nitrate series with the hope that in the course of the fractionation the bismuth would aid the separation of the small amounts of terbium from the dysprosium. After 50 series of fractionations no marked separation had taken place and the series was converted to the ethyl sulphates.

The oxides obtained by Engle and Balke[39] from the simple nitrate series were dissolved in the calculated amount of ethyl sulphuric acid which was 0.63 normal. The neutral solution so obtained was warmed gently under diminished pressure until quite concentrated and then air was blown over the surface until crystals began to form. The series was then fractionated in the usual manner, using absolute alcohol as a solvent, since the ethyl sulphates hydrolyze badly in aqueous solution, especially if a trace of free acid is present. In dissolving the crystals it was necessary to use a steam bath at a temperature no hotter than the hand could bear with comfort. If precautions are taken to prevent the hydrolysis of the ethyl sulphates, this method of fractionation is found to be very useful, since there is much less tendency to form supersaturated solutions than in a bromate or nitrate series, and in addition the separation of dysprosium is quite satisfactory. After 20 series of fractionation as the ethyl sulphates, series D indicated that practically all the neodymium

[38] J. Am. Chem. Soc., 39, p. 53; 1917.
[39] For detailed description, see J. Am. Chem. Soc., 39, p. 53; 1917.

Digitized by Google

and praseodymium had been removed at the least soluble end and the dysprosium-rich fractions contained traces of terbium.

The dysprosium-rich fractions of series C were also converted to the ethyl sulphates and fractionated for some time. High-grade dysprosium material, with some holmium and traces of terbium, was obtained from this series. At this point all fractionation of the dysprosium material was discontinued by these workers and their time directed toward the accurate determination of the atomic weight of dysprosium.

The further purification of this dysprosium material was later continued as published by Kremers, Hopkins, and Engle.[30] Series C as left by the former workers contained a fraction of 1 per cent of terbium with slight amounts of neodymium and praseodymium toward the less soluble end. Holmium was contained in all the fractions. This series was fractionated 65 times. Practically all of the neodymium and praseodymium had been removed. The color of the oxide indicated slight amounts of terbium still present. The holmium was not removed by this method.

Series D contained besides the dysprosium only traces of terbium. After 60 series of fractionations small amounts of terbium still remained, although a considerable amount had concentrated toward the least soluble end.

The dysprosium oxide was prepared as follows: The alcoholic solution of the ethyl sulphates was diluted with water, a few cubic centimeters of dilute sulphuric acid added, and the solution heated to boiling and filtered. The dysprosium was then precipitated with oxalic acid. Several alternate precipitations with ammonia and oxalic acid were given. The ammonia precipitation was carried out by passing ammonia gas over the dilute nitrate solution and agitating until precipitation was complete. The hydroxides were washed by decantation until they became colloidal and then dissolved in nitric acid preparatory to the oxalate precipitation. A hot dilute solution of oxalic acid was added to the hot nitrate solution up to the point where precipitation began. Upon allowing the solution to cool a crystalline precipitate was obtained, which was easily washed. The washed oxalate was dried and ignited in platinum if another ammonia precipitation was desired. The oxalic and nitric acids here used were especially purified as described in the published work.[31] The oxide supplied for the spectroscopic examination was taken from the best fraction of series D.

[30] J. Am. Chem. Soc., 40, p. 398; 1918.
[31] Loc. cit.

Digitized by Google

3. ERBIUM [32]

During the fractionation of the main bromate series of the yttrium group several of the individual fractions rich in erbium were removed from time to time and made up into series F, as described by Engle and Balke.[33] The fractionation of series F bromates was continued by these workers for some time, the object in view being to concentrate erbium. Finally several fractions were obtained composed only of erbium and yttrium, The erbium content was approximately 20 per cent. The fractionation of the bromates was then discontinued and the greater share of this material was subjected to other fractional methods with the hope of obtaining erbium of a high grade of purity. This latter work was undertaken by Wichers, Hopkins, and Balke.[34] The basic chloride method of Drossbach [35] was reported to give strikingly rapid results. Dr. Wichers applied this method to erbium-yttrium material of atomic weight 104. The yttrium and erbium fractions obtained had atomic weights of 95.9 and 110.6, respectively. These results, although good, were not as striking as claimed by Drossbach. The cobalticyanide method of James and Willard [36] was then tried on an erbium-yttrium mixture of atomic weight 108.5. Eleven fractions were obtained, the first and last atomic weights being 123.0 and 89.2, respectively.

Fractional precipitation with sodium nitrite has been used quite successfully by Hopkins and Balke [37] for the purification of yttrium. Dr. Wichers applied this method to a material of atomic weight of 108.5. Two series of precipitations were made, the erbium-rich material obtained from the first series being used in the second series. The best erbium material obtained in the second series of precipitations had an atomic weight of 142.9. It was apparent that none of the above methods could compare in efficiency to the nitrate fusion method.

In the fractionation of the bromates of an erbium-yttrium mixture several fractions rich in erbium and far removed from holmium on the one hand and thulium on the other had been obtained. A series of 32 nitrate fusions on this material gave the following fractions, with approximate atomic weights as indicated:

32 H	32 I	32 K	32 L	32 M	32 N	32 O	32 P
166.31	.....	.....	166.17	164.68	163.75	154.63	119.90

[32] Dr. Edward Wichers assisted in the preparation of erbium material.
[33] J. Am. Chem. Soc., 39, p. 53; 1917.
[34] J. Am. Chem. Soc., 40, p. 1615; 1918.
[35] Zeit. anorg. Chem., 76, p. 174; 1912.
[36] J. Am. Chem. Soc., 38, p. 1198; and 1497; 1916.
[37] J. Am. Chem. Soc., 38, p. 2332; 1916.

Digitized by Google

The 5 fractions richest in erbium were used by Dr. Wichers in the study of the oxide-chloride ratio for the atomic weight of erbium. A portion of fractions 32 N and 32 O, the best erbium material on hand at this time, was selected and purified to supply the oxide for the Bureau of Standards. This material was composed of only erbium and yttrium. It was purified in essentially the same way as the method used for dysprosium; that is, several alternate precipitations with ammonia and oxalic acid and final ignition in platinum.

WASHINGTON, March 31, 1921.

Digitized by Google

Digitized by Google

DEPARTMENT OF COMMERCE

SCIENTIFIC PAPERS

OF THE

BUREAU OF STANDARDS

S. W. STRATTON, DIRECTOR

No. 422

STUDIES IN COLOR SENSITIVE PHOTOGRAPHIC PLATES AND METHODS OF SENSITIZING BY BATHING

BY

FRANCIS M. WALTERS, Jr.
Associate Physicist

RAYMOND DAVIS
Photographic Technologist

Bureau of Standards

NOVEMBER 15, 1921

PRICE, 15 CENTS

Sold only by the Superintendent of Documents, Government Printing Office
Washington, D. C.

WASHINGTON
GOVERNMENT PRINTING OFFICE
1921

Digitized by Google

Digitized by Google

DEPARTMENT OF COMMERCE

LIBRARY OF THE UNIVERSITY OF CALIFORNIA

SCIENTIFIC PAPERS

OF THE

BUREAU OF STANDARDS

S. W. STRATTON, DIRECTOR

No. 422

STUDIES IN COLOR SENSITIVE PHOTOGRAPHIC PLATES AND METHODS OF SENSITIZING BY BATHING

BY

FRANCIS M. WALTERS, Jr.
Associate Physicist

RAYMOND DAVIS
Photographic Technologist

Bureau of Standards

NOVEMBER 15, 1921

PRICE, 15 CENTS
Sold only by the Superintendent of Documents, Government Printing Office
Washington, D. C.

WASHINGTON
GOVERNMENT PRINTING OFFICE
1921

Digitized by Google

Digitized by Google

Digitized by Google

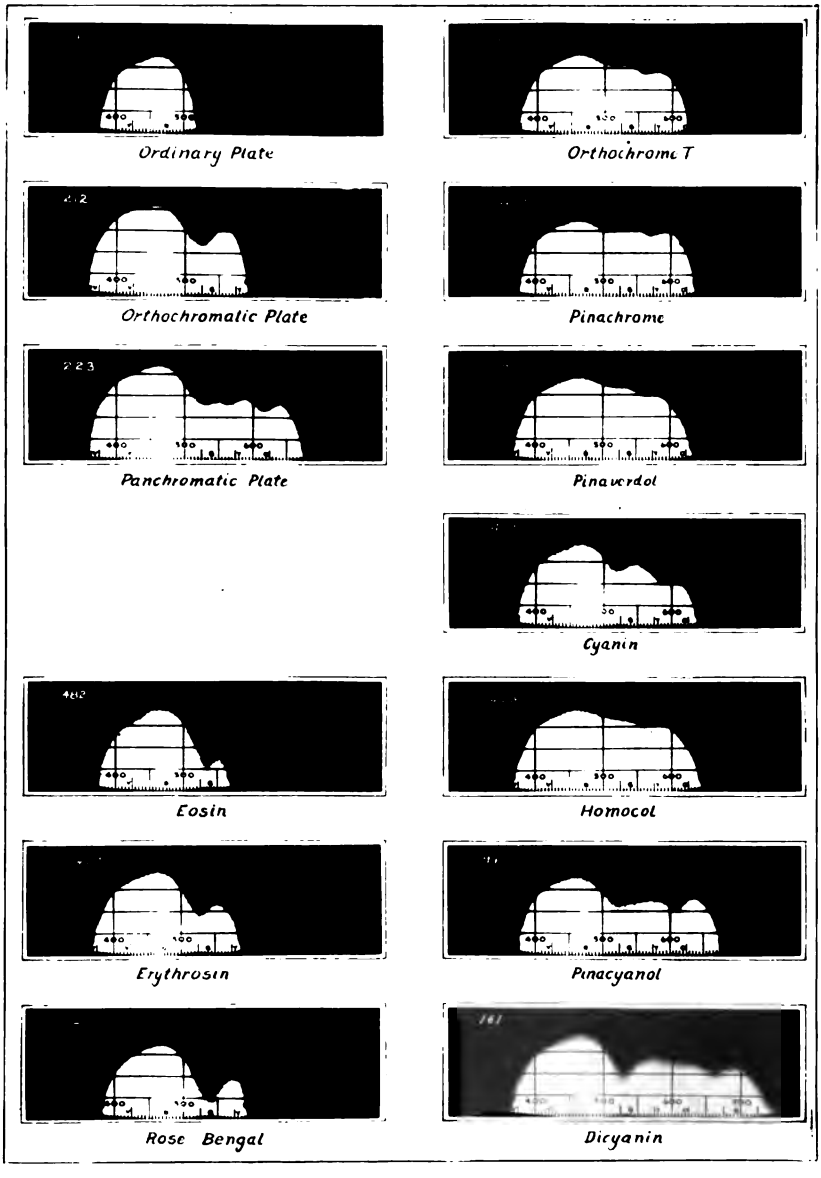

FIG. 1. *Spectrograms of commercial and bathed plates*

Spectrograms in the upper left-hand corner show the regions of color sensitativeness of the three types of commercial dry plates. The other spectrograms show the sensitiveness conferred to ordinary blue sensitive plates (Seed, 26x in this case) by bathing in solutions of sensitizing dyes. The name of the dye used is given under each spectrogram. The numbers indicate the wave length in $\mu\mu$. The letters V, B, G, Y, O, and R indicate the colors—violet, blue, green, yellow, orange, and red. They are placed at the center of the region recognized as being occupied by these colors. Beyond the violet and the red are the invisible rays, called ultra-violet and infra-red. All photographic plates are sensitive farther out into the ultra-violet than is indicated by these spectrograms. The cutting off of the ultra-violet is due to the glass used in the optical system of the spectrograph. A glass lens, such as is ordinarily used in a camera, has the same characteristic.

Digitized by Google

STUDIES IN COLOR SENSITIVE PHOTOGRAPHIC PLATES AND METHODS OF SENSITIZING BY BATHING

By Francis M. Walters, jr., and Raymond Davis

ABSTRACT

The dyes which are used in color sensitizing ordinary (blue sensitive) plates by bathing require different methods for their most successful application. Pinaverdol, pinachrome, orthochrome T, and homocol may be used in water solutions, with or without ammonia, and are very little sensitive to the presence of electrolytes. Pinacyanol may be used in water solution, if the dry plates are first thoroughly washed, but gives greater sensitizing action with more fog and poorer keeping qualities when used with water, alcohol, and ammonia. Dicyanin gives comparatively little sensitizing except when used with water and alcohol and a fairly large per cent of ammonia. Films require the use of alcohol and ammonia to give the best results with pinacyanol.

Commercial panchromatic plates have their color sensitiveness improved by washing in water, without the increase in fog which occurs when they are treated with ammonia.

CONTENTS

		Page
I.	Introduction	353
II.	General information	355
III.	Methods of studying color sensitiveness	357
	1. Spectrograph method	357
	2. Sensitometer method	358
IV.	Pinacyanol	360
	1. Water bath	360
	2. Water, alcohol, and ammonia bath	361
	3. Keeping tests	362
	4. Bathing films	363
	5. Speed of plates before and after bathing	365
V.	Dicyanin	366
VI.	Orthochromatic sensitizers	367
	1. Erythrosin	367
	2. Pinaverdol, pinachrome, orthochrome T, and homocol	368
VII.	Hypersensitizing commercial panchromatic plates	368
VIII.	Increase in speed by washing before exposure	369
IX.	The technique of plate bathing	372
X.	Procedure and formulas	373
XI.	Summary	374

I. INTRODUCTION

Photographic plates and films owe their sensitiveness to light to the silver bromide embedded in the gelatine with which they are coated. Silver bromide as found in the ordinary plate (as

Digitized by Google

well as silver chloride and silver iodide, which are also used in the preparation of photographic materials) are affected only by blue, violet, and ultra-violet light. Green, yellow, orange, and red have little or no effect, so that a photograph made on such a plate portrays blue, violet, and ultra-violet (which do not affect the eye) as white; while green (to which the eye is most sensitive), yellow, orange, and red are portrayed as black. This failure of the photographic process to render colors in black and white in the same order of luminosity as does the eye prevented for a long time the satisfactory photography of paintings, as well as the correct rendering of objects in nature.

By the addition of small amounts of certain dyes the photographic plate may, however, be made sensitive to green, yellow, orange, and red. Plates which are sensitive to the yellow-green as well as to the blue and violet are usually called orthochromatic, while plates which are sensitive also to the orange and red are called panchromatic or spectrum plates.

These three types of plates are illustrated in Fig. 1. The letters at the botton of the spectrograms indicate the centers of the radiations usually recognized by the names: V, violet; B, blue; G, green; Y, yellow; O, orange; R, red. Beyond the blue and red are found the ultra-violet and the infra-red. The numbers express the wave length of the radiation in millimicrons (1 millimicron= 0.000 000 001 meter). The sensitiveness of the plate to any particular radiation is indicated by the height of the white part of the figure; thus a height equal to 4 spaces indicates that the plate is 4 times as sensitive to that radiation as it is to radiation where the white area reaches only to the third line and 16 times as sensitive as where it reaches only the second line. This sensitiveness refers, of course, only to the sensitiveness of the plate to the particular source used in making the spectrograms and not to its sensitiveness in terms of absolute energy.

Color-sensitive plates date from Vogel's discovery in 1873[1]. In one of his experiments a collodion dry plate which had been stained yellow with aniline red to prevent halation showed, in addition to its blue and violet sensitiveness, a sensitiveness in the green. This region of sensitiveness corresponded to an absorption band in the spectrum of aniline red. He had much difficulty in the sensitizing of his plates, often obtaining only one satisfactory plate out of six attempts. With gelatine dry plates even greater

[1] Vogel, Handbuch der Photographie, 4th ed., I, p. 204; 1890.

Digitized by Google

difficulty was had until the notable discovery in 1882 of eosin [2], which made silver bromide gelatine plates much more sensitive to yellow than any dye before used. Following this encouraging discovery of the sensitizing action of eosin many other dyes were investigated by Vogel, Schumann, Eder, and others, the number investigated by Eder [3] and his students running into the hundreds. Comparatively few, however, found application in photography. The exceptions were cyanin, an orange sensitizer discovered by Vogel, and erythrosin, a strong yellow-green sensitizer discovered by Eder [4] in 1884. (See Fig. 1.) Only one of these, erythrosin, remains in use to-day. Orthochromatic photography made little real progress until 1904–05, when König introduced pinachrome, orthochrome T, and pinacyanol (Fig. 1). Pinacyanol sensitizes strongly in the red and serves as the foundation of commercial panchromatic plates.

II. GENERAL INFORMATION

Plates and films may be sensitized by two methods: (1) The dye may be incorporated in the emulsion at some stage in its preparation, usually immediately before coating, and (2) by bathing an ordinary blue sensitive dry plate in a solution of the dye. In general, the more sensitive plates result from bathing, but bathed plates often have the defect of not keeping.

The amount of dye required for sensitizing is very small. When incorporated in the emulsion, 2 to 4 mg to 100 cc of emulsion give the best results with most dyes, while in bathing the best concentration lies between 1 part in 25 000 and 1 part in 75 000, although much smaller amounts give some sensitizing action.

In order to sensitize, a dye must combine with the silver bromide itself. Further, the dyestuffs which sensitize all fall into the class of so-called substantive dyes; that is, they dye substances directly. The center of the region which is sensitized by a given dye lies about 20 millimicrons farther toward the red than the center of the absorption band of the dye.[5] Thus dyes which sensitize for the yellow-green are reddish in color, as, for example, erythrosin and pinaverdol. Dyes which sensitize for orange are purple, and red sensitizers are greenish. Eder found that the less silver iodide a silver bromide gelatin emulsion contained the better it

[2] Attout Tailfer and Clayton; French patent No. 152645 of Dec. 13, 1882, and Mar. 29, 1883.
[3] Eder, Ausführliches Handbuch der Photographie, 2, p. 443; 1898.
[4] Eder and Valenta, Beiträge zur Photochemie und Spectralanalyse, Part III, p. 174, Wien; 1904.
[5] Eder, Handbuch, 2, p. 150.

Digitized by Google

sensitized. Silver chloride sensitizes readily, but its original sensitiveness is so much less than that of silver bromide that the sensitized salt does not compare in rapidity with sensitized silver bromide.[6] An important characteristic of a dye suitable for sensitizing is its solubility. It must be soluble in water, or it must at least be capable of forming a fairly stable colloidal solution with it. Dyes soluble only in other solvents—for example, alcohol—can not penetrate the gelatine in such a manner as to dye the silver bromide. In addition, the dye should be of such a character as not to stain the gelatine so as to prevent the light from penetrating to the silver bromide. Were it not for this necessary characteristic, there are probably many dyes which would sensitize.

Before the war sensitizing dyes were principally imported from Germany. When this supply was cut off, the preparation of the dyes was undertaken by various laboratories in England and in the United States. The Ilford Co., of London, produced pinacyanol and pinaverdol, while in this country, the Eastman Kodak Co. are making orthochrome T as well. The color laboratory, Bureau of Chemistry, Department of Agriculture, has prepared pinaverdol, pinacyanol, and dicyanin. The success of these investigators has led to the preparation of entirely new sensitizers which promise marked improvement in panchromatic plates.

While commercial panchromatic plates are now sufficiently rapid for the photography of still objects and for three-color process work, there are certain problems which demand plates which are either more rapid or which are sensitive to radiations to which the panchromatic plate is not. Those who have these problems find it advisable to use ordinary plates sensitized by bathing. Important among the special problems are those in the field of spectroscopy, in which use is made of dicyanin to photograph infra-red spectra, and specially stained plates are indispensable in recording the visible spectrum of faint sources.

The directions which are furnished by the dye manufacturer for using the dye for bathing are at variance with the methods used at this Bureau and by some other workers. The work described in this paper was undertaken with the view of ascertaining the relation between the methods developed at this Bureau and the practice recommended by the dye makers.

[6] Eder, Handbuch, 2, p. 154.

Digitized by Google

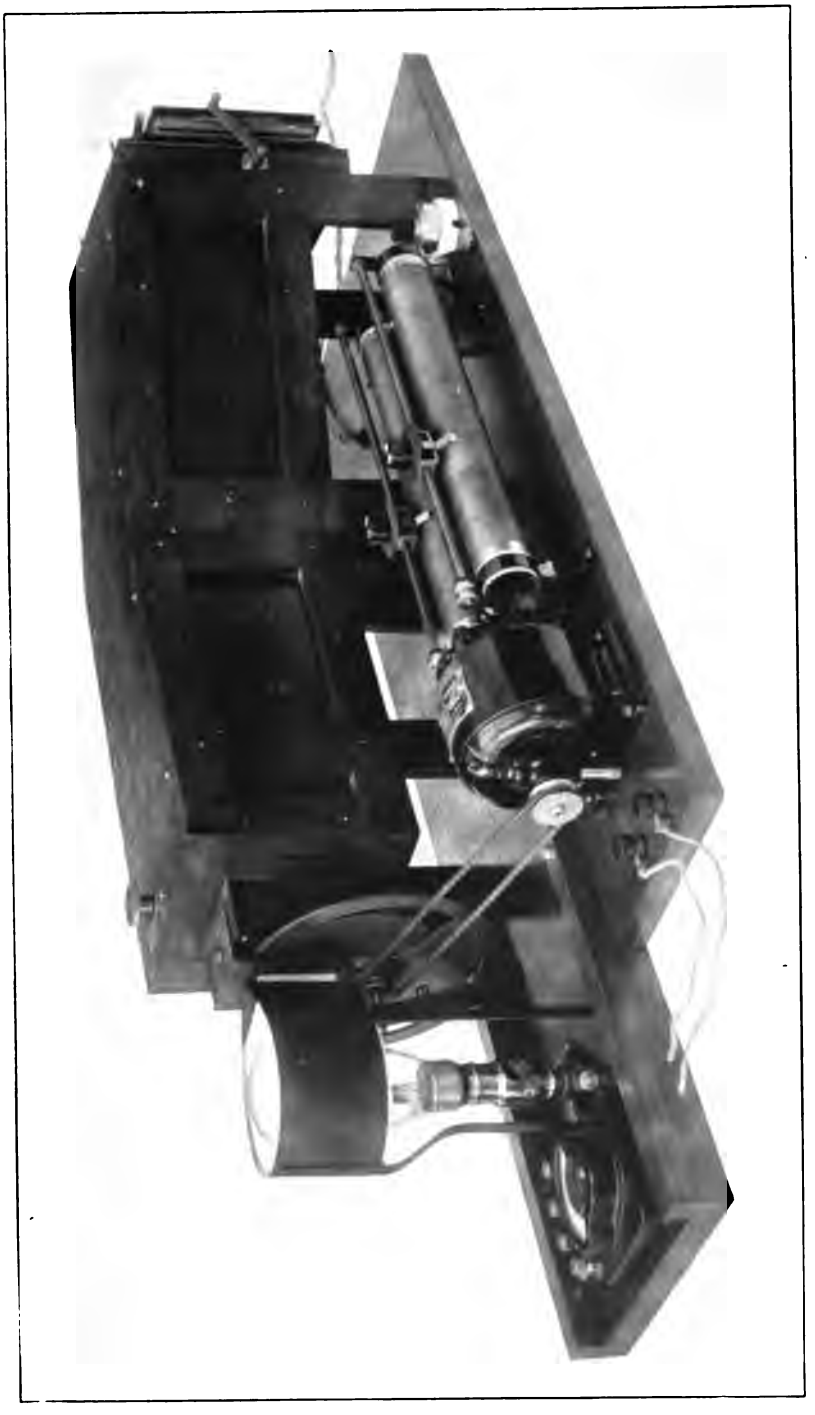

FIG. 3.—*Spectrograph to study relative color sensitiveness of plates and films*

Digitized by Google

Digitized by Google

Since pinacyanol is the most widely used red sensitizer and since good orthochromatic plates may be obtained commercially, the greater part of the investigation was done with this dye. Various methods and conditions of bathing were studied and keeping tests were made on plates sensitized by two methods of bathing. In addition to pinacyanol other important sensitizing dyes were studied.

III. METHODS OF STUDYING COLOR SENSITIVENESS

In studying the various ways of sensitizing by bathing two methods were employed: (1) The continuous spectrum of a source of white light was photographed on the plate, and (2) the

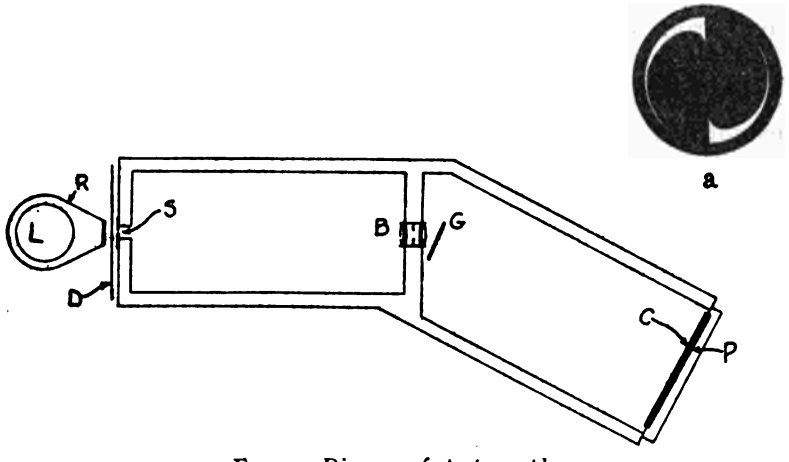

FIG. 2.—*Diagram of spectrograph*

Disk for varying exposure along the slit located at *D*. *L*, lamp; *R*, reflector; *S*, slit; *B*, lens; *G*, replica grating; *c*, the wave-length scale which is in contact with photographic plate under test.

speed of the plate to white light was measured and the filter factors of the plate with a given set of color filters were determined.

1. SPECTROGRAPH METHOD

The spectrograph shown in Fig. 2 was designed for studying the color sensitiveness of plates.

The light source (*L*) is a 100-watt tungsten lamp whose brightness is kept constant by adjusting a rheostat to maintain a constant current through the filament. Around the lamp is a white reflector (*R*), while in front of the slit is a piece of ground glass, to give uniform illumination along the slit, which is 2 inches high. Between the ground glass and the slit is placed a rotating disk (*D*), out of which is cut a variable aperture such that the exposure

Digitized by Google

along the slit varies in a fixed manner with the distance from its ends. The series of horizontal lines on the spectrograms indicate geometrically decreasing exposures. The exposure at the first line from the bottom is one-fourth that at the bottom; at the second line, one-sixteenth; at the third, one sixty-fourth; at the fourth, one two-hundred-and-fifty-sixth; and at the top, one one-thousand-and-twenty-fourth. The light from the slit passes through first a photographic lens (*B*), then a replica of a diffraction grating, which disperses it into a normal spectrum. Just in front of the plate (*P*) is a screen (*C*) bearing on it the reference lines which mark both intensities and wave lengths on the plate. The end of this screen, through which the red part of the spectrum passes, is stained with "rapid filter yellow" to screen out the second-order violet light which in the grating spectrum is superposed on the first order red.

As shown in Fig. 4, the tungsten lamp used for the investigation does not have the same spectral distribution of energy as does the sun. The tungsten lamp is deficient in the blue as compared to the sun and is relatively more intense in the red than the sun.

The spectrograph serves as a very convenient means of studying qualitatively the sensitizing action, showing as it does the regions of sensitiveness, both as to extent and as to the location of the maxima, and also, in addition to other detriments, the degree of fog induced by the process. For work of a quantitative character, however, such as a study of the time of bathing or the effect of the proportion of dye in the sensitizing bath, greater exactness is desirable. This is found in photographic sensitometry.

2. SENSITOMETER METHOD

Sensitometry consists in the exposure of a photographic material to a known source of light for definite intervals of time, the development of the material under standard conditions, and an interpretation of the blackening produced on the material in relation to the time of exposure and the intensity of the light acting. The details of the methods of sensitometry used in this work will be described in a forthcoming Bureau scientific paper.

Sensitometry is applied to the study of color sensitizing by using filters which transmit light of particular colors only. The filters used in this investigation, the relative spectrograms of which are shown in Fig. 5, are Wratten A, which gives the red sensitiveness; Wratten G, which gives very nearly the added sen-

Digitized by Google

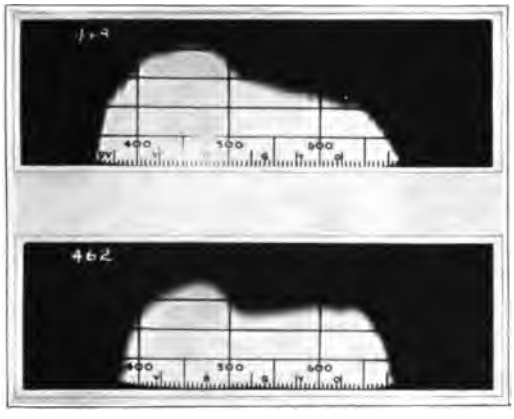

FIG. 4.—*Spectrograms showing the energy distribution of sunlight and of the tungsten lamp which was used in making the spectrograms to show the sensitizing action of the various dyes*

The vertical lines in the solar spectrum are the Fraunhofer lines. A comparison of the two spectrograms shows that the lamp has relatively more energy in the red than has the sun

Digitized by Google

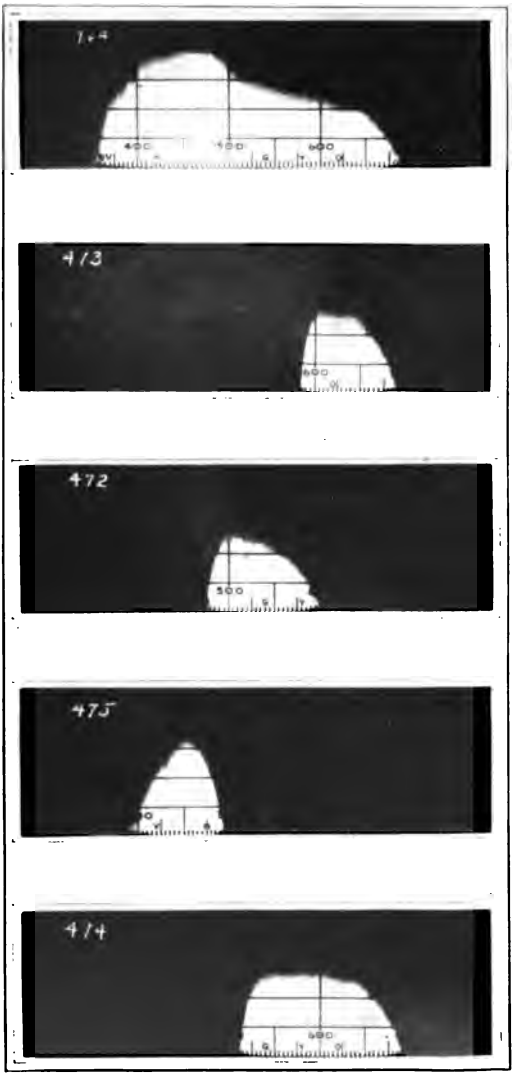

FIG. 5.—*Spectrograms (with sunlight as the source) of a commercial panchromatic plate with the filters used in the speed tests*

The A, B, and C filters select the red, green, and blue respectively, while the G transmits light of such color as to afford a measure of the added sensitiveness due to the dye

Digitized by Google

sitiveness due to the dye; Wratten B, which gives the sensitiveness to green, and Wratten C, to blue.

The speed or sensitiveness of the plate to the light transmitted by the filter may be measured by either introducing the filter between the light source and the plate in the exposing apparatus or by measuring the speed to white light and dividing this by the filter factor of the plate. When a number of filters are used, the second is the more rapid. The following procedure was, therefore, employed: Three strips from the sensitized plate were exposed in the sensitometer to a light source having approximately the spectral energy distribution of average noon sunlight, the strips were developed for different times, the densities measured and plotted against the logarithm of the time of exposure, and a speed determination made according to the method of Hurter and Driffield.[7] When used with the four Wratten filters mentioned above, two strips from the plate served to determine the factors of the plate.

The filter factors were measured as described in Bureau Scientific Paper 409. The principle of this consists in varying the intensity of the light source until equal blackening is produced with equal exposure time with and without the filter. Since the filter factor gives the ratio of the total sensitiveness of the plate to its sensitiveness to the light transmitted by the filter, the filter factor and the speed of the plate without the filter give the data necessary to determine the speed of the plate with the filter. For example, if the speed of a plate to white light (average noon sunlight) is 400 and the filter factor with the A filter is 10 the speed through the A filter is 40.

The method of stating color sensitiveness employed by Eder,[8] Sheppard and Mees,[9] and Wallace [10] gives the added or chromatic sensitiveness in terms of the blue sensitiveness. This method we believe to be unsatisfactory, because the blue sensitiveness is decreased more or less by any process of sensitizing to other colors and because the ratio of the color sensitiveness to the blue sensitiveness does not give the best basis for comparison of one plate with another. The question to be answered is, Does this method or that give the greatest sensitiveness to a given color of light, regardless of what happens to the blue? This question

[7] Ferguson, "Photographic researches of Hurter and Driffield," Royal Photographic Society, London, 1920.
[8] Eder and Valenta, Beitrage zur Photochemie II, p. 126.
[9] Sheppard and Mees; Investigations on the Theory of the Photographic Process, p. 320, London; 1907.
[10] R. J. Wallace, Astrophys. Jour., 26, p. 305; 1907.

Digitized by Google

is most directly answered by the speed of the plate to the light in question

IV. PINACYANOL

Pinacyanol is, for many purposes, the most important sensitizer. Although it is commonly used in commercial panchromatic plates in conjunction with other sensitizers which give greater sensitiveness in the yellow-green, it alone gives a fairly good panchromatic plate.

1. WATER BATH

The following is typical of the directions given by the makers for the use of pinacyanol: Dissolve 1 part of pinacyanol in 1000 parts of ethyl alcohol for the stock solution. To make red sensitive plates, bathe ordinary gelatine plates for two or three minutes in the following solutions: Water, 200 parts; stock solution, 3 parts. Wash well in running water, or frequent changes for several minutes, and dry in total darkness as quickly as possible in a current of warm, dry air free from dust.

If these directions are followed, it is found that the dye precipitates on standing after a plate has been bathed in it, or often before the plate has been sensitized, which results in the plate being spotted and lacking in sensitiveness. Pinacyanol is not soluble enough in cold water to wash away any dye deposited on the plate in the gelatine.

The addition of alum, ammonia, potassium bromide, and other electrolytes to the dye bath (water 200 cc, pinacyanol stock solution 3 cc) causes flocculation of the dye. This may indicate that the bath is not a true solution, but a colloidal solution or dispersoid.

This phenomenon suggested to the writers that the failure of the water bath in sensitizing ordinary commercial plates might be due to the presence of electrolytes in the emulsion. It is customary to add to the emulsion immediately before coating a small quantity of chrome alum to harden the gelatine, so that it will withstand alkaline development at room temperatures. There may also be present various other electrolytes, such as soluble bromides to restrain fog.[11] If present, these soluble salts would come to the surface of the plate in drying and would thus be in a position to cause the speedy flocculation of the dye bath.

Accordingly, we tried washing the plates in tap water before bathing in a water solution of pinacyanol and found that the plates then did not cause the flocculation of the dye bath. The

Digitized by Google

time for bathing is also decreased by this operation, since the gelatine swells somewhat and permits diffusion to take place more rapidly. With a washing time of five minutes the time required for sensitizing is decreased to two minutes.

While not so fast as plates sensitized in a bath containing ammonia, the water-bathed plates show considerably less initial fog and also keep much better.

Another point of importance is that if a plate be examined after removal from the dye bath there is found on it a considerable amount of the dye which is not removed by washing in water. In addition, there is a considerable staining of the gelatine, which decreases by its screening action the sensitiveness of the plate. Rinsing the plate in ethyl alcohol after the dye bath will remove to a large extent the dye dissolved in the gelatine, as well as that on the surface, while not affecting that which has combined with the silver bromide and to which the sensitizing action is due. That this is true may be shown by the fact that prolonged bathing in alcohol after sensitizing in the water bath does not decrease the color sensitiveness. It is common experience that bathed plates must be dried rapidly to secure speed and freedom from fog.[12] In addition, therefore, to furnishing cleaner plates, the rinse in alcohol aids in drying the plates. The drying is accelerated by the alcohol, which replaces to a large extent the water in the gelatine film.

2. WATER, ALCOHOL, AND AMMONIA BATH

It has been observed (particularly with erythrosin) that the addition of ammonia to the dye bath increases the sensitizing action of the dye. If ammonia be added to a water bath of pinacyanol, flocculation occurs and prevents sensitizing. However, ammonia may be safely added to the dye bath if sufficient alcohol be present. Thus the formula used at this Bureau calls for—

	Parts
Water	60
Ethyl alcohol (95 per cent)	40
Pinacyanol stock solution (1 to 1000)	4
Ammonia (28 per cent)	4

For ordinary work this quantity of ammonia usually gives too much fog and is recommended only in the case of plates which

[11] Eder, Handbuch, 3, p. 86. [12] R. J. Wallace, Astrophys. Jour., 26, p. 299; 1907.

Digitized by Google

are used for position measurements, as in spectroscopy. If the amount of ammonia be cut from 4 to 2 cc, the sensitizing action is nearly as great and the fog is much less. Compared with plates bathed in water and pinacyanol, the sensitizing action is twice as great. As shown in Fig. 6, the sensitizing action of a bath composed of water and alcohol with no ammonia is less than the bath containing water only. For use in spectroscopy the ammonia method has the particular advantage of extending the region of sensitiveness, so that lines further in the red may be photographed. (See Fig. 7.)

It should be emphasized, however, that ammonia as a sensitizer reduces the keeping qualities of plates below those of other sensitizers.

3. KEEPING TESTS

In making the test on the relative keeping quality of plates sensitized by the two methods of bathing a slow portrait plate which works fairly free from fog was used. A dozen of these were bathed by each method on a clear, dry day.

The water bathing was carried out as follows: The plates were placed in the cage of a developing tank, washed in running tap water (temperature 18° C) for five minutes, then transferred to a bath composed of tap water 1900 cc, pinacyanol stock solution (1 to 1000) 38 cc. After bathing for two minutes they were placed in alcohol for two minutes, swabbed off, and dried in a light-tight cabinet, through which air at room temperature was forced by an electric fan. When dry the plates were packed face to face in an ordinary plate box.

The other dozen plates were placed directly in a tank containing a bath composed of—

	Parts
Water	1300
Ethyl alcohol	700
Pinacyanol stock solution	40
Ammonia (28 per cent)	40

After four and one-half minutes in this bath (18° C) the plates were rinsed for two minutes in alcohol, swabbed off, and dried.

As soon as the two sets of plates were dry one of each was exposed in the sensitometer, and its filter factors were also measured. Another pair was treated in the same manner a few hours later on the same day. Then tests were made once a day for a few days and finally at intervals of about a week.

Digitized by Google

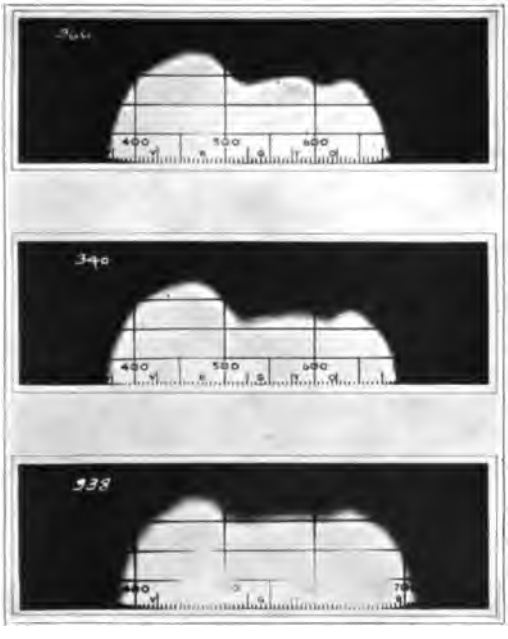

Pinacyanol and water; five minutes prewash in tap water

Pinacyanol, water, and alcohol

Pinacyanol, water, ammonia, and alcohol

FIG. 6.—*Spectrograms showing the difference in the sensitizing action of pinacyanol when used in baths of various composition*

Notice the increased action with ammonia, both in the height of the maxima and in the extension of the region of the sensitizing

Digitized by Google

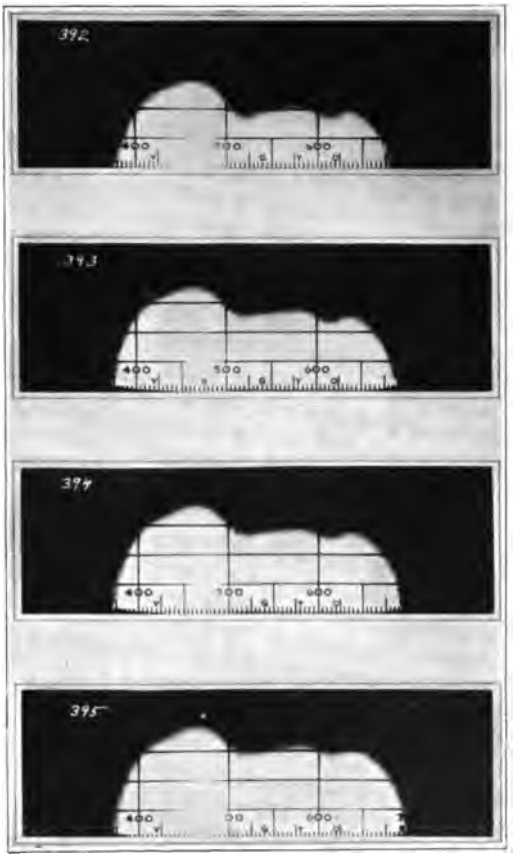

FIG. 7.—*The effect of various quantities of ammonia added to a dye bath of water and alcohol*

Note that there is comparatively little difference between the 2 cc and the 4 cc in sensitizing action. However, the fog which is not indicated in the cuts increases with the proportion of ammonia

Digitized by Google

The curves in Fig. 8 show the variation in speed [13] to white light and the fog [14] of the plates sensitized by the two methods.

Fig. 9 shows the characteristic curves for a plate sensitized with pinacyanol, water, alcohol, and ammonia when the plate was usable, while Fig. 10 shows the characteristic curves of a similar plate after it had become unfit for use.

The variation in speed through filters with time of keeping is shown in Figs. 11 and 12. If these curves be compared with those for the variation in speed to white light (Fig. 8), it will be seen that while the speed to white light was decreasing the speed due

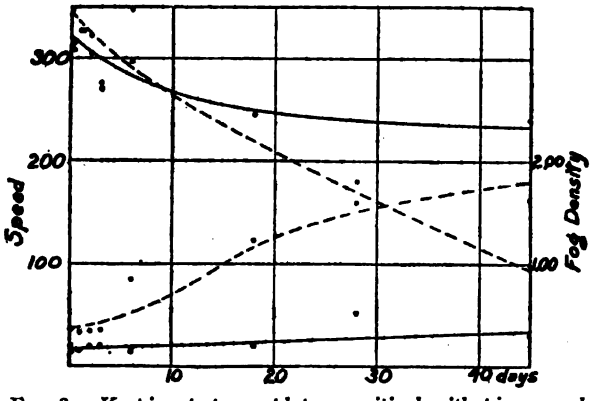

FIG. 8.—*Keeping tests on plates sensitized with pinacyanol*

The curves which start at the upper left-hand corner of the graph show the speed to white light, while those that start at the lower left-hand corner show fog (for unit development to unit contrast) measured in density. Full lines=plates sensitized in pinacyanol, water, alcohol, and ammonia.

NOTE.—The fog is given for $\gamma = 1$; that is, a development such that the contrast of the negative is the same as that of the subject.

to the added sensitiveness conferred by the pinacyanol did not decrease at quite the same rate.

4. BATHING FILMS

In sensitizing films with pinacyanol it was found that the method of prewashing and bathing in a water solution of the dye

[13] "Speed" as used here is measured by the method of Hurter and Driffield. Briefly, this is as follows: When the density due to exposure to light is plotted against the logarithm of the time of exposure some of the points will lie on a straight line. If samples of the plate which have received a set of exposures are developed for different lengths of time, their respective straight line parts extended intersect nearly in a point on the exposure axis. The value of the exposure at this intersection point is called the "inertia" of the plate. The speed numbers used by us are 10 divided by the inertia, so that the greater the speed number the faster the plate. This number was selected instead of Hurter and Driffield's 34/I because the light source employed by them (the sperm candle) is deficient in the blue as compared with our light source, which approximates average noon sunlight in its distribution of spectral energy. It should be noticed that for this reason our speed numbers are not convertible into Hurter and Driffield numbers.

[14] Fog is measured as density. Density is defined as $\log^{10}(1/T)$, where T (transmission) is the ratio of the transmitted to the incident light. Thus a fog density of 0.30 transmits one-half of the light falling on a plate; a density of 1.00, one-tenth of the incident light and a density of 2, one one-hundredth.

Digitized by Google

was not successful and that to get adequate sensitizing action it was necessary to use the bath containing water, alcohol, and ammonia. Films have a tendency to give more fog with bathing than do some plates. It has been remarked by some that any

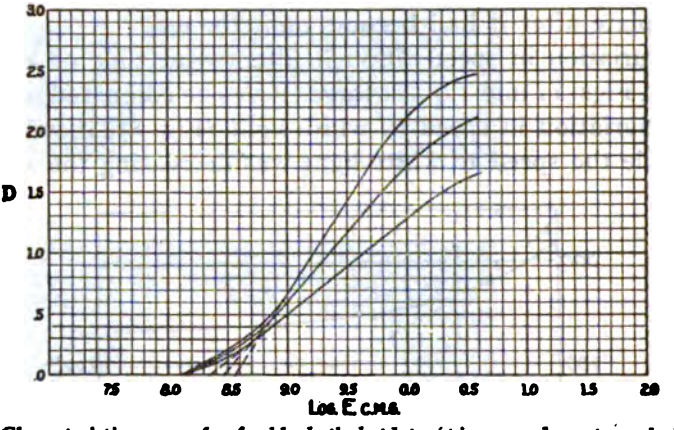

FIG. 9.—*Characteristic curves for freshly bathed plate (pinacyanol, water, alcohol, and ammonia)*

orthochromatic emulsion gives more fog when bathed than ordinary plates, and suitable films for bathing are not obtainable except with some degree of orthochromatism. In bathing films it is necessary to exercise considerable care that nothing comes in

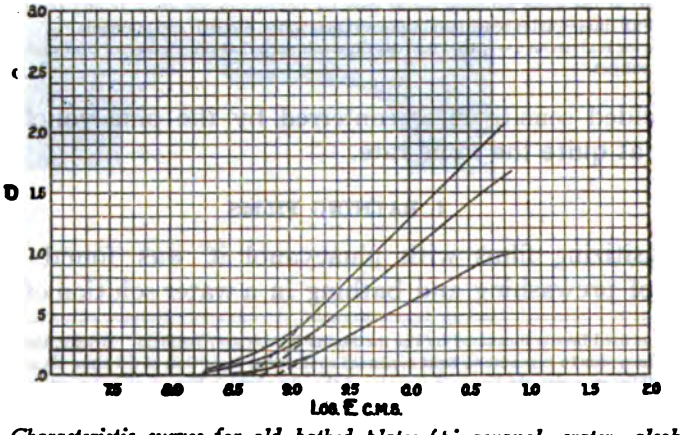

FIG. 10.—*Characteristic curves for old bathed plates (pinacyanol, water, alcohol, and ammonia)*

contact with either side of the film, since the back is usually coated with gelatine to make the film noncurling. If the back of the film becomes scratched, these scratches will cause defects in the print.

Digitized by Google

5. SPEED OF PLATES BEFORE AND AFTER BATHING

To study the comparative sensitizing action on plates having different characteristics as to speed and contrast, four plates made by the same manufacturer were selected, a fast plate, a medium-speed plate, a slow plate, and a process plate. The plates were

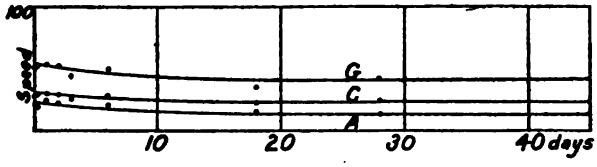

FIG. 11.—*Plates sensitised with pinacyanol and water*

sensitized in a bath containing pinacyanol, water, alcohol, and ammonia. Table 1 shows the results obtained:

TABLE 1

Plate	Initial speed	Speed after bathing	Speed with filters			
			A	B	C	G
Seed 30	500	315	26	29	28	66
Seed 26 x	400	300	28	27	25	69
Seed 23	180	155	19	17	12	47
Seed process	31	29	6	4	2	10

These results indicate that more added sensitiveness is conferred by the dye bath on slow plates than on fast ones. It may be concluded that when speed is not the factor of prime impor-

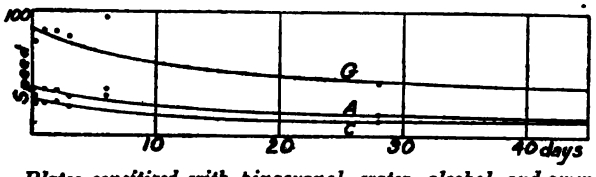

FIG. 12.—*Plates sensitised with pinacyanol, water, alcohol, and ammonia*

The *G* filter gives very nearly the added sensitiveness due to the dye. The *A* filter shows the red sensitiveness. The *C* filter shows the blue sensitiveness. If these curves be compared with those in Fig. 8, it will be observed that the color sensitiveness does not decrease as rapidly with time as the sensitiveness to white light.

tance, the plate chosen for bathing should be selected on the basis of its freedom from fog, its developing characteristics (contrast), and its resolving power.

The spectrograms of Fig. 13 show that the sensitiveness added by pinacyanol is about the same for the 30, 26×, and 23, although

Digitized by Google

the blue sensitiveness which the plates had originally still falls in the same order as the speed before bathing. Relatively the process plate has acquired a much greater sensitiveness than the other three plates, although its actual speed is far below them.

It may be remarked here that the blue sensitiveness of a plate is decreased by sensitizing. Thus the plates which were used for the keeping test had before bathing a speed of 55 with the C filter (blue), while after sensitizing with pinacyanol and water the speed dropped to 28 and after sensitizing with pinacyanol, water, alcohol, and ammonia to 26.

V. DICYANIN

The makers' instructions for the use of dicyanin call for much the same procedure as in the case of pinacyanol. However, with dicyanin, even prewashing failed to give satisfactory sensitizing with the water bath. Mees[15] states that it is necessary to bathe the plates immediately after adding the stock solution of dicyanin to the water, but even this procedure failed to give satisfactory results with the specimen of dye employed. This sample of dicyanin was about three years old.

When this sample of dicyanin was used with ammonia in the presence of enough alcohol to prevent flocculation, the sensitizing action was satisfactory. The use of ammonia has the important advantage of extending the sensitiveness to longer wave lengths, as well as increasing the action of the dye at its maxima. It is due to the use of ammonia that certain investigators[16] have been able to photograph in the infra-red as far as 1000 μ, while those who have not used ammonia with dicyanin have failed to photograph further than 800μ.

A satisfactory bath for dicyanin is as follows:

	Parts
Water	60
Ethyl alcohol (95 per cent)	40
Dicyanin stock solution (1 to 1000)	4
Ammonia (28 per cent)	4

As shown in Fig. 14, the more ammonia used the greater the sensitizing action, but the proportion of ammonia is limited by the fog it induces.

Dicyanin requires more care in its use than the other photosensitizing dyes. The solid dicyanin should be bronze green in

[15] Mees and Wratten, Photographic Jour., 58, p. 25, 1908 (Newton and Bull).
[16] B. S. Bull., 14, p. 376, 1917.

Digitized by Google

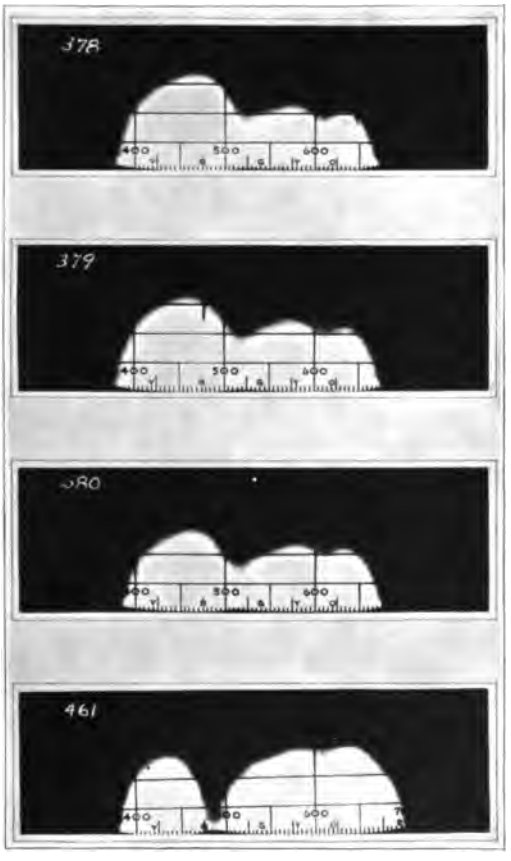

FIG. 13. *—How effect of bathing with pinacyanol varies with the type of plate bathed*

The plates shown represent the speed and contrast. It is to be observed that the faster the plate the less the added sensitiveness relatively

Digitized by Google

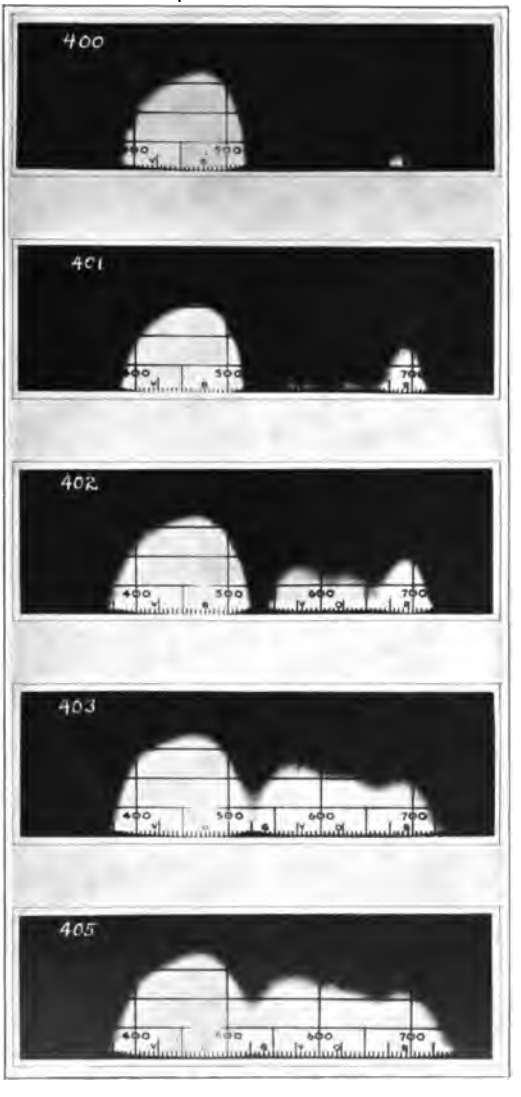

Dicyanin and water; 5 minutes prewash in tap water

Dicyanin, water, and alcohol

Dicyanin, water, alcohol, and ½ per cent ammonia

Dicyanin, water, alcohol, and 1 per cent ammonia

Dicyanin, water, alcohol, and 4 per cent ammonia

FIG. 14.—*Spectrograms showing the difference in the sensitizing action of dicyanin when used in the baths of various composition*

The use of sufficient ammonia in the bath not only increases the sensitizing action of dicyanin at its maxima, but extends its action into the infra-red as far as 1000 μμ

Digitized by Google

color. If it is not, particularly if it appears brownish, the dye has deteriorated and should not be used. The dye must be kept cool and dry in order to retain its sensitizing power. A freshly mixed bath of dicyanin is a bright blue-green color. As soon as the dye deteriorates the color changes considerably, the solution appears dull, and in addition shows a transmission band in the red. Such a solution should not be used. The temperature of the bath should not exceed 18° C, if plates reasonably free from fog are to be obtained. The alcohol rinse after bathing is decidedly beneficial.

ORTHOCHROMATIC SENSITIZERS

The other important sensitizers investigated were pinaverdol, pinachrome, homocol, orthochrome T, and erythrosin. These dyes are by no means as sensitive as pinacyanol and dicyanin to the action of electrolytes; they do not flocculate so readily in the presence of ammonia, potassium bromide, and alum. With the orthochromatic sensitizers the action of ammonia is most marked with erythrosin and homocol. The other dyes show a slight increase in sensitizing action with ammonia, but hardly enough to justify its use.

1. ERYTHROSIN

Erythrosin is stated by Eder[16] to be the best of the flourescin dyes for sensitizing. Other important representatives of this class are eosin and rose bengal. He also states that plates bathed with erythrosin are superior to plates in which the dye is incorporated in the emulsion. We were not able, however, with the sample of erythrosin used (Kahlbaum) to produce plates which were as sensitive in the yellow-green as the orthochromatic plates made by one American manufacturer. (Fig. 15.)

We found erythrosin to give the best results when used according to the directions given by Eder.[17] The plate is given a prebath for two minutes in

	Parts
Water	100
Ammonia	2

Then it is bathed for two or three minutes in a bath of

	Parts
Water	100
Stock solution (1 to 1000)	20
Ammonia	2

[16] Eder, Handbuch, 3, p. 174. [17] Eder, Handbuch, 3, p. 176.

Digitized by Google

The bathed plates should be washed in water to remove the excess dye from the gelatine. A rinse in alcohol will shorten the time required for drying.

An inspection of the spectrograms of commercial orthochromatic plates indicates that erythrosin or a dye of the erythrosin type is used in their manufacture. The advantage of erythrosin over such dyes as pinaverdol is its limited region of sensitizing action, since the sensitiveness conferred by erythrosin ceases abruptly at 580μ while the action of the other dyes continues rather farther into the red. This limited region of sensitiveness makes it possible to develop plates made sensitive with erythrosin in the light of an ordinarily good red dark-room lamp. This is a decided advantage to the practical photographer. One of the reasons that panchromatic plates have not been more generally used is that they must be developed in total, or at best in slightly modified darkness, so that the photographer is unable to judge whether or not he is carrying development to the contrast required by the subject and the printing medium to be used.

2. PINAVERDOL, PINACHROME, ORTHOCHROME T, AND HOMOCOL

These dyes are very much alike in the regions for which they sensitize. (Figs. 16 and 16*a*.) Of these four dyes, homocol has its sensitizing action increased most by the use of ammonia. Their greatest application probably lies in their use in conjunction with pinacyanol to supply the slight deficiency of the latter in the green.

VII. HYPERSENSITIZING COMMERCIAL PANCHROMATIC PLATES

The well-known action of a bath of dilute ammonia in increasing the speed of an ordinary dry plate was applied to commercial panchromatic plates in the process worked out by S. M. Burka [18] and C. C. Kiess at this Bureau in 1918. They found that commercial panchromatic plates bathed for four minutes in—

	Parts
Water	75
Ethyl alcohol (95 per cent)	25
Ammonia (20 per cent)	3.5

had the total speed increased 100 per cent and the red speed increased 200 to 800 per cent. A greater increase in speed was obtained by the use of 3.5 to 100 cc of water, with the omission of the alcohol. In this case, however, the plates dry more slowly

[18] Jour. Frank. Inst., 189, p. 25; 1920.

Digitized by Google

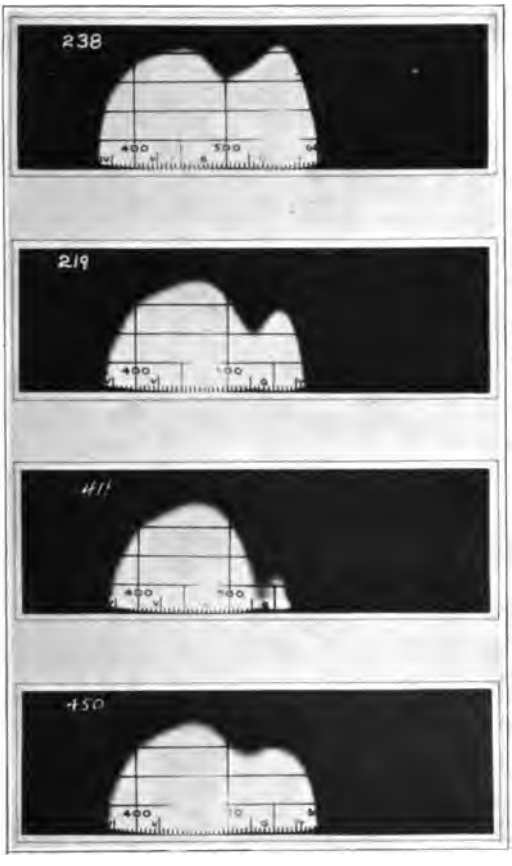

Isochromatic plate

Orthochromatic plate

Orthochromatic film

Plate bathed with erythrosin

FIG. 15.—*The comparison of commercial orthochromatic plates with a plate bathed with erythrosin shows that the latter is better than most commercial orthochromatic plates, but not as good as certain others*

Digitized by Google

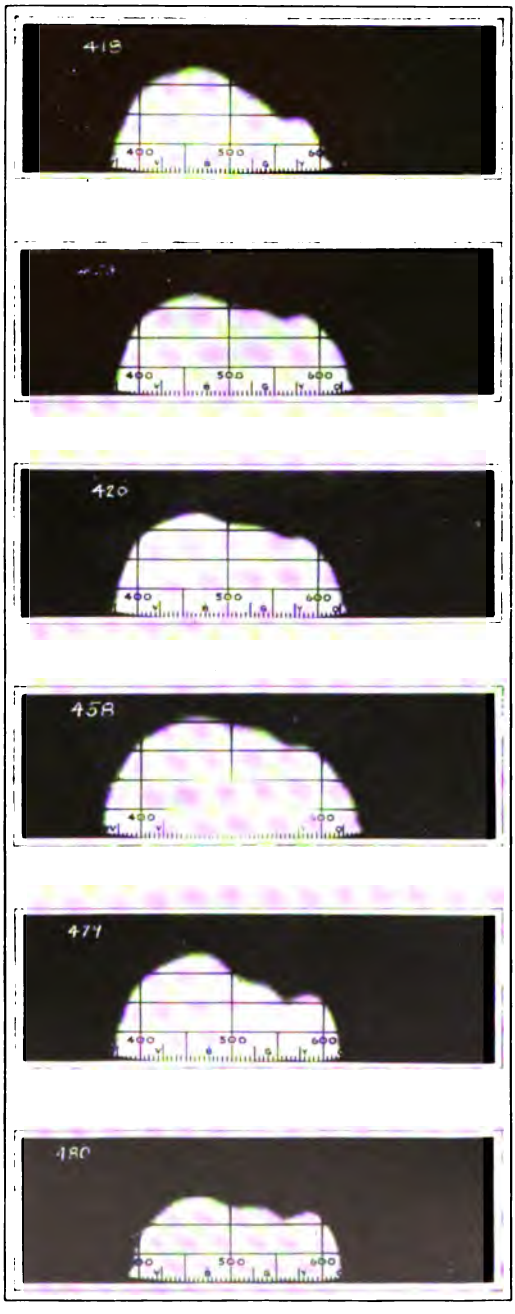

Homocol without ammonia

Homocol with ammonia

Pinaverdol without ammonia

Pinaverdol with ammonia

Orthochrome T without ammonia

Orthochrome T with ammonia

FIG. 16.—*Orthochromatic sensitizers used in water bath with and without ammonia*

The greatest effect due to ammonia is found with homocol; the other two dyes show a little extension toward the red. A comparison of these sensitizers with erythrosin shows why they are not used for orthochromatic plates. It would be difficult to devise a dark-room light which would not give considerable fog with them, while with erythrosin the sensitiveness does not extend beyond 600

Digitized by Google

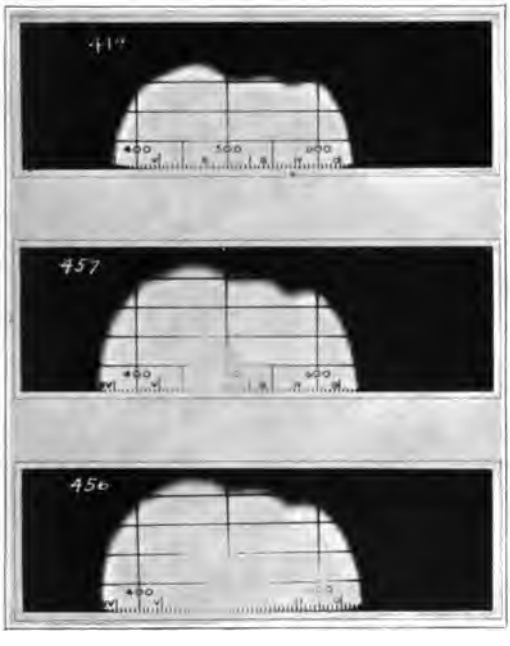

FIG. 16a.—*Pinachrome*

Digitized by Google

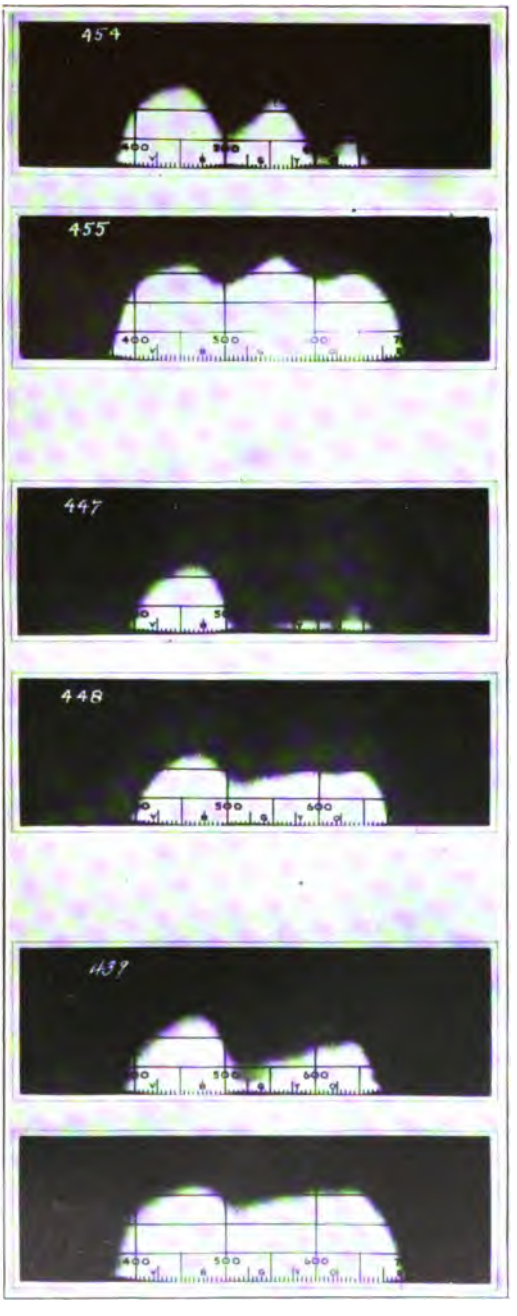

Spectrum process, unwashed; 20-minute exposure

Spectrum process, washed; 20-minute exposure

Panchromatic, d. c. unwashed

Panchromatic, d. c. washed

Pan-ortho, unwashed

Pan-ortho, washed

FIG. 18.—*Spectrograms showing increased sensitivity obtained by washing panchromatic plates*

The plates were washed in water for five minutes, dried in a cabinet, and exposed. Each was developed simultaneously with an unwashed plate of the same kind exposed for the same length of time. The spectrum-process plate was soaked in distilled water, while the other plates were washed in running tap water. It would appear that the increase in sensitiveness is due to the removal of restraining substances from the plate and not to the sensitizing action of any substance in the water

Digitized by Google

and develop more fog than when alcohol is included in the hypersensitizing bath. A rinse in alcohol after the ammonia bath will help in drying the plates more rapidly. In an early investigation of the sensitizing properties of cyanin Schumann found that bathing in a dilute solution of ammonia imparted great speed and sensitivity to a plate with cyanin incorporated in the emulsion. (See Photographische Rundschau, 3, pp. 143, 175; 1889.)

In Fig. 17 are shown the results of a keeping test made on Wratten Panchromatic Process, D. C. The plates were hypersensitized without the use of alcohol. The plates gave evidence of a slight increase in speed for a few days after hypersensitizing,

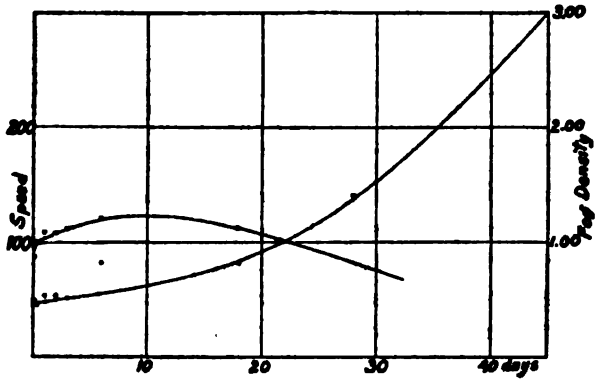

FIG. 17.—*Variation of speed and fog with time of keeping hypersensitized plates*

The fog has increased from a density of 0.45 to 3.00 in 45 days (a density of 3.00 transmits 1/1000 of the incident light).

NOTE.—The fog is given for $\gamma = 2$; that is, the development was carried until the contrast was twice that in the subject.

while the fog kept increasing from the time the plates were hypersensitized.

A comparison of the increase in speed brought about by washing and by hypersensitizing commercial panchromatic plates shows that a part of the hypersensitizing action is due to the removal of certain soluble restraining substances by washing. In Table 2 are given the results of washing and hypersensitizing three typical panchromatic plates.

VIII. INCREASE IN SPEED BY WASHING BEFORE EXPOSURE

The improvement in sensitizing by washing the ordinary plate before bathing in pinacyanol-water solution suggested that there might be a corresponding improvement in the speed of commercial panchromatic plates. Accordingly a few typical panchromatic plates were washed for five minutes in running tap water and

Digitized by Google

dried, following which the total speed to white light and the filter factors were measured. As seen from Table 2, all of the panchromatic plates showed decided improvement on being washed.

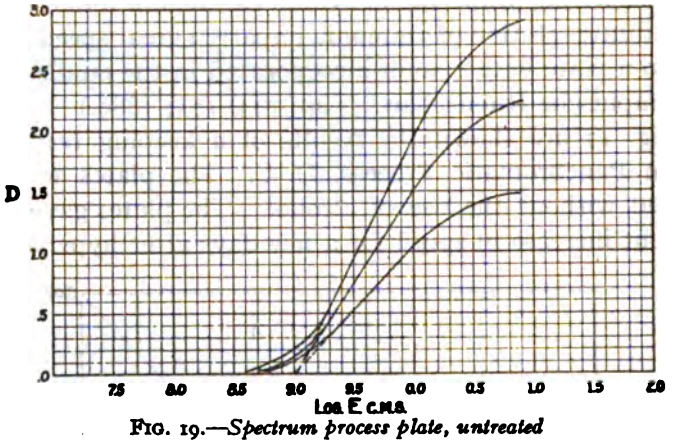

FIG. 19.—*Spectrum process plate, untreated*

That the effect is not due to a change in the rate of development is clear from an inspection of Figs. 19 and 20, which show the characteristic curves for the spectrum process plate before and after washing. Nor is the improvement due to the sensitizing action of some impurity contained in the tap water, since plates

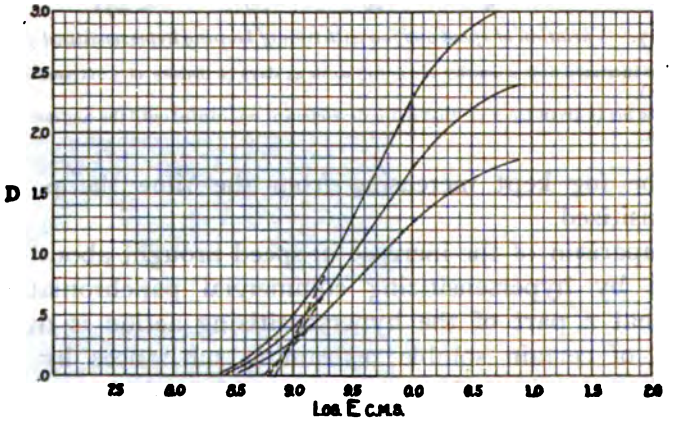

FIG. 20.—*Spectrum process plate, washed in tap water for five minutes*

washed in a few changes of distilled water showed the effect as well if not better than with tap water. That the action is not due to a variation of the water content of the plate may be concluded from the fact that the plates before exposure in the sensitometer were backed and allowed to dry for about an hour. This time is sufficient for the unwashed plate taken from the box to come to the same state of humidity as the plate which had been washed.

Digitized by Google

This increase of sensitiveness may then be concluded to result from the removal of certain restraining substances from the emulsion. From our experience with pinacyanol, chrome alum, and potassium bromide suggest themselves as the restraining substances.

The comparison of the spectrograms of unwashed and washed panchromatic plates (Fig. 18) shows that the greater part of the increase in speed to white light comes in the region of sensitiveness

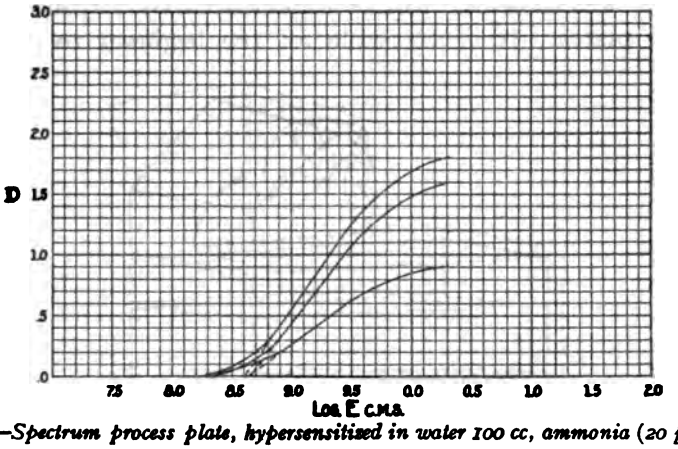

FIG. 21.—*Spectrum process plate, hypersensitized in water 100 cc, ammonia (20 per cent) 3.5 cc, and bathed four minutes*

which is due to the dyes. This is borne out by the speed measurements with the filters.

TABLE 2

Plate	Treatment	Total speed	Speed with filters				Fog density for $\gamma=1$
			A	B	C	G	
Spectrum process [a]	None	96	5	8	8	16	0.40
	Washed	155	13	19	11	40	.40
	Hypersensitized	235	22	34	16	75	1.30
Wratten panchromatic D. C.	None	180	16	15	17	36	.20
	Washed	240	32	26	19	80	.40
	Hypersensitized	380	59	50	44	140	.50
Pan-ortho	None	91	9	7	8	16	.30
	Washed	145	25	15	10	45	.40
	Hypersensitized	275	49	32	19	106	1.30

[a] The spectrum process and the pan-ortho plates were over a year old, while the Wratten plate had just been received from the factory.

The table shows that while washing does not bring the increase in speed that hypersensitizing does it does not cause the production of as much fog. The characteristic curves (Figs. 19, 20, 21)

Digitized by Google

show that washing improves the scale or rendering power of the plate, while hypersensitizing does the reverse.

Manufacturers are urged to investigate the increase of sensitiveness found by washing in water, as it may be of considerable advantage to so treat their panchromatic plates before placing them on the market.

IX. THE TECHNIQUE OF PLATE BATHING

More or less difficulty will be experienced by anyone learning to bathe plates. It is advisable for the beginner to carry out

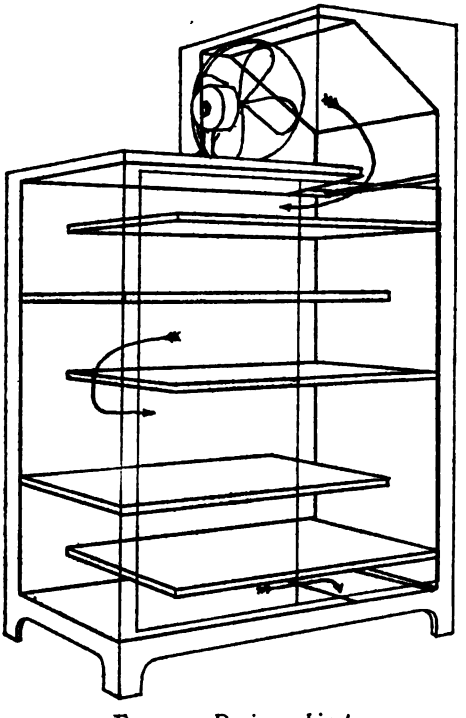

FIG. 22.—*Drying cabinet*
The outside of the cabinet is shown in light line and the inside in heavy line.

the process in full light. This will enable him to follow the process and to discover the effect of the different baths on the plate; whether or not the bathing is sufficiently long for the dye to get through the emulsion, and whether or not the rinse removes the dye well enough from the gelatine. It will tell him how much he has to rock the trays containing the baths and will give him some idea of how long it takes the plate to dry after bathing.

Digitized by Google

An essential of successful sensitizing is absolute cleanliness. Dust or particles of old dye baths remaining in the trays will cause spots and streaks. Glass trays are to be preferred to enameled trays because of the smoother surface and the less likelihood of contamination.

Foggy plates may be due to a number of causes—the choice of the wrong brand of plates for sensitizing, stray light during bathing and drying, the use of baths at too high a temperature, slow drying, or too much ammonia in the dye bath.

Slow drying sometimes gives rise to areas of varying sensitiveness on the plate, depending upon which part of the plate dries first. The rate of drying may be increased by the use of the alcohol rinse and by the use of a properly designed drying cabinet.

The drying cabinet shown in Fig. 22 has several advantages. The air driven in at the top by an electric fan passes through efficient light traps, both at the top and the bottom. Two doors form the front of the box and opening them gives access to all of the shelves, of which there are four, to hold drying racks filled with plates. The upright form of the cabinet gives it a very large capacity for the amount of floor space required. The long distance the air has to travel gives uniform distribution of the air current to all parts of the box in which plates may be placed.

X. PROCEDURE AND FORMULAS

1. Stock solutions.—Stock solutions are usually made with pure ethyl alcohol (90 per cent or stronger). Some dyes are water soluble (erythrosin), while others dissolve in methyl alcohol. The usual strength is 1 g of dye to 1000 cc of alcohol (or in the same proportion). Some dyes are less soluble than this and require from 2000 to 10 000 cc of alcohol to dissolve 1 g of dye. It is advisable to put the dye in the solvent instead of pouring the solvent on the dye, as some of the dye may stick to the bottom of the bottle and require considerable more shaking to get into solution. If the dye does not dissolve in cold alcohol, the bottle containing the dye may be placed in a water bath and heated until the alcohol boils. If it does not go into solution after boiling 30 minutes, more alcohol should be tried.

2. Water solutions.—The bath is composed of

	Parts
Water	100
Stock solution	2–6

Digitized by Google

Pinacyanol.—Wash the plate five minutes before bathing. Bathe two minutes. Rinse in alcohol until the film feels hard (three to five minutes).

Pinaverdol, Pinachrome, Orthochrome T.—Prewash optional. If prewash is omitted, bathe for four minutes.

Homocol.—Prewash optional, bathe four minutes if omitted. For increased sensitizing action, add 2 cc of ammonia.

3. Water, alcohol, and ammonia solutions. To be used when water dye bath flocculates on adding ammonia.

	Parts
Water	65
Ethyl alcohol (95 per cent)	35
Stock solution	2–4
Ammonia (twenty-eight)	2–4

In mixing this bath allow the alcohol and water to cool after mixing, add the stock solution, stir well, and then add the ammonia. Some baths work better if the minimum amount of ammonia is added before bathing the first plate, and more ammonia added as the bath loses its ammonia.

The plates are put directly in this bath, care being taken that the bath covers the entire plate. Bathe for four or five minutes and rinse in alcohol until the film is hard. Temperature should be 18° C. or less.

Pinacyanol.—As directed.

Dicyanin.—Requires full amount of ammonia.

XI. SUMMARY

An investigation of the methods of sensitizing ordinary plates by bathing shows that certain precautions are necessary with some of the modern photosensitizing dyes and not with others.

Dicyanin gives a much greater sensitiveness and extends farther into the infra-red when used in a dilute alcoholic solution with ammonia than when used with water alone.

Pinacyanol gives good results in dilute alcoholic solution with ammonia, but plates bathed in water and stock solution are almost as sensitive and keep much better, provided the plates are thoroughly washed before sensitizing, as the soluble salts contained in the emulsion prevent the sensitizing action by flocculating the dye.

Washing has a favorable action on the color sensitiveness of panchromatic plates and, while not so marked as the action of

Digitized by Google

dilute ammonia, it gives no increase in fog, which always follows the use of ammonia.

The modern orthochromatic sensitizers, pinachrome, pinaverdol, homocol, and orthochrome T, are much less sensitive to electrolytes than are pinacyanol and dicyanin. Ammonia may be added to a staining bath of water and stock solution only, but does not increase the sensitizing action appreciably except in the case of homocol.

Films are best sensitized in a bath containing water, alcohol, ammonia, and stock solution.

Certain brands of orthochromatic plates were found to be superior to plates bathed with erythrosin (Kahlbaum's), but no panchromatic plate compared favorably with pinacyanol bathed plates, except one experimental emulsion furnished by an American manufacturer.

WASHINGTON, July 12, 1921.

Digitized by Google

Digitized by Google

MAR 5 1922

DEPARTMENT OF COMMERCE

LIBRARY OF THE UNIVERSITY OF CALIFORNIA

SCIENTIFIC PAPERS

OF THE

BUREAU OF STANDARDS

S. W. STRATTON, DIRECTOR

No. 423

OPERATION OF THE MODULATOR TUBE IN RADIO TELEPHONE SETS

BY

E. S. PURINGTON, Associate Physicist

Bureau of Standards

NOVEMBER 15, 1921

PRICE, 10 CENTS

Sold only by the Superintendent of Documents, Government Printing Office, Washington, D. C.

WASHINGTON
GOVERNMENT PRINTING OFFICE
1921

Digitized by Google

Digitized by Google

MAR 5 1922

LIBRARY OF THE UNIVERSITY OF CALIFORNIA

DEPARTMENT OF COMMERCE

SCIENTIFIC PAPERS

OF THE

BUREAU OF STANDARDS

S. W. STRATTON, DIRECTOR

No. 423

OPERATION OF THE MODULATOR TUBE IN RADIO TELEPHONE SETS

BY

E. S. PURINGTON, Associate Physicist
Bureau of Standards

NOVEMBER 15, 1921

PRICE, 10 CENTS

Sold only by the Superintendent of Documents, Government Printing Office, Washington, D. C.

WASHINGTON
GOVERNMENT PRINTING OFFICE
1921

Digitized by Google

Digitized by Google

DEPARTMENT OF COMMERCE

SCIENTIFIC PAPERS

OF THE

BUREAU OF STANDARDS

S. W. STRATTON, DIRECTOR

No. 423

OPERATION OF THE MODULATOR TUBE IN RADIO TELEPHONE SETS

BY

E. S. PURINGTON, Associate Physicist

Bureau of Standards

NOVEMBER 15, 1921

PRICE, 10 CENTS

Sold only by the Superintendent of Documents, Government Printing Office, Washington, D. C.

WASHINGTON

GOVERNMENT PRINTING OFFICE

1921

Digitized by Google

Digitized by Google

OPERATION OF THE MODULATOR TUBE IN RADIO TELEPHONE SETS

By E. S. Purington

ABSTRACT

The modulator tubes of radio telephone transmitters used in commercial and military sets operate essentially as aperiodic power amplifiers of speech currents. The load on these tubes is determined approximately by the volt-ampere characteristics of the radio generating circuit, as measured at its plate power input terminals. At speech frequencies other effects occur as follows:

1. Current to the modulators and the generating circuit in parallel is supplied through an audio choke coil. The finiteness of the inductance of this coil results in an inductive component to the load.

2. The radio generating circuit contains suitable impedances to prevent consumption of radio power by the modulator tubes. These and other parts of the generating circuit may produce reactive components.

3. In consequence of the variation of the input power to the generating circuit, the desired speech variations of radio output power occur. Power must be generated to vary the electromagnetic energy associated with the output circuit, as well as to supply the resistance losses. A reaction occurs tending to produce a capacitive component to the load on the modulators.

The value of a radio telephone transmitter in conveying speech signals is measured not by the power output, but rather by the variation of power output during speech. Usually optimum results are obtained when the power rating of all the modulator tubes equals the power rating of all the radio generator tubes. Under these conditions the load upon the modulators is one into which they may operate with best efficiency.

CONTENTS

	Page
I. Introduction	378
II. Methods of modulating the radio output current of an electron-tube generating circuit	378
III. General relations in radio telephone transmitter sets using plate modulation	380
IV. The elementary functioning of the modulator unit	383
V. Load impedance as specified by wave form of plate voltage and current	385
VI. Effect of imperfections in the audio choke coil upon the performance of the set	389
VII. Effect of audio frequency impedance of parts of the generating system upon the performance of the set	390
VIII. Effects of resonance power in the radio oscillatory circuit upon the performance of the set	392
1. Power relations in resonance systems during modulation	393
2. Radio frequency phenomena in a resonance circuit carrying modulated current	397
IX. The strength of signal transmitted by a radio telephone set	402
X. Summary	405

Digitized by Google

I. INTRODUCTION

The function of a modulating device in radio communication is to vary the output current of a radio generator at a frequency or at frequencies lower than the radio frequency involved. In a certain sense practically all radio communication using single wave-length signals is by a modulation method. In continuous wave transmission, the keying by which the signals are conveyed constitutes a dot-and-dash modulation of the antenna current. In the operation of spark and other tone transmitters, the radio frequency wave trains are sent out at more or less regular intervals at an audio frequency, so that an audible note is heard upon rectification with a detecting device. In addition to this audio modulation, a second order of dot-and-dash modulation is required for conveying the telegraph signal. In radio telephony the message which is conveyed depends upon the first order modulation itself. The antenna current is made to vary, not at a single tone frequency, but with frequencies and in degrees corresponding to the pitches and intensities of the sound waves produced by the voice of the speaker. In consequence, upon rectification of the received radio signals, there are produced in the receiving telephones electrical currents which are of precisely the same nature as would be produced by communication by wire telephony.

The present paper deals with the essential electrical phenomena associated with the modulating device used in most of the present types of radio telephone transmitters employing electron tubes. The various methods of modulating the output of a generating circuit are discussed and the inherent superiority of plate modulation is pointed out. A complete radio telephone network using such plate modulation is analyzed into simpler units, and the essential and elementary operation of the modulator unit described in detail. The electrical limitations upon the proper functioning of the modulator tube are pointed out and the relative importance of these limitations discussed. The strength of speech signal conveyed by a radio telephone set is discussed, and suggestions are made as to the proper method of rating radio telephone sets as to power output.

II. METHODS OF MODULATING THE RADIO OUTPUT CURRENT OF AN ELECTRON-TUBE GENERATING CIRCUIT

With the generating device of an electron-tube circuit, speech modulation is accomplished usually by one of three general methods. The simplest is by variable absorption of the radio fre-

Digitized by Google

quency output of the circuit, as, for example, by the insertion of a speech operated microphone in the antenna lead from a continuous wave generator. A different method of variable power absorption is by shunting the generator tube, or parts of the output circuit, with another electron tube. The grid voltage of this power absorbing tube is varied at speech frequencies by the use of a microphone and speech transformer. The combination of microphone and power tube is capable of absorbing more radio power than the microphone itself would be able to handle, otherwise the operation is quite similar to modulation with a microphone directly in the antenna lead. These methods of radio power absorption are very little used in practice, largely because the generating device is required to produce much more radio power than that utilized by the actual antenna or other radiating device.

A second method of modulation is by varying the operating grid voltage of a generating tube at speech frequencies. In such apparatus the secondary of a speech transformer is inserted in the grid lead, this secondary being shunted with a radio condenser so that the operation of the generator circuit will not be influenced by the high reactance of the transformer windings. A microphone and battery in the primary of the transformer cause variations in the average grid voltage taken over successive radio cycles, and therefore change the operation of the radio generator. This method of modulation is not extensively used, chiefly because the radio frequency output of a generator circuit is usually not readily altered by varying the operating grid voltage. The grid voltage operating point is important in determining efficiency, but not the output current, provided the conditions are such that good articulation results. By reducing the operating grid voltage on a generating tube sufficiently, usually a point is reached at which the oscillation suddenly breaks and the radio output current immediately drops to zero. Grid modulation which thus cuts off the antenna current suddenly and completely results in very poor articulation. While with careful adjustments the breaking of the oscillation may be sufficiently gradual to permit good speech, this method is not considered to be one in which the modulation process is inherently reliable in telephone sets.

A third method of modulation is by varying the input plate power of a generating circuit; that is, the average plate voltage and plate current of the generating tube or tubes of a radio circuit are caused to vary at the lower or modulating frequencies. This

Digitized by Google

method is employed in practically all present commercial and military types of electron-tube radio telephone sets. It possesses the advantage over the first method that practically all the radio power output may be used in transmission of signals. On account of the nearly linear relations between cause and effect with this method, it is inherently superior to both the other methods as to articulation. In the transmission of speech signals the plate power of the generating tube is altered by the use of a power tube, which from its functioning is termed a modulator tube. It is the operation of this tube which is the center of discussion in the present paper. In connection with the discussion, however, are developed other topics, some of which are of interest in connection with any method of modulation.

III. GENERAL RELATIONS IN RADIO TELEPHONE TRANSMITTER SETS USING PLATE MODULATION

A radio telephone set using plate modulation is a more or less complicated network in which three classes of currents coexist—radio frequency, audio frequency, and direct. In Fig. 1 is shown schematically a typical radio telephone transmitter set, analyzed for purposes of discussion into four distinct units. At the extreme right is the radiator unit, which joins up the transmitter with the distant receiving station. The signal which is conveyed depends upon the nature of the wave form of current in this radiator unit, and is independent of the process by which that current is produced. The useful currents in this circuit are of radio frequency. The modulating mechanism may cause slight audio currents to flow in the radiator unit, but these produce practically no effect except at near-by stations. In the figure shown such audio currents result from the audio current flowing in the lead to the tube *O*, which is inductively coupled to the antenna or radiator circuit. During speech the radio frequency current is of variable amplitude and is known as modulated radio frequency. For the purpose of explaining the general operation of the transmitter it is unnecessary to analyze completely the wave form of this current. Curves showing the nature of the wave form with sine wave modulation are shown later in Figs. 8 and 11, and the analytical expression for such a wave form is given by equation 14, page 397.

To the left of the radiator unit is the radio generator unit. This contains electron tubes which, from the functions performed by them, are known as oscillator tubes, and also contains the other electrical equipment essential to the production of radio frequency

Digitized by Google

power from whatever power is supplied at the input $b+$ and $b-$ terminals of this unit. An essential part of any generating unit in radio telephony is a device such that the radio frequency voltage across the input terminals is small compared with other voltages of lower orders of frequency. In the present case this device is a condenser C_b, the reactance of which for radio frequencies is low compared with the ratio of average plate voltage of the oscillator tubes to the average plate current. In any continuous wave transmitter a device of this nature is required in case the radio impedance of the system supplying the plate power is so high that otherwise considerable radio voltage variations would occur across the input terminals, limiting the useful power output. In the present case the condenser C_b may be thought of as an electrical

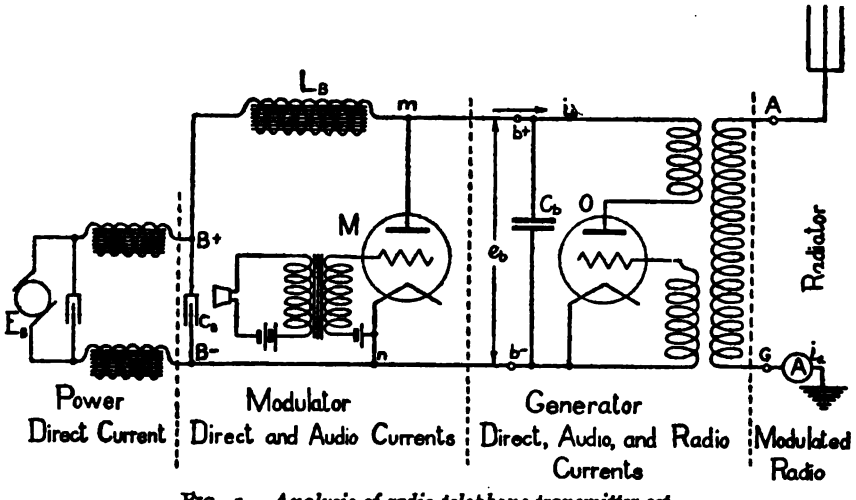

FIG. 1.—*Analysis of radio telephone transmitter set*

valve which prevents radio frequency power working back into the part of the network to the left, but which does not interfere with the lower frequency power entering the generating system. The particular type of generating circuit is known as the Meissner circuit, which is classified electrically as one with plate and grid both inductively coupled to the radio frequency circuit, using series power supply with the same radio frequency circuit flowing through the plate coupling coil as through the tube. In place of such a circuit any of a large number of other types might be used, as, for example, the type shown later in Fig. 6. In the generator unit all three types of electrical currents exist. The power entering the unit during operation is direct power and audio power. The output through the antenna and ground terminals, *A* and *G*,

Digitized by Google

is modulated radio frequency. While a tube in continuous wave telegraphy may be thought of as a converter of power from direct to radio frequency, in a radio telephone set the generator tube converts power from direct and audio to modulated radio frequency.

To the left of the generator unit is the modulator unit, the function of which is to supply audio and direct power to the generator unit, the audio power being controlled by the operator speaking into the microphone. In the case shown an electron tube is shunted across the input terminals of the generator unit, the two in parallel being supplied with direct power from a direct-current source through the iron cored choke coil L_B. The tube in this case is a speech-controlled resistance in which the instantaneous resistance, or ratio of plate voltage to plate current, is determined largely by the instantaneous grid voltage. On account of the functions it performs it is known as a modulator tube. Mechanically it is usually the same as the oscillator tube. When tubes are paralleled, approximately as many modulator tubes are used as oscillator tubes. The modulator tube is a converter of power from direct to audio frequency and the audio current and voltage output of the modulator tube is a more or less faithful reproduction of the audio voltage impressed upon the grid of the modulator tube by the use of a microphone and transformer. The modulator tube therefore functions as an aperiodic power amplifier. The audio power output may be tested, for example, by connecting a suitable resistance and stopping condenser in series across from m to n of Fig, 1, instead of the generating circuit. The power which is manifested by the heating effect upon the resistance, during speech, is entirely audio power, converted from direct power from source E_B through the agency of the modulator unit. Tubes for modulating are usually designed to operate with a negative average voltage on the grid, which in the case shown is obtained by the use of a battery in the grid lead. The choke coil L_B of the modulator circuit partially performs the same function for the modulator unit as does the condenser C_b for the generator unit. It prevents audio currents produced by the unit from working back through the input terminals $B+$ and $B-$, and in this it is aided by the condenser C_B. It performs, however, another important function.

If a fixed impedance and a variable impedance be connected in parallel and placed across a direct power source of zero internal impedance, then variations of one impedance will not disturb the

Digitized by Google

current to the other unless the two in parallel are supplied with power through a common line impedance. The generator unit may be thought of as the fixed impedance and the modulator tube as the variable impedance in parallel, both being supplied with power through the common impedance L_B. Without this impedance practically no variations in the audio frequency voltage across the $b+$ and $b-$ terminals could occur. The impedance of L_B is usually high for the average speech frequency of 800 cycles per second, in comparison with the impedance given by the ratio of the direct voltage across the $B+$ and $B-$ terminals to the direct-current constituent flowing through the choke coil. Choke coils for this purpose are usually built with an air gap in the magnetic circuit and with a large number of direct-current ampere turns per unit length of the magnetic circuit.

To the left of the modulator unit is the direct-power supply unit. In this case it consists of a direct-current generator provided with filter circuits to prevent voltage due to commutation from existing across the terminals $B+$ and $B-$. The condenser C_B functions doubly as a part of the filter network and as a device which by-passes any audio frequency current which may flow through the choke coil.

To summarize, tracing from left to right, the primary power supply to the set is direct power delivered at the $B+$ and $B-$ terminals of the modulator unit. By an audio frequency variation of the modulator tube impedance, audio power is produced and, together with direct power, is supplied to the $b+$ and $b-$ input terminals of the generator unit. As a result, the amplitude of the radio frequency output current of the generator unit is varied at speech frequencies and a wave form emitted, which upon reception gives rise again to speech currents.

IV. THE ELEMENTARY FUNCTIONING OF THE MODULATOR UNIT

The elementary and fundamental functions of the modulator tube may be readily shown by a symbolization of the adjacent units. The power supply unit is readily symbolized by a battery of voltage E_B, which represents the direct voltage across condenser C_B of Fig. 1. Across this battery is shunted in the symbolized diagram a condenser C_B to represent the capacity reactance of the filter network to an audio current flowing through the $B+$ and $B-$ terminals. The symbolization of the generator unit and

Digitized by Google

radiator unit may be by the use of experimentally determined external characteristics. Thus if the instantaneous voltage e_b across the $b+$ and $b-$ terminals be varied at a low frequency there will be corresponding changes in the current i_b through these terminals, and in the r. m. s. antenna current i_a produced by the generator system. In making such characteristics it will be understood that all controls of the generator unit, such as filament current, operating grid voltage, and couplings are left fixed. Such characteristics for a typical generator circuit are shown in Fig. 2, in which low frequency plate current and value of antenna current are plotted against the low frequency plate voltage. Over the

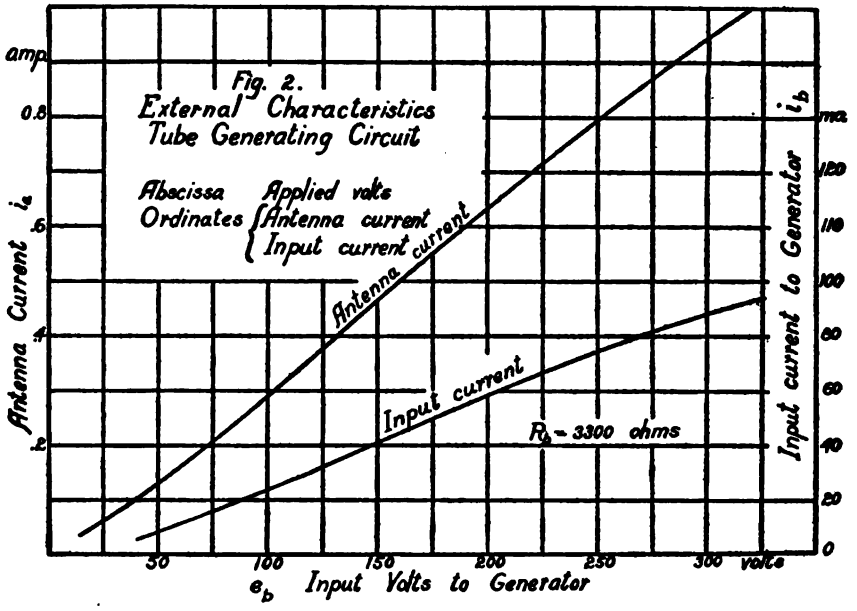

FIG. 2.—*External characteristics of tube generating circuit*

range shown, an approximately linear relation exists between these three quantities. The proportionality relation between plate voltage and plate current indicates that, as far as the modulator unit is concerned, the generating and radiator unit behave roughly as a resistance in this case of approximately 3000 ohms. This ratio of e_b to i_b may be termed the input impedance of the generator unit. The modulation characteristics for plate modulation inherently give better linear relations between cause and effect than similar characteristics for the other types of modulation.

In Fig. 3 is shown the simplified modulator diagram which may be used in discussing the elementary functioning of the modulator

Digitized by Google

tube. In this diagram the power supply unit has its representative in the battery E_b, and the generator and radiator units are symbolized by a resistance R_b. The value of this resistance is an important factor in determining how many tubes must be used in order that the modulator part of the set may operate with good electrical efficiency. Another important factor is discussed in Section IX.

V. LOAD IMPEDANCE AS SPECIFIED BY WAVE FORM OF PLATE VOLTAGE AND CURRENT

With the modulator unit as symbolized in Fig. 3, operating under the ideal conditions, with choke coil L_B of infinite impedance, the pulsations of the load current i_b and of the modulator tube current i_m will be exactly 180° out of phase with each other, since the sum of these currents will be the direct and unvarying current through the choke coil L_B. The voltages across the load e_b and across the tube e_m are obviously the same and therefore in phase. Since the load current and voltage are in phase, on account of the load being a resistance, it therefore follows that the tube alternating voltage and the alternating current are exactly 180° out of phase, with the total plate current a maximum when the plate voltage is a minimum. Moreover the load resistance is simply related to the plate voltage and current wave forms. In this simple case the maximum departure of voltage from mean divided by the maximum departure of current from mean gives the value of the load resistance R_b.

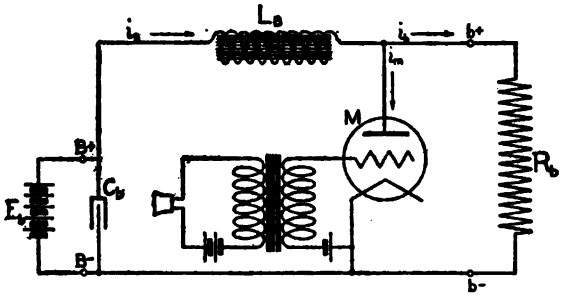

FIG. 3.—*Simplified modulator diagram*

The conception of the impedance being specified by the plate voltage and current wave forms, however, is of more general application than in this special case. Thus, in any circuit in which the tube is functioning with direct currents and voltages present as well as alternating fundamentals and harmonics, the wave forms of plate voltage and plate current with a single fundamental present must necessarily be of the form

$$e = \bar{e} + \Sigma e_n \sin(n\omega t + \theta_n) \quad (1)$$

$$i = \bar{i} + \Sigma i_n \sin(n\omega t + \phi_n) \quad (2)$$

Digitized by Google

in which $\bar{e}$ and $\bar{\imath}$ are time averages, or direct values of voltage and current, e_n and i_n are the amplitudes of the n^{th} harmonic voltage and current, and θ_n and ϕ_n are phase angles. In terms of the wave form, $\bar{e}$ and $\bar{\imath}$ are the direct values of the voltage and current supplied by the power sources jointly to the tube and its load. In the present case, the current through the choke L_B may be thought of as being in two portions, that which supplies the direct or average current to the tube and that which supplies the average current to the resistance R_b. The product $\bar{e}\,\bar{\imath}$ represents the total power delivered by the battery which is consumed in the tube structure and converted into alternating power by the tube action. By taking the product of the instantaneous tube voltage and current, and averaging over a complete cycle the power consumed by the tube is

$$\overline{e\,i} = \bar{e}\,\bar{\imath} + \Sigma \frac{e_n\,i_n}{2} \cos\,(\phi_n - \theta_n) \qquad (3)$$

The quantity $\bar{e}\,\bar{\imath}$ may be termed the direct power consumed by the tube, and the remaining terms the alternating power. For $n = 1$, the power $\frac{e_1 i_1}{2} \cos\,(\phi_1 - \theta_1)$ is the fundamental alternating power and for the higher values of n the powers are the harmonic power. Neglecting the slight plate power which may be derived from the filament heating source through the action of initial velocity of emission, and that which might in some cases be derived from the grid circuit through the agency of secondary emission, the plate battery is the only source of power which heats the plate of the tube and supplies the output power of the tube. Since the power delivered to the tube and to the alternating current load upon the tube is $\bar{e}\,\bar{\imath}$, and since analytically the direct power consumed by the tube is also this quantity, it follows that the alternating power consumed by the tube is equal in magnitude and opposite in sign to the alternating power consumed by the load on the tube. The total alternating power consumed by the tube must therefore be a negative quantity, and the actual power consumed by the tube is less than the product of the average plate voltage and the average plate current. For the fundamental output power the value $\cos\,(\phi_1 - \theta_1)$ must be a negative quantity; that is, the alternating constituents of plate voltage and plate current must differ in phase by more than 90°. Let

$$\psi_n = 180 - (\phi_n - \theta_n) \qquad (4)$$

Digitized by Google

define the angle by which current and voltage depart from being exactly 180° out of phase. The power output of the tube of any harmonic is

$$P_n = \frac{e_n\, i_n \cos \psi_n}{2} \tag{5}$$

this being determined entirely from the wave forms of tube voltage and current.

The quantities e_n i_n and ψ_n further define an output impedance of the load on the tube, the resistance and reactive components of which are given by

$$R_n = \frac{e_n}{i_n} \cos \psi_n \tag{6}$$

$$X_n = \frac{e_n}{i_n} \sin \psi_n \tag{7}$$

This resistance and reactance may in some cases correspond to what may be computed from constants of apparatus in the tube circuit. For example, if in Fig. 3 L_B is a perfect choke coil, analysis of the plate wave form will necessarily give $\psi_n = 0$ and $R_n = R_b$ for the fundamental and every harmonic frequency. In other cases when apparatus with nonlinear volt-ampere relations is used as a load, the wave forms will not correspond to any that may be computed from values of simple impedances. Thus in Fig. 3, if R_b is replaced by a resistance with nonlinear volt-ampere relations as, for example, a two-electrode electron tube, then the analysis of wave forms of plate voltage and current will give values of R_n which are not the same for all harmonics. Moreover, the values of R_n for a given harmonic will vary with the amplitude of the voltage impressed on the modulating tube. The values of R_n and X_n will nevertheless be effective values which may be used in computations of the power output and may properly represent the impedance load upon the tube.

The load impedance and power defined in this manner correspond to the entire alternating output of the system, irrespective of the localizations of the dissipation of that power. In the case of a tube in an oscillating circuit, it includes the alternating power fed back to the grid branch of the tube, determined in a similar manner from harmonic analysis of the grid voltage and current wave forms. In the case of the modulator tube, the grid alternating power is supplied from the output of the microphone and transformer, and the load impedance upon the modulator tube is

Digitized by Google

dependent upon the relation of the tube and the apparatus associated with the plate circuit only.

With the conception of the load due to the generating system given by Fig. 3, if it is assumed that the choking action of the coil L_B is perfect, then the load impedance is a pure resistance. Even if the resistance R_b is not a pure resistance but one which varies with the current (as Fig. 2), with the conception here presented the load on the modulator tube is a resistance load, although the value of this resistance is dependent on amplitude and is different for harmonic frequencies than for fundamental. If on a plane with voltage as abscissa and current as ordinate, successive simultaneous values of plate voltage and current for the modulator tube be plotted, corresponding to a complete cycle of operation, and if this trace is a line, inclosing no area, then the load is a resistance. For a specified voltage the current is the same for an increasing voltage and decreasing voltage. If this line of operation or any portion of it incloses area, then there is a reactive component to the load, so that in general a different tube current exists for an increasing voltage of a given value than for a decreasing voltage of the same value.

Neglecting harmonic currents and voltages, for a reactive load the trace on the modulator plate current plate voltage plane will be an ellipse, with a clockwise sequence of successive points for an inductive load, and a counterclockwise sequence for a condensive load. Considering total instantaneous values, however, the trace will not be elliptical. Any phenomena in the telephone set which tends to make an elliptical trace for the fundamental line of operation of the modulator tube may be said to tend to produce a reactive load.

In a telephone set of the type analyzed in Fig. 1, there are three distinct types of phenomena which prevent the load on the modulator being a resistance load. The first arises from the imperfections of the choke coil L_B, which in practice is not entirely free from audio currents. The second is due to the reactive impedance of parts of the generating system. A third effect, of a more subtle nature, and not expressible in terms of reactances of inductors or condensers, arises from the resonance phenomena in the radiator unit. These three effects will be considered in turn.

Digitized by Google

VI. EFFECT OF IMPERFECTIONS IN THE AUDIO CHOKE COIL UPON THE PERFORMANCE OF THE SET

In the modulator unit the choke coil L_B is imperfect due to the reactance not being infinite and due to the direct resistance of the windings and effects which give rise to purely alternating current power losses. On account of the reactance being finite an alternating current will pass through the choke coil when the tube is operating. Due to the resistance of the windings, a direct voltage drop occurs across the coil, so that the net direct voltage supplied to the tube, given by the average voltage $\bar{e}$ is less than the direct voltage E_B supplied by the generator or battery. These effects may be represented by the use of the diagram Fig. 4, which represents a tube circuit with the same performance as that of Fig. 3, as

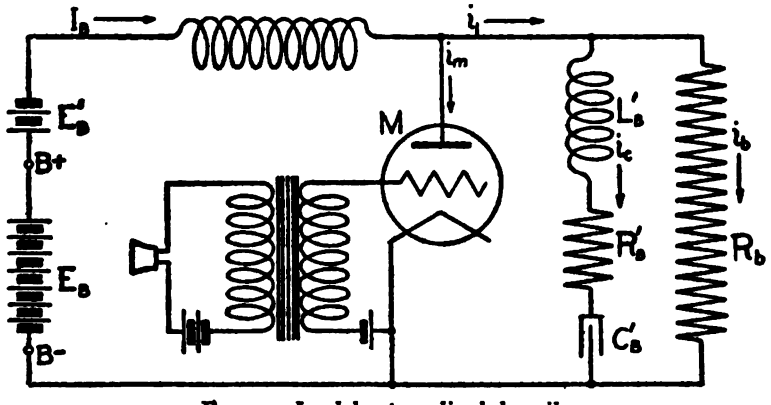

FIG. 4.—*Load due to audio choke coil*

far as tube voltage and current and the current to resistance R_b are concerned. In this latter figure, the choke coil in the battery lead is to be considered a perfect choke coil, with infinite impedance but no resistance. The battery E_B' represents a voltage opposing the main battery E_B of magnitude derived from the circuit of Fig. 3, being the product of resistance of the windings and the average current delivered by the battery. It is the difference of these two voltages which gives the net direct voltage impressed on the tube. The chain of impedances L_B' R_B' C_B' represents the effects of the finite impedance of the choke coil of Fig. 3. L_B' represents the inductance of that choke coil with the direct current flowing through the windings, and R_B represents approximately the alternating-current resistance of the choke coil, being larger than the direct-current resistance. C_B' represents the effective capacity of the power supply unit, as measured from the $B+$ and $B-$ terminals.

Digitized by Google

With the circuit of Fig. 4, the plate wave forms of voltage and current correspond to the impedance of L_B' R_B' C_B' in series, paralleled by the resistance R_b. The total load current i_l which is 180° out of phase with the modulator current i_m is composed of two portions, that passing through the choke coil i_c and the useful output current i_b through the resistance R_b. Usually the reactance of the choke coil is the greatest of the three impedances in the choke-coil chain, so that the impedance of that branch is inductive and, as a result, there is an inductive component to the load upon the tube. It results in the current pulsations in the tube current i_m being required to be greater than the pulsation in current in the useful load branch R_b. If, for example, the resistance R_b is 5000 ohms, the value of L_B' is 1.33 henry with the impedances of C_B' and R_B' negligible, then the impedance of the choke-coil branch at the speech frequency of 800 cycles is 6700 ohms. Accordingly the alternating current through the choke coil will be 75 per cent of that through the resistance R_b. The variation in the modulator tube current will in consequence be required to be 125 per cent of the variation in current to the resistance R_b. To produce, for example, an 8-milliampere variation in the useful output current of the tube, the variation of current through the tube must be 10 milliamperes. It is because a reactive component to the load limits the possible output that care must be taken to design the circuit in such a way that the tube voltage and tube current shall be approximately out of phase. To avoid excessive reactive component to the load due to the choke coil, a safe rule is to make the reactance at 800 cycles at least two or three times the value of the resistance R_b.

VII. EFFECT OF AUDIO FREQUENCY IMPEDANCE OF PARTS OF THE GENERATING SYSTEM UPON THE PERFORMANCE OF THE SET

Referring back to the diagram of Fig. 1, a source of reactive component to the load on the modulator tube has been derived due to the reactance of apparatus in the modulator unit. Similarly a second source of reactance load exists in the generating unit. Thus in the diagram, Fig. 5, condenser C_b is required to be of low reactance for the radio frequency current, but of high reactance for audio currents. If the ratio of the radio frequency to the audio frequency is low, it may not be possible to satisfy both these requirements. The characteristics of the generating system shown in Fig. 2 were for very low audio frequencies, such that

Digitized by Google

reactive effects due to the condenser are negligible. Even with the condenser present, and with actual operating audio frequencies, the current i_b may be interpreted as the average space current to the oscillator tubes during a radio cycle, corresponding to the average plate voltage e_b. However, to produce the plate voltage e_b the

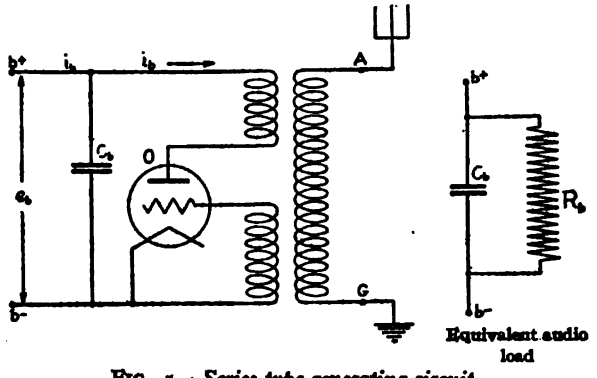

FIG. 5.—*Series type generating circuit*

modulator tubes must supply not only the conductive current i_b, but also the charging current to the condenser. As a result, the generating unit as a whole is behaving as an impedance with a capacity component.

Another type of generating circuit is shown in Fig. 6, which may be used in radio telephone sets. It may be described as a circuit

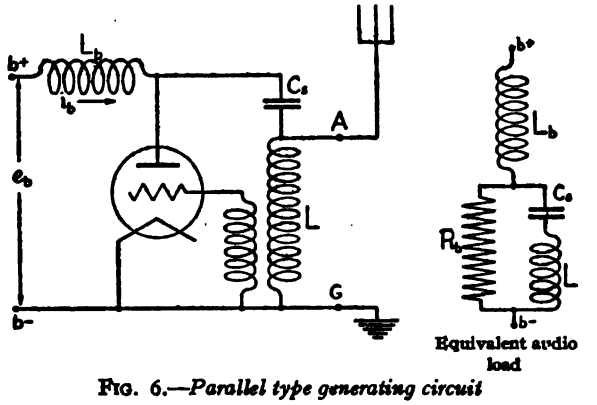

FIG. 6.—*Parallel type generating circuit*

with plate direct coupled and grid inductively coupled to the antenna circuit and with a parallel power supply. Choke coil L_b performs the same function for radio frequencies as does the choke coil L_B for audio frequencies in the modulator unit. However, there is an upper limit to the possible value of the choke coil

Digitized by Google

L_b, since it must permit the audio current to pass into the generating unit. At low ratios of radio to audio frequencies, both conditions can not be met, so that, in general, an inductive component is imposed upon the modulator tube, which may be represented as an inductance in series with the resistance R_b.

Impedances in the generating circuit other than that of a radio by-pass condenser or a choke coil may be of importance. Thus in Fig. 6, if the stopping condenser be of sufficiently high capacity, and L_b and L in series are of sufficiently high inductance, the system L_b, C_s, and L in series may constitute a series resonance circuit, which will be modified by the resistance R_b being shunted across C_s and L when the tube is operating. Such effects may give rise to distortion provided the resonance occurs within the audio-frequency range.

The choice of suitable choke coils, stopping condensers, by-pass condensers in the generator unit, depends jointly upon the radio frequency and upon the audio frequency. With too large values of the radio choke coil or by-pass condenser, a reactive load is imposed upon the modulator tube. With too low values, radio power will flow back into the modulator unit, interfering with its proper functioning as well as cutting down the radio power available for the radiator unit. In short wave-length radio telephone sets there is usually little difficulty in making a suitable choice of values, but in long wave-length sets particular care must be taken.

VIII. EFFECTS OF RESONANCE POWER IN THE RADIO OSCILLATORY CIRCUIT UPON THE PERFORMANCE OF THE SET

A third effect causing alteration of the load upon the tube from a simple resistance arises because of the energy in the electromagnetic field of the radiator unit. This effect is of a more complex nature than the other effects previously mentioned, which were expressible in terms of reactances of condensers and inductances. It is, moreover, an effect of importance not only in plate modulation methods of radio telephony, but in any method of radio communication involving modulation methods. Two methods of analysis of the phenomena will be presented. The first is based on considerations of the variations in power required to cause a specified variation in current in a radio resonance circuit. In this treatment, attention will be directed to the physical phenomena involved. The second method is based upon the analysis of the wave form of the modulated radio currents into

Digitized by Google

the carrier and side frequencies, and upon the behavior of the resonance circuit for currents of each of these frequencies.

For purposes of discussion it will be of advantage to refer to a simple type of resonance system and a simple method of modulating the current in that system. A possible method of modulating is shown in Fig. 7, involving the use of two alternating-current generators, G_r and G_a, the former turning at a speed corresponding to a radio or modulated frequency and the latter at a speed corresponding to an audio or modulating frequency. With the key K open, the field of the radio generator is excited by direct current, so that continuous radio currents flow from the armature of that generator. By closing the key, the field strength of the radio generator is varied at an audio rate, and therefore the output voltage is varied and modulated radio frequency current flows

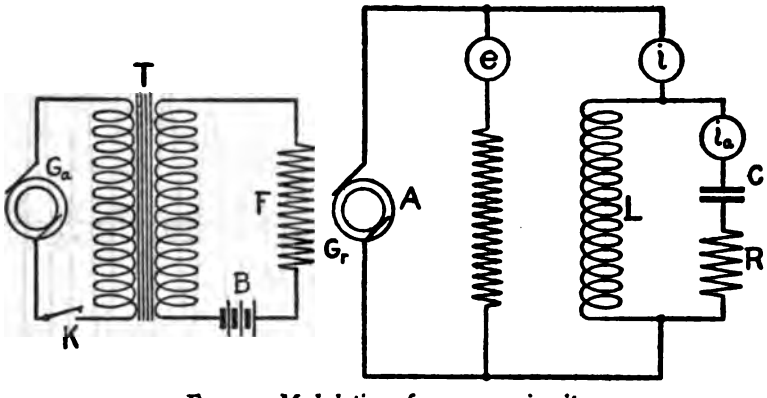

FIG. 7.—*Modulation of resonance circuit*

from the armature. The resonance load upon the radio generator is the parallel system L, C, R tuned to the frequency corresponding to the speed of rotation of the generator G_r.

1. POWER RELATIONS IN RESONANCE SYSTEMS DURING MODULATION

With the key of Fig. 7 depressed, the actual wave form of current through condenser C of the resonance system may be approximately as shown in Fig. 8, which may be described as a radio frequency current with amplitude pulsating at an audio frequency rate. For the purpose of discussing the phenomena from power considerations, imagine the instruments e, i, i_a of Fig. 7 to record root mean square values sufficiently rapidly to follow accurately an audio current, but not a radio current. Thus the instrument i_a will follow the audio variations in the antenna current, as shown by the trace i_a of Fig. 8. Similarly instruments i and e will follow

Digitized by Google

the variations in the input radio current and voltage to the resonance system. With sine wave modulation, it is apparent that all of the instruments will record sine wave forms. The relations between the three wave forms depend only upon the constants of the circuit L, C, R, and the radio and audio frequencies. For a given wave form of current i_a, the audio variations in the power which must be supplied to the oscillating circuit may be computed. This must be equal to the power registered by instruments e and i, since the resonance load behaves as a resistance for the radio frequency and the radio current through i must be in phase with the radio voltage across the circuit as determined by the current through e. Consequently the product of e and i at any time in the audio cycle gives the radio power which is being taken by the

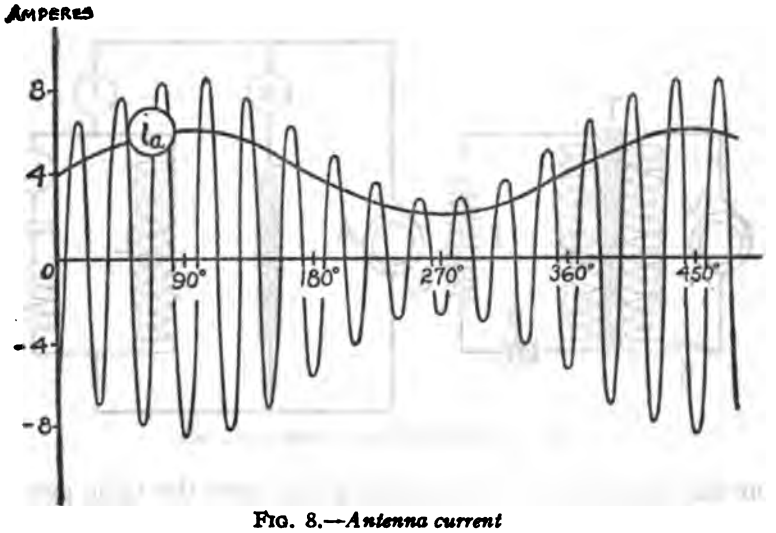

FIG. 8.—*Antenna current*

resonance circuit. It is by equating the values for power as specified by these two methods that the modulation phenomena in the resonance circuit will be examined.

For the determination of audio variation of power in terms of the current i_a and the constants L, C, R, two parts must be taken into account. At any instant in the audio cycle power must be supplied to balance the losses given by Ri_a^2, in which R is the lumped resistance and i_a is the instantaneous reading of the instrument. Power must also be supplied to change the electromagnetic energy which at any instant of the audio cycle is present in the circuit. This energy is given by Li_a^2 in which L is the lumped inductance of the circuit. During the radio cycle this energy flows back and forth from the condenser to the inductance,

Digitized by Google

the amount of energy, however, remaining constant for a fixed amplitude. With the amplitude changing, power must be supplied to alter the energy content of the circuit, given by the time rate of change of energy, the derivative being taken in the audio time scale. Consequently, the total power given is by

$$P = Ri_a^2 + \frac{d}{dt}(L\, i_a^2) \tag{8}$$

and is readily computed from the audio wave form of i_a and the lumped resistance and lumped inductance of the circuit.

As a numerical example assign the following constants to the resonance circuit:

$L = 160$ microhenries.

$C = 0.004$ microfarad.

$R = 4$ ohms.

These correspond to a resonance circuit of resonant wave length very close to 1500 meters, a log decrement per cycle of 0.063, and a resonance impedance of 10 000 ohms. Let the ratio of the audio frequency to the radio frequency be 100 to 1, so that the modulating frequency is very closely 2000 cycles per second. Let the degree of pulsation of current i_a be 50 per cent about the value 4 amperes, so that the wave form of current is

$$i_a = 4\ (1 + 0.5 \sin 12\,500\, t) \tag{9}$$

Under these conditions the audio variations in power delivered to the resonance circuit computes to be as shown in the upper curve of Fig. 9. The curve P_r gives the variations in power consumed by the resistance R, and the curve P_0 gives the variation of the power required to change the energy content. The average value of the latter is zero when taken over a complete audio cycle. The sum of the curves P_r and P_0 gives the variation of total power P_t which must be supplied to the resonance circuit to cause the wave form i_a to exist. It is this total power which must be given by the product of the pulsating sine wave forms of voltage e and input current i to the resonance system during the modulation. The problem is to find what the wave forms of e and i must be to have a product given by the curve P_t. This problem is to some extent indeterminate.

In general let the wave forms be given by

$$i_a = I_a\,[1 + k_a \sin pt] \tag{10}$$

$$e = E\,[1 + k_e \sin (pt + \phi_e)] \tag{11}$$

$$i = I\,[1 + k_i \sin (pt + \phi_i)] \tag{12}$$

Digitized by Google

in which the capital letters give average values of quantities over an audio cycle and the k's denote degrees of pulsation, and ϕ_e and ϕ_i represent phase angles with respect to the wave form of current

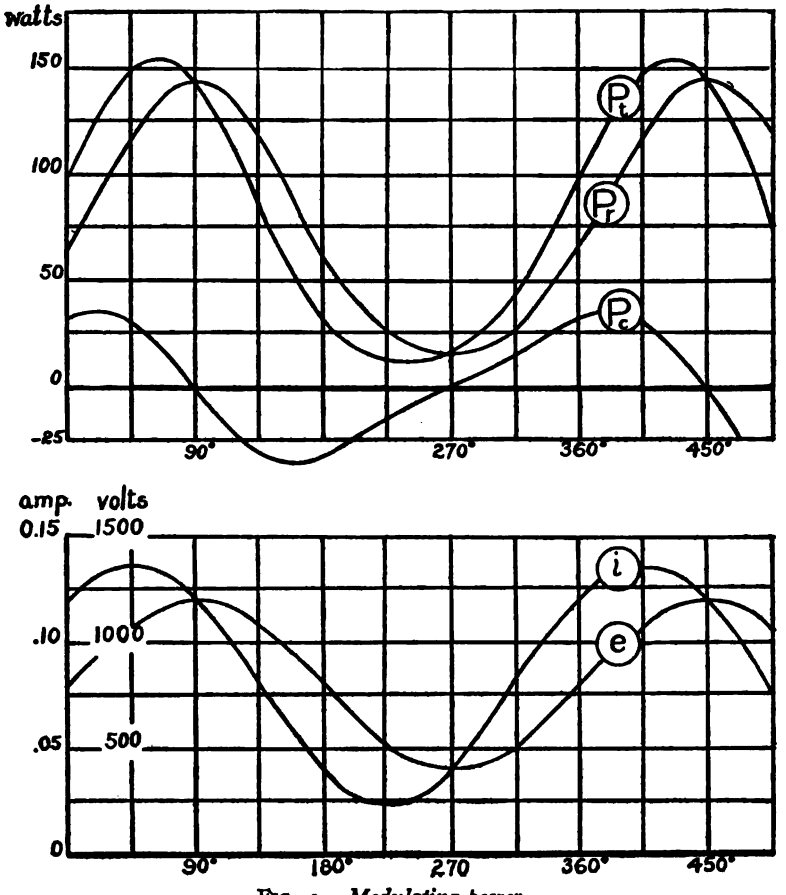

FIG. 9.—*Modulating power*

i_a. From the condition that for all instants of time in the audio cycle the identity must be satisfied

$$ei = Ri_a^2 + \frac{d}{dt}(L\, i_a^2) \qquad (13)$$

the following relations will be found;

1. Either ϕ_e must be zero or ϕ_i must be zero.
2. If $\phi_e = 0$, then $k_e = k_a$, $\phi_i = \tan^{-1} \frac{2Lp}{R}$, $k_i = k_a \sec \phi_i$
3. If $\phi_i = 0$, then $k_i = k_a$, $\phi_e = \tan^{-1} \frac{2Lp}{R}$, $k_e = k_a \sec \phi_e$

Digitized by Google

The reasons for the two possible solutions coming out of this expression is that nothing is specified as to the nature of the resonance circuit. The quantities e and i are similarly involved in the equation, and consequently two solutions arise, in one case e being in phase with i_a, and of the same degree of pulsation, and in the other i is in phase with i_a, and of the same degree of pulsation. The latter case corresponds evidently to a series resonance circuit, in which i and i_a must be of necessity the same wave form, as they are the same identical currents. The former case corresponds to resonance circuits of the parallel type in which the input voltage wave form is similar in shape to the oscillating current wave form. In this particular circuit, the ratio of e to i_a is the impedance of one branch of the resonant circuit. The solution is further incomplete because the ratio of E to I is not determined by the analysis. More detailed knowledge of the circuit must be had to determine uniquely what of the possible wave forms are correct.

For the case of the oscillating circuit as specified above, audio wave forms of radio current and voltage which are consistent with the configuration of the resonance circuit, and which when multiplied together give the total power P_t, are shown in the lower part of Fig. 9. In this case the phase angle ϕ_1 is 45°, and the degree of pulsation of input current is the square root of two times the degree of pulsation of the current i_a. The input current form is seen to lead the voltage form in the audio time scale.

2. RADIO FREQUENCY PHENOMENA IN A RESONANCE CIRCUIT CARRYING MODULATED CURRENT

To determine the relations between the radio wave forms of input current, input voltage, and condenser current, analysis must first be made of the condenser current into its radio frequency constituents. Then the performance of the resonance circuit must be determined for each of the frequencies present in the condenser current. This, then, will determine what the radio wave forms of voltage e and current i will be, corresponding to any condenser current i_a. In the present discussion these three symbols will refer to instantaneous radio frequency values of these quantities and not, as previously, to the instantaneous audio value of the effective radio values.

The wave form of a sine wave modulated radio frequency current may be expressed as

$$i_a = I\sqrt{2}\ (1 + k_a \sin pt) \sin (\omega t + \phi) \qquad (14)$$

Digitized by Google

which states that it is a radio frequency current, with an amplitude changing sinusoidally at a lower frequency. The expression may be readily expanded into

$$i_a = I\sqrt{2}\left\{\sin(\omega t+\phi) + \frac{k_a}{2}[\cos(\omega t+\phi-pt) - \cos(\omega t+\phi+pt)]\right\}$$

This latter expression states that the wave form is the sum of three currents of different frequencies, corresponding to angular velocities ω, $\omega+p$, $\omega-p$. The amplitudes of the currents of the last two frequencies are the same, and $\frac{k_a}{2}$ times the amplitude of the current of the first frequency. These three frequencies are known as the carrier and the two side frequencies. Important relations may be brought out by representing these currents vectorially as in the top diagram, Fig. 10, which represents the current flowing in condenser C of Fig. 7. Vector C represents the current of the carrier frequency, and is to be considered as rotating in a counterclockwise sense, with an angular velocity ω. The vectors $s+$ and $s-$ represent currents corresponding to the side frequencies. The vector $s+$ is rotating with an angular velocity $(\omega+p)$ and therefore at a velocity $+p$ with respect to the carrier frequency. The vector $s-$ is similarly rotating with an angular velocity $(\omega-p)$ and therefore at a velocity $-p$ with respect to the carrier frequency. The two side vectors, upon addition, lie along the vector for the carrier frequency, and this relation is maintained throughout the rotation. The degree of modulation is the ratio of the sum of the lengths of the side vectors to the carrier vector, in this case it is 50 per cent. The position of the vector C indicates the point in the radio cycle which is represented by this configuration of the vectors. In the figure, a time corresponding to 120° in the radio cycle has elapsed since the vector C was in a horizontal position. The position in the audio cycle is

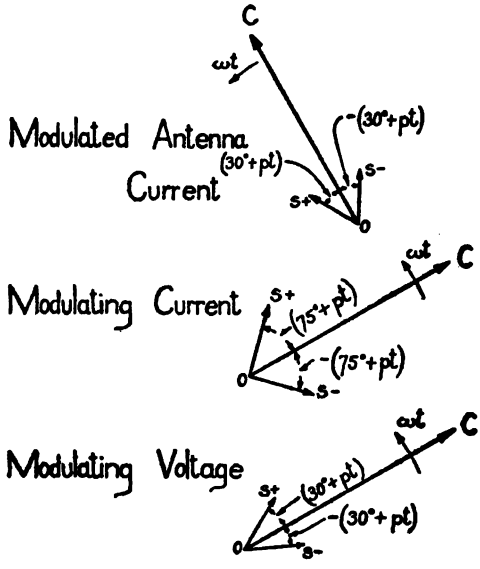

FIG. 10.—*Modulation of resonance system*

Digitized by Google

given by the angle between the carrier vector C and the side vector $s+$. Thirty degrees in the audio time scale have elapsed since the three currents were additive to give maximum instantaneous current.

Thus the diagram shown represents a particular instant of time and a particular point on the wave form of a modulated current, just as a single vector represents a point in a sine wave form. Successions of points on the modulated wave form are determined through the rotations of these vectors, the side vectors rotating slowly with respect to the carrier vector, and all three rapidly about the point O.

In order to determine the wave form of currents and voltages existing in other parts of the resonance circuit, it is necessary to know the performance of that circuit for currents of each of the three frequencies. This knowledge will enable computations and vector diagrams to be made, showing, in particular, the wave form of modulating current i and of modulating voltage e, in comparison with the wave form of output current i_2.

For convenience, the ratio of the input voltage e to input current will be termed the impedance Z of the resonance circuit. Similarly the ratio of the condenser current to the input current may be termed the transformer ratio T, since it gives the ratio by which current is increased by the resonance action. Define the resonance frequency n_0 as that frequency for which the reactance of the condenser is equal and opposite to the reactance of the inductance. Let any other frequency n be specified relative to the resonance frequency by the equation

$$n = n_0 (1 + \beta) \tag{15}$$

so that, for example, if $\beta = -0.01$, the frequency n is 1 per cent less than the resonance frequency. Let δ = the log decrement per cycle of the resonance circuit, which is π times the ratio of the series resistance of the circuit to the lumped inductive reactance.

$$\delta = \frac{\pi R}{L\omega}$$

Then, for any frequency in the resonance region it may be readily shown that the two ratios as given above are approximately

$$\frac{e}{i} = Z = \frac{Z_0}{1 + j\frac{2\pi\beta}{\delta}} \tag{16}$$

$$\frac{i_2}{i} = T = \frac{jT_0}{1 + j\frac{2\pi\beta}{\delta}} \tag{17}$$

Digitized by Google

in which Z_o and T_o are numerical values for resonance frequency at which $\beta=0$. For this type of resonance circuit, $Z_o=\frac{L}{CR}$, $T_o=\frac{L\omega_o}{R}$. For other types of parallel resonance circuits, including the case of a resonance transformer with inductive coupling but with negligible primary impedance, the values of Z_o and T_o will be different, but the ratios $\frac{Z}{Z}$ and $\frac{T}{T_o}$ will vary with frequency in quite the same manner as in the case cited.

By using the values of these ratios for the three cases $\beta=0$, $\beta=+\frac{p}{\omega}$, and $\beta=-\frac{p}{\omega}$ the carrier and side vectors may be evaluated for the input modulating current and modulating voltage. The results thus obtained for a case in which $\frac{2\pi\beta}{\delta}=1$ is shown in the last two diagrams of Fig. 10. These three diagrams show the conditions in various branches at the same instant of time.

From these diagrams the modulating current is seen to be different in wave form from either the modulating voltage or the condenser current, having a degree of modulation greater in the ratio of $\sqrt{2}$ to 1. Moreover, the audio phase of modulating current is greater by 45° than the audio phase of voltage or condenser current. The general formula for phase shift of modulation and change in degree as determined by this method is the same as that obtained, by the less complete but more general treatment given on pages 393 to 397.

As an illustration of the actual wave forms of a resonance circuit, the oscillogram, Fig. 11, shows the input current, input voltage, and the condenser current obtained by low-frequency modulation of current in a low-frequency resonance circuit, by the method shown in Fig. 7. The input current is clearly shown to be of a greater degree of modulation than the input voltage and moreover to precede it on the audio time scale. That more power is being supplied when the condenser radio current is of a given value but increasing than when of the same value but decreasing is evident, since the input current is greater in the former case than in the latter.

The effect described here is of importance in any electrical circuits in which current in a resonance system is modulated at a lower frequency. While in radio telephony the effect is not of importance at short wave lengths, it does commence to be of considerable importance at long wave lengths.

Digitized by Google

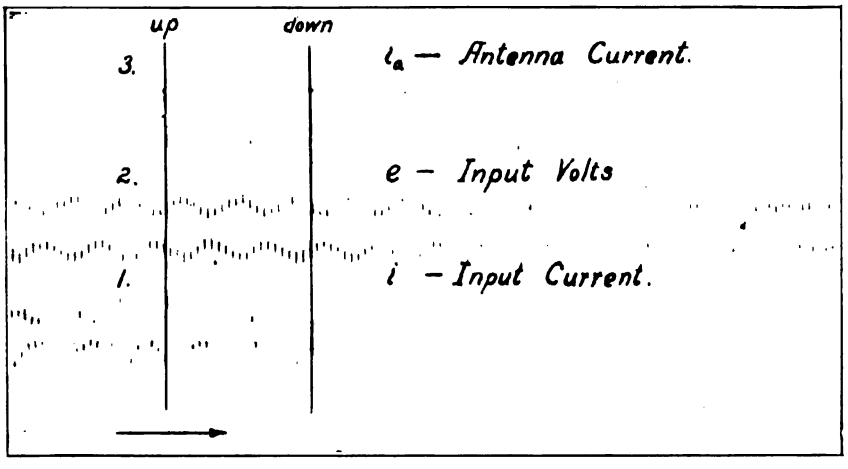

FIG. 11.—*Change of modulation. Wave form at the radiator unit*

Digitized by Google

Digitized by Google

In any modulation system whatsoever, the variation of resonance energy will of necessity influence the operation of the modulating device, since it requires greater amount of radio power to be generated when the antenna current is a given amount and increasing than when it is the same amount and decreasing. In the circuits using plate modulation, it is apparent that the radio generating circuit will react on the modulator tube by drawing more audio output current when the audio output voltage is a given value and increasing than when it is the same value but decreasing. Assuming that the effects of imperfections of the choke coil and of audio impedance of parts of the generating circuit are negligible, the line of operation on the plate voltage plate current diagram for the modulator tube will in consequence be distorted into a loop with rotation in a sense corresponding to a condensive load.

By way of summary of the effects tending to produce reactive components in the load on the modulator tube, in Fig. 12 are shown four impedances Z_1, Z_2, Z_3, and Z_4 in parallel which symbolize the load for a telephone set analyzed as in Fig. 1. The first impedance Z_1, consisting of the chain L_B', R_B', and C_B', represents the effects of imperfections of the choke coil L_B. The second impedance Z_2 represents the effect due to audio impedance of parts of the generating system, and is of very simple nature for this type of circuit. For other types as, for example, that shown in Fig. 6, the representation is more complex, and the succeeding impedances Z_3 and Z_4 would not be in parallel with Z_1 and Z_2, but be incorporated as a portion of Z_2. The third impedance Z_3 represents the equivalent condensive load due to the resonance energy in the radiator circuit. The fourth impedance Z_4 is a resistance R_b' in which most of the audio output power of the modulator tube is usually consumed. Due to the phenomena of resonance energy, the numerical value which may best represent R_b' is not necessarily the same as the value R_b of Fig. 3. Of these four impedances, the last two are possibly of the most symbolic nature, since their values depend not upon the simple electrical elements of inductance, capacity, and ohmic resistance, but rather upon the characteristics of the

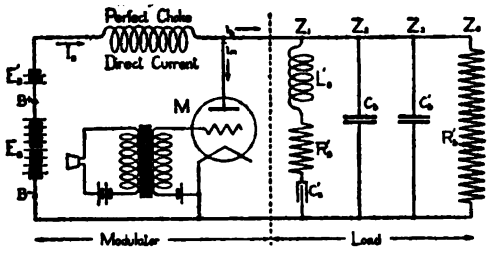

FIG. 12.—*Modulator and load*

Digitized by Google

generating tubes, values of plate and grid couplings and grid biasing voltage, and resonance impedance and decrement of the radiator circuit.

With a plate modulation set used for telegraphing, with grid voltage for the modulator tube supplied at a definite frequency either by buzzer or by use of an audio resonance circuit, it may be possible to balance out one of these impedances against another in such a manner as to produce a resistance load upon the modulator for the fundamental frequency. But for telephoning, the audio fundamentals are constantly changing in frequency and in amplitude, so that any audio frequency resonance due to balancing reactances to produce resistance load is undesirable because of the distortions which would occur. For good operation and articulation it is essential that the load impedance Z_4 be the most important throughout the speech range of frequencies.

IX. THE STRENGTH OF SIGNAL TRANSMITTED BY A RADIO TELEPHONE SET

In a continuous wave transmitter the reading of an instrument reading effective current in the antenna circuit is qualitatively an indication of the strength of signal which is being transmitted. In transmission of signals by modulation methods maximum reading of antenna current does not indicate maximum received signal. If, for example, the wave form of antenna current is one with perfect sine wave modulation, as given by equation 14, and the detection at the receiving station is according to the square law of reception, then neglecting variations of audio impedance of parts of the receiving circuit with frequency the received fundamental audio current is proportional to the product $k_a I^2$. The reading of the antenna ammeter, on the other hand, for this wave form is $I\sqrt{1+\frac{k_a^2}{2}}$. These functions are obviously not proportional.

In radio telephone transmission, however, the electrical conditions are such that sine wave modulation rarely occurs. An important factor contributing to this is the curvature of the characteristics of the generating unit as, for example, in Fig. 2. While there is no theoretical limitation upon the voltage which may be impressed upon a generating circuit, the current which can be taken by the circuit will in no case exceed the total filament emission of the generating tubes. Under conditions of efficient operation, the direct current to a tube is usually of the order of not greater than a third or half of the total emission. As a result,

Digitized by Google

if the operating plate voltage is increased, the current to the circuit can not increase indefinitely but will approach a constant value. At the same time, since the input power is no longer proportional to the square of the input voltage, the output current increases less rapidly than the input voltage, and linear relations no longer exist. The result is that during speech if a sine voltage wave is impressed upon the generating circuit by the modulator tube, the maximum increase of antenna current is less than the maximum decrease. In other words, the upward variation is less than the downward variation of antenna current.

This type of distortion at the transmitter is not necessarily detrimental to good speech transmission. In fact, with a sine wave modulation, the received audio current is not a sine wave, but contains a double frequency term, which is $\frac{k_a}{4}$ times the fundamental. It may be readily shown that the proper wave form to impress upon a detector with square law of reception in order to obtain a pure audio signal is

$$e = E\sqrt{1 + k \sin pt} \sin \omega t$$

in which k is a constant, less than unity.

Assuming there is no difference in the wave form of voltage impressed upon the detector and the wave form of current in the transmitting antenna, then to transmit a pure sine wave audio signal the transmitter antenna current should be of the form

$$i_a = I_a\sqrt{2}\sqrt{1 + k \sin pt} \sin \omega t, \; k < 1 \qquad (18)$$

The wave form of equation 18 is one which approximates that produced by transmitters in case the output current is limited by the amount of input current which is possible. If, for example, in this expression k is unity, the peak r. m. s. value of antenna current is $\sqrt{2}$ or 1.4 times the unmodulated r. m. s. value, while the minimum value is zero. In other words, this wave form is one corresponding to less upward modulation than downward modulation. Since this wave form is the proper one for transmitting a pure note and, moreover, is one which is often approached in practice, it possesses advantages over a sine wave modulated form as a basis of rating of telephone sets.

For the wave form of equation 18 the r. m. s. antenna current averaged over an audio cycle is independent of the modulation parameter k, and if this wave form is being produced, the reading of the antenna ammeter will neither rise nor fall during speech.

Digitized by Google

This is in contrast with the case of sine wave modulation (equation 14) in which the reading increases in the ratio $\sqrt{1+\frac{k_a^2}{2}}$ during speech. The upward variation of antenna power is equal to the downward variation of power, being kRI_a^2. Moreover, the received signal is also proportional to the variation of power from mean. In consequence the received signal is proportional to the difference between the peak antenna power and the minimum antenna power. The rating of a telephone set might well be specified simply by this variation of antenna power with specified speech conditions at the transmitter microphone.

These considerations of signal strength have an important bearing upon the choice of the ratio of the number of modulating tubes to the number of oscillator tubes in a transmitter set. The average antenna power which can be obtained is determined almost entirely by the number of oscillator tubes used and is quite independent of the number of modulators. On the other hand, the variation of antenna power is not determined to the same degree by the number of modulator tubes, because the number of oscillator tubes determines the nature of the load upon the modulator tubes. For example, compare the relative merits of a telephone set with three oscillators and two modulators with one using four oscillators and one modulator, using identical tubes and assuming that the sufficient grid power for the modulator tubes will be supplied in either case. The latter combination is possibly capable of producing 15 per cent greater antenna current than the former. The former, however, may be expected to produce more than twice as much audio current in the receiving telephones as the latter, first, because there are twice as many units for varying the antenna power, and second, because two modulating tubes may be expected to operate much more efficiently into the generating circuit of three tubes than one modulating tube can work into a generating circuit of four tubes.

The signal, however, can not be indefinitely improved by increase of ratio of modulator tubes to oscillator tubes, not only on account of the poor audio efficiency of the modulator under such conditions, but also because of the speech distortions which will occur due to any overmodulation. For these reasons, in constructing transmitters with tubes operating in parallel the number of modulator tubes usually about equals the number of oscillator tubes for best operation.

Digitized by Google

X. SUMMARY

1. Three methods of modulating the output current of an electron-tube generating circuit are commonly used—modulation by radio absorption, by variation of the operating grid voltage, and by variation of the operating plate voltage. Of these, the method of plate voltage modulation is the most satisfactory.

2. A telephone transmitter network may be conveniently analyzed into four units—the plate power supply, the modulator unit, the generating unit, and the radiator unit.

3. The essential operation of the modulator tube in the modulator unit is as an aperiodic power amplifier, the essential load into which the tube operates is a resistance as given by the external characteristics of the generating unit.

4. The actual load impedance of a tube acting as an amplifier, modulator, or generator is defined in terms of harmonic analysis of the wave forms of plate voltage and plate current. For modulator tubes the actual load impedance is not given exactly by the characteristics of the generating unit, on account of imperfections of the audio-choke coil, audio impedance of parts of the generating circuit, and the presence of electromagnetic energy in the radiator unit.

5. Imperfections of the audio-choke coil due to its reactance being finite tends to produce an inductive component to the load on a modulator tube. This effect can be made small as desired, and is not an essential limitation in radio telephony.

6. Audio impedance of component parts of the generating circuit may tend to produce an inductive load, resistance load, or capacity load, depending upon the nature of the generating circuit. The choice of suitable constants of condensers and inductances to function properly for radio purposes and not seriously affect the operation of the modulator tube becomes difficult only with a high ratio of modulating frequency to modulated frequency.

7. The presence of electromagnetic energy in the radiator unit requires that more power be delivered to the radiator when the antenna current is a given value and increasing than when it is the same value and decreasing. The tendency is to impose a capacitive component to the load upon the modulator tube. This effect is of more importance the greater the ratio of modulating to modulated frequency, and the less the decrement of the radiator circuit.

Digitized by Google

8. The strength of speech signal produced by a telephone transmitter set is not indicated by the reading of an ammeter in the radiator unit. The signal strength under conditions of no distortion with a receiving set with square law of reception is proportional to the difference between the peak radio power and the minimum radio power in the transmitter radiator unit. This power difference under specified speech conditions at the mouthpiece of the transmitter microphone is suggested as a suitable basis of rating radio telephone sets as to power output.

WASHINGTON, February 23, 1921.

Digitized by Google

OF THE UNIVERSITY OF CALIFORNIA

FEB 23 19

DEPARTMENT OF COMMERCE

SCIENTIFIC PAPERS

OF THE

BUREAU OF STANDARDS

S. W. STRATTON, DIRECTOR

No. 424

MATHEMATICAL THEORY OF INDUCED VOLTAGE IN THE HIGH-TENSION MAGNETO

BY

FRANCIS B. SILSBEE, Physicist

Bureau of Standards

DECEMBER 13, 1921

PRICE, 15 CENTS

Sold only by the Superintendent of Documents, Government Printing Office
Washington, D. C.

WASHINGTON
GOVERNMENT PRINTING OFFICE
1922

Digitized by Google

Digitized by Google

DEPARTMENT OF COMMERCE

SCIENTIFIC PAPERS
OF THE
BUREAU OF STANDARDS

S. W. STRATTON, DIRECTOR

No. 424

MATHEMATICAL THEORY OF INDUCED VOLTAGE IN THE HIGH-TENSION MAGNETO

BY

FRANCIS B. SILSBEE, Physicist
Bureau of Standards

DECEMBER 13, 1921

PRICE, 15 CENTS
Sold only by the Superintendent of Documents, Government Printing Office
Washington, D. C.

WASHINGTON
GOVERNMENT PRINTING OFFICE
1922

Digitized by Google

Digitized by Google

MATHEMATICAL THEORY OF INDUCED VOLTAGE IN THE HIGH-TENSION MAGNETO

By Francis B. Silsbee

ABSTRACT

Three different circuits, representing in simplified form the essential features of the high-tension magneto, are developed and equations for the electrical performance of each are given. It is shown that by the insertion of proper electrical constants in these equations the resulting performance will be substantially the same as that of an actual magneto. Methods are suggested for the experimental determination of these constants, and the agreement between this theory and observed results is shown in certain cases.

CONTENTS

	Page
Notation	408
I. Introduction	409
1. General	409
2. Cycle of operation	409
3. Historical	411
II. Double-coil model	414
1. Equations	414
2. Numerical examples	419
III. Single-coil model	426
1. Equations of model	426
2. Derivation of single-coil model from actual circuit	428
3. Single-coil model with shunting resistance	431
4. Numerical examples	433
5. Application of single-coil model to complete cycle	437
IV. Closed-coil model	439
1. Equations	439
2. Numerical example	444
3. Correlation with skin effect in iron core	447
V. Measurement of constants	451
Capacity measurement	451
1. By impulsive impedance	453
2. By computation	453
3. By resonance	453
4. By A. C. bridge	455
Resistance and inductance measurements	455
1. By ballistic galvanometer	456
2. By A. C. bridge	457
VI. Experimental confirmation of models	464
VII. Conclusions	469

Digitized by Google

NOTATION

A, B, A_1, B_1 = constants of integration.
B_1 and B_m = magnetic flux densities.
b = $\frac{R}{2L}$
C, C_1, C_2 = electrostatic capacity.
c = skin effect constant = $\sqrt{4\pi^2 f\frac{\mu}{\rho}}$
d = $\sqrt{\frac{1}{LC}}$
E, E_1, E_2 = emf of rotation or of battery.
e = base of Napierian logarithms = 2.718 . . .
f, f_1, f_2 = frequencies.
g = length of air gap.
ih = length of iron circuit.
I_0 = current at break.
i_1, i_2 = instantaneous currents.
i_w, i_s, i_c = instantaneous currents in winding, shunting resistance, and condenser.
j = $\sqrt{-1}$
K = fractional distance from terminal to effective center of C_d.
k = coefficient of coupling = $\sqrt{\frac{M^2}{L_1 L_2}}$
k_e = coefficient of coupling of eddy current circuit.
L_{12}, L_{21} = mutual inductance of double-coil model.
L, L_1, L_2 = self-inductance.
l_0 = thickness of lamination.
M = mutual inductance.
m = dependent variable in auxiliary equations.
m_1, m_2 = roots of auxiliary equations.
p = ratio of reduction from secondary to primary.
R, R_1, R_2 = resistances.
S = shunting resistance.
s = complex ratio of flux densities in skin effect.
T, T_0 = time constant $\left(\frac{L}{R}\right)$.
t = time.
v_1, v_2 = instantaneous voltage of condenser terminals.
V_s = breakdown voltage of spark gap.
V_m = maximum voltage.
X, Y = parts of complete solution of differential equations.
x = $\frac{\mu q}{h}$.
y = $\frac{\alpha_1}{\alpha_2}$.
z = impedance.
Z_1, Z_m, Z_2 = impulsive impedances = $\frac{V_m}{I_0}$.
α, α_1, α_2 = real part of roots of auxiliary equations.
β, β_1, β_2 = imaginary part of roots of auxiliary equations.
δ = small difference in roots.
θ = constant of integration (angle).
μ = permeability.
ρ = resistivity.
ϕ = phase angle of impulse.
ω = $2\pi \times$ frequency.

Digitized by Google

I. INTRODUCTION

1. GENERAL

One of the problems which has received attention from the National Advisory Committee for Aeronautics is that of the high-tension magneto, and a detailed study of this device has been carried on at the Bureau of Standards under its auspices. While in the past the magneto has been developed along empirical lines, there has recently appeared a tendency to place the design of this type of apparatus upon a more definite scientific basis, and as a foundation for such a rational design at least an approximate theory of the internal phenomena which take place within it must be available. It is the purpose of the present paper to develop from several points of view such an approximate theory for one particular period in the cycle of operation and to correlate certain of the theoretical conclusions with a few experimental results.

The magneto is an exceedingly complex electrical system which serves to transform energy from mechanical through magnetic and electrical forms into heat energy in a high-voltage spark. It is probably impossible to give a complete mathematical treatment which will permit of exact computation of all the phenomena which occur in such a device. Equations can, however, be developed for various combinations of circuits which approximate more or less closely to the actual magneto, and these abstract theoretical circuits will be referred to in the following pages as "models" of the magneto. Such models are useful for two distinct purposes: (1) The change in the performance of the model under various conditions gives a qualitative indication of the corresponding behavior of the actual magneto under similar conditions; (2) a quantitative expression for any specific property of the magneto, such, for example, as the effect of eddy currents or the magnitude of the secondary capacity, may be expressed by the numerical value of the corresponding quantity in the model, and changes made upon such properties as a result of changes in the design can thus be numerically expressed and compared.

2. CYCLE OF OPERATION

The complete operation of the magneto which leads to the production of a single spark consists of a rather complex cycle of operations, which may be divided into six distinct periods, as follows:

Digitized by Google

1. The rotation of the armature, while short circuited in the magnetic field of the permanent magnets, generates in the primary winding a certain current (2 to 4 amperes) and stores in the magnetic field thus produced a certain amount of energy ($\frac{1}{2}LI^2$). At the instant at which a spark is desired the primary contacts are separated by a cam which wholly changes the electrical characteristics of the circuit.

2. The rapid decrease in primary current which results from the separation of the contacts generates a high and increasing voltage in both primary and secondary windings. This process, which may be called period 2, continues for only a few ten-thousandths of a second until the voltage across the secondary terminals has risen to a sufficiently high value to break down the gas between the electrodes of the spark plug.

3. This breakdown of the gas in the spark gap is accompanied, first, by the very rapid discharge of the condenser formed by the leads from the magneto to the spark plug. This probably takes place in an oscillatory manner, with a frequency of several million cycles per second. This discharge may be called period 3.

4. After the rapid condenser discharge is completed there is a further interval, denoted by period 4, during which the remaining magnetic energy stored in the coil is dissipated in the spark gap by the arc which continues to exist across the gap. At high speeds the cam may allow the primary contacts to close before all of the energy has been thus dissipated.

5. In this case there must be recognized a short period 5, during which the slight charge remaining in the primary condenser is dissipated through the primary contacts, the spark is extinguished, and the residual energy transferred back to the primary winding.

6. The circuit then remains substantially dead during period 6 until the armature is rotated past the position of maximum flux and period 1 of the succeeding cycle begins.

It is the purpose of the present paper to discuss only the phenomena occurring during the very short period 2 between the separation of the primary contact points and the initiation of the spark at the secondary terminals. It is the phenomenon which occurs during this period which determines whether or not a voltage sufficient to break down the spark gap is attained, and consequently whether or not a spark is produced. The function of the magneto during this period is, of course, the same as that of an induction coil, and many of the equations discussed in the

Digitized by Google

present paper are directly applicable to such coils. The principal difference between the two types of device lies in the closer magnetic coupling between primary and secondary windings, the presence of greater amounts of unlaminated iron, and the rather higher frequencies of the oscillations involved in the case of the magneto.

3. HISTORICAL

The induction coil, having been widely used in electrical laboratories for many years, is the subject of a very extensive literature. Probably the first mathematical treatment of this device was due to Colley,[1] who assumed that the reaction of the secondary currents upon the primary was negligible, and on this basis worked out the primary and secondary currents and voltages for several cases.

A book by Armagnat[2] gives a very excellent discussion of the performance of induction coils and contains a bibliography of other work up to 1908. Since that time Taylor-Jones[3] has developed much more rigorously the mathematics of the induction coil, using what is referred to in this paper as the "double-coil model." He finds a very satisfactory agreement between the results of computations based upon this model and experimental results which he has obtained by the use of an electrostatic oscillograph.

Relatively little theoretical work had been done upon the high-tension magneto until the outbreak of the World War of 1914–1918 found the allied nations cut off from their principal supply of magnetos. The very excellent papers by Armagnat,[4] Young,[5] and Biffi[6] appeared in rapid succession, dealing with the general cycle of operations. The last of the three gives in considerable detail the mathematics of the double-coil model for an assumed case. Taylor-Jones[7] applied his induction coil equations to the magneto and by using in them constants obtained from the observed oscillations computed values of peak voltage agreeing within about 25 per cent with those directly observed. Campbell[8] at the National Physical Laboratory attempted to apply

[1] R. Colley, Wied. Ann., 44, p. 109; 1891.

[2] H. Armagnat, "The theory, design, and construction of induction coils." Trans. by O. A. Kenyon. McGraw-Hill Pub. Co.; 1908.

[3] E. Taylor-Jones, Phil. Mag., 23, p. 706, 1911; Phil. Mag., 27, p. 565, 1914; Phil. Mag., 29, p. 2, 1915; Phil. Mag., 30, p. 224, 1915; Electrician, 81, pp. 376-378, Aug. 30; pp. 396-397, Sept. 6; pp. 416-418, Sept. 13, 1918; Electrician, 82, p. 99, 1919; Electrician, 83, pp. 167-169, 201-202; 1919.

[4] H. Armagnat, Revue Electrique, 23, p. 321; 1915.

[5] A. P. Young, Automobile Engineer, 7, pp. 191, 237, 262, 298; 1917.

[6] E. Biffi, Elettrotecnica, 5, pp. 302, 326, 366, 407; 1918.

[7] E. Taylor-Jones, Phil. Mag, 36, p. 145; 1918.

[8] N. R. Campbell, Phil. Mag., 37, pp. 284, 372; 1919.

Digitized by Google

Taylor-Jones's equations to the magneto but found very considerable discrepancies which he attributed to the effect of eddy currents in the iron core. In connection with this work, however, he obtained, by means of a very elaborate point-by-point method, some actual plots of the wave form of the voltage induced in the magneto by the interruption of the primary current. These most remarkable experimental results are shown in Fig. 9, and will be referred to again later in this paper.

Bairsto[9] has treated at some length the case where the magneto secondary is shunted with a resistance. In this he uses a modification of the double-coil model which is, in effect, equivalent to the closed-coil model discussed in the paper, though developed from a different point of view.

The complexities in the electric circuits of the magneto which have led to the difficulties met by previous writers in expressing the phenomena in mathematical terms may be enumerated as follows:

1. The electrostatic capacity which exists in the secondary winding, both from one to another of the various layers of the winding, from the outer layer and leads to the frame of the machine, and to some extent from the edges of the intermediate layers to the frame, very materially affect the performance of the device. The last-mentioned component of the capacity causes the current at different parts of the secondary winding to be different in magnitude.

2. The varying magnetic permeability of the iron core at different flux densities has so far resisted all attempts at mathematical treatment, and the only practical way of handling the matter is to assume a certain average permeability or average inductance which corresponds to the particular range of magnetizing force to which the iron is subjected. Since there is always an air gap of considerable reluctance in the iron circuit, the iron never approaches the condition of saturation, and consequently the changes in permeability are not as great as would appear at first sight.

3. The changing reluctance of the magnetic circuit with changing position of the armature varies the effective inductance of the winding. This effect, however, is of little importance in a study of period 2, since the total motion of the armature in the very

[9] G. E. Bairsto, Journal (Brit.) I. E. E., 58, p. 507, June, 1920.

Digitized by Google

short interval comprising the period is so slight that the inductance can be considered a constant.

4. The rotation of both the primary and secondary winding in the magnetic field generates a certain emf not present in the induction coil and distinct from that produced by the interruption of the primary circuit, and this generated voltage also changes rather rapidly with the angular position of the armature. For a discussion of period 2, however, this voltage may be considered constant and usually of negligible magnitude.

5. The magnetic leakage between the primary and secondary windings introduces a very considerable complication into the circuit and is the principal reason for the use of the double-coil model. If this magnetic leakage could be neglected, then the simpler models discussed later in the paper would be strictly applicable.

6. The eddy currents set up in the iron core by the rapidly changing flux exert a considerable influence upon the electric phenomena, and the double-coil model discussed by previous writers contains no explicit provision for taking account of such effects. These eddy current effects are the more complex inasmuch as the frequencies of the oscillations involved are so high that the distribution of the eddy currents is subject to a skin effect analogous to that occurring in conductors carrying high-frequency currents, and the eddy currents can not be completely represented by any single tertiary circuit having fixed resistance and inductance.

7. Further complications are introduced in cases where it is desired to treat the effect of resistance in parallel with the secondary terminals, such as exists when the spark plug is fouled with carbon deposits.

In the present paper it is proposed to (1) review, for the sake of completeness, the double-coil model which has been treated by various writers and to point out in some detail the various transformations of energy which occur in it during period 2; (2) to develop a new type of model involving only a single coil and condenser. This model, of course, can not fit the performance of the actual magneto as closely as does the double-coil model, but its simplicity makes it of much greater usefulness and leads to a more easy visualization of the phenomena occurring throughout the complete cycle of operation; (3) still a third model, which may be called the closed-coil model, will be treated, which indi-

Digitized by Google

cates the effects to be expected from the eddy currents in the iron and which has been experimentally found to give a good approximation to the performance of the actual magneto. A variety of methods for determining the various constants which should be inserted in these three types of models will then be discussed in some detail, and some experiments indicating the extent to which these models represent the performance of the complete machine will be described.

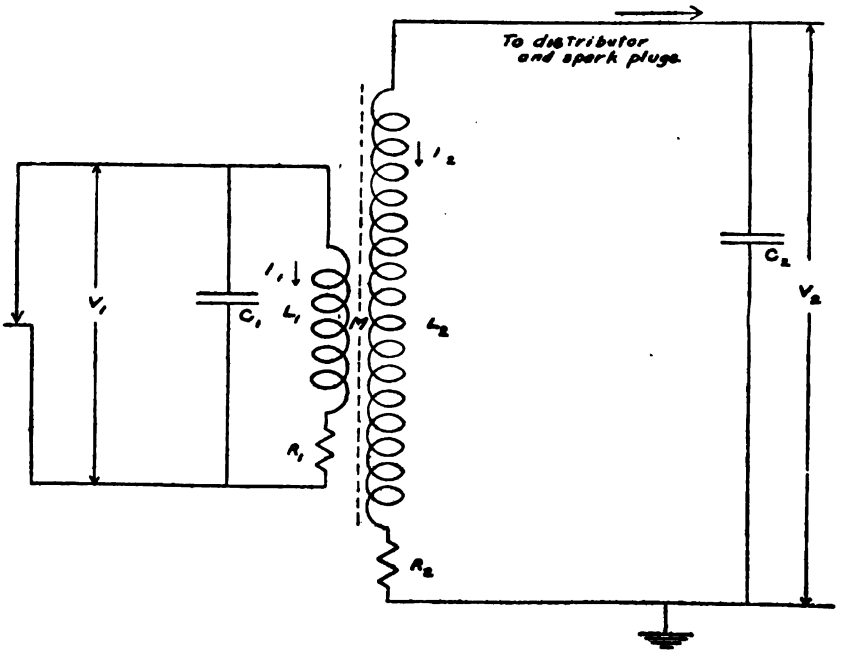

FIG. 1.—*Circuits of double-coil model as used in induction coils and in two-spark magnetos*

II. DOUBLE-COIL MODEL

1. EQUATIONS

The first and most complete type of model is that treated by previous writers on the subject and will be referred to as the double-coil model. The electric circuits may be represented in either of the two forms shown in Figs. 1 and 2. Of these, Fig. 1 corresponds to the type of circuits used in several battery ignition coils and also in so-called two-spark magnetos; i. e., magnetos intended for firing two spark plugs in the same cylinder. The second type of connection, Fig. 2, is used in certain battery systems and is widely used in magneto construction. While the equations

Digitized by Google

which result from these two types of model differ slightly in detail, the general physical phenomena which take place are the same, and most of the following discussion will be confined to the type of connection shown in Fig. 1.

In either model the coils are identified with the actual physical windings of the magneto, and consequently may be considered as having the values of self and mutual inductance possessed by the actual windings. The values of these quantities will, of course, depend upon the angular position of the armature within

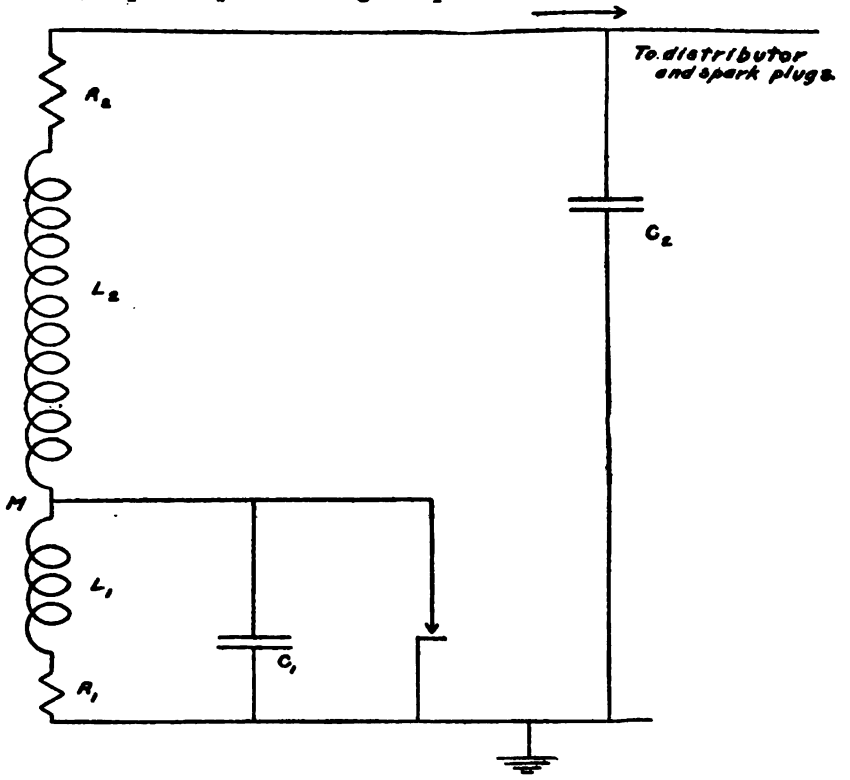

FIG. 2.—*Circuits of double-coil model as used in single-spark magnetos*

the pole pieces and upon the range of magnetizing force through which the iron is operated. It is usual to assign to the resistances R_1 and R_2 the actual resistance of the copper winding as obtained from direct-current measurements. It is possible to assign other and increased values of resistance for the purpose of representing to some degree of approximation the very greatly increased energy losses which result from the presence of eddy currents in the iron.

C_1 is identified with the capacity of the primary condenser, while C_2 represents the effect of the various secondary capacities

Digitized by Google

and is best defined as that capacity which, charged to the actual terminal voltage, will contain the same amount of energy as is actually stored in electrostatic form in the dielectric between the layers and around the terminals of the actual apparatus. In the case of a magneto by far the greater part of this capacity is actually at the terminals of the winding, and consequently the current has substantially the same value throughout the length of the secondary winding. In the case of an induction coil, where the terminal capacities are relatively smaller, this condition is not entirely fulfilled, and the current is greater at the center of the winding than at the ends. Under these conditions the mutual inductance of the secondary upon the primary is not equal to the converse effect of the primary on the secondary, and we must therefore distinguish the two coefficients of mutual induction $L_{2\,1}$ and $L_{1\,2}$. This distinction can be maintained throughout the mathematics as is done by E. Taylor-Jones,[10] but the net effect is merely to reduce the coefficient of coupling defined by

$$k^2 = \frac{L_{2\,1} L_{1\,2}}{L_2 L_1}$$

If we let i_1 and i_2 be the instantaneous currents in the primary and secondary circuits of Fig. 1, and v_1' and v_2' the corresponding instantaneous voltages at the terminals of the condensers, and also E_1 and E_2 be the emf's induced in the respective windings by the rotation of the armature, we have, applying Kirchhoff's laws to the two circuits:

$$L_1 \frac{di_1}{dt} + M \frac{di_2}{dt} + R_1 i_1 + v_1' = E_1 \tag{1}$$

$$L_2 \frac{di_2}{dt} + M \frac{di_1}{dt} + R_2 i_2 + v_2' = E_2 \tag{2}$$

We also have the relations:

$$i_1 = C_1 \frac{dv_1'}{dt} \tag{3}$$

$$i_2 = C_2 \frac{dv_2'}{dt} \tag{4}$$

[10] E. Taylor-Jones, Phil. Mag., 36, p. 145: 1918.

Digitized by Google

Combining these gives:

$$L_1C_1\frac{d^2v_1'}{dt^2}+MC_2\frac{d^2v_2'}{dt^2}+C_1R_1\frac{dv_1'}{dt}+v_1'=E_1 \tag{5}$$

$$L_2C_2\frac{d^2v_2'}{dt^2}+MC_1\frac{d^2v_1'}{dt^2}+C_2R_2\frac{dv_2'}{dt}+v_2'=E_2 \tag{6}$$

If we further let $v_1=v_1'-E_1$, and $v_2=v_2'-E_2$ and note that the rates of change of E_1 and E_2 are negligibly small compared with the exceedingly rapid rates of change of v_1 and v_2, we obtain: (7)

$$L_1C_1\frac{d^2v_1}{dt^2}+MC_2\frac{d^2v_2}{dt^2}+C_1R_1\frac{dv_1}{dt}+v_1=0 \tag{8}$$

$$L_2C_2\frac{d^2v_2}{dt^2}+MC_1\frac{d^2v_1}{dt^2}+C_2R_2\frac{dv_2}{dt}+v_2=0 \tag{9}$$

These two simultaneous differential equations may be combined to eliminate one of the variables and give the following final equation:

$$(L_1L_2-M^2)C_1C_2\frac{d^4v_2}{dt^4}+(L_1R_2+L_2R_1)C_1C_2\frac{d^3v_2}{dt^3}$$
$$+(R_1R_2C_1C_2+L_1C_1+L_2C_2)\frac{d^2v_2}{dt^2}+(R_1C_1+R_2C_2)\frac{dv_2}{dt}+v_2=0 \tag{10}$$

The corresponding equation for the type of circuit shown in Fig. 2 is

$$(L_1L_2-M^2)C_1C_2\frac{d^4v_2}{dt^4}+(L_1R_2+L_2R_1)C_1C_2\frac{d^3v_2}{dt^3}$$
$$+\{R_1R_2C_1C_2+L_1C_1+(L_2+2M+L_1)C_2\}\frac{d^2v_2}{dt^2} \tag{11}$$
$$+\{R_1C_1+(R_1+R_2)C_2\}\frac{dv_2}{dt}+v_2=0$$

These equations will be immediately recognized as the usual ones for coupled circuits so widely used in radiotelegraphy, and their application in this case differs from the more usual treatment only in the different initial condition which must be satisfied. These equations have been treated by numerous writers, among whom may be mentioned Drude,[11] Cohen,[12] and Pernot.[13] The author last named has contributed a very detailed discussion of the equations with much practical advice for their solution in numerical cases.

[11] P. Drude, Ann. Physik., 13, p. 512:: 1904.
[12] L. Cohen, Bull. Bureau of Standards, 5, p. 511:: 1909.
[13] F. E. Pernot, University of California Publications in Engineering, 1, p. 161:: 1916.

Digitized by Google

The general solution[14] for equation (10) is

$$v_2 = A_1 e^{m_1 t} + A_2 e^{m_2 t} + A_3 e^{m_3 t} + A_4 e^{m_4 t} \tag{12}$$

where m_1, m_2, m_3, m_4 are the roots of the biquadratic equation:

$$m^4 + \frac{L_1R_2 + L_2R_1}{L_1L_2 - M^2} m^3 + \frac{R_1R_2 + \frac{L_1}{C_2} + \frac{L_2}{C_1}}{L_1L_2 - M^2} m^2 + \frac{\frac{R_1}{C_2} + \frac{R_2}{C_1}}{L_1L_2 - M^2} m + \frac{1}{(L_1L_2 - M^2)C_1C_2} = 0 \tag{13}$$

Since all the coefficients in this equation are essentially positive, it may be shown from the theory of equations that (except for limiting cases) only three types of solution arise: (*a*) All the roots are real and negative; (*b*) two roots are real and negative, while the other two are complex quantities; (*c*) all the roots are complex and form two conjugate pairs. In cases (*b*) and (*c*) the real part of the complex roots is zero or negative. Most cases of actual magneto circuits come under case (*c*), and for this case the results are more conveniently expressed in the form

$$v_2 = e^{\alpha_1 t}(A_1 \sin \beta_1 t + B_1 \cos \beta_1 t) + e^{\alpha_2 t}(A_2 \sin \beta_2 t + B_2 \cos \beta_2 t) \tag{14}$$

where A_1, A_2, B_1, and B_2 are constants of integration, and $\alpha_1 \pm j\beta_1$ and $\alpha_2 \pm j\beta_2$ are the roots of equation (13). The equations for v_1, i_1, and i_2 are in the same form but with different integration constants.

Equation (14) shows that v_2 is the sum of two oscillations of frequency,

$$f_1 = \frac{\beta_1}{2\pi} \text{ and } f_2 = \frac{\beta_2}{2\pi}$$

The resulting variation of voltage and current with time is shown in Figs. 3, 5, and 7, and Curve I of Fig. 31 for typical cases. If the damping is negligible, the two frequencies are given by—

$$f^2 = \left(\frac{1}{2\pi}\right)^2 \frac{L_1C_1 + L_2C_2 \pm \sqrt{(L_1C_1 + L_2C_2)^2 - 4(L_1L_2 - M^2)C_1C_2}}{2(L_1L_2 - M^2)\,C_1C_2} \tag{15}$$

It may be seen on expanding the numerator by the binominal theorem that as the closeness of coupling is increased, f_2, corresponding to the negative root, remains approximately constant, while the other frequency, f_1, becomes larger and larger, varying roughly in proportion to $\frac{1}{L_1L_2 - M^2}$, and the corresponding term

[14] See Murray, 'Differential Equations,' p. 64, 2d ed.

Digitized by Google

in equation (14) decreases in amplitude roughly in proportion to the increase in frequency. Figs. 4, 6, and 8 show for three typical sets of values the corresponding pulsations in the energy stored in various forms in the several parts of the circuit.

2. NUMERICAL EXAMPLES

Case I corresponds to an induction coil or a very loosely coupled magneto in which the quantity k^2 has the value 0.60. The resultant curves of current and voltage show very markedly the

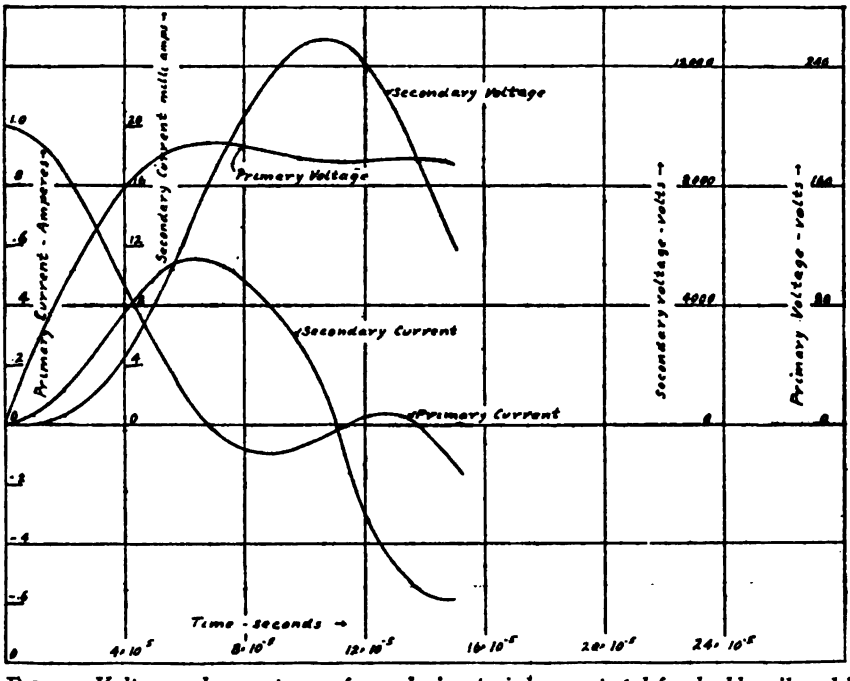

FIG. 3.—*Voltage and current wave forms during period 2 computed for double-coil model (Case I) having* R_1=0.5 Ω, L_1=0.015 *h*, C_1=0.2 *μf*, R_2=2500 Ω, L_2=36 *h*, C_2=50×10^{-6} *μf*, k^2=0.60

two oscillations which are present in such cases. It may be noted that the time $t = 11\times10^{-5}$ seconds, at which the secondary voltage V_2 is a maximum, corresponds to a time when the primary voltage V_1 is a minimum, and Fig. 4 shows that the magnetic energy—i. e., the difference between total energy and total static energy—is very small at this instant. Consequently, conditions are very favorable for the production of a high secondary voltage, and a relatively large part of the total energy supplied is available for charging the secondary condenser and producing across its terminals a high voltage.

Digitized by Google

In contrast to this we may consider Case II, which corresponds to the same circuits except that the mutual inductance between them has been increased so as to make the quantity k^2 equal 0.80. Even such an arrangement is still decidedly more loosely coupled than are the circuits in the average magneto. As shown in Fig. 5, the change in coupling has somewhat shifted the relative phase of the two oscillations, so that the maximum of the secondary volt-

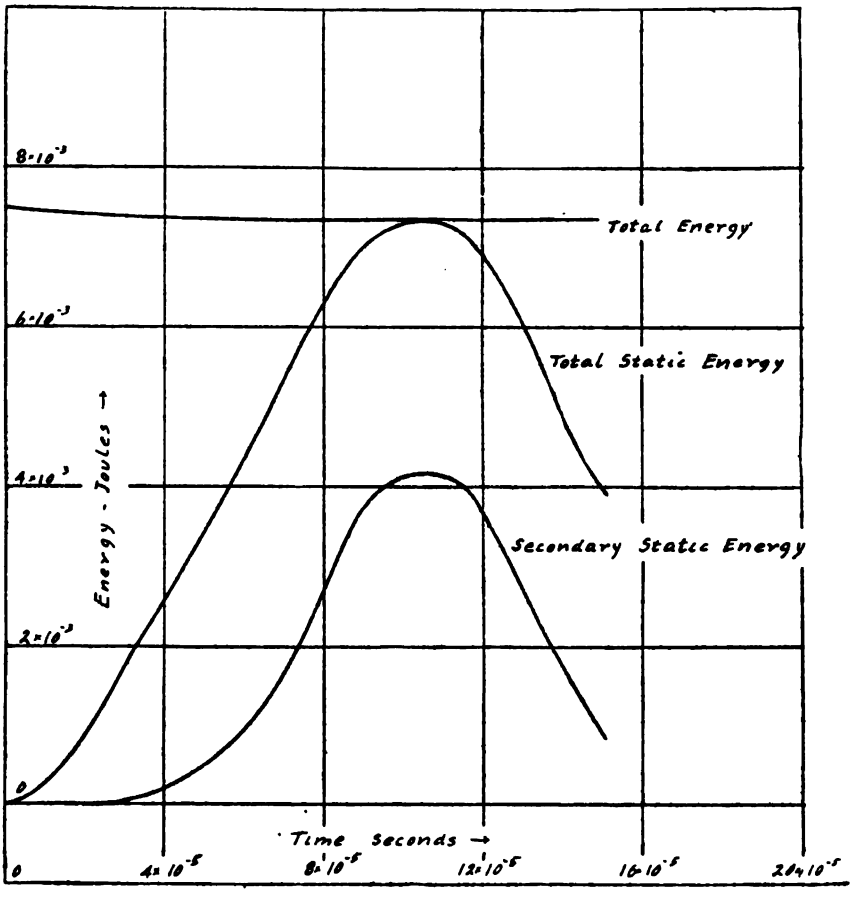

FIG. 4.—*Changes of energy with time. Double-coil model, Case I*

age no longer corresponds to a minimum of the primary voltage, and therefore at the time when the secondary voltage is a maximum ($t = 8 \times 10^{-6}$ seconds) there is a very considerable quantity of energy stored in the magnetic circuit and later in the cycle ($t = 11 \times 10^{-6}$ seconds) when this energy has been transferred to the primary condenser, some of the secondary energy has also returned to the primary, and consequently there is less available for charg-

Digitized by Google

ing the secondary condenser. It is this type of variation in the relative time at which the component oscillations have their maximum value which gives rise to the curious changes in maximum voltage shown by the curves obtained by Taylor-Jones. The curves of Figs. 3 and 5 also bring out the fact that the higher frequency component has a larger relative amplitude in the current waves than in the voltage waves. In both of these models the resistance has been taken to correspond with the actual resistance of the copper windings, and consequently the loss

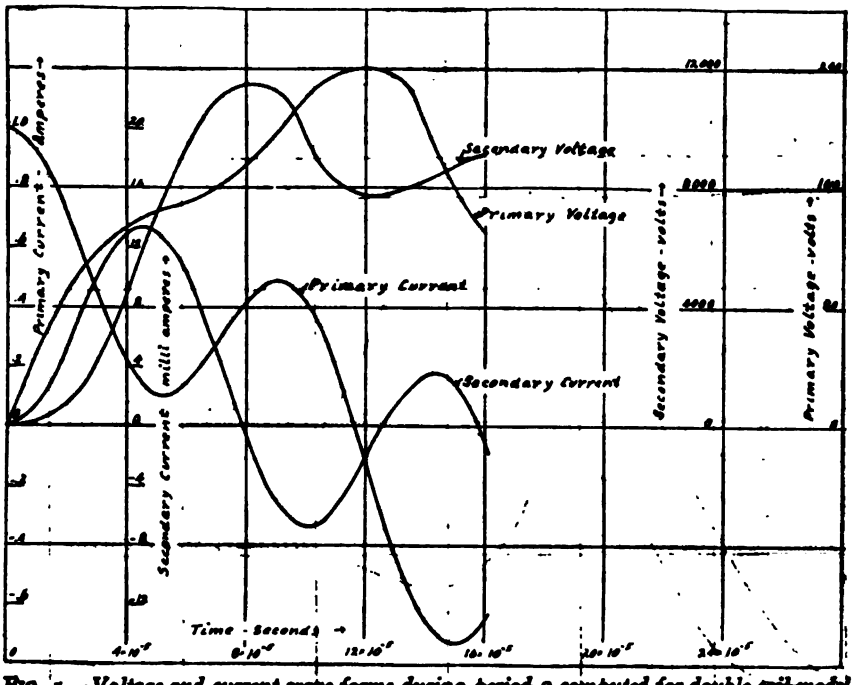

FIG. 5.—*Voltage and current wave forms during period computed for double-coil model (Case II). This case is the same as Case I except that* $k^2=0.80$

of energy as shown by the total energy curves, Figs. 4 and 6, is practically negligible, and the entire energy oscillates between the three storage regions; i. e., the coil, the primary condenser, and the secondary condenser.

Case III corresponds to the same system of circuits arranged with still closer coupling, so that $k^2=0.92$. This value is typical of many magnetos. Furthermore, the resistances of both windings have been arbitrarily increased to 50 times the value of the copper resistance in order to represent as well as possible the effect of the iron losses. It will be seen that the principal effect of the

Digitized by Google

increased closeness of coupling has been to greatly increase the frequency of the shorter period component and to materially reduce its amplitude, so that in the voltage wave it is hardly noticeable. The increase in resistance causes a rapid damping of the vibrations, and this damping is much greater for the higher frequency component, so that by the time $t = 10 \times 10^{-6}$ seconds, at which the secondary voltage has approached its maximum, the higher frequency component is practically negligible. The curves of total energy, Fig. 8, show that even with the increased damping

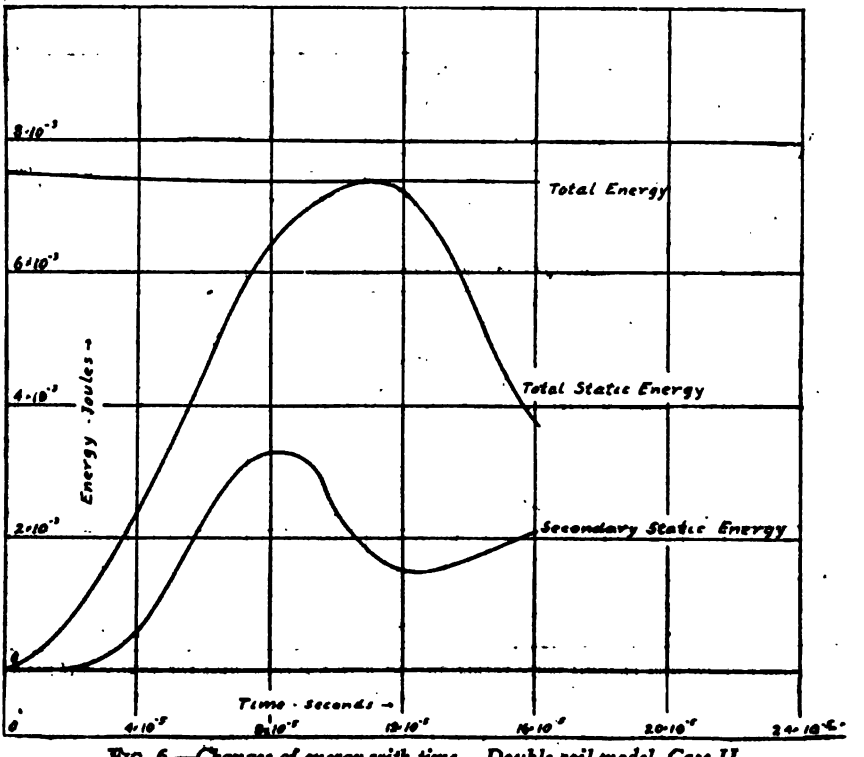

FIG. 6.—*Changes of energy with time. Double-coil model, Case II*

which results from the increased resistance the energy loss is still rather small, though it has become appreciable at the end of a complete cycle of the main wave. It is also to be noted that the primary voltage has substantially the same wave shape and is substantially in phase with the secondary voltage, and that the distribution of energy between the two at their maximum depends upon the relative capacities and turns in the windings. A comparison between Fig. 7 and Fig. 9 shows that the model for Case III, with the assumed increased resistance, roughly corresponds

Digitized by Google

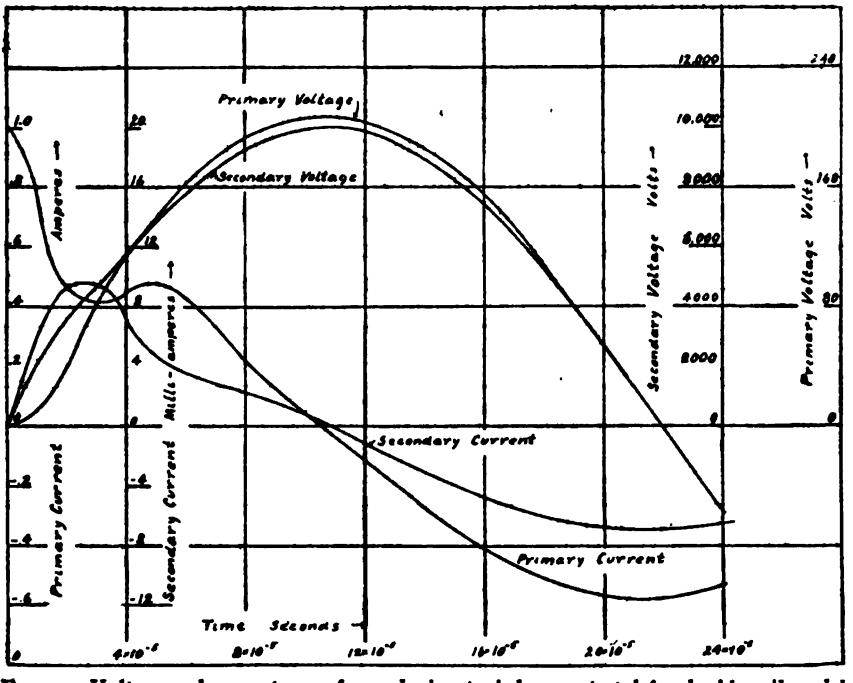

FIG. 7.—*Voltage and current wave forms during period 2 computed for double-coil model (Case III) having* $R_1=25\ \Omega$, $L_1=0.015\ h$, $C_1=0.2\ \mu f$, $R_2=125\ 000\ \Omega$, $L_2=36$, $C_2=50\times10^{-6}\ \mu f$, $k^2=0.92$

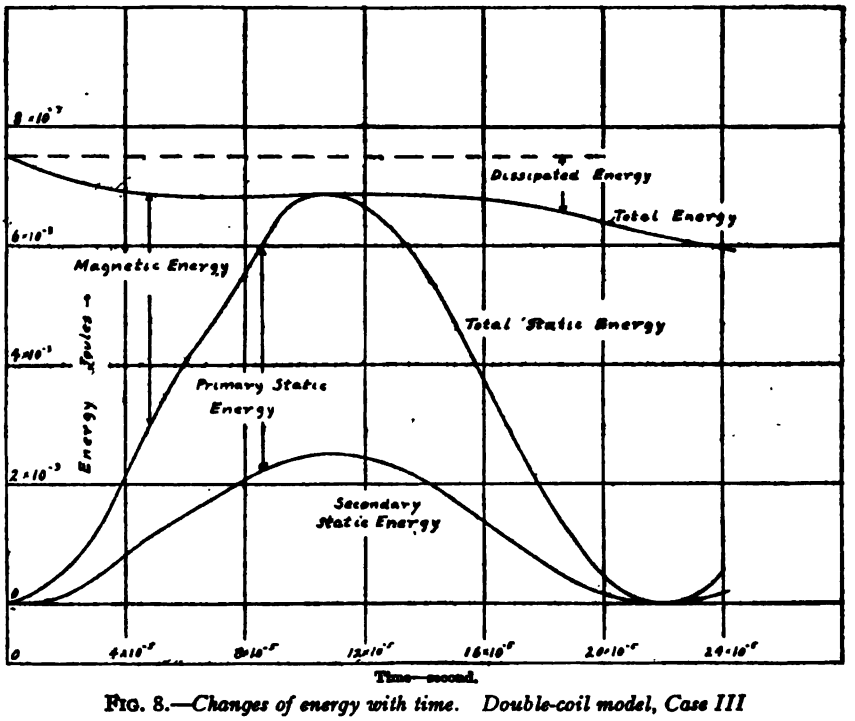

FIG. 8.—*Changes of energy with time. Double-coil model, Case III*

Digitized by Google

to the actual wave form as observed by Campbell, although the damping of the higher frequency ripple is slightly less and that of the lower frequency wave is much greater in his case.

The advantages of the double-coil model which has just been discussed are principally that it shows the effect of loose coupling between the primary and secondary. It indicates the two vibration frequencies which are present and permits the computation of their values. It is also possible with this model to take account of the fact that the current is not uniform throughout the length

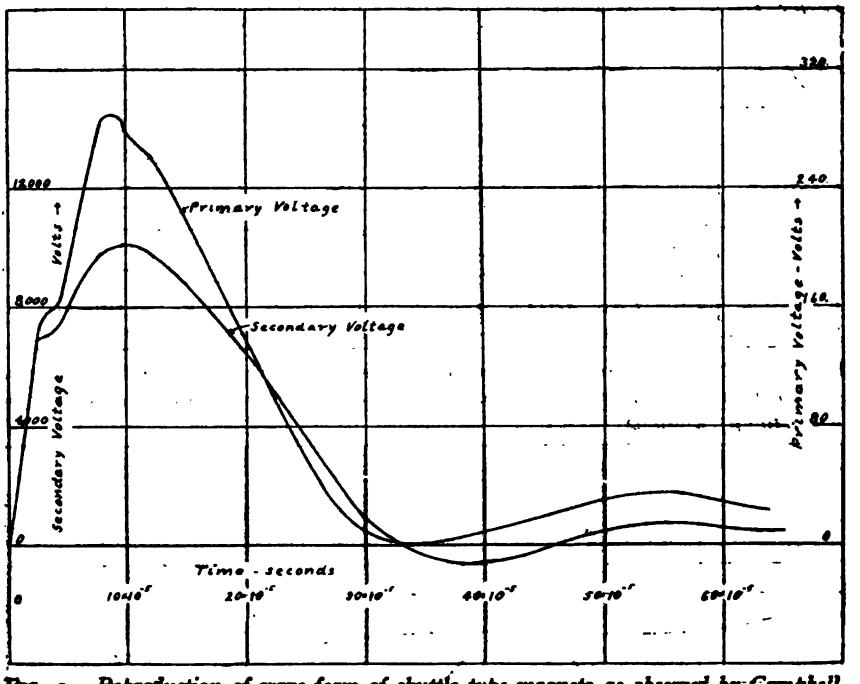

FIG. 9.—*Reproduction of wave form of shuttle type magneto as observed by Campbell.*
(From British Advisory Committee for Aeronautics Report, I. C. E. 241)

of the secondary winding. It is also possible with this double-coil model to handle cases in which a resistance R_4 exists in parallel with the secondary terminals, as would be the case with a fouled spark plug. The equations for this circuit, with the connections as in Fig. 2, are

$$L_1C_1\frac{d^2v_1'}{dt^2}+(L_1+M)\,C_2\frac{d^2v_2'}{dt^2}+R_1C_1\frac{dv_1'}{dt}+\left(\frac{L_1+M}{R_4}+R_1C_2\right)\frac{dv_2'}{dt}+\frac{R_1}{R_4}v_2'+v_1'=E_1 \tag{16}$$

Digitized by Google

$$\text{and } (L_2+M)\,C_2\frac{d^2v_2'}{dt^2}+MC_1\frac{d^2v_1'}{dt^2}+\left(\frac{L_2+M}{R_4}+R_2C_2\right)\frac{dv_2'}{dt}+\left(\frac{R_2}{R_4}+1\right)v_2'-v_1'=E_2 \tag{17}$$

The great disadvantage of this double-coil model is the excessive labor of the mathematical computations which are required in any

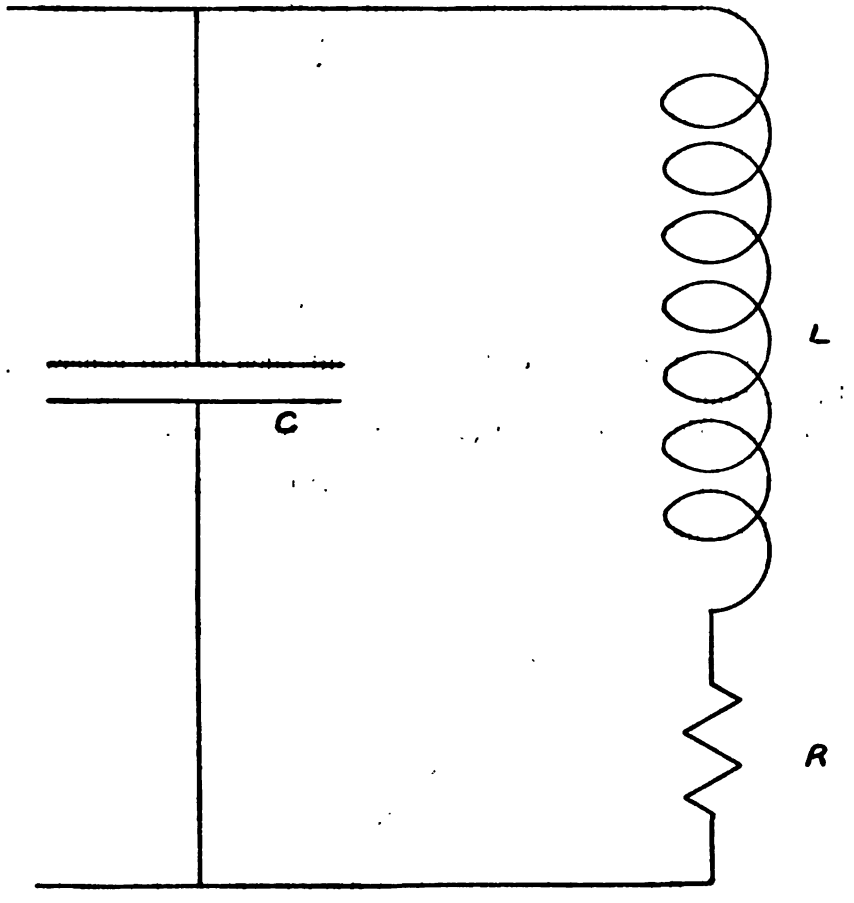

FIG. 10.—*Single-coil model circuit*

use of it, these being so great as to prohibit its frequent use in design problems. It also does not allow for the iron loss in the magnetic circuit except as the resistances may be arbitrarily increased, as was done in Case III above. There is little justification for an increase by the same factor in primary and secondary, although this is probably the most reasonable assumption to make.

Digitized by Google

III. SINGLE-COIL MODEL

As a contrast to the complex double-coil model which has just been discussed we may next consider the properties of the very simple circuit shown in Fig. 10, which may be called a single-coil model. If the coil in such a circuit is supplied with current from an external circuit which is suddenly interrupted at $t=0$, the current will at the start flow into the condenser, charging it to a continuously increasing voltage until finally the entire energy of the system is stored electrostatically in the condenser. After this the current will reverse and the circuit will oscillate in a manner analogous to either of the two circuits which constitute the double-coil model.

1. EQUATIONS OF MODEL

The differential equation for this simple type of circuit is

$$LC\frac{d^2v}{dt^2}+RC\frac{dv}{dt}+v-E=0 \tag{20}$$

where E is any constant emf in the circuit, such as that generated by rotation.

The solution of equation (20) to meet the initial conditions of condenser voltage equal to E and condenser current $C\frac{dv}{dt}$ equal to I_0 at the instant $t=o$ is:

$$v=\frac{I_0}{C(\alpha_1-\alpha_2)}(e^{\alpha_1 t}-e^{\alpha_2 t})+E \tag{21}$$

or

$$v=\frac{I_0}{\beta C}e^{\alpha t}\sin\beta t+E \tag{22}$$

where

$$\left.\begin{aligned} &I_0=\text{current at break} && \alpha_1=-b+\sqrt{b^2-d^2}\\ &b=\frac{R}{2L}=-\alpha && \alpha_2=-b-\sqrt{b^2-d^2}\\ &d=\frac{1}{\sqrt{LC}} && \beta=\sqrt{d^2-b^2}\end{aligned}\right\} \tag{23}$$

Equation (21) applies to cases where $b^2>d^2$ and equation (22) to the more usual cases where $b^2<d^2$. The maximum value attained by the voltage in the former case is

$$V_m=\frac{-I_0}{C\alpha_2}y^{\frac{y}{1-y}}+E \tag{24}$$

where

$$y=\frac{\alpha_1}{\alpha_2}$$

Digitized by Google

or if the damping is so very great that d is negligible compared to b, equation (21) reduces to

$$v = \frac{I_0 L}{RC}\left(e^{-\frac{t}{CR}} - e^{-\frac{Rt}{L}}\right) + E \tag{25}$$

and eq (24) becomes in the limit when $\frac{R^2C}{L}$ approaches ∞

$$V_m = \frac{I_0 L}{RC} + E \tag{26}$$

Similarly, in the oscillatory case ($b^2 < d^2$), the maximum voltage is

$$V_m = \frac{I_0}{dC} e^{\frac{a}{\beta}\tan^{-1}\frac{\beta}{a}} + E \tag{27}$$

If the damping is very small, equations (22) and (27) reduce to

$$v = I_0\sqrt{\frac{L}{C}}e^{-\frac{Rt}{2L}} \sin\frac{t}{\sqrt{LC}} + E \tag{28}$$

and

$$V_m = I_0\sqrt{\frac{L}{C}} + E \tag{29}$$

The variation of voltage with time indicated by equation (22) has, of course, the damped sine wave form such as those plotted in Figs. 13, 14, and Curve II of Fig. 31, and it will be noted that these figures are similar to Fig. 7, except that the higher frequency ripple is absent. It is, therefore, apparent that by suitable choice of inductance, resistance, and capacity the simple model would give in its essential features the same performance as the more complicated circuits.

It will be noted that in equations (24), (26), (27), and (29) the maximum voltage attained, V_m, appears explicitly as proportional to I_0 the current at break, if the constant term E is neglected, and it is also evident that a similar proportionality exists in the other types of model. (See, for example, equation 67.) The ratio $\frac{V_m}{I_0}$ is consequently a convenient quantity for expressing the performance of the model. Since this quantity has the physical dimensions of an impedance, it will be termed the "impulsive impedance" of the system and denoted by Z in the following discussion.

Digitized by Google

2. DERIVATION OF SINGLE-COIL MODEL FROM ACTUAL CIRCUIT

The use of this single-coil model is closely analogous to the use of the "equivalent T circuit" which is so generally and usefully applied to alternating current problems in connection with transformer design and telephone circuits. The relation between the single-coil model and the double-coil model is perhaps best brought out by considering the series of steps by which one can pass physically from one to the other. For the connection shown in Fig. 1 one may imagine the space to the right of the dotted line replaced by an imaginary region in which the various electrical quantities are indicated by "primed" letters which are related to the actually existing electrical constants by the relations

$$R_2' = \frac{R_2}{p^2},\ L_2' = \frac{L_2}{p^2},\ C_2' = p^2 C_2,\ I_2' = p i_2,\ v_2' = \frac{v_2}{p},\ E_2' = \frac{E_2}{p}, \qquad (30)$$

where p is any constant factor. In this fictitious space all the fundamental electromagnetic laws will still apply. For example,

$$i_2' = \frac{v_2'}{R_2'} \text{ (Ohm's Law)}$$

$$E_2' = -L_2' \frac{di_2'}{dt}, \text{ etc.}$$

Furthermore, if the new secondary space is coupled to the original primary circuit by a value of mutual inductance given by

$$M' = \frac{M}{p} \qquad (31)$$

the reaction of any electromagnetic phenomenon on the right upon the circuits on the left will be the same as in the original space. If the ratio p is arbitrarily chosen as equal to the ratio of secondary to primary turns, the above procedure becomes what is called in electrical engineering "referring to the primary side" and applies not only to the constants of the particular transforming device, whether it be transformer, magneto, or induction coil, but also to the constants of any other apparatus connected beyond its terminals. Thus, if V_s (= 5000 volts) is the actual breakdown voltage of a spark gap connected to the secondary, and if $p = 50$, then

$$V_s' = \frac{V_s}{p} = 100 \text{ volts}$$

is the breakdown voltage of the spark gap referred to the primary side.

Digitized by Google

This step has been purely arbitrary and mathematical, but we must now introduce the physical assumption that the primary and secondary coils are closely coupled, so that $M^2 = L_1 L_2$ or $k = 1$. If we choose $p = \frac{M}{L_1} = \frac{L_2}{M}$ then

$$L_2' = M' = L_1, \tag{32}$$

and we may then make the next step and replace the two closely coupled coils by a single coil of inductance $L = L_1 = M' = L_2'$. The only physical phenomena affected by this last change are those involving the insulation between the coils and are of no concern

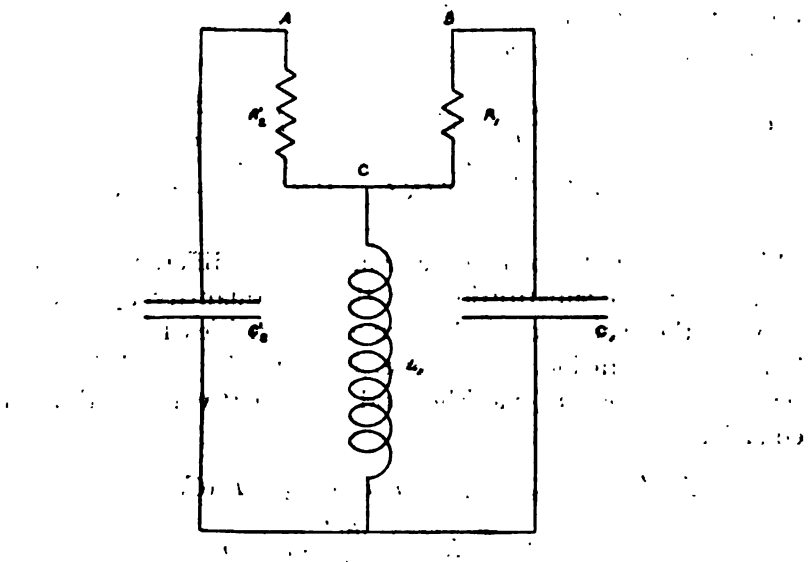

FIG. 11.—*Circuit intermediate between double-coil and single-coil models*

in the problem at hand. The result of the steps previously discussed gives a circuit shown in Fig. 11. If in any such network a current is established in the inductance coil L and left to itself, it will flow through the resistances R_1 and R_2', charging condensers C_1 and C_2'. If the relation

$$R_1 C_1 = R_2' C_2' = R_2 C_2 \tag{33}$$

holds, then the potentials of points A and B will rise together and be equal at all times like the galvanometer terminals of a Wheatstone Bridge, so that conditions will not be in any way changed if a connection is made between A and B. With such a connec-

Digitized by Google

tion in place, the circuits then become identical with those shown in Fig. 10 where $C = C_1 + C_2'$ and

$$R = \frac{R_1 R_2'}{R_1 + R_2'} \tag{34}$$

In any case the voltage established between C and either A or B is small compared to the voltage across the condenser or the coil, and the performance of the circuit shown in Fig. 11 is but little affected in case the relation (33) is not exactly fulfilled.

The justification of the single-coil model from a more mathematical point of view can be based upon equation (10) by inserting the primed quantities as defined by equation (30).

This substitution gives

$$C_1C_2'(L_1L_2' - M'^2)\frac{d^4v_2'}{dt^4} + C_1C_2'(L_2'R_1 + L_1R_2')\frac{d^3v_2'}{dt^3} + (R_1R_2'C_1C_2' + L_1C_1 + L_2'C_2')\frac{d^2v_2'}{dt^2} + (R_1C_1 + R_2'C_2')\frac{dv_2'}{dt} + v_2' = 0 \tag{35}$$

This shows that no modification of the differential equation results from the substitution and that the quantity v_2' is affected only as the insertion of the primed quantities has affected the limits of integration. As above, if $k = 1$, $(L_1 L_2' = M'^2)$ the first term of equation (35) vanishes and we are left with the third order equation

$$L_1C_1C_2'(R_1 + R_2')\frac{d^3v_2'}{dt^3} + \{R_1R_2'C_1C_2' + L_1(C_1 + C_2')\}\frac{d^2v_2'}{dt^2} + (R_1C_1 + R_2'C_2')\frac{dv_2'}{dt} + v_2' = 0 \tag{36}$$

Introducing the further physical assumption that

$$R_1C_1 = R_2C_2 = R_2'C_2' \tag{33}$$

we obtain

$$L_1R_1C_1(C_1 + C_2')\frac{d^3v_2'}{dt^3} + \{R_1^2C_1^2 + L_1(C_1 + C_2')\}\frac{d^2v_2'}{dt^2} + 2R_1C_1\frac{dv_2'}{dt} + v_2' = 0 \tag{37}$$

which can be factored, giving

$$\left(R_1C_1\frac{d}{dt} + 1\right)\left\{L_1(C_1 + C_2')\frac{d^2}{dt^2} + R_1C_1\frac{d}{dt} + 1\right\}v_2' = 0 \tag{38}$$

Digitized by Google

A complete solution of this is

$$v_2 = Ae^{-R_1C_1t} + Be^{\alpha t} \sin(\beta t + \theta) \qquad (39)$$
$$= X + Y$$

where A, B, and θ are constants of integration, and α and β are given by eq. (23) above, if we put

$$R = \frac{R_1R_2'}{R_1 + R_2'} \text{ and } C = C_1 + C_2' \qquad (40)$$

Solution X represents currents flowing from one condenser into the other without magnetizing the coil (L does not enter), while Y is the same solution as that for the single-coil model. If both condensers are initially uncharged and there is an initial current I_0 in the coil, then the constant A of equation (39) becomes zero, and consequently the single-coil model gives a complete solution.

A similar line of reasoning on either the physical or mathematical basis may be applied to the type of connection shown in Fig. 2 and leads in a similar way to the single-coil model.

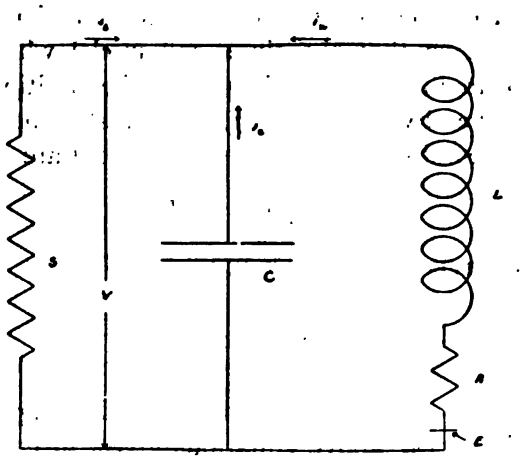

FIG. 12.—*Single-coil model with shunting resistance*

3. SINGLE-COIL MODEL WITH SHUNTING RESISTANCE

The case in which the secondary terminals are shunted by a resistance can be very readily handled by this type of model by using the substitution suggested by Mizuno.[15]

The circuit for such a case is shown in Fig. 12, and by Kirchhoff's laws we have, taking v as positive when the upper condenser plate is charged positively,

[15] F. Mizuno, Phil. Mag., 45, p. 447; 1898.

Digitized by Google

$$i_w + i_s + i_c = 0 \tag{41}$$

$$v = -i_w R - L\frac{di_w}{dt} + E \tag{42}$$

$$i_c = -C\frac{dv}{dt} \tag{43}$$

$$i_s = -\frac{v}{S} \tag{44}$$

which may be combined to give

$$\frac{d^2v}{dt^2} + \left(\frac{R}{L} + \frac{1}{SC}\right)\frac{dv}{dt} + \left(\frac{1}{LC} + \frac{R}{LSC}\right)v - \frac{E}{LC} = 0 \tag{45}$$

or

$$L_1'C'\frac{d^2v}{dt^2} + R'C'\frac{dv}{dt} + v - E' = 0 \tag{46}$$

where

$$L' = L,\ R' = R + \frac{L}{SC},\ C' = C\frac{S}{R+S},\ E' = E\frac{S}{R+S} \tag{47}$$

It will be seen that equation (46) is identical in form with equation (20) above, so that the single-coil model when shunted is equivalent to an unshunted coil having the fictitious resistance and capacity given by equation (47). It must be noted, however, that the initial conditions of the shunted model are at $t = 0$.

$$i_w = I_0 \text{ and } v = E \tag{48}$$

and are not the relations

$$C'\frac{dv}{dt} = I_0 \text{ and } v = E' \tag{49}$$

which would be obtained by strictly following through the analogy. Solving the above equations gives, in case the circuit is overdamped,

$$v = \frac{I_0}{C(\alpha_1' - \alpha_2')}\left(e^{\alpha_1' t} - e^{\alpha_2' t}\right) + E'\left[\frac{S}{R+S} + \left(\frac{1}{SC} + \frac{R\alpha_1'}{R+S}\right)\frac{e^{\alpha_1' t}}{\alpha_1' - \alpha_2'} - \left(\frac{1}{SC} + \frac{R\alpha_2'}{R+S}\right)\frac{e^{\alpha_1' t}}{\alpha_1' - \alpha_2'}\right] \tag{50}$$

or, if E is negligible,

$$v = \frac{I_0}{C(\alpha_1' - \alpha_2')}\left(e^{\alpha_1' t} - e^{\alpha_2' t}\right) \tag{51}$$

Digitized by Google

where α_1' and α_2' are obtained from L', R', and C' by equations (23). It is interesting to note that when S is so small as to produce very heavy overdamping, and make d^2 entirely negligible compared with b^2, we have the simple relation

$$V_m = I_0 S \tag{52}$$

This relation, of course, might have been obtained directly from the physical consideration that the coil will tend to send its full current I_0 through the shunting resistance S and will consequently establish across the terminals of the condenser a voltage equal to the IR drop $= I_0 S$. In most ignition circuits which are so heavily fouled as to cause misfiring this condition is quite closely approached, and a knowledge of the shunting resistance S and the sparking voltage of the gap referred to the primary side immediately gives, by comparison with the primary current at break I_0, an indication whether or not a spark will be obtained.

In case the shunting resistance is not so low as to produce excessive damping and if E is negligible, the solution of equation (46) is

$$v = \frac{I_0}{C\beta'} e^{\alpha' t} \sin \beta' t \tag{53}$$

where, as before, α' and β' are obtained from R', L', and C' by equation (23).

4. NUMERICAL EXAMPLES

From equations (21), (22), (51), and (53) above there may be computed, as shown by Figs. 13, 14, and 15, the variations of voltage, current, and of energy with time under various conditions. Case I corresponds to a circuit having $L = 0.015$ henry, $C = 0.32$ microfarad, $R = 16.8$ ohms. This circuit is that which would be obtained from that considered as Case III of the double-coil model on referring all the constants to the primary side. Case II (Fig. 13) corresponds to the same circuit when it is shunted with an additional capacity of 100 $\mu\mu f$ on the secondary side or 0.24 microfarad on the primary side. Such a shunting might well be produced by the addition of leads in a metal tube from the magneto terminal to the spark plug, or by a reasonable increase of primary condenser, such as might be thought necessary to reduce sparking at the break. It is seen that the addition of this capacity increases the period of oscillation and the time interval between the breaking of the primary current and the attainment of maximum voltage. It also produces a considerable reduction in the magnitude of the maximum which is obtained.

Digitized by Google

Cases III and IV correspond to the same circuit treated in Case I, but shunted in Case III by a resistance of 500 000 ohms on the secondary and in Case IV by 100 000 ohms on the secondary. The latter shunting is sufficient to make the oscillations aperiodic. Fig. 14 shows the very marked decrease in maximum voltage which results from the presence of the shunting resistance and Fig. 15, which shows the fluctuations in energy for Cases I, III, and IV, indicates the character of the energy transformations which take place.

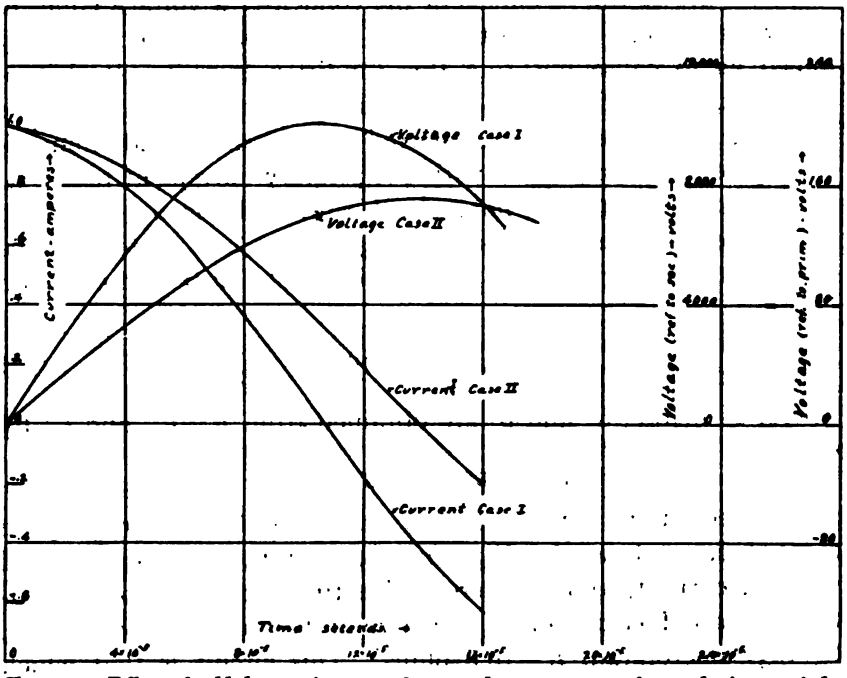

FIG. 13.—*Effect of added capacity on voltage and current wave forms during period 2 computed for single-coil model*

Case I has $L=0.015\ h$, $C=0.32\ \mu f$, $R=16.8\ \Omega$, $n=49$. Case II is for the same model with 100 micro-microfarads additional capacity in parallel with the secondary

In Case I the electrostatic energy in the condenser rises to a maximum at $t=11\times10^{-6}$ seconds, at which time all of the energy then present exists in the condenser. The drop in total energy from the initial value of 7.5×10^{-3} joules results from the dissipation of energy in the resistance. In Case III, however, we have at time $t=8\times10^{-6}$ seconds a maximum storage of energy in the condenser and a maximum voltage across its terminals. At this time the total energy has, as a result of the dissipation of energy in the shunting resistance, fallen to 4×10^{-3} joules, and

Digitized by Google

the remaining 2×10^{-3} joules are still stored as magnetic energy in the coil and are maintained in that form by the current flowing through the coil and the shunting resistance. At the later instant $t = 17 \times 10^{-6}$ seconds the current in the coil is passing through zero, but the entire energy supply has been so much depleted that at this time there is less in the condenser than at the earlier instant. Still later in the cycle the current builds up in the reverse direction and receives some of the slender store of energy which is still flowing out of the condenser. The storage

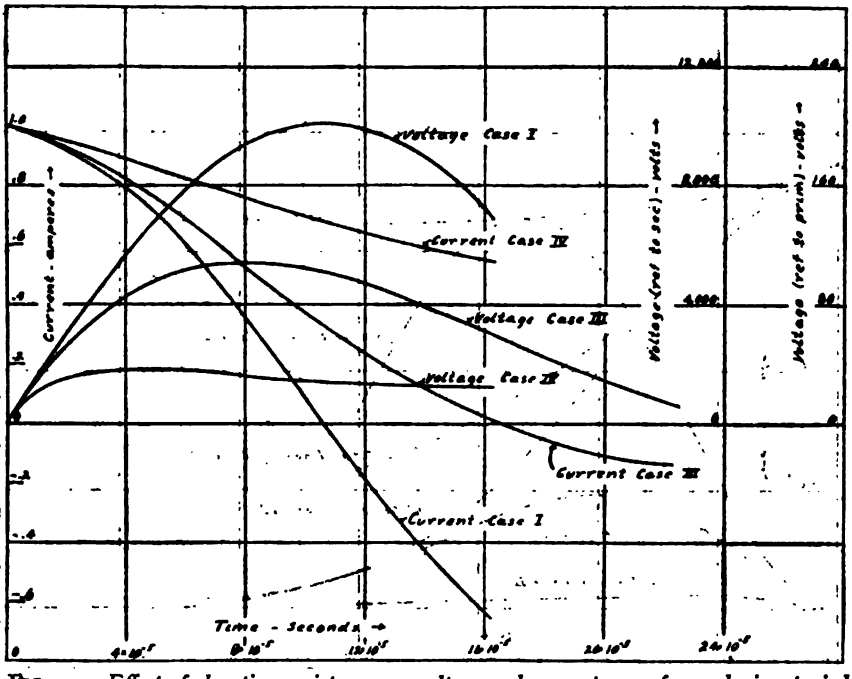

FIG. 14.—*Effect of shunting resistance on voltage and current wave forms during period 2 computed for single-coil model. Case I has $L = 0.015$ h, $C = 0.32 \mu f$, $R = 16.8\ \Omega$, $n = 49$. Case III has in addition a shunting resistance of 500 000 Ω on the secondary (equivalent to 208 Ω when referred to the primary). Case IV has a shunting resistance of 100 000 Ω on the secondary (equivalent to 41.7 Ω when referred to the primary)*

of magnetic energy in the coil by the current through the shunting resistance is closely analogous with the effect which will be discussed later of the storage of energy by the eddy currents in the core of the magneto at the instant when the currents in the windings are zero. This similarity also brings out the possibility of expressing the eddy current loss in terms of an equivalent shunting resistance and using Fig. 12 as a type of model to express these eddy current effects. It is probable, however, that in most quantitative work the alternative circuit shown in Fig. 10

Digitized by Google

with an increased value of R will be found more useful, and for a precise study of these effects the more complex "closed-coil model," to be discussed below, must be resorted to.

In most cases it is only the maximum voltage of the first oscillation which is of importance and which is given by equations (24), (26), (27), and (29), and the effect of such quantities as capacity and shunting resistance on the voltage may be represented directly by curves such as those given in Figs. 32 and 33 below, in which these physical values are compared with experi-

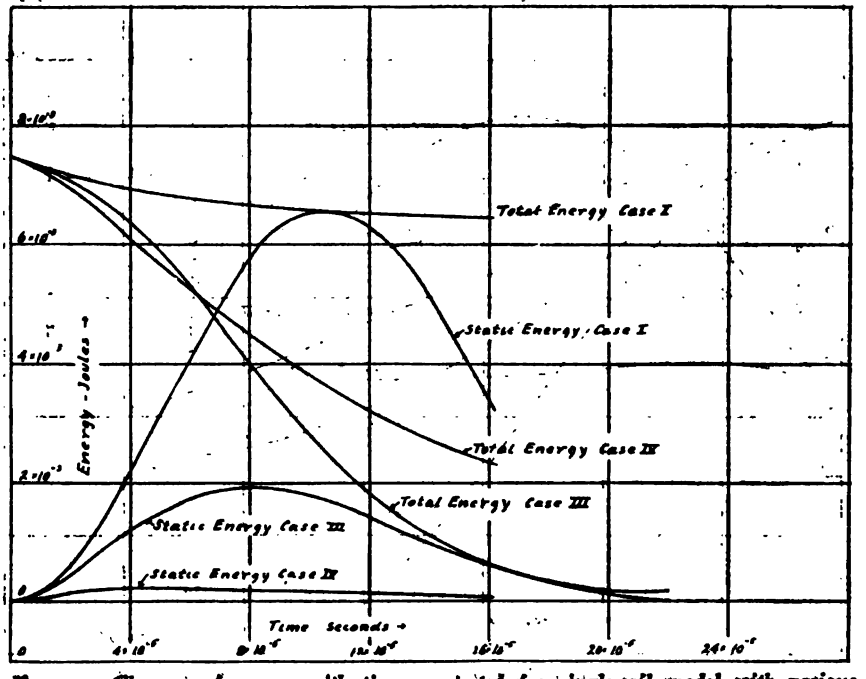

FIG. 15.—*Changes of energy with time computed for single-coil model with various shunting resistances*

mental results. The general characteristics of Fig. 32 are, of course, determined by the fact that the initial amount of energy, $\frac{1}{2} L I_0^2$, is later in the cycle stored with relatively little loss in the condenser C, and the resulting voltage may be computed from the relation

$$\frac{1}{2} L I_0^2 = \frac{1}{2} C V_m^2 \text{ or } V_m = I_0 \sqrt{\frac{L}{C}} \qquad (54)$$

The general characteristics of the curve shown in Fig. 33 are that for very high values of the shunting resistance the maximum voltage approaches a constant value given by the preceding

Digitized by Google

relation, while with very low values of the shunting resistance the simple linear relation of equation 52 applies. The dotted line shows the relation of impulsive impedance to shunting resistance on this basis.

5. APPLICATION OF SINGLE-COIL MODEL TO COMPLETE CYCLE

The relatively great simplicity of the single-coil model as compared with either the double-coil model or the closed-coil model which is discussed below renders it quite suitable for computation, and it has the further advantage of lending itself with very slight extension to a qualitative indication of the complete cycle of

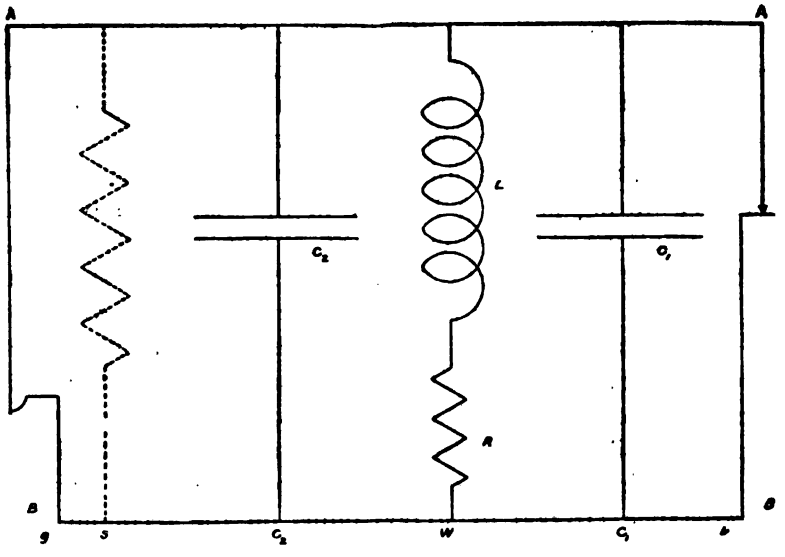

FIG. 16.—*Single-coil model extended to indicate complete cycle of operation of magneto*

operation of the magneto. Fig. 16 shows the single-coil model as thus extended by the addition of components corresponding to the primary circuit breaker and the spark gap and with its total capacity again divided into the components C_1 and C_2, of which it was originally composed.

It is seen that this model consists approximately at least of two perfect conductors or junction points A–A and B–B between which are or may be connected five circuits in parallel. At the beginning of the cycle of operation, during what may be called period 1, we have contact breaker b closed and circuits w and b of importance in the phenomenon. During this period the rotation of the armature between the magnet poles generates a

Digitized by Google

current in the circuit thus formed, which, at the instant of break, has attained a value, I_o. At the instant of break conditions are abruptly changed by the elimination of circuit *b* from the system and we then have, as has been discussed above, the coil *w*, charging the two condensers C_1 and C_2 in parallel at an initial rate I_o. This continues until at some short time later the voltage across the condenser C_2 and across the spark gap *g* has risen to a value equal to the breakdown voltage of the gap. In most cases this occurs before the current I_o has decreased very greatly and before more than a small percentage of the total magnetic energy has been stored in the two condensers. When the spark gap *g* becomes conducting, which occurs with great rapidity, we have for the very short period 3 the discharge of the two condensers through the spark gap, so that the circuit *g* in series with the combination of C_2 and C_1 in parallel only need be considered. Actually the leakage reactance of the winding, though, as explained above, nearly negligible during period 2, is of fundamental importance during period 3 because of the very high frequency of the oscillations of the circuit $g\,C_2\,C_1$. Consequently, we may expect that only condenser C_2 will be discharged at first through spark gap *g*, and that the discharge of condenser C_1 will follow at an appreciably later time after it has established the magnetic field required by the leakage flux of the winding. At the end of this entire period 3, which is of extremely short duration, we are left with the coil *w* in series with spark gap *g*, which is now broken down and which may be considered as replaced by a relatively high resistance (10 000 to 40 000 ohms on the secondary or 4 to 16 ohms referred to the primary) through which the coil can discharge. This discharge takes place during what may be called period 4 and continues usually until the entire store of energy is dissipated.

This interval of relatively long duration (0.001 to 0.008 second) is what is recorded by an oscillograph connected in series with the spark gap. If the entire supply of energy is dissipated before the contact *b* is closed, there is no further action until period 1 of the next cycle begins. If, however, the cam is so short or the magneto speed so high that the circuit breaker *b* closes before the exhaustion of the energy supply, we then have circuit *b* of relatively low resistance in parallel with circuit *g* of high resistance, both being fed by the coil *w*. The result is that most of the current flows through circuit *b* and, owing to the curious volt-ampere character-

Digitized by Google

istic of spark gaps, according to which their resistance increases rapidly as the current flow through them decreases, the entire current is actually diverted from circuit *g* to circuit *b* and the spark is extinguished with great suddenness. Furthermore the condensers which had previously been charged to the relatively low voltage (say, 1200 on secondary or 24 referred to primary) which was required to maintain the current through the spark gap now discharge themselves rapidly and probably in an oscillatory manner through circuit *b* during a short interval which may be called period 5. After the cessation of this condenser discharge the coil may still continue to send considerable current through circuit *b* during what may be called period 6 until the energy supply is finally exhausted. It will be found that this conception of a single-coil model as drawn in Fig. 16 is of great utility in analyzing the results of oscillograph tests of magnetos and indicates the reasons for the quantitative relations between corresponding changes in primary and secondary currents resulting from the opening and closing of the breaker or fluctuations in circuit resistance. It is obvious that the addition of a sixth circuit, *s*, containing resistance, as indicated by the dotted lines, serves to take account of the presence of shunting resistance across the spark plug points.

IV. CLOSED-COIL MODEL

1. EQUATIONS

The two models previously discussed can account for the energy losses in the iron of the magnetic circuit only by the device of increasing the resistance of one or both coils by some arbitrary amount. This is theoretically unsatisfactory, since it essentially implies that the energy loss is proportional to the square of the current flowing in the winding, which in general may not be correct. The iron loss consists of a certain amount of hysteresis loss, together with the dissipation of energy which results from eddy currents induced in the conducting iron core as a result of the rapid rate of change of flux. In the normal operation of the magneto the magnetic change which occurs during period 2 consists of a sudden decrease of the magnetic flux, and the energy which is lost as a consequence of this process can be estimated from the departure of the actual flux-magnetomotive force curve of the magnetic circuit from the ideal straight line which would

Digitized by Google

correspond to a circuit having no such loss. Measurements of the entire hysteresis loss for circuits of this type[16] indicate that the total amount of hysteresis loss is small relative to the energy stored in the circuit, and consequently may be neglected without introducing serious error. The larger portion of the iron loss is due to eddy currents, and consequently their effect upon the operation of the device may, to a first approximation, be represented by the presence of a closed tertiary winding which is coupled inductively to the actual physical winding of the core and which possesses certain resistance and inductance as well as a

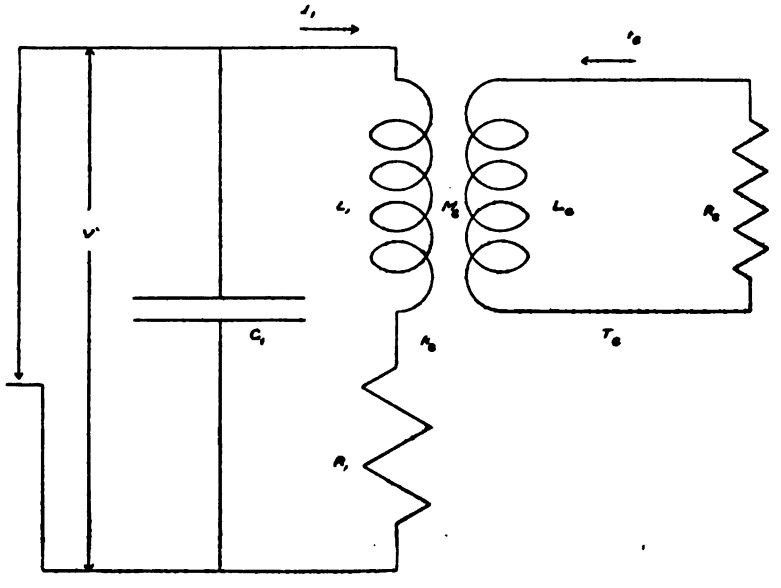

FIG. 17.—*Circuits of closed-coil model of magneto*

certain mutual inductance to the winding. The addition of such a tertiary circuit to the double-coil model would lead to an aggregation of circuits which would be too complex for useful application, and it is more valuable to add the closed tertiary circuit to the single-coil model just discussed, thus obtaining a circuit shown in Fig. 17, which will be called the "closed-coil model." A little consideration will show that the performance of the external winding will not be affected if, in place of any particular assumed tertiary circuit, an alternative circuit is substituted in which

$$L_e' = p^2 L_e, \quad M_e' = pM_e, \quad R_e' = p^2 R_e. \tag{55}$$

[16] A. P. P. Report No. 20, Nat. Advisory Comm. for Aero. Report No. 58:: 1919.

Digitized by Google

It consequently appears that the measurements and effects in the actual winding depend only upon two constants of the tertiary coil and not upon the three constants L_e, R_e, M_e, as would appear at first sight. For these two constants the most convenient ones to use are the coefficient of coupling k_e, defined as

$$k_e = \sqrt{\frac{M_e^2}{L_1 L_e}} \tag{56}$$

and the time constant T_e of the circuit defined as

$$T_e = \frac{L_e}{R_e} \tag{57}$$

Applying Kirchhoff's laws to the circuit shown in Fig. 17 gives

$$L_e \frac{di_e}{dt} + R_e i_e + M_e \frac{di_1}{dt} = o \tag{58}$$

$$L_1 C_1 \frac{d^2 v}{dt^2} + M_e \frac{di_e}{dt} + R_1 C_1 \frac{dv}{dt} + v = E_1 \tag{59}$$

which may be combined with eqs. (56) and (57) to give

$$T_e(1 - k_e^2) L_1 C_1 \frac{d^2 v}{dt^2} + \left(1 + \frac{R_1 T_e}{L_1}\right) L_1 C_1 \frac{d^2 v}{dt^2} + \left(1 + \frac{T_e}{R_1 C_1}\right) R_1 C_1 \frac{dv}{dt} + v - E_1 = o \tag{60}$$

E_1 may usually be neglected, or if its derivatives are negligible it may be eliminated by a change of variable, as was done in equation (7) above. On either basis the solution of equation (60) depends upon that of the corresponding auxiliary equation.

$$T_e(1 - k_e^2) L_1 C_1 m^3 + \left(1 + \frac{R_1 T_e}{L_1}\right) L_1 C_1 m^2 + \left(1 + \frac{T_e}{R_1 C_1}\right) R_1 C_1 m + 1 = o \tag{61}$$

The initial conditions are $v = E_1$, $i_1 = I_o$ and $i_e = o$ at $t = o$, and two cases arise, depending on whether the three roots of (61), m_1, m_2, and m_3 are all real and negative, or whether m_1 is real and negative, while m_2 and m_3 form a pair of conjugate complex quantities, so that

$$m_2 = \alpha + j\beta; \quad m_3 = \alpha - j\beta \tag{62}$$

Digitized by Google

In the former case the solution of (60) is

$$v = A_1 e^{m_1 t} + A_2 e^{m_2 t} + A_3 e^{m_3 t} \tag{63}$$

where

$$\left.\begin{aligned} A_1 &= \frac{\left(m_2 + m_3 + \frac{R_1}{(1-k_c^2)L_1}\right) I_0}{(m_1 - m_2)(m_3 - m_1) C_1} \\ A_2 &= \frac{\left(m_3 + m_1 + \frac{R_1}{(1-k_c^2)L_1}\right) I_0}{(m_2 - m_3)(m_1 - m_2) C_1} \\ A_3 &= \frac{\left(m_1 + m_2 + \frac{R_1}{(1-k_c^2)L_1}\right) I_0}{(m_3 - m_1)(m_2 - m_3) C_1} \end{aligned}\right\} \tag{64}$$

In case two of the roots (say m_1 and m_2) are nearly equal the corresponding A's become very large and equations (63) and (64) become inconvenient. If we set $m_2 = m_1 + \delta$ (65)

equation (63) becomes (assuming $\frac{R_1}{(1-k_c^2)L_1}$ to be negligible)

$$v = A_3(e^{m_3 t} - e^{m_1 t}) + \delta A_2 t e^{m_1 t} \quad \text{. . . . approx.} \tag{66}$$

if δt is small compared to 1.

When m_2 and m_3 are complex, the solution can be put in the form

$$v = I_0\left[\frac{e^{\alpha t}}{C_1\beta}\sqrt{\frac{(\alpha+m_1+A)^2+\beta^2}{(\alpha-m_1)^2+\beta^2}}\sin(\beta t - \varphi) - \frac{2\alpha+A}{C_1\{(\alpha-m_1)^2+\beta^2\}}e^{m_1 t}\right] \tag{67}$$

where α and β are defined by equation (62) and

$$A = \frac{R_1}{L_1(1-k_c^2)} \tag{68}$$

$$\varphi = \tan^{-1}\frac{\beta(A+2\alpha)}{\alpha^2 - m_1^2 - \beta^2 + A(\alpha - m_1)} \tag{69}$$

In the practical use of the closed-coil model it is seldom necessary to carry out a direct solution of the cubic equation (61), as it is usually easier to obtain one root m_1 by successive approximations. The root m_1 has the value $-\frac{1}{T_c}$ for large values of T_c and the value $\frac{1}{T_c(1-k_c^2)}$ for small values of T_c, so that an assumed value between these limits gives a good first approximation. Equation (61) may be transposed to give

$$\frac{1}{T_c} = -\left(m - \frac{k_c^2 L_1 C_1 m^3}{L_1 C_1 m^3 + R_1 C_1 m + 1}\right) \tag{70}$$

Digitized by Google

and several assumed values of m_1 can be substituted in the right-hand member and the corresponding value of T_e computed. An auxiliary graph can then be drawn with T_e as ordinate against m_1 as abscissa, and the precise value of m_1 corresponding to the original value of T_e is then read off. The cubic equation can then be depressed by dividing through by the expression $(m-m_1)$ and the resulting quadratic be easily solved by the usual methods.

It is impracticable to obtain an explicit expression for the maximum voltage of the impulse defined by equations (66) or (67), as

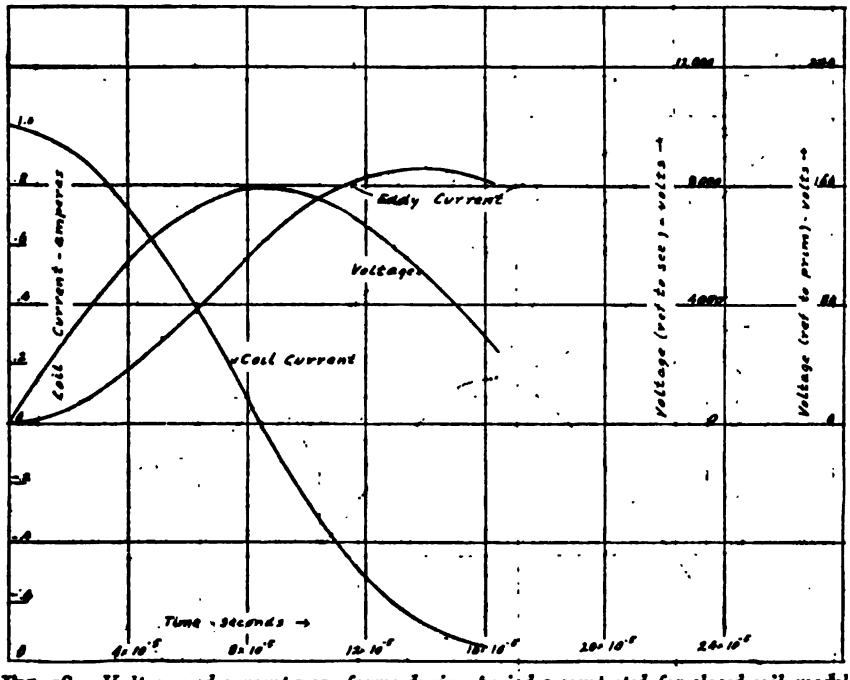

FIG. 18.—*Voltage and current wave forms during period 2 computed for closed-coil model having* $R_1=0.33\,\Omega$, $L_1=0.015$ *h*, $C_1=0.325\,\mu f$, $k_0^2=0.5$, $T_e=1.80\times10^{-4}$ *sec.*

was done in the case of the single-coil model. In a given numerical case the voltage may be computed for several values of t near the crest of the impulse and the maximum value read from an auxiliary graph of V versus t. A value of

$$t=\frac{\frac{\pi}{2}+\varphi}{\beta} \tag{71}$$

is a convenient first approximation, but is always slightly too large.

Digitized by Google

2. NUMERICAL EXAMPLE

Fig. 18 and Curve III of Fig. 31 show the general character of the variation of voltage and current in the various circuits with time and Fig. 19 the corresponding energy changes. It will be noted that the term involving e^{mt} (shown dotted in Fig. 31) in effect shifts the zero line with respect to which the damped oscil-

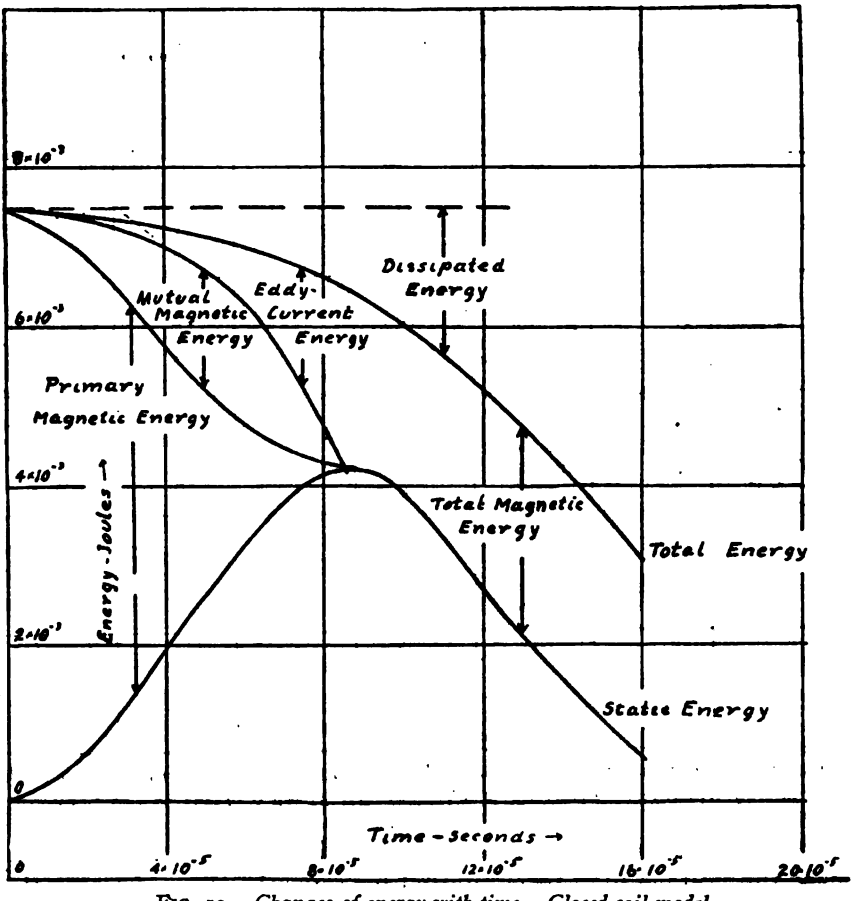

FIG. 19.—*Changes of energy with time. Closed-coil model*

lation represented by the second term occurs and gives a corresponding increase to the first positive maximum voltage and a slightly less decrease to the amplitude of the first negative maximum. This tendency is very clearly shown in the experimental curves obtained by Campbell, Fig. 9, and can not be produced by either the single or double coil models directly.

Digitized by Google

It will be noticed that in case the quantity T_0 is very large relative to $\sqrt{L_1C_1}$ that the equation (61) may be factored to give

$$\left(m+\frac{1}{T_0}\right)\left\{(1-k_0^2)L_1C_1m^2+\left(R_1C_1+\frac{k_0^2L_1C_1}{T_0}\right)m+1\right\}=0 \quad (72)$$

The difference between the approximate equation (72) and the correct equation (61) is a term $k^2_0\frac{L_1C_1}{T_0}m$, which becomes negligible in comparison with $T_0\,m$ for large values of T_0.

Similarly, if T_0 is very small, the approximate equation

$$\left(m+\frac{1}{T_0(1-k_0^2)}\right)\{L_1C_1m^2+(R_1C_1+k_0^2T_0)m+1\}=0 \quad (73)$$

may be used. The difference between equations (73) and (61) consists of the term $-k^2_0\{T_0R_1C_1+T^2_0(1-k^2_0)\}m^2$, which becomes negligible in comparison with $L_1C_1m^2$ for sufficiently small values of T_0.

The terms in the final solution corresponding to the first factor in equations (72) and (73) are negligible for the respective ranges of T_0 for which the equations apply, so the resulting solutions in these two extreme cases are in the same form as those given by the single-coil model. It is therefore evident that the substitution of proper values of L and R in the latter model will give the same results as the more complicated equation (67) above for either extreme case. It so happens, however, that in a typical shuttle armature magneto experimented with the observed values of T_0 were of the same order of magnitude as $\sqrt{L_1C_1}$, and consequently the simplified equations were not applicable.

The decrease in the coefficient of m^2 in equation (72) as compared with the analogous term in equation (73) or equation (20) can be roughly explained physically if we assume that the coupling between the tertiary coil and the main coil is direct and amounts to shunting a fraction $\frac{1}{k_0}$ of the total winding by a resistance R_0. If the time constant T_0 is made very large and consequently R_0 made very small, the net effect is to short circuit $\frac{1}{k_0}$ of the winding, leaving only a fraction of the original inductance remaining.

Fig. 20 shows the values of the real root m_1 in equation (61) for various values of T_0, and k^2_0 in a model having $L_1=0.015$ h, $R_1=0.33$ ohm, $C_1=0.325$ μf, curves being drawn for values of $k^2_0=0.1$,

Digitized by Google

0.5, 0.9, and 0.95. It may be shown that all the roots of equation (61) will be real only if k^2_e is greater than 0.889.[17]

It is seen by Fig. 20 that for such values of k^2_e, the curves of m_1 against T_e have the double bend characteristic of the cubic equation, and the three real values of m correspond to intersections of this curve with an ordinate at the proper value of T_e. The principal effect of increasing T_e at any value of k_e is to decrease the maximum voltage from the value that it has with no eddy current present to a reduced value which becomes constant for

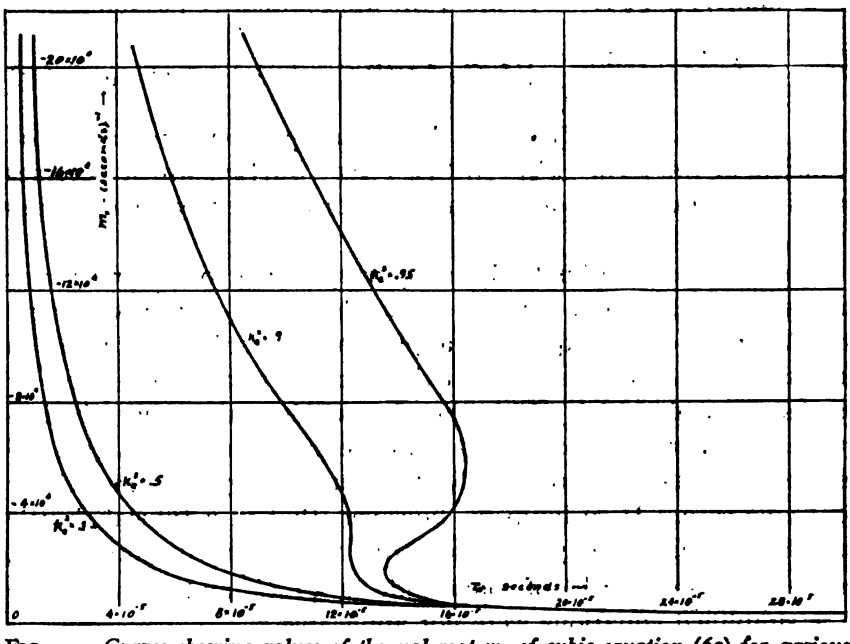

FIG. 20.—*Curves showing values of the real root m_1 of cubic equation (62) for various values of T_e and k_e^2 for circuits having R_1=0.33 Ω, L_1=0.015 h, C_1=0.325 μf*

large values of T_e. This is shown in Fig. 21, in which the crest voltage computed for a particular double-coil model (R = 0.33 ohm, L = 0.015h, C = 0.325μf) is plotted against T_e for various values of k^2_e. The lower curves indicate the contribution to this total crest voltage of the term involving $e^{m_1 t}$ of equation (67), and hence the displacement of the axis about which the oscillation corresponding to the second term takes place. It will be noted that this effect is relatively small unless k^2_e is nearly unity and T_e is greater than the limiting value at which all three roots of equa-

[17] For a discussion of the frequencies and damping coefficients in this type of closed-coil model see Iolo-Jones, Phil. Mag., 39, p. 553, May, 1920.

Digitized by Google

tion (61) are real. For smaller values of T_e the e^{mpt} term is negligibly small.

In general T_e will be proportional to the conductivity of the material, and hence will be decreased by the use of thinner laminations. It is indicated by the curve that no material change in the secondary voltage is to be expected unless the decrease in lamination thickness serves to make the value of T_e less than the value of $2\sqrt{L_1C_1}$.

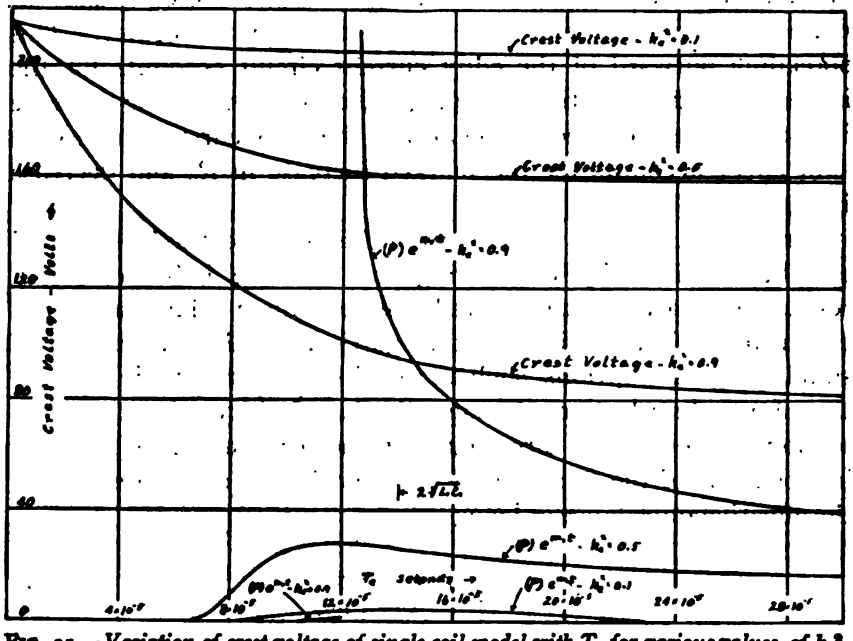

FIG. 21.—*Variation of crest voltage of single-coil model with T_e for various values of k_e^2. The lower curves show the contribution to the crest voltage of the last term* (P) e^{mpt} *of Eq. 67*

3. CORRELATION WITH SKIN EFFECT IN IRON CORE

All of the above conclusions have been based on the assumption of a single eddy current circuit of fixed constants. It is possible, however, by the alternating current bridge described below to determine what constants the equivalent tertiary coil must have in order to account for the observed resistance and inductance of the main winding at any particular frequency at which the bridge measurements are made. The results of such measurements are shown in Fig. 29, which shows the variation of T_e and k^2_e, respectively, with the frequency used in the measurements. The two sets of curves correspond to magnetos which are identical except that

Digitized by Google

in one the pole pieces are laminated, while in the other they are solid iron castings. It will be noted that the variation of T_e with frequency is very marked and that the quantity ωT_e is more nearly constant, although it increases with increase in frequency.

These variations of the tertiary coil constants with frequency are, of course, the result of the magnetic skin effect in the laminations and indicate that at higher frequencies the magnetic flux does not have time to penetrate throughout the thickness of the lamination, but that the flux density and also the eddy current density are greater near the surface than in the center. This spreading outward of the eddy current circuit accounts for the increase in the effective coupling k_e, and the resulting increase in the resistance offered to the flow of the eddy current due to the skin effect accounts for the marked increase in R_e and decrease in T_e.

A rough estimate of the amount of this skin effect to be expected can be obtained by considering the effective inductance and resistance of a uniformly wound coil containing a laminated iron core which has a relative short air gap. By making a number of simplifying assumptions, such as the absence of magnetic leakage, a uniform distribution of magnetic flux density over the cross section of the core on direct current and a permeability which is independent of the flux density we may deduce an expression for the effective impedance as being

$$Z = R + j\omega L_1 \left(\frac{h + \mu g}{sh + \mu g} \right) \tag{74}$$

where R = resistance of coil to direct current.

L_1 = inductance of coil to direct current.

μ = permeability.

s = ratio of the flux density at the surface of the iron to the mean flux density throughout the cross section. This is, in general, a complex quantity.

h = length of iron core.

g = length of air gap.

The distribution of eddy currents in an iron lamination has been worked out[18] and the relation connecting the flux density B_1 at the surface of the lamination, which is also equal to what would be produced throughout the material at zero frequency, with

[18] C. P. Steinmetz, Transient Electrical Phenomena and Oscillations, p. 365, 3d ed.

Digitized by Google

the mean flux density B_m throughout the thickness, which actually exists at the given frequency, is found to be

$$s = \frac{B_1}{B_m} = (1+j)\, cl_0 \frac{\cosh c\, l_0 \cos c\, l_0 - j \sinh c\, l_0 \sin c\, l_0}{\sinh c\, l_0 \cos c\, l_0 - j \cosh c\, l_0 \sin c\, l_0} \qquad (75)$$

where $c = \sqrt{4\pi^2 \frac{\mu}{\rho} f}$, ρ = resistivity, μ = permeability, f = frequency. (All in c g s units.)

For large values of cl_0, this reduces to

$$s = (1+j)\, cl_0 \qquad (76)$$

Inserting this value of s in the equation (74) above leads to the relations

$$\left.\begin{aligned} Z &= R + j\omega L_1 \left(\frac{1 + \frac{\mu g}{h}}{(1+j) cl_0 + \frac{\mu g}{h}} \right) \\ \text{or} \\ Z &= R + j\omega L_1 \frac{1+x}{(1+j) cl_0 + x} \end{aligned}\right\} \qquad (77)$$

if we let

$$x = \frac{\mu g}{h} \qquad (78)$$

Now, it may be shown that if alternating current of frequency f is passed through the primary of the closed coil model (Fig. 17) the apparent impedance of the coil is

$$Z = R_1 + \frac{\omega^2 k_e^2 T_e L_1}{(1+\omega^2 T_e^2)} + j\omega L_1 \left(\frac{1 + \omega^2 T_e^2 (1 - k_e^2)}{1 + \omega^2 T_e^2} \right) \qquad (79)$$

equating the two expressions (77) and (79) for the apparent impedance gives

$$k_e^2 = \frac{cl_0 (1 + \omega^2 T_e^2)}{\omega T_e (cl_0 \omega T_e + cl_0 + x)} \qquad (80)$$

and

$$T_e = \frac{-(cl_0 + x)(1 - cl_0) + c^2 l_0^2}{\omega cl_0 (1+x)} \qquad (81)$$

as being the values of k_e and T_e to be expected for coils containing such a laminated iron core.

The results of equations (80) and (81) are plotted in Fig. 22, the scale of frequency being chosen to correspond to a value of $\frac{cl_0}{\sqrt{f}}$ equal 0.1, which, in turn, is a reasonable assumption in case

Digitized by Google

the iron has a permeability $\mu = 1000$ and a resistivity $\rho = 1000$. These curves are plotted for values of x (the ratio of air gap reluctance divided by iron reluctance) of 2, 5, and 10, respectively. It will be noted that the curves connecting ωT_0 with frequency run approximately parallel with those observed for one of the magnetos tested, and that an agreement could be obtained by a suitable choice of the factor x. The agreement between the curves connecting k_0^2 with frequency is not so good, and it is possible that a decidedly different value of $\frac{cl_0}{\sqrt{f}}$ would give a better agreement.

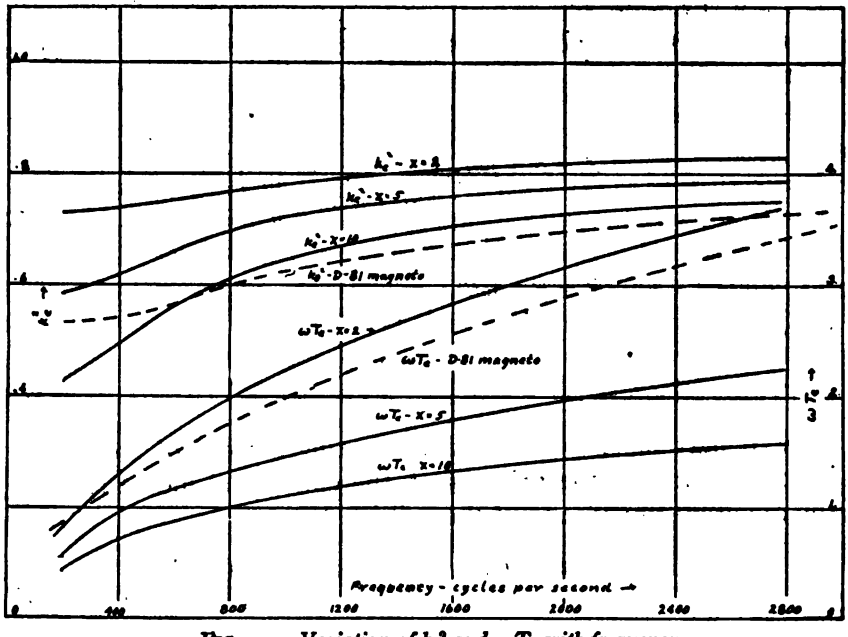

FIG. 22.—*Variation of k_0^2 and ωT_0 with frequency*

Solid curves give values computed from skin effect equations (72 and 73) for three values of $x = \frac{\text{air-gap reluctance}}{\text{iron reluctance}}$ assuming uniform laminations and that $4\pi^2 \frac{\mu}{\rho} l_0^2 = 0.01$. Dotted curves give values observed on shuttle type magneto

The general order of magnitude and the rate of increase with frequency is the same in the theoretical and actual cases, and the discrepancy probably results from the presence of large and unlaminated masses of metal in the end cheeks of the armature, the magnet poles, the supporting framework, etc., no account of which is taken in the theoretical discussion.

The energy relations between the main circuit and the tertiary circuit are shown in Fig. 19, which is a plot of the electrostatic energy in the condenser, the total magnetic energy and the amount

Digitized by Google

of energy dissipated as heat. It will be seen that at the time $t = 9 \times 10^{-6}$ seconds, at which the voltage across the condenser is a maximum, only 1.1×10^{-3} joules, or 15 per cent, of the energy has been dissipated, but 2.1×10^{-3} joules, or 28 per cent, additional is rendered unavailable by the presence of the eddy currents and is stored magnetically in that part of the iron circuit which is linked with these currents. After the breakdown of the spark gap a considerable portion of this 28 per cent may be liberated and restored to the main circuit to later appear as heat in the spark, so that from this point of view measurements of spark energy do not entirely indicate the amount of energy available for the production of voltage. This plot also indicates the similarity between the closed-coil model and the single-coil model containing a shunting resistance in parallel with its terminals. The two cases would be identical if k_0^2 were unity and the qualitative agreement is fairly close in any case.

V. MEASUREMENTS OF CONSTANTS

In determining the electrical constants R, L, C, etc., to insert in the models previously discussed two general methods are possible: (1) By independent measurements of physical dimensions or electrical quantities, such as capacity of condensers, etc.; (2) by measuring the performance of the complete device and setting up a sufficient number of equations to solve empirically for the set of constants which will best satisfy the observed results. The former type of method is, of course, desirable from the point of view of the designer or testing laboratory, while only the second type of method is applicable in cases where it is desirable to study and express in quantitative terms the performance of apparatus already in existence.

Capacity Measurement

The capacity C_1 of the primary condenser of the magneto may, of course, be easily measured by any of the standard methods and need not be referred to here. The secondary distributed capacity consists of several parts, as indicated schematically in Fig. 23: First, the capacity C_t of the condenser, which has for one "plate" the high-tension lead and the outer layer of the secondary winding, and for the other "plate" the frame of the machine, the engine ground, and any tube through which the spark-plug cable may pass. Portions of this capacity may be isolated and meas-

Digitized by Google

ured separately, but the portion between the outer layer of the winding and the frame can not be handled in this manner, since even the removal of the armature from the frame merely substitutes the ends of the core and surrounding objects for the magneto frame, and while it materially reduces C_t does not eliminate it. The next most important part of the secondary capacity is the component C_w, which is built up from the capacity between the successive layers of secondary winding connected effectively in series. The dielectric of this condenser consists of the insulation between layers, while the copper wires of the successive layers form the plates.

In addition to these two main components there is a certain amount of capacity C_d represented by condensers, one plate of which is the end turns of the successive layers of the secondary, while the other plate is the end of the armature core. This capacity is "distributed" in the strict sense of the word, and the effect of its component parts upon the entire machine performance must be weighted in proper proportion, depending upon the voltage which is applied to each successive layer.

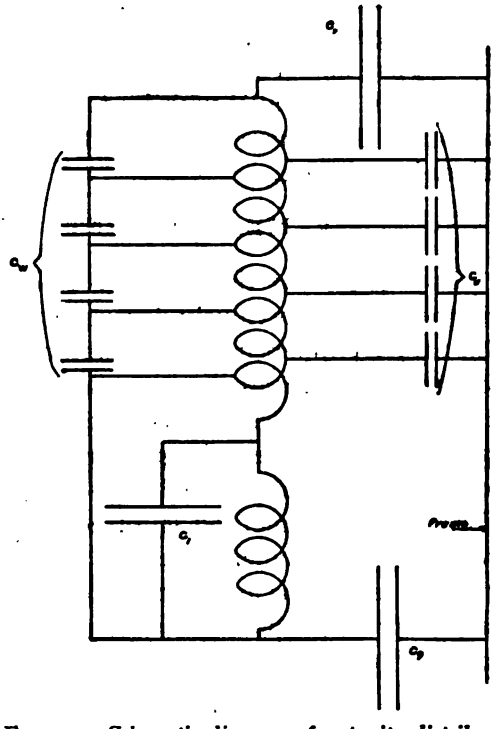

FIG. 23.—*Schematic diagram of capacity distribution in magneto.*

The equivalent capacity C_s which is desired for use as the contribution from the secondary winding in any of the models discussed above is that which would contain at the terminal voltage of the winding the same amount of electrostatic energy as is actually stored in the various portions of the dielectric, and the use of such an equivalent condenser is accurate except to the extent that there may be local oscillations of higher frequency, involving only portions of the winding and of the corresponding condensers.

Digitized by Google

1. BY IMPULSIVE IMPEDANCE

It is possible to obtain the equivalent total secondary capacity from measurements on the magneto by observing the crest voltage obtained by interrupting a known current through the primary with the primary condenser removed. This measurement should be made with a number of different values of capacity added to the secondary terminals, and the corresponding values of the impulsive impedance Z should be computed. If $\frac{1}{Z^2}$ is then plotted as ordinate against the value of the added capacity as abscissa, the results will be found to fall approximately upon a straight line, the intercept of which with the axis of abscissae will give the equivalent secondary capacity previous to the addition of the condenser.

2. BY COMPUTATION

The capacity through the winding C_w may be computed approximately from the dimensions of the winding if the dielectric constant of the insulating material is known. In this computation it is sufficiently accurate to assume the condenser to be built up of infinite parallel plates whose thickness is that of the dielectric between nearest points of the wires in adjacent layers and whose area is the product of the circumference of the mean turn multiplied by the width of the winding. Dividing this by the number of layers to allow for series connection gives the effective value which the capacity would have if the voltage gradient throughout the width of each condenser were uniform. In the actual winding, however, the dielectric at one end of the layer is subjected to a voltage $2\,e$, while that at the other end is o, if e is the voltage per layer, and the total energy stored in the condenser is greater than $\frac{1}{6}\,C\,e^2$ because of the nonuniform distribution of voltage along each layer of dielectric. Multiplying the results obtained as indicated above by the factor $\frac{4}{3}$ corrects for this condition and gives the value which should be used in conjunction with the capacity C_t obtained by other methods to give the total capacity of the winding.

3. BY RESONANCE

Another very convenient method for measuring the capacity of magneto windings is that indicated in Fig. 24, where the coil A is supplied from a suitable source with currents of radio frequency (100 000 to 500 000 cycles per second). The oscillating circuit

Digitized by Google

B, loosely coupled to A, is tuned to resonance, as indicated by a suitable hot wire instrument (A). The terminals of the winding w whose capacity is to be measured are then connected in parallel with the variable condenser C_o, and this latter is then readjusted to again establish resonance. The decrease in the condenser C_o is, of course, equal to the value of the capacity which was connected in parallel with it by the insertion of the winding. For frequencies of the magnitude indicated, the inductance of the magneto winding offers a practically infinite reactance, and only a negligible amount of current flows spirally through the winding around the core. The main part of the radio frequency current flows through the dielectric from layer to layer of condenser C_w and also supplies C_t. In using this method it is well to take readings at several different frequencies, so that if one of them coincides with a natural overtone of the coil the resulting error will be apparent from the lack of agreement with the values obtained at the other frequencies.

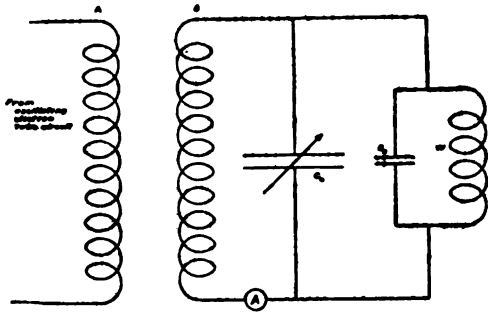

FIG. 24.—*Circuits used in measuring capacity, C_g of magneto winding W at radio frequencies*

If the grounded terminal of the primary winding can be separated from the core, the entire magneto may be regarded as having three terminals: (1) The high-tension terminal of the secondary; (2) the insulated ground terminal of the primary; (3) the frame. Any two of these terminals may be used as the terminals of a condenser to connect in parallel with C_o, while the third terminal may either be left insulated or may be connected to one of the other two. This system thus gives six possible combinations, any three of which are sufficient to determine the three capacities C_w, C_t, and C_g (C_g being the capacity between the inner layer of the primary winding and the frame). The check values obtained from the other three combinations will usually be found to agree to a few per cent.

It should be borne in mind that during these radio frequency measurements the total voltage is distributed between the layers by their respective capacities and that the voltage from any one layer to the next is uniform throughout the width of the layer,

Digitized by Google

and consequently the radio frequency values must be increased by the factor $\frac{4}{3}$ for the same reason as the computed values.

4. BY A. C. BRIDGE

Still another method for measuring C_t is obtained by the alternating current bridge method described in detail below. (See Fig. 25.) With this bridge the charging currents flowing from the winding to the frame are led off through the condenser C_e and in effect measured by it. This method gives the quantity C_t combined with an effective value of C_d weighted in proportion to the voltage applied to each element of C_d, but does not give a measure of C_w. Probably the most satisfactory values can be obtained by combining C_t obtained by this method with C_w obtained at radio frequency.

The following table gives some typical data on secondary capacity obtained by the various methods outlined in the case of two shuttle type magnetos:

Capacity	Observed at radio frequency	Computed from dimensions	A. C. bridge at 1000 cycles
Magneto D-82:			
C_t+C_d	45.3	.....	46.2
C_w	$\frac{4}{3}\times 29.3$	$\frac{4}{3}\times 27.1$	.....
C_s	258.	.....	.....
Magneto D-81:			
C_t+C_d	43.4	.....	40.7
C_w	$\frac{4}{3}\times 28.5$	$\frac{4}{3}\times 27.1$	.....
C_s	218.	.....	.....

In the case of D-82 the total effective capacity, referred to the secondary, obtained by summing the various components (including the primary condenser and secondary leads) was found to be 197 $\mu\mu f$, while the value obtained by extrapolating the line obtained by plotting $\frac{I}{Z^2_m}$ against added capacity gave 204 $\mu\mu f$.

Resistance and Inductance Measurements

The double-coil and closed-coil models involve too many constants to lend themselves readily to the determination of the numerous inductances and resistances needed by the second

Digitized by Google

method outlined above. The curve of $\frac{I}{Z^2}$ vs. capacity mentioned above should have, according to the single-coil model (see equation 27), a slope equal to $\frac{e^{-\frac{\alpha}{\beta}\tan^{-1}\frac{\beta}{\alpha}}}{L}$, and this combination of the resistance and inductance may be used in computations based upon the single-coil model or may, in fact, be used as the reciprocal of an equivalent inductance in a single-coil model of zero resistance to represent with fair accuracy the phenomenon which takes place. It might be thought that measurements of the maximum negative crest of the voltage wave, in addition to those of the positive crest, would give a value for the damping of the wave, and hence would serve to measure the resistance of the equivalent single-coil model. In the magnetos tested, however, the distortion of the base of oscillations by the eddy currents, as indicated by the term involving $e^{m_1 t}$ of equation (67) is so great that the values of resistance obtained by the method outlined are very much greater than those observed by the alternating current bridge described below and give a rather misleading indication of the amount of energy dissipation.

1. BY BALLISTIC GALVANOMETER

Measurements with reversed direct current using a ballistic galvanometer to measure the changes in flux involved serve to indicate the primary and secondary inductance and mutual inductance for such slow changes in flux, and these values are suitable for insertion in the closed-coil model, since the tertiary circuit takes care of the decrease in these inductances and the increase in resistance which occur at higher frequency. The values obtained ballistically, however, are not satisfactory for use directly in the double-coil or single-coil models. A null ballistic method may be used to obtain the coefficient of coupling k between the primary and secondary windings for use in any double coil model.[19] While the values of k obtained by this method are somewhat in error as the result of the nonuniform current distribution in the secondary winding under operating conditions, the capacity measurements indicated above show that the component C_d of capacity which causes this nonuniform current is relatively small, and the error introduced from this cause is probably negligible compared with the other errors which

[19] A. P. P. Report No. 16, National Advisory Com. for Aeronautics, Report No. 58 II.

Digitized by Google

are inherent in setting up a double-coil model equivalent to any given magneto. The changes in inductance resulting from changes in frequency are mainly dependent upon changes in the flux distribution within the iron core itself, and it is probable that they have relatively little effect upon the coefficient of coupling between the primary and secondary winding, although both L_1, and L_2 and M are individually greatly affected by an increase in frequency.

2. BY A. C. BRIDGE

The methods of measuring resistance and inductance by means of some modified form of Wheatstone bridge supplied by alternating current are rapid and convenient and may be applied to the determination of the constants for the various types of magneto models discussed above. Any such measurement, in fact, indicates the values of resistance and inductance of an equivalent circuit which, when supplied with sustained alternating current of the frequency used, shows the same magnitude and phase relation of current as does the actual apparatus tested. During the operation of a magneto in the normal manner its winding and core are subjected to an impulse which bears a close resemblance to a single half wave of sustained alternating current, and it consequently seems a reasonable assumption that the value of resistance and inductance applicable in computing such an impulse should be at least approximately the same as those observed for an alternating current of corresponding frequency.

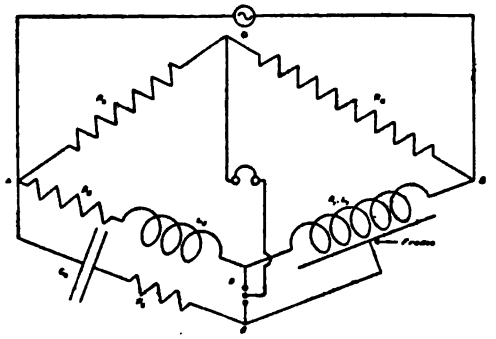

FIG. 25.—*Alternating current bridge for simultaneous measurement of effective resistance, inductance, and capacity of magneto windings*

The type of alternating current bridge which has been found convenient for such measurements is shown in Fig. 25, in which one winding, preferably the high-voltage coil, is connected as one of the four arms of a Wheatstone bridge, the primary condenser being disconnected entirely. In addition to the four normal arms, an additional circuit is connected from point A through variable condenser C_6 and a variable resistance R_6 to the frame of the magneto, which has been disconnected from the end of the

Digitized by Google

primary winding with which it is normally in contact. Inductance L_5 and resistance R_5 are then adjusted until a telephone or other suitable detector connected between points C and D shows a balance. The detector is then connected between points C and F and C_6 is adjusted for balance. When by several repetitions of this process a simultaneous balance has been obtained on both of these points, we have to a close degree of approximation the relation

$$R_1 + j\omega L_1 = \frac{R_3}{R_4}(R_5 + j\omega L_5) \tag{82}$$

from which R_1 and L_1 for each frequency can be obtained.

Equation (82) is rigorous if C_d is zero, so that the entire capacity between the winding and frame can be considered as concentrated at the ends as C_t and C_g, respectively. If this is not the case, but if the condensers C_d and C_t are free from energy loss, they may be combined to form an equivalent condenser C_k, located at a fraction K of the total length of the winding from the terminal B. Equation (82) then holds if the right-hand member is multiplied by the correction factor

$$\frac{1}{1 + K\frac{Z_5}{Z_6}} \tag{83}$$

where Z_5 and Z_6 are the impedances of arms 5 and 6, respectively, expressed in vector notation. K is given by the equation

$$K = \frac{R_3 R_6}{R_4 R_1'} \tag{84}$$

Where R_1' is that part of the coil resistance due to the copper winding only. Unfortunately, however, the condenser C_t usually has an appreciable energy loss (corresponding to a power factor of about 0.05), and a certain amount of resistance must be inserted in arm 6 to balance this loss. This resistance is often so large that the value of K computed from (84) is very seriously in error. The amount and location of the capacity C_d can be estimated roughly from the arrangement and dimensions of the windings and in the coils thus far studied is found to be negligible in its effect on equation (82).

The magnitude of the condenser C_k, which is equivalent in the bridge circuits to the combined effect of C_d and C_t, is given by

$$C_k = \frac{R_4}{R_3} \cdot \frac{C_6}{1 - K} \tag{85}$$

Digitized by Google

For use in the various artificial models, however, we desire the value of condenser, which, if connected from the secondary terminal to ground, would receive the same energy as is actually stored in the distributed capacity. This value is given by

$$C_k' = (1-K)^2 C_k = \frac{R_4}{R_3} C_6 (1-K) \tag{86}$$

In case C_d can be neglected, K becomes zero and (85) and (86) reduce to

$$C_k = \frac{R_4}{R_3} C_6$$

It will be noticed that the capacity C_g, discussed above, which may exist between the inner layer of the primary winding and the core, does not affect the measurement in any way, since it is not subjected to any difference of potential when the balance has been obtained. The component of capacity denoted above by C_w from layer to layer of the winding does not contribute to the flow of current through the arm C_6, but flows through arm 5 of the bridge. The results of equation (82) must, therefore, be corrected for this effect also by the following equations:

$$R = \frac{R'}{(1+\omega^2 L'C)^2 + \omega^2 C^2 R'^2} \tag{87}$$

$$L = \frac{L'(1+\omega^2 L'C) + CR'^2}{(1+\omega^2 L'C)^2 + \omega^2 C^2 R'^2} \tag{88}$$

In these equations R and L are the true resistance and inductance of the winding as they would be measured if the capacity C_w were absent, while R' and L' are the actual observed resistance and inductance as computed from equations (82) and (83) above. These equations are the converse of the well-known equations:

$$R' = \frac{R}{(1-\omega^2 LC)^2 + \omega^2 C^2 R^2} \tag{89}$$

$$L_p = \frac{L(1-\omega^2 LC) - CR^2}{(1-\omega^2 LC)^2 + \omega^2 C^2 R^2} \tag{90}$$

which express the effective resistance and inductance of a coil which is shunted by a condenser.

Figs. 26, 27, and 28 show typical results obtained on three shuttle-type magnetos by this method. The dotted curves give

Digitized by Google

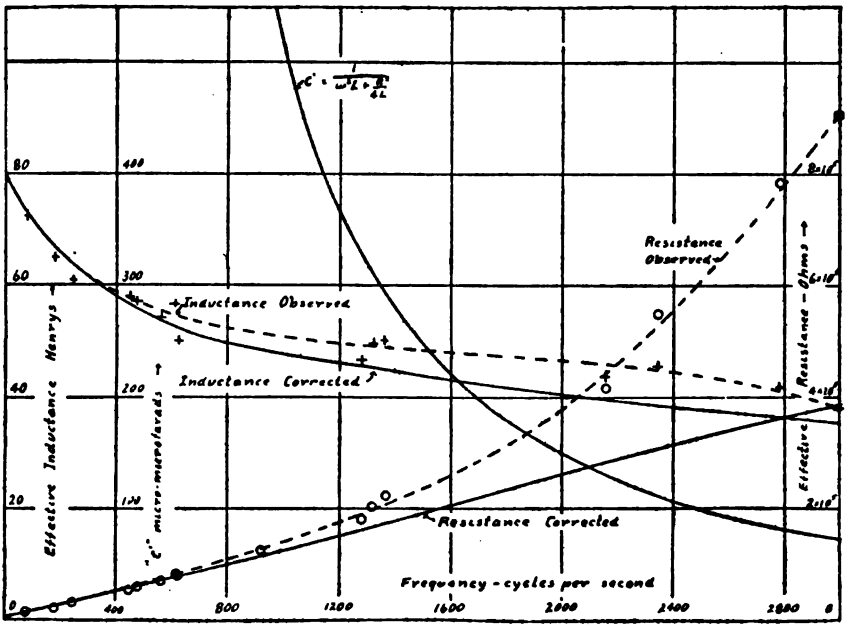

FIG. 26.—*Effective resistance and inductance of D–82 (laminated pole) magneto as measured on alternating current at various frequencies*

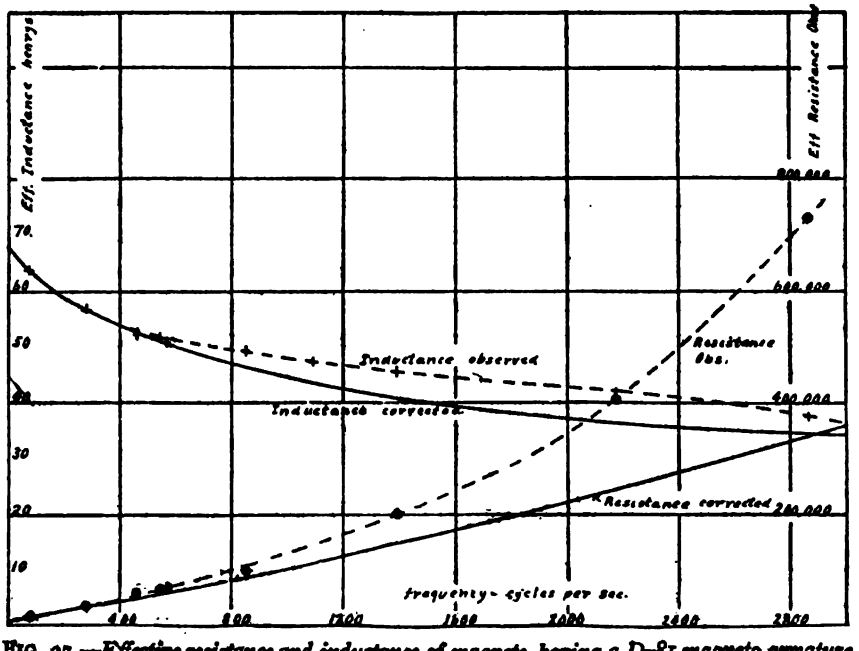

FIG. 27.—*Effective resistance and inductance of magneto having a D–81 magneto armature in a D–82 (laminated) pole structure*

Digitized by Google

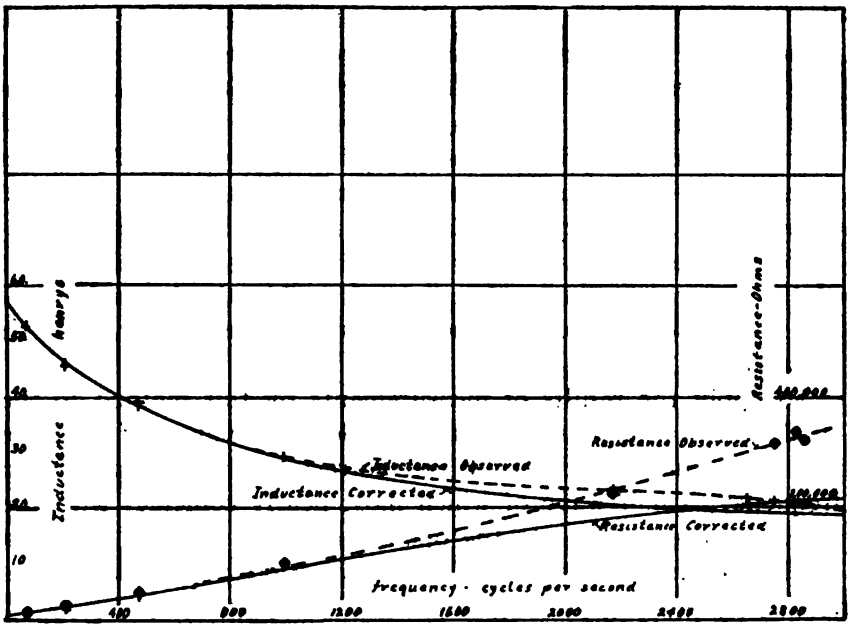

FIG. 28.—*Effective resistance and inductance of D–81 magneto (solid pole pieces)*

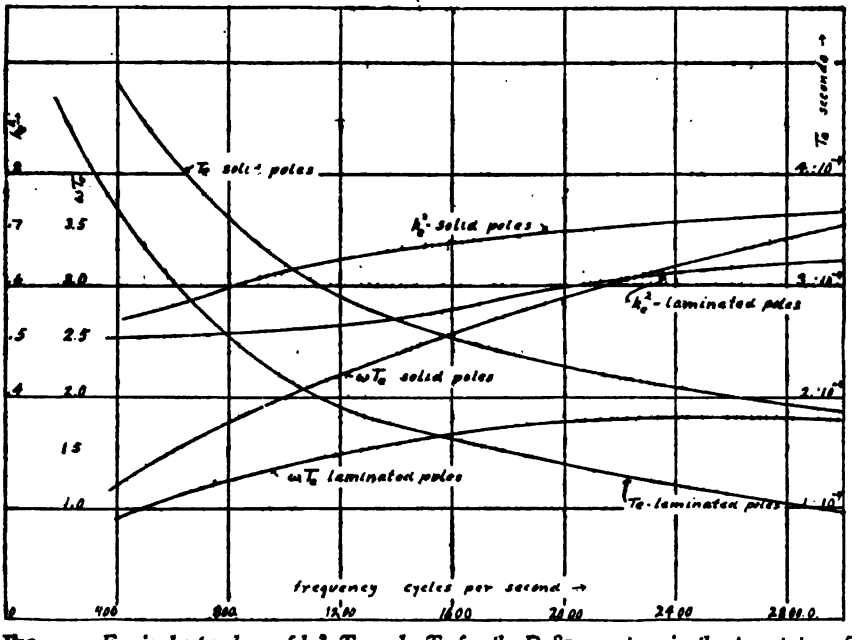

FIG. 29.—*Equivalent values of k_e^2, T_e and ωT_e for the D–81 armature in the two types of pole structure*

Digitized by Google

the observed resistance and inductance for various frequencies, while the solid curves show the corresponding values after correction has been made for the capacity C_w, which in these cases amounted to 31, 38, and 38$\mu\mu f$, respectively. It will be noted that the inductance first decreases quite rapidly from the values observed on direct current and then maintains a fairly constant value as the frequency is further increased. The effective resistance increases very rapidly to a value which is many times that of the copper winding and indicates forcibly the importance of the iron losses in effecting the dissipation of energy in such an apparatus.

To apply the results of measurements by this method to the single-coil model, it is necessary to select the values of effective resistance and inductance which correspond to the particular frequency, a half wave of which most nearly coincides with the impulse corresponding to the operation of the model. This can be done either by a series of successive approximations or more readily by plotting (see Fig. 26) the auxiliary quantity

$$C' = \frac{1}{\omega^2 L + \frac{R^2}{4L}} \tag{91}$$

C' may be defined as the capacity which, substituted in equation 23, will give as the resulting frequency $\frac{\beta}{2\pi}$ of a single-coil model the value $\frac{\omega}{2\pi}$. Hence, when the total capacity connected to the magneto is known in any specific case, the frequency corresponding to this value of C' on the auxiliary curve will be that for which R and L should be taken.

If the primary condenser is not disconnected, it produces a very marked effect upon the effective resistance and inductance, as would be expected from equations (89) and (90). Fig. 30 shows the corresponding variation of resistance and inductance with frequency and indicates that a resonance point is attained at about 2300 cycles.[30]

[30] In cases where the damping is appreciable three different frequencies of oscillation are of importance, as follows: A circuit of the single-coil type oscillating freely has a frequency, $f = \frac{1}{2\pi}\sqrt{\frac{1}{LC} - \frac{R^2}{4L^2}}$; if alternating current is applied to the terminals of the condenser of such a system, the effective inductance has the value 0 at the slightly different frequency, $f = \frac{1}{2\pi}\sqrt{\frac{1}{LC} - \frac{R^2}{L^2}}$; and the effective resistance has a maximum at a still different frequency, $f = \frac{1}{2\pi}\sqrt{\frac{1}{LC} - \frac{R^2}{2L^2}}$.

Digitized by Google

The results of A. C. bridge measurements may be correlated with the closed-coil magneto model by computing the values of k_e and T_e which a tertiary circuit must have in order to change the resistance and inductance from their D. C. values to the values which are observed at any particular frequency of A. C. The effect of such a tertiary circuit upon the main coil is indicated by equations

$$R_1' = R_1 + \frac{\omega^2 k_e^2 T_e L_1}{1+\omega^2 T_e^2} \tag{92}$$

$$L_1' = L_1 \frac{(1+\omega^2 T_e^2(1-k_e^2))}{1+\omega^2 T_e^2} \tag{93}$$

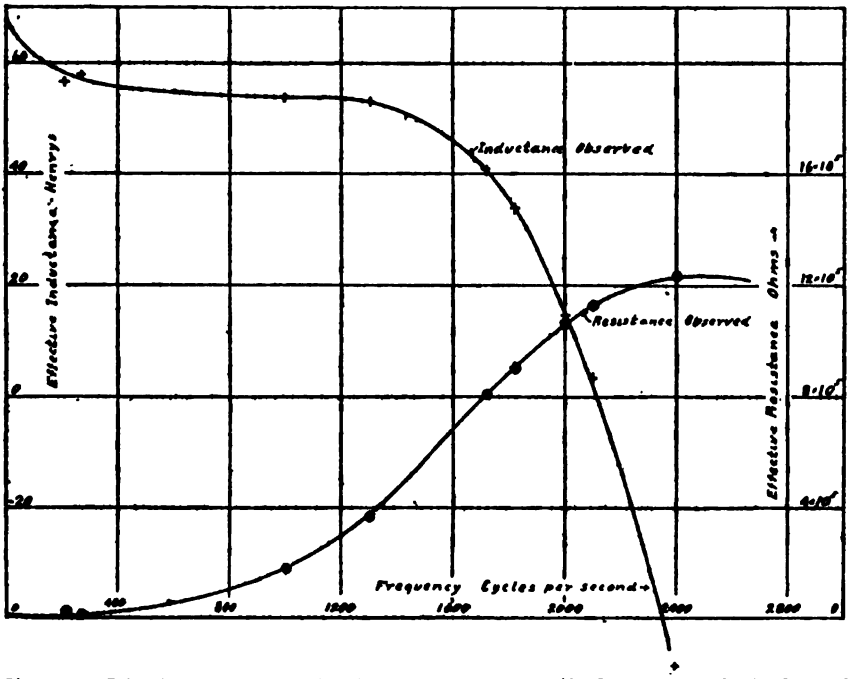

FIG. 30.—*Effective resistance and inductance of magneto (D–81 armature in D–82 field with primary condenser connected*

which result immediately from (79), and, conversely, it is possible to compute for each frequency the values of k_e and T_e by the following formulas which are derived from equations (92) and (93):

$$T_e = \frac{L_1 - L_1'}{R_1' - R_1} \tag{94}$$

$$k_e^2 = \frac{L_1 - L_1'}{L_1} + \frac{(R_1' - R_1)^2}{(L_1 - L_1')L_1\omega^2} \tag{95}$$

Digitized by Google

The resulting values of R_1, L_1, and k_e, T_e for any frequency constitute the constants of the corresponding closed-coil model. (Fig. 29.)

VI. EXPERIMENTAL CONFIRMATION OF MODELS

Probably the most searching qualitative tests of the various models discussed above is offered by the measurements at the National Physical Laboratory of the actual wave form during period 2. A comparison of Fig. 9, taken from their results, with Fig. 31 shows that the general character of a damped sinusoidal impulse can be accounted for by the single-coil model (Curve II), and that the shift of the base line of this impulse to a positive exponential curve and the consequently great reduction in the negative maximum is explained by the closed-coil model (Curve III), and that the high-frequency ripple with its relatively small amplitude can be explained by the double-coil model (Curve I).

The quantitative comparison of the models with an actual magneto is offered by tests made at the Bureau of Standards of two shuttle type Berling magnetos, models D–81 and D–82, respectively. These types are identical except that model D–82 has laminated pole pieces while D–81 has solid iron castings, and in certain of the measurements (e. g., Fig. 27) the D–81 armature was used in both frames to eliminate all other possible differences in winding. Measurements of the capacity of these magneto windings made by the radio frequency measurements are given above (p. 455), and the results of the A. C. bridge measurements made on the secondary winding of resistance, inductance, and capacity to ground are those shown in Figs. 26, 27, and 28. Throughout the alternating-current measurements the voltage applied to the bridge was varied in proportion to the frequency, so that the magnetic circuit operated at approximately the same flux density at all frequencies. Although 500 volts were applied at 3000 cycles, the flux was necessarily much less than that occurring in normal operation and corresponded to that produced by a primary current at break of 0.03 ampere. This latter value was used in the crest-voltage measurements.

The results of the experimental work are best expressed in terms of the "impulsive impedance" or ratio of the crest voltage to the current at break. While this impedance, like any other constant of the system, may be referred to either the primary or secondary circuits, it is for most purposes more convenient to use

Digitized by Google

the hybrid value given by the quotient of secondary crest voltage, divided by primary current at break. This quantity Z_m is related

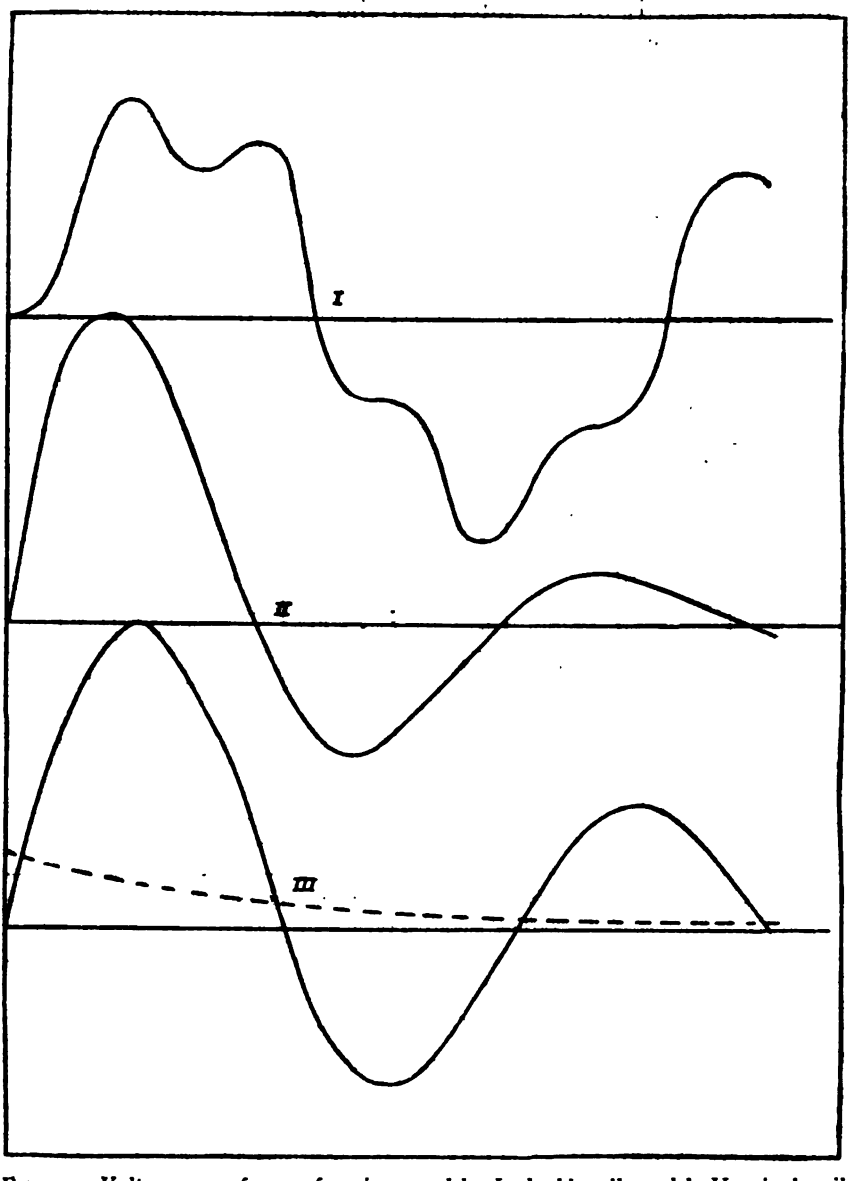

FIG. 31.—*Voltage wave forms of various models: I, double-coil model; II, single-coil model; III, closed-coil model*

to the primary (Z_1) and secondary (Z_2) impulsive impedance by the equation

$$Z_2 = n\, Z_m = n^2 Z_1 \qquad (96)$$

where n is the ratio of turns of the magneto.

Digitized by Google

Fig. 32 shows the variation of this quantity when different condensers were connected to either the primary or secondary of the magneto. It will be noted that the points indicated as circles which correspond to various additions of capacity to the primary windings lie on the same curve as those indicated by crosses which correspond to the addition of secondary capacity, this agreement constituting a very satisfactory justification of the utility of referring electrical quantities from one side to the other of the transformer, as was done in developing the single-coil model.

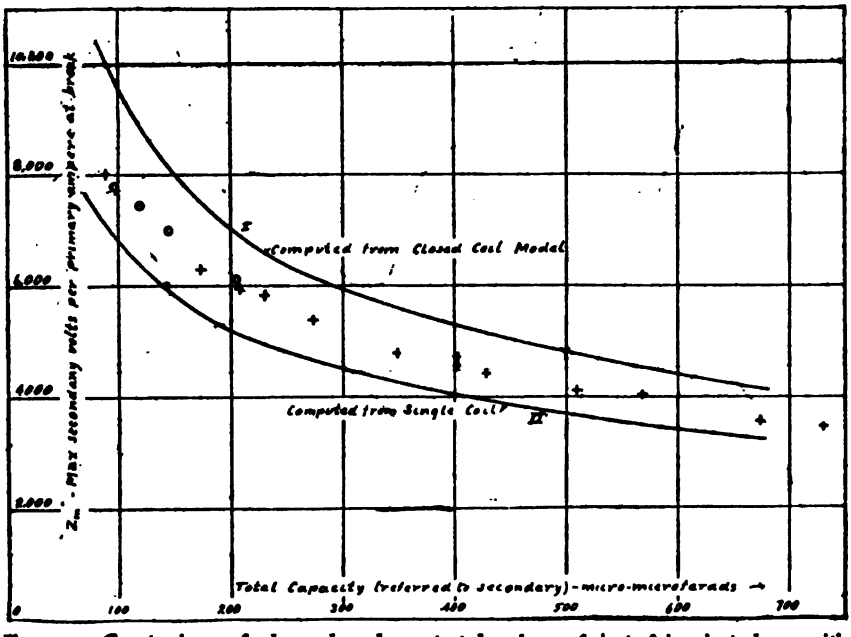

FIG. 32.—*Comparison of observed and computed values of impulsive impedance with various shunting condensers*

The solid curves are computed from data obtained by A. C. bridge measurements. The points are the result of direct crest-voltage measurements on D-82 magneto

The Curve I in Fig. 32 is drawn through points computed for the various known capacities from the single-coil model. Curve II gives similar values computed on the basis of the closed-coil model from the same A. C. bridge data. It will be seen that the discrepancy in both cases, while greater than the error of measurement and fairly constant, is by no means large when one considers that the points and the curves were obtained on entirely distinct experimental bases, there being no data common to the two sets of observations.

Digitized by Google

Fig. 33 gives a similar comparison when various shunting resistances were connected in parallel with the secondary of the magneto. The crosses represent the values of Z_m directly observed. The solid curve is computed from the single-coil model using the values of L and R, observed on the A. C. bridge at a frequency of 2200 cycles, which is the natural frequency of oscillation of the model when unshunted. When the shunting is very heavy, the observed points depart very considerably from the curve thus computed as might be expected from the slowing down of the oscillations by the shunt. If in the computation for any point the values of L and R corresponding to the actual frequency of the oscillation are used in the single-coil model, the values of Z_m indicated by the

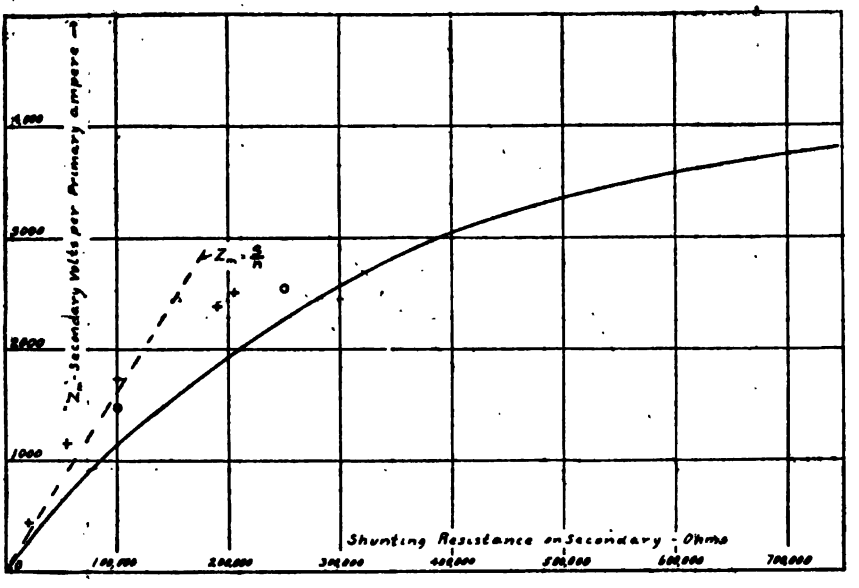

FIG. 33.—*Comparison of observed and computed values of impulsive impedance with various shunting resistances*

The solid curve is computed from the constants of a single-coil model fitting the A. C. bridge data at 2200 cycles. The circles are computed for a single coil model having the A. C. constants of the actual magneto at the particular frequency of oscillation when shunted. Crosses indicate the result of direct crest-voltage measurements on D-8a magneto.

circles are obtained, which are seen to agree much more closely with the observed values than does the solid curve. In cases where the oscillations are overdamped the values of L and R corresponding to zero frequency may be used.

Fig. 34 shows the variation of the secondary crest voltage with the magnitude of the primary current at break. The straight-line relation indicates that in spite of the presence of iron in the

Digitized by Google

magnetic circuit the variation of Z_m with current is relatively slight. This constancy of the inductance and hence of Z_m is of value inasmuch as it is not practicable to make the A. C. meas-

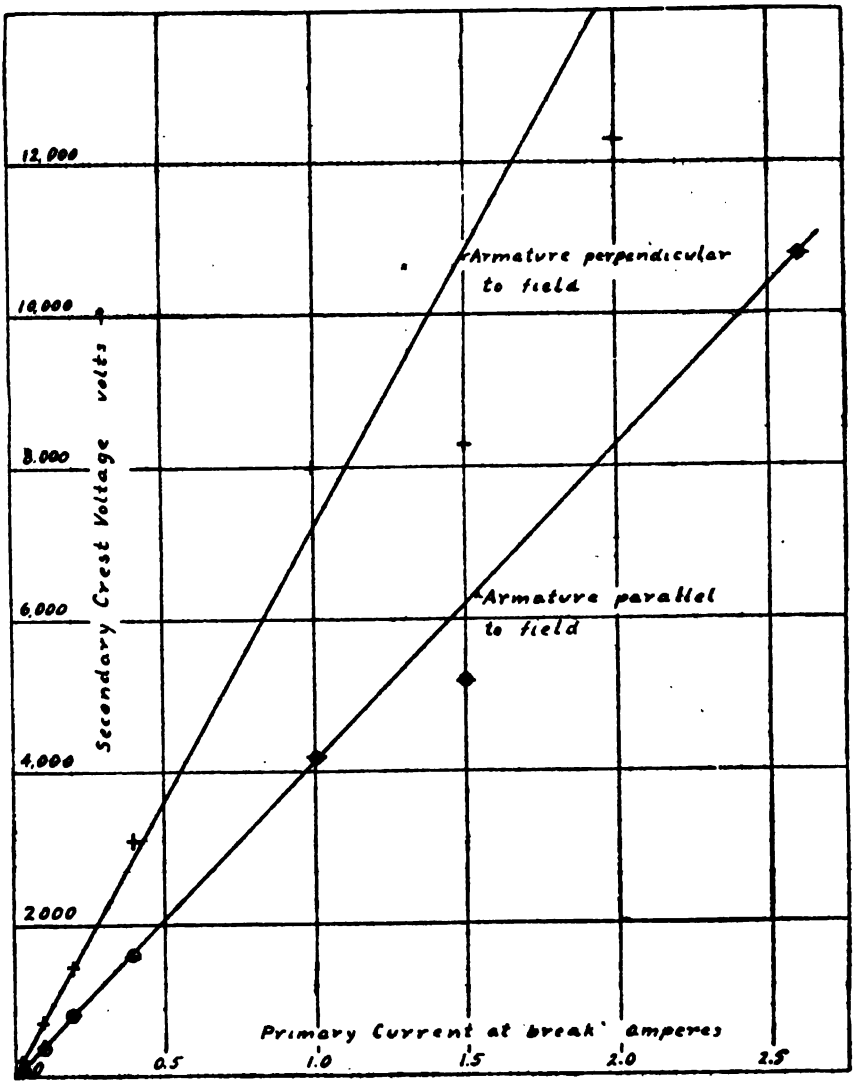

FIG. 34.—*Data showing approximate proportionality between crest voltage and primary current. (The low values at 1.5 amperes are the result of sparking at the breaker points)*

urements with as large current values as occur in actual operation of the magneto. If this were attempted, the resultant heating of the winding by the great energy loss which would occur would be excessive.

Digitized by Google

VII. CONCLUSIONS

The experimental results just described indicate that the various models proposed in this paper do not depart widely in their performance from the actual magneto, and it is hoped that the single-coil model in particular, because of its simplicity, may be found useful in designing apparatus of this type. There is a great need for experimentation by the methods suggested on a wider variety of magnetos of different types in order to confirm the validity of the models for other types of construction than the conventional shuttlewound armature and to indicate the order of magnitude of the quantities involved in typical cases. Measurements already made show that the quantity T_e is a definite quantitative measure of the effect of eddy currents, and a study of the values of this quantity in magnetos having different thickness of laminations would be of great value.

WASHINGTON, December 1, 1920.

Digitized by Google

Digitized by Google

UNIVERSITY OF CALIFORNIA
FEB 3

DEPARTMENT OF COMMERCE

SCIENTIFIC PAPERS
OF THE
BUREAU OF STANDARDS
S. W. STRATTON, DIRECTOR

No. 425

CHARACTERISTIC SOFT X-RAYS FROM ARCS IN GASES AND VAPORS

BY

F. L. MOHLER, Physicist
PAUL D. FOOTE, Physicist
Bureau of Standards

DECEMBER 17, 1921

PRICE, 10 CENTS
Sold only by the Superintendent of Documents, Government Printing Office
Washington, D. C.

WASHINGTON
GOVERNMENT PRINTING OFFICE
1922

Digitized by Google

Digitized by Google

CHARACTERISTIC SOFT X-RAYS FROM ARCS IN GASES AND VAPORS

By F. L. Mohler and Paul D. Foote

ABSTRACT

Potentials required to excite successive types of radiation in a low-pressure Wehnelt arc have been measured by observing the photoelectric effect of the arc radiation on other electrodes within the same tube. Critical radiating potentials for 11 gases and vapors have been measured in a range from 17 to 500 volts. The corresponding limiting spectral frequencies ranging from $\lambda=700$ to $\lambda=25$ *A* include the softest characteristic X-rays for all the elements considered. Critical potentials corresponding to the principle *L* series limit of sodium, magnesium, phosphorus, sulphur, and chlorine have been measured. A softer and fainter *L* limit has also been discovered in these elements. The *K* series limits of carbon, nitrogen, and oxygen have been identified, as well as the softest X-ray limits (*M* series) of potassium. Measurements of radiation from four carbon compounds gave identical results for the *K* limit of carbon.

Experiments with radiation from solids indicate the existence of soft characteristic X-radiation, with no measurable general radiation under the best vacuum conditions. Nickel shows radiation starting at 80 volts.

CONTENTS

	Page.
I. Introduction	471
II. Apparatus and methods	474
III. Results	478
1. Potassium	479
2. Sodium	481
3. Magnesium	482
4. Phosphorus	484
5. Sulphur	484
6. Carbon compounds	484
7. Air	487
8. Oxygen	488
IV. Interpretation of results	488
V. Soft X-rays from solids	493
VI. Conclusions	495

I. INTRODUCTION

The present paper is concerned with measurements of the potentials required to excite successive types of radiation in gases and vapors by electron impact. A knowledge of the physical conditions whereby different kinds of radiation may be

Digitized by Google

stimulated is of great interest in its bearing upon the various theories of atomic structure and is most essential for the rational development of certain technical engineering problems of immediate importance. The energy transformations involved in electron collision are as follows: The kinetic energy $\frac{1}{2}mv^2$ of the colliding electron is equal to Ve, where V is the potential difference through which the electron has fallen. At any potential greater than the first ionization point, collision with an atom may result in the ejection of an electron from the atom at the expense of part or all of this kinetic energy. The positive ion upon recombination with another electron will emit radiations of frequencies ν_n related to the energy E required to eject the electron as follows:

$$E = \Sigma h(\nu_1 + \nu_2 + \nu_3, \text{ etc.})$$

The highest possible frequency ν is such that $h\nu = E$. The least potential V required to eject the electron by collision and the limiting frequency ν of the resulting radiation are thus proportional, viz:

$$Ve = h\nu \text{ or } \lambda(A) = \frac{12\,345}{V \text{ (volts)}}$$

The limit ν is found to be the convergence frequency of a series of absorption lines, in all cases where the series relations are known, and in X-ray spectra it defines the edge of an absorption band. Thus either from spectroscopic measurements of the limiting frequencies of different types of radiation or from measurements of the least potential required to excite the radiation, the energy levels of the various atomic configurations may be determined.

The following transitions in the type of electron collisions take place. Above the first ionization potential one valence electron may be ejected and the arc spectrum is emitted upon recombination. At successively higher potentials two or more electrons may be ejected, with subsequent emission of the spark spectra of first or higher orders.

The electronic orbit in the atom nearest the nucleus is designated as the K orbit. Outside of this are the L, M, N, etc., orbits of successively greater diameter. Ejection of one of these electrons subsequently gives rise to the emission of X-ray spectra. If the removal is from the K ring, different lines of the K series are produced when the ejected electron returns to its equilibrium position, and similarly for the other rings.

Digitized by Google

In part because of the experimental limitations to spectroscopic analysis, but little work has been done in the investigation of the radiation from the outer X-ray orbits. The spectrum range from $\lambda = 0.1$ to $\lambda = 12$ *A* or from 100 000 to 1000 volts has been studied by the crystal spectrometer. The range of the grating spectrograph has in recent years been extended from over 20 000 *A* to less than 200 *A*, though data are very incomplete below 1200 *A*. It is, however, with this comparatively small range from 1200 to 12 *A* or from 10 to 1000 volts that all the outer X-ray orbits and probably most of the spark spectra are concerned. No X-rays have been observed from elements in the first row of the periodic table and only the *K* series in the second and third rows. It is to be expected that for the heavy elements, besides the observed *K*, *L*, and *M* series, *N* and *O* series exist, all falling in the spectral range heretofore inaccessible.

The possibility of measuring the potentials required to excite these radiations and by purely electrical measurements supplanting the meager spectroscopic data is suggested by the success of various investigators in determining resonance potentials by the radiation method.[1] In this is observed the photoelectric effect of a low-pressure Wehnelt discharge on electrodes within the same vacuum tube but electrically shielded from both positive and negative ions in the arc. The method offers a means of detecting radiation shorter than about 3000 *A*, including the region to which all materials are opaque.

An obvious difficulty in measuring the X-ray excitation potentials from a discharge in a gas is that the X radiation is superposed on the arc and spark spectra. This would not be true if the soft X-rays were obtained from solids, as in the ordinary X-ray tube. Numerous attempts of observers in the past to apply this latter method have failed, however, to show any convincing evidence of radiation characteristic of the anode material. They observed, apparently, general radiation starting at low voltage and increasing gradually with increased potential. Some experiments of the authors on radiation from solids were more successful, a brief statement of which is given in the latter part of this paper. Trouble with surface contamination of the anode, together with the requirements of the highest possible vacuum and sensitive current measurement, made the experiments very

[1] A few of the papers on this are Davis and Goucher, Phys. Rev., 10, p. 101, 1917; Horton and Davies, Proc. Roy. Soc., 95, p. 408, 1919; Mohler and Foote, B. S. Sci. Paper 400, 1920.

[2] Thomson, J. J., Phil. Mag., 28, p. 620, 1914; Laird, Ann. d. Phys., 46, p. 605, 1915; Laird and Barton, Phys. Rev., 15, p. 297, 1920; Dadourian, Phys. Rev., 14, p. 234, 1919.

Digitized by Google

difficult. It was found that in the work with vapors and gases the superposition of arc and spark radiations did not under suitable conditions mask the higher radiation potentials.

Since this work was undertaken other observers have announced fairly definite evidence of characteristic X radiation in this inaccessible range. Hollweck[3] has found evidence of selective absorption of carbon for general radiation from a solid anode. Kurth[4] has announced the measurement of the potential required to excite characteristic X-rays in the range from 12 to 400 A for five different elements used as solid targets.

In this connection it should be added that Millikan has found some of the longest X-ray emission lines in photographs of hot spark spectra with a vacuum grating spectrograph.[5]

No previous experiments have shown evidence of characteristic soft X-rays from gases. Whiddington[6] showed that there was radiation from air of a frequency range corresponding to 100 to 200 volts. The results of Richardson and Bazzoni,[7] although negative in this respect, are interesting because of the method used. They measured the maximum frequency radiated in a low-pressure arc by observing the maximum velocity attained by photoelectrons excited by this radiation. The velocity was measured by the curvature of the electron paths in a magnetic field and the frequency was computed from the Einstein equation. No radiation of frequency higher than the limit of the arc spectrum was found but the method lacked sensitivity. This at least suggests the possibility of not only measuring the potentials required to excite soft X-rays but of estimating the frequency emitted as well, by purely electrical methods.

In the present work the identification of the critical potentials observed as due to X-ray excitation rests on the agreement of observed values with the limits computed from X-ray data.

II. APPARATUS AND METHODS

Fig. 1 shows diagrammatically the arrangement of electrodes and electrical connections used to measure the radiation from arcs in gases. The electrodes *B C D* are concentric cylinders surrounding the hot wire cathode *A*. The electron current is maintained by a potential *V* between *A* and *B* and the radiation resulting

[3] C. R., 171, p. 849, 1920; 172, p. 439, 1921.
[4] Abstract, Phys. Rev., 17, p. 528, 1921; also paper read before Physical Society in April, 1921.
[5] Paper read before Nat. Acad. Sci., April, 1921. The authors lack complete data.
[6] Camb. Phil. Soc., 17, p. 144, 1913.
[7] Phil. Mag., 34, p. 285, 1917.

Digitized by Google

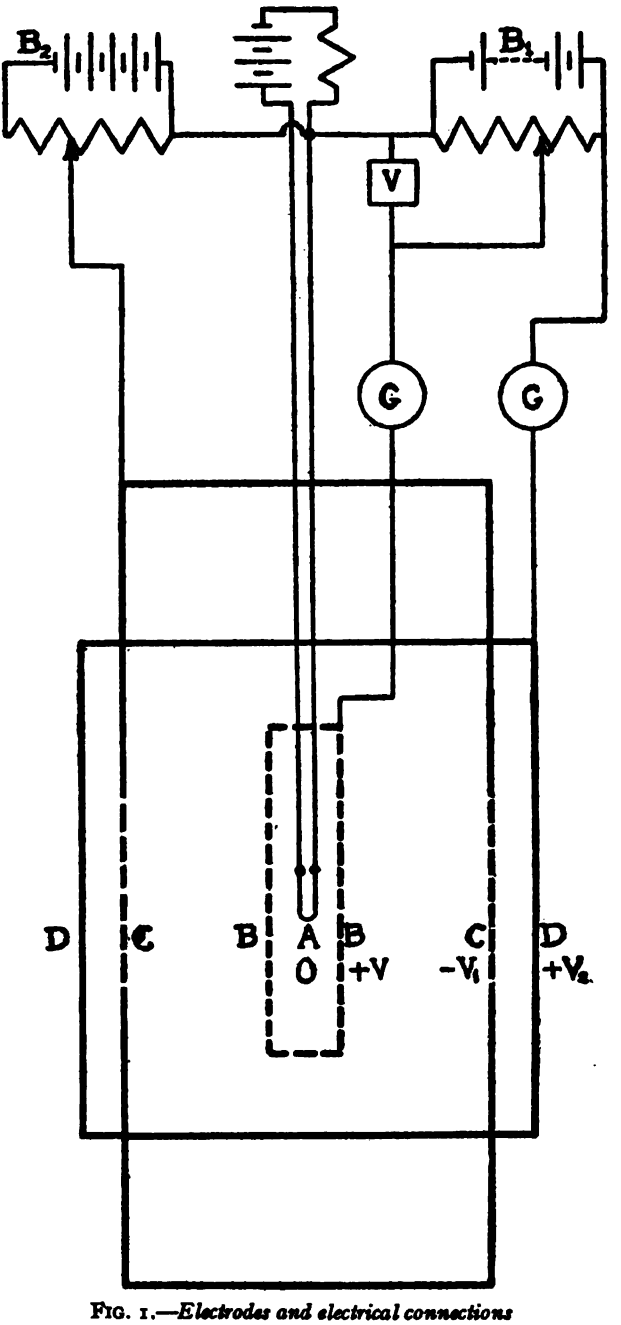

FIG. 1.—*Electrodes and electrical connections*

Digitized by Google

from electron collisions with the gas gives rise to a photoelectric current between C and D. It is essential that the electrons from the cathode actually acquire a velocity equivalent to the potential V and this is not in general the case with a current between two electrodes in a gas, on account of the loss of velocity when electrons collide with gas molecules. To insure the electrons receiving their full velocity, the grid B was mounted as closely as possible to the cathode and the gas pressure adjusted so low that nearly all collisions occurred in the space beyond the grid. This is a precaution of fundamental importance in any experiments involving the effect of potential on discharge through gases.

The shielding of the outer electrode is accomplished as follows: Consider the cathode at o potential and the grid B at $+V$. The outer grid, which almost completely incloses the inner one, is kept at a potential $-V_1$, thus preventing electrons from reaching it. Positive ions will pass through but can not reach the outer plate D when maintained at a potential $+V_2$ greater than the highest value of V used. The potential difference V_1+V_2 between C and D draws photoelectrons emitted from the outer grid to the plate.

Various evident means of testing the complete shielding of the outer electrode were frequently applied. For example, the radiation current will approach zero at low pressure while a stray electron current around C will not. Again, a stray current from the arc will change rapidly with the potential of C, while this has little effect on the radiation current.

There are several connections possible for measuring the ionization. The method most used was to put both the outer grid and plate at $-V_1$ and measure the positive current reaching them. The photoelectric current from the plate is superposed on the ion current, but as radiation currents were usually about one-hundredth as large as the positive currents this factor is negligible. The vacuum tubes were similar in design to those used previously in studying resonance potentials in gases and vapors.[8] For work with the vapors of sodium, potassium, magnesium, phosphorus, and sulphur tubes of the following type were employed:

The electrodes were suspended from a water-cooled metal top into a Pyrex glass tube about 7 cm in diameter and 40 cm long, closed at the bottom. The substance to be boiled was placed in the bottom of the tube and heated by an electric furnace. Care was taken in the suspension of the electrodes that they did not touch the hot glass walls and that the glass insulation in the top

[8] Mohler and Foote, B. S. Sci. Papers 400 and 403.

Digitized by Google

plate was shielded by outer tubes from the condensing vapor. Electrodes of sheet nickel and fine platinum gauze were used for these elements except magnesium, for which nickel gauze was employed. The outer grid was a cylinder of sheet nickel, closed at the bottom, with a zone of platinum gauze in the side. Cathodes were of oxide-coated platinum strips or of bare tungsten wire. The vapor density was controlled by varying the temperature of a furnace or, in the case of phosphorus, a water bath around the bottom of the vacuum tube.

The tube used for the carbon compounds and air was much smaller, about 4 cm in diameter, with electrodes smaller in proportion and all of platinum. The tube was of Pyrex glass with tungsten seals. Cathodes were either of tungsten or oxide-coated platinum. Gases were usually streamed through the tube through a plug of plaster of Paris. The flow was varied by changing the pressure on the high-pressure side of the plug. Liquid-air traps on each side of the discharge tube condensed all vapors. CCl_4, however, was streamed through the tube from a container at about $-70°$ C on one side to a trap in liquid air on the pump side. The temperature controlling the vapor pressure was maintained by a bath of petroleum ether with enough CCl_4 in it to make a slush at about $-60°$ C.

Several mercury-vapor pumps in series maintained the vacuum, and pressures were read on a McLeod gage sensitive to slightly less than 0.0001 mm of mercury. The electrical connections are shown in Fig. 1. The battery B_1, which supplied the arc current, was always made somewhat larger than the potential range to be studied. It is seen from the diagram how the plate is maintained at a constant potential $+V_2$ greater than V by the same battery. The retarding field maintained by B_2 was usually about 10 volts. The potential V across the arc was measured by a voltmeter with a 150-volt scale and the range increased as desired by calibrated series resistances. The current from the cathode, usually about 1 milliampere, was measured by a microammeter with a shunt resistance to regulate its sensitivity. The current to the outer plate was measured by a galvanometer, the sensitivity of which was likewise reduced by a shunt. It is interesting to note that we found the limit of sensitivity 10^{-10} amperes ample for all the work on gases and vapors.

In taking readings, for each setting of the voltage V the photoelectric current and also the current from the cathode were measured. The photoelectric current was then divided by the cathode

Digitized by Google

current and this ratio plotted against the potential V. As the radiation intensity is proportional to the cathode current for any one potential, this ratio eliminates the different characteristics of the cathode emission under changing conditions, and hence slow variations during a series of readings will not modify the results obtained. It happens that the resulting curves show nearly a straight-line relation between the photoelectric effect and the potential across the arc, with a change in slope occurring at critical potentials. The accuracy of this straight-line relation was well shown in some curves obtained in potassium. The points fall on a straight line from 23 to 140 volts, with no deviation greater than the probable experimental error of about 2 per cent. The physical significance of this property is not evident, for many factors enter, and the linear relationship is probably only an approximation. The usefulness of the relation in measuring critical potentials is, however, apparent as the critical points are the intersections of straight lines.

For an accurate determination of critical potentials it is necessary to know the correction term to be added to the applied voltage to give the effective potential through which electrons fall. This initial potential correction due to the resultant effects of potential drop along the cathode, contact difference in potential and temperature distribution of velocities of emitted electrons is usually of the order of ± 1 volt. The correction was found from the difference between the observed potential at which ionization began and the value of the ionization potentials as given in previous publications of the authors. As an accuracy of 1 volt was all that was obtainable, no great precision was required in applying such corrections. For the measurements at high voltage the only correction made was for the voltage drop across the cathode where this was large.

III. RESULTS

The following pages give results obtained for critical radiating potentials in 11 elements and compounds. Figs. 2 to 7 give typical curves and the accompanying tables the conditions of measurement and other remarks on the curves illustrated. An analysis of *all* the curves obtained which showed inflections suitable for measurement is also included. Particular care was required in some cases to secure conditions which gave definite inflections, and often many useless curves were taken before these conditions were found. Potential current readings were more or less limited to a range around the predicted potential necessary

Digitized by Google

for X-ray excitation. Thus it has happened in some instances that radiation potentials at lower voltages have been passed over entirely or only approximately located.

As X-ray excitation requires ionization of the atom, critical potentials should be indicated by an increase in the positive current as well as radiation. Careful measurements of ionization currents were made in sodium and potassium and under certain conditions the predicted effect was found as shown in some of the accompanying curves. This measurement proved more difficult than the radiation method, as the curves were never straight lines, so that in other elements ionization curves were taken only at low voltage to measure the initial potential correction.

In the statement of the mean result of observations the average precision of the observed points is given. This is doubtless always less than the probable error, but cases where systematic errors are suspected are noted. In several instances where uniformity of data permitted we have taken a number of series of readings, averaged them, and then drawn a curve through the mean points. This gives a check on the mean of separate series of readings and at least in two cases shows that what appeared to be one inflection in the separate curves was actually two, one of which was faint. As a result the mean of separate curves gave an inflection which did not agree in position with either of the inflections in the mean curve but was between the two and closer to the stronger, as should be expected.

1. POTASSIUM

The radiation potentials in potassium above the first ionization point are shown more strikingly than in any other element. There is a strong inflection at 23 volts and with higher vapor pressures a fainter inflection at 19 volts. Measurements to 140 volts show no points above 23. The pronounced change in slope does not necessarily indicate that the radiation above 23 volts is intense compared to the arc radiation, but is probably due to the fact that the arc radiation, with its high frequency limit at $\lambda=2857$, is very ineffective in producing photoelectrons from platinum. The photoelectric current measures intensity only when the spectral distribution of energy is unchanged, so that the change in slope at critical potentials is not simply related to the change in intensity. As two separate inflections were found in only 6 of the 15 curves considered, it is probable that the singly observed point at 23.3 volts was in some cases due to the overlapping effect of the two and the mean value for the upper point is

Digitized by Google

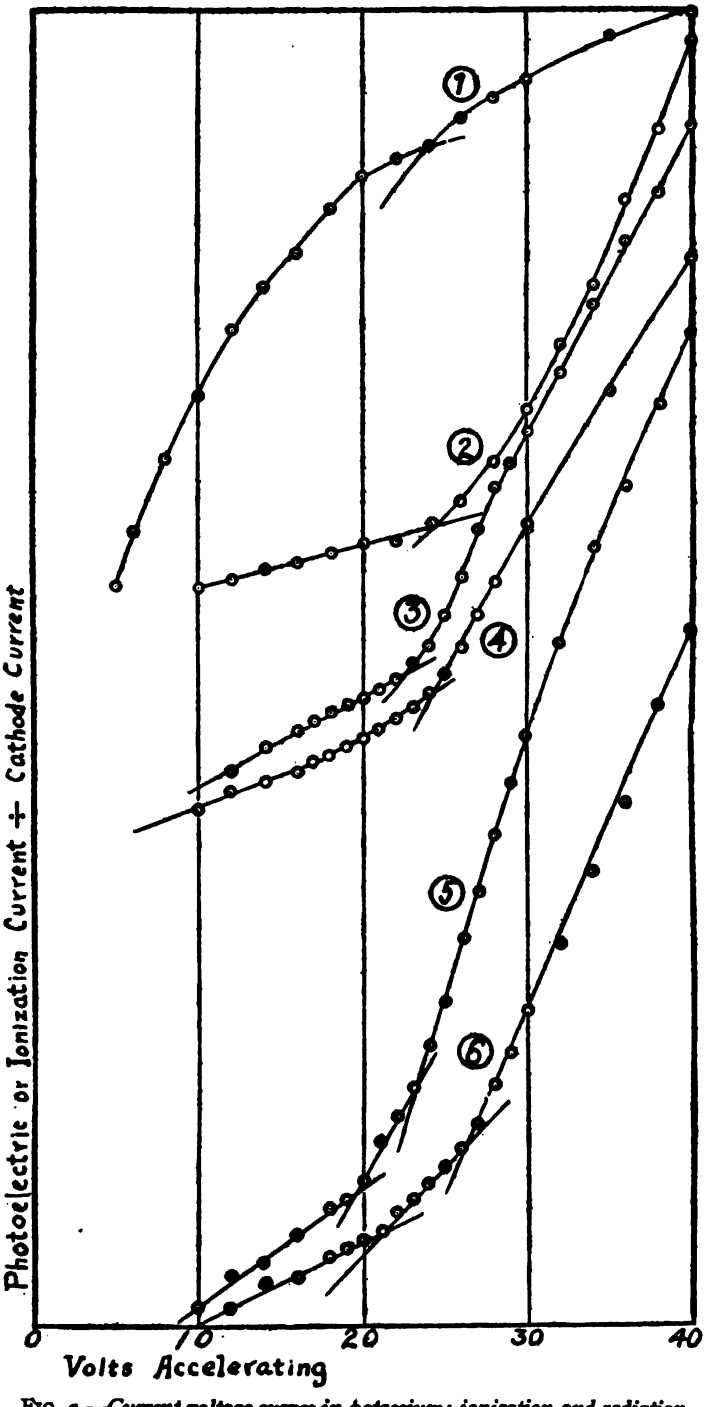

FIG. 2.—*Current-voltage curves in potassium; ionization and radiation*

Digitized by Google

accordingly too low. This may account for the rather large mean error in determining an apparently very sharp point of inflection, as shown in Table 1.

TABLE 1.—Data for Potassium Curves in Fig. 2

Curve	Temperature	Observed points	Initial potential correction
	°C	Volts	Volts
No. 1 ionization	235	24	−1
No. 2 radiation	230	24	−1
No. 3 radiation	170	23	−1
No. 4 radiation	180	24	−1
No. 5 radiation	225	19.5 23	−1.2
No. 6 radiation	240	21. 26	−1.2

Results from 15 curves (1 ionization and 14 radiation) show radiation and ionization at 23.3, mean error ±1.0; 6 curves show a lower point also at 19.3, mean error ±0.7.

2. SODIUM

Higher radiation potentials in sodium were not as marked as with potassium. They appeared sharper as the vapor density was increased, but then the currents became unsteady. Some curves at higher temperature show a marked curvature concave to the voltage axis instead of a straight line. It required long pumping to eliminate the gas evolved, and the inflection at 17 volts was at first ascribed to molecular hydrogen, which ionizes at 16 volts. It did not disappear, however, as the vacuum improved even after several days of heating, with the pumps running. Other evidence will be given later that this may be a sodium point.

TABLE 2.—Sodium Curves in Fig. 3

Curve	Temperature	Observed points	Correction
	°C	Volts	Volts
No. 1 ionization	335	38	−2
No. 2 ionization	268	36	0
No. 3 ionization	277	34	−1
No. 4 radiation	250	32	0
No. 5 radiation	315	35	0
No. 6 radiation	325	34	0
No. 7 radiation	285	16 35.5	0
No. 8 radiation	278	37	0
No. 9 radiation	285	38	−2
No. 10 radiation	280	37	−2
No. 11 radiation	255	37	−2

Results from 20 curves, 3 ionization and 17 radiation. Radiation and ionization at 35 ±1.4 volts. Eight curves showed radiation at 19 ±1.5 volts.

Digitized by Google

3. MAGNESIUM

The vapor pressure required to show higher critical potentials in magnesium necessitated a temperature of about 600° C, and the thermionic leak from the hot electrodes limited the precision.

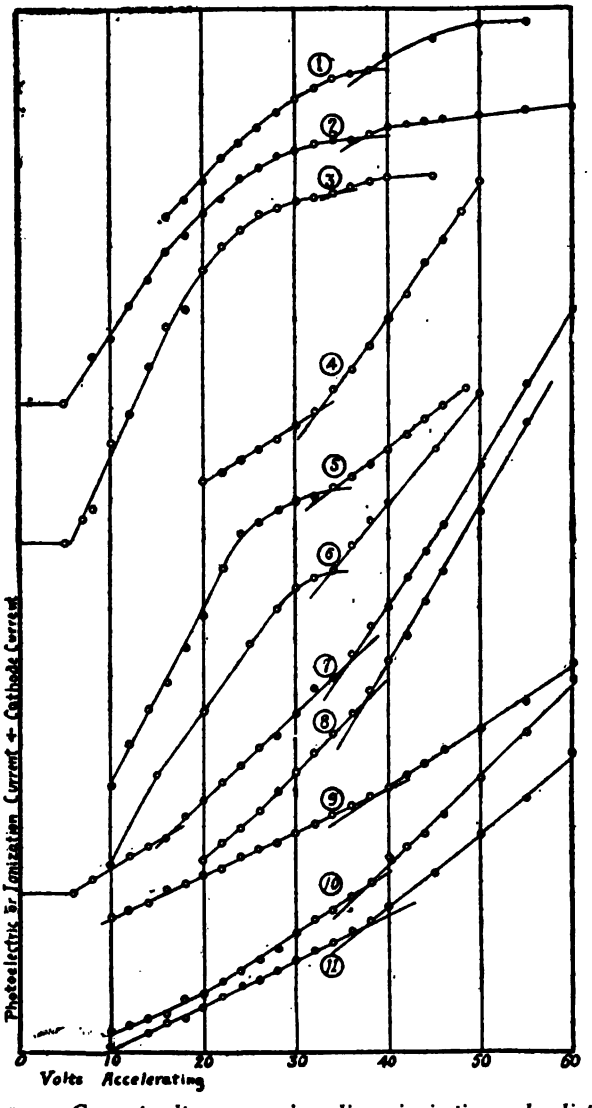

FIG. 3.—*Current-voltage curves in sodium; ionisation and radiation*

The results appear more precise, however, than with sodium. The marked curvature between 10 and 25 volts is undoubtedly due to double ionization. Theory[9] indicates that 22.6 volts are

[9] Transitions in the magnesium spectrum are described in detail in a paper by Foote, Meggers, and Mohler, to appear in Phil. Mag.

Digitized by Google

required to eject both electrons from a neutral atom and 14.95 volts to eject the second electron from a singly ionized atom. Conditions were not favorable for the measurement of these points. There may be a considerable systematic error in the 33-volt point, as the interval in readings below 30 volts was too large. The existence of this inflection was not suspected until all the data had been obtained.

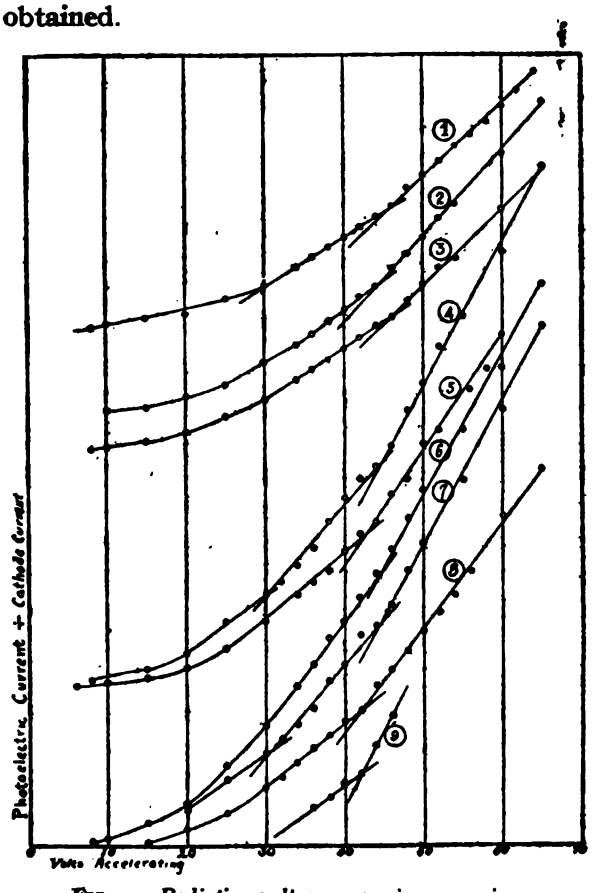

FIG. 4.—*Radiation-voltage curves in magnesium*

TABLE 3.—Magnesium Curves in Fig. 4

Curve	Temperature	Observed points	Curve	Temperature	Observed points
	°C	Volts		°C	Volts
No. 1	600	30 46	No. 6	560	44
No. 2	610	44	No. 7	560	31 44
No. 3	590	46	No. 8	615	42.5
No. 4	590	31 45	No. 9	560	42
No. 5	615	43			

Initial correction in each case +1.6. Results from 11 curves show inflection at 45.8 ±0.8; 7 curves show point at 33.5 ±1.2. A curve through the mean of 7 series of readings gives points of inflection at 47.0 and 33.6.

Digitized by Google

4. PHOSPHORUS

Results were obtained with yellow phosphorus at temperatures below 50° C. Currents were very steady and results at least for the 126-volt point fell in a small voltage range. Critical potentials at lower voltages were evident in some curves, but measurements were largely limited to a range above 80 volts. Polyvalent atoms must have many radiation potentials due to multiple ionization.

5. SULPHUR

Measurements in sulphur were difficult. The currents were unsteady at the temperatures required to give sharp inflections in the curves.

The vapor pressures must have been much higher than those used in most of the other work. The results are summarized under Table 4.

6. CARBON COMPOUNDS

These and the following substances were used in the second type of vacuum tube described. The gases CO and CO_2 were usually kept stagnant in the tube during measurements but the gas was renewed between each series. CCl_4 was streamed through the discharge chamber from a tube at the temperature given in Table 5. Data are not available for the vapor pressures corresponding to these temperatures. C_2H_2 and the other gases were streamed through a porous plug. In the case of the carbon compounds we were interested in a higher voltage range than in the foregoing elements. Consequently the field between the electrodes was so high that sparking took place under some conditions. C_2H_2 was most troublesome in this respect and measurements could be made only at low pressures. The resulting curves were least satisfactory of those obtained in carbon compounds. None were suitable for reproduction, but inflections were measurable on some and the results are tabulated. CO and CCl_4 also showed a tendency to spark when the pressure was too high. The CO measurements showed rather unsteady currents, but sharp inflections, while the CO_2 measurements were most steady, but inflections were less pronounced. CCl_4 showed inflections ascribed to chlorine as well as to carbon, but in all other cases the inflections seem to be at the same points. Apparently they are due to radiation from carbon atoms. Only a few measurements were made in a low-voltage range. The 75 volts inflection is sharp.

Digitized by Google

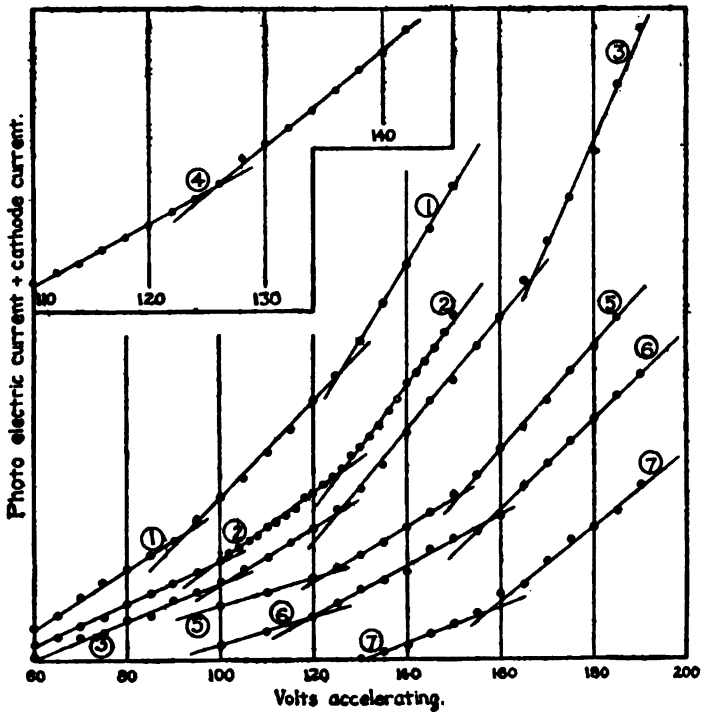

FIG. 5.—*Radiation-voltage curves in phosphorus and sulphur*

TABLE 4.—Phosphorus and Sulphur Curves in Fig. 5

Curve	Temperature	Observed points	Remarks
	°C	Volts	
No. 1 phosphorus	25	94 126	Initial correction +1 in each case
No. 2 phosphorus	40	98 126 165	
No. 3 phosphorus	40	100 125	
No. 4 phosphorus		125.5	Mean of 6 series
No. 5 sulphur		122 153	Do.
No. 6 sulphur	210	120 156	Initial correction −1 in each case
No. 7 sulphur	210	157	

PHOSPHORUS

Results from 14 curves show inflection at 126 ±0.9 volts corrected; 8 curves show a point at 99 ±2; 7 curves show a point at 163 ±2; 2 curves show a point at 109 ±1.

A mean of 7 series at 5-volt intervals gives points at 93, 111, 127, and 160. Probably the point observed in separate curves at 99 is due to the superposed effect of faint inflections at 111 and 93. The lower point is probably at 95 ±5 volts. The mean curve of 6 series at 2-volt intervals (Fig. 5, No. 4, upper scale) gives 125.5 volts.

SULPHUR

Results from 15 curves show inflections at 152 ±2.5 and at 122 ±1. A curve through the mean points of the 6 best series gives 152 and 121.

Digitized by Google

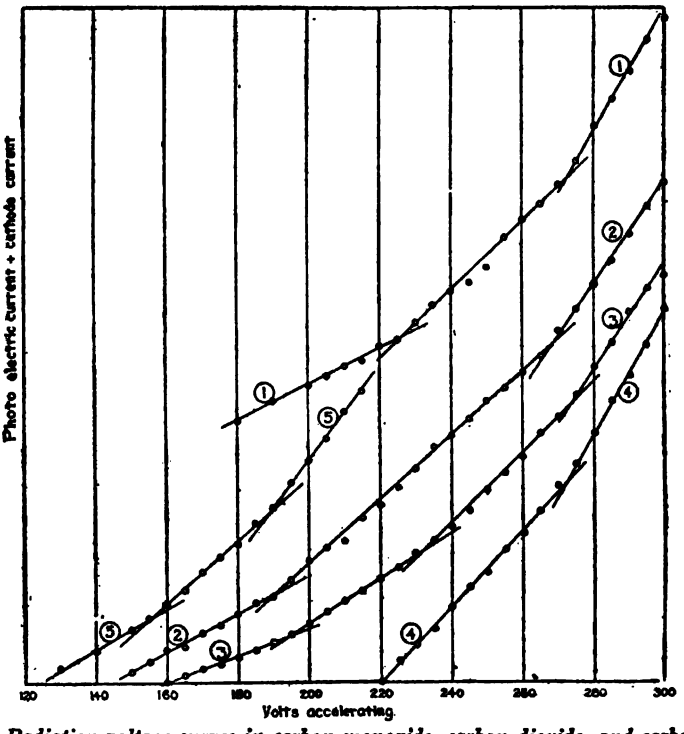

FIG. 6.—*Radiation-voltage curves in carbon monoxide, carbon dioxide, and carbon tetrachloride*

TABLE 5.—Carbon Compounds in Fig. 6

Number	Compound	Pressure or temperature	Observed points	Correction
			Volts	
1	CO	0.70 mm	225 272	.....
2	CCl_4	−73° C	190 270	+1.2
3	CCl_4	−60° C	194 230 274	+1.2
4	CO_2	0.75 mm	273	.....
5	CCl_4	−65° C	155 190	+1.2

CO

Results from 10 curves give inflections at 272.6 ±1.8; 6 curves also show a point at 229 ±3.

CO_2

Results from 8 curves give point at 273.6 ±1.9; 6 curves also show point at 234 ±2. A curve through the mean of 5 series indicates points at 272 and 235; 3 curves in low-voltage range show points near 75 and 100.

C_2H_2

Results from 4 curves show inflections at 269.5 ±0.5; 5 curves show inflections at 237 ±2. While the mean errors happen to be small, the probable error must be large, as the inflections were always faint. Three curves in low-voltage range show inflections near 75 and 110.

CCl_4

Correction +1.2 for potential across cathode. Results from 12 curves show inflection at 270.9 ±1 corrected; 12 curves give 236.2 ±2.2; 14 curves give 197.8 ±3; 2 curves give 157 ±2.

CARBON POINTS FROM ALL COMPOUNDS

271.9 ±1.9, 34 curves; 234.3 ±3.2, 29 curves; 75. approx., 6 curves.

CHLORINE POINTS

197.8 ±3, 14 curves; 157 ±2, 2 curves.

Digitized by Google

7. AIR

The study of air was for the purpose of measuring critical potentials of nitrogen. With the voltages used, sparking is avoided only by keeping the pressure low. In spite of the pressure being so low it was possible to find conditions that gave very definite inflections in the curves.

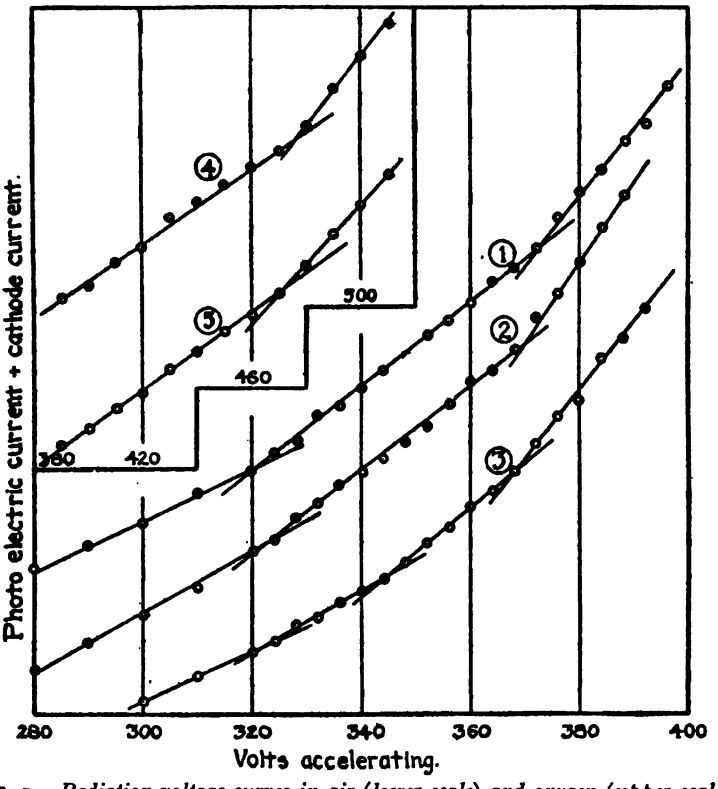

FIG. 7.—*Radiation-voltage curves in air (lower scale) and oxygen (upper scale)*

TABLE 6.—Air and Oxygen Curves in Fig. 7

Number	Pressure	Observed points	Remarks
	mm	Volts	
1 air	0.065	320 372	.....
2 air	.062	320 369	.....
3 air	.060	345 368	.....
4 oxygen	.02	477	.....
5 oxygen	.02	478	Mean of 3

NITROGEN

Twelve curves show a point at 368 ±2.5. All curves show lower points in a range between 310 and 350. Two curves of mean of 5 series each show three separate inflections as follows:

No. 1	311	353	375
No. 2	311	350	373

The mean of separate curves at 368 volts is evidently too low owing to the unresolved effect at 350. The probable value is 374 ±5.

OXYGEN

Three curves show a point at 477 ±2. The curve of the mean of these series gives 478 volts.

Digitized by Google

8. OXYGEN

Very low pressures were necessitated to avoid sparking. The results here given are only preliminary and are subject to considerable error because of the few curves taken. (See Table 6.)

Table 7 gives a summary of the observed critical potentials and the wave lengths computed from these. Fractions of volts have been omitted throughout, as they are of doubtful significance. The errors given are the mean errors in round numbers. Where none is given, the mean error has been judged too small because of systematic error or insufficient data. All values are probably subject to error of less than 5 volts.

TABLE 7

Element	Observed potentials	Corresponding wave length λ in A	Element	Observed potentials	Corresponding wave length λ in A
	Volts			Volts	
Potassium	19 ±1	650	Sulphur	122 ±1	101
	23 ±1	537		152 ±3	81.2
Sodium	17 ±2	725	Carbon	75	165
	35 ±2	353		234 ±4	52.7
Magnesium	33	374		272 ±2	45.4
	46 ±1	268	Chlorine	157	78.6
Phosphorus	95	130		198 ±3	62.3
	110	112	Nitrogen	352	35.1
	126 ±1	98.0		374	33.0
	163	77.1	Oxygen	478	25.8

IV. INTERPRETATION OF RESULTS

The following section identifies most of the observed points with X-ray series. Other potentials unrelated to X-ray series may be expected on account of multiple ionization. In none of these polyvalent elements except magnesium is there at the present time means for predicting such critical potentials.

We here use the term X-ray to denote radiation from any ring except the outer valence ring. In the case of monovalent alkali metals critical potentials above the first ionization points are accordingly due to ejection of electrons from X-ray rings and are proportional to the limiting frequency of X-ray series. Recent theories of atomic structure generally assume that the elements in the first row of the periodic table have two electron levels, in the second row three electron levels, in the third and fourth rows four electron levels, etc., corresponding to the series 2, 8, 8, 18, 18, 32 in

Digitized by Google

maximum number of electrons for each level. In the simple Bohr theory these levels may represent coplanar orbits, in more extended theories groups of crossed elliptical orbits, in the Lewis-Langmuir theory shells. Hence the X-ray spectra of the first row of elements should show only the K series, the second row K and L series, the third and fourth rows K, L, and M series, etc. The fact that there are several L and M series is explained in part by Sommerfeld as due to the existence of quantized orbits of slightly different energy value.

The radiation potentials here observed in sodium and potassium may be accordingly ascribed to the L and M series, respectively. It is possible to compute from X-ray data the L series limits for elements in the second row from magnesium to chlorine, using the Kossel relation[10] employed by Duane and Shimizu:

$$La_1 = Ka - K\alpha_1$$

where La_1 is the frequency of the principle L absorption limit, Ka the K limit, and $K\alpha_1$ the strongest K emission line. This relation corresponds to the combination law of line spectra in the visible and ultra-violet, and it is safe to assume that it holds throughout the entire spectral range. Table 8, column 4, gives the wave lengths thus computed for the elements of the second row and the corresponding potentials. The observed potentials are seen to be in fair agreement. There is an experimental error in the points computed from X-ray data comparable to that in the observed potentials because La is the difference of two frequencies of the same magnitude. The per cent error in the X-ray measurements is multiplied about twentyfold in the resulting La value.

TABLE 8.—L Limits

Atomic number	Element	Observed potential	La_1 λ in A	Computed potential	Observed potential	La_1 λ in A	Computed potential
11	Sodium	35	.....	.....	17	.....	.....
12	Magnesium	46	263.2	46.9	33	421.9	29.3
13	Aluminum	.....	177.6	69.5	.....	251.9	49.1
15	Phosphorus	126	92.2	134	95	.....	.....
16	Sulphur	152	77.1	160	122	99.9	123
17	Chlorine	198	61.9	199	157	.....	.....

K limits from measurements of Fricke, *K* lines from Siegbahn and Hjalmar, as given by Duane, Bull. N. R. C., 1 part, 6, p. 383, 1920.

[10] Phys. Rev., 14, p. 67; 1919.

Digitized by Google

A characteristic property of X-rays is the Mosely law, that the square root of the frequency of corresponding X-ray lines or limits when plotted against the atomic number gives approximately a straight line. The results for the *La* limit are so plotted in Fig. 8, upper curve. The solid points are computed from X-ray data, the circles from observed potentials. The difference between

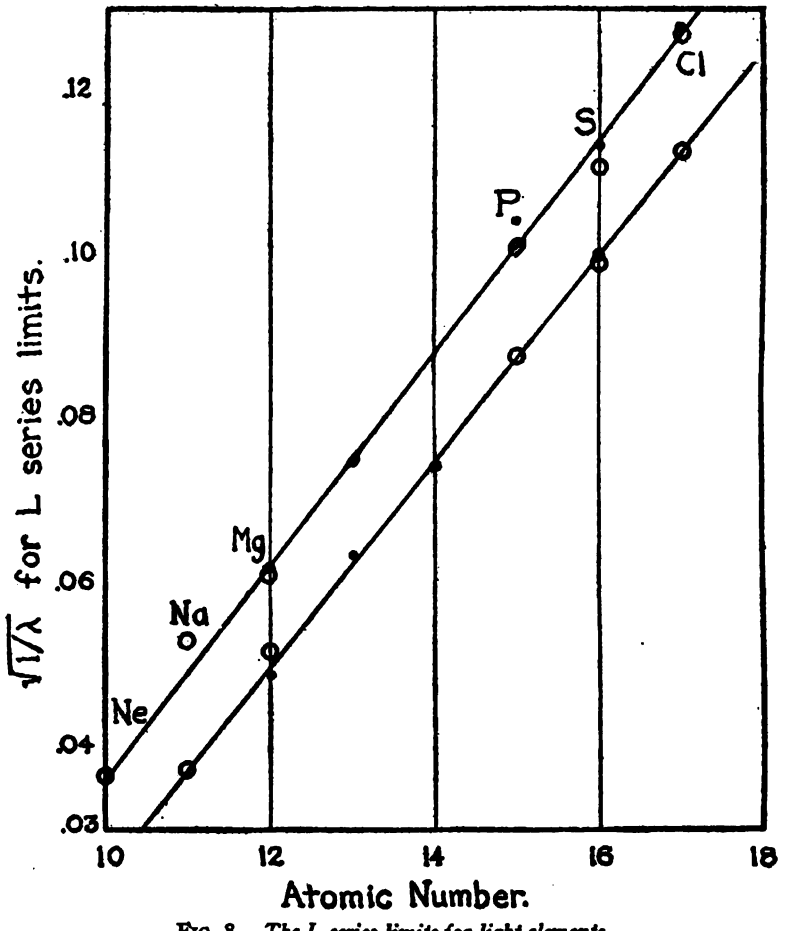

FIG. 8.—*The L-series limits for light elements*

the observed sodium point and the extrapolated straight line is greater than the probable error.

That there is an actual deviation from Mosely's law is confirmed by the results announced by Millikan from measurements of the extreme ultra-violet spectrum of sodium. He finds two isolated lines at $\lambda = 372$ and 376 A which are probably the doublet La_1 and La_2. The line 372 A corresponds to a potential of 33.2

Digitized by Google

volts, and the L limit is, of course, higher than this. The $L\alpha$ lines must be due to the valence electron falling into the L ring with an energy loss of 33 volts. Ejection of the L electron must require $33+5=38$ volts. Our observed value of 35 volts is thus probably too low rather than too high.

The deviation of the observed sulphur point is large, but the conditions for measuring this potential were unsatisfactory. The straight line between the other points is, within the estimated precision of the method, coincident with the best line through computed points.

We have included in this plot the observed first ionization potential of neon[11] at 16.7 volts, which falls exactly on the L-limit line. A similar relation has been pointed out by Kossel,[12] but he has computed the $L\alpha$ lines and used the neon point observed by Franck and Hertz at 16 volts, assuming this to be the first resonance potential.

In each of the elements of the second row a lower, relatively faint critical potential was also observed. These points plotted on the Mosely scale (lower line in Fig. 8) fall on a straight line nearly parallel to the La_1 line. The determination of these latter potentials was subject to larger errors, and the origin of the sodium point is doubtful, but the combined results seem significant. It is possible to compute from X-ray data a line nearly coincident with this. In these light elements alone a group of lines $K\alpha_3$, $K\alpha_4$, $K\alpha_5$, and $K\alpha_6$[13] have been observed. The frequencies $La_5 = Ka - K\alpha_5$ have been computed and are plotted as dots on the lower curve of Fig. 8. Table 8, right side, gives the computed wave lengths and potentials, as well as the observed points. The frequencies La_3 and La_4 fall closely together and about midway between the two lines drawn. The 110-volt point for phosphorus may be $La_{3,4}$. The computed interval $La_{,1} - La_4$ is 15 volts and the observed interval $126-110=16$ volts. In fact, we should expect a group of limits La_1, La_2 . . . . La_6, of which the first two are predominant. The pairs 1 and 2, 3 and 4, and 5 and 6 are unresolvable. The exceptionally smooth phosphorus curves showed three separate inflections, which is entirely in accord with the above prediction. For the other elements the greater experimental errors may explain the failure to resolve the inflection due to $La_{3,4}$.

[11] Horton and Davies, Proc. Roy. Soc., 98, p. 124; 1920.
[12] Zeit. f. Phys., 2, p. 470, 1920.
[13] From data of Siegbahn and Hjalmar, as given by Duane, Bull. N. R. C., 1, p. 383; 1920.

Digitized by Google

The critical potentials of carbon at 272, air 374, and oxygen 478 volts can be safely ascribed to the *K*-series limits for carbon, nitrogen, and oxygen. The evidence for this lies in part in the fact that the square root of the computed frequency plotted against atomic numbers is a straight line, as shown in Fig. 9. This line intersects the limiting frequency for helium computed from its ionization potential, 25.6 volts,[14] a relation analogous to that of neon in the *L* series. The other line in Fig. 9 is extrapolated from the *K*-series limits observed for magnesium and higher elements. The experimental points for nitrogen and oxygen fall close to this

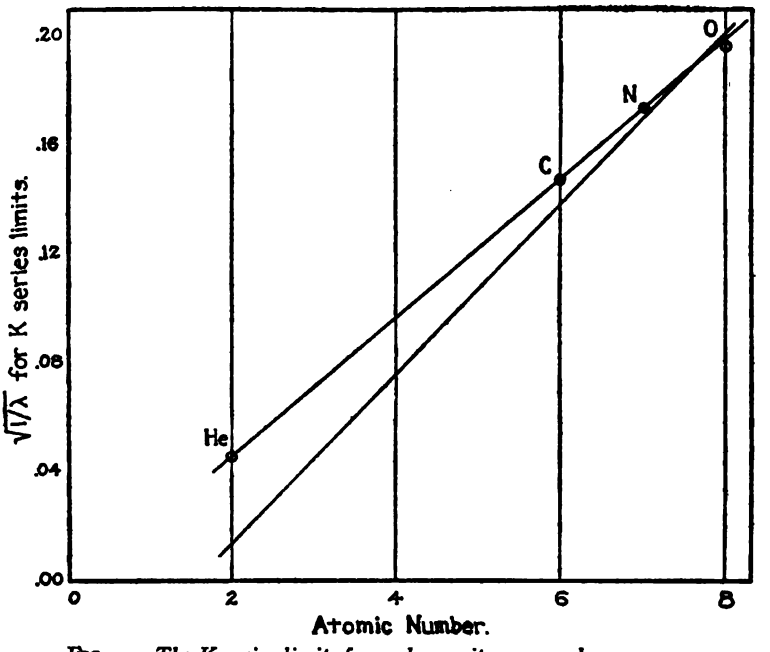

FIG. 9.—*The K series limits for carbon, nitrogen, and oxygen*

line, but the slope given by the three observed points is evidently much less. This indicates that there must be a bend in the *K* line between oxygen and magnesium.

Kurth[15] has detected critical potentials for radiation from solid carbon and oxides at $\lambda = 43.6$ and 23.8 A, respectively. The corresponding values here found are 45.4 and 25.9. The agreement is fair. Hollweck[16] has estimated the *K* limit of carbon from the absorption of thin cellulose films for radiation from a solid anode. He gives 300 volts or 41 A, but this experiment was sub-

[14] Horton and Davies, Phil. Mag. 89, p. 592; 1920.
[15] Loc. cit.
[16] C. R., 172, p. 439; 1921.

Digitized by Google

ject to much greater error than our critical potential measurements.

The two potassium points observed at 19 and 23 volts have been ascribed to the M series. It is impossible to extrapolate this series with any certainty. The relation

$$Ma = Ka - K\beta$$

gives deviations in Ma of the same order as its magnitude. All we can conclude is that the observed potentials are of the proper magnitude. It is evident that the M-series line through 19 volts will fall close to the ionization potential of argon at 15 volts, in analogous relation to the helium terminus for the K line and the neon terminus for the L line.

V. SOFT X-RAYS FROM SOLIDS

The following description of some work on the radiation from solids at low voltages is included on account of its significance in connection with the work with gases: A four-electrode tube, designed somewhat like that shown in Fig. 1, was used. The inner grid or target was an open spiral closed at the bottom by a rod of the same diameter about 5 mm below the cathode. The outer and inner grids were mounted closely together and the plate was shielded from ions in the residual gas by the same method as before. The open-grid part of the anode served to shield the cathode from the retarding field, so that the cathode current in high vacuum approached saturation at low voltage. The small outer grid confined the discharge in the residual gas to a small volume and so reduced the amount of radiation from gases.

Particular care was taken to secure the best vacuum conditions. A liquid-air trap was mounted between the pumps and vacuum tube, all closely connected by large tubing, and the apparatus was subjected to long baking at 500° C. Pressures were far below the limit of the McLeod gage (0.0001 mm.). The tube used as an ionization gage gave sensitive indications of pressure. Under the best conditions the radiation voltage curves showed no measurable radiation until a critical voltage was reached, at which point the current increased sharply. With cathode currents of over 10 milliamperes the radiation currents were measurable only with full galvanometer sensitivity (10^{-10} amperes).

Fig. 10 shows some results. Curves 1 to 7 were obtained with a nickel anode. Some indicated no measurable current to 80 volts and at this point a definite break. Curve 2 shows a small

Digitized by Google

current below 80 volts, which is probably due to gas. Curves 5, 6, and 7, however, show a definite break at 60 volts instead of 80. Previously to obtaining curve 5, the cathode temperature had been increased. At the end of the experiment it was found that the anode was coated with tungsten or some substance distilled from the tungsten cathode. Apparently it was the radiation from this coating that was observed in the latter part of the experi-

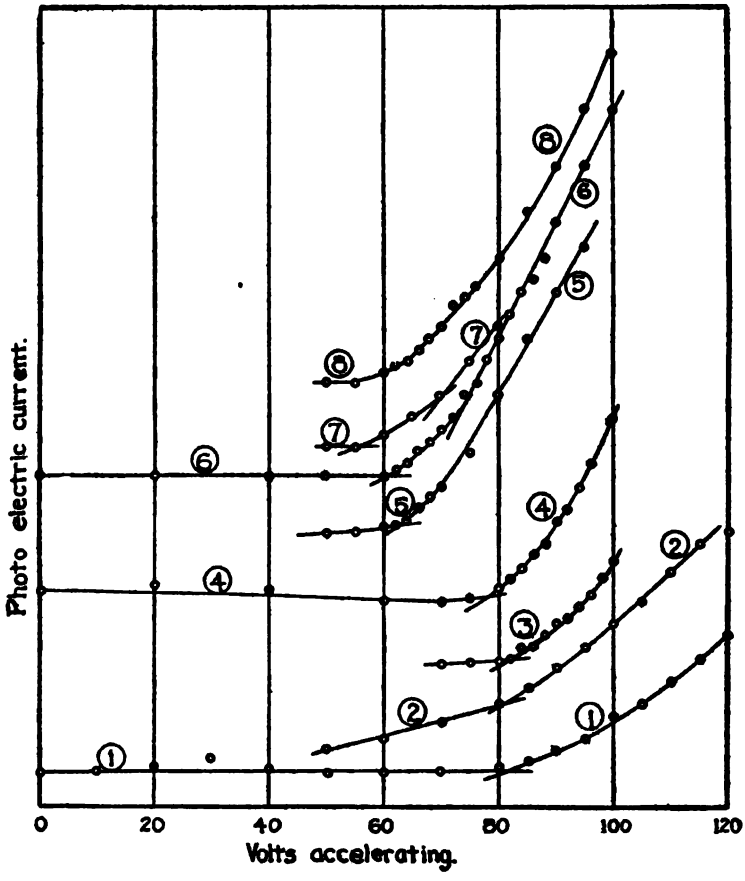

FIG. 10.—*Radiation from solids; nickel and tungsten*

ment. Curve 8, obtained with an iron anode, gives practically identical results as 5, 6, and 7 and probably for the same reason. The sharpness of inflections sometimes obtained with nickel indicates the possibilities of the method. The 80-volt point is probably the *M*-series limit. The 60-volt point can not be safely ascribed to tungsten, as some other distilled impurity may be present, for example, thorium.

Digitized by Google

Experiments were carried out with a number of metals, but the uncertainty due to surface contamination and difficulty in removing residual gas make the results of questionable value. Aluminum showed an inflection near 70 volts (probably the *L* limit), but there was always evidence of gas radiation starting at low voltage, and the point could not be accurately located.

The result, that under the best vacuum conditions there was no measurable radiation below the first critical potential, should be checked by more sensitive current measurements, as it is contrary to the work of Kurth, who always found general radiation starting at low voltage, as well as characteristic inflections.

The feebleness of the radiation from solids in comparison with that from gases precludes the possibility that the points observed in gases were due to X radiation from the inner grid.

VI. CONCLUSIONS

The present work was undertaken largely to measure the *K* and *L* limits for light elements. The *L* series is most satisfactory as a starting point, since the limits may be computed and results checked. Some general remarks on other aspects of the work follow. The elements of higher valence show evidence of many critical potentials other than X-ray limits, but these are all relatively faint. Apparently under the present conditions of measurement collisions giving multiple ionization were less probable than collisions ejecting one electron from an X-ray ring. There is evidently quite a marked difference in the probability of X-ray excitation in different gases. All these considerations of relative intensity are, of course, uncertain because of the unknown photoelectric sensitivity in this spectral region. But certainly the *L* radiation of sodium is less intense than the *M* radiation of potassium. The *L* radiation of sulphur is likewise relatively weak. Similarly marked differences are observed in the range of X-ray spectral measurements.

Comparison of the results from four different carbon compounds is also of interest. Some atomic theories indicate that X-rays of the same element in different compounds should be of different wave lengths. All four compounds give the same value for the 272-volt point within experimental error of 2 volts, or about 0.3 of an Ångström unit. It is noteworthy that all the points except the two ascribed to chlorine are shown in all the compounds and therefore must be due to carbon atoms.

Digitized by Google

Some of the results here given are only preliminary. The determination of the beginning of the *K* series is fundamental to atomic theories, and measurements with the light elements will be carried further. The extensions of the method to the *M* series and to a search for *N* and *O* series in heavy elements is also important. It is seen from the results with gases that a precision of better than 1 per cent was in some cases obtained in the potential measurements.

WASHINGTON, July, 1921.

Digitized by Google

FEB 23 192

DEPARTMENT OF COMMERCE

SCIENTIFIC PAPERS

OF THE

BUREAU OF STANDARDS

S. W. STRATTON, DIRECTOR

No. 426

THERMAL EXPANSION OF NICKEL, MONEL METAL, STELLITE, STAINLESS STEEL, AND ALUMINUM

BY

WILMER H. SOUDER, Physicist
PETER HIDNERT, Assistant Physicist
Bureau of Standards

DECEMBER 17, 1921

PRICE, 10 CENTS
Sold only by the Superintendent of Documents, Government Printing Office
Washington, D. C.

WASHINGTON
GOVERNMENT PRINTING OFFICE
1922

Digitized by Google

Digitized by Google

DEPARTMENT OF COMMERCE

SCIENTIFIC PAPERS

OF THE

BUREAU OF STANDARDS

S. W. STRATTON, DIRECTOR

No. 426

THERMAL EXPANSION OF NICKEL, MONEL METAL, STELLITE, STAINLESS STEEL, AND ALUMINUM

BY

WILMER H. SOUDER, Physicist
PETER HIDNERT, Assistant Physicist
Bureau of Standards

DECEMBER 17, 1921

PRICE, 10 CENTS
Sold only by the Superintendent of Documents, Government Printing Office
Washington, D. C.

WASHINGTON
GOVERNMENT PRINTING OFFICE
1922

Digitized by Google

Digitized by Google

THERMAL EXPANSION OF NICKEL, MONEL METAL, STELLITE, STAINLESS STEEL, AND ALUMINUM

By Wilmer H. Souder and Peter Hidnert

ABSTRACT

Data on the thermal expansion of 29 samples of commercial nickel, monel metal, stellite, stainless steel, and exceptionally pure aluminum are presented. The apparatus used was essentially the same as that described in Scientific Paper of the Bureau of Standards, No. 352.

COMMERCIAL NICKEL.—A slight irregularity was perceptible near 350° C, but there was no marked change or anomalous expansion such as was observed by previous investigators in the case of pure nickel.

MONEL METAL.—The expansion curves of monel metal were found to be fairly regular. The average coefficients of expansion of the various samples (containing from 60 to 69 per cent nickel) are all practically equal for the range from 25 to 300° C.

STELLITE.—The expansion curves show irregularities in the region between 300 and 500° C. A hammered stellite was found to have smaller coefficients of expansion than an unhammered sample of corresponding composition.

STAINLESS STEEL.—The coefficients of expansion of the annealed and the hardened sample of stainless steel are less than the coefficients of ordinary iron or steel, which is probably due to the large amount of chromium. On heating, both samples indicated critical regions which extended from approximately 825 to approximately 855° C. The transformation point on cooling occurred at about 800° C.

ALUMINUM.—The thermal expansion of the two samples of aluminum investigated between room temperature and 600° C may be represented by the following empirical equation:

$$L_t = L_0[1 + (21.90\ t + 0.0120\ t^2)\ 10^{-6}].$$

The average coefficients of expansion of the various materials for several temperature ranges are given in Table 16.

CONTENTS

	Page
I. Introduction	497
II. Apparatus	498
III. Experimental results	499
1. Nickel	499
2. Monel metal	504
3. Stellite	507
4. Stainless steel	511
5. Aluminum	514
IV. Summary	517

I. INTRODUCTION

The increasing use of nickel and nickel alloy wire in spark plugs, of monel metal for high-pressure steam valves, stems, seats, etc., of stellite for surgical and household uses, of stainless steel

Digitized by Google

for numerous purposes, such as aeroplane and automobile engine valves, pump rods, and marine fittings, and of aluminum or its alloys, almost universally, where lightness is necessary, has created a demand for data on the thermal expansion of these materials. It is necessary to properly select the materials which are component parts of accurate apparatus in order to compensate for the varying expansions of these materials. Differential expansions between nickel and porcelain in spark plugs and between monel metal and steel or brass in steam valves are important factors to be considered by manufacturers of such articles.

This paper includes original data on the thermal expansion of 10 samples of commercial nickel, 10 samples of monel metal, 5 samples of stellite, 2 samples of stainless steel, and 2 samples of exceptionally pure aluminum, in addition to the results obtained by previous observers on the expansion of nickel and aluminum.

The samples of nickel and monel metal were prepared by the International Nickel Co., Bayonne, N. J.; the stellite specimens by the Haynes Stellite Co., Kokomo, Ind., through A. W. Gray, an employee of the L. D. Caulk Co., Milford, Del.; the samples of stainless steel by the Firth-Sterling Steel Co., McKeesport, Pa.; and the samples of aluminum by the Aluminum Company of America, New Kensington, Pa. These companies also furnished the chemical compositions and previous treatments of the samples. Acknowledgment is due these companies for their cooperation and to R. L. Coleman, jr., and J. E. Wall, of the Bureau of Standards, for assistance in the tests, computations, and other work.

II. APPARATUS

The apparatus was essentially the same as that used in a similar investigation of the thermal expansion of insulating materials, to the description of which reference[1] should be made for a description of the general procedure. The electrically heated air furnace illustrated in Fig. 1 of the same paper was used for practically all of the tests. Each specimen was 30 cm in length and about 1 cm in diameter (or diagonal). In most instances the two observation wires (chromel, or alloy of platinum, and osmium), indicating the positions of the ends of the sample, were suspended from two V notches cut around and at right angles to its axis, so that the wires were prevented from

[1] B. S. Sci. Papers, No. 352; 1919.

Digitized by Google

moving laterally in the direction of the length of specimen due to the formation of oxide films or scales, if any, at high temperatures. The only desirable lateral movements of the wires were those due to the changes in temperature of the specimen.

III. EXPERIMENTAL RESULTS

The results obtained on the thermal expansion of nickel, monel metal, stellite, stainless steel, and aluminum, in addition to the determinations by previous investigators on nickel and aluminum are given in the following subsections.

1. NICKEL

In 1869 Fizeau[2] published the value 0.00001279 for the coefficient of expansion of nickel at 40° C. The sample had been previously reduced by hydrogen and compressed.

About 30 years later Tutton[3] made nine individual determinations on the thermal expansion of pure nickel. He found that the rate of expansion (or instantaneous coefficient) at any temperature t between 6 and 121° may be represented by the value

$$0.00001248 + 0.0000000148\ t, \text{ or } 10^{-8}\ (1248 + 1.48\ t).$$

Holborn and Day[4] made some measurements on the expansion of a nickel bar. From their observations, which were taken on five different days, average coefficients of expansion were computed which are given in the following table:

TABLE 1.—Coefficients of Expansion of Nickel (Holborn and Day)

Temperature range in degrees centigrade	Average coefficients of expansion × 10^6 on—				
	June 30	July 2	July 4	Sept. 18	Sept. 19
0 to 250	13.8	13.9	14.2	.....	.....
250 to 375	.....	16.2	.....	.....	.....
250 to 500	16.2	.....	16.2	.....	.....
375 to 500	.....	16.4	.....	.....	.....
500 to 750	17.9	18.0	17.9	.....	.....
0 to 750	.....	.....	.....	15.9	15.9
750 to 1000	.....	.....	.....	19.2	19.2

Before the first test the rod of nickel was 482.6 mm at 0°. After each test the sample was approximately 0.02 mm shorter than before the test.

[2] Fizeau, Comptes Rendus, 68, p. 1125, and Poggendorff's Annalen, 138, p. 30.
[3] Tutton, Proc. Roy. Soc., Nos. 415 and 419; 1899.
[4] Holborn and Day, Annalen der Physik, 89 (IV ser.), p. 104; 1901.

Digitized by Google

The observations can be represented by the following quadratic equation

$$\lambda^* = (13460\, t + 3.315\, t^2)\ 10^{-9}$$

only above 375°. Holborn and Day state that nickel undergoes a transformation in the region of 300°.

Harrison[5] determined the coefficients of expansion of a very pure specimen of nickel wire and commented as follows:

"Up to a temperature of about 365° the curve is regular. Between 365 and 380° there occurs an anomalous change in the expansion, while above 380° the curve is again regular, though now it is linear, with a different slope to the regular part of the curve which precedes it. No difference in the position or shape of the anomalous portion of this curve was noticed, whether the temperature was rising or falling. It is also worthy of notice that in every case the wire returned after heating to its original length. There was no permanent elongation."

The following table gives average coefficients of expansion for ranges between 0 and 550°:

TABLE 2.—Average Coefficients of Expansion of Nickel Wire (Harrison)

Temperature range in degrees centigrade	Average coefficients of expansion	Temperature range in degrees centigrade	Average coefficients of expansion
0 to 50	0.0000128	350 to 365	0.0000205
50 to 100	.0000136	380 to 400	.0000191
150 to 200	.0000151	400 to 450	.0000189
250 to 300	.0000174	450 to 500	.0000192
300 to 350	.0000191	500 to 550	.0000190

"The anomalous part of the curve extends from 340 to 370°, which is very approximately the range over which changes occur in the thermoelectric force and resistance of the same specimen of nickel. Moreover, it has recently been shown by the author, in some experiments not yet published, that this interval is also that over which the magnetic permeability of the same specimen changes—the actual critical temperature at which the susceptibility vanishes being just over 370°."

Harrison states that the cause of the anomalous change in expansion is to be sought for in the metal itself, although in the case of impure metals the true effect might be masked and modified by changes of a chemical nature.

* λ represents the expansion or change per unit length from 0° to any temperature t (between 375 and 1000° C.).

[5] Harrison, Phil. Mag., 7 (sixth series), p. 626; 1904.

Digitized by Google

Randall[6] made two series of determinations of the coefficients of expansion of a cylinder of pure nickel furnished by Zeiss, Jena. His results are presented in two tables and a figure, which indicates a critical region between 280 and 370°. The coefficients of expansion of the second series are less than those of the first series. Randall's values are not given here, for he states that neither set of results can justly be considered as representing the coefficient of expansion of nickel, due to the fact that he did not thoroughly anneal the sample by repeated heatings before making observations.

Henning[7] determined the linear expansion of nickel by comparing its change of length at various temperatures with the known expansion of platinum as determined by Scheel. The following table gives the linear expansion (or change in length) in millimeters of a 1 meter rod of nickel:

TABLE 3.—Expansion of Nickel (Henning)

Temperature range in degrees centigrade	Expansion of 1 meter rod	Temperature range in degrees centigrade	Expansion of 1 meter rod
	mm		mm
+16 to −191	−2.095	+16 to 500	7.336
+16 to +250	+3.268	+16 to 750	11.737
+16 to 375	5.291	+16 to 1000	16.553

From these results the average coefficients of expansion given in the following table were computed:

TABLE 4.—Coefficients of Expansion of Nickel (Henning)

Temperature range in degrees centigrade	Average coefficients of expansion	Temperature range in degrees centigrade	Average coefficients of expansion
−191 to +16	10.1×10^{-6}	16 to 500	15.2×10^{-6}
+16 to 250	14.0	500 to 750	17.6
16 to 375	14.7	500 to 1000	18.4

In the present investigation determinations were made on the thermal expansion of 10 samples of commercial nickel from room temperature to about 600° C. The nickel content varied from about 94 to 99 per cent. Five samples were hot-rolled, and the remaining five samples of corresponding compositions were hot-rolled and annealed.

[6] Randall, Phys. Rev., **20**, p. 85; 1905.
[7] Henning, Annalen der Physik, **22** (fourth series), p. 631; 1907.

Digitized by Google

The following table gives the observations of one of the samples (S653). These results are represented graphically in the accompanying figure Fig. 1, which shows a typical expansion curve:

TABLE 5.—Observations on Sample of Commercial Nickel

Observation No.	Temperature	Δl*	Observation No.	Temperature	Δl*
	°C			°C	
1	21.8	0×10⁻⁶	10	348.1	4858×10⁻⁶
2	69.6	628	11	367.7	5180
3	138.9	1591	12	383.4	5430
4	212.2	2667	13	388.0	5509
5	254.8	3327	14	504.4	7410
6	300.8	4047	15	602.2	9063
7	312.0	4239	16	447.0	6429
8	326.8	4491	17	262.6	3381
9	341.5	4756	18	30.8	80

*Represents the change per unit length from the length at the initial temperature 21.8° C.

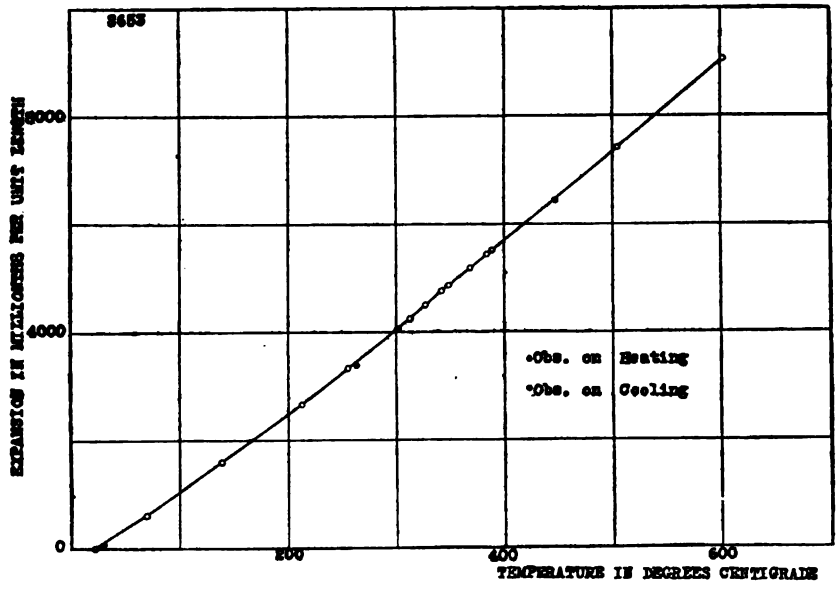

FIG. 1.—*Thermal expansion of commercial nickel*

A comparatively large number of observations were taken on each specimen between 300 and 400° C in an attempt to locate transformation regions, if any. No marked change was observed, but in most of the expansion curves of these samples a slight irregularity was perceptible in the region near 350° C. This

Digitized by Google

agrees with Harrison's[8] statement that the true effect in the case of impure metals might be masked and modified by changes of a chemical nature.

The chemical compositions and the average coefficients of expansion for various temperature ranges are given in the following table:

TABLE 6.—Chemical Compositions and Average Coefficients of Expansion of Samples of Commercial Nickel

Lab. No.	Material	Composition in per cent						
		Ni	Cu	Fe	Mn	C	Si	S
S635	Hot-rolled, ⅝-inch round	99.06	0.12	0.37	0.19	0.12	0.12	0.027
S636	Same; annealed at 1600° F for 1 hour							
S652	Hot-rolled, ⅝-inch round, low carbon	99.02	.12	.37	.22	.08	.16	.020
S653	Same; annealed at 1650° F for 1 hour							
S654	Hot-rolled, ⅝-inch round, high carbon	98.76	.17	.38	.18	.22	.26	.020
S655	Same; annealed at 1650° F for 1 hour							
S637	Hot-rolled, ¼-inch round	97.05	.15	.44	2.08	.09	.15	.029
S638	Same; annealed at 1600° F for 1 hour							
S639	Hot-rolled, ¼-inch round	94.21	.14	.46	4.92	.12	.10	.060
S640	Same; annealed at 1600° F for 1 hour							

Lab. No.	Material	Average coefficients of expansion × 10^6								
		25 to 100° C	100 to 200° C	200 to 300° C	300 to 400° C	400 to 500° C	500 to 600° C	25 to 300° C	300 to 600° C	25 to 600° C
S635	Hot-rolled, ⅝-inch round	13.2	14.4	15.3	16.8	15.5	16.9	14.4	16.4	15.4
S636	Same; annealed at 1600° F for 1 hour	13.3	14.5	15.4	16.4	16.6	16.3	14.5	16.5	15.5
S652	Hot-rolled, ⅝-inch round, low carbon	12.9	14.5	15.4	16.9	16.5	16.8	14.4	16.7	15.6
S653	Same; annealed at 1650° F for 1 hour	13.3	14.5	15.5	16.7	16.3	16.9	14.5	16.6	15.6
S654	Hot-rolled, ⅝-inch round, high carbon	13.0	14.2	15.7	15.9	15.7	14.4	14.4	15.8	14.9
S655	Same; annealed at 1650° F for 1 hour	13.3	14.2	15.6	16.3	16.2	16.3	14.5	16.3	15.4
S637	Hot-rolled, ¼-inch round	13.1	13.5	14.8	17.2	16.6	17.1	13.8	17.0	15.5
S638	Same; annealed at 1600° F for 1 hour	13.5	14.3	15.8	16.0	16.6	17.3	14.6	16.6	15.7
S639	Hot-rolled, ¼-inch round	13.2	14.1	15.4	15.9	16.7	17.3	14.3	16.7	15.5
S640	Same; annealed at 1600° F for 1 hour	13.3	14.1	15.4	15.9	16.6	17.6	14.3	16.7	15.6

From an examination of the preceding table it is apparent that the annealing of the hot-rolled samples in most cases caused a slight increase in the coefficients. The average coefficients

[8] Harrison, Phil. Mag., 7 (sixth series), p. 626; 1904.

Digitized by Google

between 25 and 300° for the samples containing 98.76 to 99.06 per cent nickel are 14.4×10^{-6} for the hot-rolled and 14.5×10^{-6} for the annealed specimens. For the range from 25 to 600° C, the coefficients of the five hot-rolled samples vary from 14.9×10^{-6} to 15.6×10^{-6}, and for the five annealed specimens from 15.4×10^{-6} to 15.7×10^{-6}. These coefficients are considerably greater than those of most of the porcelains described in Scientific Papers of the Bureau of Standards, No. 352.

The average coefficients of expansion of the 10 samples of nickel vary from 12.9×10^{-6} to 13.5×10^{-6} for the range 25 to 100° C. These coefficients are approximately 10 or 20 per cent greater than those of ordinary steel for the same range.

On cooling from the maximum temperature (about 600° C) to room temperature the observations were generally slightly below the heating curve, so that after the thermal expansion tests the specimens were shorter than before these tests. Holborn and Day[9] also found a diminution in the length of a rod of nickel after each heating and cooling. Harrison,[10] however, found that in every case nickel wire returned to its original length after heating.

The following table gives the changes in length from the original lengths after the thermal expansion tests. The minus (−) sign indicates a decrease in length:

TABLE 7.—Changes in Length Due to Heat Treatment Received During Test

Laboratory number	Change in length after test	Laboratory number	Change in length after test
	Per cent		Per cent
S635	−0.004	S655	−.018
S636	−.013	S637	−.020
S652	−.004	S638	−.004
S653	−.004	S639	−.003
S654	[a] −.064	S640	.000

[a] At any given temperature above room temperature the variation between the heating and cooling curves did not exceed this value.

2. MONEL METAL

Monel metal is a natural alloy of the approximate formula: Nickel, 67 per cent; copper, 28 per cent; and the remaining 5 per cent made up of iron, manganese, silicon, etc.

[9] Holborn and Day, Annalen der Physik, 39 (fourth series), p. 104; 1901.
[10] Harrison, Phil. Mag., 7 (sixth series), p. 626; 1904.

Digitized by Google

Measurements were made on the thermal expansion of 10 samples of monel metal from room temperature to about 600° C. Two samples were cast, and three were hot-rolled. The remaining five specimens of corresponding compositions and treatments received additional heat treatment; that is, they were annealed.

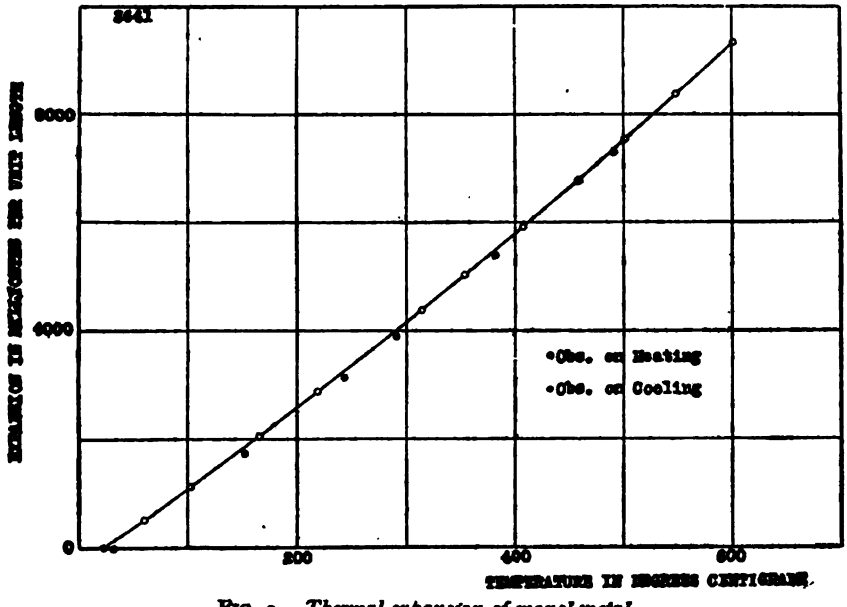

FIG. 2.—*Thermal expansion of monel metal*

A typical expansion curve (S641) is shown in Fig. 2, and the observations from which it was obtained are given in Table 8.

TABLE 8.—Observations on Expansion of a Sample of Monel Metal

Observation No.	Temperature	Δl*	Observation No.	Temperature	Δl*
	°C			°C	
1	23.4	0×10⁻⁶	10	501.2	7536×10⁻⁶
2	60.2	517	11	548.5	8370
3	102.6	1125	12	601.3	9354
4	165.6	2054	13	490.8	7300
5	218.8	2873	14	382.1	5394
6	314.6	4375	15	290.9	3890
7	353.9	5023	16	243.7	3141
8	407.6	5919	17	152.6	1734
9	457.9	6678	18	82.1	−8

* Δl represents the change per unit length from the length at the initial temperature 23.4° C.

The expansion curves on heating were found to be fairly regular. On cooling the observations were slightly below the heating curves in most cases.

Digitized by Google

The chemical compositions and the average coefficients of expansion for various temperature ranges are given in the following table:

TABLE 9.—Chemical Compositions and Average Coefficients of Expansion of Samples of Monel Metal

Lab. No.	Material	Composition in per cent							
		Ni	Cu	Fe	Mn	C	Si	S	Pb
S648	Leaded monel, cast ⅜ inch square	60.05	32.46	2.21	2.00	0.15	0.87	0.085	2.22
S649	Same; annealed 1650° F for 1 hour								
S663	Cast nonleaded monel, ⅜ inch square	66.18	28.42	2.37	2.10	.18	.70	.038	.....
S664	Same; annealed at 1650° F and slowly cooled								
S641	Hot-rolled monel wire rod, ¼ inch round	66.58	29.57	1.79	1.78	.15	.09	.090	.....
S688	Same; annealed 1600° F for 1 hour								
S650[a]	Hot-rolled monel metal, ⅜ inch rod, high carbon	67.32	28.73	1.74	1.66	[b].31	.19	.085	.....
S651	Same; annealed 1650° F for 1 hour								
S661	Hot-rolled monel ⅛ inch sheet, ⅜ inch wide	68.87	29.03	1.60	0.18	.13	.15	.027	.....
S662	Same; annealed 1600° F for 1 hour								

Lab. No.	Material	Average coefficients of expansion × 10^6							
		25 to 100° C	100 to 200° C	200 to 300° C	300 to 400° C	400 to 500° C	500 to 600° C	25 to 300° C	300 to 600° C	25 to 600° C
S648	Leaded monel, cast ⅜ inch square	13.9	15.0	15.8	16.8	17.7	20.6	15.0	18.4	16.7
S649	Same; annealed 1650° F for 1 hour	14.3	15.0	15.7	16.7	18.1	18.3	15.1	17.7	16.5
S663	Cast nonleaded monel, ⅜ inch square	13.7	15.1	15.7	16.6	17.7	18.5	15.0	17.6	16.4
S664	Same; annealed at 1650° F and slowly cooled	13.9	15.0	15.7	16.6	17.8	18.7	15.0	17.7	16.4
S641	Hot-rolled monel wire rod, ¼ inch round	14.2	14.9	15.5	16.7	17.0	18.1	14.9	17.3	16.1
S688	Same; annealed 1600° F for 1 hour	14.3	15.3	15.8	16.5	17.4	17.7	15.2	17.2	16.2
S650[a]	Hot-rolled monel metal, ⅜ inch rod, high carbon	14.5	15.1	15.9	16.4	17.1	16.2	15.2	16.6	15.9
S651	Same; annealed 1650° F for 1 hour	14.3	15.0	15.8	16.5	17.4	17.7	15.1	17.2	16.2
S661	Hot-rolled monel ⅛ inch sheet, ⅜ inch wide	14.2	14.7	15.6	16.4	17.6	17.9	14.9	17.3	16.2
S662	Same; annealed 1600° F for 1 hour	14.0	15.0	15.9	16.4	17.3	18.1	15.1	17.3	16.2

[a] The coefficients given for this sample are the average values obtained on two duplicate samples.
[b] Graphitic carbon=0.15.

Digitized by Google

It is interesting to note that the average coefficients for the range from 25 to 300° C are all practically equal. Above 300° there are some marked differences. For example, the coefficients of S648 and S649 between 500 and 600° C differ by 2.3×10^{-6}. In most cases the coefficients of the annealed and unannealed samples are equal or nearly so.

From a comparison of the average coefficients for the entire temperature range from 25 to 600° C, it is seen that the coefficients of the cast alloys are greater than those of the hot-rolled alloys, and that the leaded monel samples have the greatest coefficients.

The coefficients of expansion of monel metal are larger than those of the samples of nickel (described in the previous section). In addition to nickel monel metal contains about 30 per cent copper, which element has larger coefficients than those of the nickel or monel samples. The copper constituent, therefore, evidently raises the value of the coefficient of the alloy of copper and nickel.

3. STELLITE

This subsection includes five samples of stellite, which alloy is usually composed of cobalt, chromium, and tungsten. The alloy is sometimes modified by the addition of iron or by the substitution of molybdenum for tungsten and possibly nickel for cobalt. The discovery and other features connected with the application of this alloy have been described by the inventor.[11]

The approximate chemical compositions of the samples and the average coefficients of expansion for various temperature ranges are given in the following table:

[11] Elwood Haynes, Proc. Eng. Soc. Western Pennsylvania, 35, p. 467; Feb., 1920, and American Machinist, 53, No. 4, p. 171; July 22, 1920.

Digitized by Google

TABLE 10.—Approximate Chemical Compositions and Average Coefficients of Expansion of Samples of Stellite

Lab. No.	Material	Approximate composition in per cent					Average coefficients of expansion $\times 10^6$ in various ranges of temperature	
		Co	Cr	W	C	Fe	20 to 100° C	100 to 200° C
S521	Festel metal [a]	[b] 22.5	21.2	.....	0.7	55.3	15.6 [c] / 12.5 [c]	16.7 / 13.0
S534	Stellite, soft malleable	80	20	.....	.....	.....	14.1	15.1
S535	Stellite, hard malleable	55	40	3	2	.....	13.4	15.2
S537	Stellite, hard malleable, hammered	55	40	3	2	.....	12.2	13.1
S536	Stellite No. 2	55	35	10	.....	.....	11.0	12.3

Lab. No.	Material	Average coefficients of expansion $\times 10^6$ in various ranges of temperature						
		200 to 300° C	300 to 400° C	400 to 500° C	500 to 600° C	20 to 300° C	300 to 600° C	20 to 600° C
S521	Festel metal [a]	17.6 / 13.8	17.8 / 14.8	17.6 / 15.7	17.0	16.7 / 13.1	17.5	[d] 17.1 .....
S534	Stellite, soft malleable	16.2	15.9	16.0	18.9	15.2	16.9	16.1
S535	Stellite, hard malleable	16.0	16.3	17.5	20.2	15.0	18.0	16.5
S537	Stellite, hard malleable, hammered	14.0	14.3	15.4	17.9	13.2	15.8	14.6
S536	Stellite No. 2	13.6	13.8	13.3	16.9	12.4	14.7	[e] 13.6

[a] According to the inventor "festel metal is somewhat indefinite in its composition. The name was derived from Fe, the symbol for iron, prefixed to the first syllable of stellite, and means stellite with more or less iron added. Festel metal is a mixture of cobalt, chromium, and iron, and generally contains from 10 to 25 per cent of the latter, but may contain as high as 40 or even 50 per cent."

[b] The chemical composition of this sample of festel metal was determined by J. A. Scherrer of this Bureau. The sample also contains 0.1 per cent silicon.

[c] Values given on this horizontal line were obtained on a second test.

[d] Average coefficient of expansion between 600 and 900° C, was 19.7×10^{-6}.

[e] After this test stellite No. 2 was cooled to about −100° C; average coefficient of contraction from 19 to −94° C was 10.2×10^{-6}.

Figs. 3 to 6 show the expansion curves of four samples of stellite (S534, 535, 537, and 536) from room temperature to about 600° C. After these tests one of the specimens (S536) was cooled from room temperature to about −100° C, and the results were represented graphically in Fig. 7.

From an examination of the curves and the average coefficients of expansion it is evident that the expansion curves in most cases are irregular in the region between 300 and 500° C. For example, in the case of the soft malleable stellite (S534), the rate of expansion increases regularly with temperature up to 300° C and then decreases to a nearly constant value over the range from 300 to 500° C. At the latter temperature the average rate of expansion again increases rapidly from 500 to 600° C.

Digitized by Google

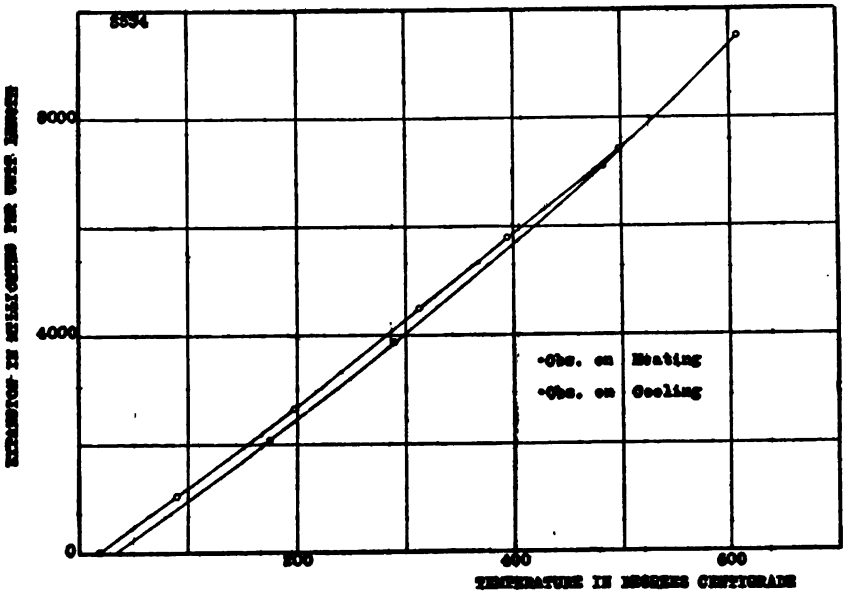

FIG. 3.—*Thermal expansion of soft malleable stellite*

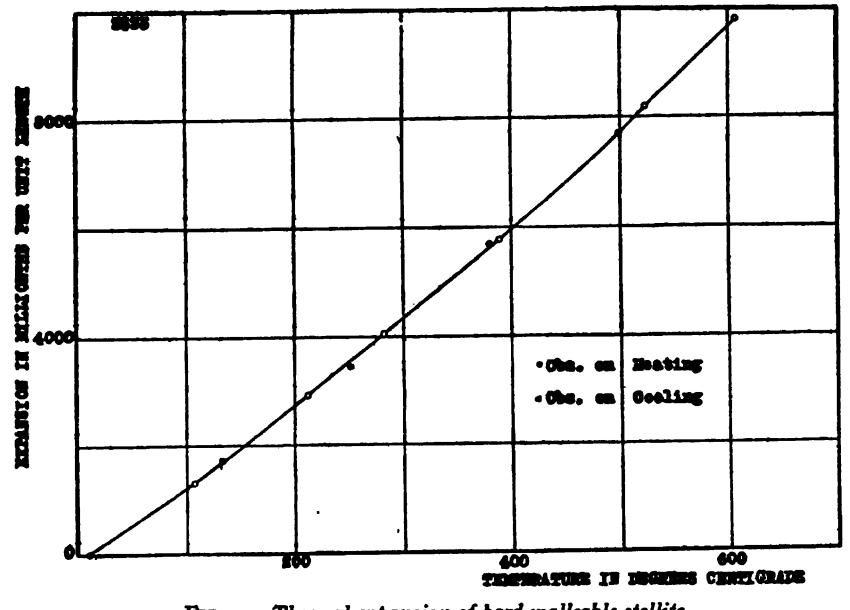

FIG. 4.—*Thermal expansion of hard malleable stellite*

Digitized by Google

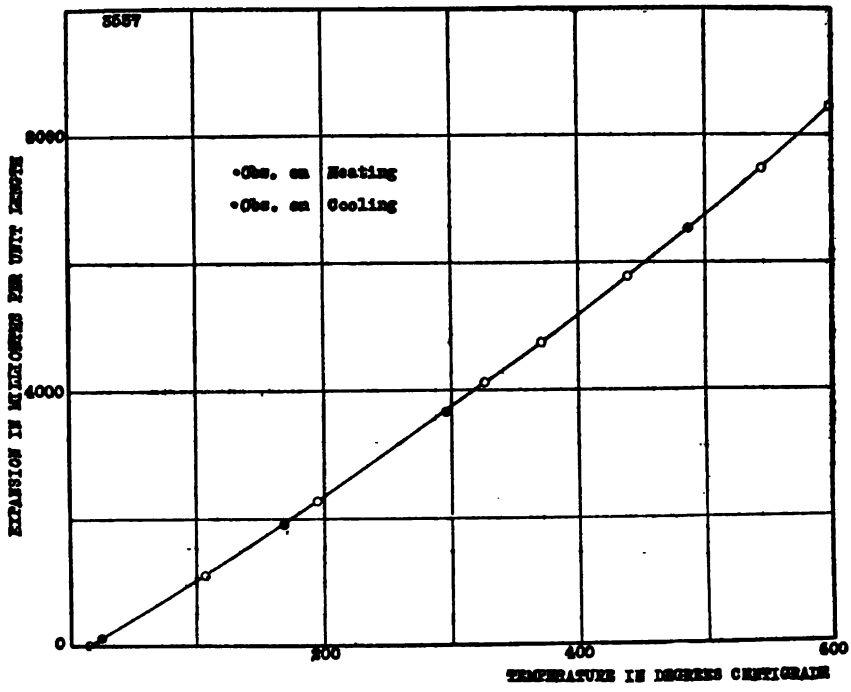

FIG. 5.—*Thermal expansion of hard malleable stellite, hammered*

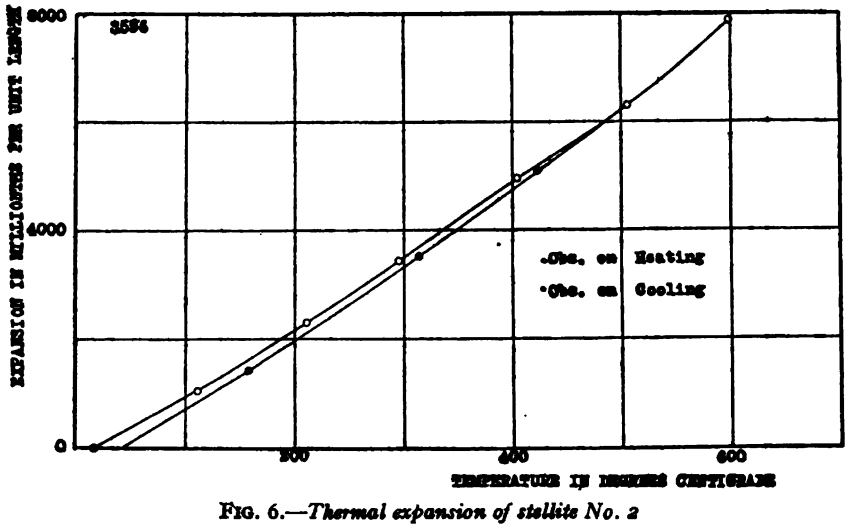

FIG. 6.—*Thermal expansion of stellite No. 2*

Digitized by Google

The stellite containing 10 per cent tungsten (S536) has the smallest coefficients of expansion of any sample investigated. The hammered stellite (S537) has smaller coefficients than the unhammered sample of corresponding composition, which indicates that hammering may lower the values of the coefficients of expansion.

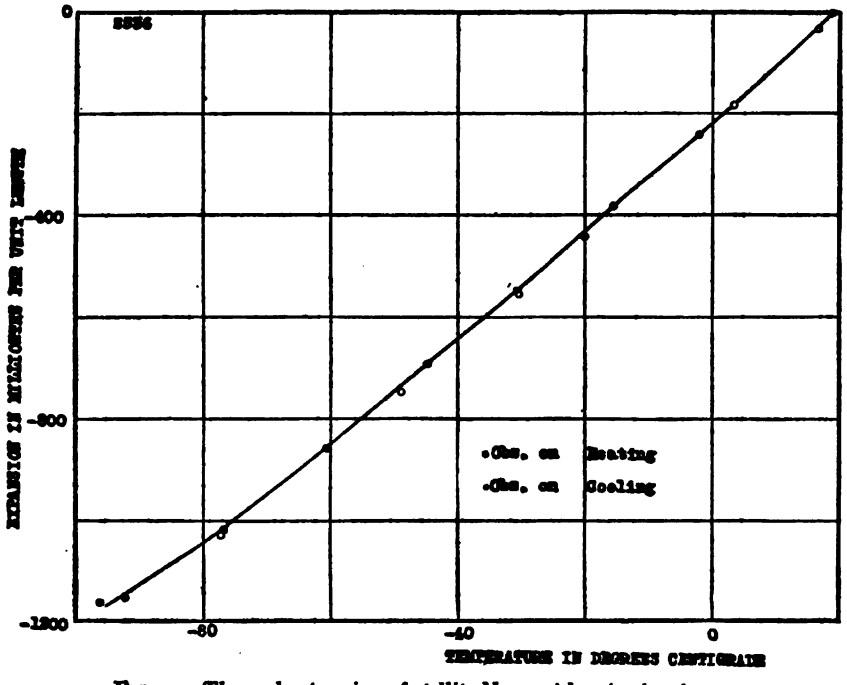

FIG. 7.—*Thermal expansion of stellite No. 2 at low temperatures*

4. STAINLESS STEEL

Determinations were made on the thermal expansion of two samples of stainless steel from room temperature to about 900° C. The composition of these specimens was as follows: Carbon, 0.30 per cent; silicon, 0.11 per cent; manganese, 0.18 per cent; sulphur, 0.011 per cent; phosphorus, 0.020 per cent; and chromium, 13.10 per cent. One of the samples (S620) was electrically melted, cast into ingots, hammer cogged, finished on rolling mill, and then annealed at 1400° F. The other sample (S680) was hardened (and not drawn). Its hardness number[12] was found to be 77.7 (scleroscope).

[12] Determined by W. B. Topping, of this Bureau.

Digitized by Google

The expansion curves of the two steels are shown in Figs. 8 and 9. On heating, both samples indicated critical regions which extended from approximately 825 to approximately 855° C. The transformation point of ordinary steel usually occurs at lower temperatures. For the two samples of stainless steel the transformation point on cooling occurred at approximately 800° C.

Up to the transformation regions the heating and cooling curves of the annealed sample are fairly regular. The cooling curve lies

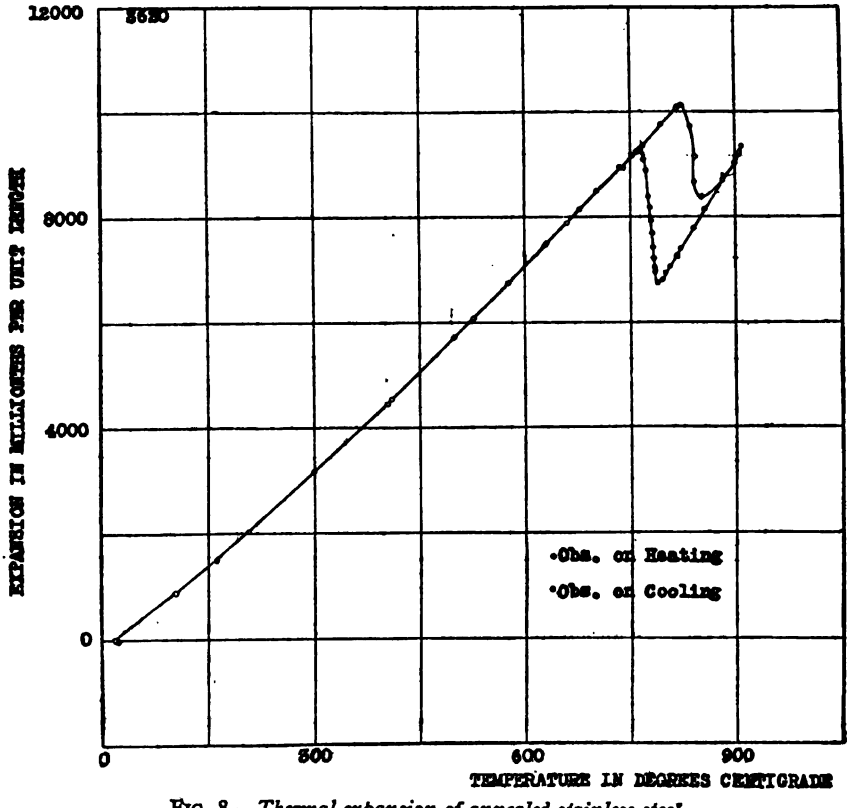

FIG. 8.—*Thermal expansion of annealed stainless steel*

slightly below the heating curve, and at the end of the test the sample was very slightly shorter than before the test, which indicates that this specimen did not suffer any great permanent deformation due to the heat treatment incident to the test.

In the case of the hardened steel the curve is irregular between 200 and 400° C, where the strains produced in hardening were probably released. Above 400° the sample behaved like the annealed specimen. This property is in agreement with the samples of carbon steel recently studied. (Complete data on these

Digitized by Google

steels will be available at a future date.) The cooling curve lies below the heating curve, and at the end of the test the sample was 0.088 per cent shorter than before the test. The cooling curve of the hardened sample is fairly regular and in close agreement with the curve of the annealed sample, as will be shown later from a comparison of the coefficients.

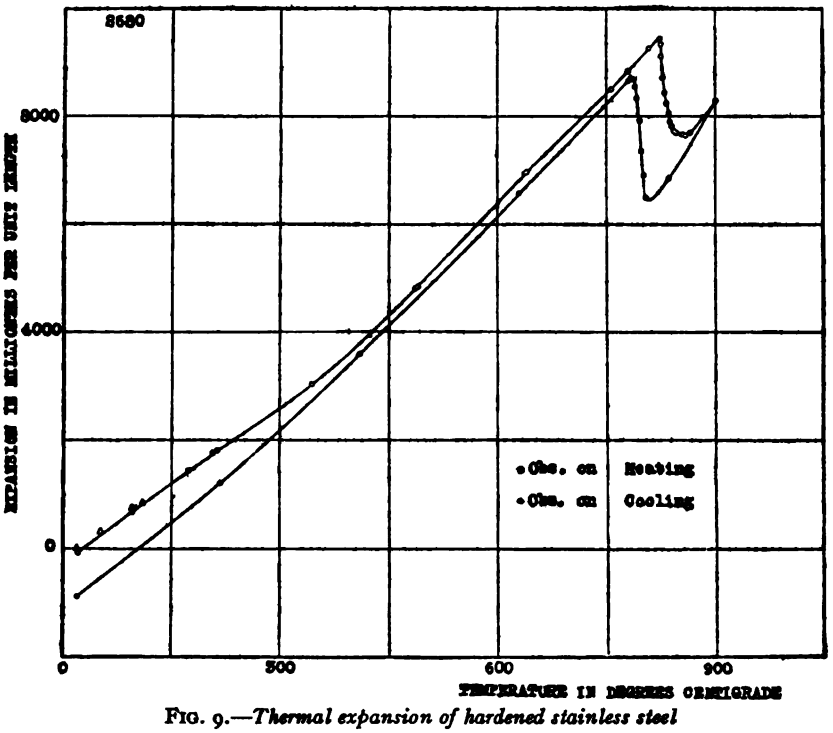

FIG. 9.—*Thermal expansion of hardened stainless steel*

The coefficients of expansion of the two samples of stainless steel for various temperature ranges are given in the following tables:

TABLE 11.—Coefficients of Expansion of Stainless Steel

Temperature range in degrees centigrade	Average coefficients of expansion × 10⁶		Temperature range in degrees centigrade	Average coefficients of expansion × 10⁶	
	Hardened	Annealed		Hardened	Annealed
20 to 100	[a] 9.6	10.3	400 to 600	13.8	13.3
	9.9		600 to 800	13.4	13.6
20 to 200	9.8	10.7	20 to 600	11.2	12.1
200 to 400	9.9	12.3			

[a] Value on first heating to about 100° C. After the sample was cooled to room temperature the test was carried to 900° C. First heating plotted at triangles. (See Fig. 9.)

Digitized by Google

Up to 400° C the coefficients of expansion of the annealed sample are appreciably larger than those of the hardened sample. Annealing, therefore, caused an increase in the values of the coefficients of the hardened sample up to 400° C.

Since the cooling curve of the annealed sample is only slightly below the heating curve, the coefficients on cooling and on heating do not materially differ. However, in the case of the hardened sample, there are appreciable differences, as may be seen by comparing the coefficients of contraction with the coefficients of expansion for corresponding temperature intervals.

TABLE 12.—Coefficients of Contraction of Hardened Stainless Steel

Temperature range in degrees centigrade	Average coefficients of contraction × 10^6	Temperature range in degrees centigrade	Average coefficients of contraction × 10^6
600 to 400	13.6	200 to 20	10.5
400 to 200	12.2	600 to 20	12.1

The coefficients of contraction of the hardened sample agree closely with the coefficients of the annealed sample. This means that the former specimen on cooling behaved like the annealed sample, as, in fact, it should, since the heat treatment constituted an annealing operation.

The coefficients of expansion of both the hardened and the annealed stainless steel are less than the coefficient of ordinary iron or steel, which is probably due to the large amount of chromium.

5. ALUMINUM

Although bearing only a slight similarity or relation to the previous nontarnishing alloys or metals reported in this paper, it is desired to record the expansion of exceptionally pure aluminum.

Some years ago Dr. R. Seligman[13] cited an example of the importance of accurate information on the thermal expansion of aluminum. "I was recently called in to examine an aluminum vacuum pan made on the Continent for a firm of oil distillers, about 10 feet long, which had collapsed. I found that the collapse was due to insufficient allowance for the difference in expansion of aluminum and iron under the influence of high temperature."

A number of investigations on the expansion of aluminum have been undertaken by various observers. Some of the results are given in this section.

[13] Trans. Far. Soc., 7, p. 228; 1911.

Digitized by Google

In 1901 Dittenberger[14] made a number of determinations on a 0.5-meter rod of pure material obtained from the Allgemeinen Elektrizitäts-Gesellschaft (of Germany). The table gives the average coefficients of expansion which were computed from his data.

TABLE 13.—Coefficients of Expansion of Aluminum (Dittenberger)

Temperature interval in degrees centigrade	Average coefficients × 10^6					Temperature interval in degrees centigrade	Average coefficients × 10^6				
	Nov. 11	Nov. 12	Nov. 13	Nov. 29	Nov. 30		Nov. 11	Nov. 12	Nov. 13	Nov. 29	Nov. 30
0-250	.....	23.7	23.6	23.8	.....	0-375	25.4	25.4	25.4	.....	.....
250-375	.....	28.8	28.8	.....	.....	0-500	26.2	26.2	26.1	26.5	.....
250-500	.....	.....	.....	29.2	.....	0-610	.....	.....	.....	.....	28.0
375-500	28.6	28.5	28.3	.....	.....						

He states that the expansion of aluminum can not be represented by a quadratic equation, especially at 250 and 610° C, and, from analogy with other metals, aluminum evidently undergoes a transformation at these temperatures.

In 1907 Henning[15] experimented with the same rod of aluminum used by Dittenberger, but obtained values which are somewhat higher than those given by the latter. The average coefficients of expansion, computed from Henning's data, are as follows:

TABLE 14.—Coefficients of Expansion of Aluminum (Henning)

Temperature interval in degrees centigrade	Average coefficients	Temperature interval in degrees centigrade	Average coefficients
+16 to −191	18.4×10^{-6}	+16 to +500	27.2×10^{-6}
+16 to +250	24.4	+16 to +610	29.0
+16 to +375	26.3		

In April, 1919, Jaeger and Scheel[16] reported data on the thermal expansion of two samples of aluminum containing, respectively, 1.2 and 0.4 per cent of impurities, chiefly iron and silicon. The expansion is summed up by the approximate formula

$$L_t = L_0 [1 + (22.9\, t + 0.009\, t^2)\ 10^{-6}]$$

between the limits −78 to 500° C.

[14] Z. Ver. deutsch. Ing., 46, p. 1532; 1902.
[15] Ann. d. Phys. (4), 22, p. 631; 1907.
[16] Elekt. Zeits. 40, p. 150, Apr. 3, 1919.

Digitized by Google

In the present investigation two samples were cut from a bar of aluminum of high purity, prepared by the Aluminum Company of America, New Kensington, Pa.

The metal was melted in an Acheson graphite crucible at a temperature which at no time exceeded 1350° F and was poured at 1300° F in a green sand mold. The bar was taken directly from the mold and received no further heat treatment before the thermal expansion tests. The analysis of samples taken from the ends of the bar after it was cast was as follows:

Silicon	0.12
Iron	0.13
Copper	0.006
Al (by diff.)	99.744

The following table gives the results obtained for the average coefficients of expansion for various temperature ranges:

TABLE 15.—Coefficients of Expansion of Aluminum

Temperature range in degrees centigrade	Average coefficients		Temperature range in degrees centigrade	Average coefficients	
	Sample 1 (S613)	Sample 2 (S615)		Sample 1 (S613)	Sample 2 (S615)
20 to 100	23.7×10^{-6}	23.8×10^{-6}	500 to 600	35.9×10^{-6}	36.2×10^{-6}
100 to 200	25.4	26.1	20 to 300	25.6	25.7
200 to 300	27.3	27.0	300 to 600	32.7	33.1
300 to 400	29.8	30.2	20 to 600	29.3	29.5
400 to 500	32.3	32.9			

The average equation

$$L_t = L_0[1 + (21.90\, t + 0.0120\, t^2)\ 10^{-6}]$$

is given as the most probable second-degree equation for the expansion of this aluminum (99.74 per cent) from room temperature to 600° C. The length at any temperature t as determined from this equation is accurate to ± 0.00004 per unit length.

Observations were taken on cooling on sample 1 (S613) and are plotted in Fig. 10. The cooling curve was found to be slightly above the heating curve, and at the end of the test the specimen was about 0.01 per cent longer than before the test. The length of the other specimen was practically the same before and after the test.

Digitized by Google

We have been unable to verify conclusively the irregularities[17] which Dittenberger indicated at 250 and 610° C. These were, perhaps, the result of impurities.

IV. SUMMARY

This paper gives data on the thermal expansion of 29 samples of commercial nickel, monel metal, stellite, stainless steel, and aluminum, in addition to the results obtained by previous observers

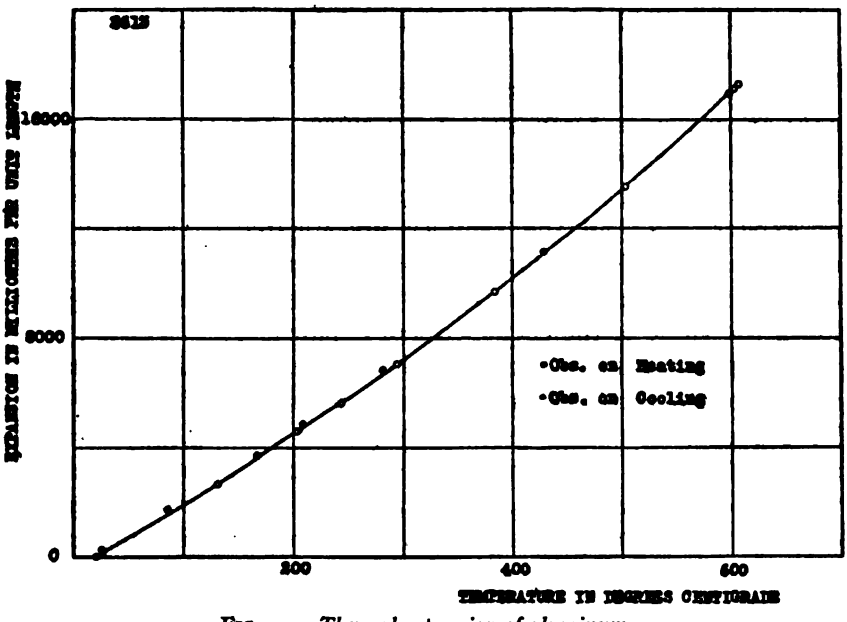

FIG. 10.—*Thermal expansion of aluminum*

on the expansion of nickel and aluminum. All of these materials except stainless steel were examined from room temperature to about 600° C. The samples of stainless steel were heated from room temperature to 900° C. The apparatus used was essentially the same as that described in Scientific Papers of the Bureau of Standards, No. 352.

NICKEL.—In most of the expansion curves of commercial nickel a slight irregularity was perceptible in the region near

[17] J. D. Edwards, of the Aluminum Co. of America, suggests a number of possible explanations for the irregularities in the thermal expansion of aluminum at 250 and 610° C. "It may be only a coincidence, but the temperature of recrystallization of aluminum is about 250° C, and if these other investigators had been using cold-rolled specimens they might have noticed a break in the curve at that temperature. The specimens sent to the Bureau were cast, and of course no recrystallization would be expected in them. Furthermore, the solubility of certain elements, such as iron and silicon in aluminum, is very low, and the presence of those impurities changing from solid solution might produce an irregularity in the results.

Digitized by Google

350° C, but there was no marked change or anomalous expansion such as was observed by previous investigators in the case of pure nickel. Annealing of the hot-rolled samples of nickel usually caused a slight increase in the values of the coefficients of expansion.

MONEL METAL.—The expansion curves of monel metal were found to be fairly regular. The average coefficients of expansion of the various samples for the range from 25 to 300° C are all practically equal. For the temperature range from 25 to 600° C, the average coefficients of the cast samples are greater than those of the hot-rolled alloys.

STELLITE.—For the samples of stellite (except festel metal) only approximate compositions are given. The expansion curves show irregularities in the region between 300 and 500° C. The stellite containing 10 per cent tungsten has the smallest coefficients of expansion of all the samples investigated. The hammered stellite has smaller coefficients than the unhammered sample of corresponding composition, which indicates that hammering may lower the value of the coefficients of expansion.

STAINLESS STEEL.—The expansion curves, including the critical regions of the annealed and the hardened sample of stainless steel, have been shown in Figs. 8 and 9. On heating, both samples indicated critical regions which extended from approximately 825 to approximately 855° C. The transformation point on cooling occurred at about 800° C. Up to the transformation regions the heating and cooling curves of the annealed sample are fairly regular. In the case of the hardened stainless steel, the curve is irregular between 200 and 400° C where the strains produced in hardening were released. Above 400° this sample behaved like the annealed specimen. The coefficients of expansion of the hardened or annealed stainless steel are less than the coefficients of ordinary iron or steel, which is probably due to the large amount of chromium.

ALUMINUM.—The thermal expansion of the two samples of aluminum investigated between room temperature and 600° C may be represented by the following empirical equation:

$$L_t = L_o [1 + (21.90\, t + 0.0120\, t^2)\ 10^{-6}].$$

The thermal expansion of aluminum was found to be approximately twice as large as that of any of the other materials discussed in this paper.

Digitized by Google

For comparison the average coefficients of expansion of the materials investigated for several temperature ranges are given in the following table:

TABLE 16.—Average Coefficients of Expansion of Nickel, Monel Metal, Stellite, Stainless Steel, and Aluminum

Materials	Average coefficients of expansion × 10^6			
	Room temperature to 100° C	Room temperature to 300° C	300 to 600° C	Room temperature to 600° C
10 samples of commercial nickel (94 to 99 per cent)	12.9 to 13.5	13.8 to 14.6	15.3 to 17.0	14.9 to 15.7
10 samples of monel metal (60 to 69 per cent Ni)	13.7 to 14.5	14.9 to 15.2	16.6 to 18.4	15.9 to 16.7
5 samples of stellite (22 to 80 per cent Co)	11.0 to 15.6	12.4 to 16.7	14.7 to 18.0	13.6 to 17.1
2 samples of stainless steel [a] (13 per cent Cr)	9.6 to 10.3			11.2 to 12.1
2 samples of aluminum	23.7 to 23.8	25.6 to 25.7	32.7 to 33.1	29.3 to 29.5

[a] The smaller values refer to a hardened sample and the larger values to an annealed sample of stainless steel. For the range from 600 to 800° C the average coefficients of expansion were 13.4×10^{-6} and 13.6×10^{-6}, respectively.

WASHINGTON, May 6, 1921.

Digitized by Google

Digitized by Google

OF THE
UNIVERSITY
OF
CALIFORNIA

FEB 23 192

DEPARTMENT OF COMMERCE

SCIENTIFIC PAPERS

OF THE

BUREAU OF STANDARDS

S. W. STRATTON, DIRECTOR

No. 427

SOME EFFECTS OF THE DISTRIBUTED CAPACITY BETWEEN INDUCTANCE COILS AND THE GROUND

BY

GREGORY BREIT, Consulting Physicist
Bureau of Standards

DECEMBER 21, 1921

PRICE, 5 CENTS
Sold only by the Superintendent of Documents, Government Printing Office
Washington, D. C.

WASHINGTON
GOVERNMENT PRINTING OFFICE
1922

Digitized by Google

Digitized by Google

SOME EFFECTS OF THE DISTRIBUTED CAPACITY BETWEEN INDUCTANCE COILS AND THE GROUND

By Gregory Breit

ABSTRACT

It is well known that the effective capacity of two condensers which are connected in series is $\frac{C_1 C_2}{C_1+C_2}$ if C_1, C_2 are the capacities of the two condensers. In the paper here presented it is shown that this rule does not always hold, and it is found that another more general relation is true. This relation depends upon the method of measuring the effective capacity. If the method used is that of resonance adjustment and if a coil symmetrical as to its two terminals is used in the resonance experiment, then it is shown mathematically and verified experimentally that $\frac{C_1 C_2}{C_1+C_2}$ is a linear function of $\frac{1}{C_1+C_2}$.

When an inductance coil is used in electrical circuits, its distributed capacity affects its behavior in various ways. Most of these are due to the capacity between various parts of the coil as well as to the capacity of the coil to ground. The two are usually indistinguishable. Thus, the effective capacity of a coil depends both on the capacity between parts of the coil and on the capacity of parts of the coil to ground. The same is true for the resistance. There appears to be one effect, however, which depends on the effective capacity of the coil to ground, primarily. This effect is observed when two condensers connected in series are connected across the coil terminals and when the common terminal of the two condensers is grounded.

Let C_1, C_2 be the capacities of the two condensers. Vary either C_1 or C_2 until resonance is obtained. If the coil had no capacity to ground, resonance would be obtained whenever $\frac{C_1 C_2}{C_1+C_2}$ had a proper value, depending on the frequency and on the inductance of the coil, but independent of the particular values of C_1 and C_2.

If the coil has capacity to ground, this is no longer true. In this case another more complicated relation takes the place of the relation

$$\frac{C_1 C_2}{C_1+C_2} = \text{const.}$$

The nature of this relation may be found by representing the distributed capacity to ground by a series of capacities, as in Fig. 1. The whole coil is here divided into n sections, and the capacity of each to ground is represented by a lumped capacity

Digitized by Google

at its end, as e. g., by C_3. The line GH represents the ground. The inductances of the various sections are written, respectively, as $L_1, L_2, \cdots L_n$. The resistances of the same sections are denoted by $R_1, R_2, \cdots R_n$. The emfs induced in the sections are written as $E_1e^{jwt}, E_2e^{jwt}, \cdots E_ne^{jwt}$, where $E_1, E_2 \cdots E_n$ are supposed to be independent of the time, where ϵ is the base of natural logarithms and where $j=\sqrt{-1}$. It is understood in writing the emfs in the complex form just used that the real part of the complex quantity written is considered only, and that in all the equations that follow the real part only of both sides will be considered. The mutual inductance between the sections having inductances L_1, L_2 will be written M_{12} and a similar notation will be used for all other sections.

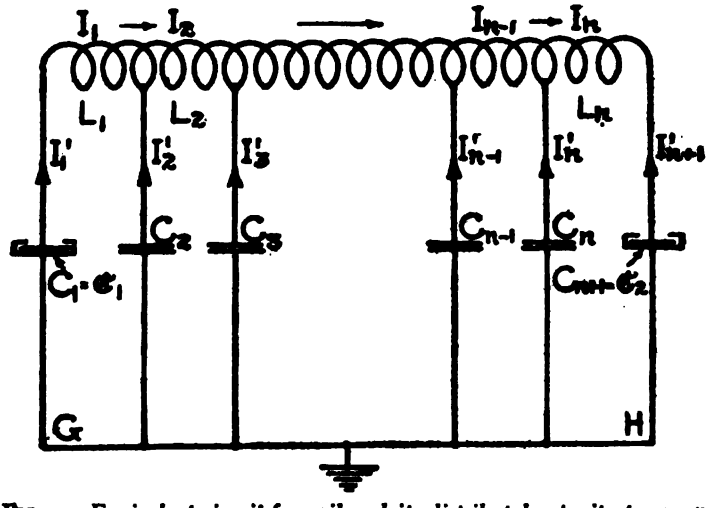

FIG. 1.—*Equivalent circuit for coil and its distributed capacity to ground*

The currents in $L_1, L_2, \cdots L_n$ are written

$$I_1e^{jwt}, I_2e^{jwt}, \cdots I_ne^{jwt}$$

The currents in $C_1, C_2, \cdots C_{n+1}$ are written as

$$I'_1e^{jwt}, I'_2e^{jwt}, \cdots I'_{n+1}e^{jwt}$$

Kirchhoff's laws, when applied to the network of Fig. 1, give

$$\begin{cases} I'_1 = I_1 \\ I'_2 + I_1 = I_2 \\ I'_3 + I_2 = I_3 \\ - - - - - \\ - - - - - \\ I'_n + I_{n-1} = I_n \\ I_n = -I'_{n+1} \end{cases} \quad (1)$$

Digitized by Google

and also

$$\left\{\begin{aligned}
&(L_1 j\omega + R_1) I_1 + M_{12} j\omega I_2 + M_{13} j\omega I_3 + \cdots + M_{1n} j\omega I_n \\
&\qquad - \frac{I'_2}{jC_2\omega} + \frac{I'_1}{jC_1\omega} = E_1 \\
&M_{12} j\omega I_2 + (L_2 j\omega + R_2) I_2 + M_{23} j\omega I_3 + \cdots + M_{2n} j\omega I_n \\
&\qquad - \frac{I'_3}{jC_3\omega} + \frac{I'_2}{jC_2\omega} = E_2 \\
&M_{n1} j\omega I_1 + \cdots + (L_n j\omega + R_n) I_n \\
&\qquad - \frac{I'_{n+1}}{jC_{n+1}\omega} + \frac{I'_n}{jC_n\omega E_n} = E_n
\end{aligned}\right. \tag{2}$$

or using (1)

$$\left\{\begin{aligned}
&\left(L_1 j\omega + R_1 + \frac{1}{j\omega C_1} + \frac{1}{j\omega C_2}\right) I_1 + \left(M_{12} j\omega - \frac{1}{j\omega C_2}\right) I_2 + M_{13} j\omega I_3 \\
&\qquad + \cdots + M_{1n} j\omega I_n = E_1 \\
&\left(M_{12} j\omega - \frac{1}{j\omega C_2}\right) I_1 + \left(L_2 j\omega + R_2 + \frac{1}{j\omega C_2} + \frac{1}{j\omega C_3}\right) I_2 \\
&\qquad + \left(M_{23} j\omega - \frac{1}{j\omega C_3}\right) I_3 + \cdots + M_{2n} j\omega I_n = E_2 \\
&\qquad \cdots\cdots\cdots\cdots\cdots\cdots\cdots\cdots \\
&\qquad \cdots\cdots\cdots\cdots\cdots\cdots\cdots\cdots \\
&M_{n1} j\omega I_1 + \cdots + \left(M_{n,n-1} j\omega - \frac{1}{j\omega C_n}\right) I_{n-1} \\
&\qquad + \left(L_n j\omega + R_n + \frac{1}{j\omega C_n} + \frac{1}{j\omega C_{n+1}}\right) I_n = E_n
\end{aligned}\right.$$

Resonance occurs when the determinant of this system of equations vanishes, provided in that determinant all the resistances are set equal to zero. This is only approximately true, but is a good approximation if the resistances are small, because for small values of the resistances the position of resonance is independent of the resistances. Thus, the condition for resonance is

$$\left|\begin{array}{llll}
L_1 - \left(\frac{1}{C_1} + \frac{1}{C_2}\right)\frac{1}{\omega^2}, & M_{12} + \frac{1}{C_2\omega^2}, & M_{13}, \cdots\cdots & M_{1n} \\
M_{12} + \frac{1}{C_2\omega^2}, & L_2 - \left(\frac{1}{C_2} + \frac{1}{C_3}\right)\frac{1}{\omega^2}, & M_{23} + \frac{1}{C_3\omega^2}, \cdots & M_{2n} \\
\cdots\cdots\cdots\cdots & \cdots\cdots\cdots\cdots & \cdots\cdots\cdots & \cdots\cdots \\
\cdots\cdots\cdots\cdots & \cdots\cdots\cdots\cdots & \cdots\cdots\cdots & \cdots\cdots \\
M_{1n} \cdots\cdots\cdots & \cdots\cdots\cdots & \cdots\cdots\cdots & L_n - \left(\frac{1}{C_n} + \frac{1}{C_{n+1}}\right)\frac{1}{\omega^2}
\end{array}\right| = 0$$

Digitized by Google

As an equation in C_1 and C_{n+1} it has the form

$$\frac{A}{C_1}+\frac{B}{C_{n+1}}+\frac{D}{C_1 C_{n+1}}+F=O \tag{3}$$

In particular, if the surroundings of the coil are symmetrical with respect to the two ends

$$A=B,$$

and hence,

$$A+\frac{D}{C_1+C_{n+1}}+F\frac{C_1 C_{n+1}}{C_1+C_{n+1}}=O \tag{4}$$

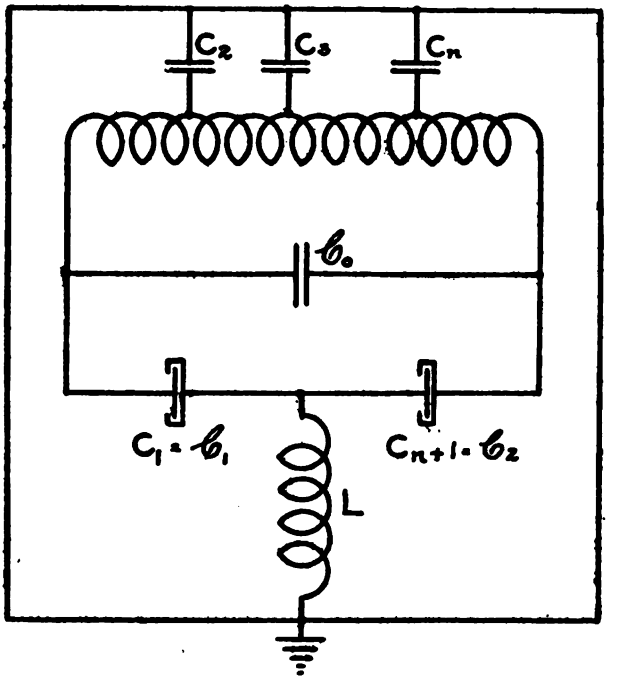

FIG. 2.—*Equivalent circuit for coil, its self-capacity, and its distributed capacity to ground*

Therefore, if for different values of C_1 proper values of C_{n+1} be found so as to secure resonance, and if $\frac{C_1 C_{n+1}}{C_1+C_{n+1}}$ be calculated, a constant number will not be obtained. However, if its value be plotted against the value of

$$\frac{1}{C_1+C_{n+1}}$$

a straight line must result according to (4).

Digitized by Google

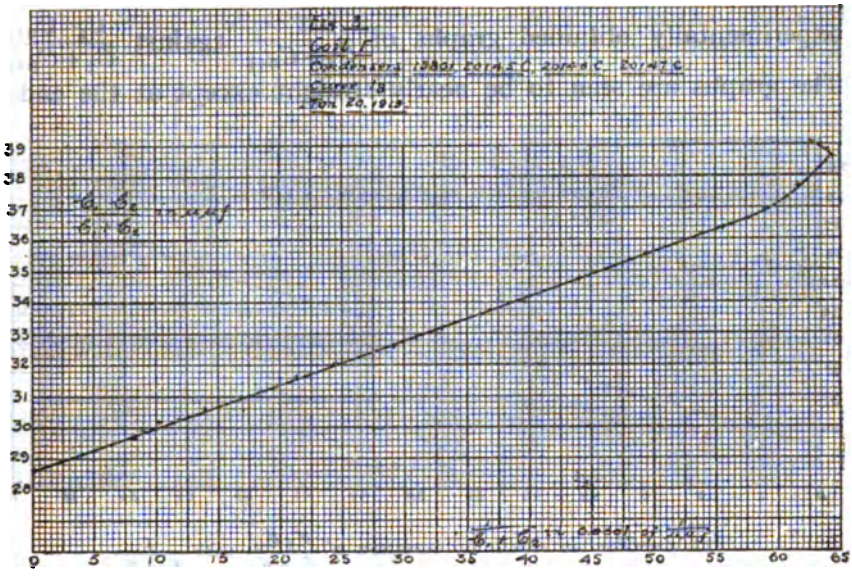

FIG. 3.—*Observed results for variation of* $\frac{C_1 C_2}{C_1+C_2}$ *with* $\frac{1}{C_1+C_2}$

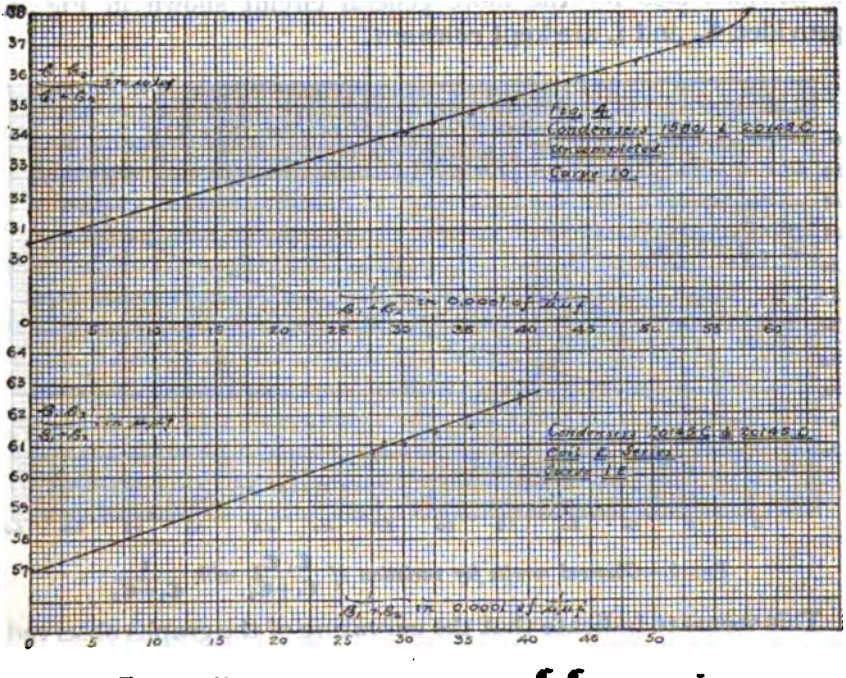

FIG. 4.—*Observed results for variation of* $\frac{C_1 C_2}{C_1+C_2}$ *with* $\frac{1}{C_1+C_2}$

Digitized by Google

Curves given as I_A, I_B, I_C, I_D, I_E (Figs. 3, 4, 5, and 6) give experimentally obtained graphs of $\frac{1}{C_1+C_{n+1}}$ against $\frac{C_1\ C_{n+1}}{C_1+C_{n+1}}$. The graphs are seen to be nearly straight except at the ends,

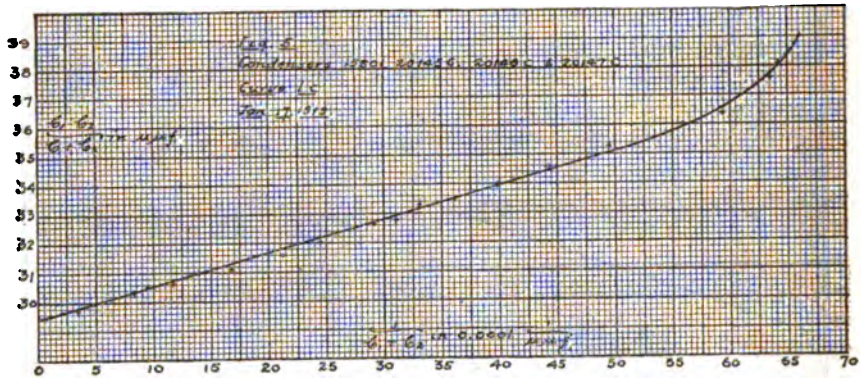

FIG. 5.—*Observed results for variation of* $\frac{C_1 C_2}{C_1+C_2}$ *with* $\frac{1}{C_1+C_2}$

where they have a bend. This bend is probably due to a dissymmetry in the surroundings.

By similar reasoning it is found that a relation of the form (3) is satisfied also for the more general circuit shown in Fig. 2, provided C_0 and L are kept constant.

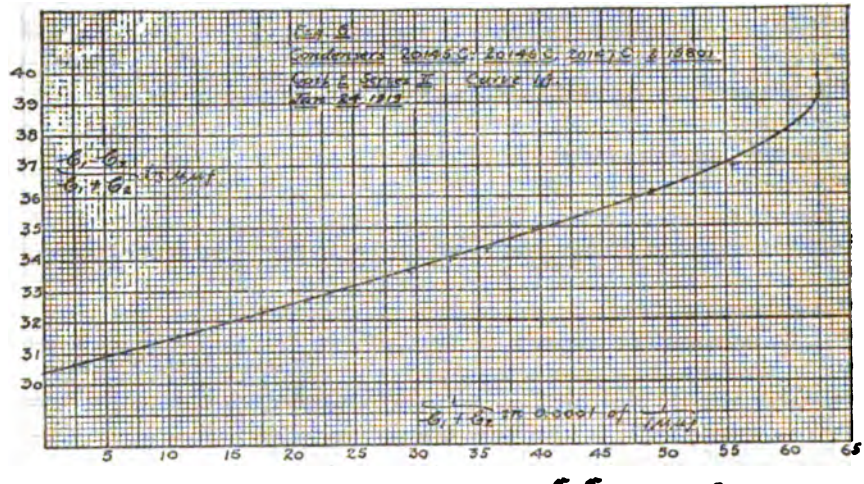

FIG. 6.—*Observed results for variation of* $\frac{C_1 C_2}{C_1+C_2}$ *with* $\frac{1}{C_1+C_2}$

This seems to indicate that the curvature of the graphs observed is due to dissymmetry in the surroundings, because distributed capacity effects between different parts of the coil are probably taken account of by the above-mentioned calculation.

Digitized by Google

SUMMARY

When two condensers connected in series with common terminal grounded are connected across the terminals of an inductance coil, their effective capacity in series is not equal to their effective capacity so far as resonance of the coil is concerned. If the capacity of one condenser is $\mathbb{C}_1$ and of the other $\mathbb{C}_2$, the quantity

$$\frac{\mathbb{C}_1 \mathbb{C}_2}{\mathbb{C}_1 + \mathbb{C}_2}$$

is the effective capacity of the two condensers in series. As stated, it does not stay constant when $\mathbb{C}_1$ is changed arbitrarily and $\mathbb{C}_2$ is readjusted for resonance. However, $\frac{\mathbb{C}_1 \mathbb{C}_2}{\mathbb{C}_1 + \mathbb{C}_2}$ is linearly related to $\frac{1}{\mathbb{C}_1 + \mathbb{C}_2}$.

WASHINGTON, May 6, 1921.

Digitized by Google

Digitized by Google

APR 22 1922

DEPARTMENT OF COMMERCE

SCIENTIFIC PAPERS

OF THE

BUREAU OF STANDARDS

S. W. STRATTON, DIRECTOR

LIBRARY UNIVERSITY OF CALIFORNIA

No. 428

THE RADIO DIRECTION FINDER AND ITS APPLICATION TO NAVIGATION

BY

FREDERICK A. KOLSTER, Physicist
FRANCIS W. DUNMORE, Associate Physicist
Bureau of Standards

JANUARY 16, 1922

PRICE, 15 CENTS

Sold only by the Superintendent of Documents, Government Printing Office
Washington, D. C.

WASHINGTON
GOVERNMENT PRINTING OFFICE
1922

Digitized by Google

Digitized by Google

THE RADIO DIRECTION FINDER AND ITS APPLICATION TO NAVIGATION

By Frederick A. Kolster and Francis W. Dunmore

ABSTRACT

The radio direction finder is a simple instrument by means of which the direction of a radio transmitting station may be determined.

A practical form of direction finder has been developed by the Bureau of Standards, in cooperation with the Bureau of Lighthouses, for use on shipboard, and tests have proved it to be a very useful nautical instrument.

Sound and visual signaling devices have been used at light stations for many years, but during fog, when they are most needed, they fail to give reliable information. The radio direction finder is not affected by fog, and has the further advantage that it will operate over much greater distances.

This paper deals briefly with the principles of the operation of the direction finder, but is primarily concerned with practical development, which has made possible a device sufficiently simple and accurate for use as an aid to navigation, and with practical applications which have been made.

The system described includes the use of the radio direction finder on shipboard in connection with automatically operated radio transmitting apparatus installed at light stations. The paper describes in detail a direction finding system of this type, including radio transmitting apparatus which is in operation on light stations at the entrance to New York harbor and the direction finder installed on shipboard.

As a result of extensive tests, which are described, this method of installing the direction finder on shipboard has been found to have numerous advantages over another system of direction finding, in which each ship transmits radio signals to a number of direction finders located on shore.

The paper points out the importance of establishing as soon as possible radio transmitting stations at the other important light stations on the Atlantic and Pacific coasts and the installation of radio compass equipment on shipboard.

CONTENTS

	Page
I. Introduction	529
II. The radio direction finder	532
1. Fundamental principles	532
2. Design	535
3. Operation	541
4. Unidirectional characteristics	544
5. Experimental results	546
III. Practical application to navigation	551
IV. Conclusion	564

I. INTRODUCTION

Sound and visual signaling devices have been employed for many years as aids to navigation. Lighthouses and lightships, with their characteristic light flashes and sound signals, are estab-

Digitized by Google

lished and maintained along the coasts and at harbor entrances in order that shipping may be carried on with maximum safety.

Unfortunately, however, during fog or thick weather, when the greatest need for these aids to navigation exists, they fail to serve their purpose adequately. Light does not penetrate fog, and it is well known that sound signals are extremely unreliable and can not be depended upon to indicate direction or distance. Furthermore, even under favorable conditions, the most modern devices for visual or sound signaling are limited to comparatively short distances.

The utilization of electric waves such as are employed in radio communication for fog-signaling purposes has been suggested from time to time, and although early experiments have been made both in this country and abroad for the purpose of determining the practicability of fog signaling by radio no serious attempt has been made to encourage the adoption of the scheme until recently.

In May, 1913, one of the authors of this paper, acting as a representative of the Department of Commerce on the Interdepartmental Radio Committee on Safety at Sea, strongly advocated that serious consideration be given to the possibilities of radio signaling as an aid to navigation and that the matter be brought before the International Conference on Safety at Sea, which was held in London during that year.

It is well known that electric waves penetrate fog and can be transmitted over much greater distances than light or sound waves. Any lighthouse equipped with a suitable radio transmitting equipment, therefore, becomes an effective radio fog-signaling station whose characteristic signals are readily received by all ships within range irrespective of weather conditions.

Since 1913 the radio laboratory of the Bureau of Standards has given a great deal of attention to the practical development of methods and devices for radio fog signaling and particularly to the development of a suitable instrument for use on shipboard by means of which the direction or bearing of the signaling station may be determined.

It is the purpose of this paper to describe the radio fog-signaling system and especially the direction-finding instrument or radio compass, as it is sometimes called, and to give the principles upon which its operation is based as well as the results obtained in practical use. Under normal conditions this publication would have been released several years ago, but because of the important

Digitized by Google

military value of the direction finder, so effectively demonstrated during the war, the Navy Department, in 1915, requested that publication as well as civil application be delayed. During the war many naval vessels were equipped with the radio direction finder.

More recently the Navy Department has established an extensive system of direction-finder stations on shore, the purpose of which is to furnish to ships, upon request, radio bearings taken by two or more such stations. In the Navy system the ship whose position is to be determined becomes the signaling station from which radio bearings are taken at two or more direction-finder stations located on shore. The bearings thus obtained are then communicated to the ship by radio.

The system advocated and developed by the Bureau of Standards in cooperation with the Bureau of Lighthouses is the reverse of the Navy system. Lighthouses and light vessels whose location on sailing charts are accurately shown are equipped with radio fog-signaling apparatus, which automatically transmit their respective characteristic signals during fog or at such times as may be necessary. The direction finder is then required to be installed on shipboard, where it may be operated directly by the navigating officer, who can take bearings at any time and as often as he desires on any one or more of the radio fog-signaling stations established and operated by the Bureau of Lighthouses.

Extensive tests have been conducted with the view of determining the practicability of the Bureau of Standards system. So successful have been the results that it is predicted that within a short time every important lighthouse and light vessel will become a radio fog-signaling station, and the radio direction finder will become as much a part of a ship's equipment as the magnetic compass. An extremely effective aid to navigation will thus be provided which, if universally adopted, will result in more adequately protecting life and property at sea.

The cost of a direction finder for shipboard installation is so small as compared with the benefits which may be derived therefrom, perhaps in a single instance, where life, property, or even time may be saved, that it can not enter into consideration. Likewise the cost to the Government of establishing radio-signaling stations at lighthouses and on light vessels is small as compared to their value as substantial aids to navigation, particularly since no additional personnel is required in their operation and maintenance.

Digitized by Google

International recognition of the future importance of radio fog-signaling has been recorded in the report of the Interallied Radio Commission which met in Paris in 1919 and later in the report of the Universal Electrical Communications Union which met in Washington in 1920.

The following recommendations concerning the operation of radio fog-signaling or radio-beacon stations, based upon practical experience obtained during actual tests, were submitted to the Communications Union by the Bureau of Standards for international consideration.

SERVICE OF RADIO BEACON STATIONS

Each administration which shall install radio beacons shall observe the following conditions:

Radio beacons adopted for the needs of navigation shall be divided into three classes:

1. Short-range radio beacons.
2. Long-range radio beacons.
3. Radio beacons on shipboard.

The transmitting wave length for these three classes of beacons shall be 1000 meters, spark or interrupted continuous waves.

Short-range shore beacons shall be limited in power such that accurate radio bearings can be taken at a distance of 30 miles. During fog or at such times as may be determined by the administration, these beacons shall transmit characteristic signals whose form, frequency, and tone shall be fixed by the administration.

Long-range shore beacons shall be limited in power such that accurate radio bearings can be taken at a distance of 300 miles. These long-range beacons shall be limited in number and shall operate at infrequent intervals during fog or at such times as may be determined by the administration. The form, frequency, and tone of the characteristic signal transmitted by these stations shall be determined by the administration.

Radio beacons on shipboard shall be limited in power such that accurate radio bearings may be taken at a distance of 10 miles. During fog or thick weather, shipboard beacons shall transmit characteristic signals at frequent intervals commencing with the call signal repeated for 30 seconds and terminating with the indication of the ship's course and speed.

Radio beacons on permanently moored vessels, such as light ships, shall be considered as shore beacons.

BUREAU OF STANDARDS RADIO LABORATORY.

WASHINGTON, D. C., October 15, 1920.

II. THE RADIO DIRECTION FINDER

1. FUNDAMENTAL PRINCIPLES

The fundamental radio circuit is made up of inductance and capacity. These elements appear in various forms, and in the ideal circuit, as shown diagrammatically in Fig. 1, the inductance

Digitized by Google

is entirely concentrated or lumped in the coil L, and the capacity is likewise concentrated or lumped in the condenser C.

Power may be supplied to such a circuit either by applying a resonant voltage across the condenser C or by inducing a resonant voltage in the coil L, or by action of both in proper phase relation.

In the ordinary antenna circuit, as used in present-day radio communication, we find, generally speaking, that the inductance is substantially concentrated in the form of a coil L, and that the capacity is formed by a conductor or group of conductors elevated above the ground, the elevated conductors forming one plate of the condenser and the ground or counterpoise forming the other plate, as shown in Fig. 2.

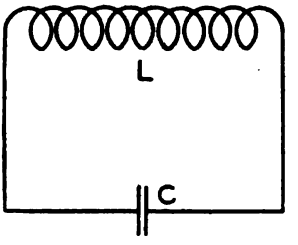

FIG. 1.—*Simple radio circuit*

It may be said, therefore, that energy is received in the ordinary radio antenna system by virtue of the fact that its capacity is exposed to the incoming electromagnetic wave or, in other words, that energy enters the system by way of its capacity, thereafter to be transferred to its inductance. The electrical capacity of an antenna as well as the potential impressed upon it by the incoming electromagnetic wave depends largely upon its physical dimensions, generally the size and height of its elevated area and in special types of antennas, mainly upon the length of the antenna wires.

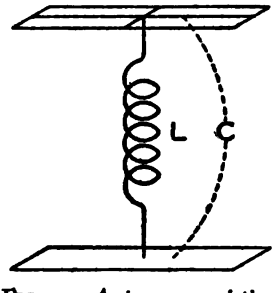

FIG. 2.—*Antenna consisting of elevated conductors (condenser type)*

Referring now to Fig. 3, we have what may be considered as the reverse of the antenna system shown in Fig. 2. In this case energy is received in the system by virtue of the fact that its inductance L is exposed to the incoming electromagnetic wave or, in other words, energy enters the system by way of its inductance, thereafter to be transferred to its capacity.

The inductance of coil L depends upon the number of turns, the area inclosed, and the spacing of the turns. The current in the receiving circuit depends largely upon these factors as well as the resistance of the circuit. For given physical dimensions, however, any value of inductance may be obtained by winding the proper number of turns in the coil L, so that the electrical dimensions of the coil system are not so dependent upon its physi-

Digitized by Google

cal dimensions as is the ordinary antenna system. As a matter of fact, a coil system of very small dimensions as compared with an antenna may be used for the reception of radio signals.

Although the coil-receiving system is superior in many respects to the antenna system, its chief advantage lies in its directive properties. If the coil *L* in Fig. 3, for example, is rotated about its vertical axis *ab*, the received signal intensity from any given source of transmission will vary approximately in accordance with the diagram shown in Fig. 4.

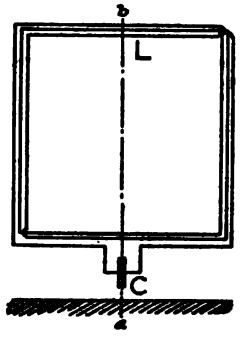

FIG. 3.—*Antenna consisting of closed coil (inductance type)*

Maximum signal intensity *OP* or *OM* is obtained when the plane of the coil *L* lies in the direction of the source of transmission *A* or *B*. If the source is in the direction *C* or *D*, or exactly normal or at right angles to the plane of the coil *L*, then the signal intensity is zero. In all other directions the intensity varies in accordance with the figure-of-eight characteristics in Fig. 4. For example, in directions *OE* or *OF*, *OG* or *OH*, the distances *ON* or *OQ* respectively represent the relative signal intensities as compared with the maximum *OM* or *OP*.

It is immediately apparent, therefore, that if the coil *L* in Fig. 3 is of sufficiently small dimensions to permit rotation about its vertical axis, signals transmitted from any given source will be received with gradually varying degrees of intensity until the coil becomes normal or at right angles to the direction in which the transmitting source lies, at which time the signal intensity becomes zero. This position of silence is critical, and therefore may be used to indicate, with great accuracy, the line of direction of the source.

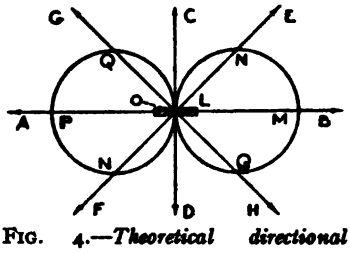

FIG. 4.—*Theoretical directional characteristic of closed coil antenna*

It is upon these simple principles that the direction finder as developed at the Bureau of Standards is based. The theory of its design and operation presents a number of interesting problems, however, and it is not until these problems are thoroughly understood that the ideal conditions for accurate direction finding can be realized.

Digitized by Google

In the matter of design it is of importance to determine under given practical conditions the number of turns and the spacing of the turns which will give maximum received signal intensity for the wave length or range of wave lengths to be received.

In the matter of operation it is of importance to obtain as nearly as possible the ideal figure-of-eight characteristic with its critical or sharply defined position of zero signal intensity. The operating circuit adjustments and the method of reading bearings must be simple and rapid.

2. DESIGN

The main electrical circuit of the direction finder or coil receiving system is nothing more nor less than a simple radio circuit containing inductance, resistance, and capacity, and may be treated as such in every respect. No new theory enters into its electrical behavior, and in determining best circuit conditions it is only necessary to define the practical requirements.

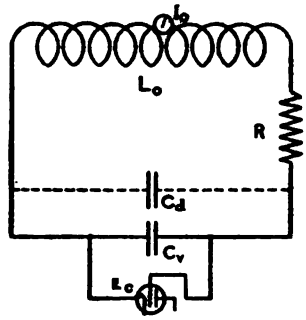

FIG. 5.—*Coil antenna circuit showing distributed capacity and resistance*

Without going into the theory in great detail, we shall consider for the purpose of illustration two cases involving different initial requirements. In both cases the dimensions of the coil, the number of turns, and the spacing between turns are fixed. It will then be the purpose in one case to determine the wave length or range of wave lengths which will give maximum received current in the coil and in the other case to determine the wave length or range of wave lengths which will give maximum potential difference across the tuning condenser. A constant source of undamped or continuous wave transmission will be assumed.

CASE 1.—To determine the wave length which will produce maximum current at center of coil L_0. (See Fig. 5.)

L_0 = 20 turns, 4 feet by 4 feet, high-frequency cable 48 strands No. 38 wire. One-half inch separation between turns.

R = resistance of circuit measured at center of coil.

C_d = effective distributed capacity of coil L_0 = 39 micromicrofarads.

C_v = variable tuning condenser.

Digitized by Google

For given undamped wave transmission, the received current in the coil L_0 may be expressed in terms of the circuit constants.

$$I = \text{constant} \times \frac{AN}{R\sqrt{L_0 C_0}} = \text{constant} \times \frac{AN}{R\lambda}$$

where

A = area of coil.
N = number of turns.
R = resistance.
L_0 = inductance of coil.
C_0 = total capacity = $C_d + C_v$.
λ = wave length in meters.

Since in the case in question the area and number of turns are fixed we need only to consider the variation of current with

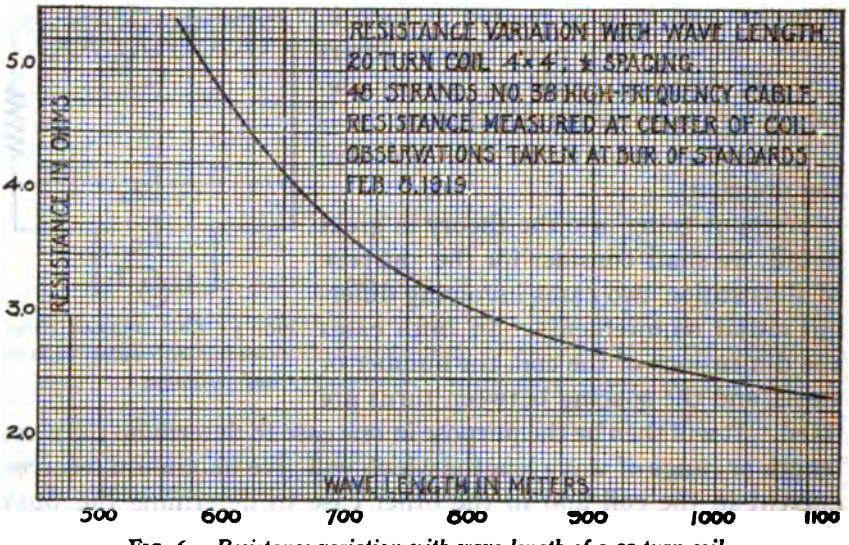

FIG. 6.—*Resistance variation with wave length of a 20-turn coil*

resistance and wave length. This involves the measurement of the high-frequency resistance of the coil, and if the current were uniformly distributed throughout the coil this resistance could be measured at any point in the coil, but due to the inherent distributed capacity of the coil which, although very small as compared to the tuning condenser capacity at the longer wave lengths when the tuning condenser is large, has appreciable effect at the shorter wave lengths when the tuning capacity is small, the resistance should be measured with reference to the part of the coil in which the current is to be determined. In this case the current at the center of the coil will be determined and therefore the resistance measurements are made at the center.

Digitized by Google

The resistance variation with wave length thus measured is shown in Fig. 6 and the calculated data for the current variation, proportional to $\frac{1}{\lambda R}$, is given in Table 1.

TABLE 1.—Data for Case 1

λ (meters)	$C_0=C_d \pm C_v$ ($\mu\mu f$)	R (ohms)	$\frac{10^6}{\lambda R}$
550	89	5.70	319
600	105	4.80	347
700	145	3.75	380
800	189	3.13	399
900	240	2.75	404
1000	295	2.50	400
1100	355	2.40	378
1200	423	2.35	354

The current variation is shown in Fig. 7, and it will be seen that maximum current is obtained at a wave length of 900 meters.

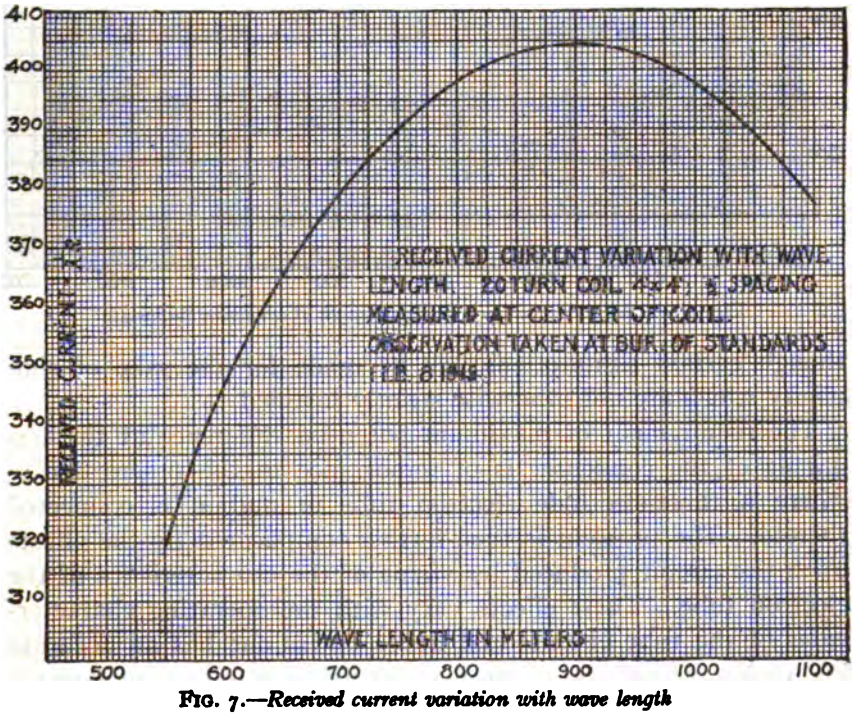

FIG. 7.—*Received current variation with wave length*

This case serves as an example of a practical case where the detector circuit is associated inductively with the coil L_0 and preferably at the center of the coil, and if it be assumed that no

Digitized by Google

appreciable increase in resistance is introduced because of the loosely coupled detector circuit, then the coil system above described would function with maximum efficiency when receiving a wave length of 900 meters.

CASE 2.—Maximum potential at terminals of condenser.

Due to the distributed capacity of the coil and the consequent nonuniform distribution of current through the coil at the shorter wave lengths this case presents somewhat more difficulty in its treatment than case 1. However, the data given in what follows will serve sufficiently well for the purpose intended even

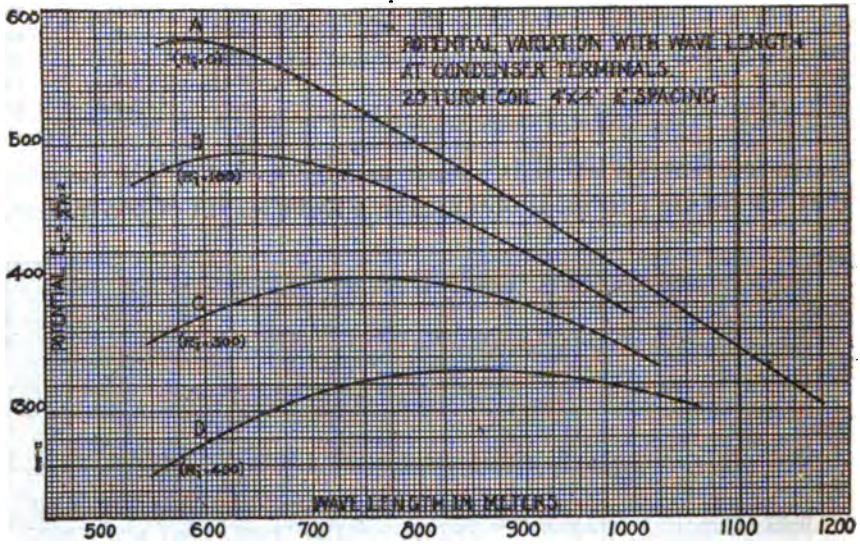

FIG. 8.—*Potential variation with wave length at condenser terminals*

though certain assumptions will be made for the sake of simplicity which are not otherwise strictly justified.

The requirement of maximum potential difference at the terminals of the condenser is of importance in the practical case where a three-electrode electron tube or audion is connected thereto. The problem is then further complicated by the effects upon the circuit produced by virtue of the characteristics of the electron tube. These effects vary with the operating characteristics of the tube circuits and hence unless one has an accurate knowledge of how the electron tube with its auxiliary apparatus will modify the coil system under all conditions, no accurate nor definite determination of the conditions for maximum potential difference can be made.

Digitized by Google

Let us take by way of example the case wherein it is desired to determine the variation with wave length of the voltage at the terminals of the condenser in the coil system described in case 1. The assumption will be made that the distributed capacity of the coil L_0, Fig. 5, can be represented as a perfect condenser C_d in parallel with the perfect tuning condenser C_v, giving a total capacity $C_0 = C_d + C_v$. Furthermore, it will be assumed that the current variation with wave length in the combined condenser paths will be as determined in case 1 and shown by the curve in Fig. 7.

Then if $I = \text{constant} \times \frac{AN}{R\lambda}$

then $E_c = \frac{I}{C_0\omega} = \text{constant} \times \frac{AN}{RC_0} = \text{constant} \times \frac{ANL}{R\lambda^2}$

For the case in question where A, N, and L are given and remain constant,

$$E_c = \text{constant} \times \frac{1}{R\lambda^2}$$

TABLE 2.—Data for Case 2

λ (meters)	$C_0 = C_d + C_v$ ($\mu\mu f$)	R (ohms)	$\frac{10^9}{R\lambda^2}$
550	89	5.70	580
600	105	4.80	578
700	145	3.75	543
800	189	3.13	498
900	240	2.75	448
1000	295	2.50	400
1100	355	2.40	344
1200	423	2.35	295

This variation of voltage with wave length is given by the curve A in Fig. 8, which shows that the maximum potential is obtained across the capacity of the coil system when receiving a wave length of about 550 meters.

In the practical case this condition would be true if the detecting apparatus connected to the terminals of the condenser were purely potentially operated and absorbed no energy from the coil system. The above example, therefore, serves to illustrate the practical conditions which would exist in the case where a vacuum tube circuit having zero input resistance is connected to the condenser C_v.

Digitized by Google

The potential variations with wave length for cases where the input resistance of the electron-tube circuit has an appreciable positive value, which it will be assumed remains constant over the wave-length range, are shown in Fig. 8 by curves *B*, *C*, and *D*.

The data from which these curves were drawn were obtained by considering the input circuit of the electron tube as equivalent to a capacity C_i in series with a resistance R_i. The complete coil system may then be shown as in Fig. 9.

Having obtained the coil circuit resistance R for various wave lengths by measurement as in case 1, the effective increase in circuit resistance ΔR due to the input resistance R_i may be calculated from the formula:

$$\Delta R = R_i \times \left(\frac{C_i}{C_0}\right)^2,$$

where C_0 is the total capacity $C_d + C_v + C_i$.

Here again the assumption is made that the capacities C_d and C_v are in the nature of perfect condensers and that currents in the three condenser branches are substantially in phase.

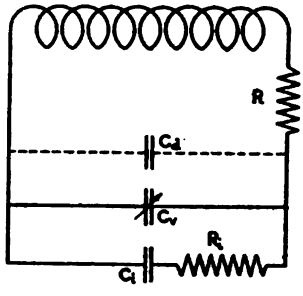

FIG. 9.—*Equivalent coil system*

In Fig. 8, curves *B*, *C*, and *D* give the variation with wave length of the voltage across a condenser $C_0 = C_d + C_v + C_i$, when the coil circuit resistance is $R + \Delta R$, R being given by the curve in Fig. 6 and ΔR being calculated for $R_i = 100$ ohms for case *B*, 300 ohms for case *C*, and 600 ohms for case *D*.

The value of R_i in practice depends, of course, upon the type of electron-tube circuits employed and the operating adjustments used for each wave length. In fact, when the inductance in the plate circuit becomes larger than a certain value a reduction of circuit resistance is effected; that is, ΔR becomes negative.

It is seen, therefore, that the design of a coil system in which the electron-tube apparatus is to be directly connected across the tuning condenser is thoroughly dependent upon the characteristics and adjustments of the electron-tube circuits. Generally speaking, however, best receiving efficiency for a given coil is obtained at the shorter wave lengths where small condenser capacities are required. For example, in the case of the 20-turn

Digitized by Google

coil herein described, for which let us take curve *A* in Fig. 8 as being a fair representation of a practical case, it is seen that a received wave length of between 500 and 600 meters will give maximum effect. The natural wave length of the coil as determined by its inductance and distributed capacity is approximately 400 meters.

3. OPERATION

Naturally the operation of the coil system as a direction finder depends upon its design, and although it is desirable to obtain as nearly as possible the conditions for maximum receiving efficiency, good direction-finding characteristics are of first importance. Best receiving conditions are often obtained at wave lengths close to the natural wave length of the coil when using the voltage operated detector system, but under these conditions good direction-finding qualities are not generally obtained.

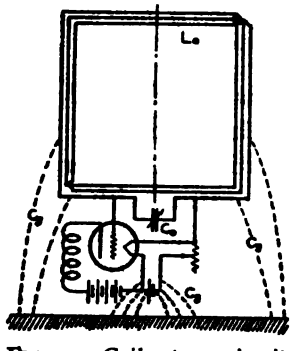

FIG. 10.—*Coil antenna circuit, showing asymmetry of distributed capacity to earth*

An important factor which up to this point has not been considered enters into the operation of the coil system, particularly in its use as a direction finder. This has to do with the effects produced in the coil system by virtue of the fact that the coil structure has an appreciable capacity to earth. Furthermore, the entire coil system, including the detector circuits, connected thereto, is electrically unsymmetrical with respect to earth. This results in a distortion of the ideal figure-of-eight signal intensity characteristic obtained by rotation of the coil about its vertical axis. The critical position of zero signal intensity no longer exists and the directive qualities of the coil system are obscured.

An examination of Fig. 10 will show that the electron-tube circuit connected to the condenser C_0 will be operated upon by the potential across the condenser as produced by the current received in the coil L_0 by the direct action upon the coil of the incoming electromagnetic wave. It will also be operated upon to a lesser extent by the voltage applied to the electron tube due to direct action upon it of the incoming wave through the earth capacities C_g. Furthermore, because of the electrically unsymmetrical relation of the coil system with respect to earth, an appreciable current will be set up in the coil circuit by the incoming wave acting through the earth capacities C_g. The potential produced

Digitized by Google

by this current across the condenser C_0 will likewise operate upon the electron tube.

The ideal figure-of-eight signal intensity characteristic is therefore distorted by these additional effects, the degree of distortion depending upon their relative magnitudes. In practice it often happens that the signal intensity produced by direct action through the earth capacity is sufficient to destroy the critical zero signal characteristic of the coil when its plane is at right angles to the incoming wave front. This effect is illustrated by Fig. 11, in which the dotted tangential circles or figure-of-eight represents the ideal variations of signal intensity for various positions of the coil with respect to a given source, and the small circle represents the variation of signal intensity produced by direct action through the earth capacities. It is seen that this signal is independent of coil position. Furthermore, it is produced by a voltage which is in quadrature with the condenser voltage which produces the figure-of-eight signal variation. The characteristic shown in full line is therefore the resultant effect.

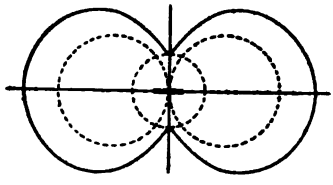

FIG. 11.—*Coil characteristic, showing effect of direct action through earth capacity*

The further effect produced by the voltage operating upon the electron tube as the result of a current set up in the coil by the action of the incoming wave through the earth capacity is shown in Fig. 12.

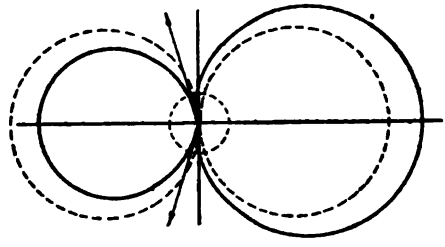

FIG. 12.—*Coil characteristic, showing effect of current set up in coil by capacity to earth*

In this case the constant signal intensity represented by the small circle is produced by a voltage which is either in phase or 180° out of phase with the condenser potential giving the figure-of-eight signal characteristic, depending upon the relative position of the coil with respect to the incoming wave. The resultant characteristic is given by the full-line figure. It will be noted that the positions of zero signal intensity are no longer at right angles to the plane of the coil, nor do they coincide with the axis of the coil as in the ideal case. This is a very common occur-

Digitized by Google

rence in practice which leads to considerable annoyance if not properly taken care of.

Finally, we have in Fig. 13 a representation of the signal variation characteristic which results when both effects described with reference to Figs. 11 and 12 are present.

For accurate direction finding such conditions can not be tolerated, and means must therefore be applied to minimize or entirely eliminate these undesirable effects.

First of all, it is essential to avoid using the direction finder at or near the natural wave length of the coil where the above-described effects are likely to be magnified. At the same time receiving efficiency must not be sacrificed to too great an extent.

The complete solution of the problem depends upon obtaining exact electrical symmetry of the entire coil system, including the auxiliary electron-tube apparatus, with respect to earth.

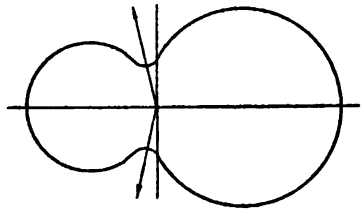

FIG. 13.—*Resultant coil characteristic*

The capacity with respect to earth of a direction-finder coil depends upon its physical dimensions and its height above earth. For a coil of given area and placed at a given height above earth, this capacity will vary with the spacing of the turns. If the windings of the coil are widely separated, the axial length of the coil is great, and its capacity to earth is increased.

In Fig. 14 the variation of capacity to earth with spacing of turns for a coil 5 by 5 feet wound with 12 turns is given for two cases. Curve 1 gives the value of earth capacity for various spacings when the coil was 2 feet above earth and curve 2 when 5 feet above earth.

In determining the best spacing of turns in the matter of design there are, therefore, two factors to be considered. The distributed capacity of the coil and hence its natural wave length must be reduced by separating the windings. However, this should not be carried so far as to make the axial length and hence the capacity to earth too great.

As stated above, for direction-finding purposes the coil system should be electrically symmetrical with respect to earth. This condition can be brought about by proper adjustment of the condensers C_1 and C_2 in Fig. 15. Furthermore, the condensers

Digitized by Google

C_0, C_1, and C_2, together with all other auxiliary apparatus, should be shielded as shown by S.

The electrical symmetry can further be improved by avoiding direct connection of the electron tube to the circuit as shown in Fig. 16. In this case the electron tube is connected to the second-

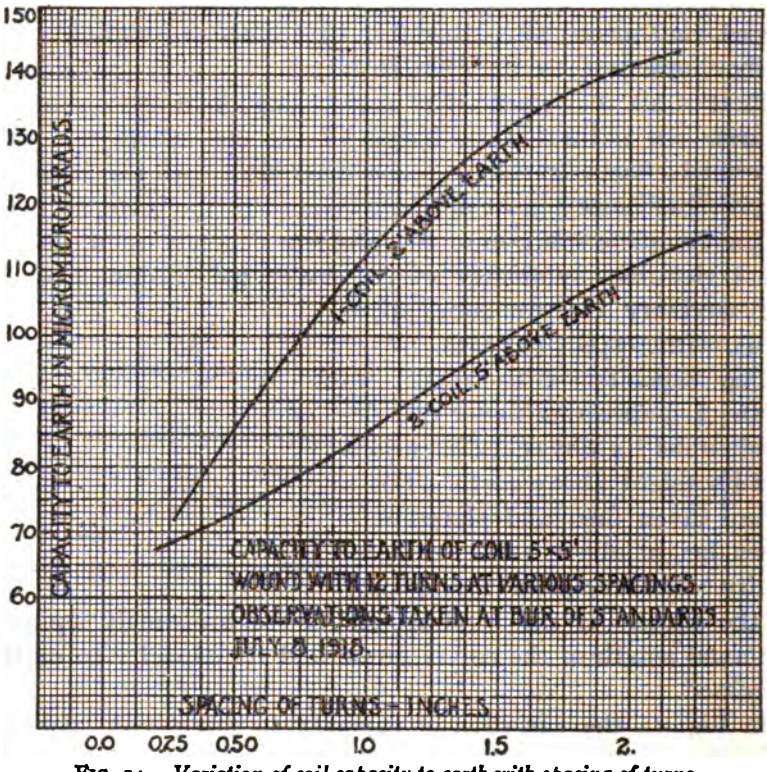

FIG. 14.—*Variation of coil capacity to earth with spacing of turns*

ary winding of a suitable transformer, the primary of which is connected to the condenser C_0.

The arrangement shown in Fig. 17, wherein a double-grid and double-plate electron tube is used, affords excellent symmetry.

In any case it is of the greatest importance that the electron-tube system which in practice usually consists of a detector tube with one or more stages of radio and audio amplification shall be operated upon only by the direct action of the incoming wave upon the coil L_0.

4. UNIDIRECTIONAL CHARACTERISTICS

The rotatable coil system with its critical position of zero signal intensity is a direction finder to the extent that the line of direction in which a radio transmitting source lies can be accurately

Digitized by Google

determined. The sense of direction, however, is not indicated; that is to say, it is known that the source lies on the axis of the coil but it is not known whether it lies to one side or the other of the plane of the coil.

To provide simple means of determining the sense as well as the line of direction is of practical importance, for example, in locating and proceeding to the aid of a ship in distress.

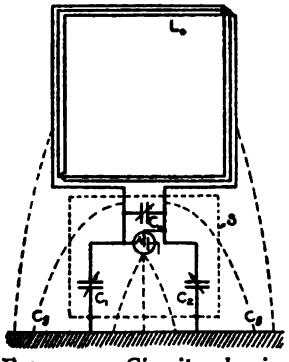

FIG. 15.—*Circuit showing method of obtaining symmetry of coil capacity to earth, using balancing condensers*

By accentuating and utilizing the effect described in connection with Fig. 12 where the received signal results from the combined effects of the current set up in the coil by direct action of the incoming wave together with that produced indirectly through the earth capacity, a unidirectional characteristic may be obtained by virtue of which the sense of direction is readily determined.

This can be accomplished by the system shown in Fig. 18, in which a tuning inductance L_g is inserted in the earth connection between the condensers C_1 and C_2. If now, the electrical symmetry of the coil system with respect to earth is upset by reducing the capacity C_1 and increasing the capacity C_2 or vice versa, a current will be set up in the coil L_o by indirect action through the tuned path including L_g and C_g. The signal intensity produced by this current is independent of the relative position of the coil L_o with respect to the transmitting source and may be made equal to that produced by direct action upon coil L_o when its plane is in the line of direction of the source. Because of the phase relation of the currents set up in coil L_o the signal intensities resulting therefrom will be accumulative or differential depending upon whether the source of transmission is at A or at B in Fig. 19. This unidirectional effect may be utilized for the purpose of determining the sense of direction of a transmitting source. For example, if the direction of a source of transmission is found to be in the line AB, Fig. 19, the fact that it is at B and not at A is determined by observing the direction indicated by the arrow S attached to the coil L_o, when maximum signal is obtained.

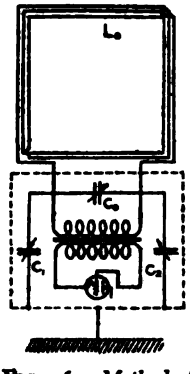

FIG. 16.—*Method of obtaining symmetry of coil capacity to earth, using balancing condensers and coupling transformer*

Digitized by Google

Another method of accomplishing the same result without disturbing the electrical symmetry of the coil system with respect to earth is shown in Fig. 20. In this case the indirect action upon the coil circuit L_0 C_0 is produced by inductively coupling

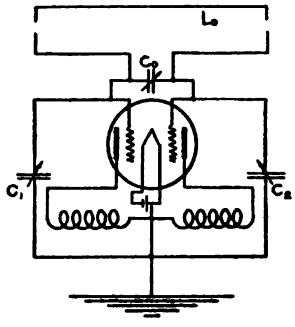

FIG. 17.—*Use of double-grid tube to obtain symmetry of coil system*

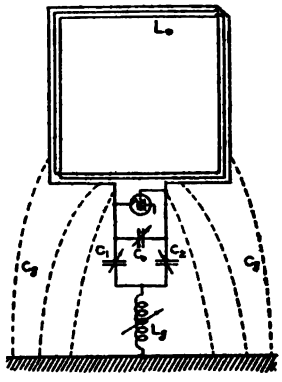

FIG. 18.—*Unidirectional coil antenna system, using unbalanced method*

the earth circuit L_g C_g to the coil circuit through the coupling coils l_g and l_2. In order to maintain electrical symmetry the coil l_1 is used to balance the effect of the similar coil l_2.

In the system described in connection with Fig. 19, the unidirectional characteristic is controlled entirely by adjusting the condensers C_1 and C_2 in opposite sense, while in that shown in Fig. 20 it is controlled by the degree of coupling between coils l_2 and l_g.

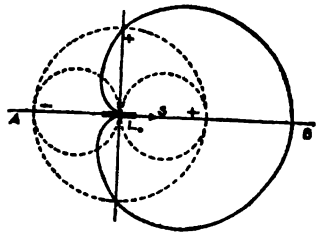

FIG. 19.—*Unidirectional coil characteristic*

The receiving efficiency of the earth circuit L_g C_g is in some cases not sufficient to produce complete unidirectional effect as shown in Fig. 19. This difficulty can be corrected by utilizing an additional capacity area in combination with the coils L_0 as shown in Fig. 21 in which the capacity area A is connected to the middle point of the coil L, thereby increasing the earth capacity C_g and maintaining, when desired, perfect electrical symmetry.

5. EXPERIMENTAL RESULTS

A large number of tests have been conducted to determine the accuracy of the coil system herein described when used as a direction finder. For example, in Fig. 22 results of field tests are

Digitized by Google

shown wherein the direction of a transmitting source located at the Bureau of Standards was observed by means of a portable direction finder set up at various points in the vicinity of the Bureau.

It will be seen upon examination of Fig. 22 that with the exception of two cases the direction of the source was observed with considerable accuracy. Observations made at the north end of the Sixteenth Street bridge and at the intersection of Ingomar Street and Belt Road gave directions several degrees out. These locations were purposely chosen in order to show the distorting effect upon the wave front of large structures and of

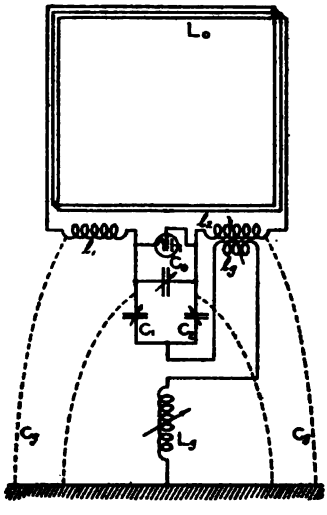

FIG. 20.—*Unidirectional coil antenna system, using balanced method and coupling*

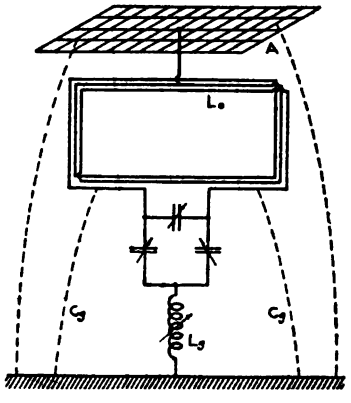

FIG. 21.—*Unidirectional coil antenna system, using elevated capacity area*

telephone and power lines. In all other cases care was taken in choosing locations free from obstructions, although in several cases the direction finder was set up in rather thickly wooded sections. Trees apparently have little distorting effect.

The portable direction finder used in these tests was designed and constructed at the Bureau of Standards. It has several interesting features and is very convenient for field work. The coil is wound in two sections of five turns each sewed in waterproof canvas. A switch is provided by means of which the five-turn sections may be connected either in parallel or series. With a tuning condenser, having a maximum capacity of approximately one-thousandth microfarad, a wave-length range of from 300 to 1500 meters is thus readily obtained.

Digitized by Google

Several views of the portable direction finder are shown in Figs. 23, 24, and 25. In Fig. 25 the magnetic compass needle and degree scale are shown.

When setting up the direction finder the zero degree mark of the scale is set to coincide with the magnetic north-and-south line and the scale then clamped. The direction of the transmit-

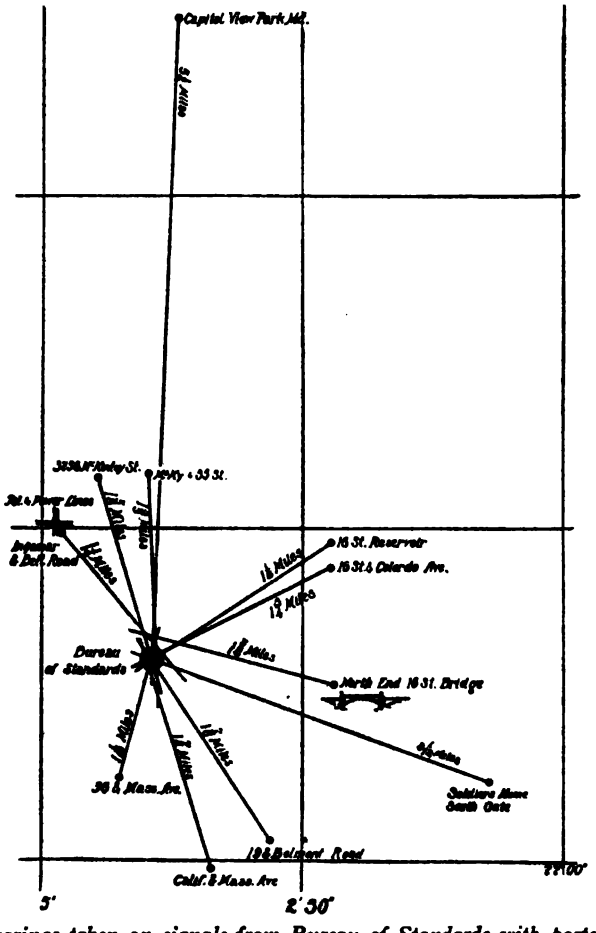

FIG. 22.—*Bearings taken on signals from Bureau of Standards with portable direction finder*

ting source is then observed by rotating the coil to the position of critical silence at which position the scale reading is noted. The direction of the source is thus given with respect to magnetic north.

Coming back now to the matter of wave distortion caused by the proximity of large metallic structures and other energy-absorbing

Digitized by Google

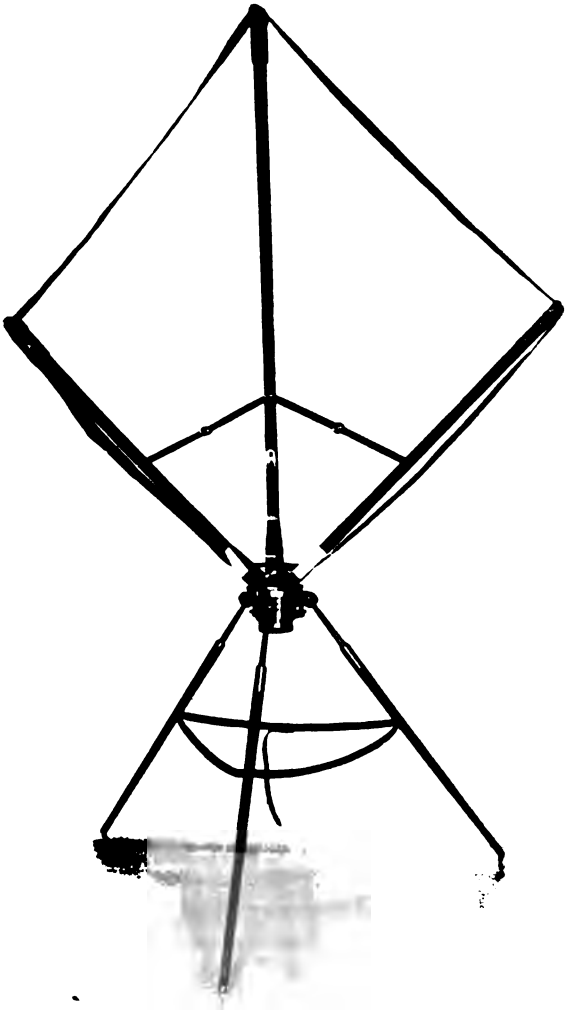

FIG. 23. *Collapsible type of direction finder for field use*

FIG. 24.—*Collapsible type of direction finder ready for transportation*

Digitized by Google

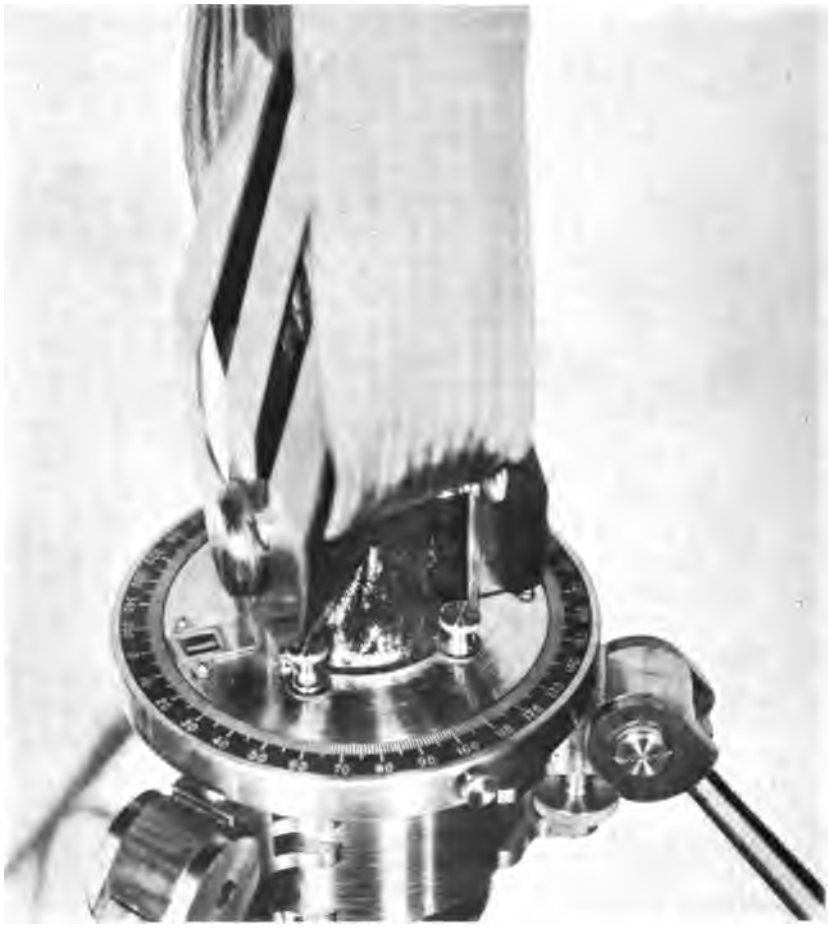

FIG. 25.—*Scale and magnetic compass as used on direction finder for field use*

Digitized by Google

systems, it is of interest to study the results obtained in the case where observations of direction were made near the Washington Monument. The Monument is about 555 feet high and has within it an elevator and stairway which form what may be considered as a fairly efficient antenna.

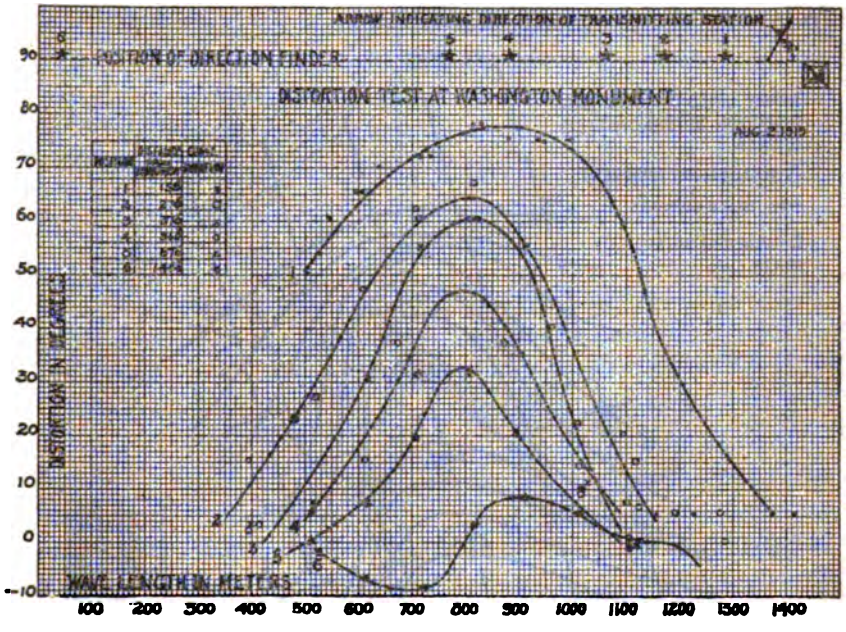

Position	Distance from monument	Curve notation
	Feet.	
1	158	●
2	270	□
3	370	×
4	560	○
5	670	△
6	1,400	*

FIG. 26.—*Distortion of radio waves caused by Washington Monument*

The results of tests made near the Monument are given in Figs. 26 and 27, which are self-explanatory.

An interesting fact is brought out by the curves given in Fig. 26, which show that maximum distortion occurs at a wave length of about 800 meters. This is apparently the natural wave length of the Monument. In other words, the Monument considered as an antenna is in resonance or in tune at this wave length.

Digitized by Google

Another interesting case is given in Fig. 28 which shows the distorting effects of a tuned antenna upon the incoming wave as observed at various distances from the lead-in wire of the antenna, indicated by positions 1, 2, 3, and 4 in the figure. The dimensions of the antenna were small as compared with the wave length used in this test, and when the antenna was out of tune no distorting effects were observed even at position 1.

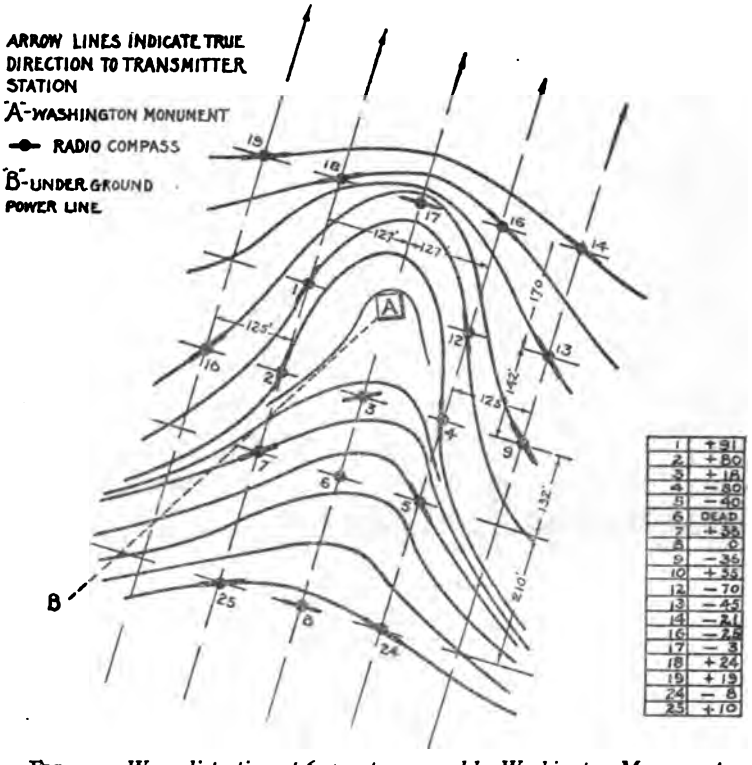

FIG. 27.—*Wave distortion at 625 meters caused by Washington Monument*

Although the experiments briefly described above were conducted under more or less exaggerated conditions, they serve nevertheless to show that great care must be taken in locating direction-finding stations on land and that in cases where distorting structures or systems can not be avoided a calibration of the direction finder must be made in order that the proper corrections may be applied to the observations taken under given conditions. This matter of calibration will be discussed in greater detail in the following section in which the use of the direction finder on shipboard is described.

Digitized by Google

III. PRACTICAL APPLICATION TO NAVIGATION

Although the coil receiving system and direction finder have been effectively used for many practical purposes, particularly during the war, its application to navigation is perhaps the most

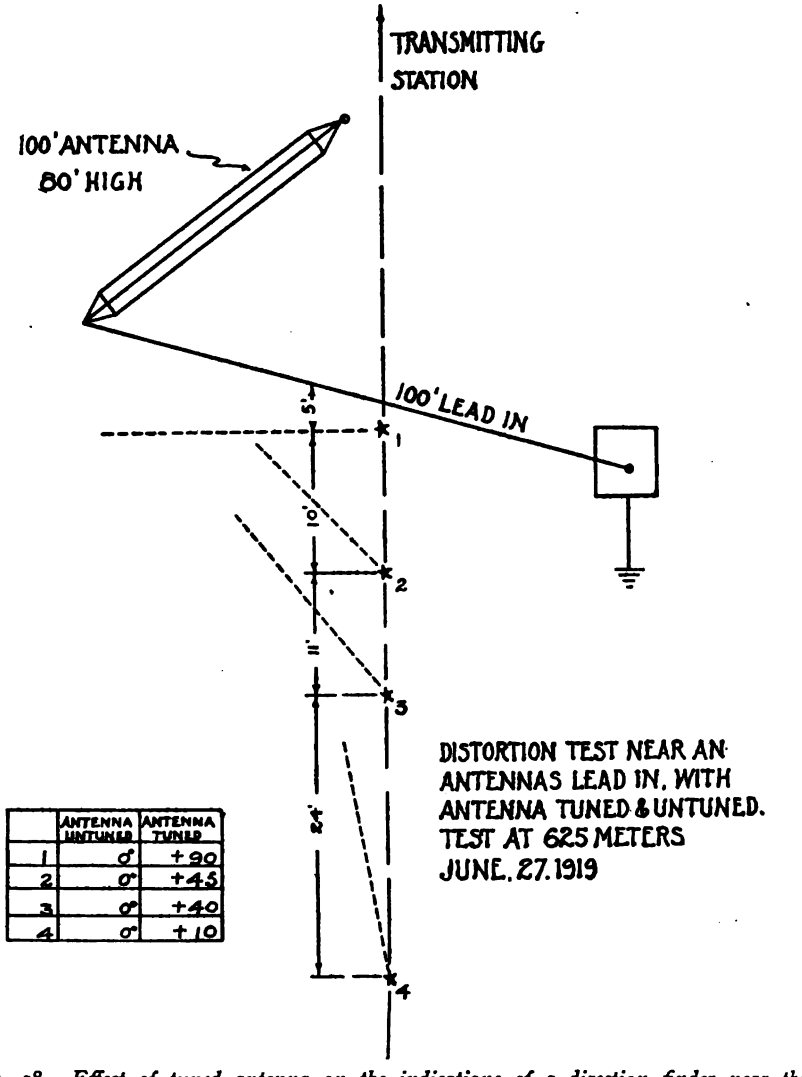

	ANTENNA UNTUNED	ANTENNA TUNED
1	0°	+90
2	0°	+45
3	0°	+40
4	0°	+10

FIG. 28.—*Effect of tuned antenna on the indications of a direction finder near the antenna lead-in*

important, and it was originally for this purpose that its development was undertaken by the Bureau of Standards.

The first practical tests of the radio fog-signaling and radio direction-finding system were begun in 1916 when the Navesink

Digitized by Google

light station at Atlantic Highlands, N. J., was equipped with an automatically operated radio transmitting set. At the same time a direction finder was installed on the lighthouse tender *Tulip*.

The transmitter installed at Navesink is shown in Fig. 29. A transmitting coil consisting of three turns 10 feet square, shown in Fig. 30, was used instead of the customary antenna.

The results obtained in these early tests were very successful, but further progress was stopped because of the war. Immediately after the armistice, however, this work was revived, and in the fall of 1919 more elaborate tests were made in Chesapeake Bay.

For these tests the lighthouse tender *Arbutus*, shown in Fig. 31, was equipped with an experimental type of direction finder, shown in Fig. 32. Three lighthouses, namely, Smith Point, Windmill Point, and Wolf Trap, were equipped with radio transmitters, two of the rotary spark type and one of the electron-tube type. The maximum sending range of these signaling stations was only about 20 miles as their radiating power was limited by the size of the antennas, which it will be seen in Fig. 35 was necessarily small.

Considerable attention was given during these tests to the matter of calibration of the direction finder in order to determine the nature and magnitude of wave distortion caused by the metallic mass of the ship. All calibrations were made with the ship's radio antenna out of tune with the signaling wave length and grounded to the ship's hull so that it became essentially a part of the metallic mass of the ship, which, taken as a whole, had an electrical period far different from that of the signaling wave.

The direction finder was placed approximately amidships and on its center line so that the mass of the ship was approximately symmetrically arranged with respect to the direction finder. Under these conditions calibration or correction curves were obtained as shown in Fig. 33. It is seen, therefore, that the radio direction finder on shipboard requires calibration just as does the ship's magnetic compass. A correction must be applied to the observed radio direction, either added or subtracted and varying in amount from zero to a maximum depending upon the fore-and-aft positions of the ship with respect to the direction of approach of the signaling wave.

To illustrate the accuracy with which the position of a ship may be determined by means of the direction finder, there is shown in Fig. 34 an actual case in which radio bearings were taken on the *Arbutus* from each of the three signaling stations or radio beacons.

Digitized by Google

FIG. 29.—*Early type of automatic radio beacon transmitter, installed at Navesink Lighthouse, 1916*

FIG. 30.—*Coil aerial transmitter used at Navesink Lighthouse, 1916*

Digitized by Google

FIG. 31.—*Lighthouse tender "Arbutus," showing experimental type of direction finder just aft of pilot house*

FIG. 32.—*Experimental type of direction finder on lighthouse tender "Arbutus"*

Digitized by Google

The intersection of these bearings drawn on the chart from each of the light stations gives the observed position of the ship. A

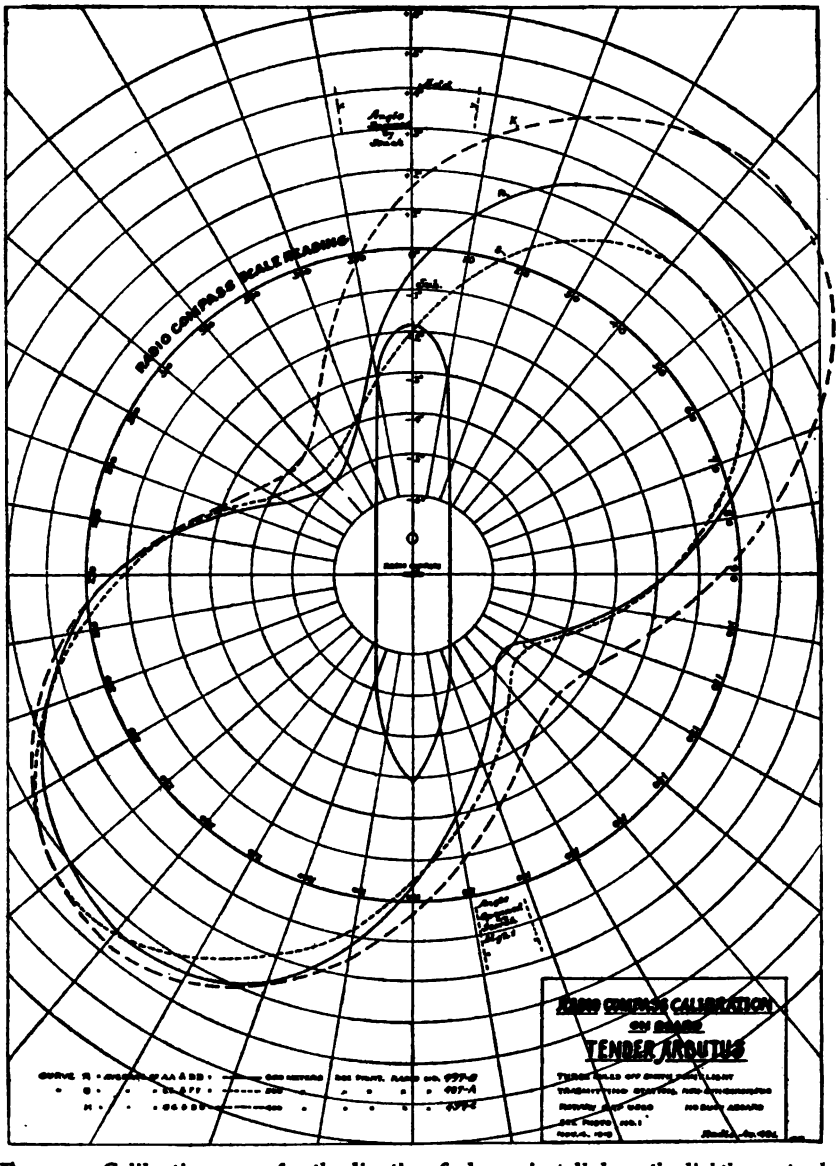

FIG. 33.—*Calibration curve for the direction finder as installed on the lighthouse tender "Arbutus"*

fourth check bearing taken from the naval radio station at Norfolk is also shown. The actual position of the ship was at buoy 10 C.

Digitized by Google

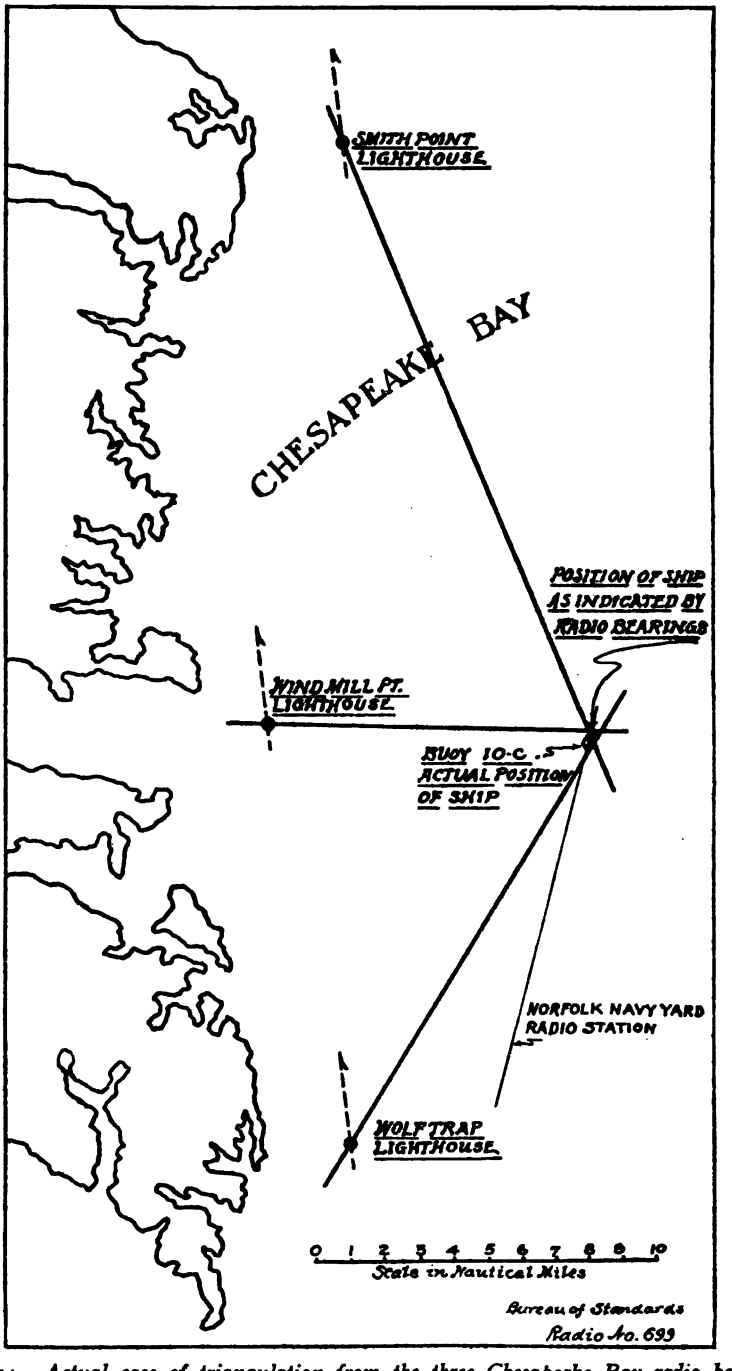

FIG. 34.—*Actual case of triangulation from the three Chesapeake Bay radio beacons*

Digitized by Google

FIG. 35.- *Smith Point Lighthouse equipped experimentally as a radio beacon*

Digitized by Google

Digitized by Google

The success of the Chesapeake Bay tests has led to the permanent installation of radio fog-signaling equipment on the Fire Island and Ambrose Channel light vessels, and at the Sea Girt light station on the New Jersey coast below Asbury Park. The Sea Girt radio beacon station is shown in Fig. 36 and the signaling apparatus in Fig. 37. The radio transmitter is of the quenched-spark type supplied from a 500-cycle, 1-kw generator. The automatic signaling system is shown to the right of the figure and is designed to transmit a characteristic signal consisting of three dots sent out in rapid succession at frequent intervals. The Fire Island and Ambrose Channel light vessels are equipped with similar apparatus, but having different signal characteristics.

Dot-signal characteristics have been adopted because of the ease with which they can be distinguished by the observer who may not be a radio operator. The signal characteristic of the Fire Island light vessel is two dots sent out in rapid succession and that of the Ambrose Channel light vessel, single dots. In each case the signaling station transmits for a given interval of time and then remains silent for a given interval of time, these time intervals being different for each station. The wave length used is 1000 meters which has been tentatively chosen by international agreement. It is possible, however, that it will be found necessary in cases where the three radio beacons are comparatively close together, to use wave lengths slightly different from each other, as, for example, 950, 1000, and 1050 meters, in order to overcome the difficulty of interference, although in general this difficulty is satisfactorily solved by the proper choice of the signaling and silent periods for each station. The signaling apparatus as installed on the Fire Island and Ambrose Channel light vessels is entirely automatic in its operation and is designed to be operated by the personnel of the station with only occasional inspection by a radio engineer attached to the office of the superintendent of the lighthouse district.

As an example of a direction-finder equipment for shipboard installation, that of the lighthouse tender *Tulip* is of interest and will be described in connection with the results obtained in a series of tests conducted during the summer and fall of 1920.

The direction-finder coil is shown in Fig. 38 and consists of 11 turns of insulated wire wound on a rigid skeleton frame 4 feet square. The coil is attached to a shaft which extends into the pilot house through suitable bearings and which is supported on ball bearings in order to permit ease and uniformity of rotation.

Digitized by Google

Another view of the direction-finder coil is shown in Fig. 39 where it is seen directly over the pilot house and on the center line of the ship. The interior view of the pilothouse, Fig. 38, illustrates the method of attaching the direction finder to the binnacle carrying the magnetic compass. By means of this arrangement radio bearings are observed in a simple and direct manner. The exterior coil is rotated from within the pilot house by means of a handwheel, and the bearing of the signaling station is read directly on the magnetic compass card. In Fig. 40 the captain of the *Tulip* is seen taking the radio bearing of the Fire Island light vessel.

A calibration or correction curve for the *Tulip* direction finder was obtained by taking simultaneous visual and radio bearings on one of the light vessels while the *Tulip* made a circular course at a distance of a few miles from the light vessel. This correction curve is shown in Fig. 41, and it will be noted that it approaches very nearly a sine curve. It will be noted further that maximum deviation from true direction occurs when the direction of approach of the signaling wave is approximately at 45° with the ship's center line; that is, when the mass of the ship assumes an unsymmetrical relation with respect to the approaching wave front. In the fore-and-aft direction and directly abeam the deviation is zero or nearly so because of the more or less symmetrical arrangement of the ship's mass with respect to the direction of approach of the wave front. This, of course, holds true only when the direction finder is located approximately amidships.

Once the correction curve has been obtained for the particular wave length assigned to the radio fog-signaling stations or radio beacons, a correction scale may be made in accordance with the curve, which, if attached to the binnacle as shown in Fig. 42, provides convenient means for reading the bearing and correction simultaneously.

The electrical circuit of the direction finder is given in Fig. 43. The variable condenser C_0 together with the coil L_0 form the main receiving circuit which is tuned to the signaling wave length. Connected across the condenser C_0, either directly or through a potential transformer P, is the vacuum tube amplifying and detecting apparatus D. This consists of a three-stage radio-frequency amplifier, a detector, and a two-stage audio-frequency amplifier made up as a unit with a minimum number of operating adjustments.

Digitized by Google

FIG. 36.—*The Sea Girt Lighthouse equipped as a radio beacon*

FIG. 37.—*Radio beacon transmitter with automatic signaling key for giving the beacon characteristic*

Digitized by Google

FIG. 40. —*The captain of the lighthouse tender "Tulip" operating the radio direction finder*

Digitized by Google

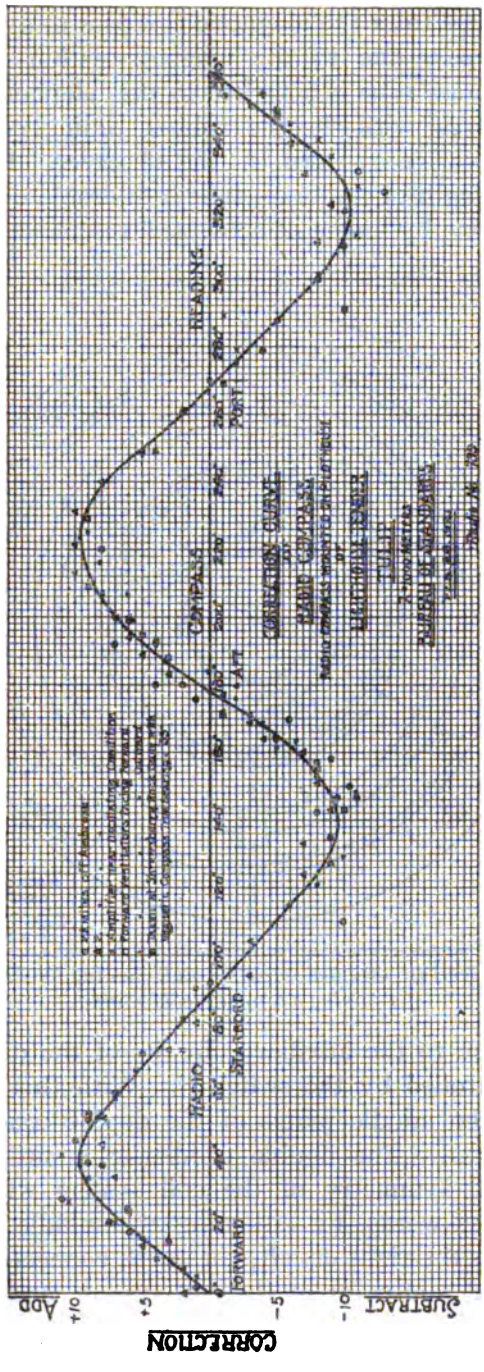

FIG. 41.—*Correction curve for direction finder installed on lighthouse tender "Tulip"*

Digitized by Google

The telephone receivers T are located in a fixed position at a sufficient distance from the magnetic compass to avoid any effect upon the compass due to the magnets within the telephone receivers. A brass tube is attached to the telephone receivers as shown in Fig. 44 with flexible rubber tubing completing the circuit to the earpieces worn by the observer. By the proper choice of the length of the brass tube a desirable quality is given to the signal tone by virtue of acoustical resonance.

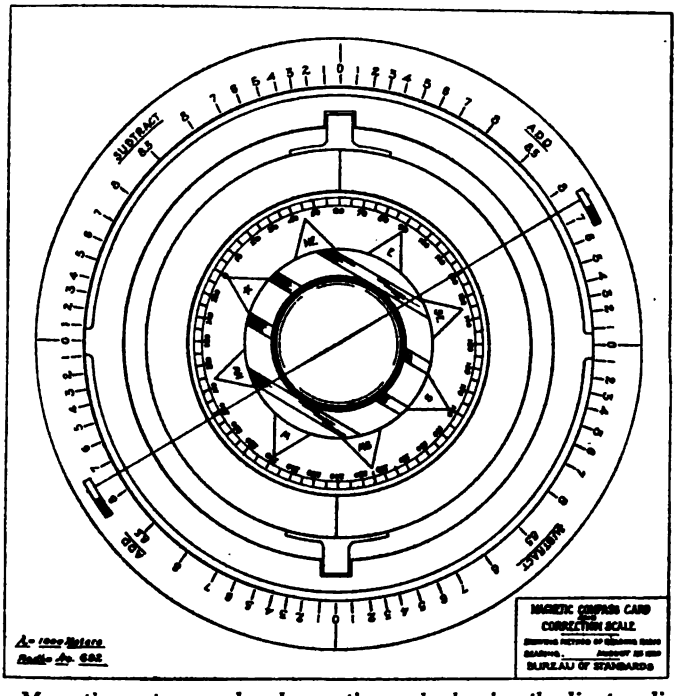

FIG. 42.—*Magnetic compass card and correction scale showing the direct-reading method of obtaining a corrected radio bearing*

We now come to the auxiliary circuits of the direction finder which are controlled by the switch S. With this switch closed to the right, the middle plates of the double condenser C_3 are directly grounded. The double condenser is utilized to bring about electrical symmetry of the coil system with respect to earth. In other words, by adjusting the middle plates of the condenser C_3 to the right or left, the earth connection is brought to the electrical mid-point of the coil system, and the parasitic effects described earlier in the paper are eliminated, that is to say, the signal received in the telephones T results only from the energy directly received in the coil L_0.

Digitized by Google

With the switch S closed to the left, a small condenser C_2 is connected across half of the double condenser C_3 and the inductance L_1 and tuning condenser C_1 are inserted in the ground lead. Under these conditions, the coil system is no longer electrically symmetrical with respect to earth, and received energy enters the coil circuit L_0C_0 indirectly through the tuned

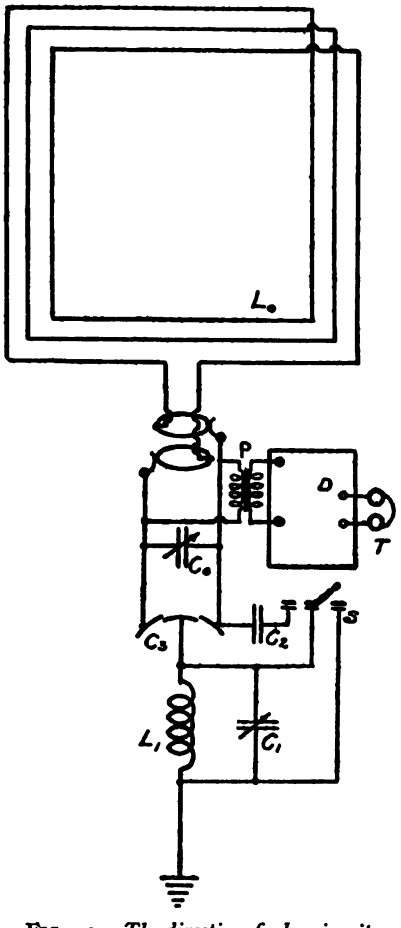

FIG. 43.—*The direction finder circuit*

ground circuit of which the capacity of the complete coil system to earth forms a part.

By the proper adjustment of the capacity C_2 and the circuit L_1C_1, a complete unidirectional effect can be obtained as previously described.

In the practical operation of the direction finder, all tuning adjustments remain set for the 1000-meter wave length of the

Digitized by Google

signaling stations. Switch *S* is closed to the right when observing the line of direction of a given signaling station and to the left when it is desired to determine the sense of direction. In other words, to determine the line of direction of a station, the coil system which is directly grounded at its electrical mid-point by throwing switch *S* to the right is rotated to the position of critical silence, at which time the plane of the coil is normal to the direction of approach of the signaling wave. To determine the sense of direction of the station, switch *S* is closed to the left and the coil rotated to the position of maximum signal intensity at which time the plane of the coil is in the direction of approach of the signaling wave and pointing toward the signaling station as indicated by an index pointer provided for that purpose. The complete direction finder system is shown with details in Fig. 45.

The results of actual tests conducted under most practical conditions are shown by the charts, Figs. 46 and 47, which are self-explanatory.

The 45-mile run shown in Fig. 46 was made on radio bearings taken from the signaling station on the Fire Island light vessel. During this run the direction finder was operated and all bearings taken by the captain of the tender *Tulip*, who had had no previous experience in the operation of any kind of radio apparatus.

In Fig. 47 the estimated positions of the *Tulip* at quarter-hour intervals are given during the south-by-west course taken from Jones Inlet buoys. The true position of the ship, as determined by radio bearings taken on two of the three signaling stations, is also shown in several instances.

The accuracy with which the position of a ship may be determined by triangulation, resulting from bearings taken by radio on two or more signaling stations, depends, of course, upon the sense, whether positive or negative, and order of magnitude of the possible error made in observing the radio bearing of each of the signaling stations. Theoretical triangulations are shown in Fig. 48, in which an exaggerated error of plus or minus 2 degrees is assumed in each case. Any set of three observations or bearings will locate the ship within a triangular area, but the true position of the ship may be entirely outside of this area but within a star-shaped area formed as shown in Fig. 48, the details of which are shown in Fig. 49.

Digitized by Google

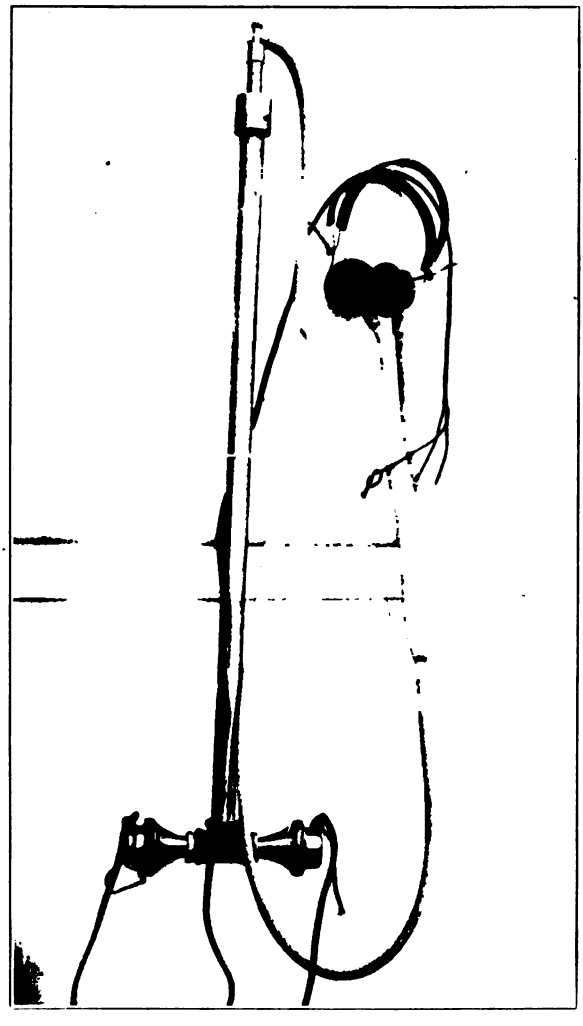

FIG. 44.—*Method of keeping telephone receivers at a fixed distance from the magnetic compass*

Digitized by Google

Digitized by Google

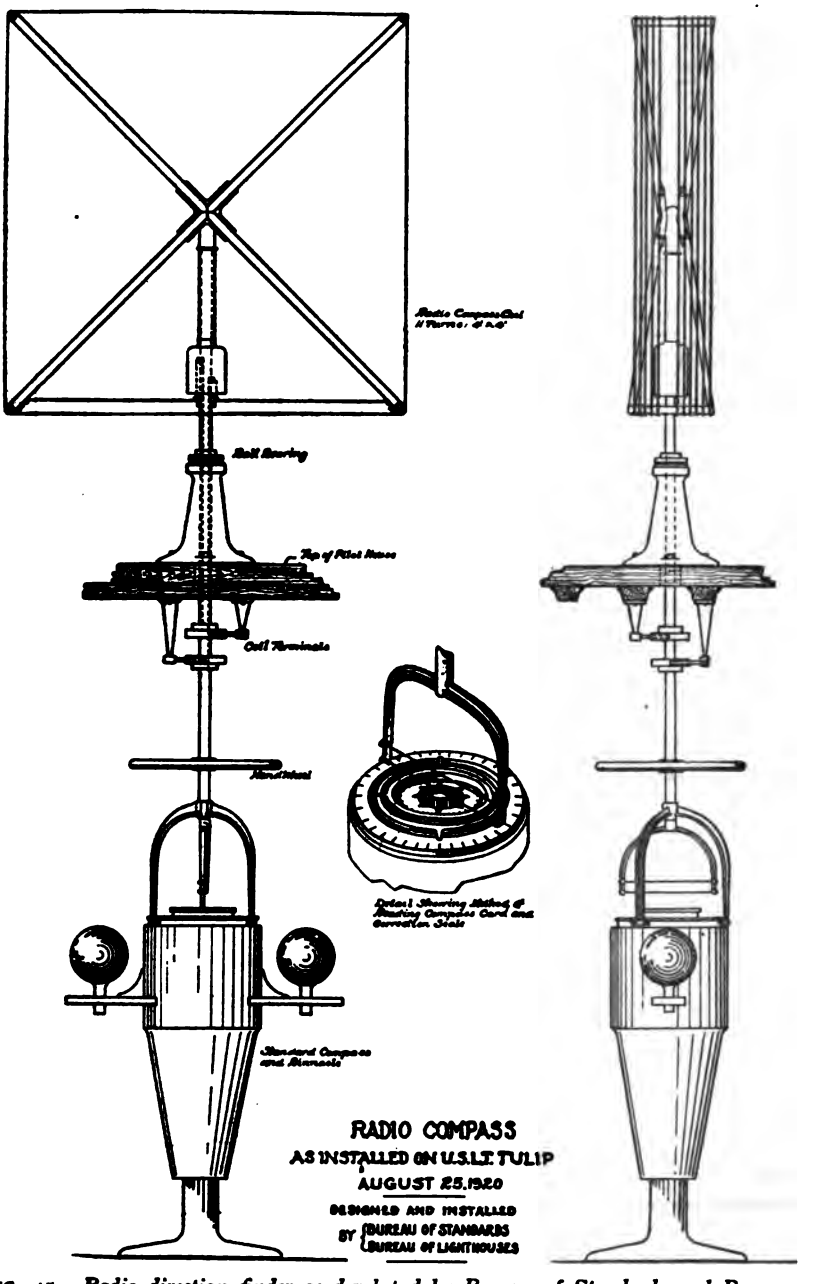

FIG. 45.—*Radio direction finder as developed by Bureau of Standards and Bureau of Lighthouses*

Digitized by Google

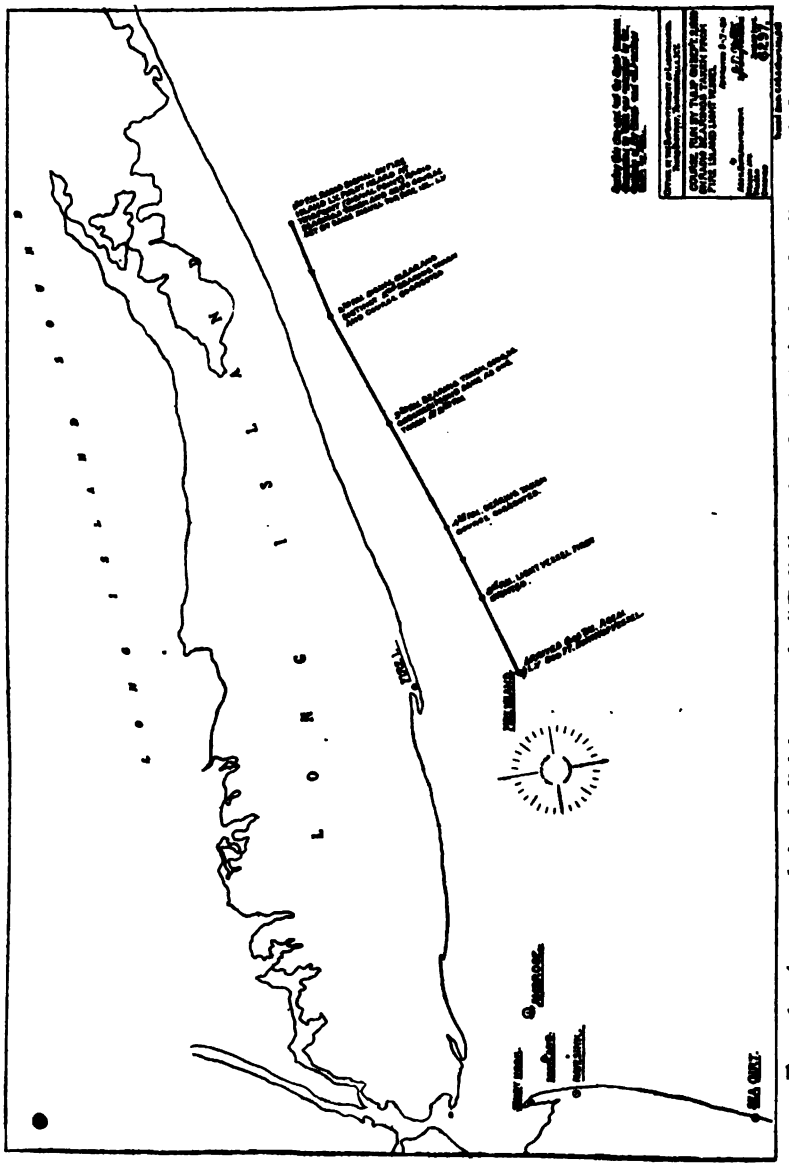

FIG. 46.—*A run made by the lighthouse tender "Tulip" navigated entirely by the radio direction finder*

Digitized by Google

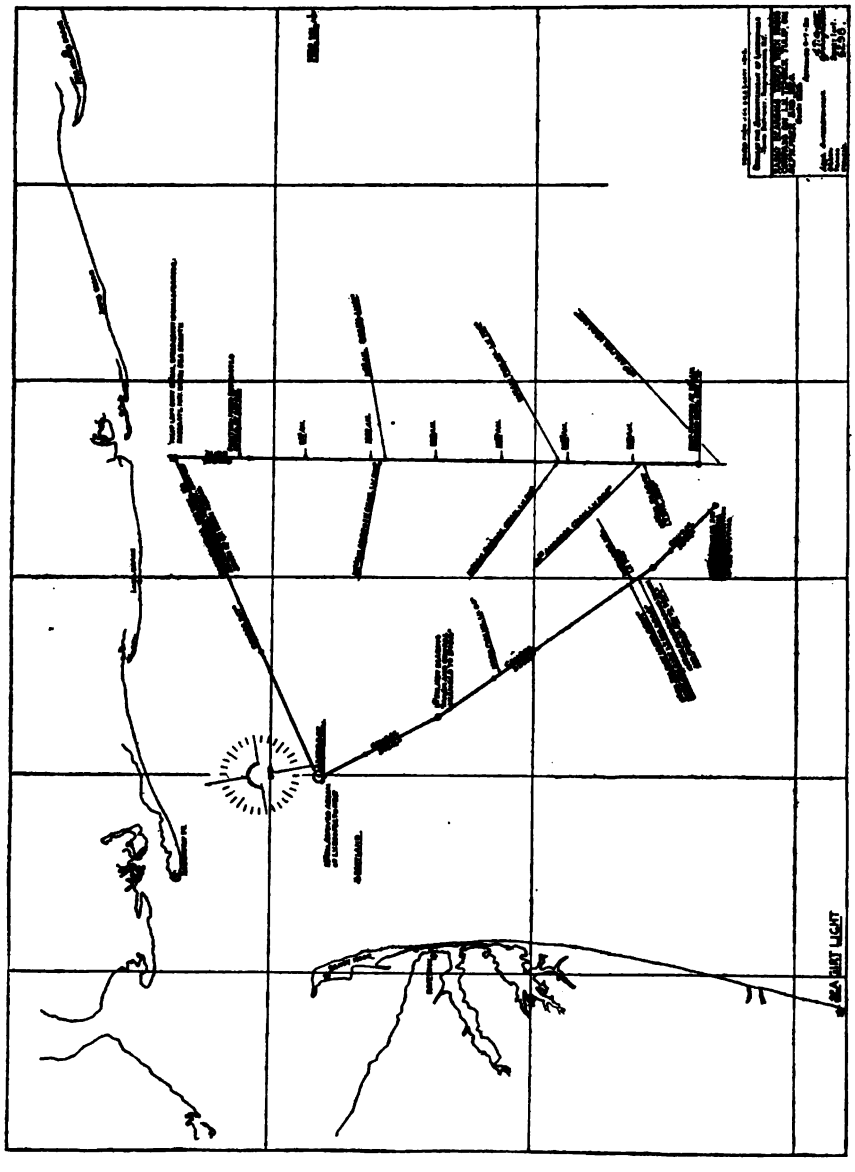

FIG. 47.—*Runs made by the authors entirely by radio bearings*

Digitized by Google

IV. CONCLUSION

In conclusion it may be definitely stated that the radio direction finder, or radio compass, as herein described, is an extremely effective aid to navigation, particularly in fog or thick weather. If properly constructed, installed, and calibrated, it can be depended upon to give reliable results. The device is essentially a nautical instrument and should be installed on shipboard, where it may be used directly by the navigator in taking bearings on

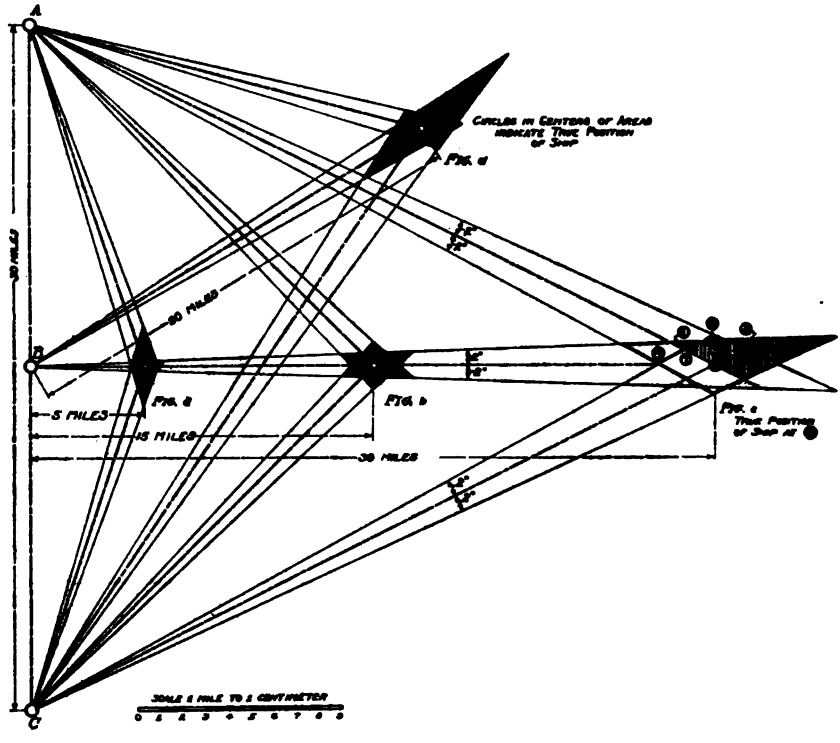

FIG. 48.—*Accuracy of radio triangulation*

signaling stations established on shore or on light vessels. Bearings may thus be taken at any time and as often as desired.

The reverse method of locating direction-finder stations on shore and requiring the navigator of a ship to make a request for his bearing or position from time to time, as conditions may permit, is fundamentally wrong. Delays and errors are inherent, and even under the most favorable conditions the time consumed in making a request for bearings, taking bearings, and getting the information into the navigator's hands, is too great.

Digitized by Google

The maintenance of a 24-hour service at the required number of shore direction-finder stations requires a large operating personnel, continually on watch but only occasionally called upon for service. This places great responsibility and expense upon the Government.

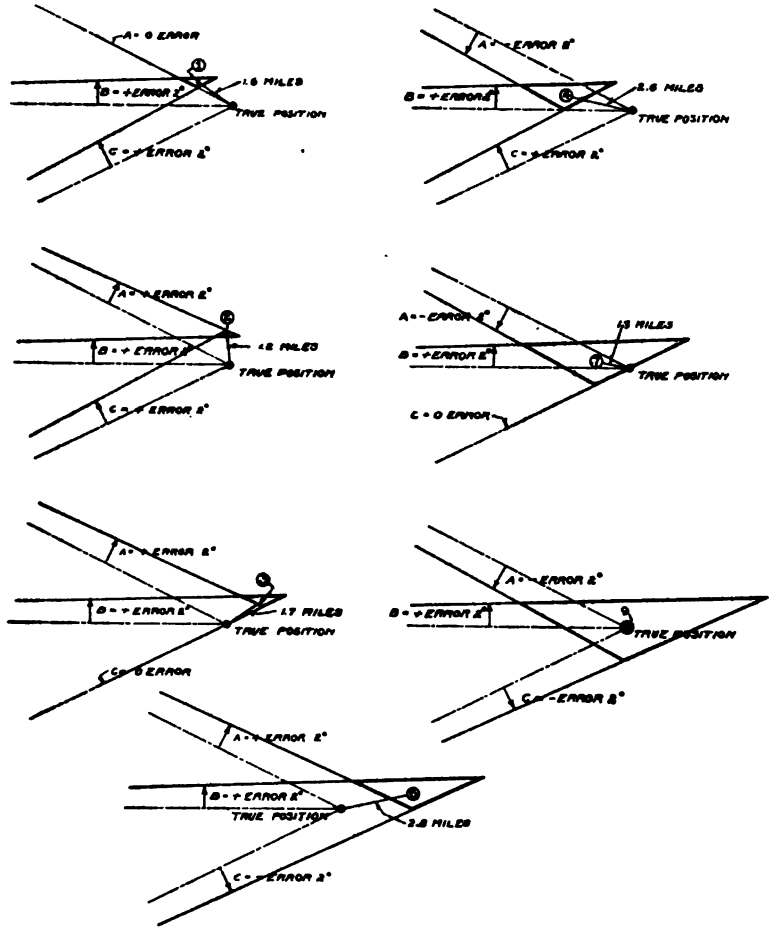

FIG. 49.—*Accuracy of radio triangulation, showing true and observed position*

Signaling stations, whose locations are accurately shown on mariners' charts, may be established at lighthouses and on light vessels at very little expense. Such stations would thus become a part of an already well-established service whose function is strictly that of maintaining aids to navigation. No additional personnel is required since the operation and maintenance of the radio-signaling apparatus would be the duty of the light keeper.

Digitized by Google

The cost of the radio direction-finder equipment for shipboard installation is so small as compared with the benefits which may be derived therefrom, perhaps in a single instance, where life, property, or even time may be saved, that it can not enter into consideration.

The utility of the direction finder on shipboard goes further than that of taking bearings on known stations on or near shore. Other ships at sea, perhaps in distress or in fog, can be located and their course determined. As a matter of safety, every ship at sea in fog should send out radio fog signals at frequent intervals, effective over a distance of at least 10 miles. This would enable another ship within range equipped with a radio direction finder to determine the direction and course of the signaling ship and thereby proceed with safety and without delay.

The work of the Bureau of Standards herein described has been conducted with the assistance and close cooperation of the Bureau of Lighthouses and particularly of the lighthouse depot at Tompkinsville, N. Y.

WASHINGTON, July 9, 1921.

Digitized by Google

LIBRARY OF THE UNIVERSITY OF CALIFORNIA

MAR 9 1922

DEPARTMENT OF COMMERCE

SCIENTIFIC PAPERS

OF THE

BUREAU OF STANDARDS

S. W. STRATTON, DIRECTOR

No. 429

NOTE ON THE PREPARATION OF MANNOSE

BY

E. P. CLARK, Associate Sugar Chemist

Bureau of Standards

JANUARY 16, 1922

PRICE, 5 CENTS

Sold only by the Superintendent of Documents, Government Printing Office
Washington, D. C.

WASHINGTON
GOVERNMENT PRINTING OFFICE
1922

Digitized by Google

Digitized by Google

NOTE ON THE PREPARATION OF MANNOSE

By E. P. Clark

ABSTRACT

A method is described by which mannose may be prepared easily and economically. Ivory-nut shavings or sawdust are treated with dilute NaOH, washed, and dried. Five hundred grams of the material thus prepared are digested for a day with 75 per cent sulphuric acid, then dissolved in water to make 5.5 liters. This mixture is boiled for two and one-half hours, neutralized with $BaCO_3$, concentrated, and the sugar crystallized from glacial acetic acid, giving a yield of 42 to 45 per cent of the treated meal.

A method for the preparation of mannose from ivory-nut shavings has recently been described by Horton.[1] In his procedure the shavings are first treated with dilute sodium-hydroxide solution, whereby gums and extractives are removed. This preliminary step is a great improvement over previous methods, as it gives a product of higher purity and eliminates the disadvantage of excessive foaming when the solution is concentrated. However, the mass of detail prescribed for subsequent steps offsets the advantage gained; hence the method, as a whole, is no improvement over that of Hudson and Sawyer.[2]

The writer has on various occasions prepared mannose by a very simple process which, when applied to ivory-nut shavings that have first been treated with sodium hydroxide, gives a yield that is considerably higher than either author has reported. This method is given below, as its simplicity and economy will appeal to workers who have to prepare this sugar.

Sifted ivory-nut shavings are added to 10 times their weight of boiling 1 per cent sodium-hydroxide solution. The mixture is at once removed from the source of heat and stirred occasionally during one-half hour. The shavings are then washed thoroughly with running water until neutral and clear, and dried.

Five hundred grams of the material thus prepared are thoroughly mixed with 500 g of 75 per cent sulphuric acid and allowed to stand until the next day. This mass is dissolved in water, making a volume of 5.5 liters, and boiled under a reflux for two

[1] Horton, Paul M., J. Ind. and Eng. Chem., 13, No. 11, p. 1040; 1921.
[2] Hudson C. S., and Sawyer, H. L., J. Am. Chem. Soc., 39, p. 470; 1917.

82509°—22

Digitized by Google

and one-half hours. While the liquid is still boiling, it is neutralized with a thin paste of precipitated barium carbonate. The solution is at once filtered through a thin layer of active carbon placed on moistened filter paper in a Büchner funnel. The filtrate generally contains a little barium, probably in combination with organic acids. This is removed by adding a few cubic centimeters of dilute sulphuric acid until no further precipitate is formed. The barium sulphate is filtered off and the solution evaporated under reduced pressure to 87 to 88 per cent total solids.[3] An equal volume of glacial acetic acid is added and thoroughly mixed by warming and shaking. The sirup is seeded, placed in an ice box overnight for crystallization to start, and is then frozen with an ice-salt mixture. The frozen mass is placed in a refrigerator at or near 0° C where it will thaw out slowly. After about a day the greater portion of the sugar will often have crystallized, but generally a week is required for complete crystallization. The yield is uniformly 42 to 45 per cent of the treated meal used.

WASHINGTON, December 12, 1921.

[3] Horton directs that the final sirup shall be concentrated to 96 per cent total solids. It is difficult and tedious to get such a thick mixture into solution in acetic acid, and it is obviously impractical where a dozen or more kilos of mannose are to be made at one time. A concentration of 87 to 88 per cent total solids is amply heavy, and offers no difficulty either in dissolving in the acid or in subsequent crystallization.

Digitized by Google

MAY 22 1922

DEPARTMENT OF COMMERCE

LIBRARY OF THE UNIVERSITY OF CALIFORNIA

SCIENTIFIC PAPERS

OF THE

BUREAU OF STANDARDS

S. W. STRATTON, DIRECTOR

No. 430

HIGH-FREQUENCY RESISTANCE OF INDUCTANCE COILS

BY

GREGORY BREIT, Consulting Physicist

Bureau of Standards

FEBRUARY 24, 1922

PRICE, 5 CENTS

Sold only by the Superintendent of Documents, Government Printing Office
Washington, D. C.

WASHINGTON
GOVERNMENT PRINTING OFFICE
1922

Digitized by Google

Digitized by Google

HIGH-FREQUENCY RESISTANCE OF INDUCTANCE COILS

By Gregory Breit

ABSTRACT

The definition of the resistance of a coil is simple for direct current and may be given directly in terms of Ohm's Law. Similarly, the computation of the resistance of a coil made of a wire of known length, cross section, and material is quite easy for direct current. The same problem becomes difficult if an alternating current of high frequency is used instead of a direct current.

It is shown in this paper that a different definition of resistance must be given; that the value of the resistance thus defined depends upon the point in the coil with respect to which the resistance is defined; and it is shown how the resistance-variation method, described in Bureau of Standards Circular 74, may be employed to measure the resistance thus defined.

A formula is derived for the value of the current at any point of the coil when the emf induced in any portion of the coil is known. This formula is compared with the experimental results obtained on coil aerials. This formula presupposes the knowledge of the resistance measured by the resistance-variation method with respect to all points on the coil. In order to know this resistance, it is sufficient to know the resistance as measured with respect to one point and also to know the distribution of current in the coil. The value of the resistance with respect to one point of the coil is worked out and the result is verified experimentally.

CONTENTS

	Page
Introductory	569
I. Meaning of the term "resistance" at high frequencies	570
II. Simplifying assumption	571
III. Properties of nondissipative systems	572
IV. Application of properties of nondissipative systems to coils	574
1. Resistance inserted in coil	576
2. Resistance-variation method of measuring resistance	576
3. Computation of current at one point of the coil due to emf at a different point	577
4. Application to coil aerials	579
5. Law of increase of resistance near the natural period	582
(a) Case of grounded coil	586
(b) Experimental test of resistance formulas	586
V. Summary	587

INTRODUCTORY

At low frequencies there is little difficulty in discussing the resistance of a coil. At sufficiently high frequencies, however, some difficulty is encountered. There are two effects which cause

Digitized by Google

the difficulty. The first is the skin effect and the second is the capacity effect. It is the purpose of this discussion to treat the capacity effect. It is believed that the modifications introduced in this treatment by skin effect are only minor.

The capacity effect consists in the collection of charges on the wires of the coil and in the nonuniform distribution of current in the coil which these charges cause.

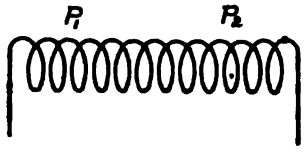

FIG. 1.—*Inductance coil*

If P_1, P_2 are two points of the coil (see Fig. 1), a certain charge collects on the wire between P_1 and P_2. If the current entering the section $P_1 P_2$ at P_1 is i_1, and if the current leaving the section at P_2 is i_2, and if Q should denote the charge in the section $P_1 P_2$ then

$$i_1 = \frac{dQ}{dt} + i_2$$

by the conservation of charge.

The quantity Q is determined mainly by the potential differences between the section $P_1 P_2$ and the remaining parts of the coil. These potential differences are roughly proportional to $\frac{di}{dt}$ where i is the average current in the coil.

This, of course, is true only provided there are no appreciable phase differences between the induced emf's due to various portions of the coil; i. e., provided the dimensions of the coil are small in comparison with the wave length used, and also provided the coil may be regarded as a perfect conductor. Thus, the difference between i_1 and i_2 is roughly proportional to i and the square of the frequency. For high frequencies, therefore, the current distribution is very nonuniform and for low frequencies it is practically uniform.

The nonuniformity of current affects the resistance of the coil. It is the purpose here to find the modification to be introduced in the ordinary treatment of resistance by the nonuniform current distribution.

I. MEANING OF THE TERM "RESISTANCE" AT HIGH FREQUENCIES

In alternating-current theory the resistance is taken to be the real part of a complex quantity z (called the complex impedance), which is such that if the current i is the real part of $Ie^{j\omega t}$, and and if the emf e is the real part of $Ee^{j\omega t}$, where I and E are real or

Digitized by Google

complex quantities independent of the time t, where $j=\sqrt{-1}$, and where ϵ is the base of natural logarithms, then

$$E=zI.$$

This definition applies to circuits consisting of series combinations of inductances, resistances, and capacities independently of where the emf e is applied or where the current i is measured. If, however, the circuits consist of parallel combinations of resistance, inductance, and capacity, it is no longer immaterial where the emf e or the current i are measured.

In the case of the coil, also, it is not immaterial where e is inserted and where i is measured, because i is not the same at different points of the coil and because the effect of e on i at a given place may depend upon the place where e is inserted. This compels one to define the resistance not for the coil as a whole, but only for a particular point of the coil. One can imagine the wire cut at that point, the two faces of the cut separated by a very small gap and an emf inserted in that gap, and one can also imagine the current measured at that gap. Call the emf e and the current i and write

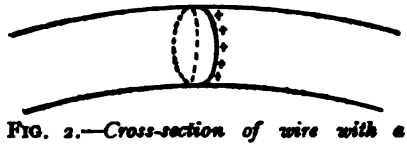

FIG. 2.—*Cross-section of wire with a double layer of charge*

$$e=Ee^{j\omega t}, \qquad i=Ie^{j\omega t}.$$

The impedance of the coil, together with the circuit connected across its terminals with reference to the point at which the gap was made, will be defined, as usual, by the equation

$$z=\frac{E}{I}.$$

The real part of the impedance will be termed the resistance and the coefficient of j in the imaginary part will be called the reactance.

It may be shown in the usual manner that the resistance R thus defined is such that i^2R is the power lost in the coil where i, R are measured at the point where the emf is applied.

II. SIMPLIFYING ASSUMPTION

In radiotelegraphy it is usually legitimate to assume that the coils are made of perfect conductors when it is desired to find the current distribution in the coils. A perfect conductor is an ideal substance whose properties are the limit of the properties ap-

Digitized by Google

proached by a conductor having a finite conductivity when the conductivity becomes infinite. For a perfect conductor the electric intensity at the surface is normal to the surface and the magnetic intensity at the surface is tangential to the surface.

The energy losses in a system consisting of perfect conductors are entirely energy losses due to radiation. In the case of a coil these energy losses are negligible, and so the coil itself, so far as its current distribution is concerned, can be looked at as a nondissipative system; i. e., a system in which no energy is dissipated.

It is well known that there is a very close analogy between electrical and dynamical systems, and that to most of the propositions of dynamics one can give an electrical interpretation. The analogy between dynamical and electrical systems becomes complete if charges are taken as coordinates. Then the energy stored up in the electric field is regarded as potential energy and the energy of the magnetic field of the currents is regarded as kinetic energy. Of course, in a consideration of a continuous system, such as a coil, the number of coordinates is infinite, so that the system should be considered as the limiting case of another system with a finite number of coordinates, as this number is increased indefinitely. In the case of the coil the wire may be subdivided into small portions along each length and the charges on these portions are then coordinates. As the number of sections is increased indefinitely the number of coordinates also increases indefinitely, and in the limit the coordinates represent the coil correctly. This is precisely analogous to the treatment of the vibrations of a string of finite and uniform density by replacing it by a weightless string with beads spaced along its length.

Nondissipative dynamical systems have been studied, their properties are known, and will be here applied to the case of the coil made out of a perfect conductor. A brief review of these properties will now be given.

III. PROPERTIES OF NONDISSIPATIVE SYSTEMS

Consider, then, a dynamical system whose kinetic energy T and whose potential energy V are given, respectively, by

$$T = \tfrac{1}{2}\,(a_{11}\dot{q}_1^2 + a_{22}\dot{q}_2^2 + \cdots + 2a_{12}\dot{q}_1\dot{q}_2 + \cdots)$$

$$V = \tfrac{1}{2}\,(b_{11}q_1^2 + b_{22}q_2^2 + \cdots + 2b_{12}q_1q_2 + \cdots)$$

where

$$q_1, q_2, q_3, \cdots, q_n$$

Digitized by Google

are the coordinates of the system and where

$$\dot{q}_1, \dot{q}_2, \cdots, \dot{q}_n$$

are the derivatives of the coordinates as to the time. The behavior of the system is given by Lagrange's equations

$$\frac{d}{dt}\left(\frac{\partial L}{\partial \dot{q}_r}\right) - \frac{\partial L}{\partial q_r} = Q_r, \quad (r = 1, 2, \cdots, n)$$

where L is the kinetic potential defined by

$$L = T - V$$

and where Q_r is the component of generalized force corresponding to q_r. These equations when the values of T and V are substituted take the form

$$\left(a_{1r}\frac{d^2q_1}{dt^2} + b_{1r}q_1\right) + \left(a_{2r}\frac{d^2q_2}{dt^2} + b_{2r}q_2\right) + \cdots + \left(a_{nr}\frac{d^2q_n}{dt^2} + b_{nr}q_n\right) = Q_r$$

$$(r = 1, 2, \cdots n)$$

or symbolically

$$\left(a_{1r}\frac{d^2}{dt^2} + b_{1r}\right)q_1 + \left(a_{2r}\frac{d^2}{dt^2} + b_{2r}\right)q_2 + \cdots + \left(a_{nr}\frac{d^2}{dt^2} + b_{nr}\right)q_n = Q_r$$

If one deals with purely periodic motions of frequency ω in 2π seconds, then differentiation as to t when repeated twice amounts to multiplication by $-\omega^2$. Hence the equations of motion become

$$(-a_{1r}\omega^2 + b_{1r})q_1 + (-a_{2r}\omega^2 + b_{2r})\,q_2 + \cdots + (-a_{nr}\omega^2 + b_{nr})\,q_n = Q_r$$

The solution of this system of equations gives for the coordinates

$$q_s = \frac{\Delta_s}{\Delta}$$

where

$$\Delta = \begin{vmatrix} -a_{11}\omega^2 + b_{11}, & -a_{12}\omega^2 + b_{12}, & \cdots, & -a_{1n}\omega^2 + b_{1n} \\ -a_{12}\omega^2 + b_{12}, & -a_{22}\omega^2 + b_{22}, & \cdots, & -a_{2n}\omega^2 + b_{2n} \\ -a_{13}\omega^2 + b_{13}, & -a_{23}\omega^2 + b_{23}, & \cdots, & -a_{3n}\omega^2 + b_{3n} \\ \cdots & \cdots & \cdots & \cdots \\ \cdots & \cdots & \cdots & \cdots \\ -a_{1n}\omega^2 + b_{1n}, & -a_{2n}\omega^2 + b_{2n}, & \cdots, & -a_{nn}\omega^2 + b_{nn} \end{vmatrix}$$

and where Δ_s is the result of changing in Δ the elements of the s^{th} column into $Q_1, Q_2, \cdots, Q_n$.

Digitized by Google

The condition for resonance is

$$\Delta = 0.$$

This is an equation in ω^2. It has n roots and gives the n natural periods of the system.

If $\Delta = O$, then provided neither of its first minors is zero, and provided neither of the quantities Q_s is zero, all of the quantities q_s become infinite. Similarly, their derivatives become infinite (provided $\omega \neq O$) and also all linear combinations of the coordinates or of their derivatives, which are not identically zero, become infinite.

Thus, for a nondissipative system resonance is independent of the relative values of the components of generalized force, and it is also independent of the quantity measured in detecting resonance as long as the quantity used increases when the coordinates increase. Thus, this criterion may be the maximum value of one coordinate or of the derivative of the coordinate as well as of a linear combination of several coordinates (not vanishing identically) or, finally, a linear nonvanishing combination of the several velocities.

IV. APPLICATION OF PROPERTIES OF NONDISSIPATIVE SYSTEMS TO COILS

A physical system is never a nondissipative system. However, if the dissipation of energy is sufficiently small its properties approach those of a nondissipative system.

The inductance coil made of copper wire has some energy losses. If, however, the resistance between any two points of it is negligible compared to the reactance between these two points, the coil may be considered for some purposes as a nondissipative system. The smaller the resistance is made in comparison with the reactance the more nearly is the coil nondissipative.

In the theory that follows it will be assumed that the reactance is sufficiently high and the resistance sufficiently low to make the coil nondissipative. For any actual coil this assumption must, of course, be justified. It is generally justified if the resistance of any part of the coil is negligible compared to its reactance. Under these conditions the presence of the resistance affects the current only to the second order of the resistance, as may be seen by expanding the impedance by Taylor's theorem.

Digitized by Google

The current distribution also is determined, primarily, by the reactance and is affected only to the second order by the resistance. To this order, then, the current distribution is the same as if the coil were nondissipative. Now, in a nondissipative system the ratios of the coordinates are independent of the distribution of generalized forces as resonance is approached.

To see the truth of this statement observe that the ratio of two coordinates, say, q_1 and q_2, is the ratio of corresponding determinants, say Δ_1, Δ_2. Here

$$\Delta_1 = Q_1 \mathfrak{C}_{11} + Q_2 \mathfrak{C}_{12} + \cdots + Q_n \mathfrak{C}_{1n}$$
$$\Delta_2 = Q_1 \mathfrak{C}_{21} + Q_2 \mathfrak{C}_{22} + \cdots + Q_n \mathfrak{C}_{2n}$$

where $\mathfrak{C}_{rs}$ is the minor of $-a_{rs}\omega^2 + b_{rs}$ in Δ.

However, Δ is a symmetrical determinant. Further, for resonance Δ vanishes. But if a symmetrical determinant vanishes then all the second minors of the complimentary determinant vanish. Hence

$$\frac{\mathfrak{C}_{11}}{\mathfrak{C}_{12}} = \frac{\mathfrak{C}_{12}}{\mathfrak{C}_{22}} = \frac{\mathfrak{C}_{13}}{\mathfrak{C}_{23}} = \cdots = \frac{\mathfrak{C}_{1n}}{\mathfrak{C}_{2n}} = \mathfrak{C}$$

say. And consequently

$$\frac{q_1}{q_2} = \frac{\Delta_1}{\Delta_2} = \mathfrak{C}$$

The ratio $\frac{q_1}{q_2}$ is therefore independent of the values of $Q_1, Q_2, \ldots, Q_n$ provided the resonance condition

$$\Delta(\omega) = 0$$

is fulfilled, and also provided it is legitimate, for resonance, to compute the ratios of various q's on the assumption that the system is nondissipative. The latter proviso requires careful consideration, because for resonance the reactance of a circuit vanishes and consequently the current is determined mainly by the resistance and not by the reactance.

Nevertheless, in practice this does not give difficulty, because the only root of $\Delta(\omega)$ to be considered is the lowest, so that the reactance vanishes only for the whole circuit considered in series. Hence, even though the absolute value of the current due to an emf applied at a point P_1 (see Fig. 1) will depend on the resistance, still the distribution of current will be determined mainly by the very high reactances of the various parts of the coil. Thus,

Digitized by Google

considering the portion of the coil between P_1 and P_2, the current may either be used up in charging that portion or else in passing through it and charging portions of the coil beyond P_1 P_2. The relative proportion of the parts of the current which are used in these ways is determined by the impedances of the part P_1 P_2 (used as a condenser) and the parts beyond P_1 P_2. If the conductivity of the material is high, the impedances are not distinguishable from the reactances, and therefore the proviso is satisfied. *It thus has been shown that the current distribution for resonance is independent of the distribution of emf's and that it is the same as if the system were nondissipative.*

These facts may also be extended to systems in which the total dissipation is not negligible, provided the emf is not induced in the parts which are not perfect conductors. For, the current distribution in the parts in which the conductors are nearly perfect is still the same. Thus, if a short resistance of negligible capacity be inserted in a cut made in the coil, the current distribution is not affected thereby, because the current entering the resistance is equal to the current leaving it and because everywhere outside the resistance the coil is nearly nondissipative.

1. RESISTANCE INSERTED IN COIL

As explained, a resistance inserted at some point in the coil does not affect the current distribution. It therefore cuts down the current in the same ratio at all points in the coil. Hence it follows that if the coil has been brought into resonance by adjusting the condenser it will still be in resonance when a resistance is inserted at any point.

In fact, let this point be P. Let an emf e be applied very near to P. Whether the condenser is tuned or not, if a resistance be inserted at P the absolute value of the current must be cut down because, with reference to the point, the coil and the condenser together have a certain impedance, say, $z=R+jX$. Whether or not R is equal to zero, an increase in R increases the absolute value of z, viz: $|z|=\sqrt{R^2+X^2}$
and therefore decreases the absolute value of the current.

2. RESISTANCE-VARIATION METHOD OF MEASURING RESISTANCE

This suggests a method of measuring the quantity R at any point in the coil. This method is known as the resistance-variation method. It is described for the case of the coil terminal in Bureau of Standards Circular 74, pages 180 to 185. It consists in

Digitized by Google

bringing the coil into resonance by a proper adjustment of the tuning condenser and measuring the current I. Then, a resistance R_1 is inserted and a new current I_1 is observed.

As explained the ratio $\frac{I}{I_1}$ does not depend on the way in which the emf is induced. Therefore, one can imagine the emf induced very close to the point where the resistance R_1 is inserted. If the resistance with reference to this point is R and if the emf is E, then

$$I=\frac{E}{R}, \qquad I_1=\frac{E}{R+R_1}$$

whence

$$R=\frac{R_1}{\frac{I}{I_1}-1} \quad \ldots . \tag{1}$$

Here I and I_1 are measured at the point where R_1 is inserted. However, their ratio was shown to be independent of the place where they are measured. Thus, I, I_1 may be measured at an arbitrarily chosen point in the coil. If the place where R_1 is inserted is varied, different values of R are obtained. If x be a parameter along the wire of the coil, R is then a function of x, say, $R(x)$.

3. COMPUTATION OF CURRENT AT ONE POINT OF THE COIL DUE TO EMF AT A DIFFERENT POINT

The function $R(x)$ is such that the current at x, due to an emf e applied at x, is $\frac{e}{R(x)}$ provided the coil is tuned. Suppose that an emf e is applied at x_1. It is desired to know the current at x_2. The currents at x_2 and x_1 are always in the same ratio, which may be conveniently written as $\frac{f(x_2)}{f(x_1)}$.

The current at x_1 due to e at x_1 is $\frac{e}{R(x_1)}$

Therefore, the current at x_2 due to e at x_1 is $\frac{e}{R(x_1)} \cdot \frac{f(x_2)}{f(x_1)}$. If, now, a resistance R_0 be inserted at x_2, the current at x_2 must be decreased to $\frac{R(x_2)}{R(x_2)+R_0}$ of its former value. Consequently, at x_1 also it

Digitized by Google

has been decreased to that fraction of its former value. Therefore, at x_1 after the resistance R_0 has been inserted the current is

$$i_1' = \frac{e}{R(x_1)} \cdot \frac{R(x_2)}{R(x_2)+R_0} \qquad (2)$$

Again, compare the result of inserting R_0 at x_1 with the result of inserting it at x_2 when the same current flows through the coil. In the second case the amount of energy lost per second is $\left(\frac{f(x_2)}{f(x_1)}\right)^2$ of what it is in the first case. Therefore, in terms of the current i_1 at x_1, the energy lost per second in R_0 when R_0 is inserted at x_2 is

$$R_0\left(\frac{f(x_2)}{f(x_1)}\right)^2 i_1^2$$

but the resistance $R(x_1)$ is such a quantity that the power lost in the coil is

$$R(x_1)\, i_1^2.$$

Therefore, the total power lost in both the coil and R_0 is

$$\left[R(x_1)+R_0\frac{f(x_2)^2}{f(x_1)^2}\right] i_1^2$$

Thus, when R_0 is inserted at x_2 the coil appears to have a resistance

$$R(x_1)+R_0\frac{f(x_2)^2}{f(x_1)^2}$$

with reference to x_1. Consequently, after R_0 is inserted the current at x_1 becomes

$$i_1' = \frac{e}{R(x_1)+R_0\frac{f(x_2)^2}{f(x_1)^2}} \qquad (3)$$

Comparing (2) and (3)

$$R(x_1)\, f(x_1)^2 = R(x_2)\, f(x_2)^2 \qquad (4)$$

Hence, also,

$$\frac{f(x_2)}{f(x_1)} = \sqrt{\frac{R(x_1)}{R(x_2)}} \qquad (5)$$

Digitized by Google

Further, the current at x_2 due to an emf e at x_1 is

$$i_2 = \frac{e}{R(x_1)} \frac{f(x_2)}{f(x_1)}$$

and therefore by (5) is

$$i_2 = \frac{e}{\sqrt{R(x_1) R(x_2)}} \tag{6}$$

If, then, x be a point of the coil and if in an element dx an emf $e(x)\,dx$ be induced, then the current at x_0 is

$$i_0 = \frac{1}{\sqrt{R(x_0)}} \int_{x_1}^{x_2} \frac{e(x)\,dx}{\sqrt{R(x)}} \tag{7}$$

where now x_1, x_2 denote the terminal values of x.

(A different and shorter proof of this may be given with the aid of Lord Rayleigh's reciprocal theorem.)

4. APPLICATION TO COIL AERIALS

Coil aerials are inductance coils used for receiving signals in radiotelegraphy. The emf due to the incident wave is distributed uniformly through the coil aerial. Thus, formula (7) may be used to compute the current at any point.

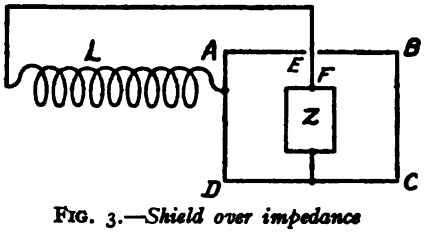

FIG. 3.—*Shield over impedance*

Qualitative checks of this theory are given by the experimental results on signal intensities obtained by means of coil aerials for the Signal Corps. The theory was also verified by some special experiments performed in the yard of the Bureau of Standards.

A coil aerial was wound on a wooden frame and placed between the two large rectangular coils of an electron tube generating set. The coils were so arranged as to give an approximately uniform field. The coil was tuned to the wave length of the generating set by means of a condenser across its terminals. An electrostatic voltmeter was connected across the condenser terminals. The tuning of the condenser was effected from a distance by a pulley and the voltmeter was read from a distance by means of a telescope. This eliminated the effect of the observer's body.

Leaving the wave length of the generating set unchanged, turns were cut off from the coil, alternately from both sides. It

Digitized by Google

was retuned each time and the voltmeter reading was noted. Then, on the same frame a similar coil was wound and, using the same condenser, resistance measurements were made with reference to the condenser terminal and also with reference to a point exactly in the middle of the coil. The apparent inductance of the coil was also measured.

Now, it will be shown presently that if

N is the number of turns

L_a is the apparent inductance

and

$$R_e = \frac{R_o}{1 + \frac{2}{3}\left(\sqrt{\frac{R_o}{R_m}} - 1\right)}$$

R_o, R_m being respectively the resistance with reference to the terminal and with reference to the middle, then $\frac{NL_a}{R_e}$ must be proportional to the reading of the voltmeter. This was verified experimentally, as will be described presently. The relation can be derived as follows:

The reading is $\frac{i_o}{C\omega}$ where i_o is the current through the joint capacity of the condenser and voltmeter and where C is that joint capacity. By the definition of apparent inductance this is the same as $i_o L_a \omega$. By equation (7)

$$i_o = \frac{1}{R_o}\int_{x_1}^{x_2} e(x)\sqrt{\frac{R_o}{R(x)}}\,dx$$

But $e(x)$ is constant if x denotes the length along the wire. Therefore, letting $e = \int_{x_1}^{x_2} e(x)\,dx$

$$i_o = \frac{e}{R_o}\frac{\int_{x_1}^{x_2}\sqrt{\frac{R_o}{R(x)}}\,dx}{x_2 - x_1} = \frac{e}{R_o}\left(1 + \theta\left(\sqrt{\frac{R_o}{R_m}} - 1\right)\right)$$

where $\theta\left(\sqrt{\frac{R_o}{R_m}} - 1\right)$ denotes the mean value of $\sqrt{\frac{R_o}{R(x)}} - 1$

Digitized by Google

In the case of an ungrounded coil such as has been used R_m is the least value of $R(x)$. Thus, $\theta < 1$.
Further, by (5)

$$\sqrt{\frac{R_o}{R(x)}} - 1 = \frac{i(x)}{i_o} - 1$$

The quantity $\frac{i(x)}{i_o} - 1$ when plotted against x is nearly a parabola.[1]
Taking this approximation

$$\theta = \frac{2}{3}$$

This, of course, is only an approximation.
Thus,

$$i_o = \frac{\epsilon}{R_e}$$

where

$$R_e = \frac{R_o}{1 + \frac{2}{3}\left(\sqrt{\frac{R_o}{R_m}} - 1\right)}$$

Here e itself is proportional to the number of turns N. Thus, the voltmeter reading is proportional to

$$\frac{NL_a}{R_e}$$

The results of the experiment on a 3-foot coil wound with No. 18 wire, spaced 1 cm and used at 437 meters, are:

Number of turns	Ratio of experimental to theoretical voltage
6	0.98
7	1.00
8	1.01
9	1.04
10	1.12

Considering the fact that the resistances measured with reference to the middle and to the terminal may differ by a factor of 2, and that a slight dissymmetry was introduced in the resistance measurements by the thermocouple and galvanometer used in

[1] G. Breit, "The distributed capacity of inductance coils," Phys. Rev., 17, pp. 672, 673, Figs. 6, 7, 8; June, 1921.

Digitized by Google

measuring the current, that the value of θ is only an approximation, and that the experiment was performed outdoors, where the humidity has a variable effect on the resistance, this agreement may be regarded as satisfactory.

Formula (5) has been verified directly by means of thermogalvanometers calibrated at 60 cycles.

5. LAW OF INCREASE OF RESISTANCE NEAR THE NATURAL PERIOD

So far measured values of resistance have been relied upon. It now becomes necessary to compute the resistance without measuring it. The whole coil may be imagined to be divided into a number of parts. The points of division may be so chosen that the mutual inductance of each part to the whole coil is the same.

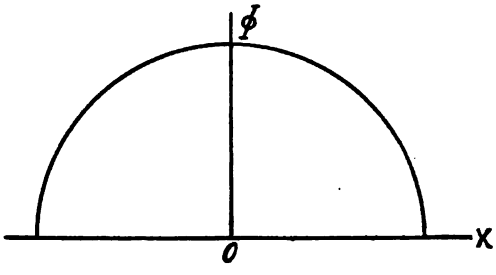

FIG. 4.—*Graphical representation of the function* ϕ

If the coil is wound closely, the current in any section, say the mth, is

$$i_m = i_o + \phi(m)\omega^2\bar{i} \quad . \quad . \quad . \quad . \quad . \quad (8)$$

where

$$\bar{i} = \frac{i_1 + i_2 + \cdot \cdot \cdot \cdot \cdot \cdot + i_n}{n}$$

where n is the total number of parts.[2]

Let

$$\Phi = \frac{\sum_{m=1}^{n} \phi(m)}{n}$$

Then, summing (8) and dividing by n

$$\bar{i} = i_o + \Phi\omega^2\bar{i}$$

that is,

$$\bar{i} = \frac{i_o}{1 - \Phi\omega^2}$$

and

$$i_m = i_o\left[1 + \frac{\phi(m)\omega^2}{1 - \Phi\omega^2}\right]$$

[2] G. Breit, "The distributed capacity of inductance coils," Phys. Rev., 17, pp. 669, 671, June, 1921; Section, explanation of constancy of C_o, equation (28a).

Digitized by Google

In the limit when the subdivision becomes very fine one can write

$$i(x) = i_0\left[1 + \frac{\phi(x)\omega^2}{1-\Phi\omega^2}\right] \tag{9}$$

where x, as before, is a parameter along the wire. Again, for a closely wound coil the length of the elementary section is independent of its order. Hence, the parameter x must be taken as the length or else it must be a constant times the length along the wire.

Let $R(x)dx$ be the resistance of the section between x and $x+dx$ at the frequency in question with the particular current distribution which flows through the section.

The power lost in the section is

$$R(x)[i(x)]^2dx$$

The power lost in the whole coil is

$$i_0^2\int_{x_1}^{x_2} R(x)\left(\frac{i(x)}{i_0}\right)^2 dx$$

Therefore, the resistance with reference to the point x_0 is

$$R_0 = \int_{x_1}^{x_2} R(x)\left(\frac{i(x)}{i_0}\right)^2 dx$$

This by (9) becomes

$$R_0 = \int_{x_1}^{x_2} R(x)dx + \frac{2\omega^2}{1-\Phi\omega^2}\int_{x_1}^{x_2} R(x)\phi(x)dx + \frac{\omega^4}{(1-\Phi\omega^2)^2}\int_{x_1}^{x_2} R(x)[\phi(x)]^2dx \cdots \tag{10}$$

In particular if $R(x)$ is independent of x

$$R_0 = \left[1 + \frac{2\omega^2\Phi}{1-\Phi\omega^2} + \frac{\omega^4\,\overline{\phi^2}}{(1-\Phi\omega^2)^2}\right]\int_{x_1}^{x_2} R(x)dx \tag{11}$$

where $\overline{\phi^2}$ is the average of ϕ^2 with respect to x.

If x_0 is a terminal point Φ is $\frac{1}{\omega_0^2}$ where ω_0 is 2π times the natural frequency of the coil, for

$$\bar{i} = \frac{i_0}{1-\Phi\omega_0^2}$$

Digitized by Google

and since for the natural frequency the terminal current vanishes $i_0 = o$ for a finite $\bar{I}$ which necessitates

$$\Phi = \frac{I}{\omega_0^2}$$

Thus, (11) may be also written as

$$R_0 = \left[1 + \frac{2\frac{\omega^2}{\omega_0^2}}{1 - \frac{\omega^2}{\omega_0^2}} + \frac{\frac{\omega^4 \overline{\phi^2}}{\omega_0^4 \Phi^2}}{\left(1 - \frac{\omega^2}{\omega_0^2}\right)^2} \right] \int_{x_1}^{x_2} R(x)dx \quad \cdots \quad (12)$$

or, if it is preferred to use wave lengths

$$R_0 = \left[1 + \frac{2}{\frac{\lambda^2}{\lambda_0^2} - 1} + \frac{\frac{\overline{\phi^2}}{\Phi^2}}{\left(\frac{\lambda^2}{\lambda_0^2} - 1\right)^2} \right] \int_{x_1}^{x_2} R(x)dx \quad (13)$$

Now, $\int_1^{x_2} R(x)dx$ is the resistance which the coil would have if there were no capacity effect. The knowledge of skin effect is sufficient for its computation. Assuming the change in resistance due to skin effect to be known, it remains to find $\frac{\overline{\phi^2}}{\Phi^2}$ and λ_0 in order to find the coil resistance.

If the current distribution in a coil is known the ratio $\frac{\overline{\phi^2}}{\Phi^2}$ may be calculated.

CALCULATION OF $\frac{\overline{\phi^2}}{\Phi^2}$ FOR SPECIAL CASES

The special case considered is that of a short, closely wound, solenoid when used ungrounded.

The quantity $\frac{\overline{\phi^2}}{\Phi^2}$ clearly depends only on the shape of the $\phi(x)$,x curve. It remains unchanged if $\phi(x)$ is multiplied by a constant factor.

It was shown in "The distributed capacity of inductance coils" (loc. cit.) that the quantity called there $\alpha(x)$ is

$$\alpha(x) = -\frac{10^{-11} KLl}{35.956 \pi a} \coth u_0 \frac{\cos v}{\sin v}$$

Digitized by Google

It is therefore proportional to

$$\frac{\cos v}{\sqrt{\sin v}}$$

The quantity $\alpha(x)$ is so chosen that $\left(\frac{di}{dt}\right)\alpha(x)dx$ is the charge in the segment of the coil between x and $x+dx$. Also, in the notation of the paper cited x is proportional to a length along the wire. The quantity v may be regarded as defined by

$$a \cos v = x$$

In order to obtain the current distribution from $\alpha(x)$ it suffices to note that

$$\frac{\partial i}{\partial x} = -\left(\frac{di}{dt}\right)\alpha(x)$$

Thus

$$i = -\frac{di}{dt}\int_a^x \alpha(x)dx$$

Hence

$$\phi \text{ is proportional to } \int_a^x \frac{xdx}{\sqrt{a^2-x^2}} = -\sqrt{a^2-x^2}$$

Thus, ϕ may be represented by a semicircular arc. The average value of $\sqrt{a^2-x^2}$ is then $\frac{\pi a}{4}$, and the square of the average value is $\frac{\pi^2 a^2}{16}$

The square of $\sqrt{a^2-x^2}$ is a^2-x^2, and its average is $\frac{2a^2}{3}$

Thus

$$\frac{\overline{\phi^2}}{\Phi^2} = \frac{32}{3\pi^2} = 1.080$$

With the aid of this expression, formula (13) for the case of a short single layer solenoid becomes

$$R_0 = \left[\left(\frac{1}{1-\frac{\lambda^2_0}{\lambda^2}}\right)^2 + \frac{0.080}{\left(\frac{\lambda^2}{\lambda_0^2}-1\right)^2}\right]\int_{x_1}^{x_2} R(x)dx \qquad (14)$$

It is worth while to call attention to the fact that this formula is true, independently of whether the solenoid is in an elliptical shield or not because the term coth u_0 occurring in $\alpha(x)$ does not affect the result.

Digitized by Google

(*a*) CASE OF GROUNDED COIL.—In the case of a grounded coil it is easiest to compute the resistance with reference to the ungrounded terminal, because if i_0 is the current at the terminal, $i_0 = 0$ is the condition which must be satisfied for λ_0. From this resistance the resistance at any other point may be derived.

This remark is to serve as a caution not to take the grounded terminal as the terminal x_0. The formula (14) is then modified only inasmuch as the factor 0.080 is changed.

(*b*) EXPERIMENTAL TEST OF RESISTANCE FORMULAS.—Formula (14) is a convenient one for experimental verification.

If λ is not too near to λ_0 the second term in the parentheses may be neglected. Then (14) takes the simplified form

$$R_0 = \frac{\int_{x_1}^{x_2} R(x)dx}{\left(1 - \frac{\lambda_0^2}{\lambda^2}\right)^2} \qquad (14')$$

This is formula (35) of Lindemann (loc. cit.). It is seen, however, from the derivation that in the case of a shielded condenser it holds only for the resistance measured in the ungrounded lead. Also, it is apparent from formula (14) that (14′) is not an exact expression even for the case of a coil made of a perfect conductor and with constant skin effect throughout its length. Thus, for the case of perfect linkage, nearly perfect conductivity, but variable skin effect, formula (10) holds.

Since the influence of the place in which the resistance is inserted does not seem to have been realized in Lindemann's work, a new verification of formula (14′) was thought advisable. This verification was carried out on a coil designed to satisfy the assumptions made in deriving (14′). The coil was a single-layer coil wound with stranded wire (litz). The number of strands was 32, and each strand was insulated from the other.

According to a calculation made by Lindemann [3] the ratio of the increase of the resistance of a wire due to skin effect to its direct current resistance is

$$\frac{\pi^2\omega^2 z^2 r^6}{2\sigma^2 R^2}$$

where z = number of strands;
r = radius of a strand;
R = radius of the wire;
σ = resistivity in cgs electromagnetic units.

[3] R. Lindemann, Jahrbuch. d. drahtl. Tel., 4, p., 574 (28); 1910–1911.

Digitized by Google

Using this formula, and also the measured value of λ_0, which proved to be 200 meters, the ratios of increase of resistance in comparison with the direct-current resistance as well as the measured values are as below:

Wave-length (meters)	Skin effect factor	Capacity factor	Measured R	Apparent direct-current resistance
			Ohms	Ohms
717	1.142	1.176	6.65	4.94
781	1.120	1.146	6.42	4.99
800	1.114	1.139	6.25	4.93
908	1.089	1.103	5.94	4.94
1139	1.056	1.065	5.71	5.07
1255	1.046	1.051	5.47	4.97
Mean				4.97

In the last column is given the result of dividing the measured values recorded in the column before the last by the numbers given in the second and the third columns. For example—

$$4.94 = \frac{6.65}{1.142 \times 1.176}$$

The measured direct-current resistance is 4.84 ohms. It is less than the mean of the last column by 0.13 ohm, which is a deviation of 2.7 per cent. The values used are values measured with reference to the ungrounded lead.

V. SUMMARY

There has been discussed the meaning of the term "resistance" when applied to a coil in which high-frequency current is flowing. It was shown that the term must be applied only with reference to a particular point in the circuit.

The computation of the current at a given point in the circuit when an emf is arbitrarily induced in it and when the circuit is tuned has been carried through. The results have been checked experimentally.

The resistance of a coil has been computed on the assumption that the effect on it of skin effect is known. The formula has been checked experimentally.

Acknowledgment is due to Dr. C. Snow, R. S. Ould, and C. T. Zahn for reading the manuscript and for suggestions which have led to a clearer presentation of the subject.

WASHINGTON, July 18, 1921.

Digitized by Google

Digitized by Google

Digitized by Google

Digitized by Google

LIBRARY OF THE UNIVERSITY OF CALIFORNIA

MAY 22 1922

DEPARTMENT OF COMMERCE

SCIENTIFIC PAPERS

OF THE

BUREAU OF STANDARDS

S. W. STRATTON, DIRECTOR

No. 431

[Part of Vol. 17]

THE FIELD RADIATED FROM TWO HORIZONTAL COILS

BY

GREGORY BREIT, Consulting Physicist

Bureau of Standards

MARCH 10, 1922

PRICE, 5 CENTS

Sold by the Superintendent of Documents, Government Printing Office, Washington, D. C.

WASHINGTON

GOVERNMENT PRINTING OFFICE

1922

Digitized by Google

Digitized by Google

THE FIELD RADIATED FROM TWO HORIZONTAL COILS

By Gregory Breit

ABSTRACT

The landing of airplanes can be facilitated by emitting from the landing field a vertical beam of electromagnetic radiation of a radio frequency. A type of transmitting coil antenna has been devised for this purpose by J. A. Willoughby, of the Bureau of Standards. The behavior of this transmitting coil antenna is calculated in the following paper. Formulas are worked out for the current received in a coil aerial and in an antenna oriented in a known manner at a sufficient distance from the transmitter. It is found that for coil reception if—

I_s=sending current.
n_s=number of turns in either coil of the transmitter.
h=distance between the planes of the two coils of the transmitter.
M_s=area of either transmitting coil.
l=distance from transmitter to receiver.
θ=angle made by the length l with the vertical.
ϕ=angle made by plane of receiving coil with length l.
λ=wave length used.
R=resistance of receiving coil.
n_r=number of turns in receiving coil.
M_r=area of receiving coil.
I_r=received current.

Then

$$I_r=4.675\times10^4\frac{I_s\,n_s\,n_r\,M_s\,M_r\,h_s\sin\theta\cos\theta\cos\phi}{\lambda^4\,l\,R}$$

and for open antenna reception

$$I_r=\frac{7.44\times10^3\,I_s\,n_s\,M_s\,h_s\,h_r\,\sin\theta\cos\theta\cos\alpha}{\lambda^3\,R\,l}$$

where h_r=length of antenna.
α=angle made by antenna with normal to plane of l and vertical.
R=resistance of antenna.

It is found that if a vertical coil aerial is used for reception and if the airplane flies horizontally a maximum signal is obtained when the distance l makes an angle of 30° with the vertical. The influence of the earth is also discussed for the case when the earth may be considered as a perfect conductor. In both cases it was found that the energy was sent out by the transmitter into a region which is very similar to what would be obtained by constructing two coaxial circular cones having a common apex and a vertical axis, the cones themselves being inverted and cut off at a proper height (perhaps a mile or more, depending on the sensitivity of the receiving apparatus).

CONTENTS

	Page
I. Introduction	590
II. Calculation of field intensity	590
(1) Circular coils	592
(2) Rectangular coils	596
III. Applications	599
(1) Region of audible signal	599
(2) Current in receiving coil	603
IV. Summary	605
V. List of symbols	605

Digitized by Google

I. INTRODUCTION

The usefulness of a beam of radio waves directed upward from an airplane landing field for assisting an airplane to locate the landing area in times of poor visibility is apparent. During the course of some experimental work along this line J. A. Willoughby, then laboratory assistant at the Bureau of Standards, suggested the use of a special type of antenna for this purpose. The theory of the radiation from such an antenna is given in the present paper.

Mr. Willoughby proposed the use of an antenna consisting of two horizontal coils, one placed somewhat above the other, the current in one coil flowing in the opposite direction to that of the current in the other. The current was intended to be of a fairly high radio frequency, such as is ordinarily employed in radio communication with airplanes, so that signals could be received with an ordinary radio receiving set.

In general, it was believed that the waves would radiate in the form of a beam or inverted cone above the antenna. Experiment showed this to be true, signals being received on the airplane only when it was nearly above and in the immediate vicinity of the transmitting antenna.

To determine from theoretical considerations the nature of the radiated field and the region over which signals can be heard at various heights above such an aerial, the following calculation was made. The calculation justifies the belief that the radiation would form a beam in the form of an inverted cone above the transmitting antenna. The results of the calculation are expressed in inverse powers of the distance from the transmitting antenna. The lowest power gives the radiation component of the field. The next higher power may be looked at as a first approximation to the induction component. In the final formulas it is always assumed that the dimensions of the transmitting coils and the distance between them are small in comparison with the wave length used. However, it has been made sure by additional computations that the directional properties of the radiation do not depend on this approximation within a wide range.

II. CALCULATION OF FIELD INTENSITY

The principle of the calculation is based on the solution of Lorentz of the general problem of finding the electric field intensity **E** and the magnetic field intensity **H** at a given point if

Digitized by Google

the distribution of charges and currents is known. The fundamental equations of the electromagnetic field are:

$$\text{curl } \mathbf{H} = \frac{4\pi}{c}\left(\rho \mathbf{v} + \frac{K}{4\pi}\frac{\partial \mathbf{E}}{\partial t}\right)$$

$$\text{curl } \mathbf{E} = -\frac{\mu}{c}\frac{\partial \mathbf{H}}{\partial t}$$

$$\text{div } \mathbf{E} = \frac{4\pi\rho}{K}$$

$$\text{div } \mathbf{H} = O$$

where ρ is the volume density of charge, K the dielectric constant, μ the permeability, t the time, $\mathbf{E}$ the electric intensity, $\mathbf{H}$ the magnetic intensity, c a constant depending upon the choice of units, and $\mathbf{v}$ is the velocity of the charge.[1]

A solution of this system of equations is

$$\mathbf{H} = \text{curl } \mathbf{A}$$

$$\mathbf{E} = -\frac{\mu}{c}\frac{\partial \mathbf{A}}{\partial t} - \Phi$$

where

$$\mathbf{A} = \frac{1}{c}\int \frac{\{\rho \mathbf{v}\}}{r} d\tau$$

$$\Phi = \frac{1}{K}\int \frac{\{\rho\}}{r} d\tau$$

the symbol $\{\psi\}$ denoting the value of ψ at the element of volume $d\tau$ at the time $t - \frac{r\sqrt{K\mu}}{c}$, r being the distance from the element of volume $d\tau$ to the point at which $\mathbf{A}$ or Φ is computed. The integrals are to be extended throughout all space. A surface distribution of charge is only a special case of volume distribution. Thus, the above solution for volume distribution applies in all cases.

[1] In the Gaussian system in this notation $K=1$ and $\mu=1$ for air, and c is numerically equal to the velocity of light (approximately 3×10^{10}). For the electromagnetic system $\mu=1$, $K=\frac{1}{(\text{velocity of light})^2}$ for air, and $c=1$. On the electrostatic system $c=1$, and for air $K=1$, $\mu=\frac{1}{(\text{velocity of light})^2}$. Results in the international system of electric and magnetic units can not be obtained from this set of equations.

Digitized by Google

•Out of the infinite variety of shapes which the coils of the transmitting aerial which is under consideration can have there are two most easily amenable to analysis. These are: (1) Circular coils, (2) rectangular coils. The first has the advantage of symmetry; the second has the advantage of easy practical construction and of the possibility of obtaining particular solutions by elementary means, which also hold to the first order of magnitudes for the general case.

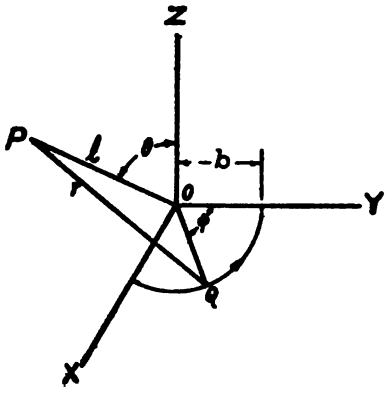

FIG. 1.—*Reference system used in discussing radiation from single circular coil*

1. CIRCULAR COILS

Consider a single circular coil of radius b in the plane of XY, with its center at the origin of coordinates. (See Fig. 1.) Let the dielectric constant of the space around the coil be K.

Let P be any point in the XZ plane,

Q any point on the circle.

Also denote

$\angle QOY$ by ϕ
$\angle POZ$ by θ
OP by l
PQ by r

If the current in the coil is in the sense indicated by the arrow, and if its amount is $I \cos \omega t$ at all points in the wire, then the components of the vector potential $\mathbf{A}$ at P along OX, OY, OZ are

$$A_x = -\frac{I}{c}\int_0^{2\pi} \frac{b \cos \omega\left(t - \frac{r}{V}\right)\cos\phi \, d\phi}{r} = 0$$

$$A_y = \frac{I}{c}\int_0^{2\pi} \frac{b \cos \omega\left(t - \frac{r}{V}\right)\sin\phi \, d\phi}{r}$$

$$A_z = 0$$

because the only currents which exist are horizontal, and therefore $A_z = 0$; A_x is also zero, as can be seen from considerations

Digitized by Google

of symmetry. It is sufficient, therefore, to consider only the expression for A_y.

The integral in this expression can be written as a power series in $\frac{1}{l}$ for large values of l. From the triangle PQO we have

$$r = \sqrt{l^2 + b^2 - 2bl \sin\theta \sin\phi}$$

$$r = l\left[1 - \frac{b}{l}\sin\theta\sin\phi + \frac{b^2}{2l^2}(1 - \sin^2\theta\sin^2\phi) \cdots\cdots\right]$$

and

$$\frac{1}{r} = \frac{1}{l}\left[1 + \frac{b}{l}\sin\theta\sin\phi - \frac{b^2}{2l^2}(1 - 3\sin^2\theta\sin^2\phi) \cdots\right]$$

Consequently, $\cos\omega\left(t - \frac{r}{V}\right) =$

$$\cos\left[\omega\left(t - \frac{l}{V} + \frac{\omega b}{V}\sin\theta\sin\phi - \frac{\omega b^2}{2Vl}(1 - \sin^2\theta\sin^2\phi)\right) \cdots\cdots\right]$$

Neglecting the terms $\frac{b}{2l}(1 - \sin^2\theta\sin^2\phi)$ and $\frac{b}{2l^2}(1 - 3\sin^2\theta\sin^2\phi)$

$$A_y = \frac{I\cos\omega\left(t - \frac{l}{V}\right)}{c}\int_0^{2\pi} b\cos\left(\frac{\omega b\sin\theta\sin\phi}{V}\right)\sin\phi\left[\frac{1}{l} + \frac{b}{l^2}\sin\theta\sin\phi\right]d\phi$$

$$-\frac{I\sin\omega\left(t - \frac{l}{V}\right)}{c}\int_0^{2\pi} b\sin\left(\frac{\omega b\sin\theta\sin\phi}{V}\right)\sin\phi\left[\frac{1}{l} + \frac{b}{l^2}\sin\theta\sin\phi\right]d\phi$$

But

$$\int_0^{2\pi}\cos\left(\frac{\omega b\sin\theta\sin\phi}{V}\right)\sin\phi\, d\phi = 0$$

$$\int_0^{2\pi}\cos\left(\frac{\omega b\sin\theta\sin\phi}{V}\right)\sin^2\phi\, d\phi$$

$$= \frac{1}{2}\int_0^{} \cos\left(\frac{\omega b\sin\theta\sin\phi}{V}\right)(1 - \cos 2\phi)\, d\phi$$

$$= \pi\left\{J_0\left(\frac{\omega b\sin\theta}{V}\right) - J_2\left(\frac{\omega b\sin\theta}{V}\right)\right\}$$

$$= 2\pi J_1'\left(\frac{\omega b\sin\theta}{V}\right)$$

Digitized by Google

where J_n denotes the Bessel function of the first kind of order n and J_n' is the first derivative of that function as to its argument.

Also

$$\int_0^{2\pi} \sin\left(\frac{\omega b \sin\theta \sin\phi}{V}\right) \sin\phi \, d\phi = 2\pi J_1\left(\frac{\omega b \sin\theta}{V}\right)$$

while

$$\int_0^{2\pi} \sin\left(\frac{\omega b \sin\theta \sin\phi}{V}\right) \sin^2\phi \, d\phi = 0$$

Therefore

$$A_y = \frac{2\pi I b^2 \sin\theta}{l^2 c} J_1'\left(\frac{\omega b \sin\theta}{V}\right) \cos\omega\left(t - \frac{l}{V}\right) - \frac{2\pi I b}{lc} J_1\left(\frac{\omega b \sin\theta}{V}\right) \sin\omega\left(t - \frac{l}{V}\right)$$

Since Φ is constant

$$E_y = -\frac{\mu}{c}\frac{\partial A_y}{\partial t} = \frac{2\pi\mu I b^2 \omega \sin\theta}{l^2 c^2} J_1'\left(\frac{\omega b \sin\theta}{V}\right) \sin\omega\left(t - \frac{l}{V}\right) + \frac{2\pi\mu I b\omega}{lc^2} J_1\left(\frac{\omega b \sin\theta}{V}\right) \cos\omega\left(t - \frac{l}{V}\right) \quad \ldots\ldots\ldots\ldots\ldots (1)$$

As l increases the second term becomes much more important than the first. For sufficiently large values of l it is the only term of importance. For this reason it can be called the radiation component of E. It must be remembered here that although attention was confined to one special point in the OXZ plane the treatment does not lose any generality on that account, because the OXZ plane can always be made to pass through any required point. The whole expression gives the electric intensity associated with a single circular current correctly to terms involving $\frac{1}{l^2}$. For points very close to the transmitting antenna it breaks down, because the terms involving $\frac{1}{l^3}, \frac{1}{l^4}$, etc., should be taken into account. The expression can be used to calculate the effect of two circular currents by superposing the effects due to each individually.

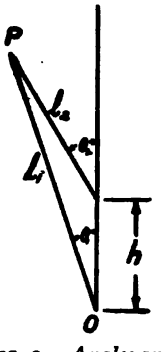

FIG. 2.—*Angles and distances used in the case of two circular coils*

Digitized by Google

If the current in the two coils is $I \cos \omega t$ at any instant, and if the quantities l, θ have values l_1, θ_1 for the first coil and l_2, θ_2 for the second coil, then the resultant value of E_y is

$$E_y = \frac{2\pi\mu\omega b^2}{c^2} I \left\{ \frac{\sin \omega\left(t - \frac{l_1}{V}\right)}{l_1^2} J_1'\left(\frac{\omega b \sin \theta_1}{V}\right) \sin \theta_1 - \frac{\sin \omega\left(t - \frac{l_2}{V}\right)}{l_2^2} J_1'\left(\frac{\omega b \sin \theta_2}{V}\right) \sin \theta_2 \right\}$$
$$+ \frac{2\pi\mu\omega b I}{c^2} \left\{ \frac{\cos \omega\left(t - \frac{l_1}{V}\right)}{l_1} J_1\left(\frac{\omega b \sin \theta_1}{V}\right) - \frac{\cos \omega\left(t - \frac{l_2}{V}\right)}{l_2} J_1\left(\frac{\omega b \sin \theta_2}{V}\right) \right\}$$

This is a general expression, which is correct if terms involving $\frac{1}{l^3}$ can be neglected. For special cases it can be simplified. For example, if the centers of the two circles are both on OZ, if their planes are parallel, and if the distance between their planes is h (see Fig. 2), then

$$l_1 = l_2 + h \cos \theta \cdots$$

and $\sin \theta_1 = \frac{l_2}{l_1} \sin \theta_2 = (1 - \frac{h}{l} \cos \theta) \sin \theta$

θ being approximately the mean of θ_1 and θ_2. Therefore, neglecting powers of h higher than the first,

$$\frac{\sin \theta_1}{l_1^2} \sin \omega\left(t - \frac{l_1}{V}\right) J_1'\left(\frac{\omega b \sin \theta_1}{V}\right) - \frac{\sin \theta_2}{l_2^2} \sin \omega\left(t - \frac{l_2}{V}\right) J_1'\left(\frac{\omega b \sin \theta_2}{V}\right)$$
$$= h \cos \theta \frac{\partial}{\partial l} \left\{ \frac{\sin \theta}{l^2} J_1'\left(\frac{\omega b \sin \theta}{V}\right) \sin \omega\left(t - \frac{l}{V}\right) \right\}$$
$$- \frac{h \sin \theta \cos \theta}{l} \frac{\partial}{\partial (\sin \theta)} \left\{ \frac{\sin \theta}{l^2} J_1'\left(\frac{\omega b \sin \theta}{V}\right) \sin \omega\left(t - \frac{l}{V}\right) \right\}$$

and $$\frac{\cos \omega\left(t - \frac{l_1}{V}\right)}{l_1} J_1\left(\frac{\omega b \sin \theta}{V}\right) - \frac{\cos \omega\left(t - \frac{l_2}{V}\right)}{l_2} J_1\left(\frac{\omega b \sin \theta_2}{V}\right)$$
$$= \left[h \cos \theta \frac{\partial}{\partial l} - \frac{h \sin \theta \cos \theta}{l} \frac{\partial}{\partial (\sin \theta)} \right] \left\{ \frac{\cos \omega\left(t - \frac{l}{V}\right)}{l} J_1\left(\frac{\omega b \sin \theta}{V}\right) \right\}$$

Digitized by Google

Performing the differentiations and substituting

$$E_y = \frac{2\pi\mu I b\omega^2 h\cos\theta}{Vc^2} J_1\left(\frac{\omega b\sin\theta}{V}\right)\frac{\sin\omega\left(t-\frac{l}{V}\right)}{l}$$

$$-\frac{2\pi\mu I b\omega h\cos\theta}{l^2 c^2}\left\{J_1\left(\frac{\omega b\sin\theta}{V}\right)+2\frac{b\omega\sin\theta}{V}J_1'\left(\frac{\omega b\sin\theta}{V}\right)\right\}\cos\omega\left(t-\frac{l}{V}\right)$$

If, in addition, $\frac{\omega b}{V}$ is small compared to unity, $J_1\left(\frac{\omega b\sin\theta}{V}\right)$ can be set equal to $\frac{\omega b\sin\theta}{2V}$, while $J_1'\left(\frac{\omega b\sin\theta}{V}\right)$ can be replaced by $\frac{1}{2}$.

Therefore, if h and b are both sufficiently small

$$E_y = \frac{\pi\mu I b^2\omega^3 h\sin\theta\cos\theta}{V^2 c^2}\frac{\sin\omega\left(t-\frac{l}{V}\right)}{l}$$

$$-\frac{3\pi\mu I b^2\omega^2 h\sin\theta\cos\theta}{Vc^2}\frac{\cos\omega\left(t-\frac{l}{V}\right)}{l^2}$$

$$E_y = \frac{M\mu I h\sin\theta\cos\theta}{c^2}\left[\frac{\omega^3\sin\omega\left(t-\frac{l}{V}\right)}{lV^2}-\frac{3\omega^2\cos\omega\left(t-\frac{l}{V}\right)}{l^2 V}\right]\cdots(2)$$

where $M=\pi b^2$ = the area of either loop.

The expression for E_y given in equation (2) enables one to compute the electric field intensity at any point whose distance from the coils is large compared with their radii and their distance apart. This is obtained in terms of the current, its frequency, the distance from the coils, the velocity of light, and the angle between the line joining the point to the coils and the vertical line through the coils.

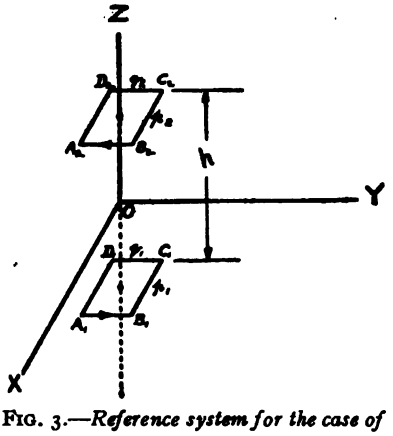

FIG. 3.—*Reference system for the case of two rectangular coils*

2. RECTANGULAR COILS

Let the sides of the two coils be parallel to each other, the lengths of the sides of one being p_1, q_1, and the lengths of the corresponding sides of the other being p_2, q_2. Let the centers of the two coils be on a line perpendicular to the planes of the coils, the planes themselves being parallel and a distance h apart. (See Fig. 3.)

Digitized by Google

Let the origin of coordinates be at a point midway between the planes of the two coils, the axis of X being parallel to the sides p_1, p_2, the axis of Y parallel to q_1, q_2, and the axis of Z being drawn in such a sense as to make the system right-handed. Let the currents in the two coils in the directions indicated by the arrowheads on Fig. 2 be $I \cos \omega t$. Consider the effect at a point (X, O, Z) in the OXZ plane. As before, $A_x = A_z = 0$. In computing A_y it is to be noted that the distance from (X, O, Z) to A_2B_2 is

$$\sqrt{\left(X-\frac{p_2}{2}\right)^2+\left(Z-\frac{h}{2}\right)^2}=l-\frac{p_2X}{2l}-\frac{hZ}{2l}$$

where l is the distance of (X, O, Z) from the origin and the expression for the distance does not take into account terms of higher order than the first in p_2 and h. Similarly, the distances from the same point to C_2D_2 is

$$l+\frac{p_2X}{2l}-\frac{hZ}{2l},$$

to A_1B_1 is

$$l-\frac{p_1X}{2l}+\frac{hZ}{2l},$$

and to C_1D_1 is

$$l+\frac{p_1X}{2l}+\frac{hZ}{2l}.$$

Thus, since the contributions of the sides A_1D_1, B_1C_1, A_2D_2, B_2C_2 to the vector potential at (X, O, Z) are equal and opposite, and since the distance of any point in A_1B_1 from (X, O, Z) is to the first power of q the same as the distance from A_1B_1 to (X, O, Z)

$$\begin{aligned}A_y = &\frac{q_1 I \cos\omega\left(t-\frac{l}{V}+\frac{p_1X}{2lV}-\frac{hZ}{2lV}\right)}{c\left(l-\frac{p_1X}{2l}+\frac{hZ}{2l}\right)}\\ &-\frac{q_2 I \cos\omega\left(t-\frac{l}{V}+\frac{p_2X}{2lV}+\frac{hZ}{2lV}\right)}{c\left(l+\frac{p_2X}{2l}-\frac{hZ}{2l}\right)}\\ &+\frac{q_2 I \cos\omega\left(t-\frac{l}{V}-\frac{p_2X}{2lV}+\frac{hZ}{2lV}\right)}{c\left(l+\frac{p_2X}{2l}-\frac{hZ}{2l}\right)}\\ &-\frac{q_1 I \cos\omega\left(t-\frac{l}{V}-\frac{p_1X}{2lV}-\frac{hZ}{2lV}\right)}{c\left(l+\frac{p_1X}{2l}+\frac{hZ}{2l}\right)}\end{aligned} \qquad (3)$$

Digitized by Google

If we are interested in the radiation component only, it is justifiable to write the denominators of all the foregoing fractions as l, because

$$\frac{1}{l+\delta}=\frac{1}{l}-\frac{\delta}{l^2}+, \text{ etc., where } \delta<l.$$

$$\text{Thus, } A_y=\frac{-2q_1I}{cl}\sin\omega\left(t-\frac{l}{V}-\frac{hZ}{2lV}\right)\sin\frac{\omega p_1X}{2lV}$$

$$+\frac{2q_2I}{cl}\sin\omega\left(t-\frac{l}{V}+\frac{hZ}{2lV}\right)\sin\frac{\omega p_2X}{2lV}$$

Now let $\frac{\omega p_1}{V}$ and $\frac{\omega p_2}{V}$ be small compared to unity. Then, since $\frac{X}{l}<1$ we can write as an approximation

$$A_y=\frac{\omega}{clV}\frac{X}{l}\left[p_2\,q_2\sin\omega\left(t-\frac{l}{V}+\frac{hZ}{2lV}\right)-p_1\,q_1\sin\omega\left(t-\frac{l}{V}-\frac{hZ}{2lV}\right)\right]$$

If now $p_1\,q_1=p_2\,q_2=M$

$$A_y=2\frac{\omega M}{clV}\frac{X}{l}\cos\omega\left(t-\frac{l}{V}\right)\sin\left(\frac{hZ\omega}{2lV}\right)$$

And, again, if $\frac{\omega h}{V}$ is small compared to unity then since $\frac{Z}{l}<1$

$$A_y=I\frac{\omega^2Mh}{cV^2l}\frac{X}{l}\frac{Z}{l}\cos\omega\left(t-\frac{l}{V}\right)$$

Therefore

$$E_y=-\frac{\mu}{c}\frac{\partial A_y}{\partial t}=I\frac{\omega^3\mu Mh}{c^2V^2l}\frac{X}{l}\frac{Z}{l}\sin\omega\left(t-\frac{l}{V}\right)$$

$$E_y=I\frac{\omega^3\mu Mh}{c^2V^2l}\sin\theta\cos\theta\sin\omega\left(t-\frac{l}{V}\right) \qquad (4)$$

in the notation of the first case. To the first power of $\frac{1}{l}$, this is precisely the same as formula (2) of the first case. This shows that for sufficiently low frequencies the shape of the coils is immaterial as long as their area is kept the same. Moreover, if in the expression (4) we carry out the calculation to the second power of $\frac{1}{l^2}$ we get in addition to the terms so far obtained in A_y

$$\left(\frac{p_1X}{2l^2}-\frac{hZ}{2l^2}\right)\frac{q_1}{c}I\cos\omega\left(t-\frac{l}{V}+\frac{p_1X}{2lV}-\frac{hZ}{2lV}\right)$$

Digitized by Google

$$-\left(\frac{p_2X}{2l^3}+\frac{hZ}{2l^3}\right)\frac{q_2}{c}I\cos\omega\left(t-\frac{l}{V}+\frac{p_2X}{2lV}+\frac{hZ}{2lV}\right)$$

$$+\left(\frac{hZ}{2l^3}-\frac{p_2X}{2l^3}\right)\frac{q_2}{c}I\cos\omega\left(t-\frac{l}{V}-\frac{p_2X}{2lV}+\frac{hZ}{2lV}\right)$$

$$+\left(\frac{p_1X}{2l^3}+\frac{hZ}{2l^3}\right)\frac{q_1}{c}I\cos\omega\left(t-\frac{l}{V}-\frac{p_1X}{2lV}-\frac{hZ}{2lV}\right)$$

which after a few reductions gives on replacing the sines of small quantities by the quantities themselves and the cosines by 1

$$\frac{3Mh\omega}{l^2cV}\frac{Z}{l}\frac{X}{l}I\sin\omega\left(t-\frac{l}{V}\right)$$

which contributes to E_y

$$\frac{-3Mh\omega^2\mu}{l^2c^2V}I\cos\theta\sin\theta\cos\omega\left(t-\frac{l}{V}\right)$$

Thus, it is seen that this also agrees with formula (2) of the first case. Therefore, the value of E_y is the same for both circular and rectangular coils within terms in the second power of $\frac{1}{l}$. It may be well to recall again the conditions under which these first terms may be taken as approximating the actual value of E_y. These are:

1. $\frac{\omega h}{V}$ is small compared to unity. This amounts to saying that the wave length is large compared to the distance between the coils.

2. $\frac{\omega q}{V}$, $\frac{\omega p_1}{V}$, $\frac{\omega p_2}{V}$ are small compared to unity. This means that the wave length is large compared to the dimensions of each coil.

3. The distance of the airplane from the coils is large compared to the dimensions of the coils and their distance apart.

The same general method will also apply to the calculation of the field radiated by any number of coils.

III. APPLICATIONS

1. REGION OF AUDIBLE SIGNAL

If an airplane is flying over the two horizontal coils, the strength of the signal received on the airplane depends on the type of receiving apparatus and upon the orientation of the aerial. A type commonly used consists of a vertical coil aerial fixed rigidly to the frame of the machine.

Digitized by Google

For simplicity assume that the airplane is so far from the transmitter that $\frac{\omega}{V}$ is large compared to $\frac{1}{l}$.

Then

$$E_y = \frac{M\mu Ih \sin\theta\cos\theta}{c^2} \cdot \frac{\omega^3 \sin\omega\left(t-\frac{l}{V}\right)}{lV^2}$$

Let there be a receiving coil placed at P with its plane parallel to OY and let the angle which its plane makes with the plane POY be ϕ. Then the emf induced in the coil is

$$n_r M_r \frac{M\mu Ih \sin\theta\cos\theta}{c^2} \cdot \frac{\omega^4 \cos\omega\left(t-\frac{l}{V}\right)}{lV^2} \cos\phi$$

where M_r is the area of the coil, n_r is the number of turns.

The units in which this result is given depend on the choice of system of units, as explained at the beginning of this paper. The result is given in volts by

$$4.675\times 10^{-4} \frac{n_r M_r MIh \sin\theta\cos\theta\cos\phi}{l\lambda^4} \cos\omega\left(t-\frac{l}{V}\right)$$

in which I is in amperes, $\lambda = \frac{2\pi V}{\omega}$, and the lengths are in any unit, provided the same unit is used for all including λ and the dimensions entering into M_r and M.

If I, ω, and the constants of the two circuits are unchanged, this expression is proportional to $\frac{\sin\theta\cos\theta\cos\phi}{l}$

If $\phi = 0$, i. e., if the receiving coil is kept vertical, this number is $\psi = \frac{\sin\theta\cos^2\theta}{l}$

Consider now the variations in ψ as the position of P is varied. The variation most likely to occur in practice is a displacement of P parallel to the planes of the two coils; i. e., along OX. Mathematically this amounts to making Z a constant and since $r = \frac{Z}{\cos\theta}$

$$\psi = \frac{1}{Z}\sin\theta\cos^3\theta$$

This attains a maximum when $\cos^4\theta - 3\cos^2\theta\sin^2\theta = 0$, i. e., when (neglecting the minimum corresponding to $\theta = \frac{\pi}{2}$)

$$\sin\theta = \frac{1}{2}, \quad \text{or } \theta = 30°.$$

Digitized by Google

Thus, if the airplane moves horizontally with the receiving coil vertical the signal is loudest when the airplane subtends at the transmitter an angle of 30° with the vertical.

In terms of the coordinates X and Z

$$\psi = \frac{XZ^3}{[Z^2+X^2]^3} = \frac{\frac{X}{Z}}{Z\left[1+\frac{X^2}{Z^2}\right]^3} = \frac{1}{Z}\frac{\xi}{(1+\xi^2)^3} \text{ where } \xi = \frac{X}{Z}$$

Fig. 4 shows the graph of the function $\frac{\xi}{(1+\xi^2)^3}$ plotted against $\xi = \frac{X}{Z}$. It represents the variation of the electromotive force with the distance traversed by the airplane on a scale which would correspond to a unit distance of the airplane above the ground.

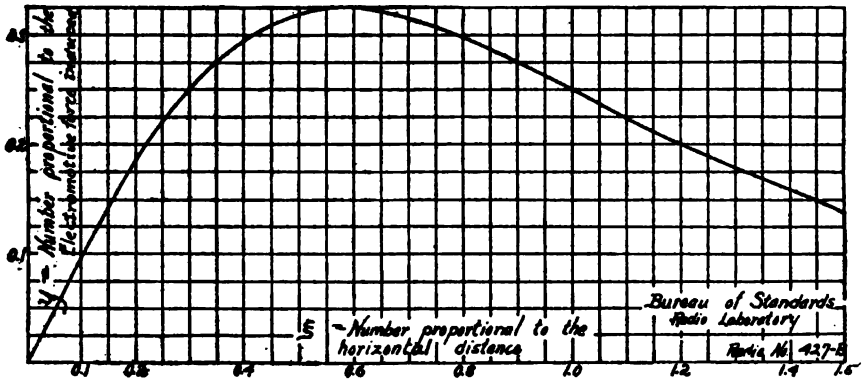

FIG. 4.—*Relation between electromotive force induced in a vertical coil and the distance traversed by the airplane in horizontal flight*

This curve can be used to find the surface within which the signal is audible and outside of which it is not audible. In fact, for points on the surface, $\frac{1}{Z}\frac{\xi}{(1+\xi^2)^3}$ must have a definite value K. Let a given value be assigned to $\frac{\xi}{(1+\xi^2)^3}$ and the two corresponding values of ξ be located on the curve. Let these be ξ_1 and ξ_2. Since $Z = \frac{1}{K}\frac{\xi}{(1+\xi^2)^3}$ this gives at once the values of X corresponding to ξ_1 and ξ_2, which are $\frac{\xi_1}{K}\frac{\xi}{(1+\xi^2)^3}$ and $\frac{\xi_2}{K}\frac{\xi}{(1+\xi^2)^3}$. If it is desired merely to determine the shape of the resulting surface, we can set $K = 1$ and plot $\frac{\xi_1\xi}{(1+\xi^2)^3}$, and $\frac{\xi_2\xi}{(1+\xi^2)^3}$ against $\frac{\xi}{(1+\xi^2)^3}$

Digitized by Google

where ξ_1 and ξ_2 are values of ξ corresponding to $\frac{\xi}{(1+\xi^2)^2}$. Looked on in a different light this means that the curve can be traced by the parametric equations

$$Z=\frac{\xi}{(1+\xi^2)^2}, \qquad X=\frac{\xi^2}{(1+\xi^2)^2}.$$

The properties of the curve can thus be easily traced from these expressions. Thus, if $\xi=0$, both Z and X are zero and, moreover, X is infinitesimal compared to Z. Consequently, here the curve is tangent to the axis of Z. Again, when $\xi=\infty$, $Z=X=0$ but now Z is infinitesimal compared to X, and hence the curve touches the axis of X. The curve is shown as curve a in Fig. 5.

Table 1 gives values of X and Z corresponding to a series of values of ξ.

TABLE 1

ξ	$Z=\frac{\xi}{(1+\xi^2)^2}$	$X=\frac{\xi^2}{(1+\xi^2)^2}$	$Z_1=\frac{\xi}{(1+\xi^2)^{2.5}}$	$X_1=\frac{\xi^2}{(1+\xi^2)^{2.5}}$
0	0	0	0	0
0.1	0.098	0.098	0.098	0.0098
.2	.1849	.03699	.1812	.3629
.3	.253	.0756	.2447	.0724
.4	.2972	.1189	.2761	.1105
.5	.3202	.1601	.2891	.1446
.6	.3242	.1944	.2779	.1671
.7	.3150	.2203	.2581	.1807
.8	.2973	.2379	.2321	.1859
.9	.2748	.2471	.2043	.1839
1.0	.2500	.2500	.1769	.1769
1.1	.2252	.2476	.1516	.1666
1.2	.2015	.2419	.1290	.1548
1.3	.1796	.2337	.1095	.1425
1.5	.1421	.2131	.0789	.1189
2.0	.0800	.1599	.0358	.0716
3.0	.03	.09	.00950	.02849
4.0	.0137	.0554	.003323	.01344

If the earth were a perfect conductor, its effect could be replaced by the effect of the images of the two coils in the surface of the earth. The whole transmitting system can then be replaced by four coils, the two on the inside carrying currents in the same direction and the two on the outside carrying currents in a direction opposite to that of the inside coils.

Digitized by Google

In this case the emf induced can be shown to be proportional to $\frac{\sin\theta\cos^4\theta}{Z}$. There is, therefore, a maximum signal for horizontal flight with a vertical receiving coil when

$$\cos^5\theta - 4\sin^2\theta\cos^2\theta = 0$$

or when

$$\sin\theta = \frac{1}{\sqrt{5}},\quad \theta = 26^\circ 34'$$

In order to trace the volume within which the signal is just audible, we must trace the curve

$$\frac{XZ^2}{r^5} = K, \text{ which becomes on letting } X = \xi Z$$

$$X = \frac{1}{K}\frac{\xi^2}{(1+\xi^2)^{2.5}}$$

$$Z = \frac{1}{K}\frac{\xi}{(1+\xi^2)^{2.5}}.$$

The surface is obtained by revolving this curve about OZ and is shown as curve b in Fig. 5. The general properties of the curve are the same as those for the case when the earth is negligible.

2. CURRENT IN RECEIVING COIL

In international electric units the current received in the coil is, within certain limitations, depending on the properties of the coil,

$$I_r = \frac{4.67\times 10^4\, I_s n_s n_r M_s M_r h_s \sin\theta\cos\theta\cos\phi}{\lambda^4 l R} \tag{5}$$

where the symbol s refers to the sending system, R is the resistance of the receiving coil circuit, and where the same unit of length is used for λ, l, M_s, M_r, h_s. If instead of the closed aerial an open antenna is used for receiving

$$I_r = \frac{7.44\times 10^2\, I_s n_s M_s h_s h_r \sin\theta\cos\theta\cos\alpha}{\lambda^3 R l} \tag{6}$$

where R is the resistance of the antenna circuit and α is the angle made by the antenna with the local direction of $\mathbf{E}$, the other quantities being the same as for equation (5).

The derivation of this paper neglects the reflection of the waves from the surface of the earth and the effect of eddy currents in the earth in the neighborhood of the transmitting set.

Digitized by Google

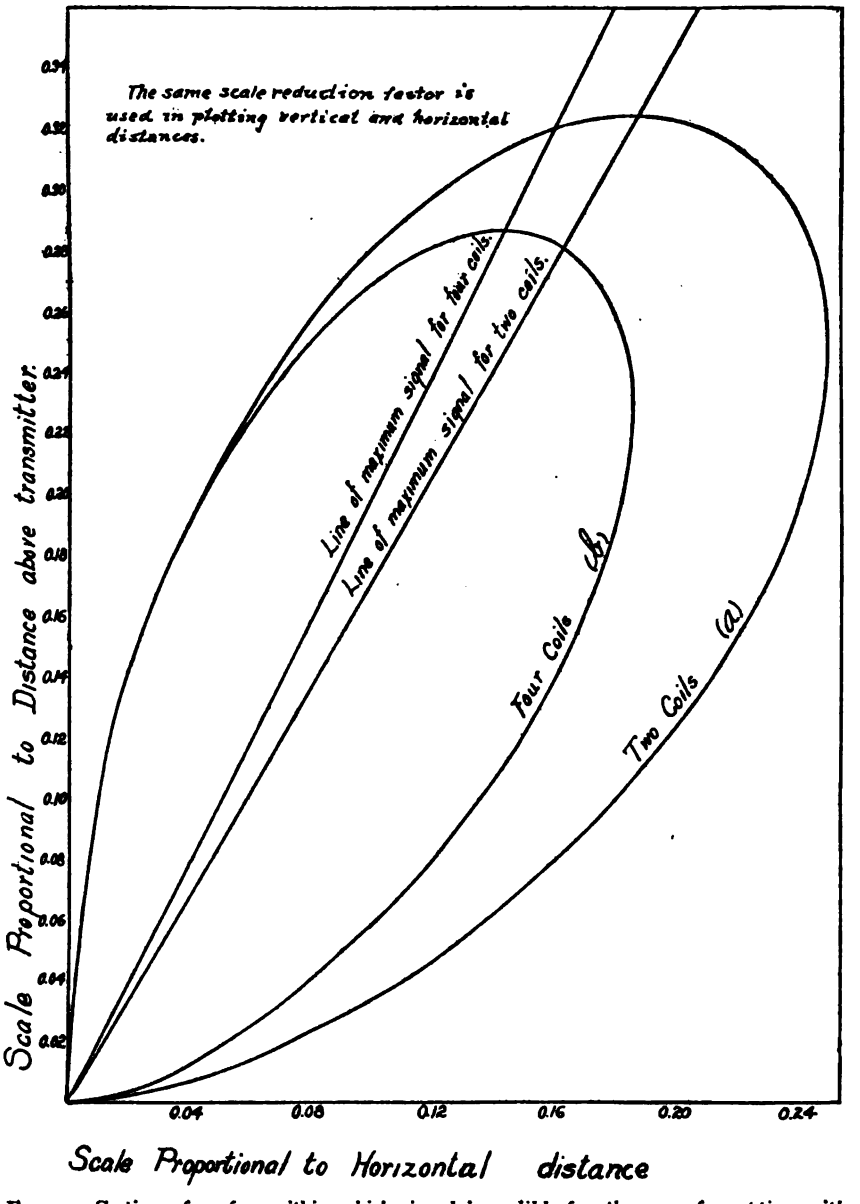

FIG. 5.—*Section of surface within which signal is audible for the case of reception with plane of coil vertical*

Digitized by Google

IV. SUMMARY

The nature of the field radiated by two horizontal coils has been calculated. The currents received in such a field by means of a coil aerial and by means of an open antenna have been computed.

The case of a receiving station installed on an airplane has been considered in detail. The portions of space where the signal is heard have been ascertained. The angle with the vertical at which the signal is a maximum has been calculated. It was found to be 30° for the case of a vertical receiving coil.

The more complicated case of four transmitting coils has been studied. Two of these coils were taken to be the image of the other two in a horizontal plane. In this case the maximum is shifted still closer to the vertical, namely, to 26° 34′. This calculation can be applied to the case of two coils situated above a perfectly conducting plane. If the earth were a perfect conductor, it would apply to the case of two coils above the surface of the earth. It is improbable that in ordinary cases the conductivity of the earth is sufficiently high to justify such an approximation. Since, however, both in the case of an earth having a perfect conductivity and in the case of an earth having zero conductivity the maximum signal strength is found approximately at 30° with the vertical, this can also be expected for ordinary conductivities.

Acknowledgment is due Dr. J. H. Dellinger and L. E. Whittemore, of the Bureau of Standards, and to Dr. F. D. Murnaghan, of the Johns Hopkins University, for reading the manuscript and for suggestions as to the choice of symbols used in the paper.

V. LIST OF SYMBOLS

$\mathbf{H}$ = magnetic intensity.
c = a constant depending upon the choice of units.
$\mathbf{v}$ = velocity of charge.
K = dielectric constant.
$\pi = 3.1416$.
t = time.
$d\tau$ = element of volume.
$\mathbf{E}$ = electric intensity.
μ = permeability.
ρ = volume density of charge.
$\mathbf{A}$ = vector potential at P.
$\phi = \angle QOY$ (p. 592) (Fig. 1).

Digitized by Google

A = absolute value of vector potential at P.
r = distance from element of volume $d\tau$ to the point at which $\mathbf{A}$ or ϕ is computed.
b = radius of circular coil aerial.
V = velocity of light.
R = resistance of receiving circuit.
l = distance from transmitting to receiving apparatus.
A_x = component of vector potential in direction OX.
A_y = component of vector potential in direction OY.
A_z = component of vector potential in direction OZ.
$\omega = 2\pi \times$ frequency.
(r) is a subscript referring to the receiving system.
(s) is a subscript referring to the sending system.
M_r = area of receiving coil.
M_s = area of sending coil.
n_s = number of turns in transmitting coil.
n_r = number of turns in receiving coil.
h_r = height of receiving antenna.
$h = h_s$ = distance between transmitting coils.
λ = wave length.

WASHINGTON, July 14, 1921.

Digitized by Google

JUN 22 1922

LIBRARY OF THE UNIVERSITY OF CALIFORNIA

DEPARTMENT OF COMMERCE

SCIENTIFIC PAPERS

OF THE

BUREAU OF STANDARDS

S. W. STRATTON, DIRECTOR

No. 432

[Part of Vol. 17]

AN IMPROVED METHOD FOR PREPARING RAFFINOSE

BY

E. P. CLARK, Associate Technologist

Bureau of Standards

APRIL 8, 1922

PRICE, 5 CENTS

Sold only by the Superintendent of Documents, Government Printing Office
Washington, D. C.

WASHINGTON
GOVERNMENT PRINTING OFFICE
1922

Digitized by Google

Digitized by Google

AN IMPROVED METHOD FOR PREPARING RAFFINOSE

By E. P. Clark

ABSTRACT

Owing to the demands made by chemists and bacteriologists for specifications and standards for raffinose, a convenient and economical method for its preparation has been developed so this may be brought about.

Cottonseed meal is extracted with water, the liquor freed from impurities with basic lead acetate, and the raffinose present is removed from the liquid as an insoluble lime compound. This raffinosate is decomposed with CO_2, and the free sugar resulting is crystallized from its concentrated sirup by means of alcohol.

A device for carbonating, which is useful for many other purposes, is also described.

Several methods have been proposed for the preparation of raffinose.[1] All these procedures, however, with the exception of the method of Hudson and Harding, as these authors have well pointed out, have many serious disadvantages. The latter method, while it is a decided improvement over all others and gives fairly good results on very small lots, nevertheless has objectionable features when applied to the preparation of larger quantities of the sugar. Chief among these may be mentioned the tedious procedure in extracting the meal, the necessity of evaporating large quantities of water due to the excessive dilution of the extract, and the quantity and cost of the reagents required. The following method overcomes these disadvantages and enables one to prepare relatively large quantities of this sugar by a convenient and economical process.

Five kilograms of coarsely ground cottonseed meal are thoroughly moistened with 2 liters of water and allowed to stand overnight. The meal is then loosely packed in a cylindrical percolator, and sufficient water added to saturate the meal and leave a stratum above it. When the liquid begins to run from the percolator, more menstruum is added from time to time until a sample of the percolate, after defecation with dry basic lead acetate, has an optical rotation of not more than 1° in a 2 dm tube.[2] The process is then stopped, and the percolate is treated with a solution of basic lead acetate until no more precipitate is formed. The yellow precipitate is filtered off upon large folded filters and finally washed on the filter with a little water. The filtrate and

[1] E. O. Von Lippmann, Die chemie der zuckerarten 3rd ed., p. 1627–1630; 1904. C. S. Hudson and T. S. Harding, J. Am. Chem. Soc., 36, No. 10, p. 2110; 1914. H. E. Zitkowski, American Sugar Industry, 12, p. 324; 1910.

[2] As there are substances in the meal which are extracted much more slowly than the sugar, and which cause difficulty in the subsequent steps, as well as give an inferior product, it is essential to obtain a quite rapid percolation, consuming not more than 30 to 35 minutes; and it is not expedient to carry the extraction beyond where the optical rotation of the liquid is less than 1° in a 2 dm tube.

Digitized by Google

washings, which should have a volume of 12 to 13 liters, are freed from the excess of lead with oxalic acid. The lead oxalate is removed and washed on the filter with a little water. The filtrate and washings are thoroughly mixed, measured, and the optical activity of the liquid determined. It is then made distinctly alkaline to litmus with sodium hydroxide. The precipitate thus formed flocks out and settles to the bottom of the vessel in a few minutes. The supernatant liquid is next filtered through a Buchner funnel provided with a thin layer of decolorizing carbon on filter paper. The filtration is rapid under these conditions, and when all has passed through, the precipitate is placed on the filter and drained.

The raffinose is next removed from the solution by forming the insoluble calcium raffinosate. To conveniently accomplish this the liquor is cooled to 10° C or lower, placed in a jar or other suitable container, and rapidly stirred with a mechanical stirring device. As it is being agitated a quantity of powdered active lime, preferably 200 mesh, but not coarser than 100 mesh, sufficient to precipitate all the sugar is slowly sifted in. After all has been added, the stirring is continued for about five minutes. If the lime is active and the optical activity of the solution is calculated to raffinose hydrate with a specific rotation of about 105°, 1 g of lime to 1 g of raffinose is sufficient for complete precipitation. However, unless the activity of the lime is known, it is advisable to test the liquid to see if all the sugar has been removed; if not, more lime should be added. The calcium raffinosate is filtered off, washed by grinding up to a smooth paste with 2½ liters of cold lime water, and again filtered.

It is next carbonated to neutrality. Emphasis is to be laid upon accomplishing this easily and quickly. The device illustrated in Fig. 1 was used for this purpose.[3] The cake of raffinosate is

[3] The design is essentially that developed by C.W. Doherty, of the Great Western Sugar Co., for carbonating beet juices. It consists of an ordinary stirring apparatus that may be clamped to any rigid laboratory support stand. The stirring shaft, *A*, is made of steel tubing 8 mm inside diameter. Just below the shaft support is a union, *B*, to which is joined another section of shafting of the desired length. For most laboratory work a length of 45 cm is sufficient. Attached to the lower end are two triangular plates. These plates, which are 2 mm thick and whose sides are 75 mm long, are held 2 mm apart by 3 rivets near the apex of the angles. The plate attached to the shafting has an opening connecting with the stirring rod. The bottom plate has no opening. *C* is a stuffing box made by simply attaching to the stirring shaft a short piece of good rubber tubing in which is placed a well oiled, closely fitting cork cylinder, *D*, through which a piece of glass tubing, *E*, is inserted. The glass tube is held rigid by means of a clamp, *F*. The cork thus arranged may be made gas tight, and still turn freely, by tightening the rubber tubing about it with a wire. Incidentally, this apparatus may be used to advantage for a number of purposes. In the work described in this paper, where any stirring was done or where precipitates were ground up with water in order to wash them, the stuffing box attachment was removed and the upper orifice of the turning shaft corked. The precipitate was placed in a suitable container with the liquid used to wash it and the apparatus turned for 1 or 2 minutes. At the end of this time the mixture was a perfectly smooth paste, all lumps being completely broken up. It has also been used very effectively in decomposing lead precipitates with hydrogen sulphide. Quantities of lead precipitates which would normally require from 3 to 4 hours for complete decomposition have been decomposed completely in 15 to 20 minutes.

Digitized by Google

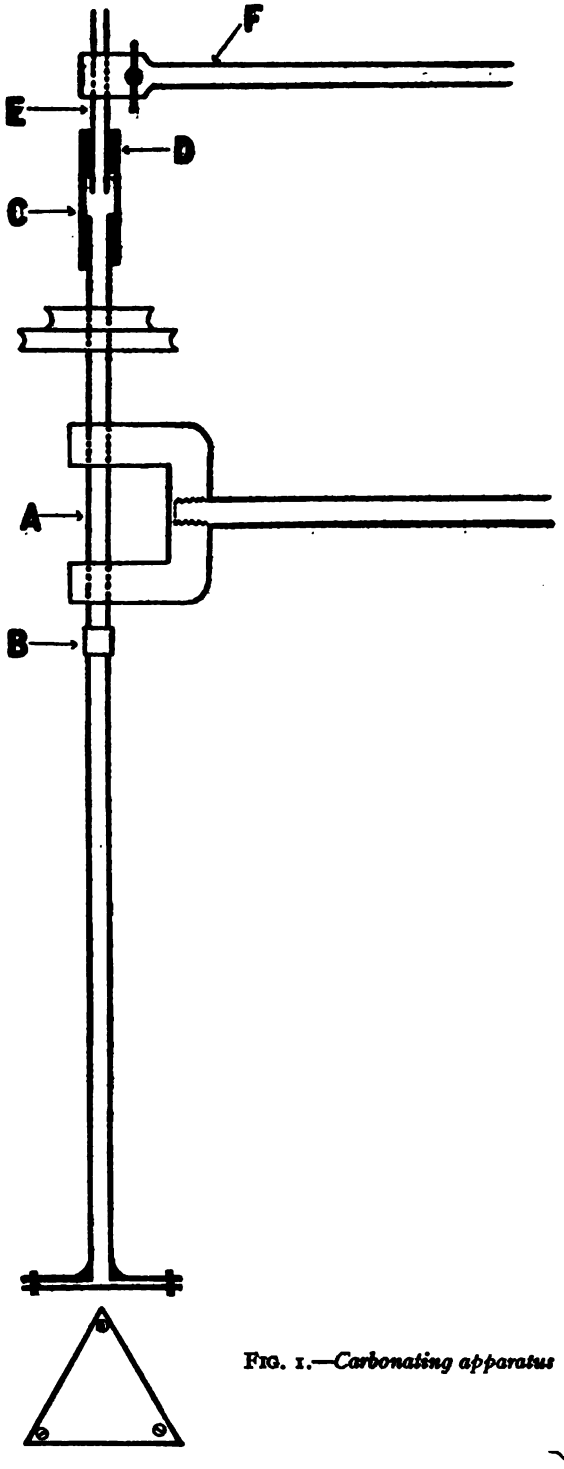

FIG. 1.—*Carbonating apparatus*

Digitized by Google

placed in a deep, narrow can of about 8 liters capacity and filled three-fourths full of water at 50° C, and a lively stream of carbon dioxide is passed through the apparatus while it is being turned about 1500 rpm. In this way the gas is centrifugally distributed and neutralizes the lime in 4 or 5 minutes without any loss of CO_2. The solution is filtered while hot, and the precipitate is washed by grinding up with 2 liters of water and again filtering. The combined liquors are evaporated under diminished pressure to 70 to 75 per cent total solids and warmed to about 60° C. To this sirup 95 per cent ethyl alcohol is added just to saturation. The alcoholic solution is then warmed on the water bath to about 60° C and filtered through a small Buchner funnel in which has been placed a mat of washed asbestos. The filtrate, which is brilliantly clear, is seeded and placed in the ice box to crystallize. Two days are generally sufficient for complete crystallization.

The raffinose is filtered off from the mother liquor, washed first with 80 per cent, then 95 per cent, alcohol, and dried. The yield varies considerably, according to the amount of sugar in the meal; but from a number of different experiments in which different meals were used, yields from 2.3 per cent to 4 per cent were obtained. The crude sugar thus prepared is quite pure, containing only from 0.06 to 0.08 per cent ash.

To purify crude raffinose, a 40 per cent solution (anhydrous sugar) is made by dissolving it in distilled water at 70° C. The warm solution is filtered through a mat of asbestos and placed in the ice box to crystallize. The crystals are freed from mother liquor, washed with 80 per cent, then 95 per cent, alcohol, and dried. A sample of air-dried material thus purified contained 0.005 per cent ash.

An alternative method of recrystallization is to concentrate the above 40 per cent solution under reduced pressure to 70 per cent total solids, warm to 70° C, and add two volumes of 95 per cent alcohol with constant stirring. Crystallization begins almost at once and is complete in a few hours. The crystals are filtered off, washed with 95 per cent alcohol, and dried.

An air-dried sample thus prepared contained 0.015 per cent ash, and its rotation, after being completely dehydrated, was

$$[\alpha]_D^{20} = 123.23 \text{ (10.0136 g per 100.00 cc)};$$
$$[\alpha]_{\lambda 5461.1}^{20} = 144.95 \text{ (10.0136 g per 100.00 cc)}$$

WASHINGTON, October 7, 1921.

Digitized by Google

LIBRARY OF THE UNIVERSITY OF CALIFORNIA

DEPARTMENT OF COMMERCE

SCIENTIFIC PAPERS

OF THE

BUREAU OF STANDARDS

S. W. STRATTON, DIRECTOR

No. 433

[Part of Vol. 17]

THERMAL EXPANSION OF A FEW STEELS

BY

WILMER SOUDER, Physicist
PETER HIDNERT, Associate Physicist
Bureau of Standards

APRIL 10, 1922

PRICE, 5 CENTS
Sold only by the Superintendent of Documents, Government Printing Office
Washington, D. C.

WASHINGTON
GOVERNMENT PRINTING OFFICE
1922

Digitized by Google

Digitized by Google

DEPARTMENT OF COMMERCE

SCIENTIFIC PAPERS

OF THE

BUREAU OF STANDARDS

S. W. STRATTON, DIRECTOR

No. 433

[Part of Vol. 17]

THERMAL EXPANSION OF A FEW STEELS

BY

WILMER SOUDER, Physicist
PETER HIDNERT, Associate Physicist
Bureau of Standards

APRIL 10, 1922

PRICE, 5 CENTS
Sold only by the Superintendent of Documents, Government Printing Office
Washington, D. C.

WASHINGTON
GOVERNMENT PRINTING OFFICE
1922

Digitized by Google

Digitized by Google

THERMAL EXPANSION OF A FEW STEELS

By Wilmer Souder and Peter Hidnert

ABSTRACT

Thermal expansion data are given on 28 specimens of iron and steel. Most of the specimens were heated above 900° C. Tables and curves are used to summarize the results. The tests were made by direct measurements of the length changes and not relative to some other substance or element. The observations were made without disturbing the furnace or specimen and therefore give correct relative values for all temperature intervals.

Variations in length changes, contraction and expansion reversals while passing through the critical regions, and similar changes are compared and discussed.

An attempt is made to throw some light on the magnitude of the tendency toward warping or surface cracking as related to the rate of cooling and width of critical regions.

Expansion coefficients are tabulated for the various alloys and for various temperature intervals.

Data on one specimen of vacuum electrolytic iron and one of gray cast iron are recorded. The length changes incident to the drawing of a sample of hardened steel are shown in a curve.

A brief review of some of the previous work on expansion is included.

CONTENTS

		Page
1.	Introduction	611
2.	Previous work	612
3.	Apparatus	614
4.	Results	615
5.	Summary	626

1. INTRODUCTION

The anomalous expansion of iron and certain steels when heated over the range 600 to 1000° C has been known for a number of years. The structural changes taking place at or near these points of nonuniform expansion have been given considerable attention within the last decade. In addition to the irregularities in expansion, which are influenced by these changes, there are numerous other physical properties which are modified during the passage through the above temperature range. Among the effects which have been used to more accurately chart this region are: Changes in electrical, magnetic, elastic, and thermal

Digitized by Google

properties, changes in microstructure, hardness, and rate of expansion.

The present paper presents additional data on the last-named property, and while the emphasis will not be placed on the structural or molecular phases often accompanying the variations in expansivity, it is felt that the data may be of sufficient accuracy to warrant their use for certain parts of such study should one care to make such use of them. The results represent direct measurement of expansion on a number of selected specimens and are perhaps above the average in accuracy for direct, continuous measurements of thermal expansion.

The principles of hardening and heat treatments of steel are dependent to some degree upon the proper handling while within the above range. Our comments on the dimensional changes will bear upon the physical effects which may be expected to accompany these dimensional irregularities. The shrinkage, warping, surface cracking, and usual lack of highest accuracy of dimensions met in heat-treated work render data on expansion and contraction worthy of careful consideration.

2. PREVIOUS WORK

Svedelius, Le Chatelier, Charpy and Grenet, Guillaume, Driesen, Honda, and other investigators have done work on the thermal expansion of iron and steel. Since a satisfactory review of their work would require considerable space in comparison with that of the other sections of this paper, it was decided to point out only a few of the results or conclusions of some of the previous observers. For additional information, reference should be made to the original papers.

CHARPY AND GRENET [1] found that, if small samples of medium steels (0.6 to 1 per cent C) and of high-carbon steels were heated above 900° C and quenched in water, the expansion curves of the former show abrupt contraction of about 1 per cent between 250 and 350° C, and the curves of the high-carbon steels indicate two contractions, one at about 150 and the other at 300° C.

In a later paper [2] these authors compare results obtained in the critical regions of steels by three different methods. The following tables show the comparative values:

[1] Charpy and Grenet, C. R., **136**, pp. 92–94; Jan. 12, 1903.
[2] Charpy and Grenet, C. R., **139**, pp. 567–568; Oct. 10, 1904.

Digitized by Google

TABLE 1.—Comparison of Electrical Resistance and Dilatation Methods (Charpy and Grenet)

Carbon content	Electrical resistance method		Dilatation method	
	Transformation begins	Transformation ends	Contraction begins	Contraction ends
	°C	°C	°C	°C
0.82 per cent	730	760	735	745
1.06 per cent	730	760	740	750
1.15 per cent	739	739	735	740
1.38 per cent	750	750	735	755

TABLE 2.—Comparison of Thermoelectric and Dilatation Methods (Charpy and Grenet)

Carbon content	Thermoelectric method		Dilatation method	
	Maximum of $\frac{dE}{dt}$	Minimum of $\frac{dE}{dt}$	Contraction begins	Contraction ends
	°C	°C	°C	°C
0.28 per cent	720	840	720	820
0.62 per cent	700	760	743	760
0.92 per cent	700	800	737	760
1.14 per cent	708	780	747	760
1.30 per cent	680	740	725	740

CHARPY AND CORNU [3] found that more than 1.3 per cent Si in low-carbon steels (0.1 per cent C, 0.3 Mn), caused the expansion curve to be almost rectilinear from 0 to 900° C, without an indication of a critical region. However, for an alloy containing 0.35 per cent C and 0.8 per cent Mn, it required 4.5 per cent Si to show a similar phenomenon.

DRIESEN [4] states that above the critical region, the coefficients of expansion of carbon steels are practically constant for samples containing less than 0.85 per cent C. This conclusion is in agreement with the results of Charpy and Grenet.[5] The carbon steel containing 0.33 per cent C showed the maximum change of length during the critical region. Honda [6] gives data which are in close agreement with this result, for he found that a steel containing 0.31 per cent C indicated the maximum contraction in the trans-

[3] Charpy and Cornu, C. R., **156**, pp. 1240–1243; Apr. 21, 1913.
[4] Driesen, Ferrum, **11**, pp. 129–138, Feb., and pp. 161–169, Mar., 1914; Rev. de Mét., **14**, pp. 683–706, Sept.–Oct., 1917.
[5] Charpy and Grenet, C. R., **134**, p. 540; 1902.
[6] Honda, Tôhoku Univ., Sci. Reports, **6**, pp. 203–212, Nov., 1917.

Digitized by Google

formation region. Driesen also found that steels containing more than 0.65 per cent carbon and quenched from above 900° C contract on reheating to about 300° C, and with steels containing more than 1 per cent carbon a similar phenomenon is also observed at 100 to 150° C.

ŌKŌCHI AND SATŌ [7] determined the growth of gray cast iron on repeated heatings. They found that permanent growth is never produced below the transformation temperature. They state the rapid expansion from about 650° C to near the transformation point in the first heating is due to the separation of free carbon from cementite. There are two periods of growth: (1) During the transformation, and (2) at temperatures above the transformation.

Benedicks and others have used certain modifications of the thermal expansive relations to more accurately define transformations in structure, etc. However, since these tests are, in general, only differential tests of expansivity, no claims being made for the absolute values of thermal expansion, or since their application has been limited to metallurgical considerations, it is not within the province of this review to discuss their results.

In many instances we have been prevented from making more detailed comparisons of this work with that of other investigators because of the more complex composition of these steels. While the agreement on carbon content, for example, may be good, the included manganese, vanadium, or chromium may have introduced an unknown effect. These steels were selected with the idea of securing representative specimens rather than any special series of some one alloying element.

3. APPARATUS

The apparatus [8] of the Bureau's expansivity laboratory was used. The specimens were 30 cm in length and about 1 cm in diameter. The platinum-osmium position wires were placed in sharp V-notches cut near each end and at right angles to the axis of the specimens. In this manner the oxide which always formed did not influence the longitudinal separation of the vertical position wires. Attempts to gold plate the specimens or to use neutral gases in the furnace were not successful, due perhaps to the occluded gases which could not be displaced; hence the above method of setting the wires in notches was adopted and proved quite satisfactory.

[7] Ōkōchi and Satō, Tokyo Univ. Coll. of Eng., J. 10, pp. 53–71, Feb., 1920.
[8] Described in B. S. Sci. Papers, No. 352.

Digitized by Google

4. RESULTS

This work (with one or two exceptions) deals with annealed alloys. The specimens were carried through the transformations at a slow rate of temperature change, usually less than 1 degree per minute. The length changes showed little, if any, lag for temperature variations. Intentional reversals in temperature gradient were accompanied by corresponding reversals in length changes and without a lag of more than 2 minutes. A further confirmation of the uniformity of temperature throughout the entire specimen is found in the sharp breaks in the expansion curves, indicating that practically all parts began the transformation at the same instant. This uniformity of temperature is more readily maintained at high temperatures than at lower temperatures because of the rapid increase in rate of transfer of radiant energy with increase of temperature.

In some instances the tests were disturbed before all data were taken, and in repeating the test only a few points were taken within the range of the previous test. These points usually agreed with the previous test, and in such cases the second run is shown in the curve as a dotted or broken line. (See Fig. 15.) Heating values are indicated by open center circles and cooling values by dark center circles. Where the observations were so numerous that these circles interfered with each other the curve has been omitted. The specimen was watched constantly to see that no smaller variations were overlooked. When the expansion or contraction appeared to be regular these intervening observations were not recorded, or if recorded were not used in the plots.

The cast-iron specimen S483 (Fig. 17) is included to show the rapid growth at high temperature. Additional work is being planned to cover this field more thoroughly. The specimen of hardened steel (Fig. 16) gives a graphical picture of the shrinkages accompanying the drawing process.

Little if any of the above work can be considered as new information. It is perhaps a further confirmation of the findings of other observers, many of which were using entirely different lines of attack. The results will indicate the accuracy and ease with which it is possible to investigate materials at higher temperatures by this method of thermal analysis. Doubtless much of the value of these data will be worked out by those more closely connected with the industrial applications of such.

The results of the expansion measurements are given by the curves of Figs. 2 to 22 and the data relating thereto are assembled

Digitized by Google

TABLE 3.—Results of Analyses and Measurements of the Samples

PART 1.—RESULTS OF CHEMICAL ANALYSES

Lab. No.	C	Mn	P	S	Si	Cr	V	Ni	Miscellaneous
S546	0.35	1.42	0.013	0.037	0.20	1.00	0.11	.....	
S547	.49	1.21	.05	.050	.12	.....	.....	.....	
S548	.41	.64	.052	.061	.086	.....	.....	.....	
S549	.44	.57	.013	.033	.161	.....	.14	.....	
S550	.59	.92	.024	.033	.25	.....	.....	.....	
S551	.35	.08	.010	.027	.110	1.17	.14	.....	
S552	.36	.46	.011	.029	.09	.57	.12	.....	
S553	.168	.01	.010	.026	.135	2.50	.39	3.94	
S554	.410	1.11	.053	.049	.115	.....	.....	2.00	
S555	.144	.10	.03	.035	.034	1.15	.21	.....	Cu 1.85
S556	.252	.06	.012	.035	.007	.....	.....	.....	
S557	.168	.08	.010	.029	.038	.92	.24	.....	Mo .64
S558	.122	.05	.020	.040	.846	.85	.23	.....	
S559	.326	.78	.014	.035	.094	.....	.....	3.59	
S560	.342	.28	.01	.043	.094	.82	.26	.....	Cu 2.70
S561	.396	.25	.012	.023	.095	.....	.....	.....	W 3.96
S562	.380	1.17	.055	.067	.10	.....	.....	.81	
S563	.388	1.21	.010	.043	1.04	.....	.....	3.67	
S564	.512	.42	.016	.021	1.45	.....	.....	.....	W 1.58
S565	.30–.40	.....	.....	.....	.....	13.00	.....	.....	
S566	.418	.68	.012	.025	.23	.....	.....	.....	
S507	.02	nil	nil	.007	.006	(Co, Cu, Ni, total 0.014)			
S482	1.28	.37	.....	.....	.....	.19	.....	.....	
S504	.20	1.10	.05	.05	.....	.5	.....	.5	
S483	3.08	.....	.....	.....	1.68	.....	.....	.....	
S484	.14	.....	.....	.....	.....	.....	.....	34.52	
S457	.09	.19	.....	.....	3.70	1.76	.005–	.05–	
S614[a]	.85	1.00	<.02	.....	.25	.50	.....	.....	W .45

PART 2.—AVERAGE COEFFICIENTS OF EXPANSION ON HEATING (TEMPERATURES INDICATED) × 10^6

Lab. No.	25 to 100° C	100 to 200° C	200 to 300° C	300 to 400° C	400 to 500° C	500 to 600° C	600 to 700° C	25 to 300° C	300 to 600° C	25 to 600° C
S546	12.4	12.8	14.4	15.1	15.9	15.9	16.2	13.3	15.6	14.5
S547	11.3	12.2	14.2	16.3	17.7	15.4	16.7	12.7	16.5	14.7
S548	11.1	12.2	14.3	15.8	15.7	16.0	16.6	12.7	15.8	14.3
S549	11.2	12.4	14.3	15.4	16.4	16.5	16.8	12.7	16.1	14.5
S550	11.1	12.5	14.6	15.4	16.1	16.8	16.6	12.9	16.1	14.6
S551	11.0	12.3	14.8	15.6	15.9	16.5	16.2	12.9	16.0	14.5
S552	11.8	12.6	14.4	15.1	16.0	16.6	16.8	13.1	15.9	14.5
S553	10.8	11.7	13.5	14.0	14.5	14.4	.....	12.1	14.3	13.3
S554	11.6	11.9	14.0	16.2	13.7	16.5	16.4	12.6	16.1	14.4
S555	11.2	12.6	13.8	15.6	15.6	16.0	16.7	12.7	15.7	14.3
S556	11.1	12.0	14.2	15.5	15.9	16.6	16.9	12.5	16.0	14.3
S557	11.3	11.8	13.9	15.3	13.7	16.6	16.1	12.5	15.9	14.2
S558	11.6	12.5	13.7	14.6	15.2	16.0	15.8	12.7	15.2	14.0
S559	10.9	11.5	13.6	15.2	15.1	15.7	.....	12.1	15.3	13.8
S560	11.6	12.6	14.2	16.0	15.9	16.4	16.9	12.9	16.1	14.6
S561	11.1	12.0	14.0	15.1	15.7	16.4	16.5	12.5	15.7	14.2
S562	11.2	12.7	14.3	15.2	16.2	16.7	16.4	12.9	16.1	14.5
S563	11.6	12.0	13.2	14.2	15.2	15.6	.....	12.3	15.0	13.7
S564	10.4	12.1	13.7	15.9	15.7	16.1	.....	12.2	15.9	14.2
S565	10.0	10.6	12.0	12.6	13.5	13.9	13.7	11.0	13.3	12.2
S566	9.4	12.0	14.3	15.3	16.4	17.1	16.8	12.1	16.2	14.3
S507	12.0	13.0	14.5	15.3	15.9	16.8	17.4	13.3	15.9	14.7
S482	11.0	11.6	13.6	15.1	16.3	16.1	17.0	12.0	15.9	14.1
S504	12.3	12.9	14.2	15.9	16.2	16.5	16.8	13.2	16.5	14.9
S483[b]	8.4	11.7	14.2	15.6	14.3	Growing		11.6	Growing	
S484	3.7	8.4	14.1	16.6	18.4	18.8	19.1	9.2	18.2	13.6
S457	11.1	12.4	13.3	14.0	15.6	16.0	16.9	12.6	15.3	14.0

[a] Hardened from 850° C; scleroscope 60; shortened 1.2 mm per meter.

[b] Expansion values must be considered as approximate only, since the values doubtless contain a percentage of growth in addition to expansion.

Digitized by Google

TABLE 3—Continued

PART 3.—CRITICAL REGION DATA

Lab. No.	Heating				Cooling			
	Temp. contraction began	Temp. contraction ended	Contraction	Average rate of heating	Temp. expansion began	Temp. expansion ended	Expansion	Average rate of cooling
	°C	°C	μ/m	°C/minute	°C	°C	μ/m	°C/minute
S546	742	792	1255	0.38	682	661	1475	0.49
S547	723	771	1495	.80	667	640	1540	.....
S548	722	780	1440	.37	.....	665	.....	.....
S549	735	790	1495	.71	746	675	1525	.79
S550	729	799	1605	.73	685	659	1590	.79
S551	759	806	1910	.57	769	717	1805	.69
S552	744	811	1535	.67	763	695	1605	.68
S553	711	790	860	.84	431	332	1515	.50
S554	730	817	740	.76	781	715	695	.93
S555	764	826	1135	.54	785	704	1415	.78
S556	734	823	1410	.82	806	732	90	.87
S557	774	858	700	1.55	839	757	795	2.35
S558	806	811	.....	.53	.....	.....	.....	.82
S559	688	742	1730	.90	621	542	1205	1.01
S560	738	794	1310	.50	746	685	1450	.68
S561	758	837	820	.65	817	738	1010	.67
S562	718	787	1300	.50	730	637	1200	.83
S563	694	730	970	.61	550	540	.....	.56
S564	735	770	1580	.72	738	676	1335	.90
S565	864	886	605	.92	846	805	835	1.14
S566	725	768	1710	.83	721	665	1725	.75
S507	912	917	1310	.67	906	903	163	.50
S482	732	742	1000	.32	712	694	660	2.78
S504	722	833	1230	.36	747	648	1020	.89
S483	790	810	Indet.	.30	775	746	2120	.54
S484	None	None	None	.....	.....	.....	.....	.....
S457	None	(Coeff. 800 to 900 = 17.7; 900 to 1000 = 18.9; 25 to 1000 = 15.3)						

PART 4.—EXPANSION DATA

Lab. No.	Average coefficient of expansion (× 10^6) above critical region				Coefficient on cooling 600 to 25° C	Increase in length at 25° C	Maximum difference in heating and cooling curves	Temp. of maximum difference
	Heating	Temp. range	Cooling	Temp. range				
		°C		°C			μ/m	°C
S546	23.4	825–900	22.7	900–725	14.5 × 10^{-6}	−1202	−1250	513–555
S547	.....	.....	22.7	900–700	14.6	− 462	− 630	485–515
S548	22.7	800–900	22.7	900–800	14.5	− 110	− 125	363–393
S549	22.8	800–900	22.8	900–800	14.4	− 82	− 145	505–525
S550	24.0	800–900	23.1	900–725	14.5	− 400	− 465	343–380
S551	24.1	825–900	22.8	900–800	14.3	− 270	− 355	585–613
S552	24.0	825–900	22.6	900–800	14.4	− 90	− 195	640
S553	.....	.....	22.3	900–550	10.7 (275–25°C)	− 680	.....	290
S554	.....	.....	21.9	900–800	14.5	− 198	− 225	405–423
S555	.....	.....	22.0	900–805	14.2	+ 343	+ 380	85–150
S556	.....	.....	23.0	895–820	14.3	− 593	− 730	675
S557	.....	.....	.....	.....	13.9	+ 98	+ 160	180–225
S558	.....	.....	.....	.....	14.0	+ 346	+ 360	90–160
S559	22.2	800–900	22.8	900–700	13.1 (500–25°C)	− 727	− 875	515–525
S560	.....	.....	.....	.....	14.5	+ 335	+ 380	125–195
S561	.....	.....	.....	.....	14.1	+ 18	+ 110	182–223
S562	.....	.....	22.7	900–800	14.5	− 200	− 225	515–520
S563	22.6	800–900	21.1	900–600	10.9 (500–25°C)	− 920	−2080	525–590
S564	23.0	800–900	23.0	900–800	14.2	− 148	− 180	408–455
S565	.....	.....	.....	.....	12.1	− 63	− 100	570–615
S566	22.6	800–900	23.1	900–800	14.5	− 366	− 366	25
S507	23.4	905–945	23.4	917–945	13.3	− 120	−1500	912
S482	34	750–875	28.6	875–713	14.3	.....	− 825	712
S504	23.4	833–850	21.6	950–760	14.8	− 430	− 510	600
S483	37	815–900	25	900–775	14.1	+9040	+9340	300
S484	.....	.....	.....	.....	13.6	.....	.....	.....
S457	.....	.....	.....	.....	12.6	0	0	.....

Digitized by Google

in Table 3. These results can be more readily interpreted by classifying them under the characteristics of the theoretical curve of Fig. 1. This curve represents the critical regions within which anomalous length changes occur. Most of the specimens followed the sequence of expansion as shown by the curve A, B, C, D, E, F, G of this figure. The length increments were usually quite regular up to point B, where they reversed sign and were recorded as contractions until point C was reached. From point C the expansion was usually greater than at any previous point. On cooling from D to E the contraction corresponded to the expansion on heating. At E the contraction ceased and an expansion was recorded until point F was approached. Below this point the contraction was again similar to the corresponding expansion recorded on heating.

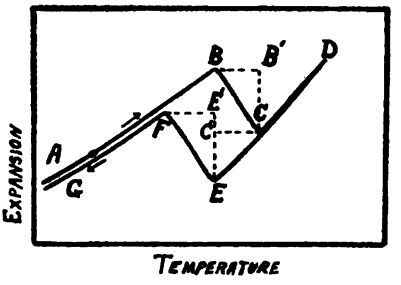

FIG. 1.—*Theoretical expansion curve for range 600 to 900° C*

The values for vacuum electrolytic iron [9] (S507, Fig. 2) may serve as reference values for the alloys. The temperature interval of contraction with heating (B, B' of Fig. 1) extended from 912 to 917° C. The corresponding interval of expansion with cooling (E', F) extended from 906 to 903° C. These intervals of temperature represent the retardations due to inherent resistances to this change, to impurities present, to our finite rate of heating or cooling. Where the retardations exceed these limits they may be assumed to be the results of alloying elements.

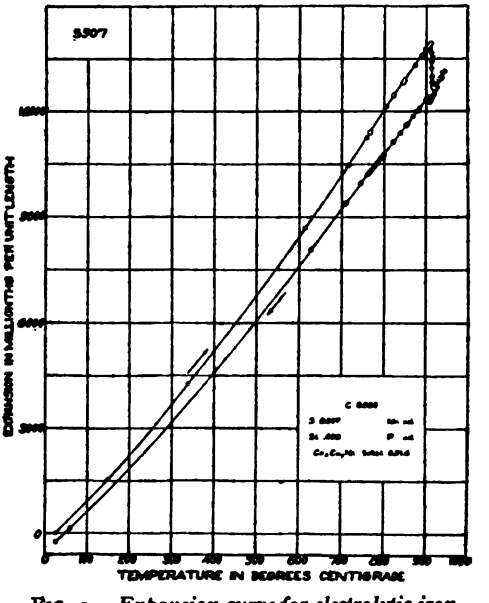

FIG. 2.—*Expansion curve for electrolytic iron*

[9] Made by Dr. A. W. Owen, of this Bureau.

Digitized by Google

The temperature interval between points C and E (CC') is not constant and varies fron 11° C for iron to an indefinite value of about 350° C on specimen S553 (Fig. 3). Specimen S484 (Fig. 4) is not included in this comparison because of the lack of proper temperature range necessary to bring out these differences.

The low expansivity of invar at room temperatures is due to the fact that this E, F region has been lowered to corresponding temperatures. Other specimens of nickel steel showing this lowering of the E, F region are: S559 (Fig. 5) and S563 (Fig. 6). These curves, including S484, give their relations to other steels at high temperatures. Excluding nickel steels, the greatest displacements are given by S546 (Fig. 7), S547 (Fig. 8), and S504 (Fig. 9). On S556 (Fig. 10) this difference is only 17° C, whereas on S546 (Fig. 7) it amounts to 110° C. Now, the usual procedure in hardening steel is to quench from some temperature a certain number of degrees above the temperature of the irregularities of the heating curve. Should it develop that the most desirable quality is present in the steel at point E (after having passed point C) rather than at point C, it is conceivable that errors approaching 100° C may have entered the quenching values.

Alloys showing the maximum differences between temperatures B and C (BB') are S504 (Fig. 9), S556 (Fig. 10), and S554 (Fig. 11). Similarly between E and F ($E'F$) we have S504 (Fig. 9), S562 (Fig. 12), and S553 (Fig. 3). Cast iron is excluded because of the indefiniteness due to growth.

Perhaps one of the most important variations is that of length change between E and F (EE'). If we assume the usual stress-strain relations as applying in this case then the stresses set up within a specimen, the outer shell of which has passed through this range before the inner, will be proportional to the length (EE'). This feature will be discussed later in connection with the results of a hardened specimen (S614). Specimens S551 (Fig. 13) and S566 (Fig. 14) illustrate this maximum expansion on cooling. The rate at which this stress is applied depends upon the value of EE', the value of $E'F$, and the rate of cooling of the different sections of the specimen.

It is interesting to note that the specimen of high silicon steel S457 (Fig. 15) gave only slight if any reversals although heated to 1002° C.

The coefficient of expansion of iron over the range 25 to 100° C is 12.0×10^{-6}. The average value for 25 of the steels tested is 11.2×10^{-6}, and the deviations (excluding high chromium and

Digitized by Google

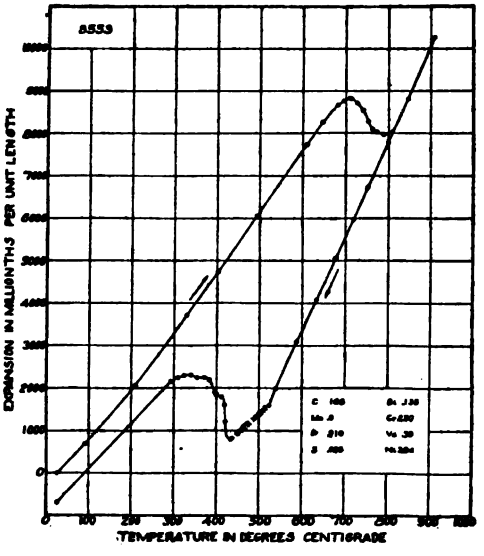

FIG. 3.—*Expansion curve for nickel steel.*

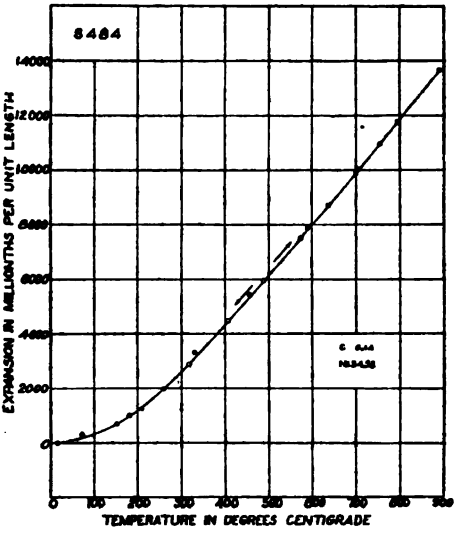

FIG. 4.—*Expansion curve for nickel steel*

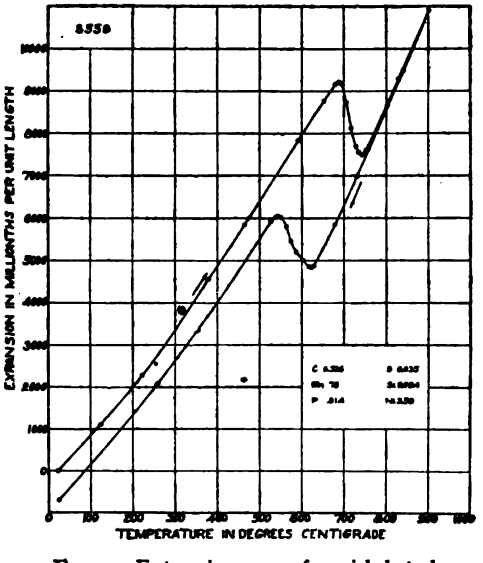

FIG 5.—*Expansion curve for nickel steel*

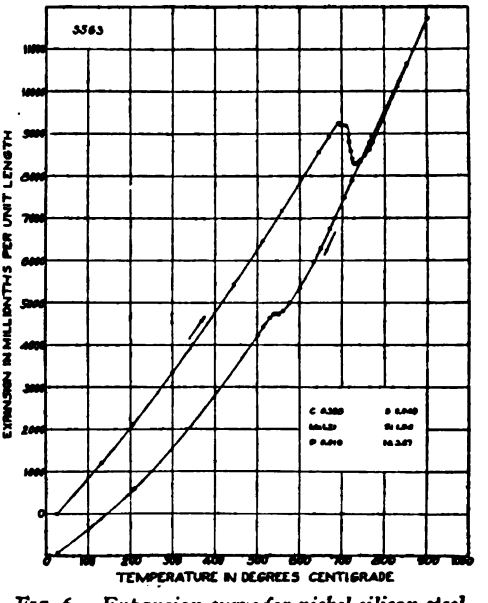

FIG. 6.—*Expansion curve for nickel-silicon steel*

Digitized by Google

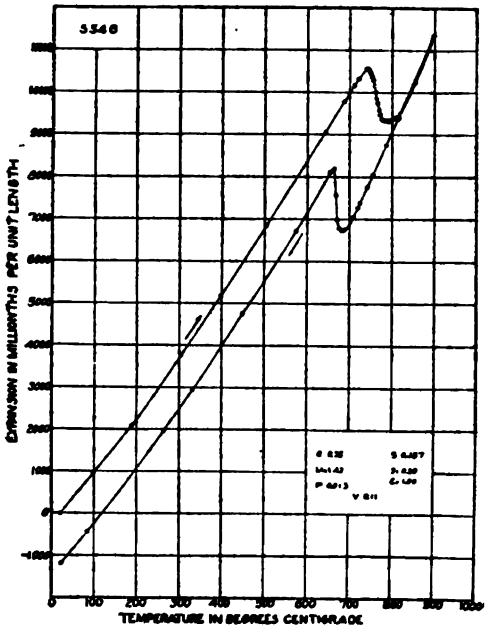

FIG. 7.—*Expansion curve for steel showing large variations between heating and cooling critical regions*

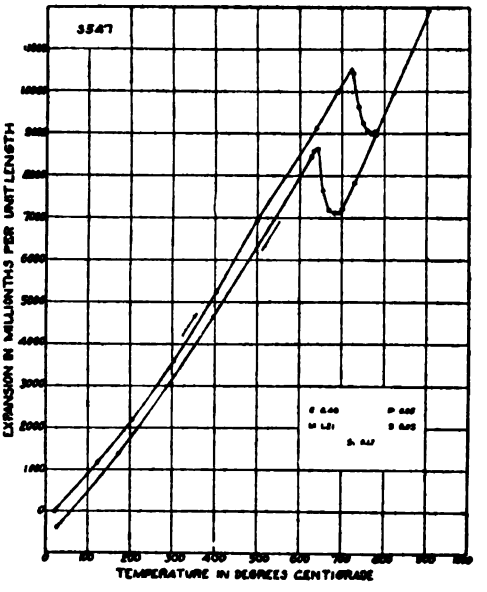

FIG. 8.—*Expansion curve for steel showing large variations between heating and cooling critical regions*

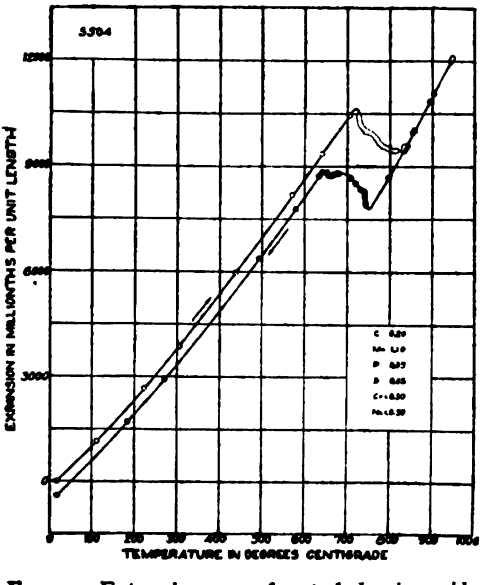

FIG. 9.—*Expansion curve for steel showing wide critical regions*

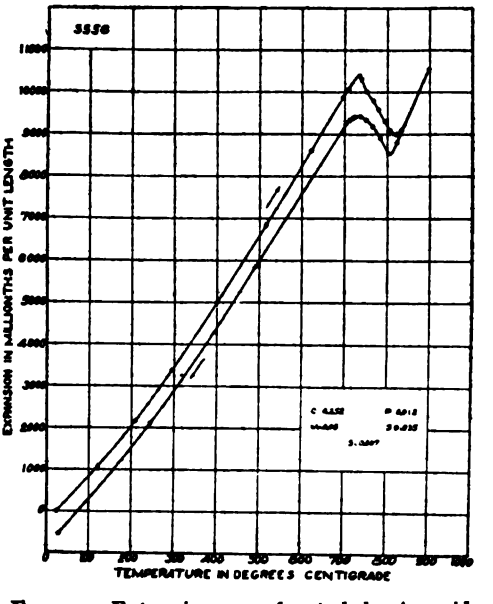

FIG. 10.—*Expansion curve for steel showing wide critical regions*

Digitized by Google

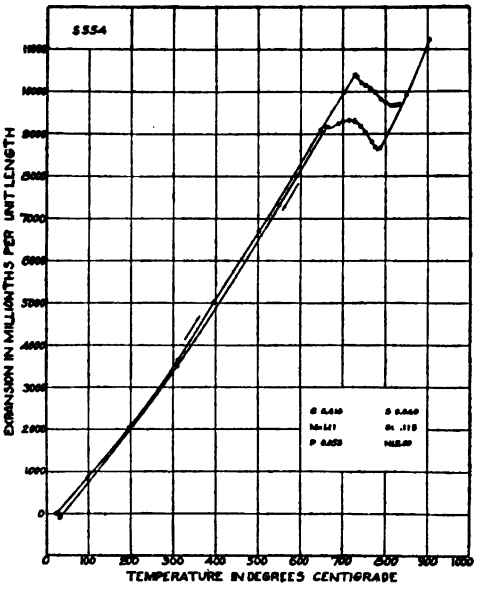

FIG. 11.—*Expansion curve for steel showing wide critical regions*

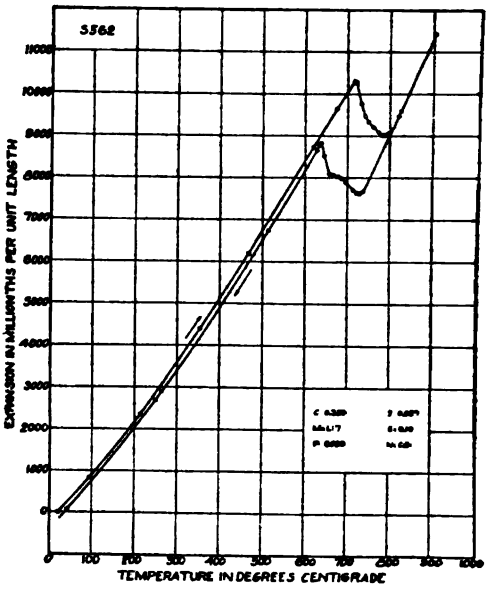

FIG. 12.—*Expansion curve for steel showing wide critical regions*

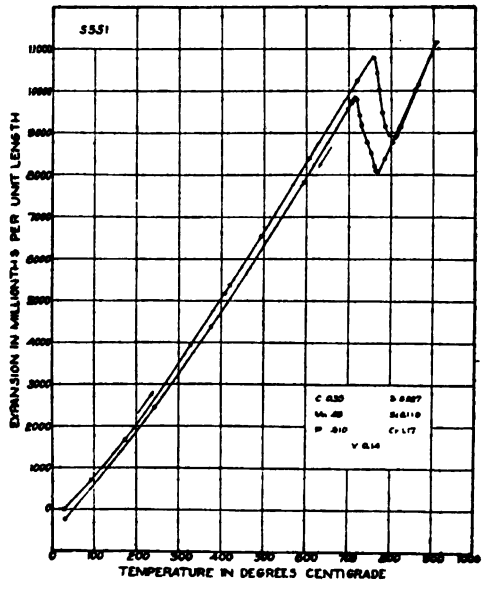

FIG. 13.—*Expansion curve for steel showing large change of dimension at critical regions*

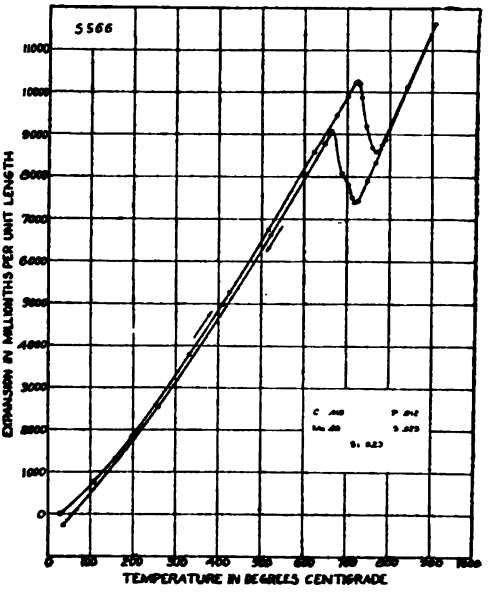

FIG. 14.—*Expansion curve for steel showing large change of dimension at critical regions*

Digitized by Google

nickel steels) are small. The average value from 25 to 600° C is 14.2×10^{-6}. Above the critical regions the values jump to values between 22.6×10^{-6} and 24.1×10^{-6}. The special high carbon, nickel, and silicon steels are not included within this range. The cooling coefficients are closely related. Within the critical region the coefficient is quite different, usually reversing sign. This reversal of sign, or expansion on cooling, may set up stresses in the hardened steel which if not properly released will cause cracking or distortion. The higher the temperature above the critical region from which the specimen is quenched and the faster the rate of cooling, the greater should be the tendency to these defects. Undoubtedly the coarser grain structure of the higher temperatures has some influence; but the cooling of the outer layer before the interior cools will set up stresses, since this outer layer adapts itself about the interior before the interior has passed through the critical region where it will tend to expand, and to stretch or crack the outer shell. The release of this stress of outer shell is shown in S614 (Fig. 16). The relative amount of this stress can be compared in the column headed "Expansion μ/m (cooling)."

The works of Honda,[10], Chevenard,[11] and others show that quenching steel may carry point E several hundred degrees below the normal slow-cooling position recorded in our tests. If we apply the coefficient 23×10^{-6} for the contraction rate over these several hundred degrees range for the retarded or undercooled phase of the outer surface, and apply the normal coefficient (approximately) 16×10^{-6} for the inner portions where the cooling has been sufficiently slow to permit the transformations, we justify an intensification of the above stresses.

When variations in the ratios of quenching of different parts of a surface exist, the above-mentioned inequalities in the time and rate of expansion or contraction may readily manifest their effects in warping or local cracking.

Steel No. S614, Fig. 16, is included to show the effects of hardening as related to length changes. This specimen was heated to 850° C and quenched in oil. Upon heating above 50° C we found the curve departing from the annealed-steel curve (see dotted lines for average annealed steel). The specimen was carried from 50 to 100° C and back in about 200 minutes and gave a shrinkage of about 250 microns per meter. This shrink-

[10] Honda, Tôkohu University, Scientific Reports, 8, pp. 181–205. Honda, Matsushita and Idei, J. Iron and Steel Inst., 108, pp. 251–269.

[11] P. Chevenard, C. R., 165, pp. 59–62; Rev. de Mét., 16, pp. 17–19.

Digitized by Google

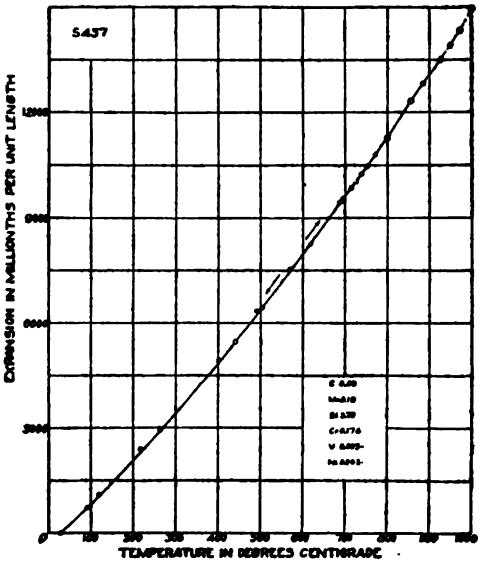

FIG. 15.—*Expansion curve for silicon steel*

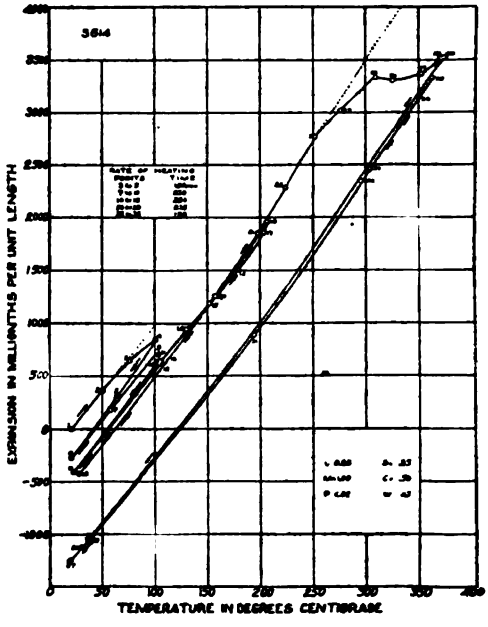

FIG. 16.—*Expansion curve for steel showing release of strains in drawing*

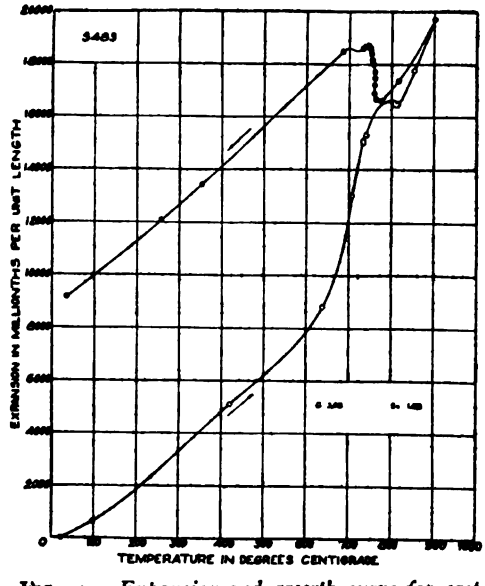

FIG. 17.—*Expansion and growth curve for cast iron*

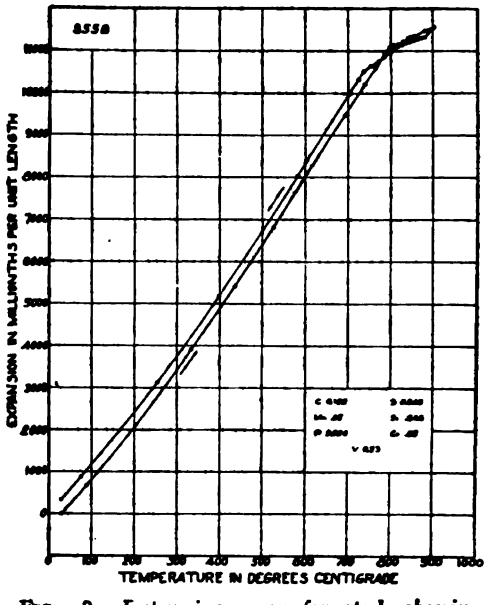

FIG. 18.—*Expansion curve for steel, showing small change of dimension at critical regions*

Digitized by Google

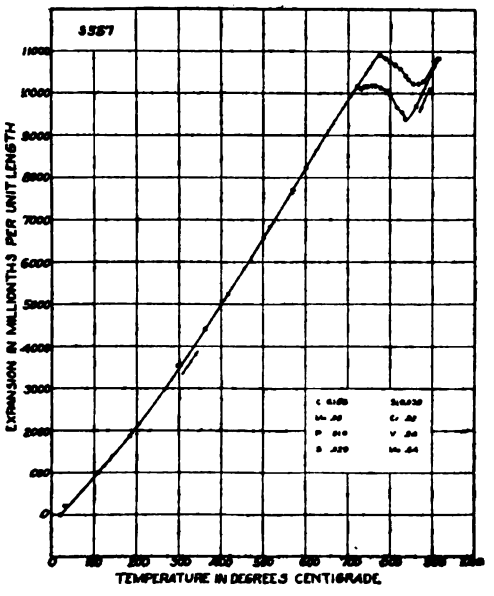

FIG. 19.—*Expansion curve for steel*

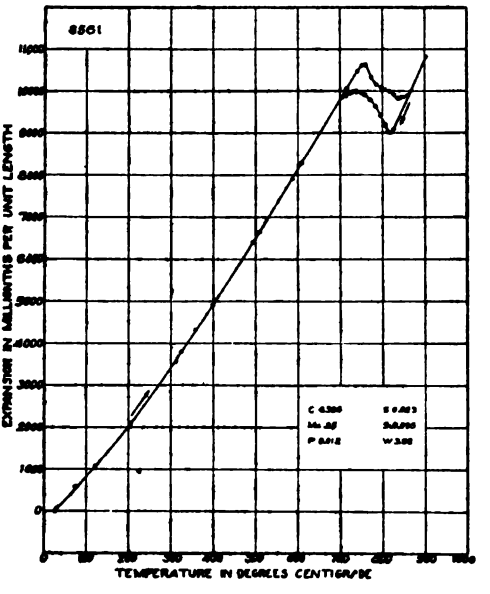

FIG. 20.—*Expansion curve for steel*

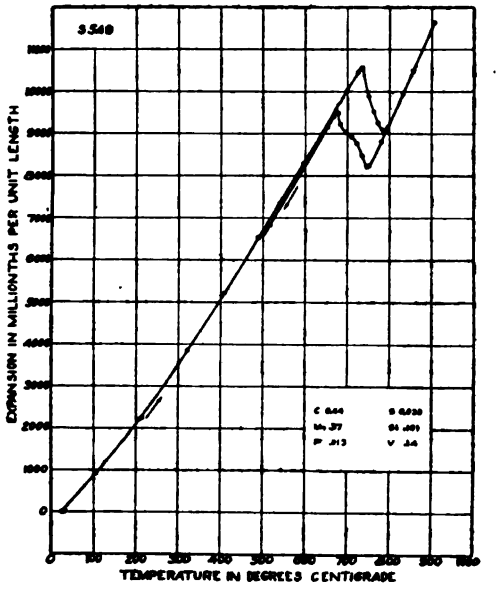

FIG. 21.—*Expansion curve for steel*

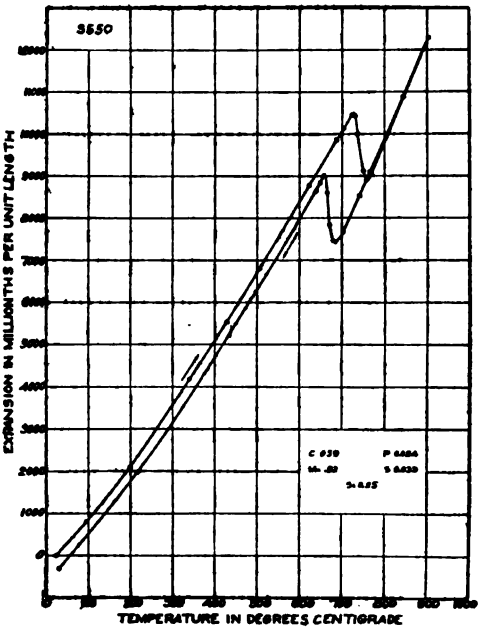

FIG. 22.—*Expansion curve for steel*

Digitized by Google

age is to be expected since the outer shell was stressed by the central portions passing through the (expanding) critical regions after the outer layers had passed this stage and had started on the regular contraction. Reheating to 100° C and holding for about 4 hours was sufficient to release additional stresses, and the specimen then showed a total shrinkage at 25° C of 400 microns per meter, or in more general terms 400 millionths per unit length. This heat treatment appears to have released practically all the stresses possible to release at or near 100° C, for additional heating to 200° C gave very little additional shrinkage. The cooling curve from 200° C crosses the heating at about 150° C; no explanation is evident for this phenomenon. Reheating to 250° C and above renewed the shrinkages, and at 310 to 350° C the effect was very pronounced. At 370° C the effect appeared to be complete and upon return to room temperature gave a total shrinkage of 1250 microns per meter, or one-eighth of 1 per cent.

This shrinkage has been shown for a specimen of chrome steel [12] on which the observations were carried beyond the critical ranges. The present curve gives greater detail of the changes.

The increase or decrease in length on cooling to 25° C was usually small and, in a large degree, indicates the lack of perfect annealing before the test was started. The maximum differences between the heating and cooling curves are closely related to the permanent length changes.

Figs. 18, 19, 20, 21, and 22 are included as additional specimens which emphasize the differences previously mentioned.

5. SUMMARY

1. Data on the anomalous expansion of a few steels and irons have been recorded, and made available for reference.

2. The expansion of iron has been determined over the range 25 to 945° C. The expansion from 25 to 100° C was found to be 12.0×10^{-6}. The average expansion of a number of steels, over this same range was found to be 11.2×10^{-6}, and for the range 25 to 600° C, 14.2×10^{-6}.

3. The coefficient for the ordinary steels which we have heated above the critical regions have been evaluated as approximately 23×10^{-6}.

4. The shrinkages and warpages of drawn steels have been interpreted in terms of the rate of expansion and rate of temperature reduction on passing through the critical regions.

WASHINGTON, November 8, 1921.

[12] B. S. Sci. Papers, No. 426, p. 513.

Digitized by Google

JUN 22 1922

DEPARTMENT OF COMMERCE

SCIENTIFIC PAPERS

OF THE

BUREAU OF STANDARDS

S. W. STRATTON, DIRECTOR

No. 434

[Part of Vol. 17]

ELECTROMOTIVE FORCE OF CELLS AT LOW TEMPERATURES

BY

G. W. VINAL, Physicist
F. W. ALTRUP, Assistant Physicist
Bureau of Standards

APRIL 17, 1922

PRICE, 5 CENTS
Sold only by the Superintendent of Documents, Government Printing Office
Washington, D. C.

WASHINGTON
GOVERNMENT PRINTING OFFICE
1922

Digitized by Google

Digitized by Google

ELECTROMOTIVE FORCE OF CELLS AT LOW TEMPERATURES

By G. W. Vinal and F. W. Altrup

ABSTRACT

The practical importance of a knowledge of the electromotive behavior of dry cells and storage batteries at low temperatures has arisen from their use in the Arctic and at high altitudes. Measurements on dry cells and storage batteries cooled to −72° C by carbon dioxide snow and to −170° C by the use of liquid air were made. The Gibbs-Helmholtz equation was applied to the observations, and excellent agreement between theory and observation was found. At the lowest temperatures high values of voltage were sometimes observed, and the polarity was often reversed. A possible explanation based on the Nernst equation is given.

The practical importance of a knowledge of the electromotive behavior of dry cells and storage batteries at low temperatures has arisen from their use in the Arctic and at high altitudes. In June, 1921, the Department of Terrestrial Magnetism of the Carnegie Institution, through Dr. S. J. Mauchly, requested the Bureau of Standards to furnish information in answer to the following questions: (1) What is the open circuit voltage of dry cells at approximately 0° F and below? (2) Are dry cells fit for use after they have been frozen and thawed out again? Since there was no reliable information available on this subject, some experimental work was undertaken, which included observations on storage batteries also. In the first experiments the temperature range was extended to −72° C, and as the open circuit voltage of the cells was not materially changed by cooling them to this temperature the work was extended to −170° C because of the theoretical interest in the application of the Gibbs-Helmholtz and Nernst equations to these cells.

Two methods for cooling the cells were employed. For the range +25 to −72° C the cells were submerged in a gasoline bath to which small amounts of carbon dioxide snow were added gradually until the lowest temperature attainable was reached, when an excess of the snow was packed around the cells. For the range +20 to −170° C liquid air was used for cooling. The dry cells

Digitized by Google

were placed in a double-walled glass jacket similar to a Dewar vessel, but having air at atmospheric pressure between the walls. This was submerged in liquid air contained in a larger Dewar flask. The storage cell, contained in a glass test tube, was similarly arranged with the addition of a ground cork packing to protect it from breakage. By this means the cooling was gradual, about two hours being required for the cells to fall from room temperature to the lowest temperature available.

The temperatures were measured by a thermocouple of standardized constantan and copper wire. Since it was not practicable to insert the thermocouple in the dry cells of which the emf was measured, the thermocouple was placed at the center of a similar dry cell which was grouped symmetrically with the other cells. The temperature of the storage cell was measured by placing the thermocouple, protected by a thin-walled glass tube, in the electrolyte between the positive and negative plates of the cell. The electromotive forces of the thermocouples were read on a high-resistance potentiometer.

The dry cells were ¾ inch diameter by 2⅛ inches high and were taken from flashlight batteries of a well-known make. A few experiments on silver chloride dry cells were made also. The storage cells were made by cutting strips of suitable size from the pasted plates of an automobile starting and lighting battery. These were placed in test tubes about 1 inch in diameter, with perforated hard-rubber separators and a few glass beads. The electrolyte was adjusted to a specific gravity of 1.275 to 1.280 at the end of five days of continuous charging at 0.4 ampere.

TABLE 1.—Open Circuit Voltages of Cells

[For values below −70° C, see Fig. 2]

Temperature (°C)	Ordinary dry cell [a]	Storage cell [a]	Silver chloride cell [b]	Temperature (°C)	Ordinary dry cell [a]	Storage cell [a]	Silver chloride cell [b]
	Volts	Volts	Volts		Volts	Volts	Volts
20	1.540	2.116	1.06	−30	1.508	2.100	1.01
10	1.537	2.113	1.05	−40	1.530	2.096	1.00
0	1.533	2.111	1.04	−50	1.540	2.092	.99
−10	1.523	2.107	1.03	−60	1.540	2.087	.98
−20	1.512	2.103	1.02	−70	1.526	2.081	.97

[a] Based on potentiometer readings.
[b] Interpolated values based on electrometer readings.

The voltage of the cells during test was measured by three different methods, but the open circuit measurements at the lowest

Digitized by Google

temperatures could be made only by an electrometer. This instrument was loaned to us by the Department of Terrestrial Magnetism. The open circuit voltages were also measured on a 20 000 ohm potentiometer, which afforded a very sensitive method

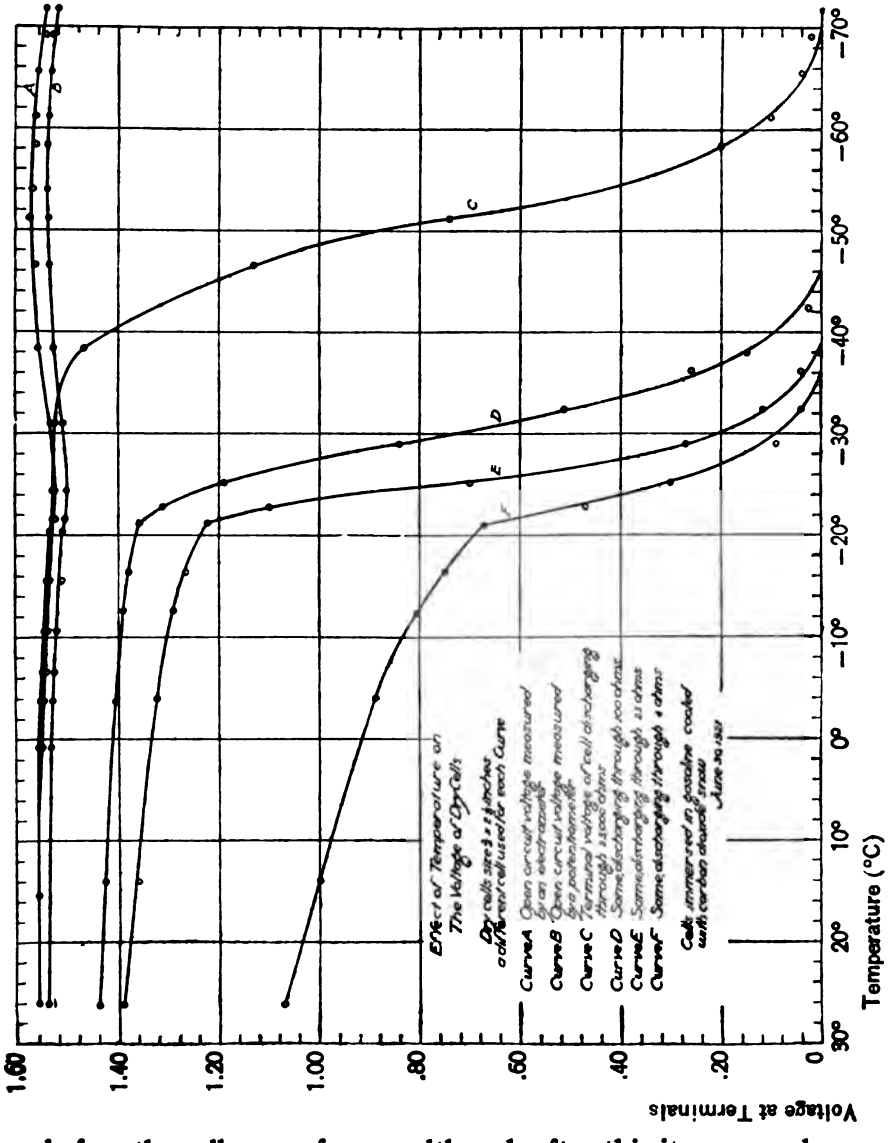

FIG. 1.—*Effect of temperature on the voltage of dry cells*

before the cells were frozen, although after this it was nearly useless. A voltmeter having a scale of 2.5 volts and a resistance of 25 000 ohms was used for some of the measurements.

The results of experiments with dry cells of the ordinary type are shown in Table 1 and Fig. 1. Curves *A* and *B* represent the

Digitized by Google

open circuit voltages as measured for two different cells by the electrometer and the potentiometer. Curves *C*, *D*, *E*, and *F* represent the terminal voltage when the cells were discharging through 25 000, 100, 25, and 4 ohms, respectively. The curves indicate the existence of a critical point at about $-21°$ C.

The open circuit voltage curves indicate that changes in the temperature coefficient occur at certain temperatures. Between $+26$ and 0° C the coefficient was found to be constant and somewhat less than a millivolt per degree. The coefficient is positive; that is, increase in temperature is accompanied by increase in voltage. Between 0 and $-20°$ C the coefficient is still positive but larger. At $-20.4°$ C a break occurs. The temperature coefficient becomes much larger during the next few degrees and then changes to negative at about $-24°$ C. At $-54°$ C the coefficient again becomes positive. It is interesting to note that at $-54°$ C the voltage is higher than at ordinary temperatures.

Curves *C*, *D*, *E*, and *F* show that the ordinary dry cell can deliver current down to about $-20°$ C, below which the voltage falls off rapidly to zero.

Silver chloride dry cells were measured in a similar manner, and the open circuit voltages are given in Table 1. When the voltage was measured by the 25 000-ohm voltmeter, however, the terminal voltage began to fall rapidly from 0° C downward. At -10 C it was 0.9 volt, and from this point it decreased nearly linearly to 0.05 volt at $-50°$ C.

Experiments were also made to determine the voltage of storage cells within the range $+25$ to $-72°$ C, using the electrometer, the potentiometer, and the voltmeter to measure the voltage. As freezing did not occur within this range, the potentiometer gave the most accurate results, as shown in Table 1, but the results of all methods were in good agreement. The temperature coefficient was small and constant. This fact permitted an accurate estimate of the temperature coefficient to be made, since the cell had sufficient time for thermal equilibrium to be established at the beginning and end of this range. The temperature coefficient was found to be 0.000398 volts per degree C.

It is interesting to compare this result with the value computed from the available thermochemical data and the Gibbs-Helmholtz equation. This equation is usually written

$$Q = W - T\frac{dW}{dT}, \tag{1}$$

Digitized by Google

where Q is the heat of the reaction, W the available work, and T the absolute temperature. This equation is applicable to a reversible cell in which the passage of current does not involve any appreciable change in volume. If E denotes the open circuit voltage of the cell, W equals 96 500 E volt coulombs [1] for one equivalent. Q expressed in calories may be converted to volt coulombs by multiplying by 4.183, and the equation becomes:

$$\frac{dE}{dT} = \frac{1}{T}(E - 0.000021674\,Q). \qquad (2)$$

Both E and Q are dependent on the concentration of the electrolyte, which for this experiment was of 1.280 sp. gr. The value of E corresponding to the initial value T was observed directly. The value for Q may be calculated from published thermochemical data.

The commonly accepted reaction of the lead accumulator during discharge may be described by the following equation:

$$\left.\begin{array}{l}\text{Positive plate, } PbO_2 + H_2SO_4 \\ \text{Negative plate, } Pb + H_2SO_4\end{array}\right\} + N.H_2O \rightarrow 2PbSO_4 + (N+2)\ H_2O,$$

where N is the number of molecules of water to 2 molecules of sulphuric acid in the original solution. The corresponding thermochemical equation is

$$PbO_2 + Pb + 2H_2SO_4 + N.H_2O = 2\ PbSO_4 + (N+2)H_2O + Q_N,$$

where Q_N, the heat of the reaction, depends on the dilution of the acid, which is fixed by N. Since the chemical reaction must take H_2SO_4 from the dilute electrolyte, the energy represented by Q_N for other strengths of acid will be less in amount by the quantity of heat evolved by dilution of the acid, or Q_N will be greater if the concentration is greater.

Values for Q have been determined by Streintz [2] and Tscheltzow [3] to be 87 000 and 88 600 calories, respectively. The mean of their determinations is 87 800 calories. Dolezalek [4] states that these values apply to dilute sulphuric acid (1 mol of H_2SO_4 to about 400 mols of H_2O), and hence a correction for the heat of dilution is necessary. The heat of dilution [5] of the acid solution from a

[1] The value 96 500 coulombs is based on recent determinations with the silver and iodine voltameters by Vinal and Bates at the Bureau of Standards, B. S. Sci. Papers, No. 218.
[2] Wied. Ann., 58, p. 698; 1894.
[3] C. R., 100, p. 1458; 1885.
[4] Theory of the lead accumulator, p. 29.
[5] Thomsen's data, Landolt and Bornstein tables, 4 ed., p. 885.

Digitized by Google

specific gravity of 1.280 as used in our experiment to the concentration equivalent to 1 mol of acid to 399 mols of water is 2210 calories per mol. Two mols are involved, and hence the value for the heat of the reaction for an electrolyte of 1.280 specific gravity is 87 800 + 4420 = 92 220 calories.

The value for E at 25° C and electrolyte of specific gravity 1.280 was 2.120 volts. The temperature, 25° C, corresponds to 298° absolute. Substituting these values for T, E, and Q in equation (2) the value for the temperature coefficient $\frac{dE}{dT}$ is found to be 0.000407. The results of the experiment showed a decrease in the open circuit voltage of 0.0386 volts when the temperature was decreased 97° C, from which $\frac{dE}{dT} = 0.000398$.

The agreement of this observed value with that calculated from thermochemical data is better than would be expected and gives a striking proof of the validity of the Gibbs-Helmholtz equation over a wide range of temperature.

A second series of measurements extending the temperature range down to −170° C was then made. Only the electrometer readings are of value at this low temperature. The results on a dry cell and a storage cell are shown graphically in Fig. 2. These are the open circuit voltages measured electrostatically. The storage cell showed marked undercooling of the electrolyte before freezing began. The dry cell showed a considerable increase in voltage at −112° C over the normal value. The most remarkable facts are the reversal of voltages and the extraordinarily large values of voltage exhibited by the storage cell, exceeding 10 volts at the lowest temperatures. The current was, of course, vanishingly small.

Nernst's equation applied to the storage battery in accordance with Liebenow's theory [6] is as follows:

$$E = \frac{RT}{2} \ln \frac{C_p C_n}{[Pb^{++}]\ [PbO_2^{--}]},$$

where C_p and C_n are the solution tensions of the positive and negative active material and the bracketed values represent the corresponding ionic concentrations. It is evident that a decrease in the ionic concentrations would result in an increase in the value of E if other quantities remained the same.

[6] Zs. f. Elektrochem., 8, p. 525; 1897.

Digitized by Google

The freezing of the electrolyte reduces the mobility of the ions practically to zero. If, then, the ions which are in immediate contact with the surface of the electrodes are discharged, they can not be replaced by the migration of other ions from the electro-

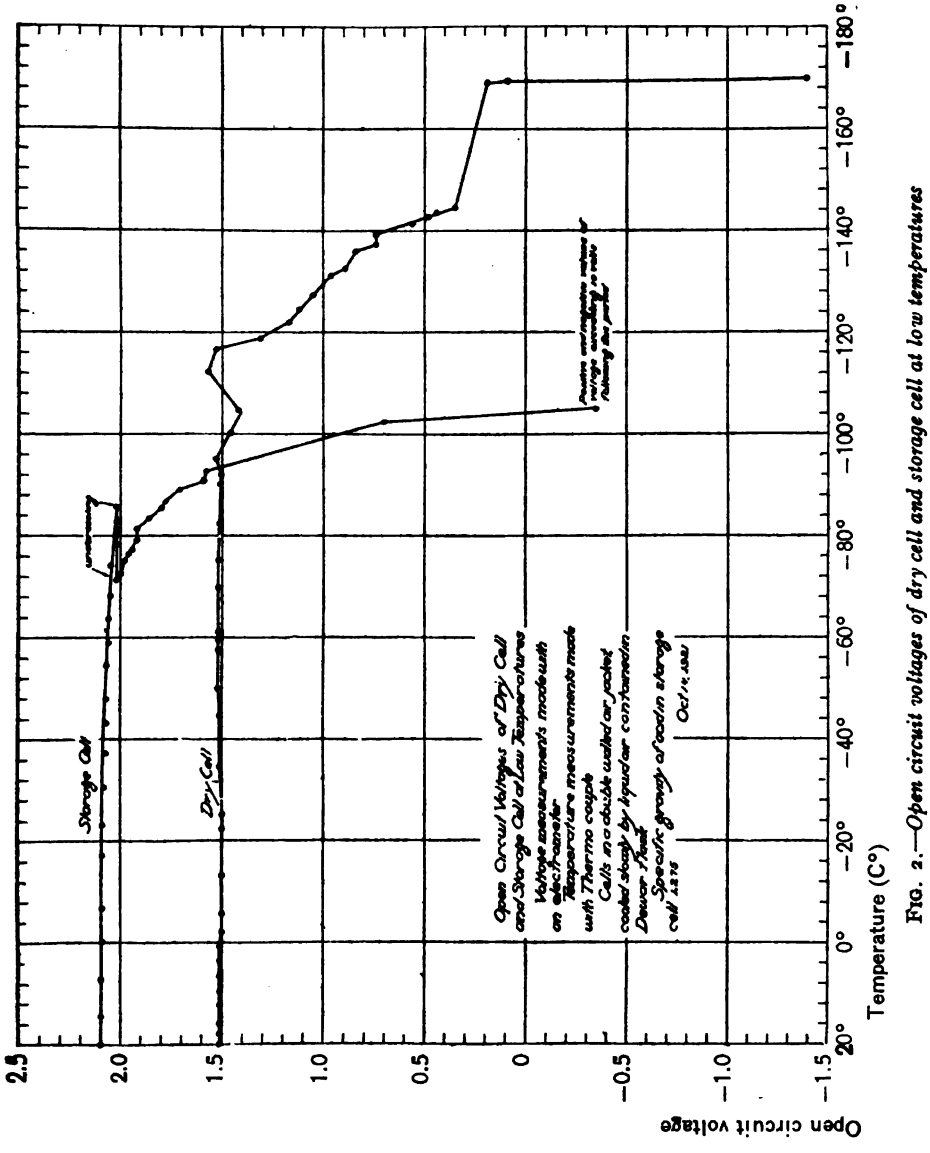

FIG. 2.—*Open circuit voltages of dry cell and storage cell at low temperatures*

lyte, and the effect in the region of the electrodes is essentially a decrease in the ionic concentrations. The equation, therefore, suggests the possibility of increased values of E as was observed after the freezing occurred.

Digitized by Google

No ready explanation of the reversal of voltage is available unless it be assumed that the variation of solution tension of each electrode with temperature is such that curves representing them would intersect at the temperature at which reversal occurs. Pressure may have had something to do with the voltage variations, since the electrometer showed violent fluctuations whenever the frozen electrolyte of the storage cell "ticked." Ice below the freezing temperature sometimes makes a similar ticking sound.

The genuineness of the reversed voltage was shown by the following observations: The dry cell after showing a steady reversed voltage of about 1.4 volts was removed from the liquid air, and in the course of a few minutes the reversed voltage decreased steadily, passed through zero, and increased to a normal positive value. Secondly, the potentiometer used for simultaneous measurements with the electrometer on the storage cell retained enough sensibility to show that the potential was reversed at the same time that the electrometer showed a reversed reading.

All of the cells, including the ordinary type of dry cell, the silver chloride cells, and the storage cells, appeared to be entirely normal after being thawed out. The glass test tube containing the storage cell was not broken.

The experiments in the range $+25$ to $-72°$ C answer completely the practical questions which prompted the investigation. The thermodynamic theory as expressed in the Gibbs-Helmholtz equation is accurately confirmed by the measurements on a storage cell. At temperatures down to $-170°$ C points of theoretical interest were found. These suggest that potential differences of normal value at ordinary temperatures may be greatly magnified at extremely low temperatures when the current is vanishingly small. High atmospheric potentials sometimes observed may have some relation to this effect.

We wish to acknowledge the loan of the electrometer by Dr. L. A. Bauer, Director of the Department of Terrestrial Magnetism, and the assistance of Dr. Mauchly in taking some of the observations; also valuable suggestions by Dr. E. Buckingham.

WASHINGTON, January 6, 1922.

Digitized by Google

DEPARTMENT OF COMMERCE

SCIENTIFIC PAPERS

OF THE

BUREAU OF STANDARDS

S. W. STRATTON, Director

No. 435

(Vol. 18)

METALLOGRAPHIC ETCHING REAGENTS

II. FOR COPPER ALLOYS, NICKEL, AND THE ALPHA ALLOYS OF NICKEL

BY

HENRY S. RAWDON, Physicist
MARJORIE G. LORENTZ, Assistant Physicist

APRIL 16, 1921

PRICE 10 CENTS

Sold only by the Superintendent of Documents, Washington, D. C.

WASHINGTON
GOVERNMENT PRINTING OFFICE
1921

Digitized by Google

Digitized by Google

DEPARTMENT OF COMMERCE

SCIENTIFIC PAPERS

OF THE

BUREAU OF STANDARDS

S. W. STRATTON, DIRECTOR

No. 435

[Part of Vol. 17]

METALLOGRAPHIC ETCHING REAGENTS

II. FOR COPPER ALLOYS, NICKEL, AND THE ALPHA ALLOYS OF NICKEL

BY

HENRY S. RAWDON, Physicist
MARJORIE G. LORENTZ, Assistant Physicist
Bureau of Standards

APRIL 27, 1922

PRICE, 15 CENTS
Sold only by the Superintendent of Documents, Government Printing Office
Washington, D. C.

WASHINGTON
GOVERNMENT PRINTING OFFICE
1922

Digitized by Google

Digitized by Google

METALLOGRAPHIC ETCHING REAGENTS:

II. FOR COPPER ALLOYS, NICKEL, AND THE ALPHA ALLOYS OF NICKEL

By Henry S. Rawdon and Marjorie G. Lorentz

ABSTRACT

This investigation constitutes the second part of the general study of metallographic etching reagents at this Bureau. The following were used as typical materials for etching: Copper alloys, including all the typical copper-zinc alloys, bronze and aluminum bronze, nickel and the α alloys of nickel, monel metal, cupro-nickel, and nickel brass.

Experimental results are given to show the importance of films varying in thickness upon the different crystals in a metallographic specimen in producing a "contrast etch pattern." This is clearly shown by separating the filming and the etching operations, both sulphide and oxide films being used.

The α copper alloys resemble copper in their general behavior upon etching. Aluminum bronze was found to be the most unsatisfactory of such alloys of copper to etch.

Nickel is etched with considerable difficulty. Strong oxidizing acids, such as nitric, or other acids to which oxidizing agents have been added may be used, but there is usually considerable pitting of the surface and a very noticeable lack of contrast in the resulting etch pattern. Concentrated hydrochloric acid, however, gives excellent results in both these respects. Monel metal and cupro-nickel resemble nickel in their etching characteristics, though they are etched more readily. The nickel brasses are much more like the brasses and bronzes and are readily etched by reagents used for these alloys.

Copper alloys, like copper, are readily etched by ammoniacal, acid, and some neutral solutions which otherwise would have only a slight effect upon them provided a stream of oxygen is passed through the solution while the specimen is immersed. Nickel, cupro-nickel, and monel metal are not materially affected in the rate of etching by the use of oxygen gas.

CONTENTS

	Page
I. Introduction	636
II. Materials used	636
III. Results	639
IV. Nature of contrast etching	643
V. Etching characteristics of copper alloys	646
1. Brass	646
(*a*) α brass	646
(*b*) $\alpha\beta$ brass	653
(*c*) High-zinc alloys	655
2. Bronze	658
3. Aluminum bronze	658
VI. Etching characteristics of nickel and of α nickel alloys	658
1. Nickel	658
2. Nickel alloys	666
VII. Effect of oxygen upon the rate of etching	673
VIII. Summary	075

Digitized by Google

I. INTRODUCTION

The work herein described forms part of the general investigation of metallographic etching reagents in progress at the Bureau of Standards. In a previous article [1] the authors summarized the results obtained with typical etching regents when copper was used as the metal which was etched. The results reported below were obtained in the extension of this investigation to the important industrial alloys of copper, the brasses and bronzes, to nickel, and to the common nickel-rich alloys. Since the present work was a direct continuation of the former study, the general method of investigation was similar to that previously employed. In addition to the reagents of the previous investigation certain others which were found to be particularly suited to some of the new materials were also used. The results obtained with copper suggested strongly the importance of oxidation in the successful etching of metallographic specimens. It was shown that most of the metallographic etching reagents used for etching copper and its alloys are oxidizing in their nature, the efficiency of the reagent depending largely upon this characteristic feature of the solution. Reagents which have at best only a very slight effect upon copper can be made to etch fairly readily either by passing oxygen through the liquid while the specimen is immersed or by adding an oxidizing agent. The character of the etched surface produced—that is, whether of the plain or of the contrast type—depends almost entirely upon the results of the oxidation which aids and accompanies the solution of the metal. In general, the results obtained in the present investigation with the typical copper-rich alloys chosen serve to confirm and to substantiate the conclusions reached in the former study. The alloys containing nickel are usually considerably more resistant to etching reagents than are the alloys of copper. This is particularly true for nickel itself, which is often satisfactorily etched only with extreme difficulty.

II. MATERIALS USED

The alloys which were used to illustrate the action of the different typical etching reagents prepared are listed in Table 1.[2]

[1] Henry S. Rawdon and Marjorie G. Lorentz, Metallographic etching reagents: I. for copper, B. S. Sci. Papers No. 399, 1920.

[2] Most of the rolled copper alloys were furnished for this investigation by W. H. Bassett, technical superintendent American Brass Co., and W. B. Price, chief chemist, Scovill Manufacturing Co., Waterbury, Conn. The nickel and the nickel-rich alloys were furnished by P. D. Merica, director of research, International Nickel Co., and by the Driver-Harris Co. The help thus given is here acknowledged.

Digitized by Google

TABLE 1.—Alloys Used in the Determination of Their Etching Characteristics

Number	Type of alloy	Percentage of principal constituents [a]										Physical state of alloy
		Cu	Zn	Sn	Pb	Al	Ni [b]	Fe [b]	Mn	C	Si	
1	α brass	95	4.9					0.05				Rolled sheet, 18 gage; annealed 1 hour at 500° C
2 [c]	do	94.3	5.6					.08				Rolled sheet, 11 gage; annealed 1½ hours at 650° C
3	do	92.6	6.5	0.8				.05				Rolled sheet, 22 gage; annealed 3 hours at 750° C
4	do	90	9.9					.07				Rolled sheet, 18 gage; annealed 1 hour at 500° C
5	do	84.8	15.1		0.01		0.09					Rolled sheet, 12 gage; annealed 1½ hours at 650° C
6	do	75	24.9					.10				Do.
7 [c]	α brass+lead	73	24.3		2.6			.08				Rolled sheet, 11 gage; annealed 1½ hours at 650° C
8 [c]	α brass	72.3	27.6					.07				Rolled sheet, 18 gage; annealed 1 hour at 500° C
9 [c]	α brass + tin	72	26.8	1.2				.04				Rolled sheet; 18 gage; annealed 3 hours at 750° C
10	α brass	69.2	30.7		.01		.03					Rolled sheet, 8 gage; 1½ hours at 650° C
11	do	67.38	31.7		.7			.15				Rolled sheet, 12 gage; annealed 1½ hours at 650° C
12	do	66.1	33.7		.01			.03				Rolled sheet, 18 gage; annealed 1 hour at 500° C
13 [c]	α β brass	61.7	38.1		.01			.03				Do.
14	do	61.3	37.8	.8	.01		.02					Rolled sheet, 18 gage; annealed 3 hours at 750° C
15	do	61	38.8		.2			.02				Rolled sheet, 18 gage; annealed 1 hour at 500° C (quenched in water)
16 [c]	β brass	53.9	45.67	.3	.08			.02				Cast
17 [c]	β γ brass	44.7	54.24		1.06							Do.
18	γ brass	39.9	60.02		.08							Do.
19	γ ε brass	28.5	70.99	.48	.03							Do.
20	ε brass	16.5	83.41	.04	.05							Do.
21 [c]	ε η brass	4.5	95.5									Do.
22	α bronze	91.3		8.7				.1				Rolled sheet, 18 gage; annealed 1½ hours at 650° C
23 [c]	do	89.3		10.7				.1				Rolled sheet, 16 gage; annealed 1½ hours at 650° C
24 [c]	Zinc bronze	88	2	10								Cast
25 [c]	Aluminum bronze	92				8						Rolled sheet, 20 gage; annealed 1¼ hours at 550° C
26 [c]	do	92				8						Cast
27	do	96.9		.4		2.4		Trace				Do.
28	Electrolytic nickel	.10					99.7	.14	[d]			Electrolytically deposited
29 [c]	Cast nickel	.13					99.3	.25	[d]	0.10	0.05	Cast
30	Nickel	.21					99.2	.39	0.04	.03	.11	Cold drawn, ½ inch in diameter

[a] The authors are indebted to J. A. Scherrer, associate chemist of this Bureau, for the analysis of these alloys, except numbers 24, 51, 52, and 53, the percentage compositions of which are only approximate.

[b] In each case this was reported as being "less than" the figure given.

[c] Representative micrographs of the alloys indicated thus are given in the following sections.

[d] Not detected.

Digitized by Google

TABLE 1—Continued

Number.	Type of alloy	Percentage of principal constituents										Physical state of alloy
		Cu	Zn	Sn	Pb	Al	Ni	Fe	Mn	C	Si	
31	Nickel	0.18					98.7	0.52	0.14	0.4	0.09	Hot rolled, 5/8-inch plate
32 [c]	Monel metal	28.5					66.3	2.49	1.85	.12	.73	Cast
33 [c]	do	29.3					66.6	1.90	1.76	.13	.18	Hot-rolled rod, 3/4 inch in diameter
34 [c]	do	28.7					67	2.00	1.70	.18	.18	Cold-drawn rod, 3/4 inch in diameter
35 [c]	Nickel						99.4	.20		.12	.03	Sheet, 10 gage
36	do	.35					99.1	.40	.05	.03	.08	Sheet, 20 gage
37 [c]	do [e]											Electrolytic, remelted in vacuo and cast
38 [c]	Cupro-nickel	53.7					44.4	.69	.81	.11	.04	Cast
39	do	72.1					27.8	.22	.02			Do.
40	Nickel brass	68.7	14.6				16.4	.26	.02			Rod, 1/4 inch in diameter
41	do	48.9	36.9	0.45	1.5		11	.18	.98			Rod, 1/2 inch in diameter
42	do	54.1	19.5				26	.19	.19			Sheet, 24 gage
43	do	64.6	25				10	.17	.17			Sheet, 18 gage
44 [c]	Cupro-nickel	79.8					19.6	.30	.14			Sheet, 20 gage
45 [c]	Nickel brass	65.5	17.2				17	.30	.02			Sheet, 18 gage
46 [c]	do	65.5	17.2				17	.30	.02			Sheet, 18 gage, annealed 835° C
47	do	65.6	16.30		.90		17	.20	.03			Sheet, 18 gage
48	do	65.6	16.30		.90		17	.2	.03			Sheet, 18 gage, annealed 835° C
49	do	65.80	27.4		1.20		5.30	.16	.02			Sheet, 18 gage
50	do	65.80	27.4		1.20		5.30	.16	.02			Sheet, 18 gage, annealed 835° C
51	Nickel						99.15					Rod, 1/8 inch in diameter
52 [c]	Manganese nickel						97		3			Rod, 1/2 inch in diameter
53	Invar						35					

[c] Representative micrographs of the alloys indicated thus are given in the following sections.

[e] Compare No. 28.

Digitized by Google

A great many of the industrially used brasses and bronzes are of relatively simple microstructure, inasmuch as they consist of only one constituent. For this reason several copper-zinc alloys with zinc content greater than that of industrial brasses were prepared. Several of the zinc-rich brasses are of a duplex structure, and thus illustrate the etching characteristics of alloys containing constituents which differ considerably in their electrochemical properties.

In the study of the nickel alloys only the industrially important α alloys were considered. The group of nickel-chromium alloys, though of very considerable importance from an industrial viewpoint, was not considered in this investigation. It is very probable that their characteristic structural features result from other conditions besides the nickel or chromium content. The various types of etching reagents employed are listed in Table 2.

TABLE 2.—Etching Reagents Used

Number	Reagent	Nature of etching solution
1	10 volumes concentrated ammonium hydroxide and 1 volume hydrogen peroxide (3 per cent solution)	Ammoniacal oxidizing solution
2	2 volumes concentrated ammonium hydroxide and 3 volumes potassium permanganate solution (4 g per 1000 cm ^{3} water)	Do.
3	1 volume sulphuric acid (sp. gr. 1.84) and 10 volumes hydrogen peroxide (3 per cent solution)	Acid oxidizing solution
4	1 volume sulphuric acid (sp. gr. 1.84) and 5 volumes saturated solution of potassium dichromate	Do.
5	1 volume sulphuric acid (sp. gr. 1.84) and 5 volumes potassium permanganate solution (4 g per 1000 cm ^{3} water)	Do.
6	10 per cent aqueous solution of ammonium persulphate	Do.
7	Concentrated nitric acid	Oxidizing acid
8	Saturated solution chromic acid	Do.
9	10 g ferric chloride, 30 cm ^{3} hydrochloric acid (sp. gr. 1.19), 120 cm ^{3} water	Acid oxidizing solution
10	Same as 9, in 120 cm ^{3} alcohol	Do.
11	5 g copper—ammonium chloride, 120 cm ^{3} water, concentrated ammonium hydroxide added until precipitate which forms redissolves	Electrochemical action
12	Same as 11 in alcoholic solution	Do.
13	Saturated aqueous solution of bromine	Oxidizing solution
14	2 per cent aqueous solution of silver nitrate	Electrochemical action
15	Concentrated hydrochloric acid	Nonoxidizing acid
16	Nitric acid + acetic acid; 50 per cent nitric acid, 25 per cent glacial acetic acid, 25 per cent water	Oxidizing acid
17	Concentrated ammonium hydroxide and oxygen	Oxidation and an ammoniacal solvent
18	10 per cent sulphuric acid and oxygen	Oxidation and an acid solvent
19	Ammonium chloride and oxygen	Neutral salt solution and oxidation

III. RESULTS

One of the limitations in an investigation like the present one, in which the records are obtained almost entirely by means of micrographs, is the difficulty of concisely summarizing these results. The reproduction of all of the micrographs illustrating the results obtained for the different alloys with each of the etch-

Digitized by Google

ing methods used is out of the question. For this reason there is given in Table 3 a resumé of the general action of the different etching reagents upon the various alloys used. The following symbols have been employed for the purpose: e, excellent; g, good; f, fair; p, poor; n, no action. This forms the first letter of the key. The general nature of the etching action—that is, whether results of the contrast or of the plain type were obtained—has been indicated by c or p as the second letter of the key. The numerals show the approximate etching period required, in seconds, unless indicated otherwise. Although in the majority of cases the etching period was determined quite accurately, the figures given should be regarded as approximate only for the material in general. In some cases, particularly for nickel, the etching period was found to vary in a manner which could not be accounted for easily. After a specimen had been etched once satisfactorily, the etching period for subsequent etching was usually considerably less than at first. Further details concerning the various reagents and their action upon different alloys are given in some of the following sections.

Since the greater number by far of examinations of microstructure carried out are made at magnifications in the neighborhood of 100 diameters, this value was selected as standard for the examinations to be made in this investigation. Examinations at high magnifications are usually made for a very special purpose, and the specimen must be etched accordingly. The conclusions and opinions expressed in the following sections do not necessarily hold in all cases for examinations at high magnifications.

Digitized by Google

TABLE 3.—Etching Characteristics of Alloys Examined

Key. First letter: e, excellent; g, good; f, fair; p, poor; n, no action; x, reagent not used. Second letter: c, contrast etch pattern; p, plain etch pattern. Numerals indicate average etching period in seconds, except * minutes and ** hours

Number	Type	Reagent number [a]															
		1	2	3	4	5	6	7	8	9	10	11	12	13	14	15	16
1	α brass	gc 30	pc 2½*	pc 10	fc 20	fc 2*	fc 3*	pc	pp 1*	gc 30	pc 30	fc 30	n 2*	fp 20	pp	pc 30*	x
2[b]	do	gp 15	fc 2½*	gc 30	fc	fc 2*	gc 30	ec 5	gp 15	gc 20	ec 25	gc	fc 10*	n 20	gp	pc 30*	x
3[b]	do	ec 15	pp 2½*	pc 30	pc 10	gp 25	gc 25	gp 5	fp 15	fc 25	pc 1*	fc 25	pc 25	gc 10	fp	fc 30*	x
4	do	gc 30	pc 2½*	pc 1*	gc 10	fc 1½*	gp 2½*	fp 5	ep 10	fc 45	pc 1*	pc 30	fc 1*	pc 10	ep	x	x
5[b]	do	gc 15	pc 2½*	fc 30	n 20	fc 2*	fc 30	ec 5	gp 15	fc 20	gc 25	gc 20	pc 10*	n	gp	pc 30*	x
6	do	fc 20	pc 12*	fc 1½*	pc 45	fc 30	fc 2*	pc 4	gp 10	ec 40	ec 1½*	gc 45	ec 5*	pp 30	pp	pc 30*	x
7	do	ec 20	pc 1½*	ec 45	fc 10	gc 2½*	ec	fc 4	fp 20	gc 30	gc 1*	ec 40	fc 5*	pc 20	n	pc 30*	x
8	do	gc 20	pc 1*	fp 20	gc 15	pc 30	gc 20	gp 25	gp 10	fc 20	fc 30	gc 10	fc 20	pc 20	gp	pc 30*	x
9[b]	do	fc 30	pc 4*	fc 2x	gc 25	gp 1½*	gp 1½*	gc 5	gp 30	fc 1*	fc 1*	gc 1*	fc 3*	pc 30	gp	pc 30*	x
10	do	gc 30	pp 45	gp 45	fc 1½*	g 1½*	gc 5*	gc 3	ep 20	gc 30	ec 1*	gc 30	gc 5*	pp 20	ep	pc 30*	x
11	do	gc 20	pc 2½*	gc 2½*	pc 30	pc 2*	gc 2½*	gc 4	gp 10	fp 40	fc 1½*	gc 1*	pc 4*	gp 30	pp	pc 30*	x
12	do	fc 15	fc 1*	gc 30	pc 15	pc 30	fc 2*	gc 5	gp 10	gc 15	gc 30	fc 30	pc 45	pc 20	gp	pc 30*	x
13[b]	α β brass	fc 15	fc 1*	gc 30	fc 15	gc 30	gc 30	gc 3	fp 10	pc 20	gc 20	pc 20	pc 30	gc 15	pp	x	x
14[b]	do	pc 45	pc 1½*	gc 45	pp 1½*	gc 1½*	gp 4*	fp 4	gp 20	fp 30	fc 1*	gc 30	pc 5*	pc 20	gp	fc 30*	x
15[b]	do	gc 10	gc 1*	gc 30	gc 15	gc 20	gc 30	gc 3	gp 5	gc 5	fc 10	gc 20	pc 30	fc 15	gc	x	x
16[b]	β brass	gc 15	gc 1½*	pc 30	x	gc 30	pp 40	x	gp 20	x	x	gc 20	x	x	fp	x	x
17	β γ brass	gc 15	fc 5*	fc	pc 20	gc 3½*	fc 2½*	ep	gc 10	fc 15	gc 20	fc 15	fc 20	pc 2	ec	x	x
18	γ brass	pp 5	pp 5*	pc	pp 30	fc 3*	pp 2*	ec 3	gp 7	fc 15	gc 15	fc 15	gc 20	gc 3	gp	x	x
19	γ ε brass	gc 15	gc 2*	ec 20	ec 10	gc 20	ec 20	fc	gc 3	ec 15	pp 5	pc 25	ec 60	pc 2	fc	x	x
20	ε brass	gc 5	n 2*	pc 3	fc 5	pc 3	fp 10	pc 3	gc 5	pp 10	pc 15	n 20	n 10	fp 10	n	x	x
21	ε η brass	gc 30	pc 3*	ec 3	fc 5	gc 5	gc 15	pc 3	gc 10	gc 10	ec 15	pc 20	pc 10	gc 10	pc	x	x
22[b]	Bronze	gp 15	pc 3*	pc 1*	ep 20*	gp 2	fc 3*	fc 4	gp 15	ec 15	ec 15	pp 4*	gp 5*	x	x	fc 2**	x
23[b]	do	gp 30	pc 3*	fp 1*	gc 2*	gc 2*	fp 3*	fc 4	gp 40	ec 15	ec 15	pp 6½*	gp 10*	x	x	ec 30	x
24[b]	Cast bronze	fc 20	fc 1½*	fp 45	fc 25	fp 25	fc 30	fc 3	fc 20	fc 20	fc 45	pc 30*	pc 1½*	x	pc	ec 30	x
25[b]	Al bronze	fp 15	pc 2½*	fp 40	fc 20	fc 20	gp 40	fp 4	pp 20	fc 20	pp 30	fp 20	n 30	x	n	x	x
26[b]	Cast al bronze, 8 per cent	ec 20	pc 6½*	ec 45	gc 30	fp 2½*	fp 45	fp 5	pp 20	ec 30	pc 45	fc 30	pc 45	pp	n	gc 15*	x
27[b]	Cast al bronze, 3 per cent	gc 20	pc 2½*	fc 50	gc 30	fc 2½*	gc 45	ec 5	pc 20	pc 20	fp 30	pp 30	fc 45	fp 20	fp	x	x
28	Electrolytic nickel	n	n	ec 4*	n	pp 8*	n	gc 5	n	n	pc ½*	n	n	n	n	n	ec 15
29	Cast nickel	n	n	gc 30	n	gp 1*	pp 15*	ep 15	n	fc 1*	pc 4*	n	n	n	n	ec 1**	ep 45
30	Drawn nickel	n	n	pp 30	pp 50	n	fc 5*	gc 15	n	gc 2*	pp 6*	n	n	n	n	ec 1**	gp 15

[a] See Table 2.

[b] The etching period for these alloys was estimated; for all others it was accurately timed.

88775°—22——2

Digitized by Google

TABLE 3—Continued

Alloy		Reagent number															
Number	Type	1	2	3	4	5	6	7	8	9	10	11	12	13	14	15	16
31	Rolled nickel	n	n	pp 40	pp 50	n	fp 8*	fp 30	n	fc 1½*	pp 6*	n	n	n	n	ec 1**	gp 15
32	Cast monel metal	n	n	fc 2*	n	gc 5*	gc 1½**	fp 5	n	gc 3*	gc 3*	n	n	fc 1*	fc	ec 1**	gp 15
33	Rolled monel	n	n	gc 1½*	pp 25*	pc 28*	fp 25*	fp 3	n	ec 2½*	fc 4*	n	n	n	n	ec 1**	ep 15
34	Drawn monel	n	n	ec 1½*	pp 25*	fc 28*	fp 25*	ep 3	n	gc 15*	fc 4*	n	n	n	n	ec 1**	ep 15
35	Nickel sheet	n	n	pc 1*	pp 10*	n	fc 20*	fp 20*	n	gc 15*	pc 20*	n	n	n	n	ec 1**	gp 2*
36	do	n	n	fc 1*	fp 8*	n	n		fc 20	n	gc 4*	fc 6*	n	n	n	gp 1**	gp 2½*
37	Electrolytic nickel, remelted and cast.	n	n	gp	n	n	pp	gp	n	pp 3*	n		n	n	n	pp 2**	ep
38	Cast cupro-nickel	n	n	gp 1*	pp 20	fp 1*	pp 10*	fp 3	fp 3*	gp 20	fp 45	n	n	gp 3	n	ec 1**	gp 3
39	do	fp	fc	pp	pp	fp	gp	gp	fc	gc	fp	fp	fc	pc	gc	fp 15*	gc 5
40	Nickel brass	pc 1½*	n	gp 1*	pp 20	fp 20	fp 8*	gp 3	gp 30	gc 10	fc	fc 1½*	pc 2*	pc 3	pp	fc 30*	fp 40
41	do	gp 10	pc 2*	gp 15	pc 8	gp 20	fp 1*	fp 2	fp 10	gp 5	fp 20	gp 15	pp 25	pp 5	gp	pc 20*	pp 5
42	do	n	pp 9*	ep 5*	gp 2*	pp 2½*	ec 9*	pc 15	ep 1*	fc 15	ec 45	pp 5*	n 3*	pp 45	pp	fc 30*	gc 15
43	do	ec 5	pc 2*	gp 1*	pp 45	fc 3½*	fc 5*	ep 5	fp 15	pc 2*	fc 7*	pp 1*	pp 4*	pp 45	gp	gc 20*	ep 15
44	Cupro-nickel	fp 10*	pc 2*	fp 1½*	pp 30	pp 3*	fp 4*	pp 3	pp 1½*	fp 2*	fc 45	pp 45	n	pc 10	n 4*	fc 20*	gc 15
45	Nickel brass	pp 10*	pc	ep 1*	pp 40	gp 1*	ep 5*	pp 10	pp 1*	gc 45	ec 45	pp 2*	pc 1*	pp 10	pp	pc 15*	pp 40
46	do	gc 6*	pc 1½*	gp 1½*	pp	gc 3*	fp 4*	pp 3	pp 45	gc 25	ec 45	fp 2*	n	n 15	n	fc 30*	ep 20
47	do	pp 30	n	fp 40	pp 45	fp 2*	fp 3*	pp 15	pp 1*	pp 30	pp 45	pp 2*	n 2*	n 15	pp 5*	n 15*	pp 25
48	do	pc 12*	pc 2½*	gp 1*	fp 45	gp 1½*	gp 5*	fp 10	fp 1*	gc 30	gc 1*	fp 1½*	n 5*	n 15	fp 5*	pc 30*	ep 45
49	do	pc 10	pc 2*	pp 2½*	pp 1*	n 2*	pp 2*	fp 10	pp 30	pc 30	pp 45	fc 30	pp 10*	n 30	pp 3*	pc	pp 30
50	do	ec 10	fc 2½*	fp 1½*	pc 1*	pp 1*	gc 3*	gc 10	ep 1*	ec 30	gc 1*	gc 1*	pc 10*	pp 30	pp 3½*	pc 15*	gc 30
51	Nickel	n	n	fp 30	n	n	p 5*	fp 5	n	fc 5*	gc 5*	n	n	n	n	gc 1**	fp 15
52	Manganese nickel	n	n	fc 20	n	n	n 4½*	gp 10	n	n 5*	gp 12*	n	n	n	n	ec 1**	gp 30
53	Invar	n	n	fp 10	pp 30	n	fp 3½*	fp 15	n	fc 7*	gp 20	n	n	n	n	x	x

Digitized by Google

IV. NATURE OF CONTRAST ETCHING

The terms "contrast" and "plain" etching are used to designate the character of the results obtained with different reagents upon any type of alloy and particularly those consisting of only one constituent, such as the metals, the α brasses and bronzes, β brass, γ brass, etc. Microscopic examination of such materials after plain etching usually reveals only the grain boundaries as a network of black lines, together with such extraneous features as inclosures. The grains show no "individuality" other than that of size and shape. However, in the same material after contrast etching, each grain has an individuality of its own which is the result in a large measure of its relative brightness as compared to the neighboring grains.

Such contrast may be developed in at least two very different ways. If the polished surface of the specimen is etched sufficiently, a differential roughening of the various grains will result as the crystalline facets are revealed within the boundaries of the different grains. Since the orientation of all the facets within any particular grain is the same, it follows that the light incident upon such an etched section of a crystal will be reflected in a definite manner. The direction of the reflected beam varies for different grains and depends upon the orientation of the crystalline facets. Thus, a crystal will appear dark or light according to the position of the eye of the observer with respect to the beam reflected by this crystal.

Fig. 1 shows the appearance of a very deeply etched brass. The contour of the etched surface was revealed by using sections perpendicular to the etched surface, precautions being first taken to protect it by means of a coating of electrolytically deposited copper. The micrographs plainly show the regularity in the roughening of the section of a crystal and also that it conforms to the crystalline orientation of the grain as revealed by the etching pits. This means of producing contrast in etching is well understood and has been frequently described. The second method, which is given below, is not so well known.

It is often desirable in the study of the microstructure of metals to produce contrast without much roughening of the surface. This may be accomplished by the use of reagents which cause the formation of a very thin film on the surface, the thickness of which varies from grain to grain. This effect has deen described in considerable detail for copper [3] and is usually attributed to

[3] See footnote 1

Digitized by Google

oxidation films. The part that such films play in contrast etching may be demonstrated rather strikingly, as is shown in Figs. 2, 3, and 4, by a double etching process.

Hydrogen sulphide was used as a convenient means for producing a thin film on the specimen, and an aqueous solution of silver nitrate was used as the reagent for etching, which of itself produces little, if any, contrast (Fig. 2*a*). When the slightly warmed polished brass specimen (No. 11, Table 1) was suspended in a bottle of hydrogen sulphide gas, to which a drop of concentrated hydrochloric acid had been added to accelerate the attack, a film having the appearance shown in Fig. 2*b* was produced. No evidence of crystalline structure was revealed. On

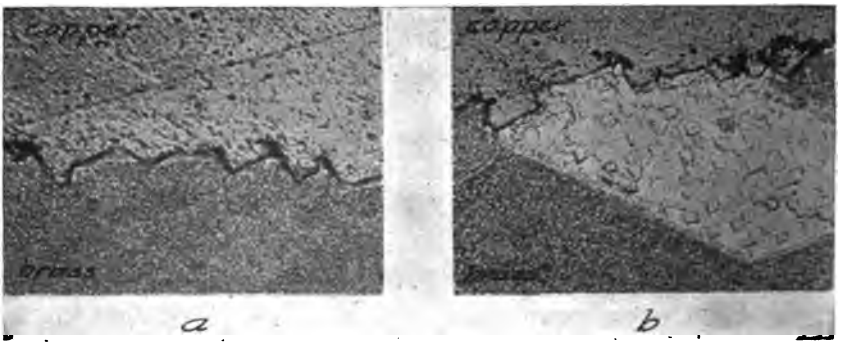

FIG. 1.—*Roughening of the surface of crystals of brass as a result of prolonged etchings of a polished surface.* × 500

A polished section of an α brass (alloy 10, Table 1) was etched 12 hours in 50 per cent copper ammonium chloride and a section perpendicular to the etched face was then examined after etching with copper ammonium chloride. Note the similarity in orientation of the notches in the etched surface of (*a*), which represents a portion entirely within a single crystal. Note in (*b*) how the orientation of the notches of the etched surface is the same as that of the etching pits within the crystal.

the other hand, when a specimen etched by the means of silver-nitrate solution was suspended in the hydrogen sulphide the sulphide film formed on certain crystals with greater readiness

EXPLANATION OF FIG. 2, PAGE 645

(*a*) α brass (alloy 11, Table 1) etched with 10 per cent solution of silver nitrate. Note the absence of contrast.

(*b*) Same specimen as (*a*), which after polishing was suspended in an atmosphere of hydrogen sulphide for 1 minute. Note the surface film of sulphide. The black spots mark the location of the inclusions of lead in the alloy.

(*c*) The specimen (alloy 11) after being etched as in (*a*) was placed in hydrogen sulphide as in (*b*). The contrast of the etch pattern produced was much less pronounced than in (*d*).

(*d*) The specimen (alloy 11) after being filmed by means of hydrogen sulphide as in (*b*) was etched with silver nitrate solution as in (*a*). Note the brilliant contrast which resulted.

(*e*) α β brass (alloy 14, Table 1) etched with 10 per cent silver nitrate solution.

(*f*) Same specimen as (*e*) which after polishing was placed in an atmosphere of hydrogen sulphide.

(*g*) Same specimen as (*e*), etched with silver nitrate solution and then filmed with sulphide as in (*f*).

(*h*) Same specimen as (*e*), filmed with hydrogen sulphide as in (*f*), then etched with silver nitrate as in (*e*). Note the definite contrasted etch pattern.

Digitized by Google

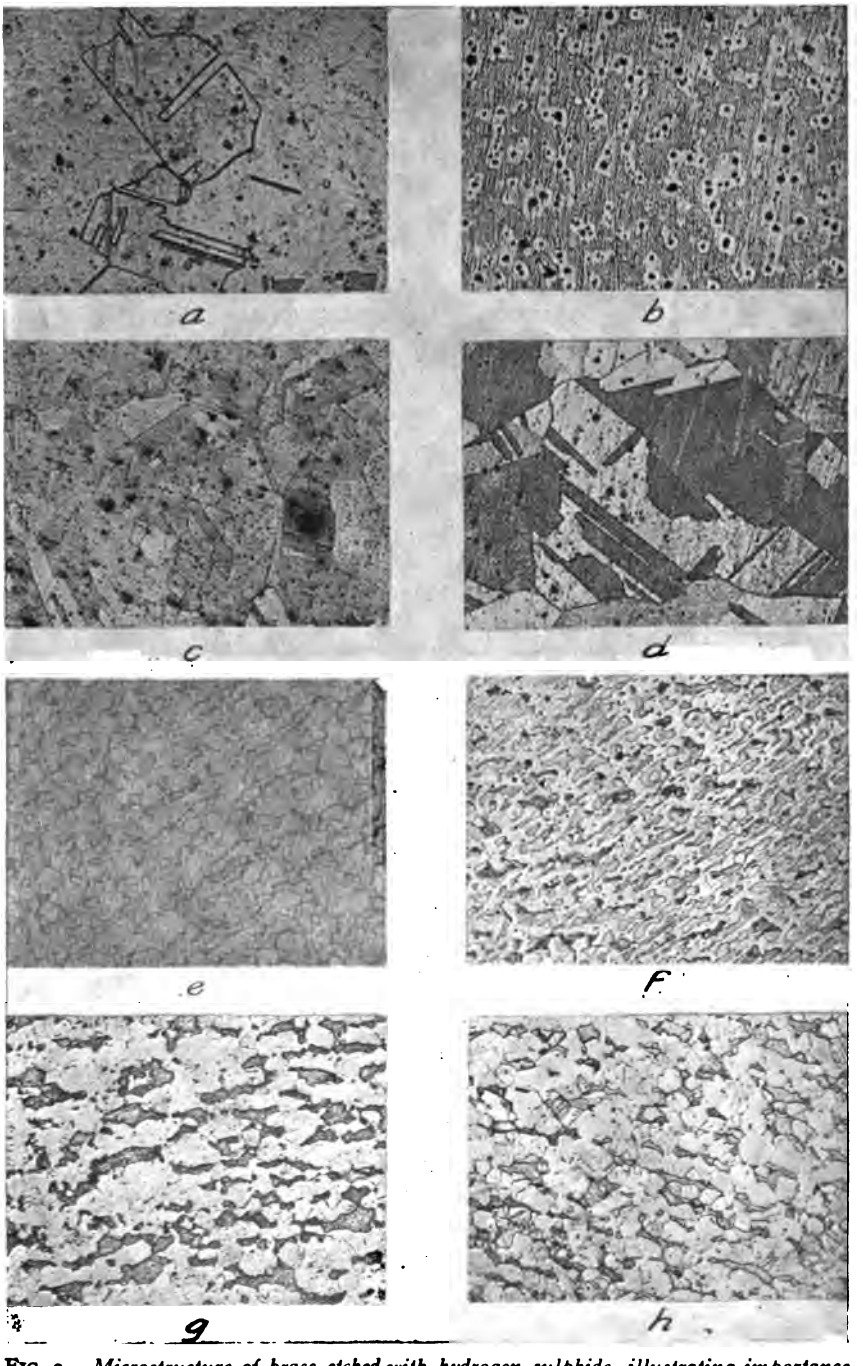

FIG. 2.—*Microstructure of brass etched with hydrogen sulphide, illustrating importance of a surface film in producing contrast between crystals of etched surface.* × 100

[For further explanation of Fig. 2, see p. 644]

Digitized by Google

than on others, so that a slightly contrasted etch pattern resulted. However, by far the best results were obtained by first producing a uniform sulphide film on the surface of the polished specimen and then etching the filmed sample in the silver-nitrate solution (Fig. 2*d*). Such a procedure gave excellent results with all the α and the $\alpha\beta$ brasses. With cast zinc bronze the best results were obtained by producing the sulphide film upon the etched surface rather than etching the previously filmed surface (Fig. 3).

The fact that the results given above are of rather general application and do not depend upon any peculiar properties of the sulphide film was demonstrated by using oxide films instead of sulphide. The specimens were gently heated in the air until a uniform thin coating of oxide had formed and were then etched with silver-nitrate solution. Fig. 4 shows the results obtained with some of the specimens. For demonstration purposes, one is somewhat restricted in the choice of reagents, since it is necessary that the solution used be one that produces a "plain" etch pattern. For practical use, of course, this limitation does not hold.

V. ETCHING CHARACTERISTICS OF COPPER ALLOYS

1. BRASS

(*a*) α BRASS.—There is nothing strikingly different in the etching characteristics of the α brasses from those of copper. Figs. 5 and 6 show the general effect of the different reagents upon two of the alloys used. The results shown are quite representative of the behavior of the other α brasses of a different copper-zinc ratio toward the same reagents. The data summarized in Table 3 show this in a general way. Although some differences were observed in the etching period for α brasses differing in their zinc content, they were not pronounced and systematic enough to permit any generalization being made. From the results obtained it appears that the addition of tin to an α brass in amounts of approximately 1 per cent renders the etching of the specimen more difficult than that of a similar brass containing no tin. Not only was the etching period lengthened, but the general appearance of the etched surface was not nearly so satisfactory as that of a similar alloy containing no tin. Fig. 7 illustrates this. The presence of particles of lead in an α brass did not seriously affect its etching characteristics, although with a very few reagents, as shown in Fig. 8 and Fig. 2*b*, an unetched

Digitized by Google

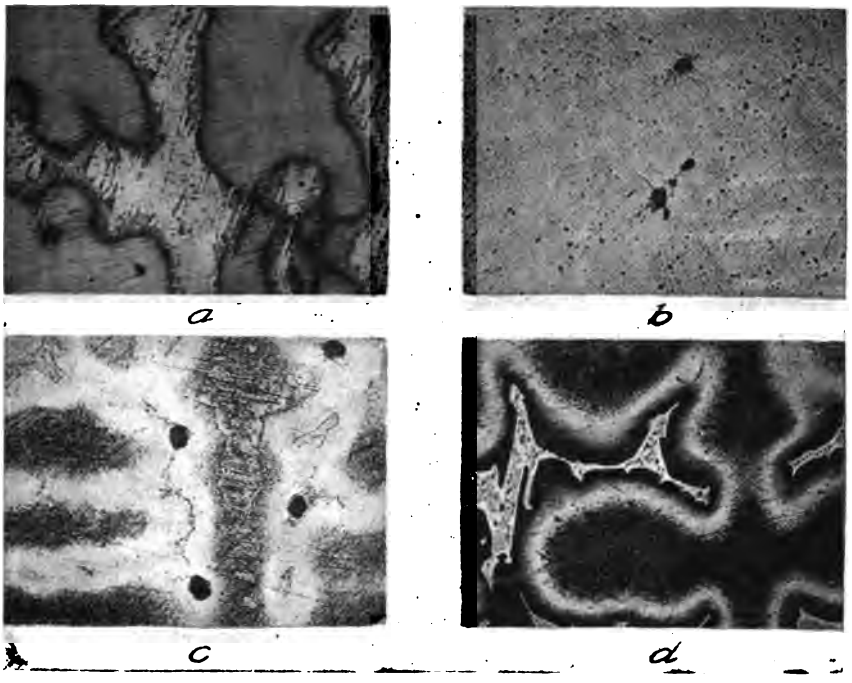

FIG. 3.—*Microstructure of cast bronze illustrating the importance of surface films in producing contrast upon etching.* × 100

(*a*) Cast zinc bronze (alloy 24, Table 1) etched with 10 per cent solution of silver nitrate. Note the adhering silver covering the eutectoid constituent.

(*b*) Specimen (*a*) which, after polishing, was placed in an atmosphere of hydrogen sulphide for 1 minute.

(*c*) Specimen (*a*) filmed by hydrogen sulphide as in (*b*), then etched with silver nitrate as in (*a*).

(*d*) Specimen (*a*) etched with silver nitrate and then exposed in hydrogen sulphide as in (*b*). Note the brilliant contrast produced. The adhering silver covering the eutectoid—see (*a*)—protects this constituent from the action of the sulphide and thus increase the contrast.

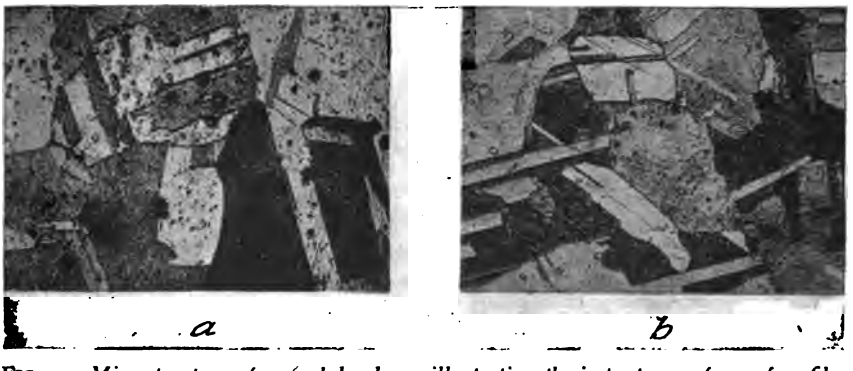

FIG. 4.—*Microstructure of annealed α brass illustrating the importance of a surface film produced by oxidation in producing contrast.* × 100

The polished specimens were heated for 10 minutes on a hot plate in the air, so as to produce a uniform oxide film. The oxidized specimens were then etched with 10 per cent silver nitrate solution.

(*a*) Alloy 11, Table 1. See Fig. 2 (*a*).

(*b*) Alloy 6, Table 1.

Digitized by Google

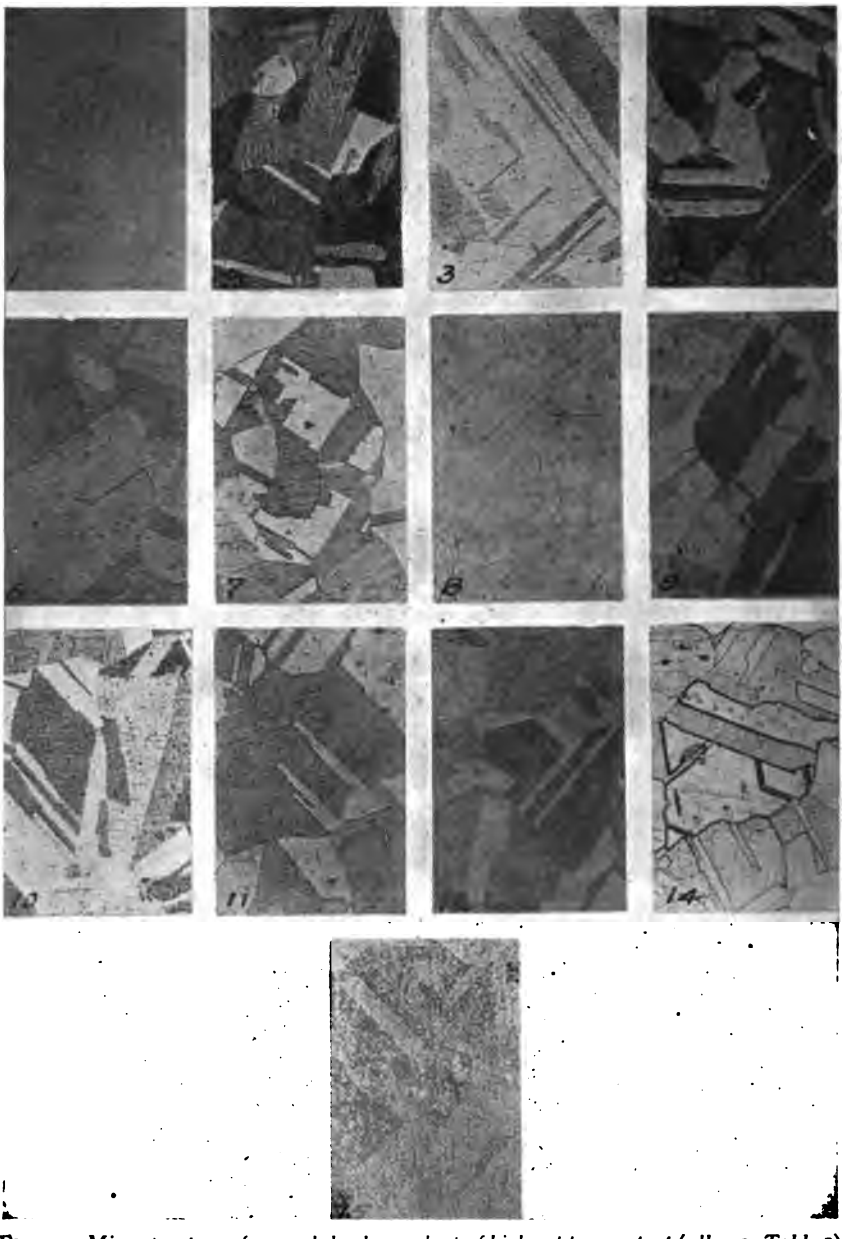

FIG. 5.—*Microstructure of annealed α brass sheet of high copper content (alloy 2, Table 1) illustrating the etching characteristics of the material.* × 100

The numbers indicate the etching reagent used. See Table 2.

Digitized by Google

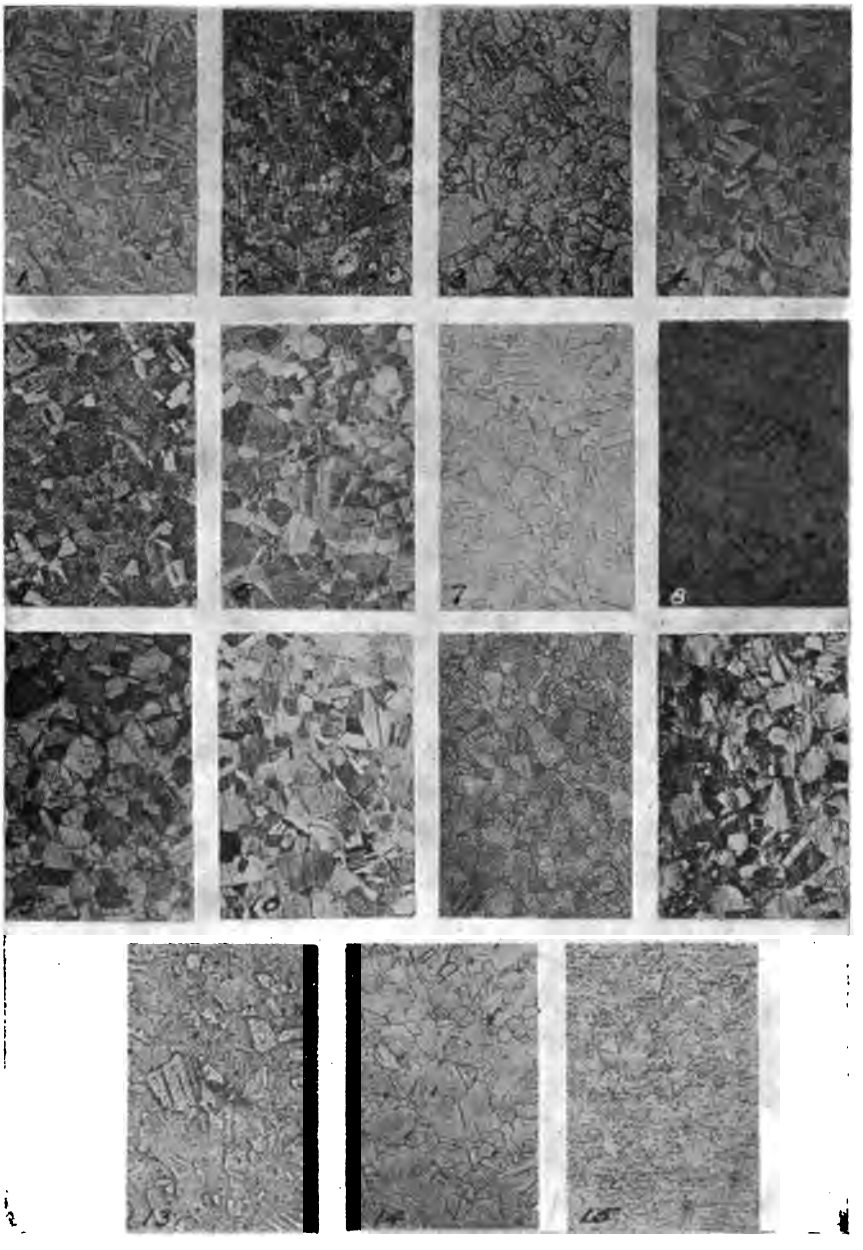

FIG. 6.—*Microstructure of annealed α brass sheet of low copper content (alloy 8, Table 1) illustrating the etching characteristics of the material.* × 100

The numbers indicate the etching reagent used, see Table 2. Compare with Figs. 7 and 8.

Digitized by Google

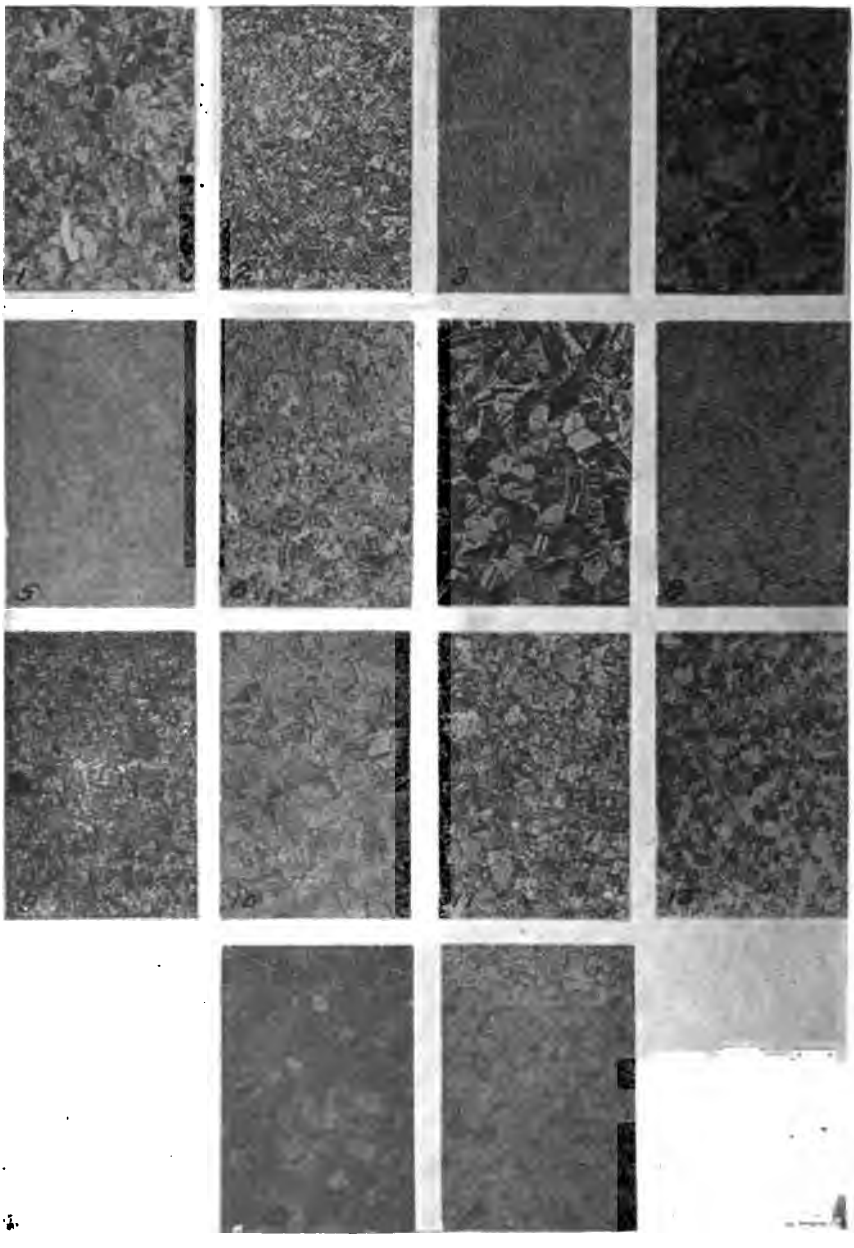

FIG. 7.—*Microstructure of annealed α brass sheet of low copper content containing tin (alloy 9, Table 1) illustrating the etching characteristics of the alloy.* × 100

The number on each micrograph indicates the etching reagent used (Table 2). Compare with Figs. 6 and 8.

Digitized by Google

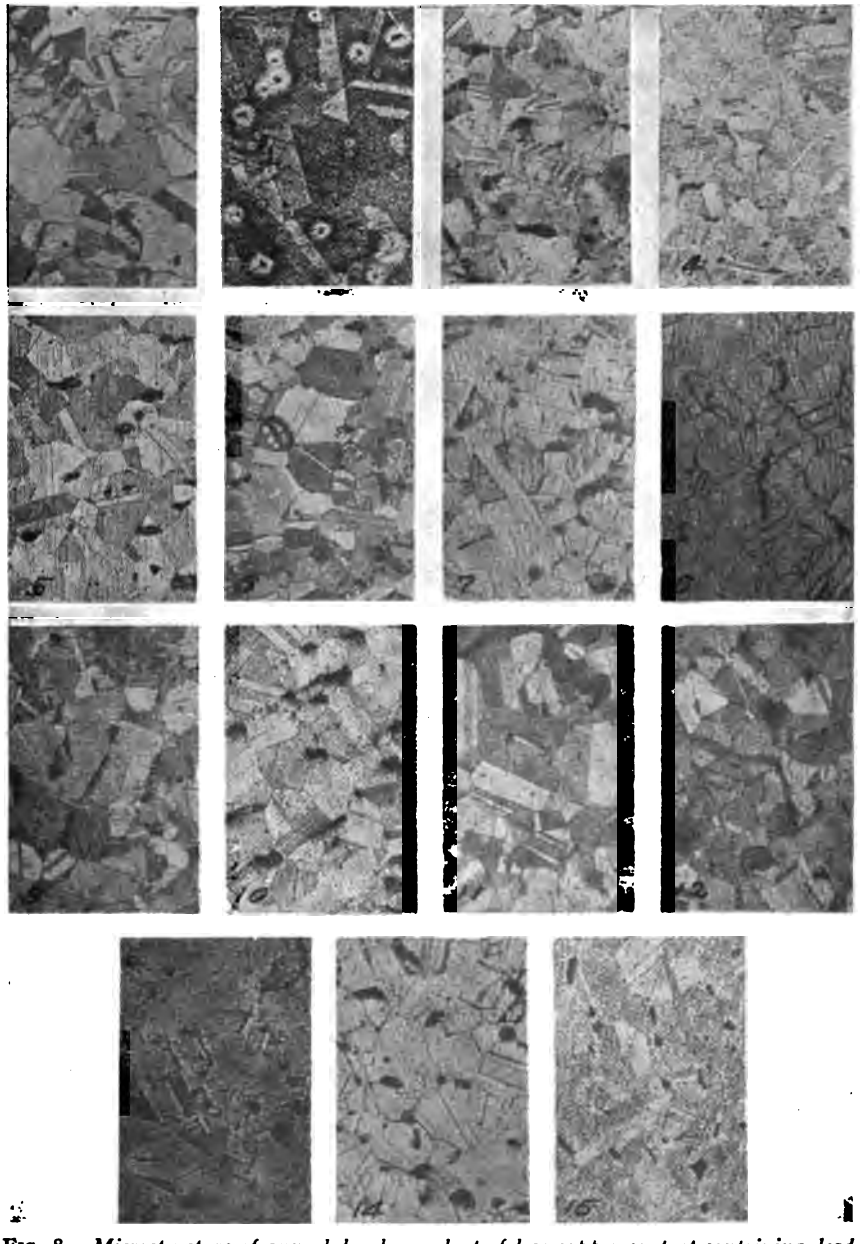

FIG. 8.—*Microstructure of annealed α brass sheet of low copper content containing lead (alloy 7, Table 1) illustrating the etching characteristics of the alloy.* × *100*

The number on each micrograph indicates the etching reagent used (Table 2). Compare with Figs. 6 and 7.

Digitized by Google

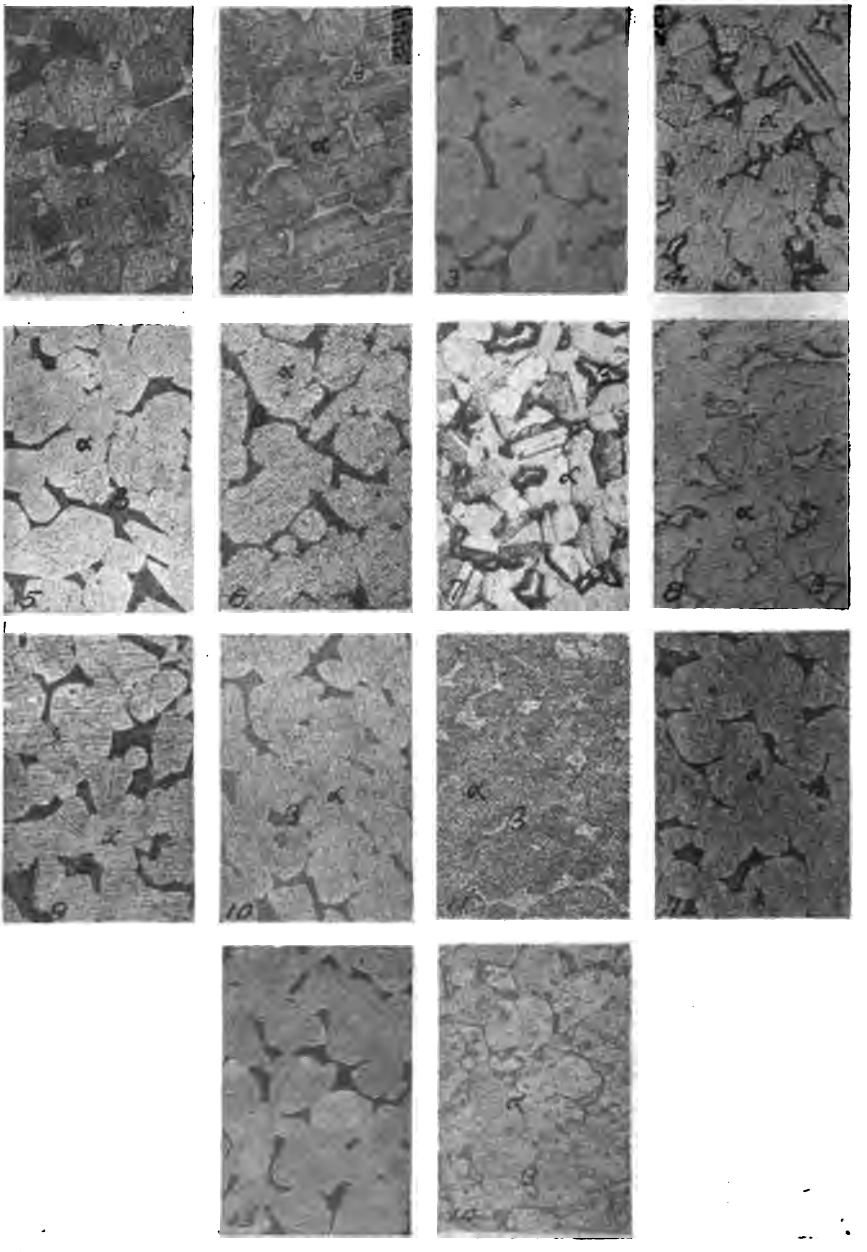

FIG. 9.—*Microstructure of annealed α β brass sheet (alloy 13, Table 1) illustrating the etching characteristics of this alloy.* × 100.

The number on each micrograph indicates the etching reagent used (Table 2).

Digitized by Google

"halo" surrounded each isolated globule of lead. However, this effect was not pronounced or general enough to be considered of much significance.

(*b*) $\alpha\ \beta$ BRASS.—The introduction of a second metallographic constituent modifies very considerably the etching properties of brass. Fig. 9 shows the microscopic appearance of an $\alpha\ \beta$ brass (specimen 13, Table 1) after being etched with the various types of reagents. The results shown may be considered as typical for brasses of this type. The relative amounts of the two constituents vary in different alloys according to the copper-zinc ratio and the form and arrangement of the two constituents according to the treatment of the alloy.

As will be noted in Fig. 9, the relative intensity of the attack of the two constituents varied with different solutions. By reagents which have a strong solvent action, such as nitric acid or sulphuric acid containing potassium dichromate, the β constituent was found to be readily attacked, so that, on account of the difference in level which resulted, this constituent appeared dark and the α matrix, in which the grain boundaries had been developed, light. Other reagents which were of a milder nature were found to color the β grains so that they appeared dark in the light structureless α matrix. With a few reagents for the same specimen this effect was reversed so that the β constituent appeared as uncolored areas in a slightly darkened background of the α matrix. In other cases each of the constituents remained uncolored and only the grain boundaries were revealed. Of course in such a case the two could be readily distinguished from each other upon visual examination by their difference in color. A further complication was sometimes noted in the case of alloys in which the α constituent was in considerable excess. The grains constituting the α matrix were found to etch in the manner previously described, so that considerable contrast between the different α grains resulted. This rendered the β constituent relatively inconspicuous, particularly so in the micrograph.

The fact that the difference in the behavior of the β constituent is not entirely dependent upon the nature of the etching reagent employed is illustrated by the results shown in Fig. 10. The alloy used was of the following composition: Copper, 60.06 per cent; tin, 0.58 per cent, nickel, manganese, and phosphorus, not detected; zinc, by difference, 39.26 per cent, and had been rolled into a "round" of 3½ inches diameter. In numerous streaks in

Digitized by Google

the central portion the β constituent was etched dark, while in adjacent portions this constituent appeared light-colored. Apparently these streaks corresponded to the large crystals of the ingot and had suffered no change other than that of shape by the rolling of the material. The difference in the etching properties of the β constituent were shown best by such reagents as ammonium copper chloride, ferric chloride, sulphuric acid containing an oxidizer such as potassium dichromate or potassium permanganate. With some other reagents, for example, silver nitrate and chromic acid, the β constituent was etched uniformly

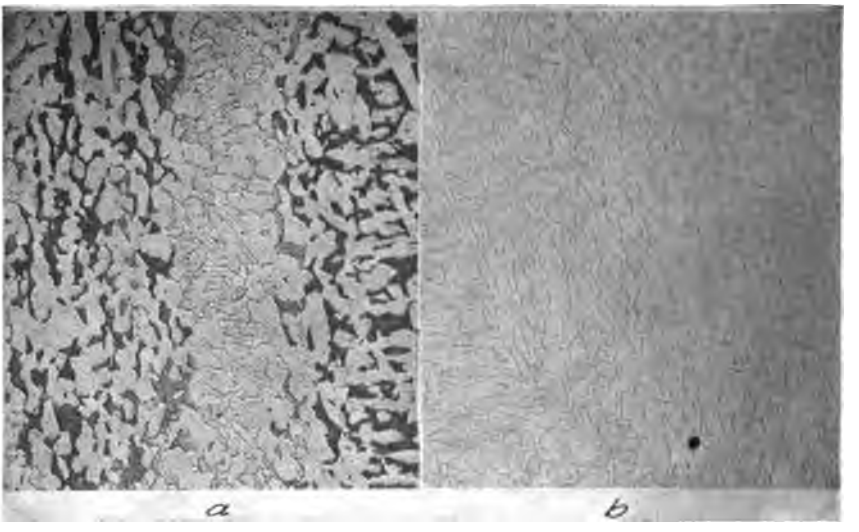

FIG. 10.—*Microstructure of α β brass etched with different reagnets illustrating the anomalous behavior of the β constituent.* × 100

(*a*) Etching reagent, copper ammonium chloride solution (No. 11, Table 2). Note the darkened appearance of the β constituent in certain streaks; in other portions this constituent remained uncolored. This difference in etching properties was characteristic and persisted after the specimen was annealed.

(*b*) Same specimen as (*a*); etching reagent, chromic acid solution (No. 8, Table 2). Note uniform appearance of the two constituents across the entire surface.

in all of the crystals. This difference in the etching properties of the β constituent was found to persist after the material had been annealed. Heating the specimen for four hours at approximately 450° C did not materially affect the etching properties of the alloy. It may be concluded, then, that the anomalous behavior of the β constituent in different crystals can not be attributed to internal stresses which might exist within the wrought material. There is some evidence, however, which suggests that the direction in which the crystal was sectioned has a bearing upon the relative etching properties of the two constituents

Digitized by Google

(*c*) HIGH ZINC ALLOYS.—Of the copper-zinc alloys of relatively high zinc content only the β alloy is of any considerable industrial importance. However, in order to demonstrate their relative etching characteristics, alloys representative of each of the different structural types were prepared and examined. In etching β brass the same question arises, as to a plain or a contrast effect as with the α alloys. Fig. 11 shows the results obtained with this alloy when etched with several different types or reageants.

Figs. 12 and 13 are given to illustrate the characteristics of two of the high zinc alloys of duplex structure, the $\beta\gamma$ and $\epsilon\ \eta$, the latter

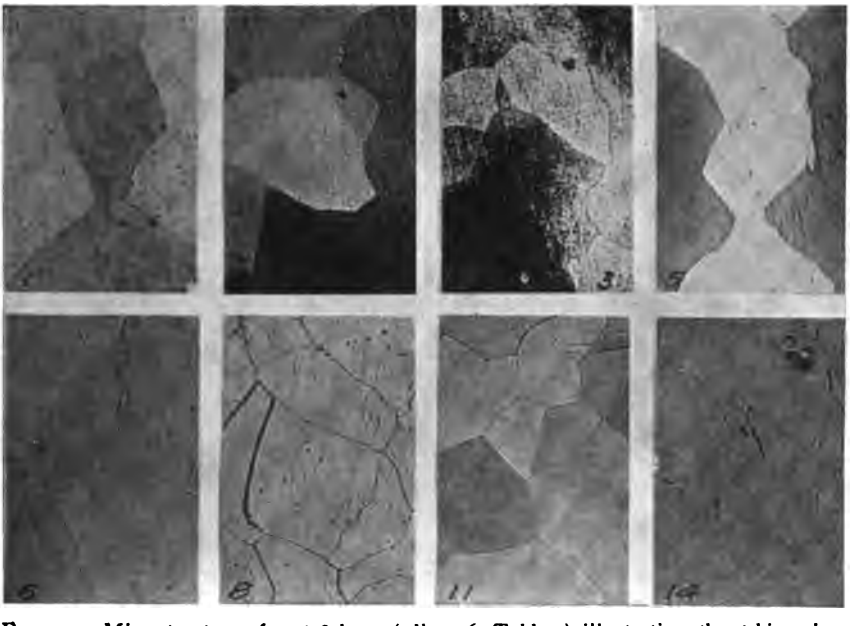

FIG. 11.—*Microstructure of cast β brass (alloy 16, Table 1) illustrating the etching characteristics of the alloy.* × 100

The number on each micrograph indicates the etching reagent used (Table 2).

one being one of very high zinc content. It will be noted that, although as a rule the zinc-rich constituent was the one which was darkened, with several reagents a reversal in the etching effect of the two constituents occurred. As might be expected, the alloys of high zinc content resemble zinc in their properties more than copper and were readily etched by some reagents—for example, ammonium chloride—which had no effect upon the alloys of high copper content. The use of oxygen or strong oxidizers in the etching reagents was not so necessary for the high zinc alloys as for those of high copper content.

Digitized by Google

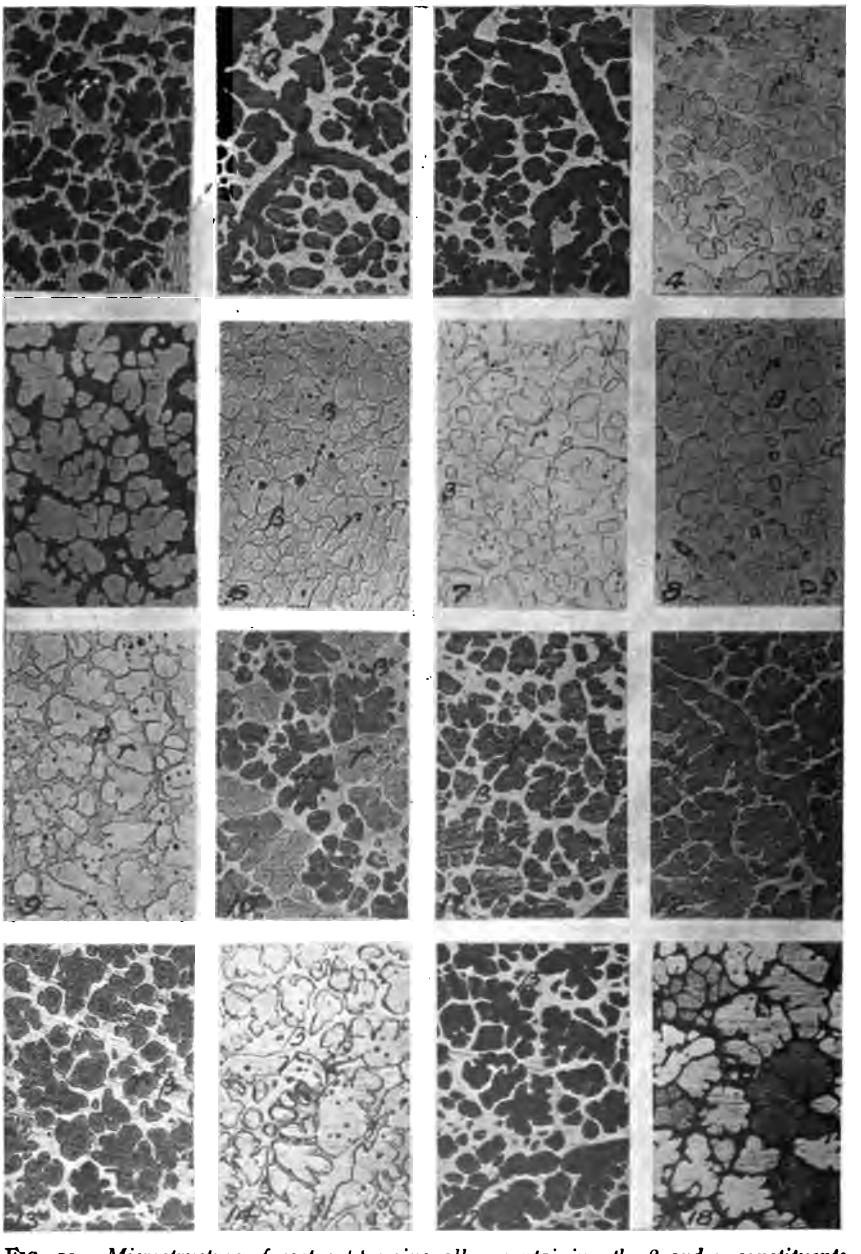

FIG. 12.—*Microstructure of cast copper-zinc alloy containing the β and γ constituents (alloy 17, Table 1) illustrating the etching characteristics of the alloy.* × 100

The number on each micrograph indicates the etching reagent used (Table 2). In the unetched state the γ nodules appear gray in a yellow matrix of the β constituent.

Digitized by Google

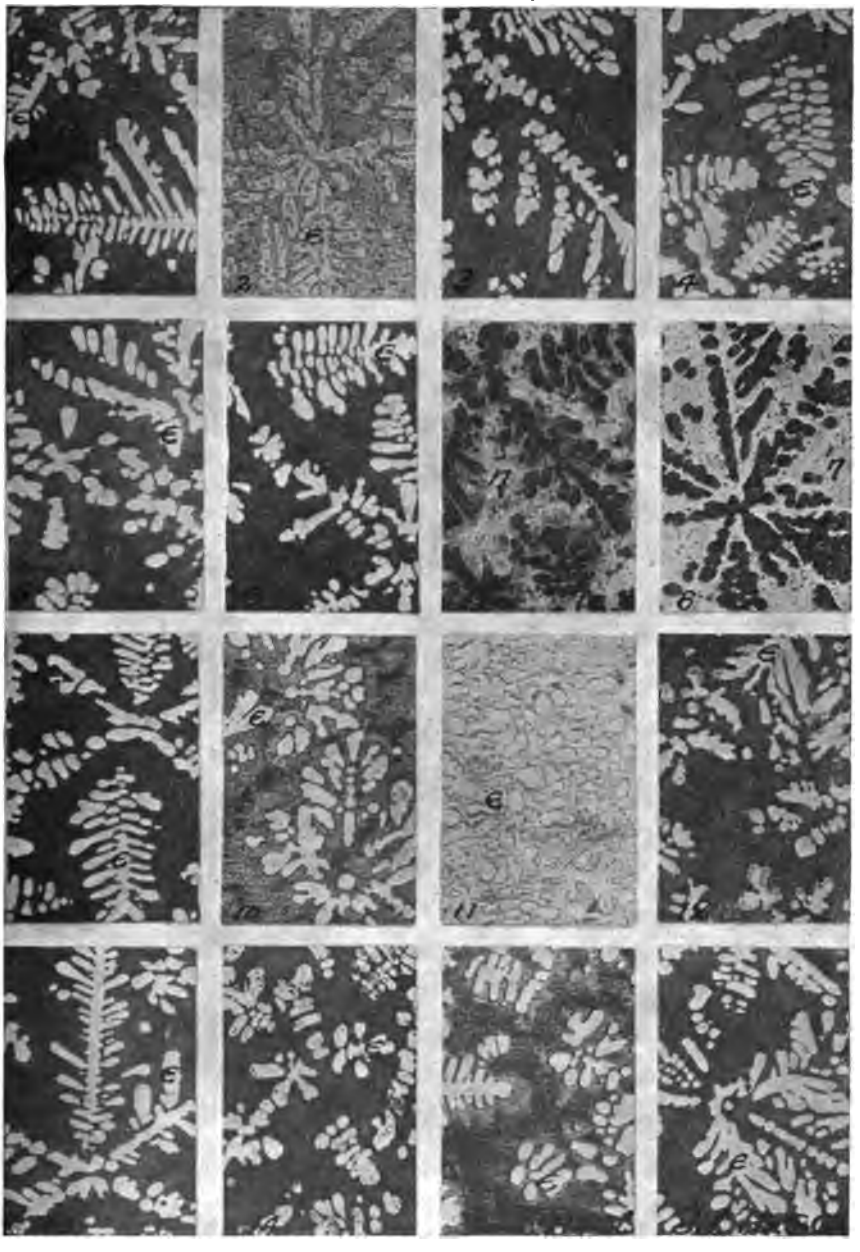

FIG. 13.—*Microstructure of cast copper-zinc alloy containing the ε and η constituents (alloy 21, Table 1) illustrating the etching characteristics of the material.* × 100

The number on each micrograph indicates the etching reagent (Table 2) used.

Digitized by Google

2. BRONZE

The α bronzes presented no difficulties in etching other than those already discussed for the corresponding brasses, and, in general, the results were very similar. Fig. 14 shows the results for the different types of etching reagents and illustrates which reagents are suitable for producing either a contrast or a plain etching.

The cast bronze shown in Fig. 15 has a more complex structure, so that the variations in its behavior with different types of etching reagents were much more pronounced. The micrographs illustrate this much more forcibly than can be done in words. Incidentally they also show the care which should be used in the choice of an etching reagent according to the features of the structure of an alloy which it is desired to emphasize.

3. ALUMINUM BRONZE

Of all the copper alloys used, aluminum bronze (specimen 25, Table 1) was found to be the most unsatisfactory in its behavior toward the various types of etching reagents used. This was true particularly for the metal in the rolled condition; when cast the alloy was etched very satisfactorily with no difficulty. Figs. 16 and 17 show the results obtained for the material in the rolled state and for the same alloy in the cast condition. The best results by far were obtained by passing oxygen through the etching reagent. By this means the boundaries of the crystals of the rolled material were clearly outlined and considerable contrast of the different crystals was developed. When etched with the other reagents, these features were lacking (Fig. 16).

VI. ETCHING CHARACTERISTICS OF NICKEL AND OF ALPHA NICKEL ALLOYS

1. NICKEL

This metal is very much more resistant to etching than is copper or the alloys of copper just discussed. Not only are there fewer reagents that can be used for etching purposes, but also the results obtained are often far from satisfactory. Since nickel is so resistant in its chemical properties a very active reagent—for example, nitric acid—must be employed, and consequently pitting of the surface very often results. Each slight inclusion acts as a center from which the surrounding metal is dissolved, and the pits which form are often the most conspicuous of the microstructural features. There is usually a lack of contrast between the different crystals after etching, the etch pattern being of the "plain" type.

Digitized by Google

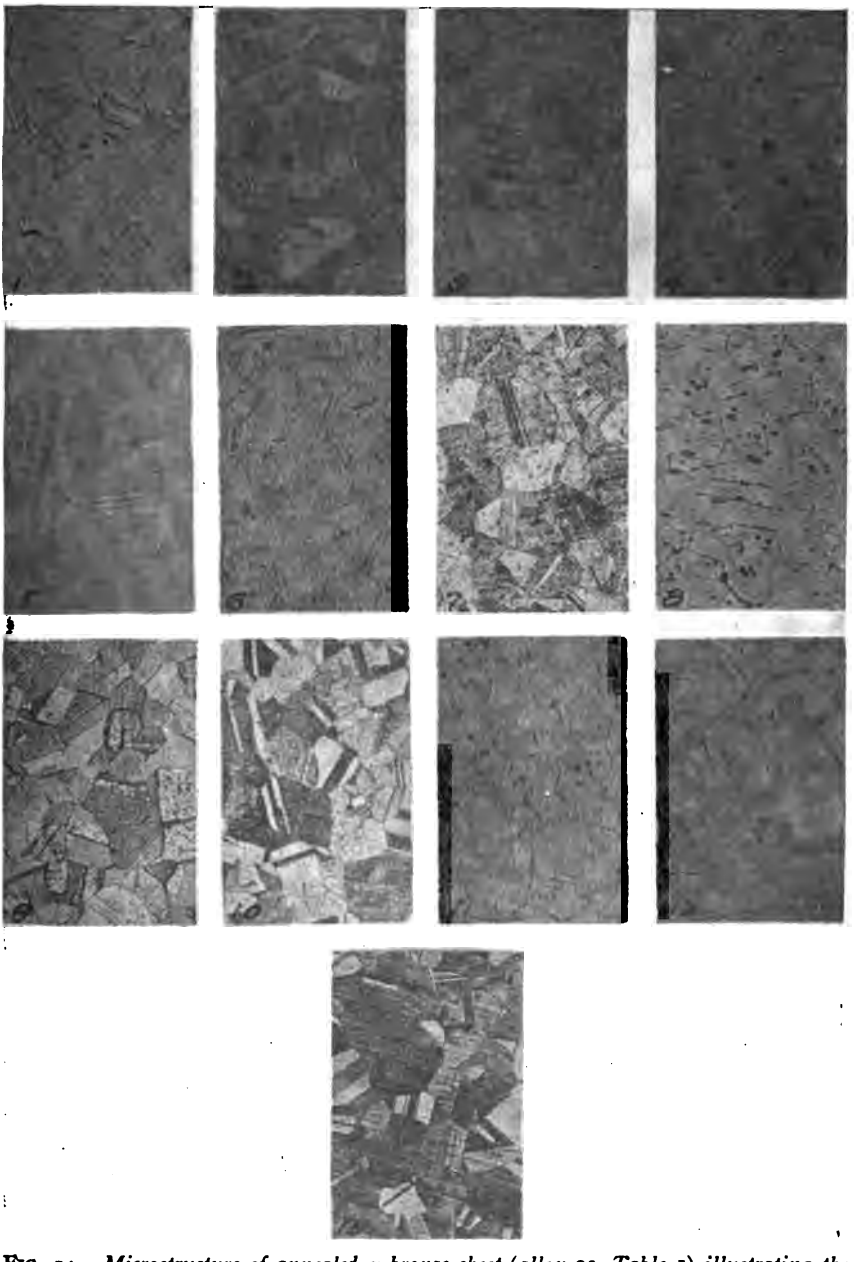

FIG. 14.—*Microstructure of annealed α bronze sheet (alloy 23, Table 1) illustrating the etching characteristics of this alloy.* × 100

The number on each micrograph indicates the etching reagent (Table 2) used.

Digitized by Google

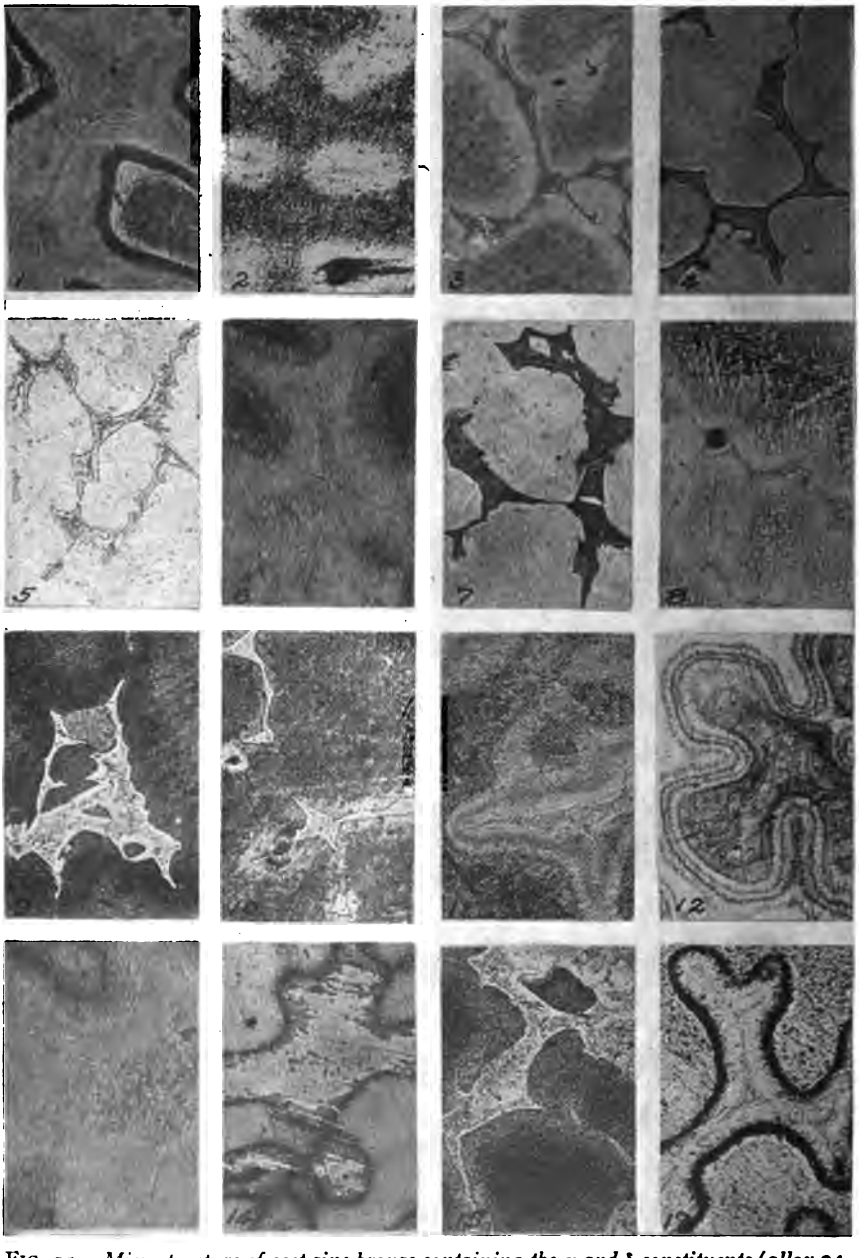

FIG. 15.—*Microstructure of cast zinc-bronze containing the α and δ constituents (alloy 24, Table 1) illustrating the etching characteristics of the alloy.* × 100

The number on each micrograph indicates the etching reagent used (Table 2).

Digitized by Google

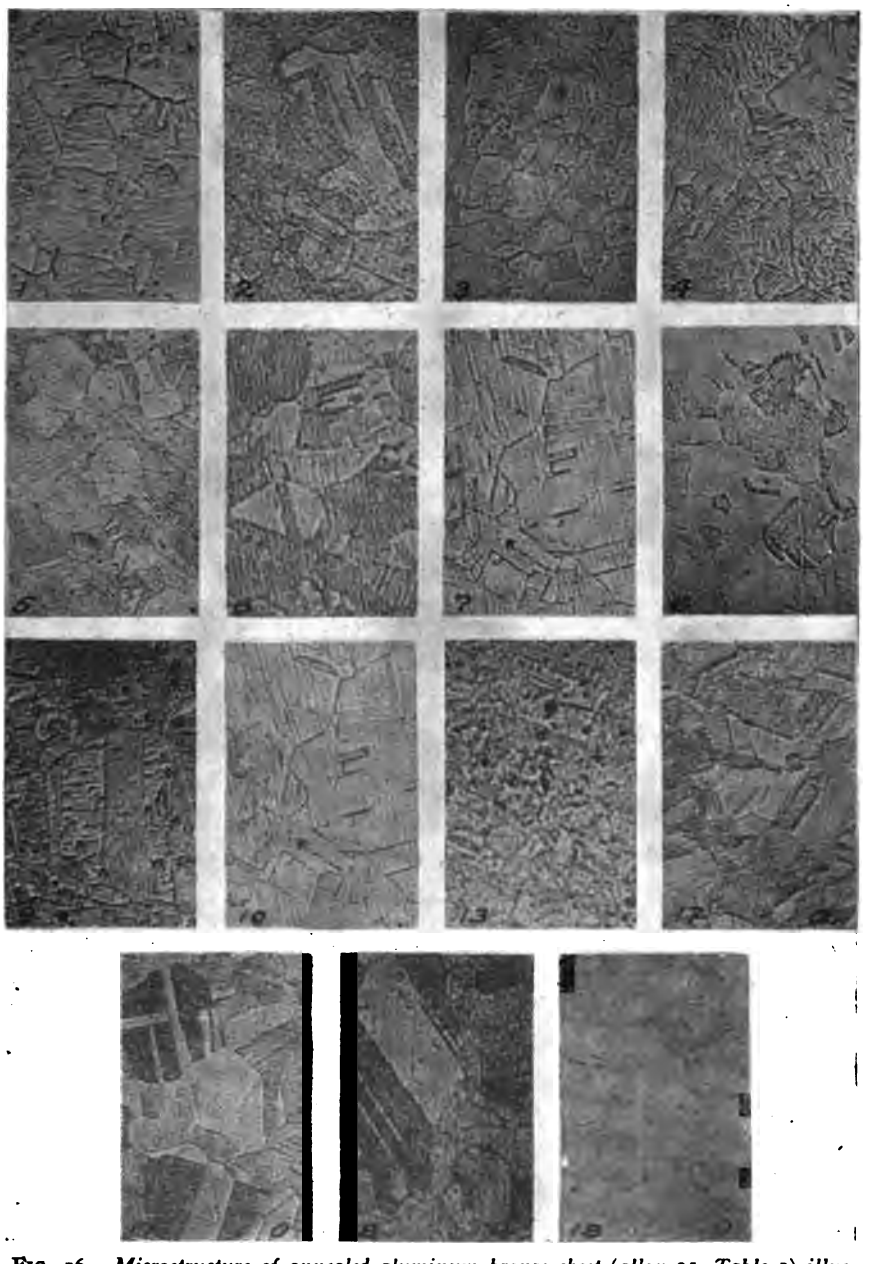

FIG. 16.—*Microstructure of annealed aluminum bronze sheet (alloy 25, Table 1) illustrating the etching characteristics of the alloy.* × 100

The number on each micrograph indicates the etching reagent used (Table 2). In micrographs 17 and 18, *d* indicates "directly in current of oxygen," *o* "outside oxygen current."

Digitized by Google

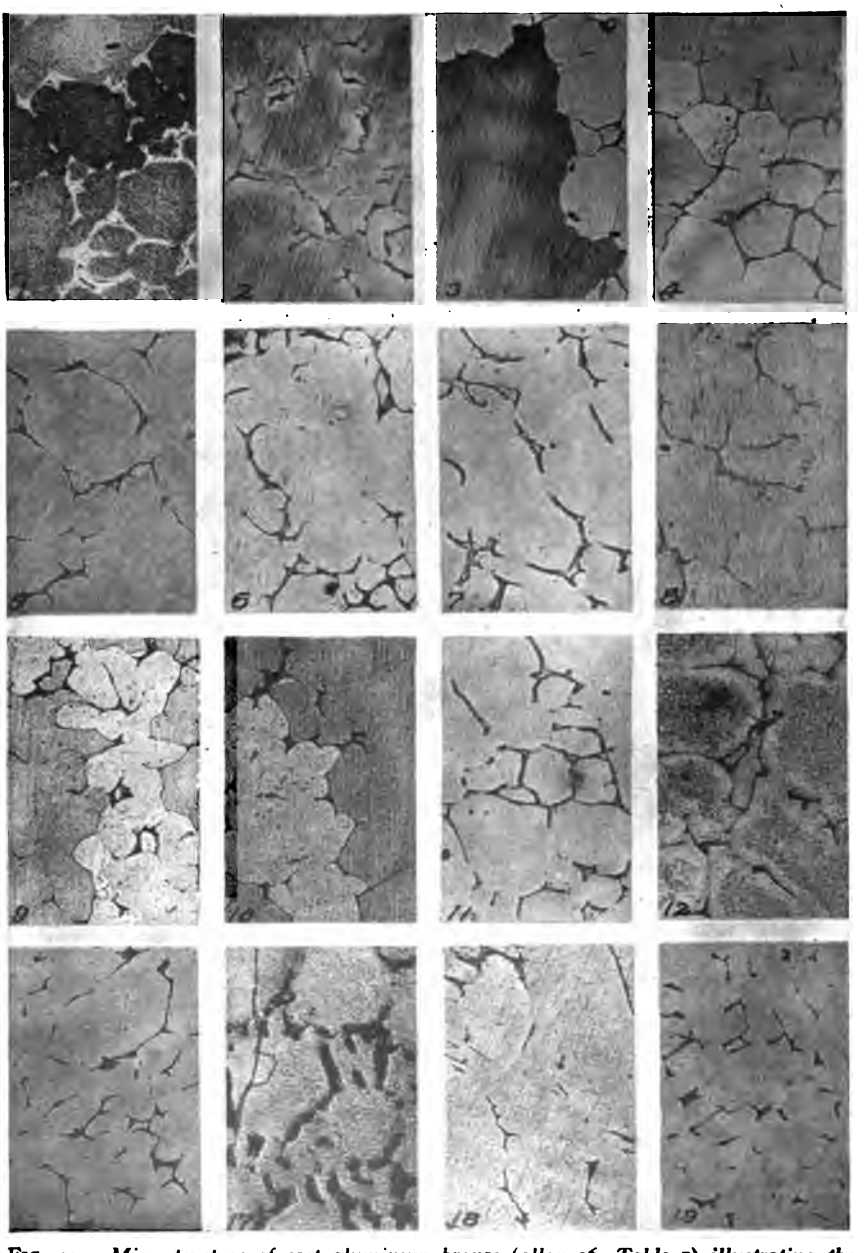

FIG. 17.—*Microstructure of cast aluminum bronze (alloy 26, Table 1) illustrating the etching characteristics of the alloy.* × 100

The number on each micrograph indicates the etching reagent used (Table 2).

Digitized by Google

The following materials (Table 1) were used as representative of the different forms of the metal: Electrolytically deposited nickel, the same after being remelted in vacuo, commercial cast nickel containing oxide, cast nickel which had been deoxidized, hot and cold rolled materials, and a specially treated material termed "manganese nickel." Representative micrographs of cast and rolled nickel are shown in Figs. 18 and 19.

The readiness with which cast nickel will etch depends to a very large extent upon the purity of the metal. Electrolytic nickel remelted in vacuo was found to etch with very much more difficulty than the commercial cast metal. It was also noted for several different specimens that the first time the surface was etched after grinding and polishing the etching period required was usually much longer than that necessary after a slight repolishing of a previously etched surface. It was often necessary to disregard the results of the first etching entirely and depend upon those obtained after the surface had been repolished.

It will be noted from the micrographs (Figs. 18 and 19) that the addition of an oxidizing agent is often sufficient to make a solution which otherwise would have no appreciable action upon nickel a very fair etching reagent. This does not always answer the purpose, however, and the etching characteristics of nickel appear to be much more "erratic" than do those of copper or even of the alloys of nickel.

One of the more satisfactory reagents for producing a plain etching consists of nitric acid diluted with acetic acid and has been described by Merica.[4] The most satisfactory reagent for etching nickel and producing contrast with a minimum amount of pitting was found to be concentrated hydrochloric acid. The use of this acid in concentrated form for etching purposes for developing microstructure of nickel and related alloys is new so far as the authors are aware. The only disadvantage in its use is the long time required. In some cases (Table 3) an etching period of one hour was required to develop the structure satisfactorily. However, one of the principal requirements for etching nickel satisfactorily appears to be a very slow uniform action. A solution of ferric chloride produces results somewhat similar to concentrated hydrochloric acid in a much shorter time but, on the whole, is not so desirable, as the pitting of the specimen is sometimes excessive with this reagent. Hydrochloric acid was found

[4] Circular 100, Nickel, p. 16.

Digitized by Google

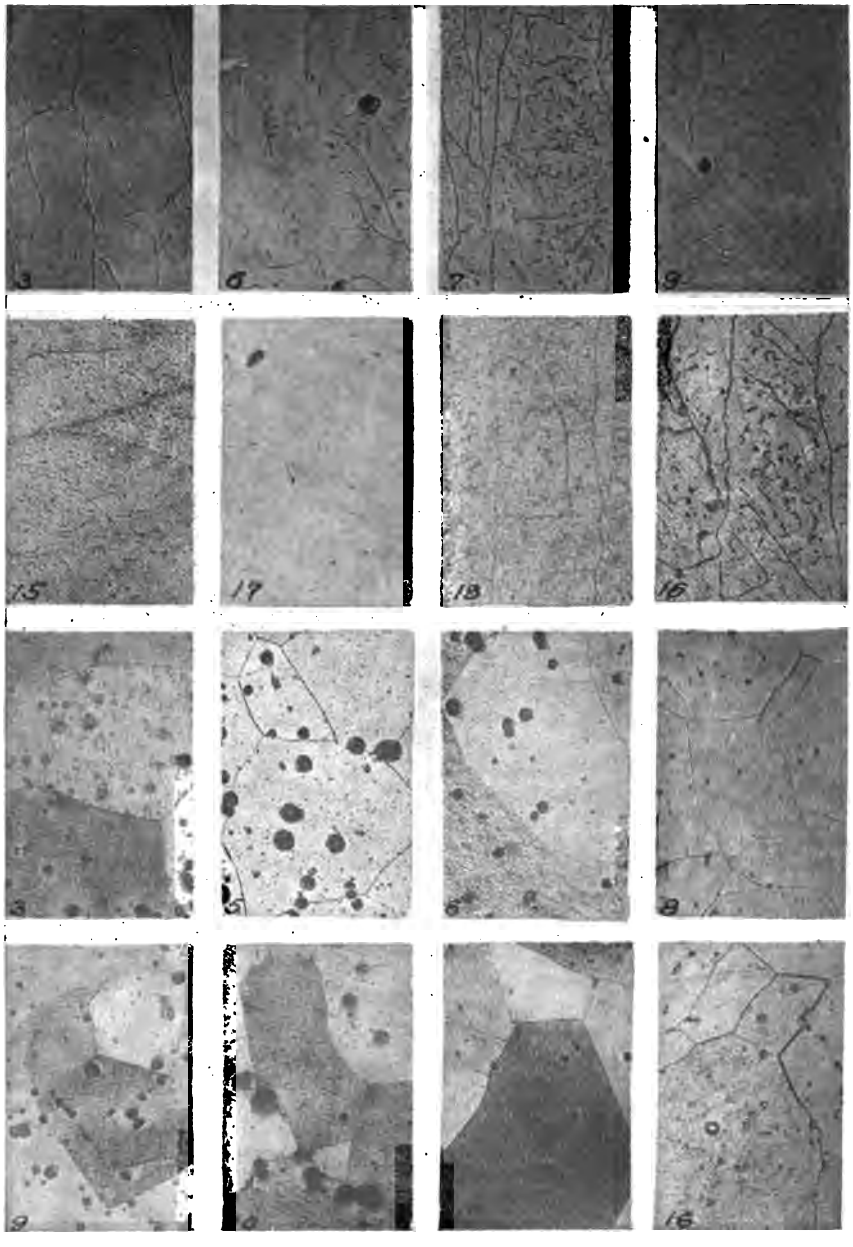

FIG. 18.—*Microstructure of cast nickel illustrating the etching characteristics of this metal.* × 100

The two upper rows of micrographs are of electrolytic nickel melted in vacuo (specimen 37, Table 1); the two lower rows show the appearance of commercial cast nickel (specimen 29, Table 1).

The number on each micrograph indicates the etching reagent used (Table 2).

Digitized by Google

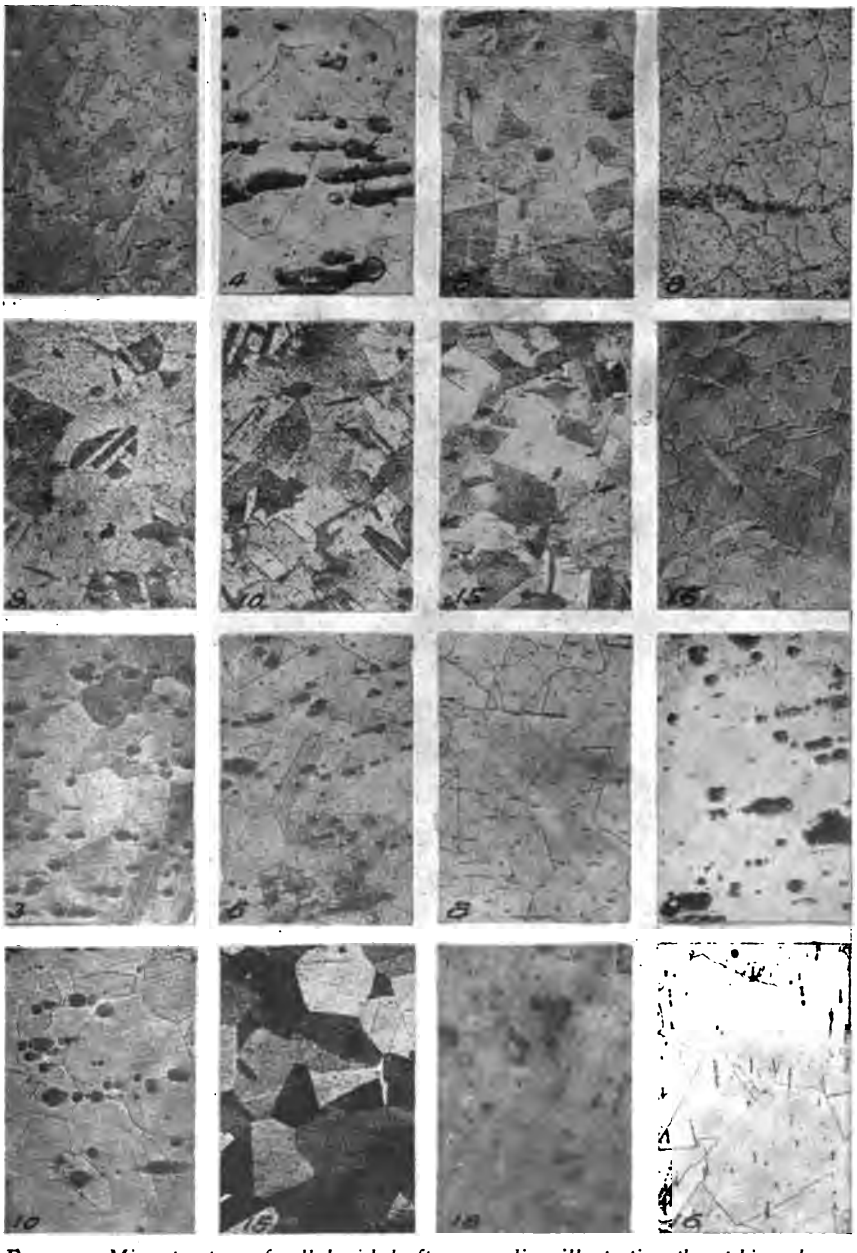

FIG. 19.—*Microstructure of rolled nickel after annealing illustrating the etching characteristics of this metal.* × *100*

The two upper rows of micrographs show the structure of sheet nickel (alloy 35, Table 1); the two lower rows, manganese-nickel rod (alloy 52, Table 1). The number on each micrograph indicates the etching reagent used (Table 2).

Digitized by Google

to be useful also for some of the copper alloys, particularly those in the cast state, and representative micrographs have been given in some of the preceding figures. The period required for etching the copper alloys with hydrochloric acid was, of course, very much shorter than for nickel, a period somewhat less than a minute usually being sufficient.

2. NICKEL ALLOYS

The alloys chosen as representative were those in common industrial use and all were of the α type of structure. The list included cupro-nickel, monel metal, nickel brass (nickel silver, formerly German silver) and high nickel steel (invar).

The nickel alloys of the types examined etch very much more readily than does nickel. All of the alloys excepting invar contained a considerable percentage of copper, and the etching characteristics were affected accordingly, so that, though they were not etched so readily as were the copper alloys, they resembled them in their behavior more closely than they did nickel. Practically all the reagents which were found useful for the copper alloys were useful also for the alloys of nickel.

Figs. 20 and 21 show the characteristic appearance of cupro-nickel in the cast and the wrought state after etching with various types of reagents. The results produced with the same reagents upon monel metal are shown in Figs. 22, 23, and 24. The micrographs show that the "cored" or dendritic structure of the cupro-nickel is readily revealed by nearly all the reagents used, but not so with monel metal. A point worthy of note concerning the cored structure of nickel alloys is the fact that it appears to be independent of the network of the grain boundaries. It may be noted in some of the micrographs of cast monel metal given that the grain boundary cuts across the dendritic pattern instead of inclosing a complete dendrite entirely within a single grain.

The high nickel "cores" persist after mechanical working of the alloy as "work lines" extending in the direction of rolling or forging. These lines are readily revealed by the vigorously acting reagents, such as nitric acid, and form a very characteristic feature of the microstructure of nickel alloys particularly in the hot-rolled or unannealed state. When an oxidizing reagent was used, there was often a pronounced difference in the intensity of the film produced upon these "work lines" and upon the intermediate streaks, so that the surface had a banded appear-

Digitized by Google

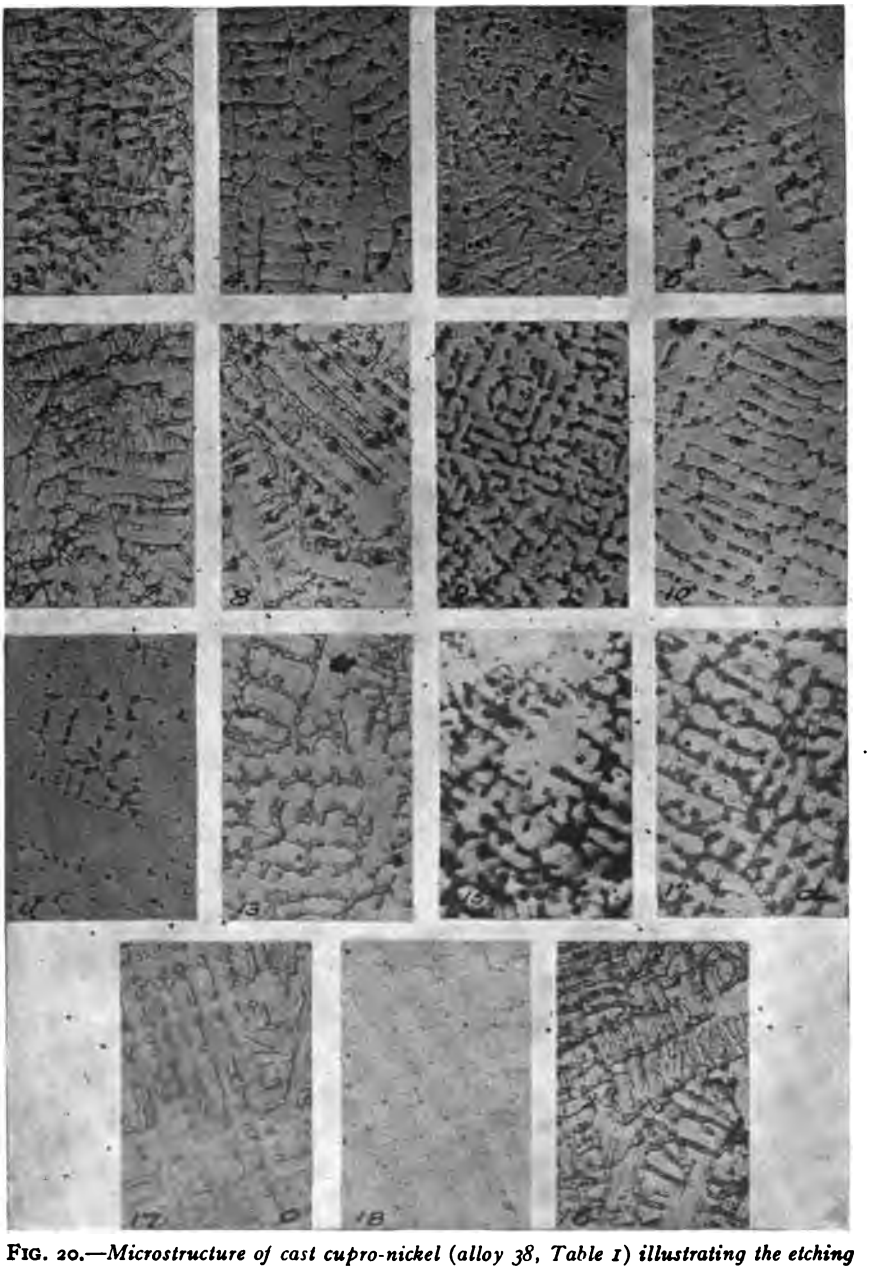

FIG. 20.—*Microstructure of cast cupro-nickel (alloy 38, Table 1) illustrating the etching characteristics of the alloy.* × *100*

The number on each micrograph indicates the etching reagent (Table 2) used. In micrograph 17, *a* indicates "directly in oxygen current"; *o* "outside oxygen current."

Digitized by Google

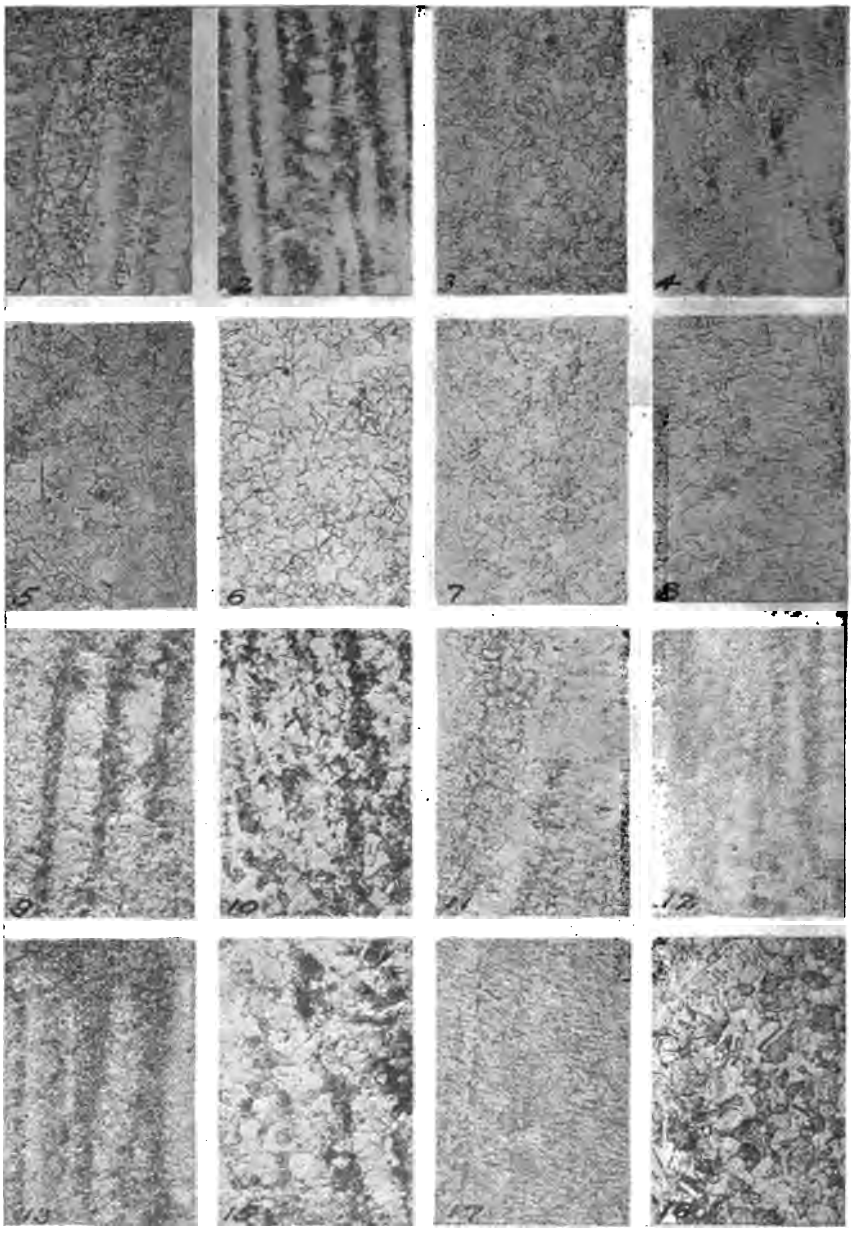

FIG. 21.—*Microstructure of cold rolled cupro-nickel sheet (alloy 44, Table 1) illustrating the etching characteristics of the material.* × *100*

The number on each micrograph indicates the etching reagent (Table 2) used.

Digitized by Google

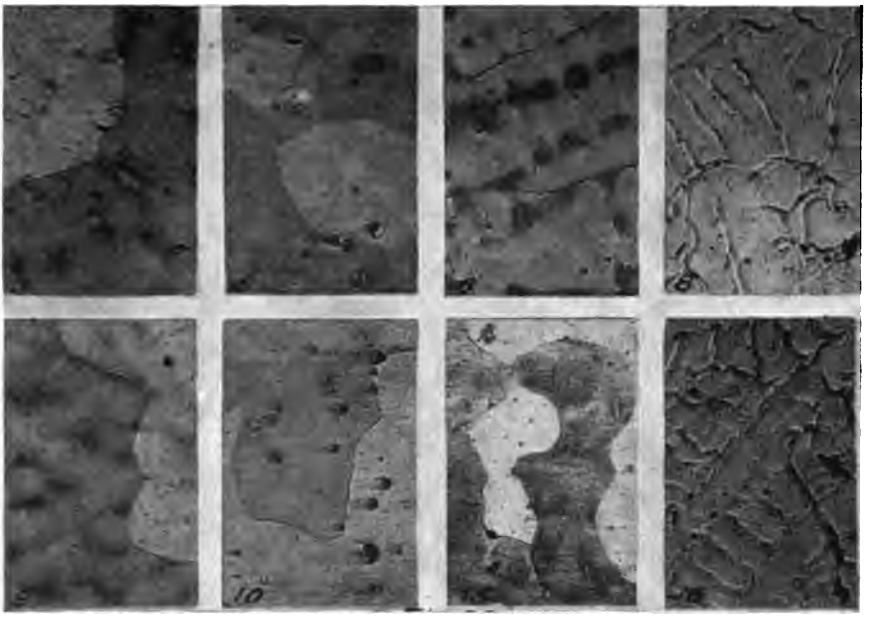

FIG. 22.—*Microstructure of cast monel metal (alloy 32, Table 1) illustrating the etching characteristics of the metal.* × 100

The number on each micrograph indicates the etching reagent (Table 2) used.

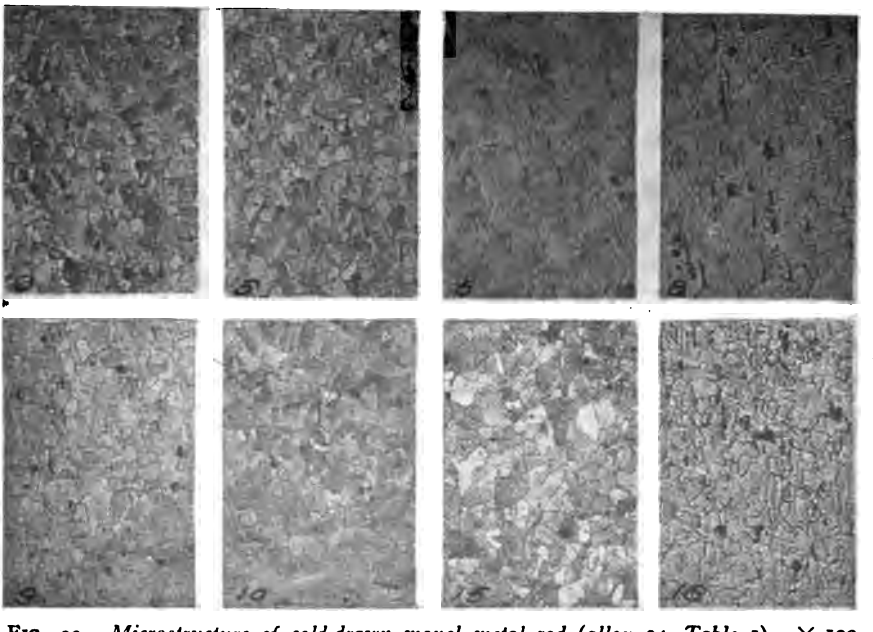

FIG. 23.—*Microstructure of cold-drawn monel metal rod (alloy 34, Table 1).* × 100

The number on each micrograph indicates the etching reagent (Table 2) used.

Digitized by Google

ance though otherwise unetched. This was sometimes very pronounced when oxygen was passed through the etching solution, as is shown in Fig. 24.

Figs. 25 and 26 show the results obtained with nickel brass (No. 45, Table 1) in the cold-rolled state and the same after

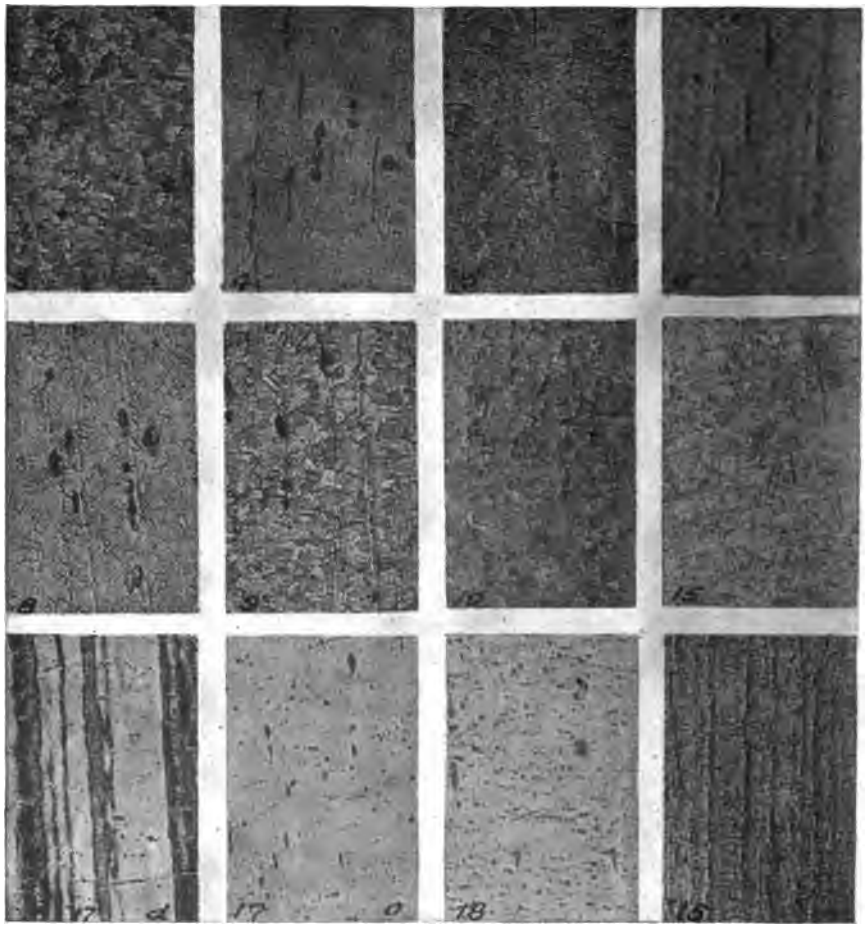

FIG. 24.—*Microstructure of hot-rolled monel metal plate (alloy 33, Table 1) illustrating the etching characteristics of the alloy.* × 100

The number on each micrograph indicates the etching reagent used (Table 2). In micrograph 17, *d* indicates "directly in oxygen current," *o* "outside the current oxygen."

annealing. The general behavior of alloys of this group varies with the nickel content. The specimens low in nickel were found, as might be expected, to be very similar to the copper-zinc alloys in their etching characteristics although not quite so readily attacked. The contrast produced and the general appearance of the etched surface were quite similar, however.

Digitized by Google

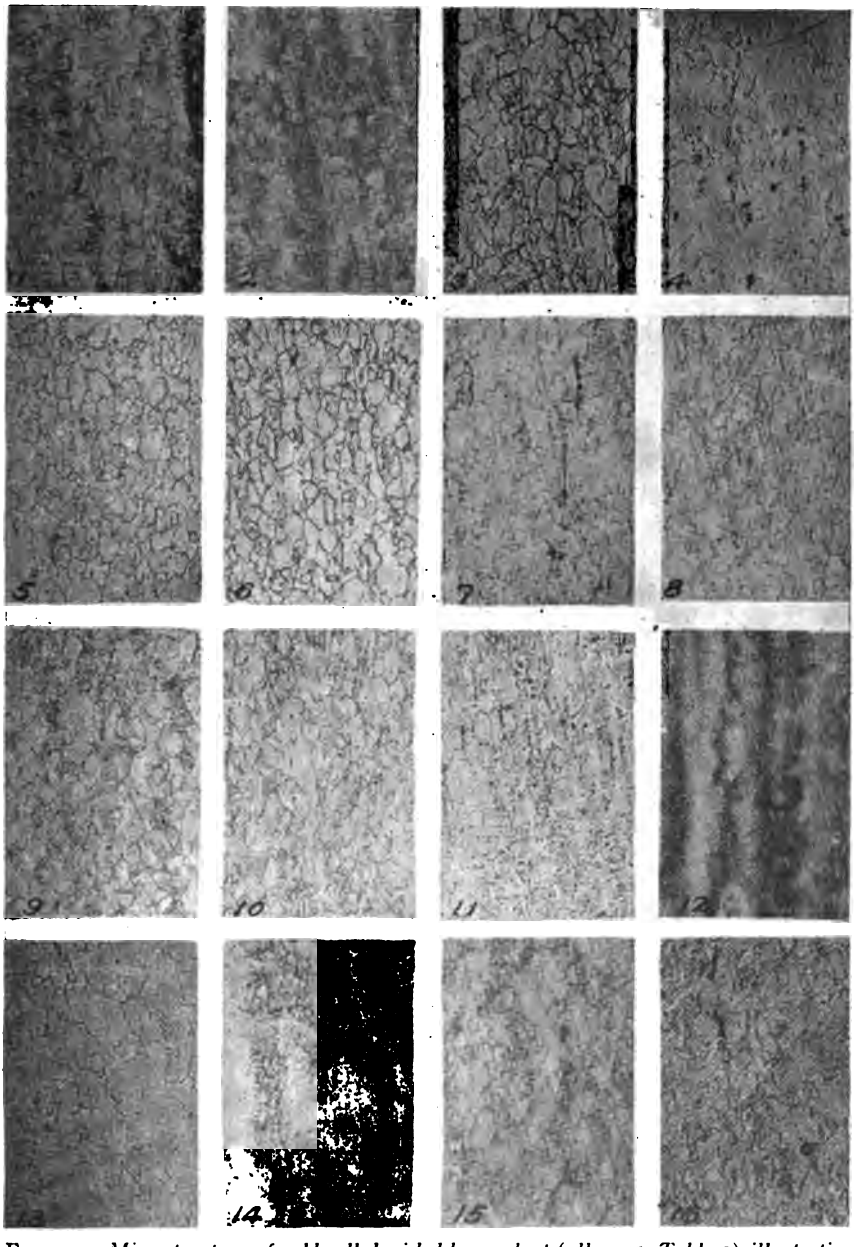

FIG. 25.—*Microstructure of cold-rolled nickel-brass sheet (alloy 45, Table 1) illustrating the etching characteristics of the alloy.* × 100

The number on each micrograph indicates the etching reagent (Table 2) used.

Digitized by Google

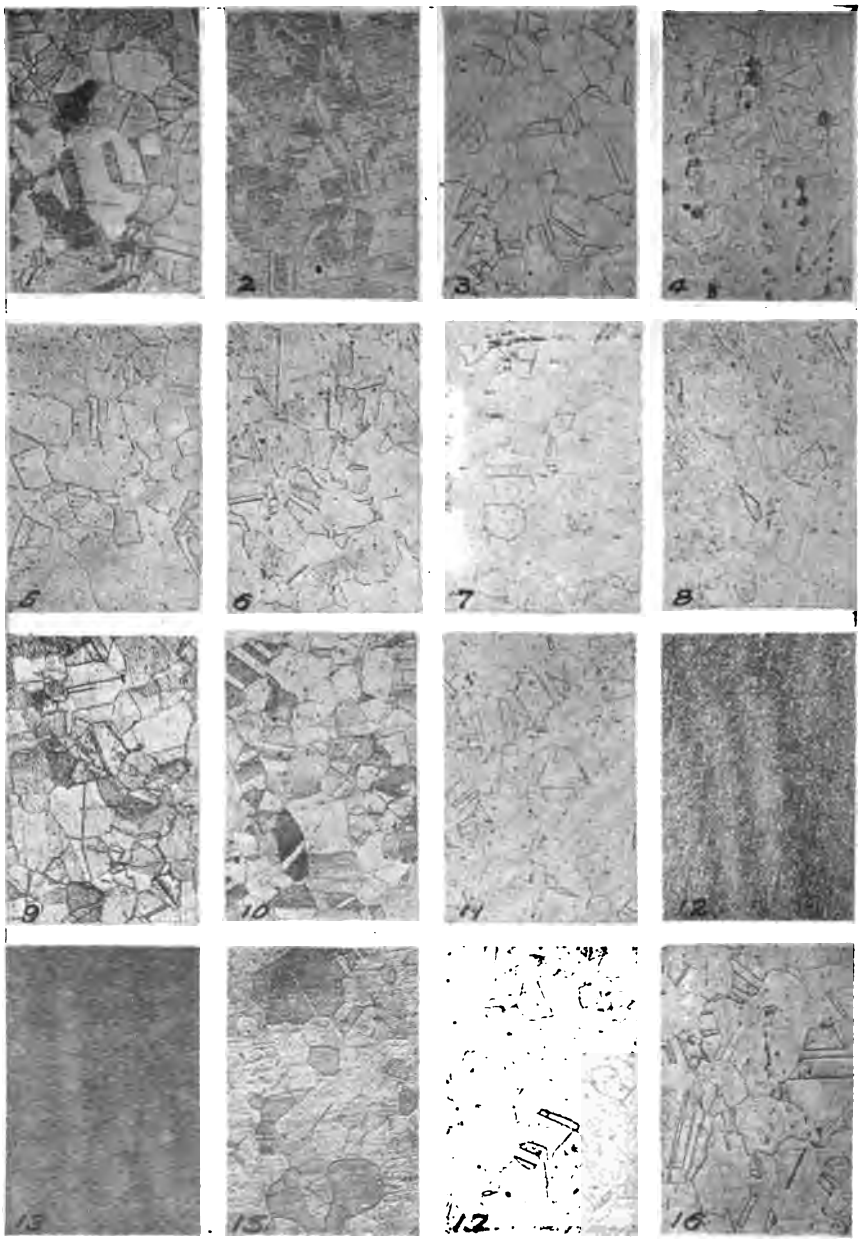

FIG. 26.—*Microstructure of annealed nickel-brass sheet (alloy 46, Table 1) illustrating the etching characteristics of the alloy.* × 100

The number on the micrograph indicates the etching reagent (Table 2) used.

Digitized by Google

VII. EFFECT OF OXYGEN UPON THE RATE OF ETCHING

The importance of oxygen in metallographic etching reagents has been previously discussed.[5] In order to verify and confirm the conclusions which appeared to be justified by the results obtained upon etching copper with reagents through which oxygen was bubbled, specimens representative of the different copper and nickel alloys and of various forms of nickel were etched in a similar manner. Three typical reagents were used—ammonium hydroxide, dilute sulphuric acid, and a solution of ammonium chloride. A stream of oxygen was passed through each after the specimen had been immersed and the bubbles were directed against the surface to be etched.

The results obtained with the α copper alloys, on the whole, confirmed those for copper and need not be considered in detail here. Some typical micrographs are given in Fig. 27. It was noted that when a specimen was etched with ammonium hydroxide and oxygen the most intense attack was in the central portion of the area against which the stream of gas was directed. The best contrast, however, was usually found in the annular portion surrounding the central area where the action was somewhat less vigorous. Those portions of the surface which were not near the oxygen stream remained almost entirely unetched. With dilute sulphuric acid and oxygen the etching action was confined almost entirely to the annular portion, the spot against which the gas was directed remaining bright and unetched. This effect was probably largely the results of mechanical causes. The bubbles of gas in passing through ammonium hydroxide become saturated with ammonia and hence have a pronounced effect; but, since the sulphuric acid is not volatile, a similar condition does not obtain with this reagent, and it is only where the acid solution becomes saturated with oxygen that the metal is attacked. Ammonium chloride and oxygen resembled ammonium hydroxide, although the action was much less intense.

When the duplex copper-zinc alloys were etched by the use of oxygen, the general tendency was for the more soluble (zinc-rich) constituent to oxidize more readily than the other. Thus, the β constituent was found to darken in all reagents much more readily than the α. A few exceptions were noted, however—as, for example, in α β brass—in which the oxidation was reversed in the acid solution as compared with the ammoniacal one (Fig. 27). Oxygen as a gas appears to have an almost negligible

[5] See footnote 1.

Digitized by Google

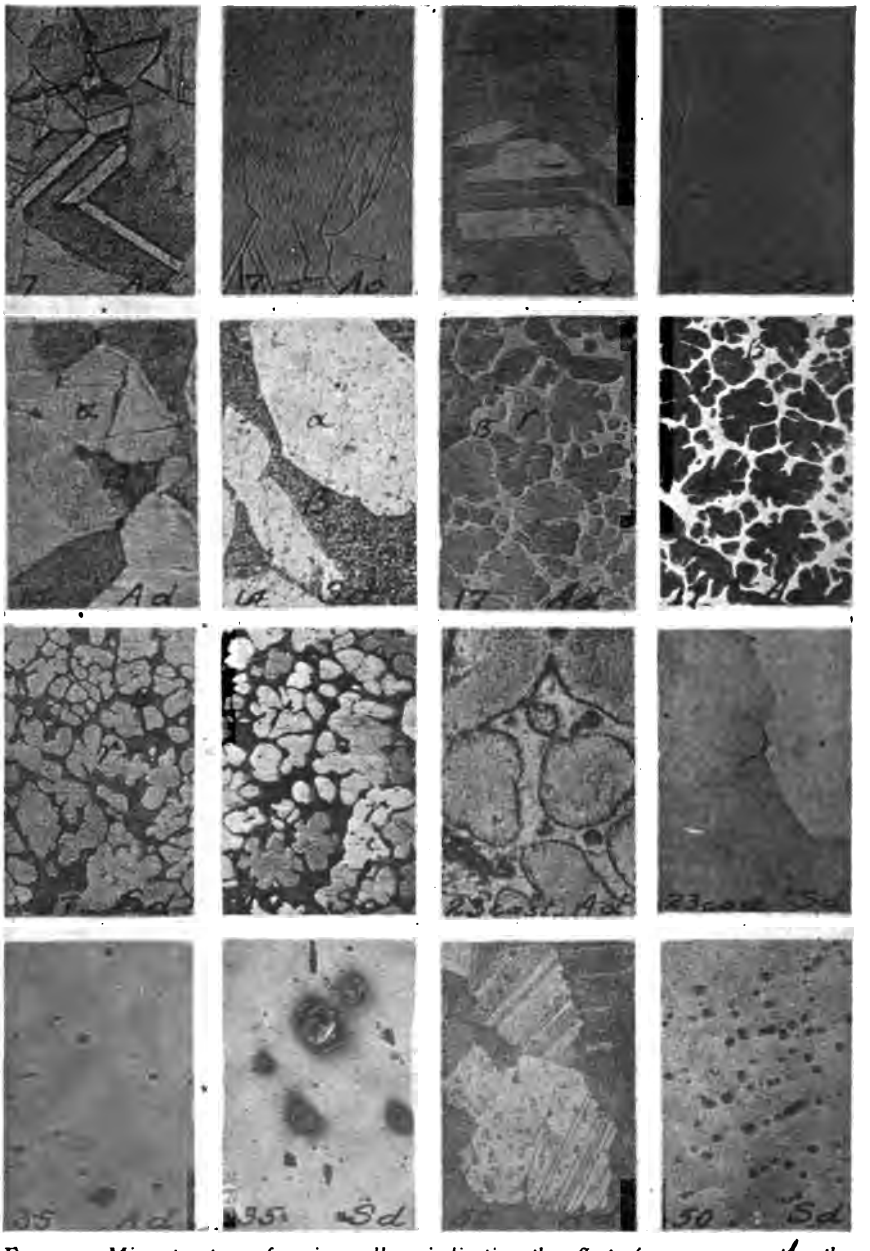

FIG. 27.—*Microstructure of various alloys indicating the effect of oxygen gas upon the etching of copper alloys, nickel, and nickel brass.* × 100

The number on each micrograph indicates the alloy (Table 1). The etching solution is shown on each micrograph. *A* indicates concentrated ammonium hydroxide; *S* dilute sulphuric acid; *d* directly in the oxygen current; *o* outside the oxygen current.

Digitized by Google

influence upon the etching of nickel. The action of sulphuric acid was found to be slightly intensified on account of the attack by the acid on the inclusions in the metal and the formation of pits. The action of ammonium hydroxide and oxygen is very slight and may be disregarded entirely. The behavior of cupro-nickel and monel metal was very similar to that of nickel under the same conditions. These results are of importance from a practical viewpoint in that they demonstrate in a striking and simple manner the noncorrodibility of these materials.

The nickel brasses were found to be etched very appreciably by ammonium hydroxide and oxygen. Sulphuric acid and oxygen, however, have but little effect upon them.

VIII. SUMMARY

1. This article constitutes the second part of the general investigation of metallographic etching reagents in progress at this Bureau. It is closely related to the one already published on copper in the methods employed and results obtained. The following materials were used: Copper alloys, including brasses, bronze, and aluminum bronze; nickel; and the α alloys of nickel, monel metal, cupro-nickel, and nickel brass.

2. The results of some further experimental work are given to show the importance of films in producing contrast in etching. Oxide and sulphide films were used, and it was shown by separating the etching and the filming operations that films varying in thickness on the individual crystals are produced by certain reagents, giving rise to "contrast." The better understood method for producing contrast by a differential roughening of the crystals upon etching is also illustrated.

3. The α copper alloys closely resemble copper in their general behavior upon etching and in the character of the results produced. The addition of tin to brass appears to render it slightly less responsive to etching reagents than the same alloy without tin. Aluminum bronze in the rolled condition was the most unsatisfactory of the copper alloys examined to etch. A series of copper-zinc alloys representative of all the types of structure in this series was examined. The alloys rich in zinc resemble this metal in their etching characteristics more than they do the copper-rich alloys, in that highly oxidizing etching reagents do not appear to be necessary for the successful etching of the alloy.

Digitized by Google

4. Nickel, particularly when of high purity, is etched with considerable difficulty. Oxidizing acids, such as nitric, and acids to which strong oxidizers had been added, were found effective for a quick etching. For producing a contrast etch pattern with freedom from pitting a long immersion in concentrated hydrochloric acid was found to give excellent results.

5. Of the α nickel alloys examined monel metal and cupro-nickel were found to resemble nickel in their etching properties though they etched more readily. The nickel brasses (nickel silver) resemble the α copper alloys in many respects and were readily etched by the reagents used for the brasses and bronzes.

6. The copper alloys behave very similarly to copper in their behavior toward etching reagents through which oxygen was bubbled. They were readily etched by reagents—ammoniacal, acid, or neutral—which otherwise would have but slight effect upon them provided a stream of oxygen was passed through the solution while the specimen was immersed. Nickel was found not to be affected materially in its rate of etching by the use of oxygen gas except in the degree of pitting produced in some specimens. Cupro-nickel and monel metal resemble nickel in this respect, and the nickel brasses are somewhat like the copper alloys. They respond to the ammoniacal solutions containing oxygen though not to acid solutions and oxygen.

7. The large number of microscopic examinations which the investigation has necessitated, of which it is possible to present only a relatively small number of the micrographs, has rendered the summarizing of the results a rather difficult matter. Only the more obvious and general features have been discussed.

WASHINGTON, August 26, 1921.

Digitized by Google

DEPARTMENT OF COMMERCE

SCIENTIFIC PAPERS

OF THE

BUREAU OF STANDARDS

S. W. STRATTON, Director

No. 436

[PART 21]

INTERFERENCE METHODS FOR STANDARDIZING AND TESTING PRECISION GAGE BLOCKS

BY

C. G. PETERS, Associate Physicist
H. S. BOYD, Assistant Physicist

MAY 5, 1921

WASHINGTON
GOVERNMENT PRINTING OFFICE
1921

Digitized by Google

Digitized by Google

DEPARTMENT OF COMMERCE

SCIENTIFIC PAPERS

OF THE

BUREAU OF STANDARDS

S. W. STRATTON, DIRECTOR

No. 436

(Part of Vol. 17)

INTERFERENCE METHODS FOR STANDARDIZING AND TESTING PRECISION GAGE BLOCKS

BY

C. G. PETERS, Associate Physicist
H. S. BOYD, Assistant Physicist
Bureau of Standards

MAY 2, 1922

PRICE, 10 CENTS

Sold only by the Superintendent of Documents, Government Printing Office
Washington, D. C.

WASHINGTON
GOVERNMENT PRINTING OFFICE
1922

Digitized by Google

Digitized by Google

INTERFERENCE METHODS FOR STANDARDIZING AND TESTING PRECISION GAGE BLOCKS

By C. G. Peters and H. S. Boyd

ABSTRACT

Precision gages, which are blocks of metal (usually steel), having two opposite faces plane, parallel, and a specified distance apart, are used in the shop as reference end standards for checking micrometers and other measuring instruments, and also as distance pieces or size blocks for precise mechanical work. The extensive use of precision gages necessitated by the small tolerances allowed in the manufacture of interchangeable machine parts has required more accurately determined end standards and more rapid and precise methods for comparing gages with these standards than have been previously available.

Since comparisons of end standards with line standards by means of micrometer-microscopes and of precision gages with end standards by means of contact instruments are subject to appreciable errors, methods which make use of the interference of light waves were used in making these measurements. With the interference methods described in this article the planeness and parallelism errors of precision surfaces can be measured, and the length of standard gages can be determined by direct comparison with the standard light waves with an uncertainty of not more than a few millionths of an inch. The errors of other gages can be determined by comparison with these calibrated standards with equal precision. This process makes the standard light waves, which have been determined to one part in four or five million relative to the international meter the standards of length for this work.

The apparatus used for calibrating standards and comparing other gages with these standards is illustrated by line drawings and thoroughly explained.

CONTENTS

	Page
I. Introduction	678
II. Optical method	679
III. Interference of light	681
IV. Test for planeness of surfaces	684
1. Perpendicular incidence	684
2. Errors of interpretation	688
V. Adherence of surfaces	690
VI. Test for parallelism of surfaces	692
VII. Calibration of end standards with the Fabry and Perot interferometer	693
1. General plan pf apparatus	693
2. Source of light	694
3. Interferometer	694
4. Constant-temperature chamber	695
5. Spectrograph	695
6. Photographic	695
7. Determination of the order of interference	696

Digitized by Google

Page

VII. Calibration of end standards with Fabry and Perot interferometer—Con.
8. Correction of λ 697
9. Correction for the thickness of the platinum films 698
10. Correction for nonparallelism of the gage surfaces 698
11. Computations 699
12. Accuracy and sources of error 699
VIII. Comparison of gages with standards 704
1. Comparison of length 704
2. Comparison of parallelism of surfaces 706
IX. Intercomparison of three gages 708
X. Development of standard gages 710
XI. Comparison between gages and other objects 712
XII. Summary 713

I. INTRODUCTION

Precision gages, which are blocks of metal (usually steel) having two opposite faces plane, parallel, and a specified distance apart are used in the shop as reference end standards for checking micrometers and other measuring instruments, and also as distance pieces or size blocks for precise mechanical work. The extensive use of precision gages necessitated by the small tolerances allowed in the manufacture of interchangeable machine parts, and the development of the process of making these gages with errors of construction that seldom amount to 0.5 micron (0.00002 inch)—in most cases to not more than 0.25 micron (0.00001 inch)—have created a need for more rapid and precise methods of test and also for more accurately determined reference standards than have been available. Since tests of the accuracy of precision gages can be most readily made by comparison with secondary end standards of the same size and shape, gage blocks with very nearly perfect surfaces can be used in the testing laboratory as secondary end standards when they have been accurately calibrated relative to some fundamental standard of length and when it has been proved that they retain their dimensions for a considerable period of time.

The fundamental standard of length, the International Prototype Meter, is a line standard whose length is the distance between two lines ruled on a platinum-iridium bar carefully preserved in a special vault at the International Bureau of Weights and Measures near Paris. A duplicate of this bar, Meter No. 27, which is kept at the Bureau of Standards, is the primary standard of length for the United States. Other similar bars, graduated in various subdivisions of a meter and calibrated relative to the primary standards, are used as secondary or working standards. In calibrating these secondary and intermediate line standards errors of 0.2 micron

Digitized by Google

(0.000008 inch) are possible, due to imperfections in the ruled lines.

The end standards of the Bureau of Standards have been calibrated heretofore by comparison with these line standards by the methods of Fizeau [1] and Fischer.[2] These methods, requiring the use of microscopes, are subject to errors of measurement which may amount to 0.5 micron (0.00002 inch).

The comparisons between the secondary end standards and the precision gages are usually made with contact comparators subject to errors of 0.5 micron (0.00002 inch).

Inasmuch as the tolerance on some machine work is ±2.5 microns (±0.0001 inch), requiring the precision gage of the shop to be correct within 0.25 to 0.5 micron (one or two hundred-thousandths of an inch), this degree of precision in the gages requires the secondary end standards of the testing laboratory to be correct within a few hundredths of a micron (millionths of an inch). This tolerance also requires that the errors of measurement in making the comparison between the gages and the standards should likewise be limited to a few hundredths of a micron. It is impossible to attain this precision in measuring the irregularities in the surfaces of gages or end standards with any micrometric apparatus, in calibrating end standards by comparison with line standards, or or in making comparisons between end standards and precision gages with any contact apparatus, because in each case the error of measurement may be several times the allowable error. The error of measurement in the step from the standard meter to the gage should not be more than 0.02 to 0.06 micron (one to three millionths of an inch).

In December, 1917, we undertook to develop an optical method for making these measurements, and in a short time, by applying methods which make use of the interference of light waves, succeeded in solving the problem.[3]

II. OPTICAL METHOD

Instead of calibrating the end standards by direct comparison with line standards derived from the meter the lengths of standard light waves were chosen as the primary standards. These

[1] Travaux et Mémoires du Bureau International des Poids et Mesures, 10.

[2] Bull. Phil. Soc. of Washington, 18, p. 241; 1898.

[3] Reports on these methods have been given at the following meetings: Peters, American Society of Mechanical Engineers, New York, Dec. 5, 1918. Peters and Boyd, American Physical Society, Washington, Apr. 25, 1919; American Society of Mechanical Engineers, Washington, May 30, 1919; and Philosophical Society of Washington, May 29, 1920. A popular article on the methods was published by Peters and Boyd in the American Machinist, Sept. 30 and Oct. 7, 1920.

Digitized by Google

waves possess all the necessary properties of fundamental units of length, the most important of which are constancy, reproducibility, accuracy of measurement, and ease of application. As to their constancy, reproducibility, and accuracy of determination little need be said. The wave lengths of red, yellow, and green radiations from cadmium have been determined by direct comparison with the standard meter by Michelson [4] in 1893 and redetermined by Fabry and Benoit [5] in 1907, the values obtained from these two independent determinations agreeing to one part in sixteen million when corrected to similar conditions.

Numerous comparisons made by spectroscopists between these fundamental wave lengths and the wave lengths emitted by other luminous substances prove that the light waves are the most dependable length units known. Their work has placed at our disposal a large number of light sources which can be easily obtained and operated and which emit radiations whose wave lengths are known to one part in four or five million. The only remaining requirement is the easy application of these waves in the calibration of end standards.

In making this application incandescent neon and helium gases, giving wave lengths ranging from 0.40 to 0.75 micron (0.000016 to 0.000030 inch) were used. These have been determined [6] with an accuracy of one part in four or five million and found to be exactly reproducible within the limits of observational error. For an accuracy of one millionth of an inch a comparison with these waves is therefore exactly equivalent to a comparison with the standard meter.

Three sets of carefully selected gages, each containing 81 blocks of various lengths from 0.05 to 4 inches, were chosen as the secondary end standards for gage calibration by interference methods. The planeness and parallelism of the surfaces and length of the gages were determined by means of the interference fringes seen in monochromatic light. To test for planeness, a glass true plane was placed over each gage surface and the curvature of the interference fringes in monochromatic light was determined by means of the Pulfrich instrument described below. Each gage was then made the separator for two interferometer plates, thus forming a Fabry and Perot interferometer. Lack of parallelism of the sur-

[4] Michelson, Travaux et Mémoires du Bureau International des Poids et Mesures, 2; 1895.
[5] Fabry and Benoit, Travaux et Mémoires, 15; 1913.
[6] Burns, Meggers, and Merrill, B. S. Sci. Papers, No. 329; 1918.

Digitized by Google

faces was determined on moving the eye across the plates by the expansion or contraction of the circular (Haidinger) rings, produced when the interferometer was illuminated with radiation from a helium source. The distance between the interferometer plates was determined from measurements on the diameters of these rings. From this determination, by applying corrections for the density of the air, lack of parallelism of the gage surfaces, and thickness of the metallic film on the interferometer plates, the length of the gage was obtained.

Several independent determinations made the same day on a given gage agreed to 0.025 micron (0.000001 inch). Intercomparisons between similar gages from different sets and between combinations of different gages proved that errors in the determinations of these gages were in no case greater than 0.07 micron (0.000003 inch), and these errors were due in most cases to irregularities in the surfaces of the gages. With perfect gages and accurately controlled conditions the precision of the measurements should be comparable with the highest precision obtainable in wave-length measurements.

After these end standards were calibrated a large number of precision gages were compared with them by means of an interferometer comparator. With this instrument one person is able to test the planeness and parallelism of the surfaces and length of about 100 gages per day with an uncertainty of not more than 0.07 micron (0.000003 inch). During the past year about 30 000 precision gages have been tested at the Bureau of Standards by two workers, which shows that the method is sufficiently rapid for quantity work.

Thus it has been possible to originate, by the method fully described below, end standards directly from the standard light waves and to compare large numbers of commercial gages with these standards by means of light interference, with an accuracy far greater than can be attained in the manufacturing shops of the country.

III. INTERFERENCE OF LIGHT

The sensation of light is due to transverse waves radiated by luminous bodies. These waves vary in length, giving rise to different color sensations. The range of the wave lengths visible to the eye is from about 0.4 micron (0.000016 inch) for blue light to 0.7 micron (0.000028 inch) for red.

Digitized by Google

If two trains of waves from one point in a source having traversed different paths fall upon a point on the retina of the eye, the resultant amplitude of vibration determines the brightness. If they are "in step," maximum brightness results. If, however, the troughs of the one arrive with the crests of the other, destructive interference takes place, resulting in relative darkness. If the two trains travel different distances, so that the difference in path is some whole number of wave lengths, then the waves will reach the eye in phase. If the difference in path is equal to some whole number of wave lengths plus one-half wave length, the waves in the two trains will be in opposite phase, so that destructive interference takes place. The conditions for interference are realized when light from an extended source S, Fig. 1, falls on a thin transparent film. Part of the light is reflected from the first surface, $ABCD$, and the remainder is transmitted to the second surface, $ABGF$, where partial reflection again takes place. Since the wave trains reaching E from these two reflections have traveled over different distances, reinforcement or destructive interference can, therefore, occur. When white light is used and the film is sufficiently thin, a few brightly colored bands are seen across its surface. If monochromatic light—that is, light of one color or of very limited spectral extent—be employed, alternate light and dark bands or interference fringes may be observed to cross the film.

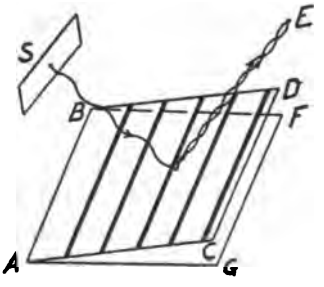

FIG. 1.—*Interference of light reflected from the surfaces of a thin film*

If one of the surfaces of the film be plane, the shape of the other surface can be obtained from measurements of the film thickness at several points. To derive the relation between the film thickness t and the shape of the interference fringes, consider the thin film formed by the two plane surfaces which are represented by the traces AC and AG, Fig. 2, inclined at a slight angle ϕ. Observing the film at an angle θ with the normal, rays of light originating at the point S in the source and reflected by the two surfaces AC and AG will appear to come from the two sources S_1 and S_2. The difference in path of two rays reaching E is $N\lambda$, where N is the "order of interference" or number of waves in the

Digitized by Google

distance S_2K and λ is the wave length of the monochromatic light. Let the distance between the two images of the source $S_1S_2 = h$.

$$\begin{aligned} N\lambda &= h\cos(\theta+\alpha) \\ &= h\cos\theta\cos\alpha - h\sin\theta\sin\alpha \\ &= 2(a+b)\sin\phi\cos\theta - 2d\sin\phi\sin\theta \\ &= 2(a+b)\sin\phi\cos\theta - 2b\sin\phi\cos\theta \\ &= 2a\sin\phi\cos\theta \\ &= 2t\cos\theta. \end{aligned} \qquad (1)$$

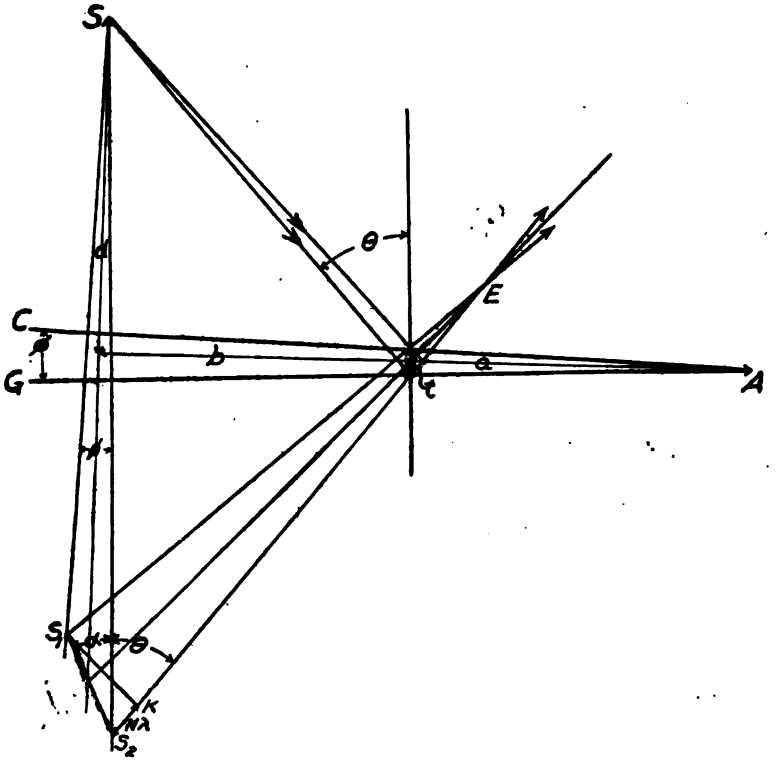

FIG. 2.—*Relation between the film thickness and the order of interference*

If N is an integer, the two wave trains will be opposite in phase, due to the phase change $\left(\frac{\lambda}{2}\right)$ by reflection at the denser medium,[7] and the point observed will in that case appear dark. The locus of the points for which N is a given integer is the interference fringe of the Nth order and appears as a dark band across the film.

[7] Only under special cases is this phase change exactly a half wave length; but it is not necessary in the present case to determine its exact value.

Digitized by Google

Equation (1) may also be expressed in the form

$$t = N \frac{\lambda}{2} \frac{l}{P}, \tag{2}$$

where P represents the perpendicular distance from E to the film and l the distance from E to the point at which t is taken.

IV. TEST FOR PLANENESS OF SURFACES

1. PERPENDICULAR INCIDENCE

In testing the planeness of polished surfaces, such as are produced on prisms, surface plates, precision gages, or micrometer anvils, a test plate is placed in close contact with and slightly inclined to the surface to be tested, thus forming a thin wedge-shaped film discussed in the previous section. This test plate is of glass, one surface of which has been polished accurately true plane and tested against a master true plane or liquid surface of large extent. The accuracy of the test is, of course, limited by the irregularities of the test-plate surface. It is very difficult to make glass surfaces 50 to 75 mm (2 to 3 inches) in diameter plane within 0.25 micron (0.000010 inch), and to reduce this error requires exceptional skill. For ordinary work, however, test plates plane within 0.25 micron (0.00001 inch) are sufficient, but when it is necessary to determine irregularities of a few hundredths of a micron (millionths of an inch) in the surface under test, great care must be exercised in selecting and testing the test plate.

In order to give a definite value to the wave length λ, the thin wedge-shaped film of air formed between the plane surface of the test plate and the surface under test is illuminated with monochromatic light. A convenient source of monochromatic light is a Bunsen flame, in which is inserted a piece of asbestos soaked in a salt solution, or a ground glass plate illuminated either by a helium lamp operated on a 5000-volt ac circuit, or by a mercury vapor lamp covered with a green glass screen. The wave lengths of the most effective visible radiation from these sources are approximately:

Sodium (yellow) = 0.589 micron (0.0000232 inch).
Helium (yellow) = 0.588 micron (0.0000231 inch).
Mercury (green) = 0.546 micron (0.0000215 inch).

A colored glass screen illuminated by an incandescent lamp or ordinary daylight may be used as a source if high precision is not

Digitized by Google

desired, but the light will not be sufficiently monochromatic to allow assignment of a definite value to the most effective wave length.

A very convenient instrument for illuminating the film and at the same time viewing the interference fringes on the film is one designed by Pulfrich[8] and shown in Fig. 3. The light from a helium lamp H is focused upon a small total reflection prism p. After being collimated by the lens O_1 it is reflected by the prism R down to the interferometer ABD, which is in the focal plane of the lens O_1. The rays reflected by the film surfaces are brought to a focus by the lenses O_1 and O_2 upon the slit S, and images of the interference pattern and the reference marks on the test plate are viewed with the eyepiece C. The direct-vision prism K separates the fringe patterns due to the helium light of different wave lengths. A pair of cross wires located at S and operated

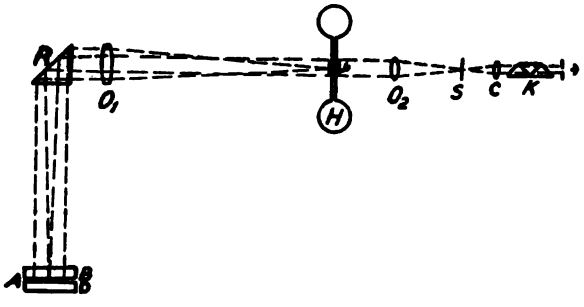

FIG. 3.—*Optical system of the Pulfrich instrument*

by a micrometer head make it possible to measure small displacements of the fringes from the straight reference lines ruled on the test plate AB. With this instrument and an exceedingly true test plate the planeness of an unknown surface can be measured with an accuracy of 0.025 micron (0.000001 inch). The only objection to the instrument is that the field is limited to about 2.5 cm (1 inch), so in testing a large surface only a small portion can be seen at one time. Instruments of similar optical design described by Schultz[9], Schönrock[10], and Laurent[11] eliminate this objection by having fields of view as large as 25 cm (10 inches). With these four instruments the rays of light coming from the source to the film surfaces are made parallel by the lens systems and when reflected back to the eye pass along the perpendicular

[8] Pulfrich, Zeits. f. Inst., 18, p. 261; 1898.
[9] Schultz, Zeits. f. Inst., 36, p. 252; 1914.
[10] Brodhun and Schönrock, Zeits. f. Inst., 22, p. 355; 1902.
[11] Laurent, C. R., 96, p. 1035; 1883.

Digitized by Google

to, say, the first surface, and this condition holds over the whole field of view. Under such conditions, in equation (1) $\cos\theta = 1$, and

$$2t = N\lambda, \tag{3}$$

which states that the difference in path of the two interfering trains is simply equal to the double thickness of the film (the double distance signifying that the light travels down and back through the film). From this equation it is evident that where N is constant—that is along any one fringe—t is also constant. Hence, the fringes trace lines of equal separation of the two surfaces.[12] Starting from the line of contact AB of the two plane surfaces, Fig. 4, and moving to a wider part of the film, when $2t = \lambda$ interference occurs causing the first dark fringe f_1 which is a straight line parallel to AB. When $2t = \frac{3}{2}\lambda$, the wave trains reinforce each other and a bright fringe is produced. Moving to a still thicker part of the wedge, where $2t = 2\lambda$, a second dark fringe f_2 will occur, etc. From this it is evident that if the surfaces are plane the fringes will be straight lines, equally spaced, and parallel to the line of intersection of the surfaces. The next dark fringe always occurs on passing to where the double separation increases by λ. Hence, the distance between fringes depends on the inclination of the surfaces.

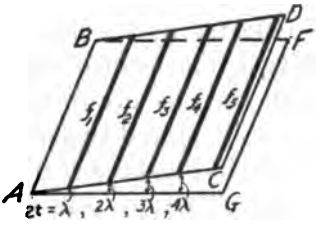

FIG. 4.—*Interference fringes, plane surface*

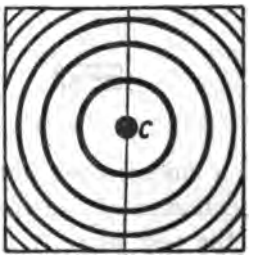

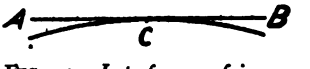

FIG. 5.—*Interference fringes, convex spherical surface*

If a plane surface be brought in contact with a convex spherical surface, Fig. 5, then at C the point of contact $2t$ is equal to zero. Radially from this point the separation of the surfaces increases uniformly in all directions, so the fringes, and hence the lines on which $2t = N\lambda$, are concentric circles around the point of contact as a center. On any ring the distance of the spherical surface

[12] The fact should be stressed here, however, that the fringe marks the line of constant thickness of the film only when the direction of view is perpendicular to the film over the whole film. Observed obliquely, straight fringes do not indicate that the tested surface is plane, as shown below.

Digitized by Google

from the plane is equal to the number of the ring, counting from the point of contact, times $\frac{\lambda}{2}$. By pressing down at A the plane surface can be made to roll on the spherical surface, shifting the point of contact and with it the center of the ring system in the direction of A or toward the point of application of the pressure. With a convex surface, therefore, the center of the ring system lies at the point of minimum separation.

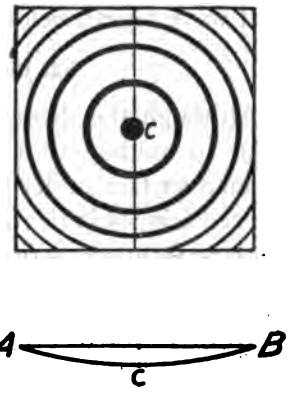

FIG. 6.—*Interference fringes, concave spherical surface*

If one of the surfaces be concave and spherical, Fig. 6, a similar system of concentric circular fringes is produced, but in this case the center of the system lies at the point of maximum separation. Pressing down on A causes the center of the ring system to shift toward B, the direction of increasing separation, away from the point of application of the pressure. Thus, a slight pressure on one edge of the plane surface AB serves to indicate whether the curved surface is convex or concave.

With one surface plane and the other irregular the fringes are irregular, each of which follows the line of equal separation of the surfaces. Whether the irregularity is a projection or depression can be determined by applying a slight pressure to one edge of the upper surface and noting the direction of shift of the fringes.

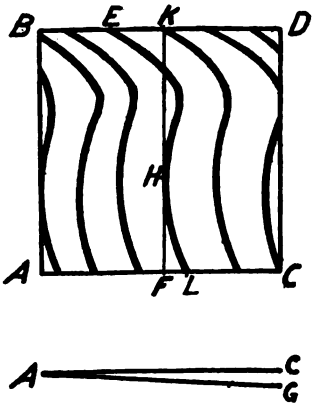

FIG. 7.—*Interference fringes, irregular surface*

The amount a curved surface deviates from a true plane can be readily estimated as follows: Draw a straight line FK, Fig. 7, across the center of the true plane surface, parallel to the line of contact AB of the surfaces. Bring this line tangent to one of the fringes at, say, the point H. It is evident that this line represents the direction a fringe through H would take if the irregular surface could be converted into a plane tangent to the irregular surface at H. The fractional

Digitized by Google

part of the distance between two fringes by which the fringe EL deviates from the straight line FK gives the fractional part of a half wave length by which the irregular surface deviates along FK from true plane. With AB as the line of contact, the point F is estimated to be one-fourth wave length above and K one-half wave length below the plane surface tangent at H.

2. ERRORS OF INTERPRETATION

Although the theory is quite explicit, it is a very common mistake to assume that straight fringes always indicate planeness when a surface under test is placed on a true plane, and conversely curved fringes indicate that the surface is not a true plane. Both of these interpretations may be wrong. For example, the operator may view the light reflected obliquely by the film, and to make sure that the fringes are straight he may lower his eye to sight along them. Or, the fringes from one position appearing curved, he may shift to another and find them quite straight, then draw his conclusions from what he observes under these, to him, best conditions.

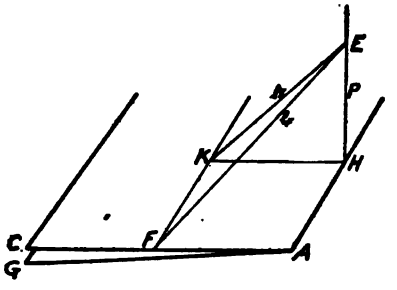

FIG. 8.—*Errors of interpretation caused by viewing the film obliquely*

It is important to know something about the magnitude of the errors which may be introduced by the assumption that straight fringes always indicate planeness and curved ones indicate curvature of the surface tested. The treatment of this falls under the general case shown in Fig. 2, where the thickness of the film at any point is given by equation (2)

$$t = \frac{N\lambda}{2}\frac{l}{P}, \tag{2}$$

which goes, for normal incidence, into equation (3)

$$t = \frac{N\lambda}{2}. \tag{3}$$

Suppose from the point E, Fig. 8, a straight fringe is observed along FK which is drawn parallel to AH. With one of the film surfaces plane, how much does the other diverge from plane

Digitized by Google

between F and K? Using (3) instead of (2) in determining the thickness of the film at any point gives

$$t' = \frac{N\lambda}{2}. \tag{4}$$

The error introduced is

$$t - t' = t'\left(\frac{l}{P} - 1\right). \tag{5}$$

The actual deviation from planeness between F and K is

$$\Delta t = t_F - t_K. \tag{6}$$

The observed deviation from (3) is

$$\Delta t' = t'_F - t'_K. \tag{7}$$

The error introduced by using (3) instead of (2) is

$$S = \Delta t - \Delta t' = \left(\frac{l_F}{P} - 1\right)t'_F - \left(\frac{l_K}{P} - 1\right)t'_K = \left(\frac{l_F}{P} - 1\right)\Delta t' + \frac{t'_K}{P}\Delta l \tag{8}$$

Where $\Delta l = l_F - l_K$.

This equation is seen to be consistent in that S becomes zero for normal incidence at both F and K, in which both $\left(\frac{l_F}{P} - 1\right)$ and Δl are zero.

Sighting along a line from a normal position over K, $l_K = P$;

$$S = t'_F\left(\frac{l_F}{P} - 1\right),$$

which states that the error in determining how much the tested surface deviates from the plane is simply equal to that in determining the thickness of the film at F, equation (5).

If one observes the fringe obliquely at both F and K, l_F and l_K increasing and at the same time approaching equality, we have for a given length FK the error represented by the term that contains $\Delta t'$, increasing with θ, while that represented by the term containing t'_K is decreasing. Take some numerical examples:

(*a*) With the eye 10 inches above the center of a 6-inch surface being tested on a true plane and viewing a diametrical fringe, $P = 10$, $l_F = 10.445$, $l_K = P$, applying (8)

$$S = 0.044\,\Delta t' + 0.044\,t'_K.$$

Digitized by Google

(*b*) With the eye moved back 10 inches in a direction at right angles to the fringe, P remaining constant, and viewing the center K and the farthest edge F, $l_F = 14.46$ $l_K = 14.14$ we have from (8)

$$S = 0.446\,\Delta t' + 0.032\,t'_K.$$

(*c*) With the eye moved back 20 inches instead of 10, $l_F = 22.56$, $l_K = 22.36$,

$$S = 1.256\,\Delta t' + 0.020t'_K.$$

A comparison of (*a*), (*b*), and (*c*) shows that the error arising from the actual deviation in planeness increases rapidly with oblique inspection, while the error rising from the thickness of the film decreases. Both these effects cause the fringes to straighten with increasing θ. Therefore, using oblique incidence slightly reduces the error of measurement if the surface under test is plane and greatly increases the error if the surface deviates from plane. An improvement on the customary apparatus is made by the addition of a thin plate of glass P, set at an angle of 45 degrees to the perpendicular EH from the eye to the surface, Fig. 9. With this arrangement the error due to deviation of the surface from plane is eliminated and a correction can be applied for error due to the film thickness.

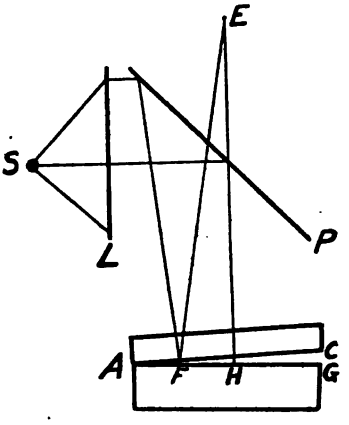

FIG. 9.—*Optical system for testing surfaces*

V. ADHERENCE OF SURFACES

When the plane surfaces of two gages, or of a gage and a glass plate, are brought into intimate contact, they adhere to each other, necessitating considerable force to separate them. To cause this adherence the surfaces are first washed with benzol, then with alcohol, and finally wiped with clean cotton to remove all traces of grease and dust. The surface of the plate is brought in contact with the gage surface and pressed on tightly to force out the film of air. A drop of alcohol when placed on the plate against the gage will spread out around the gage and pull the two surfaces into very close contact. Any excess of liquid can be forced out by sliding the surfaces on each other. When they

Digitized by Google

come into close contact the adhesive force causes them to grip each other and resist a large separating force.

A large number of measurements we have made show that when two very plane surfaces are brought into contact in this manner the separating film is not more than 0.025 micron (0.000001 inch) thick. Doubtless the surfaces come into intimate contact at the high points, the liquid filling the fine furrows or scratches left by the finishing laps. Our tests show that two gages with the ordinary lapped finish when brought into contact as described require to separate them a pull in the direction perpendicular to the surfaces of from 2.5 to 2.8 kg, per square centimeter (35 to 40 pounds per square inch).

With gages possessing a high optical polish more intimate contact is possible—that is, the capillary film is much thinner—and the required separating force ranges between 6.7 to 7 kg. per square centimeter (95 and 100 pounds per square inch). Considering the extreme thinness of the separating film when good contact exists, the need of exceedingly plane surfaces is apparent. A nick or burr on the edge or a small surface elevation which holds the two surfaces 0.25 micron (0.00001 inch) apart makes adherence almost impossible. Two surfaces will also adhere when covered with a film of grease or with moisture from the hand. The thickness of these films, however, is a rather indefinite quantity, in most cases about 0.07 micron (0.000003 inch), and while considerable force is required to slide the gages on each other they can be pulled apart by a force of 5 to 10 pounds per square inch. With gages having slight surface imperfections the oil film assists somewhat in holding them together and for the ordinary uses of gages the existence of the oil or grease film introduces no appreciable error, but in making accurate calibration of the gages themselves it should be eliminated.

The results obtained with two different combinations of gages are given in Table 1 to illustrate the effect produced by the film between the gages. The five gages in the first set were brought into contact as described above. The measured length of the combination differed from the sum of lengths of the individual gages by four millionths of an inch. The nine gages in the second set were first brought into contact as described above. In this case the measured length of the combination A differs from the sum of the lengths of the individual gages by six millionths of an

Digitized by Google

inch. The gages were then separated, rubbed across the wrist, and brought into contact again. The measured length B shows that the length of the combination increased by thirty-four millionths of an inch. This indicates that a film of moisture about three to four millionths of an inch in thickness had been introduced between each pair of gages.

TABLE 1.—Comparison of the Measured Lengths of Gage Combinations

Designation of length	Inches
Gages 0.30+0.25+0.20+0.125+0.120 inch:	
Sum of individual lengths	0.995011
Measured length of combination	.995015
Gages 0.15+0.25+0.30+0.35+0.40+0.45+0.55+0.60+0.90 inch:	
Sum of individual lengths	4.000079
Measured length of combination A	4.000073
Measured length of combination B	4.000107

VI. TEST FOR PARALLELISM OF SURFACES

The arrangement of the apparatus used to test the parallelism of the surfaces of a standard gage is shown in Fig. 10. Two

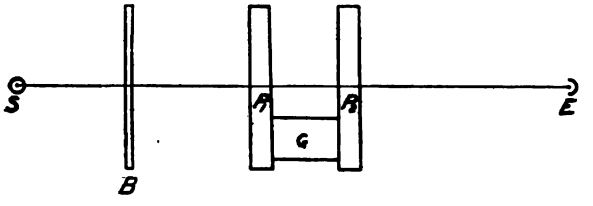

FIG. 10.—*Optical system for testing parallelism of gage surfaces*

accurately plane interferometer plates P_1 and P_2 have a semi-transparent film of platinum on their inner faces. Near one edge of each a strip of the platinum about one-half inch wide is removed. This clear area on P_1 is brought in contact with one end of the gage, G, and that of P_2 with the other end of the gage. This combination of plates and gage constitutes a Fabry and Perot interferometer. When this interferometer is placed in front of the ground glass screen B illuminated with monochromatic light from the source S, and viewed from E along a line SE perpendicular to the platinized surfaces, concentric interference rings known as "Haidinger rings" are seen. When the eye E is moved in a direction perpendicular to the line of sight SE, the system of rings moves across the plates in the same direction, the center of the system always remaining on the perpendicular from the eye

Digitized by Google

to the surface. If, now, the interferometer surfaces are parallel to each other, which means that the two gage surfaces which are in contact with them must also be parallel, each ring will retain its original diameter when the eye is moved as designated. If the plates are not parallel, the rings expand on moving opposite points of greater separation and contract as the eye is moved in the direction of smaller separation. Suppose that when the eye is shifted, so that the center of the ring system moves across the plates from one edge to the other, the first central ring expands and takes the place originally occupied by the second (a new ring forming within); then the distance between the two interferometer plates has increased by one-half wavelength, which for yellow helium light is about 0.29 micron (0.000011 inch). If the width of the gage is one-fourth that of the platinized space, this would mean a difference of about 0.07 micron (0.000003 inch) between the gage lengths along opposite sides. Since an expansion of

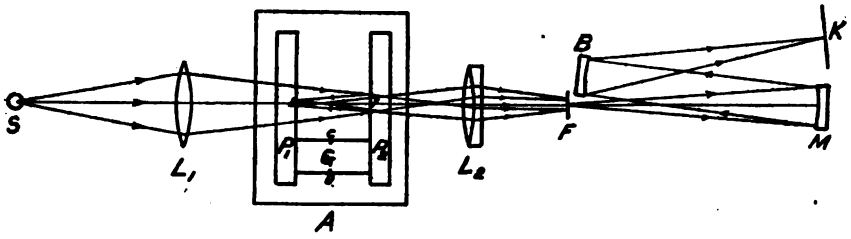

FIG. 11.—*Optical system for determining the length of a gage by means of light waves*

the rings can be estimated to one-fourth of the diameter of the first ring, an error of 0.025 micron (0.000001 inch) in the parallelism of the gage surfaces can be detected. To realize this precision, however, special care must be taken to have the surfaces of the gage in very close contact with the plates.

VII. CALIBRATION OF END STANDARDS WITH THE FABRY AND PEROT INTERFEROMETER

1. GENERAL PLAN OF APPARATUS

The arrangement of the apparatus used to measure gages in wave lengths is shown in Fig. 11. The interferometer formed by the gage and plates of Fig. 10 is placed within a constant temperature chamber A in front of the slit of a grating or prism spectrograph. Light from the neon lamp S is focussed by the lens L_1 upon the interferometer P_1P_2. Part of the light is transmitted directly through the interferometer, part is reflected by the

Digitized by Google

platinized surface of P_2 to the platinized surface of P_1, where it is again partially reflected, and then a part of it passes on through P_2, and so on through a large number of multiple reflections and transmissions. The reflected and directly transmitted parts when combined produce a system of interference rings which is focussed by the lens L_2 upon the slit F of the spectrograph. The images of the slit corresponding to the different radiations from neon are separated by the grating B and recorded on the photographic plate K.

2. SOURCE OF LIGHT

The source of light used in this work was an electric discharge tube filled with neon gas and operated on a 10 000 volt ac circuit. Wave lengths between 0.58 and 0.70 micron (0.000023 and 0.000028 inch) were used in making the determinations. The radiations from neon gas are very homogeneous and show good interference with large path differences, making it possible to measure gages 5 cm (2 inches) in length without difficulty. Longer gages can be measured if a telescope is used in making the interferometer adjustments. A limit on the maximum length of gage which can be compared directly with light waves by this interference method is imposed by the fact that no spectral lines are ideally homogeneous or monochromatic. Under ordinary conditions the neon lines fail to show interference when the retardation exceeds 300 000 waves. This permits direct comparison with 10 cm gages. The spectral lines of krypton are sharper and would allow 20 cm gages to be measured by this method.

3. INTERFEROMETER

The interferometer plates were glass disks 42 mm (1.7 inches) in diameter and 8 mm (0.3 inch) in thickness, or glass plates 5 cm (2 inches) square and 1 cm (0.4 inch) thick. These plates were covered with thin platinum films by the method of sputtering from a platinum electrode in a vacuum. Bringing a gage in contact with the platinum film causes the film to scale off, making adherence impossible. To eliminate this difficulty, a strip of the platinum a little larger than the gage surface was removed from each plate and the gage surface brought into contact with the clear glass surface. The gages which formed the separators or étalons for the interferometer plates varied in length from 1 mm to 5 cm and from 0.05 to 2 inches.

Digitized by Google

4. CONSTANT-TEMPERATURE CHAMBER

Since the length of a gage varies with the temperature, it is necessary to measure and specify the length at 20° C, which has been chosen as the standard temperature for measuring instruments. This was accomplished by placing the interferometer in a chamber *A* surrounded by a thermostated bath previously described.[13] The temperature of the bath was brought to the desired point and held for a period of at least one-half hour before beginning the photographic exposures in order to allow the gage to assume a steady state.

5. SPECTROGRAPH

Dispersing apparatus of some kind is required in order that length measurements may be made with various colors or spectral lines such as are emitted by luminous neon gas. For this purpose either a prism spectrograph or a diffraction grating may be used, but the concave grating mounted in parallel light with the aid of a mirror has certain advantages in stability, achromatism, and minimum astigmatism over any other type of spectrograph which might be considered as suitable for these measurements.

For most of the work the grating spectrograph of the spectroscopic laboratory was used. *M* is a speculum concave mirror and *B* a concave grating. The mirror and grating each have a radius of curvature of about 640 cm. (21 feet). The grating was ruled by Dr. Anderson and has 39 800 lines on a distance of 13.2 cm. (5.2 inches). The linear dispersion at *K* with this apparatus is about 10 A per millimeter in the spectrum of the first order.

6. PHOTOGRAPHIC

The spectrum of neon between the wave length limits 0.58 and 0.70 micron (0.000023 and 0.000028 inch) was recorded on Seed 27 photographic plates after staining with pinacyanol.[14] The exposure times ranged from 5 to 10 minutes. Since the slit was illuminated by radiations, each of which produced a system of interference rings, the photograph of the spectrum shows the images of the slit crossed by arcs of the ring systems. The diameters of the interference rings were measured by means of a micrometer screw with a head graduated to 5 microns. By substituting a micrometer eyepiece for the photographic plate visual observations could be made on the diameters of monochromatic

[13] Meggers and Peters, B. S. Sci. Papers, No. 327, p. 713; 1918.
[14] Meggers and Stimson, J. Op. Soc. Am., 4, No. 3; 1920.

Digitized by Google

fringes, but a photographic impression of the interference phenomena is generally to be preferred.

7. DETERMINATION OF THE ORDER OF INTERFERENCE

Neglecting here any difference in phase change by reflection at the surfaces (treated in section 9) the thickness of the air space between the two interferometer plates is given by the equation

$$t = \frac{N\lambda}{2} = (n+n')\frac{\lambda}{2}, \tag{9}$$

where N is the order of interference at the center of the ring system, n that of the first ring, and hence n' the fraction difference in order between the first ring and the center of the system. In carrying out the computations n' is calculated as the fraction part of the order by which *any* given ring differs from N. The formula for calculating this is given by Meggers [15]

$$n' = \frac{n\omega^2 d^2}{8r^2}, \tag{10}$$

where d is the diameter of any given ring image, r the corresponding length of the image of a stop placed across the slit, and ω the angle subtended by this stop at the lens, L_2, which projects the ring system on the slit. It is obvious that the approximate value of n obtained by using the nominal length of the gage which separates the plates is sufficient for calculating the value of n'.

The exact value of n is obtained as follows: If T be the nominal length of the gage, the approximate value of n is, for any given wave length,

$$n_1 = \frac{2T}{\lambda_1}.$$

From this

$$n'_1 = \frac{n_1\omega^2 d^2}{8r^2},$$

which, together with n_1, gives a tentative value T_1 for the thickness. This value T_1 is then used to calculate the trial value $N_c = n_c + n'_c$ of the order for each wave length used. From these approximate values of n and the measured diameters of the rings, n' for each wave length is obtained by substitution in (10). We

[15] Meggers, B. S. Sci. Papers, No. 251; 1915.

Digitized by Google

now have two values for the fraction part of the order—one, n', obtained from the measured diameter of the rings, and the other, n'_0, from the trial thickness of the gage. If these magnitudes coincide for the various wave lengths within the limits of experimental accuracy, it shows that n_1 has been correctly chosen. Otherwise n_1 must be corrected by some whole number, y, which may be determined as follows:

Let $R = \frac{\lambda_1}{\lambda}$ be the ratio of the wave length used for obtaining the trial value to the wave length being used to correct it. Since changing n_1 by the whole number y changes N for a wave length λ by Ry, and hence n' by $(1-R)y$, we have the difference between the observed and calculated values

$$n' - n'_0 = (1-R)y,$$

from which

$$y = \frac{n' - n'_c}{1-R}.$$

This serves to calculate for λ_1 a value t_1 for the thickness, which is subject only to the errors of measurements, not to the inaccuracy in the nominal length of the gage.

$$t_1 = \frac{\lambda_1}{2}(n_1 + y + n'_1).$$

From this corrected thickness the order of the first ring is readily computed for each wave length. These values of n and the computed fraction n' are then substituted in (9). Each wave length thus furnishes independently a value for t, from which the mean value is finally obtained.

8. CORRECTION OF λ

The wave lengths which are given for standard conditions of 15° C and 760 mm pressure vary with changes in the density of the air. The wave lengths must therefore be corrected to the existing temperature and pressure conditions. Since this correction and the dispersion of the air are small, it is sufficient to apply the correction factor

$$f = \frac{\mu_{15}}{\mu_t}, \text{ where } \mu_t = 1 + \frac{(\mu_{15} - 1)\, P\, 288}{760\, T},$$

Digitized by Google

to the mean value of the thickness t, given above, to obtain the optical thickness t_p of the space at EF between the two platinum films.

9. CORRECTION FOR THE THICKNESS OF THE PLATINUM FILMS

With unplatinized interferometer plates the distance t_g (at EF, Fig. 11, between the two glass surfaces as computed above from measurements of the rings would be the true distance between the plates, because the phase change of π due to the two air-glass reflections is eliminated in the determination of n. With the platinized surfaces, however, t_g differs from t_p by a small correction $x = t_g - t_p$, which is equal to the thickness of the films plus or minus the change in the optical path due to the difference in phase change for air-glass and air-platinum reflections. To measure x, a glass test plate is placed over each interferometer plate so as to cover both the clear and platinized parts. Each gives a system of fringes arising from the interference between the front and back surfaces of the thin air films inclosed. The system over the platinized area, owing to the combined effect of difference in thickness of the air film and difference in phase change by reflection, is displaced (less than one order) relative to the system from the clear portion. Multiplying by $\frac{\lambda}{2}$ the combined displacement resulting at the two plates, when tested with the light in the same direction as under working conditions, gives the correction x to be applied to the thickness of the gage as calculated in section 8.

10. CORRECTION FOR NONPARALLELISM OF THE GAGE SURFACES

If the gage surfaces are parallel, the interferometer plates will be parallel, and the length L of the gage is

$$L = t_g = t_p + x.$$

If the gage surfaces are not parallel, a correction must be applied to t_g to obtain L. Having the difference $z = L_C - L_D$ in the length of the gage along the two opposite sides C and D, Fig. 11, obtained as explained in section VI, and making the distance from EF to the gage at C equal to the width of the gage, the length along C is obviously

$$L_C = t_g - z,$$

and along D is

$$L_D = t_g - 2z.$$

Digitized by Google

11. COMPUTATIONS

An illustration of the method for making the computations for a 25.4 mm (1 inch) gage is shown in Table 2. Column 1 gives the wave lengths used; 2, the measured diameter d of the first and second rings, respectively; 5, the fractional part n' of the order at the center of each ring system; 6, the order of interference N or number of waves in the double distance between the plates at the center of the ring $N=n+n'$; and 7, the double optical thickness of the air film or $N\lambda$.

TABLE 2.—Computing Method for a 25.4 mm Gage

1 λ in Ångstrom units	2[a] d	3 d^2	4 $\frac{d^2\omega^2}{8r^2}$	5 n'	6 N	7 $2t$ in microns
5852.488	455 676	207 457	93 205	0.807 1.779	86 802.793	50 801.2304
5944.834	341 602	116 362	52 162	.444 1.384	85 454.414	50 801.2306
6096.163	551 746	304 557	136 205	.133 1.083	83 333.108	50 801.2210
6143.062	495 713	245 508	110 228	.910 1.885	82 693.898	50 801.2254
6334.428	409 667	167 445	75 199	.601 1.596	80 199.599	50 801.2251
6506.528	295 612	87 375	39 168	.304 1.312	78 077.308	50 801.2191
6678.276	344 631	118 398	53 178	.403 1.354	76 069.379	50 801.2308
$f=1.0000102$						
Mean value of $2t$						50 801.2261
Corrected for density of air, $2t\times f=2t_p$						50 801.7442
t_p						25 400.8721
Correction for film thickness, x						.0701
Distance between glass plates, t_g						25 400.9422
Correction for slant of gage surface, $-z$						.0367
Length of gage at C, L_C						25.4009789 mm 1.0000365 inch
Length of gage at D, L_D						25.4010156 mm 1.0000380 inch

[a] In columns 2 to 5, the figures in each group of two refer, respectively, to the first and second rings.

12. ACCURACY AND SOURCES OF ERROR

A comparison of the values obtained for the thickness of the air film, Table 2, column 7, shows that the maximum variation of t for the several wave lengths is about one part in five million when using a 1-inch separator. The correction for the change in λ arising from a change in density of the air is about one part in one hundred thousand. With the accurate values of the refractive index of air[16] available, this correction should not introduce an

[16] Meggers and Peters, B. S. Sci. Papers, No. 327; 1918.

Digitized by Google

error of one part in ten million in the total length. The combined thickness and phase difference effect of the platinum films is about 0.07 micron (0.000003 inch), and the probable error in measuring this thickness about 0.003 micron (0.0000001 inch), which would introduce an error in the value of the distance between the plates of about one part in ten million. Therefore, using a 25 mm (1 inch) étalon and making measurements with several wave lengths, the value of the distance t_g between the glass surfaces at *EF* should be correct relative to the International meter to about 1 part in four or five million.

Transferring this measured distance to the gage introduces the greatest error. With a perfect gage and perfectly plane interferometer plates the only sources of error are the films between the gage surfaces and the plates. If the surfaces are thoroughly cleaned and carefully brought into contact, the separation is less than 0.025 micron (0.000001 inch). It is probable that slight projections on the surfaces are in intimate contact and that the liquid film exists in the intervening spaces. Therefore, with carefully controlled conditions, the error in the measurement of perfect gages should be less than 0.025 micron (0.000001 inch).

In actual practice, however, most interferometer plates obtainable deviate from true plane by about 0.05 micron (0.000002 inch), and the surfaces of carefully selected gages deviate from true plane and parallelism by about 0.13 micron (0.000005 inch) on the average. Therefore, in transferring t_g to the gage the error introduced depends largely upon imperfections of the gage. With carefully selected gages the errors in the values of the length along the C and D sides range from 0.025 to 0.075 micron (one to three millionths inch).

The measurements made on one of our standards (1-inch, set 7) shown in Table 3 are representative of the values obtained for several hundred other standards. Each value given is the result of a single determination made after a separate assembling of the interferometer and adjustment of the spectrograph. The first determination of January 11, 1921, was made with the grating spectrograph shown in Fig. 11. The second determination of that date was made with a different pair of interferometer plates and a prism spectrograph.

Digitized by Google

TABLE 3.—Length of 1-Inch Gage of Set 7 at 20° C

Date	Length	Date	Length
	Inches		Inches
Feb. 4, 1918	1.0000008	Feb. 7, 1918	0.9999992
Feb. 7, 1918	.9999996	Mar. 17, 1920	.9999983
Do	.9999990	Jan. 11, 1921	.9999974
Do	.9999993	Do	.9999968

Another very important source of error that may be overlooked is the thermal expansion of the material. A 25 mm (1-inch) length of steel expands about 0.32 micron (0.000013 inch) per degree Centigrade rise in temperature. The gage must therefore be held at the constant temperature of 20° C within a few hundredths of a degree. If the measurements are made at any other temperature, this must be accurately measured and the expansivity of the material known in order to reduce the length to standard conditions. We have found expansion coefficients ranging from 0.000011 to 0.000013 for gage steels of various compositions, hardness, and previous heat treatment. This shows that it is unsafe to assume a value for the expansivity when measuring the absolute length of a gage or comparing an unknown gage with a standard at a temperature that differs very much from 20° C.

TABLE 4.—Thermal Expansion of Several Precision Gages

Gage	Temperature interval	Coefficient of expansion $\times 10^4$	Gage	Temperature interval	Coefficient of expansion $\times 10^4$
	°C			°C	
Johansson, set 5813, 10 mm	20 –50	0.129	Bureau of Standards:		
Do	20 –50	.129	Steel A, 0.4 inch	24.0–76.9	0.132
Johansson, set 5813, 9 mm	20 –50	.125	Steel B, 0.4 inch	33.0–82.8	.129
Do	20 –50	.125	Pratt & Whitney, 0.375 inch	21 –78	.135
Johansson, set 20, 0.4 inch	19.8–75.5	.124	Schuchardt and Schutte, 0.5		
Do	32.8–76.5	.123	inch	5.8–46.0	.116
Johansson, set 7, 0.4 inch	56.3–79.6	.131	Do	5.8–46.0	.115
Do	19.6–79.6	.132			
Johansson, set 7, 0.35 inch	21.3–82.4	.128			
Do	20.6–82.4	.127			

In Table 4 is shown the thermal expansion of several precision gages. These measurements were made with the interferometer and electrical furnace previously described in our publication [17]

[17] Peters and Cragoe, B. S. Sci. Papers, No. 393; 1920.

Digitized by Google

on the dilatation of optical glass. Column 1 gives the designation of the gage under investigation; column 2, the temperature interval; and column 3, the coefficient of expansion.

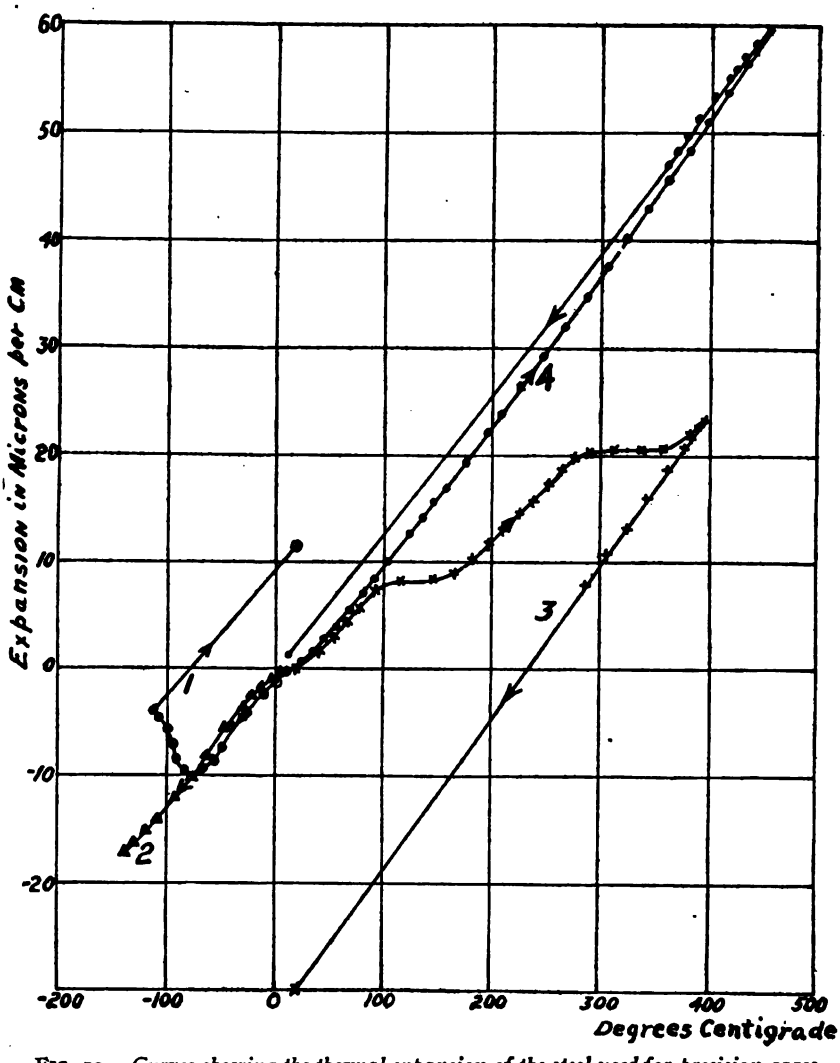

FIG. 12.—*Curves showing the thermal expansion of the steel used for precision gages*

The composition of steel B which is used for precision gages at the Bureau of Standards is C, 1.00 to 1.10 per cent; Mn, 0.30 to 0.40 per cent; P, 0.025 per cent; S, 0.025 per cent; Si, 0.20 to 0.30 per cent; Cr, 1.30 to 1.50 per cent; balance, Fe. This is almost identical with the compositions that have been published

Digitized by Google

for the steels used in the Johansson and the Pratt & Whitney gages.

The thermal expansion of a gage about 1 cm long and 2 cm in diameter made from steel B is shown in Fig. 12. It was hardened by heating to 850° C and quenching in oil. The original hardness was 95 as measured with a scleroscope, and length was 11.024 mm. The sample was first cooled to −114° C, the change in length being represented by curve *1*. On returning to room temperature the hardness was 94.5 and the length 11.035 mm; that is, the length had increased 12 microns due to this treatment. After cooling again to −135° C, represented by curve *2*, and returning to room temperature the hardness was 94 and length 11.035 mm. No further change in length took place. The sample was then heated to 392° C and allowed to cool to 20° C, change in length being represented by curve *3*. The final hardness was 76 and length 11.004 mm. This treatment caused a permanent shortening of about 31 microns. The sample was then heated to 450° C and allowed to cool to 20° C. The change in length is represented by curve *4*.

TABLE 5.—Changes of Length with Time

Gage	Date	Length	Gage	Date	Length
		Inches.			Inches.
1.000 inch	Mar. 1, 1919	1.000000	2.000 inches	Mar. 19, 1920	1.999993
	June 3, 1919	.999998		May 22, 1920	1.999992
	July 19, 1919	.999992			
	Aug. 19, 1919	.999992	3.000 inches	Feb. 20, 1919	3.000000
	Oct. 16, 1919	.999993		Apr. 28, 1919	2.999975
	Mar. 20, 1920	.999988		Aug. 20, 1919	2.999900
	May 21, 1920	.999988		Sept. 19, 1919	2.999877
				Mar. 18, 1920	2.999856
1.000 inch	May 21, 1919	1.000000		May 21, 1920	2.999851
	May 29, 1919	1.000018			
	June 17, 1919	1.000022	4.00 inches	Apr. 29, 1919	4.000000
	Aug. 19, 1919	1.000034		June 2, 1919	3.999998
	Oct. 17, 1919	1.000038		July 19, 1919	3.999992
	Jan. 7, 1920	1.000043		Aug. 19, 1919	3.999980
	Mar. 20, 1920	1.000044		Oct. 16, 1919	3.999980
	May 22, 1920	1.000047		Mar. 18, 1920	3.999971
				May 21, 1920	3.999970
2.000 inches	Mar. 1, 1919	2.000000			
	May 29, 1919	1.999976	4.00 inches	May 7, 1919	4.000000
	July 19, 1919	1.999966		June 3, 1919	4.000014
	Aug. 19, 1919	1.999963		Aug. 20, 1919	4.000025
	Oct. 16, 1919	1.999951		Nov. 26, 1919	4.000021
	Mar. 18, 1920	1.999938		May 21, 1920	4.000025
	May 21, 1920	1.999935			
			4.00 inches	Dec. 22, 1919	4.000000
2.000 inches	Sept. 24, 1919	2.000000		Mar. 18, 1920	3.999999
	Oct. 16, 1919	2.000002		May 21, 1920	3.999993
	Jan. 9, 1920	2.000000			

Unless the material from which the standards are made is exceedingly stable the high accuracy of the length determination is soon lost due to changes in the length with time. While we have found many steel gages that retain their dimensions remark-

Digitized by Google

ably well, others have been found to change several microns—or hundred thousandths of an inch—in a few months. A few examples of gages that have undergone changes of length with time are given in Table 5. The fact that these changes may take place requires frequent intercomparisons and redeterminations of the gages used as standards.

VIII. COMPARISON OF GAGES WITH STANDARDS

1. COMPARISON OF LENGTH

The accurate comparison of two gages, *A* and *B*, Fig. 13 (front), of supposedly the same length, is made by the following method:

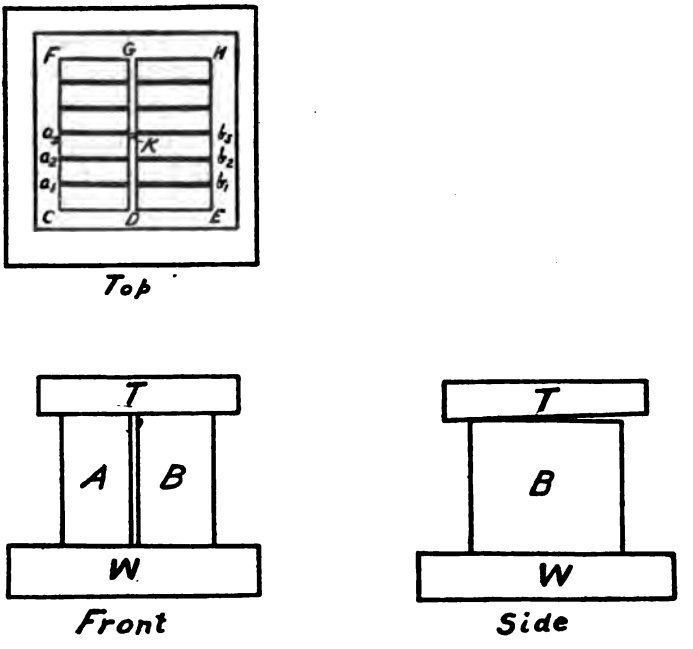

FIG. 13.—*Intercomparison of two similar gages of equal length*

The two gages are placed side by side in intimate contact, as described in *V* above, with the true plane surface of a glass plate *W*. The lower surfaces of the two gages being in the same plane, the problem is then simply to determine the distance between the planes of the two upper surfaces. This is done by placing a test plate *T* in contact with the gages along the line *CDE*, Fig. 13 (top), and somewhat inclined to these surfaces. This gives side by side two thin wedge-shaped films. When illuminated and viewed as shown in Figs. 3 or 9, two sets of straight fringes parallel

Digitized by Google.

to the edge of the wedge are seen; see top view, Fig. 13. Since it is only necessary then to determine the difference in thickness of these films at some adjacent position, say K, we can assume zero phase changes at the surfaces and calculate the distance at that point between the planes of the two gage surfaces. If the two gages are of the same length, their upper surfaces will lie in the same plane, so when we pass to the thicker part of the wedge from the line of contact CDE, the first fringe a_1 on A will coincide with the first fringe on b_1 on B, the second with the second, etc.

Consider the point K, where there is coincidence between the third fringes on the two gages. For perpendicular view the optical thickness of the film at any point is given by equation (3)

$$t = \frac{N\lambda}{2}.$$

In this case the distance t from the test plate to each gage would be $\frac{3\lambda}{2}$ at K, which means that the gages are of equal length.

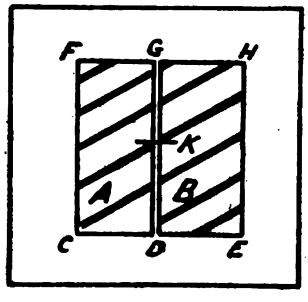

FIG. 14.—*Intercomparison of two similar gages of slightly different length.*

Suppose the gages are unequal in length, say B is shorter than A. The test plate will then come in contact with A at the point D and with B at the point E and the fringes appear, as in Fig. 14. If at K, we have the second fringe over A coinciding with the fourth over B, the distance at that point between the test plate and A is $\frac{2\lambda}{2}$ and between the test plate and B is $\frac{4\lambda}{2}$. Therefore, the distance between the planes of the two gage surfaces is $\frac{2\lambda}{2}$. If we are using a helium lamp for a source, $\frac{\lambda}{2}$ is about 0.3 micron (0.000012 inch), hence B is about 0.6 micron (0.000024 inch) shorter than A. If A is a calibrated standard, we immediately have the length of the unknown gage B. By estimating the displacement of the fringes to one or two tenths of the distance between two bands measurements of still greater refinement can be made. In making these measurements it is absolutely essential that the fringes be viewed with the Pulfrich or other instruments previously referred to, or as shown in Fig. 9; that is, normally to

Digitized by Google

the gage surfaces. If they are viewed at an angle to the perpendicular, then the thickness is not equal to $\frac{N\lambda}{2}$, but equal to $\frac{N\lambda}{2}\frac{l}{P}$, so that an incorrect interpretation of the distances is made.

When observing with the unaided eye, as shown in Fig. 9, it is not advisable to make comparisons between gages that differ in length by more than five or six wave lengths. With the aid of the Pulfrich instrument, however, comparisons between gages that differ in length as much as ½ inch may be made. With this method the fractional orders n' at the point K over each gage are measured for several different radiations of helium gas. The orders of interference N for each wave length are then computed from these fractions and the approximate distance between the test plate and the upper surface of each gage by the method described in Section VII, which holds for straight fringes as well as for Haidinger rings.[18]

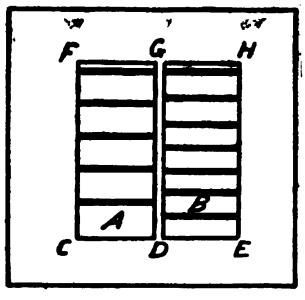

FIG. 15.—*Test for parallelism of gage surfaces. B shorter at GH than DE*

The absolute length of a gage is found in the same way. The gage is brought in contact with a steel base plate and the thicknesses of the air columns over the gage and base plate, respectively are measured. The distance between the test plate and the base plate minus the distance from the test plate to the gage gives the length of the gage. The steel base plate is used in order to eliminate any difference in phase losses on reflection. This method was used in calibrating most of the end standards less than 5 mm (½ inch) in length, because the operation of making the measurement and computations requires only about one-third the time consumed when using the circular fringe method.

2. COMPARISON OF PARALLELISM OF SURFACES

The test for parallelism of the two surfaces of an unknown gage B is made along with the length comparison. Assuming that the two surfaces of the standard gage A, Fig. 15, are plane and parallel, the test plate brought in contact with it along CD gives straight fringes over A which are parallel to CD and equally spaced. If the upper surface of the gage B is parallel to the plane of the upper surface of A, the fringes over B will be parallel to those over

[18] Peters, J. of Wash. Acad. of Sci., 9, p. 282; 1919.

Digitized by Google

A and have the same spacing. If, however, the length of B at GH is less than at DE, then the wedge over B will be steeper than over A and the fringes closer together. Therefore, if as indicated 7 fringes are observed over B and 5 over A, GH is $\frac{2\lambda}{2}$ below DE, or the gage is about 0.000022 inch shorter on the GH side than on the DE side. If the length of B at GH is greater than at DE, then the wedge over B will be thinner than over A and the fringes farther apart. If the surfaces of the standard A are not parallel, then to determine the true slant or lack of parallelism of the surfaces of B along DG, the apparent slant is determined as described above. Letting A_{FG}, B_{GH}, etc., also denote the lengths of the gages along those sides, we have $B_{GH} - B_{DE} = s$. If now from other sources it is known that the slant of A is $A_{FG} - A_{CD} = a$, then the true slant of B is

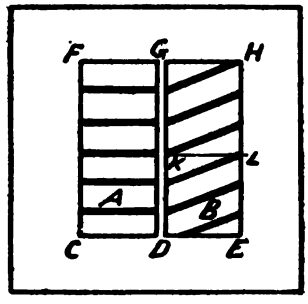

FIG. 16.—*Test for parallelism of gage surfaces. B longer at HE than at GD*

$$b = a + s, \tag{11}$$

a, b, and s being positive or negative, as the case may be.

Suppose, as in Fig. 16, that the edge GD of B is parallel to the plane of the upper surface of A, but the surface of B slopes slightly, so that HE is above GD. Since the fringes lie along lines of equal thickness of the air film, they will extend across B at an angle to those over A, being deflected toward the open end of the film or toward H. If HE is below GD, the fringes on B will be deflected toward the thin edge of the film or toward E, as in Fig. 17. If we draw a line KL parallel to CE from the left end of any fringe over B, the displacement of the other end of that fringe from KL divided by the distance between two consecutive fringes gives the difference in height between GD and HE in half wave lengths. This difference gives the slant between the upper surface of A and the upper surface of B. If the two surfaces of A are perfectly parallel, it is also the slant between the two surfaces of B. If the

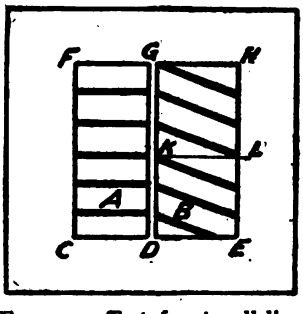

FIG. 17.—*Test for parallelism of gage surfaces. B shorter at HE than at GD*

Digitized by Google

two surfaces of A are not parallel, but the slant $A_{GD}-A_{FC}=c$, using the same expression for length as above, then the true slant of B is equal to the observed apparent slant $B_{DG}-B_{HE}=d$ minus kc, where k is the ratio of the widths of the gages B and A; that is,

$$f=d-kc. \tag{12}$$

The slant of the two surfaces of B can also be determined by measuring the perpendicular distances between them, say, at the middle points of all four edges of B, by bringing them successively contiguous to A at the point K.

When determining the length of a gage or standard with the Pulfrich instrument, the fringes over the gage should be parallel to and equally spaced with those over the base plate. Any deviation from such a condition signifies that the gage surfaces are not parallel, in which case the amount of nonparallelism may be determined by the method just described on making a and c equal to zero in the formulas (11) and (12).

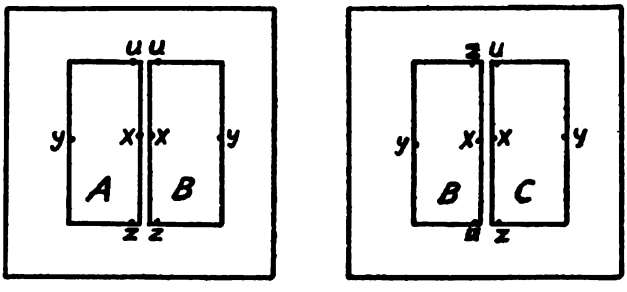

FIG. 18.—*Test for relative length of gages and parallelism of the surfaces by the intercomparison of three similar gages*

IX. INTERCOMPARISON OF THREE GAGES

The lack of parallelism of the two faces at each of three unknown gages, A, B, and C, can be accurately determined and an intercomparison between their lengths made by bringing them in contact with the base plate two at a time. Let A_x, B_x, C_x, A_y, etc., denote the lengths of the gages at the points x, y, z, u, indicated in Fig. 18, and

$$A_K=A_u-A_z, \qquad A_S=A_x-A_y,$$
$$B_K=B_u-B_z, \qquad B_S=B_x-B_y,$$
$$C_K=C_u-C_z, \qquad C_S=C_x-C_y,$$

represent, respectively, the slants of the gages A, B, and C in the two perpendicular directions uz and xy. If the gages A and B are brought into contact with the base plate, so that A_u and B_u,

Digitized by Google

A_x and B_x, and A_z and B_z are adjacent, as in Fig. 18 (left) (gage A face up and B face down), then one can make the comparisons between the lengths of the gages:

$$A_u - B_u = r,^{19}$$
$$A_z - B_z = s,$$
$$A_x - B_x = l,$$

and observe the apparent slant $B_x - B_y = a$ on B. Gage B can then be replaced by C and a similar comparison made

$$A_u - C_u = t,$$
$$A_z - C_z = q,$$
$$A_x - C_x = m,$$
$$C_x - C_y = b \text{ (apparent slant)}.$$

Then B replaces A, so that B_z and C_u, B_u and C_z, and B_x and C_x are adjacent (both gages face down), Fig. 18 (right). The final comparisons to be made are:

$$B_z - C_u = v,$$
$$B_u - C_z = w,$$
$$B_x - C_x = n,$$
$$C_x - C_y = c \text{ (apparent slant)}.$$

Solving these twelve equations:

(1) $$m - l = n$$

showing that this method gives a comparison of the lengths of the gages at the corresponding x-points, and a check on this comparison.

(2)
$$A_K = r - q + w,$$
$$= t - s - v,$$
$$B_K = A_K - r + s,$$
$$C_K = A_K - t + q,$$

giving two determinations of the slant of each gage in the direction *uz*, the mean of which may be taken as the true value with an error of one-half an algebraic combination of the errors of the six measurements.

[19] The small letters represent the measured quantities.

Digitized by Google

(3) If B and C are f and h times as wide as A, respectively, then C is $\frac{h}{f}$ times as wide as B and

$$B_s = a - f\,A_s,$$
$$C_s = b - h\,A_s,$$
$$C_s = c - \frac{h}{f}\,B_s,$$
$$A_s = \frac{f\,(b-c) + ah}{2\,fh},$$
$$B_s = \frac{f\,(c-b) + ah}{2\,h},$$
$$C_s = \frac{h\,(b+c) - ah}{2\,f}.$$

If the gages are all the same width, then $f = h = 1$ and

$$A_s = \frac{b-c+a}{2},$$
$$B_s = \frac{c-b+a}{2},$$
$$C_s = \frac{b+c-a}{2},$$

showing that the error of each determination is one-half the algebraic combination of the individual errors. Thus, the method of intercomparing three gages enables one to determine easily and accurately the relative merits of each, their planeness errors having been previously determined, so that the best one can be chosen as a secondary standard of length and the others as working standards for use in the laboratory.

X. DEVELOPMENT OF STANDARD GAGES

Having established the fact that two plane surfaces can be brought into contact, so that the separation is less than two hundredths of a micron (one millionth of an inch), and having the interference method for comparing two gages of nearly equal length, it is possible to calibrate long gages from line standards and make comparisons between these long gages and equal combinations of two or more shorter ones. The arrangements used by Fischer[20] and Perard[21] for comparing a long end standard with a line standard are shown in Fig. 19. Two gages, A and B, are brought into close contact, and two fine lines, C and D, are ruled

[20] Phil. Soc. Wash., Bull., 12, p. 241; 1898.
[21] C. R., 154, p. 1586; 1912.

Digitized by Google

on them parallel to their plane of contact, EF. The distance X between the lines C and D is determined by comparison with the line standard. A is then brought into contact with one surface of the long gage G which is to be calibrated and B with the opposite surface of G. The distance Y between the two lines C and D is

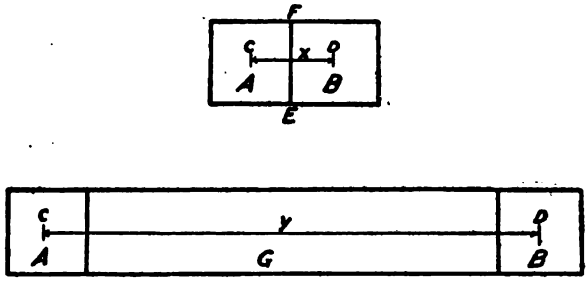

FIG. 19.—*Calibration of end standards relative to line standards*

again determined by comparison with the line standard. The difference in the two distances $Y-X$ gives the length of the gage G in terms of the line standard.

After the length of G has been accurately determined by comparison with the line standard or by direct measurement with the light waves, combinations of shorter gages can be compared with it by using the interference comparator, as follows: Suppose G is 6 inches long and we have three gages, A, B, and C, each very nearly 3 inches in length. G is brought into contact with the plane base plate W, Fig. 20, B is also placed in contact with W, and A with the upper surface of B. The difference a in the lengths of G and the combination of A and B is obtained from the relative displacement of the interference fringes as described in section VIII. The combined length of A and B is equal to that of G plus a. In the same way the observed difference b between the combined lengths of B and C and that of G is obtained. Likewise c for gages C and A. Letting the designation of the gages also represent their lengths, we have

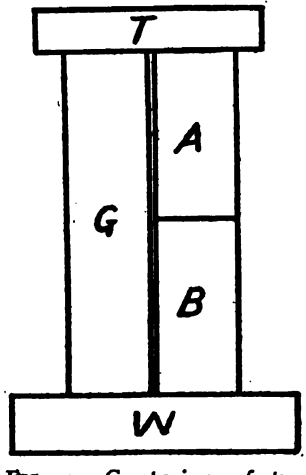

FIG. 20.—*Comparison of two short gages with one long gage*

$$A+B=G+a,$$
$$B+C=G+b,$$
$$C+A=G+c,$$

Digitized by Google

where G is the known length of the standard and a, b, and c are measured. These equations can be readily solved for the unknowns, A, B, and C. Similarly, with four gages, A, B, C, and D, each nearly 2 inches long, we would have

$$A + B + C = G + a,$$
$$B + C + D = G + b,$$
$$C + D + A = G + c,$$
$$D + A + B = G + d.$$

Since the four independent simultaneous equations contain four unknowns, the length of each unknown gage can be computed.

In general, given $n+1$ unknown gages of nearly equal length, n of which when combined are nearly equal to the known gage G, there will be $n+1$ combinations which may be compared with G. Hence, the length of each unknown gage can be obtained by this comparison method. Intermediate sizes may be measured by comparing the combined lengths of a known and unknown gage with a known.

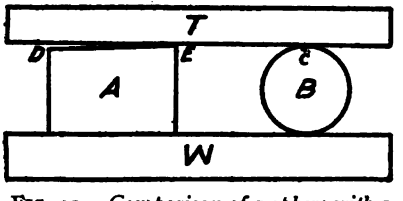

FIG. 21.—*Comparison of a sphere with a gage block*

XI. COMPARISON BETWEEN GAGES AND OTHER OBJECTS

An accurate determination of the dimensions of any body, say a sphere, can be made by comparison with a gage of nearly the same size. For this the gage A and the sphere B are placed in contact with the base plate W, Fig. 21, and the test plate T laid over them. If B is slightly smaller than A, the test plate will touch the gage along the edge E and the sphere at the point C. When illuminated and viewed as shown in Fig. 3 or 9, straight fringes parallel to E will be seen to cross the upper surface of the gage. The number of fringes N across the face of the gage from D to E multiplied by $\frac{\lambda}{2}$ gives the distance between the cover plate and the gage surface at D. If the distance CE is equal to DE, then the point C must be $\frac{N\lambda}{2}$ below the plane of the surface of the

Digitized by Google

gage, and hence the diameter of the sphere $\frac{N\lambda}{2}$ less than the length of the gage. If B is larger than A, the upper plate will touch the gage along the edge D and be $\frac{N\lambda}{2}$ above E. C would then be $\frac{2N\lambda}{2}$ above the plane of the surface of the gage and the diameter of B equal to the length of the gage plus $N\lambda$.

XII. SUMMARY

The extensive use of precision gages as reference standards for precise mechanical work has required more accurately determined end standards and more rapid and precise methods for comparing gages with these standards than have been previously available. Since comparison of end standards with line standards by means of micrometer-microscopes and of precision gages with end standards by means of contact instruments are subject to appreciable errors, methods which make use of the interference of light waves were used in making these measurements. With the interference methods described in this article, the planeness and parallelism errors of precision surfaces can be measured and the length of standard gages determined by direct comparison with the standard light waves with an uncertainty of not more than a few millionths of an inch. The errors of other gages can be determined by comparison with these calibrated standards with equal precision. This process makes the standard light waves which have been determined to one part in four or five million relative to the international meter, the standards of length for this work. Three sets of gages each containing 81 blocks were selected for end standards. These were tested for surface errors and calibrated by comparison with the light waves and have been recalibrated every few months because changes with wear or time are known to occur in material gages. Large numbers of precision gages have been compared with these end standards with sufficient speed and precision to meet all requirements.

WASHINGTON, May 3, 1921.

Digitized by Google

Digitized by Google

AUG (1922

DEPARTMENT OF COMMERCE

SCIENTIFIC PAPERS

OF THE

BUREAU OF STANDARDS

S. W. STRATTON, DIRECTOR

No. 437

THE SOLUBILITY OF DEXTROSE IN WATER

BY

RICHARD F. JACKSON, Associate Chemist
CLARA GILLIS SILSBEE, Assistant Chemist
Bureau of Standards

MAY 5, 1922

PRICE, 5 CENTS

Sold only by the Superintendent of Documents, Government Printing Office
Washington, D. C.

WASHINGTON
GOVERNMENT PRINTING OFFICE
1922

Digitized by Google

Digitized by Google

THE SOLUBILITY OF DEXTROSE IN WATER

By Richard F. Jackson and Clara Gillis Silsbee

ABSTRACT

The solubilities of dextrose, in addition to their scientific interest, have become of fundamental importance in controlling the processes of manufacture. They have been determined over a range of temperatures extending to 90° C. Three solid phases are capable of existence, namely, ice, α-dextrose monohydrate, and anhydrous α-dextrose. From the freezing point curve, computed from existing data, and the saturation curve of dextrose hydrate, the cryohydric point was found. Dextrose hydrate is stable between −5.°3 C and 50° C; its solubility has a high temperature coefficient.

The transition from dextrose hydrate to anhydrous dextrose is shown to occur at 50° C. Above this temperature anhydrous dextrose is the solid phase. Its temperature coefficient is relatively small. Below the transition temperature the anhydrous form may persist in unstable equilibrium, even at a temperature as low as 28° C.

CONTENTS

		Page.
1.	Introductory	715
2.	Historical	716
3.	General description of solubility measurements	716
4.	The solid phase; ice	718
5.	The cryohydric point	719
6.	The solid phase; α-$C_6H_{12}O_6.H_2O$	719
7.	The melting point of dextrose hydrate	721
8.	The transition point	723
9.	The solid phase; α-$C_6H_{12}O_6$	723
10.	Summary	724

1. INTRODUCTORY

In very recent times it has been found commercially feasible to crystallize dextrose from water solution and to separate the crystals from the mother liquor by centrifugal machines in much the same manner as the corresponding step in cane sugar manufacture is carried out. A similar process [1] was attempted about forty years ago, but the effort resulted in failure. With the advent of modern machinery and more scientific methods, however, the

[1] Making crystalline dextrose, C. E. G. Porst, Sugar, 23, p. 380; 1921. Louisiana Planter, 67, p. 14; July 2, 1921.

Digitized by Google

industry is at present being revived on a large scale with every prospect of success.

As a fundamental basis for calculating supersaturation coefficients, for estimating crystallizer performance, and the more extended investigation of the effect of nonsugars in the process of crystallization, the solubility of the pure substance in water assumes a technical as well as scientific importance. To serve these purposes we have undertaken the determination of solubilities over a wide range of temperatures.

2. HISTORICAL

A survey of the literature revealed but one solubility measurement, and that at only one temperature. Anthon [2] in 1883 found that at 15° C 100 parts of water dissolved 81.68 parts of anhydrous dextrose, giving a solution of 44.96 per cent. Aside from this, no data are in existence. Maquenne,[3] however, states that at 100° C dextrose and water are miscible in all proportions.

3. GENERAL DESCRIPTION OF SOLUBILITY MEASUREMENTS

The solubility measurements were made by agitating the mixture of dextrose and water with a large proportion of the solid phase in a rotating frame under the water of an electrically operated thermostat. After equilibrium had been reached, the solution was separated from the crystals and analyzed. The separation of the finely divided crystals from the viscous saturated solution was accomplished by filtration under pressure through an asbestos mat, the arrangement of which is shown diagrammatically in Fig. 1.

The filtration tube *A* was constructed of glass tubing 20 mm inside diameter with walls 3 mm thick. In this was inserted the perforated brass disc *B* which was edged with lead and covered with an asbestos mat. For temperatures much removed from that of the laboratory, the transference from the solubility bottle *C* was accomplished as shown in position *I*. The solubility bottle was removed from the rotating frame with a pair of tongs and its mouth held above the liquid of the thermostat and wiped dry. A rubber stopper was inserted which carried the wide bore glass tube *D*, which extended nearly to the bottom of the bottle. The glass tube passed through another stopper into the filtration tube,

[2] V. Lippmann, Die chemie der zuckerarten, 1, p. 266; 1904.
[3] Les sucres et principaux dérivés, p. 479; 1900.

Digitized by Google

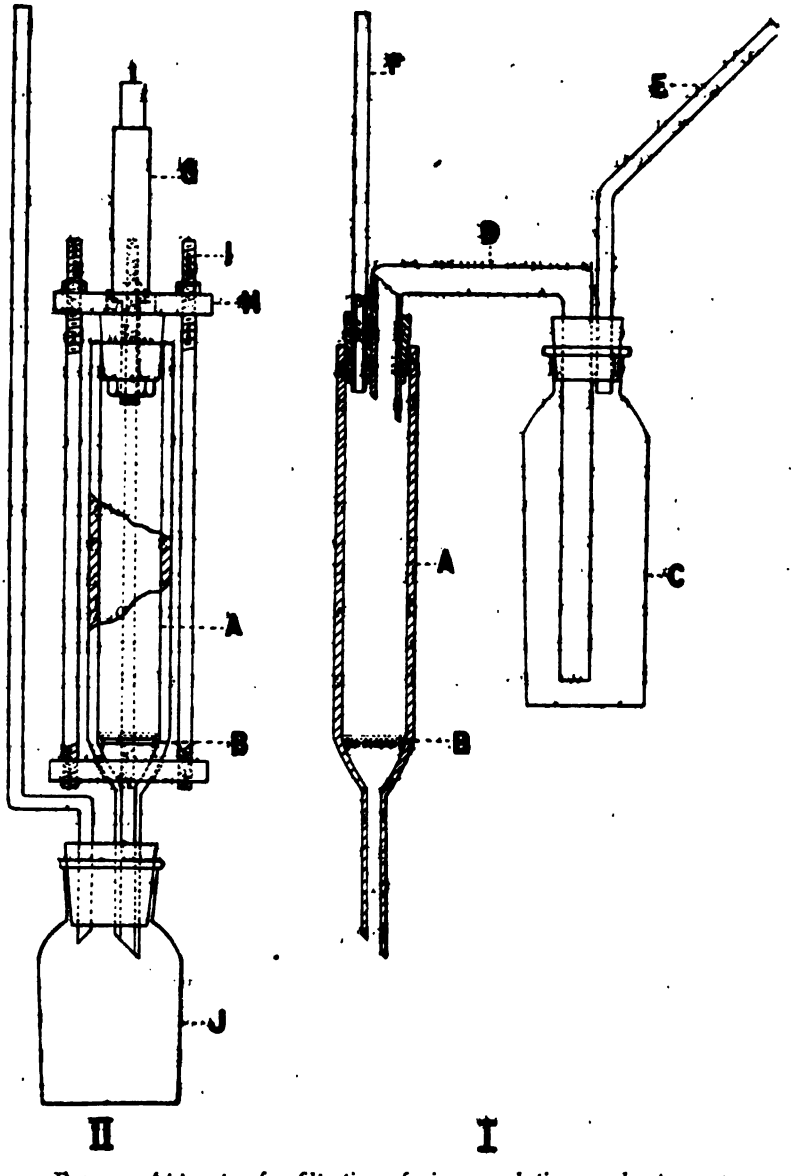

FIG. 1.—*Apparatus for filtration of viscous solutions under pressure*

Digitized by Google

the latter being arranged with respect to the remaining parts of the apparatus as shown in position *II*, with the exception of the valve *G* and brass plate *H*. The whole apparatus, with the exception of the upper parts of the two small glass tubes *E* and *F*, was then immersed in the water of the thermostat and allowed to take its temperature. A slight air pressure transmitted through the tube *E* sufficed to drive the crystal mixture into the filter tube without even a momentary change in temperature.

After the transference the upper edge of the filter tube *A* was raised above the surface of the liquid of the thermostat and wiped dry. The valve *G* and stopper were inserted in the filter tube and held tightly by the brass plate *H*, which was held in place by the three brass posts *I*. An ordinary bicycle pump supplied sufficient pressure to force the saturated solution through the asbestos filter into the weighed container *J*, which was finally dried, brought to the temperature of the balance case, and weighed.

The weighed sample was transferred to a weighed 100 cc volumetric flask, made to volume at 20° C and weighed. The solution was allowed to stand over night in order to complete the mutarotation which occurs to some extent upon dilution of a concentrated syrup, and was polarized in a Bates-Frič saccharimeter at 20° C. By this procedure we obtained a densimetric and polariscopic determination of the dextrose in the sample. An agreement by these two methods was assumed to be an indication of the accuracy of the analytical work.

For the normal weight of dextrose the value 32.231 g, as previously determined by one of us,[4] was used. The densities of dextrose solutions which were determined incidentally to this same investigation were used as standards. All analytical results in this paper are expressed in terms of anhydrous dextrose.

4. THE SOLID PHASE; ICE

Starting with the freezing point of pure water we may plot the freezing point curve of dextrose solutions by using the data of Roth[5] for the more dilute solutions, and of Abegg[6] for the more concentrated solutions. Abegg's determinations are expressed in terms of volume concentrations at the freezing point temperatures, with no accessory data by which to calculate the concentrations by weight. It was consequently necessary to determine the densi-

[4] Jackson, B. S. Bulletin, 12, p. 633, 1916 (or B. S. Sci. Papers, No. 293).
[5] Landolt and Börnstein Tabellen, p. 820; 1912.
[6] Zeit. Phys. Chem., 15, 222; 1894.

Digitized by Google

ties of the solutions which possessed the same concentrations per volume at the respective temperatures as those concerned in his freezing point determinations. Two such solutions were prepared and their densities at 0° C and their expansion coefficients were accurately determined. From these data their densities and volume concentrations were computed for the temperatures at which Abegg's freezing point determinations were made. In both cases the volume concentrations as thus determined approximated Abegg's very closely, and a slight interpolation to his precise concentration was possible without appreciable error. The solution containing 188.02 g per liter at −2°.305 C had a density $\left(\frac{-2°.305\ C}{4°C}\right)$ of 1.0740 and a weight composition of 17.586 per cent; that containing 378.0 g per liter at −5°.605 C had a density $\left(\frac{-5°.605\ C}{4°\ C}\right)$ of 1.1464 and a weight composition of 33.015 per cent.

The above data are plotted in Fig. 2. The essential agreement between Roth's and Abegg's determinations is shown by the smoothness of the connecting curve.

5. THE CRYOHYDRIC POINT

At the intersection of the freezing point curve with the extrapolated solubility curve of hydrated dextrose occurs the cryohydric point. The temperature and composition as determined graphically proved to be −5°.3 C and 31.75 per cent.

Since no solubility measurements were made below 0° C, the possibility is not excluded that a new solid phase may be stable between 0 and −5°.3 C.

6. SOLID PHASE; α-$C_6H_{12}O_6.H_2O$

At and above the cryohydric temperature the stable solid phase of the sugar is the monohydrate. The region of stability of this phase extends from −5°.3 C to exactly 50° C. The solubilities are assembled in Table 1 and are shown graphically in Fig. 2. As appears from the diagram, Anthon's solubility measurement at 15° C is in good agreement with our curve.

This phase on crystallization from water solution in general forms minute plates of a lustrous silky appearance. The crystals, however, are capable of good development. We are informed by Mr. W. B. Newkirk, of the Corn Products Refining Co., that when

Digitized by Google

the substance is allowed to crystallize slowly during the process of large scale manufacture, crystals of considerable magnitude are obtained. Mr. F. P. Phelps, of this Bureau, has succeeded in growing perfectly formed crystals 6–7 mm in length.

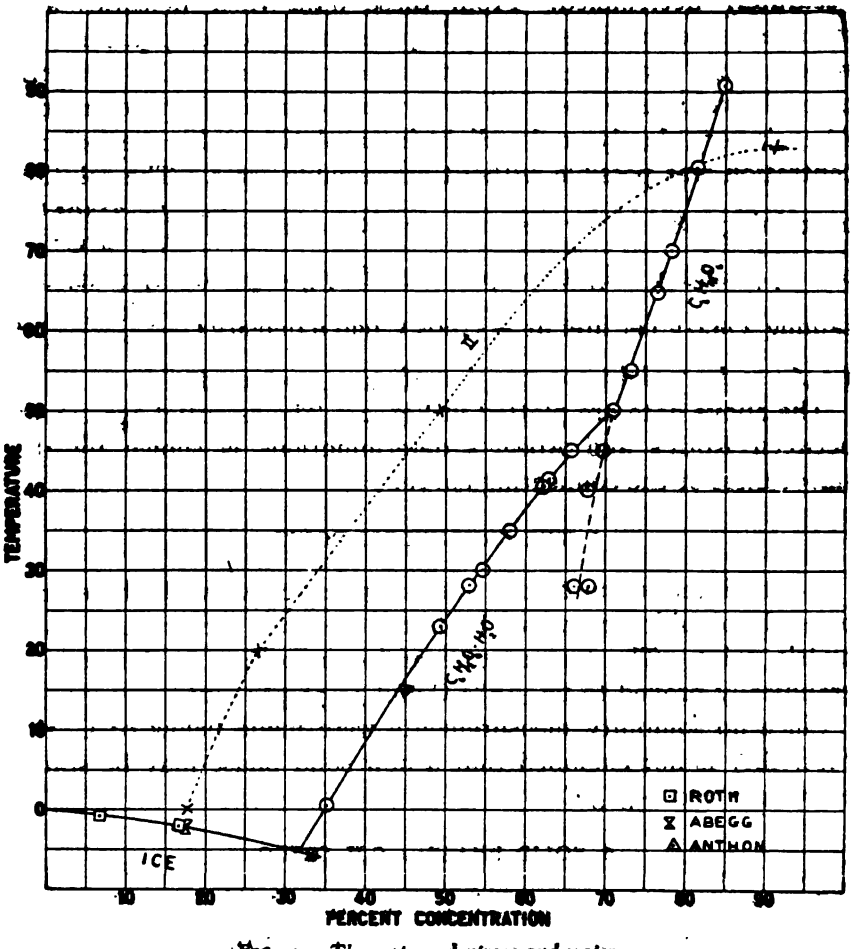

FIG. 2.—*The system, dextrose and water*

The solid curves show the final equilibria with respect to the solid phases, ice, dextrose hydrate, and anhydrous dextrose. The dotted curve shows the instantaneous solubility before mutarotation. All data are expressed in terms of anhydrous dextrose.

The temperature coefficient of the solubility is very large. Thus, if the solubilities in Table 1 are stated in terms of the parts of dextrose dissolved by a constant weight of water, it is seen that 100 g of water dissolve, at 0°.5 C, 54.32; at 30° C, 120.46; and at 50° C, 243.76 g of dextrose.

Digitized by Google

TABLE 1.—The Solubility of Dextrose in Pure Water

Temperature in degrees centigrade	Solid phase	Dextrose in solution [a]	Temperature in degrees centigrade	Solid phase	Dextrose in solution [a]
		Per cent			Per cent
−0.772 [b]	Ice	6.83	28.00	α-$C_6H_{12}O_6$ Metastable	66.0
−2.117 [b]		16.65	28.00		67.9
−2.305 [c]		17.59	40.00		67.6
−5.605 [c]		33.02	45.00		69.69
−5.3	Cryohydrate	31.75	55.22	α-$C_6H_{12}O_6$	73.08
			64.75		76.36
+ 0.50	α-$C_6H_{12}O_6.H_2O$	35.2	70.2		78.23
15.00 [d]		44.96	80.5		81.49
22.98		49.37	90.8		84.90
28.07		52.99			
30.00		54.64			
35.00		58.02			
40.40		62.13			
41.45		62.82			
45.00		65.71			
50.00	Transition	70.91			

[a] Estimated as anhydrous sugar.
[b] Roth, Zeit. Phys. Chem., 43, p. 552; 1903.
[c] Abegg, Zeit. Phys. Chem., 16, p. 222; 1894.
[d] Anthon, v. Lippmannn, Die Chemie der Zuckerarten, I, p. 266; 1894.

7. THE MELTING POINT OF DEXTROSE HYDRATE

The melting point of dextrose hydrate as observed in a capillary tube in the usual manner has been found to lie in the vicinity of 80–90° C, the values reported by different observers [1] being strikingly at variance with one another. We have found that if the capillary containing the sample is plunged into the bath which had previously been brought to about 83° C, incipient fusion occurred, although it was found impossible to obtain reproducible results.

At its melting point dextrose hydrate is in equilibrium with a solution of its own composition. In other words, the solubility as thus determined is 90.9 per cent at 80–85° C. It is at once apparent from Fig. 2 that by no manner of extrapolation can our solubility curve of the hydrate be made to pass through this point, and that the discrepancy is so great that some explanation is required.

When crystalline dextrose is dissolved in water, it immediately undergoes a partial stereochemical transformation into the β-form at a rate which depends upon the temperature. All of the present measurements were made under equilibrium conditions, the time of agitation of the crystals being continued until the reaction,

$$\underset{\text{crystals}}{\alpha\text{-dextrose}} \rightleftharpoons \underset{\text{saturated solution}}{\alpha\text{-dextrose}} \rightleftharpoons \underset{\text{solution}}{\beta\text{-dextrose}}$$

[1] V. Lippmann, Die Chemie der Zuckerarten, I, p. 263; 1904.

Digitized by Google

had reached equilibrium. The final solubility is consequently that of α-dextrose, not in water, but in a solution of β-dextrose. On the other hand, at the melting point or the temperature of incipient fusion, the composition of the crystals represents the solubility of α-dextrose in water, since no β-dextrose can be formed until after the crystal has begun to fuse. Even after fusion the complete transformation to the equilibrium requires several minutes, during which time the melting point is undergoing rapid variation, both because of the formation of the β-compound and because of the rapid efflorescence of the hydrate. With these two disturbing effects, it is not surprising that the melting point should fail of reproducibility. It is now of interest to inquire if, on the basis of the above discussion, we may reconcile our solubility curve with the observed melting point. If we could plot the solubility curve of α-dextrose hydrate in pure water—that is, the instantaneous solubility before mutarotation has begun—such a curve should pass through the observed melting point.

On this curve two points are experimentally realizable. One of these is the melting point itself. The other point is the instantaneous solubility at 0° C. The possibility of obtaining experimental data at 0° C depends upon the fact that the rate of mutarotation is an important function of temperature. Thus the velocity constant of mutarotation which, expressed in decimal logarithms and minutes, is 0.00662[8] at 20°.7 C, becomes about the order of 0.001 at 0° C.[9] The reaction being so slow, it is possible to obtain a solubility measurement of the pure α-hydrate in water before its transformation has become considerable by violently agitating a large excess of solid phase in the presence of its solution for short periods of time. The mean of three such determinations which were in agreement within 3 per cent indicated that the instantaneous solubility was 17.5 per cent.

A concentrated aqueous solution of dextrose after the completion of the mutarotation contains the two isomers[10] in the ratio of about 40 per cent α- and 60 per cent β-. We may therefore from our solubility measurements make an approximate calculation of the solubility of the α-dextrose in pure aqueous solution. An example will suffice.

At 20° C the final solubility is 47.5 per cent. One hundred grams of the solution then contains 19.0 g α-dextrose, 28.5 g

[8] Levy, Zeit. Phys. Chem., 17, p. 301; 1895.

[9] Nelson and Beegle, J. Amer. Chem. Soc., 41, p. 565; 1919, report 0.00092 at 0.°15 C. and p_H 6.84.

[10] Armstrong, The simple carbohydrates and glucosides, p. 17; 1919. Hudson, J. Amer. Chem. Soc., 39, p. 1018; 1917.

Digitized by Google

β-dextrose, and 52.5 g water. We find the solubility of the α-form in pure water to be about 26.6 per cent. Proceeding in this way we may compute roughly the solubilities of the α-dextrose in pure water, as shown in the dotted curve II. This curve, which is obviously little more than qualitative in character, is seen to be compatible with the observed melting point of 80–85° C.

8. THE TRANSITION POINT

At 50° C duplicate measurements were made of the solubility approached from supersaturation and from undersaturation, respectively. The solubility proved to be 71.06 per cent. The solid phases from which samples of the solution had been taken were rapidly purged with aqueous alcohol followed by ether. They were then air died and analyzed for their water content. One of these was completely anhydrous; the other contained exactly one molecule of water of crystallization. Since these two solid phases were in equilibrium with solutions of the same composition at the same temperature, it is evident that the temperature of 50° C is the "transition point" from the hydrated to the anhydrous crystalline form, in the presence of the solution. It should, however, be remarked that this is only a pseudo-transition point. The true transition point would be that temperature at which α-dextrose is in equilibrium with a solution containing only α-dextrose. The solution actually contains about 60 per cent of β-dextrose, which thus lowers the true transition point by a perfectly definite amount. The true transition temperature would be of so fugitive a character that its measurement not only would involve great experimental difficulties, but would be of little practical significance.

9. THE SOLID PHASE; α-$C_6H_{12}O_6$

At temperatures above 50° C anhydrous dextrose becomes the stable solid phase. Its solubility rises in very nearly linear relation and, compared with that of the hydrate, with a small temperature coefficient. It forms hard crystals which are capable of development to a considerable size. The solubility measurements are assembled in Table 1 and plotted in Fig. 2.

The solubility curve produced to the 100 per cent ordinate shows a melting point for the anhydrous form below 135° C, whereas the observed melting point is 144–146° C.[11] Here again

[11] Maquenne, Les sucres et principaux dérivés, p. 478; 1900.

Digitized by Google

the melting point, as indicated by extension of the solubility curve, is that of the mixture of α- and β-dextrose, while the observed is that of the pure α-dextrose.

Below the transition temperature it is possible to maintain the anhydrous form as the solid phase in a metastable state. We have succeeded in extending the solubility measurements down to 28° C. Our data on this branch of the curve must be considered approximate, since the experimental difficulties were considerable.

In the vicinity of 100° C the anhydrous β-dextrose becomes the stable solid phase. We have not attempted to determine the transformation point or the solubilities. It is possible to predict, however, that the solubility curve of the β-compound lies very close to the prolongation of the α-, since their observed melting points are very close together. The β-dextrose melts at 148° C, the α- at 146° C.

10. SUMMARY

The equilibria in the system, dextrose and water have been determined. For temperatures below 90° C three solid phases are capable of existence, namely, ice, α-dextrose monohydrate, and anhydrous α-dextrose. The freezing point curve was computed from the data of Roth and of Abegg. The cryohydric point, determined graphically, was found to lie at the temperature $-5°.3$ C and concentration 31.75 per cent dextrose. The solid phase, α-dextrose monohydrate, which occurs in lustrous plates, is stable between $-5°.3$ C and 50° C. Its solubility shows a very high temperature coefficient. Thus, at 0°.5 C, 100 parts of water dissolve 54.32 parts; at 50° C, 243.76 parts of dextrose. The observed melting point, 80–90° C, although located far from the extrapolated solubility curve, is shown to be compatible with the measurements, on the theory that β-dextrose is present in the saturated solution and absent during a melting point determination. Above the transition point, 50° C, the anhydrous form becomes stable. Its solubility shows a small temperature coefficient. The solubility measurements of this phase in metastable state were continued down to 28° C.

WASHINGTON, January 7, 1922.

Digitized by Google

[illegible]

DEPARTMENT OF COMMERCE

SCIENTIFIC PAPERS
OF THE
BUREAU OF STANDARDS

S. W. STRATTON, Director

No. 438

TESTS OF STELLAR RADIOMETERS AND MEASUREMENTS OF THE ENERGY DISTRIBUTION IN THE SPECTRA OF 16 STARS

BY

W. W. COBLENTZ, Physicist

Bureau of Standards

MAY 14, 1921

PRICE 15 CENTS

Sold only by the Superintendent of Documents, Government Printing Office
Washington, D. C.

WASHINGTON
GOVERNMENT PRINTING OFFICE
1921

Digitized by Google

Digitized by Google

DEPARTMENT OF COMMERCE

SCIENTIFIC PAPERS

OF THE

BUREAU OF STANDARDS

S. W. STRATTON, DIRECTOR

No. 438

TESTS OF STELLAR RADIOMETERS AND MEASUREMENTS OF THE ENERGY DISTRIBUTION IN THE SPECTRA OF 16 STARS

BY

W. W. COBLENTZ, Physicist

Bureau of Standards

MAY 12, 1922

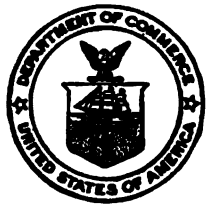

PRICE, 10 CENTS

Sold only by the Superintendent of Documents, Government Printing Office
Washington, D. C.

WASHINGTON
GOVERNMENT PRINTING OFFICE
1922

Digitized by Google

Digitized by Google

TESTS OF STELLAR RADIOMETERS AND MEASUREMENTS OF THE ENERGY DISTRIBUTION IN THE SPECTRA OF 16 STARS

By W. W. Coblentz

ABSTRACT

In this paper an account is given (1) of new tests of stellar radiometers, (2) of new measurements of the total radiation of stars in the region of 0 hrs. to 12 hrs. in right ascension, not previously measured, and (3) of tests of a method of determining the spectral energy distribution of stars by means of transmission screens, which, either singly or in combination, are placed in front of a vacuum thermocouple used as a radiometer.

The results obtained verify previous observations showing that red stars emit three to four times as much total radiation as blue stars of the same visual magnitude.

By means of a series of transmission screens (of yellow and red glass, of water, and of a thick plate of quartz) wide spectral regions were isolated, and the radiation intensities in the spectrum from 0.3μ to 0.43μ, 0.43μ to 0.6μ, 0.6μ to 1.4μ, 1.4μ to 4.1μ, and 4.1μ to 10μ were determined. In this manner the energy distribution in the complete spectrum of 16 stars was determined.

The observed spectral radiation components were compared with similar data computed for a black body at various temperatures. In this manner it was found that the temperature which a complete radiator or so-called black body would have to attain in order to emit a spectral energy distribution similar to that observed varies from 3000° K for red, class M, stars, to 10 000° K, or even higher, for blue, class B, stars.

The water-cell transmission of binary stars, having companions of low luminosity, is low, indicating that the companion stars emit considerable infra-red radiation.

CONTENTS

	Page
I. Introductory statement	726
II. Apparatus and methods	727
1. Subsidiary investigations in stellar radiometry	728
2. Recent tests of thermocouple material	728
3. Description of vacuum thermocouples used in the present work	731
4. Description of the transmission screens	733
5. The reflecting telescope	736
III. Measurement of the total radiation from stars	737
IV. Measurement of the spectral radiation of 16 stars	739
1. Spectral energy data on 16 stars	740
2. The water cell transmission data	743
3. The quartz cell transmission data	744
4. Binary stars	744
5. Stellar temperatures	745
V. Summary	749

Digitized by Google

I. INTRODUCTORY STATEMENT

During the past summer, through the generosity of the Lowell Observatory, Flagstaff, Ariz. (altitude 7300 ft.), the writer was given an opportunity to try out new devices for stellar radiometry and to make new stellar radiation intensity measurements. Not only was an otherwise busy program interrupted but, furthermore, Dr. C. O. Lampland personally operated the telescope, thus insuring speed and efficiency in accomplishing results. It is a pleasure to record here my grateful acknowledgments for the many courtesies extended me by various members of the Lowell Observatory.

The whole experience is an excellent object lesson in what may be accomplished by physicists and astronomers (or, for that matter, by laboratories having a common problem but incomplete apparatus) by combining their forces in trying out new devices, thus saving time and the expense that would be required in building up complete equipment, which in the end may or may not prove satisfactory.

In a previous paper [1] data were given on a comparison of stellar radiometers and radiometric measurements of 110 stars, using the Crossley reflector of the Lick Observatory at Mount Hamilton, Calif., the altitude being about 4000 ft. Quantitative measurements were made on stars down to magnitude 5.3 and qualitative measurements to magnitude 6.7. It was found that red stars emit from 2.5 to 3 times as much *total* radiation as blue stars of the same visual magnitude.

These observations were verified by an independent method which consisted in measuring the transmission of stellar radiation through a 1 cm cell of water, having quartz windows. By this means it was shown that of the *total* radiation emitted blue stars have about 2 times as much *visible* radiation as yellow stars and about 3 times as much *visible* radiation as red stars.

The purpose of the present investigation was (1) to verify previous results, (2) to measure the radiation intensities of the bright stars in the region of 0 hrs. to 12 hrs. in right ascension, not previously measured, thus completing the survey of the whole sky (in this latitude), and (3) to determine the feasibility of the method of obtaining the spectral energy distribution of stars by means of transmission screens which either singly or in combination are placed in front of the vacuum thermocouple which was used

[1] Coblentz, B. S. Bulletin, 11, p. 613; 1914.

Digitized by Google

to measure the thermal radiation intensity. By means of these transmission screens it was possible to obtain for the first time an insight into the radiation intensities in the complete spectrum of a star.

Data on the spectral energy distribution of stars as related to that of a black body are very meager. They are the results practically of the spectrophotometric measurements of Wilsing[2] and of Nordmann,[3] and the spectral energy curves determined photographically by Plaskett,[4] all of which relate to the visible spectrum. From the data obtained on the radiation intensities in the visible spectrum, these experimenters have obtained estimates of stellar temperatures of 3000° for red stars to 25 000° or even higher for blue stars.

In view of the subject matter to be discussed in this paper, it is relevant to recall that in previous papers it was indicated that, in comparison with the photoelectric cell, the thermocouple is far less sensitive and hence more limited in its application as to the number of stars that can be measured. (Neither instrument can tell us the size or distance of stars). But the thermocouple enables one to obtain information not obtainable by other instruments. Combined with an absorption cell (of water) one can detect the presence of dark companions of binary stars.

This device gives us a new means for studying planetary radiation and temperature conditions. If the surface of a planet becomes warmed by the sun's rays and in turn emits radiation (which will be entirely of long wave lengths), the amount of radiation transmitted through the water cell will be less than when the reflecting surface remains cool. Data of this type were previously obtained on the moon. Applied to the planet Mars, if the polar cap is snow then the transmission of reflected sunlight should be higher than that observed from the dark areas, if the latter are bare ground. On the other hand, if the dark areas contain green vegetation (similar to that of our earth) the temperature rise will be small, the water-cell transmission will be high, and the results may be difficult of interpretation.

II. APPARATUS AND METHODS

Under the present caption is given a recapitulation of results obtained in the improvement of stellar radiometers as well as a general description of the instruments used in the present work.

[2] Wilsing, Scheiner, and Münch, Publ. Astrophys. Obs., Potsdam, 24, No. 74; 1920.
[3] Nordmann and LeMorvan, C. R., 178, p. 72; 1921.
[4] Plaskett, Monthly Notices, R. A. S., 80, p. 771; 1920.

Digitized by Google

1. SUBSIDIARY INVESTIGATIONS IN STELLAR RADIOMETRY

At various times during the seven years which have elapsed since making the previous stellar radiation measurements attention was given to the improvement of stellar radiometers. A study was made of magnetic shielding, and of some of the problems that will be encountered in using a vacuum galvanometer.[5]

An investigation was made of selective radiometers (photoelectric cells). A new multiple bolometer receiver was described, consisting of two bolometer receivers, one back of the other, which increased the sensitivity by 50 per cent. A new combination was described, consisting of a bolometer, back of which was placed a thermocouple.[6] These devices will aid materially in increasing the sensitivity. However, owing to the complexity of operation, no attempt was made to utilize them in a temporary installation such as was used in the present work. In fact, owing to the temporary nature of the present radiometric installation, it was not possible to use the full sensitivity that was available in the equipment employed.

Among the photoelectric receivers, Case's thalofide cell was investigated.[7] This cell has a sharp maximum of sensitivity for radiation of wave lengths at about 1μ, which property may prove of interest in some lines of stellar radiometry.

2. RECENT TESTS OF THERMOCOUPLE MATERIAL

Before making up the vacuum thermocouples for the present investigation it was of interest to try material of different thermoelectric power to determine the effect of heat conduction upon the radiation sensitivity. Some material of great ductility but low thermoelectric power was obtainable in much smaller diameters than the wires of bismuth and bismuth alloys previously used. It was therefore of interest to determine whether by using the finest wire to reduce conduction, and thus conserve the heat at the juncture, the efficiency of the receiver could be increased. In making the test samples of various metals were joined in series, thus eliminating the question of internal resistance, which remained the same throughout the test.

The materials tested were connected in series as follows: 60 Au +40 Pd: 90 Pt+10 Rh: Bi: 95 Bi+5 Sn: 97 Bi+3 Sb: 90 Pt+10 Rh. The gold-palladium and the platinum-rhodium alloy wires[8]

[5] B. S. Bulletin, 13, p. 423; 1916.
[6] J. Wash. Acad. Sci., 6, p. 473; 1916. B. S. Bulletin, 14, p. 532; 1918.
[7] B. S. Sci. Papers, 16, p. 253; 1920.
[8] From Baker and Co., Newark, N. J.

Digitized by Google

were 0.02 mm in diameter. The alloys of bismuth-tin and bismuth-antimony were in the form of fine wire[9], 0.025 mm in diameter.

The pure bismuth was in the form of a strip made by pressing a wire flat between glass plates and cutting it with a razor, as described in the previous paper.[10] The strip was approximately 0.07 mm wide by 0.01 to 0.02 mm thickness. From previous tests it appears that the low radiation sensitivity of this sample (see Table 1) was owing to its large cross section. Moreover the receiver did not appear to be thoroughly covered with lampblack. The receivers were about 0.5 mm in diameter, made of small globules of tin (or Woods alloy for the bismuth alloys), pressed flat (while molten) between thin plates of mica, as described in previous papers, and painted with lampblack.

The radiation sensitivity test was made in air by focusing upon the receiver an artificial star, which consisted of a pinhole in a thin aluminum plate in front of an acetylene flame.

The results of this test are summarized in Table 1, in which column 2 gives the thermoelectric power in microvolts, column 3 gives the ratio of the emf's, and column 4 gives the ratio of galvanometer deflections in terms of that of the thermojunction of Au+Pd : Pt+Rh, taken as a standard.

TABLE 1.—Comparison of Stellar Thermocouples

Elements	Thermo-electric power	Ratio of emf's	Radiation sensi-tivity
	mv		
Au+Pd : Pt+Rh	32	1.0	1.0
Pt+Rh : Bi	85	2.65	2.85
Bi : Bi+Sn	137	4.28	3.65
Bi+Sn : Bi+Sb	129	4.04	5.35
Bi+Sb : Pt+Rh	74	2.31	2.56

The results are interesting in showing that the radiation sensitivity is closely proportional to the thermoelectric power (which is to be expected), but there seems to be no marked gain in sensitivity from reduction of thermal conduction. In the case of the pure bismuth the wire was not as thin as it could be made, and hence there is reason for believing that the efficiency would have been higher if a finer wire had been used. The thermocouples of the bismuth-alloy wire are interesting in having a radiation sensitivity

[9] From Adam Hilger (Ltd.), 75 A Camden Road, London, England.
[10] B. S. Bulletin, 11, p. 623; 1914.

Digitized by Google

about 20 per cent higher than would be expected from the thermoelectric power. This seems to show an improvement in sensitivity as a result of elimination of heat conduction. However, there is one more factor to be considered, namely, internal resistance. In changing from pure bismuth to the bismuth alloys the thermal emf is increased only about 60 per cent, whereas the internal resistance is increased threefold to fourfold. Hence, from the nature of the thermocouple required for stellar radiometry it appears to be more efficient to use the pure bismuth wire. This conclusion is substantiated by the tests described in previous papers and by the results on the thermocouples used in the present investigation. For example, the data in Table 2 show that the stellar thermocouple of Au + Pd alloy in mounting No. 10 (evacuated and ready for use) was only half as sensitive as the thermocouple of Bi in mounting No. 7, which was used seven years ago. Furthermore, the radiation sensitivity of the thermocouples of the alloys of Bi is not markedly higher than that of the pure Bi, although they have a 57 per cent higher thermoelectric power.

In a recent test of a thermocouple of silver and 0.13 mm tellurium (from Dr. P. W. Bridgeman) against a similar couple of 0.1 mm bismuth (receivers of tin 1.2 by 2.2 mm) the radiation sensitivity of the tellurium-silver couple was only twice that of the standard bismuth-silver couple, whereas its resistance was more than 10 times that of the bismuth couple.

In view of the results mentioned on a preceding page, showing an increased radiometer efficiency as a result of utilizing reradiation of one receiver upon another (one receiver back of the other), it is of interest to describe some observations showing the effect of convection in reducing the radiation sensitivity when one receiver is back of the other.

In the present tests a regular stellar thermocouple was used, with receivers (0.5 mm in diameter) blackened on the front and bright on the rear side. The left (*L*) receiver, which was used as a standard of comparison, was a trifle larger than the right (*R*) receiver, which was under investigation. A reflector consisting of a small globule of tin attached to a fine wire for a support and pressed flat (0.5 mm diameter) but unpainted was placed at different distances back of the right (*R*) receiver. The tests were made in air at atmospheric pressure. In a vacuum convection and conduction would be reduced. It was found that when the reflector was 0.5 mm from the receiver the radiation sensitivity was reduced by 30 per cent, while at a distance of 1 mm the

Digitized by Google

reduction in sensitivity is still appreciable (15 per cent). The intention was to paint the rear side of the front receiver (which, however, would increase its emissivity) with lampblack in order to absorb the reradiated energy which was returned by the reflector, placed back of the receiver as just described. However, from the tests just described it seemed doubtful whether, in this particular form of radiometer, the addition of a reflector to utilize the reradiated energy would accomplish much more than to compensate for the increased emissivity caused by blackening the rear side of the receiver. Hence the receivers were used without reflectors.

3. DESCRIPTION OF VACUUM THERMOCOUPLES USED IN THE PRESENT WORK

The vacuum containers for the thermocouples were of the same general design used in the previous work. Four containers were taken to the observatory, a distance of 2500 miles, without breakage. No vacuum pump was taken (and none was available without going a long distance from the observatory) in order to demonstrate that metallic calcium is a reliable means of vacuum maintenance.[11]

An electric heater was provided for heating the metallic calcium to incandescence. It consisted of a thin porcelain tube about 10 cm long and 1.5 cm internal diameter. On the outside of this tube was wound about 2 m of thin (0.2 mm) platinum wire, having a resistance of 12 ohms. This was covered with alundum cement, such as is used in pyrometric work. A small rheostat was provided and the whole operated on a 110-volt circuit. It required less than 2 amperes to raise this heater to a low red temperature, and being of low heat capacity this was accomplished in a few minutes.

The evacuation was tested by means of an induction coil as previously described. The containers leaked but little, as was evidenced by the cathode fluorescence of the glass that continued for days when the calcium was not heated. In practice, the calcium evacuator was heated on the afternoon preceding the observations.

Container No. 7 remained the same as used in the previous measurements, except that about two years ago a new quartz tube containing new metallic calcium was provided.[12] The

[11] B. S. Sci. Papers, 17, p. 187; 1921.
[12] B. S. Sci. Papers, 17, p. 187; 1921.

Digitized by Google

thermocouples were of flat material as described in the previous paper.

Container No. 8 was No. 6, previously used, but with new thermocouples (see Table 2).

Containers Nos. 9 and 10 were new with the fluorite windows attached by means of Boltwood's [13] low vapor pressure cement. This cement has a low melting point which enables one to attach the fluorite without cracking it.

The mounted container is shown in Fig. 1, in which *Ca* represents the quartz tube containing the metallic calcium, *F* the fluorite window, *T* the thermopile, and *P* the potential terminals for testing the evacuation by means of an induction coil, automobile spark coil, or a transformer of 2000 to 10 000 volts. For further details of construction and manipulation the reader is referred to previous papers.[14]

Two thermocouples were placed in each of the three new mountings. Either one of these could be used without delay in changing the connections. As shown in the lower left-hand corner of Fig. 4 these thermocouples were bent U-shaped, so that the two junctures were close (0.5 to 1 mm) together, in order to facilitate exposing them alternately to the star image, as previously described.[15] Only fine wires of the alloys of bismuth (with tin and with antimony) were at hand, and these were very brittle, especially the alloys with antimony. Furthermore, difficulty was experienced in attempting to solder the Bi + Sb wire to the silver wire (used to reduce the resistance) with Wood's alloy. As finally constructed the central U-shaped part of the thermocouple was made of Bi + Sb wire about 2 mm long and the two end pieces of Bi + Sn wire about 1.5 mm long. The junctures were made by means of globules of Wood's alloy, pressed flat between thin plates of mica, as already described. These couples were then soldered to the silver wires, which were coiled to take up any mechanical vibrations caused by handling. Even with this precaution mounting No. 8 had to be remade four times, involving the construction of at least 20 thermocouples before a pair was obtained for shipment. It may be added that this material was so fragile that the receptacle containing the four mountings was carried by hand to the observing station.

---

[13] From Prof. B. B. Boltwood, Yale University, New Haven, Conn.

[14] B. S. Bulletin, 11, p. 131, 1914; 11, p. 613; 1915.

[15] See Fig. 2, B. S. Bulletin, 11, p. 622; 1914.

Digitized by Google

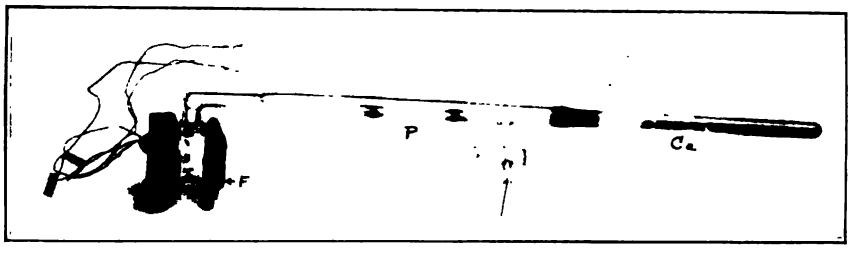

FIG. 1—*Stellar thermocouple, T, in evacuated glass container*

Digitized by Google

Digitized by Google

A summary of the constants, including the radiation sensitivity, of the (freshly evacuated) thermocouples is given in Table 2. They are of interest in showing the uniformity of radiation sensitivity that may be expected in thermocouples constructed of the same material. The receivers were made 0.5 mm in diameter, which was larger than previously used, thinking it might be more efficient in case of change in focus of the star image. But this proved detrimental, because the time to attain a maximum deflection was greatly prolonged. Receiver No. 1 of mounting No. 10 was the quickest acting (2 secs.) of the U-shaped couples, and it was used for all the measurements recorded in this paper.

TABLE 2.—Summary of Data on Stellar Thermocouples

Mounting	Thermocouple	Size of receiver	Resistance of couple	Galvanometer deflection	Remarks
		mm	ohms	cm	
No. 7	No. 1	0.4	11.3	68	Bi+Sn : Bi+Sb
	No. 2	.3	4.6	60	Bi : Pt
No. 8	No. 1	.6	22.7	68	Bi+Sn : Bi+Sb
	No. 2	.4	16.2	76	Bi+Sn : Bi+Sb
No. 9	No. 1	.6	19.8	58	Bi+Sn : Bi+Sb
	No. 2	.4	15.2	60	Bi+Sn : Bi+Sb Good action
No. 10	No. 1	.3	19.3	68	Bi+Sn : Bi+Sb Best; quickest action
	No. 2	.5	2.43	29	Au+Pd : Pt+Rh

4. DESCRIPTION OF THE TRANSMISSION SCREENS

The function of the screens is to transmit radiation extending over fairly narrow regions of the spectrum. By means of such screens, which, either singly or in combination, are placed in front of the thermocouples, one can obtain some idea of the spectral energy distribution of stars. Screens were selected which had a uniformly high transmission over a fairly narrow region of the spectrum, terminating abruptly in complete opacity in the rest of the spectrum. By proceeding in this manner no correction was necessary to the observations other than that for surface reflection, which amounts to about 9 per cent for the two surfaces of the screen. A slight amount of dust will raise the reflection losses to 10 per cent, or even higher. The screens selected have the following properties:

FLUORITE, which was used as the window of the vacuum container, transmits uniformly all radiations from the extreme ultra-violet to 10μ in the infra-red.

Digitized by Google

QUARTZ, thickness 4.77 mm, is transparent to all radiations from the extreme ultra-violet to 4.1μ in the infra-red (see curve A, Fig. 2). This gives the spectral radiation extending from 0.3μ to 4.1μ

WATER, thickness 1 cm, in a cell containing thin quartz windows, is transparent from the extreme ultra-violet to 1.4μ in the infra-

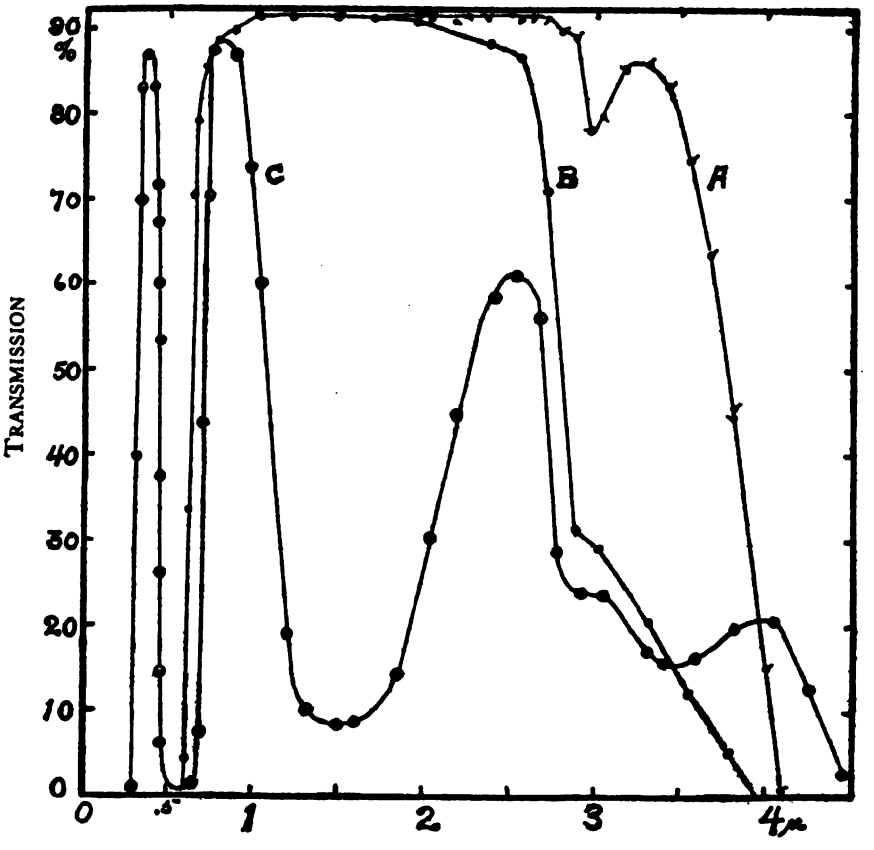

FIG. 2.—*Transmission curves of screens: A, quartz; B, red glass; C, blue-purple glass*

red (see curve *C*, Fig. 3). Used as a screen this gives the spectral radiation between 0.3μ and 1.4μ.

YELLOW GLASS, Schott's Jena 5560, thickness 2.97 mm, is opaque to radiations of wave lengths less than 0.43μ (see curve *A*, Fig. 3). The infra-red transmission is not very abrupt. Hence it was used in combination with the water cell, giving the spectral radiation between 0.43μ and 1.4μ.

RED GLASS, Schott's Jena 4512, thickness 1.97 mm, is opaque to radiations of wave lengths less than 0.6μ (see curve *B*, Fig. 2).

Digitized by Google

It was used in combination with the water cell, giving the spectral radiation between 0.6μ and 1.4μ. The difference between the galvanometer deflection when the water cell is interposed and when the water cell plus the red glass are interposed (corrected for reflection) gives the radiation in the spectral region from 0.3μ to 0.6μ. Similarly, the difference between the galvanometer deflec-

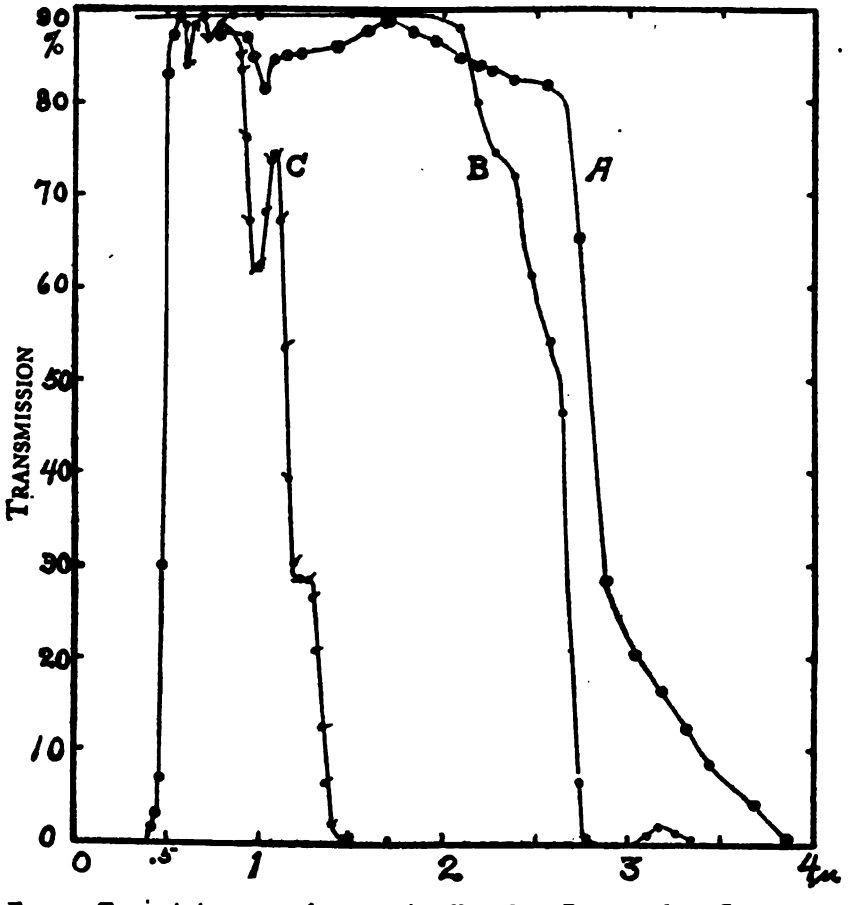

FIG. 3.—*Transmission curves of screens: A, yellow glass; B, pyrex glass; C, water, 1 cm in thickness*

tion for the water cell plus yellow glass and the deflection for the water cell plus red glass represents the spectral radiation between 0.43μ and 0.60μ.

PYREX GLASS, Corning, thickness 1.19 cm, terminates very abruptly in its transmission at 2.8μ (see curve *B*, Fig. 3). However, the sample used contained striæ and it was used in the measurements of the radiation from only one star.

Digitized by Google

BLUE-PURPLE-ULTRA GLASS, Corning, G 585, thickness 3.15 mm, when used in combination with the water cell gives the radiation in two high narrow transmission bands, at 0.36μ and 0.83μ, respectively (see curve *C*, Fig. 2). Using in addition the above-mentioned red or yellow glass, the radiation in the spectral region from 0.7μ to 1.4μ is obtained. Hence, by proper combination of the data one can obtain the radiation intensities between 0.6μ and 0.7μ and between 0.3μ and 0.4μ. Owing to a constant change in galvanometer sensitivity, which required so much time in repeating observations when using the various screens, this blue-purple screen was used in only one series of measurements of stellar radiation.

By means of these screens it was possible to obtain the radiation intensity in the spectrum from the extreme ultra-violet (which is limited by atmospheric transmission and the low reflectivity of the mirrors) at 0.3μ to 0.43μ, 0.43μ to 0.60μ, 0.60μ to 1.4μ, 1.4μ to 4.1μ, and 4.1μ to 10μ.

These screens, which were in the form of disks 25 mm in diameter, were mounted in brass supports, which in turn were mounted upon brass rods and sleeves, as shown in Fig. 4. Each rod and sleeve could be rotated independently by means of a lever. In this manner the various screens could be interposed (either singly or in combination) in the optical path.

In Fig. 4 the vacuum thermocouple mounting of Fig. 1 is shown in its holder. The small eyepiece to the right is for setting the thermojunction on the star image. The incandescent lamp is for illuminating the levers when operating the transmission screens. The whole mounting takes the place of the plate holder in the telescope, and it required only a few minutes to interchange it with the plate holder.

5. THE REFLECTING TELESCOPE

The telescope used in this investigation was the 40-in. (100 cm) reflector of the Lowell Observatory, which is at an elevation of 7300 ft. The focal length is 221 in. (550 cm). There is a diagonal mirror which reflects the star image to the side of the tube. The mirrors were newly silvered and in an excellent condition. The elevation being almost twice that of the station previously used, atmospheric scattering and absorption should be appreciably reduced. At this station there is a rainy season during two of the summer months, and this summer the cloudiness

Digitized by Google

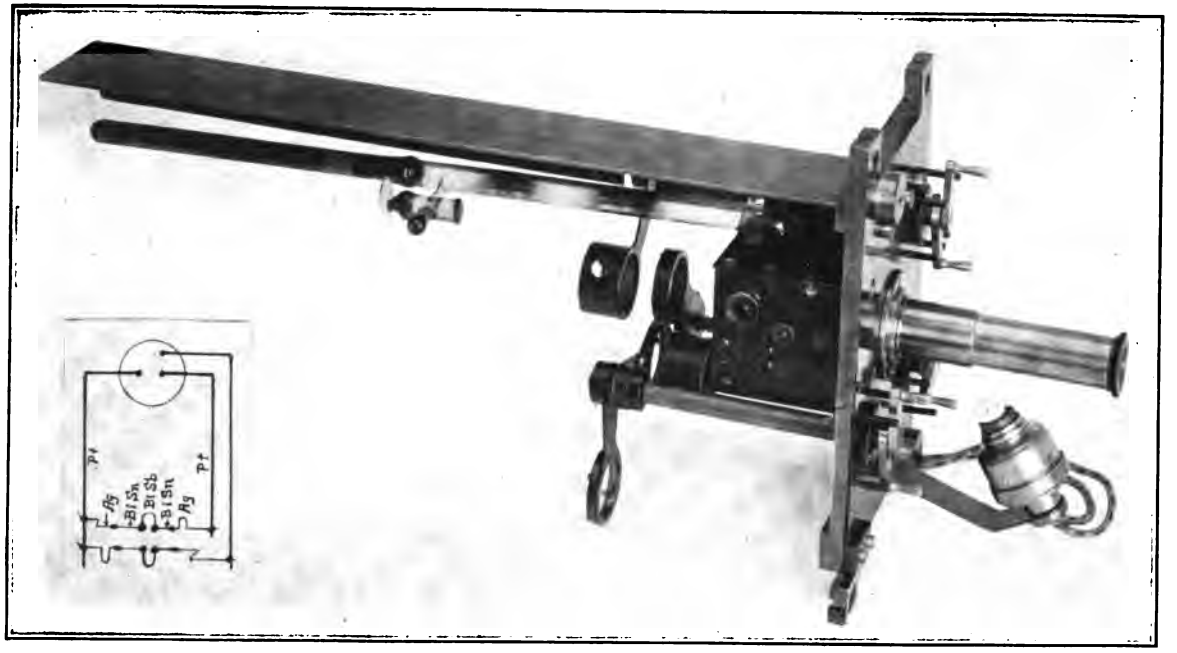

FIG. 4.—*Mounting for stellar thermocouple container (see Fig. 1) and transmission screens; inset, diagram of thermocouples*

Digitized by Google

Digitized by Google

continued longer than usual, thus encroaching upon the time set for making the experiments. For this reason the observations were not made under such ideal conditions from night to night as was hoped. However, observations made on the same night are consistent in showing small gradations in the infra-red component radiation, corresponding with the small gradations in spectral types (for example, B2 and B8) of stars. There are apparently slight inconsistencies in the water cell transmissions in comparing class B and class A stars. While this may really be true, and perhaps is to be expected, further observations will be necessary to decide this question. This form of stellar radiometer is very sensitive to slight changes in atmospheric transparency which are scarcely perceptible to the eye of even an experienced astronomer.

III. MEASUREMENT OF THE TOTAL RADIATION FROM STARS

The method of observation consisted in projecting the star image alternately upon the two junctures of the thermocouple by turning the slow motion screws of the plate holder and noting the change in the galvanometer deflection as observed with the telescope scale, which was at a distance of 2 m.

In the present investigation the total radiation measurements seemed of little interest. They constitute the measurements made without the transmission screens, and they are given in Table 3. The size of the deflections are of the same order as previously observed, verifying previous conclusions that red stars emit far more total radiation than blue stars of the same visual magnitude. For example, the observations of October 6 show that μ Geminorum emits about four times as much total radiation as ϵ Geminorum, which has the same visual magnitude,

The great difference in the total radiation from stars is well illustrated in Table 4, which gives a comparison of the total radiation from groups of stars having closely the same visual magnitude.

Observations of total radiation were made on 13 stars not previously observed. Since considerable time was required to complete a series of observations in order to determine the spectral radiation, no attempt was made to observe faint stars.

Digitized by Google

TABLE 3.—Total Radiation From Stars; also Transmission through a 1 cm Cell of Water. The Time is "Standard Mountain Time"

Object	Date (1921)	Hour	Magnitude	Observed deflection	Maximum deviation from the mean value	Galvanometer sensitivity $i = k \cdot 10^{-10}$	Galvanometer deflection for $i = 1 \cdot 10^{-10}$	Spectral class of star	Transmission of water cell
				cm			cm		Per cent
α Aquilae	Sept. 27	7:15	0.9	1.70	0.15	1.11	1.89	A5	73
	Oct. 5	8:30		1.61	.04	1.16	1.87	.....	69
α Scorpii	Sept. 27	7:45	1.22	7.60	.18	1.16	8.82	Map	33
α Lyrae	Sept. 27	8:45	.14	3.05	.15	1.18	3.60	Ao	75
β Andromedae	Sept. 27	11:45	2.37	2.33	.15	1.05	2.45	Ma	41
α Tauri	Sept. 27	13:15	1.06	5.80	.20	1.04	6.03	K5	42
α Aurigae	Oct. 3	12:30	.21	3.81	.10	1.29	4.91	Go	57
β Tauri	Oct. 3	13:00	1.78	.66	.06	1.18	.78	B8	79
γ Orionis	Oct. 3	13:15	1.70	.53	.04	1.21	.64	B2	82
α Orionis	Oct. 3	13:30	.92	12.40	.20	1.21	15.00	Ma	34
β Orionis	Oct. 3	14:30	.34	2.08	.05	1.39	2.89	B8 p	63
θ Orionis (Nebula)	Oct. 3	15:00	.....	± .02	.....	.....	.....	.....	.....
α Canis Majoris	Oct. 3	15:30	−1.58 8.5	6.40	.20	1.66	10.62	Ao	65
α Boötis	Oct. 5	7:15	.24	7.10	.25	1.14	8.10	Ko	47
α Cygni	Oct. 5	9:45	1.4	1.06	.04	1.26	1.34	A2	76
ε Orionis	Oct. 6	14:00	1.75	.43	.07	1.54	.66	Bo	81
α Persei	Oct. 6	14:20	1.90	.45	.04	1.66	.75	F5	74
α Canis Minoris	Oct. 6	15:00	.48 13.5	1.70	.08	1.57	2.67	F5	64
β Canis Minoris	Oct. 6	15:15	3.09	.25	.03	1.51	.38	B8	.....
γ Geminorum	Oct. 6	15:30	1.98	.47	.04	1.51	.71	Ao	.....
β Geminorum	Oct. 6	15:45	1.21	1.46	.07	1.50	2.19	Ko	58
α Geminorum	Oct. 6	16:00	1.99 2.85	.50	.05	1.55	.78	Ao	82
μ Geminorum	Oct. 6	16:15	3.19	1.36	.09	1.55	2.11	Ma	41
ε Geminorum	Oct. 6	16:45	3.18	.38	.03	1.52	.58	G5	66
α Leonis	Oct. 6	17:00	1.3	.48	.09	1.63	.78	B8	.....
γ Leonis	Oct. 6	17:15	2.61 3.80	.61	.09	1.63	.99	Ko	.....
Mars	Oct. 6	17:25	.....	.75	.07	1.63	1.22	.....	67
Venus	Oct. 6	17:40	.....	60.20	.10	1.63	98.30	.....	.....
β Lyrae	Oct. 10	8:00	var.	.21	.05	1.25	.26	B8 p	.....
λ Aquarii	Oct. 10	8:45	3.84	.65	.08	1.16	.75	Ma	47
β Pegasi	Oct. 10	9:10	2.61	2.28	.12	1.30	2.96	Mb	38

By increasing the sensitivity—say, 5 times—thus obtaining deflections of 15 to 20 mm instead of 3 to 5 mm as previously observed, it will be possible to determine the spectral energy distribution of a large number of stars which could not be measured accurately with the present temporary radiometric installation. As already explained, the present apparatus was hastily assembled to try out a specific problem, and advantage could not be taken of the full sensitivity available.

The measurements of the total radiation, and of the transmission through the water cell are given in columns 7 and 9, respectively, of Table 5. The latter are the ratio of the observed galvanometer deflections without correction for losses by reflection, etc. The

Digitized by Google

numerical values are somewhat higher than previously observed. They would be still higher for blue stars if a correction were made for absorption by the silver mirrors.

TABLE 4.—Comparison of the Total Radiation from Stars Having Closely the Same Visual Magnitude

Star	Spectral class	Visual magnitude	Galvanometer deflection	Star	Spectral class	Visual magnitude	Galvanometer deflection
			cm				cm
ϵGeminorum	G5	3.18	0.58	δOphiuchi	Ma	3.03	1.37
μGeminorum	Ma	3.19	2.11	γLeonis	Ko	2.61	.99
						3.80	
βGeminorum	Ko	1.21	2.19	βPegasi	Mb	2.61	2.96
αScorpii	Ma	1.22	8.82				
				αCoronae Borealis	Ao	2.32	.48
αAquilae	A5	.90	1.89	βUrsae Majoris	Ao	2.44	.37
αTauri	K5	1.06	6.03	γDraconis	K5	2.42	1.65
αOrionis	Ma	.92	15.0				
				αAurigae	Ge	.21	4.91
ρOphiuchi	Ko	2.94	.37	αBootis	Ko	.24	8.10

IV. MEASUREMENT OF THE SPECTRAL RADIATION OF 16 STARS

Under this caption are gathered all the observations of the spectral radiation measurements on 16 stars and various comments relating thereto. A typical example of the spectral component radiation data is given in Table 5, tabulated as follows: Column r gives the range of the spectrum transmitted by the various transmission screens used on a particular star; column 2 gives the observed galvanometer deflections, corrected for losses (9 per cent) by reflection from the surfaces of the transmission screens; column 4 gives the "reduced deflection" obtained from column 2, arranged in consecutive order in the spectral ranges given in column 3. After applying a correction for absorption by the two silvered mirrors, column 5, and an additional correction for atmospheric absorption (entirely uncertain at 4 to 10μ), column 6, the data in the various spectral regions are calculated in per cent of the total radiation, columns 7 and 8. Finally, in column 9 are given the calculated spectral components in percentage of the total radiation emitted by a black body at the temperature indicated at the top of the column. For this purpose the constant $C_2 = 14\,320$ was used. The calculated spectral energy curve, for, say, 3000° K, was drawn to a large scale on cross-section paper. Similar curves were drawn after applying the spectral transmission data of the various screens.

Digitized by Google

TABLE 5.—Spectral Component Radiation Data of β Orionis (Rigel)

Magnitude 0.34 ; Class B8p

Observed spectral transmission ranges	Observed galvanometer deflection	Galvanometer deflection				Percentage of total radiation		
		Consecutive spectral ranges	Reduced deflection	Corrected for mirrors	Corrected for mirrors and atmosphere	Observed		Calculated for 10 000° K
						Corrected for mirrors	Corrected for mirrors and atmosphere	
μ	cm	μ	cm	cm	cm	Per cent	Per cent	Per cent
0.3 to 10.....	2.08	0.3 to 0.43	0.73	1.22	1.52	45.7	51.3	49.5
.3 to 4.1.....	1.90	.43 to .6	.39	.46	.53	17.2	17.9	17.5
.3 to 1.4.....	1.47	.6 to 1.4	.35	.37	.37	13.9	12.5	21.4
.43 to 1.4.....	.74	1.4 to 4.1	.43	.44	.54	16.5	18.3	10.8
.6 to 1.4.....	.35	4.1 to 10	.18	.18	.....	6.7	.....	.8

The areas of these curves are proportional to the radiation transmitted by the screens. Hence a comparison can be made between the computed and observed data. Since atmospheric absorption terminates the spectrum at 0.3μ, the calculated spectral energy curves were similarly terminated at 0.3μ. This has no effect upon the spectral energy curves at 3000° K. But for temperatures of 8000 to 10 000° K an appreciable amount of the calculated energy lies at wave lengths less than 0.3μ.

The data herewith presented represent spectral energy curves of stars as observed at an altitude of 7300 ft (2250 m.). In view of the preliminary nature of the measurements, sufficient time was not available to work out fine corrections for atmospheric absorption pertaining to the particular screens used, and thus obtain a more accurate energy distribution of stars as it is outside the earth's atmosphere. In the case of the Sun, in spite of numerous attempts, it has not been possible [16] to work out satisfactorily the relative spectral energy distribution as it is outside the atmosphere, and it would be even more difficult for blue stars in which the maximum radiation intensity lies in the ultra-violet. Since air is opaque to radiation of wave lengths less than about 0.29μ, it is not known whether radiation of wave lengths less than 0.29μ is emitted by stars.

1. SPECTRAL ENERGY DATA ON 16 STARS

The spectral radiation components are given in Table 6. The data are arranged according to spectral class, the date of observation being given in Table 3. Comments on special features of these observations are made under separate captions.

[16] Abbot and Fowle, Ann. Astrophys. Obs., 8, p. 139; 1913.

Digitized by Google

TABLE 6.—Spectral Radiation Components of 16 Stars in Per Cent of the Total Observed Radiation. Corrected for all Losses Except Atmospheric Absorption (Which May Be Obtained from Table 5)

Observed spectral range	β Orionis, Mag. 0.34; Class B8p	ε Orionis, Mag. 1.75; Bo	α Canis Majoris, Mag. 1.6 and 8.5; Ao	α Lyrae, Mag. 0.14; Ao	α Cygni, Mag. 1.4; A2	α Aquilae, Mag. 0.9; A5	α Canis Minoris, Mag. 0.48 and 13.5; F5	α Aurigae, Mag. 0.21; Go	α Boötis, Mag. 0.24; Ko	β Geminorum, Mag. 1.21; Ko	α Tauri, Mag. 1.06; K5	α Orionis, Mag. 0.92; Ma	α Scorpii, Mag. 1.22; Map	β Andromedae, Mag. 2.37; Ma	μ Geminorum, Mag. 3.19; Ma	β Pegasi, Mag. 2.61; Mb
μ																
0.3 to 0.43	45.7	59.3	36.2	41.1	41.0	38.7	23.5	18.4	16.1	29.9	10.6	7.0	.....	.....	22.7	.....
.3 to .6	.....	.....	.....	.....	.....	.....	.....	.....	.....	.....	.....	.....	10.8	20.2	.....	16.4
.43 to .6	17.2	.....	20.1	19.0	20.2	17.8	20.0	18.2	5.7	10.9	4.3	3.1	.....	.....	5.2	.....
.43 to 1.4	.....	32.2	.....	.....	.....	.....	.....	.....	.....	.....	.....	.....	.....	.....	.....	.....
.6 to 1.4	13.9	.....	20.2	24.1	26.1	23.1	30.0	30.6	33.8	28.7	31.0	29.4	27.8	30.4	22.7	27.0
1.4 to 4.1	16.5	.....	21.1	13.2	9.7	19.5	24.0	26.4	38.1	25.3	52.0	57.7	56.4	33.2	40.3	52.5
1.4 to 10	.....	8.5	.....	.....	.....	.....	.....	.....	.....	.....	.....	.....	.....	.....	.....	.....
4.1 to 10	6.7	.....	2.4	2.6	3.0	.9	2.5	6.4	6.3	5.2	2.1	2.8	5.0	16.2	9.1	4.1

TABLE 6A.—Examples of the Comparison of Observed and Calculated Spectral Radiation Components in Percentage of the Total.

Spectral range	α Lyrae 8000 K		α Cygni 8000 K		α Canis Minoris 6000 K		α Orionis 3000 K		α Scorpii 3000 K		β Orionis 10 000 K	
	Observed	Calculated	Observed	Calculated	Observed	Calculated	Observed	Calculated	Observed	Calculated	Observed	Calculated
μ												
0.3 to 0.43	41.1	41.0	41.0	41.0	23.5	28.0	7.0	5.2	.....	.....	45.7	49.5
.3 to .6	.....	.....	.....	.....	.....	.....	.....	.....	10.8	8.1	.....	.....
.43 to .6	19.0	19.9	20.2	19.9	20.0	19.5	3.1	2.9	.....	.....	17.2	17.5
.6 to 1.4	24.1	25.3	26.1	25.3	30.0	30.5	29.4	27.9	27.8	27.8	13.9	21.4
1.4 to 4.1	13.2	13.0	9.7	13.0	24.0	21.0	57.7	55.0	56.4	55.0	16.5	10.8
4.1 to 10	2.6	.8	3.0	.8	2.5	1.0	2.8	9.0	5.0	9.0	6.7	.8

Digitized by Google

In comparing the observed with the calculated spectral components no attempt is made to obtain agreement in the ultra-violet (0.3μ to 0.43μ) and the extreme infra-red (4.1μ to 10μ). In a few cases where the calculated and the computed data are not very close, the temperature is arrived at from a consideration of the ratio of intensities of the spectral ranges 0.43μ:0.6μ and 0.6μ: 1.4μ or 1.4μ: 4.1μ.

In some cases the observed ultra-violet component is extremely large in comparison with the calculated value; for example, μ Geminorum, which appears to have a peculiar spectral energy distribution. In this case the galvanometer deflections were small and the galvanometer sensitivity was changing. Hence, some of the disagreement is, no doubt, owing to errors of observation. Similarly, β Geminorum, α Andromedae and β Pegasi appear to have a complex spectral energy distribution. In β Pegasi the ultra-violet component seems large. The other components indicate a spectral energy distribution similar to that of a black body at 3000 to 3300° K.

In numerous cases the agreement between the observed and the calculated values was found to be very close; as, for example, in the α-stars of Lyra, Cygnus, Aquila, Canis Minor, Taurus, Orion, and Scorpio. In the latter the spectral components of wave lengths 4.1μ to 10μ is small, but this may be owing to absorption by the large air mass (see Table 6A.)

In the case of binary stars having large companions of low luminosity—as, for example, α Canis Majoris and β Orionis (see Table 5)—the agreement between the observed and the calculated spectral components is not very close. The short wave length components are similar to those of a radiator at 8000 to 10 000° K, whereas the infra-red components are in agreement with those of a radiator at 4000° K. This, however, does not cast doubt upon the method, but substantiates the conclusions drawn from the transmission observations, made with only the water cell, which show that there is an excess of infra-red radiation in binary stars having companions of low luminosity. This is similar to the radiation from a gas flame—for example, an acetylene flame in which the incandescent carbon particles have their maximum emission in the short wave lengths—whereas the products of combustion, CO_2 and water vapor, have their maximum emission (CO_2 at 4.4μ) in the infra-red.

Digitized by Google

2. THE WATER CELL TRANSMISSION DATA

The measurement of the stellar radiation transmitted by the water cell is a quick and an efficient means of determining the infra-red radiation from stars. The observed transmissions for the blue, B and A class stars (which have no dark companion stars), are as high as 82 per cent, and if a correction had been made for absorption by the silvered mirrors the transmission would be still higher. Since the maximum observable transmission through the water cell can be only about 91 per cent, and since the water cell absorbs but little radiation of wave lengths less than 0.9μ, it appears from this high transmission that in blue stars there is but little infra-red radiation of wave lengths greater than 1μ. Assuming that the energy distribution is similar to that of a black body, the transmission data indicate that the maximum emission must lie in the ultra-violet. From this it appears that much information on the spectral energy distribution of blue stars can be obtained by means of the photographic plate.

In Table 7 the water cell transmissions are arranged in the order of the spectral class of the star. These data confirm previous measurements showing that the red stars are losing heat by radiation much faster than blue stars of the same visual magnitude. In this same table data are given on the absolute magnitudes and the luminosities [17] of some of the stars. As is to be expected, these data do not contribute much to the present problem.

TABLE 7.—Transmission of Stellar Radiation Through 1 cm Layer of Water

Star	Magnitude		Luminosity	Spectral type	Transmission	Remarks
	Relative	Absolute				
					Per cent	
ϵ Orionis	1.75	.....	.....	Bo	81	
γ Orionis	1.70	.....	.....	B2	82	
β Tauri	1.78	.....	.....	B8	79	
β Orionis	.34	.....	.....	B8 p	*63	(Rigel) spectroscopic binary
α Geminorum	1.99 2.85	.....	.....	Ao	82	(Castor)
α Lyrae	.14	.....	.....	Ao	75	(Vega)
α Canis Majoris	−1.58 8.5	.....	.....	Ao	*65	(Sirius) binary
α Cygni	1.4	.....	.....	A2	76	(Deneb)
α Aquilae	.9	.....	.....	A5	71	(Altair)
α Persei	1.9	+0.3	75.9	F5	74	(Suspected binary)
α Canis Minoris	.48 13.5	+3.1	5.75	F5	*64	(Procyon) binary
α Aurigae	.21	+ .3	75.9	Go	*57	(Capella) spectroscopic binary
ϵ Geminorum	3.18	−1.0	251.	G5	66	
β Geminorum	1.21	+ .8	47.9	Ko	58	(Pollux)
α Boötis	.24	+ .9	43.7	Ko	47	(Arcturus)
α Tauri	1.06	+ .9	43.7	K5	42	(Aldebaran)
λ Aquarii	3.84	.....	.....	Ma	47	
μ Geminorum	3.19	.....	.....	Ma	41	
β Andromedae	2.37	+1.6	22.9	Ma	41	
α Orionis	.92	.....	.....	Ma	34	(Betelgeux)
α Scorpii	1.22	−3.0	1584.	Ma p	*33	(Antares) spectroscopic binary
β Pegasi	2.61	+1.3	30.2	Mb	38	

[17] Adams and Joy, Astrophys. J., 46, p. 313; 1917.

Digitized by Google

3. THE QUARTZ CELL TRANSMISSION DATA

The transmission measurements made with the quartz cell corrected for reflection indicate a small amount of infra-red radiation of wave lengths greater than 4μ. In the case of blue stars this amounts to only 2 to 5 per cent. In some cases the observed radiation is greater than the computed, as, for example, in α Lyrae. This is partly owing to errors of observation and also because the correction of 9 per cent for reflection and scattering is too low. The correction for reflection of a screen which is slightly dusty is 10 to 11 per cent.

In the case of red stars some measurements indicate the presence of infra-red radiations, of wave lengths greater than 4μ, to the extent of 10 per cent or more of the total. In some cases the data seem inconsistent (for example, Antares and Aldebaran), but this is probably owing to the large air mass, and hence the large absorption of infra-red rays. On the other hand, in some of the blue stars the low emissivity at 4μ to 10μ is probably owing to selective emission.

The data on β Orionis (Table 5) confirm the water-cell transmission measurements, showing a large percentage of infra-red radiation from binary stars. Since only a small proportion of the total radiation from stars is of wave lengths greater than 4.5μ, it appears that radiometers with thin quartz windows can be used in stellar radiometry.

4. BINARY STARS

In Table 7 the stars marked thus (*) are binaries with companions of low luminosity and so close to the primary star that they could not be measured separately. In all cases the water-cell transmissions are low, showing the large amount of infra-red radiation contributed by the dark companion in comparison with the total radiation incident upon the thermocouple. This is especially conspicuous in the case of Sirius. In this connection the following excerpts from Aitken [18] are appropriate (italics inserted by the writer):

> The magnitude of Sirius on the Harvard scale is -1.58. Estimates of the brightness of the companion vary, but it is probably not far from 8.5 on the same scale, a difference of 10.1 magnitude. Accepting these figures, *Sirius radiates more than 11 000 times as much light as its companion;* and, if the parallax 0.376″ is correct, fully 30 times as much as our Sun. Yet, according to the best mass determinations, the bright star is only 2.56, the companion 0.74 times as massive as the Sun; and Adams finds that the smaller star, which to the eye seems decidedly the yellower, has the same spectrum (class A) as the bright star. These are facts, as Campbell says, "we are powerless to explain at present."

[18] Aitken, The binary stars, p. 229; 1918.

Digitized by Google

From Table 7 it may be noticed that although the visible radiation from the companion is less than $\frac{1}{11,000}$th that of Sirius, the infra-red radiation is sufficient to reduce the transmission of a class A star from 80 to 65 per cent. In other words, the infra-red radiation from the companion star is much (2 to 3 times) greater than that of Sirius.

The method of analysis by means of the water cell may be useful in obtaining information concerning doubtful cases of spectroscopic binaries. For example, Campbell [19] lists α Persei (class F5) as having a suspected variation in radial velocity caused by a companion star. The water-cell transmission is high (74 per cent) and of the order to be expected for a star of its class. Hence, we may infer that the companion star is of the same or a later class (for example, class A), or, what is more likely, that there is no companion star.

5. STELLAR TEMPERATURES

The radiation emanating from the photosphere of a star is complex. In some cases—as, for example, γ Cassiopeiae (class B 0 p)—recently studied by Plaskett,[20] there are bright emission lines of hydrogen or helium superposed upon a continuous spectrum. It is therefore difficult to determine the spectral energy distribution of the radiation from such stars.

From laboratory experience it is known that in the spark spectra (hypothetical temperature 10 000°K) of metals the maximum emisssion is in the ultra-violet.[21] Similarly, the emission spectrum of an arc between metal electrodes and in the carbon arc (3600°K) is in the near infra-red -0.8 to 1μ. The quartz-mercury arc has its maximum emission at 0.365μ. For vacuum tube radiation, hydrogen has its most intense emission lines in the visible and ultra-violet; nitrogen,[22] in the region of 1μ, while the radiation from incandescent helium is confined almost entirely to the emission line at 1.08μ.[23] The radiation from highly attenuated material at a high temperature (for example the incandescent particles of carbon in an acetylene flame) is the most saturated for the short wave lengths.[24] Even for incandescent solids in the form of rods[25] (Nernst glowers) it was found that saturation of radiation seems

[19] Lick Obs. Bulletin, 6, p. 17; 1910. Goos, Astronom. Nachtr., 180, p. 57; 1909.
[20] Plaskett, Mo. Notices, Roy. Astro. Soc., 80, p. 771; 1920.
[21] Pflüger, Ann. der Phys. (4), 18, p. 890; 1904.
[22] Investigation of infra-red spectra, Publ. No. 35, Carnegie Inst. of Wash., 1905.
[23] B. S. Bulletin, 9, p. 93; 1912.
[24] B. S. Bulletin, 7, p. 253, 1911; 9, p. 98, 1912. B. S. Sci. Papers, 15, p. 639; 1920.
[25] B. S. Bulletin, 9, p. 102; 1912.

Digitized by Google

to begin in the short wave lengths. Whether in stars of low density but of infinite thickness of the radiating layer the spectral energy distribution is that of a complete radiator or so-called black body remains to be determined. In the case of stars showing bright spectral lines the emission is evidently highly selective. In the case of incandescent helium the infra-red radiometric measurements on stars might show a peculiar energy distribution owing to the strong emission line at 1.08μ. From these as well as other considerations one can hardly expect to obtain exact agreement between the calculated and the observed results.

An estimate of the effective temperature of a star was obtained by two methods. The first method consisted in making all corrections to the observations, excepting those for atmospheric absorption, and comparing them with the calculated values, using a solar type star (α Aurigae, class Go) as a standard. This seems permissible in view of the fact that the observed temperature (6000°K) of α Aurigae was found to be in close agreement with that assigned to the sun. The stellar temperatures estimated in this manner are given in column 4 of Table 8.

The second method consisted in applying all corrections to the observations, including the one for atmospheric absorption, and comparing the results with the calculated values. Applying factors for atmospheric absorption introduces great irregularities in the observed spectral radiation components. This, no doubt, is owing partly to selective emission of the star and partly to the use of improper transmission factors, which, because of lack of time, could not be determined directly.

The temperature of a star, as estimated from the spectral energy components outside of the atmosphere, extends over a wide range, the average value of which is in good agreement with that obtained by the first method. (See column 3 of Table 8. For each star, the maximum temperature is obtained from the shortest component radiation.)

In the B and A class stars the effective temperatures are no doubt somewhat higher than herewith recorded because of lack of proper corrections for atmospheric absorption.

In the case of the Sun an estimate of the effective temperature of the photosphere has been arrived at by various methods. The estimated temperature varies from 5740° K, for the total radiation, to 6140° K, for the spectral radiation method.[26] Unfortunately,

[26] See recalculations by Coblentz, J. Op. Soc. Am., 5, p. 272; 1921.

Digitized by Google

the writer was not equipped to test the present apparatus on the Sun at the station used for measuring stellar radiation. However, the temperatures of the solar type stars (class G) are in good agreement with that of the Sun. For example, the observed temperature of α Aurigae is between 5500° K (see Table 8) and 6000° K. By making proper corrections for atmospheric absorption the effective temperature of the stellar photosphere as observed outside the earth's atmosphere would be several hundred degrees higher. Hence, a conservative estimate is 6000° K.

TABLE 8.—Stellar Temperatures

Star	Class	Coblentz		Wilsing, Scheiner, and Münch	Nordmann and Le Morvan	Nordmann	Saha
		Calculated	Class Go as standard				
		°K	°K	°K	°K	°K	°K
α Orionis	Bo	13 000–14 000	13 000	.....	.....	.....	18 000
β Orionis	B8p	10 000–12 000	10 000	.....	.....	.....	.....
α Lyrae	Ao	8000–10 000	8000	9400	.....	12 200	.....
α Canis Majoris	Ao	8000–11 000	8000	.....	.....	.....	12 000
α Cygni	A2	8000–10 000	9000	9400	.....	.....	.....
α Aquilae	A5	7000–9000	8000	8100	.....	.....	.....
α Canis Minoris	F5	5500–7500	6000	7200	.....	.....	.....
α Aurigae	Go	5300–6500	6000	7100	.....	.....	7000
α Bootis	Ko	3500–4500	4000	3700	.....	.....	.....
β Geminorum	Ko	4500–7000	5500	4900	.....	.....	.....
α Tauri	K5	2800–4500	3500	3500	3600	3500	.....
α Orionis	Ma	2800–3300	3000	3000	.....	.....	5000
α Scorpii	Map	2500–3200	3000	.....	.....	.....	.....
β Andromedae	Ma	3500–4500	4000	3200	4300	3700	.....
μ Geminorum	Ma	2500–3300	3500	3100	3200	.....	.....
β Pegasi	Mb	2500–3200	3000	2800	.....	.....	.....
Sun	Go	.....	[a]5800–6200	.....	.....	5320	.....

[a] Recalculated from Abbot and Fowle, Jour. Opt. Soc. Am., 5, p. 272; 1921.

In Table 8 are assembled various determinations of the effective stellar temperatures by Nordmann,[27] and by Nordmann and Le Morvan;[28] also determinations by Wilsing, Scheiner, and Münch,[29] and calculated values by Saha[30] on the basis of ionization theory.

The various methods used to obtain stellar temperatures give different results. For example, Plaskett (see footnote 20) obtained an effective temperature of 6800° K for γ Cassiopeiae (class Bop) by considering the continuous spectrum, and 10 600° K by considering the bright line spectrum of hydrogen and Bohr's theory of the energy and frequency required to ionize the hydrogen atom. In view of the fact that his continuous spectrum measure-

[27] Nordmann, C. R., 149, p. 1038; 1909.
[28] Nordmann and Le Morvan, C. R., 178, p. 72; 1921.
[29] Wilsing, Scheiner, and Münch, Publ. Astrophys. Obs., Potsdam, 24, No. 74; 1920.
[30] Saha, Proc. Roy. Soc. London (A), 99, p. 135; 1921.

Digitized by Google

ments terminated at 0.42μ, where also is the maximum spectral energy, it is possible that the higher temperature, estimated on the basis of ionization theory, is the more nearly correct.

Wilsing, Scheiner, and Münch [30] also obtained a temperature of 6800° K for γ Cassiopeiae. Their temperature measurements for various stars of class B vary from 7000 to 15 000° K; class A, vary from 8000 to 12 000° K; class F, vary from 5000 to 7000° K; class G, from 4000 to 5000° K; and class M, 3000 to 3500° K.

While it is to be expected that the various methods used must give different results, it is extremely interesting to find a rather close agreement in the estimated temperature as shown in Table 8. The agreement is especially close for stars of classes G, K, and M; that is, stars having a low temperature.

In conclusion, it may be added that, owing to the nature of the spectral energy distribution of stars at low temperatures as a result of atmospheric absorption, the observed maximum emission is no doubt shifted farther toward the short wave lengths than is the true maximum. Hence, the temperatures may be several hundred degrees lower than here recorded. Similarly, for the B and A classes of stars, which have their maximum emission in the ultra-violet, the temperatures may be considerably higher than here recorded owing to atmospheric absorption, which shifts the observed (ultra-violet) maximum emission farther toward the visible spectrum than is the true maximum, but which has little effect, relatively, on the infra-red spectral radiation component.

Most of the stars measured are no doubt giants, of which Russell [31] says: "The mean densities of the giant stars diminish rapdly with increasing redness, from one-tenth that of the Sun for class A to less than one twenty-thousandth that of the sun for class M." To those given to speculation concerning the nature of stellar radiation and temperatures it no doubt is of interest to find that the observed radiometric data seem conclusive in showing that the early type (class M) stars are losing heat by radiation three to four times as fast as the more dense but hotter late type (class B, A) stars. The least dense, class M, stars must therefore be losing heat by radiation, in which conduction can not contribute very materially in maintaining the surface at a given temperature. This is an interesting subject which should be given further attention.

In the dense stars the shape of the spectral energy curve, and hence our inferences of the effective temperature, is determined by

[31] Russell, Pop. Astron., 22, Nos. 5 and 6; 1914.

Digitized by Google

the spectral emissivity of the surface, while in the less dense stars the radiation emanates from great depths. Hence, as a matter of caution, it seems well to point out that the present meager data can not safely be used in considering the giant and the dwarf stars of the same class.

V. SUMMARY

The object of the present investigation was: (1) To test new stellar thermocouples, (2) to verify previous measurements of stellar radiation, (3) to measure the radiation intensities of bright stars in the region of 0 hrs. to 12 hrs., of right ascension, not previously measured, and (4) to determine the feasibility of the method of obtaining the spectral energy distribution of stars by means of transmission screens which, either singly or in combination, are placed in front of the vacuum thermocouple.

By means of vacuum thermocouples measurements were made on the total radiation intensities of 13 bright stars not observed in 1914, thus completing the survey of the whole sky. A total of 30 celestial objects were measured, including Venus and Mars.

By means of a series of transmission screens (of yellow and red glass, of water, and of a thick plate of quartz) wide spectral regions were isolated and the radiation intensities in the spectrum from 0.3μ to 0.43μ, 0.43μ to 0.6μ, 0.6μ to 1.4μ, 1.4μ to 4.1μ, and 4.1μ to 10μ were determined. In this manner the distribution of energy in the spectra of 16 stars was determined, thus obtaining for the first time an insight into the radiation intensities in the complete spectrum of a star.

By means of these transmission screens it was found that in the B and A class stars, the maximum radiation intensity lies in the ultra-violet (0.3μ to 0.4μ), while in the cooler, K and M class, stars the maximum emission lies at 0.7μ to 0.9μ in the infra-red. In the case of single stars, at all temperatures, the spectral energy distribution is selective as compared with a black body.

A calculation is made of the spectral component radiations of a black body at various temperatures, using the spectral transmission data on these screens. From a comparison of the observed and the calculated spectral radiation components it appears that the black body temperature (that is, the temperature which a black body would have to attain in order to emit a similar relative spectral energy distribution) varies from 3000° C for red, class M, through 6000° K for the yellow, solar-type stars, to 10 000° K or perhaps even higher for blue, class B, stars. Owing to selective

Digitized by Google

emission the true temperatures are higher than these values for black body radiation.

The observing station being much higher than previously used (7300 ft. as compared with 4000 ft.), the atmospheric scattering of light was greatly reduced, and consequently the transmissions in the violet are somewhat higher than previously observed when the water cell was interposed. However, all the data verify previous measurements, showing that red stars emit three to four times as much total radiation as blue stars of the same visual magnitude. Moreover, observations made on the same night (same weather conditions) are consistent in showing small gradations in the infra-red radiation component, corresponding with the small gradations (say, B2 and B8) in spectral classes.

For binary stars having companions of low luminosity the water-cell transmissions are low, indicating that the companion stars emit considerable infra-red radiation.

The measurements made with the water cell show that, in blue and yellow stars, practically all the energy lies in that part of the spectrum to which the photographic plate is sensitive. Hence, since the effect on the photographic plate is cumulative, and the time for exposure is relatively unlimited, the spectral energy distribution of many faint stars can be mapped, which will not be possible by any other methods known to us at the present day.

Among the subsidiary investigations made with a view to the improvement of stellar radiometers this paper gives data on the radiation sensitivity of thermocouples of alloys of gold-palladium, platinum-rhodium, bismuth-tin, bismuth-antimony, and also of pure bismuth.

WASHINGTON, December 16, 1921.

Digitized by Google

INDEX TO VOLUME 17.

A.

Page.

Absolute measurement of reflection and transmission factors 1
Air, liquid, production 277
Alloys, nickel, also copper, etching reagents. 635
Alloys of copper, thermal expansion 91
Alpha alloys of nickel, etching reagents 635
Altrup, F. W., G. W. Vinal, and, Electromotive force of cells at low temperatures ... 627
Aluminum, thermal expansion 497
Ammonia, liquid 287
Annealed eutectoid carbon steel 65
Arc spectra of yttrium, lanthanum, and cerium 317
Arc spectra, wave-lenth measurements 161
Arcs in gases and vapors 471
Argon spectrum 193

B.

Black body, thermal radiation 7
Boyd, H. S., C. G. Peters, and, Interference methods for standardizing and testing precision gage blocks 677
Breit, Gregory, High-frequency resistance of inductance coils 569
——, Some effects of the distributed capacity between inductance coils and the ground .. 521
——, The field radiated from two horizontal coils 589

C.

Capacity, distributed, between inductance coils and the ground 521
Carbon steel, annealed eutectoid 65
Cells at low temperatures, voltage 627
Cerium, arc spectrum 317
Characteristic soft X rays from arcs in gases and vapors 471
Cheney, W. L., C. Nusbaum, and, Effect of the rate of cooling on the magnetic and other properties of an annealed eutectoid carbon steel 65
Clark, E. P., An improved method for preparing raffinose 607
——, Note on the preparation of mannose 567
——, Preparation of galactose 227
Coblentz, W. W., A portable vacuum thermopile 187
——, Present status of the constants and verification of the laws of thermal radiation of a uniformly heated inclosure 7
——, Spectrophotoelectrical sensitivity of proustite 179
——, Spectroradiometric investigation of the transmission of various substances, II 267
——, Tests of stellar radiometers and measurements of the energy distribution in the spectra of 16 stars 725
Coils, horizontal, for electromagnetic radiation 589
Color sensitive photographic plates 353
Constants of thermal radiation of a black body 7
Construction of platinum resistance thermometers 49
Cook, J. W., The production of liquid air on a laboratory scale 277
Cooling, effect, on properties of carbon steel .. 65
Copper alloys, etching reagents 635
Copper and its alloys, thermal expansion 91
Crapoe, C. S., and D. R. Harper, 3d, Specific volume of liquid ammonia 287

D.

Davis, Raymond, A new method for the measurement of photographic filter factors. 79
—— *and Francis M. Walters, jr.*, Studies in color sensitive photographic plates and methods of sensitizing by bathing 353
Dextrose, solubility in water 715
Direction finder, radio 529
Distributed capacity between inductance coils and the ground 521
Dunmore, Francis W., Frederick A. Kolster, and, The radio direction finder and its application to navigation 529

E.

Earth elements, rare 317
Effect of cooling on properties of carbon steel. 65
Electromotive force of cells at low temperatures 627
Energy distribution in spectra of 16 stars 725
Etching reagents, metallographic 635
Eutectoid carbon steel 65
Expansion, thermal, of a few steels 611
Expansion, thermal, of copper 91
Expansion, thermal, of nickel, monel metal, stellite, stainless steel, and aluminum 497

F.

Factors, photographic filter 79
Factors, reflection and transmission 1, 203
Field from two horizontal coils 589
Filter factors, photographic 79
Foote, Paul D., F. L. Mohler, and, Characteristic soft X rays from arcs in gases and vapors 471

G.

Gages, precision, standardizing and testing .. 677
Galactose, preparation 227
Gases, X rays, from arcs in 471
Gray sensation 231

Digitized by Google

H.

Page.

Harper, D. R., 3d, C. S. Cragoe, and, Specific volume of liquid ammonia..... 287
Hidnert, Peter, Thermal expansion of copper and some of its important industrial alloys. 91
——, *Wilmer H. Souder, and*, Thermal expansion of a few steels..... 611
——, *Wilmer H. Souder, and*, Thermal expansion of nickel, monel metal, stellite, stainless steel, and aluminum..... 497
High-frequency resistance of inductance coils 569
High-tension magneto..... 407
Horizontal coils for electromagnetic radiation. 589

I.

Improved method for preparing raffinose.... 607
Induced voltage in high-tension magneto... 407
Inductance coils, high-frequency resistance.. 569
Industrial alloys of copper..... 91
Infra-red spectrum, wave-length measurements..... 161
Instrument for measuring reflection and transmission factors..... 1
Interference measurements in spectra of argon, krypton, and xenon..... 193
Interference methods for standardizing and testing precision gage blocks..... 677

J.

Jackson, Richard F., and Clara Gillis Silsbee, The solubility of dextrose in water..... 715

K.

Karrer, Enoch, Use of the Ulbricht sphere in measuring reflection and transmission factors..... 203
Kiess, C. C., B. S. Hopkins, and H. C. Kremers, Wave lengths longer than 5500 A in the arc spectra of yttrium, lanthanum, and cerium and the preparation of pure rare earth elements..... 317
Kolster, Frederick A., and Francis W. Dunmore, The radio direction finder and its application to navigation..... 529
Krypton spectrum..... 193

L.

Lanthanum, arc spectrum..... 317
Laws of thermal radiation of a black body... 7
Light, white..... 231
Liquid air production..... 277
Liquid ammonia..... 287
Lorentz, Marjorie G., Henry S. Rawdon, and, Metallographic etching reagents: II, for copper alloys, nickel, and the alpha alloys of nickel..... 635
Low temperatures affecting voltage of cells.. 627

M.

Magnetic properties of annealed eutectoid carbon steel..... 65
Magneto, high-tension..... 407
Mannose, preparation..... 567
Mathematical theory of induced voltage in high-tension magneto..... 407
Measuring energy distribution in spectra of 16 stars..... 725
Measuring interference in spectra of argon, krypton, and xenon..... 193
Measuring photographic filter factors..... 79
Measuring reflection and transmission factors 1, 203
Measuring wave lengths in arc spectra..... 161
Meggers, W. F., Interference measurements in the spectra of argon, krypton, and xenon. 193
Metallographic etching reagents..... 635
Modifications in platinum resistance thermometers..... 49
Modulator tube and radio telephone sets..... 377
Mohler, F. L., and Paul D. Foote, Characteristic soft X rays from arcs in gases and vapors..... 471
Monel metal, thermal expansion..... 497

N.

Navigation by radio direction finder..... 529
Nickel, etching reagents..... 635
Nickel, thermal expansion..... 497
Nusbaum, C., and W. L. Cheney, Effect of the rate of cooling on the magnetic and other properties of an annealed eutectoid carbon steel..... 65

O.

Operation of modulator tube in radio telephone sets..... 377

P.

Peters, C. G., and H. S. Boyd, Interference methods for standardizing and testing precision gage blocks..... 677
Photographic filter factors..... 79
Photographic plates, color sensitive..... 353
Platinum-resistance thermometers..... 49
Portable instrument for measuring reflection and transmission factors..... 1
Portable vacuum thermopile..... 187
Precision gage blocks, standardizing and testing..... 677
Preparing galactose..... 227
Preparing mannose..... 567
Preparing pure rare earth elements..... 317
Preparing raffinose..... 607
Priest, Irwin G., The spectral distribution of energy required to evoke the gray sensation 231
Producing liquid air on a laboratory scale... 277
Properties of annealed eutectoid carbon steel 65
Proustite, spectrophotoelectrical sensitivity.. 179
Pure rare earth elements..... 317
Purington, E. S., Operation of the modulator tube in radio telephone sets..... 377

R.

Radiation, thermal, of a black body..... 7
Radio direction finder and its application to navigation..... 529
Radio signaling at airplane landing field..... 589
Radio telephone modulator tubes..... 377

Digitized by Google

Page.

Radiometers, stellar 725
Raffinose, preparation 607
Rare earth elements 317
Rawdon, Henry S., and Marjorie G. Lorents, Metallographic etching reagents: II, for copper alloys, nickel, and the alpha alloys of nickel 635
Reagents for metallographic etching 635
Red spectrum, wave-length measurements ... 161
Reflection factors 1, 203
Resistance, high-frequency, of inductance coils 569
Resistance thermometers, platinum 49

S.

Sensation, gray 231
Sensitivity, spectrophotoelectrical, of proustite 179
Sensitizing photographic plates to color 353
Silsbee Clara Gillis, Richard F. Jackson, and, The solubility of dextrose in water 725
Silsbee, Francis B., Mathematical theory of induced voltage in the high-tension magneto 407
Sligh, T. S., jr., Recent modifications in the construction of platinum-resistance thermometers 49
Soft X rays from arcs in gases and vapors 471
Solubility of dextrose in water 725
Some effects of the distributed capacity between inductance coils and the ground 521
Souder, Wilmer, and Peter Hidnert, Thermal expansion of a few steels 611
——, *and Peter Hidnert,* Thermal expansion of nickel, monel metal, stellite, stainless steel, and aluminum 497
Specific volume of liquid ammonia 287
Spectra, arc, of yttrium, lanthanum, and cerium 317
Spectra of argon, krypton, and xenon 193
Spectra of 16 stars, measuring energy distribution in 725
Spectra, wave-length measurements 161
Spectral distribution of energy required to evoke the gray sensation 231
Spectrophotoelectrical sensitivity of proustite 179
Spectroradiometric investigation of the transmission of various substances 267
Sphere, Ulbricht 203
Stainless steel, thermal expansion 497
Standardizing precision gage blocks 677
Stars, measuring energy distribution in spectra 725
Steel, annealed eutectoid carbon 65
Steels, thermal expansion 611
Stellar radiometers, tests 725
Stellite, thermal expansion 497
Substances, transmission data 267

T.

Page.

Taylor, A. H., A simple portable instrument for the absolute measurement of reflection and transmission factors 1
Testing precision gage blocks 677
Tests of stellar radiometers 725
Theory of induced voltage in high-tension magneto 407
Thermal expansion of a few steels 611
Thermal expansion of copper 91
Thermal expansion of nickel, monel metal, stellite, stainless steel, and aluminum 497
Thermal radiation of a black body 7
Thermometers, resistance 49
Thermopile, vacuum, portable 187
Transmission data for various substances ... 267
Transmission factors 1, 203
Transmitters, radio telephone, modulator tubes 377
Telephone, radio, modulator tubes 377

U.

Ulbricht sphere 203
Uniformly heated inclosure, thermal radiation 7

V.

Vacuum thermopile, portable 187
Vapors, X rays from arcs in 471
Verifying laws of thermal radiation of a black body 7
Vinal, G. W., and F. W. Altrup, Electromotive force of cells at low temperatures ... 627
Voltage, induced, in high-tension magneto ... 407
Voltage of cells at low temperatures 627
Volume, specific, of liquid ammonia 287

W.

Walters, Francis M., jr., Wave-length measurements in arc spectra photographed in the yellow, red, and infra-red 161
—— *and Raymond Davis,* Studies in color-sensitive photographic plates and methods of sensitizing by bathing 353
Wave-length measurements in arc spectra ... 161
Wave lengths in arc spectra of yttrium, lanthanum, and cerium 317
White light 231

X.

Xenon spectrum 193
X rays from arcs in gases and vapors 471

Y.

Yellow spectrum, wave-length measurements 161
Yttrium, arc spectrum 317

Digitized by Google

Digitized by Google

Digitized by Google

Digitized by Google

Digitized by Google

RETURN TO the circulation desk of any
University of California Library
or to the
NORTHERN REGIONAL LIBRARY FACILITY
Bldg. 400, Richmond Field Station
University of California
Richmond, CA 94804-4698

ALL BOOKS MAY BE RECALLED AFTER 7 DAYS

- 2-month loans may be renewed by calling (510) 642-6753
- 1-year loans may be recharged by bringing books to NRLF
- Renewals and recharges may be made 4 days prior to due date.

DUE AS STAMPED BELOW

APR 18 2001
RETURNED

MAR 19 2000

JUN 21 2007

12,000 (11/95)

MAR 28 1963

MAR 11 1966 44
REC'D LD

LD 21A-50m-4,'60
(A9562s10)476B

General Library
University of California
Berkeley

Digitized by Google

U.C. BERKELEY LIBRARIES

C006693071

THE UNIVERSITY OF CALIFORNIA LIBRARY

Digitized by Google